VOLUME 29 / NUMBER 23
DECEMBER 8, 1991
ACC. NOS. N91-31078 TO N91-32031

STAR
AN ABSTRACT JOURNAL

Scientific and Technical Aerospace Reports

PRODUCED BY THE
SCIENTIFIC AND TECHNICAL
INFORMATION
PROGRAM

NASA

NATIONAL AERONAUTICS AND SPACE ADMINISTRATION

***Scientific and Technical Aerospace Reports* (*STAR*)** is an abstract journal that provides comprehensive coverage of worldwide aerospace-related reports. It is a major product of the International Aerospace Database managed by the NASA Scientific and Technical Information (STI) Program. The coverage includes reports on aeronautics, space, and supporting disciplines. *STAR* lists current, publicly available reports entered into the NASA STI Database during the 2-week period preceding publication. A typical citation and abstract appear on page viii. They explain how to read the items that are announced in this journal.

NASA sponsors a companion journal, *International Aerospace Abstracts* (*IAA*), that lists abstracts of the open literature on aerospace subjects available worldwide. *IAA* is available through the American Institute of Aeronautics and Astronautics.

Entries found in *STAR* and *IAA* are available through NASA's online service, RECON, as the International Aerospace Database and through DIALOG as the Aerospace Database.

Information on aerospace and related subjects is gathered by the NASA STI Program through national and international agreements and exchanges and is made available to the NASA community as well as to the public in many forms through various outlets. The section on NASA STI Program Products and Services contains additional information.

US ISSN 0036-8741

Volume 29 Number 23 / DECEMBER 8, 1991

TABLE OF CONTENTS

AERONAUTICS For related information see also *Astronautics.*

01 AERONAUTICS (GENERAL) **3781**

02 AERODYNAMICS **3781**
Includes aerodynamics of bodies, combinations, wings, rotors, and control surfaces; and internal flow in ducts and turbomachinery. For related information see also *34 Fluid Mechanics and Heat Transfer.*

03 AIR TRANSPORTATION AND SAFETY **3785**
Includes passenger and cargo air transport operations; and aircraft accidents. For related information see also *16 Space Transportation* and *85 Urban Technology and Transportation.*

04 AIRCRAFT COMMUNICATIONS AND NAVIGATION **3786**
Includes digital and voice communication with aircraft; air navigation systems (satellite and ground based); and air traffic control. For related information see also *17 Space Communications, Spacecraft Communications, Command and Tracking* and *32 Communications and Radar.*

05 AIRCRAFT DESIGN, TESTING AND PERFORMANCE **3788**
Includes aircraft simulation technology. For related information see also *18 Spacecraft Design, Testing and Performance* and *39 Structural Mechanics.* For land transportation vehicles see *85 Urban Technology and Transportation.*

06 AIRCRAFT INSTRUMENTATION **3791**
Includes cockpit and cabin display devices; and flight instruments. For related information see also *19 Space craft Instrumentation* and *35 Instrumentation and Photography.*

07 AIRCRAFT PROPULSION AND POWER **3791**
Includes prime propulsion systems and systems components, e.g., gas turbine engines and compressors; and onboard auxiliary power plants for aircraft. For related information see also *20 Spacecraft Propulsion and Power, 28 Propellants and Fuels,* and *44 Energy Production and Conversion.*

08 AIRCRAFT STABILITY AND CONTROL **3797**
Includes aircraft handling qualities; piloting; flight controls; and autopilots. For related information see also *05 Aircraft Design, Testing and Performance.*

09 RESEARCH AND SUPPORT FACILITIES (AIR) **3798**
Includes airports, hangars and runways; aircraft repair and overhaul facilities; wind tunnels; shock tubes; and aircraft engine test stands. For related information see also *14 Ground Support Systems and Facilities (Space).*

ASTRONAUTICS For related information see also *Aeronautics.*

12 ASTRONAUTICS (GENERAL) ..... **N.A.**
For extraterrestrial exploration see *91 Lunar and Planetary Exploration.*

13 ASTRODYNAMICS **3800**
Includes powered and free-flight trajectories; and orbital and launching dynamics.

14 GROUND SUPPORT SYSTEMS AND FACILITIES (SPACE) ..... **N.A.**
Includes launch complexes, research and production facilities; ground support equipment, e.g., mobile transporters; and simulators. For related information see also *09 Research and Support Facilities (Air).*

15 LAUNCH VEHICLES AND SPACE VEHICLES **3800**
Includes boosters; operating problems of launch/space vehicle systems; and reusable vehicles. For related information see also *20 Spacecraft Propulsion and Power.*

16 SPACE TRANSPORTATION **3800**
Includes passenger and cargo space transportation, e.g., shuttle operations; and space rescue techniques. For related information see also *03 Air Transportation and Safety* and *18 Spacecraft Design, Testing and Performance.* For space suits see *54 Man/System Technology and Life Support.*

17 SPACE COMMUNICATIONS, SPACECRAFT COMMUNICATIONS, COMMAND AND TRACKING . **N.A.**
Includes telemetry; space communications networks; astronavigation and guidance; and radio blackout. For related information see also *04 Aircraft Communications and Navigation* and *32 Communications and Radar.*

N.A.—no abstracts were assigned to this category for this issue.

18 SPACECRAFT DESIGN, TESTING AND PERFORMANCE **3801**
Includes satellites; space platforms; space stations; spacecraft systems and components such as thermal and environmental controls; and attitude controls. For life support systems see *54 Man/System Technology and Life Support.* For related information see also *05 Aircraft Design, Testing and Performance, 39 Structural Mechanics,* and *16 Space Transportation.*

19 SPACECRAFT INSTRUMENTATION ..... **N.A.**
For related information see also *06 Aircraft Instrumentation* and *35 Instrumentation and Photography.*

20 SPACECRAFT PROPULSION AND POWER **3802**
Includes main propulsion systems and components, e.g., rocket engines; and spacecraft auxiliary power sources. For related information see also *07 Aircraft Propulsion and Power, 28 Propellants and Fuels, 44 Energy Production and Conversion,* and *15 Launch Vehicles and Space Vehicles.*

CHEMISTRY AND MATERIALS

23 CHEMISTRY AND MATERIALS (GENERAL) **3805**

24 COMPOSITE MATERIALS **3805**
Includes physical, chemical, and mechanical properties of laminates and other composite materials. For ceramic materials see *27 Nonmetallic Materials.*

25 INORGANIC AND PHYSICAL CHEMISTRY **3809**
Includes chemical analysis, e.g., chromatography; combustion theory; electrochemistry; and photochemistry. For related information see also *77 Thermodynamics and Statistical Physics.*

26 METALLIC MATERIALS **3813**
Includes physical, chemical, and mechanical properties of metals, e.g., corrosion; and metallurgy.

27 NONMETALLIC MATERIALS **3817**
Includes physical, chemical, and mechanical properties of plastics, elastomers, lubricants, polymers, textiles, adhesives, and ceramic materials. For composite materials see *24 Composite Materials.*

28 PROPELLANTS AND FUELS **3821**
Includes rocket propellants, igniters and oxidizers; their storage and handling procedures; and aircraft fuels. For related information see also *07 Aircraft Propulsion and Power, 20 Spacecraft Propulsion and Power,* and *44 Energy Production and Conversion.*

29 MATERIALS PROCESSING **3822**
Includes space-based development of products and processes for commercial application. For biological materials see *55 Space Biology.*

ENGINEERING For related information see also *Physics.*

31 ENGINEERING (GENERAL) **3851**
Includes vacuum technology; control engineering; display engineering; cryogenics; and fire prevention.

32 COMMUNICATIONS AND RADAR **3852**
Includes radar; land and global communications; communications theory; and optical communications. For related information see also *04 Aircraft Communications and Navigation* and *17 Space Communications, Spacecraft Communications, Command and Tracking.* For search and rescue see *03 Air Transportation and Safety,* and *16 Space Transportation.*

33 ELECTRONICS AND ELECTRICAL ENGINEERING **3858**
Includes test equipment and maintainability; components, e.g., tunnel diodes and transistors; microminiaturization; and integrated circuitry. For related information see also *60 Computer Operations and Hardware* and *76 Solid-State Physics.*

34 FLUID MECHANICS AND HEAT TRANSFER **3864**
Includes boundary layers; hydrodynamics; fluidics; mass transfer and ablation cooling. For related information see also *02 Aerodynamics* and *77 Thermodynamics and Statistical Physics.*

35 INSTRUMENTATION AND PHOTOGRAPHY **3872**
Includes remote sensors; measuring instruments and gauges; detectors; cameras and photographic supplies; and holography. For aerial photography see *43 Earth Resources and Remote Sensing.* For related information see also *06 Aircraft Instrumentation* and *19 Spacecraft Instrumentation.*

36 LASERS AND MASERS **3875**
Includes parametric amplifiers. For related information see also *76 Solid-State Physics.*

37 MECHANICAL ENGINEERING **3879**
Includes auxiliary systems (nonpower); machine elements and processes; and mechanical equipment.

38 QUALITY ASSURANCE AND RELIABILITY **3882**
Includes product sampling procedures and techniques; and quality control.

39 STRUCTURAL MECHANICS **3883**
Includes structural element design and weight analysis; fatigue; and thermal stress. For applications see *05 Aircraft Design, Testing and Performance* and *18 Spacecraft Design, Testing and Performance.*

GEOSCIENCES For related information see also *Space Sciences.*

42 GEOSCIENCES (GENERAL) ..... **N.A.**

43 EARTH RESOURCES AND REMOTE SENSING **3887**
Includes remote sensing of earth resources by aircraft and spacecraft; photogrammetry; and aerial photography. For instrumentation see *35 Instrumentation and Photography.*

44 ENERGY PRODUCTION AND CONVERSION **3888**
Includes specific energy conversion systems, e.g., fuel cells; global sources of energy; geophysical conversion; and windpower. For related information see also *07 Aircraft Propulsion and Power, 20 Spacecraft Propulsion and Power,* and *28 Propellants and Fuels.*

45 ENVIRONMENT POLLUTION **3891**
Includes atmospheric, noise, thermal, and water pollution.

46 GEOPHYSICS **3893**
Includes aeronomy; upper and lower atmosphere studies; ionospheric and magnetospheric physics; and geomagnetism. For space radiation see *93 Space Radiation.*

47 METEOROLOGY AND CLIMATOLOGY **3896**
Includes weather forecasting and modification.

48 OCEANOGRAPHY **3897**
Includes biological, dynamic, and physical oceanography; and marine resources. For related information see also *43 Earth Resources and Remote Sensing.*

LIFE SCIENCES

51 LIFE SCIENCES (GENERAL) **3897**

52 AEROSPACE MEDICINE **3898**
Includes physiological factors; biological effects of radiation; and effects of weightlessness on man and animals.

53 BEHAVIORAL SCIENCES **3900**
Includes psychological factors; individual and group behavior; crew training and evaluation; and psychiatric research.

54 MAN/SYSTEM TECHNOLOGY AND LIFE SUPPORT **3901**
Includes human engineering; biotechnology; and space suits and protective clothing. For related information see also *16 Space Transportation.*

55 SPACE BIOLOGY ..... **N.A.**
Includes exobiology; planetary biology; and extraterrestrial life.

MATHEMATICAL AND COMPUTER SCIENCES

59 MATHEMATICAL AND COMPUTER SCIENCES (GENERAL) ..... **N.A.**

60 COMPUTER OPERATIONS AND HARDWARE **3907**
Includes hardware for computer graphics, firmware, and data processing. For components see *33 Electronics and Electrical Engineering.*

61 COMPUTER PROGRAMMING AND SOFTWARE **3908**
Includes computer programs, routines, algorithms, and specific applications, e.g., CAD/CAM.

62 COMPUTER SYSTEMS **3915**
Includes computer networks and special application computer systems.

63 CYBERNETICS **3917**
Includes feedback and control theory, artificial intelligence, robotics and expert systems. For related information see also *54 Man/System Technology and Life Support.*

64 NUMERICAL ANALYSIS **3919**
Includes iteration, difference equations, and numerical approximation.

65 STATISTICS AND PROBABILITY **3922**
Includes data sampling and smoothing; Monte Carlo method; and stochastic processes.

66 SYSTEMS ANALYSIS **3923**
Includes mathematical modeling; network analysis; and operations research.

67 THEORETICAL MATHEMATICS ..... **N.A.**
Includes topology and number theory.

PHYSICS For related information see also *Engineering.*

70 PHYSICS (GENERAL) ..... **N.A.**
For precision time and time interval (PTTI) see *35 Instrumentation and Photography;* for geophysics, astrophysics or solar physics see *46 Geophysics, 90 Astrophysics,* or *92 Solar Physics.*

71 ACOUSTICS **3923**
Includes sound generation, transmission, and attenuation. For noise pollution see *45 Environment Pollution.*

72 ATOMIC AND MOLECULAR PHYSICS **3925**
Includes atomic structure, electron properties, and molecular spectra.

73 NUCLEAR AND HIGH-ENERGY PHYSICS **3926**
Includes elementary and nuclear particles; and reactor theory. For space radiation see *93 Space Radiation.*

74 OPTICS **3927**
Includes light phenomena and optical devices. For lasers see *36 Lasers and Masers.*

75 PLASMA PHYSICS **3929**
Includes magnetohydrodynamics and plasma fusion. For ionospheric plasmas see *46 Geophysics.* For space plasmas see *90 Astrophysics.*

76 SOLID-STATE PHYSICS **3930**
Includes superconductivity. For related information see also *33 Electronics and Electrical Engineering* and *36 Lasers and Masers.*

77 THERMODYNAMICS AND STATISTICAL PHYSICS ..... **N.A.**
Includes quantum mechanics; theoretical physics; and Bose and Fermi statistics. For related information see also *25 Inorganic and Physical Chemistry* and *34 Fluid Mechanics and Heat Transfer.*

SOCIAL SCIENCES

80 SOCIAL SCIENCES (GENERAL) ..... **N.A.**
Includes educational matters.

81 ADMINISTRATION AND MANAGEMENT **3934**
Includes management planning and research.

82 DOCUMENTATION AND INFORMATION SCIENCE **3935**
Includes information management; information storage and retrieval technology; technical writing; graphic arts; and micrography. For computer documentation see *61 Computer Programming and Software.*

83 ECONOMICS AND COST ANALYSIS ..... **N.A.**
Includes cost effectiveness studies.

84 LAW, POLITICAL SCIENCE AND SPACE POLICY ..... **N.A.**
Includes NASA appropriation hearings; aviation law; space law and policy; international law; international cooperation; and patent policy.

85 URBAN TECHNOLOGY AND TRANSPORTATION ..... **N.A.**
Includes applications of space technology to urban problems; technology transfer; technology assessment; and surface and mass transportation. For related information see *03 Air Transportation and Safety, 16 Space Transportation,* and *44 Energy Production and Conversion.*

SPACE SCIENCES For related information see also *Geosciences.*

88 SPACE SCIENCES (GENERAL) **3937**

89 ASTRONOMY **3937**
Includes radio, gamma-ray, and infrared astronomy; and astrometry.

90 ASTROPHYSICS **3939**
Includes cosmology; celestial mechanics; space plasmas; and interstellar and interplanetary gases and dust. For related information see also *75 Plasma Physics.*

91 LUNAR AND PLANETARY EXPLORATION **3940**
Includes planetology; and manned and unmanned flights. For spacecraft design or space stations see *18 Spacecraft Design, Testing and Performance.*

92 SOLAR PHYSICS **3940**
Includes solar activity, solar flares, solar radiation and sunspots. For related information see *93 Space Radiation.*

93 SPACE RADIATION ..... **N.A.**
Includes cosmic radiation; and inner and outer earth's radiation belts. For biological effects of radiation see *52 Aerospace Medicine.* For theory see *73 Nuclear and High-Energy Physics.*

GENERAL

Includes aeronautical, astronautical, and space science related histories, biographies, and pertinent reports too broad for categorization; histories or broad overviews of NASA programs.

99 GENERAL **3940**

SUBJECT INDEX **I-1**

PERSONAL AUTHOR INDEX **I-63**

CORPORATE SOURCE INDEX **I-71**

CONTRACT NUMBER INDEX **I-83**

REPORT/ACCESSION NUMBER INDEX **I-91**

APPENDIX **A-1**

TYPICAL CITATION AND ABSTRACT

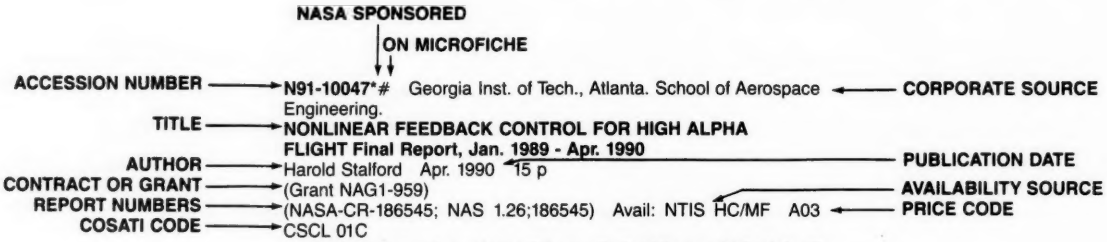

Analytical aerodynamic models are derived from a high alpha 6 DOF wind tunnel model. One detail model requires some interpolation between nonlinear functions of alpha. One analytical model requires no interpolation and as such is a completely continuous model. Flight path optimization is conducted on the basic maneuvers: half-loop, 90 degree pitch-up, and level turn. The optimal control analysis uses the derived analytical model in the equations of motion and is based on both moment and force equations. The maximum principle solution for the half-loop is poststall trajectory performing the half-loop in 13.6 seconds. The agility induced by thrust vectoring capability provided a minimum effect on reducing the maneuver time. By means of thrust vectoring control the 90 degrees pitch-up maneuver can be executed in a small place over a short time interval. The agility capability of thrust vectoring is quite beneficial for pitch-up maneuvers. The level turn results are based currently on only outer layer solutions of singular pertrubation. Poststall solutions provide high turn rates but generate higher losses of energy than that of classical sustained solutions.

Author

VOLUME 29 NUMBER 23 / DECEMBER 8, 1991

Scientific and Technical Aerospace Reports

A Semimonthly Publication of the National Aeronautics and Space Administration

01 AERONAUTICS (GENERAL)

N91-31078*# National Aeronautics and Space Administration. Ames Research Center, Moffett Field, CA.
VIBRATION ANALYSIS OF THE SA349/2 HELICOPTER
Ruth Heffernan, Dominique Precetti, and Wayne Johnson (Johnson Aeronautics, Palo Alto, CA.) Jan. 1991 102 p
(NASA-TM-102794; A-90083; NAS 1.15:102794) Avail: NTIS HC/MF A06 CSCL 01B

Helicopter airframe vibration is examined using calculations and measurements for the SA349/2 research helicopter. The hub loads, which transmit excitations to the fuselage, are predicted using a comprehensive rotorcraft analysis and correlated with measuring hub loads. The predicted and measured hub loads are then coupled with finite element models representing the SA349/2 fuselage. The resulting vertical acceleration at the pilot seat is examined. Adjustments are made to the airframe structural models to examine the sensitivity of predicted vertical acceleration to the model. Changes of a few percent to the damping and frequency of specific models lead to large reductions in predicted vibration, and to major improvements in the correlations with measured pilot-seat vertical acceleration. Author

N91-31079# Naval Postgraduate School, Monterey, CA.
AN INTEGER PROGRAMMING MODEL FOR NAVY'S MARITIME PATROL AVIATION FLEET M.S. Thesis
Robert W. Drash Sep. 1990 78 p
(AD-A239464) Avail: NTIS HC/MF A05 CSCL 05/1

This thesis details an integer programming model to aid in the modernization of the Navy's Maritime Patrol Aviation fleet. Over a user specified time horizon, the model provides a schedule for when to retire, perform avionics upgrades, or transfer current inventory aircraft from the USN to the USNR. Additionally, the model determines when to open a new aircraft production line and the number of aircraft to procure each year. The model optimizes the modernization schedule while taking into consideration required inventory, minimum required percentage of aircraft containing modern avionics, maximum desired mean aircraft age, budgetary limitations, and production line restrictions. The model minimizes the procurement, operating and maintenance costs using the X-System solver. GRA

02 AERODYNAMICS

Includes aerodynamics of bodies, combinations, wings, rotors, and control surfaces; and internal flow in ducts and turbomachinery.

For related information see also *34 Fluid Mechanics and Heat Transfer.*

N91-31080 Oklahoma Univ., Norman.
COMPUTATIONAL ANALYSIS OF HYPERSONIC FLOWS PAST ELLIPTIC-CONE WAVERIDERS Ph.D. Thesis
Bok-Hyun Yoon 1990 307 p
Avail: Univ. Microfilms Order No. DA9119183

A comprehensive study for the inviscid numerical calculation of the hypersonic flow fields past a class of elliptic-cone derived waveriders is presented. The theoretical background associated with hypersonic small disturbance theory (HSDT) is reviewed. Several approximation formulas for the waverider compression surface are established. A computational fluid dynamics (CFD) algorithm is used to calculate flow fields for the on-design case and a variety of off-design cases. The results are compared with (HSDT), experiment, and other CFD results. The unknown flow patterns that were discovered show the power and utility of CFD for investigating novel hypersonic configurations such as waveriders. Dissert. Abstr.

N91-31081# National Aerospace Lab., Amsterdam (Netherlands). Informatics/Aerodynamics Div.
DEVELOPMENT AND VALIDATION OF CHARACTERISTIC BOUNDARY CONDITIONS FOR CELL-CENTERED EULER FLOW CALCULATIONS WITH A SHOCK-FREE AIRFOIL
J. I. vandenBerg and J. W. Boerstoel 30 Oct. 1989 16 p
Presented at 8th GAMM Conference on Numerical Methods in Fluid Mechanics, Delft, Netherlands, Sep. 1989 Sponsored by Netherlands Agency for Aerospace Programs
(NLR-TP-89360-U; ETN-91-99647) Copyright Avail: NTIS HC/MF A03

An overview of the development, analysis, and numerical validation of a solid wall boundary condition for cell centered Euler flow calculations is presented. This solid wall boundary condition is provided by the theory of characteristics, and is based on a central difference scheme. The boundary condition was developed to clarify the question of what the effect is of various boundary condition algorithms on the accuracy of calculation results for three dimensional Euler flows around delta wings. A mathematical analysis of the boundary condition was performed. It consists of a theoretical study to the consistency, well-posedness, and stability. The numerical validation consists of a comparison of calculation results with various boundary conditions with each other. Discretization and convergence errors were investigated. ESA

N91-31082*# National Aeronautics and Space Administration. Langley Research Center, Hampton, VA.
USER'S GUIDE TO A SYSTEM OF FINITE-ELEMENT SUPERSONIC PANEL FLUTTER PROGRAMS
Christine L. Woolley and John T. Batina Jul. 1991 54 p
(NASA-TM-104109; NAS 1.15:104109) Avail: NTIS HC/MF A04 CSCL 01A

The utilization and operation of a set of six computer programs for the prediction of panel flutter at supersonic speeds by finite element methods are described. The programs run individually to determine the flutter behavior of a flat panel where the finite elements which model the panel each have four degrees of freedom (DOF), a curved panel where the finite elements each have four DOF, and a curved panel where the finite elements each have six DOF. The panels are assumed to be of infinite aspect ratio and are subjected to either simply-supported or clamped boundary conditions. The aerodynamics used by these programs are based on piston theory. Application of the program is illustrated by sample cases where the number of beam finite elements equals four, the in-plane tension parameter is 0.0, the maximum camber to panel length ratio for a curved panel case is 0.05, and the Mach number is 2.0. This memorandum provides a user's guide for these programs, describes the parameters that are used, and contains sample output from each of the programs. Author

N91-31083*# North Carolina State Univ., Raleigh.
A COMPUTATIONAL AND EXPERIMENTAL INVESTIGATION OF A THREE-DIMENSIONAL HYPERSONIC SCRAMJET INLET FLOW FIELD Ph.D. Thesis
Scott Douglas Holland 1991 676 p
(Grant NAGw-1072)
(NASA-CR-188788; NAS 1.26:188788) Copyright Avail: NTIS HC/MF A99 CSCL 01A

A combined computational and experimental parametric study of the internal aerodynamics of a generic three dimensional sidewall compression scramjet inlet configuration was performed. The study was designed to demonstrate the utility of computational fluid dynamics as a design tool in hypersonic inlet flow fields, to provide a detailed account of the nature and structure of the internal flow interactions, and to provide a comprehensive surface property and flow field database to determine the effects of contraction ratio, cowl position, and Reynolds number on the performance of a hypersonic scramjet inlet configuration. Author

N91-31084# National Aerospace Lab., Amsterdam (Netherlands). Aerodynamics Div.
A EUROPEAN COLLABORATIVE INVESTIGATION OF THE THREE-DIMENSIONAL TURBULENT SHEAR LAYERS OF A SWEPT WING
B. vandenBerg 19 Sep. 1988 24 p Presented at the AGARD Fluid Dynamics Panel Symposium on Fluid Dynamics on Three-Dimensional Turbulent Shear Flows and Transition, Cesme, Turkey, 3-6 Oct. 1988 Previously announced as N90-10380
(NLR-MP-88054-U; GARTEUR-AD(AG07)-TP048; ETN-91-99655) Avail: NTIS HC/MF A03

An extensive and detailed experiment in progress is described on the turbulent shear layers of a swept wing. The measurements comprise both the upper and lower wing surface boundary layer as well as the three dimensional near wake behind the wing. Starting from required viscous flow properties, a wing geometry was designed by flow calculations. The theoretical wing design was checked by pilot model tests. The results suggest that the viscous flow in this experiment may become an interesting test case for turbulence models for three dimensional shear flows. The measurements in the turbulent shear layers comprise mean flow quantities, skin friction data and the six Reynolds stress tensor components. To establish the measurement accuracy, several data checks were performed, including independent tests with similar models in two different wind tunnels. ESA

N91-31085# Max-Planck-Inst. fuer Stroemungsforschung, Goettingen (Germany, F.R.).
THE EFFECT OF JET BLEED ON BASE PRESSURE DISTRIBUTION, SHEDDING FREQUENCY, AND MEAN VELOCITY PROFILES IN THE WAKE BEHIND A TWO-DIMENSIONAL BLUNT MODEL
V. L. Zhdanov and H. Eckelmann Jun. 1990 37 p Sponsored in part by Max-Planck-Gesellschaft
(MPIS-12/1990; ISSN-0436-1199; ETN-91-99738) Avail: NTIS HC/MF A03

A two dimensional body with a semicircle front followed by a parallel sided body with a blunt trailing edge is investigated at a free stream velocity of 14 m/s in an open return wind tunnel with a cross section of 280 by 1400 square mm. The cord length, base height and spanwise width of the body are 200 mm, 40 mm and 280 mm, respectively. By means of a slot in the near surface of the body a base bleed is achieved. The slot width is changed from 0.75 mm to 3.8 mm, and the bleed coefficient varies between zero and 0.24. Base pressure and Strouhal number distributions as well as mean velocity profiles in the wake of the body are presented. ESA

N91-31086# Messerschmitt-Boelkow-Blohm G.m.b.H., Ottobrunn (Germany, F.R.). Unternehmensbereich Verteidigungssysteme.
AEROTHERMODYNAMICAL PROJECT OF HYPERSONIC PROJECTILES [AERO-THERMODYNAMISCHER ENTWURF VON HYPERSCHALL-PROJEKTILEN]
Horst Schneider 1990 10 p In GERMAN
(MBB-UA-1193-90-PUB; OTN-032766; ETN-91-99754) Avail: NTIS HC/MF A02

The development method of the aerothermodynamical configurations of hypersonic projectiles is presented. They can be used in electromagnetic or electrothermal guns. Comparison calculations are used to determine the dependability of the project program. Aero and thermodynamic requirements are discussed, with reference to a parameter study. The project of a basic configuration with its main aerothermodynamic properties is presented, using optimization. From an aerothermodynamical point of view, the configuration presented should correspond to about Mach 10, with regard to requirements for high launching velocities. Tungsten is to be used as penetration material, so low ablation is to be expected in the stagnation point field. ESA

N91-31087# Messerschmitt-Boelkow-Blohm G.m.b.H., Munich (Germany, F.R.). Kommunikationssysteme und Antriebe.
A SHOCK-FITTING ALGORITHM FOR THE SIMULATION OF INVISCID FLOWS IN CHEMICAL NON-EQUILIBRIUM
M. Pfitzner 30 Jan. 1990 33 p Presented at the 12th ICNMFD, Oxford, England, 1990
(MBB-UK-0131-90-PUB; OTN-033083; ETN-91-99756) Avail: NTIS HC/MF A03

An upwind finite difference algorithm based on the integration of the quasi conservative Euler equations for the simulation of inviscid flow in chemical non-equilibrium is described. Shock fitting is applied to deal with the strong bow shock present in hypersonic flows. Post correction techniques are used. An explicit Runge-Kutta time stepping scheme is applied with the chemical source terms treated point implicity where necessary. Convergence is accelerated using a local time step and enthalpy correction. In the supersonic part of the flow field the pseudo space marching technique is applied. The algorithm is implemented in two dimensional and three dimensional codes. Results of several test cases are presented. ESA

N91-31088# Messerschmitt-Boelkow-Blohm G.m.b.H., Munich (Germany, F.R.). Hubschrauber und Flugzeuge.
VISCOUS EFFECTS
E. H. Hirschel 1 Feb. 1991 38 p Presented at Space Course 1991, Aachen, Fed. Republic of Germany, 20 Feb. 1991
(MBB-FE202/S/PUB/441; ETN-91-99764) Avail: NTIS HC/MF A03

Viscous effects play a large role in hypersonic aerothermodynamics, especially for airbreathing cruise vehicles. Four basic classes of viscous hypersonic flow are identified and discussed. Their influence on aerothermodynamic vehicle design and performance is sketched. The fact that viscous effects must be seen in the broader context of diffusive context of diffusive transport mechanisms is illustrated. Selected phenomena are discussed in more detail and qualitative and quantitative results are given. ESA

N91-31089# Office National d'Etudes et de Recherches Aerospatiales, Paris (France). Direction des Grands Moyens d'Essais.
TRANSITION LENGTH DETERMINATION IN THE F1 WIND TUNNEL, TEST REPORT [DETERMINATION DE LA LONGUEUR DE TRANSITION DANS LA SOUFFLERIE F1. PROCES VERBAL D'ESSAIS]
Christian Pelissier May 1990 46 p In FRENCH
(Contract STPA-8595009)
(ONERA-PV-1/8571-GY; ETN-91-99907) Avail: NTIS HC/MF A03

A study of the length of natural transition in the F1 wind tunnel is presented. A cone of UREOL resin with a 10 degree angle at the summit is used and the main investigation method is thermographic visualization. Results confirm that at a given Mach number the generating pressure is not accompanied by parasitic effects perturbing the natural boundary layer transition. The studies of effects due to variation of the Reynolds numbers carried out in F1 are therefore really significant. ESA

N91-31090# METRAVIB, Lyon (France). Dept. Materiaux.
VAUDREUIL (FRANCE) LARGE HYDRODYNAMIC TUNNEL: ACOUSTIC CHAMBER DAMPING [GRAND TUNNEL HYDRODYNAMIQUE DU VAUDREUIL: AMORTISSEMENT DE LA CHAMBRE ACOUSTIQUE]
M. Salvia 31 May 1990 63 p In FRENCH
(Contract DRET-88-509)
(METRAVIB-RDS-1-007-67; ETN-91-99910) Avail: NTIS HC/MF A04

Principle techniques used in the damping of the tunnel walls are described. Results of a parametric study of the structural damping of the wall and the energy distribution between the propagated, reflected, and trapped waves in the structure are given. The wave damping is optimized using calculations of damped sandwich structures of viscoelastic materials used near to their vitreous transition. The energy distributions for the basic structure and damped structures (multilayer structures) are evaluated using the SAM software code. ESA

N91-31091# Ecole Centrale de Lyon (France). Lab. de Mecanique des Fluides et d'Acoustique.
CONTRIBUTION OF LOW WAVE NUMBERS TO THE WALL PRESSURE FIELD IN A TWO DIMENSIONAL TURBULENT BOUNDARY LAYER: COMPARISON OF DIFFERENT EXPERIMENTAL TECHNIQUES Ph.D. Thesis
Philippe Ibars 1990 135 p In FRENCH; ENGLISH summary
(ECL-90-15; ETN-91-99919) Avail: NTIS HC/MF A07

Three techniques to obtain the interspectral density of the wall pressure field induced by a turbulent boundary layer in the frequency and wave number domain are studied. The first uses a vibrating structure excited by the flow as a spatial-temporal filter; the second uses a network (or antenna) of pressure sensors; and the third uses fast Fourier transformation processing of previously calculated pressure signals. Particular attention is given to practical problems of development and gauging of the components. Measurements are conducted in wind tunnel at the same flow conditions. ESA

N91-31092# Office National d'Etudes et de Recherches Aerospatiales, Paris (France). Direction de l'Aerodynamique.
EXPLOITATION OF OAT15A PROFILE TESTS IN THE T2 WIND TUNNEL: EXPERIMENTAL DETERMINATION OF THE WAVE DRAG Final Summary Report [EXPLOITATION DES ESSAIS DU PROFIL OAT15A DANS LA SOUFFLERIE T2: DETERMINATION EXPERIMENTALE DE LA TRAINEE D'ONDE. RAPPORT DE SYNTHESE FINAL]
H. Bezard Jul. 1990 46 p In FRENCH
(Contract DRET-89-34-001)
(ONERA-RSF-88/1685-AY-158-A; ETN-91-99929) Avail: NTIS HC/MF A03

Results and exploitation of OAT15A profile tests in the T2 wind tunnel with laser velocimetry flow analysis are presented with the aim of experimentally determining the wave drag on the profile. The shock is determined for different contours by integrating the amount of movement. The influences of contour dimensions and the precision on velocity measurements are studied. Comparisons are carried out with different viscous computation methods. ESA

N91-31093# Office National d'Etudes et de Recherches Aerospatiales, Paris (France). Direction de l'Aerodynamique.
VALIDATION OF TWO DIMENSIONAL DRAG PREDICTION METHODS Final Summary Report [VALIDATION DES METHODES DE PREVISION DE LA TRAINEE EN BIDIMENSIONNEL. RAPPORT DE SYNTHESE FINAL]
A. M. Rodde Mar. 1990 40 p In FRENCH
(ONERA-RSF-85/1685-AY; ETN-91-99930) Avail: NTIS HC/MF A03

Drag on different profiles is analyzed and results are compared to other research tests. Three profiles are studied: the OAT15A, for which detailed results obtained in transonic wind tunnels are used; the NACA0012 and RAE2822 profiles, for which published tests results and computations are used. The potential non conservative strong coupling method is shown to obtain for the most part comparable results to NASA research. ESA

N91-31094# Office National d'Etudes et de Recherches Aerospatiales, Paris (France).
ATSF SUPERSONIC AIRCRAFT INTAKE. REVIEW OF THE ANALYSES OF SOME PARTICULAR PROBLEMS, TECHNICAL SUMMARY [ENTREES D'AIR POUR L'AVION SUPERSONIQUE ATSF. REVUE DES MOYENS D'ETUDES ET DE QUELQUES PROBLEMES PARTICULIERS. RAPPORT TECHNIQUE DE SYNTHESE]
C. Sans Aug. 1990 96 p In FRENCH
(ONERA-RTS-134/2149-AY-640-A; ETN-91-99931) Avail: NTIS HC/MF A05

A survey and application examples of codes (semi-empirical and numerical) for computing internal flow in two dimensional supersonic air intakes are presented. Air intake drag reduction and flow stability (effects of pumping) are considered. Industrially proposed air intake definitions are analyzed. Existing test methods are reviewed. ESA

N91-31095# Office National d'Etudes et de Recherches Aerospatiales, Paris (France). Direction Scientifique de la Resistance des Structures.
THREE DIMENSIONAL EXTENSION OF A NUMERICAL METHOD FOR RESOLVING SMALL TRANSONIC PERTURBATIONS IN UNSTRUCTURED MESH [EXTENSION 3D D'UNE METHODE NUMERIQUE DE RESOLUTION DES PETITES PERTURBATIONS TRANSSONIQUES EN MAILLAGE NON STRUCTURE]
F. Bangui Mar. 1990 69 p In FRENCH
(Contract DRET-89-34-001)
(ONERA-RT-50/3064-RY-093-R; ETN-91-99936) Avail: NTIS HC/MF A04

A method to solve the Euler equations in small transonic perturbations using a mixed formulation, and entropic and physical variables, is presented. The problem is solved with a finite element scheme. The algebra for a discretized system, the structure of the edge-profile operator and the condition imposed on the profile, and the resolution algorithm are described. Numerical applications and validations are presented for the steady case. ESA

N91-31096# Office National d'Etudes et de Recherches Aerospatiales, Toulouse (France). Dept. d'Etudes et de Recherches en Aerodynamique.
STUDY OF THE FLOW AROUND THE GARTEUR AD/AG07 WING: FIRST F2 TEST CAMPAIGN RESULTS Final Report [ETUDE DE L'ECOULEMENT AUTOUR DE L'AILE GARTEUR AD/AG07: RESULTATS DE LA PREMIERE CAMPAGNE D'ESSAIS AF2]
C. Gleyzes Jun. 1990 134 p In FRENCH
(Contract STPA-89-95-004-52)
(ONERA/DERAT-37/5025-26; ETN-91-99941) Avail: NTIS HC/MF A07

Three dimensional shear flow around the Garteur AD/AG07 wing was studied. Attention was paid to the preparation, model equipment (pneumatic and electric), and development of different measurement methods. The study focused principally on a parametric study to define the final configuration for final tests. The transition triggering system performance was verified. Wall pressure measurements and friction direction measurements in an incidence region around the nominal theoretic incidence (0.5 deg) were made. Three dimensional boundary layer soundings were taken within scanners installed on the model in the 0.5 deg configuration. ESA

N91-31097# Association Aeronautique et Astronautique de France, Paris.
MEASUREMENT OF SIX COMPONENT EFFORTS IN TRANSITION FLOW [MESURES D'EFFORTS SIX COMPOSANTS EN ECOULEMENT TRANSITOIRE]
Marc Stojanowski 1989 35 p In FRENCH Presented at the

26th Colloque d'Aerodynamique Appliquee, Toulouse, France, 23-25 Oct. 1990 Previously announced in IAA as A90-21049
(AAAF-NT-89-01; ISBN-2-7170-0962-0; ISSN-0243-0177;
ETN-91-99942) Avail: NTIS HC/MF A03; CEDOCAR, Section des Diffusions, 26 Blvd Victor, 75996 Paris Armees, France, HC 30 francs

An inertial correction method using accelerometer measurements to measure six aerodynamic coefficients of transition and unsteady flow is presented. The increased field of flight corresponding to high altitudes up to 120 km and high speed of 7 to 8 km/s is studied for the hypersonic flow field of the reentry trajectories of the Hermes Manned Spaceplane. First results on longitudinal elements are encouraging, notably where expected effects are obtained. The study was therefore turned to new forms of Hermes while integrating acquired experience, so as the optimize to accelerometric corrections. ESA

N91-31098# Association Aeronautique et Astronautique de France, Paris.
RADAC MODEL DEFORMATION MEASUREMENT SYSTEM: FIRST RESULTS AT THE F1 WIND TUNNEL [DISPOSITIF RADAC DE MESURE DES DEFORMATIONS DE MAQUETTE: PREMIERS RESULTATS EXPERIMENTAUX DANS LA SOUFFLERIE F1]
B. Lamiscarre, B. Sidoruk, C. Castan, and M. Bazin (Office National d'Etudes et de Recherches Aerospatiales, Paris, France) 1989 21 p In FRENCH Presented at the 26th Colloque d'Aerodynamique Appliquee, Toulouse, France, 23-25 Oct. 1990 Previously announced in IAA as A91-19595
(AAAF-NT-89-03; ISBN-2-7170-0936-1; ISSN-0243-0177;
ETN-91-99944) Avail: NTIS HC/MF A03; CEDOCAR, Section des Diffusions, 26 Blvd Victor, 75996 Paris Armees, France, HC 15 francs

The RADAC (French acronym for altitude and deformation reconstruction) measurement system enables determination of the model and test assembly deformations under aerodynamic forces. The principles of stereo reconstruction of three dimensional shapes are described. Tests results and first results obtained during qualification tests in the F1 pressurized wind tunnel are presented. ESA

N91-31099# Association Aeronautique et Astronautique de France, Paris.
CONDITIONAL SAMPLING [LE PRELEVEMENT CONDITIONNEL]
C. Armand and R. Selvaggini (Office National d'Etudes et de Recherches Aerospatiales, Modane, France) 1989 21 p In FRENCH Presented at the 26th Colloque d'Aerodynamique Appliquee, Toulouse, France, 23-25 Oct. 1990 Previously announced in IAA as A90-21047
(AAAF-NT-89-04; ISBN-2-7170-0937-X; ISSN-0243-0177;
ETN-91-99945) Avail: NTIS HC/MF A03; CEDOCAR, Section des Diffusions, 26 Blvd Victor, 75996 Paris Armees, France, HC 15 francs

A conditional sampling method to overcome parametric uncertainties in wind tunnel experimental conditions is presented. The method consists of permanently measuring the parameter to be regulated and allows measurement of pressure distribution on wing configurations to be carried out precisely since the measurement are synchonized and acquired in desired conditions. The method is applied to two tests: wing pressure measurement and aerodynamic measurements on a demi-model. ESA

N91-31100# Association Aeronautique et Astronautique de France, Paris.
LASER VELOCIMETRY AT THE CEAT AERODYNAMIC GROUP: APPLICATION TO UNSTEADY MEASUREMENTS ON A FLUID FLAP PROFILE [LA VELOCIMETRIE LASER AU GROUPE AERODYNAMIQUE DU CEAT: APPLICATION AUX MESURES INSTATIONNAIRES SUR UN PROFIL A VOLET FLUIDE]
J. Humbertclaude and P. Dufour 1989 44 p In FRENCH Presented at 26th Colloque d'Aerodynamique Appliquee, Toulouse, France, 23-25 Oct. 1990
(AAAF-NT-89-05; ISBN-2-7170-0938-8; ISSN-0243-0177;
ETN-91-99946) Avail: NTIS HC/MF A03; CEDOCAR, Section des Diffusions, 26 Blvd Victor, 75996 Paris Armees, France, HC 30 francs

The use of laser velocimetry to analyze unsteady conditions (helicopter profile or canard surface incidence oscillation) is discussed. A solution that can be used in periodic test cases is addressed. A synchronization housing triggers conditional acquisition during each cycle. An application of results obtained in a test campaign on a pulsed fluid flap profile is presented. ESA

N91-31101# Association Aeronautique et Astronautique de France, Paris.
LOW LEVEL TURBULENCE DETECTION BY A LASER VELOCIMETRY TECHNIQUE: APPLICATION TO TRANSONIC FLOWS [DETECTION DE BAS NIVEAUX DE TURBULENCE PAR UNE TECHNIQUE DE VELOCIMETRIE LASER: APPLICATION AUX ECOULEMENTS TRANSSONIQUES]
V. Mercier, P. Szeger, R. Leblanc, M. Riethmuller, and R. Decuypere (Ecole Royale Militaire, Brussels, Belgium) 1989 17 p In FRENCH Presented at 26th Colloque D'Aerodynamique Appliquee, Toulouse, France, 23-25 Oct. 1989
(Contract DRET-87-1187)
(AAAF-NT-89-07; ISBN-2-7170-0940-X; ISSN-0243-0177;
ETN-91-99948) Avail: NTIS HC/MF A03; CEDOCAR, Section des Diffusions, 26 Blvd Victor, 75996 Paris Armees, France, HC 15 francs

The development of a laser velocimetry technique to detect the boundary layer transition in transonic flow is described. The turbulence measurement relies on analyzing the number of particles passing from one spot to another and more precisely on the correlation between them. The minimum turbulence detectable by LDV (Laser Doppler Velocimetry) in percentage, approaches the percentage given by LTV (Laser Transit Velocimetry) for certain applications. A mathematical model confirms the sensitivity of the obtained characteristic parameter. The method is transposed for transonic wind tunnel measurements. ESA

N91-31102# Association Aeronautique et Astronautique de France, Paris.
LOCAL MEAN MASS VOLUME MEASUREMENT AROUND A MODEL WITH LATERAL JET IN SUPERSONIC FLOW [MESURE DE LA MASSE VOLUMIQUE MOYENNE LOCALE AUTOUR D'UNE MAQUETTE MUNIE D'UN JET LATERAL EN ECOULEMENT SUPERSONIQUE]
L. Bobin (Institut Franco-Allemand de Recherches, Saint-Louis, France) 1989 13 p In FRENCH Presented at 26th Colloque d'Aerodynamique Appliquee, Toulouse, France, 23-25 Oct. 1989
(AAAF-NT-89-08; ISBN-2-7170-0941-8; ISSN-0243-0177;
ETN-91-99949) Avail: NTIS HC/MF A03; CEDOCAR, Section des Diffusions, 26 Blvd Victor, 75996 Paris Armees, France, HC 15 francs

The model consists of a revolving 40 mm diameter cylinder-cone, without incidence. The cylinder part has a profiled pipe of 4 mm diameter exit, which ejects a cold jet of methane normally to the wind tunnel flow (M = 2). The convergence study was carried out by measuring the mean spontaneous Raman diffusion and the mean local mass volume of the air and injected methane. The results agree with predictions for flow without jet. Other results will be used to develop mathematical models of perturbed flows by a transverse jet. This new experiment confirms the importance of spontaneous Raman diffusion as a non intrusive aerodynamic measuring method. ESA

N91-31103# Association Aeronautique et Astronautique de France, Paris.
LASER FOURIER DENSITOMETRY AND LASER INDUCED PHOTOCHEMICAL ANEMOMETRY IN SUPERSONIC FLOW [LA DENSITOMETRIE DE FOURIER PAR LASER ET L'ANEMOMETRIE PAR EFFET PHOTOCHIMIQUE INDUIT PAR LASER EN ECOULEMENT SUPERSONIQUE]
J. P. Bonnet, B. Cabrit, R. E. Falco, G. Gemaux, and D. Gresillon (Ecole Polytechnique, Palaiseau, France) 1989 40 p In FRENCH Presented at 26th Colloque d'Aerodynamique Appliquee, Toulouse, France, 23-25 Oct. 1990
(Contracts DRET-86-095; DRET-DS/SSR-88-1441)
(AAAF-NT-89-09; ISBN-2-7170-0942-6; ISSN-0243-0177; ETN-91-99950) Avail: NTIS HC/MF A03; CEDOCAR, Section des Diffusions, 26 Blvd Victor, 75996 Paris Armees, France, HC 30 francs

Laser Fourier Densitometry (LFD) and Laser Induced Photochemical Anemometry (LIPA) flow analysis techniques are presented. LFD is a nonintrusive method adapted to hypersonic or supersonic compressible turbulent flows. In LIPA a pulsed UV laser is developed and photochemical substances are used to create a mesh of simultaneous measurements. LFD is applied to the study of planar transition in hypersonic flow. The LIPA method is tested using a supersonic wake/jet flow. ESA

N91-31104# Association Aeronautique et Astronautique de France, Paris.
AIRFOIL-VORTEX INTERACTION: UNSTEADY WALL PRESSURE MEASUREMENT [INTERACTION ENTRE UN TOURBILLON ET UN PROFIL: MESURE DE PRESSIONS PARIETALES INSTATIONNAIRES]
J. L. Peube, B. Ferret, and S. Gabard (Poitiers Univ., France) 1989 27 p In FRENCH Presented at the 26th Colloque d'Aerodynamique Appliquee, Toulouse, France, 23-25 Oct. 1990 Previously announced in IAA as A91-19593
(AAAF-NT-89-13; ISBN-2-7170-0946-9; ISSN-0243-0177; ETN-91-99954) Avail: NTIS HC/MF A03; CEDOCAR, Section des Diffusions, 26 Blvd Victor, 75996 Paris Armees, France, HC 30 francs

Problems encountered at the metrology level of wall pressure and different solutions studied for correcting the measurement component are presented. A theoretic study to determine the optimal position of a mechanical restrictor along the length of a pneumatic connecting tube is given. Experimental results from unsteady pressure measurements are presented. ESA

N91-31105# Association Aeronautique et Astronautique de France, Paris.
BOUNDARY LAYER TRANSITION DETECTION AND MEASUREMENT METHODS AT CERT/DERAT [MOYENS DE DETECTION ET DE MESURES DE LA TRANSITION DE LA COUCHE LIMITE UTILISES AU CERT/DERAT]
J. C. Juillen and D. Arnal (Centre d'Etudes et de Recherches, Toulouse, France) 1989 40 p In FRENCH Presented at the 26th Colloque d'Aerodynamique Appliquee, Toulouse, France, 23-25 Oct. 1990 Previously announced in IAA as A91-19592
(AAAF-NT-89-14; ISBN-2-7170-0947-7; ISSN-0243-0177; ETN-91-99955) Avail: NTIS HC/MF A03; CEDOCAR, Section des Diffusions, 26 Blvd Victor, 75996 Paris Armees, France, HC 30 francs

A nonexhaustive list of methods to detect and measure boundary layer transition is prepared. Results that can be expected from each method and various application examples and results are given: swept wing transition in wind tunnel; transition in incompressible flow on a flat plate in wind tunnel (hot wire and microphone); transonic flight transition; hypersonic swept cylinder transition; and liquid crystal visualization. ESA

N91-31106*# National Aeronautics and Space Administration. Lewis Research Center, Cleveland, OH.
EXPERIMENTAL INVESTIGATION OF TURBULENT FLOW THROUGH A CIRCULAR-TO-RECTANGULAR TRANSITION DUCT Ph.D. Thesis - Washington Univ.
David O. Davis Sep. 1991 217 p
(Grant NAG3-376)
(NASA-TM-105210; E-6522; NAS 1.15:105210) Avail: NTIS HC/MF A10 CSCL 01A

Steady, incompressible, turbulent, swirl-free flow through a circular-to-rectangular transition duck was studied experimentally. The cross-sectional area remains the same at the exit as at the inlet, but varies through the transition section to a maximum value approximately 15 percent above the inlet value. The cross-sectional geometry everywhere along the duct is defined by the equation of a superellipse. Mean and turbulence data were accumulated utilizing pressure and hot-wire instrumentation at five stations along the test section. Data are presented for operating bulk Reynolds numbers of 88,000 and 390,000. Measured quantities include total and static pressure, the three components of the mean velocity vector, and the six components of the Reynolds stress tensor. In addition to the transition duct measurements, a hot-wire technique which relies on the sequential use of single rotatable normal and slant-wire probes was proposed. The technique is applicable for measurement of the total mean velocity vector and the complete Reynolds stress tensor when the primary flow is arbitrarily skewed relative to a plane which lies normal to the probe axis of rotation. Author

03 AIR TRANSPORTATION AND SAFETY

Includes passenger and cargo air transport operations; and aircraft accidents.

For related information see also *16 Space Transportation* and *85 Urban Technology and Transportation.*

N91-31107 Vibro-Meter S.A., Fribourg (Switzerland).
PROCESS FOR DETECTING THE LIKELIHOOD OF ICE FORMATION, ICE WARNING SYSTEM FOR CARRYING OUT THE PROCESS, AND UTILIZATION THEREOF Patent
Martin Lustenberger, inventor 7 Mar. 1989 15 p
(Patent-1-250-926; Int-Patent-Class-G08B-108; CTN-91-60144)
Copyright Avail: Micromedia Ltd., Technical Information Centre, 165 Hotel de Ville, Place du Portage, Phase 2, Hull, Quebec J8X 3X2, Canada HC $4.00 CAN, MMF $2.75 CAN

This invention relates to a process and apparatus for detecting the likelihood of natural ice formation on the surface of an aircraft, to a warning system, and to a utilization thereof. The process consist of: positioning a diaphragm having a fundamental resonant frequency and harmonic frequencies on an exposed surface of the aircraft; exciting the diaphragm at one of its resonance frequencies; alternately cooling and heating the diaphragm such that its temperature falls below and rises above the temperature of the exposed surface to alternately create and melt an accretion of ice when the ambient temperature is near or below the freezing point; and measuring any variation in the resonant frequency of the vibration of the diaphragm which occurs during the heating and cooling steps. The fundamental resonance frequency will decrease and the harmonic frequencies increase in the presence of an accretion of ice. An alarm is set off when the variation exceeds a predetermined value. In addition, the process measures the ambient temperature, measures the temperature of the diaphragm, and controls the heating and cooling cycle such that the duration of the cycle is dependant on the ambient temperature. CISTI

N91-31108 Leigh Instruments Ltd., Ottawa (Ontario).
BEACON ACTIVATION DEVICE Patent
Geoffrey Dobbs, inventor 4 Jul. 1989 15 p
(Patent-1-256-916; Int-Patent-Class-G01S-104; CTN-91-60168)
Copyright Avail: Micromedia Ltd., Technical Information Centre, 165 Hotel de Ville, Place du Portage, Phase 2, Hull, Quebec J8X 3X2, Canada HC $4.00 CAN, MF $2.75 CAN

Crash position indicators (CPIs) are radio beacons which begin automatically to broadcast distress signals upon crashing of the aircraft. They are usually designed such that the beacon is biased

to the on-broadcast position. Auxiliary batteries, called shut-off batteries, counterbalance the on bias during normal operation. A number of factors other than crash activation, including human error and shut-off battery failure, can incapacitate the shut-off function and cause the CPI to transmit. This invention provides a CPI that is as reliable as existing systems in its activation, but is also very reliable in holding the beacon in a deactivated mode during flight and ground servicing. It is comprised of a radio transmitter, a battery, and a normally open switch. The device is releasably attached to the aircraft co-acting with an ejector such that in the event of a crash the ejector releases the device from the aircraft. The ejector closes the switch when it operates, thereby turning on the beacon. In a second embodiment the device is equipped with a normally open switch which is deformable. The switch is positioned such that the switch is permanently deformed into a closed position when the ejector operates, thus activating the beacon. CISTI

N91-31109# Materials Research Labs., Ascot Vale (Australia).
TROPICAL TESTS OF A SEAWATER MARKER
R. J. Swinton and E. Gellert 1991 20 p
(MRL-TR-90-19) Copyright Avail: NTIS HC/MF A03

A series of tests on the MRL seawater marker were carried out under tropical conditions for the following reasons: (1) to examine the performance of fluorescein in tropical conditions; (2) to compare the MRL marker with commercially available dye marker; and (3) to test a prototype, helicopter-deployed marker device. Results confirmed that fluorescein, in the form used in the commercially available markers, perform poorly in tropical conditions, whilst the MRL marker was vastly superior. The helicopter marker device was deployed from a height of 50 m and was successful in creating a fast-acting, long-duration dye stain over a large area. Author

N91-31110# National Transportation Safety Board, Washington, DC.
ANNUAL REVIEW OF AIRCRAFT ACCIDENT DATA. US AIR CARRIER OPERATIONS, CALENDAR YEAR 1988
18 Apr. 1991 77 p
(PB91-176040; NTSB/ARC-91/01) Avail: NTIS HC/MF A05

The record of aviation accidents is presented involving revenue operations of U.S. Air Carriers including Commuter Air Carriers and On Demand Air Taxis for calendar year 1988. Three major sections are presented according to the federal regulations under which the flight was conducted: 14 CFR 121, 125, 127, Scheduled 14 CFR 135, or Nonscheduled 14 CFR 135. In each section tables are presented to describe the losses and characteristics of 1988 accidents to enable comparison with prior years. Author

N91-31111# Office National d'Etudes et de Recherches Aerospatiales, Paris (France).
STUDY OF LIGHTNING STRIKES ON AN AIRCRAFT IN FLIGHT. ELECTROMAGNETIC MEASUREMENTS Final Report [ETUDE DE FOUDROIEMENT D'UN AVION EN VOL. MESURES ELECTROMAGNETIQUES]
J. P. Moreau and L. Gautier Jun. 1990 109 p In FRENCH
(Contract DRET-89-001-19)
(ONERA-RF-25/7234-PY; ETN-91-99939) Avail: NTIS HC/MF A06

Seventeen lightning strikes in flight obtained with the Transall 04 instrumented aircraft were analyzed. Simultaneously recorded electric and magnetic fields relating to discharge current measurements provide basic elements for interpretation of phenomena associated with lightning strikes. High cadence video cameragrams bring an important validation to the proposed physical processes. ESA

N91-31112# Office National d'Etudes et de Recherches Aerospatiales, Paris (France). Direction de la Physique Generale.
STUDY OF LIGHTNING STRIKES ON AN AIRCRAFT IN FLIGHT. ELECTRIC MEASUREMENTS Final Report [ETUDE DU FOUDROIEMENT D'UN AVION EN VOL. MESURES ELECTRIQUES]
A. Delannoy, P. Blanchet, and P. Laroche Jun. 1990 82 p In FRENCH
(Contract DRET-89-001-19)
(ONERA-RF-98/7154-PY; ETN-91-99940) Avail: NTIS HC/MF A05

At the time of the Transall aircraft tests campaign of lightning strike study, numerous electric measurements were taken to characterize the atmospheric environment and to determine criteria for lightning initiation. Measurements of the atmospheric electric field, electric conductivity, hydrometeor charges and liquid and solid water prescence are analyzed. ESA

N91-31113* National Aeronautics and Space Administration. Ames Research Center, Moffett Field, CA.
AIRBORNE RESCUE SYSTEM Patent
Leonard A. Haslim, inventor (to NASA) 4 Jun. 1991 12 p
Filed 6 Oct. 1989 Supersedes N91-23095 (29 - 15, p 2367)
(NASA-Case-ARC-11909-1; US-Patent-5,020,742;
US-Patent-Appl-SN-418320; US-Patent-Class-244-137.2;
US-Patent-Class-441-83; Int-Patent-Class-B64D-1/08;
Int-Patent-Class-B64D-9/00; Int-Patent-Class-B64C-1/22;
Int-Patent-Class-B63C-9/01) Avail: US Patent and Trademark Office CSCL 01C

The airborne rescue system includes a boom with telescoping members for extending a line and collar to a rescue victim. The boom extends beyond the tip of the helicopter rotor so that the victim may avoid the rotor downwash. The rescue line is played out and reeled in by winch. The line is temporarily retained under the boom. When the boom is extended, the rescue line passes through clips. When the victim dons the collar and the tension in the line reaches a predetermined level, the clips open and release the line from the boom. Then the rescue line can form a straight line between the victim and the winch, and the victim can be lifted to the helicopter. A translator is utilized to push out or pull in the telescoping members. The translator comprises a tape and a rope. Inside the telescoping members the tape is curled around the rope and the tape has a tube-like configuration. The tape and rope are provided from supply spools.
Official Gazette of the U.S. Patent and Trademark Office

04 AIRCRAFT COMMUNICATIONS AND NAVIGATION

Includes digital and voice communication with aircraft; air navigation systems (satellite and ground based); and air traffic control.

For related information see also *17 Space Communications, Spacecraft Communications, Command and Tracking* and *Communications and Radar.*

N91-31114# Flight Digital Co., Las Cruces, NM.
DEVELOPMENT OF A GEOGRAPHIC NAVIGATIONAL DISPLAY DEVICE FOR GENERAL AVIATION AIRCRAFT Final Report
M. P. Squires Feb. 1991 126 p Sponsored by New Mexico Research and Development Inst., Albuquerque
(PB91-170282; NMRDI-2-76-5622) Avail: NTIS HC/MF A07 CSCL 17G

The goal was to produce a pilot friendly, relatively inexpensive navigation display unit for general aviation aircraft which would diminish the navigational workload by quickly providing a vast amount of data while demanding minimal attention from the pilot. The project began in March 1988, ending in December 1990, with the NavScreen Model FD-100 accepted by the FAA for installation in certified aircraft. The NavScreen is an exciting, new, low cost way of displaying navigation information, using LORAN position data to show pilots at a glance, on a moving map display, where they are, where they are going, and where they have been with respect to all airports 100 nm from their present location. Over 11,000 U.S. airport diagrams are contained on one easily updated 3-1/2 inch diskette which slides in the front of the unit. The

NavScreen fits a standard 4 x 6 inch avionics slot in the instrument panel. GRA

N91-31115 Litton Systems, Inc., Beverly Hills, CA.
ENHANCED GLOBAL POSITIONING SYSTEM DELTA-RANGE PROCESSING Patent
Alison Brown, inventor 23 May 1989 24 p
(Patent-1-254-637; Int-Patent-Class-G01S-502; CTN-91-60171) Copyright Avail: Micromedia Ltd., Technical Information Centre, 165 Hotel de Ville, Place du Portage, Phase 2, Hull, Quebec J8X 3X2, Canada HC $4.00 CAN, MF $2.75 CAN

The NAVSTAR Global Positioning System (GPS) is a satellite based radio navigation system providing accurate three dimensional positioning and precise time. Using GPS data, position can be derived from measurement of the changes in the carrier phase over a fixed period of time. This is called delta range (DR) measurement. It normally takes approximately 24 hours of observations to obtain reasonable accuracy using DR data. The present invention reduces the amount of time required to obtain an accurate location of the receiver by improving the method or delta range measurement. In this system, DR measurements are first accumulated over one second, then over two seconds, over three seconds, and so on. The accumulation of DRs for each new time interval and all old time intervals eliminates many errors created when measuring a DR for an individual time period. By processing the data accumulated by adding information for previous measurements to the newest measurement it is possible to get an accurate position measurement in eight hours. CISTI

N91-31116 Grumman Aerospace Corp., Bethpage, NY.
PASSIVE RANGING OF AN AIRBORNE EMITTER BY A SINGLE NON-MANEUVERING OR STATIONARY SENSOR Patent
Martin Golinsky, inventor 16 May 1989 19 p
(Patent-1-254-292; Int-Patent-Class-G01S-302; Int-Patent-Class-G015-352; CTN-91-60173) Copyright Avail: Micromedia Ltd., Technical Information Centre, 165 Hotel de Ville, Place du Portage, Phase 2, Hull, Quebec J8X 3X2, Canada HC $4.00 CAN, MF $2.75 CAN

The present invention relates to a passive range sensor which is capable of measuring the range of a moving target, such as an aircraft from a stationary platform, an air traffic control tower, or from another aircraft moving along a linear trajectory at a constant velocity. The system uses a succession of bearing and frequency measurements obtained on an appropriate sensor at discrete periods of time from a radiant signal emitted by the target vehicle. The emitted radiation may be continuous or pulsed. The sensor collects frequency and bearing information on the emitter at discrete intervals. As a result of the combined movement of the target and sensor there is produced a geometric pattern of rays of received radiation which can be used to derive the desired range information. Its velocity and direction of travel may also be determined. The system may be used by ships employing sonic sensors and by satellites employing optical sensors. For the system to be accurate the target must not be maneuvering, and the test vehicle must be located sufficiently far from the target that they can be assumed to be in the same horizontal plane. CISTI

N91-31117# Technische Univ., Delft (Netherlands). Werkeenheid Fotogrammetrie en Remote Sensing.
LARGE SCALE CAESAR IMAGES USING INERTIAL NAVIGATION AND PRESSURE ALTITUDE MEASUREMENT. ACCURACY DEFORMATIONS AND POSSIBILITIES FOR A GLOBAL POSITIONING SYSTEM (GPS) Thesis [GROOTSCHALIGE CAESAR-OPNAMEN MET GEBRUIKMAKING VAN TRAAGHEIDSNAVIGATTE EN DRUKHOOGTEMETING. NAUWKEURIGHEID, VERVORMINGEN EN MOGELIJKHEDEN VOOR GPS]
Michel deLaat May 1990 79 p In DUTCH; ENGLISH summary
(ETN-91-99418) Avail: NTIS HC/MF A05

The geometric accuracy of large scale CAESAR images was investigated. A test flight was carried out with the following onboard: a CAESAR line scanner, a local level inertial navigation system, a strapped down inertial reference system, an instrument that determines the altitude by measuring pressure differences, and a GPS (Global Positioning System). A differential GPS receiver was placed on one of the ground control points. Using six ground control points, the accuracy of the images of one strip were determined after two different geometric corrections without the use of GPS. The effects of errors of the auxilliary instruments on the scale of the images are indicated, together with ways in which GPS can be used to prevent these scale errors. It turns out that an interesting application of GPS is the absolute orientation of CAESAR images during the geometric correction procedure. ESA

N91-31118# Technische Univ., Delft (Netherlands). Orbital Mechanics Section.
INVESTIGATIONS ON THE USE OF GPS FOR GEODETIC AND ORBIT DETERMINATION APPLICATIONS
E. T. Hesper Feb. 1991 301 p Sponsored by NAL
(LR-649; ISBN-90-6275-660-3; ETN-91-99614) Copyright Avail: NTIS HC/MF A14

The results of an investigation of the characteristics of the NAVSTAR/GPS (Global Positioning System) and an exploration of its use for various applications, through numerical simulations and offline processing of observations obtained by operational GPS receivers, are reported. The report covers: operational principles and characteristics; results of an observation campaign using the Bernese second generation software package; Hermes navigation/localization GPS/DRS (Data Relay Satellite) simulations; mathematical description of the real time relative orbit determination of two space vehicles using the Oasis system. ESA

N91-31119# National Aerospace Lab., Amsterdam (Netherlands). Flight Informatics Div.
BAYESIAN MULTI-SENSOR TRACKING FOR ADVANCED AIR-TRAFFIC CONTROL SYSTEMS
H. A. P. Blom, R. A. Hogendoorn, and F. J. vanSchaik 8 May 1988 12 p Presented at the Guidance and Control Panel AGARDograph 301 on Computation, Prediction and Control of Aircraft Trajectories Previously announced as N91-11003 Sponsored by Dutch Organization of Civil Aviation
(NLR-MP-88056-U; ETN-91-99656) Avail: NTIS HC/MF A03

An overview of a Bayesian tracking system for a multisensor environment is given. The main modules perform track initiation, track continuation, and systematic error estimation, respectively. The track continuation module plays the most important role for air traffic control. It consists of a combination of those approximate Bayesian methods that proved to be the most efficient for the main problems of track continuation: extended Kalman filtering for nonlinear dynamics, probabilistic data association for unassociated measurements, and interacting multiple model filtering for sudden maneuvers. Comparisons of this new tracking system with alpha-beta, Kalman based, and state of the art tracking systems show its superiority for application to air traffic control surveillance. The advantages of this system are given. ESA

N91-31120* National Aeronautics and Space Administration. Langley Research Center, Hampton, VA.
AIRPLANE TAKEOFF AND LANDING PERFORMANCE MONITORING SYSTEM Patent
David B. Middleton, inventor (to NASA), Raghavachari Srivatsan, inventor (to NASA), and Lee H. Person, Jr., inventor (to NASA) 10 Sep. 1991 28 p Filed 6 Aug. 1987 Supersedes N88-24621 (26-18, p 2462) Continuation-in-part of US-Patent-Appl-SN-082766
(NASA-Case-LAR-13854-1-CU; US-Patent-5,047,9421-CU; US-Patent-Appl-SN-192562; US-Patent-Appl-SN-082766; US-Patent-Class-364-427; US-Patent-Class-364-428; US-Patent-Class-73-178T; Int-Patent-Class-G06F-15/50) Avail: US Patent and Trademark Office CSCL 17G

The invention is a real-time takeoff and landing performance monitoring system for an aircraft which provides a pilot with graphic and metric information to assist in decisions related to achieving

rotation speed within the safe zone of a runway, or stopping the aircraft on the runway after landing or takeoff abort. By comparing the present performance of the aircraft with a predicted nominal performance based upon given conditions, performance deficiencies are detected by the system. The system provides a head-down display and a head-up display. The head-up display is projected onto a partially reflective transparent surface through which the pilot views the runway. Hence, the system supplies the pilot with critical status information while allowing the pilot to continue to view the runway.

Official Gazette of the U.S. Patent and Trademark Office

N91-31121# Massachusetts Inst. of Tech., Cambridge.
ORIGINS OF GPS SURVEYING Technical Report, 29 Apr. 1986 - 24 Apr. 1991
C. C. Counselman 26 Apr. 1991 27 p
(Contract F19628-86-K-0009)
(AD-A239676; PL-TR-91-2088; SR-10) Avail: NTIS HC/MF A03 CSCL 17/7

Conceptually, Global Position System (GPS) geodetic surveying is a descendant of hyperbolic radio positioning systems such as LORAN and Omega, of the very long baseline interferometry technique of radio astronomy, and of satellite Doppler tracking. Satellite Doppler positioning systems such as TRANSIT may have paved the way for GPS politically and economically, but conceptually they were strongly opposed to and probably retarded the development of GPS geodetic surveying. GRA

N91-31122# Analytic Sciences Corp., Reading, MA.
PERFORMANCE ASSESSMENT AND COVERAGE EVALUATION (PACE) WORKSTATION (USER MANUAL)
George R. Desrochers 15 Dec. 1990 89 p
(Contract DTCG23-89-C-20008)
(AD-A239723; TIM-5834-2-1; USCG/ONSCEN-01-91) Avail: NTIS HC/MF A05 CSCL 17/7

The Performance Assessment and Coverage Evaluation (PACE) Workstation is a microcomputer based tool to assist Omega Navigation System Center (ONSCEN) personnel in answering questions regarding Omega system performance. The workstation implements a probabilistic model of Omega system availability for user-selected coverage and other criteria. This memorandum provides information on the operation of the PACE workstation. GRA

N91-31123# Analytic Sciences Corp., Reading, MA.
OMEGA SYSTEM PERFORMANCE ASSESSMENT AND COVERAGE EVALUATION (PACE) WORKSTATION DESIGN AND IMPLEMENTATION, VOLUME 2
George R. Desrochers 15 Feb. 1991 476 p
(Contract DTCG23-89-C-20008)
(AD-A239724; TIM-5834-2-2-Vol-2; USCG/ONSCEN-02.2-91-Vol-2) Avail: NTIS HC/MF A21 CSCL 17/7

The Performance Assessment and Coverage Evaluation (PACE) workstation is a microcomputer based tool to assist Omega Navigation System Center personnel in answering questions regarding Omega system performance. The workstation implements a probabilistic model of Omega system availability for user-selected coverage and other criteria. This memorandum provides information on the design and implementation of the PACE workstation software. GRA

N91-31124# Analytic Sciences Corp., Reading, MA.
ANALYSIS AND EVALUATION OF SELECTED PACE APPLICATIONS Final Report, Dec. 1990 - Apr. 1991
P. B. Morris Apr. 1991 57 p
(Contract DTCG23-89-C-20008)
(AD-A239726; TIM-5834-4-1; USCG/ONSCEN-4-91) Avail: NTIS HC/MF A04 CSCL 12/5

Selected applications of the Omega System Availability model are analyzed and compared. These applications illustrate the range and scope of issues which may be addressed by the System Availability model. Three general applications at the primary Omega frequency of 10.2 kHz are described in terms of scenarios which postulate specific system conditions or configurations. These applications make use of the PACE workstation which incorporates the new 24-hour/4-month/2-frequency signal coverage database. The applications analyzed in this report include: (1) comparison of system availability using the previous (2-hour/4-month/2-frequency) and new signal coverage databases, (2) comparison of global and regional system availability and the sensitivity of system availability to signal coverage access criteria thresholds, and (3) comparison of system availability as interpreted by conventional airborne Omega receiver/processor signal deselection algorithms and PACE with baseline signal coverage access criteria. For most of the applications, system performance is examined in terms of three system station power level configurations: (1) all transmitting stations at full power, (2) a 6 dB power reduction at the Hawaii station (all other transmitting stations at full power), (3) Hawaii permanently off-air (all other transmitting stations at full power). GRA

05 AIRCRAFT DESIGN, TESTING AND PERFORMANCE

Includes aircraft simulation technology.

For related information see also *18 Spacecraft Design, Testing and Performance* and *39 Structural Mechanics*.For land transportation vehicles see *85 Urban Technology and Transportation.*

N91-31125# National Aeronautical Establishment, Ottawa (Ontario). Structures and Materials Lab.
PHOTOELASTIC COATING STUDY OF REDESIGNED CT114 COUPON JOINT TEST SPECIMEN FOR HORIZONTAL STABILIZER REAR ATTACHMENT FITTING TO VERTICAL STABILIZER REAR SPAR
J. P. Komorowski 15 Mar. 1989 13 p
(NAE-LTR-ST-1701; CTN-91-60026) Copyright Avail: NTIS HC/MF A03

As part of a program of life extension for the CT-114 aircraft, an experimental investigation was initiated of the durability and damage tolerance of the horizontal stabilizer rear attachment fitting and its attached components from the vertical stabilizer rear spar in the tail assembly. Photoelastic studies under static loads were carried out. Specimens from earlier studies were used with redesigned fasteners to provide more representative transfer of load through the structure. A strain survey was carried out to see if significant slippage and redistribution of strain occurred depending on the type of fastener used. The fastener installations were shown to result in large tensile strains to the doubler plate. It was recommended that further tests be carried out with fastener pitch increased and a full width doubler used to better simulate the structure. CISTI

N91-31126 Beech Aircraft Corp., Boulder, CO.
METHOD FOR FASTENING AIRCRAFT FRAME ELEMENTS TO SANDWICH SKIN PANELS COVERING SAME USING WOVEN FIBER CONNECTORS Patent
Paul J. Jonas, inventor 18 Sep. 1990 25 p
(Patent-1-274-075; Int-Patent-Class-B64C-318; CTN-91-60135)
Copyright Avail: Micromedia Ltd., Technical Information Centre, 165 Hotel de Ville, Place du Portage, Phase 2, Hull, Quebec J8X 3X2, Canada HC $4.00 CAN, MF $2.75 CAN

An invention for joining frame elements to fibre reinforced composite skin panels is described. It is comprised of a three dimensional woven fiber strap or band of H-shaped cross section which takes maximum advantage of the ability of the yarn strands of endless filament bundles to carry large tension loads. The crossbar portion of the H projects laterally beyond the upright portion. It forms the means for bridging the gap formed on the inner face of a skin panel when a groove is routed adjacent to the frame element which is to be fastened. Strands of the crossbar section are adhesively bonded to the inner facesheet adjacent to the groove edges reestablishing its continuity across the joint.

The upright portion of the strap likewise establishes an adhesively bonded woven bridge interconnecting the edges of the core exposed at the sides of the groove in the skin panel and the faces of the frame element. Any chordwise bending load tending to widen the gap in the inner facesheet is resisted by the filaments in the crossbar section. Any load tending to pull the spar out of the channel formed by the crossbar and upright portion of the H is resisted by the entire upright portion of the H connector. The joint thus formed can give way only by breaking or stretching the adhesive bond. CISTI

N91-31127 Grumman Aerospace Corp., Bethpage, NY.
TORSION RESISTANT GROOVED JOINT Patent
Aldo Arena, inventor and Robert L. Benoit, inventor 22 Aug. 1989 11 p
(Patent-1-258-589; Int-Patent-Class-F16B-400; CTN-91-60164)
Copyright Avail: Micromedia Ltd., Technical Information Centre, 165 Hotel de Ville, Place du Portage, Phase 2, Hull, Quebec J8X 3X2, Canada HC $4.00 CAN, MF $2.75 CAN

Torque or torsion members are commonly used in aircraft or aerospace vehicles by connecting the ends of a tubular member to a preformed member adapted to fasten the assembled torsion member to the elements between which torque or torsion is to be transmitted. This allows a substantial reduction of the overall weight of the assembly. This invention provides a torque tube assembly wherein the torsional strength of the end connection exceeds the torsional strength of the tube comprising a pair, or end members interconnected by a tubular member. The grooving and forming arrangement of a pushrod are adapted to torque or to torsion transmitting tubes, and a member is produced such that the torsion strength of the tube at the end connection exceeds the torsional buckling and failure strength of the tube itself. The invention is obtained by extending the grooves axially of the tube, and by maintaining the groove side walls at an angle within prescribed limits; the number of grooves to the outer diameter of the end fitting and groove width at a prescribed ratio; the groove depth to the groove width at a prescribed ratio; and the axial length of the grooves longer than the circumferential groove width. CISTI

N91-31128 Kansas Univ., Lawrence.
FIGHTER AGILITY METRICS Ph.D. Thesis
Randall Keith Liefer 1990 206 p
Avail: Univ. Microfilms Order No. DA9119093

Proposed new metrics to assess fighter aircraft agility are collected and analyzed. A framework for classification of these new agility metrics is developed and applied. A complete set of transient agility metrics is evaluated with a high fidelity, nonlinear F-18 simulation provided by NASA-Dryden. Test techniques and data reduction methods are proposed. A method of providing cuing information to the pilot during flight test is discussed. The sensitivity of longitudinal and lateral agility metrics to deviations from the pilot cues is studied in detail. The metrics are shown to be largely insensitive to reasonable deviations from the nominal test pilot commands. Instrumentation required to quantify agility via flight test is also considered. With one exception, each of the proposed new metrics may be measured with instrumentation currently available. Simulation documentation and user instructions are provided in an appendix. Dissert. Abstr.

N91-31129 Oklahoma Univ., Norman.
MODEL OF AN AEROSPACE PLANE BASED ON AN IDEALIZED CONE-DERIVED WAVERIDER FOREBODY Ph.D. Thesis
Hyung-Koo Park 1990 161 p
Avail: Univ. Microfilms Order No. DA9119180

The flow field of an idealized cone-derived waverider is axisymmetric. This feature is preserved for the rest of the vehicle, including the inlet, cowl, combustor, and nozzle. Researchers thus have a tip to tail model in which both the external and internal flows are axisymmetric. The assumption of axial symmetry provides a major simplification for the analysis and allows for a systematic integration of the propulsion unit with the aerodynamics. A novel design concept is used for the nozzle that avoids shock waves, minimizes the nozzle length, and tends to maximize the thrust. The model is designed to provide lift, thrust, drag, and fuel consumption data for a vehicle cruising at a hypersonic Mach number. Despite its idealized, inviscid limitations, it provides a reasonably self-consistent representation of both the aerodynamics and the scramjet/nozzle powerplant of the vehicle in a fully integrated configuration. In addition to describing the model, a range of parametric studies are presented. Dissert. Abstr.

N91-31130# Aeritalia S.p.A., Turin (Italy). Defence Aircraft Group.
INLET EDGE FUNNEL OF A CIVIL AIRCRAFT GONDOLA ENGINE [IMBUTITURA DEL BORDO DI ENTRATA DI UNA GONDOLA MOTORE DI UN VELIVOLO CIVILE]
A. Formisano and G. L. Raffeto (Espri MARC, Genoa, Italy) 1990 40 p In ITALIAN Presented at the Conferenza Italiana degli Utenti MARC, Padua, Italy, 27-28 Sep. 1990
(ETN-91-99775) Copyright Avail: NTIS HC/MF A03

A finite element code to investigate the elastoplastic behavior of the aluminum material Al 2219T0 for its application in an inlet edge funnel is presented. The structure and forming processing are outlined. The geometry of the problem is described. The results agree with experimental and theoretical predictions. ESA

N91-31131# National Aerospace Lab., Amsterdam (Netherlands). Informatics Div.
DESIGN AND TESTING OF A MULTIBLOCK GRID-GENERATION PROCEDURE FOR AIRCRAFT DESIGN AND RESEARCH
J. W. Boerstoel, J. M. J. W. Jacobs, A. Kassies, A. Amendola, R. Tognaccini, and P. L. Vitagliano (Aeritalia S.p.A., Turin, Italy) 19 May 1989 21 p Presented at 64th AGARD Fluid Dynamics Panel on Applications of Mesh Generation to Complex 3D Configurations, Loen, Norway, 24-25 May 1989 Previously announced as N90-21984
(Contract NIVR-1604N)
(NLR-TP-89146-U; ETN-91-99643) Avail: NTIS HC/MF A03

A multiblock grid generation procedure embedded in a numerical flow simulation system is described. Major features of the grids are: they are suitable for complex aerodynamic configurations; the grid lines are continuous, in particular, over block faces; the grid lines are not slope-continuous over block faces; the topology and geometry of block decomposition are specified first, and then the grid-point distributions; the application and transfinite interpolation and elliptic techniques. It is possible to construct multiblock grids around complex configurations with 250 to 1000 blocks, and to computer (Euler) flows on such grids. New technical concepts are proposed, to improve the accuracy of the flow simulation results, and to reduce manhour investments in the construction of multiblock grids. ESA

N91-31132# National Aerospace Lab., Amsterdam (Netherlands).
[ACTIVITIES REPORT OF THE NATIONAL AEROSPACE LABORATORY] Annual Report, 1989 [STICHTING NATIONAAL LUCHT- EN RUIMTEVAARTLABORATORIUM: VERSLAG OVER HET JAAR, 1989]
1989 110 p In DUTCH
(ETN-91-99438) Avail: NTIS HC/MF A06

Theoretical and numerical methods were developed for the investigation of the aerodynamics of new configurations. Flight tests were performed for the evaluation and certification of the Fokker 50 and Fokker 100. Aircraft structures and materials were tested. Instrumentation for astronautical applications was developed. Software and hardware were developed for applied informatics. Technical equipment was developed for flow studies, flight mechanics research, constructions and materials, aeronautical research, applied informatics, and mechanical techniques. ESA

N91-31133# National Aerospace Lab., Amsterdam (Netherlands). Flight Div.
FLIGHT TESTING IN THE NETHERLANDS: AN OVERVIEW
J. T. M. vanDoorn and R. L. vanderVelde 1 Sep. 1988 29 p

Presented at the 73rd AGARD Flight Mechanics Panel-Symposium on Flight Test Techniques, Edwards Air Force Base, CA, 17-20 Oct. 1988
(NLR-MP-88053-U; ETN-91-99654) Avail: NTIS HC/MF A03

An overview of the flight test activities and capabilities in the Netherlands is given. A general description of the flight tests programs of the last decades with civil and military aircraft, helicopters and research aircraft is given. Some of the highlights of the more recent programs are presented, i.e., the type certification of the Fokker 50 and Fokker 100 civil transport aircraft, evaluation and certification trials with the military F216 fighter aircraft, helicopter ship compatibility testing and the determination of the mathematical model of the Cessna citation 500 for the phase 2 flight simulator. Furthermore a short description of the flight test instrumentation and flight test techniques that have become available in the Netherlands during the last decade is given. ESA

N91-31134# Messerschmitt-Boelkow-Blohm G.m.b.H., Munich (Germany, F.R.).
NOXIOUS MATTER MINIMIZATION AS A PROJECT CRITERION FOR AIRCRAFT [SCHADSTOFFMINIMIERUNG ALS ENTWURFSKRITERIUM FUER FLUGZEUGE]
Horst Prem 1990 9 p In GERMAN Presented at the Internationaler Kongress 'Umweltfreundlkicher Verkehr durch moderne Verkehrstechnologien', Nuernberg, Fed. Republic of Germany, 24-25 Sep. 1990
(MBB-Z-0337-90-PUB; OTN-030880; ETN-91-99759) Avail: NTIS HC/MF A02

Environmental conditions taken into account during aircraft development where the emphasis is on the verification of technical possibilities and efficiency improvement are considered. It appears necessary to transfer, on a European scale, the technology and verification program for laminar wings, hydrogen aircraft and corresponding airport infrastructure. It is shown that a better blade geometry could reduce helicopter noise and that hydrogen propulsion will change aircraft configuration. ESA

N91-31135# Messerschmitt-Boelkow-Blohm G.m.b.H., Munich (Germany, F.R.). Airplane Div.
ENHANCED FIGHTER MANEUVERABILITY AIRCRAFT (X-31A) WING AND THRUST VECTORING VANE DESIGN
H. Lonsinger, G. Guenther, and J. Schweiger Nov. 1990 12 p
(MBB-FE22/S/PUB/0433/A; ETN-91-99763) Copyright Avail: NTIS HC/MF A03

The X-31A experimental aircraft configured to explore the maneuverability and flying qualities in the high angle of attack and post stall regime using a digital fly by wire flight control system (FCS) and carbon carbon thrust vectoring vanes is described. Advanced NARMCO 5245/T800 chlorofluorocarbons (CFC) epoxy materials are used for the monolithic wing box covers and cocured control surfaces whereas carbon carbon composite is used for the three high temperature affected thrust vectoring vanes. The wing is designed with an optimization program for minimum weight. Primary design parameters are buckling and strain limits, while a high flutter margin is required to reduce the effort for aeroelastic qualification programs. The structural development including the optimization process is described. General design criteria, material selection, material allowables, component design, and manufacturing principles are discussed. ESA

N91-31136# Office National d'Etudes et de Recherches Aerospatiales, Paris (France). Direction de la Physique Generale.
VORTEX-BLADE INTERACTION ON A HELICOPTER PRINCIPAL ROTOR. VALIDATION OF THE S2DI COMPUTATION PROGRAM AND STUDY OF VORTEX MODELS [BRUIT D'INTERACTION PALE-TOURBILLON SUR UN ROTOR PRINCIPAL D'HELICOPTERE. VALIDATION DU PROGRAMME DE CALCUL S2DI ET ETUDE DE MODELES DE TOURBILLON]
G. Rahier Aug. 1990 31 p In FRENCH
(Contract DRET-89-34-001)
(ONERA-RT-92/5094-PY; ETN-91-99937) Avail: NTIS HC/MF A03

A 2-D singularities method of computing the pressures on a profile is tested for the case of steady flows, degrees of incidence, pitching oscillations and undulating flow. Results validate the computation code, which proves to be fast and reliable. Study of different vortex interaction models shows that in a 2-D computation it is necessary to have a vortex representation which allows for deformation in order to correctly predict the strong interactions and collisions. ESA

N91-31137# Association Aeronautique et Astronautique de France, Paris.
SECOND GENERATION SUPERSONIC TRANSPORT AIRCRAFT: LOW SPEED AERODYNAMICS [AVION DE TRANSPORT SUPERSONIQUE DE SECONDE GENERATION: AERODYNAMIQUE BASSES VITESSES]
P. Carlier, C. Pujol, and F. Begin 1989 43 p In FRENCH Presented at 26th Colloque d'Aerodynamique Appliquee, Toulouse, France, 23-25 Oct. 1990
(AAAF-NT-89-02; ISBN-2-7170-0963-9; ISSN-0243-0177; ETN-91-99943) Avail: NTIS HC/MF A03; CEDOCAR, Section des Diffusions, 26 Blvd Victor, 75996 Paris Armees, France, HC 30 francs

The ATSF (French acronym for future supersonic transport aircraft) program, to find better subsonic/supersonic performance compromises and to optimize the wing configuration for low speed, taking turbulent phenomena into account, is outlined. Aerodynamics of wings at low, medium and high angles of incidence, and the influence of sideslip are studied. Lateral and longitudinal turbulent coefficients are considered. The Concorde aircraft is specifically addressed. First wind tunnel flow visualization tests for the ATSF preproject are reported. ESA

N91-31138*# National Aeronautics and Space Administration. Langley Research Center, Hampton, VA.
TWO ALTERNATIVE WAYS FOR SOLVING THE COORDINATION PROBLEM IN MULTILEVEL OPTIMIZATION
Jaroslaw Sobieszczanski-Sobieski Aug. 1991 17 p
(NASA-TM-104036; NAS 1.15:104036) Avail: NTIS HC/MF A03 CSCL 01C

Two techniques for formulating the coupling between levels in multilevel optimization by linear decomposition, proposed as improvements over the original formulation, now several years old, that relied on explicit equality constraints which were shown by application experience as occasionally causing numerical difficulties. The two new techniques represent the coupling without using explicit equality constraints, thus avoiding the above diffuculties and also reducing computational cost of the procedure. The old and new formulations are presented in detail and illustrated by an example of a structural optimization. A generic version of the improved algorithm is also developed for applications to multidisciplinary systems not limited to structures. Author

N91-31139*# National Aeronautics and Space Administration. Langley Research Center, Hampton, VA.
A TECHNIQUE FOR LOCATING FUNCTION ROOTS AND FOR SATISFYING EQUALITY CONSTRAINTS IN OPTIMIZATION
Jaroslaw Sobieszczanski-Sobieski Aug. 1991 9 p
(NASA-TM-104037; NAS 1.15:104037) Avail: NTIS HC/MF A02 CSCL 01C

A new technique for locating simultaneous roots of a set of functions is described. The technique is based on the property of the Kreisselmeier-Steinhauser function which descends to a minimum at each root location. It is shown that the ensuing algorithm may be merged into any nonlinear programming method for solving optimization problems with equality constraints. Author

N91-31140* National Aeronautics and Space Administration. Langley Research Center, Hampton, VA.
ROTATABLE NON-CIRCULAR FOREBODY FLOW CONTROLLER Patent
Cary A. Moskovitz, inventor (to NASA) 24 Sep. 1991 11 p Filed 10 Aug. 1990

(NASA-Case-LAR-14212-1-CU; US-Patent-5,050,819; US-Patent-Appl-SN-565090; US-Patent-Class-244-75R; US-Patent-Class-244-87; US-Patent-Class-244-88; US-Patent-Class-244-199; US-Patent-Class-244-120; Int-Patent-Class-B64C-19/00) Avail: US Patent and Trademark Office CSCL 01C

The invention is a rotatable, non-circular forebody flow controller. The apparatus comprises a small geometric device located at a nose of a forebody of an aircraft and a non-circular cross-sectional area that extends toward the apex of the aircraft. The device is symmetrical about a reference plane and preferably attaches to an axle which in turn attaches to a rotating motor. The motor rotates the device about an axis of rotation. Preferably, a control unit connected to an aircraft flight control computer signals to the rotating motor the proper rotational positioning of the geometric device.

Official Gazette of the U.S. Patent and Trademark Office

N91-31141# Naval Air Development Center, Warminster, PA. Air Vehicle and Crew Systems Technology Dept.

EFFECT OF WIND OVER DECK CONDITIONS ON AIRCRAFT APPROACH SPEEDS FOR CARRIER LANDINGS Summary Report

Richard P. Micklos 1 Sep. 1991 36 p
(AD-A239511; NADC-91027-60) Avail: NTIS HC/MF A03 CSCL 01/2

Aircraft Approach Speeds measured during NADC photographic surveys of operational carrier landings have been higher than anticipated when compared to NATOPS recommended approach speed curves. The cause of this increase in approach speed is identified as the increase in the wind over deck, above minimum recovery head wind requirements, available during actual carrier landings. GRA

06 AIRCRAFT INSTRUMENTATION

Includes cockpit and cabin display devices; and flight instruments.

For related information see also *19 Spacecraft Instrumentation* and *35 Instrumentation and Photography.*

N91-31142 International Superconductivity Technology Center, Tokyo (Japan).

STEERABLE WINDOWED ENCLOSURES Patent

John N. Leavitt, inventor 26 Sep. 1989 27 p
(Patent-1-262-653; Int-Patent-Class-G01C-1916; CTN-91-60160) Copyright Avail: Micromedia Ltd., Technical Information Centre, 165 Hotel de Ville, Place du Portage, Phase 2, Hull, Quebec J8X 3X2, Canada HC $4.00 CAN, MF $2.75 CAN

A design is provided of a steerable windowed enclosure for a gyro-stabilized sensor mounted within the enclosure and including a relatively small window through which the gyro-stabilized sensor can view the exterior and which can be moved in conformity with the controlled movements of the mechanism so that the sensor and the window remain registered with one another. The gyro-stabilized sensors may include photoelectric scanners, television cameras, infrared imagers, or directional antennas and may be carried by a truck or suspended by a boom from a dirigible, an aircraft, or, particularly, a helicopter. The gyro-stabilized imager thus attached is capable of delivering sharp steady images as though attached to an earth-based tripod. The steerable enclosure is mounted, steered, and controlled so that it responds to changes in the orientation of the imager by a compensatory movement so that the window remains aligned with line of sight of the imager. It is thereby possible to provide an enclosure with a smaller window than was heretofore possible without obstructing the view of the imager. This means the window can be made less fragile, easier to clean, and have a longer operating life. More importantly, the optical properties of the window can be better controlled. CISTI

N91-31143*# National Aeronautics and Space Administration. Langley Research Center, Hampton, VA.

FLIGHT TESTS WITH A DATA LINK USED FOR AIR TRAFFIC CONTROL INFORMATION EXCHANGE

Charles E. Knox and Charles H. Scanlon Sep. 1991 38 p
(NASA-TP-3135; L-16936; NAS 1.60:3135) Avail: NTIS HC/MF A03 CSCL 17B

Previous studies showed that air traffic control (ATC) message exchange with a data link offers the potential benefits of increased airspace system safety and efficiency. To accomplish these benefits, data link can be used to reduce communication errors and relieve overloaded ATC voice radio frequencies, which hamper efficient message exchange during peak traffic periods. Flight tests with commercial airline pilots as test subjects were conducted in the NASA Transport Systems Research Vehicle Boeing 737 airplane to contrast flight operations that used current voice communications with flight operations that used data link to transmit both strategic and tactical ATC clearances during a typical commercial airflight from takeoff to landing. The results of these tests that used data link as the primary communication source with ATC showed flight crew acceptance, a perceived reduction in crew work load, and a reduction in crew communication errors.

Author

07 AIRCRAFT PROPULSION AND POWER

Includes prime propulsion systems and systems components, e.g., gas turbine engines and compressors; and onboard auxilliary power plants for aircraft.

For related information see also *20 Spacecraft Propulsion and Power, 28 Propellants and Fuels,* and *44 Energy Production and Conversion.*

N91-31144# Advisory Group for Aerospace Research and Development, Neuilly-Sur-Seine (France). Propulsion and Energetics Panel.

LOW TEMPERATURE ENVIRONMENT OPERATIONS OF TURBOENGINES (DESIGN AND USER'S PROBLEMS)

1990 373 p Partly in FRENCH and ENGLISH Presented at the Propulsion and Energetics Panel 76th Symposium, Brussels, Belgium, 8-12 Oct. 1990
(AGARD-CP-480; ISBN92-835-0618-9) Copyright Avail: NTIS HC/MF A16; Non-NATO Nationals requests available only from AGARD/Scientific Publications Executive

The papers presented at the Propulsion and Energetic Panel 76th Symposium and the discussions represent a significant contribution to improved cold weather tolerant and anti-icing design and to safer aircraft operation in a low temperature environment. The following subject areas are covered: cold weather operational experience and requirements, system design considerations, fuel effects and lubricants behavior, and icing condition and testing. For individual titles, see N91-31145 through N91-31173.

N91-31145# Army Air Corps, Stockbridge (England). School of Aeronautical Engineering.

LOW TEMPERATURE ENVIRONMENT OPERATION OF TURBO ENGINES: A MILITARY OPERATOR'S EXPERIENCE AND REQUIREMENTS

M. Summerton *In* AGARD, Low Temperature Environment Operations of Turboengines (Design and User's Problems) 1990 3 p (For primary document see N91-31144 23-07)
Copyright Avail: NTIS HC/MF A16; Non-NATO Nationals requests available only from AGARD/Scientific Publications Executive

The United Kingdom's commitment to NATO includes the regular use of Royal Marine and Army helicopters in low temperature conditions. The operation of the Westland LYNX helicopter is addressed with its Rolls Royce GEM engines during winter deployments in Norway where the near-arctic conditions present certain operating and working difficulties. These difficulties are considered both generally, from a human and physical point of view, and then more specifically with regard to the engines

themselves. Finally, a few areas for improvements are discussed, with the emphasis on reliability, ease of maintenance, and effective development and testing before entry into service. Author

N91-31146# Canadian Forces Base Cold Lake, Medley (Alberta). Base Aircraft Maintanence Engineering Organization.
LOW TEMPERATURE ENVIRONMENT OPERATIONS OF TURBO ENGINES
Christian Ouellette *In* AGARD, Low Temperature Environment Operations of Turboengines (Design and User's Problems) 1990 3 p (For primary document see N91-31144 23-07)
Copyright Avail: NTIS HC/MF A16; Non-NATO Nationals requests available only from AGARD/Scientific Publications Executive

The following subject areas are covered: (1) the climate conditions in Canada; (2) a summary of the Operational and Maintenance community of the Canada Armed Forces operational role and commitments; (3) maintenance problems and practices associated with the cold weather environment; (4) the 'Hung Start' problem associated with CF-18. GE-F404 engines; and (5) the status of the infamous J-85-CAN-15 compressor stall problem. Author

N91-31147# Flugplatz Butzweilerhof, Cologne (Germany, F.R.).
ANALYSIS OF STARTING PROBLEMS IN COLD WEATHER WITH ASTAZOU TYPE TURBINE ENGINES IN HELICOPTERS [ANALYSE DES PROBLEMES DE DEMARRAGE PAR TEMPS FROID AVEC LES TURBOMOTEURS D'HELISOPTERE DE TYPE ASTAZOU]
W. Pieters *In* AGARD, Low Temperature Environment Operations of Turboengines (Design and User's Problems) 1990 6 p In FRENCH; ENGLISH summary (For primary document see N91-31144 23-07)
Copyright Avail: NTIS HC/MF A16; Non-NATO Nationals requests available only from AGARD/Scientific Publications Executive

During the heavy winter periods in the beginning of the 80th, the Belgian army had considerable starting problems on its helicopters ALOUETTE equipped with ASTAZOU turbo engines. The different detection methods of the phenomena employed by the users, the immediate actions undertaken by the army, and the solutions worked out in collaboration with the constructors as well as their budgetary consequences are discussed. Author

N91-31148# Fokker B.V., Schipol-Oost (Netherlands). Environmental Control and Ice Protection Systems.
VULNERABILITY OF A SMALL POWERPLANT TO WET SNOW CONDITIONS
R. Meijn *In* AGARD, Low Temperature Environment Operations of Turboengines (Design and User's Problems) 1990 6 p (For primary document see N91-31144 23-07)
Copyright Avail: NTIS HC/MF A16; Non-NATO Nationals requests available only from AGARD/Scientific Publications Executive

Several temporary flame-out incidents were experienced in descent through light icing conditions and precipitation during regular scheduled flights. Extensive ground testing of the engine indicated less tolerance to ice ingestion than was demonstrated in engine certification tests. Powerplant ice protection was enhanced by additional anti-icing of the engine flexible seal by bleed air. Factors are discussed influencing unexpected ice formation and associated uncertainties in the qualification process of a small turboprop powerplant. Author

N91-31149# Boeing Canada, Toronto (Ontario).
ICE TOLERANT ENGINE INLET SCREENS FOR CH113/113A SEARCH AND RESCUE HELICOPTERS
R. B. Jones and W. A. Lucier *In* AGARD, Low Temperature Environment Operations of Turboengines (Design and User's Problems) 1990 11 p Sponsored in part by National Research Council of Canada (For primary document see N91-31144 23-07)
Copyright Avail: NTIS HC/MF A16; Non-NATO Nationals requests available only from AGARD/Scientific Publications Executive

The Canadian Forces CH113/113a Search and Rescue Helicopters occasionally encounter unavoidable icing conditions in their operating environment, The original engine inlet safeguards were not designed form nor capable of sustained operations in icing environments, necessitating removal of the inlet screens in these conditions. This arrangement resulted in unacceptable risk of foreign object damage to the engine, and compromised operational safety. Ice tolerant inlet screens were developed as a remedy for this problem. The flat faced, inverted cone screens with a bypass opening accommodate progressive ice congestion during the various operational modes with minimum engine performance degradation. Author

N91-31150# Sundstrand Turbomach, San Diego, CA.
COLD STARTING SMALL GAS TURBINES: AN OVERVIEW
C. Rodgers *In* AGARD, Low Temperature Environment Operations of Turboengines (Design and User's Problems) 1990 22 p (For primary document see N91-31144 23-07)
Copyright Avail: NTIS HC/MF A16; Non-NATO Nationals requests available only from AGARD/Scientific Publications Executive

The requirements to operate aircraft gas turbines over a large range of environmental conditions prove particularly demanding to the systems designer, especially when rapid starting of a cold engine is stipulated at sub-zero ambient temperature. As a consequence the occurrence of cold climatic extremes are discussed and a trend is observed toward designing aircraft for specific areas and deployment, rather than worldwide usage. Cold engine cranking torque characteristics are basically controlled by the lubricant viscous drag in the mechanical drive train and accessories. This viscous drag is dependent upon the magnitude of the applied start torque. Experience with start system for small gas turbine Auxiliary Power Units (APU's) showed that the total weight required for successful starting at -54 C can approach the weight of the APU powerhead itself. As a consequence, most cold start requirements are relaxed to -40 C or higher. Methods for reducing APU viscous drag and start energy requirements that deserve future study are the all electric gearbox-less APU, and the possibility of a self-start combustor concept. Author

N91-31151# Hans-Sachs-Str., Groebenzell (Germany, F.R.).
COLD START OPTIMIZATION ON A MILITARY JET ENGINE
H. Gruber *In* AGARD, Low Temperature Environment Operations of Turboengines (Design and User's Problems) 1990 5 p (For primary document see N91-31144 23-07)
Copyright Avail: NTIS HC/MF A16; Non-NATO Nationals requests available only from AGARD/Scientific Publications Executive

Cold-starting testing at temperatures of approximately -40 C was performed on 2 RB 199 engines at a West Germany altitude test facility. The engines were of the same build standard with exception of the seal configuration (labyrinth or brush), and running times. One part of the test was performed with F34 fuel, the other with F40. The facilities, test methods, and test results are presented. Author

N91-31152# Pratt and Whitney Aircraft of Canada Ltd., Mississauga (Ontario).
COLD WEATHER IGNITION CHARACTERISTICS OF ADVANCED SMALL GAS TURBINE COMBUSTION SYSTEMS
I. Critchley, P. Sampath, and F. Shum *In* AGARD, Low Temperature Environment Operations of Turboengines (Design and User's Problems) 1990 7 p (For primary document see N91-31144 23-07)
Copyright Avail: NTIS HC/MF A16; Non-NATO Nationals requests available only from AGARD/Scientific Publications Executive

Low temperature and high altitude starting requirements of present day small aero-gas turbine engines are discussed from the viewpoint of their influence on the design of the combustors and ignition systems. Use of electric starters, common in small engines, creates particular challenges to starting especially under cold soak sea level and altitude startup conditions. The main factors in combustion system design affecting starting performance are discussed, including combustor sizing, fuel placement, fuel atomization, fuel scheduling, and igniter selection. Low emission requirements may adversely affect starting performance,

necessitating use of elaborate fuel/ignition systems, some recent developments are described. Author

N91-31153# General Electric Co., Peebles, OH.
COLD WEATHER JET ENGINE STARTING STRATEGIES MADE POSSIBLE BY ENGINE DIGITAL CONTROL SYSTEMS
R. C. Wibbelsman *In* AGARD, Low Temperature Environment Operations of Turboengines (Design and User's Problems) 1990 14 p (For primary document see N91-31144 23-07)
Copyright Avail: NTIS HC/MF A16; Non-NATO Nationals requests available only from AGARD/Scientific Publications Executive

The advent of the computing power of digital controls now makes it possible to achieve a major step forward in the controls systems ability to cope with the multiplicity of situations confronting the engine starting system designer. One of strategies that could be employed is presented, used by the GE and CFMI Commercial Family of large high bypass ratio turbofan engines. Numerous variations of this basic concept could be employed. Author

N91-31154# KHD Luftfahrttechnik G.m.b.H., Oberursel (Germany, F.R.). Thermodynamics and Performance Dept.
COLD START INVESTIGATION OF AN APU WITH ANNULAR COMBUSTOR AND FUEL VAPORIZERS
K. H. Collin *In* AGARD, Low Temperature Environment Operations of Turboengines (Design and User's Problems) 1990 18 p (For primary document see N91-31144 23-07)
Copyright Avail: NTIS HC/MF A16; Non-NATO Nationals requests available only from AGARD/Scientific Publications Executive

The combustor of the APU (Auxiliary Power Unit) for the Tornado fighter aircraft is described. As this APU has to cope with the narrow space in the fuselage it must be of a small size. An annular combustor is favorable as it is short and can be integrated into the envelope of the outer diameter. The fuel vaporizing system is chosen because of its great advantages with combustion. The ignition process is described which is difficult because no fuel is actually vaporized when the start is initiated. Theoretical background and experimental steps of a development program are reported. The result was perfect starting of this system down to -40 C and a very high 'First Start Reliability' which means no false start leading to several start procedures. Author

N91-31155# Pratt and Whitney Aircraft, West Palm Beach, FL.
CONTROL SYSTEM DESIGN CONSIDERATIONS FOR STARTING TURBO-ENGINES DURING COLD WEATHER OPERATION
Robert R. Pollak *In* AGARD, Low Temperature Environment Operations of Turboengines (Design and User's Problems) 1990 10 p (For primary document see N91-31144 23-07)
Copyright Avail: NTIS HC/MF A16; Non-NATO Nationals requests available only from AGARD/Scientific Publications Executive

Starting turbo-engines at climatic extremes has always presented challenges to the systems engineer. The wide range of both ambient and engine internal temperatures experienced by many influential variables increase the complexity of the startup process both on the ground and in the air. The content of this paper provides the current status of advanced control methods designed specifically to address combustor ignition and quick, stall-free acceleration to idle. Sensitivity of combustor ignition limits to cold conditions as well as fuel types was accommodated by both the combustor fuel delivery system and control system design. Specific attention is also given to starting at cold altitude conditions with extremely hot as well as extremely cold internal engine temperatures. Successfully meeting these requirements was accomplished by designing the control system to automatically monitor external influential variables as well as engine internal parameters both prior to and during the actual startup cycle and using these data to continuously adjust fuel scheduling to obtain optimum startup characteristics. Author

N91-31156# Pratt and Whitney Aircraft of Canada Ltd., Mississauga (Ontario).
COLD START DEVELOPMENT OF MODERN SMALL GAS TURBINE ENGINES AT PRATT AND WHITNEY AIRCRAFT OF CANADA LTD.
D. S. Breitman and F. K. Yeung *In* AGARD, Low Temperature Environment Operations of Turboengines (Design and User's Problems) 1990 7 p (For primary document see N91-31144 23-07)
Copyright Avail: NTIS HC/MF A16; Non-NATO Nationals requests available only from AGARD/Scientific Publications Executive

Engine cold start capability is essential for aircraft in Arctic or winter operations. Demonstration of this capability is part of the engine development and certification requirements. Variables such as the combustor design, the diffuser exit flow characteristics, and the compressor performance at sub-idle conditions all affect the cold start capability of an engine. How these factors are usually optimized is briefly described, and an overview of the successful PW305 Engine cold start development (with an electric starter) is presented. The PW305 is a new turbofan engine from Pratt & Whitney of Canada in the 5000 lb thrust range. Author

N91-31157# Wehrtechnische Dienststelle fuer Luftfahrzeuge, Manching (Germany, F.R.).
DESIGN CONSIDERATIONS BASED UPON LOW TEMPERATURE STARTING TESTS ON MILITARY AIRCRAFT TURBO ENGINES
H.-F. Feig *In* AGARD, Low Temperature Environment Operations of Turboengines (Design and User's Problems) 1990 16 p (For primary document see N91-31144 23-07)
Copyright Avail: NTIS HC/MF A16; Non-NATO Nationals requests available only from AGARD/Scientific Publications Executive

Test experience on engine low temperature starting was obtained in the course of multinational and national trials to assess weapon system performance. The objective of the trials was to recommend a clearance for the weapon system. In order to carry out these tests adequately, the operational role of the weapon system had to be considered and the operational limits of the engines and associated systems had to be known. Parameters influencing low temperature start capabilities were reviewed and experience gained from the tests was discussed. Author

N91-31158# Canadian Forces Headquarters, Ottawa (Ontario).
CLIMATIC CONSIDERATIONS IN THE LIFE CYCLE MANAGEMENT OF THE CF-18 ENGINE
R. W. Cue and D. E. Muir (GasTOPS Ltd., Ottawa, Ontario) *In* AGARD, Low Temperature Environment Operations of Turboengines (Design and User's Problems) 1990 15 p (For primary document see N91-31144 23-07)
Copyright Avail: NTIS HC/MF A16; Non-NATO Nationals requests available only from AGARD/Scientific Publications Executive

The Canadian Forces have developed an Engine Parts Life Tracking System (EPLTS) to define the scheduled maintenance requirement of CF-18 aircraft engine components. Up to 64 components are tracked by this system, 26 of which are life limited on the basis of 8 different Life Usage Indices defined by the engine manufacturer and evaluated during each operational mission by the aircraft's Inflight Engine Condition Monitoring System. Data on the rates of component life consumption collected by the EPLTS during a full 12 month time span were analyzed. The manner and extent to which seasonal effects might influence these life consumption rates and hence the life cycle management of the engine are presented and discussed. Author

N91-31159# Rolls-Royce Ltd., Leavesden (England).
APPLICATION OF A WATER DROPLET TRAJECTORY PREDICTION CODE TO THE DESIGN OF INLET PARTICLE SEPARATOR ANTI-ICING SYSTEMS
D. L. Mann and S. C. Tan (Cranfield Inst. of Tech., Bedford, England) *In* AGARD, Low Temperature Environment Operations of Turboengines (Design and User's Problems) 1990 11 p Sponsored in part by Ministry of Defence (For primary document

see N91-31144 23-07)
Copyright Avail: NTIS HC/MF A16; Non-NATO Nationals requests available only from AGARD/Scientific Publications Executive

Over the past five years, a dust particle trajectory code has been developed. Recent work on the code to include an ice accretion prediction model suitable for use as a design aid for a wide variety of gas turbine engine inlets, but particularly for particle separator geometries is described. The calculation of the local heat transfer coefficient is seen to be critical to the success of the ice accretion prediction. The incorporation of a suitable model is described, and a series of validation tests, carried out on a full scale rig, were shown to satisfactorily verify the code. A second series of validation experiments, carried out in an icing facility, further shows the prediction model to be appropriate. Author

N91-31160# General Motors Corp., Indianapolis, IN. Gas Turbine Div.
DEVELOPMENT OF AN ANTI-ICING SYSTEM FOR THE T800-LHT-800 TURBOSHAFT ENGINE
Gary V. Bianchini *In* AGARD, Low Temperature Environment Operations of Turboengines (Design and User's Problems) 1990 13 p (For primary document see N91-31144 23-07)
Copyright Avail: NTIS HC/MF A16; Non-NATO Nationals requests available only from AGARD/Scientific Publications Executive

The T900-LHT-800 is a modern technology 1200 hp (900 kW) class turboshaft engine developed for the U.S. Army's LH helicopter and various civil applications. One of its significant features is an integral inlet particle separator (IPS). The presence of an IPS significantly complicates development of an anti-icing system for protection against the hazards associated with ice formation during operation in environmental icing conditions. The T800 engine is described, and the anti-icing system requirements, design evolution, and validation testing are discussed. The final anti-icing system configuration resulting from the development effort is presented. Author

N91-31161# Rolls-Royce Ltd., Derby (England).
ENGINE ICING CRITICALITY ASSESSMENT
E. Brook *In* AGARD, Low Temperature Environment Operations of Turboengines (Design and User's Problems) 1990 6 p (For primary document see N91-31144 23-07)
Copyright Avail: NTIS HC/MF A16; Non-NATO Nationals requests available only from AGARD/Scientific Publications Executive

Assessment of an engine design for icing risk is important at both the design stage and for development and certification testing. Icing must be included with aerodynamic and noise constraints during the design phase to minimize the risk of design change during development, and the compromise tested must be tested at the extremes of the atmospheric icing, and aircraft and engine operating envelopes most appropriate to the particular components. The type of assessment necessary is addressed and illustrated mainly by reference to high bypass ratio turbofans. The approach to identifying critical conditions is presented and areas where research can provide basic data for the development of design methods are discussed. Author

N91-31162# General Electric Co., West Lynn, MA. Aircraft Engines Div.
ICE INGESTION EXPERIENCE ON A SMALL TURBOPROP ENGINE
L. W. Blair, R. L. Miller, and D. J. Tapparo *In* AGARD, Low Temperature Environment Operations of Turboengines (Design and User's Problems) 1990 9 p (For primary document see N91-31144 23-07)
Copyright Avail: NTIS HC/MF A16; Non-NATO Nationals requests available only from AGARD/Scientific Publications Executive

Modern high technology turbine aircraft engines often employ high rotor speed compressors with thin advanced blading designs to achieve better performance. The engine designer is faced with a tradeoff between optimum compressor performance and on-wing durability. During the engine/aircraft development stage, certain assumptions are made regarding the icing environment and the testing required to confirm compatibility with it. Often, the true impact of the design trade-off is not realized until the engine is exposed to its service environment. Despite successful engine test cell and aircraft natural icing certification tests, in 1984 General Electric Aircraft Engines Company began to experience an unacceptable level of foreign object damage (FOD) caused by ingested ice with its CT7-5/-7 family of turboprop engines.The purpose of this paper is to: (1) address the issue of Stage one compressor rotor blade ice FOD in the CT7 engine; (2) explain the methods and techniques used in assessing the icing environment; (3) explain the lessons learned from test and analysis; and (4) define the final resolution of the compressor maintenance problem which simultaneously created accelerated performance deterioration for the engine. The first part of this paper deals with the airframe icing environment and its impact on the engine inlet system. The second part concentrates on the design improvement and durability testing of the Stage one compressor blade. Author

N91-31163# Ministry of Defence, London (England).
FUELS AND OILS AS FACTORS IN THE OPERATION OF AERO GAS TURBINE ENGINES AT LOW TEMPERATURES
G. L. Batchelor *In* AGARD, Low Temperature Environment Operations of Turboengines (Design and User's Problems) 1990 7 p (For primary document see N91-31144 23-07)
Copyright Avail: NTIS HC/MF A16; Non-NATO Nationals requests available only from AGARD/Scientific Publications Executive

Two factors strongly influence the low temperature behavior of aero gas turbine fuels and oils: viscosity and state or phase change - i.e. whether the material is liquid or solid. In fact, the question is whether solids are, or are not, present because, although the whole may cease to flow at some designated temperature, the lighter components of hydrocarbon and other organic mixtures are likely to be liquids under all natural circumstances. Terms such as freezing point, pour point, and the like, will be familiar enough; the chemical and physical realities underlying such parameters are examined, and their impact on aero gas turbine engine performance is considered. For the purposes of this paper, fuels and oils will be treated quite separately. Author

N91-31164# Southwest Research Inst., San Antonio, TX.
THE EFFECT OF FUEL PROPERTIES AND ATOMIZATION ON LOW TEMPERATURE IGNITION IN GAS TURBINE COMBUSTORS
D. W. Naegeli, L. G. Dodge, and C. A. Moses *In* AGARD, Low Temperature Environment Operations of Turboengines (Design and User's Problems) 1990 10 p Sponsored in part by Naval Air Propulsion Center (For primary document see N91-31144 23-07)
(Contracts DAAK70-85-C-0007; DAAK70-87-C-0043)
Copyright Avail: NTIS HC/MF A16; Non-NATO Nationals requests available only from AGARD/Scientific Publications Executive

Experiments were conducted in a T63 engine combustor to gain a better understanding of the role played by volatility and atomization in low temperature ignition. Eight test fuels were used, some of which were specially blended to vary either viscosity or volatility while holding the other constant. Six atomizers were used to vary the fuel spray characteristics, and average drop sizes, represented by Sauter mean diameter (SMD), were measured. Air temperatures were varied from 239 to 310 K. Ignition comparisons were made by the minimum fuel-air ratios necessary to achieve ignition. Significant results included: (1) viscosity, which determined atomization characteristics, was more important than volatility in the ignition process; (2) ignition depended more on achieving a critical drop size than on reaching the lean-limit fuel-air ratio; and (3) fuel temperature was found to be more important than air temperature for low-temperature ignition, an effect due principally to viscosity and atomization rather than evaporization. A practical implication is that fuel heating would give a much greater improvement in cold-start performance than heating the combustor inlet air. Author

N91-31165# Royal Military Coll. of Canada, Kingston (Ontario). Dept. of Mechanical Engineering.
THE INFLUENCE OF FUEL CHARACTERISTICS ON HETEROGENEOUS FLAME PROPAGATION
M. F. Bardon, J. E. D. Gauthier, and V. K. Rao *In* AGARD, Low Temperature Environment Operations of Turboengines (Design and User's Problems) 1990 9 p (For primary document see N91-31144 23-07)
Copyright Avail: NTIS HC/MF A16; Non-NATO Nationals requests available only from AGARD/Scientific Publications Executive

A theoretical study of flame propagation through mixtures of fuel vapor, droplets, and air under conditions representative of cold starting in gas turbunes is discussed. Two previously developed models are described: one for heterogeneous flame propagation and the other for describing the complex evaporative behavior of real fuel blends. Both models were validated against experimental data. The combined model incorporates the effects of pressure, temperature, droplet diameter, turbulence intensity, delivered equivalence ratio, fuel prevaporization, and fuel type on flame propagation. Differences in the combustion performance of Jet A1, JP-4, and two single component reference fuels are compared. Conclusions are drawn regarding the use of pure compounds to represent real fuel blends, and the relative importance of various engine conditions and spray parameters on combustion. Author

N91-31166# Naval Air Propulsion Test Center, Trenton, NJ.
THE DEVELOPMENT OF A COMPUTATIONAL MODEL TO PREDICT LOW TEMPERATURE FUEL FLOW PHENOMENA
R. A. Kamin, C. J. Nowack, and B. A. Olmstead (Boeing Military Airplane Development, Seattle, WA.) *In* AGARD, Low Temperature Environment Operations of Turboengines (Design and User's Problems) 1990 13 p Sponsored by ONR (For primary document see N91-31144 23-07)
Copyright Avail: NTIS HC/MF A16; Non-NATO Nationals requests available only from AGARD/Scientific Publications Executive

Fuel availability studies indicated that the relaxation of the F-44 freeze point specification could greatly increase the yield of F-44 per ballel of crude. A thorough analysis was initiated to insure that the higher freeze point fuel would not form solid wax precipitates during low temperature operations that could impact aircraft mission performance. In order to evaluate the effects of a potential change in the freeze point specification over the entire inventory of United States naval aircraft, a general three dimensional computational fluid dynamics code, PHOENICS 84, was modified for use. Inputs into the code include tank geometry, mission profile, and fuel properties. Outputs from the model include fuel cooldown and holdup, as a function of time in the tank. The accuracy of the code was verified by experimental data obtained during flight and simulator testing of instrumented tanks. Author

N91-31167# Naval Air Propulsion Test Center, Trenton, NJ.
ENVIRONMENTAL ICING TESTING AT THE NAVAL AIR PROPULSION CENTER
William H. Reardon and Vito J. Truglio *In* AGARD, Low Temperature Environment Operations of Turboengines (Design and User's Problems) 1990 18 p (For primary document see N91-31144 23-07)
Copyright Avail: NTIS HC/MF A16; Non-NATO Nationals requests available only from AGARD/Scientific Publications Executive

A comprehensive Environmental Icing Simulation System developed by the Naval Air Propulsion Center (NAPC) is discussed. The system accommodates the testing of ducted and free stream mounted engines and free stream mounted engine inlets. The Navy specification icing test procedures, success criteria and rationale for the requirements are discussed. Also discussed are the capabilities of the NAPC icing facilities in terms of critical icing cloud parameters such as liquid water content, mean effective droplet diameter, humidity and inlet air temperature. How the icing environment is established, calibrated prior to testing, and verified during testing are covered. NAPC test experience in the Navy qualification programs for the T406, T700, and F404, as well as demonstration and development test programs performed with the TOMAHAWK Cruise Missile inlet and the F-14A aircraft inlet duct are discussed. Author

N91-31168# Rolls-Royce Ltd., Derby (England).
ICING RESEARCH RELATED TO ENGINE ICING CHARACTERISTICS
S. J. Riley *In* AGARD, Low Temperature Environment Operations of Turboengines (Design and User's Problems) 1990 12 p (For primary document see N91-31144 23-07)
Copyright Avail: NTIS HC/MF A16; Non-NATO Nationals requests available only from AGARD/Scientific Publications Executive

Physical properties and characteristics of ice formed by accretion were investigated experimentially to provide a database relevant to civil turbofan engine and powerplant surfaces. Part of that work, relating to unheated surfaces, including observations of ice accretion on various bodies over a range of conditions, and measurement of the adhesive strength of ice samples is discussed. Author

N91-31169# Centre d'Essais des Propulseurs, Orsay (France).
NUMERICAL MODEL OF EVOLUTION IN SUPERCOOLED CLOUD OF WATER DROPLETS IN A CASE OF ICING [MODELISATION NUMERIQUE DE L'EVOLUTION D'UN NUAGE DE GOUTTELETTES D'EAU EN SURFUSION DANS UN CAISSON GIVRANT]
Paul Creismeas and Joel Courquet (Office National d'Etudes et de Recherches Aerospatiales, Toulouse, France) *In* AGARD, Low Temperature Environment Operations of Turboengines (Design and User's Problems) 1990 10 p In FRENCH; ENGLISH summary (For primary document see N91-31144 23-07)
Copyright Avail: NTIS HC/MF A16; Non-NATO Nationals requests available only from AGARD/Scientific Publications Executive

A computational tool, called M.A.GI.C., developed as a tool for icing tests is discussed. In order to compare numerical results from M.A.GI.C. to physical measurements, an analysis based on granulometry measurement of droplets inside a wind tunnel was performed. The results of the comparison were acceptable. Author

N91-31170# Sverdrup Technology, Inc., Arnold AFS, TN.
ICING TEST CAPABILITIES FOR AIRCRAFT PROPULSION SYSTEMS AT THE ARNOLD ENGINEERING DEVELOPMENT CENTER
C. Scott Bartlett, J. Richard Moore, Norman S. Weinberg, and Ted D. Garretson (Arnold Engineering Development Center, Arnold Air Force Station, TN.) *In* AGARD, Low Temperature Environment Operations of Turboengines (Design and User's Problems) 1990 9 p (For primary document see N91-31144 23-07)
Copyright Avail: NTIS HC/MF A16; Non-NATO Nationals requests available only from AGARD/Scientific Publications Executive

Icing test capabilities for the full scale turbine engine propulsion systems at the Engine Test Facility (ETF) at the Arnold Engineering Development Center (AEDC) are discussed. The methods and hardware used to inject liquid spray into a cold airstream to simulate in-flight icing conditions are discussed. The spray manifold systems and spray injection nozzles currently in use at AEDC are described. Test experiences in both direct and free-jet connect icing tests are addressed. Recent ice accretion scaling techniques and test results, and developments and observations in cloud liquid water content and droplet sizing are briefly discussed. Uses of real time ice accretion detectors for facility calibration and test article ice accretion rate monitoring are addressed. Author

N91-31171# Aero and Industrial Technology Ltd., Burnley (England). Combustion Technology Centre.
ICING TEST PROGRAMMES AND TECHNIQUES
E. Carr and D. Woodhouse *In* AGARD, Low Temperature Environment Operations of Turboengines (Design and User's Problems) 1990 8 p (For primary document see N91-31144 23-07)
Copyright Avail: NTIS HC/MF A16; Non-NATO Nationals requests available only from AGARD/Scientific Publications Executive

Described here are the capabilities of an altitude test facility with a main chamber 4m diameter by 12 m long and capable of providing air flows up to 5kg/s and simulating altitudes up to 15 km. The experience obtained on icing programs since the plant was commissioned in 1953 is described. Examples of the procedures used to establish the susceptibility of equipment to icing are given. The examples cover the use of scale models, the evaluation of probes, and the testing of complete helicopter engine intakes. Author

N91-31172# Deutsche Forschungsanstalt fuer Luft- und Raumfahrt, Oberpfaffenhofen (Germany, F.R.). Inst. for Atmospheric Physics.

A DOCUMENTATION OF VERTICAL AND HORIZONTAL AIRCRAFT SOUNDINGS OF ICING RELEVANT CLOUDPHYSICAL PARAMETERS **c46**

H.-E. Hoffmann *In* AGARD, Low Temperature Environment Operations of Turboengines (Design and User's Problems) 1990 14 p (For primary document see N91-31144 23-07)

Copyright Avail: NTIS HC/MF A16; Non-NATO Nationals requests available only from AGARD/Scientific Publications Executive

In a homogeneous st-cloud (in a high pressure area) the total water content (TWC) is nearly linearly increasing with increasing distance from the cloud base and obtains its largest value near the top (0.39 respectively 0.49 g/cu m). The median volume diameter (MVD) is nearly remaining constant and has predominantly small values (between 15 and 23 microns). The phase of particles in all st-clouds, evaluated up to now, was fluid. Such a regularity was not found in any of the other types of inhomogeneous clouds of a warm front. Apart from temperature (T), which is decreasing nearly linearly in these clouds too, the course of TWC and MVD is very irregular. Both the parameters can have several maxima at different distances from the base. The maxima values of TWC can be up to 0.45 g/cu m and those of the MVD up to 460 microns. The phase of the particles could vary between fluid and solid. Not only the vertical structures, but also the horizontal structures show great differences in the particle distributions. In the clouds of a high pressure area more than 90 percent of the particles had diameters between 2 and 32 microns. Author

N91-31173# Royal Aerospace Establishment, Farnborough (England). Propulsion Dept.

DEVELOPMENTS IN ICING TEST TECHNIQUES FOR AEROSPACE APPLICATIONS IN THE RAE PYESTOCK ALTITUDE TEST FACILITY **c09**

M. Holmes, V. E. W. Garratt, and R. G. T. Drage *In* AGARD, Low Temperature Environment Operations of Turboengines (Design and User's Problems) 1990 15 p (For primary document see N91-31144 23-07)

Copyright Avail: NTIS HC/MF A16; Non-NATO Nationals requests available only from AGARD/Scientific Publications Executive

The altitude test facilities at the Royal Aerospace Establishment at Pyestock are used in support of clearance of aero-engines, intakes, and helicopter rotors to operate under severe icing conditions. An important aspect of the work is the simulation of the wet icing cloud in terms of water concentration, mean droplet size and spectrum. Water spray rakes or booms were developed for this activity and individual nozzles were calibrated in a wind tunnel built for this purpose. A laser particle sizer was used to calibrate typical spray nozzles and attempts were made to establish a traceable standard. The development of cloud simulations is discussed as well as facilities for monitoring ice formation and shedding. Author

N91-31174 Boeing Canada, Toronto (Ontario).

SEGMENTED ROTATABLE NOZZLES Patent Application

Douglas Garland, inventor 8 Feb. 1990 37 p

(CA-Patent-Appl-SN-2-009-634; Int-Patent-Class-F02G-140; Int-Patent-Class-B64C-2900; CTN-91-60136) Copyright Avail: Micromedia Ltd., Technical Information Centre, 165 Hotel de Ville, Place du Portage, Phase 2, Hull, Quebec J8X 3X2, Canada HC $4.00 CAN, MF $2.75 CAN

A thrust deflector is provided for use with vertical/short take off and landing (VSTOL) aircraft having pressurized gas generators. The thrust deflector consists of a number of adjacent nozzles. Each of the nozzles has a body with a first and a second face. The nozzles further have an inlet for receiving pressurized gas from the gas generator and at least one outlet connected to the inlet for discharging pressurized gas from the nozzle. Each of the nozzles is rotatable from a first position in which the outlet directs pressurized gas downward to a second position in which the outlet directs pressurized gas rearward. In the first position, the first and second faces of the bodies of adjacent nozzles are spaced apart to permit air to flow between the nozzles. In the second position, the first and second faces of adjacent nozzles are in contact preventing air passage between adjacent nozzles. The thrust deflector may be mounted on stub wings along either side of the fuselage or in a chordwise arrangement in the main wing of the aircraft. Lower ejector doors may be rotatably mounted adjacent to the nozzles distal to the fuselage and the nozzles suitably spaced to cause thrust augmentation according to the ejector principle. CISTI

N91-31175 Boeing Canada, Toronto (Ontario).

SEGMENTED VECTORING CRUISE NOZZLES Patent Application

Douglas Garland, inventor and Joseph E. Farbridge, inventor 8 Feb. 1990 36 p

(CA-Patent-Appl-SN-2-009-635; Int-Patent-Class-F02K-178; CTN-91-60137) Copyright Avail: Micromedia Ltd., Technical Information Centre, 165 Hotel de Ville, Place du Portage, Phase 2, Hull, Quebec J8X 3X2, Canada HC $4.00 CAN, MF $2.75 CAN

A thrust vectoring structure is provided for vertical/short take off and landing (VSTOL) aircraft having a pressurized gas generator and at least one rearward facing outlet with an opening for discharging pressurized gas from the pressurized gas generator. This structure has a plurality of horizontal dividers extending between the sides of the opening. A front flap is rotatably mounted adjacent to the front edge of the dividers and a rear flap is similarly mounted adjacent the rear edge of the dividers. The flaps are rotatable from a horizontal position to a vertical position. In the horizontal position the pressurized gas is directed rearwardly. In the vertical position the pressurized gas is directed downwardly in a number of discrete segmented jets. The flaps are further rotatable so that they diverge outwardly in either the horizontal or the vertical positions. In one embodiment, the top of the outlet is also rotatable toward or away from the bottom to vary the cross sectional area of the outlet. CISTI

N91-31176 Boeing Canada, Toronto (Ontario).

VENTRAL SEGMENTED NOZZLES Patent Application

Joseph E. Farbridge, inventor, Douglas Garland, inventor, A. R. Schexnayder, inventor, Brian E. Meyer, inventor, and Charles F. Ritchie, inventor 8 Feb. 1990 21 p Prepared in cooperation with Canadian General Electric Co. Ltd., Toronto, Ontario

(CA-Patent-Appl-SN-2-009-636; Int-Patent-Class-F02K-100; Int-Patent-Class-B64C-2900; CTN-91-60138) Copyright Avail: Micromedia Ltd., Technical Information Centre, 165 Hotel de Ville, Place du Portage, Phase 2, Hull, Quebec J8X 3X2, Canada HC $4.00 CAN,M F $2.75 CAN

A thrust directing system is provided for vertical or short takeoff and landing (VSTOL) aircrafts having a pressurized gas generator. The thrust directing system consists of a number of spaced, downwardly facing openings along the bottom of the fuselage. The openings are fluidly connected with the outlet of the aircraft engine so that pressurized gas from the aircraft engine is discharged through the openings and away from the fuselage in discrete, spaced jets. The openings can be provided with at least one vectoring flap for further directing the heat being discharged through the opening. The flap is movable to direct the heat from a vertical direction to at least one rearward direction. Air introduction means may also be provided which fluidly communicate with the space between the nozzles. CISTI

N91-31177 Boeing Co., Seattle, WA.
REMOVABLE SLIDER SHOE FOR A TRANSLATING SLEEVE USED ON A JET ENGINE COWL AND DUCT Patent
Alfred H. Greiert, inventor 3 Jan. 1989 12 p
(Patent-1-247-868; Int-Patent-Class-F16C-2902; CTN-91-60151)
Copyright Avail: Micromedia Ltd., Technical Information Centre, 165 Hotel de Ville, Place du Portage, Phase 2, Hull, Quebec J8X 3X2, Canada HC $4.00 CAN, MF $2.75 CAN

An improved low friction bearing surface for a translating sleeve used on a jet engine cowl and duct was devised. It consists of a removable slider shoe for mounting on a translating sleeve of a jet engine cowl and duct. The sleeve has a slider which moves in a track on the cowl. The shoe is comprised of: a removable element adapted for receipt of a slider for sliding along the length of the track; a second removable element having a portion of its outer periphery adapted for receipt of the slider for sliding along the length of the track; a low friction surface on the outer periphery of each shoe element; and removable means for securing and replacing the shoe elements and the slider. The claimed shoe elements are made from a low friction rub surface bonded to aluminum. This invention eliminates the time and expense of removing a solid molded shoe attached to the slider when the slider becomes worn. The removable shoe can be quickly removed and replaced. CISTI

N91-31178*# National Aeronautics and Space Administration. Lewis Research Center, Cleveland, OH.
A HIGH-FREQUENCY SERVOSYSTEM FOR FUEL CONTROL IN HYPERSONIC ENGINES
Donald L. Simon Aug. 1991 11 p
(DA Proj. 1L1-61102-AH-45)
(NASA-TM-104333; E-6098; NAS 1.15:104333;
AVSCOM-TR-91-C-016) Avail: NTIS HC/MF A03 CSCL 21E

A hydrogen fuel-flow valve with an electrohydraulic servosystem is described. An analysis of the servosystem is presented along with a discussion of the limitations imposed on system performance by nonlinearities. The response of the valve to swept-frequency inputs is experimentally determined and compared with analytical results obtained from a computer model. The valve is found to perform favorably for frequencies up to 200 Hz. Author

N91-31179# Aeronautical Research Labs., Melbourne (Australia).
FIELD EVALUATION OF SIX PROTECTIVE COATINGS APPLIED TO T56 TURBINE BLADES AFTER 500 HOURS OF ENGINE USE
S. G. Russo Jun. 1991 26 p
(ARL-MAT-TM-405; AR-006-615) Copyright Avail: NTIS HC/MF A03

The evaluation of several protective coatings that were applied to IN738-LC first stage turbine blades in two military gas turbines for an interval of 500 flight hours indicated variations in the extent of hot-corrosion resistance. The coatings included two conventional nickel aluminides, an aluminide modified with chromium, a platinum-modified aluminide, an aluminide modified with silicon and a platinum/rhodium-modified aluminide. The aim of this trial is to find a coating that will withstand up to 3000 engine operating hours. Detailed metallographic examinations as well as scanning electron microscopy were employed in the evaluation. Results indicated that the precious metal aluminides offered the best protection with the chromium-aluminide being the most susceptible to hot-corrosion. The conflicting results of the basic aluminide coatings reaffirms the point that no firm conclusions can be made solely on one assessment. Furthermore, there was no apparent cracking in any of the coatings. Author

N91-31180# Ecole Centrale de Lyon (France).
CALCULATING THE FLOW IN A TURBOMACHINE WITH CLEBSCH VARIABLES AND A FINITE ELEMENT METHOD Ph.D. Thesis [CALCUL D'ECOULEMENT DANS UNE TURBOMACHINE A L'AIDE DES VARIABLES DE CLEBSCH ET PAR UNE METHODE D'ELEMENTS FINIS]
El Mostafa ElGhazzani 1990 145 p In FRENCH; ENGLISH summary
(ETN-91-99918) Avail: NTIS HC/MF A07

A three dimensional computation method for the analysis of the inviscid flow through any isolated, fixed or rotating turbomachinery component is presented. A Clebsch formulation, completely equivalent to the Euler equations set, is implemented from the Eulerian type variational principle. The formulation includes a loss scheme and the numerical processing uses a finite element discretization. The method is applied to transport equations and a relaxation scheme is used. Boundary conditions implementation is studied and integrated in the computation. Calculations were performed on a fixed geometry, on a mixed flow runner and on a Francis turbine runner. Results are compared to experimental data and quasi three dimensional and Navier-Stokes calculation results. ESA

N91-31181*# National Aeronautics and Space Administration. Lewis Research Center, Cleveland, OH.
JET-A REACTION MECHANISM STUDY FOR COMBUSTION APPLICATION
Chi-Ming Lee, Krishna Kundu, and Waldo Acosta (Army Aviation Systems Command, Cleveland, OH.) 1991 13 p Presented at the 27th Joint Propulsion Conference, Sacramento, CA, 24-27 Jun. 1991; cosponsored by AIAA, SAE, ASME, and ASEE Previously announced in IAA as A91-45810
(DA Proj. 1L1-62211-A-47A)
(NASA-TM-104441; E-6279; NAS 1.15:104441;
AVSCOM-TR-91-C-029; AIAA-91-2355) Avail: NTIS HC/MF A03 CSCL 21E

Simplified chemical kinetic reaction mechanisms for the combustion of Jet A fuel was studied. Initially, 40 reacting species and 118 elementary chemical reactions were chosen based on a literature review. Through a sensitivity analysis with the use of LSENS General Kinetics and Sensitivity Analysis Code, 16 species and 21 elementary chemical reactions were determined from this study. This mechanism is first justified by comparison of calculated ignition delay time with the available shock tube data, then it is validated by comparison of calculated emissions from the plug flow reactor code with in-house flame tube data. Author

08 AIRCRAFT STABILITY AND CONTROL

Includes aircraft handling qualities; piloting; flight controls; and autopilots.

For related information see also *05 Aircraft Design, Testing and Performance.*

N91-31182 Societe Nationale Industrielle Aerospatiale, Paris (France).
PROCEDURE FOR STEERING A LOW-SPEED MISSILE, WEAPON SYSTEM, AND MISSILE FOR IMPLEMENTATION OF THE PROCEDURE Patent
Jean Guillot, inventor, Jacques Raynaud, inventor, Michel Maree, inventor, Robert Vaillant, inventor, and Jean Ansaldi, inventor 20 Feb. 1990 25 p
(Patent-1-265-947; Int-Patent-Class-F42B-15033;
Int-Patent-Class-G05D-110; CTN-91-60131) Copyright Avail: Micromedia Ltd., Technical Information Centre, 165 Hotel de Ville, Place du Portage, Phase 2, Hull, Quebec J8X 3X2, Canada HC $4.00 CAN, MF $2.75 CAN

The present invention pertains to a procedure for steering a missile of the man-pack type having a range of up to 2000 m with an initial low-speed that is suitable for firing from a confined area. Missile speed increases from about 20 m/s at launch to high subsonic values at the end of the flight. Beyond a range of 300 m, corrections must be made in the trajectory of the missile. The missile is steered solely by force upon launching with this method being effective at low initial velocities, and then by changing the center of gravity, the shift is made to mixed steering (combination of steering by force and aerodynamic steering) when

flight speed has increased sufficiently. The weapon system comprises a launch tube and a missile, with the latter being equipped with a propulsion system and control devices. This propulsion system includes at least one integrated booster, the combustion of which ends before the missile leaves the tube, and at least one flight propulsion unit which is equipped with lateral nozzles for steering by force. The unit is equipped with control surfaces which are capable of deflecting the thrust vector of the jet. It is possible to mount the flight propulsion unit and the combat payload such that the center of gravity changes during flight in a way that contributes to the desired steering effect and increases the distance of the flight. CISTI

N91-31183# Messerschmitt-Boelkow-Blohm G.m.b.H., Ottobrunn (Germany, F.R.). Unternehmensbereich Verteidigungssysteme.
POSSIBILITIES OF SIMULATION AND OPTIMIZATION FOR GUIDED MISSILE SYSTEMS [BEDIENBARKEIT VON LENKFLUGKOERPERSYSTEMEN SIMULATION UND OPTIMIERUNG]
Gottfried Scharfenberg and Illobrand v.Ludwiger 1990 4 p In GERMAN
(MBB-UA-1201-90-PUB; OTN-032795; ETN-91-99755) Avail: NTIS HC/MF A01

It is shown that by using a system operating concept, system relevant parameters such as operator number, operator qualification, automatization degree, function extent, and information quantities can be acknowledged and specified in the form of rapid prototyping, so that costly project mockups become unnecessary. Optimal system efficiency can only be reached by adapting technical system components to the capacities and limits of system operators. ESA

N91-31184# Societe de Fabrication d'Instruments de Mesure, Massy (France).
ROBUSTNESS AND TECHNIQUES OF MULTIVARIABLE CONTROL FOR HELICOPTER PILOTING. DISPATCH 3: INCLUSION REGIONS TECHNIQUE ON LINEAR MODEL [ROBUSTESSE ET TECHNIQUES DE COMMANDE MULTIVARIABLE POUR LE PILOTAGE DE L'HELICOPTERE. LOT 3: TECHNIQUE DES REGIONS D'INCLUSION SUR MODELE LINEAIRE]
29 Aug. 1990 84 p In FRENCH
(RD/PA-14-227; ETN-91-99975) Avail: NTIS HC/MF A05

The inclusion regions method is applied to the basic stability design of an automatic helicopter pilot. The basis of an inclusion regions approach is the localization of real values of a perturbed system from a nominal system. Two types of regions are distinguished: robust but conservative regions obtained by normal approximations; E contours, which are fields obtained from the so-called real values of the nominal system and the size of perturbation. Techniques to reduce the extent of these regions at a given frequency are studied. Problems using the method with prohibitively sized perturbations are discussed. ESA

09 RESEARCH AND SUPPORT FACILITIES (AIR)

Includes airports, hangars and runways; aircraft repair and overhaul facilities; wind tunnels; shock tubes; and aircraft engine test stands.

For related information see also *14 Ground Support Systems and Facilities (Space).*

N91-31185# Deutsche Forschungsanstalt fuer Luft- und Raumfahrt, Brunswick (Germany, F.R.). Abt. Systemtechnik und Navigation.
THE EFFECTS OF DIFFERENT SEQUENCING STRATEGIES ON THE CAPACITY OF AIRPORTS
Ingrid Gerdes Sep. 1990 28 p In GERMAN; ENGLISH summary
(DLR-Mitt-90-18; ISSN-0939-298X; ETN-91-99561) Avail: NTIS HC/MF A03; DLR, Wissenschaftliches Berichtswesen, VB-PL-PO, Postfach 90 60 58, 5000 Cologne, Fed. Republic of Germany, HC 13 DM

Analytical models for the sequencing problem of a single runway are developed. The model runway capacity is computed for various input data and a sequence length ranging from two to ten aircrafts. The results are discussed. Connections between the theoretical models and the Computer Oriented Metering Planning and Advisory Systems (COMPAS) which includes an algorithm for the planning of sequences are shown. Various Sequencing (SEQ) and Modified Sequencing (MSEQ) processes are developed and compared with the First Come First Served (FCFS) process. It was established that MSEQ is the best COMPAS approximation. ESA

N91-31186# Messerschmitt-Boelkow-Blohm G.m.b.H., Munich (Germany, F.R.).
SIMULATION OF DISTANCE-DEPENDENT FUNCTIONS IN VISUAL SYSTEMS FOR TRAINING SIMULATORS USING THE Z-BUFFER TECHNIQUE
Gerhard Brune and Wolfgang Metze 1990 4 p Presented at the International Training Equipment Conference, Birmingham, England, Apr. 1990
(MBB-UA-1190-90-PUB; OTN-032762; ETN-91-99751) Avail: NTIS HC/MF A01

The use of the z buffer technique to correctly depict mutually occulting objects in the scene is described. The distance information, which is calculated and stored in the z buffer for this purpose, can then be advantageously used to support other range dependent functions of the simulator both within the visual system (simulation of limited visibility, point lights, and its own landing lights) as well as other simulator functions (laser range finder, radar altimeter, and collision detection). ESA

N91-31187# Association Aeronautique et Astronautique de France, Paris.
INSTRUMENTATION UNDER DEVELOPMENT FOR THE ONERA F4 WIND TUNNEL [INSTRUMENTATION EN COURS DE DEVELOPPEMENT POUR LA SOUFFLERIE F4 DE L'ONERA]
A. Girard, A. Boutier, J. P. Chevallier, and G. Francois (Office National d'Etudes et de Recherches Aerospatiales, Paris, France) 1989 28 p In FRENCH Presented at the 26th Colloque d'Aerodynamique Appliquee, Toulouse, France, 23-25 Oct. 1990 Previously announced in IAA as A90-19596
(AAAF-NT-89-11; ISBN-2-7170-0944-2; ISSN-0243-0177; ETN-91-99952) Avail: NTIS HC/MF A03; CEDOCAR, Section des Diffusions, 26 Blvd Victor, 75996 Paris Armees, France, HC 30 francs

The instrumentation associated to the F4 tunnel is based on: a strioscopic component whose 500 mm diameter mirrors are inside the test chamber emptied before the gust; a six component inertial compensation type balance. The use of a certain number of other techniques is foreseen and particular attention is given to means for studying the effects of real gas. One such technique is electron beam excited fluorescence. Metrological development effort relies equally on holographic interferometry, high cadence infrared thermography, and laser diode spectroscopy. ESA

N91-31188# Association Aeronautique et Astronautique de France, Paris.
A FIRST HOT WIRE SCANNER [UN PREMIER SCANNER A FILS CHAUDS]
J. L. Peube and B. Nayroles (Institut de Mecanique de Grenoble, France) 1989 25 p In FRENCH Presented at 26th Colloque d'Aerodynamique Appliquee, Toulouse, France, 23-25 Oct. 1990
(AAAF-NT-89-16; ISBN-2-7170-0949-3; ISSN-0243-0177; ETN-91-99957) Avail: NTIS HC/MF A03; CEDOCAR, Section des Diffusions, 26 Blvd Victor, 75996 Paris Armees, France, HC 15 francs

The question of scanning, to measure a scalar field defined in a continuous medium which occupies a spatial field, is explained. The feasibility of experiments with a hot wire scanner was examined

hypothetically at very low frequencies. A simple physical study of the system which validates the hypotheses was carried out. Theoretical comments on resolution algorithm and a numerical exploration of its possibilities for the case of a larger number of wires are presented. Experiments carried out in a wind tunnel with a 12 wire and 9 mesh scanner are described. ESA

N91-31189# Ecole Polytechnique, Palaiseau (France). Lab. de Physique des Milieux Ionises.
DEVELOPMENT OF AN INFRARED LASER FOURIER DENSITOMETER (LFD) AND FIRST WIND TUNNEL TESTS Final Report [REALISATION D'UN DENSITOMETRE DE FOURIER PAR LASER (DFL) INFRAROUGE, ET PREMIER ESSAIS EN SOUFFLERIE]
D. Gresillon, B. Cabrit, J. P. Bonnet, and G. Gemaux Jun. 1990 45 p In FRENCH
(Contract DRET-86-095)
(PMI-2335; ETN-91-99976) Avail: NTIS HC/MF A03

The principle and definition and sensitivity of the obtained signal of LFD (Laser Fourier Densitometry) are presented. A mobile optical bench adapted to studies in jet pipe, its characteristics, and the obtained signals are described. Wind tunnel observations in supersonic flows are presented: two studies of supersonic wake at Mach 1.6 and 4.2; a study of the turbulent boundary layer interaction with shock wave at Mach 2.25; first observation of the turbulence in a boundary layer in hypersonic flow. ESA

N91-31190# Oak Ridge National Lab., TN.
A MULTIFUNCTION ION-IRRADIATION/SURFACE MODIFICATION ULTRAHIGH VACUUM CHAMBER SYSTEM
R. A. Buhl Apr. 1991 113 p
(Contract DE-AC05-84OR-21400)
(DE91-016819; ORNL/TM-11746) Avail: NTIS HC/MF A06

A modular ultrahigh vacuum chamber system has been built to facilitate experiments at the Triple Ion Beam Accelerator Facility at the Oak Ridge National Laboratory (ORNL). The system currently consists of three chambers, linked by ultrahigh vacuum valves through which groups of specimens are transferred via a track-type shuttle mechanism. A loading/vapor deposition dual purpose chamber serves not only as a vacuum interlock for loading and unloading groups of specimens, but also as a dual-electron gun-type metal vapor deposition station. The ion-irradiation chamber, located adjacent to the loading chamber, is positioned at the intersection of beam lines from three Van de Graaff accelerators. An Auger surface analyzer with an in situ differentially pumped sputter-gun assembly is located in the third chamber. The chambers are mounted on a frame with 'airfloat' pads beneath the feet so that a lateral translation permits the beam lines to be connected to other chambers in the system. The modular assembly concept in conjunction with the lateral mobility and the specimen transfer mechanism enhances the ability to accommodate future expansion in the system. A Hewlett Packard (HP) Vectra PC connected via an IEEE-488 interface to an upgraded HP 3852A controller provides data acquisition and control. DOE

N91-31191# Air Force Inst. of Tech., Wright-Patterson AFB, OH.
A KNOWLEDGE-BASE FOR REHABILITATION OF AIRFIELD CONCRETE PAVEMENTS Ph.D. Thesis
Wayne J. Seiler 1991 263 p
(AD-A239354; AFIT/CI/CIA-91-004d) Avail: NTIS HC/MF A12 CSCL 01/5

Airfield pavement knowledge captured in this research showed that knowledge-based techniques can be used to quickly select and design rehabilitation alternatives for runways, taxiways or aprons. The AIRfield PAvement Consultant System (AIRPACS) uses the knowledge of planners, constructors, airfield managers and designers to solve difficult jointed plain concrete pavement (JPCP) design problems. This expert system focuses on aircraft safety and pavement structural capacity which are key issues for all pavement design participants. During the validation tests, AIRPACS recommendations were compared to results that were obtained using current empirical and mechanistic design procedures. The results demonstrate that the knowledge acquired and represented in AIRPACS will allow knowledgeable pavement engineers to quickly perform airport rehabilitation designs. GRA

N91-31192# Naval Postgraduate School, Monterey, CA.
TOUCH SCREEN USE ON FLIGHT SIMULATOR INSTRUCTOR/OPERATOR STATIONS M.S. Thesis
Alan A. Vazquez Sep. 1990 79 p
(AD-A239524) Avail: NTIS HC/MF A05 CSCL 05/9

The goal was to aid designers in selecting the best data input device for the design of Instructor/Operator Stations (IOSs). A literature review of touch screen, mouse, and trackball technologies is provided. IOS users were surveyed to evaluate the use of touch screens with several military flight simulators. IOS users' experience level, frequency of touch screen interaction, and familiarity with touch screen, mouse, and trackball devices are provided, along with data on the tasks performed, required accuracy, parallax, arm fatigue, and feelings toward touch screen use. It is concluded that, although touch screens are being used by persons with too much experience and for tasks reported in the literature to be inappropriate, results are generally satisfactory. However, it is recommended that input devices should be matched with the tasks performed. GRA

N91-31193# Harry Diamond Labs., Adelphi, MD.
ELECTRON-BEAM-PINCH EXPERIMENT AT HARRY DIAMOND LABORATORIES: PROVIDING FOR A HIGH-DOSE-RATE FLASH X RAY FACILITY FOR TRANSIENT RADIATION EFFECTS ON ELECTRONICS (TREE) TESTING OF PIECEPARTS Final Report, May - Jul. 1990
Dale N. Robertson, Marc S. Litz, Steven M. Blomquist, James C. Blackburn, and Gregory K. Ovrebo Aug. 1991 15 p
(AD-A239558; HDL-TM-91-11) Avail: NTIS HC/MF A03 CSCL 18/7

The peak photon-radiation dose rate of the High-Intensity Flash X-Ray facility has been increased by at least a factor of five through the use of custom beam-pinching hardware. With this hardware, the facility can now routinely provide a dose rate of 2.7 x 10(exp 11) rads(Si)/s, at a distance of 1/4 in. from the drift-tube face, while providing excellent radial drop-off to minimized irradiation of items surrounding the device under test. The experimental results show the optimum operating parameters of the beam-pinching hardware to be a drift-tube length equal to 6 cm with an internal nitrogen gas pressure of 0.1 Torr. GRA

N91-31173# Royal Aerospace Establishment, Farnborough (England). Propulsion Dept.
DEVELOPMENTS IN ICING TEST TECHNIQUES FOR AEROSPACE APPLICATIONS IN THE RAE PYESTOCK ALTITUDE TEST FACILITY
M. Holmes, V. E. W. Garratt, and R. G. T. Drage *In* AGARD, Low Temperature Environment Operations of Turboengines (Design and User's Problems) 1990 15 p (For primary document see N91-31144 23-07)
Copyright Avail: NTIS HC/MF A16; Non-NATO Nationals requests available only from AGARD/Scientific Publications Executive

N91-31632*# National Aeronautics and Space Administration. Langley Research Center, Hampton, VA.
REVIEW OF TYPICAL APPLICATIONS: WIND TUNNELS
James F. Meyers *In* VKI, Laser Velocimetry, Volume 2 1991 43 p (For primary document see N91-31625 23-36)
Copyright Avail: NTIS HC/MF A10 CSCL 14B

N91-31730 British Aerospace Public Ltd. Co., Bristol (England). Sowerby Research Center.
THE SOWERBY RESEARCH CENTRE AND UNIVERSITY LIAISON
J. Ackroyd *In its* BAe University Round Table on Gravitational Research Nov. 1990 3 p (For primary document see N91-31729 23-46)
Copyright Avail: British Aerospace (Military Aircraft) Ltd., Warton Aerodrome, Preston, Lancashire PR4 1AX, England

12 ASTRONAUTICS (GENERAL)

For extraterrestrial exploration see *91 Lunar and Planetary Exploration.*

No abstracts in this category.

13 ASTRODYNAMICS

Includes powered and free-flight trajectories; and orbital and launching dynamics.

N91-31194*# National Aeronautics and Space Administration. Langley Research Center, Hampton, VA.
AUTOMATIC SATELLITE TRACKING SYSTEM FOR THE NASA SATELLITE PHOTOMETRIC OBSERVATORY
Glenn H. Mucklow 23 Aug. 1991 36 p Conference held in Melbourne, FL, 20 Sep. 1980
(NASA-TM-105037; NAS 1.15:105037) Avail: NTIS HC/MF A03 CSCL 22A

The development of an Automatic TV Tracking System for NASA's mobile 61 cm aperture Satellite Photometric Observatory is described. The analysis techniques used to match the FOV and resolutions to changing seeing conditions are covered in details. Theoretical reasons for such matching of general interest are discussed. It is shown that the energy density in a satellite image is 11 times greater during good seeing conditions than during typical seeing conditions. The Z7987 image tube is shown to be able to detect 16th magnitude objects under ideal seeing conditions using only 8 percent of the light collected by the main telescope. Experimental results show that the SPO equipped with a Z7987 camera can track a satellite at any orbital velocity with less than 0.14 mr accuracy using the DBA Series 606 TV Tracker. The manual system used prior to the installation of the Automatic TV Tracking System could maintain track at 1.1 mr accuracy for comparison. Author

14 GROUND SUPPORT SYSTEMS AND FACILITIES (SPACE)

Includes launch complexes, research and production facilities; ground support equipment, e.g., mobile transporters; and simulators.

For related information see also *09 Research and Support Facilities (Air).*

No abstracts in this category.

15 LAUNCH VEHICLES AND SPACE VEHICLES

Includes boosters; operating problems of launch/space vehicle systems; and reusable vehicles.

For related information see also *20 Spacecraft Propulsion and Power.*

N91-31195# Centre National d'Etudes Spatiales, Toulouse (France).
CALCULATION OF FRAGMENT EJECTION VELOCITIES ON EXPLOSION OF A LAUNCHER [CALCUL DE LA VITESSE D'EJECTION DES FRAGMENTS LORS D'UNE EXPLOSION DE LANCEUR]
Francois Desclaux Sep. 1990 80 p In FRENCH; ENGLISH summary Original contains color illustrations
(CNES-NT-128; ETN-91-99535) Copyright Avail: NTIS HC/MF A05

Fragment ejection velocities resulting from the explosion of an Ariane launcher are estimated. Many assumptions are made to simplify the model. The assumptions overestimate the consequences, so as to achieve a safety margin. The fragments are ejected under the pressure of gases issuing from the explosion. Two modeling approaches are oriented and compared. The first utilizes spherical symmetry to obtain global equations of the phenomenon. The second method is more precise but requires greater computer time. It models the Euler equations for fluids in a two dimensional moving grid system, and uses a Harten type numerical scheme. Certain cases corresponding to an explosion of an Ariane 4 type launcher are presented. ESA

N91-31196*# National Aeronautics and Space Administration. Lewis Research Center, Cleveland, OH.
THE INTERNATIONAL SPACE UNIVERSITY'S VARIABLE GRAVITY RESEARCH FACILITY DESIGN
Sheila G. Bailey, Francis P. Chiaramonte, and Kenneth J. Davidian Sep. 1991 36 p
(NASA-TM-105224; E-6541; NAS 1.15:105224) Avail: NTIS HC/MF A01 CSCL 22B

A manned mission to Mars will require long travel times between Earth and Mars. However, exposure to long-duration zero gravity is known to be harmful to the human body. Some of the harmful effects are loss of heart and lung capacity, inability to stand upright, muscular weakness and loss of bone calcium. A variable gravity research facility (VGRF) that would be placed in low Earth orbit (LEO) was designed by students of the International Space University 1989 Summer Session held in Strasbourg, France, to provide a testbed for conducting experiments in the life and physical sciences in preparation for a mission to Mars. This design exercise was unique because it addressed all aspects concerning a large space project. The VGRF design was described which was developed by international participants specializing in the following areas: the politics of international cooperation, engineering, architecture, in-space physiology, material and life science experimentation, data communications, business, and management. Author

16 SPACE TRANSPORTATION

Includes passenger and cargo space transportation, e.g., shuttle operations; and space rescue techniques.

For related information see also *03 Air Transportation and Safety* and *18 Spacecraft Design, Testing and Performance.* For space suits see *54 Man/System Technology and Life Support.*

N91-31197# Technische Univ., Berlin (Germany, F.R.). Inst. fuer Luft- und Raumfahrt.
THE QUESTION OF AN EFFICIENT SPACE TRANSPORTATION SYSTEM FOR EXTRATERRESTRIAL MATERIALS [ZUR FRAGE DER WIRTSCHAFTLICHKEIT DES IMPORTES EXTRATERRESTRISCHER ROHSTOFFE]
Michael Reichert 1 Dec. 1990 85 p In GERMAN
(ILR-MITT-252(1990); ETN-91-99743) Avail: NTIS HC/MF A05

A sensitivity analysis shows the great dependency of the transportation costs of both DILETS (Direct Lunar Earth Transportation System) and EXLETS (Extended Lunar Earth Transportation System) on the specific transportation, on the costs of the NEPTUNE carrier system, and, to a lesser degree on the costs of a man year installation. It is shown that the selection of one of the two transportation systems depends on the transportation requirements. If, for instance, the payload transportation on the distance Moon-Earth is dominated by raw material exploitation and industrial production on the moon for the terrestrial world market, the DILETS system is to be chosen, on account of its lower specific transportation costs. Conversely, the EXLETS system is to be selected for the exploitation of a large cislunar infrastructure with lunar material and products fabricated

on the Moon in Geostationary Earth Orbit (GEO), Low Earth Orbit (LEO) and Lunar Orbit (LO), for instance for the construction of a great orbital solar power plant in GEO. ESA

N91-31198# Messerschmitt-Boelkow-Blohm G.m.b.H., Ottobrunn (Germany, F.R.).
THE SAENGER CONCEPT AND THE GERMAN HYPERSONIC TECHNOLOGY PROGRAM [SAENGER UND DAS DEUTSCHE HYPERSCHALL-TECHNOLOGIEPROGRAMM]
Heribert Kuczera 1991 3 p In GERMAN Presented at VDI-GIS Syposium Raumfahrtaktivitaeten in der Bundesrepublik Deutschland Neuorientierung - Ziele - Anforderungen - Mittelstand, Bonn, Fed. Republic of Germany, 14-15 Mar. 1991
(MBB-UK-0132-91-PUB; OTN-030547; ETN-91-99757) Avail: NTIS HC/MF A01

The SAENGER concept is described as a two stage space transportation system which can be launched and landed in European airports. The first stage is a hypersonic carrier aircraft using liquid hydrogen. Its operation will not need more than one thousand people, as compared to the 7000 people in attendance for the American shuttle. The full reusabilility of the space transportation system allows sharp reduction of operation and transportation costs. SAENGER could be ready for service in 2010. ESA

17 SPACE COMM., SPACECRAFT COMM., COMMAND & TRACKING

Includes telemetry; space communications networks; astronavigation and guidance; and radio blackout.

For related information see also *04 Aircraft Communications and Navigation* and *32 Communications and Radar.*

No abstracts in this category.

18 SPACECRAFT DESIGN, TESTING AND PERFORMANCE

Includes satellites; space platforms; space stations; spacecraft systems and components such as thermal and environmental controls; and attitude controls.

For life support systems see *54 Man/System Technology and Life Support.* For related information see also *05 Aircraft Design, Testing and Performance, 39 Structural Mechanics,* and *16 Space Transportation.*

N91-31199 Routes, Inc., Kanata (Ontario).
STUDY OF SPACE QUALIFICATION SPECIFICATIONS Final Report
William Payne, Ronald Buckingham, Frederick Daniels, and Peter E. Townsend 17 Apr. 1990 347 p
(Contract NDH-3600-1-9-3594-01-SV)
(CTN-91-60201) Avail: NTIS HC A15

Spacecraft design, manufacture, environmental testing, launch and mission operations all require precise specifications. Space-based projects involving hardware or software procurement require both standard specifications and project specific specifications. This document contains a compilation of reference material and information sources on space environmental qualification which may be used to establish environmental specifications for Canadian Forces space-based hardware procurement. Sources evaluated fall into three main classes: standard military documents, documents available from government agencies and institutions, and commercially produced documents. They include: peer review technical journals, hard copy abstract services, trade magazines, standard reference works, and newsletters. A list of 244 publications related to military satellite procurement and space system engineering is provided. In addition aerospace related collections in libraries in the Ottawa area are described and evaluated. Canadian, American and European sources from which relevant technical documents may be purchased are described. Online search services and document ordering services are evaluated and online databases of special relevance are listed. CISTI

N91-31200*# Contel Federal Systems, Inc., Chantilly, VA.
TRAFFIC MODEL FOR ADVANCED SATELLITE DESIGNS AND EXPERIMENTS FOR ISDN SERVICES Final Report, 13 Sep. 1990 - 30 Sep. 1991
Gerard R. Pepin and E. Paul Hager Washington NASA 30 Sep. 1991 32 p
(Contract NASw-4520)
(NASA-CR-188802; NAS 1.26:188802) Avail: NTIS HC/MF A03 CSCL 22B

The data base structure and fields for categorizing and storing Integrated Services Digital Network (ISDN) user characteristics is outlined. This traffic model data base will be used to exercise models of the ISDN Advanced Communication Satellite to determine design parameters and performance for the NASA Satellite Communications Applications Research (SCAR) Program. Author

N91-31201*# National Aeronautics and Space Administration. Langley Research Center, Hampton, VA.
RESTRUCTURED FREEDOM CONFIGURATION CHARACTERISTICS
Patrick A. Troutman, Michael L. Heck, Renjith R. Kumar, and Daniel D. Mazanek (Analytical Mechanics Associates, Inc., Hampton, VA.) Jun. 1991 66 p
(NASA-TM-104057; NAS 1.15:104057) Avail: NTIS HC/MF A04 CSCL 22B

In Jan. 1991, the LaRc SSFO performed an assessment of the configuration characteristics of the proposed pre-integrated Space Station Freedom (SSF) concept. Of particular concern was the relationship of solar array operation and orientation with respect to spacecraft controllability. For the man-tended configuration (MTC), it was determined that torque equilibrium attitude (TEA) seeking Control Moment Gyroscope (CMG) control laws could not always maintain attitude. The control problems occurred when the solar arrays were tracking the sun to produce full power while flying in an arrow or gravity gradient flight mode. The large solar array articulations that sometimes result from having the functions of the alpha and beta joints reversed on MTC induced large product of inertia changes that can invalidate the control system gains during an orbit. Several modified sun tracking techniques were evaluated with respect to producing a controllable configuration requiring no modifications to the CMG control algorithms. Another assessment involved the permanently manned configuration (PMC) which has a third asymmetric PV unit on one side of the transverse boom. Recommendations include constraining alpha rotations for MTC in the arrow and gravity gradient flight modes and perhaps developing new non-TEA seeking control laws. Recommendations for PMC include raising the operational altitude and moving to a symmetric configuration as soon as possible. Author

N91-31202# Centre National d'Etudes Spatiales, Toulouse (France).
CHOICE OF A DIFFERENTIAL METHOD FOR ATTITUDE RESTITUTION WITH DYNAMIC IMBALANCE [CHOIX D'UNE METHODE DIFFERENTIELLE POUR LA RESTITUTION D'ATTITUDE AVEC BALOURD DYNAMIQUE]
E. Cazala-Hourcade Jun. 1990 47 p In FRENCH; ENGLISH summary Revised
(CNES-NT-126; CNES-CT/DTI/MS/CM/290; ETN-91-99533)
Copyright Avail: NTIS HC/MF A03

Van Der Ha's formalism is used to develop a method of differential correction using pseudo measurement to take the imbalance of a spin stabilized biliquid satellite into account. The imbalance of spin stabilized biliquid satellites such as Inmarsat 2 and Telecom 2 must be taken into account for attitude determination. In Van Der Ha's formalism, the imbalance is a source

of error and he evaluates the sensitivity of pseudo measurements with respect to the imbalance in order to assess the final error induced on attitude determination. ESA

N91-31203# Technische Univ., Munich (Germany, F.R.). Lehrstuhl fuer Raumfahrttechnik.
CONTRIBUTIONS TO A SPACE STATION FOR FLIGHTS IN THE NEAR FIELD AND TOWARDS GEOSTATIONARY EARTH ORBIT Ph.D. Thesis [BEITRAEGE ZUR RAUMSTATION ALS BAHNHOF FUER FLUEGE IN DEN NACHBEREICH UND NACH GEO]
Michael Kirschner 1990 130 p In GERMAN
(ETN-91-99744) Avail: NTIS HC/MF A07

Missions and their boundary conditions were described. The Orbital Transfer Vehicle (OTV) carries out all orbital maneuvers with its rocket motors. Missions were executed, using a one stage and a two stage OTV. A mathematical coupling of disturbances by Earth gravitation and atmosphere was carried out. Parametric mission examinations are described for Low Earth Orbit (LO)/Geostationary Earth Orbit (GEO), OTV, Aeroassisted Orbital Transfer Vehicle (AOTV). Comparisons and discussions are reported on LEO/GEO and LEO/LEO missions. ESA

N91-31204*# Science Applications International Corp., Huntsville, AL.
OPTIMIZATION TECHNIQUES APPLIED TO PASSIVE MEASURES FOR IN-ORBIT SPACECRAFT SURVIVABILITY Interim Report, period ending 30 Jun. 1991
Robert A. Mog and D. Marvin Price Jun. 1991 192 p
(Contract NAS8-37378)
(NASA-CR-184198; NAS 1.26:184198) Avail: NTIS HC/MF A09 CSCL 22B

Spacecraft designers have always been concerned about the effects of meteoroid impacts on mission safety. The engineering solution to this problem has generally been to erect a bumper or shield placed outboard from the spacecraft wall to disrupt/deflect the incoming projectiles. Spacecraft designers have a number of tools at their disposal to aid in the design process. These include hypervelocity impact testing, analytic impact predictors, and hydrodynamic codes. Analytic impact predictors generally provide the best quick-look estimate of design tradeoffs. The most complete way to determine the characteristics of an analytic impact predictor is through optimization of the protective structures design problem formulated with the predictor of interest. Space Station Freedom protective structures design insight is provided through the coupling of design/material requirements, hypervelocity impact phenomenology, meteoroid and space debris environment sensitivities, optimization techniques and operations research strategies, and mission scenarios. Major results are presented.
Author

N91-31205# Air Force Inst. of Tech., Wright-Patterson AFB, OH.
APPLICATION OF SEMIANALYTIC SATELLITE THEORY TO MANEUVER PLANNING M.S. Thesis
Carole A. Jablonski May 1991 152 p
(AD-A239417; AFIT/CI/CIA-91-049; CSDL-T-1086) Avail: NTIS HC/MF A08 CSCL 22/3

The high precision mean element (semianalytic) satellite theory developed at Draper Laboratory is more efficient than conventional numerical methods and more accurate than the current generation of analytic theories. This efficiency, along with its portability to a variety of computing environments makes the semianalytic theory a natural choice for maneuver planning applications. These applications will become more important in the future as the capability of individual platforms to maneuver, the number of platforms in space, and the requirements for rapid response to requests for data all increase. The application of semianalytic satellite theory to an Earth Observation satellite in an orbit similar to that expected for LANDSAT 6 is investigated. Orbit constraints such as sun synchronous, repeat ground track, frozen orbit, and non-impulsive maneuver capabilities are included in this analysis. Applications of maneuver planning to past and future satellite missions that include at least two of the listed orbit constraints are discussed. Since atmospheric drag is the primary uncertain disturbing acceleration to the nominal satellite orbit, upper and lower limits of a density confidence interval were determined. Two methods were analyzed; it was found that using forecast and actual solar flux and geomagnetic activity data from the years 1986 to 1990 resulted in a conservative but realistic confidence interval. The upper limit is utilized to compute the time of the orbit adjust burn. GRA

19 SPACECRAFT INSTRUMENTATION

For related information see also *06 Aircraft Instrumentation* and *35 Instrumentation and Photography.*

No abstracts in this category.

20 SPACECRAFT PROPULSION AND POWER

Includes main propulsion systems and components, e.g., rocket engines; and spacecraft auxilliary power sources.

For related information see also *07 Aircraft Propulsion and Power, 28 Propellants and Fuels, 44 Energy Production and Conversion,* and *15 Launch Vehicles and Space Vehicles.*

N91-31206 Department of National Defence, Ottawa (Ontario).
ASBESTOS-FREE INSULANT FOR ROCKET MOTORS Patent
Guy J. E. Couture, inventor, Denis J. Sanschagrin, inventor, and Pierre J. Carignan, inventor 28 Nov. 1989 18 p
(Patent-1-263-227; Int-Patent-Class-F16L-5900; CTN-91-60153) Copyright Avail: Micromedia Ltd., Technical Information Centre, 165 Hotel de Ville, Place du Portage, Phase 2, Hull, Quebec J8X 3X2, Canada HC $4.00 CAN, MF $2.75 CAN

An asbestos free, thermal insulant material for high temperature applications is described. In particular, it is intended as an insulant to rocket motors which have a metal casing and employ a solid propellant. The insulant is comprised of a carboxyl terminated polybutadiene based binder, a thermally stable reinforcing organic fiber material comprising a mixture of an aromatic polyamide fiber material, a heat stabilized poly acrylonitrile fiber material, such as Kevlar 29, and a powdered siliceous filler, preferably kaolin. The thermal insulant is self-adhesive to the metal casing of the rocket. The total solids loading of the composition varies from 55 to 75 percent weight comprised of 25 to 65 percent powdered siliceous material and 35 to 75 percent fibers. CISTI

N91-31207 Department of National Defence, Ottawa (Ontario).
ROCKET BOOSTED TARGET Patent
Henry P. Hudema, inventor, Stanley K. Burton, inventor, Alexander B. Markov, inventor, and Clayton G. Coffey, inventor 16 May 1989 16 p
(Patent-1-254-289; Int-Patent-Class-F02K-995; Int-Patent-Class-F02K-930; Int-Patent-Class-F42B-1512; CTN-91-60174) Copyright Avail: Micromedia Ltd., Technical Information Centre, 165 Hotel de Ville, Place du Portage, Phase 2, Hull, Quebec J8X 3X2, Canada HC $4.00 CAN, MF $2.75 CAN

The use of self propelled aerial targets, including expendable rocket boosted targets, is an aspect of weapons training. The present invention concerns an improved expendable target and components of an improved target system. Specifically, a plurality of rocket motors are mounted on a rocket, and a motor ignition means is carried on the body for firing the rocket motors in selected groups at selected time intervals. The sequential firing of the rocket motors provides a quasi maneuverable target with a long flight time and range. The present invention concerns a rocket firing

system to be carried on the rocket propelled vehicle for controlling the firing of groups of rocket motors. The sequential firing of the rocket boosted targets is controlled by a timing system which can be preprogrammed. This timing system can be activated by a means external to the vehicle. CISTI

N91-31208*# National Aeronautics and Space Administration. Lewis Research Center, Cleveland, OH.
NONLINEAR COMBUSTION INSTABILITY MODEL IN TWO- TO THREE-DIMENSIONS
Richard J. Priem (Priem Consultants, Inc., Cleveland, OH.) and Kevin J. Breisacher 1989 11 p Presented at the 26th JANNAF Combustion Meeting, Pasadena, CA, 23-27 Oct. 1989
(NASA-TM-102381; E-5097; NAS 1.15:102381) Avail: NTIS HC/MF A03 CSCL 21H

A model is developed on using quasi-steady state equations for the injection, atomization, and vaporization processes that consider the instantaneous local pressures, temperatures, density, and gas velocity vector associated with a 3-D wave. The coupled sets of equations are solved to determine frequency and growth rate of the oscillations as a function of wave amplitude. Calculated results are used to explain the observed instabilities in a 40 Klb LOX/Methane combustor. Author

N91-31209*# Sverdrup Technology, Inc., Brook Park, OH.
SPACE ENGINE SAFETY SYSTEM Final Report
William A. Maul and Claudia M. Meyer Cleveland, OH NASA Sep. 1991 11 p Presented at the Conference on Advanced Space Exploration Initiative Technologies, Cleveland, OH, 4-6 Sep. 1991; sponsored by AIAA, NASA, and OAI
(Contract NAS3-25266)
(NASA-CR-187219; E-6565; NAS 1.26:187219; AIAA-91-3604)
Avail: NTIS HC/MF A03 CSCL 21H

A rocket engine safety system was designed to initiate control procedures to minimize damage to the engine or vehicle or test stand in the event of an engine failure. The features and the implementation issues associated with rocket engine safety systems are discussed, as well as the specific concerns of safety systems applied to a space-based engine and long duration space missions. Examples of safety system features and architectures are given, based on recent safety monitoring investigations conducted for the Space Shuttle Main Engine and for future liquid rocket engines. Also, the general design and implementation process for rocket engine safety systems is presented. Author

N91-31210# Los Alamos National Lab., NM.
AN INVESTIGATION OF DUAL-MODE OPERATION OF A NUCLEAR-THERMAL ROCKET ENGINE
W. L. Kirk, J. C. Hedstrom, S. W. Moore, R. D. McFarland, M. A. Merrigan, J. J. Buksa, M. W. Cappiello, D. L. Hanson, and K. A. Woloshun Jun. 1991 38 p
(Contract W-7405-eng-36)
(DE91-015977; LA-12102) Avail: NTIS HC/MF A03

A preliminary assessment of the technical feasibility and mass competitiveness of a dual-mode nuclear propulsion and power system based on Rover-type reactors has been completed. Earlier studies have indicated that dual-mode systems appear attractive for electrical power levels of a few kilowatts. However, at the megawatt electrical power level considered in this study, it appears that extensive modifications to the nuclear-thermal engines would be required, the feasibility of which is unclear. Mass competitiveness at high electrical power levels is also uncertain. Further study of reactor and shield design in conjunction with mission and vehicle studies is necessary in order to determine a useful dual-mode power range. DOE

N91-31211# Los Alamos National Lab., NM.
A REVIEW OF THE LOS ALAMOS EFFORT IN THE DEVELOPMENT OF NUCLEAR ROCKET PROPULSION
F. P. Durham, W. L. Kirk, and R. J. Bohl 1991 9 p Presented at the AIAA/NASA/OAI Conference on Advanced SEI Technologies, Cleveland, OH, 3-4 Sep. 1991
(Contract W-7405-eng-36)
(DE91-016036; LA-UR-91-2295; CONF-9109226-1) Avail: NTIS HC/MF A02

This paper reviews the achievements of the Los Alamos nuclear rocket propulsion program and describes some specific reactor design and testing problems encountered during the development program along with the progress made in solving these problems. The relevance of these problems to a renewed nuclear thermal rocket development program for the Space Exploration Initiative (SEI) is discussed. DOE

N91-31212*# National Aeronautics and Space Administration. Lewis Research Center, Cleveland, OH.
MASS COMPARISONS OF ELECTRIC PROPULSION SYSTEMS FOR NSSK OF GEOSYNCHRONOUS SPACECRAFT
Vincent K. Rawlin and Gregory A. Majcher (Cleveland State Univ., OH.) 1991 48 p Presented at the 27th Joint Propulsion Conference, Sacramento, Ca, 24-27 Jun. 1991; sponsored by AIAA, SAE, ASME, and ASEE Previously Announced in IAA as A91-45808
(NASA-TM-105153; E-6438; NAS 1.15:105153; AIAA-91-2347)
Avail: NTIS HC/MF A03 CSCL 21H

A model was developed and exercised to allow wet mass comparisons of three axis stabilized communication satellites delivered to geosynchronous transfer orbit. The mass benefits of using advanced chemical propulsion for apogee injection and north-south stationkeeping (NSSK) functions or electric propulsion (hydrazine arcjets and xenon ion thrusters) for NSSK functions are documented. A large derated ion thrusters is proposed which minimizes thruster lifetime concerns and qualification test times when compared to those of smaller ion thrusters planned for NSSK applications. The mass benefits, which depend on the spacecraft mass and mission duration, increase dramatically with arcjet specific impulse in the 500 to 600 s range, but are nearly constant for the derated ion thruster operated in the 2300 to 3000 s range. For a given mission, the mass benefits with an ion system are typically double those of the arcjet system; however, the total thrusting time with arcjets is less than 1/3 that with ion thrusters for the same thruster power. The mass benefits may permit increases in revenue producing payload or reduce launch costs by allowing a move to a smaller launch vehicle. Author

N91-31213*# Rockwell International Corp., Canoga Park, CA. Rocketdyne Div.
HYDROGEN TEST OF A SMALL, LOW SPECIFIC SPEED CENTRIFUGAL PUMP STAGE Final Report
May 1991 46 p
(Contract NAS3-23164)
(NASA-CR-187117; NAS 1.26:187117; RI/RD-87-164) Avail: NTIS HC/MF A03 CSCL 21H

A small, low specific speed centrifugal pump stage with a 2 inch tip diameter, .030 inch tip width shrouded impeller and volute collector was tested with liquid hydrogen as the pumped fluid. The hydrodynamic design of the pump stage is summarized and the noncavitating and cavitating performance results are presented. Test speeds were 60 and 80 percent of the 77,000 rpm design speed. Liquid hydrogen test results are compared with data from previous tests of the stage in water. Author

N91-31214*# Rockwell International Corp., Canoga Park, CA. Rocketdyne Div.
FLOW INDUCED VIBRATIONS IN THE SSME INJECTOR HEADS Final Interim Report
Frank A. Lepore Jun. 1991 91 p
(Contract NAS8-36195)
(NASA-CR-184209; NAS 1.26:184209; RI/RD-91-157) Avail: NTIS HC/MF A05 CSCL 21H

A description is given of the flowfield in the Space Shuttle Main Engine (SSME) powerhead, the mechanisms which control flow-induced vibrations, and previous experimental work. An in-depth description is given of the development phase of the program , which includes the analysis, design, and fabrication of liquid oxygen (LOX) posts models used in the experimental phase,

as well as test facilities, equipment, and procedures used. Also covered is the experimental data analysis, which includes overall steady state powerhead flowfield as well as the high frequency response of the LOX posts. Author

N91-31215*# Spectra Research Systems, Inc., Huntsville, AL. Systems Technology Div.

EVALUATION OF UNDEVELOPED ROCKET ENGINE CYCLE APPLICATIONS TO ADVANCED TRANSPORTATION Final Report

29 Mar. 1990 94 p

(Contract NAS8-36643)

(NASA-CR-184205; NAS 1.26:184205; SRS/STD-TR89-90)

Avail: NTIS HC/MF A05 CSCL 21H

Undeveloped pump-fed, liquid propellant rocket engine cycles were assessed and evaluated for application to Next Manned Transportation System (NMTS) vehicles, which would include the evolving Space Transportation System (STS Evolution), the Personnel Launch System (PLS), and the Advanced Manned Launch System (AMLS). Undeveloped engine cycles selected for further analysis had potential for increased reliability, more maintainability, reduced cost, and improved (or possibly level) performance when compared to the existing SSME and proposed STME engines. The split expander (SX) cycle, the full flow staged combustion (FFSC) cycle, and a hybrid version of the FFSC, which has a LOX expander drive for the LOX pump, were selected for definition and analysis. Technology requirements and issues were identified and analyses of vehicle systems weight deltas using the SX and FFSC cycles in AMLS vehicles were performed. A strawman schedule and cost estimate for FFSC subsystem technology developments and integrated engine system demonstration was also provided. Author

N91-31216*# National Aeronautics and Space Administration. Lewis Research Center, Cleveland, OH.

MEDIUM POWER HYDROGEN ARCJET PERFORMANCE

Francis M. Curran, S. Ray Bullock, Thomas W. Haag, Charles J. Sarmiento, and John M. Sankovic 1991 22 p Presented at the 27th Joint Propulsion Converence, Sacramento, CA, 24-27 Jun. 1991; sponsored by AIAA, SAE, ASME, and ASEE

(NASA-TM-104533; E-6409; NAS 1.15:104533; AIAA-91-2227)

Avail: NTIS HC/MF A03 CSCL 21H

An experimental investigation was performed to evaluate hydrogen arcjet operating characteristics in the range of 1 to 4 kW. A series of nozzles were operated in modular laboratory thrusters to examine the effects of geometric parameters such as constrictor diameter and nozzle divergence angle. Each nozzle was tested over a range of current and mass flow rates to explore stability and performance. In the range of mass flow rates and power levels tested, specific impulse values between 650 and 1250 sec were obtained at efficiencies between 30 and 40 percent. The performance of the two larger half angle (20, 15 deg) nozzles was similar for each of the two constrictor diameters tested. The nozzles with the smallest half angle (10 deg) were difiicult to operate. A restrike mode of operation was identified and described. Damage in the form of melting was observed in the constrictor region of all the nozzle inserts tested. Arcjet ignition was also difficult in many tests and a glow discharge mode that prevents starting was identified. Author

N91-31217*# National Aeronautics and Space Administration. Lewis Research Center, Cleveland, OH.

ADVANCED POWER SYSTEMS FOR EOS

Sheila G. Bailey, Irving Weinberg, and Dennis J. Flood 1991 8 p Presented at the 26th Intersociety Energy Conversion Engineering Conference, Boston, MA, 4-9 Aug. 1991; cosponsored by ANS, SAE, ACS, AIAA, ASME, IEEE, and AIChE

(NASA-TM-105222; E-6536; NAS 1.15:105222) Avail: NTIS HC/MF A02 CSCL 21H

The Earth Observing System, which is part of the International Mission to Planet Earth, is NASA's main contribution to the Global Change Research Program. Five large platforms are to be launched into polar orbit: two by NASA, two by the European Space Agency, and one by the Japanese. In such an orbit the radiation resistance of indium phosphide solar cells combined with the potential of utilizing 5 micron cell structures yields an increase of 10 percent in the payload capability. If further combined with the Advanced Photovoltaic Solar Array, the total additional payload capability approaches 12 percent. Author

N91-31218*# National Aeronautics and Space Administration. Lewis Research Center, Cleveland, OH.

THIN FILM, CONCENTRATOR AND MULTIJUNCTION SPACE SOLAR CELLS: STATUS AND POTENTIAL

Dennis J. Flood 1991 12 p Presented at the European Space Power Conference, Florence, Italy, 3-6 Sep. 1991; sponsored by ESA, the Italian Space Agency, and the European Power Electronics

(NASA-TM-104505; E-6366; NAS 1.15:104505) Avail: NTIS HC/MF A03 CSCL 21H

Recent, rapid advances in a variety of solar cell technologies offer the potential for significantly enhancing, or enabling entirely new, mission capabilities. Thin film solar cells are of particular interest in that regard. A review is provided of the status of those thin film cell technologies of interest for space applications, and the issues to be resolved before mission planners can consider them. A short summary is also given of recent developments in concentrator and multijunction space solar cell and array technology. Author

N91-31219*# Rockwell International Corp., Canoga Park, CA. Rocketdyne Div.

REUSABLE ROCKET ENGINE INTELLIGENT CONTROL SYSTEM FRAMEWORK DESIGN, PHASE 2 Final Report

Ed Nemeth, Ron Anderson, Joe Ols, and Mark Olsasky Sep. 1991 191 p

(Contract NAS3-25557)

(NASA-CR-187213; NAS 1.26:187213; RI/RD-91-158-Phase-2)

Avail: NTIS HC/MF A09 CSCL 21H

Elements of an advanced functional framework for reusable rocket engine propulsion system control are presented for the Space Shuttle Main Engine (SSME) demonstration case. Functional elements of the baseline functional framework are defined in detail. The SSME failure modes are evaluated and specific failure modes identified for inclusion in the advanced functional framework diagnostic system. Active control of the SSME start transient is investigated, leading to the identification of a promising approach to mitigating start transient excursions. Key elements of the functional framework are simulated and demonstration cases are provided. Finally, the advanced function framework for control of reusable rocket engines is presented. Author

N91-31220*# National Aeronautics and Space Administration. Lewis Research Center, Cleveland, OH.

ECCENTRICITY EFFECTS ON LEAKAGE OF A BRUSH SEAL AT LOW SPEEDS

Julie A. Schlumberger, Margaret P. Proctor, and Robert C. Hendricks 1991 9 p Proposed for presentation at the 1991 Winter Annual Meeting of the ASME, Atlanta, GA, 1-6 Dec. 1991

(NASA-TM-105141; E-6414; NAS 1.15:105141) Avail: NTIS HC/MF A02 CSCL 13K

The effects of eccentricity on brush seal leakage at low rotational speeds were investigated. Included are the leakage results for ambient temperature air and nearly saturated streams at three different rotor eccentricities at both 0 and 400 rpm. A brush seal with a nominal bore diameter of 13.647 cm. (5.3730 in.) was used. It had a radial concentric interference of 0.071 cm (0.0028 in.) and a fence height of 0.0927 cm (0.0365 in.). There were 1060 bristles per centimeter of circumference (2690 bristles per inch of circumference). Rotor eccentricities of 0.003, 0.010, 0.038, and 0.043 cm (0.001, 0.004, 0.015, and 0.017 in.) were achieved by using bushings with different offsets. The results were compared with an annular seal model (FLOWCAL) for air and to a standard labyrinth seal model for steam. The annular seal model was also compared with a bulk flow model of a concentric brush seal in air. Large eccentricities did not damage the brush seals or

their Haynes 25 bristles. However, the 304 stainless steel rotor did not show wear, indicating a harder surface is needed. Only the stream data showed hysteresis and were affected by shaft rotation. The brush seal had lower leakage rates than those predicted for comparable annular and labyrinth seals (conventional) because of the large clearances those seals require to accommodate large shaft excursions. Author

N91-31221# Sandia National Labs., Albuquerque, NM.
NUCLEAR THERMAL ROCKETS: A SYSTEMS STUDY
L. W. Connell 1991 9 p Presented at the AIAA/NASA/OAI Conference on Advanced SEI Technologies, Cleveland, OH, 3-4 Sep. 1991
(Contract DE-AC04-76DP-00789)
(DE91-017066; SAND-91-1659C; CONF-9109226-7) Avail: NTIS HC/MF A02

One of the principal findings of the Synthesis Group was the importance of nuclear thermal rocket propulsion for the successful manned exploration of Mars. Solid core Nuclear rocket concepts are examined. The NTR with the highest level of technology readiness is the NERVA Derivative Reactor (NDR). Advanced NTRs based on the Particle Bed Reactor (PBR) offer the potential for improving the key NTR performance parameters of thrust-to-weight ratio and specific impulse over those of the NDR. The sensitivity of spacecraft mass to improvements in these parameters will be computed. A direct comparison of the NDR and PBR concepts is also performed. DOE

23 CHEMISTRY AND MATERIALS (GENERAL)

N91-31222# Department of Energy, Washington, DC. Chemical Sciences Div.
SUMMARIES OF FY 1991 RESEARCH IN THE CHEMICAL SCIENCES
Aug. 1991 137 p Prepared in cooperation with DOE, Oak Ridge, TN
(DE91-011221; DOE/ER-0144/9) Avail: NTIS HC/MF A07

These summaries provide the scientific and technical public, as well as the legislative and executive branches of the Government, information, either generally or in some depth, about the Chemical Sciences program. Areas of research supported are indicated in the section headings, the 'Selected Topics of General Interest' list, and the summaries themselves. Energy technologies that may be advanced by use of the basic knowledge generated in this program are included in the 'Selected Topics of General Interest' list. DOE

N91-31223# Edgerton, Germeshausen and Grier, Inc., Idaho Falls, ID.
PRODUCTION OF ORGANIC CHEMICALS VIA BIOCONVERSION: A REVIEW OF THE POTENTIAL
S. A. Leeper, T. E. Ward, and G. F. Andrews Jul. 1991 80 p
(Contract DE-AC07-76ID-01570)
(DE91-015524; EGG-2645) Avail: NTIS HC/MF A05

The U.S. should develop alternative feedstocks for production of organic chemicals as a step in reducing dependence on foreign oil and to protect the US economy from oil supply disruptions. Potential alternative feedstocks include lignocelliulose, poly-saccharides, and sugars. These feedstocks include lignocellulose, to organic chemicals via bioconversion; sources include feedstock crops (lignocellulosic, polysac-charide, and sugar crops grown specifically for use as feedstocks in organic chemicals production) and industrial, municipal, and agricultural wastes. A wide range of chemicals can be produced via bioconversion, including existing commodity chemicals and entirely new chemicals and polymers. In this review, potential feedstocks are described and are shown to be sufficient to support a bioconversion-based organic chemicals industry. In addition, the current U.S. organic chemicals industry is briefly described. The potential of bioconversion for production of existing commodity chemicals and entirely new chemicals and polymers is discussed. DOE

24 COMPOSITE MATERIALS

Includes physical, chemical, and mechanical properties of laminates and other composite materials.
For ceramic materials see *27 Nonmetallic Materials.*

N91-31224 United Technologies Corp., East Hartford, CT.
METHOD FOR STABILIZING THICK HONEYCOMB CORE COMPOSITE ARTICLES Patent
Gary J. Jacaruso, inventor 2 May 1989 13 p
(Patent-1-253-424; Int-Patent-Class-B32B-312; CTN-91-60139)
Copyright Avail: Micromedia Ltd., Technical Information Centre, 165 Hotel de Ville, Place du Portage, Phase 2, Hull, Quebec J8X 3X2, Canada HC $4.00 CAN, MF $2.75 CAN

The use of honeycomb core structures to act as lightweight structural members in fiber reinforced composite articles is well known. These honeycomb structures are laid up with the resin matrix in the uncured stage. The composite is subsequently heated under vacuum and pressure during which process the honeycomb structure frequently deforms or collapses. A method is disclosed for stabilizing honeycomb core structures such that upon final curing of the composite layup, no substantial lemon seeding occurs. The method comprises bonding a layer of resin impregnated, continuous woven graphite fibers to at least one of the open cell surfaces of the honeycomb core; curing the resin to form the stabilized honeycomb cure; cutting the stabilized core to net shape and then forming the desired article by applying the desired layers of additional composite material onto the core; and curing to form the final composite article. The graphite fibers should be woven such that the longest length is oriented in the direction of greatest compressive force. CISTI

N91-31225 Texas A&M Univ., College Station.
AN ANALYTICAL PREDICTION OF MATRIX CRACKING IN FIBROUS COMPOSITE LAMINATES Ph.D. Thesis
Jong-Won Lee 1990 127 p
Avail: Univ. Microfilms Order No. DA9118263

An analytical procedure based on the principal of minimum potential energy is developed for predicting the effect of matrix cracking on the monotonic and cyclic res onses of fibrous composite laminates. The following items, which the composite material society has focused considerable research efforts on, are modeled: (1) the degraded stiffness tensor for an off-axis angle-ply in a laminate subjected to in-plane monotonic loadings and constant temperature change as an explicit function of the average matrix crack density and the undamaged ply properties; (2) the monotonic matrix cracking evolution criterion to correlate the applied average axial stress, thermal residual stresses due to curing, and the average matrix crack density in cross-ply laminates; and (3) a hypothetical form of the cyclic matrix cracking evolution criterion for cross-ply laminates for predicting matrix cracking due to tension-tension fatigue loading. In addition to the above topics, a relationship between the strain-like internal state variable and the damage potential is provided. A number of experimental and theoretical studies are compared with the present research for demonstrating the practical applicability of the present study. as an engineering tool. Dissert. Abstr.

N91-31226 Texas A&M Univ., College Station.
AN INVESTIGATION INTO THE EFFECTS OF DAMAGE ON THE STRESSES IN A COMPOSITE LAMINATE Ph.D. Thesis
Eric Walter Nottorf 1990 165 p
Avail: Univ. Microfilms Order No. DA9118279

A general constitutive framework based on continuum damage mechanics with constraints imposed by thermodynamics for composite laminates is presented. Several methods for the calculation of matrix crack and delamination damage variables at a given damage state are presented and compared. A methodology

for the prediction of matrix crack and delamination damage variable evolution is developed and shown to have the ability to model experimental data for several cross ply laminates. The damage effects are incorporated into the model by tensor-valued internal state variables for both matrix cracking and delaminations, respectively. Adjacent damage dependent ply stresses are crucial in influencing the initiation and growth of delaminations in composite laminates. A new method for determining the damage dependent stresses in the adjacent piles is presented along with the calculated stress changes due to matrix cracking and interply delaminations. Along with this stress calculation method, a general framework is formulated for the determination of delamination growth using fracture mechanics along with several methods for determining the energy release rate of delaminations. Dissert. Abstr.

N91-31227 Delaware Univ., Newark.
PROCESSING AND CHARACTERIZATION OF CONTINUOUS FIBER-REINFORCED GLASS AND GLASS-CERAMIC MATRIX COMPOSITES Ph.D. Thesis
Shaio-Wen Wang 1990 203 p
Avail: Univ. Microfilms Order No. DA9120450

An investigation of the processing and mechanical behavior, particularly damage evolution and failure mechanisms, of continuous fiber reinforced glass and glass-ceramic composites was conducted. The processing effort utilized a slurry infiltration/hot pressing technique to fabricate carbon fiber reinforced borosilicate glass and Nicalon SiC fiber reinforced borosilicate glass composites. A slurry infiltration prepregging setup was designed and successfully operated. Processing parameters including slurry composition, binder burnout cycle and hot pressing schedule were systematically studied and optimized. Mechanical behavior studies were conducted on Nicalon SiC/Calcium Aluminosilicate (CAS) composites. The nature and the strength of the fiber/matrix interface was first characterized using a variety of fiber indentation test methods and transmission electron microscopy. Dissert. Abstr.

N91-31228 Delaware Univ., Newark.
THE INFLUENCE OF INTERPHASE REGIONS ON LOCAL THERMAL STRESSES AND DEFORMATIONS IN COMPOSITES Ph.D. Thesis
Nancy R. Sottos 1990 175 p
Avail: Univ. Microfilms Order No. DA9120463

Computational and theoretical modeling as well as experimental investigation are discussed of the influence of the interphase region on the local thermal stresses and deformations which may arise during processing of polymer matrix composites. A numerical approach is adopted to predict the sensitivity of the micro-thermal stresses to fiber spacing and local variations in material properties. Experimental studies centered on the development of a scanning micro-interferometer for in-situ measurements of thermal displacements in the interphase. Author

N91-31229 Virginia Polytechnic Inst. and State Univ., Blacksburg.
A METHOD FOR THE GEOMETRICALLY NONLINEAR ANALYSIS OF COMPRESSIVELY LOADED PRISMATIC COMPOSITE STRUCTURES Ph.D. Thesis
Frederick Stoll 1991 221 p
Avail: Univ. Microfilms Order No. DA9120404

A method was developed for the geometrically nonlinear analysis of the static response of thin-walled stiffened composite structures loaded in uniaxial or biaxial compression. The method was applicable to arbitrary prismatic configurations composed of linked plate strips, such as stiffened panels and thin-walled columns. The longitudinal ends of the structure are assumed to be simply supported, and geometric shape imperfections can be modeled. The method can predict the nonlinear phenomena of post buckling strength and imperfection sensitivity which are exhibited by some buckling-dominated structures. The method is computer based and semi-analytic in nature, making it computationally economical in comparison to finite element methods. Dissert. Abstr.

N91-31230# Sandia National Labs., Albuquerque, NM.
THE MECHANICAL RESPONSE OF WOVEN KEVLAR FABRIC
W. E. Warren 1991 3 p Presented at the 22nd Midwestern Mechanics Conference, Rolla, MO, 6-9 Oct. 1991
(Contract DE-AC04-76DP-00789)
(DE91-010581; SAND-91-0652C; CONF-911070-2) Avail: NTIS HC/MF A01

Woven Kevlar fabrics exhibit a number of beneficial mechanical properties which include strength, flexibility, and relatively low density. The desire to engineer or design Kevlar fabrics for specific applications has stimulated interest in the development of theoretical models which relate their effective mechanical properties to specific aspects of the fabric morphology and microstructure. In this work the author provides a theoretical investigation of the large deformation elastic response of a plane woven Kevlar fabric and compares these theoretical results with experimental data obtained from uniaxially loaded Kevlar fabrics. The theoretical analysis assumes the woven fabric to be a regular network of orthogonal interlaced yarns and the individual yarns are modeled as extensible elastica, thus coupling stretching and bending effects at the outset. This comparison of experiment with theory indicates that the deformation of woven fabric can be quite accurately predicted by modeling the individual yarns as extensible elastica. DOE

N91-31231# Aerospatiale, Suresnes (France). Centre Commun de Recherches Louis-Bleriot.
RELATION BETWEEN FIBER PROPORTION AND MECHANICAL CHARACTERISTICS OF CARBON-RESIN COMPOSITES Final Report [RELATION ENTRE TAUX DE FIBRES ET CARACTERISTIQUES MECANIQUES DES COMPOSITES CARBONE-RESINE]
D. Guedra and J. Levrier 10 Jul. 1989 182 p In FRENCH
(Contract STPA-87-96-008-00-471-75-81)
(RE-50-345/F; ETN-91-99911) Avail: NTIS HC/MF A09

Different fiber resin systems are studied in order to evaluate the influence of fiber proportion on the mechanical properties. An influence limited to a few percent in relation to the standard fiber proportion is established when examining theoretical thicknesses, and less than 10 when examining real thicknesses. Delaminating was investigated in two modes: (1) the force necessary to propagate a crack opening; and (2) the force necessary to propagate a delamination by interlaminary shearing. Only the tensile strength in mode 2 (G sub 2c) is affected. A perceptible fall of G sub 2c is observed with a raise of the proportion of fibers, whatever the material. ESA

N91-31232# Ecole Superieure de Physique et de Chimie Industrielles, Paris (France). Lab. de Physicochimie Structurale et Macromoleculaire.
COMPOSITE MATRIX DEFORMATION PROCESS IN RELATION TO MOLECULAR STRUCTURE Final Summary Report [PROCESSUS DE DEFORMATION DES MATRICES DE COMPOSITE EN RELATION AVEC LEUR STRUCTURE MOLECULAIRE]
Serge Cukierman, Rene-Paul Eustache, Jean-Louis Halary, Francoise Laupretre, and Lucien Monnerie 1990 120 p In FRENCH
(Contract DRET-87-140)
(ETN-91-99915) Avail: NTIS HC/MF A06

The viscoelastic behavior of resins is characterized and molecular motion is studied by NMR (Nuclear Magnetic Resonance) of high resolution C-13 in solids. The preparation of the diepoxides studied is described. The influence of chemical and structural properties on water intake and the evolution of associated mechanical properties is studied, in parallel with an analysis on the formation of shear bands. ESA

N91-31233# Lille Univ. (France). Lab. de Structures et Propriete de l'Etat Solide.
PLASTIC DEFORMATION PROCESSES IN RELATION TO MOLECULAR STRUCTURE Final Report [PROCESSUS DE DEFORMATION PLASTIQUE DE MATRICES DE COMPOSITES EN RELATION AVEC LEURS STRUCTURES MOLECULAIRES]
F. Fernagut, J. M. Lefebvre, and B. Escaig 1990 37 p In FRENCH
(Contract DRET-87-140)
(ETN-91-99916) Avail: NTIS HC/MF A03

Non-elastic deformation behavior of epoxy model networks is examined from the point of view of sheared microregion nucleation propagation. The molecular structure (chain flexibility, degree of reticulation, nature of the diamine, local mobility) is correlated with macroscopic mechanical characteristics measured by compression tests. The roles of these different structural characteristics on the evolution of mechanical response are identified. ESA

N91-31234# Office National d'Etudes et de Recherches Aerospatiales, Paris (France). Direction Scientifique de la Resistance des Structures.
COMPOSITE MATERIALS DAMAGE. TRANSVERSE CRACKING AND DELAMINATION [ENDOMMAGEMENT DES MATERIAUX. FISSURATION TRANSVERSE ET DELAMINAGE]
J. L. Chaboche Aug. 1989 59 p In FRENCH
(ONERA-RT-6/7256-RY-080-R; ETN-91-99932) Avail: NTIS HC/MF A04

Transverse cracking in laminates with weak orientations enclosed by stiffeners is addressed. Different methods of nondestructive tests (X-rays, ultrasound, optical microscopy) are used to show the cracking. Delamination is studied and different methods used to calculate dissipated energy levels are compared. ESA

N91-31235*# National Aeronautics and Space Administration. Lewis Research Center, Cleveland, OH.
EXPERIMENTAL AND ANALYTICAL ANALYSIS OF STRESS-STRAIN BEHAVIOR IN A (90/0 DEG)2S, SiC/Ti-15-3 LAMINATE
Bradley A. Lerch, Matthew E. Melis, and Mike Tong (Sverdrup Technology, Inc., Brook Park, OH.) Aug. 1991 11 p
(NASA-TM-104470; E-6319; NAS 1.15:104470) Avail: NTIS HC/MF A03 CSCL 11D

The nonlinear stress strain behavior of 90 degree/0 degree sub 2s, SiC/Ti-15-3 composite laminate was numerically investigated with a finite element, unit cell approach. Tensile stress-strain curves from room temperature experiments depicted three distinct regions of deformation, and these regions were predicted by finite element analysis. The first region of behavior, which was linear elastic, occurred at low applied stresses. As applied stresses increased, fiber/matrix debonding in the 90 degree plies caused a break in the stress-strain curve and initiated a second linear region. In this second region, matrix plasticity in the 90 degree plies developed. The third region, which was typified by nonlinear, stress-strain behavior occr red at high stresses. In this region, the onset of matrix plasticity in the 0 degree plies stiffened the laminate in the direction transverse to the applied load. Metallographic sections confirmed the existence of matrix plasticity in specific areas of the structure. Finite element analysis also predicted these locations of matrix slip. Author

N91-31236* National Aeronautics and Space Administration. Pasadena Office, CA.
COMPOSITE FLEXIBLE BLANKET INSULATION Patent
Demetrius A. Kourtides, inventor (to NASA), William C. Pitts, inventor (to NASA), Howard E. Goldstein, inventor (to NASA), and Paul M. Sawko, inventor (to NASA) (Jet Propulsion Lab., California Inst. of Tech., Pasadena.) 13 Aug. 1991 39 p Filed 21 Sep. 1989 Patent jointly owned by Eloret Corp., Palo Alto, CA
(NASA-Case-NPO-11907-1-NP; US-Patent-5,038,693; US-Patent-Appl-SN-410576; US-Patent-Class-112-440; US-Patent-Class-428-285; Int-Patent-Class-B32B-7/08) Avail: US Patent and Trademark Office CSCL 11D

Composite flexible multilayer insulation systems (MLI) were evaluated for thermal performance and compared with the currently used fibrous silica (baseline) insulation system. The systems described are multilayer insulations consisting of alternating layers of metal foil and scrim ceramic cloth or vacuum metallized polymeric films quilted together using ceramic thread. A silicon carbide thread for use in the quilting and the method of making it are also described. These systems are useful in providing lightweight insulation for a variety of uses, particularly on the surface of aerospace vehicles subject to very high temperatures during flight. Official Gazette of the U.S. Patent and Trademark Office

N91-31237# Sandia National Labs., Albuquerque, NM.
EFFECTS OF TRAPPED GASES ON CERAMIC-FILLED-GLASS COMPOSITE DENSIFICATION
K. G. Ewsuk 1991 11 p Presented at the International Symposium on the Science and Technology of Sintering, Vancouver, British Columbia, 24-27 Jul. 1991
(Contract DE-AC04-76DP-00789)
(DE91-015850; SAND-90-2054C; CONF-910755-1) Avail: NTIS HC/MF A03

The effects of trapped gases within closed pores on ceramic-filled-glass (CFG) composite densification during final-stage, non-reactive, liquid-phase sintering (NLPS) have been assessed on the basis of how pore gas pressure affects the driving force for sintering. Gas pressure within close pores counteracts the (ideal) surface tension driving force for pore shrinkage, and decreases the driving force for CFG composite densification. For a gas that cannot diffuse through the composite matrix, the pore gas pressure increases with increasing density, and ultimately counterbalances the surface tension driving force for pore shrinkage. As a result, the rate of densification decreases with increasing density, and densification ultimately ceases at an end point density less than 100 percent theoretical density (TD). The effect is appreciable for greater than 1 micron radius pores, and becomes more pronounced with increasing pore size. Trapped gases in less than 1 micron pores have a relatively insignificant effect on final-stage densification. DOE

N91-31238# Oak Ridge National Lab., TN.
INTERLAMINAR DEFORMATIONS ON THE CYLINDRICAL SURFACE OF A HOLE IN LAMINATED COMPOSITES BY MOIRE INTERFEROMETRY
Raymond G. Boeman 1991 8 p Presented at the 2nd International Conference on Photomechanics and Speckle Metrology, San Diego, CA, 21-26 Jul. 1991
(Contract DE-AC05-84OR-21400)
(DE91-015922; CONF-9107157-1) Avail: NTIS HC/MF A02

Moire interferometric techniques were adapted to facilitate studies on 25.4 mm (1 in.) diameter holes. A replication scheme was developed to produce a high-frequency diffraction grating on the cylindrical surface of a hole. Techniques were developed to interrogate the specimen grating to obtain the in-plane deformations on the hole surface. The application of the technique to the measurement of interlaminar deformations on the cylindrical surface of a hole in a laminated composite plate is presented. The techniques can be generalized for investigations on both convex and concave singly-curved surfaces. DOE

N91-31239# Utah Univ., Salt Lake City. Dept. of Materials Science and Engineering.
ALUMINA REINFORCED TETRAGONAL ZIRCONIA (TZP) COMPOSITES
D. K. Shetty 1991 9 p
(Contract DE-FG02-87ER-45312)
(DE91-016748; DOE/ER-45312/4) Avail: NTIS HC/MF A02

This progress report/continuation proposal summarizes the highlights of research results obtained in the past year in the DOE-supported research project entitled, Alumina Reinforced Tetragonal Zirconia (TZP) Composites, and proposes additional research to be conducted during the period July 1, 1991 through June 30, 1992. Several significant research results were obtained in the past year. (1) The role of MnO additive in grain growth

kinetics, phase stability and transformation toughening of Ce-TZP/Al2O3 composites was established. (2) It was shown that the monotonic and homogeneous transformation plasticity obtained in the Ce-TZP/Al2O3 composite led to crack-tip transformation zones more efficient in zone shielding than similar commercial grades. (3) A method for evaluating rising crack-growth-resistance behavior (R-Curve) of toughened ceramics based on stable crack growth measurements was demonstrated and shown to be superior to current techniques based on strength measurements. (4) A nonlinear shear-lag model developed for assessing fiber-matrix interfacial sliding friction was employed to analyze single filament pullout and pushout tests on model SiC-borosilicate glass composites. The two tests gave identical sliding friction coefficient and residual clamping stress only when the Poisson contraction/expansion of the filaments in the pullout and the pushout tests, respectively, were taken into account via the new shear-lag theory. DOE

N91-31240# Oak Ridge National Lab., TN.
EFFECTS OF OXIDATION AND COMBUSTION ENVIRONMENTS ON THE PROPERTIES OF NICALON/SiC COMPOSITES
R. A. Lowden and R. D. James (Clemson Univ., SC.) 1991 14 p Presented at the 5th Annual Conference on Fossil Energy Advanced Research and Technology Development (AR/TD) of Materials, Oak Ridge, TN, 13-16 May 1991
(Contract DE-AC05-84OR-21400)
(DE91-016778; CONF-9105184-12) Avail: NTIS HC/MF A03

The stability of Nicalon/SiC composites with a graphic carbon interface layer at elevated temperatures in oxidizing and simulated fossil fuel environments has been investigated. Composite specimens with and without an external SiC surface coating have been oxidized in air and have been exposed to a variety of combustion environments at a temperature of 1273 K. A burner rig furnace was constructed for simulating corrosive fossil fuel environments containing water vapor, sulfur, and sodium. Post-exposure room temperature flexure tests were performed to measure the strengths of the samples, and optical and electron microscopy have been employed to analyze corrosion, glass layer formation, and compositional changes at the surface of the specimens and at the fiber-matrix interface. Correlations between exposure environment, the interface, and mechanical properties of the composites were examined. DOE

N91-31241# Air Force Inst. of Tech., Wright-Patterson AFB, OH.
EFFECT OF PORCELAIN SURFACE PRETREATMENTS ON COMPOSITE RESIN-PORCELAIN SHEAR BOND STRENGTH M.S. Thesis
Harvey H. Breckner, III May 1991 186 p
(AD-A239359; AFIT/CI/CIA-91-062) Avail: NTIS HC/MF A09 CSCL 06/5

The bond between composite resin and dental porcelain is important in dentistry because without it porcelain restorations could not be bonded to tooth structure and it would be more difficult to repair defective porcelain restorations intraorally. The objectives of this research were to determine the effects that six dental porcelain surface pretreatments, two types of silanes, and thermocycling had on composite resin-porcelain shear bond strength. GRA

N91-31242# National Inst. of Standards and Technology, Gaithersburg, MD. Corrosion Group.
THE INFLUENCE OF MOISTURE AND PRESSURE ON THE MECHANICAL PROPERTIES OF A GLASS-EPOXY MATRIX COMPOSITE AND A GRAPHITE-EPOXY MATRIX COMPOSITE Technical Report No. 2, 1 Feb. 1989 - 1 Feb. 1991
M. R. Stoudt, E. Escalante, and R. E. Ricker Jul. 1991 30 p
(Contract N00014-89-F-0072)
(AD-A239509; NIST-855-05-91-34) Avail: NTIS HC/MF A03 CSCL 11/4

The influence of exposure to water at ambient pressure and at elevated pressure was evaluated on the mechanical properties of a glass fiber-epoxy matrix composite and a graphite fiber-epoxy matrix composite. The mechanical properties of three different fiber orientations for each material were measured in the dry condition, after exposure to water at ambient pressure and after exposure to water at 5.9 MPa. In order to determine if the observed degradation was permanent, the mechanical properties were also measured after the absorbed water was removed. During exposure, the rate and extent of water absorption and desorption was evaluated by measuring the weight change at periodic intervals. Substantial reductions in the yield strength and ultimate strength were observed in the wet condition for the glass epoxy samples at both pressures, while the strength of the graphite epoxy composite was found to be insensitive to the water exposure. The wet strength of the glass epoxy composite was found to be independent of water pressure during absorption and upon desorption, complete recovery of the dry strength was shown. Evidence of compression induced failure was observed for the graphite-epoxy composite in the wet condition. GRA

N91-31243# Naval Research Lab., Washington, DC.
MODELLING THE RESPONSE OF THICK COMPOSITE MATERIALS DUE TO AXISYMMETRIC SHOCK LOADING
J. A. Nemes and P. W. Randles 5 Aug. 1991 85 p
(AD-A239531; NRL-MR-6856) Avail: NTIS HC/MF A05 CSCL 11/4

Preliminary efforts for developing a methodology to predict the response of thick composite materials to axisymmetric shock loading are presented. Consideration is given to material layups that result in transversely isotropic behavior in the plane of the fibers. The response of thick graphite/epoxy composite plates subjected to underwater explosive loadings is solved numerically using a transient finite-element code. Both spherical and plane shock waves are considered. Results are compared to analytical results, where possible, along with computed results using steel as the plate material. A continuum damage model appropriate for thick composite materials subjected to high rate loading is developed to consider the response of the composite materials in the nonlinear range. The model considers two different damage parameters, one to represent delamination type cracks and the other to represent matrix cracking. The model is applied initially for different types of homogeneous deformation and then applied to the response of the composite plate subjected to the underwater explosive loading. GRA

N91-31244# Virginia Polytechnic Inst. and State Univ., Blacksburg.
THE FORMATION OF NOVEL THERMOPLASTIC COMPOSITES FROM LIQUID CRYSTALLINE POLYMERS AND THEIR BLENDS Final Report, 1 Jun. 1988 - 30 Jun. 1991
D. G. Baird, T. Sun, A. M. Sukhadia, A. Datta, and H. ODonnell Jul. 1991 27 p
(Contract DAAL03-88-K-0104)
(AD-A239546; ARO-25344.14-MS) Avail: NTIS HC/MF A03 CSCL 11/4

The miscibility of several liquid crystalline polymers (LCPs) blended with polyetherimide (PEI) was found to have a significant effect on the mechanical properties of the blend. Although the properties are higher than the matrix PEI, it has been found that immiscible blends of PEI with some LCPs show a negative deviation from the law of mixtures for flexural properties and tensile properties. In contrast, other LCPs which are partially miscible with PEI show a positive deviation from this law. The partial miscibility is probably responsible for the synergistic enhancement of some of the physical properties. Additionally, the LCP reinforcement was found to substantially lower the torsional creep compliance of the blend and blending with PEI increases the thermoformability of some of the LCPs. The reinforcing LCP fibrils and their molecular orientation were retained in the blends when thermoformed above the melting point of the LCPs. Secondly, a mixing process was developed which would generate continuous LCP fibrils in the matrix polymer during processing and allow blending of polymers such as LCPs with other matrices, which usually do not have overlapping processing temperatures, such

as polypropylene and poly(ethylene terepthalate). The blending process allows us to impart separate thermal histories to the matrix and the LCP to yield a favorable viscosity ratio. The tensile moduli of the blends made by this approach had significantly improved properties than physical blends. GRA

N91-31245# Army Lab. Command, Watertown, MA. Material Technology Lab.
RESPONSE OF AN ALUMINA FIBER REINFORCED ALUMINUM COMPOSITE TO COMBINED TENSION-TORSION Final Report
Nikos Tsangarakis, Gary P. Pelletier, and Marc S. Pepi Jul. 1991 20 p
(DA Proj. 1L1-62105-AH-42)
(AD-A239560; MTL-TR-91-27) Avail: NTIS HC/MF A03 CSCL 11/4

The introduction of fiber reinforced composites in structural design has generated the need to develop new test procedures for rating these materials. The assessment of the performance of such composites under combined tensile-torsional loading should increase their reliability. Specimens such as the cruciform, the thin wall cylinder, and the center cracked plate have been used extensively to investigate the response of isotropic materials to biaxial loading. These specimens, however, may not be appropriate for all types of fiber reinforced composites. It has been shown that, in certain composites, premature failure by fiber debonding can occur at points of stress concentration or where there is a change in the specimen's contours. Because of these trends, the cruciform and the center cracked plate could be poor candidates for combined tensile-torsional testing of fiber reinforced composites. On the other hand, the thin wall cylindrical specimen could be promising for certain applications (e.g. pressure vessels). Aluminum coupons reinforced unidirectionally with continuous alumina fibers were loaded in combined tension-torsion. Experimental results indicated that the superimposition of a 0.0025 shear strain reduced the tensile strain to failure by 67 pct. Similarly, the superimposition of a 0.0007 tensile strain reduced the shear strain to failure by 81 pct. GRA

25 INORGANIC AND PHYSICAL CHEMISTRY

Includes chemical analysis, e.g., chromatography; combustion theory; electrochemistry; and photochemistry.

For related information see also *77 Thermodynamics and Statistical Physics.*.

N91-31246# Wright Lab., Wright-Patterson AFB, OH.
AN EXPERT SYSTEM FOR THE IDENTIFICATION OF SILICON IMPURITIES USING FTIR SPECTROSCOPY Final Report, Jan. 1989 - Jun. 1990
Ronald E. Perrin and Steven B. Fairchild 30 Apr. 1991 121 p
(AD-A236504; WL-TR-91-4012) Avail: NTIS HC/MF A06 CSCL 20/5

A expert-system for the analysis of the infrared spectra of silicon based electronic materials was developed. The Fourier Transform Infrared Spectroscopy System produces characteristic spectral lines for impurities present in silicon materials under analysis. A MicroVax workstation with a commercially available expert-system shell is attached to the spectrometer. By examining these spectral line patterns the expert-system is able to deduce the identities and concentrations of the unknown impurities. The use of this program greatly reduces the analysis time required for each sample and produces more consistent results. GRA

N91-31247# Pacific Northwest Lab., Richland, WA.
CATALYSIS-BY-DESIGN IMPACTS ASSESSMENT
L. L. Fassbender, J. K. Young, and R. K. Sen (Sen, R. K. and Associates, Washington, DC) May 1991 99 p
(Contract DE-AC06-76RL-01830)
(DE91-013280; PNL-7694) Avail: NTIS HC/MF A05

Catalyst researchers have always recognized the need to develop a detailed understanding of the mechanisms of catalytic processes, and have hoped that it would lead to developing a theoretical predictive base to guide the search for new catalysts. This understanding allows one to develop a set of hierarchical models, from fundamental atomic-level ab-initio models to detailed engineering simulations of reactor systems, to direct the search for optimized, efficient catalyst systems. During the last two decades, the explosions of advanced surface analysis techniques have helped considerably to develop the building blocks for understanding various catalytic reactions. An effort to couple these theoretical and experimental advances to develop a set of hierarchical models to predict the nature of catalytic materials is a program entitled Catalysis-by-Design (CRD). In assessing the potential impacts of CBD on US industry, the key point to remember is that the value of the program lies in developing a novel methodology to search for new catalyst systems. Industrial researchers can then use this methodology to develop proprietary catalysts. Most companies involved in catalyst R&D have two types of ongoing projects. The first type, what we call market-driven R&D, are projects that support and improve upon a company's existing product lines. Project of the second type, technology-driven R&D, are longer term, involve the development of totally new catalysts, and are initiated through scientists' research ideas. The CBD approach will impact both types of projects. However, this analysis indicates that the near-term impacts will be on market-driven projects. The conclusions and recommendations presented in this report were obtained by the through personal interviews with individuals involved in a variety of industrial catalyst development programs and through the three CBD workshops held in the summer of 1989. DOE

N91-31248# Sandia National Labs., Albuquerque, NM.
HVOF: PARTICLE, FLAME DIAGNOSTICS, AND COATING CHARACTERISTICS
K. A. Kowalsky, D. R. Marantz (Flame-Spray Industries, Inc., Port Washington, NY.), M. F. Smith, and W. L. Oberkampf 1990 7 p Presented at the 3rd National Thermal Spray Conference and Exposition, Long Beach., 21-24 May 1990
(Contract DE-AC04-76DP-00789)
(DE91-014654; SAND-90-0844C; CONF-900520-6) Avail: NTIS HC/MF A02

Dual focus laser velocimetry (L2F), photographic techniques, and pressure measurements were used to investigate particle and flame characteristics of a high velocity oxygen/fuel (HVOF) flame spray gun known as CDS. Velocities of alumina, tungsten carbide, and Triballoy particles within the HVOF effluent stream have been measured using L2F techniques. Photographs of the exiting gases were used to determine the local Mach numbers within the gas stream. Measurements of Mach angles in the photographs were used to determine the actual gas velocity in the free jet of the device. Pressure measurements were made on the HVOF device which enabled calculations of the gas content, R, and the specific heat ratio. These calculations combined with estimates of gas temperature are used to calculate gas velocities at Mach 1 (nozzle exit). The HVOF device was used to produce dense WC/12 wt. percent Co and Triballoy T-400 coatings. For the two gas flow conditions examined, higher hardness values and densities were observed for coatings deposited at the higher gas flow rates. DOE

N91-31249# Laser Science, Inc., Ames, IA.
LASER DEPOSITION OF CUBIC BORON NITRIDE ON ELECTRONIC MATERIALS Progress Report, 15 Jun. - 14 Jul. 1991
Arul Molian, Madhav Rao, and P. Molian 12 Jul. 1991 7 p
(Contract N00014-91-C-0102)
(AD-A238313) Avail: NTIS HC/MF A02 CSCL 07/4

This interim report describes the work performed during the first month of research on the laser ablation methodology of cubic boron nitride deposition on electronic materials. Specifically, the report presents our initial efforts dealing with material procurement, experimental design and setup, preliminary experiments, results and some discussion. The work shows the potential of laser for the synthesis of cubic boron nitride. GRA

N91-31250# Argonne National Lab., IL.
THE CHEMISTRY OF TRANSITION METAL CLUSTERS
S. J. Riley 1991 36 p Presented at the NATO Advanced Study Institute Conference, Acquafredda di Maratea, Italy, 11-21 Jun. 1991
(Contract W-31-109-eng-38)
(DE91-015108; ANL/CP-73328; CONF-9106180-1) Avail: NTIS HC/MF A03

This paper reviews the basic aspects of metal cluster generation, the procedures for studying the gas phase chemical reactions of clusters, and the techniques of cluster detection. Examples of large cluster-size dependence of chemical reactivity are presented. Experiments in which clusters are saturated with adsorbate molecules are discussed, showing how such studies can often provide information about cluster structure. Thermodynamic measurements of cluster-adsorbate binding energies and entropies are presented. Processes in which adsorbed molecules decompose on cluster surfaces are considered. Measurements of cluster ionization potentials, by both chemical and physical means, are discussed. DOE

N91-31251# Allied-Signal Aerospace Co., Kansas City, MO.
DETERMINATION OF AQUEOUS PROCESSABLE PHOTORESIST IN TIN-LEAD PLATING SOLUTIONS
R. E. Smith Jul. 1991 29 p
(Contract DE-AC04-76DP-00613)
(DE91-015575; KCP-613-4371) Avail: NTIS HC/MF A03

A method based on reverse phase liquid chromatography has been developed for determining the solubility of Dynachem's HG aqueous processable photoresist in tin-lead plating baths. This photoresist is processed with aqueous products, alleviating the need for chlorinated solvents previously used with non-aqueous resists. It is separated from other plating solution components on a poly(styrene/divinylbenzene) column using a 90 percent acetonitrile eluent. An ultraviolet (UV) detector at 252 nm was used for quantitation. Five replicate analyses had a relative standard deviation of 4.63 percent. This method was used to measure photoresist drag-in the current production tin-lead plating bath, which contains peptone (Tank Number TL-25), and in three different tin-lead baths that are being evaluated as replacements. Spectroscopic analysis of Dynachem HG indicated that it contains a bis azide photoinitiator that cross-links with an acrylate polymer upon exposure to ultraviolet light. The final purpose of this method was to determine if the tin-lead chemistries were compatible with Dynachem HG aqueous photoresist. DOE

N91-31252# Lawrence Livermore National Lab., CA.
EXPERIMENTAL DETERMINATION OF THE TEMPERATURE AND DENSITY OF OPACITY SAMPLES
T. S. Perry, D. Bach, F. Serduke, R. E. Stewart, R. Wallace, R. Lee, J. Kilkenny, S. J. Davidson, J. Foster, and C. C. Smith (Ministry of Defence, Aylesbury, England) 1991 23 p Presented at the International LTE Opacity Workshop and Code Comparison Study, Paris, France, 3-7 Jun. 1991
(Contract W-7405-eng-48)
(DE91-015686; UCRL-JC-107736; CONF-9106249-1) Avail: NTIS HC/MF A03

Point projection spectroscopy has been successfully used to measure the opacities of several elements. To critically compare the experiments with opacity calculations it is necessary to know the sample conditions. Several techniques have been used in the past year to characterize the temperature and density of opacity samples. These techniques include DANTE measurements, streaked 22X x-ray microscope measurements, and ion balance measurements using point projection spectroscopy. Temperatures are now known to an accuracy of - or + 10 percent and densities to - or + 20 percent. In the future evenmore precise measurements will be made by measuring the opacity, temperature, and density simultaneously. DOE

N91-31253# State Univ. of New York, Buffalo. Dept. of Chemistry.
DETERMINATION OF SOLVATION KINETICS IN SUPERCRITICAL FLUIDS
F. V. Bright 1991 25 p
(Contract DE-FG02-90ER-14143)
(DE91-016096; DOE/ER-14143/1) Avail: NTIS HC/MF A03

The proposed research centers on improving our understanding of solvation processes in pure and entrainer-modified supercritical fluids. Specific topics are: (1) kinetics for solvation in supercritical media; (2) influence of entrainers on solvation; (3) reversibility of the solvation process (i.e., can equilibrium information be recovered); (4) effects of solvation on solute-solute interaction kinetics; and (5) impact of fluid density on these processes. Because of its inherent sensitivity, selectivity, and time resolution, we propose to investigate these processes with time-resolved fluorescence spectroscopy. The results from this project should provide insight into the kinetics and mechanisms of solute-fluid, solute-entrainer, and solute-solute interactions in supercritical media. In turn, this information can lead to a more accurate molecular understanding of supercritical fluid solvation. DOE

N91-31254# California Univ., Berkeley. Lawrence Berkeley Lab.
VIRIAL COEFFICIENTS AND EQUATIONS OF STATE FOR MIXED FLUIDS; APPLICATION TO CH4-H2O
K. S. Pitzer, A. Anderko, and S. M. Sterner Jun. 1991 16 p Presented at the 11th Symposium on Thermophysical Properties, Boulder, CO, 23-27 Jun.1991
(Contract DE-AC03-76SF-00098)
(DE91-016248; LBL-30899; CONF-9106176-4) Avail: NTIS HC/MF A03

The statistical mechanics of both pure and mixed fluids yields expressions in terms of virial expansions. The composition dependencies of various virial coefficients are well established as are the integrals expressing their values in terms of intermolecular potentials. These expressions are simple for the second virial coefficient but increase in complexity so rapidly for higher coefficients that it is not yet feasible to generate a complete equation of state from intermolecular potentials by this method. But it will be shown that these properties for the second, third, and fourth virial coefficients can be combined in a very useful manner with information from the complete equations of state for the component pure fluids to yield a form for the equation for the mixed fluid which maintains consistency with all of the pertinent principles and has a minimum number of parameters to be evaluated empirically. The system CH4-H2O is presented here as an example and other very recent applications are cited. DOE

N91-31255# Texas A&M Univ., College Station. Dept. of Chemistry.
CORRELATIONS BETWEEN SURFACE STRUCTURE AND CATALYTIC ACTIVITY/SELECTIVITY
D. W. Goodman Jul. 1991 26 p
(Contract DE-FG05-88ER-13954)
(DE91-016453; DOE/ER-13954/3) Avail: NTIS HC/MF A03

The goal of this research is to address those issues which are keys to understanding the relationship between surface properties and catalytic activity/selectivity. These issues also impact the understanding of the origins of the enhanced catalytic properties of mixed-metal catalysts. The experimental approach utilizes a microcatalytic reactor contiguous to a surface analysis system, an arrangement which allows in vacuo transfer of the catalyst from one chamber to the other. Topics studied include: reaction kinetics of methanol from syngas, CO oxidation by dioxygen, and ethane hydrogenolysis; electronic properties of bimetallic systems; synthesis and characterization of ultra-thin MgO films on Mo(100); and vibrational studies of ultra-thin metal and metal oxide films. DOE

N91-31256# Texas A&M Univ., College Station. Dept. of Chemistry.
HIGH PRESSURE CATALYTIC REACTIONS OVER SINGLE-CRYSTAL METAL SURFACES
J. A. Rodriguez and D. W. Goodman 1991 238 p
(Contract DE-FG05-88ER-13954)
(DE91-016475; DOE/ER-13954/T1) Avail: NTIS HC/MF A11

Studies dealing with high-pressure catalytic reactions over single-crystal surfaces are reviewed. The coupling of an apparatus for the measurement of reaction kinetics at elevated pressures with an ultrahigh vacuum system for surface analysis allows detailed study of structure sensitivity, the effects of promoters and inhibitors on catalytic activity, and, in certain cases, identification of reaction intermediates by post-reaction surface analysis. Examples are provided which demonstrate the relevance of single crystal studies for modeling the behavior of high surface area supported catalysts. Studies of CO methanation and CO oxidation over single crystal surfaces provide convincing evidence that these reactions are structure insensitive. For structure-sensitive reactions (ammonia synthesis, alkane hydrogenolysis, alkane isomerization, water-gas shift reaction, etc.) model single crystal studies allow correlations to be drawn between surface structure and catalytic activity. The effects of both electronegative (S and P) and electropositive (alkali metals) impurities upon the catalytic activity of metal single crystals for ammonia synthesis, CO methanation, alkane hydrogenolysis, ethylene epoxidation and water-gas shift are discussed. The roles of 'ensemble' and 'ligand' effects in bimetallic catalysts are examined in light of data obtained using surfaces prepared by vapor-depositing one metal onto a crystal face of a dissimilar metal. DOE

N91-31257# Allied-Signal Aerospace Co., Kansas City, MO.
ANALYSIS OF PRODUCTION SOLUTIONS BY POLAROGRAPHY
M. J. Bronson Jul. 1991 21 p
(Contract DE-AC04-76DP-00613)
(DE91-016479; KCP-613-4367) Avail: NTIS HC/MF A03

Polarographic methods were developed for zinc (II) and for stannous chloride in tin. Statistical analyses were performed using the polarographic methods on zinc (II) and for tin (II). Because polarography was determined to be a very troublesome and not very repeatable method, its usefulness for routine analyses and control of production plating process solutions was not demonstrated. DOE

N91-31258* National Aeronautics and Space Administration. Ames Research Center, Moffett Field, CA.
ETCHING METHOD FOR PHOTORESISTS OR POLYMERS
Patent
Narcinda R. Lerner, inventor (to NASA) and Theodore J. Wydeven, Jr., inventor (to NASA) 16 Apr. 1991 13 p Filed 4 May 1989 Continuation-in-part of US-Patent-Appl-SN-150169, filed 29 Jan. 1988
(NASA-Case-ARC-11873-2; US-Patent-5,007,983;
US-Patent-Appl-SN-347591; US-Patent-Appl-SN-150169;
US-Patent-Class-156-643; US-Patent-Class-156-668;
US-Patent-Class-156-345; US-Patent-Class-437-229;
US-Patent-Class-204-192.32; Int-Patent-Class-H01L-21/306)
Avail: US Patent and Trademark Office CSCL 07D

A method for etching or removing polymers, photoresists, and organic contaminants from a substrate is disclosed. The method includes creating a more reactive gas species by producing a plasma discharge in a reactive gas such as oxygen and contacting the resulting gas species with a sacrificial solid organic material such as polyethylene or polyvinyl fluoride, reproducing a highly reactive gas species, which in turn etches the starting polymer, organic contaminant, or photoresist. The sample to be etched is located away from the plasma glow discharge region so as to avoid damaging the substrate by exposure to high energy particles and electric fields encountered in that region. Greatly increased etching rates are obtained. This method is highly effective for etching polymers such as polyimides and photoresists that are otherwise difficult or slow to etch downstream from an electric discharge in a reactive gas.
Official Gazette of the U.S. Patent and Trademark Office

N91-31259# Los Alamos National Lab., NM.
WATER TRANSPORT PROPERTIES OF FUEL CELL IONOMERS
T. A. Zawodzinski, Jr., T. E. Springer, J. Davey, J. Valerio, and S. Gottesfeld 1991 13 p Presented at the 180th Meeting of the Electrochemical Society, Phoenix, AZ, 13-18 Oct. 1991
(Contract W-7405-eng-36)
(DE91-016015; LA-UR-91-2389; CONF-911047-5) Avail: NTIS HC/MF A03

We will report transport parameters measured for several available perfluorosulfonate membranes. The water sorption characteristics, diffusion coefficient of water, electroosmotic drag, and conductivity will be compared for these materials. The intrinsic properties of the membranes will be the basis of our comparison. An objective look at transport parameters should enable us to compare membranes without the skewing effects of extensive features such as membrane thickness. DOE

N91-31260# Southern Research Inst., Birmingham, AL.
ELECTROSTATIC PRECIPITATION OF CONDENSED ACID MIST
R. S. Dahlin Apr. 1991 59 p
(Contract DE-AC22-88PC-88867)
(DE91-016530; DOE/PC-88867/T10;
SRI-ENV-91-292-6657-XXXIV) Avail: NTIS HC/MF A04

This report deals with the second part (Phase 2) of a two-phased study of the control of acid mist emissions using a compact, wet electrostatic precipitator (WESP). The goal of the study was to determine the degree of acid mist control that could be achieved when a compact WESP was used to replace or augment the mist eliminators in a flue gas desulfurization (FGD) system. Phase 1 of the study examined the electrical operation of a lab-scale WESP collecting an acid mist from a coal combustion pilot plant equipped with a spray chamber. The results of this study were used to develop and validate a computer model of the WESP. In Phase 2, measurements were made at two utility scrubber installations to determine the loadings of acid mist, fly ash, and scrubber carryover. These measurements were used as input to the computer model to project the performance of retrofitted WESPs at both of the utility test sites. Phase 1 results showed that excellent electrical operating conditions could be achieved, but very high loadings of acid mist or the fine fly ash tended to degrade electrical operation because of space charge suppression of the corona current. Measurements made at the utility sites under Phase 2 showed that acid mist accounted for 40 to 57 percent of the total particulate mass, while fly ash and scrubber solids accounted for 40 to 55 percent and 1.0 to 3.4 percent. Impactor samples from both test sites showed an increase in acid content with decreasing particle size. DOE

N91-31261# Pennsylvania State Univ., University Park. Energy and Fuels Research Center.
CATALYST DISPERSION AND ACTIVITY UNDER CONDITIONS OF TEMPERATURE-STAGED LIQUEFACTION
A. Davis, H. H. Schobert, G. D. Mitchell, and L. Artok Jun. 1991 17 p
(Contract DE-AC22-89PC-89877)
(DE91-016602; DOE/PC-89877/6) Avail: NTIS HC/MF A03

Objectives (1) to investigate the use of highly dispersed catalysts for the pretreatment of coal by mild hydrogenation, (2) to identify the active forms of the catalysts under reaction conditions and (3) to clarify the mechanisms of catalysis. The experimental program will focus upon the development of effective methods of impregnating coal with catalysts, evaluating the conditions under which the catalysts are most active and establishing the relative impact of improved impregnation on conversion and product distributions obtained from coal hydrogenation. Four catalyst materials have been selected for this investigation: ammonium tetrathiomolybdate, ferrous sulfate, molybdenum hexacarbonyl, and

iron pentacarbonyl. Results are presented for liquefaction experiments performed on pre-swollen coals with and without catalysts at 275 C. DOE

N91-31262# Colorado State Univ., Fort Collins. Dept. of Chemistry.
CHEMICALLY MODIFIED ELECTRODES AND RELATED SOLUTION STUDIES
C. M. Elliott 1991 15 p
(Contract DE-FG02-87ER-13666)
(DE91-016740; DOE/ER-13666/T3) Avail: NTIS HC/MF A03

The following subject areas are covered: water oxidation catalysis by doubly linked mu-oxo ruthenium complexes; polymer films formed by oxidation of transition metal electrodes into solutions of bisbipyridine alkane ligands; polymer films containing (CpMo(mu-S))2S2CHR dinuclear clusters; conducting polymer films for catalyst incorporation; and Ru4/Fe complexes of tetra (4'-methyl-2.2'-bipyridine) porphyrin - catalytic epoxidation of olefins. DOE

N91-31263# Washington Univ., Seattle. Dept. of Physics.
X RAY AND GAMMA RAY SPECTROSCOPY OF SOLIDS UNDER PRESSURE
R. L. Ingalls 30 Jun. 1991 6 p
(Contract DE-FG06-84ER-45163)
(DE91-016948; DOE/ER-45163/26) Avail: NTIS HC/MF A02

Studies are summarized of various materials at high pressures by means of x ray and gamma ray absorption spectroscopy. It is to be recalled that pressure is a fundamental thermodynamic variable. In particular it enables one to control the state of the material, such as liquid or solid, insulating or conducting, para- or ferromagnetic, etc. High pressure techniques were developed which are suitable for use with XAFS (X ray Absorption Fine Structure) studies utilizing synchrotron radiation such as the Stanford Synchrotron Radiation Laboratory (SSRL). Such work is being continued, as well as studies involving the Mossbauer effect. Currently, no beam time has been received at SSRL, however time has been scheduled in two weeks for one week, at which time advantage will be taken of the new injector. The new injector is expected to finally make it possible to achieve three or four runs per year, in contrast to recent years where the rate was less than one per year. DOE

N91-31264# Colorado State Univ., Fort Collins. Dept. of Chemistry.
MASS RESOLVED EXCITATION SPECTROSCOPY OF BENZYL AND PHENYLNITRENE RADICALS
E. R. Bernstein and H. S. Im 30 Jul. 1991 15 p
(Contract N00014-89-J-1237)
(AD-A239394; TR-74) Avail: NTIS HC/MF A03 CSCL 07/3

Two-color mass resolved excitation spectra are obtained for the benzyl and phenylnitrene radicals. The spectrum previously assigned to the benzyl radical is generated by a species with mass 91 amu. This finding is consistent with the proposed (C6H5C*H2) benzyl radical structure. The origin of transition lies at 21,997/cm. The ionization energy for the benzyl radical is approximately 7.236 eV. The phenylnitrene radical spectrum is associated with a species of 90 amu. The phenylnitrene designation is not appropriate for this mass number: the suggested cyanocyclopentadienyl radical species (C5H4CN) is consistent with this mass. This radical has an ionization threshold of approximately 9.05 eV. Lifetimes are reported for a number of the vibronic states of both radicals. GRA

N91-31265# Naval Research Lab., Washington, DC.
CHEMICAL REDUCTION OF INTERMODULATION INTERFERENCE CAUSED BY METAL-OXIDE-METAL JUNCTIONS ABOARD SHIP
Robert Hynes, Homer W. Carhart, and John C. Cooper 31 Jul. 1991 30 p
(AD-A239530; NRL-9344) Avail: NTIS HC/MF A03 CSCL 20/5

Intermodulation interference from metal oxide metal nonlinear junctions near high frequency transmitters and receivers is suppressed effectively by application of chemical mixtures that provide an alternate, low impedance current path across the junction. The chemical formulations incorporate conductive and high dielectric constant materials into polymers. The mixtures clean metal oxides from surfaces, inhibit further corrosion, and can be used as additives to MILSPEC paints and lubricants. The approach greatly reduces intermodulation interference from electromagnetically active junctions in shipboard applications. Specific Topics include Electromagnetic interference, Chemical suppression, Broadband noise, and Intermodulation interference. GRA

N91-31266# Pittsburgh Univ., PA. Surface Science Center.
ATOMIC HYDROGEN DRIVEN HALOGEN EXTRACTION FROM Si(100): ELEY-RIDEAL SURFACE KINETICS
C. C. Cheng, S. R. Lucas, H. Gutleben, W. J. Choyke, and J. T. Yates, Jr. 12 Jul. 1991 23 p
(Contract N00014-82-K-0280)
(AD-A239544; TR-41) Avail: NTIS HC/MF A03 CSCL 20/5

The interaction of atomic hydrogen with halogen-terminated Si(100) surfaces was studied by Auger electron spectroscopy (AES) and temperature programmed desorption (TPD) mass spectroscopy. Efficient removal of surface halogen has been observed when the halogen-terminated Si(100) surface was exposed to atomic hydrogen at a substrate temperature, 630 K. The reaction rate constants for halogen extraction on the Si(100) surface follow the trend kI greater than kBr greater than kCl. In addition, the halogen extraction kinetics are found to be first order in both the surface coverage of halogen and in the atomic hydrogen flux. Studies of the temperature dependence of the halogen extraction rate show the activation energies for the extraction of Cl and Br are 2.1 and 1.6 kcal mol-1, respectively. The extremely low activation energy for the reaction demonstrates that the H-extraction process follows an Eley-Rideal reaction mechanism where the surface reaction is mainly driven by the high internal energy of incident atomic hydrogen instead of thermal excitation from the Si(100) solid surface. GRA

N91-31267# California Inst. of Tech., Pasadena. Graduate Aeronautical Labs.
A COMPARISON OF SEVERAL THEORIES WHICH USE JET SCALING TO PREDICT LIFTOFF HEIGHTS OF TURBULENT-JET FLAMES
Jay A. Hammer 31 Dec. 1990 26 p
(Contract N00014-89-J-1991)
(AD-A239717; GALCIT-FM-90-3) Avail: NTIS HC/MF A03 CSCL 21/4

In this paper several previously developed theories for predicting liftoff heights of turbulent-jet flames are examined and compared. The five theories are: a turbulent flame speed theory, a cascade mixing time theory, a strain-rate theory, a scalar dissipation-rate theory and an empirical correlation. Each theory uses far-field scaling of isothermal, turbulent jets. Through a systematic algebraic development, the predictions of the theories are presented in a common form. They are then compared for their ability to predict the experimentally observed linear dependence of liftoff height on nozzle exit velocity. Following this, their ability to correctly predict the relative liftoff heights of different fuels is examined. Finally, the theories are extended to predict blowout and their predictions are compared to experimental results of several fuels. GRA

N91-32026# Keuring van Electrotechnische Materialen N.V., Arnhem (Netherlands). Dept. of Chemical Research.
THE SELECTIVE CATALYTIC OXIDATION OF AMMONIA TO N2 AND H2O OVER SILICA-SUPPORTED MOLYBDENA CATALYSTS
F. J. J. G. Janssen and J. J. P. Biermann *In its* KEMA Scientific Reports, Volume 8, Number 2, 1990 Apr. 1990 p 105-108
(For primary document see N91-32023 23-99)
Avail: NTIS HC/MF A04

N91-32029# Keuring van Electrotechnische Materialen N.V., Arnhem (Netherlands). Dept. of Chemical Research.
SOME APPLICATIONS OF X-RAY PHOTOELECTRON SPECTROSCOPY AND SECONDARY-ION MASS SPECTROSCOPY
F. J. J. G. Janssen and H. M. Weijers *In its* KEMA Scientific Reports, Volume 8, Number 2, 1990 Apr. 1990 p 131-141 (For primary document see N91-32023 23-99)
Avail: NTIS HC/MF A04

N91-32030# International Flame Research Foundation, Ijmuiden (Netherlands).
ADJUSTMENT OF THE MIXING-RATE CONSTANT IN THE EDDY BREAK-UP MODEL FOR A JET FLAME
B. M. Visser and G. Koopmans (Keuring van Electrotechnische Materialen N.V., Arnhem, Netherlands) *In* Keuring van Electrotechnische Materialen N.V., KEMA Scientific Reports, Volume 8, Number 2, 1990 Apr. 1990 p 143-147 (For primary document see N91-32023 23-99)
Avail: NTIS HC/MF A04

26 METALLIC MATERIALS

Includes physical, chemical, and mechanical properties of metals, e.g., corrosion; and metallurgy.

N91-31268 General Electric Co., Fairfield, CT.
FATIGUE-RESISTANT NICKEL-BASE SUPERALLOYS Patent
Keh-Minn Chang, inventor 2 May 1989 33 p
(Patent-1-253-363; Int-Patent-Class-C22C-1905; Int-Patent-Class-C22F-110; CTN-91-60140) Copyright Avail: Micromedia Ltd., Technical Information Centre, 165 Hotel de Ville, Place du Portage, Phase 2, Hull, Quebec J8X 3X2, Canada HC $4.00 CAN, MF $2.75 CAN

Nickel based superalloys are extensively used in the production of large scale critical components for aircraft engines, such as turbine disks. This invention presents a strengthened nickel based superalloy composition which, when forged and properly heat treated, exhibits essentially time independent fatigue cracking resistance coupled with very good tensile and rupture strength properties. Parts, such as turbine disks, can be fabricated in large scale from these alloys using conventional hot forging techniques without encountering difficulties in forging and heat treating operations. These alloys contain nickel, chromium, cobalt, molybdenum, tungsten, aluminum, titanium, niobium, zirconium, and boron with the gamma prime precipitate phase being present in an amount ranging from 42 to 48 percent by volume. The processing protocol is as follows: final forging must begin at a temperature 5 to 25 C higher than the gamma prime precipitate solvus; solution annealing is carried out at 5 to 15 C above the recrystallization temperature; cooling from the annealing temperature is to be at a rate from 80 to 150 C per minute. After annealing, the alloy is aged at temperatures between 600 and 800 C for 8 to 24 hours. CISTI

N91-31269 Kaiser Aluminum and Chemical Corp., Oakland, CA.
COMPOSITE INGOT CASTING Patent
George J. Binczewski, inventor 21 Feb. 1989 27 p
(Patent-1-250-128; Int-Patent-Class-B22D-1100; CTN-91-60145) Copyright Avail: Micromedia Ltd., Technical Information Centre, 165 Hotel de Ville, Place du Portage, Phase 2, Hull, Quebec J8X 3X2, Canada HC $4.00 CAN, MF $2.75 CAN

This invention relates to the casting of lithium aluminum alloys. These alloys have highly desirable weight and modulus properties which suit them well for the manufacture of aircraft parts. Expensive alloying processes necessitated by the presence of highly reactive lithium in these alloys have delayed their exploitation. A process for continuously or semicontinuously casting lithium containing alloys, especially lithium aluminum alloys, is claimed. In addition, a casting method wherein the alloy is cast within a precast solid metal shell which prevents direct contact between the alloy and the coolant. The outer shell, which is preferably an aluminum alloy, can be cast continuously and simultaneously with the encased alloy core resulting in more efficient operations and in better control of various metallurgical conditions. This cladding provides a protective environment for the alloy, eliminating the need for an inert atmosphere for processing. It also reduces ingot cracking due to thermal stress. This improved process and system advantageously allows the subsequent fabrication and processing of the final composite or metal clad ingot by way of conventional rolling, extruding, or forging equipment. CISTI

N91-31270 General Electric Co., Fairfield, CT.
RAPIDLY SOLIDIFIED NICKEL ALUMINIDE OF IMPROVED STOICHIOMETRY AND DUCTILIZATION Patent
Alan I. Taub, inventor, Shyh-Chin Huang, inventor, and Keh-Minn Chang, inventor 1 Aug. 1989 15 p
(Patent-1-257-987; Int-Patent-Class-C22C-903; Int-Patent-Class-C22C-102; CTN-91-60165) Copyright Avail: Micromedia Ltd., Technical Information Centre, 165 Hotel de Ville, Place du Portage, Phase 2, Hull, Quebec J8X 3X2, Canada HC $4.00 CAN, MF $2.75 CAN

Nickel aluminide has good physical properties at temperatures above 1000 F making it suitable for use in jet engines. However, it has displayed poor strength properties at room temperature. A process is described for the preparation of rapidly solidified annealed nickel aluminide having an aluminum concentration between 0.235 and 0.245. With such an aluminum nickel ratio it is possible to achieve higher levels of boron doping (between 0.5 and 1.5 percent). This boron doped, aluminum poor aluminide has higher tensile strength and significantly improved ductility over nickel aluminides with higher aluminum concentrations. CISTI

N91-31271 General Electric Co., Fairfield, CT.
METHOD FOR IMPARTING STRENGTH TO INTERMETALLIC PHASES Patent
Shyh-Chin Huang, inventor, Keh-Minn Chang, inventor, and Alan I. Taub, inventor 20 Jun. 1989 17 p
(Patent-1-255-929; Int-Patent-Class-C22C-1900; CTN-91-60169) Copyright Avail: Micromedia Ltd., Technical Information Centre, 165 Hotel de Ville, Place du Portage, Phase 2, Hull, Quebec J8X 3X2, Canada HC $4.00 CAN, MF $2.75 CAN

Nickel aluminum alloys containing the intermetallic Ni3Al exhibit excellent strength at high temperatures but are very brittle at low temperatures. It has been found that the boron doping significantly improves the room temperature tensile strength and ductility. A process is presented for the preparation of a boron doped alloy which has a L1 subscript 2 type crystal structure and an approximate composition of 0.75 parts nickel, 0.20 parts aluminum, 0.05 parts a substitute metal which may be either vanadium or silicon. The alloy is rapidly cooled at a rate of at least 1000 C per second. The resulting alloy has significant ductility and yield strength, exhibits improved high temperature performance, and is capable of operating at high temperatures for sustained periods of time. CISTI

N91-31272# Sandia National Labs., Albuquerque, NM.
A COMPARISON OF TECHNIQUES FOR THE METALLOGRAPHIC PREPARATION OF THERMAL SPRAYED SAMPLES
M. F. Smith, D. T. McGuffin, J. A. Henfling, and W. J. Lenling (Thermal Spray Technologies, Watertown, WI.) 1991 13 p Presented at the 4th National Thermal Spray Conference and Exposition, Pittsburgh, PA, 5-10 May 1991
(Contract DE-AC04-76DP-00789)
(DE91-014704; SAND-90-3032C; CONF-9105107-1) Avail: NTIS HC/MF A03

Metallographic preparation of thermal spray coated samples is often difficult because hard and soft materials, which normally require different polishing techniques, are commonly present in a single spray-coated sample. In addition, the microstructures of many spray-deposited materials make them prone to pull-out damage during cutting, grinding, and polishing operations. We have compared alternative metallographic techniques to prepare three common types of thermal sprayed coatings: (1) a plasma sprayed

alumina-titania wear coating, (2) a plasma sprayed zirconia thermal barrier coating, and (3) an HVOF (High Velocity Oxy-Fuel) sprayed tungsten carbide/cobalt (WC/Co) hardcoating. Each coating was deposited onto a steel substrate and was prepared with metallographic protocols based on: (a) silicon carbide (SiC) papers, (b) bonded diamond platens, and (c) diamond slurries. Polishing with SiC papers generally produced edge rounding and significant pull-out that increased the apparent porosity of the coatings. Polishing with bonded diamond platens produced better results, but some pull-out was still observed. In addition, this method is typically the most expensive due to the limited lifetime and high cost of the platens. Preparation by diamond slurry lapping produced the best overall results at a reasonable cost per sample. Porosity artifacts produced by polishing with SiC papers and bonded diamonds platens also resulted in spuriously low hardness values for the WC/Co samples, but hardness results for the two ceramic coatings were not affected by the polishing method. DOE

N91-31273 Rensselaer Polytechnic Inst., Troy, NY.
THE INFLUENCE OF PLASTIC-STRAIN-INDUCED ANISOTROPY ON STRESS DISTRIBUTIONS IN THE FINITE DEFORMATION OF DUCTILE METALS Ph.D. Thesis
Yeong Sung Suh 1990 204 p
Avail: Univ. Microfilms Order No. DA9120246

The influence of plastic strain induced anisot ropy on stress distributions in the finite deformation of ductile metals, modeled as combined isotropic-kinematic hardening, a particular form of anisotropic hardening, is presented for several different types of straining such as simple shear, tension-torsion, and axisymmetric extrusion. For combined isotropic-kinematic hardening, the anisotropy generated by plastic flow is expressed by the back stress. The evolution equation for this contains form-invariant isotropic functions of the plastic strain rate and back stress, and also involves the spin associated with induced anisotropy. A numerical fitting procedure allowed the author to show that circles modeled as combined isotropic-kinematic hardening around the nose are in good agreement with the experimental yield loci taken from the nonproportional straining. Dissert. Abstr.

N91-31274# Lawrence Livermore National Lab., CA.
CREEP DEFORMATION AND FRACTURE OF A TWO-PHASE TiAl INTERMETALLICS
J. S. Huang and Young-Won Kim Apr. 1991 8 p Presented at the Symposium on Physical Metallurgy of Intermetallic Compound, Cincinnati, OH, 20-24 Oct. 1991
(Contract W-7405-eng-48)
(DE91-011963; UCRL-JC-106770; CONF-9110103-1) Avail: NTIS HC/MF A02

Gamma TiAl (L1(sub o) structure), which is stable up to about 1460 C, exhibits good specific strength, modulus, and oxidation resistance at high temperature service such as is required for heat engines. Due to its inherent brittleness at ambient temperature, extensive efforts have been made in recent years to develop more ductile alloys. A number of researchers have studied the deformation behavior of single-phase TiAl alloys, while there are only limited number of reports on the deformation behavior of two-phase alloys. Although TiAl alloys have good oxidation resistance, it has been reported that inward diffusion of oxygen causes embrittlement of the alloys. This presents a problem when the materials undergo creep in an oxygen environment. The embrittlement could facilitate crack initiation and growth (creep crack growth) from the surface and shorten the creep rupture life of the material at high temperature. To better understand the effect of oxidation on deformation and fracture at high temperature, we studied the creep behavior of a two- phase alloy in vacuum and in air. DOE

N91-31275# Los Alamos National Lab., NM.
DYNAMIC STRENGTH AND STRAIN RATE EFFECTS ON FRACTURE BEHAVIOR OF TUNGSTEN AND TUNGSTEN ALLOYS
A. K. Zurek and G. T. Gray, III 1991 9 p Presented at the 3rd International Conference on Mechanical and Physical Behavior of Materials Under Dynamic Loading, Strasbourg, France, 14-18 Oct. 1991
(Contract W-7405-eng-36)
(DE91-013029; LA-UR-91-1652; CONF-911069-3) Avail: NTIS HC/MF A02

An investigation of the stress-strain response as a function of strain rate, spall strength, and dynamic fracture behavior of pure W, W-26Re, W-Ni-Fe and W-Ni-Fe-Co has been performed. Spall strength measurements, obtained in symmetric-impact tests, showed an increase in spall strength from 0.4 GPa for pure tungsten to 3.8 GPa for 90W- 7Ni-3Fe. Concurrent with increase in spall strength was a change in fracture mode from cleavage (for pure W) to a mixture of transgranular and intergranular fracture for the alloyed systems. Compression testing performed at strain rates from 10(exp minus 3) s(exp minus 1) to 3000 s(exp minus 1) showed that pure tungsten exhibits a large strain rate sensitivity and almost no work hardening at tested strain rates. In contrast, W-26Re and W-Ni-Fe-Co displayed significant work hardening at all strain rates. DOE

N91-31276# Los Alamos National Lab., NM.
INFLUENCE OF LOADING RATE ON THE MECHANICAL RESPONSE AND SUBSTRUCTURE EVOLUTION OF SHOCK-LOADED COPPER
G. T. Gray, III and C. E. Morris 1991 7 p Presented at the 3rd International Conference on Mechanical and Physical Behavior of Materials Under Dynamic Loading, Strasbourg, France, 14-18 Oct. 1991
(Contract W-7405-eng-36)
(DE91-013390; LA-UR-91-1723; CONF-911069-6) Avail: NTIS HC/MF A02

Shock recovery experiments on copper have been conducted to investigate the influence of loading rate and stress amplitude on defect storage and post-shock mechanical properties. The shock risetimes varied approximately from one nanosecond for the shock experiments to one microsecond for quasi-isentropic loading experiments. All the experiments had the same peak pressure and pulse duration. Decreasing the strain-rate of loading is shown to increase both the defect storage and post-shock yield strength of copper. The effect of loading rate on post-shock substructure and mechanical response of impacted copper is postulated to be directly related to the amount of dislocation motion before interaction with other dislocations and to the amount of reversible dislocation motion and resultant annihilation during the rarefaction portion of the shock-release cycle. DOE

N91-31277# Oak Ridge National Lab., TN.
NON-EQUILIBRIUM SOLIDIFICATION IN AUSTENITIC STAINLESS STEEL WELDS
J. M. Vitek and S. A. David 1991 9 p Presented at the Fall Meeting of the Minerals, Metals and Materials Society of AIME and Materials Week of the American Society of Metals, Cincinnati, OH, 20-24 Oct. 1991
(Contract DE-AC05-84OR-21400)
(DE91-014279; CONF-911003-1) Avail: NTIS HC/MF A02

Recent studies have shown that non-equilibrium solidification may occur in a wide range of stainless steel alloy compositions. The non-equilibrium microstructures that are found are commonly produced in laser and electron beam-welded materials but they can also be observed, in some cases, in welds produced by conventional arc welding. In general, non-equilibrium solidification extends the range of compositions in which fully austenitic or fully ferritic microstructures are observed, while the range over which duplex microstructures are observed is reduced. These experimental results are explained in terms of thermodynamic considerations. Calculations, as well as experimental evidence, indicate that rapid solidification conditions result in sufficient undercooling to allow for competition between primary ferrite and primary austenite solidification. Under such conditions, primary austenite formation is kinetically favored. In addition, rapid cooling can inhibit the equilibrium solid state transformation of ferrite to austenite, leading to the retention of fully ferritic microstructures for some alloy compositions. Finally, over a limited range of

compositions, fully austenitic microstructures have been found without any evidence of a solidification substructure. These microstructures may be produced by a massive transformation from ferrite to austenite in the solid state. Alternatively, these microstructures can be explained in terms of solidification behavior. Further research is required to clarify this subject. DOE

N91-31278# Argonne National Lab., IL.
FORMATION OF DEFECT STRUCTURES IN METALS DURING IRRADIATION
H. Wiedersich and V. Naundorf Jun. 1991 4 p Presented at the International Conference on Physics of Irradiation Effects in Metals, Siofok, Hungary, 20-24 May 1991
(Contract W-31-109-eng-38)
(DE91-015548; ANL/CP-73552; CONF-9105130-5) Avail: NTIS HC/MF A01

Four main areas with good potential for impact on radiation effects research in the next few years were addressed: (1) in-situ, real time experimentation; (2) computer experiments; (3) impact of high resolution and analytical electron microscopy on radiation effects research; and (4) defect production in metals by electronic losses. Recollections from the session assembled with the help of view graphs kindly provided by some of the discussion participants are included. DOE

N91-31279# California Univ., Berkeley. Lawrence Berkeley Lab.
MAGNETIC FIELD-INDUCED FRACTURE CHANGES IN METASTABLE AUSTENITES AT 4.2 K Ph.D. Thesis
Jin Wah Chan Jun. 1991 84 p
(Contract DE-AC03-76SF-00098)
(DE91-016263; LBL-30942) Avail: NTIS HC/MF A05

Austenitic stainless steels have been used as structural alloys in high field superconducting magnets. Some of the candidate structural alloys for the next generation of magnetic confinement fusion reactors are of this type. In this application the alloys sustain high stresses in high strength magnetic fields at 4.2 K. It is known that plastic deformation at low temperatures induces a martensitic transformation in some of these alloys and that the presence of a strong magnetic field enhances the transformation. If such potentially metastable alloys are selected for this application, their mechanical behavior under service conditions has to be examined closely. Work on the tensile behavior of 18-8 type stainless steels under conditions of cryogenic temperatures and high-strength magnetic fields indicates that the tensile behavior does not undergo large changes in an engineering sense. However, fatigue and fracture properties have not yet been examined closely. This work addresses the fracture behavior of 18-8 type austenitic alloys at 4.2 K in an 8 T magnetic field. The fracture toughness is found to change with the application of the magnetic field. The direction of the fracture toughness change is related to enhanced transformation due to the reduction in the stability of the alloy in the magnetic field. Materials of low stability decrease in toughness and materials of intermediate stability increase in toughness; fully stable alloys showed no change. Several mechanisms that contribute to the observed differences are identified. These include: formation of low toughness martensite regions, strain hardening rate increases due to the transformation, transformation toughening, magnetostatic interactions, and changes in the slip characteristics. The timing of the transformation influences the relative strength of the operative mechanisms and determines the direction and amount of fracture toughness change. DOE

N91-31280# Oak Ridge National Lab., TN.
WELDABILITY AND HOT DUCTILITY OF IRON ALUMINIDES
D. I. Ash, G. R. Edwards, and S. A. David May 1991 137 p Prepared in cooperation with Colorado School of Mines, Golden
(Contract DE-AC05-84OR-21400)
(DE91-016343; ORNL/SUB-85-27421/04; MT-CWR-091-012)
Avail: NTIS HC/MF A07

The weldability of iron aluminide alloys is discussed. Although readily welded with electron beam (EB) and gas-tungsten arc (GTA) techniques, iron aluminides are sometimes susceptible to cracking during cooling when welded with the GTA welding process. Taken into account are the effects of microstructural instability (grain growth), weld heat input (cooling rate), and environment on the hot ductility of an iron aluminide alloy designated FA-129. DOE

N91-31281# Florida Atlantic Univ., Boca Raton. Alloy Research Center.
THEORETICAL STUDIES OF METALLIC ALLOYS
J. S. Faulkner and L. T. Wille Jul. 1991 18 p
(Contract DE-FG05-89ER-45392)
(DE91-016486; DOE/ER-45392/3) Avail: NTIS HC/MF A03

A new method to predict and understand the structure and phase stability of solid-solution alloys from a knowledge only of the atomic numbers of the constituent atoms is being developed. The coherent potential approximation will be used to obtain the electronic contribution to the energy and the Monte Carlo method of statistical mechanics will be used for the thermodynamic part of the calculation. An improved coherent potential approximation will be developed by combining the standard approach with the quadratic KKR (QKKR) band theory method. This will make it easier to predict the properties of alloys from first principles. The QKKR method will be developed further. DOE

N91-31282# National Aerospace Lab., Amsterdam (Netherlands). Structures and Materials Div.
CORROSION FATIGUE CRACK ARREST IN ALUMINIUM ALLOYS
R. J. H. Wanhill and L. Schra 4 Aug. 1988 42 p Presented at the ASTM Symposium on Evaluation and Techniques in Fractography, Atlanta, GA, Nov. 1988 Sponsored by Netherlands Agency for Aerospace Programs
(NLR-MP-88050-U; ETN-91-99652) Avail: NTIS HC/MF A03

Corrosion fatigue crack retardation and arrest in two high strength aluminum alloys was investigated. Results indicate that two mutually competitive processes, hydrogen embrittlement and crack tip blocking by corrosion products, have opposing effects on low stress intensity fatigue. Crack blocking is dominant at the lowest stress intensities. Prospects for enhancing corrosion fatigue crack arrest, and hence the durability of aircraft structures, are reasonable. It is suggested that multifunctional inhibitors could be added to the environment and metal surface treatments to promote corrosion product build up and prevent hydrogen entry at the crack tip. ESA

N91-31283# Forschungszentrum Juelich G.m.b.H. (Germany, F.R.). Inst. fuer Angewandte Werkstofforschung.
MECHANICAL BEHAVIOR OF A NICKEL BASED ALLOY UDIMET 700 FABRICATED BY POWDER METALLURGY [MECHANISCHES VERHALTEN DER PULVERMETALLURGISCH HERGESTELLTEN NICKELBASISLEGIERUNG UDIMET 700]
Dimitrios Moulatsiotis Dec. 1990 212 p In GERMAN
(JUEL-2414; ISSN-0366-0885; ETN-91-99742) Avail: NTIS HC/MF A10

The mechanical behavior of UDIMET 700 was examined at high temperatures. UDIMET 700 powder was compacted in two grain size distributions for three different production processes, and heat treated with a view to material optimization. It was shown that the use of coarses powder leads to an increase of strength for the final product. The percentage purity of the process gas takes particular importance in the fabrication of UDIMET 700, using vacuum plasma sprayers. The values obtained for tensile strength and failure strain in warm tensile tests can be compared to the corresponding values of reference material. ESA

N91-31284# Institut National des Sciences Appliquees, Lyon (France). Groupe d'Etudes de Metallurgie Physique et de Physique des Materiaux.
DEVELOPMENT AND CHARACTERIZATION OF LOW TEMPERATURE Cu-Al-Be SHAPE MEMORY ALLOYS Ph.D. Thesis [ELABORATION ET CARACTERISATION DE NOUVEAUX ALLIAGES A MEMOIRE DE FORME BASSE

TEMPERATURE TYPE CU-AL-BE]
Soliman Belkahla 1990 131 p In FRENCH
(ISAL-90-0093; ETN-91-99746) Avail: NTIS HC/MF A07

The dynamic characteristics of a Cu-Al-Be shape memory alloy are described. Addition of low percentages of berrylium to the alloy produces a significant drop in the temperature at which martensic transformation occurs. The percentages of the metals giving maximum stability in the beta phase shows practically no variation. No matter the Ms temperature chosen, resistance to ageing of the beta phase stays the same. This property makes the alloy particularly interesting for industrial purposes as it can replace Cu-Al-Ni alloys at low transformation temperatures between -200 and 60C. The shape memory properties of the alloy are comparable to those found for Cu-Zn-Al and Cu-Al-Ni alloys.
ESA

N91-31285# Institut National Polytechnique, Toulouse (France). Lab. de Materiaux.
STRESS CORROSION CRACKING OF 2091 AD 8090 ALUMINUM-LITHIUM ALLOYS IN CHLORIDE CONTAINING AQUEOUS SOLUTIONS. INFLUENCE OF SULPHATE AND NITRATE ADDITIONS Ph.D. Thesis
Sylvie Marsac 1991 142 p In FRENCH; ENGLISH summary
(Rept-431/91; ETN-91-99925) Avail: NTIS HC/MF A07

The susceptibility to stress corrosion cracking of 8090 and 2091 Al-Li alloys in 0.6 M NaCl solutions with sulphate or nitrate additions was investigated using slow strain rate tests in total immersion and constant load tests in alternate emersion-immersion. In only chloride solution, the 2091 T851 shows little susceptibility: no failure occurs for the 2091 T8X and the 8090 T851 alloys. Sulphate addition produces an increase of cracking: its effect is greater for very low content (8 ppm) and decreases when sulphate content increases. Nitrate addition has a similar influence but only for a very critical content. Electrochemical impedance measurements were performed to specify the role of nitrate ions on the mechanism of passive film development and deterioration.
ESA

N91-31286# Oak Ridge National Lab., TN.
DUAL ION IMPLANTATION EFFECTS ON FATIGUE PROPERTIES OF Fe-13Cr-15Ni ALLOYS
G. R. Rao, E. H. Lee, and B. A. Chin (Auburn Univ., AL.) 1991 20 p Presented at the 7th International Conference on Surface Modification of Metals by Ion Beams (SMMIB-7), Washington, DC, 15-19 Jul. 1991
(Contract DE-AC05-84OR-21400)
(DE91-015930; CONF-910707-3) Avail: NTIS HC/MF A03

Bend fatigue tests and microhardness measurements were carried out on eight complex Fe-13Cr-15Ni alloys based on the composition Fe-13Cr-15Ni-2Mo-2Mn-0.2Ti-0.8Si-0.06C, implanted simultaneously with 400 keV boron and 550 keV nitrogen ions to a dose of 2.3 x 10(exp 16) ions/sq cm for each ion. For all eight alloys, the dual implantation improved surface hardness but reduced the fatigue life. Optical microscopy revealed that the implantation suppressed slip band formation and slip band crack initiation. Transmission electron microscopy was used to characterize the near surface microstructures. It is evident that the suppression of slip band formation promoted grain boundary cracking to relieve stresses developed in the grains, thus leading to a reduced fatigue life. A similar study of four simple alloys based on the ternary Fe-13Cr-15Ni indicated that while dual implantation improved fatigue life, up to 250 percent in one case, triple implantation with boron, nitrogen and carbon ions reduced fatigue life, again due to a shift to grain boundary cracking. Improvement in fatigue properties of polycrystalline alloys by multiple ion implantation thus is limited by the presence of grain boundaries.
DOE

N91-31287# Los Alamos National Lab., NM.
MODEL DESCRIPTION OF TRANSITION METALS USING THE ROTATED SECOND MOMENT APPROXIMATION
J. D. Kress and A. F. Voter 25 Jun. 1991 14 p Presented at the International Energy Agency (IEA) Workshop on the Use of Molecular Dynamics in Modeling Radiation Effects and Other Non-Equilibrium Phenomena, La Jolla, CA, 6-8 May 1991
(Contract W-7405-eng-36)
(DE91-016043; LA-UR-91-2259; CONF-9105172-3) Avail: NTIS HC/MF A03

An interatomic potential is described, the rotated second moment approximation (RSMA), which incorporates directional bonding through energy moments evaluated over directional atomic orbitals. When non-directional orbitals are used, RSMA reduces to the standard SMA, and is thus capable of describing metallic systems. A model RSMA potential is demonstrated for 3d transition metals, with only first neighbor shell interactions, which can correctly predict the experimental trend in the relative stability of the fcc and hcp structures. A generalization of RSMA is proposed that is related in the same way that the embedded atom method (EAM) is related to the SMA. A generalized fcc RSMA potential is constructed for which the Cauchy pressure can be made negative by systematically adjusting one parameter. This behavior results from the angular (directional) forces and not from a physically-unreasonable embedding function.
DOE

N91-31288# California Univ., Berkeley. Lawrence Berkeley Lab.
METASTABLE AUSTENITES IN CRYOGENIC HIGH MAGNETIC FIELD ENVIRONMENTS
Jin Wah Chan, D. Chu, A. J. Sunwoo, and J. W. Morris, Jr. Jun. 1991 6 p
(Contract DE-AC03-76SF-00098)
(DE91-016420; LBL-30520) Avail: NTIS HC/MF A02

The fracture behavior of austenitic stainless steels of differing stability, AISI31OS, 304, and 304L, in a 4.2 K, 8T magnetic field environment are examined. 304L specimens with different amounts of work at different rolling temperatures are also examined. The different rolling conditions are used to produce stability differences independent of those inherent to chemistry differences. The application of an 8T magnetic field at 4.2 K leads to measured fracture toughness above and below that without an applied field in the metastable alloys, with the amount and direction of change a function of the stability of the alloy. Stable 310S alloy does not exhibit significant fracture toughness changes. This difference in fracture behavior is attributed to the enhancement of martensitic transformation about the crack tip during the fracture process in a magnetic field.
DOE

N91-31289# Virginia Polytechnic Inst. and State Univ., Blacksburg. Dept. of Chemical Engineering.
INFLUENCE OF SURFACE DEFECTS AND LOCAL STRUCTURE ON OXYGENATE REACTION PATHWAYS OVER METAL OXIDE SURFACES
D. F. Cox Jul. 1991 4 p
(Contract DE-FG05-90ER-14129)
(DE91-016600; DOE/ER-14129/1) Avail: NTIS HC/MF A01

The surface chemistry is studied of the C1 oxygenates (methanol, formaldehyde, formic acid), and its dependence on surface defects and tin cation coordination numbers on the SnO2(110) surface. These initial C1 studies will be completed and work will be initiated on understanding the scrambling of lattice oxygen into the oxidation products from the C1 molecules. This upcoming work will utilize the preferential labeling of bridging lattice oxygen positions on the SnO2(110) surface with O-18 so that the specific crystallographic origin of the oxidizing atoms can be determined.
DOE

N91-31290# Oregon Graduate Center for Study and Research, Beaverton.
DEFORMATION INDUCED MICROSTRUCTURAL AND MICROCHEMICAL CHANGES DURING THERMOMECHANICAL TREATMENT
D. G. Atteridge, L. E. Murr, W. E. Wood, and S. M. Bruemmer (Pacific Northwest Lab., Richland, WA.) 1990 53 p
(Contract DE-AC06-86NE-37963)
(DE91-016949; DOE/NE-37963/16) Avail: NTIS HC/MF A04

An important aspect of this program was the continued study into modeling the effects of deformation on isothermally induced

grain boundary chromium depletion (GBCD) in mill annealed (MA) and solution annealed (SA) stainless steel (SS) material. An understanding of this subject is academically important to this program as well as commercially important to the industrial community. DOE

27 NONMETALLIC MATERIALS

Includes physical, chemical, and mechanical properties of plastics, elastomers, lubricants, polymers, textiles, adhesives, and ceramic materials.

For composite materials see *24 Composite Materials*.

N91-31291# Oak Ridge National Lab., TN.
INITIAL DETERMINATION OF THE MICROMECHANICAL PROPERTIES OF OXIDE SCALES
P. F. Tortorelli, J. R. Keiser, W. C. Oliver, and K. R. Willson (Geneva Coll., Beaver Falls, PA.) 1990 12 p Presented at the 4th Conference on Fossil Energy Materials, Oak Ridge, 15-17 May 1990
(Contract DE-AC05-84OR-21400)
(DE90-012164; CONF-900546-7) Avail: NTIS HC/MF A03

A depth-sensing submicron identation technique is being used to characterize the mechanical response of oxide scales. The method has been applied to studies of chromia-rich and alumina scales grown on a stainless steel and an iron aluminide respectively. Results on room temperature micromechanical properties (elastic modulus, hardness, etc.) are presented to provide data for determining scale fracture criteria, to evaluate models, and to propose reactive element additions to alloys modify the mechanical behavior of oxide scales and thereby improve scale adherence. Average values of elastic moduli for thin chromia-rich scales formed on 20-25-Nb steels were in good agreement with that for the bulk chromia. However, the elastic modulus of the alumina scale grown on an Fe-21.4 wt percent Al alloy differed significantly from that reported for bulk Al2 sub 3. The addition of 0.13 percent Ce to the 20-25-Nb steel, which significantly improves scale adherence, did not affect the elastic modulus, hardness, strength, or plasticity of the oxide scale. Therefore, these findings did not support the subject models of scale adherence for cerium. Nevertheless, the technique of depth-sensing submicron indentation testing appears to offer promise as a method of characterizing oxide scales and their ability to protect alloys from high temperature corrosion and environmental degradation. DOE

N91-31292# Sandia National Labs., Albuquerque, NM.
PROCESS FOR PRODUCING PLASMA SPRAYED CARBIDE-BASED COATINGS WITH MINIMAL DECARBURIZATION AND NEAR THEORETICAL DENSITY
W. J. Lenling (Fisher-Barton, Inc., Watertown, WI.), M. F. Smith, and J. A. Henfling 1990 10 p Presented at the 3rd National Thermal Spray Conference and Exposition, Long Beach., 21-24 May 1990
(Contract DE-AC04-76DP-00789)
(DE91-012016; SAND-90-0845C; CONF-900520-4) Avail: NTIS HC/MF A02

Plasma spray deposition of carbide/metal hardcoatings is difficult because complex chemical transformations can occur while spraying, especially in the presence of oxygen. A commercial plasma spray torch has been modified to simultaneously inject carbide powder and a metal alloy powder at two different locations in the plasma stream. Composite hardcoatings of tungsten carbide/cobalt with a nickel-base alloy matrix have been produce with this dual-injection spray process and compared to coatings sprayed with a conventional plasma spray process. X-ray diffraction revealed very little change in the carbide phase composition of dual-injection coatings as compared to the original composition of the carbide spray powder. Conversely, the conventionally sprayed coatings showed significant transformation of the WC phase to the less desirable W2C phase, and secondary oxy-carbide phases were also clearly evident. Porosity in the dual-injection coatings was consistently less than 2 percent, as measured by image analysis of polished metallographic samples. Microhardness results for the dual injection coatings also compared very favorably with values for the conventional coatings. Preliminary results from an ongoing abrasive wear study indicate that the dual-injection coatings are more wear resistant than the conventional coatings, but further research is needed. DOE

N91-31293# Sandia National Labs., Albuquerque, NM.
BENEFICIAL EFFECTS OF AUSTEMPER POST-TREATMENT ON TUNGSTEN CARBIDE BASED WEAR COATINGS
W. J. Lenling (Fisher-Barton, Inc., Watertown, WI.), M. F. Smith, and J. A. Henfling 1990 14 p Presented at the 3rd National Thermal Spray Conference and Exposition, Long Beach., 21-24 May 1990
(Contract DE-AC04-76DP-00789)
(DE91-013260; SAND-90-0846C; CONF-900520-5) Avail: NTIS HC/MF A03

A post-deposition austemper heat treatment has been found to have several beneficial effects on the properties of plasma sprayed, tungsten carbide-based wear coatings. Four different tungsten carbide-based coatings were plasma spray deposited onto AISI 5150 steel substrates and then heat treated using an austemper process. Compared to the as-deposited condition, x-ray analyses indicated that the percentage of the desirable WC phase was increased by the heat treatment, while the less desirable W2C and other complex carbide phases were eliminated. Microscopic inspection of polished metallographic section showed a change in the coating/substrate bonding mechanism from mechanical to metallurgical bonding after heat treatment, and significant increases in coating hardness were also observed. When properly controlled, the heat treated coatings exhibited beneficial residual compressive stresses to varying degrees. As evidenced by improved performance in bending and impact tests, the heat treatment enhanced the durability of the wear coatings. Preliminary abrasive wear test results also indicate improved wear performance after the austemper heat treatment. DOE

N91-31294 Michigan Technological Univ., Houghton.
CERAMIC COMPOSITION Patent
Tseng-Ying Tien, inventor 31 Jan. 1989 48 p
(Patent-1-249-609; Int-Patent-Class-C04B-3510; CTN-91-60147)
Copyright Avail: Micromedia Ltd., Technical Information Centre, 165 Hotel de Ville, Place du Portage, Phase 2, Hull, Quebec J8X 3X2, Canada HC $4.00 CAN, MF $2.75 CAN

An improved ceramic composition is described particularly relative to the high temperature properties required in such applications as ceramic engines or ceramic lined engines. The material should be suitable for application as a light diesel engine cylinder and head liner, in hot adiabatic engines, gas turbine engines, and recuperator heat exchanger applications. The matrix phase of the ceramic is selected for the group consisting of solid solutions characterized by the formula Al2O3.(x)Cr2O3 and the formula 3Al2O3.2SiO2 + (x) (Cr2O3.2SiO2) where (x) is the relative mole fraction of Cr2O3 or Cr2O3.2SiO2. The disperse phase is characterized by the formula ZrO2.(y)HfO2 where (y) is the relative mole fraction of HfO2. These ceramics exhibit significantly improved hardness and fracture toughness, as well as low thermal conductivity at ultrahigh combustion temperatures, and high resistance to thermal shock, wear, and corrosion. CISTI

N91-31295 Nova Scotia Research Foundation Corp., Dartmouth.
CHARACTERIZATION OF FIRE RESISTANT GRP'S BY MECHANICAL PROPERTIES DETERMINATION
T. Betancourt and M. Robicheau 6 Mar. 1988 154 p
(Contract DREA-W7707-7-7935-01-OSC)
(DREA-CR-88-421; CTN-91-60216) Avail: NTIS HC A08

Results presented here are from monitoring the residual mechanical properties in 25 flame retarded glass reinforced plastics (GRPs) after their exposure to elevated temperatures. These plastics were prepared from three different polyester resins, one vinylester and one epoxy resin. Flame retardants included antimony trioxide, zinc borate, aluminum trihydrate and Nyacol. Over 1400 tests were performed in order to determine the tensile, flexural,

impact and shear properties and deflection temperatures in these plastics after their exposure to 23 C, 150 C, 225 C, and 300 C. Room temperature mechanical properties of GRPs are usually degraded to various degrees by additions of different fire retardants. Some loss of room temperature mechanical properties due to retardants can be recovered by exposing the fire reinforced GRPs for a short period to elevated temperatures of about 150 C. Heating at 300 C destroyed the flexural properties of all but six GRPs. Five of these, however, had some of their properties seriously affected by this treatment. The only plastic which did not have its residual properties seriously degraded at this temperature was the vinyl ester resin with 5 percent Nyacol added. Author (CISTI)

N91-31296 Texas A&M Univ., College Station.
FRACTURE TOUGHNESS CHARACTERIZATION OF POLYMERS Ph.D. Thesis
Michael Scott Cayard 1990 180 p
Avail: Univ. Microfilms Order No. DA9118199

The effect of various precracking techniques on the measured value of fracture toughness is examined, and it is demonstrated that alternate methods to fatigue precracking can lead to suitable crack tip conditions. Also, the appropriate size requirements necessary for a valid application of linear elastic fracture mechanics (LEFM) were experimentally determined on two polymer systems exhibiting differing degrees of strain softening. An attempt is then made to numerically predict the load displacement response of single edged notched three point bend specimens on one of these polymer systems using an existing model which accounts for the large inelastic deformation of glassy polymers. The model predictions correlated well for specimen sizes which exhibited a linear elastic response. However, as a greater percentage of the total volume exhibited strains approaching yield, the model was unable to predict the increased nonlinearity in the load displacement curves. Dissert. Abstr.

N91-31297 Texas A&M Univ., College Station.
ROBUST IMPEDANCE CONTROL OF ROBOT MANIPULATORS Ph.D. Thesis
Gun-Woong Bae 1990 116 p
Avail: Univ. Microfilms Order No. DA9118178

The objective was to design a controller for robot manipulators that could achieve a desired target impedance robustly and could follow the desired trajectory, even when disturbances and parameter uncertainties exist. Typical assumptions such as the so-called matching condition, full state feedback, and information about interacting forces at the end effector are necessary to robustly linearize the nonlinear dynamics of a robot manipulator to a desired linear dynamics (target impedance). After linearization, a simple linear controller can be applied in an outer loop to carry out fine maneuvers. The robustness of this control scheme is demonstrated. Provided the input to the linearization, interacting force, disturbances, and parameter uncertainties are bounded, and the outer control loop can be designed to make the total system stable, then the linearization will be robust. To linearize a nonlinear system with parameter uncertainties and disturbance to a desired linear system robustly, input/output (I/O) linearization and sliding mode control (SMC) are combined into a technique which was named robust sliding linearization (RSL) and the impedance control which uses RSL to achieve target impedance is named robust impedance control (RIC). To avoid saturation of the actuators, the desired trajectory can be modified by monitoring the input torque to the actuators. In this manner, the stability of the total system is guaranteed while the saturation of actuators is taken into account. The fact that a nonlinear system can behave like a linear mass-spring-damper system in specified directions is a promising technique to be applied to manufacturing processes, in particular, light machining operations such as deburring. Simulation of a robot manipulator with disturbance at the end effector shows a variety of features of RSL. A deburing simulation with an irregular surface shows the applicability of RIC. Dissert. Abstr.

N91-31298# Lawrence Livermore National Lab., CA.
DYNAMIC YIELD STRENGTH OF A PALLADIUM ALLOY METALLIC GLASS
C. F. Cline and J. E. Reaugh 15 May 1991 10 p Presented at the 3rd International Conference on Mechanical and Physical Behavior of Materials Under Dynamic Loading, Strasbourg, France, 14-18 Oct. 1991
(Contract W-7405-eng-48)
(DE91-015111; UCRL-JC-106047; CONF-911069-7) Avail: NTIS HC/MF A02

Taylor anvil tests in the reverse ballistic mode have been carried out to determine the dynamic yield strength of a Pd(77.5)Cu(6.0)Si(16.5) metallic glass. Scanning electron microscopy has been utilized to evaluate the details of the rod and anvil interface after impact. Computer simulations have also been carried out to interpret and confirm the results and conclusions. DOE

N91-31299# Argonne National Lab., IL.
MECHANICAL CHARACTERIZATION OF SEISMIC BASE ISOLATION ELASTOMERS
R. F. Kulak and T. H. Hughes 1991 12 p Presented at the 11th International Conference on Structural Mechanics in Reactor Technology, Tokyo, Japan, 18-23 Aug. 1991
(Contract W-31-109-eng-38)
(DE91-015680; ANL/CP-72558; CONF-910817-20) Avail: NTIS HC/MF A03

From the various devices proposed for seismic isolators, the laminated elastomer bearing is emerging as the preferred device for large buildings/structures, such as nuclear reactor plants. The laminated bearing is constructed from alternating thin layers of elastomer and metallic plates (shims). The elastomer is usually a carbon filled natural rubber that exhibits damping when subjected to shear. Recently, some blends of natural and synthetic rubbers have appeared. Before candidate elastomers can be used in seismic isolation bearings, their response to design-basis loads and beyond- design-basis loads must be determined. This entails the development of constitutive models and and then the determination of associated material parameters through specimen testing. This paper describes the methods used to obtain data for characterizing the mechanical response of elastomers used for seismic isolation. The data provides a data base for use in determining material parameters associated with nonlinear constitutive models. In addition, the paper presents a definition for a damping ratio that does not exhibit the usual reduction at higher strain cycles. DOE

N91-31300# Oak Ridge K-25 Site, TN.
DEVELOPMENT OF CERAMIC MEMBRANES FOR GAS SEPARATION: FY 1990 DEVELOPMENT ACTIVITIES
D. E. Fain, G. E. Roettger, and D. E. White Jun. 1991 18 p
(Contract DE-AC05-84OT-21400)
(DE91-015915; K/QT-413) Avail: NTIS HC/MF A03

Work is being carried out at the Oak Ridge K-25 Site to develop a ceramic membrane having very small pores for separating hydrogen at high temperatures from the mixture of gases produced by coal gasification processes. This report summarizes progress made during FY 1990 in developing a ceramic membrane for this application. During FY 1990 more than 200 experimental alumina membranes were fabricated and characterized as part of development effort aimed at achieving smaller pore size. Improvements made in membrane fabrication during the year were successful in reducing the mean pore radius of alumina membranes from about 15 Angstroms to about 7 Angstroms. Studies carried out as part of the development tests identified further process modifications that should be capable of reducing the pore size to less than 5 Angstroms. To begin studying the effects of membrane pore size on separation factor, pure gas flow measurements were made on two series of alumina membranes having mean pore radii ranging between about 7 and 22 Angstroms. The results indicated that other transport mechanisms (in addition to Knudsen transport) were active in this small pore size range. In preparation for testing membranes at elevated temperatures, metal ferrules

were fabricated from a sulfidation resistant stainless steel and tests were begun on an active metal brazing technique for sealing the metal ferrules to the ceramic membranes. Substantial progress was made in developing a mathematical model for gas transport through small-pored inorganic membranes. Separation factors calculated from the model closely approximate the empirical data over the range of pore sizes for which data are available. The model predicts that very high separation factors can be achieved with membranes having slightly smaller pore size than those currently available. DOE

N91-31301# Oak Ridge National Lab., TN.
DEVELOPMENT OF TOUGHENED CERAMICS FOR ELEVATED TEMPERATURES
P. F. Becher, H. T. Lin, and K. B. Alexander 1991 8 p Presented at the International Symposium on Ceramics, Yokohama (Japan), 16-18 Oct. 1991
(Contract DE-AC05-84OR-21400)
(DE91-015923; CONF-911084-1) Avail: NTIS HC/MF A02

The fracture toughness of ceramics can be substantially increased by crack bridging mechanisms introduced by discontinuous reinforcing phases. Examples of the toughening achieved by various discontinuous reinforcing phases (e.g., whiskers, matrix grains) are used to illustrate the effects on the material properties. The critical material parameters are defined by the analysis of crack bridging contributions due to elastically and frictionally bridging reinforcements and pullout processes. In addition for many of these ceramics and composites, the mechanical properties appear to be retained with increase in temperature. The key issue in their use at elevated temperatures is their creep resistance. Results of creep studies reveal that changes in the material characteristics can be used to further improve the creep resistance of these materials. These findings can then be incorporated into the design of toughened ceramics for elevated temperature applications. DOE

N91-31302# Sandia National Labs., Albuquerque, NM.
DEFECT DIFFUSION IN ION IMPLANTED GLASSES
G. W. Arnold, G. Battaglin, A. Boscolo-Boscoletto, F. Caccavale, G. DeMarchi, P. Mazzoldi, and A. Miotello (Trento Univ., Povo, Italy) 1991 13 p Presented at the 6th Conference on Radiation Effects in Insulators, Weimar (Germany), 24-28 Jun. 1991
(Contract DE-AC04-76DP-00789)
(DE91-016119; SAND-91-1296C; CONF-910646-4) Avail: NTIS HC/MF A03

Ion implantation in glasses produces structure modifications at depths greater than those of the implanted ion range. Such a result is evidenced by means of leaching experiments, alkali element depletion, distribution of gaseous implanted species, etching rate as function of depth. A systematic study with the aim to evidence a threshold in the nuclear deposited energy for defect diffusion is presented. Fourier transform infrared spectroscopy measurements confirm the glass modifications at extended depths. DOE

N91-31303# Sandia National Labs., Albuquerque, NM.
ION-IMPLANTATION INDUCED CRYSTALLIZATION OF GLASS
G. W. Arnold 1991 32 p Presented at the 1991 Dalian International Conference on Glass, Dalian (China), 18-20 Jun. 1991
(Contract DE-AC04-76DP-00789)
(DE91-016121; SAND-91-0379C; CONF-9106253-1) Avail: NTIS HC/MF A03

Controlled crystallization of glass through ion-implantation technology provides a means of altering near-surface physical properties, e.g., composition, hardness, reactivity, and refractive index. These changes may be desirable from the standpoint of electro-optical device fabrication technology. We have achieved crystallization through ion-implantation and appropriate thermal annealing. Three approaches have been used: (1) catalyzed precipitation of the crystalline phase on colloidal implanted metal (Au, Ag) in a lithia-alumina-silica (LAS) glass; (2) crystalline quartz growth on Li-implanted fused silica; and (3) crystallization of Li20.2SiO2 glass by inert gas ion implantation. The processing methods and our understanding of the phenomenology are discussed in detail. DOE

N91-31304# Messerschmitt-Boelkow-Blohm G.m.b.H., Munich (Germany, F.R.). Unternehmensbereich Verteidigungssysteme.
ADHESION OF THICK LAYER SYSTEMS ON CERAMIC BASED PRECIOUS METALS IN HYBRID MICROELECTRONIC CIRCUITS [HAFTUNG VON DICKSCHICHTSYSTEMEN AUF EDEL METALL-KERAMIK-BASIS BEI HYBRID-MIKROELEKTRONIKEN]
Ruediger Huch and Werner Moeller 1990 6 p In GERMAN Presented at the Vortrags- und Diskussionstagung Haftung bei Verbundwerkstoffen und Werkstoffverbunden, Konstanz, Fed. Republic of Germany, 21-22 Jun. 1990
(MBB-UA-1191-90-PUB; OTN-032763; ETN-91-99752) Avail: NTIS HC/MF A02

The solder adhesion of conductor layers, resistance layers, and dielectric layers on ceramic substrates determines the quality and durability of hybrid electronics, and was examined with regard to materials used, processes, and stresses. It was shown that adhesion is mainly determined by the coefficient of expansion, sinter behavior, crystallization behavior of glass, and further soldering. The influences of operation and aging on adhesion were considered. ESA

N91-31305# Aerospatiale, Suresnes (France). Centre Commun de Recherches Louis-Bleriot.
INFLUENCE OF ADHESIVE POLYMERIZATION CONDITIONS ON THE DURABILITY OF ADHESIVE JOINTS [ETUDE DE L'INFLUENCE DES CONDITIONS DE POLYMERISATION DES ADHESIFS SUR LA DURABILITE DES ASSEMMBLAGES COLLES]
J. M. Cuntz, A. Cavedon, and P. P. Villatte 3 Apr. 1990 33 p In FRENCH
(Contract STPA-88-96-009)
(DCR/I-03357-90; ETN-91-99912) Avail: NTIS HC/MF A03

The influence of the presence of unused Dicyandiamide (DDA) at the time of adhesive polymerization on the long term holding strength of aluminum joint bonded structures is considered. The adhesives FM73MO6 and EA9628 NWO6 are tested. Except for hardness, their chemical compositions are comparable: only EA9628 contain DDA. Despite the presence of unused DDA at EA9628 polymerization (verified by chemical analysis), no impact on the performance of bonded joints is observed, comparative to the tests with FM73. The adhesive tests show, on the other hand, that the prime role played by the presence of the primary BR127 in fighting against the initiation and development of corrosion in bonded joints. ESA

N91-31306# Ecole Nationale Superieure des Mines, Valbonne (France).
FIELD 3, THEME 1: STRUCTURAL MATERIALS. POST 2: THERMOTROPIC LIQUID CRYSTAL POLYMERS Final Summary Report [DOMAINE 3, THEME 1: MATERIAUX STRUCTURAUX. POSTE 22: POLYMERES A CRISTAUX LIQUIDES THERMOTROPES]
Edith Peuvrel and Patrick Navard 1990 83 p In FRENCH
(Contract DRET-89-017-01)
(ETN-91-99982) Avail: NTIS HC/MF A05

The feasibility of Liquid Crystal Polymers (LCP)/long fibers crossply composites is addressed. The flow of LCP around one or several obstacles is studied. An experimental setup to observe the flow along a capillary flow is studied. The manufacture of composites with different fiber/matrix plys is studied. ESA

N91-31307* National Aeronautics and Space Administration. Langley Research Center, Hampton, VA.
ETHYNYL TERMINATED IMIDOTHIOETHERS AND RESINS THEREFROM Patent
Paul M. Hergenrother, inventor (to NASA), John W. Connell, inventor (to NASA), and R. Gerald Bass, inventor (to NASA) (Virginia

Commonwealth Univ., Richmond.) 4 Jun. 1991 8 p Filed 4 May 1989 Division of US-Patent-Appl-SN-218792, filed 14 Jul. 1988
(NASA-Case-LAR-13910-2-CU; US-Patent-5,021,518; US-Patent-Appl-SN-347558; US-Patent-Appl-SN-218792; US-Patent-Class-525-422; US-Patent-Class-525-471; Int-Patent-Class-C08F-283/04; Int-Patent-Class-C08F-283/00; Int-Patent-Class-C08G-73/10; Int-Patent-Class-C08G-16/00)
Avail: US Patent and Trademark Office CSCL 11C

Ethynyl terminated imidothioethers (ETIs) are prepared by the reaction of a dimercaptan, such as 4,4'-dimercaptodiphenyl ether, and an ethynyl containing maleimide, such as N-(3-ethynylphenyl)maleimide. Blends of these ETIs and ethynyl terminated polymeric materials, such as ethynyl terminated sulfones and ethynyl terminated arylene ethers, are also prepared. These resin blends exhibit excellent processability, and the cured blends show excellent fracture toughness and solvent resistance, as well as excellent adhesive and composite properties.
Official Gazette of the U.S. Patent and Trademark Office

N91-31308# Oak Ridge National Lab., TN.
ION BEAM ENHANCED ADHESION OF IRON FILMS TO SAPPHIRE SUBSTRATES
J. E. Pawel, L. J. Romana, C. J. McHargue, and J. J. Wert (Vanderbilt Univ., Nashville, TN.) 1991 11 p Presented at the 7th International Conference on Surface Modification of Metals by Ion Beams (SSMIB-7), Washington, DC, 15-19 Jul. 1991
(Contract DE-AC05-84OR-21400)
(DE91-015931; CONF-910707-4) Avail: NTIS HC/MF A03

The effect of implantation of different ion species on the adhesion of iron films to sapphire substrates has been investigated. The implantation energies were adjusted to ensure the ion concentration profiles, damage profiles, and recoil distributions were the same for each species. For all implantations, the peak ion concentration was at the film-substrate interface. The adhesion of the films was measured by pull test and a scratch test. For a fluence of 1 x 10(exp 15) ions/sq cm, implantation of Cr (300 keV) and Fe (320 keV) increased the bond strength whereas implantation of Ni (340 keV) did not. The effect is proposed to be due to changes in the interfacial energy resulting from the presence of the ion species at the interface. Only a narrow zone is affected; the mixing at the interface is less than 10 nm. DOE

N91-31309# Sandia National Labs., Albuquerque, NM.
ELASTIC WAVE DISPERSION IN HIGH-STRENGTH CERAMICS
M. E. Kipp and D. E. Grady 1991 5 p Presented at the 1991 American Physical Society (APS) Conference on Shock Compression of Condensed Matter, Williamsburg, VA, 17-20 Jul. 1991
(Contract DE-AC04-76DP-00789)
(DE91-016648; SAND-91-0061C; CONF-9107105-49) Avail: NTIS HC/MF A01

Impact experiments are reported that provide load-release paths and spall data in high strength ceramics shocked to states below the Hugoniot Elastic Limit. The data are in the form of particle velocity histories. Wave code calculations are used to check the consistency of measured ultrasonic elastic velocities with the sound speed in a linear shock velocity-particle velocity relationship required to obtain accurate pulse width and release wave structure. The calculations are also used to estimate the spall strength of the ceramics. The dispersion observed during release from elastic states in some high strength ceramics is significantly more extensive than what is normally associated with elastic solids. The materials considered here are boron carbide, silicon carbide, and zirconium dioxide. DOE

N91-31310# Pennsylvania Univ., Philadelphia. Dept. of Chemistry.
APPLICATION OF MICROWAVE CAVITY PERTURBATION TECHNIQUES IN CONDUCTING POLYMERS Technical Report, 1 Jan. - 31 Oct. 1991
Z. H. Wang, H. H. Javadi, and A. J. Epstein 9 Aug. 1991 15 p
(Contract N00014-90-J-1559)
(AD-A239376; TR-1991-18) Avail: NTIS HC/MF A03 CSCL 07/6

Microwave cavity perturbation (MCP) techniques have been applied to measure complex microwave conductivities of conducting polymers. We find MCP is suitable for polymers with a large range of conductivities. In our experiment, it is possible to determine the parameter within 5 percent for fairly conducting samples through the extrapolation of normalized frequency shift to the high conducting limits (i.e., high temperature limit) and/or the comparison with DC conductivity. For all cases, the experimentally determined values are very close to the calculated ones based on the measurement of sample geometry. Some potential microwave applications of the conducting polymers are discussed. GRA

N91-31311# Army Lab. Command, Watertown, MA. Material Technology Lab.
STRUCTURE PROPERTY RELATIONSHIP OF ALIPHATIC POLYURETHANE ELASTOMERS PREPARED FROM CHDI Final Report
Catherine A. Byrne, C. H. Desper, and Joey L. Mead Jul. 1991 42 p
(AD-A239397; MTL-TR-91-26) Avail: NTIS HC/MF A03 CSCL 07/6

Aliphatic polyurethane elastomers were prepared from trans-1,4 diisocyanato cyclohexane, poly (tetramethylene oxide), 1,4-butanediol and optionally trimethylolpropane. CHDI is a compact symmetrical diisocyanate which is responsible for remarkable properties in these polymers. They are nearly transparent elastomers with low glass transition temperatures of approx. -80 C, and high final softening temperatures up to 270 C, for polymers with low hard phase contents of 20 to 30 pct. They are well phase separated and exhibit either paracrystallinity or crystallinity with small crystallite size after preparation. Considerable crystallinity develops after scanning up in temperature to 275 C or holding at 150 to 160 C for six hours. The polymers are insoluble even when heated in polymer solvents and this is attributed to ordering even in the as-synthesized polymers. They have excellent mechanical properties compared to other polyurethane elastomers and retain their modulus up to high temperatures. Because of their excellent phase separation and low hard segment content, with the resultant discrete domains, they exhibit very low hysteresis in compression and tension. GRA

N91-31312# Air Force Inst. of Tech., Wright-Patterson AFB, OH.
EFFECT OF THICKNESS AND BRAND OF METAL CERAMIC PORCELAIN ON COLOR M.S. Thesis
Douglas J. Wasson May 1991 142 p
(AD-A239398; AFIT/CI/CIA-91-026) Avail: NTIS HC/MF A07 CSCL 06/12

An essential aspect of any successful metal ceramic restoration is to provide an acceptable shade match to adjacent teeth or restorations. Generally, the dentist will select a shade from a prefabricated shade guide and write a work order for the lab to match that shade with the metal ceramic restoration. Two of the many factors that can affect the ultimate shade of a metal ceramic restoration are the brand of porcelain and the thickness of dentin porcelain used in the final restoration. The effects were examined of thickness and brand on the shade of dentin porcelain. Two hundred eighty-eight metal ceramic specimens were made using a custom shade tab device. Three Vita Lumin shades (A3.5, B1, and C3) of three commercially available dental porcelains that reportedly use shade matched opaques (Microbond, Ceramco II, and Jelenko) and one commercially available dental porcelain that does not use shade matched opaques (Vita VMK 68) were used to make six specimens in each of four thicknesses (0.3 mm opaque only, and 0.3, 0.6, and 0.9 mm of dentin porcelain). GRA

N91-31313# Massachusetts Inst. of Tech., Cambridge.
STRATEGIES FOR BIOPOLYMER ENGINEERING OF PHB-LIKE MATERIALS Final Technical Report

Anthony J. Sinskey, Oliver P. Peoples, and Chokyun Rha 16 Aug. 1991 30 p
(Contract N00014-87-K-0378)
(AD-A239690) Avail: NTIS HC/MF A03 CSCL 07/6

The overall objective of this proposal is to study the genetics and enzymology of polyhydroxybutyrate (PHB) biosynthesis at the molecular level in order to provide strategies for the development of new PHB-like biopolymers. Specific aims are to: (1) control the chain length of the PHB polymers produced in fermentation processes through genetic manipulation; (2) incorporate different monomers into PHB producing co-polymers with different physical properties; and (3) examine the physical/rheological properties of these new biopolymers in order to develop criteria at the molecular level. GRA

28 PROPELLANTS AND FUELS

Includes rocket propellants, igniters, and oxidizers; their storage and handling procedures; and aircraft fuels.

For related information see also *07 Aircraft Propulsion and Power, 20 Spacecraft Propulsion and Power,* and *44 Energy Production and Conversion.*

N91-31314# Lawrence Livermore National Lab., CA.
THE AUTOIGNITION CHEMISTRY OF PARAFFINIC FUELS AND PRO-KNOCK AND ANTI-KNOCK ADDITIVES: A DETAILED CHEMICAL KINETIC STUDY
C. K. Westbrook, W. J. Pitz, and W. R. Leppard (General Motors Research Labs., Warren, MI.) 1991 57 p Presented at the Society of Automotive Engineers International Fuels and Lubricants Meeting and Exposition, Toronto, Ontario, 7-10 Oct. 1991
(Contract W-7405-eng-48)
(DE91-014992; UCRL-JC-107388; CONF-911025-1) Avail: NTIS HC/MF A04

A numerical model is used to examine the chemical kinetic processes which lead to knocking in spark-ignition internal combustion engines. The construction and validation of the model is described in detail, including the low temperature reaction paths involving alkylperoxy radical isomerization. The numerical model is then applied to C1 to C7 paraffinic hydrocarbon fuels, and a correlation is developed between the Research Octane Number (RON) and the computed time of ignition for each fuel. Octane number is shown to depend on the rates of OH radical production through isomerization reactions, and factors influencing the rate of isomerization such as fuel molecule size and structure are interpreted in terms of the kinetic model. The knock behavior of fuel mixtures is examined, and the manner in which pro-knock and anti-knock additives influence ignition is studied numerically. The kinetics of methyl tert-butyl ether (MTBE) is discussed in particular detail. DOE

N91-31315# Lawrence Livermore National Lab., CA.
PERFORMANCE EVALUATION OF INSENSITIVE EXPLOSIVES
R. L. Simpson, J. W. Kury, A. L. Nichols, III, R. D. Breithaupt, and P. C. Crawford 31 May 1991 14 p Presented at the 2nd International Symposium on Pyrotechnics, Beijing (Peoples Rep. of China), 28-31 Oct. 1991
(Contract W-7405-eng-48)
(DE91-015767; UCRL-JC-106143; CONF-9110164-1) Avail: NTIS HC/MF A03

A calculational and experimental approach is described for characterizing explosive performance using quantities of 50 to 100 g. Thermochemical calculations are used to estimate the energy released for the isentropic expansion of the detonation products. LLNL's 1-D metal acceleration test has been modified to measure both detonation velocity and the high pressure behavior of the products. Calculational accuracy of the BKWR and CHEQ equations of state are examined by comparison with results from cylinder test experiments for a range of explosives. preliminary results for the modified one-dimensional metal acceleration experiment are presented for RDX and TATB. DOE

N91-31316# Lawrence Livermore National Lab., CA.
UNDERSTANDING COMPOSITE EXPLOSIVE ENERGETICS
W. C. Tao, C. M. Tarver, D. R. Breithaupt, and D. L. Omellas 3 Jun. 1991 13 p Presented at the 27th JANNAF Combustion Meeting, Cheyenne, WY, 5-9 Nov. 1990
(Contract W-7405-eng-48)
(DE91-015770; UCRL-JC-104280; CONF-9011119-5) Avail: NTIS HC/MF A03

We investigated the first series of bicomponent composite explosives, PETN/Al and TNT/Al, loaded with different weight percent of 5 (mu)m spherical aluminum. The metal acceleration techniques chosen for this study proved to be quite versatile in detailing the reaction zone length for the reaction between the aluminum and the detonation products. We have been able to incorporate a calculational method, which involves reactive flow modelling and thermodynamic calculations with TIGER, to predict the extent of aluminum reaction within the early time expansion. We performed additional Ta plate-push and impedance-matching particle velocity measurements on PETN/Al compositions with longer charges filled with 18-micron aluminum particles. It is our goal to understand the different physical, chemical, and thermal mechanisms influencing the complex kinetics associated with composite explosive systems in hope that we can tailor the rate of explosive energy delivery for various applications. We are developing a reaction zone model (ZND), in contrast to a CJ model, which will provide a realistic and useful description of the hydrodynamic response in composite explosives. From the particle velocity measurements using either a LiF or NaCl impedance-matching crystal, we found that the previous CJ reactive flow model with instantaneous energy release often overestimates the early time Ta velocity profile. The new ZND reaction zone model with the incorporation of aluminum burn is able to describe the particle velocity histories. At short run distances the detonation within these metal filled compositions is not steady-state, and the ZND model slightly underestimates the Ta plate velocities. At longer distances, the ZND model is able to resolve the two dimensional effects from radial rarefaction. The aluminum reaction in both the 5- and 18-micron composite formulations with PETN follows a simple diffusion mechanism. DOE

N91-31317# Messerschmitt-Boelkow-Blohm G.m.b.H., Ottobrunn (Germany, F.R.). Unternehmensbereich Verteidigungssysteme.
THE PHYSICAL PROPERTIES OF A PYROTECHNICAL CIRCUIT ELEMENT [DIE PHYSIKALISCHEN EIGENSCHAFTEN EINES PYROTECHNISCHEN SCHALTELEMENTES]
Karl-Heinz Ilg 1990 12 p In GERMAN
(MBB-UA-1192-90-PUB; OTN-032764; ETN-91-99753) Avail: NTIS HC/MF A03

The ignition of the circuit was examined with regard to the energy, in the field of 1.7 to 24 mJ. It was found that ignition times show a strong dependency on the duration and amplitude of voltage pulse. Ignition times were extended up to a factor of 1.6 by thermal preloading. Dynamic ignition measurements show clearly that the minimum ignition energy from 300 nanoseconds of pulse width moves between 1.9 and 3.5 mJ. Heat dissipation takes place over 10 milliseconds, so that an already high ignition energy is required for ignition. Ignition times dependent on input quantities, such as power and pulse width can be determined by equations. ESA

N91-31318*# National Aeronautics and Space Administration. Lewis Research Center, Cleveland, OH.
TECHNICAL PROSPECTS FOR UTILIZING EXTRATERRESTRIAL PROPELLANTS FOR SPACE EXPLORATION
Diane L. Linne and Michael L. Meyer 1991 20 p Presented at the 42nd International Astronautical Congress, Montreal, Quebec, 5-11 Oct. 1991; sponsored by International Astronautical Federation
(NASA-TM-105263; E-6594; NAS 1.15:105263) Avail: NTIS HC/MF A03 CSCL 21I

NASA's LeRC has supported several efforts to understand how lunar and Martian produced propellants can be used to their best

advantage for space exploration propulsion. A discussion of these efforts and their results is presented. A Manned Mars Mission Analysis Study identified that a more thorough technology base for propellant production is required before the the net economic benefits of in situ propellants can be determined. Evaluation of the materials available on the moon indicated metal/oxygen combinations are the most promising lunar propellants. A hazard analysis determined that several lunar metal/LOX monopropellants could be safely worked with in small quantities, and a characterization study was initiated to determine the physical and chemical properties of potential lunar monopropellant formulations. A bipropellant metal/oxygen subscale test engine which utilizes pneumatic injection of powdered metal is being pursued as an alternative to the monopropellant systems. The technology for utilizing carbon monoxide/oxygen, a potential Martian propellant, was studied in subscale ignition and rocket performance experiments. Author

N91-31319# Department of Energy, Washington, DC.
ASSESSMENT OF COSTS AND BENEFITS OF FLEXIBLE AND ALTERNATIVE FUEL USE IN THE US TRANSPORTATION SECTOR
Jul. 1991 88 p
(DE91-015451; DOE/PE-0098P) Avail: NTIS HC/MF A05

The Alternative Motor Fuels Act of 1988 (Public Law 100-494), Section 400EE, states that the Secretary of Energy shall study methanol plants, including the costs and practicability of such plants that are (1) capable of utilizing current domestic supplies of unutilized natural gas, (2) relocatable, or (3) suitable for natural gas to methanol conversion by natural gas distribution companies. Unutilized gas within the lower 48 states is characterized and an economic analysis is performed of methanol plants required by the act. The approach with regard to unutilized lower 48 gas is to (1) compare the costs of converting such gas to methanol against the expected price of gasoline over the next 20 years, and (2) compare the economics of converting such gas to methanol against the economics of using the gas as a pipeline transported fuel. It is concluded that remote gas and low-Btu gas generally cannot be converted to methanol at costs near the expected competitive value of gasoline because of the poor economies of scale of small methanol plants. DOE

N91-31320# Brookhaven National Lab., Upton, NY.
CONVERSION OF BIOMASS AND FOSSIL FUELS TO METHANOL AND ITS EFFECT ON CO2 EMISSIONS
M. Steinberg Apr. 1991 4 p Presented at the 1991 International Conference on Coal Conversion, New Castle, England, 16-20 Jun. 1991
(Contract DE-AC02-76CH-00016)
(DE91-015846; BNL-46300; CONF-9106255-1) Avail: NTIS HC/MF A01

The purpose for this report is to present a preliminary analysis of various processes for conversion of biomass to methanol fuel with the objective of determining the effect of these processes on net CO2 emissions. The analysis is made primarily on the basis of first principles of mass and energy balances. There are at least four systems that can produce methanol from biomass (defined as wood or lignocellulose). They are: destructive distillation of wood; conventional steam-oxygen gasification of wood; higher temperature pyrolysis of wood; and coprocessing of biomass with fossil fuel using the hydrocarb process. DOE

29 MATERIALS PROCESSING

Includes space-based development of products and processes for commercial applications.

For biological materials see *55 Space Biology*.

N91-31321# European Space Agency, Paris (France).
SUMMARY REVIEW OF SOUNDING ROCKET EXPERIMENTS IN FLUID SCIENCE AND MATERIAL SCIENCES: TEXUS 1 TO 20; MASER 1 AND 2
Olivier Minster and Brigitte Kaldeich, ed. Noordwijk, The Netherlands ESTEC Feb. 1991 346 p Original contains color illustrations
(ESA-SP-1132; ISBN-92-9092-104-08; ETN-91-99531) Copyright Avail: NTIS HC/MF A15; EPD, ESTEC, Noordwijk, Netherlands, HC 75 Dutch guilders

Summary reports of experiments carried out on the Technology Experiments Under Microgravity (TEXUS)-Technologische Experimente Unter Schwerelosigkeit flights from 1977 (TEXUS 1) to 1988 (TEXUS 20) and on the Swedish Materials Science Experiment Rocket (MASER) 1 and 2 (1987 and 1988) are presented. The major areas covered include: (1) capillarity; (2) fluid dynamics; (3) physical chemistry; (4) diffusion; (5) phase transition and critical point phenomena; (6) crystal growth from the melt; (7) crystal growth of proteins; (8) metals and alloys; (9) systems with a miscibility gap in the liquid state; (10) composites with solid particles; (11) composites with gases; (12) technological experiments; and (13) containerless processing. For individual titles, see N91-31322 through N91-31469.

N91-31322# Fraunhofer-Gesellschaft e.V., Stuttgart (Germany, F.R.). Inst. fuer Grenzflaechen und Bioverfahrenstechnik.
LIQUID MOTION IN CAPILLARY TUBES (TEXUS 3) **c34**
P. J. Sell, E. Maisch, and J. Siekmann (Essen Univ., Germany, F.R.) *In* ESA, Summary Review of Sounding Rocket Experiments in Fluid Science and Materials Sciences: TEXUS 1 to 20; MASER 1 and 2 Feb. 1991 p 20-21 (For primary document see N91-31321 23-29)
Copyright Avail: NTIS HC/MF A15; EPD, ESTEC, Noordwijk, Netherlands, HC 75 Dutch guilders

The Technological Experiments Under Microgravity (TEXUS) 3 Investigation of the free surface and the dynamics of liquids in capillary systems which aimed at predicting their behavior in porous media is summarized. This study is also relevant to certain materials science systems and liquid systems in space. The apparatus consisted of a reservoir equipped with five stand pipes. Once microgravity conditions were established, the reservoir was filled with delaminated water from a supply tank. The stand pipes served to stabilize the free surface of the liquid and to form flat menisci into which capillary glass tubes with cylindrical, sinusoidal, or conical shapes were lowered. The rise of the liquid allowed the visualization of the velocity field both in the bulk and close to the rising menisci. For comparison, the experiment was simulated on Earth using two immiscible liquids of the same density, in a Plateau setup. The menisci observed in space were less stable than those observed on Earth and deviated from the hemispherical shape, due to hydrodynamical effects. As a result of these effects, the capillary force was reduced and the liquid rise time was longer than observed on Earth. In addition, wetting aids mounted in the stand pipes increased unexpectedly the convective forces. The observations agreed well with theoretical predictions, when account is taken of the fluid velocities and the apparent contact angles in the Gauss-Laplace and Navier-Stokes equations. ESA

N91-31323# Fraunhofer-Gesellschaft e.V., Stuttgart (Germany, F.R.). Inst. fuer Grenzflaechen und Bioverfahrenstechnik.
LIQUID MOTION IN CAPILLARY TUBES (TEXUS 5) **c34**
P. J. Sell, D. Renzow, and E. Maisch *In* ESA, Summary Review of Sounding Rocket Experiments in Fluid Science and Materials Sciences: TEXUS 1 to 20; MASER 1 and 2 Feb. 1991 p 22-23 (For primary document see N91-31321 23-29)
Copyright Avail: NTIS HC/MF A15; EPD, ESTEC, Noordwijk, Netherlands, HC 75 Dutch guilders

The Technological Experiments Under Microgravity (TEXUS) 5 observation of the capillary rise of water in tubes of large diameters and of different shapes under microgravity conditions is summarized. A planar water/air interface was achieved in a cuvette under microgravity conditions by means of wetting and nonwetting coatings. Five glass tubes of conical, cylindrical, or sinusoidal shape were simultaneously lowered into the cuvette. The process was filmed with a cine camera. The water rose up as soon as the end of each tube came in contact with the liquid surface, and menisci of different shapes were formed. The water rose up with different

velocities depending on the diameter and the shape of the tubes. The behavior of the rising liquid was in good agreement with computer simulations. ESA

N91-31324# Fraunhofer-Gesellschaft e.V., Stuttgart (Germany, F.R.). Inst. fuer Grenzflaechen und Bioverfahrenstechnik.
BUBBLES AND FOAMS (TEXUS 10) ESA **c34**
P. J. Sell, D. Renzow, and K. F. Gebhardt *In* ESA, Summary Review of Sounding Rocket Experiments in Fluid Science and Materials Sciences: TEXUS 1 to 20; MASER 1 and 2 Feb. 1991 p 24 (For primary document see N91-31321 23-29)
Copyright Avail: NTIS HC/MF A15; EPD, ESTEC, Noordwijk, Netherlands, HC 75 Dutch guilders

The Technological Experiments Under Microgravity (TEXUS) 10 experiment to study the growth and coalescence of gas bubbles and the formation of polyhedral foams is summarized. Four cells with different aqueous solutions of sodium dodecylsulfate were employed to investigate the transition from spherical foams under microgravity conditions. Bubbles were formed in each cell by means of a gas jet. By reducing the liquid in the cells, the bubbles were forced into contact and finally formed a polyhedral foam. The process was observed by means of a cine camera. Simulation experiments performed on Earth allowed the study of the foam stability and the determination of the dynamic surface properties. As the bubbles detached from the gas input nozzle relatively easily, it was possible to produce a spherical foam. The latter observation gave information on the role of the Plateau-border, which caused the liquid to be sucked from the reservoir into the foam and lamellae as external forces, due to gravity or artificial low pressure, were reduced. ESA

N91-31325# Escuela Tecnica Superior de Ingenieros Aeronauticos, Madrid (Spain). Lab. de Aerodinamica.
LONG LIQUID BRIDGES ABOARD SOUNDING ROCKETS (TEXUS 12) ESA
I. Martinez and A. Sanz *In* ESA, Summary Review of Sounding Rocket Experiments in Fluid Science and Materials Sciences: TEXUS 1 to 20; MASER 1 and 2 Feb. 1991 p 26-29 (For primary document see N91-31321 23-29)
Copyright Avail: NTIS HC/MF A15; EPD, ESTEC, Noordwijk, Netherlands, HC 75 Dutch guilders

The Technological Experiments Under Microgravity (TEXUS) 12 experiment is summarized. Microgravity experimentation with liquid bridges is of great potential value for the understanding of basic phenomena related to a variety of disciplines. Important applications include, for example, the growth of single crystals from a molten bridge as used to purify silicon in the semiconductor industry. Many materials science applications involve very slow mass and heat diffusion processes over long periods. The same was thought initially about experimentation with large free liquid masses, although experiments with small liquid bridges (about 1 cubic cm) have been carried out since the first sounding rocket flights. Several mechanisms were proposed for the formation of free liquid brigdes in microgravity, each aimed at minimizing both the time taken and the residual motions in the liquid. This experiment showed that only 10 of the microgravity periods available aboard a sounding rocket is consumed in establishing long liquid bridge (60 cubic cm in this case), thus leaving 90 free for scientific investigations. ESA

N91-31326# Escuela Tecnica Superior de Ingenieros Aeronauticos, Madrid (Spain). Lab. de Aerodinamica.
FREEZING OF A LONG LIQUID COLUMN (TEXUS 18) ESA
I. Martinez and A. Sanz *In* ESA, Summary Review of Sounding Rocket Experiments in Fluid Science and Materials Sciences: TEXUS 1 to 20; MASER 1 and 2 Feb. 1991 p 30-31 (For primary document see N91-31321 23-29)
Copyright Avail: NTIS HC/MF A15; EPD, ESTEC, Noordwijk, Netherlands, HC 75 Dutch guilders

The Technological Experiments Under Microgravity (TEXUS) 18 experiment to measure the contact angle between the free liquid surface and the solid/liquid interface during the longitudinal solidification of a liquid column is summarized. The good resolution of the television pictures during ground tests could not be reproduced during flight and a precise measurement of the reducing angle could not be achieved. The solidification front seemed to remain plane. Although the thermal gradient measured in the liquid was of the order of 10 C/mm and the thermal coefficient of the surface tension of water is high, no convection occurred (the tracers stayed nearly at rest). This is interpreted as the effect of impurities which strongly reduced the surface tension of water. A temporary opacity of the liquid was observed close to the cooling support just before the appearance of the first ice crystal. A peak in the temperature recordings of the cool support seems to indicate the occurrence of undercooling and subsequent release of solidification enthalpy. The reentry of the rocket caused the breakage of the remaining liquid part of the column. The ice crystal obtained, which stayed on the cooling support, was 13 mm long, as anticipated. During future microgravity experiments, the growth of a single crystal should be triggered in order to assess the influence of the crystallographic orientation on the receding angle. ESA

N91-31327# Technische Univ., Berlin (Germany, F.R.). Inst. fuer Nichmetallische Anorganische Werkstoffe.
INTERFACIAL CONVECTION (TEXUS 1)
R. Brueckner *In* ESA, Summary Review of Sounding Rocket Experiments in Fluid Science and Materials Sciences: TEXUS 1 to 20; MASER 1 and 2 Feb. 1991 p 36-37 (For primary document see N91-31321 23-29)
Copyright Avail: NTIS HC/MF A15; EPD, ESTEC, Noordwijk, Netherlands, HC 75 Dutch guilders

The Technological Experiments Under Microgravity (TEXUS) 1 experiment to investigate the mass transfer between two immiscible liquids by interfacial convection and without density instability is summarized. The experimental cell (25 mm in diameter, 3 mm deep) was separated into two halves by a movable teflon partition. One half was filled with a solution of acetic acid in amyl alcohol, the other with water colored with methyl orange. The cell was filmed with a cine camera through a Schlieren optic system. Under microgravity conditions, the partition was retracted to bring the immiscible liquids into contact and to allow the transfer of acetic acid from amyl alcohol into water. The amyl alcohol-acetic acid solution spread along the surface of the partition due to a better wetting of the teflon by the organic solution than by water. The interface was strongly deformed and violent interfacial convection occurred. The curvature of the interface was then stabilized with a radius of 2 cm. The convection decreased slowly but was maintained for 170 s since the liquids at the interface were renewed by the hydrodynamic flows generated by the initial convection. Thereafter, the interface remained immobile except for some disturbances induced by the residual accelerations of the rocket. A similar experiment carried out on Earth showed that the interfacial convection does not stop under normal gravity. Also, when starting with an aqueous solution of acetic acid and pure amyl alcohol (stable configuration with respect to the densities), a quick decay of the interfacial convection was observed (less than 30 s) under gravity. It was concluded that the interfacial effects are also particularly strong in microgravity. ESA

N91-31328# Technische Univ., Berlin (Germany, F.R.). Inst. fuer Nichtmetallische Anorganische Werkstoffe.
INTERFACIAL CONVECTION (TEXUS 2)
R. Brueckner *In* ESA, Summary Review of Sounding Rocket Experiments in Fluid Science and Materials Sciences: TEXUS 1 to 20; MASER 1 and 2 Feb. 1991 p 38-39 (For primary document see N91-31321 23-29)
Copyright Avail: NTIS HC/MF A15; EPD, ESTEC, Noordwijk, Netherlands, HC 75 Dutch guilders

The Technological Experiments Under Microgravity (TEXUS) 2 experiment to study interfacial instabilities induced by two phase three component boundaries at the interface, or by local heating is summarized. The experimental set up used for the previous experiment on TEXUS 1 was slightly modified in order to investigate the interfacial convection induced by injecting a drop of glycerin at the interface between amyl alcohol and water or by heating locally the interface. A small heating element was installed in

order to create a hot spot at the interface. The local temperature was to be recorded by means of a thermocouple. The partition consisted of a tube with a steel tip to prevent a total wetting by amyl alcohol. Motions induced by spreading effects were clearly visible. They decayed very rapidly each time the heater was switched off. Similar experiments were carried out on the ground. The densities were matched by adding Cs2CO3 to the water. The concentration induced interfacial convection was twice as fast as in microgravity but this can result from the increase of the interfacial tension by the salt. Little thermally induced interfacial convection could be observed since gravity driven buoyancy convection was dominant. ESA

N91-31329# Technische Univ., Berlin (Germany, F.R.). Inst. fuer Nichtmetallische Anorganische Werkstoffe.
DIFFUSION-INDUCED INTERFACIAL CONVECTION (TEXUS 3)
R. Brueckner *In* ESA, Summary Review of Sounding Rocket Experiments in Fluid Science and Materials Sciences: TEXUS 1 to 20; MASER 1 and 2 Feb. 1991 p 40-41 (For primary document see N91-31321 23-29)
Copyright Avail: NTIS HC/MF A15; EPD, ESTEC, Noordwijk, Netherlands, HC 75 Dutch guilders

The Technological Experiments Under Microgravity (TEXUS) 3 experiment aimed at assessing the validity of the criterion proposed by Sternling and Scriven for the prediction of the stability of a liquid-liquid interface during the transfer of a solute from one liquid into the other is summarized. The transfer of acetone from a volume of solution consisting of 31.4 vol toluene and 68.6 vol acetone into an identical volume of pure water was investigated. The teflon partition was equipped with a steel tip to avoid the preferential wetting of teflon by one of the liquids. Once microgravity conditions were established, the partition was retracted in 23 s. Although not in the center of the cell, the interface formed was reasonably plane. A strong initial interfacial convection was induced, which lasted for 43 s and suddenly stopped; 79 s later, interfacial convection occurred in steps. Periods of intense activity alternated with relatively long periods of almost no activity. This pseudoperiodic transfer of matter was driven by the Marangoni effect. It led to concentration of acetone of 24 vol in water at the end of the microgravity period, and the interface progressed towards the toluene. In a similar carried out on Earth, the transfer of acetone after the decay of the perturbations induced by the retraction of the partition was only driven by diffusion since the configuration was stable with respect to the density differences. Also, the influence of the partition motion and the extent of the Schlieren are less important than in microgravity. The qualitative results of these experiments appear to be in contradiction with the prediction of the theory of Sternling and Scriven. ESA

N91-31330# Technische Univ., Berlin (Germany, F.R.). Inst. fuer Nichtmetallische Anorganische Werkstoffe.
THERMALLY INDUCED INTERFACIAL CONVECTION (TEXUS 4)
R. Brueckner *In* ESA, Summary Review of Sounding Rocket Experiments in Fluid Science and Materials Sciences: TEXUS 1 to 20; MASER 1 and 2 Feb. 1991 p 42-43 (For primary document see N91-31321 23-29)
Copyright Avail: NTIS HC/MF A15; EPD, ESTEC, Noordwijk, Netherlands, HC 75 Dutch guilders

The Technological Experiments Under Microgravity (TEXUS) 4 experiment to study the stability of a liquid/liquid interface submitted to a thermal gradient is summarized. The experimental cell was 28 mm high, 30 mm wide, and 10 mm deep with the front and the back walls made of optical glass. One lateral wall was heated in order to achieve a temperature difference of 30 C across the cell. The cell contained identical volumes of n-dodecan and water which were initially separated by a movable partition. After a delay of 180 s in microgravity to allow, first, the decay of the convection generated in the liquids by the launch and despin of the rocket and, secondly, the establishment of a linear thermal gradient, the partition was to be retracted to create a liquid/liquid interface. The cell was observed by means of a He-Ne laser differential interferometer. The fringe patterns were recorded with a 16 mm camera. During ground reference tests, the interferograms showed that uniform regions are established in the liquids with boundary layers at the set walls. The retraction of the partition failed. However, the interferograms recorded in microgravity showed that the establishment of a linear thermal gradient required about 100 s whereas numerical simulations indicated that the convection in the liquids was damped about 15 s after the beginning of the microgravity period. The time needed for the establishment of a linear temperature profile is therefore the determining factor for the timing of such experiments. ESA

N91-31331# Technische Univ., Berlin (Germany, F.R.). Inst. fuer Nichtmetallische Anorganische Werkstoffe.
DIFFUSION-INDUCED INTERFACIAL CONVECTION (TEXUS 8)
R. Brueckner and H. Christ *In* ESA, Summary Review of Sounding Rocket Experiments in Fluid Science and Materials Sciences: TEXUS 1 to 20; MASER 1 and 2 Feb. 1991 p 44 (For primary document see N91-31321 23-29)
Copyright Avail: NTIS HC/MF A15; EPD, ESTEC, Noordwijk, Netherlands, HC 75 Dutch guilders

The Technological Experiments Under Microgravity (TEXUS) 8 experiment to investigate the reverse of TEXUS 3, i.e. transport of acetone from a water acetone mixture into toluol, which, according to theory, should result in different convection modes at the interface, is summarized. The same acetone concentration (water to acetone: 1 to 2 in volume) as in the previous experiment was chosen in order to obtain quantitatively comparable results. The cell was also observed through a Schlieren optics system with a cine camera. The formation and continuous growth of two convection cells on each side of the interface was observed for about 40 s after withdrawing the partition. Then one cell was progressively absorbed by its neighbor on each side of the interface. The two remaining cells continued to grow further, until filling the whole volume of liquid with a double whirl, which disappeared as the concentration equilibrium was reached. The results obtained were in qualitative agreement with theory (Sterling and Scriven, Sanfeld et al). The magnitude of the vortices estimated on the basis of the theory was only derived for low concentrations, whereas large concentrations were used in the experiment. ESA

N91-31332# Technische Univ., Berlin (Germany, F.R.). Inst. fuer Nichtmetallische Anorganische Werkstoffe.
DIFFUSION-INDUCED INTERFACIAL CONVECTION (TEXUS 11)
R. Brueckner and H. Christ *In* ESA, Summary Review of Sounding Rocket Experiments in Fluid Science and Materials Sciences: TEXUS 1 to 20; MASER 1 and 2 Feb. 1991 p 46-47 (For primary document see N91-31321 23-29)
Copyright Avail: NTIS HC/MF A15; EPD, ESTEC, Noordwijk, Netherlands, HC 75 Dutch guilders

The Technological Experiments Under Microgravity (TEXUS) 11 experiment, which was the third experimental study on the concentration dependence of mass transfer by convection at the interface between two fluids using the model system toluol water acetone and aimed at studying the transfer of acetone from an aqueous solution into toluol but with an initial acetone concentration difference reduced to 30 vol in order to investigate the instability mechanisms involved when the concentration equilibrium is approached, is summarized. The main result of this analysis is that the instability observed during this experiment and also during the TEXUS 8 experiment is not oscillatory. The oscillations are imposed due to purely hydrodynamical effects. Nevertheless, this non-oscillatory instability becomes weaker and weaker when the concentration equilibrium is approached, and disappears when two diffusion layers with sufficient thickness are built. ESA

N91-31333# Justus Liebig-Univ., Giessen (Germany, F.R.). Physikalisches Inst.1.
OSCILLATORY MARANGONI CONVECTION (TEXUS 3A AND 3B)
D. Schwabe and A. Scharmann *In* ESA, Summary Review of Sounding Rocket Experiments in Fluid Science and Materials Sciences: TEXUS 1 to 20; MASER 1 and 2 Feb. 1991

p 48-51 (For primary document see N91-31321 23-29)
Copyright Avail: NTIS HC/MF A15; EPD, ESTEC, Noordwijk, Netherlands, HC 75 Dutch guilders

The Technological Experiments under Microgravity (TEXUS) 3A and 3B Experiemts to study the Marangoni convection in a floating zone held between two plates are summarized. The transition from a laminar to an oscillatory regime occurs on Earth when a critical temperature difference is imposed between the two plates, and when a critical Marangoni number is reached. The experiment aimed at verifying the occurrence of such a transition under microgravity conditions. Since the same oscillatory regime of Marangoni convection occurred under microgravity conditions and on Earth, it was concluded that the thermocapillary convection does not need interaction with buoyancy forces to become time dependent. ESA

N91-31334# Justus Liebig-Univ., Giessen (Germany, F.R.). Physikalisches Inst. 1.
CRITICAL MARANGONI NUMBER (TEXUS 5)
D. Schwabe and A. Scharmann *In* ESA, Summary Review of Sounding Rocket Experiments in Fluid Science and Materials Sciences: TEXUS 1 to 20; MASER 1 and 2 Feb. 1991 p 52-53 (For primary document see N91-31321 23-29)
Copyright Avail: NTIS HC/MF A15; EPD, ESTEC, Noordwijk, Netherlands, HC 75 Dutch guilders

The Technological Experiments Under Microgravity (TEXUS) 5 experiment to determine the transition from steady to oscillatory Marangoni flow in a floating zone corresponding to a critical Marangoni number is summarized. A cylindrical sample of NaNO3 (diameter 6 mm, length 3.7 mm) held between two independently heated graphite supports of the same diameter was investigated both on Earth and in space. The sample was melted and the temperature difference dT between the graphite supports was increased during 120 s at a rate of 0.1 C/s, starting from dT = 10 C. The transition from steady to oscillatory flow was detected by means of a thermocouple located in the middle of the melt. The microgravity experiment was slightly disturbed by the vibrations of the cine cameras of a neighboring experiment and the exactly identical critical Marangoni numbers measured on ground and in microgravity are interpreted as accidental. The spectrum of oscillation frequencies at 1 g and 0 g are comparable with a main frequency at 0.5 Hz. However, the precision of the measure at 0 g is reduced by low and high frequency noise besides this main frequency. ESA

N91-31335# Justus Liebig-Univ., Giessen (Germany, F.R.). Physikalisches Inst. 1.
CRITICAL MARANGONI NUMBER (TEXUS 8)
D. Schwabe and A. Scharmann *In* ESA, Summary Review of Sounding Rocket Experiments in Fluid Science and Materials Sciences: TEXUS 1 to 20; MASER 1 and 2 Feb. 1991 p 54-55 (For primary document see N91-31321 23-29)
Copyright Avail: NTIS HC/MF A15; EPD, ESTEC, Noordwijk, Netherlands, HC 75 Dutch guilders

The Technological Experiments Under Microgravity (TEXUS) 8 Experiment to investigate the transition from steady to oscillatory Marangoni convection in a floating zone is summarized. A floating zone of NaNO3 (melting point 307 C, radius 3 mm, length 3.2 mm) was formed between to coaxial cylindrical heaters under microgravity conditions. After melting and thermal equilibration, the temperature difference between the heaters was increased from 15 to 35 C at a rate of 0.085 C/s. A thermocouple located in the center of the zone was employed to detect the transition from steady to oscillatory Marangoni convection. A ground reference experiment was carried out for comparison. The critical temperature difference in microgravity was 22.7 C whereas it was 27.3 C on Earth. The corresponding critical Marangoni numbers are 8500 and 10,200. The critical Marangoni number is definitely smaller in microgravity than on Earth. The oscillation frequencies are also smaller in microgravity. Since the zones were heated from above, these results could be explained by the stabilizing effect of gravity. ESA

N91-31336# Deutsche Forschungs- und Versuchsanstalt fuer Luft- und Raumfahrt, Goettingen (Germany, F.R.).
THERMAL MARANGONI CONVECTION IN A FLOATING ZONE (TEXUS 3)
C.-H. Chun and W. Wuest *In* ESA, Summary Review of Sounding Rocket Experiments in Fluid Science and Materials Sciences: TEXUS 1 to 20; MASER 1 and 2 Feb. 1991 p 56-57 (For primary document see N91-31321 23-29)
Copyright Avail: NTIS HC/MF A15; EPD, ESTEC, Noordwijk, Netherlands, HC 75 Dutch guilders

The Technological Experiments Under Microgravity (TEXUS) 3 Experiment to observe thermally induced Marangoni convection under microgravity conditions is summarized. A floating zone of silicone oil (10 mm high and 10 mm in diameter) was formed under microgravity conditions between the flat ends of two copper rods. One rod was fixed while the other rod was progressively moved on the required 10 mm in 30 s. The silicone oil, containing Ti and TiO2 tracer particles, was transferred from a reservoir into the floating zone. The floating zone was left at rest before the movable rod was heated, first up to 36 C for 2 mm, then up to 48 C. A laser beam, 0.1 mm thick, illuminated a meridian plane of the zone which was observed with a 16 mm cine camera. The temperature differences recorded between the two rods were first 7.8 and then 18.9 C. The corresponding Marangoni numbers were 6000 and 16,000 respectively. Although the particles had a tendency to stick to the rods, they allowed the visualization of the convective flows in the floating zone. A thin thermal boundary layer could be observed along the gas/liquid interface (Marangoni layer). In the case of the high thermal gradient, two velocity maxima could be measured near the hot and cold ends of the zone. This was in agreement with the theoretical predictions. A smaller corner vortex embedded in the large vortex could also be clearly observed. ESA

N91-31337# Deutsche Forschungs- und Versuchsanstalt fuer Luft- und Raumfahrt, Goettingen (Germany, F.R.).
OSCILLATORY AND TURBULENT FLOW REGIMES DUE TO MARANGONI CONVECTION (TEXUS 7)
C.-H. Chun *In* ESA, Summary Review of Sounding Rocket Experiments in Fluid Science and Materials Sciences: TEXUS 1 to 20; MASER 1 and 2 Feb. 1991 p 58-59 (For primary document see N91-31321 23-29)
Copyright Avail: NTIS HC/MF A15; EPD, ESTEC, Noordwijk, Netherlands, HC 75 Dutch guilders

The Technological Experiments Under Microgravity (TEXUS) 7 Experiment aimed at determining whether, at Marangoni numbers far beyond the critical one, Marangoni convection in a circular floating zone remains oscillatory or becomes turbulent is summarized. The influence of the aspect ratio 1/d of the floating zone on the instabilities was also to be investigated. Two cylindrical floating zones of methanol of 3.3 mm and 10 mm in length were investigated, which correspond respectively to Marangoni numbers of 9,4000 and 12,4000. In the first zone, and for a temperature difference of 7.6 C, a regular oscillatory flow was detected with three distinct frequencies (0.59, 0.86, 1.16 Hz). The Marangoni vortex close to the surface can be seen on the film traveling up and down. Both when the zone length was increased up to 10 mm and when the temperature difference was increased up to 10 C, irregular fluctuations occurred which had no distinct frequency and correspond on the film to a clearly full turbulent convection with large structure fluctuations. Employing a physical model concept, the criteria for the occurrence of higher oscillation modes and for their development into turbulent non periodic structures, including the influence of the aspect ratio, were shown. ESA

N91-31338# Brussels Univ. (Belgium). Chemical Physics.
INFLUENCE OF A SURFACE TENSION MINIMUM ON THE MARANGONI EFFECT (TEXUS 8) ESA
J. C. Legros, G. Petre, and M. C. Limbourg-Fontaine *In* ESA, Summary Review of Sounding Rocket Experiments in Fluid Science and Materials Sciences: TEXUS 1 to 20; MASER 1 and 2 Feb. 1991 p 60-61 (For primary document see N91-31321 23-29)

Copyright Avail: NTIS HC/MF A15; EPD, ESTEC, Noordwijk, Netherlands, HC 75 Dutch guilders

Some liquid systems have the particular property to present a surface tension minimum as a function of temperature, at which the Marangoni number vanishes. It was expected that, in microgravity, the remaining motions would be slowed down and their pattern would be strongly modified. Also, the onset of oscillatory convection can occur only at higher temperature differences. The Technological Experiments Under Microgravity (TEXUS) 8 Experiment, which aimed to confirm that the velocity field is reversed in the temperature range where the surface tension increases with temperature, is summarized. The cell employed to observe the motions at the surface and in the bulk of an aqueous solution of n-heptanol was 3 cm long, 2 cm high, and 1 cm wide. Special attention was paid to avoiding the contamination of the solution. The side walls were heated prior to the launch up to 45 and 65 C respectively (minimum surface tension at 40 C). Anticreeping barriers allowed the retention of a plane surface when filling the cell with 3 cc of solution under microgravity conditions. Tracer particles were included in the solution. The whole process was recorded by a 16 mm cine camera. As expected, the tracers moved from the cold region (low surface tension) towards the hot region (high surface tension) of the surface and their motion started near the hot wall. A single convection cell grew but the microgravity period was too short to reach a steady state. With temperatures measured at the side walls of the cell of respectively 46 and 66 C, the velocity at the surface of the liquied was 0.8 mm/s about five minutes after the cell was filled. At steady state on ground, the velocities were of the order of 5 mm/s. ESA

N91-31339# Brussels Univ. (Belgium). Chemical Physics.
INFLUENCE OF A SURFACE TENSION MINIMUM ON THE MARANGONI EFFECT (TEXUS 9) ESA
J. C. Legros, G. Petre, and M. C. Limbourg-Fontaine *In* ESA, Summary Review of Sounding Rocket Experiments in Fluid Science and Materials Sciences: TEXUS 1 to 20; MASER 1 and 2 Feb. 1991 p 62-63 (For primary document see N91-31321 23-29)
Copyright Avail: NTIS HC/MF A15; EPD, ESTEC, Noordwijk, Netherlands, HC 75 Dutch guilders

The previous experiment confirmed that the motion induced by the thermal Marangoni effect at the free surface of a fluid is oriented from the cold towards the hot region when the surface tension increases with temperature. The Technological Experimemnts Under Microgravity (TEXUS) 9 Experiment, aimed at observing the behavior of a fluid presenting a surface tension minimum (as a function of temperature) in the middle of its free surface, in anticipation of a D-1 experiment, is summarized. Unexpectedly, a convection cell developed in the hot region only, with a motion from the cold to the hot region on two thirds of the surface. The order of magnitude of the velocity was 0.5 mm/s at the free surface after five minutes of heating. The remaining third of the surface in the cold region was almost at rest. However, no steady state could be reached due to the short duration of the microgravity period. The same occurred on Earth, where the 'opening of the surface' is also numerically predicted when the temperature of the walls is respectively lower and higher than the temperature corresponding to the surface tension minimum. Only a motion from the cold to the hot part was observed. However, velocity gradients were higher than in microgravity. As the temperature at the free surface was not measured, no quantitative analysis could be achieved. ESA

N91-31340# Brussels Univ. (Belgium). Chemical Physics.
INFLUENCE OF A SURFACE TENSION MINIMUM ON THE MARANGONI EFFECT (TEXUS 19) ESA
M. C. Limbourg-Fontaine, J. C. Legros, and G. Petre *In* ESA, Summary Review of Sounding Rocket Experiments in Fluid Science and Materials Sciences: TEXUS 1 to 20; MASER 1 and 2 Feb. 1991 p 64-65 (For primary document see N91-31321 23-29)
Copyright Avail: NTIS HC/MF A15; EPD, ESTEC, Noordwijk, Netherlands, HC 75 Dutch guilders

The Technological Experiments Under Microgravity (TEXUS) 19 Experiment, aimed at a quantitative investigation of the convection in a layer of a liquid presenting a surface tension minimum at the temperature Tm, submitted to a thermal gradient parallel to its free surface and with T1 less than TM less than T2, is summarized. Velocities were measured at the middle of the liquid/gas interface and close to the hot side. The velocity at the interface was a maximum before the inversion of the large central roll. After the inversion, the velocity was about one third of the maximum value and remained stable up to the end of the experiment. The interpretation of a single interferogram with some assumptions about the fluid temperature at the sides of the cell showed that the surface tension minimum is close to the point where the surface opens between two contrarotative rolls. The main actual result is the inversion of the flow direction at the interface in the presence of a surface tension minimum. It is not yet possible to ascertain whether the inversion is due to the displacement along the interface of the isotherm Tm corresponding to the surface tension minimum. Also, the influence of the gaseous phase on the surface concentration is not clear and could have contributed to the inversion. ESA

N91-31341# Naples Univ. (Italy). Inst. U. Nobile.
THERMAL MARANGONI CONVECTION IN A FLOATING ZONE (TEXUS 9) ESA
R. Monti, G. Mannara, and L. G. Napolitano *In* ESA, Summary Review of Sounding Rocket Experiments in Fluid Science and Materials Sciences: TEXUS 1 to 20; MASER 1 and 2 Feb. 1991 p 66-67 (For primary document see N91-31321 23-29)
Copyright Avail: NTIS HC/MF A15; EPD, ESTEC, Noordwijk, Netherlands, HC 75 Dutch guilders

The Technological Experiments Under Microgravity (TEXUS) 9 Experiment to collect quantitative data on transient thermofluid dynamic fields in floating zones at high Peclet (or Marangoni) numbers is summarized. A liquid bridge (1.8 cm long 1.8 cm in diameter) of silicone oil seeded with tracers (150 microns in diameter) was established between two copper disks under microgravity conditions. One disk was heated and the other was equipped with thermocouples for heat flux measurements. A set of five thermocouples was immersed in the zone 40 s after its formation to detect the temperature fluctuations in the liquid. A meridian section of the zone was illuminated by a laser beam and observed with a cine camera. The results seem to indicate that the onset of turbulence occurs first in the boundary layer near the free surface. Then oscillations are triggered through the coupling with the temperature field. The transition could be predicted when the surface Reynolds number reaches a critical value. ESA

N91-31342# Naples Univ. (Italy). Inst. U. Nobile.
EXPERIMENTAL RESULTS ON MICROGRAVITATIONAL FLUID DYNAMICS (TEXUS 14b) ESA
R. Monti and R. Fortezza *In* ESA, Summary Review of Sounding Rocket Experiments in Fluid Science and Materials Sciences: TEXUS 1 to 20; MASER 1 and 2 Feb. 1991 p 68-73 (For primary document see N91-31321 23-29)
Copyright Avail: NTIS HC/MF A15; EPD, ESTEC, Noordwijk, Netherlands, HC 75 Dutch guilders

The Technological Experiments Under Microgravity (TEXUS) 14b Experiment to study the onset of Marangoni oscillations in a liquid bridge but with lower heating rates than in the previous experiment is summarized. Telescience was implemented in order to maximize the results obtained within the microgravity period available. The possibility of modifying parameters during the flight permitted the definition of a flexible experimental procedure. As anticipated, the onset of oscillations was observed twice during the flight. The microgravity period ended before the decay of the second oscillating regime. The velocity field 197 s after liftoff was deduced from the tracer motions, and is shown. The onset of oscillations is related to the value of the dynamic Weber number using criterion based on experimental observations and on plausible causes for the transition to occur. Numerical calculations were performed with the temperature/time profiles of the supports as inputs and compared with the experimental results. ESA

N91-31343# Groningen Rijksuniv. (Netherlands). Dept. of Chemical Engineering.
THREE-DIMENSIONAL MARANGONI CONVECTION (MASER 1) ESA
J. H. Lichtenbelt and H. A. Dijkstra *In* ESA, Summary Review of Sounding Rocket Experiments in Fluid Science and Materials Sciences: TEXUS 1 to 20; MASER 1 and 2 Feb. 1991 p 74-75 (For primary document see N91-31321 23-29)
Copyright Avail: NTIS HC/MF A15; EPD, ESTEC, Noordwijk, Netherlands, HC 75 Dutch guilders

Mass transfers are of great importance in technological processes but the theoretical models used generally assume linear variations of the mass transfer coefficients. In fact, surface tension and density effects induce convection flows in the liquids, usually thin films, which deeply modify these coefficients. The Materials Science Experiment Rocket (MASER) 1 experiment to visualize Marangoni convection flows coupled to a mass transfer from a liquid to a gas is summarized. The results are interpreted as depending on the air flow velocity. For high air flows, the acetone concentration is approximately zero in the bubble and the convection pattern originates from Marangoni instabilities; for small air flows, the acetone concentration in the gas increases along the bubble and generates concentration and thus surface tension gradients at the liquid surface (lower surface tension near the outlet pipe). ESA

N91-31344# Groningen Rijksuniv. (Netherlands). Dept. of Chemical Engineering.
THREE-DIMENSIONAL MARANGONI CONVECTION (MASER 2) ESA
L. P. B. M. Janssen and H. C. J. Hoefsloot *In* ESA, Summary Review of Sounding Rocket Experiments in Fluid Science and Materials Sciences: TEXUS 1 to 20; MASER 1 and 2 Feb. 1991 p 76-77 (For primary document see N91-31321 23-29)
Copyright Avail: NTIS HC/MF A15; EPD, ESTEC, Noordwijk, Netherlands, HC 75 Dutch guilders

Marangoni convection cells generated by mass transfer in the liquid bulk around a bubble were observed in previous microgravity experiments. The Material Science Experiment Rocket (MASER) 2 experiment to assess the influence of the bubble diameter on the convective patterns is summarized. Observations show that the convective patterns do depend on the bubble size. The differences to previous observations are interpreted as the result of air flow differences. The mechanical shear stress in the interface increases with an increasing air flow and becomes dominant in the case of the 5 and the 7 mm bubbles in this experiment. In the case of the 5 mm bubble in MASER 1 where the air flow was weaker, the surface tension effects counteracted this shear stress. The single spot Marangoni flows around the 3 mm bubble are not yet clearly understood but are thought to originate in microscale effects. ESA

N91-31345# Essen Univ. (Germany, F.R.). Fachbereich 12-Mechanik.
THERMOCAPILLARY DROP MOTION, 1 (MASER 1) ESA
G. Wozniak and J. Siekmann *In* ESA, Summary Review of Sounding Rocket Experiments in Fluid Science and Materials Sciences: TEXUS 1 to 20; MASER 1 and 2 Feb. 1991 p 78-79 (For primary document see N91-31321 23-29)
Copyright Avail: NTIS HC/MF A15; EPD, ESTEC, Noordwijk, Netherlands, HC 75 Dutch guilders

The Material Science Experiment Rocket (MASER) 1 experiment to verify the experimental set up for the observation of the thermocapillary motion of droplets in a low gravity environment, to verify the current theory for droplets at low Reynolds (Re) and Marangoni (Mg) numbers and to collect data for the development of numerical models at higher Re and Mg, is summarized. Paraffin oil drops were injected in a 26 by 60 by 12 cu mm test cell filled with an aqueous ethanol solution and submitted to a thermal gradient. It is thought that the interfacial properties of the first drop were deeply affected by the prolonged contact with the ethanol solution prior to and during the launch and that no thermocapillary effect could occur. Evidently, the second drop was from pure paraffin oil. It is believed that its motion was exclusively due to the Marangoni effect and not residual accelerations. Its behavior was in accord with theoretical models. ESA

N91-31346# Essen Univ. (Germany, F.R.). Fachbereich 12-Mechanik.
THERMOCAPILLARY DROP MOTION, 2 (MASER 2) ESA
G. Wozniak and J. Siekmann *In* ESA, Summary Review of Sounding Rocket Experiments in Fluid Science and Materials Sciences: TEXUS 1 to 20; MASER 1 and 2 Feb. 1991 p 80-81 (For primary document see N91-31321 23-29)
Copyright Avail: NTIS HC/MF A15; EPD, ESTEC, Noordwijk, Netherlands, HC 75 Dutch guilders

The thermocapillary motion of a drop was observed in a previous microgravity experiment. A Material Science Experiment Rocket (MASER) 2 experiment aimed at collecting data to verify current theory at low Reynolds (Re) and Marangoni (Mg) numbers and to validate numerical models at higher Re and Mg is summarized. A 26 by 60 by 15 cu mm cell was filled with an ethanol aqueous solution and submitted to a thermal gradient. Unexpectedly, air bubbles of up to 56.5 mm in diameter entered into the cell during the launch and migrated towards the hot side wall of the cell once microgravity conditions were established. Although the temperature gradients measured at both lateral walls were nominal, it is possible that the air bubbles partly isolated the heating wall, thus decreasing locally the thermal gradient. After a 5 mm microgravity period, the injection needle was pushed into the cell through a membrane. Three successive bubbles were formed properly, which ranged from 1.6 to 2.4 mm in diameter. All of them migrated as expected towards the hot side of the cell and parallel to the thermal gradient. The results showed that the current theory at low Re and Mg is a good approximation. However, uncertainties remained with regard to the gradient and the liquid properties, which prevented the validation of numerical models. ESA

N91-31347# Forschungsinstitut fuer Edelmetalle und Metallchemie, Schwaebisch Gmuend (Germany, F.R.).
ELECTROLYTIC HYDROGEN FORMATION (TEXUS 1)
C. J. Raub and W. Wospernov *In* ESA, Summary Review of Sounding Rocket Experiments in Fluid Science and Materials Sciences: TEXUS 1 to 20; MASER 1 and 2 Feb. 1991 p 84-85 (For primary document see N91-31321 23-29)
Copyright Avail: NTIS HC/MF A15; EPD, ESTEC, Noordwijk, Netherlands, HC 75 Dutch guilders

The Technological Experiments Under Microgravity (TEXUS) 1 experiment to observe electrolytic formation of hydrogen under microgravity conditions is summarized. Due to the abscence of buoyancy forces, the hydrogen bubbles formed at the surface of the cathode should not be removed and the formation of a hydrogen film completely isolating the electrode could result. The electrolysis of a Na2SO4 solution with a Cu anode and a Au coated Pt cathode was achieved under microgravity conditions. The cell was observed with a cine camera. A residual rotation of the electrolyte could be observed during the two first minutes of the experiment. The bubbles formed at the surface of the cathode were smaller than under normal gravity thereby indicating that their coalescence can be hampered in microgravity. Part of this foam like layer of hydrogen bubbles migrated towards the top of the cell whereas dust particles stayed stable. This could be due to surface tension driven convection induced by a local heating by the illumination system or, most probably, to the residual accelerations of the rocket. The bubbles did not isolate the electrode and the potential drop through the cell at constant current was not altered. This indicated that the electrolyte films formed between the bubbles were still conducting. ESA

N91-31348# Forschungsinstitut fuer Edelmetalle und Metallchemie, Schwaebisch Gmuend (Germany, F.R.).
ELECTROLYTICALLY GENERATED HYDROGEN BUBBLES (TEXUS 6) Abstract Only
C. J. Raub *In* ESA, Summary Review of Sounding Rocket Experiments in Fluid Science and Materials Sciences: TEXUS 1

to 20; MASER 1 and 2 Feb. 1991 p 86 (For primary document see N91-31321 23-29)
Copyright Avail: NTIS HC/MF A15; EPD, ESTEC, Noordwijk, Netherlands, HC 75 Dutch guilders

The Technological Experiments Under Microgravity (TEXUS) 6 experiment to observe the nucleation, growth and coalescence of hydrogen bubbles on a cathode under microgravity is summarized. It was also expected to observe the passivation of the electrode. The electrolysis at constant current of a Na2SO4 solution was achieved under microgravity conditions. The formation of hydrogen bubbles on both an Au and a Pt cathode was observed with a cine camera. The growth of the hydrogen bubbles was most rapid at the initial stage since the supersaturation is the largest during, and just after, the nucleation. The size of the bubbles depended on the cathode material. When a bubble separated from the electrode, its size decreased with time due to the dissolution of the hydrogen in the electrolyte. The bubbles are uncharged, as determined by means of additional electrodes. Neither a passivation, nor a variation of the potential drop over the cell were induced when the cathode was recovered by hydrogen bubbles. This unexpected result indicated that electrolytic processes under microgravity conditions may well be viable.
ESA

N91-31349# Kiel Univ. (Germany, F.R.). Metallkunde-Labor.
INTERMITTENT POLARIZATION (TEXUS 2)
G. Mix *In* ESA, Summary Review of Sounding Rocket Experiments in Fluid Science and Materials Sciences: TEXUS 1 to 20; MASER 1 and 2 Feb. 1991 p 88-89 (For primary document see N91-31321 23-29)
Copyright Avail: NTIS HC/MF A15; EPD, ESTEC, Noordwijk, Netherlands, HC 75 Dutch guilders

The Technological Experiments Under Microgravity (TEXUS) 2 experiment to study the influence of convection on the electrochemical corrosion is summarized. The corrosion of Cu electrodes immersed in a 1 m KCL solution was investigated in two cells. Tylose was added in one cell in order to increase the viscosity of the solution. A voltage of 100 mV was intermittently applied to the cells before, during, and after the launch and during the reentry of the rocket. The intensity through the cells during on cycles and the voltage drop during off cycles were recorded. Tylose additions effectively reduce the convection, since little influence of gravity was detected in the corresponding cell. In the other cell, the influence of an increased gravity level, during the launch, was clearly visible. After the damping of the residual convection during the microgravity phase, the results indicated the spreading of a diffusion boundary layer. This layer yielded a marginal current at the end of the polarization phases 40 less than on Earth. The increasing gravity level during the reentry of the rocket rapidly had a strong effect on the convection in the cell and thus on the current values.
ESA

N91-31350# Battelle Inst., Frankfurt am Main (Germany, F.R.).
DISPERSION LAYERS BY ELECTRODEPOSITION (TEXUS 1)
J. Ehrhardt *In* ESA, Summary Review of Sounding Rocket Experiments in Fluid Science and Materials Sciences: TEXUS 1 to 20; MASER 1 and 2 Feb. 1991 p 90-91 (For primary document see N91-31321 23-29)
Copyright Avail: NTIS HC/MF A15; EPD, ESTEC, Noordwijk, Netherlands, HC 75 Dutch guilders

The Technology Experiments Under Microgravity (TEXUS) 1 experiment to assess the suitability of a microgravity environment for the investigation of the electrodeposition of dispersions and to study the behavior of the suspended particles during the electrolysis is summarized. A suspension of alpha Al2O3 (10 g/l, about 0.3 microns in diameter) in a Ni(NH2SO3)2, 4H2O based electrolyte was investigated. The suspension was stirred during the ascent phase of the rocket and electrolysis was started shortly after microgravity conditions were established. A 5 micron thick Ni layer containing Al2O3 particles was deposited on the profiled cathode. However, the stirring unit did not work as expected, and the concentration of suspended particles was too low. Conclusions could be drawn on the behavior of the particles in the electrolyte from their distribution in the deposited Ni layer. The electric current appeared to be 10 less efficient than an Earth (more hydrogen was formed) but the throwing power of the electrolyte was higher. The corrosion resistance of the layer deposited under microgravity conditions was much higher. It was thus demonsrated that it is possible to perform electrodeposition experiments under microgravity conditions and to investigate the incorporation of particles in the absence of buoyancy-driven convection and sedimentation.
ESA

N91-31351# Battelle Inst., Frankfurt am Main (Germany, F.R.).
DISPERSION ELECTROLYSIS (TEXUS 4)
J. Ehrhardt *In* ESA, Summary Review of Sounding Rocket Experiments in Fluid Science and Materials Sciences: TEXUS 1 to 20; MASER 1 and 2 Feb. 1991 p 92-93 (For primary document see N91-31321 23-29)
Copyright Avail: NTIS HC/MF A15; EPD, ESTEC, Noordwijk, Netherlands, HC 75 Dutch guilders

The Technological Experiments Under Microgravity (TEXUS) 4 experiment to clarify whether the particles coagulate in microgravity or drift towards the cathode separately as on Earth, and to get a thorough knowledge of mechanisms which would allow the improvement of ground processes, is summarized. A suspension of Al2O3 particles (about 0.3 microns in diameter) in a Ni sulphamate electrolyte was investigated. The electric current through the cell, as well as the gas pressure and the temperature variations in the cell, were recorded. Hydrogen bubbles formed at the cathode during the electrolysis. The layer deposited in microgravity was partially detached due to the contamination of the gold coated cathode before the launch. It appeared that, in space, the particles also drifted towards the cathode without any prior coagulation, as in Earth based experiments. The 7 micron thick Ni layer deposited in microgravity contained a more homogeneous distribution of particles. It also had a higher density than the 7 to 9 micron thick layer obtained on Earth, which had a surface density of particles of 40,000/sq cm. In addition, the layer deposited in space was almost amorphous and was much less prone to corrosion by artificial sea water than the layer deposited on Earth. In the latter, the Ni grains were large enough to exhibit a crystalline behavior.
ESA

N91-31352# Battelle Inst., Frankfurt am Main (Germany, F.R.).
DISPERSION ELECTROLYSIS (TEXUS 7)
J. Ehrhardt and G. Walter *In* ESA, Summary Review of Sounding Rocket Experiments in Fluid Science and Materials Sciences: TEXUS 1 to 20; MASER 1 and 2 Feb. 1991 p 94-95 (For primary document see N91-31321 23-29)
Copyright Avail: NTIS HC/MF A15; EPD, ESTEC, Noordwijk, Netherlands, HC 75 Dutch guilders

The Technological Experiments Under Microgravity (TEXUS) 7 experiment aimed at determining whether particle transport is dominated by electrophoresis or is mainly driven by diffusion is summarized. The deposition of Ni from an electrolyte containing Al2O3 particles onto a highly clean, gilt brass cathode was investigated both under microgravity conditions and on the ground. Contrary to the previous experiment, the development of hydrogen bubbles could be avoided and a high current efficiency (about 98 percent) was reached. But surprisingly, except for a few loosely built agglomerates, almost no Al2O3 particles were deposited with the well adherent, totally crack free and 89 microns thick Ni layer. Particle coagulation also occurred on Earth. Since the available time (340 s) was too short to allow the diffusion of the agglomerates and as only a few of them got embedded in the Ni layer, it was concluded that electrophoresis is not the dominating force of the transport. Furthermore, since in this experiment the cathode surface was free from hydrogen bubbles, it was concluded that, in the previous experiment, the single particles which were codeposited with the Ni layer were detached from loosely coagulated particles by motions in the electrolyte induced by the formation of the hydrogen bubbles.
ESA

N91-31353# Battelle Inst., Frankfurt am Main (Germany, F.R.).
DISPERSION ELECTROLYSIS (TEXUS 9)

J. Ehrhardt *In* ESA, Summary Review of Sounding Rocket Experiments in Fluid Science and Materials Sciences: TEXUS 1 to 20; MASER 1 and 2 Feb. 1991 p 96-97 (For primary document see N91-31321 23-29)
Copyright Avail: NTIS HC/MF A15; EPD, ESTEC, Noordwijk, Netherlands, HC 75 Dutch guilders

Previous space experiments showed that the coagulation of particles prevents their deposition in an electrolytically deposited metallic layer. They also showed that a very weak shear stress should be sufficient to separate single particles which are then deposited. The Technological Experiments Under Microgravity (TEXUS) 9 experiment to verify this assumption by performing the electrolysis in two phases, first with the electrolyte at rest and then with a smooth stirring, is summarized. The electrolysis of a solution of nickel sulphate containing alpha-Al2O3 particles (60 g/l, 0.3 microns in size) with an anode of nickel (30 sq cm) and a disk shaped cathode of brass (10 sq cm) was investigated under microgravity conditions and on Earth. During the first phase, the electrolyte was kept still and the suspended particles coagulated very fast as expected, so that no single particles were available for codeposition. During the second phase, the electrolyte was mechanically stirred and single particles were incorporated in the deposited Ni layer. The experiment showed that, in microgravity, a weak shearing force is sufficient to release single particles from noncompact coagulates for galvanic codeposition. ESA

N91-31354# Technische Univ., Munich (Germany, F.R.). Inst. A fuer Thermodynamik.
NUCLEATE POOL BOILING (TEXUS 3)
J. Straub and A. Weinzierl *In* ESA, Summary Review of Sounding Rocket Experiments in Fluid Science and Materials Sciences: TEXUS 1 to 20; MASER 1 and 2 Feb. 1991 p 98-99 (For primary document see N91-31321 23-29)
Copyright Avail: NTIS HC/MF A15; EPD, ESTEC, Noordwijk, Netherlands, HC 75 Dutch guilders

As soon as the value of the gravity related components exceeds zero, the following heat transfer mechanisms are involved: free convection; enthalpy transfer by buoyancy induced detachment; and flotation of bubbles. In order to elucidate the relative contributions of these mechanisms, the behavior of bubbles on boiling and the related heat transfer were investigated in microgravity. For a duration of 360 s, all gravity related mechanisms can be physically decoupled, so that the experiment can concentrate on the three main heat and matter transfer mechanisms, which are: evaporation/condensation; interface convection; and heat conduction. Steady nucleate boiling was established within 0.5 s. The pressure increase was about 5000 Pa. The bubbles moved along the wire during their lifetime of a few tenths of a second, and mass transport by evaporation/condensation could be observed. The heat transfer coefficient appeared to be equal or even greater in the absence of gravity. These results proved the dominating role of Marangoni convection in the boiling heat transport in microgravity. ESA

N91-31355# Technische Univ., Munich (Germany, F.R.). Inst. A fuer Thermodynamik.
BUBBLE FORMATION, 1 (TEXUS 5)
J. Straub and A. Weinzierl *In* ESA, Summary Review of Sounding Rocket Experiments in Fluid Science and Materials Sciences: TEXUS 1 to 20; MASER 1 and 2 Feb. 1991 p 100-101 (For primary document see N91-31321 23-29)
Copyright Avail: NTIS HC/MF A15; EPD, ESTEC, Noordwijk, Netherlands, HC 75 Dutch guilders

The previous boiling experiment showed the occurrence of a steady state heat transfer under microgravity conditions. An experiment aimed at investigating several heat fluxes into a subcooled liquid in order to observe the onset of boiling, and condensation effects at the bubble surface is summarized. A stepwise increase up to 50 W/sq cm of the heat flux from a Pt wire (25 mm long, 0.2 mm in diameter) into subcooled Freon 113 (bulk temperature: 25 C) was achieved. Nine discrete heat fluxes were investigated under microgravity conditions. The bubble formation at the wire was recorded by a cine camera. Each power level was maintained constant for 13 s in order to reach a steady state. The onset of boiling started by the formation of a 'vapor hose' around the wire and at a superheating 25 higher than on Earth where a steady state is reached long before, owing to natural convection. After removal of the initial bubble, a steady state boiling occurred which was significantly stabilized by Marangoni convection at the surface of the bubbles. The steady state boiling heat transfer in subcooled Freon 113 seems to be almost independent of gravity. ESA

N91-31356# Technische Univ., Munich (Germany, F.R.). Inst. A fuer Thermodynamik.
BUBBLE FORMATION, 2 (TEXUS 10)
J. Straub and M. Zell *In* ESA, Summary Review of Sounding Rocket Experiments in Fluid Science and Materials Sciences: TEXUS 1 to 20; MASER 1 and 2 Feb. 1991 p 102-103 (For primary document see N91-31321 23-29)
Copyright Avail: NTIS HC/MF A15; EPD, ESTEC, Noordwijk, Netherlands, HC 75 Dutch guilders

A previous investigation of the boiling heat transfer from a heated platinum wire in microgravity had shown no significant change in steady state boiling compared with results on Earth. An experiment aimed at investigating the boiling heat transfer from a plate in order to assess the influence of the geometry of the heater is summarized. The experimental set up was therefore slightly modified for the investigation of the bubble nucleation, bubble dynamics, phase change, and Marangoni transport with respect to the stability of boiling heat transfer from a plate in microgravity. In microgravity, the onset of boiling in the subcooled liquid occurred at a superheating higher than on Earth but the activation of the first nucleation site required only 45 of the heat flux. Also, the spreading of nucleate boiling was 20 times faster than on Earth. However, the duration of the thermal transition to steady state increased up to several seconds, due to the long time required for the condensation of the initial 'vapor explosion'. When the heat input to the plate was increased above 5 W/sq cm, the limits of the heat transport mechanisms in microgravity (dissipation of the condensation enthalpy from the top of the bubbles towards the subcoolded bulk by thermocapillary flows and bubble dynamics) were exceeded and a film boiling regime was set up. The experiment ended with the burn out of the heater, as it was isolated by a layer of vapor. ESA

N91-31357# Technische Univ., Munich (Germany, F.R.). Inst. A fuer Thermodynamik.
BUBBLE FORMATION, 2. MICROGRAVITY MEASUREMENTS OF THE BOILING HEAT TRANSFER FROM FLAT HEATING SURFACES (TEXUS 11)
J. Straub and M. Zell *In* ESA, Summary Review of Sounding Rocket Experiments in Fluid Science and Materials Sciences: TEXUS 1 to 20; MASER 1 and 2 Feb. 1991 p 104-107 (For primary document see N91-31321 23-29)
Copyright Avail: NTIS HC/MF A15; EPD, ESTEC, Noordwijk, Netherlands, HC 75 Dutch guilders

An experiment to investigate the boiling process in a saturated liquid, during the transition from a saturated to a subcooled liquid, and in a subcooled liquid, is summarized. Results on saturated boiling, transition from saturated to subcooled boiling, and subcooled boiling are discussed. Conclusions are: on bubble formation and growth, the impulse forces are overcome by the adhesion forces on the heating surface; using subcooled boiling in microgravity, the condensation at the top of the bubble guarantees their stability but with a reduced critical heat flux; in the case of flat heating surfaces, the influence of Marangoni convection on the heat transfer seems to be negligible; and the current boiling process models, which are generally based on gravity mechanism, should be reconsidered especially regarding the real influence of gravity. ESA

N91-31358# Technische Univ., Munich (Germany, F.R.). Inst. A fuer Thermodynamik.
INST. A FUER THERMODYNAMIK.
J. Straub and M. Zell *In* ESA, Summary Review of Sounding

Rocket Experiments in Fluid Science and Materials Sciences: TEXUS 1 to 20; MASER 1 and 2 Feb. 1991 p 108-109 (For primary document see N91-31321 23-29)
Copyright Avail: NTIS HC/MF A15; EPD, ESTEC, Noordwijk, Netherlands, HC 75 Dutch guilders

An experiment designed to allow the observation of single vapor bubbles under different conditions in the liquid (saturated, subcooled) is summarized. The bubbles were formed at a spot heater (Au thin film on a glass substrate) where they grew under controlled thermal gradients. A differential interferometer was used for the determination of the temperature field around the bubble without contact and thermal inertia. The images were recorded with a cine camera. The spot heater temperature, the heat flux, the fluid temperature, and the pressure in the cell where also recorded. A quantitative analysis of the optical record was only possible during two short sequences where a single bubble could be generated in microgravity. With a low subcooling in microgravity, the bubbles grew fast and the intensity of the interfacial convection varied periodically. This is reflected by the temperature/time profile of the heating surface which is inversely proportional to the heat transfer coefficient. The minima which occurred periodically correspond to the ceasing of the interfacial convection. The observation of the dynamical behavior of the surface of vapor bubbles during boiling to be tested. ESA

N91-31359# Technische Hochschule, Aachen (Germany, F.R.). Inst. fuer Physikalische Chemie.
ULTRASOUND ABSORPTION IN MOLTEN SALTS (TEXUS 14b)
E. Kirschbaum and J. Richter *In* ESA, Summary Review of Sounding Rocket Experiments in Fluid Science and Materials Sciences: TEXUS 1 to 20; MASER 1 and 2 Feb. 1991 p 110-111 (For primary document see N91-31321 23-29)
Copyright Avail: NTIS HC/MF A15; EPD, ESTEC, Noordwijk, Netherlands, HC 75 Dutch guilders

An experiment to investigate the absorption of a 25 MHz ultrasound wave by a binary mixture of RbNO3 67 pct - AgNO3 33 pct (mole fraction) at a temperature of 230 C, on Earth and in a microgravity in convection free conditions, is summarized. A stainless steel cell was used which was equiped with optical glass windows and with a volume compensation system. The cell was preheated for 1.5 h before the launch in order to ensure well-stabilized thermal conditions during flight. The absorption coefficient deduced from the measurements was 19 pct higher in space than on the ground. This difference was well beyond the accuracy of the method. This was contrary to expectations, since the absence of convection should have led to higher intensities and thus lower absorption values. ESA

N91-31360# Technische Hochschule, Aachen (Germany, F.R.). Inst. fuer Physikalische Chemie.
ULTRASOUND ABSORPTION IN MOLTEN SALTS (TEXUS 17) ESA
E. Kirschbaum and J. Richter *In* ESA, Summary Review of Sounding Rocket Experiments in Fluid Science and Materials Sciences: TEXUS 1 to 20; MASER 1 and 2 Feb. 1991 p 112-113 (For primary document see N91-31321 23-29)
Copyright Avail: NTIS HC/MF A15; EPD, ESTEC, Noordwijk, Netherlands, HC 75 Dutch guilders

The previous experiment yielded unexpectedly low absorption values in microgravity. An experiment to confirm and extend the results is summarized. The same experimental hardware was used. A binary mixture of RbNO3 50 pct - AgNO3 50 pct (mole fraction) was investigated at a temperature of 230 C both on Earth and in microgravity. When compared with the ground results, the flight results showed again that a higher absorption of ultra sound (25 MHz) occurred in microgravity. The absorption coefficient deduced from the flight measurements was 14 pct higher than the one obtained on Earth, which was in agreement with the previous space results. These values cannot be explained as the result of the absence of convection in microgravity. In addition, the ground results were confirmed by using two different methods: the Debye-Sears method and the pulse transmission method and by performing measurements with the laboratory equipment (both methods) and in the flight module on the ground (Debye-Sears method). It is therefore believed that the higher absorption was strictly a microgravity effect whose further study may allow some insights into the structure of liquids. ESA

N91-31361# Chalmers Univ. of Technology, Goeteborg (Sweden).
THERMAL CONDUCTIVITY OF LIQUIDS (MASER 1) ESA
S. Aalto *In* ESA, Summary Review of Sounding Rocket Experiments in Fluid Science and Materials Sciences: TEXUS 1 to 20; MASER 1 and 2 Feb. 1991 p 114-115 (For primary document see N91-31321 23-29)
Copyright Avail: NTIS HC/MF A15; EPD, ESTEC, Noordwijk, Netherlands, HC 75 Dutch guilders

An experiment to measure the heat conductivity of ethanol by using the transient hot wire technique in the absence of gravity is summarized. In principle a thick heated layer should be obtained around the wire, which can however be destabilized by other effects than gravity driven ones. The difference between the data at the very beginning originated in the heating of the wire itself. Then, up to 13 s, the data were in good agreement, thereby yielding the value of the heat conductivity of ethanol: 0.179 plus or minus 0.0045 W/Km at 28 C. After 13 s, there was a slight change in slope and after 120 s, the wire temperature decreased drastically. This was interpreted as the result of the onset of a convective regime probably induced by the accumulation of the effects of the radial component of the residual accelerations of the rocket. ESA

N91-31362# Technische Univ., Eindhoven (Netherlands). Lab. of Colloid Chemistry.
COLLOID CHEMISTRY (TEXUS 17) ESA
H. N. Stein *In* ESA, Summary Review of Sounding Rocket Experiments in Fluid Science and Materials Sciences: TEXUS 1 to 20; MASER 1 and 2 Feb. 1991 p 116-117 (For primary document see N91-31321 23-29)
Copyright Avail: NTIS HC/MF A15; EPD, ESTEC, Noordwijk, Netherlands, HC 75 Dutch guilders

The coagulation of quartz particles (0.015 vol. pct. of quartz particles with a diameter of 1.25 microns in a 0.5 M NaCl solution) was investigated in nine cells under various shear rates. After homogenization of the solutions by ultrasonic mixing, four shear rates were achieved in duplicate under microgravity conditions in eight cells by means of rotating magnets stirring the liquid at different speeds: 0, 50, 100 and 200 rpm. In these eight cells, the transmission of a laser beam was measured, which yielded the evolution of the particle density with the time. In the ninth cell, the flow pattern in the liquid at different shear rates was recorded with a cine camera. Whereas the flight and ground results were comparable at 220 rpm the light transmission measurements increased further in microgravity (increased coagulation) than on Earth, at lower shear rate. Also, the shape of the curves was different. That the Brownian motions are more important in microgravity was not a satisfactory explanation of these results and nothing indicated that the damping of the residual flows should have been slower in the flight cells than in the same cells on the ground. ESA

N91-31363# Technische Univ., Clausthal-Zellerfeld (Germany, F.R.). Inst. fuer Nichtmetallische Werkstoffe.
REACTION KINETICS IN GLASS MELTS (TEXUS 1)
G. H. Frischat *In* ESA, Summary Review of Sounding Rocket Experiments in Fluid Science and Materials Sciences: TEXUS 1 to 20; MASER 1 and 2 Feb. 1991 p 120-121 (For primary document see N91-31321 23-29)
Copyright Avail: NTIS HC/MF A15; EPD, ESTEC, Noordwijk, Netherlands, HC 75 Dutch guilders

Two cylindrical samples of Na2O.3SiO2 and Rb2O.3SiO2, maintained in close contact, were remelted under microgravity conditions. An effective reaction temperature of 1160 C in the glass melts was achieved for an effective reaction time of 135 s. The samples were then rapidly cooled before the end of the microgravity period. The resulting diffusion profiles were analyzed

with an electron microprobe. The formation of gas bubbles at the interface between the samples caused local flow and some minor disturbances of the diffusion profiles. However, the interdiffusion coefficient which ranges between 0.000001 and 0.00001 cu cm/s depending on the concentration, could be determined. The precision was a significant improvement on the ground reference which was strongly influenced by buoyancy convection. ESA

N91-31364# Technische Univ., Clausthal-Zellerfeld (Germany, F.R.). Inst. fuer Nichtmetallische Werkstoffe.
REACTION KINETICS IN GLASS MELTS: CORROSION OF SiO2 (TEXUS 4)
G. H. Frischat, W. Beier, and M. Braedt *In* ESA, Summary Review of Sounding Rocket Experiments in Fluid Science and Materials Sciences: TEXUS 1 to 20; MASER 1 and 2 Feb. 1991 p 122-123 (For primary document see N91-31321 23-29)
Copyright Avail: NTIS HC/MF A15; EPD, ESTEC, Noordwijk, Netherlands, HC 75 Dutch guilders

An experiment to study the corrosion process of refractory materials by molten glasses, in the absence of buoyancy convection, is summarized. The corrosion of SiO2 glass by two different glass melts (Na2O.3SiO2 and Na2O.2SiO2) was investigated. An effective reaction temperature of 1420 C was achieved under microgravity conditions in an isothermal furnace and for an effective reaction time of 182 s. The SiO2 glass was transformed into cristobalite (crystalline phase). However, the diffusion controlled profiles were determined by means of an electronmicrophobe. The space samples exhibit the expected undisturbed profiles and the following interdiffusion coefficients could be evaluated: D equals 2.8 times 10 to the minus 7th power sq cm/s for Na2O.3SiO2; D equals 6 times 10 to the minus 7th power sq cm/s for Na2O.2SiO2. In contrast, the ground processed samples showed apparently shorter diffusion profiles and smaller interdiffusion coefficients, due the gravity driven convection. ESA

N91-31365# Technische Univ., Clausthal-Zellerfeld (Germany, F.R.). Inst. fuer Nichtmetallische Werkstoffe.
REACTION KINETICS IN GLASS MELTS: SODIUM SELF-DIFFUSION IN ALKALI-SILICATE MELTS (TEXUS 6)
G. H. Frischat and M. Braedt *In* ESA, Summary Review of Sounding Rocket Experiments in Fluid Science and Materials Sciences: TEXUS 1 to 20; MASER 1 and 2 Feb. 1991 p 124-125 (For primary document see N91-31321 23-29)
Copyright Avail: NTIS HC/MF A15; EPD, ESTEC, Noordwijk, Netherlands, HC 75 Dutch guilders

An experiment to determine the self diffusion coefficient of sodium in alkali silicate melts in the absence of convection is summarized. Sodium self diffusion in Na2O.3SiO2 and 0.5 Na2O.0.5 Rb2O.3SiO2 glass melts was studied at an effective temperature of 1200 C for an effective diffusion time of 125 s. The diffusion samples were placed in Pt containers, and the radioactive isotope Na-22 was used for the measurements. The diffusion profiles were analyzed and yielded the following diffusion coefficients: D(Na)* equals (2.5 + or - 0.4) 0.00001 cu cm/s in Na2O.3SiO2; D(Na)* equals (2.05 + or - 0.6) 0.00001 cu cm/s in 0.5Na2O.0.5 Rb2O.3SiO2. These values may be considered as intrinsic data, whereas the experiments conducted on Earth were disturbed by buoyancy convection and yielded only unrealistically high (apparent) values. In the case of the space experiments, the contact zones between the two samples were smooth, whereas some distortions were observed in the ground reference samples. ESA

N91-31366# Technische Univ., Clausthal-Zellerfeld (Germany, F.R.). Inst. fuer Nichtmetallische Werkstoffe.
SELF- AND INTERDIFFUSION IN ALKALI-SILICATE MELTS (TEXUS 11 AND 12)
G. H. Frischat, V. Braetsch, and M. Meier *In* ESA, Summary Review of Sounding Rocket Experiments in Fluid Science and Materials Sciences: TEXUS 1 to 20; MASER 1 and 2 Feb. 1991 p 126-129 (For primary document see N91-31321 23-29)
Copyright Avail: NTIS HC/MF A15; EPD, ESTEC, Noordwijk, Netherlands, HC 75 Dutch guilders

Results showing that a ground processed sample exhibits a strongly disturbed concentration profile, whereas a space processed sample exhibits, apart from the border zones, isoconcentration lines roughly parallel to the initial interface, are presented. These experiments aimed at getting diffusion data complementary to those obtained on previous space flights. The three experiments carried out in TEM-01 furnaces aimed at determining self and interdiffusion coefficients in the system xNa2O.(1-x)RbO2.3SiO2 at 1545 K, 1610 K and 1680 K The design of the samples is shown. Annealing was achieved in microgravity for about 150 s. The interdiffusion samples were analyzed according to the Boltzmann-Matano principle, the self diffusion samples using the residual activity technique. Results gave a deviation from the Arrhenius law for which no explanation could be given because of few experimental data and inherent lack of accuracy. ESA

N91-31367# Technische Univ., Clausthal-Zellerfeld (Germany, F.R.). Inst. fuer Nichtmetallische Werkstoffe.
SELF- AND INTERDIFFUSION IN ALKALI-SILICATE MELTS (TEXUS 13)
G. H. Frischat, V. Braetsch, and M. Meier *In* ESA, Summary Review of Sounding Rocket Experiments in Fluid Science and Materials Sciences: TEXUS 1 to 20; MASER 1 and 2 Feb. 1991 p 130-131 (For primary document see N91-31321 23-29)
Copyright Avail: NTIS HC/MF A15; EPD, ESTEC, Noordwijk, Netherlands, HC 75 Dutch guilders

A microgravity experiment within a series to investigate pure diffusive processes, i.e., without buoyancy convection which is superimposed on them on Earth, is summarized. The sample consisted of an interdiffusion part and a tracer diffusion part, the latter with an intermediate layer of Na-22 tracer. The sample was contained in platinum and processed in a Ni cartridge. It was annealed under microgravity conditions at a temperature of 1425 K for an effective time of 250 s. The interdiffusion part of the sample was analyzed with a microprobe and the undisturbed profile of the tracer diffusion part by the residual activity method. The tracer diffuion coefficient obtained was in very good agreement with those obtained previously. A comparison between the interdiffusion coefficient obtained with the Boltzman-Matano formula and those obtained previously is shown. This value confirmed the results of experiments carried out in TEXUS and FSLP. In contrast to what is observed in this system below 1300 K, no significant concentration dependence of the coefficient can be detected. The validity of one of the more recent theoretical productions, namely the relationship between between self- and inter-diffusion coefficients, could not be verified, mainly due to the lack of precise values of D sub Rb*. ESA

N91-31368# Technische Univ., Clausthal-Zellerfeld (Germany, F.R.). Inst. fuer Nichtmetallische Werkstoffe.
REACTION KINETICS IN MOLTEN GLASSES: SELF-DIFFUSION IN ALKALI-SILICATE MELTS (TEXUS 20)
G. H. Frischat and M. Meier *In* ESA, Summary Review of Sounding Rocket Experiments in Fluid Science and Materials Sciences: TEXUS 1 to 20; MASER 1 and 2 Feb. 1991 p 132-133 (For primary document see N91-31321 23-29)
Copyright Avail: NTIS HC/MF A15; EPD, ESTEC, Noordwijk, Netherlands, HC 75 Dutch guilders

An experiment to investigate the Rb-86 tracer diffusion coefficient (D sub Rb) in glass melts without interference of convective mass transport is summarized. The self diffusion of Rb in the glass system xNa2O-(1-x)Rb2O-3 SiO2, with the compositions x equals 0.75 and x equals 0.5, was investigated using the radioactive isotope Rb-86. ESA

N91-31369# Technische Univ., Clausthal-Zellerfeld (Germany, F.R.). Inst. fuer Nichtmetallische Werkstoffe.
SPECIAL REFRACTIVE INDEX PROFILES IN GLASSES OBTAINED BY ION EXCHANGE (TEXUS 19) ESA
G. H. Frischat, W. Beier, and U. Horst *In* ESA, Summary Review of Sounding Rocket Experiments in Fluid Science and Materials Sciences: TEXUS 1 to 20; MASER 1 and 2 Feb. 1991

p 134-135 (For primary document see N91-31321 23-29)
Copyright Avail: NTIS HC/MF A15; EPD, ESTEC, Noordwijk, Netherlands, HC 75 Dutch guilders

An experiment to investigate the possibility of obtaining buried silver profiled in glasses in a one step process by diffusive ion exchange between glasses and molten salts is summarized. Two polished glass samples (61/33/6 mole pct SiO2/Na2O/Al2O3) with a layer of salt (10/90 mole pct AgNO3/NaNO3) in between were processed in a Ni cartridge. There was provision for volume expansion of the salt on melting. The glass samples ware maintained at 350 C in microgravity and diffusive silver/sodium exchanges occurred for effective times of 222 s and 219 s respectively. Penetration depths of about 40 microns were obtained. Deconvolution calculations were performed which turned out to increase the steepness of the profile flank, thus demonstrating that buried silver profiles cannot be produced in this way. However, as a thin layer of molten salt wetted unexpectedly one of the glass samples, a silver concentration profile was found on the side opposite to the initial salt layer. This profile exhibited a maximum at a depth of about 14 microns. This showed that buried silver profiles can be obtained by a single diffusion process using thin films of nitrate melt which act as a limited ion source. ESA

N91-31370# Technische Univ., Delft (Netherlands). Lab. of Metallurgy.
SULPHUR DIFFUSION IN LIQUID CAST IRON (TEXUS 6) ESA
T. Luyendijk and H. Nieswaag *In* ESA, Summary Review of Sounding Rocket Experiments in Fluid Science and Materials Sciences: TEXUS 1 to 20; MASER 1 and 2 Feb. 1991 p 136-137 (For primary document see N91-31321 23-29)
Copyright Avail: NTIS HC/MF A15; EPD, ESTEC, Noordwijk, Netherlands, HC 75 Dutch guilders

An experiment to determine the diffusion coefficient of sulphur in liquid cast iron in comparison to that of phosphorus is summarized. The capabilities of the ceramic skin technology applied to cast iron were also to be assessed prior to a Spacelab experiment. The sample was made of several diffusion welded cylinders of white cast iron (carbon: 4.2 to 4.3 wt. pct, no silicon) with various concentrations of sulphur and phosphorus. It was coated with a plasma sprayed Al2O3 skin and enveloped in alumina wool before being inserted in a TMZ cartridge. The temperature at the outer surface of the cartridge was measured by three thermocouples. The temperature difference within the sample was previously determined on the ground. The sample was preheated up to 1000 C before the launch and melted and resolidified under microgravity conditions. A diffusion period of about 180 s was thus achieved, with however a thermal gradient of approximately 10 C/cm between the top of the sample (first melted) and its bottom (last melted). The alumina skin showed many cracks. These were due to the volume expansion of the sample on melting. Nevertheless, no reaction occurred between the cast iron and the alumina skin. ESA

N91-31371# Technische Hochschule, Aachen (Germany, F.R.). Inst. fuer Physikalische Chemie.
VENTILATION AND FILLING OF AN OPTICAL DIFFUSION CELL (TEXUS 8)
J. Richter, J. Hermanns, and W. Merkens *In* ESA, Summary Review of Sounding Rocket Experiments in Fluid Science and Materials Sciences: TEXUS 1 to 20; MASER 1 and 2 Feb. 1991 p 138-139 (For primary document see N91-31321 23-29)
Copyright Avail: NTIS HC/MF A15; EPD, ESTEC, Noordwijk, Netherlands, HC 75 Dutch guilders

An experiment to bring two columns of molten salts into contact and to observe the subsequent diffusion processes is summarized. The ventilation and filling procedure of the 'flowing junction' cell employed was to be tested precursory to an experiment on, D-1. The cell, made of stainless steel, was equipped with quartz glass windows (40 by 10 by 5 cu mm) to allow the observation with a cine camera. The cell was filled with two mixtures of sodium nitrate and silver nitrate with mole fractions of silver nitrate of 0.84 and 0.86. The two salt mixtures were injected under microgravity by means of pneumatically operated pistons. The melts flowed from both sides of the cell towards each other and came into contact where the interface was to be located. Since the quartz glass was badly wetted by the molten salts a plane interface free of gas inclusion suitable for diffusion studies was formed. ESA

N91-31372# Space Technology Corp., Tokyo (Japan).
SOLUTAL DIFFUSION MEASUREMENTS IN LIQUID PbSnTe UNDER MICROGRAVITY (TEXUS 19)
M. Katayama, M. Kaneko, and J. Sato *In* ESA, Summary Review of Sounding Rocket Experiments in Fluid Science and Materials Sciences: TEXUS 1 to 20; MASER 1 and 2 Feb. 1991 p 140-141 (For primary document see N91-31321 23-29)
Copyright Avail: NTIS HC/MF A15; EPD, ESTEC, Noordwijk, Netherlands, HC 75 Dutch guilders

An experiment to measure the diffusion coefficient in liquid Pb(1-x)Sn(x)Te in the absence of buoyancy driven convection is summarized. The Sn distribution in the flight sample showed that mixing occurred. The dendritic microstructure was coarse in the outer shell and fine in the center of the sample. The temperature recordings indicated that the cooling rate was much slower than anticipated, and that the solidification heat release occurred only 27 s after the end of the microgravity period. The Sn distribution along longitudinal lines at the outer surface of the flight sample varied markedly with the angular location of the line. If the sample remained molten after the end of the microgravity period, the varying reentry accelerations would have caused an unusual mixing of the two liquids. The large scatter of the data suggested that the cooling rate influences the accuracy of diffusion measurements. The use of capillary tubes in space experiments is therefore strongly recommended. ESA

N91-31373# Goettingen Univ. (Germany, F.R.). Inst. fuer Metallphysik.
DIFFUSION OF Ni IN Cu-Au AND Cu-Al ALLOYS (TEXUS 20)
J. Urbanek, C. Koestler, and T. Hehenkamp *In* ESA, Summary Review of Sounding Rocket Experiments in Fluid Science and Materials Sciences: TEXUS 1 to 20; MASER 1 and 2 Feb. 1991 p 142-143 (For primary document see N91-31321 23-29)
Copyright Avail: NTIS HC/MF A15; EPD, ESTEC, Noordwijk, Netherlands, HC 75 Dutch guilders

An experiment to measure the diffusion coefficient of Ni in Cu and in CuAu and CuAl alloys in anticipation of an experiment on D-2 is summarized. Diffusion profiles were measured along the sample length with an electron microprobe. The homegeneity of the Al and Au atoms distribution in the Cu alloys was assessed. Periodical variations of the Ni concentration were detected close to the solid/liquid interfaces. These are clearly due to the dentritic structure of the solidified alloys, particularly at higher concentrations of the alloying element. The diffusion coefficients obtained were about 0.000019 cm/s, i.e. one order of magnitude lower than those measured on Earth in capillaries. No significant dependence of the diffusion coefficient on the Al concentration was detected whereas it was found to decrease at increasing Au concentration. No satisfactory explanation can be given yet. ESA

N91-31374# Technische Univ., Munich (Germany, F.R.). Inst. fuer Thermodynamik.
PHASE TRANSITION (TEXUS 8)
J. Straub, R. Lange, and K. Nitsche *In* ESA, Summary Review of Sounding Rocket Experiments in Fluid Science and Materials Sciences: TEXUS 1 to 20; MASER 1 and 2 Feb. 1991 p 148-149 (For primary document see N91-31321 23-29)
Copyright Avail: NTIS HC/MF A15; EPD, ESTEC, Noordwijk, Netherlands, HC 75 Dutch guilders

At a critical point, many physical properties of fluids are strongly modified and measurements of their behavior can be difficult or inaccurate under Earth gravity. An experiment aimed at observing phenomenologically the phase transition of a fluid cooled through its critical state, and at studying a fluid passing the critical point along the critical isochoire from its two phase to its one phase region is summarized. The kinetics of the critical phase transition of sulfur hexafluoride was investigated under microgravity conditions. The temperature of the fluid container wall was

accurately controlled and the temperature response in the center of the fluid was measured. The phase transition was observed by means of a 16 mm cine camera. The analysis of the temperature/time profile obtained showed no significant delay of the thermal response in the center of the fluid on heating and cooling the container wall through the critical temperature. This indicated that the thermal equilibrium in the critical region was much more enhanced than had been expected, as the thermal diffusivity tends to be zero at Tc. This surprising result was particularly evident on the cine pictures where the homogeneous onset of the phase transition throughout the whole volume of the cell was observed. ESA

N91-31375# Central Electricity Research Labs., Leatherhead (England).
IONIC SOLUTIONS NEAR THE CRITICAL POINT OF WATER (TEXUS 10) ESA
D. J. Turner *In* ESA, Summary Review of Sounding Rocket Experiments in Fluid Science and Materials Sciences: TEXUS 1 to 20; MASER 1 and 2 Feb. 1991 p 150-153 (For primary document see N91-31321 23-29)
Copyright Avail: NTIS HC/MF A15; EPD, ESTEC, Noordwijk, Netherlands, HC 75 Dutch guilders

Aqueous ionic solutions behave very abnormally in the temperature region between 300C and the critical point of water. Consistent patterns in the anomalous behavior of a variety of thermodynamic and transport properties of high temperature salt solutions have been noted. These suggest that the anomalies result from the high compressibility of the solvent and that the same effects explain the gravity induced stratification which has been observed in salt solutions near the critical point. An experiment to achieve a better understanding of these compressibility effects is summarized. Reference experiments on the ground (by turning the cell upside down) confirmed earlier observations of a very significant stratification under conditions where a normal fluid mixture would have been homogeneous. The flight solution exhibited unexpected phenomena in the pre-equilibrium stage before the launch (the measurements were made at the bottom of the cell). This is interpreted as the result of a temporary and only slowly reversible precipitation of salt between the electrodes. During the flight, a microgravity related increase in solution resistance and time dependent resistence resulting from salt redissolution were observed. ESA

N91-31376# Central Electricity Research Labs., Leatherhead (England).
IONIC SOLUTIONS NEAR THE CRITICAL POINT OF WATER (TEXUS 12) ESA
D. J. Turner *In* ESA, Summary Review of Sounding Rocket Experiments in Fluid Science and Materials Sciences: TEXUS 1 to 20; MASER 1 and 2 Feb. 1991 p 154-155 (For primary document see N91-31321 23-29)
Copyright Avail: NTIS HC/MF A15; EPD, ESTEC, Noordwijk, Netherlands, HC 75 Dutch guilders

A follow up to the Technological Experiments Under Microgravity (TEXUS) 10, the TEXUS 12, experiment is summarized. The difficulty addressed was an increase in solution resistance under microgravity partially obscurred by the the prescence of NaCl at launch. The resistance measurements on the solution were made in the autoclave employed for the TEXUS 10 experiment. To avoid the presence of solid NaCl at launch, the prelaunch heating profile was modified and extended, and a solution whose density was significantly closer to critical (0.97 instead of 0.92 of the critical density of water) was used. An improvement in the purity of the solution was also achieved by ensuring that nothing but gold, a platinum rhodium alloy and synthetic sapphire were in contact with it. The most important conclusions were the demonstration of a large effect of microgravity and the fact that equilibrium in the low gravitational field takes more than 6 minutes. For further experiments of this type, an effective method of mixing the solution during the ascent of the rocket would be required. ESA

N91-31377# Commissariat a l'Energie Atomique, Saclay (France). Centre d'Etudes Nucleaires.
PHASE SEPARATION OF A BINARY FLUID NEAR ITS CRITICAL POINT (TEXUS 11)
D. Beysens, P. Guenoun, and F. Perrot *In* ESA, Summary Review of Sounding Rocket Experiments in Fluid Science and Materials Sciences: TEXUS 1 to 20; MASER 1 and 2 Feb. 1991 p 156-157 (For primary document see N91-31321 23-29)
Copyright Avail: NTIS HC/MF A15; EPD, ESTEC, Noordwijk, Netherlands, HC 75 Dutch guilders

The first of a series of experiments to study phase separation in binary fluids under microgravity is summarized. On Earth, the experiment was performed with a critical mixture of deuterated cyclohexane, cyclohexane and methanol with matched densities. In microgravity, a critical mixture of deuterated cyclohexane and methanol was investigated. Just before launch, the critical temperature was determined accurately by cooling the mixture by steps of 1 mK up to observing its opalescence. The flight temperature/time profile was subsequently preprogrammed. Nothing but the vapor bubble could be seen in the flight cell even 6 mm after the quench, whereas macroscopic spinodal structures were clearly visible in the ground cell. The behavior of the mixtures appeared very different although convection flows were essentially suppressed in both cases. Two possible explanations are summarized. ESA

N91-31378# Commissariat a l'Energie Atomique, Gif-sur-Yvette (France). Centre d'Etudes Nucleaires.
PHASE SEPARATION IN MICROGRAVITY OF BINARY FLUIDS NEAR THE CRITICAL POINT (TEXUS 13)
D. Beysens, P. Guenoun, and F. Perrot *In* ESA, Summary Review of Sounding Rocket Experiments in Fluid Science and Materials Sciences: TEXUS 1 to 20; MASER 1 and 2 Feb. 1991 p 158-161 (For primary document see N91-31321 23-29)
Copyright Avail: NTIS HC/MF A15; EPD, ESTEC, Noordwijk, Netherlands, HC 75 Dutch guilders

An experiment to investigate the phase separation of a binary fluid near its critical point using a strict isodensity system and to validate the microgravity like conditions by experiments in microgravity is summarized. Mixtures of three components, cyclohexane, deuterated cyclohexane, and methanol, with a density difference either large or very small were investigated. These mixtures behave with respect to the phase transition like a binary fluid. Five experiments were compared which were performed on Earth (g equals 1) and in microgravity (g equals 0.0001) under the same conditions. Results showed that, on Earth, the gravity induced flows in the isodensity system can be neglected when compared to the capillary flows, at least for a 6 mm duration of the experiment. There is therefore a possibility of carefully studying the phase separation of fluids on Earth, at least in the critical region as it would occur in space where gravity induced convection is suppressed. ESA

N91-31379# Deutsche Forschungsanstalt fuer Luft- und Raumfahrt, Cologne (Germany, F.R.). Inst. for Space Simulation.
SPINOIDAL DECOMPOSITION (TEXUS 17)
H. Klein, G. Schmitz, and D. Woermann *In* ESA, Summary Review of Sounding Rocket Experiments in Fluid Science and Materials Sciences: TEXUS 1 to 20; MASER 1 and 2 Feb. 1991 p 162-163 (For primary document see N91-31321 23-29)
Copyright Avail: NTIS HC/MF A15; EPD, ESTEC, Noordwijk, Netherlands, HC 75 Dutch guilders

Analogies between phase transitions suggest that the spinodal decomposition of a single component fluid can be studied by means of light scattering techniques in the same way as a spinodal decomposition of binary liquid mixtures. An experiment carried out in microgravity which exactly reflected one carried out on Earth is summarized. The results obtained were similar to those obtained on Earth, thus demonstrating that the process was not influenced by gravity during that short persistence time. It was concluded that spinodal decomposition is much more affected by a finite quenching rate in a single component fluid than in binary mixture.

This is due to the fact that the relaxation time of the density fluctuations in the former is smaller than the relaxation time of the concentration fluctuations in the latter. ESA

N91-31380# Deutsche Forschungsanstalt fuer Luft- und Raumfahrt, Cologne (Germany, F.R.). Inst. for Materials Research.

DIRECTIONAL SOLIDIFICATION OF DOPED GERMANIUM (TEXUS 4) ESA

H. U. Walter *In* ESA, Summary Review of Sounding Rocket Experiments in Fluid Science and Materials Sciences: TEXUS 1 to 20; MASER 1 and 2 Feb. 1991 p 166-167 (For primary document see N91-31321 23-29)

Copyright Avail: NTIS HC/MF A15; EPD, ESTEC, Noordwijk, Netherlands, HC 75 Dutch guilders

An experiment to demonstrate the feasibility of sounding rocket flights for the preparation of homogeneously doped semiconductor material is summarized. Marangoni convection was to be excluded by avoiding free melt surfaces. Crystals of Ge(Ga) alloy (concentration of 10 to the 17th power to 10 to the 19th power Ga atoms/cu cm) were prepared. In order to avoid Marangoni convection induced by surface tension gradients at the liquid gas interface, the crystals were grown by the Bridgeman technique, which means that the melt was encapsuled without any free surface. The seeds were prepared by the Czochralski method. Four identical gradient furnaces were employed where solidification was achieved by cooling down. The projected values of solidification rate (50 microns/s) and temperature gradient (60 K/cm) were maintained within the order of magnitude to the end of the solidification. The cooling rate increased from the initial value of approximately 0.1K/s to about 0.3K/s. Apart from radial segregation, which was due to the furnace properties, steady state growth could be achieved within seconds after microgravity conditions were established. Striations were not observed in materials grown in microgravity (less than 10 (exp -4) g). Growth appeared to be less sensitive to axial than to radial accelerations. ESA

N91-31381# Deutsche Forschungsanstalt fuer Luft- und Raumfahrt, Cologne (Germany, F.R.). Inst. for Materials Research.

STRIATIONS IN GERMANIUM (TEXUS 6) ESA

H. U. Walter *In* ESA, Summary Review of Sounding Rocket Experiments in Fluid Science and Materials Sciences: TEXUS 1 to 20; MASER 1 and 2 Feb. 1991 p 168 (For primary document see N91-31321 23-29)

Copyright Avail: NTIS HC/MF A15; EPD, ESTEC, Noordwijk, Netherlands, HC 75 Dutch guilders

The chemical homogeneity of doped semiconductors and alloys is strongly affected by growth rate variations due the thermal instabilities or convection. The feasibility of conducting simple crystal growth experiments within the constraints of sounding rocket flights was to be investigated using the model system germanium doped with gallium. Two samples of Ga doped Ge (5 times 10 to the 17th power/cc and 5 times to the 18th power/cc) were encapsulated in BN crucibles in tantalum cartridges. The samples were processed in a gradient furnace using power reduction to control directional solidification. Interface markings were achieved by current pulsing through the samples. Prior to the launch, the samples were melted to the seed crystal. The directional solidification process was then initiated and approximately 2 cm of material were solidified prior to liftoff. The process was continued throughout the flight of the rocket, so that the solidifying samples were exposed to acceleration levels ranging from 20 g to 10 (exp -4) g. The analysis of longitudinal sections of the single crystals obtained releaved an excellent homogeneity in the 2 cm long section corresponding to the 6 minutes of microgravity conditions. Striations were observed in the segments grown on the ground (gravity driven convection) and in the section corresponding to the despin of the rocket (forced convection). ESA

N91-31382# Centre National de la Recherche Scientifique, Grenoble (France).

SINGLE CRYSTALS OF CeMg3 (TEXUS 7) ESA

J. Pierre, J. Baruchel, M. Schlenker, and E. Siaud *In* ESA, Summary Review of Sounding Rocket Experiments in Fluid Science and Materials Sciences: TEXUS 1 to 20; MASER 1 and 2 Feb. 1991 p 170 (For primary document see N91-31321 23-29)

Copyright Avail: NTIS HC/MF A15; EPD, ESTEC, Noordwijk, Netherlands, HC 75 Dutch guilders

On Earth, the growth of single crystals of the compound CeMg3 using the vertical Bridgman technique is impeded by the sedimentation of the denser component, cerium, which leads to the formation of the CeMg phase at the bottom of the crucible. By operating under microgravity conditions and thus avoiding the segregation of cerium, it was expected to obtain large single crystals of CeMg3. The sample was heated up to 800 C and remained molten for about 4 min before it solidified. A similar sample was processed in the same way on the ground for comparison. Whereas the ground reference sample exhibited CeMg impurities, the space sample consisted entirely of the CeMg3 phase. This showed that the segregation of Ce results from the density difference and not from the diffusion of atoms under a thermal gradient. However, the thermal profile inside the furnace was rather inhomogeneous and resulted in a radial rather than axial crystallization, thus preventing the growth of large single crystals. ESA

N91-31383# Centre National de la Recherche Scientifique, Grenoble (France).

GROWTH OF RARE EARTH-MAGNESIUM CRYSTALS (TEXUS 12)

J. Pierre and E. Siaud *In* ESA, Summary Review of Sounding Rocket Experiments in Fluid Science and Materials Sciences: TEXUS 1 to 20; MASER 1 and 2 Feb. 1991 p 172-173 (For primary document see N91-31321 23-29)

Copyright Avail: NTIS HC/MF A15; EPD, ESTEC, Noordwijk, Netherlands, HC 75 Dutch guilders

Following on the TEXUS 7 experiment where a polycrystalline sample of CeMg3, could be obtained owing to the absence of sedimentation of cerium, this experiment aimed at obtaining large crystals of CeMg3 by processing the sample under well controlled thermal conditions. In the Earth grown crystal, the precipitates were more randomly distributed, forming polygonal cells with a size of about 0.1 to 0.2 mm as previously observed during the ground tests. Clearly the coherence was greater in the space grown crystal. This could be related to the absence of convection flows in the melt in microgravity. Backscattering X-ray Laue patterns indicated a good crystallinity of the sample, with a restricted mosaicity. The Earth grown sample yielded X-ray patterns of worse quality, with a local mosaicity of the order of 3 to 4 degrees. The neutron transmission Laue patterns indicated a coherent orientation of the flight sample, whereas the reference sample contained clearly crystals of different orientations. The rocking curves and neutron topography of the space sample showed that it consisted of two groups of elements with an internal mosaicity of about 4 degrees and disoriented by about 10 degrees. This was interpreted as the result of the nucleation of several crystals at the conical end of the crucible. ESA

N91-31384# Freiburg Univ. (Germany, F.R.). Kristall. Inst.

FLOATING-ZONE GROWTH OF A SILICON SINGLE CRYSTAL (TEXUS 7)

A. Eyer and H. Leiste *In* ESA, Summary Review of Sounding Rocket Experiments in Fluid Science and Materials Sciences: TEXUS 1 to 20; MASER 1 and 2 Feb. 1991 p 174-175 (For primary document see N91-31321 23-29)

Copyright Avail: NTIS HC/MF A15; EPD, ESTEC, Noordwijk, Netherlands, HC 75 Dutch guilders

An experiment aimed at demonstrating the feasibility in microgravity of the floating zone growth of silicon crystals by radiation heating in a single ellipsoid mirror furnace, and comparing the dopant distribution obtained on Earth and in space, is summarized. A silicon single crystal (8 mm in diameter, 90 mm long, P doped, resistivity 0.03 Ohm/cm) was grown over a length

of 25 mm under microgravity conditions. The crystal was mounted wall-free in a fused silica ampoule. The power/time profile was preprogrammed, but with the possibility of manual override. A similar experiment was carried out on the ground for comparison. The lack of convective cooling in the furnace in the absence of gravity caused an anticipated increase of the length of the zone and eventually its rupture. The rupture was further promoted by a decreasing diameter of the grown part of the crystal, due to the absence of hydrostatic pressure in microgravity. The lower part of the melt crystallized in a conical shape, the upper part in a spherical shape. Both longitudinal sections of the space and found samples exhibited striations. It can thus be concluded that these striations are essentially due to Marangoni convection. ESA

N91-31385# Freiburg Univ. (Germany, F.R.). Kristall. Inst.
GROWTH OF A Si CRYSTAL COVERED WITH A SiO2 SKIN (TEXUS 12)
A. Croell, W. Mueller, and R. Nitsche *In* ESA, Summary Review of Sounding Rocket Experiments in Fluid Science and Materials Sciences: TEXUS 1 to 20; MASER 1 and 2 Feb. 1991 p 176-177 (For primary document see N91-31321 23-29)
Copyright Avail: NTIS HC/MF A15; EPD, ESTEC, Noordwijk, Netherlands, HC 75 Dutch guilders

An experiment to compare the dopant distributions in crystals processed on Earth and in microgravity is summarized. The experimental concentration profiles were compared with profiles calculated with the assumption of a hemispherical diffusion of the dopant. In the case of the crystal grown in space, the similarity between experimental and calculated profiles leads to the conclusion that purely diffusive conditions were achieved in microgravity. On the contrary, the important discrepancy observed in the case of the crystal pulled on Earth shows that laminar convection occurred. This convection could only be driven by gravity. Any contribution of interfacial tension effects would have been also observed in the space grown crystal. It was thus shown that Marangoni convection during float zoning on Earth can be effectively prevented by covering the sample surface, but that a considerable gravity driven laminar convection occurs with such a zone geometry. ESA

N91-31386# Erlangen-Nuremberg Univ. (Germany, F.R.). Inst. fuer Werkstoffwissensch 6.
FLOATING ZONE GROWTH OF GaAs CRYSTALS (TEXUS 20)
G. Mueller and R. Rupp *In* ESA, Summary Review of Sounding Rocket Experiments in Fluid Science and Materials Sciences: TEXUS 1 to 20; MASER 1 and 2 Feb. 1991 p 178-179 (For primary document see N91-31321 23-29)
Copyright Avail: NTIS HC/MF A15; EPD, ESTEC, Noordwijk, Netherlands, HC 75 Dutch guilders

An experiment to perform a floating zone experiment with a GaAs crystal using a specially designed growth ampoule, and to verify numerical simulations which predicted the occurrence of nonstationary convection flows, and thus dopant striations in the space grown crystal, is summarized. To a major extent, and in spite of the oxidizing atmosphere and of the very high pulling speed, a single crystal was grown in space. Contrary to the expectations, no striations could be detected. This could have been due to the presence of a thin oxide skin at the surface of the floating zone, which damped the convection flows in the bulk. Also, the relatively low dopant concentration (3 times 10 to the 16th power at/cu cm) made striations difficult to reveal. Photoluminescence intensities were measured at the surface of a longitudinal section of the sample. The intensities measured in the nonmelted region were more than ten times as high as the intensities measured in the space grown region. This can be interpreted as a consequence of the unusually high pulling speed achieved during the flight which yielded a crystal with a highly disturbed structure. ESA

N91-31387# Royal Inst. of Tech., Stockholm (Sweden). Dept. of Casting of Metals.
FLOATING ZONE CRYSTAL GROWTH OF Ga-DOPED GERMANIUM (TEXTUS 10) ESA
T. Carlberg *In* ESA, Summary Review of Sounding Rocket Experiments in Fluid Science and Materials Sciences: TEXUS 1 to 20; MASER 1 and 2 Feb. 1991 p 180-181 (For primary document see N91-31321 23-29)
Copyright Avail: NTIS HC/MF A15; EPD, ESTEC, Noordwijk, Netherlands, HC 75 Dutch guilders

Two rod shaped 5 mm in diameter single crystals of Ga doped Ge (1.5 times 10 to the 18th power at/cu cm) were processed in mirror furnaces. Once microgravity conditions were established, a floating zone was formed in each sample. The samples were then pulled at 3 mm/mm on 5 mm and 5 mm/mm on 7 mm respectively. Current pulsing with a frequency of 1 Hz was applied for the marking of the growing solid/liquid interface. The longitudinal section of both samples showed a polycrystalline structure starting from a strongly curved initial solid/liquid interface. The growth rate along the samples could be deduced from the interface demarcations and segregation profiles could be measured. These profiles clearly showed that convective mixing occurred in the liquid zones. But the absence of striations indicated that the driving force of the convection levels in the space samples and in reference samples showed the importance of the contribution of surface tension forces to the convection flows in liquid zones on the ground. ESA

N91-31388# Royal Inst. of Tech., Stockholm (Sweden). Dept. of Casting Metals
FLOATING-ZONE EXPERIMENTS WITH GERMANIUM CRYSTALS (TEXUS 12) ESA
T. Carlberg *In* ESA, Summary Review of Sounding Rocket Experiments in Fluid Science and Materials Sciences: TEXUS 1 to 20; MASER 1 and 2 Feb. 1991 p 182-183 (For primary document see N91-31321 23-29)
Copyright Avail: NTIS HC/MF A15; EPD, ESTEC, Noordwijk, Netherlands, HC 75 Dutch guilders

The experiments were performed in mirror furnaces. The samples consisted of 5 mm diameter Ge crystals doped with 5 times 10 to the 18th power at/cu cm of Ge. The most striking results were the radial concentration profiles exhibited by the coated space sample, which has inverted profiles compared to the others. This can only be interpreted as the result of a very weak convection, which was not strong enough to homogenize the melt but which caused a flow of solute from regions close to the surface towards the center. For the three other samples, where the Ga concentration is higher close to the surface region, the results can be explained by outwards diffusion along the curved solid/liquid interface which occurred in the boundary layer while the bulk melt is assumed to be homogeneous due to convective mixing. ESA

N91-31389# Royal Inst. of Tech., Stockholm (Sweden). Dept. of Casting Metals.
FLOATING ZONE GROWTH OF GERMANIUM CRYSTALS (TEXUS 14b) ESA
T. Carlberg and E. Tillberg *In* ESA, Summary Review of Sounding Rocket Experiments in Fluid Science and Materials Sciences: TEXUS 1 to 20; MASER 1 and 2 Feb. 1991 p 184-185 (For primary document see N91-31321 23-29)
Copyright Avail: NTIS HC/MF A15; EPD, ESTEC, Noordwijk, Netherlands, HC 75 Dutch guilders

The previous experiments showed unambiguously that convection occurs in liquid zones during growth in microgravity. An experiment to investigate the influence of the length of the liquid zone and thereby also of the shape of the growing interface (the longer the zone, the more planar the interface) in order to get more data on the interaction between segregation at curved interfaces and convection is summarized. The convection was expected to vary also with the zone length. It was of interest to reproduce the anomalous results obtained with a previous space sample without free surfaces. ESA

N91-31390# Royal Inst. of Tech., Stockholm (Sweden). Dept. of Casting Metals.
SEMI-CONFINED BRIDGMAN GROWTH OF Ga-DOPED Ge (MASER 2)
T. Carlberg and E. Tillberg *In* ESA, Summary Review of Sounding Rocket Experiments in Fluid Science and Materials Sciences: TEXUS 1 to 20; MASER 1 and 2 Feb. 1991 p 186-187 (For primary document see N91-31321 23-29)
Copyright Avail: NTIS HC/MF A15; EPD, ESTEC, Noordwijk, Netherlands, HC 75 Dutch guilders

An experiment to investigate the dopant segregation during the growth of Ga-doped Ge crystals using a semi-confined Bridgman configuration with different thermal gradients is summarized. Different levels of Marangoni convection were expected thus to be achieved. From this possibly, the critical Marangoni number corresponding to the onset of oscillatory flows could be evaluated. The space crystals were grown under thermal gradients of 130 and 90 K/cm respectively. The axial segregation profile in the high gradient sample corresponded to an effective partition coefficient of 0.75 and indicated that only a weak convection occurred during the growth. In the low gradient sample, a strong coupling occurred between the instable growth rate and the concentration as well as a strong radial segregation, both of which indicated a low convection level. This was contrary to expectations, since the Marangoni numbers were of the order of 10,000 when the growth started, and significant convection, including oscillatory flows, should have occurred. This result could be explained by the presence of a native oxide layer on the surface of the samples. The layer cracked on melting and only a small free surface area could generate Marangoni convection. ESA

N91-31391# Commissariat a l'Energie Atomique, Grenoble (France). Centre d'Etudes Nucleaires.
SEMI-CONFINED BRIDGMAN GROWTH OF Ga-DOPED Ge (MASER 2)
D. Camel and P. Tison *In* ESA, Summary Review of Sounding Rocket Experiments in Fluid Science and Materials Sciences: TEXUS 1 to 20; MASER 1 and 2 Feb. 1991 p 188-189 (For primary document see N91-31321 23-29)
Copyright Avail: NTIS HC/MF A15; EPD, ESTEC, Noordwijk, Netherlands, HC 75 Dutch guilders

Thermocapillary flows have a strong influence on the segregation of a dopant during floating zone crystal growth. An experiment to study this influence in a Bridgman configuration with a partially floating melt in order to avoid interaction with a melting interface and to allow the comparison between segregations obtained with and without free surfaces is summarized. A sharp maximum of the radial concentration profile could be observed at a well defined position all along the uncovered region of the sample. This maximum, induced by convection, was not located on the sample axis, due the asymmetry of the oxide skin, and due also to the local contribution to the mixing of a large bubble in the covered region. According to theory, a boundary layer flow regime was established with a maximum velocity of the liquid of the order of 8 cm/s. This value was probably not reached due to the surface oxide layer, but the mixing efficiency does not depend only on the maximum velocity. ESA

N91-31392# Antwerp Univ. (Belgium). Lab. voor Chem. en Fys. Mineralogie.
CRYSTALLISATION EXPERIMENTS WITH SALTS (TEXUS 13)
R. Vochten *In* ESA, Summary Review of Sounding Rocket Experiments in Fluid Science and Materials Sciences: TEXUS 1 to 20; MASER 1 and 2 Feb. 1991 p 190 (For primary document see N91-31321 23-29)
Copyright Avail: NTIS HC/MF A15; EPD, ESTEC, Noordwijk, Netherlands, HC 75 Dutch guilders

The difference in crystal structures between space and ground grown (001) oriented Ge-S0.98-Se0.02 single crystals was reported previously. An experiment aimed at performing a preliminary qualitative study of the variation of the cell parameters after fusion and crystallization under microgravity conditions is summarized. Well pronounced differences were observed for HgI2, HgBr2 and the two eutectic mixtures HgBr2-HgCl2 (0.52 to 0.48 in mol pct) and HgI2-HgBr2 (0.41 to 0.59 in molpct), the samples crystallized under microgravity conditions yielding less X-ray deflections lines. It could not be excluded that decomposition actually occurred at 270 C. In order to confirm the value of the results obtained and to calculate the lattice parameters of the single components, further ground experiments with the same rate of freon cooling but at different temperatures are needed. If decomposition does not occur it is clear that another crystallographic phase was formed under microgravity conditions. ESA

N91-31393# Space Technology Corp., Tokyo (Japan).
SOLUTION GROWTH OF GaAs SINGLE CRYSTALS (TEXUS 19)
S. Kodama and Y. Suzuki *In* ESA, Summary Review of Sounding Rocket Experiments in Fluid Science and Materials Sciences: TEXUS 1 to 20; MASER 1 and 2 Feb. 1991 p 192-195 (For primary document see N91-31321 23-29)
Copyright Avail: NTIS HC/MF A15; EPD, ESTEC, Noordwijk, Netherlands, HC 75 Dutch guilders

An experiment aimed at growing a GaAs single crystal from a metallic solution in microgravity is summarized. It is expected to obtain crystals of better quality from solutions at temperatures below the melting point of GaAs. The absence of unstable liquid flows in microgravity should also contribute to the improvement of the crystal quality. On the ground, the melt was homogenized by buoyancy convection flows. The crystals exhibited a lateral growth morphology with no hillock or type 1 striations, except in the crystal layer which was rapidly grown at the end of the experiment. These observations confirmed that purely diffusive growth conditions were achieved in microgravity. ESA

N91-31394# Space Technology Corp., Tokyo (Japan).
VAPOUR GROWTH OF AN InP CRYSTAL (TEXUS 20)
T. Kimura, T. Nishimura, K. Mizuguchi, T. Murotani, and Y. Yukimoto *In* ESA, Summary Review of Sounding Rocket Experiments in Fluid Science and Materials Sciences: TEXUS 1 to 20; MASER 1 and 2 Feb. 1991 p 196-197 (For primary document see N91-31321 23-29)
Copyright Avail: NTIS HC/MF A15; EPD, ESTEC, Noordwijk, Netherlands, HC 75 Dutch guilders

It was expected that growing an InP crystal from the vapor phase under microgravity, and thus under purely diffusive conditions, would result in an expitaxial layer of highly uniform thickness. The source of S doped InP and the substrate of Fe doped InP, both 10 sq mm in size, were located at the ends of an evacuated quartz ampoule 5 mg of InCl3 were used as a transport agent. A TEM-01 furnace was specially adapted to process the ampoule under gradient conditions. Heating started 270 s before launch. At the beginning of the microgravity period, the temperature of the source and the substrate were 720 C and 630 C respectively. Transport and growth were achieved for 260 s. The ampoule was cooled by injecting helium before reentry. Photoluminescence measurements with the sample at room temperature exhibited a peak at a wavelength corresponding to the energy gap of InP. This emission could come only from a S doped InP layer, and not from the Fe doped substrate. SIMS analysis indicated the presence of S over depth of about 0.1 microns, beyond which the signal was reduced to a background level. SEM pictures of a cross section of the sample showed indeed a 0.1 microns thick epitaxial layer. ESA

N91-31395# Freiburg Univ. (Germany, F.R.). Chemisches Lab.
DIFFUSION-CONTROLLED GROWTH OF PROTEIN SINGLE CRYSTALS: B-GALACTOSIDASE (TEXUS 3)
W. Littke *In* ESA, Summary Review of Sounding Rocket Experiments in Fluid Science and Materials Sciences: TEXUS 1 to 20; MASER 1 and 2 Feb. 1991 p 200-201 (For primary document see N91-31321 23-29)
Copyright Avail: NTIS HC/MF A15; EPD, ESTEC, Noordwijk, Netherlands, HC 75 Dutch guilders

Solving the three dimensional structure of organic macromolecular compounds is often impossible due to the

difficulties encountered in obtaining single crystals large enough and with a high degree of perfection for X-ray analysis. A comparison of the growth of single crystals of the same protein under terrestrial and microgravity conditions was to be performed. This experiment aimed at testing the apparatus and at verifying whether diffusion controlled conditions are achieved in microgravity. On the ground, turbulent convection was observed and only amorphous protein material was obtained. Under microgravity conditions, a strictly laminar diffusion process could be observed, and crystallites of the order of one micron ion size were grown. Due to the short crystallization time available (about 6 min), the crystals grown in space are of inferior quality than, but still comparable to, those obtained on Earth after several days. This can be tentatively explained as a result of a near range order close to the order in crystallized material, which is established in the solution in the absence of convection. ESA

N91-31396# Freiburg Univ. (Germany, F.R.). Chemisches Lab.
DIFFUSION-CONTROLLED GROWTH OF PROTEIN SINGLE CRYSTALS: INVESTIGATION OF B-GALACTOSIDASE AT LOW TEMPERATURE (TEXUS 4)
W. Littke *In* ESA, Summary Review of Sounding Rocket Experiments in Fluid Science and Materials Sciences: TEXUS 1 to 20; MASER 1 and 2 Feb. 1991 p 202 (For primary document see N91-31321 23-29)
Copyright Avail: NTIS HC/MF A15; EPD, ESTEC, Noordwijk, Netherlands, HC 75 Dutch guilders

An experiment aimed at assessing the temperature range of protein crystallization under microgravity conditions is summarized. The same apparatus and experimental procedure as in TEXUS 3 (Technological Experiments under Microgravity) were employed but at a temperature of -8 C instead of +20 C. The melting points of the solutions were lowered by adding glycerol. Again strictly laminar diffusion process was observed. But the tendency for protein to crystallize at -8 C was reduced and nothing was obtained but a precipitate if amorphous protein material. ESA

N91-31397# Freiburg Univ. (Germany, F.R.). Chemisches Lab.
DIFFUSION-CONTROLLED GROWTH OF SINGLE CRYSTALS OF PROTEIN (TEXUS 5)
W. Littke *In* ESA, Summary Review of Sounding Rocket Experiments in Fluid Science and Materials Sciences: TEXUS 1 to 20; MASER 1 and 2 Feb. 1991 p 204-205 (For primary document see N91-31321 23-29)
Copyright Avail: NTIS HC/MF A15; EPD, ESTEC, Noordwijk, Netherlands, HC 75 Dutch guilders

An experiment aimed at determining the reproducibility of the promising results obtained in TEXUS 3 (Technological Experiments under Microgravity) prior to a Spacelab 1 experiment, is summarized. The same experimental conditions as in TEXUS 3 were reproduced and yielded the same promising results. Some rod shaped single crystals of the enzyme B galactosidase, molecular weight 465,000 D, embedded in amorphous protein material were obtained within the 6 minutes of the costing phase of the rocket. The linear dimensions are about three times larger than those of crystals grown on Earth over a period of 60 hours. ESA

N91-31398# Technische Univ., Brunswick (Germany, F.R.). Inst. fuer Werkstoffkunde u. Herstellungsverfahren.
ALLOY FORMATION (TEXUS 5)
F. Haessner and P. Wehr *In* ESA, Summary Review of Sounding Rocket Experiments in Fluid Science and Materials Sciences: TEXUS 1 to 20; MASER 1 and 2 Feb. 1991 p 208-209 (For primary document see N91-31321 23-29)
Copyright Avail: NTIS HC/MF A15; EPD, ESTEC, Noordwijk, Netherlands, HC 75 Dutch guilders

An experiment to study the formation of alloys under microgravity conditions, regarding in particular the mutual dissolution rate of metals, the influence of surface layers, the microstructures obtained and the heat of alloying reactions, is summarized. This experiment was carried out prior to the Spacelab project 'non contact measuring technique, determination of enthalpies of reaction in zero gravity'. On the basis of numerous measurements, 35 pairs of metallic samples were selected, each with a CuTi alloy acting as solvent. The samples contained in alumina crucibles were processed in an isothermal furnace. In each crucible, a weak contact was pre-established between the solvent alloys and the metal to be dissolved. Ground reference tests were carried out under the same experimental conditions. Macroscopic and microscopic inspection of the microstructures, as well as SEM and X-ray microanalysis were achieved. A summary of the results obtained both on Earth and in space is presented. ESA

N91-31399# Hamburg Univ. (Germany, F.R.).
SOLIDIFICATION OF A HYPEREUTECTIC ALLOY (TEXUS 1)
H. Ahlborn *In* ESA, Summary Review of Sounding Rocket Experiments in Fluid Science and Materials Sciences: TEXUS 1 to 20; MASER 1 and 2 Feb. 1991 p 210-211 (For primary document see N91-31321 23-29)
Copyright Avail: NTIS HC/MF A15; EPD, ESTEC, Noordwijk, Netherlands, HC 75 Dutch guilders

Primary crystals formed in a melt are submitted on Earth to thermal convection and gravity driven sedimentation of flotation. This experiment aimed at studying the influence of a diffusion controlled solidification process on the structure of a hypereutectic alloy. A sample of hypereutectic alloy (60 wt percent Sb-40 wt percent Ag) was melted and solidified under microgravity conditions and in the chamber on an acoustic levitator. A cine camera was used to observe the behavior of the sample and its shape alterations during melting and solidification. The acoustic levitator did not work as expected. The sample was processed while free floating but it touched the prepositioning wire cage before it solidified. The metallographic analysis of the sample showed that, as expected, no gravity driven sedimentation occurred. The primary crystals are unexpectedly larger and the eutectic structure finer than in the samples processed on ground. The undisturbed solidification achieved under microgravity conditions resulted in bigger primary crystals and deeper undercooling, therefore in a finer structure of the eutectic. ESA

N91-31400# Royal Inst. of Tech., Stockholm (Sweden). Dept. of Casting of Metals.
SOLIDIFICATION OF ALLOYS (TEXUS 1)
H. Fredriksson and T. Carlberg *In* ESA, Summary Review of Sounding Rocket Experiments in Fluid Science and Materials Sciences: TEXUS 1 to 20; MASER 1 and 2 Feb. 1991 p 212-213 (For primary document see N91-31321 23-29)
Copyright Avail: NTIS HC/MF A15; EPD, ESTEC, Noordwijk, Netherlands, HC 75 Dutch guilders

An experiment studying the structure of eutectic and hypereutectic alloys solidified in the absence of convection sedimentation is summarized. Various samples were either processed isothermally in mirror furnaces (sample size: 7 mm diam., 12 mm length) or solidified directionally in gradient furnaces (sample size: 8 mm diam., 80 mm length). Sn-Zn eutectic was isothermally processed. The normally fan shaped structure of this eutectic is probably due to the fragmentation of growing plates, which generate new plates oriented in a slightly shifted direction. When compared with the reference sample processed on the ground, the space sample exhibited in its center a larger proportion of this normal eutectic structure (90 percent instead of 60 percent) and a coarser arrangement. It is therefore concluded that convection influences strongly the formation of such structures. Al-Al2Cu eutectic was solidified directionally. No significant differences between the structures of the space and reference samples were observed as the solidification rates were rather high and the accuracy of the measurement of the fault density in the cellular structures obtained was low. Al-15 percent Cu (hypereutectic) was solidified directionally. The transition between a columnar and an equiaxed structure was observed. The length of the zone with directed columnar dendrites was 38 mm long in the space sample and only 25 mm in the ground reference sample. This is thought to be due to the more stable conditions in microgravity with a reduced convection in the melt. ESA

N91-31401# Royal Inst. of Tech., Stockholm (Sweden). Dept. of Casting of Metals.
SOLIDIFICATION OF ALLOYS (TEXUS 2)
H. Fredriksson and T. Carlberg *In* ESA, Summary Review of Sounding Rocket Experiments in Fluid Science and Materials Sciences: TEXUS 1 to 20; MASER 1 and 2 Feb. 1991 p 214 (For primary document see N91-31321 23-29)
Copyright Avail: NTIS HC/MF A15; EPD, ESTEC, Noordwijk, Netherlands, HC 75 Dutch guilders

The AlSi eutectic alloy exhibits on Earth a plate like fan shaped structure resulting from the fragmentation and further growth of crystals. The fragmentation occurs due to temperature fluctuations or convection effects and is thus related to the stability of the melt during the process. Under stabilized conditions, i.e. in microgravity, a more or less normal eutectic structure should be obtained. A sample of Al-12.5 percent Si was heated up to 650 C and cooled down in a mirror furnace under microgravity conditions. About 80 percent of the space processed sample exhibited a fan shaped structure which was interpreted as the result of an incomplete dissolution of small Si crystals in the melt before cooling down. In ground processed samples, it was clearly shown that the amount of fan shaped structure obtained depends on the melting time. In addition, the dissolution rate was slower in microgravity due to the absence of convection flows. ESA

N91-31402# Royal Inst. of Tech., Stockholm (Sweden). Dept. of Casting of Metals.
MACROSEGREGATION IN Ag-Sn ALLOYS (MASER 1)
H. Fredriksson, H. Shahani, and R. W. Smith (Queens Univ., Kingston, Ontario) *In* ESA, Summary Review of Sounding Rocket Experiments in Fluid Science and Materials Sciences: TEXUS 1 to 20; MASER 1 and 2 Feb. 1991 p 216-217 (For primary document see N91-31321 23-29)
Copyright Avail: NTIS HC/MF A15; EPD, ESTEC, Noordwijk, Netherlands, HC 75 Dutch guilders

Macrosegregation is thought to be mainly due to interdendritic flows generated by buoyancy forces and shrinkage as well as to the sedimentation of the primary crystals. A microgravity experiment intended to investigate the macrosegregation in directionally solidified hypereutectic Ag-Sn alloys (less than 48 wt percent of Ag, primary precipitation of Ag3Sn below 480 C and eutectic reaction at 221 C) is summarized. No macrosegregation and, due to significant radial heat losses, no orientation of the primary precipitates occurred in the flight samples. In the solid down sample, the platelike primary precipitates of AgSn were thicker and more numerous in the lower part of the sample. The very top consisted of pure eutectic. Probably due to the fact that the primary precipitates were well attached to each other, no macrosegregation was observed in the solid up sample. A model was developed to describe the flow generated by the primary precipitation of AgSn ahead of the solidification front, assuming that the macrosegregation was due to interdendritic flows only. The results of the calculations were in good agreement with the experimental observations. ESA

N91-31403# Royal Inst. of Tech., Stockholm (Sweden). Dept. of Casting of Metals.
DIRECTIONAL SOLIDIFICATION OF Al-Cu ALLOYS (MASER 2)
H. Shahani and H. Fredriksson *In* ESA, Summary Review of Sounding Rocket Experiments in Fluid Science and Materials Sciences: TEXUS 1 to 20; MASER 1 and 2 Feb. 1991 p 218-219 (For primary document see N91-31321 23-29)
Copyright Avail: NTIS HC/MF A15; EPD, ESTEC, Noordwijk, Netherlands, HC 75 Dutch guilders

The mechanism of the columnar equiaxed transition process is strongly influenced by the natural convection in the melt. Free crystals can grow ahead of the solidification front when the cooling rate is sufficiently high and the solidification rate sufficiently slow. These crystals can then block the columnar growth by adhering to the front. According to this theory, the columnar zone should be longer under microgravity. Two samples of AlCu (20 and 43 wt percent Cu), 4 mm diameter and 60 mm long, were processed in gradient furnaces. Typical temperature gradients, solidification rates and cooling rates are plotted. The lengths of the columnar zones are given. It is thought that, due to the low gradients, the length of the 'mushy' zone was up to several cm and that an extended network was formed ahead of the front. Due to the small size of the samples, convection was hampered on ground and similar structures were obtained. ESA

N91-31404# Commissariat a l'Energie Atomique, Grenoble (France). Centre d'Etudes Nucleaires.
DIRECTIONAL SOLIDIFICATION OF EUTECTICS (TEXUS 6)
J. J. Favier and J. deGoer *In* ESA, Summary Review of Sounding Rocket Experiments in Fluid Science and Materials Sciences: TEXUS 1 to 20; MASER 1 and 2 Feb. 1991 p 220-221 (For primary document see N91-31321 23-29)
Copyright Avail: NTIS HC/MF A15; EPD, ESTEC, Noordwijk, Netherlands, HC 75 Dutch guilders

An experiment to assess the influence of gravity on the structure of lamellar and fiber like eutectic alloys is summarized. One lamellar eutectic sample (Al2Cu-Al) and one fiber like eutectic sample (Al3NiAl) were directionally solidified in gradient furnaces under microgravity conditions. Their structure was studied and the lamellar or fibrous spacings were measured by laser diffraction along the whole of each sample. No appreciable modification of the regularity of the eutectic structures between 1 g and 0 g could be observed. This was contrary to results obtained in Skylab eutectic Al2Cu-Al. However, no steady state growth conditions were achieved in these experiments due to the non steady thermal conditions (increasing rate of solidification) which induced a rapid morphological destabilization of the solidification front after a few tens of seconds under microgravity conditions. ESA

N91-31405# Erlangen-Nuremberg Univ. (Germany, F.R.). Inst. of Materials Science.
DIRECTIONAL SOLIDIFICATION OF EUTECTICS InSb-NiSb (TEXUS 10)
G. Mueller and P. Kyr *In* ESA, Summary Review of Sounding Rocket Experiments in Fluid Science and Materials Sciences: TEXUS 1 to 20; MASER 1 and 2 Feb. 1991 p 222-223 (For primary document see N91-31321 23-29)
Copyright Avail: NTIS HC/MF A15; EPD, ESTEC, Noordwijk, Netherlands, HC 75 Dutch guilders

An experiment to determine the influence of convection on the growth and the structure of fiber like eutectic alloys is summarized. An InSb-NiSb eutectic alloy (97.7 and 2.3 wt percent respectively) was melted in a mirror furnace and directionally solidified, starting before the launch of the rocket and under microgravity conditions. Demarcation of the solid/liquid interface was achieved during the whole growth period by means of current pulses through the sample. The analysis of the microstructures along a longitudinal section of the sample showed that the initial interface was practically plane. 11 mm of sample were resolidified before the launch, which induced a growth discontinuity. At that time, the interface was then slightly convex. 4 mm of sample were solidified under microgravity conditions. The corresponding microstructure confirmed the results of the previous space experiment. The average spacing between the NiSb needles decreased by 20 percent during the flight. This result has again been quantitatively confirmed in experiments on D-1 and can be examined by the theory of eutectic growth. ESA

N91-31406# Technische Hochschule, Aachen (Germany, F.R.). Foundry Inst.
BOUNDARY LAYERS IN TRANSPARENT MELTS (TEXUS 10)
A. Ecker and P. R. Sahm *In* ESA, Summary Review of Sounding Rocket Experiments in Fluid Science and Materials Sciences: TEXUS 1 to 20; MASER 1 and 2 Feb. 1991 p 224-227 (For primary document see N91-31321 23-29)
Copyright Avail: NTIS HC/MF A15; EPD, ESTEC, Noordwijk, Netherlands, HC 75 Dutch guilders

An experiment to determine concentration band temperature distribution in a solidifying transparent melt is summarized. Investigation of their time dependence and their interaction with the solidification front was addressed. The transparent model alloy

succinonitrile, 15 wt percent ethanol, was directionally solidified with a dendritic interface. The concentration distribution was measured by means of an interferometer, the interferograms being recorded by a cine camera. The temperature distribution was determined by means of thermistors located in the melt. Large differences were observed between the temperature and concentration profiles recorded on microgravity and those recorded on Earth. These differences were shown to be due, on Earth, to rising droplets of the ethanol rich phase resulting in a concentration profile which is not yet described by any known theory. In contrast the concentration profile recorded in microgravity agrees well with the existing theories and thus supports the text-book expectation. ESA

N91-31407# Ruhr Univ., Bochum (Germany, F.R.).
SEGREGATION BEHAVIOUR OF RARE EARTHS UNDER MICROGRAVITY AND NORMAL GRAVITY CONDITIONS (TEXUS 13)
S. Sprenger, H. Bach, and S. Methfessel *In* ESA, Summary Review of Sounding Rocket Experiments in Fluid Science and Materials Sciences: TEXUS 1 to 20; MASER 1 and 2 Feb. 1991 p 228-233 (For primary document see N91-31321 23-29)
Copyright Avail: NTIS HC/MF A15; EPD, ESTEC, Noordwijk, Netherlands, HC 75 Dutch guilders

The still incompletely known Eu-La phase diagram was determined experimentally by Differential Thermal Analysis (DTA). In contrast to the theoretical predictions, a miscibility gap was found over a reduced concentration interval and the critical temperature was about 960 C. The experiment is summarized and results, including those with Mossbauer measurements, are discussed. For a better understanding of the parameters dominating the separation, further experiments are needed which will measure the surface tension and the viscosity as a function of the temperature and concentration. ESA

N91-31408# Deutsche Forschungs- und Versuchsanstalt fuer Luft- und Raumfahrt, Cologne (Germany, F.R.). Inst. for Materials Research.
COMPOSITE MATERIALS, 1 (TEXUS 1)
H. U. Walter and G. Ziegler *In* ESA, Summary Review of Sounding Rocket Experiments in Fluid Science and Materials Sciences: TEXUS 1 to 20; MASER 1 and 2 Feb. 1991 p 236-237 (For primary document see N91-31321 23-29)
Copyright Avail: NTIS HC/MF A15; EPD, ESTEC, Noordwijk, Netherlands, HC 75 Dutch guilders

Due to the absence of sedimentation and buoyancy effects, the stability of multicomponent systems with one and more fluid phases was postulated under microgravity conditions. There are, however, additional mechanisms that are not based on gravitational forces which could lead to the regrouping or separation of components during liquid phase processing such as mechanisms based in intermolecular forces. An experiment to identify those mechanisms for liquid-liquid gas systems, using model systems for the investigation is summarized. The model systems investigated consisted of Ag with additions of Na-glass (4:1); pore volumes were of the order of 10 percent. The melting point of Ag is at 960.8 C and the viscosity of the Na glass at 1100 C is 10(exp 3) P. The sample was rapidly melted and resolidified after a melting time of 1 min in microgravity. The mixture was quantitatively separated into a large drop of Ag without any inclusion or pores and a single pore, both surrounding by a layer of glass. These results indicated that separation can take place under microgravity conditions as well and can be driven by surface tension gradients. The preparation of heterogeneous alloys or composites from powder mixtures is, therefore, not possible with mixtures having non-wetting components and pore volume or with degassing materials. ESA

N91-31409# Deutsche Forschungs- und Versuchsanstalt fuer Luft- und Raumfahrt, Cologne (Germany, F.R.). Inst. for Materials Research.
COMPOSITE MATERIALS, 2 (TEXUS 2)
H. U. Walter and G. Ziegler *In* ESA, Summary Review of Sounding Rocket Experiments in Fluid Science and Materials Sciences: TEXUS 1 to 20; MASER 1 and 2 Feb. 1991 p 238-239 (For primary document see N91-31321 23-29)
Copyright Avail: NTIS HC/MF A15; EPD, ESTEC, Noordwijk, Netherlands, HC 75 Dutch guilders

An experiment to investigate mechanisms causing component separation, drop coalescence, drop and bubble migration during liquid phase processing of heterogeneous mixtures in the absence of gravity driven sedimentation, is summarized. The model systems investigated were: (1) 80 percent Ag-20 percent glass and (2) 35 percent Ag-65 percent glass. The samples were prepared from carefully degassed powder mixtures by hot isostatic pressing to theoretical density. They were melted and resolidified under microgravity conditions. The tendency for glass to reach the energetically favorable crucible walls was again observed, although in the absence of pores. Sample 2 was quantitatively separated. However, only a partial separation of the components was observed in sample 1 where glass inclusions remained in the Ag core. This was interpreted as the result of the formation of a three dimensional network of particles which tended to gather all inclusions toward the crucible walls. Due to the lower glass concentration in sample 1 some particles were not reached by the network and remained in the Ag matrix. This indicates also that Stokes migration of particles was not predominant. ESA

N91-31410# Deutsche Forschungs- und Versuchsanstalt fuer Luft- und Raumfahrt, Cologne (Germany, F.R.). Inst. for Materials Research.
IMMISCIBLES, 1 (TEXUS 3)
H. U. Walter *In* ESA, Summary Review of Sounding Rocket Experiments in Fluid Science and Materials Sciences: TEXUS 1 to 20; MASER 1 and 2 Feb. 1991 p 240 (For primary document see N91-31321 23-29)
Copyright Avail: NTIS HC/MF A15; EPD, ESTEC, Noordwijk, Netherlands, HC 75 Dutch guilders

The mechanisms governing component separation in liquid-liquid mixtures are of interest in view of the results of microgravity experiments dealing with the preparation of dispersions from binary systems exhibiting a miscibility gap in the liquid state. Due to the complexity of these systems and due to the variety of mechanisms which may contribute to coarsening and component separation, the analysis that could be performed was rather limited. The present experiment series is aimed, therefore, at investigating and isolating some of these mechanisms using a simple model system: Ag/Na silicate glass. Complete separation of the components was observed with the glass coating the inside of the stainless steel and the Ag forming the core of sample. Since Marangoni transport was absent and all coarsening mechanisms related to nucleation and growth of nuclei were avoided thanks to a system of mutually insoluble components, it was concluded that the separation observed was due to coalescence and wetting of the rather high volume fraction chosen. It could be demonstrated theoretically that a coherent network of interconnected particles forms in dispersions having a volume fraction of the minority component of more than 12 percent. This was the case and the remelting of such dispersions resulted in coalescence and redistribution according to wetting conditions. The preparation of dispersions using immiscible systems is therefore not posiible at high volume fractions. ESA

N91-31411# Deutsche Forschungs- und Versuchsanstalt fuer Luft- und Raumfahrt, Cologne (Germany, F.R.). Inst. for Materials Research.
IMMISCIBLES, 2 (TEXUS 5)
H. U. Walter *In* ESA, Summary Review of Sounding Rocket Experiments in Fluid Science and Materials Sciences: TEXUS 1 to 20; MASER 1 and 2 Feb. 1991 p 242-243 (For primary document see N91-31321 23-29)
Copyright Avail: NTIS HC/MF A15; EPD, ESTEC, Noordwijk, Netherlands, HC 75 Dutch guilders

An experiment to investigate the stability of liquid liquid dispersions as a function of the volume fraction of the minority component is summarized. Previous experiments conducted in

microgravity resulted in samples where at 35, 20 and 17 vol percent resp. of glass in an Ag matrix complete separation of the components was observed. This experiment aimed at investigating lower volume fractions. Metallurgically prepared powder samples of borosilicate glass dispersed in an Ag matrix were remelted and solidified in an isothermal furnace during the coasting period of the rocket. The volume percentage of glass in the samples was: 11, 9, 7, 5, 3 and 1 percent resp. With increasing volume fraction, increasing coarsening of glass inclusions was observed. The initial dispersion was preserved with samples having a volume fraction of glass below 5 percent only. This result proved that coalescence of neighboring, contacting particles due to statistical distribution is of major importance with regard to coarsening. Computer-generated statistical distributions of spherical particles showed similarly that chains and three dimensional grouping of particles in contact with each other dominate above 12 vol percent. The larger number of particles was isolated only below 12 percent. ESA

N91-31412# Deutsche Forschungs- und Versuchsanstalt fuer Luft- und Raumfahrt, Cologne (Germany, F.R.). Inst. for Materials Research.

DISPERSION ALLOYS (TEXUS 7)

H. U. Walter *In* ESA, Summary Review of Sounding Rocket Experiments in Fluid Science and Materials Sciences: TEXUS 1 to 20; MASER 1 and 2 Feb. 1991 p 244-245 (For primary document see N91-31321 23-29)

Copyright Avail: NTIS HC/MF A15; EPD, ESTEC, Noordwijk, Netherlands, HC 75 Dutch guilders

Previous experiments with model systems and powder metallurgically prepared samples allowed the study of the stability of liquid liquid dispersions and in particular the influence of the volume fraction. They showed that the stability of liquid dispersions can be obtained only for volume fractions below 10 pct. An experiment to check the feasibility of producing metallic dispersions with systems having a miscibility gap in the liquid state is summarized. Eight samples of three binary systems with a miscibility gap in the liquid state (Al-Pb, Al-In and Al-Bi) were investigated under microgravity conditions. Even though the volume fraction of the minority component was kept below 10 percent, no dispersion with statistical distribution of inclusions was obtained. The major transport of droplets was clearly due to Marangoni convection since the minority component was found in the hottest region of the samples. The interaction of inclusions with the solidification front resulted in either linear or cellular structures, depending on the thermal gradient during solidification. This showed that the dispersions needed for technological applications cannot be produced by simply cooling through the miscibility gap even in microgravity. Marangoni transport has to be counteracted or minimized. ESA

N91-31413# Daelen und Loos G.m.b.H., Wiesbaden-Schierstein (Germany, F.R.). Glyco-Metall-Werke.

Al-Pb BEARING ALLOY (TEXUS 1)

E. Hodes and M. Steeg *In* ESA, Summary Review of Sounding Rocket Experiments in Fluid Science and Materials Sciences: TEXUS 1 to 20; MASER 1 and 2 Feb. 1991 p 246-247 (For primary document see N91-31321 23-29)

Copyright Avail: NTIS HC/MF A15; EPD, ESTEC, Noordwijk, Netherlands, HC 75 Dutch guilders

Al-Pb dispersions hold promise for industrial applications since they are expected to show excellent properties. But homogeneous Al-Pb alloys cannot be obtained by casting due to the gravity driven sedimentation of Pb. An experiment under microgravity conditions expected to obtain a fine liquid-liquid dispersion and to conserve it in the solid by fast cooling, is summarized. A compact powder mixture (Al-8 percent Pb, 3.5 percent Si, 1.5 percent Cu, 1 percent Sn in wt) was heated under microgravity conditions up to 1100 C, i.e. above the miscibility gap. The temperature was decreased to below 1000 C to form the liquid-liquid dispersion which was then rapidly solidified. Pores were formed due to an insufficient densification and/or degassing of the initial material, and gathered between the border region, with an irregular grain structure, and the dendritic bulk. Oxide layers around the particles prevented the creation of a homogeneous melt and the sample processed on the ground and in space exhibited similar features. However, the size of the Pb particles was significantly smaller in the space sample than in the ground sample. ESA

N91-31414# Krupp (Fried.) G.m.b.H., Essen (Germany, F.R.).

FUNDAMENTAL STUDIES IN THE MANGANESE-BISMUTH SYSTEM (TEXUS 2)

P. Pant *In* ESA, Summary Review of Sounding Rocket Experiments in Fluid Science and Materials Sciences: TEXUS 1 to 20; MASER 1 and 2 Feb. 1991 p 248-249 (For primary document see N91-31321 23-29)

Copyright Avail: NTIS HC/MF A15; EPD, ESTEC, Noordwijk, Netherlands, HC 75 Dutch guilders

The manganese-bismuth system exhibits a miscibility gap in the liquid state. At 445 C the intermetallic ferromagnetic compound MnBi forms peritectically. On ground, melting and solidification result in a complete separation of the primary constituent. This is accumulated, via buoyancy driven flotation, in the upper part of the sample so that the proportion of MnBi obtained is less than 20 wt percent. An experiment aimed at clarifying whether the separation process can be avoided in microgravity, thus allowing the peritectic reaction to run its course so as to obtain pure MnBi is summarized. Manganese-bismuth specimens produced by special processes under terrestrial conditions were investigated. They were melted at 1150 C in an isothermal furnace and cooled down at a rate of 400 K/min. Both samples did not exhibit any signs of segregation. The MnBi phase was uniformly distributed and present in the form of small crystallites. This favorable constellation of the structure induced a considerable increase of the coercivity values when compared with the values in specimens processed on the ground. This experiment with manganese bismuth as a model system proved that, in microgravity, it is possible to allow peritectic reactions in systems with miscibility gap in the liquid state to proceed to completion. ESA

N91-31415# Royal Inst. of Tech., Stockholm (Sweden). Dept. of Casting of Metals.

SOLIDIFICATION OF IMMISCIBLE ALLOYS: ZnBi (TEXUS 2)

H. Fredriksson and T. Carlberg *In* ESA, Summary Review of Sounding Rocket Experiments in Fluid Science and Materials Sciences: TEXUS 1 to 20; MASER 1 and 2 Feb. 1991 p 250-251 (For primary document see N91-31321 23-29)

Copyright Avail: NTIS HC/MF A15; EPD, ESTEC, Noordwijk, Netherlands, HC 75 Dutch guilders

An experiment to investigate the solidification of immiscible alloys under microgravity conditions is summarized. ZnBi alloys (8, 24 and 38 wt percent Bi) were prepared by casting and reprocessed in microgravity either under isothermal conditions in mirror furnaces or under thermal gradient in resistance heated furnaces. The calculations of the diffusion controlled growth rate of the particles during cooling through the miscibility gap yielded results considerably smaller that the experimental ones. This showed that the migration of the particles (Stokes and Marangoni effects) and the coalescence processes have to be taken into account in the theoretical models. The formation of the surface layer was believed to be due to residual accelerations which originated in the sedimentation of Bi rich droplets. ESA

N91-31416# Royal Inst. of Tech., Stockholm (Sweden). Dept. of Casting of Metals.

THE COALESCENCE PROCESS IN IMMISCIBLE ALLOYS (TEXUS 3)

H. Fredriksson and A. Bergman *In* ESA, Summary Review of Sounding Rocket Experiments in Fluid Science and Materials Sciences: TEXUS 1 to 20; MASER 1 and 2 Feb. 1991 p 252-253 (For primary document see N91-31321 23-29)

Copyright Avail: NTIS HC/MF A15; EPD, ESTEC, Noordwijk, Netherlands, HC 75 Dutch guilders

An experiment to study the precipitation process as well as the coalescence process of droplets in a liquid matrix is summarized. Eleven samples of Zn-Bi alloys were processed. Three different compositions (4, 6 and 9 wt percent) and different initial

size distributions (obtained by using different quenching rates during their preparation) were investigated under isothermal conditions in mirror furnaces. The samples were heated up to a temperature just above the monotectic temperature. The holding time inside the miscibility gap ranged from 10 to 110 s before the samples cooled down naturally. The droplet distributions in the flight samples were compared with the droplet distributions in reference samples. It appeared that the coalescence process was much faster than expected when considering only Ostwald ripening and collision processes. The larger the volume fraction of the droplets, the larger was the difference between predictions and observations. The precipitated liquid even formed a surface layer around some samples in which the collision of the droplets was enhanced accordingly. ESA

N91-31417# Royal Inst. of Tech., Stockholm (Sweden). Dept. of Casting of Metals.
THE COALESCENCE PROCESS IN IMMISCIBLE ALLOYS (TEXUS 5)
H. Fredriksson and A. Bergman *In* ESA, Summary Review of Sounding Rocket Experiments in Fluid Science and Materials Sciences: TEXUS 1 to 20; MASER 1 and 2 Feb. 1991 p 254 (For primary document see N91-31321 23-29)
Copyright Avail: NTIS HC/MF A15; EPD, ESTEC, Noordwijk, Netherlands, HC 75 Dutch guilders

An experiment to study the precipitation process as well as the coalescence process of droplets in a liquid matrix is summarized. Seven Zn-4 percent Bi samples were investigated with different initial size distributions obtained by using two quenching techniques during their preparation. The samples were contained in either boron nitride or graphite crucibles and were isothermally processed in mirror furnaces under microgravity conditions. They were held at a temperature above the monotectic temperature for a given time and then cooled down naturally. The droplet distributions in the flight samples and in samples processed on the ground were compared. Again, the coalescence process was much faster than expected when considering only Ostwald ripening and collision processes. This was attributed to a Marangoni movement of the droplets. No influence of the crucible materials on the coalescence process could be detected. The larger was the initial droplet size in the samples, the faster was to coalescence process. ESA

N91-31418# Royal Inst. of Tech., Stockholm (Sweden). Dept. of Casting of Metals.
UNIDIRECTIONAL SOLIDIFICATION OF IMMISCIBLE ALLOYS (TEXUS 5)
H. Fredriksson and A. Bergman *In* ESA, Summary Review of Sounding Rocket Experiments in Fluid Science and Materials Sciences: TEXUS 1 to 20; MASER 1 and 2 Feb. 1991 p 256-257 (For primary document see N91-31321 23-29)
Copyright Avail: NTIS HC/MF A15; EPD, ESTEC, Noordwijk, Netherlands, HC 75 Dutch guilders

An experiment to analyze the effect of a temperature gradient on the precipitation of droplets in immiscible alloys is summarized. Two Cu-Pb samples (36 and 42 wt percent Pb, respectively) were placed in 0.8 mm thick graphite crucibles, 65 mm in length and 4 mm inner diameter, which were closed at their top with cement. The samples were processed in gradient furnaces under microgravity conditions. The bottom of each sample was threaded to a 6 mm copper rod in contact with a phase change heat sink. After switching off the furnace, unidirectional extraction of the heat from the samples was achieved and thus directional solidification. The temperature was measured in each sample at three different locations. Reference samples were processed in the same furnaces. It was observed that, in the space samples, the droplets migrated towards the hotter region during the precipitation process. In the ground processed samples, a gravity induced sedimentation of the droplet occurred. A theoretical treatment of the experimental results was performed. The theory related the movement of the droplets to the temperature dependence of the interfacial tension between the liquid droplets and the liquid matrix. ESA

N91-31419# Royal Inst. of Tech., Stockholm (Sweden). Dept. of Casting of Metals.
UNIDIRECTIONAL SOLIDIFICATION OF IMMISCIBLE ALLOYS (TEXUS 7)
H. Fredriksson *In* ESA, Summary Review of Sounding Rocket Experiments in Fluid Science and Materials Sciences: TEXUS 1 to 20; MASER 1 and 2 Feb. 1991 p 258 (For primary document see N91-31321 23-29)
Copyright Avail: NTIS HC/MF A15; EPD, ESTEC, Noordwijk, Netherlands, HC 75 Dutch guilders

An experiment to analyze the effect of a temperature gradient and of the composition on the precipitation of droplets in immiscible alloys is summarized. Three Zn-Bi based samples (with addition of 3 percent of Cu or 3 percent of Mg) were placed in graphite crucibles, whose tops were closed with cement. The samples were processed in gradient furnaces under microgravity conditions. After melting, the furnaces were switched off and the unidirectional extraction of heat from the bottom of the samples was achieved by means of copper rods in contact with a phase-change heat sink. Reference samples were processed under normal gravity conditions in the same furnaces. During the precipitation process in microgravity, the droplets migrated towards the hotter region of the samples due to the Marangoni effect. The theoretical treatment of the experimental results relates the motion of the droplets to their interfacial tension. The different behavior observed in Cu-Pb and Zn-Bi alloys is due to the different temperature dependence of their interfacial tension. ESA

N91-31420# Royal Inst. of Tech., Stockholm (Sweden). Dept. of Casting of Metals.
UNIDIRECTIONAL SOLIDIFICATION OF Zn-Bi SAMPLES (TEXUS 14b)
H. Fredriksson *In* ESA, Summary Review of Sounding Rocket Experiments in Fluid Science and Materials Sciences: TEXUS 1 to 20; MASER 1 and 2 Feb. 1991 p 260-261 (For primary document see N91-31321 23-29)
Copyright Avail: NTIS HC/MF A15; EPD, ESTEC, Noordwijk, Netherlands, HC 75 Dutch guilders

The structures observed in alloys with a miscibility gap in the liquid state depend on the temperature gradient applied during the solidification process and on gravity. In gradient experiments performed under normal and reduced gravity it is possible to distinguish between these two effects. Samples of Zn-Bi with 4, 6 and 8 wt percent Bi were investigated. In the reference sample a few numbers of large inclusions were found from 2 to 3.5 cm from the bottom and a large number of small inclusions from 3.5 cm to the very top. In the space samples, no droplets were found up to 3.5 cm. Above that level an increasing number of droplets with increasing size could be observed. The difference in distribution profile between the reference and flight sample could be related to the gravitational effect in the former and to the Marangoni effect in the latter. However, the existence of a droplet free area at the bottom of each sample could not be explained. ESA

N91-31421# Royal Inst. of Tech., Stockholm (Sweden). Dept. of Casting of Metals.
DIRECTIONAL SOLIDIFICATION OF IMMISCIBLE ALLOYS Zn-Pb (MASER 2)
H. Fredriksson, H. Shahani, A. Bergman, and A. Eliasson *In* ESA, Summary Review of Sounding Rocket Experiments in Fluid Science and Materials Sciences: TEXUS 1 to 20; MASER 1 and 2 Feb. 1991 p 262-263 (For primary document see N91-31321 23-29)
Copyright Avail: NTIS HC/MF A15; EPD, ESTEC, Noordwijk, Netherlands, HC 75 Dutch guilders

An experiment to analyze the influence of immiscible alloys is summarized. Following on experiments with the systems Cu-Pb and Zn-Bi, Zn-Pb samples were investigated. Two samples of Zn-2.5 percent Pb and Zn-4 percent Pb contained in graphite crucibles (65 mm long, 4 mm inner diameter) were processed in gradient furnaces under microgravity. The metallographic analysis of the samples indicated that the precipitated droplets migrated as expected towards the hottest regions of the samples due to

interfacial tension gradients. A theoretical analysis could be performed by correlating the observations with the thermal profile recorded during the flight. The different migration velocities observed between the systems Zn-Pb, Zn-Bi and Cu-Pb could be related to the different temperature dependences of the corresponding interfacial tensions. The migration velocity of the droplets increases with an increasing temperature dependence of the interfacial tension (accordingly, the higher velocities were observed in the Cu-Pb system). In a Zn-Bi sample processed on the ground under thermally stabilizing conditions (hottest region at the top of the sample), the Marangoni effect even balanced the gravity-driven sedimentation of Bi-rich droplets of given size.
ESA

N91-31422# Fulmer Research Inst. Ltd., Stoke Poges (England). Materials Processing Section.
IMMISCIBLE ALLOY SYSTEM Al-Pb (TEXUS 7)
P. D. Caton and W. G. Hopkins *In* ESA, Summary Review of Sounding Rocket Experiments in Fluid Science and Materials Sciences: TEXUS 1 to 20; MASER 1 and 2 Feb. 1991 p 264-265 (For primary document see N91-31321 23-29)
Copyright Avail: NTIS HC/MF A15; EPD, ESTEC, Noordwijk, Netherlands, HC 75 Dutch guilders

An experiment to demonstrate the increased stability of dispersions under microgravity conditions where the gravity driven sedimentation force is reduced, and to get some indications on the importance of surface effects on the agglomeration and solidification front inclusion when the distorting effects of gravity are removed, is summarized. Three aluminum samples containing lead in the range 6 to 8 wt percent (monotectic temperature 660 C) were prepared by melting under partial pressure of inert gas and casting into a copper mold in order to get a fine initial dispersion. The samples processed on the ground exhibit the expected agglomerations of lead in the direction of gravity. In space, in sample 1, a fine dispersion was produced and retained, with however a denuded region of the surface believed to result from solidification rate variations. Sample 3 also showed particles pushed in the direction of solidification but with an unexpected rim of larger droplets within the denuded region on the surface. Sample 2 showed an unexpected segregation of large droplets in the last frozen liquid. In view of the low of solubility of Pb in Al at the monotectic point (1.5 wt percent), and the rapid solidification of the samples, it was possible to analyze the stability of the dispersion and its interaction with the solidification front as it swept through.
ESA

N91-31423# Battelle Inst., Frankfurt am Main (Germany, F.R.).
ACOUSTIC MIXING (TEXUS 5)
H. Heide and D. Langbein *In* ESA, Summary Review of Sounding Rocket Experiments in Fluid Science and Materials Sciences: TEXUS 1 to 20; MASER 1 and 2 Feb. 1991 p 266-267 (For primary document see N91-31321 23-29)
Copyright Avail: NTIS HC/MF A15; EPD, ESTEC, Noordwijk, Netherlands, HC 75 Dutch guilders

An experiment to test an acoustic mixing system and to prepare a dispersion alloy with a binary alloy presenting a miscibility gap in the liquid state is summarized. A sample consisting of 95 wt percent Zn + 5 wt percent Pb (monotectic temperature 418 C, eutectic temperature 318 C) was heated in a crucible up to 518 C and directionally solidified. The dispersion formed was intermittently held dispersed by means of an ultrasonic generator. The activation of the generator was controlled by thermocouples: it was switched off when the solidification front reached thermocouple 1, and reactivated when the solidification front reached the thermocouple 2. The diameter of the Pb rich particles clearly increased in the central region. This proved the feasibility of the experiment concept.
ESA

N91-31424# Battelle Inst., Frankfurt am Main (Germany, F.R.).
SOLIDIFICATION OF IMMISCIBLE ALLOYS (TEXUS 8)
D. Langbein and W. Heide *In* ESA, Summary Review of Sounding Rocket Experiments in Fluid Science and Materials Sciences: TEXUS 1 to 20; MASER 1 and 2 Feb. 1991 p 268-269 (For primary document see N91-31321 23-29)
Copyright Avail: NTIS HC/MF A15; EPD, ESTEC, Noordwijk, Netherlands, HC 75 Dutch guilders

An experiment aimed at obtaining a fine dispersion by using acoustic mixing in an alloy containing a critical concentration of the minority component is summarized. Samples of Zn-15 wt percent Pb were heated up to 518 C and directionally solidified in a gradient furnace under microgravity conditions. The ultrasonic mixing tool was in direct contact with the melt and controlled by two thermocouples. The mixer was deactivated when the solidification front reached the first thermocouple and reactivated when the front reached the second one. The sections processed with acoustic mixing contained a fairly homogeneous distribution of Pb rich particles with diameters of up to 50 microns in the space sample, whereas in the ground reference sample their diameter was up to 120 microns. When the acoustic mixer was switched off, the particle size increased up to 200 to 300 microns in the space sample, but only up to 150 microns in the ground reference sample. Also, the volume content of lead in the sections solidified during mixing was lower than the initial lead content. This showed that, with a critical concentration of the minority component, rapid and extreme coagulation occurs, and that the use of an acoustic mixer to produce a fine dispersion gives better results in microgravity than on Earth.
ESA

N91-31425# Battelle Inst., Frankfurt am Main (Germany, F.R.).
SEPARATION OF TRANSPARENT FLUIDS DUE TO MARANGONI CONVECTION (TEXUS 7)
D. Langbein and W. Heide *In* ESA, Summary Review of Sounding Rocket Experiments in Fluid Science and Materials Sciences: TEXUS 1 to 20; MASER 1 and 2 Feb. 1991 p 270-271 (For primary document see N91-31321 23-29)
Copyright Avail: NTIS HC/MF A15; EPD, ESTEC, Noordwijk, Netherlands, HC 75 Dutch guilders

An experiment to observe the nucleation, growth, transport and coalescence of droplets during the unidirectional cooling of a transparent immiscible systems from above its critical temperature, is summarized. A mixture of 65 wt percent of methanol and 35 wt percent of cyclohexane (near critical concentration) was investigated in a transparent test cell. The cell was heated up to 50 C, i.e. above the critical temperature (45.6 C), before the launch. Once microgravity conditions were established, one side of the cell was cooled down to 10 C. The separation of the two fluids near the cool side of the cell was observed by means of a camera using a background illumination. The propagation of the cooling front, the growth of cyclohexane particles behind the cooling front, and after about 30 s, strong Marangoni convection towards the cooling front were all observed. Marangoni convection was induced by both thermal and solutal gradients. The behavior observed during the experiment fitted well with the theoretical predictions of many of the physical effects which contribute to the separation. A collective, frontlike migration of the droplets was observed which was stimulated by the temperature and concentration transport induced by Marangoni convention.
ESA

N91-31426# Battelle Inst., Frankfurt am Main (Germany, F.R.).
MARANGONI TRANSPORT OF DROPLETS AT A SOLIDIFICATION FRONT (TEXUS 9)
D. Langbein and W. Heide *In* ESA, Summary Review of Sounding Rocket Experiments in Fluid Science and Materials Sciences: TEXUS 1 to 20; MASER 1 and 2 Feb. 1991 p 272-273 (For primary document see N91-31321 23-29)
Copyright Avail: NTIS HC/MF A15; EPD, ESTEC, Noordwijk, Netherlands, HC 75 Dutch guilders

An experiment to observe the nucleation and growth of droplets and their transport by thermal Marangoni flow as well as their interaction with the solidification front of a transparent binary system with a miscibility gap in the liquid phase is summarized. A mixture of 5 wt percent of methanol and 95 wt percent of cyclohexane was investigated in a transparent cell. The cell was homogeneously heated up to 50 C before the launch. Once microgravity conditions were established, one side of the cell was cooled down to -5 C in order to solidify directionally the liquid matrix of cyclohexane.

The cooled side of the cell was observed with a 16 mm cine camera. The film showed that the initial nucleation front of droplets of the minority component (fog of methanol), which corresponded to the cooling front, was plane, thereby indicating a convection free heat flow. After about 30 s, the droplets had grown sufficiently (up to about 0.2 mm) and started to migrate rapidly toward the top of the cell due to thermal and solutal Marangoni convection. They moved along the driving temperature and concentration field, thus resulting in a collective migration. However, the methanol droplets exhibited a strong tendency to coagulate. A few seconds later, when the cyclohexane solidification started at the bottom of the cell, the methanol droplets formed at the cooled wall detached rapidly. This indicated that solid cyclohexane is perfectly and completely wetted by liquid cyclohexane. ESA

N91-31427# National Research Inst. for Metals, Ibaraki (Japan).
SOLIDIFICATION OF AN Al-Pb-Bi ALLOY UNDER MICROGRAVITY (TEXUS 13)
K. Togano, Y. Yoshida, K. Tachikawa, and K. Nii (National Research Inst. for Metals, Tokyo, Japan) *In* ESA, Summary Review of Sounding Rocket Experiments in Fluid Science and Materials Sciences: TEXUS 1 to 20; MASER 1 and 2 Feb. 1991 p 274-277 (For primary document see N91-31321 23-29)
Copyright Avail: NTIS HC/MF A15; EPD, ESTEC, Noordwijk, Netherlands, HC 75 Dutch guilders

The Al-Pb-Bi ternary alloy system is of monotectic type with a large miscibility gap in the liquid state. On Earth, the Al rich melt and the Pb-Bi alloy tend to separate from each other due to their large density difference, resulting in a large segregation in the alloy ingot. An experiment to obtain an Al-Pb-Bi ingot with a homogeneous dispersion of superconducting Pb-Bi particles in an Al matrix is summarized. This dispersed alloy was to be cold worked into a wire, thus deforming the Pb-Bi particles into fine fibers arrayed parallel in the Al matrix. The resulting composite wire was expected to have good superconducting properties. X-ray perspective views did not show any appreciable gas holes and shrinkage voids inside of the samples except for the top of the reference one. The contour of the samples showed that the BN was not wetted by the molten Al-Pb-Bi alloy which, in addition, was easily removed from the crucibles. A significant difference in microstructure seen between the flight and the ground processed samples is reported. ESA

N91-31428# Consiglio Nazionale delle Ricerche, Genoa (Italy).
MENISCUS STABILITY IN IMMISCIBLE METALS (MASER 1)
A. Passerone, R. Sangiorgi, and F. Rossito (Politecnico di Milano, Italy) *In* ESA, Summary Review of Sounding Rocket Experiments in Fluid Science and Materials Sciences: TEXUS 1 to 20; MASER 1 and 2 Feb. 1991 p 278-279 (For primary document see N91-31321 23-29)
Copyright Avail: NTIS HC/MF A15; EPD, ESTEC, Noordwijk, Netherlands, HC 75 Dutch guilders

A theoretical model predicts that liquid bridges formed in microgravity by immiscible metals are stable as long as the ratio L(exp 3)/V (L-length and V-volume of the bridge) is kept below a critical value which depends on the wetting angle of the interface on the support plates. An experiment aimed at testing this stability criteria and evaluating the wetting conditions of a liquid/liquid interface on different ceramic materials is summarized. The grace of a nearly perfect liquid bridge between two silica plates could be observed. This was considered as the first experimental evidence of the possibility to form stable liquid bridges in immiscible metals. However, the bridge profiles were disturbed on cooling and cannot be reliably compared to computed ones. Also, the contraction of the Zn rich phase on cooling led to the penetration of Bi rich liquid along the ceramic plates and resulted in a pseudo wetting pattern. An even distribution of Zn needles could be seen in the Bi rich phases, contrary to what is observed on Earth. ESA

N91-31429# Metallgesellschaft, A.G., Frankfurt am Main (Germany, F.R.).
DEMIXING OF A MONOTECTIC TERNARY ALLOY (TEXUS 20)
B. Prinz *In* ESA, Summary Review of Sounding Rocket Experiments in Fluid Science and Materials Sciences: TEXUS 1 to 20; MASER 1 and 2 Feb. 1991 p 280-281 (For primary document see N91-31321 23-29)
Copyright Avail: NTIS HC/MF A15; EPD, ESTEC, Noordwijk, Netherlands, HC 75 Dutch guilders

Some Al based monotectic alloys; where a monotectic minority phase is embedded in a multiphase matrix, are expected to have significantly improved properties. On Earth however, the investigation of such alloys is impeded by the rapid sedimentation of the droplets of the denser minority phase (up to 20 mm/s with 40 microns diameter droplets), and their coagulation at the bottom of the sample. A project to study how a network of primary dendrites could stabilize the dispersed minority phase in a ternary monotectic alloy is summarized. The ternary system Al-Si-Bi was studied. Three compositions were investigated in the range of the technically interesting composition. It was show, that the Si concentration has a strong influence on the number and the size of the Bi rich particles. With an appropriate Si concentration, the sedimentation of the Bi rich phase is reduced on Earth, and the Bi enrichment of the center of the samples due to thermal gradients is impeded in microgravity. ESA

N91-31430# Deutsche Forschungs- und Versuchsanstalt fuer Luft- und Raumfahrt, Cologne (Germany, F.R.). Inst. for Materials Research.
COMPOSITE MATERIALS, 1 (TEXUS 1)
H. U. Walter and G. Ziegler *In* ESA, Summary Review of Sounding Rocket Experiments in Fluid Science and Materials Sciences: TEXUS 1 to 20; MASER 1 and 2 Feb. 1991 p 284-285 (For primary document see N91-31321 23-29)
Copyright Avail: NTIS HC/MF A15; EPD, ESTEC, Noordwijk, Netherlands, HC 75 Dutch guilders

Due to the absence of sedimentation and buoyancy effects, the stability of multicomponent systems with one or more fluid phases has been postulated under microgravity conditions. There are, however, additional mechanisms that are not based on gravitational forces which could lead to the regrouping or separation of components during liquid phase processing such as mechanisms based on intermolecular forces. An experiment to identify those mechanisms for solid liquid gas systems using model systems for the investigation is summarized. The model system investigated consisted of Ag with additions of Al2O3 or W; the pore volumes were of the order of 30 percent. Almost complete separation of the components was observed in the systems having a wetting angle higher than 90 deg (e.g. Ag-Al2O3) whereas little separation was found in, the systems having a wetting angle below 90 deg (e.g. Al-W). These results indicated that separation can take place under microgravity conditions as well. The preparation of heterogeneous alloys or composites from powder mixtures is, therefore, not possible with mixtures having nonwetting components and pore volume or degassing materials. ESA

N91-31431# Deutsche Forschungs- und Versuchsanstalt fuer Luft- und Raumfahrt, Cologne (Germany, F.R.). Inst. for Materials Research.
COMPOSITE MATERIALS, 2 (TEXUS 2)
H. U. Walter and G. Ziegler *In* ESA, Summary Review of Sounding Rocket Experiments in Fluid Science and Materials Sciences: TEXUS 1 to 20; MASER 1 and 2 Feb. 1991 p 286-287 (For primary document see N91-31321 23-29)
Copyright Avail: NTIS HC/MF A15; EPD, ESTEC, Noordwijk, Netherlands, HC 75 Dutch guilders

An experiment to investigate the mechanisms causing component separation, drop coalescence, particle agglomeration, drop and bubble migration during liquid phase processing of heterogeneous mixtures in the absence of gravity driven sedimentation is summarized. The model systems investigated were the following: (1) 80 percent Ag with wetting agents (Cu, Ni) 20 percent W, (2) 80 vol. percent Ag, 20 percent W; (3) 80 percent Ag, 20 percent Al2O3 in TZM crucibles. Contrary to the previous experiment, the samples were prepared from carefully degassed and deoxidized powder mixtures hot isostatically pressed to

theoretical density. They were melted under microgravity conditions and resolidified after a thermal soak period of 1 min at 100 C. The remelting of sample (1) resulted in a homogeneous particle reinforced composite, as capillarity and coalescence processes were of no importance. Partial separation of the components was observed in sample (2) due to voids resulting from the removal of some Ag melt form the crucible, and in sample (3) where the bigger particles (2 mm) accumulated in one side of the crucible due to the residual accelerations of the rocket and the smaller ones (0.5 mm) remained in the matrix. ESA

N91-31432# Krupp (Fried.) G.m.b.H., Essen (Germany, F.R.).
ALLOYS WITH OXIDE INCLUSIONS (TEXUS 2)
D. Neuschuetz and J. Poetschke *In* ESA, Summary Review of Sounding Rocket Experiments in Fluid Science and Materials Sciences: TEXUS 1 to 20; MASER 1 and 2 Feb. 1991 p 288-289 (For primary document see N91-31321 23-29)
Copyright Avail: NTIS HC/MF A15; EPD, ESTEC, Noordwijk, Netherlands, HC 75 Dutch guilders

An experiment to prepare a eutectic alloy with oxide inclusions under microgravity conditions is summarized. Two samples of hot isostatically pressed powder of AlCu33 containing 1 percent of Al2O3 particles (75 percent between 20 and 100 microns in diameter, 25 percent less than 20 microns) were remelted and solidified in boron nitride crucibles under microgravity conditions. One of the two crucibles cracked and a large part of the melt flowed out of it. Part of this melt formed a large drop (about 10 mm in diameter), which solidified with free surfaces. The analysis of the samples shows that the alumina suspension was stable for the 90 s melting period in microgravity. The displacement of the alumina particles by the eutectic cells could be observed in some places but in the majority of cases there was no connection between the structure and the arrangement of the alumina particles. Moreover, the structure formation was not affected by the alumina particles in suspension. ESA

N91-31433# Krupp (Fried.) G.m.b.H., Essen (Germany, F.R.).
THE BEHAVIOUR OF ALUMINA-COPPER SUSPENSIONS (TEXUS 3A AND 3B)
J. Poetschke and K. Hohenstein *In* ESA, Summary Review of Sounding Rocket Experiments in Fluid Science and Materials Sciences: TEXUS 1 to 20; MASER 1 and 2 Feb. 1991 p 290-291 (For primary document see N91-31321 23-29)
Copyright Avail: NTIS HC/MF A15; EPD, ESTEC, Noordwijk, Netherlands, HC 75 Dutch guilders

According to theory, solid particles are repelled by a solidification front provided that their radius does not exceed a critical value. An experiment aimed at studying the stability of molybdenum and alumina inclusions in liquid copper under microgravity conditions is summarized. Three cylindrical samples were processed during each flight: two Cu samples, 4.6 mm in diameter, with Al2O3 particles and contained in sintered corundum crucibles; one Cu sample containing Mo particles and coated by a 50 microns thick Al2O3 skin. The Al2O3 particles were spherical, less than 100 microns in diameter (mostly between 20 and 63 microns). The Mo particles were 30 microns in diameter. The particles were initially homogeneously dispersed. The samples were located nonsymmetrically along the axis of the furnace, parallel to each other. It is assumed that, during their directional solidification, the three samples followed the same temperature/time profile as the Cu-Mo sample which was monitored by means of four thermocouples. The samples remained molten for about 2 minutes. The residual accelerations were the order of 0.2 g and 10(exp -4) g during the first and the second flight respectively. The dispersions remained stable at 10(exp -4) g while they segregated at 0.2 g. ESA

N91-31434# Krupp (Fried.) G.m.b.H., Essen (Germany, F.R.).
COPPER-ALUMINA SUSPENSIONS (TEXUS 5)
J. Poetschke *In* ESA, Summary Review of Sounding Rocket Experiments in Fluid Science and Materials Sciences: TEXUS 1 to 20; MASER 1 and 2 Feb. 1991 p 292-293 (For primary document see N91-31321 23-29)
Copyright Avail: NTIS HC/MF A15; EPD, ESTEC, Noordwijk, Netherlands, HC 75 Dutch guilders

An experiment to investigate the interaction between Al2O3 particles (less than 100 microns) and a solidification front of pure Cu is summarized. The objectives of these experiment were: to investigate the interaction with a planar solidification front; to study the behavior of particles presenting a large apex ratio; to assess the influence of the crucible material/ Powder metallurgy prepared samples of Cu (O2 less than 30 ppm) containing Al2O3 particles (1 vol percent, less than 20 microns in size with an apex ratio in the range of 5 to 10) were processed in tantalum crucibles. The samples were partially melted and then directionally solidified under an axial thermal gradient of 80 to 120 K/cm and at a rate of 0.05 cm/s in order to achieve a planar solidification front. The CO2 remaining in the samples provoked the formation of elongated pores during the space processing. The majority of the rod shaped Al2O3 particles were rotated in the melt when interacting with the solidification front so that they were embedded transverse to the growth direction. No such interactions as above was observed with spherical particles. ESA

N91-31435# Krupp (Fried.) G.m.b.H., Essen (Germany, F.R.).
COPPER-MOLYBDENUM SUSPENSION (TEXUS 9)
J. Poetschke and P. Pant *In* ESA, Summary Review of Sounding Rocket Experiments in Fluid Science and Materials Sciences: TEXUS 1 to 20; MASER 1 and 2 Feb. 1991 p 294-295 (For primary document see N91-31321 23-29)
Copyright Avail: NTIS HC/MF A15; EPD, ESTEC, Noordwijk, Netherlands, HC 75 Dutch guilders

Previous space experiments demonstrated that alumina particles smaller than 10 microns in a copper matrix are pushed by a solidification front with with a velocity lower than 500 microns/s. On Earth, molybdenum spheres of 30 microns in diameter also showed interactions at solidification rates lower than 1 micron/s. The experiment investigated the latter system in microgravity in order to get more precise and more reliable data. A copper sample (50 x 8 sq mm) containing Mo particles (1 vol percent, 2 to 20 microns) in uniform distribution was melted under microgravity conditions and directionally solidified. A similar reference sample was processed under the same thermal conditions on Earth. As expected, the suspension remained stable under microgravity conditions. However, it was also stable on Earth. It was therefore believed that the molybdenum particles built a network, although their concentration should have been too low for the formation of such a skeleton. ESA

N91-31436# Katholieke Univ. te Leuven (Belgium).
METALLIC COMPOSITES WITH PARTICLES (TEXUS 6)
A. Deruyttere and L. Froyen *In* ESA, Summary Review of Sounding Rocket Experiments in Fluid Science and Materials Sciences: TEXUS 1 to 20; MASER 1 and 2 Feb. 1991 p 296-297 (For primary document see N91-31321 23-29)
Copyright Avail: NTIS HC/MF A15; EPD, ESTEC, Noordwijk, Netherlands, HC 75 Dutch guilders

An experiment to study the rearrangement of solid particles in a matrix during melting and solidification under microgravity conditions is summarized. Special attention was paid to the influence of the wetting of the crucible by the molten matrix. Three Cu samples containing 0.25 vol percent of SiC particles (angular shaped, 125 to 160 microns) and prepared by hot extrusion were investigated. The samples were processed in TZM crucibles, well wetted, or in a graphite crucible badly wetted by liquid copper. They were rapidly melted and solidified in an isothermal furnace under microgravity conditions. The liquid copper was sucked out of the two TZM crucible by capillarity due to the formation of small gaps round the cover which was not welded on the crucible. This induced flows in the liquid. The particles were found in gas holes inside the samples. In the sample contained in a graphite crucible which did not leak, the particles were found at the periphery of the Cu matrix. It appeared that in the Cu system having a low volume fraction of coarse SiC particles, the separation had already occurred on melting independent of gravity. Extensive dissolution

of SiC and the diffusion of Si in Cu took place on heating up. The melting point of the matrix round the particles was thus lowered and the volume expansion induced by partial melting of the alloyed zones caused internal pressures and, further, convection flows. The SiC particles were thus exuded even before the matrix was completely melted. If the crucible is wetted by the matrix the particles are gathered in gas holes. In the case of non-wetting, they are located at the crucible-matrix interface. ESA

N91-31437# Katholieke Univ. te Leuven (Belgium).
METALLIC COMPOSITES WITH PARTICLES (TEXUS 7)
A. Deruyttere and L. Froyen *In* ESA, Summary Review of Sounding Rocket Experiments in Fluid Science and Materials Sciences: TEXUS 1 to 20; MASER 1 and 2 Feb. 1991 p 298-299 (For primary document see N91-31321 23-29)
Copyright Avail: NTIS HC/MF A15; EPD, ESTEC, Noordwijk, Netherlands, HC 75 Dutch guilders

An experiment to identify the forces which cause the displacement of particles in a metallic melt, paying attention to the mutual wetting behavior between the molten matrix, the particles and crucible materials, is summarized. Three copper based samples were processed in an isothermal furnace. Two powder metallurgy prepared Cu samples with 1.1 vol percent of SiO2 particles (angular shaped, 32 to 45 microns, badly wetted by liquid copper), one (a) in a TZM crucible, well wetted, and the other (b) in a graphite crucible, badly wetted by liquid copper. The third Cu sample (c) contained 30 vol percent of W particles (less than 45 microns in diameter, well wetted by liquid copper) with well defined positions (loose skeleton) and was inserted in a pure copper shell to avoid direct interaction of the particles with the crucible wall during the first phase of the experiment. The samples were rapidly melted under microgravity conditions and resolidified 3 minutes later. Contrary to what is obtained on Earth where buoyancy induced flotation occurs, sample (a) exhibited a quite uniform distribution of the particles after space processing. In sample (b), the particle either agglomerated or clung to gas holes. In sample (c), the initial arrangement of the W particles was almost maintained. The main conclusion was that an uniform dispersion of non-wetting particles can be maintained in a molten matrix under microgravity conditions, provided that the matrix wets the crucible. ESA

N91-31438# Katholieke Univ. te Leuven (Belgium).
MELTING AND SOLIDIFICATION OF METALLIC COMPOSITES (TEXUS 9)
A. Deruyttere and L. Froyen *In* ESA, Summary Review of Sounding Rocket Experiments in Fluid Science and Materials Sciences: TEXUS 1 to 20; MASER 1 and 2 Feb. 1991 p 300-301 (For primary document see N91-31321 23-29)
Copyright Avail: NTIS HC/MF A15; EPD, ESTEC, Noordwijk, Netherlands, HC 75 Dutch guilders

The influence of the mutual wetting behaviors between a molten matrix, particles and the crucible material on the stability of metallic dispersions was studied in previous space experiments. An experiment to study the role of the moving solid/liquid interface of the solidifying matrix, by processing identical samples under different thermal conditions, is summarized. The difference in behavior between badly wetted (SiO2) and well wetted (Mo) particles in liquid and solidifying copper was obvious. The separation of the badly wetted SiO2 particles from the copper matrix which also badly wets graphite was due to interface energies. Thermal gradient and low gravity conditions appeared to be suitable for obtaining stable Cu-Mo dispersions. ESA

N91-31439# Katholieke Univ. te Leuven (Belgium).
METAL MATRIX COMPOSITES (TEXUS 14b)
A. Deruyttere and L. Froyen *In* ESA, Summary Review of Sounding Rocket Experiments in Fluid Science and Materials Sciences: TEXUS 1 to 20; MASER 1 and 2 Feb. 1991 p 302-303 (For primary document see N91-31321 23-29)
Copyright Avail: NTIS HC/MF A15; EPD, ESTEC, Noordwijk, Netherlands, HC 75 Dutch guilders

An experiment was intended to obtain a better understanding of the sedimentation process and the formation of a particle skeleton in metal matrix composites during melting and solidification is summarized. The importance of the redistribution of the dispersed phase has been shown before. Two Al-SiC (0.4 vol percent SiC, 0 to 3 microns) composite samples were prepared by powder metallurgy and hot extrusion. The cooling rates were calculated on the basis of the microscopic examination of the dendrite arm spacings and of the thermal gradients measured in the samples: 8 microns/s and 0.4 microns/s. Large holes were unexpectedly found in both the flight and the reference samples. No such hole formation had ever been observed during the extensive ground tests. They were therefore attributed to defects and inhomogeneities introduced during the sample preparation. The temperature recordings differed from what had been predicted on the basis of the ground preparatory test results and of computer simulations. However, the qualitative results were satisfactory. As predicted by the expulsion model, macroscopic interaction occurred in microgravity between the particles and the solidification front. ESA

N91-31440# Katholieke Univ. te Leuven (Belgium).
METAL MATRIX COMPOSITES (TEXUS 20)
A. Deruyttere and L. Froyen *In* ESA, Summary Review of Sounding Rocket Experiments in Fluid Science and Materials Sciences: TEXUS 1 to 20; MASER 1 and 2 Feb. 1991 p 304-305 (For primary document see N91-31321 23-29)
Copyright Avail: NTIS HC/MF A15; EPD, ESTEC, Noordwijk, Netherlands, HC 75 Dutch guilders

An experiment to investigate and the interaction between W particles and the solid/liquid interface of an Ag matrix and to study the accompanying fluid flows in the melt and the particle agglomeration process is summarized. The sample was prepared by powder metallurgy from Ag and W particles (2.8 vol percent) including hot pressing and degassing. Dimensional control and radiographic inspection of the samples did not reveal any significant gas evolution. A longitudinal section was then analyzed metallographically. No macro sedimentation of the solid liquid suspension was observed in the flight sample. The uniform initial distribution of the W particles had changed to an arrangement of the particle around small spheres. The distribution was more uniform in the regions containing Ni, which is a wetting promoting element. The reference sample exhibited a pronounced layered sedimentation. ESA

N91-31441# Surrey Univ., Guildford (England). Dept. of Metallurgy and Mat. Tech.
SOLIDIFICATION OF FINE DISPERSIONS IN MICROGRAVITY (TEXUS 14b)
N. J. E. Adkins and P. J. Goodhew *In* ESA, Summary Review of Sounding Rocket Experiments in Fluid Science and Materials Sciences: TEXUS 1 to 20; MASER 1 and 2 Feb. 1991 p 306-307 (For primary document see N91-31321 23-29)
Copyright Avail: NTIS HC/MF A15; EPD, ESTEC, Noordwijk, Netherlands, HC 75 Dutch guilders

An experiment to directionally solidify under microgravity conditions an aluminum melt containing insoluble alumina fibers is summarized. On Earth, heating of such a dispersion above the melting point of the matrix would be followed rapidly by sedimentation and agglomeration of the particles. If the parameters governing this behavior can be determined it may be possible to develop new processing routes which preserve very fine particle dispersions while simplifying their production. Additionally the theory of particle engulfment by a moving solidification front should be verifiable from the microgravity results, if appropriate cooling rates and particles sizes can be achieved. The theory predicts that with the smallest particles and the average dendrite velocities achieved in this experiment, particle pushing should have occurred in only the slow and medium solidification rate specimens. This was confirmed in particle distribution histograms, although the theory predicts a critical velocity approximately three times slower than in the experiment. ESA

N91-31442# Maschinenfabrik Augsburg-Nuernberg A.G., Munich (Germany, F.R.).
DISPERSION ALLOYS (TEXUS 19)
W. Amende and G. Vael *In* ESA, Summary Review of Sounding Rocket Experiments in Fluid Science and Materials Sciences: TEXUS 1 to 20; MASER 1 and 2 Feb. 1991 p 308-309 (For primary document see N91-31321 23-29)
Copyright Avail: NTIS HC/MF A15; EPD, ESTEC, Noordwijk, Netherlands, HC 75 Dutch guilders

An experiment to study the behavior of small non metallic particles dispersed in a metallic matrix during melting and directional solidification in microgravity is summarized. The samples consisting of pure Ag or of an Ag matrix with uniformly dispersed W or WC particles (0.5 wt percent, average size 1 micron), were powder metallurgically prepared. The longitudinal sections of the Ag-0.5W and the Ag-0.5WC samples looked similar. Spherical pores formed, in particular close to the sample/crucible interface. These pores were clearly due to a gas formation in the samples, although this was contrary to what had been observed during the preparatory tests. Single particles surrounded by a Ni-rich layer (which improved significantly their wettability) were observed close to the crucible wall along the sample and in porous regions further from the walls. The latter observation indicated that convection flows occurred, probably due to liquid free surfaces submitted to a thermal gradient. The particle enrichment at the top of the sample indicated rather that particles were pushed by the solidification front. It was concluded that the particle/melt interfacial tension plays an important role during the processing of dispersion alloys. ESA

N91-31443# Politecnico di Milano (Italy).
LIQUID PHASE SINTERING (TEXUS 8)
F. Rossitto *In* ESA, Summary Review of Sounding Rocket Experiments in Fluid Science and Materials Sciences: TEXUS 1 to 20; MASER 1 and 2 Feb. 1991 p 310-311 (For primary document see N91-31321 23-29)
Copyright Avail: NTIS HC/MF A15; EPD, ESTEC, Noordwijk, Netherlands, HC 75 Dutch guilders

An experiment to assess the role of capillary forces in the rearrangement of metallic particles in a metallic molten matrix and to get better information on the liquid meniscus shape and stability in the absence of gravity by using model systems (spheres and wires) is summarized. 16 different samples consisting of W spheres (150 or 300 microns in diameter) or W technical powders (25 microns average diameter) all coated with Cu or Ag (liquid volume fraction 15 or 30 percent) were investigated. The space samples showed a very good homogeneity in the sphere arrangement and in the second phase distribution, high densification (up to the theoretical density), and isotropy in the shrinkage. The final sphere arrangement was axially homogeneous and radial variations could be correlated with the local amount of the second phase, with transitions at the predicted values of the liquid volume fraction. The ground processed samples presented a marked instability in the second phase distribution, due to the expulsion of the liquid that induced the coalescence of the liquid bridges with continuous variation of the spatial arrangement along the sample and, accordingly, both radial and axial anisotropy of the shrinkage. ESA

N91-31444# National Defence Research Establishment, Stockholm (Sweden).
TUNGSTEN COMPOSITES (TEXUS 10)
L. B. Ekbom and H. Fredriksson (Royal Inst. of Tech., Stockholm, Sweden) *In* ESA, Summary Review of Sounding Rocket Experiments in Fluid Science and Materials Sciences: TEXUS 1 to 20; MASER 1 and 2 Feb. 1991 p 312-313 (For primary document see N91-31321 23-29)
Copyright Avail: NTIS HC/MF A15; EPD, ESTEC, Noordwijk, Netherlands, HC 75 Dutch guilders

Two samples of Ni-Fe-W matrix (Ni-58:Fe-24:W-15:Co-2.2 percent, 70 microns in diameter) and W particles (25 and 50 vol percent, about 2.5 microns in size) were prepared by powder metallurgy techniques. They were processed in plasma sprayed alumina crucibles in high temperature mirror furnaces under microgravity conditions. The samples were kept molten above 1460 C for 12 s (25 vol percent) and 60 s (50 vol percent). Both samples exhibited large shrinkage holes in their central part. However, there was an even distribution of W particles, showing that no surface tension driven segregation occurred. The initially uneven distribution had become even during the short liquid phase sintering period. This indicated that the particles were well wetted by the molten matrix and that the disintegration of the agglomerates was effective. Due to a nonequilibrium reaction, some of the particles dissolved in the molten matrix, through its W content increased to 27 percent. The W particles took a spherical shape and their size increased from 2.5 microns to about 8 microns in diameter in less than one minute. In both samples, W particles partly joined by a grain boundary or separated only by a narrow layer of matrix can be observed. This could be result of a surface tension driven reaction. ESA

N91-31445# National Defence Research Establishment, Stockholm (Sweden).
TUNGSTEN COMPOSITES (TEXUS 19) ESA
L. B. Ekbom and H. Fredriksson (Royal Inst. of Tech., Stockholm, Sweden) *In* ESA, Summary Review of Sounding Rocket Experiments in Fluid Science and Materials Sciences: TEXUS 1 to 20; MASER 1 and 2 Feb. 1991 p 314-315 (For primary document see N91-31321 23-29)
Copyright Avail: NTIS HC/MF A15; EPD, ESTEC, Noordwijk, Netherlands, HC 75 Dutch guilders

An experiment to study the sintering mechanism with W-Ni-Fe samples with a low content of W particles is summarized. The previous short duration (less than 1 mm) experiment had shown that composites can be produced with a fairly homogeneous distribution of particles, but there were still agglomerates at a microscopic scale. This experiment aimed at performing a longer sintering process with a lower W content. Two samples with W particle fractions of 10 pct and 20 pct were prepared from a powder mixture of W45 pct-Ni35 pct-Fe20 pct (size 2 to 5 microns). In samples processed on Earth, the W particles had sedimented towards the bottom and were grown by exchange with the matrix to a diameter of 8 to 9 microns. In the flight samples, the particle distribution was quite homogeneous. However, the rapid separation already observed in the previous short duration space experiment was not followed by further separation. As the initial liquid was not in equilibrium with the particles, the wetting and separation of the particles was again effective. But when the equilibrium was reached, the wetting angle of the molten matrix on the particles increased and the particles started to join again. This was especially the case when the crystallographic orientations of the two neighboring particles was favorable. ESA

N91-31446# Krupp (Fried.) G.m.b.H., Essen (Germany, F.R.).
LIQUID PHASE SINTERING (TEXUS 19) ESA
V. Rogge, J. Poetschke, W. Graf, and F. Deuerler *In* ESA, Summary Review of Sounding Rocket Experiments in Fluid Science and Materials Sciences: TEXUS 1 to 20; MASER 1 and 2 Feb. 1991 p 316-317 (For primary document see N91-31321 23-29)
Copyright Avail: NTIS HC/MF A15; EPD, ESTEC, Noordwijk, Netherlands, HC 75 Dutch guilders

An experiment to study the liquid phase sintering mechanism with respect to sedimentation, convection and Brownian motions, with the possibility of producing hard metals with a lower fraction of reinforcing particles than is currently achieved on Earth, is summarized. Three samples of Co-WC with the same volume fraction of WC particles (34 pct) but with different particle sizes (1.3 and 6 m) were prepared by powder metallurgy. The samples were liquid phase sintered at 1400 C for 240 s. In the flight samples, the medium and large size particles were homogeneously distributed, whereas the small size particles had clearly built a macroscopic network. However, the microstructures in the meshes of this network exhibited WC particles homogeneously distributed in the matrix and were therefore similar to the one in the two other samples. In the reference samples, the WC particles formed networks whatever their size. The bigger the particle size, the

smaller the network mesh and the better the microstructure homogeneity or degree of dispersion. In the samples with small size particles, the network mesh was bigger in the ground sample than in the flight sample. ESA

N91-31447# Hochschule der Bundeswehr, Hamburg (Germany, F.R.). Lab. fuer Werkstoffkunde und Schweisstechnik.
PORES IN ALUMINIUM ALLOYS (TEXUS 3)
H. Hoffmeister and J. Ruediger *In* ESA, Summary Review of Sounding Rocket Experiments in Fluid Science and Materials Sciences: TEXUS 1 to 20; MASER 1 and 2 Feb. 1991 p 320-321 (For primary document see N91-31321 23-29)
Copyright Avail: NTIS HC/MF A15; EPD, ESTEC, Noordwijk, Netherlands, HC 75 Dutch guilders

An experiment to study the interaction between gas bubbles and a solidification front in a metallic melt under microgravity conditions is summarized. This experiment was a precursor to an arc welding experiment. The increase of the total pore volume and of the porosity, induced by the pressure drop during the solidification process, is also applicable to the preparation of metal foams. Three Al based cyclindrical samples, (1) Al 99.999, (2) Al-2.27 wt Mg, and (3) Al-0.67 wt Mg were processed in a cartridge under an atmosphere of N2-H2 (9:1). At the beginning of the experiment, the cumulative frequency was 50 pct for a pore diameter of 0.48, 0.34 and 0.28 mm in sample (1), (2) and (3) respectively. These values were enlarged at the end of the experiment by a factor 1.32, 1.27 and 1.25 respectively. The total pore number dropped during the experiment. It was concluded that the bubbles coagulated in the melt. It was assumed that the gas pressure was a maximum just before the beginning of the solidification and that the increase of the pore volume between th ebottom and the top of the samples was induced by the axial thermal gradient. ESA

N91-31448# Krupp (Fried.) G.m.b.H., Essen (Germany, F.R.). Hauptabt. Metallurgische Verfahren.
MANUFACTURE OF STEEL FOAM (TEXUS 4)
J. Poetschke and P. Pant *In* ESA, Summary Review of Sounding Rocket Experiments in Fluid Science and Materials Sciences: TEXUS 1 to 20; MASER 1 and 2 Feb. 1991 p 322-323 (For primary document see N91-31321 23-29)
Copyright Avail: NTIS HC/MF A15; EPD, ESTEC, Noordwijk, Netherlands, HC 75 Dutch guilders

Steel foam manufactured directly from the melt could find applications as a high strength but light material, e.g. for sound proofing or energy absorbing components. However, there was no reference to steel foam preparation in the literature and it was not known to what extent the fundamentals of foam manufacture established in aqueous and organic chemistry could be applied to steel. Preliminary tests showed that liquid steel presents no surface elasticity and thus, that only spherical foams stable for less than 1 s can be formed. An experiment to determine if the capillary forces, which are very large due to the high surface tension of steel, play a role in the instability of the foams is summarized. Four steel samples (4.7-Cr, 4.9-Mo, 2-V, 0.63-W, 1.05-C, 0.7-Si, 0.001-O, 0.34-N in wtpct) supersaturated with nitrogen were processed in Al2O3 crucibles in an isothermal furnace. The samples were melted for 120 or 240 s and solidified under microgravity conditions. All samples were free of gas bubbles. It was concluded that a two-phase steel foam is just as unstable in microgravity as on Earth. ESA

N91-31449# Krupp (Fried.) G.m.b.H., Essen (Germany, F.R.). Hauptabt. Metallurgische Verfahren.
MANUFACTURE OF STEEL FOAM (TEXUS 6)
J. Poetschke and P. Pant *In* ESA, Summary Review of Sounding Rocket Experiments in Fluid Science and Materials Sciences: TEXUS 1 to 20; MASER 1 and 2 Feb. 1991 p 324-325 (For primary document see N91-31321 23-29)
Copyright Avail: NTIS HC/MF A15; EPD, ESTEC, Noordwijk, Netherlands, HC 75 Dutch guilders

The results of the previous experiment showed that two phase foams are as unstable in space as on Earth. An experiment to prevent the coalescence of the gaseous inclusions by means of a third phase consisting of a graphite lamellar network is summarized. Two powder metallurgy prepared samples were investigated: Fe-4.8 pct C + 1.53 pct SiO2; Fe-4.8 pct C + 0.11 pct Al + 1.53 pct SiO2. The first was only partially melted and its density decreased from 7.21 to 6.86 g/cu cm (foaming ratio of 5 pct). The second was completely melted for only 10 s and its density decreased from 7.21 to 6.35 g/cu cm (foaming ratio of 12 pct). Since the material was only molten for a few seconds, there was not enough gas produced to form real foams. Only the initial stages of bubble nucleation and graphite lamellae growth were reached. It was shown that the graphite lamellae could grow independent from the gas bubbles but that their nucleation was easier at the surface of the bubbles. As the gas bubbles adhered to the graphite due to a bad wetting of the liquid, their coalescence was prevented. Therefore, it could be expected to obtain foams more stable than without graphite. ESA

N91-31450# Krupp (Fried.) G.m.b.H., Essen (Germany, F.R.). Hauptabt. Metallurgische Verfahren.
MANUFACTURE OF IRON FOAM (TEXUS 7)
J. Poetschke and P. Pant *In* ESA, Summary Review of Sounding Rocket Experiments in Fluid Science and Materials Sciences: TEXUS 1 to 20; MASER 1 and 2 Feb. 1991 p 326-327 (For primary document see N91-31321 23-29)
Copyright Avail: NTIS HC/MF A15; EPD, ESTEC, Noordwijk, Netherlands, HC 75 Dutch guilders

An experiment to check whether the coalescence of gas bubbles in the melt can be prevented by means of a solid network for a longer duration than in the previous experiment is summarized. Two samples were processed in an isothermal furnace. One consisted of Fe-4.3 pct P + 0.13 pct N2 and was processed at a temperature where a solid liquid gas system forms. The other sample consisted of Fe-4.8 pct C + 1.53 pct SiO2 (as in the previous experiment). The first sample exhibited a foaming efficiency of 44 pct which is the same as under terrestrial conditions. With the second sample, a foam consiting of a fine iron network interlaced by graphite was obtained, which was however very brittle. In the ground reference sample, the melt was sucked out of the graphite skeleton due to the gravity. It was concluded that foams consisting of three phases of melting are more stable than those consisting of two phases. However, the size and the distribution of the bubbles cannot be controlled using reactive gases, even in microgravity. This could, however, be possible with inert gases. ESA

N91-31451# Dornier System G.m.b.H., Friedrichshafen (Germany, F.R.).
METALLIC FOAMS (TEXUS 5)
W. Schaefer *In* ESA, Summary Review of Sounding Rocket Experiments in Fluid Science and Materials Sciences: TEXUS 1 to 20; MASER 1 and 2 Feb. 1991 p 328-329 (For primary document see N91-31321 23-29)
Copyright Avail: NTIS HC/MF A15; EPD, ESTEC, Noordwijk, Netherlands, HC 75 Dutch guilders

Under microgravity conditions, the absence of buoyancy could allow the preparation of metallic foams and metal samples with a high porosity. An experiment to prepare a metallic foam is summarized. A sample consisting of 3 g of CuSn6 with additions of CuO and C was processed in an Al2O3 crucible. The sample was heated in an isothermal furnace up to about 1090 C which is above the liquids temperature and where the following reaction accurs: CuO + C is converted to Cu + CO. The sample was then rapidly cooled down below the solidus temperature before the end of the microgravity period. Reference samples were processed on the ground following the same temperature/time profile. The comparison between the space and the ground samples was as follows: for reference, maximum pore diameter = 0.05 mm, porosity = 0.8; for flight, maximum pore diameter = 2 mm, porosity 11 pct. It was concluded that the stability of a metallic foam is enhanced under microgravity. ESA

N91-31452# Dornier System G.m.b.H., Friedrichshafen (Germany, F.R.).
PREPARATION OF ALUMINIUM FOAMS (TEXUS 9)
W. Schaefer *In* ESA, Summary Review of Sounding Rocket Experiments in Fluid Science and Materials Sciences: TEXUS 1 to 20; MASER 1 and 2 Feb. 1991 p 330-331 (For primary document see N91-31321 23-29)
Copyright Avail: NTIS HC/MF A15; EPD, ESTEC, Noordwijk, Netherlands, HC 75 Dutch guilders

The stability of pores in a metallic matrix was investigated in a previous space experiment. An experiment to investigate the stability of aluminum foams containing a solid lamellar structure is summarized. Two aluminum samples were processed under microgravity conditions in an isothermal furnace. One sample contained additions of TiH2 in order to produce hydrogen gas bubbles by the reaction: 3 Al + TiH2 is converted to Al3Ti + H2. The Al3Ti thus obtained should form a solid lamellar structure which should prevent the coalescence of the bubbles. The other sample was previously melted on Earth and already contained gas pores. Both samples were melted and resolidified in alumina crucibles under microgravity conditions. Similar samples were processed under the same thermal conditions on the ground. The sample melted for the first time under microgravity had about the same porosity as the corresponding sample processed on Earth (61 and 67 percent respectively). However, the porosity of the sample already melted on Earth and reprocessed under microgravity increased by a factor of 1.5 (from 48 pct to 74 pct). ESA

N91-31453# Krupp (Fried.) G.m.b.H., Essen (Germany, F.R.).
GAS BUBBLES IN A COPPER-ALUMINA SUSPENSION (TEXUS 11)
J. Poetschke *In* ESA, Summary Review of Sounding Rocket Experiments in Fluid Science and Materials Sciences: TEXUS 1 to 20; MASER 1 and 2 Feb. 1991 p 332-333 (For primary document see N91-31321 23-29)
Copyright Avail: NTIS HC/MF A15; EPD, ESTEC, Noordwijk, Netherlands, HC 75 Dutch guilders

Cu samples with 0.1 pct of Al2O3 particles (average diameter 0.05 microns) were powder metallurgically prepared, including mixing of the wet components, compression, vacuum outgassing, sintering and extrusion. They were processed in alumina crucibles in an isothermal furnace equipped with a cooled pedestal. The flight sample was preheated to 800 C before launch. Once microgravity conditions were established, it was almost completely molten and resolidified directionally under a thermal gradient of 60 K/cm. The initial objective of the experiment was to study the interaction between alumina particles and the advancing solidification front of a copper matrix. Due to the unexpected formation of gas bubbles, this objective could not be reached and the samples were analyzed with respect to the nucleation growth and coalescence of the gas bubbles. ESA

N91-31454# Krupp (Fried.) G.m.b.H., Essen (Germany, F.R.).
BUBBLE FORMATION, GROWTH, AND EXPANSION DURING THE LIQUID PHASE SINTERING OF A WC-Co SAMPLE
W. Graf *In* ESA, Summary Review of Sounding Rocket Experiments in Fluid Science and Materials Sciences: TEXUS 1 to 20; MASER 1 and 2 Feb. 1991 p 334-335 (For primary document see N91-31321 23-29)
Copyright Avail: NTIS HC/MF A15; EPD, ESTEC, Noordwijk, Netherlands, HC 75 Dutch guilders

An experiment to demonstrate that the WC particles deagglomerate during the liquid phase sintering of a WC-Co alloy in microgravity, and that a fine dispersion alloy can be obtained after solidification, is summarized. Unexpectedly, bubbles formed during the process and their nucleation, growth and coalescence were finally studied. The bubble morphology indicated that expansion processes occurred: coalescence and Ostwald ripening were noted. As the convection was greatly reduced, the coalescence probably stopped at the end of the bubble growth phase. The clear spots, which often still contain a bubble in their center, are a qualitative proof that gas bubbles disappeared by Ostwald ripening. They contain only cobalt and no WC particles. A theory of Ostwald ripening of gas bubbles was developed which confirmed semiquantitatively this assumption. ESA

N91-31455# Maschinenfabrik Augsburg-Nuernberg A.G., Munich (Germany, F.R.).
SKIN TECHNOLOGY (TEXUS 1)
H. Sprenger and K. Schweitzer (Motoren- und Turbinen-Union Muenchen G.m.b.H., Germany, F.R.) *In* ESA, Summary Review of Sounding Rocket Experiments in Fluid Science and Materials Sciences: TEXUS 1 to 20; MASER 1 and 2 Feb. 1991 p 338-339 (For primary document see N91-31321 23-29)
Copyright Avail: NTIS HC/MF A15; EPD, ESTEC, Noordwijk, Netherlands, HC 75 Dutch guilders

The shape of casts or powder compacts remelted or reprocessed under microgravity conditions can be preserved by means of a passive, refractory layer which can be extemely thin (order of microns). This process could be used to produce high grade engine components (e.g. turbine blades) with improved mechanical or thermal properties due to the elimination of sedimentation and buoyancy effects under microgravity conditions. Due also to the absence of convection and the greatly reduced thermal mass of the mould, the process could be better controlled. An experiment aimed at demonstrating the shape preservation capability of thin oxide skins is summarized. An IN-100 superalloy sample (4 by 7 by 30 mm) coated with 50 microns Ni-18Cr-6Al + 75 microns Al2O3 was processed in an evacuated TZM cartridge. The sample was preheated prior to liftoff and its upper half was melted and resolidified directionally during the microgravity period. The sample was slightly deformed due to the volume change on melting as is schematically explained. This deformation mechanism should be easily prevented by adapting the sample geometry. ESA

N91-31456# Maschinenfabrik Augsburg-Nuernberg A.G., Munich (Germany, F.R.).
SKIN TECHNOLOGY (TEXUS 2)
H. Sprenger and K. Schweitzer (Motoren- und Turbinen-Union Muenchen G.m.b.H., Germany, F.R.) *In* ESA, Summary Review of Sounding Rocket Experiments in Fluid Science and Materials Sciences: TEXUS 1 to 20; MASER 1 and 2 Feb. 1991 p 340-341 (For primary document see N91-31321 23-29)
Copyright Avail: NTIS HC/MF A15; EPD, ESTEC, Noordwijk, Netherlands, HC 75 Dutch guilders

An experiment to demonstrate the sample shape preservation on melting by means of a thin refractory skin and to attempt to produce a cast structure starting from a powder metallurgy prepared sample in microgravity is summarized. An IN 100 superalloy sample and a powder metallurgy prepared sample of IN 738 with Y2O3 particles were processed in vacuum sealed TZM cartridges. Both samples were coated with a 50 microns thick plasma sprayed Al2O3 skin. A cavity was drilled through the skin at the top of each sample to allow for the 3 volume expansion on melting. The samples were to be directionally melted and resolidified in microgravity. The anticipated temperatures were not reached and only an intermediary state between liquid and solid was reached (solid particles in a liquid matrix). The IN 100 sample detached from its pedestal and was unexpectedly free floating during the process. It came into contact with the TZM cartridge with which it reacted. However, the cavity compensated the volume expansion as expected. The IN 738 sample was slightly deformed due to the unexpected formation of gas bubbles. The Y2O3 particles were agglomerated at the grain boundaries of the matrix alloy. A possible explanation was that they had been pushed by the solidification front. ESA

N91-31457# Maschinenfabrik Augsburg-Nuernberg A.G., Munich (Germany, F.R.).
SKIN TECHNOLOGY (TEXUS 3)
H. Sprenger and K. Schweitzer (Motoren- und Turbinen-Union Muenchen G.m.b.H., Germany, F.R.) *In* ESA, Summary Review of Sounding Rocket Experiments in Fluid Science and Materials Sciences: TEXUS 1 to 20; MASER 1 and 2 Feb. 1991 p 342

(For primary document see N91-31321 23-29)
Copyright Avail: NTIS HC/MF A15; EPD, ESTEC, Noordwijk, Netherlands, HC 75 Dutch guilders

A thin solid protecting skin (0.1 to 10 microns thick) can be used to preserve the shape of a sample on melting under microgravity conditions. However, secondary forces such as surface and interface tensions, volume changes induced by melting and solidification, increase of the pressure in the melt (e.g. by the creation of bubbles or by chemical reactions) and convection in the melt can disturb the process. The contribution of these deformation of a molten sample coated by a ceramic skin is investigated. The AlMg3 samples processed on the ground with a 10 to 20 micron thick SnO2 skin exhibited no leakage, thus showing that the deformation could only be induced by the volume increase during melting. An AlMg3 sample coated with a 0.3 micron thick SnO2 skin was successfully melted and resolidified under microgravity conditions. However, the surface of the cavity was unexpectedly oxidized and the oxide layer formed was as rigid as the SnO2 skin. This prevented the melt from expanding properly and the sample was heavily deformed. ESA

N91-31458# Maschinenfabrik Augsburg-Nuernberg A.G., Munich (Germany, F.R.).
SKIN TECHNOLOGY (TEXUS 4)
H. Sprenger and K. Schweitzer (Motoren- und Turbinen-Union Muenchen G.m.b.H., Germany, F.R.) *In* ESA, Summary Review of Sounding Rocket Experiments in Fluid Science and Materials Sciences: TEXUS 1 to 20; MASER 1 and 2 Feb. 1991 p 344-345 (For primary document see N91-31321 23-29)
Copyright Avail: NTIS HC/MF A15; EPD, ESTEC, Noordwijk, Netherlands, HC 75 Dutch guilders

The Technological Experiments Under Microgravity (TEXUS) 4 experiment was carried out only a few days after the recovery of the TEXUS 3b sample. Since it was first concluded that the deformation of this sample was due to an incomplete solidification at the end of the microgravity period, the experiment was repeated, but with a ten times thicker SnO2 coating layer. The same arrangement as in TEXUS 3b was used. The thickness of the SnO2 skin was 3 microns. Surprisingly, the deformation of the sample was very pronounced, although not as important as the one of the TEXUS 3b sample (0.3 microns thick skin). A careful examination of the temperature/time profile showed that no major deviation from the preprogrammed profile had occurred and that the sample had been melted and solidified under microgravity conditions. Later ground investigations revealed that the deformation was due to the insufficient stiffness of thin skins with respect to the deformation forces which still remain in space. These forces originated in the unexpected formation of an oxide layer on the free surface of the molten alloy which rendered the volume compensation cavity inefficient when the sample melted. ESA

N91-31459# Maschinenfabrik Augsburg-Nuernberg A.G., Munich (Germany, F.R.).
SKIN TECHNOLOGY (TEXUS 9)
H. Sprenger *In* ESA, Summary Review of Sounding Rocket Experiments in Fluid Science and Materials Sciences: TEXUS 1 to 20; MASER 1 and 2 Feb. 1991 p 346-347 (For primary document see N91-31321 23-29)
Copyright Avail: NTIS HC/MF A15; EPD, ESTEC, Noordwijk, Netherlands, HC 75 Dutch guilders

An experiment to control the shape of an alloy sample during reprocessing in microgravity by using a badly wetted thin solid skin with a hole at the top to compensate for volume changes during the process and to prevent the oxidization of the free surface of the alloy is summarized. A silver sample coated with a 20 micron thick layer of TiO2/Ni was partially melted and solidified under microgravity conditions. The wetting angle of molten Ag on the coating skin is about 150 C. Under the operating conditions, no formation of oxides at the free surface could occur. The shape of the thin skin was not affected during the process, thereby demonstrating that volume compensation had been effective. However, due to the bad wetting, the shape of the reprocessed alloy sample did not coincide anymore with the square shape of the skin. Due to capillary forces, the upper part of the melt had been detached from the corners and edges. Therefore, it was concluded that the optimum design of the skin coating is to have a well wetted skin in the regions where the shape conservation of the sample is required and a badly wetted skin for the volume compensation. ESA

N91-31460# Maschinenfabrik Augsburg-Nuernberg A.G., Munich (Germany, F.R.).
SKIN TECHNOLOGY (TEXUS 11 AND 12)
H. Sprenger *In* ESA, Summary Review of Sounding Rocket Experiments in Fluid Science and Materials Sciences: TEXUS 1 to 20; MASER 1 and 2 Feb. 1991 p 348-350 (For primary document see N91-31321 23-29)
Copyright Avail: NTIS HC/MF A15; EPD, ESTEC, Noordwijk, Netherlands, HC 75 Dutch guilders

The results of previous microgravity experiments showed that the sample shape conservation requires the control of the volume variations on melting and the compensation of the surface forces. This can be achieved by using a skin rigid enough (i.e. thick enough) and by letting the sample expand in a badly wetted free volume on melting. The importance of a good wetting of the molten sample on the skin has also been recognized. Two experiments with the following objectives are summarized. Conservation of the sample shape by means of a suitable volume compensation system and of a well wetted skin: study of the behavior of model dispersion alloys during melting and solidification. (In particular, the influence of the wetting behavior of the Cu matrix on both the Mo skin and the dispersed particles (AlO3 and Mo) was to be studied). ESA

N91-31461# Bundesanstalt fuer Materialpruefung, Berlin (Germany, F.R.).
BRAZING OF CAPILLARY GAPS (TEXUS 2)
W. Bathke, N. Philippovich, R. Stickler, and K. Frieler (Technische Univ., Vienna, Austria) *In* ESA, Summary Review of Sounding Rocket Experiments in Fluid Science and Materials Sciences: TEXUS 1 to 20; MASER 1 and 2 Feb. 1991 p 352-353 (For primary document see N91-31321 23-29)
Copyright Avail: NTIS HC/MF A15; EPD, ESTEC, Noordwijk, Netherlands, HC 75 Dutch guilders

An experimentation to investigate the effects of microgravity on vacuum brazing is summarized. The specimen consisted of four Ni cylinders arranged inside each other in order to from both a 200 micron thick annular gap and a sickle shaped gap (0 to 2 mm tick). The brazing metal was a near eutectic Ag-Cu alloy containing a small amount of Li to promote spreading (58-Ag, 39-Cu, 3-Li at pct) as well as a trip of radioactive Ag tracers. The experiment was carried out in an isothermal furnace and the specimen was analyzed by both autoradiography and metallography. It was concluded that: extremely wide gaps of up to 2 mm could be filled under microgravity owing to capillary forces, although the shrinkage porosity increased in the largest area of the brazing seam; in large sickle shaped gaps, interface instabilities led to the entrapment of bubbles; the autoradiography of the specimen showed that considerable mixing of the molten brazing material had taken place even under microgravity conditions; chamfers were not sufficient to prevent the spilling over of the brazing material under microgravity; the microstructure of the Ni/Ag-Cu system investigated was not fundamentally different in the space and the ground samples except for an increased precipitation of the primary phase in the space sample which was due to a reduced mass transport in microgravity. ESA

N91-31462# Royal Inst. of Tech., Stockholm (Sweden). Dept. of Casting of Metal.
SOLDERING IN MICROGRAVITY (TEXUS 5)
T. Carlberg and M. Liljendahl *In* ESA, Summary Review of Sounding Rocket Experiments in Fluid Science and Materials Sciences: TEXUS 1 to 20; MASER 1 and 2 Feb. 1991 p 354-355 (For primary document see N91-31321 23-29)
Copyright Avail: NTIS HC/MF A15; EPD, ESTEC, Noordwijk, Netherlands, HC 75 Dutch guilders

An experiment to study the capillary flow of solder in gaps of variable width and to investigate the dissolution of the base material, is summarized. Three copper samples were processed, two with a conical gap increasing in width from the reservoir of solder (Sn-Ag, Tf = 221 C), and one with a cyclindrical gap. The samples were heated up to 260 C and then cooled naturally. The following results were obtained: in a cylindrical sample, which presented a gap width of 0.50 mm, nearly all the solder contained in the reservoir was sucked into the gap (this was not the case in the ground processed samples); the conical sample presenting a gap from 0.20 mm to 0.70 mm was evenly filled up to a width of 0.56 mm; and the conical sample where the gap increased from 0.20 mm to 1.00 mm was filled up to 0.58 mm. It was concluded that a maximum gap width of close to 0.6 mm can be filled with the system Cu/Sn-Ag. In the corresponding reference samples processed on Earth, the gaps were never uniformly filled up to this width. The space and ground samples exhibited different microstructures, particularly with respect to the volume fraction of the Cu-Sn phase, but this could be interpreted as the effect of slightly different temperature/time profiles. No influence of convection could be seen. ESA

N91-31463# Chalmers Univ. of Technology, Goeteborg (Sweden). Dept. of Engineering Metals.
ADHESION OF METALS ON CERAMIC SUBSTRATES (MASER 2) ESA
L. Kozma and R. Warren *In* ESA, Summary Review of Sounding Rocket Experiments in Fluid Science and Materials Sciences: TEXUS 1 to 20; MASER 1 and 2 Feb. 1991 p 356-357 (For primary document see N91-31321 23-29)
Copyright Avail: NTIS HC/MF A15; EPD, ESTEC, Noordwijk, Netherlands, HC 75 Dutch guilders

The efficiency of the brazing of ceramic materials with each other or with metals by means of metallic alloys depends largely on the wetting capability of the alloys. The adhesion characteristics are often improved by adding chemically active metals to the braze. A microgravity experiment to investigate the component distribution in the braze, to determine the attractive forces between the braze and the substrate, and to assess the influence of the surface roughness on the wetting behavior of the braze, is summarized. It was concluded that the interfacial segregation of Ti, which is of prime importance for the mechanical strength of brazed joints, can be more accurately adjusted, and the influence of the alloys composition can be better studied in a microgravity environment. ESA

N91-31464# Battelle Inst., Frankfurt am Main (Germany, F.R.).
ACOUSTIC POSITIONING OF A MOLTEN ALLOY SAMPLE (TEXUS 1)
E. G. Lierke *In* ESA, Summary Review of Sounding Rocket Experiments in Fluid Science and Materials Sciences: TEXUS 1 to 20; MASER 1 and 2 Feb. 1991 p 360-361 (For primary document see N91-31321 23-29)
Copyright Avail: NTIS HC/MF A15; EPD, ESTEC, Noordwijk, Netherlands, HC 75 Dutch guilders

An experiment to test an acoustic positioning system with a molten metallic sample under microgravity conditions is summarized. The acoustic levitator was accomodated in an isothermal resistance furnace. The temperature dependence of the acoustic wave pattern was compensated by injecting high or low density gas. The process was controlled by a reflector pick-up signal. During heating up to 650 C, a heavy gas (krypton) was injected into the furnace. An active gas cooling (nitrogen) system was employed. The spherical sample (hypereutectic alloy Ag 40-Sb 60 in wt, melting temperature: 485 C) was 8 mm in diameter an prepositioned in a wire cage. The sample processing was observed by means of a cine camera. Although the electronic monitor outputs indicated no malfunction during the flight, the cine recording showed that no stable positioning was achieved and that the sample touched the cage. Either the wave pattern was not stable or the gas which acted as an acoustic wave carrier was blown out of the furnace in the low pressure environment of the flight. ESA

N91-31465# Battelle Inst., Frankfurt am Main (Germany, F.R.).
ACOUSTIC POSITIONING (TEXUS 9) ESA
E. G. Lierke and R. Grossbach *In* ESA, Summary Review of Sounding Rocket Experiments in Fluid Science and Materials Sciences: TEXUS 1 to 20; MASER 1 and 2 Feb. 1991 p 362-363 (For primary document see N91-31321 23-29)
Copyright Avail: NTIS HC/MF A15; EPD, ESTEC, Noordwijk, Netherlands, HC 75 Dutch guilders

Containerless processing under high purity conditions favours the extensions of the undercooling range of metallic melts and can result in metastable crystalline or amorphous (glassy) phases with unique physical properties. Microgravity conditions facilitate the containerless processing of samples and prevent the the sedimentation of denser components. An acoustic levitator had been developed, adapted to an ELLI mirror furnace and partially tested during short-duration (10 s) parabolic aircraft flights. An experiment aimed at testing the performance of the system for longer durations is summarized. A sample of Pd 77.5 - Cu6 - Si 16.5 (8 mm in diameter, 2.84 g) was prepositioned in a wire cage in the focus of the mirror furnace. The experiment was performed in the temperature range 760 C (melting point) to 1000 C with heating rates of 10 to 20 C/s. The sample was monitored with a charge coupled device camera for automatic and telecommand control. The positioning test was only marginally successful. The sample was effectively free floating while completely melted. However, it started to rotate and oscillate during the cooling phase and came into contact with the wire cage several times. Finally, it remained attached to the cage while still molten and solidified. ESA

N91-31466# Deutsche Forschungs- und Versuchsanstalt fuer Luft- und Raumfahrt, Cologne (Germany, F.R.). Inst. for Space Simulation.
CONTAINERLESS SOLIDIFICATION OF A Pd-Cu-Si SAMPLE (TEXUS 9) ESA
D. M. Herlach and R. Wilnecker *In* ESA, Summary Review of Sounding Rocket Experiments in Fluid Science and Materials Sciences: TEXUS 1 to 20; MASER 1 and 2 Feb. 1991 p 364-365 (For primary document see N91-31321 23-29)
Copyright Avail: NTIS HC/MF A15; EPD, ESTEC, Noordwijk, Netherlands, HC 75 Dutch guilders

An experiment to melt and solidify containerlessly a PdCuSi glass forming alloy by means of an acoustic positioning device accomodated in a mirror furnace is summarized. The analysis of the microstructure of the sample showed that the alloy was completely molten during the microgravity period. The Si contained in the sample was oxidized indicating the atmosphere had not been pure enough. The solidification started from the contact point with the wire cage and resulted in a lamellar eutectic structure. The size of the lamellae was increasing with the distance from the contact point, indicating that heteorogeneous nucleation and high cooling rate had occurred at the contact point. Comparative differential scanning calorimetry measurements showed that the undercooling prior to solidification had been less than 190 K. ESA

N91-31467# Battelle Inst., Frankfurt am Main (Germany, F.R.).
ACOUSTIC POSITIONING (TEXUS 14b) ESA
E. G. Lierke and R. Grossbach *In* ESA, Summary Review of Sounding Rocket Experiments in Fluid Science and Materials Sciences: TEXUS 1 to 20; MASER 1 and 2 Feb. 1991 p 366-367 (For primary document see N91-31321 23-29)
Copyright Avail: NTIS HC/MF A15; EPD, ESTEC, Noordwijk, Netherlands, HC 75 Dutch guilders

An experiment to test a single axis positioner under steep thermal gradient by processing a spherical sample in the focus of a mirror furnace is summarized. Temperatures of up to 900 C were to be reached with heating rates ranging from 6 to 20 K/s and cooling rates between 4 and 8 K/s. Also, the experiment aimed at reaching undercooling values as high as possible with an easy glass forming eutectic alloy, PdCuSi. A video recording showed radial oscillations of the sample during the heating up period and that contacts occurred between the sample and its

support. However, these oscillations vanished at high temperatures and a quiet and contactless positioning of the molten sample in the focus of the mirror was achieved. Oscillations occurred again during the cooling phase which led to contacts between the sample and the support. ESA

N91-31468# Deutsche Forschungs- und Versuchsanstalt fuer Luft- und Raumfahrt, Cologne (Germany, F.R.).
CONTAINERLESS UNDERCOOLING OF A Pd-Cu-Si ALLOY (TEXUS 14b) ESA
D. M. Herlach, R. Wilnecker, and F. Gillessen *In* ESA, Summary Review of Sounding Rocket Experiments in Fluid Science and Materials Sciences: TEXUS 1 to 20; MASER 1 and 2 Feb. 1991 p 368-369 (For primary document see N91-31321 23-29)
Copyright Avail: NTIS HC/MF A15; EPD, ESTEC, Noordwijk, Netherlands, HC 75 Dutch guilders

An experiment to reach high undercooling values is summarized. A period of about 40 s without any contact between the molten sample and the support was achieved. The temperature time profile was deduced from reference measurements and the video recording. There was a temperature plateau corresponding to melting before overheating at 1225 K and then cooling. The sample solidification started at an undercooling of about only 170 K, again due to oscillations and to contact with the support. This was confirmed by the analysis of the sample section, where two crystalization points can be seen from which the eutectic grew towards the center of the sample. An undercooling of 70 K was achieved with a sample processed on Earth in a quartz tube, thereby demonstrating that containerless processing allows significantly higher undercooling values to be reached. Auger analyses of the sample surface showed that the undercooling was limited by reactions between the melt and the surrounding atmosphere. It was therefore concluded that further experiments should be performed under very high purity conditions. ESA

N91-31469# Battelle Inst., Frankfurt am Main (Germany, F.R.).
ELECTROSTATIC POSITIONING FOR CONTAINERLESS PROCESSING OF A LI-SILICATE GLASS (TEXUS 10) ESA
E. G. Lierke, R. Grossbach, G. H. Frischat, and K. Fecker *In* ESA, Summary Review of Sounding Rocket Experiments in Fluid Science and Materials Sciences: TEXUS 1 to 20; MASER 1 and 2 Feb. 1991 p 370-371 (For primary document see N91-31321 23-29)
Copyright Avail: NTIS HC/MF A15; EPD, ESTEC, Noordwijk, Netherlands, HC 75 Dutch guilders

An experiment intended to test an electrostatic positioning system by processing containerlessly a Li silicate glass sample is summarized. The crystallization and demixing of such a glass is strongly influenced by the heterogeneous nucleation occurring at the crucible wall. Melting and resolidification under containerless conditions was expected to yield a glass with a better homogeneity. A disalignement of one of the charge coupled devices (CCD's) occurred during the launch. The sample detection system of this CCD then identified a corner of the observation window as the sample. The electrodes were wrongly activated and no proper positioning was achieved. The sample moved irregularly between the electrodes and, therefore was not always in the mirror focus. It was estimated that the outer shell of the sample reached a temperature of only 500 to 700 C, instead of the target 1150 C, before it stuck to one of the electrodes. Nuclei did not dissolve and phase separation could occur. The initially transparent blue sample turned to blue opaque. It is proposed to retest the electrostatic levitator during parabolic aircraft flights with an improved sample position detection system using diode arrays to have a faster response. ESA

N91-31736 Commercial Space Technologies Ltd., London (England).
REVIEW OF MICROGRAVITY
Per Anders Hansson *In its* BAe University Round Table on Gravitational Research Nov. 1990 10 p (For primary document see N91-31729 23-46)
Copyright Avail: British Aerospace (Military Aircraft) Ltd., Warton Aerodrome, Preston, Lancashire PR4 1AX, England

31 ENGINEERING (GENERAL)

Includes vacuum technology; control engineering; display engineering; cryogenics; and fire prevention.

N91-31470*# Planning Research Corp., Edwards, CA.
PREDICTED THERMAL RESPONSE OF A CRYOGENIC FUEL TANK EXPOSED TO SIMULATED AERODYNAMIC HEATING PROFILES WITH DIFFERENT CRYOGENS AND FILL LEVELS Final Report
Gregory J. Hanna (Hanna Technology Resources, Boulder, CO.) and Craig A. Stephens Washington NASA Sep. 1991 19 p Presented at the AIAA Session of the ASME/AICHE National Heat Transfer Conference, Minneapolis, MN, 28-31 Jul. 1991 Previously announced in IAA as A91-45461
(Contract NAS2-12722)
(NASA-CR-4395; H-1738; NAS 1.26:4395; AIAA-91-4007) Avail: NTIS HC/MF A03 CSCL 13B

A two dimensional finite difference thermal model was developed to predict the effects of heating profile, fill level, and cryogen type prior to experimental testing the Generic Research Cryogenic Tank (GRCT). These numerical predictions will assist in defining test scenarios, sensor locations, and venting requirements for the GRCT experimental tests. Boiloff rates, tank-wall and fluid temperatures, and wall heat fluxes were determined for 20 computational test cases. The test cases spanned three discrete fill levels and three heating profiles for hydrogen and nitrogen.
Author

N91-31471 Rensselaer Polytechnic Inst., Troy, NY.
INTER-GEN: A HYBRID APPROACH TO ENGINEERING DESIGN OPTIMIZATION Ph.D. Thesis
David John Powell 1990 183 p
Avail: Univ. Microfilms Order No. DA9120237

A large portion of engineering design optimization involves the time consuming process of running iterative simulation codes to predict the performance of a design. An optimization approach based on the interdigitation of three optimization technologies is presented. The approach, Inter-GEN, is an interdigitation of genetic algorithms, expert systems, and numerical optimization. Inter-GEN uses a control strategy to couple and switch among optimization technologies to get the greatest optimization improvement in as few runs of the simulation code as possible. There are two search phases in the Inter-GEN approach: Knowledge directed and knowledge supplementation. Knowledge directed search uses expert system technology tightly coupled with numerical optimization techniques. Knowledge supplementation search phase supplements the engineer's incomplete knowledge of the parameter space by coupling genetic algorithms and numerical optimization to explore and exploit the parameter space efficiently. Inter-GEN was implemented and tested using a single control strategy on a diverse set of eleven test cases. The results show Inter-Gen to be a more efficient and robust optimization approach than other approaches alone. Dissert. Abstr.

N91-31472# Sandia National Labs., Albuquerque, NM.
SILICON MICROMACHINING BASED ON POROUS SILICON FORMATION
M. J. Kelly, T. R. Guilinger, and J. O. Stevenson 1991 2 p Presented at the 180th Meeting of the Electrochemical Society, Phoenix, AZ, 13-18 Oct. 1991
(Contract DE-AC04-76DP-00789)
(DE91-013744; SAND-91-0910C; CONF-911047-3) Avail: NTIS HC/MF A01

The mechanical strength of silicon, in combination with the sophisticated silicon wafer processing techniques developed to produce silicon integrated circuits, makes it an ideal candidate for the development of a microelectromechanical device technology. We describe a new electrochemical processing technique based

on porous silicon that can produce surface and buried insulators, conductors, and sacrificial layers required for sensor, micromotor, and membrane fabrication. DOE

N91-31473# California Univ., Berkeley. Lawrence Berkeley Lab.
A JET POLISHING TECHNIQUE FOR THINNING TWO PHASE MATERIALS
M. J. Witcomb (Witwatersrand Univ., Johannesburg, South Africa) and U. Dahmen Nov. 1990 2 p Presented at the Annual Electron Microscopy Society of South Africa (EMSSA) Conference, Grahamstad (South Africa), 3-7 Dec. 1990
(Contract DE-AC03-76SF-00098)
(DE91-016422; LBL-29967; CONF-9012103-2) Avail: NTIS HC/MF A01

A common problem in the preparation of thin foils for transmission electron microscopy is the different thinning rate in two-phase materials. Often this leads to foils in which the majority, or matrix, phase is evenly polished while the minority, or precipitate, phase is either etched out or stands proud of the surrounding material. In the present report, we describe a two-stage jet polishing technique that has been used successfully on different relatively coarse two-phase structures. DOE

N91-31474# Centre National d'Etudes Spatiales, Toulouse (France).
SOLDERING OF COMPLEX MULTILAYER PRINTED BOARDS [BRASSAGE DES CARTES IMPRIMES MULTICOUCHES COMPLEXES]
Jean-Marie Garrigue and Jean-Francois Braun (MATRA Espace, Toulouse, France) Sep. 1990 68 p In FRENCH; ENGLISH summary Original contains color illustrations
(CNES-NT-127; ETN-91-99534) Copyright Avail: NTIS HC/MF A04

The soldering limits of complex multilayer printed boards used for spaceborne electronic equipment are presented. 6400 configurations related to board design, component's lead characteristics and manual and wave soldering parameters, are tested. Choices and recommendations are suggested to overcome these limits. Quality and reliability aspects of the soldered joints are broached, and research topics are proposed. Soldering problems are found to develop beyond 8 to 10 layers of circuits in components with connection conductivities of less than 1 to 2 W per cm over temperature in degrees centigrade. ESA

N91-31475# Centre Aeroporte de Toulouse (France).
LOW ALTITUDE EJECTION RELEASE (TOTAL MASS BETWEEN 1,660 AND 5,600 KG) [LARGAGE PAR EJECTION A FAIBLE HAUTEUR (MASSE TOTALE COMPRISE ENTRE 1.660 KG ET 5.600 KG)]
M. Josse Apr. 1990 82 p In FRENCH
(Rept-90/05; ETN-91-99980) Avail: NTIS HC/MF A05

Design studies on the process of release by ejection at low altitude of loads whose total mass are between 1,660 and 5,600 kg are reported. The feasibility and definition phases and definition synthesis and selection are covered. The characteristics of the release process thus defined are detailed and the process is recommended for evaluation. ESA

N91-31476* National Aeronautics and Space Administration. Langley Research Center, Hampton, VA.
APPARATUS AND METHOD FOR EXPLOSIVE BONDING TO EDGE OF FLYER PLATE Patent
Laurence J. Bement, inventor (to NASA) and Anne C. Kushnick, inventor (to NASA) 24 Sep. 1991 11 p Filed 2 Oct. 1990
(NASA-Case-LAR-14096-1; US-Patent-5,050,789; US-Patent-Appl-SN-591644; US-Patent-Class-228-107; US-Patent-Class-228-2.5; Int-Patent-Class-B23K-20/08) Avail: US Patent and Trademark Office CSCL 13H

The invention is an apparatus and a process for the explosive joining of a flyer plate and a base plate. The apparatus consists of a flyer plate positioned over a base plate. The flyer plate has a notch containing a filler material in intimate contact with the flyer plate. An adhesive means holds a ribbon explosive partially overlapping the notch in the flyer plate. A detonating means initiates the ribbon explosive that drives the flyer plate to accomplish a high velocity, angular collision between the mating surfaces. This collision creates surface melts and effacing bonding, resulting in electron sharing linkups between the plates. An unbonded tab fractures at a base of the notch leaving a bond to an edge of the attached flyer plate.
Official Gazette of the U.S. Patent and Trademark Office

N91-31477# Los Alamos National Lab., NM.
FINITE ELEMENT MODELING OF ORTHOGONAL MACHINING USING AN ELASTIC-VISCOPLASTIC MATERIAL MODEL
B. A. Laake and C. A. Anderson Aug. 1991 52 p
(Contract W-7405-eng-36)
(DE91-016815; LA-12151-MS) Avail: NTIS HC/MF A04

An orthogonal machining operation is modeled using an elastic-viscoplastic constitutive law in an Eulerian formulation. To perform this analysis, an existing finite element code was modified to include features applicable to the machining problem. A viscosity relationship based on an overstress, viscoplastic failure criterion is used. A routine for automatic remeshing is used. It allows the mesh to follow streamlines, thus predicting final chip geometry. The code is first verified by comparing results with analytical solutions for a Couette-type flow problem with viscoplastic material law. Finite element results for the machining problem are compared with solutions from machining theory, experimental data, and other numerical solutions from the literature. DOE

N91-32025# Keuring van Electrotechnische Materialen N.V., Arnhem (Netherlands). Dept. of Physical Research.
THE CRITICAL TEMPERATURE FOR DRYING-OUT OF SOILS AROUND POWER CABLES AS A FUNCTION OF LOCAL CONDITIONS
G. Koopmans and J. Kuiper *In its* KEMA Scientific Reports, Volume 8, Number 2, 1990 Apr. 1990 p 97-103 (For primary document see N91-32023 23-99)
Avail: NTIS HC/MF A04

32 COMMUNICATIONS AND RADAR

Includes radar; land and global communications; communications theory; and optical communications.

For related information see also *04 Aircraft Communications and Navigation* and *17 Space Communications, Spacecraft Communications, Command and Tracking.* For search and rescue see *03 Air Transportation and Safety,* and *16 Space Transportation.*

N91-31478# Atlantis Scientific Systems Group, Inc., Ottawa (Ontario).
UPDATES TO THE DREO AIRBORNE RADAR SIMULATOR
Karen A. Vineberg and Ronald H. Saper Jun. 1989 43 p
(Contract DREO-W7714-7-5353)
(ASSGI-167; CTN-91-60129) Avail: NTIS HC A03

The airborne radar simulator (ABRSIM) code comprises a detailed video simulation for modeling the performance of coherent pulsed radar system in an airborne environment. The simulation is quite general in its capabilities and can account for ambiguous performance in both frequency and range. Clutter cancellation involving more than one phase center was investigated. Radar performance was studied as a function of phase center position using the optimal and the MTI two pulse canceller binomial weighting signal processors. Performance was measured in terms of signal to interference ratios (SIR). Interference represents the combined effect of system noise and clutter. Both forward looking and side looking cases were examined. The phase center was varied in elevation and in azimuth. The MTI system which does a simple subtraction, performs well only the phase centers were aligned with the direction of aircraft motion and the matching condition was met. Thus, this was not an effective way of cancelling clutter. The optimal processor performed well under several

different geometries. The SIR ratio was only marginally worse with changes in elevation but degraded quickly with changes in azimuth. It is suggested that this performance pattern was a result of sidelobe nulling. CISTI

N91-31479 COM DEV Ltd., Cambridge (Ontario).
DIELECTRIC IMAGE-RESONATOR MULTIPLEXER Patent
Wai-Cheung Tang, inventor, Richard J. Cameron, inventor, and David M. T. Bryant, inventor 28 Mar. 1989 34 p
(Patent-1-252-835; Int-Patent-Class-H03H-970; Int-Patent-Class-H04J-102; CTN-91-60143) Copyright Avail: Micromedia Ltd., Technical Information Centre, 165 Hotel de Ville, Place du Portage, Phase 2, Hull, Quebec J8X 3X2, Canada HC $4.00 CAN, MF $2.75 CAN

This invention relates to microwave multiplexers for use in satellite communications. A multiplexer has two to four channels and each channel has one bandpass filter. The multiplexer has a common cavity and contains a dielectric cut resonator for each channel. The dielectric resonators function as bandpass filter elements for frequencies between 1 and 4 GHz. The common cavity provides a common junction and contains means to couple electromagnetic energy between the various channels. Reductions in volume of 75 percent and almost as much in mass were achieved over the equivalent single mode dielectric resonator filter. Furthermore, wide passband filter characteristics which require the stronger couplings may be realized. Unwanted modes of resonance are suppressed within the cavity assuring a wide spurious free reject band. The multiplexer can be operated to realize symmetric and asymmetric cross coupling through the use of probes or loops. CISTI

N91-31480 Communications Satellite Corp., Washington, DC.
ELECTROMAGNETICALLY COUPLED MICROSTRIP ANTENNAS HAVING FEEDING PATCHES CAPACITIVELY COUPLED TO FEEDLINES Patent
Amir I. Zaghloul, inventor 21 Nov. 1989 21 p
(Patent-1-263-181; Int-Patent-Class-H01Q-904; Int-Patent-Class-H01Q-138; Int-Patent-Class-H01Q-2106; CTN-91-60158) Copyright Avail: Micromedia Ltd., Technical Information Centre, 165 Hotel de Ville, Place du Portage, Phase 2, Hull, Quebec J8X 3X2, Canada HC $4.00 CAN, MF $2.75 CAN

With the advent of microwave integrated circuits (MIC), monolithic microwave integrated circuits (MMIC), and direct broadcast satellites, a need for inexpensive, easily fabricated antennas operating over a wide bandwidth and for antennas which operate at different frequency bands has arisen. A design is described for a microstrip antenna which displays the desired characteristics. In addition, it operates in either linear or circular polarization mode, has circularly polarized elements with a low axial ratio and linearly polarized elements with a high axial ratio, and is simple and inexpensive to manufacture. The antenna has a plurality of radiating and feeding patches, each having perturbation segments, the feeding patches being capacitively coupled to the radiating patches, and the feedline capacitively coupled to the feeding patch. The feed network also can comprise active circuit components implementing MIC or MMIC techniques, such as amplifiers and phase shifters to control the power distribution, the sidelobe levels, and the beam direction of the antenna. The design can be scaled to operate in any frequency band such as L-band, S-band, X-band, Ku-band, or Ka-band. CISTI

N91-31481 Department of National Defence, Ottawa (Ontario).
RADOME-LENS EHF ANTENNA DEVELOPMENT Patent
Yung L. Chow, inventor and Sujeet K. Chaudhuri, inventor 31 Oct. 1989 19 p
(Patent-1-262-571; Int-Patent-Class-H01Q-142; CTN-91-60159) Copyright Avail: Micromedia Ltd., Technical Information Centre, 165 Hotel de Ville, Place du Portage, Phase 2, Hull, Quebec J8X 3X2, Canada HC $4.00 CAN, MF $2.75 CAN

A radome is a thin shell of uniform thickness used to protect an antenna from the weather. It has heretofore been regarded as a hinderance to the radiation performance of the antenna. An antenna which is capable of scanning 90 deg of the sky is highly desirable as it would allow two antennas to scan the whole sky. It has been found that a radome can be configured in such a manner that it not only eliminates the refraction problems normally encountered from radomes, but employs that characteristic to amplify transmitted and/or received rays to enable the scanning of the whole sky with two antennas. The design for such a radome lens is described. The resulting radome continues to provide protection for the antenna and also functions as a lens that amplifies a scan angle of less than 90 deg to 90 deg or more without much spherical abberation. In an aperture planar phased array with electronic scanning, such amplification enables the array to retain substantial antenna gain and partial dual polarization capability. CISTI

N91-31482 COM DEV Ltd., Cambridge (Ontario).
ANTENNA STUDY FOR 60 GHz INTERSATELLITE LINK Final Report
Subir Ghosh 26 Apr. 1989 102 p
(Contract DREO-W7714-8-5734/01-ST)
(CD-RPT-ITL-5043-003; CTN-91-60178) Copyright Avail: NTIS HC A06

This report describes a detailed study of the antenna design and operation for the 60 GHz intersatellite cross links to a geostationary relay satellite. Intersatellite links will be used extensively in the future to achieve global connectivity of satellite constellations. Scenarios for inter-orbital linkages were examined with respect to the following antenna characteristics: inter-orbital link parameters, pointing and tracking requirements, radio frequency (RF) design encompassing transmission and receiving links, tracking and anti-jamming measures, mechanical and thermal design, positioner mechanism, mounting and deployment, and signal routing. A comparative study of the options is given wherever appropriate, to highlight the key features. The key features of the proposed antenna system are: (1) a rotating reflector design to allow tracking with a fast moving satellite; (2) a beam waveguide arrangement which allows the transmitter and receiver equipment to be entirely located in a controlled environment; (3) a multi-function feed system (transmit receive, beacon) inside the antenna boom ensures a reliable and compact feed network; and (4) positional mechanisms for azimuth and elevation tracking that allow unconstrained RF signal routing through beam waveguides. Author (CISTI)

N91-31483 Software Kinetics Ltd., Stittsville (Ontario).
THE AUTOMATIC SURVEILLANCE, TRACKING, AND IMAGING PROGRAM. USER MANUAL
Joe A. Szozda 31 Mar. 1989 98 p
(Contract DREO-66ER-7-0003/E2-ER)
(SK-1600-44-001-02-0; DREO-W7714-8-5620; CTN-91-60179)
Avail: NTIS HC A05

The automatic surveillance, tracking and imaging program (ASTIP) is a phased-array radar system which carries out surveillance of a designated field of view, and acquires and tracks multiple targets in its surveillance space. The user manual provides a detailed description of the device and file preparations that must be completed before ASTIP is run. The device and file preparations are summarized as an acquisition of resources list for quick reference by operators familiar with ASTIP. A detailed explanation of the preparations are presented in subsequent sections of the user manual. Each option in the menu-driven operator interface is discussed in detail. Diagrams of the ASTIP menus are located in the appendices. The error condition section explains the errors that are typically encountered and provides possible solutions to each of the problems. Finally, the procedures required to maintain the ASTIP software are explained in the building ASTIP section of the user manual. Author (CISTI)

N91-31484 Atlantis Scientific Systems Group, Inc., Ottawa (Ontario).
IMPROVEMENTS TO PROGRAMS FOR SYSTEM STUDIES OF SPACE-BASED RADAR Final Report

Ronald H. Saper 30 Mar. 1990 19 p
(Contract DRE-W7714-9-9272)
(DRE-179; CTN-91-60199) Avail: NTIS HC A03

This report provides details of a project in which two computer programs for systems studies of space-based radar, a pulse Doppler detection simulator (PDDS) and integrated surveillance simulator (ISS), were evaluated and upgraded. The validity and accuracy of the various routines was checked and errors were corrected when found. User Compatible Front End (UCFE), a generic user interface, was tailored to the PDDS and ISS simulators. This interface is flexible and easy to use, allows easy entry of input parameters for a PDDS of ISS run, provides full line editing, online help, and screen management functions. In addition, output formats were modified, and the code was modified to enhance efficiency. It was recommended that post processing improvements to the ISS be undertaken to simplify and speed the execution of parameteric studies of reliability of systems, swath schemes and radar baseline detection. CISTI

N91-31485 Atlantis Scientific Systems Group, Inc., Ottawa (Ontario).
BEHAVIOUR OF THE SIR FOR SPACE-BASED DPCA RADAR UNDER VARIOUS SPATIAL CLUTTER DISTRIBUTIONS
Leonard Lightstone Feb. 1988 48 p
(Contract DREO-W7714-7-5271)
(CRC-W7714-7-5271; CTN-91-60203) Avail: NTIS HC A03

This report presents an examination of the effects of the statistical nature of clutter reflectivity on the signal to interference ratio (SIR) of a space-based displaced phase center antenna (DPCA) system. Also included is the interference effect of discrete scatterers. Earlier studies have evaluated the SIR using optimal filters. These linear systems are designed to statistically minimize the effect of interference on the detection performance of the radar and are based on the covariance matrix of the clutter and system noise. The resulting SIR curves provide the expectation of the SIR values as a function of target Doppler speed. Due to the statistical nature of clutter patch reflectivity, actual SIR values, evaluated on a burst by burst basis, will vary about the SIR expectation curve. To gain a better understanding of the effects of the random nature of clutter on these SIR values, a more detailed clutter model has been developed which allows calculation of the actual clutter return signal. An extension provided to the clutter model is the inclusion of discrete scatterers. These scatterers may be thought of as strong specular reflectors such as buildings or, on a larger scale, cities. The potential for very large radar cross-section (RCS) values associated with discrete scatterers may have serious degradation effects on the SIR performance. Preliminary simulation results indicate the following: (1) significant difference can exist between mean and stochastic SIR values; (2) the exact nature of the clutter spatial statistics is unimportant indicating that the central limit theorem applies; (3) variation of the SIR values about the mean curve decrease with increasing mean SIR value; and (4) with optimal filtering, discrete scatterers only act to cause an overall degradation in the SIR curve. Two important extensions of the analysis which have not been considered here are the effects of non-optimal filters and the internal motion of clutter. CISTI

N91-31486 Atlantis Scientific Systems Group, Inc., Ottawa (Ontario).
PULSE DOPPLER RADAR SIMULATION STUDY Final Technical Report
Murray Gibb, Leonard Lightstone, and Ronald H. Saper Oct. 1988 285 p
(Contract DND-14SV-W7714-7-5353)
(ASSGI-14SV-W7714-7-5353; ASSGI-TR-20; CTN-91-60204)
Avail: NTIS HC A13

In the past several years two different models have been produced for predicting detection performance of space-based and airborne coherent pulsed radars. The present work describes enhancements incorporated in the software including: (1) conversion of the code to ANSI standard FORTRAN-77; (2) development and implementation of a suitable algorithm for the evaluation of the clutter covariance matrix of an array processor; (3) derivation and coding of the linear frequency modulated (LFM) waveform simulation capability for radar system performance evaluation; and (4) implementation of a Monte Carlo code to study receiver imperfections for the non-frequency modulated (NFM) waveform as well as the derivation of analytical expressions describing the effects of linear receiver imperfections on this waveform. Single precision accuracy was found to be close to that of double precision. The looping of the clutter patches was found to be the time limiting process in the clutter calculations and hence little run time was gained by use of single precision. Evaluation of the LFM waveform showed range velocity coupling and a nonstationary behaviour or the return signal. Detection performance of the LFM waveform is consistently better than that of the NFM waveform. CISTI

N91-31487 Old Dominion Univ., Norfolk, VA.
INTEGRATED CONTROL OF THERMALLY DISTORTED LARGE SPACE ANTENNAS Ph.D. Thesis
Robert Heath Tolson 1990 100 p
Avail: Univ. Microfilms Order No. DA9118082

Studies on controlling the thermal distortion of large space antennae have generally studied a single orbital position and have optimized actuator locations based on minimizing the RMS surface deviation from the original parabolic shape. One study showed the benefits of directly using far zone electric field characteristics as the performance measure; but, this approach resulted in a nonlinear programming problem. The objective of the current study is to develop an approach to designing a control system that recognizes the time dependence of the distortion and controls variables that are directly related to far field performance in a quadratic cost sense. The first objective, to include time dependence, is accomplished using a principal component analysis to expand an aperture phase function into components that are orthogonal in space and time. The approach for the second objective is to expand the far zone electric field in a Zernike-Bessel series. For surface distortions of less than 1/4 wavelength, it is shown that the coefficients of this series provide a reliable measure of far field performance. Dissert. Abstr.

N91-31488*# Contel Federal Systems, Inc., Chantilly, VA. Federal Systems Div.
INTERIM SERVICE ISDN SATELLITE (ISIS) NETWORK MODEL FOR ADVANCED SATELLITE DESIGNS AND EXPERIMENTS Report, 25 Sep. 1990 - 15 Sep. 1991
Gerard R. Pepin and E. Paul Hager 13 Sep. 1991 41 p
(Contract NASw-4520)
(NASA-CR-186565; NAS 1.26:186565) Avail: NTIS HC/MF A01 CSCL 17B

The Interim Service Integrated Services Digital Network (ISDN) Satellite (ISIS) Network Model for Advanced Satellite Designs and Experiments describes a model suitable for discrete event simulations. A top-down model design uses the Advanced Communications Technology Satellite (ACTS) as its basis. The ISDN modeling abstractions are added to permit the determination and performance for the NASA Satellite Communications Research (SCAR) Program. Author

N91-31489# Universiteit Twente, Enschede (Netherlands). Faculty of Applied Mathematics.
SOME ORDER DIMENSION BOUNDS FOR COMMUNICATION COMPLEXITY PROBLEMS
U. Faigle and Walter Kern Feb. 1991 17 p
(MEMO-938; ISSN-0169-2690; ETN-91-99736) Avail: NTIS HC/MF A03

A general (0,1) matrix M is associated with an ordered set P(M). Lower and upper bonds for the deterministic communication complexity of M in terms of the order dimension of P(M) are derived. The special class of communication matrices M obtained as cliques versus stable sets incidence matrices of comparability graphs G is considered. Their complexity is bound by O ((log d).(log n)), where n is the number of nodes of G and d is the

order dimension of an orientation of G. In this special case, the bound is shown to improve other well known bounds obtained for the general cliques versus stable set problem. ESA

N91-31490# Sandia National Labs., Albuquerque, NM.
RADAR-CROSS-SECTION MEASUREMENT ERRORS CAUSED BY TEST OBJECT INTERACTION WITH LOW-DIELECTRIC-CONSTANT SUPPORTS
B. C. Brock, W. E. Patitz, K. W. Sorensen, and D. H. Zittel 1991 5 p Presented at the 13th Annual NIST Meeting on Antenna Measurements Techniquest Association (AMTA), Boulder, CO, 7-11 Oct. 1991
(Contract DE-AC04-76DP-00789)
(DE91-015340; SAND-91-0955C; CONF-9110159-1) Avail: NTIS HC/MF A01

In the search for an ideal test-object support for simulated free-space radar-cross-section (RCS) measurements, low-density polystyrene foam has achieved considerable popularity. However, significant error can be introduced into a measurement by the use of an inappropriately designed support. Although low back-scatter radar cross section (RCS) can be obtained with this material, interactions can occur between the test object and the mount which will cause measurement errors in excess of several dB. We present results of measurements performed on a simple test object supported on a low-density foam column which demonstrate this effect. As we discuss, this error can be incorrectly interpreted to be caused by poor alignment of the test object with the radar-range coordinate system. Finally, we show that the error can be explained by differential propagation effects. In addition, this simple theory provides the insight necessary to devise appropriate measures to minimize the errors caused by the presence of the support. DOE

N91-31491# Los Alamos National Lab., NM.
ABSTRACTS OF PAPERS PRESENTED AT THE FIRST LOS ALAMOS SYMPOSIUM ON ULTRA-WIDEBAND RADAR
Abstracts Only
B. W. Noel, comp. Jul. 1991 41 p Symposium held in Los Alamos, NM, 5-8 Mar. 1990
(Contract W-7405-eng-36)
(DE91-015976; LA-12128-C; CONF-900397-Absts) Avail: NTIS HC/MF A03

To provide an open and unbiased forum for exchanging ideas and research results among specialists in the field of radar and related topics, the First Los Alamos Symposium on Ultra-Wideband Radar was held at Los Alamos National Laboratory March 3 to 7, 1990. This document contains copies of the abstracts of the papers presented at the symposium. More than 200 scientists and engineers from the United States, Canada, and Great Britain attended the symposium. They heard 75 papers that I tried to categorize into seven subject areas: fundamental topics, computational electromagnetics, applications, new technologies, signal propagation, signal processing, and testing. Of the 75 papers, roughly 45 of the full texts are scheduled to be published in book form by CRC Press. DOE

N91-31492*# Kansas Univ. Center for Research, Inc., Lawrence. Radar Systems and Remote Sensing Lab.
A NUMERICAL PROCEDURE FOR RECOVERING TRUE SCATTERING COEFFICIENTS FROM MEASUREMENTS WITH WIDE-BEAM ANTENNAS
Qinglin Wang and S. P. Gogineni Sep. 1991 34 p
(Contract NAGw-1984; N00014-89-J-1456)
(NASA-CR-186042; NAS 1.26:186042; RSL-TR-8240-2) Avail: NTIS HC/MF A03 CSCL 20N

A numerical procedure for estimating the true scattering coefficient, sigma(sup 0), from measurements made using wide-beam antennas. The use of wide-beam antennas results in an inaccurate estimate of sigma(sup 0) if the narrow-beam approximation is used in the retrieval process for sigma(sup 0). To reduce this error, a correction procedure was proposed that estimates the error resulting from the narrow-beam approximation and uses the error to obtain a more accurate estimate of sigma(sup 0). An exponential model was assumed to take into account the variation of sigma(sup 0) with incidence angles, and the model parameters are estimated from measured data. Based on the model and knowledge of the antenna pattern, the procedure calculates the error due to the narrow-beam approximation. The procedure is shown to provide a significant improvement in estimation of sigma(sup 0) obtained with wide-beam antennas. The proposed procedure is also shown insensitive to the assumed sigma(sup 0) model. Author

N91-31493# Universiteit Twente, Enschede (Netherlands). Dept. of Informatics.
REFINING INTERFACES OF COMMUNICATING SYSTEMS
Ed Brinksma, Bengt Jonsson, and Fredrik Orava (Swedish Inst. of Computer Science, Uppsala.) Feb. 1991 18 p Sponsored in part by Swedish Board for Technical Development
(MEMO-INF-91-19; TIOS-91/003; ISSN-0923-1714; ETN-91-99700) Avail: NTIS HC/MF A03

There are now several theories for describing and reasoning about the behavior of communicating systems, where the behavior of a communicating system is described in terms of its capabilities to perform communication actions in cooperation with its environment. In such theories, preorders or equivalences are defined as criteria for when one system is an acceptable substitute or implementation of another. Existing theories of communicating systems define preorders or equivalence relations only between systems with identical sets of communication actions. In many practical design situations, however, it may be desirable to refine a system by changing its set of communication actions. A simple method for carrying out such refinements is presented. The method is first formulated in a general setting, and then elaborated in more detail in the trace model and a simple version of the failure model. The usefulness of the method is demonstrated by an application to I.451, an ISDN (Integrated Services Digital Network) access protocol. ESA

N91-31494# Federal Aviation Administration, Atlantic City, NJ.
SOLID-STATE RADAR BEACON DECODER (SSRBD) MASTER TEST PLAN (MTP)
Leonard H. Baker and Thomas D. Bratton Sep. 1991 37 p
(DOT/FAA/CT-TN91/33) Avail: NTIS HC/MF A03

The Master Test plan (MTP) establishes the basic framework to guide and direct the Solid-State Radar Beacon Decoder (SSRBD) test program. The MTP explains the relationship between all test phases and also concerns the SSRBD system's readiness to be integrated into the National Airspace System (NAS). Sufficient detail is provided to define and direct the development of the next lower level of documentation. The MTP addresses the responsibilities of the SSRBD contractor and the Federal Aviation Administration (FAA). Author

N91-31495# Federal Aviation Administration, Atlantic City, NJ.
AERONAUTICAL MOBILE SATELLITE SERVICE (AMSS) TEST PLAN
Sean M. Sandlin (Computerized Technoiogies, Inc., Columbus, OH.) May 1991 49 p
(NASA Order T-0704-F)
(DOT/FAA/CT-TN91/20) Avail: NTIS HC/MF A03

A test program is described which will be conducted by the Federal Aviation Administration to support the validation of Standards and Recommended Practices being developed for the Aeronautical Mobile Satellite Service by the International Civil Aviation Organization. A description of the Communication Test Facility is also presented which will be used to perform the tests. A brief description is also included of each test to be performed along with setup and data to be recorded. Author

N91-31496 Physics and Electronics Lab. TNO, The Hague (Netherlands).
INTRODUCTION TO RADAR POLARIMETRY Final Report
J. S. Groot 23 Apr. 1991 70 p
(FEL-91-B122; TD-91-2021; ETN-91-90006) Copyright Avail:

Physics and Electronics Lab. TNO, P.O. Box 96864, 2509 JG, The Hague, Netherlands

An introduction is made to polarimetry with microwaves, i.e., radar polarimetry. Basic relevant electromagnetic theory is considered and the definition of polarization is given. Polarization is a two parameter quantity for which several representations exist. Some are given, together with a few methods to generate a wave with an arbitrary polarization. How the polarization of a wave can be changed by several different physical mechanisms is discussed. The scattering matrix describes the way in which the polarization of a wave is altered by scattering. Some properties and examples are given. The problem of minimization and maximization of the power received by a radar illuminating an object with a given scattering matrix is solved. The scattering matrix describes the scattering by a single stationary target, it cannot be used to describe the scattering by a time varying or distributed target. The Stokes matrix should be used instead. The definition and some properties of this matrix are considered. ESA

N91-31497 Royal Netherlands Meteorological Inst., De Bilt. Physical Meteorology Dept.

COORDINATE CONVERSIONS FOR PRESENTING AND COMPOSITING WEATHER RADAR DATA

H. R. A. Wessels 1990 15 p

(KNMI-TR-129; ISSN-0169-1708; ETN-91-90008) Copyright Avail: Royal Netherlands Meteorological Inst., P.O. Box 201, 3730 AE De Bilt, Wilhelminalaan 10, Netherlands

The transformation of radar data to a polar stereographic grid is discussed. One of the reasons to choose this projection was its acceptance as a standard for the COST-73 composite radar products. Special attention is given to the errors involved in certain approximations. In the appendices acccurate computing schemes are given for the two so called principal problems of geodesy: computing the coordinates of a target with given range and azimuth, and the inverse problem: the computation of azimuth and distance of a given target. ESA

N91-31498# Loughborough Univ. of Technology (England). Dept. of Electrical and Electronic Engineering.

AIRBORNE ESM RECEIVERS: TECHNIQUES AND TECHNOLOGIES M.S. Thesis

P. R. Mercer 1989 242 p

(ETN-91-99988) Copyright Avail: NTIS HC/MF A11

The techniques and technologies used in airborne Electric Support Measures (ESM) receivers designed for operation at microwave frequencies are explained. Detailed descriptions of ESM antennas and receivers are given. Potential antenna-receiver combinations are considered. Significant areas having an impact on future designs are reviewed: extension to millimeter wave operation, the use of artificial intelligence techniques in processors and the move towards integrated defensive aids suites. ESA

N91-31499*# Stanford Telecommunications, Inc., Reston, VA.

THE DATA DISTRIBUTION SATELLITE SYSTEM Final Report

Ronald C. Bruno and Aaron Weinberg Sep. 1991 122 p

(Contract NAS3-25091)

(NASA-CR-187172; NAS 1.26:187172) Avail: NTIS HC/MF A06 CSCL 17B

The Data Distributed Satellite (DDS) will be capable of providing the space research community with inexpensive and easy access to space payloads and space data. Furthermore, the DDS is shown to be a natural outgrowth of advances and evolution in both NASA's Space Network and commercial satellite communications. The roadmap and timescale for this evolution is described along with key demonstrations, proof-of-concept models, and required technology development that will support the projected system evolution toward the DDS. Author

N91-31500# Sandia National Labs., Albuquerque, NM.

ELECTROMAGNETIC PENETRATION OF SLOT APERTURES WITH DEPTH AND LOSSES

L. K. Warne and K. C. Chen 1991 4 p Presented at the 1991 International Conference on Electromagnetics in Aerospace Applications (ICEAA), Torino (Italy), 17-20 Sep. 1991

(Contract DE-AC04-76DP-00789)

(DE91-016401; SAND-91-1737C; CONF-9109228-1) Avail: NTIS HC/MF A01

Typical aerospace joints lead to apertures which are very narrow and thick. We develop a systematic analytical treatment of this type of aperture (precise conditions of validity given in the text), although the results are also applicable to apertures on a thin conducting body. An antenna integral equation with an equivalent antenna radius is used to describe the voltage across a narrow and thick aperture in a perfectly conducting plane. The result shows the voltage across the aperture has very high Q (quality-factor) resonances, because the equivalent radius is exponentially small. Transmitted power also exhibits similar behavior. When metallic and gasket losses are included, a nonlocal antenna model together with a local transmission line model is used to describe the voltage across the aperture. Good metallic walls, such as aluminum, are found to significantly reduce the penetration of an aperture of typical dimensions. Gaskets with relatively small loss tangents also result in significant penetration reductions. A simple transmission line with uniform loading is used to approximate the governing equation. In the lossless limit and for moderate fatness parameter this simple transmission line model is comparable in accuracy to King's three-term theory. The loading of the bolts or hinges is demonstrated to act in many cases as a short. Finally, the low frequency penetration for a narrow slot aperture of arbitrary depth is characterized by the equivalent polarizabilities (dominating longitudinal component) as a function of the ratio of the depth to the width and ratio of the length to the width. A general relationship is shown to exist between the equivalent radius and the transverse line dipole moments of a slot aperture with depth. The longitudinal equivalent polarizabilities of antennas and slot apertures are used to derive a coupling energy bound for a step function EMP. DOE

N91-31501# Naval Research Lab., Washington, DC.

THEORY AND APPLICATION OF THE WAVELET TRANSFORM TO SIGNAL PROCESSING Report, for May - Oct. 1990

David M. Drumheller 31 Jul. 1991 49 p

(AD-A239533; NRL-9316; ONT-90-165) Avail: NTIS HC/MF A03 CSCL 12/1

Recently, a new representation of square summable functions has been found that displays some sense of locality in time. Its continuous version is called the wavelet transform, and discrete version is called the wavelet expansion. This report presents several theoretical and practical aspects of these new representations in the context of signal theory and a signal processing. On the theoretical level, some new results are proved regarding the properties of wavelets. The work of others has also been extended. Two practical applications of the wavelet expansion are also presented. The first is the equivalent to passband filtering of analog signals, and the second is the derivation of an iterative restoration algorithm used to estimate the impulse response of a linear system. Author (GRA)

N91-31502# Naval Research Lab., Washington, DC.

INTEGRATION LOSSES AND CLUTTER-DOPPLER SPREAD FOR A SPACE BASED RADAR CAUSED BY IONOSPHERIC SCINTILLATION DURING A SOLAR MAXIMUM Final Report

Eric L. Mokole 31 Jul. 1991 14 p

(AD-A239534; NRL-9343) Avail: NTIS HC/MF A03 CSCL 17/9

Estimates are obtained of the effect of worst-case, ionospheric scintillation on the combined, coherent-noncoherent, integration process and on the clutter-Doppler spread for a specific waveform and a space based radar in a 1030-km orbit. The experiments are representative of worst-case scintillation conditions. The results of these data, which correspond to a period of solar maximum, are compared to earlier results for a period of severe scintillation but minimal solar activity. The frequency-diverse waveform consists of bursts (coherent pulse trains) of 0.256-s duration at four distinct frequencies per look and six looks per dwell. The space based radar will suffer a combined integration loss not exceeding 2.54

dB, 0.70 dB, and 0.06 dB at VHF, UHF, and L band, respectively, for 95 percent of the time in worst-case conditions. In addition, the clutter Doppler spread that is induced by ionospheric scintillation is less than 4.90 Hz, 1.58 Hz, and 0.26 Hz at the same frequencies and under the same conditions as for 95 percent of the time. GRA

N91-31503# Range Commanders Council, White Sands Missile Range, NM. Frequency Management Group.
FLIGHT TEST DIGITIZED/COMPRESSED VIDEO SPECTRUM ALLOCATION
Aug. 1991 4 p
(AD-A239535; RCC/FMG-702-91) Avail: NTIS HC/MF A01 CSCL 14/3

A common, recommended frequency band is identified for the operation of range flight test digitized/compressed video systems. In the early 1980s, the National Security Agency (NSA) recommended that all test range communications transmissions be secured. At the time, all range flight test video transmissions were made using nonencrypted conventional analog video systems. To use standard NSA encryptors, it became necessary to digitize and compress these analog video signals. By the late 1980s, it became obvious that a standard digitized/compressed video system, operating in a common portion of the frequency spectrum, needed to be developed. This task was initiated to determine the common frequency spectrum to be used by this digitized/compressed video system. GRA

N91-31504# Massachusetts Inst. of Tech., Cambridge.
TIME DOMAIN ELECTROMAGNETIC WAVES IN MULTILAYERED MEDIA Final Report, 1 May 1988 - 30 Apr. 1991
J. A. Kong 15 Jul. 1991 40 p
(Contract DAAL03-88-K-0057)
(AD-A239545; ARO-25089.12-EL) Avail: NTIS HC/MF A03 CSCL 20/14

The time domain response was studied of electromagnetic wave radiation, transmission and coupling in multilayered media. The following problems are pursued: (1) extensions and modifications to the double deformation technique; (2) propagation in nonconventional transmission structures; (3) signal distortion at discontinuities; (4) the effects of anisotropic material and nonlinear loads; and (5) limitation of quasi-TEM approximation. A powerful transform-domain formulation is emphasized and refined, (the double deformation technique) in order to have a unified way of interpreting the results. Yet other techniques such as the space-time domain integral equation method, the transmission line matrix method, the method of characteristics, and the method of moments are also to be applied to different problems as demanded by efficiency or ease of formulation. The research results can be applied to computer aided design of high speed microelectronic integrated circuits, as well as to time-domain geophysics sub-surface probing, and active remote sensing with transient radar pulses. GRA

N91-31505# Colsa, Inc., Huntsville, AL.
HYBRID ELECTRO-OPTIC PROCESSOR Final Report, Sep. 1988 - Sep. 1989
Stephen T. Welstead and Michel J. Ward Jul. 1991 45 p
(Contract F30602-88-D-0027)
(AD-A239547; RL-TR-91-164) Avail: NTIS HC/MF A03 CSCL 09/5

This report describes the design of a hybrid electro-optic processor to perform adaptive interference cancellation in radar systems. The processor is designed to process wideband interference signals as well as multipath copies of these signals. The optical components in the processor include acousto-optic cells used as delay lines, a charge coupled device linear detector array, and a transmissive liquid crystal display spatial light modulator. The spatial light modulator is driven by an electronic microprocessor. A new way of achieving improved dynamic range for such a spatial light modulator is reported. Included in this report is a discussion of the design, partial fabrication in the laboratory, and partial testing of the hybrid electro-optic processor. A follow on effort is planned to complete the construction and testing of the processor. The work described in this report is the combined effort of RADC in-house project 4600P103 and Contract F30602-88-D-0027. Author (GRA)

N91-31506# General Accounting Office, Washington, DC. National Security and International Affairs Div.
ELECTRONIC WARFARE: FAULTY TEST EQUIPMENT IMPAIRS NAVY READINESS
Jun. 1991 27 p
(AD-A239562; GAO/NSIAD-91-205) Avail: NTIS HC/MF A03 CSCL 17/4

The Navy equips its tactical aircraft with electronic warfare systems, such as radar warning receivers and jammers, to protect them from hostile weapons. The radar warning receiver alerts the pilot that the aircraft is being tracked by a hostile radar, and the jammer transmits electronic signals to deceive or otherwise interfere with the radar. The Navy believes that these systems are important for the aircraft to be able to accomplish their mission and survive in a wartime environment. Therefore, ensuring that these systems are maintained and operating properly is critical to accomplishing the Navy's mission. GRA

N91-31507# Range Commanders Council, White Sands Missile Range, NM.
SPECTRUM MONITORING PROCEDURES AND TECHNIQUES
Jul. 1990 439 p
(AD-A239567; RCC-701-90) Avail: NTIS HC/MF A19 CSCL 20/14

The first step towards operating an emitter on a test range is to contact the local frequency manager to establish a schedule. Since restricted radio frequency bands and operations are different at each test range location, most testing is accomplished by sharing the spectrum available with all range users. The telemetry bands in particular require spectrum activity scheduling. The objective is to resolve scheduling conflicts prior to operations. When two programs or projects request to use the same spectrum, their activity can be separated by quard bands, discrete frequencies, time, or operating locations (terrain masking). Priorities assigned to each program usually dictate which program will be scheduled first; however, use of priorities to schedule activities should be avoided and only considered as a last resort. When a scheduling conflict cannot be resolved using these techniques, it is brought to the attention of the responsible program managers. When scheduling activities involve other federal or nonfederal agencies, it is in the best interest of program managers to be as flexible as possible. GRA

N91-31508# Naval Research Lab., Washington, DC.
PERFORMANCE OF AN ANGLE-OF-ARRIVAL ESTIMATOR IN THE PRESENCE OF A MAINBEAM INTERFERENCE SOURCE
Feng-Ling C. Lin and Frank F. Kretschmer, Jr. 12 Aug. 1991 16 p
(AD-A239629; NRL-9345) Avail: NTIS HC/MF A03 CSCL 17/3

Mainbeam interferences present a serious target tracking problem for array antennas. A technique is studied that is capable of providing information on target angle of arrival when a single interference source enters the antenna mainbeam. In-depth evaluation of the technique shows that its performance in angle estimation accuracy is comparable with that obtained by other more sophisticated methods, yet its implementation is relatively simple. The resultant angular estimation errors are quite close to the theoretical Cramer-Rao bounds previously derived. GRA

N91-31509# Ohio State Univ., Columbus.
ADAPTIVE ARRAYS IN PACKET RADIO NETWORKS Final Report, 1 Mar. 1989 - 3 Aug. 1990
R. T. Compton 31 Jul. 1991 5 p
(Contract DAAL03-89-K-0073)
(AD-A239636; ARO-26274.1-EL) Avail: NTIS HC/MF A01 CSCL 25/2

This research considered the use of adaptive antennas in packet radio networks (PRNs). By using an adaptive array at a packet radio terminal, the receiving pattern of a terminal can change in response to each received packet. For example, in a slotted system, a terminal with an adaptive array can receive one or more packets correctly in a slot even when the slot contains colliding packets, because the array automatically nulls the colliding packets. The performance was first studied of a single packet radio terminal using a multibeam adaptive array. The throughput-delay performance of the packet terminal was evaluated for both slotted and unslotted channels. In addition, the throughput delay performance was also studied of a small slotted network that uses a single beam adaptive array at each terminal. GRA

N91-31510# Naval Ocean Systems Center, San Diego, CA.
ARCTIC VLF/LF DATA ACQUISITION Final Report, Aug. 1987 - Dec. 1990
T. Hepner and J. E. Bickel Feb. 1991 96 p
(AD-A239704; NOSC/TD-2052) Avail: NTIS HC/MF A05
CSCL 20/14

This report describes VLF/LF signal data recorded in the Arctic at fixed sites in Fairbanks, Alaska, and Thule, Greenland; on the icebreakers Polarbjorn and USCGC Northwind; and on P-3 aircraft. The various recording sites and platforms, recording equipment and data types are described, as are the methods used to calibrate the recorded data to absolute field intensity. Problems encountered during data collection, data editing, and radiated power measurements are also discussed. Near-field radiated power measurements and the overall accuracy of the VLF/LF data collected are also discussed. The observational data recorded and discussed are to be used in verifying or modifying theoretical propagation prediction models used to determine communication coverage. GRA

33 ELECTRONICS AND ELECTRICAL ENGINEERING

Includes test equipment and maintainability; components, e.g., tunnel diodes and transistors; microminiaturization; and integrated circuitry.

For related information see also *60 Computer Operations and Hardware* and *76 Solid-State Physics.*

N91-31511 Department of National Defence, Ottawa (Ontario).
HIGH SPEED DIGITAL DIRECT ACCESS FILTER FOR TRACKING OR EXCISION OF PARAMETRIC SIGNAL DATA Patent
James F. Mickeal, inventor 3 Jul. 1990 30 p
(Patent-1-271-231; Int-Patent-Class-G06F-702; CTN-91-60133)
Copyright Avail: Micromedia Ltd., Technical Information Centre, 165 Hotel de Ville, Place du Portage, Phase 2, Hull, Quebec J8X 3X2, Canada HC $4.00 CAN, MF $2.75 CAN

This invention relates to signal processing apparatus and particularly to a circuit for processing digital signal data for signal sources such as sensors in a radar system. Adaptive signal tracking and excision systems report their measurements in the form of parameter packets. Data within these signal packets represent a set of uniquely different measurements of the signal characteristics, such as frequency or amplitude. If signal parameters from a particular source do not change rapidly and are distinct from those of other sources, the signal can be filtered on the basis of the values of the detected parameters. The filtering process involves comparing the parameters of a packet with those of a predetermined set of data (a data window) where data may be rejected or forwarded for further processing. If the filtered data is sent to a signal processor, the processor can set the filter criteria based on some sort of adaptive criteria. In this invention, both the hardware and the comparison time are minimized by use of a directly accessed array of RAM memories. Speeds of 20 MHz are achieved. CISTI

N91-31512 Department of National Defence, Ottawa (Ontario).
FILTER SYSTEM FOR RADAR APPLICATIONS Patent
Robert J. Inkol, inventor 28 Aug. 1990 31 p
(Patent-1-273-409; Int-Patent-Class-G01S-7295; CTN-91-60134)
Copyright Avail: Micromedia Ltd., Technical Information Centre, 165 Hotel de Ville, Place du Portage, Phase 2, Hull, Quebec J8X 3X2, Canada HC $4.00 CAN, MF $2.75 CAN

Receivers in radar electronic support systems can receive considerable quantities of data. These signals typically include parameters such as time of arrival, amplitude, frequency, angle of arrival, and pulse width, which can be associated with a discrete emitter. This invention relates to a filter system for radar applications which permits observed data measurements for a multiplicity of radar emitters to be deinterleaved and stored in a buffer memory organized to allow data corresponding to any one of the radar emitters to be efficiently accessed for further analysis. The filter processes data at a very high speed so as to reduce overhead associated with the intercommunication function. CISTI

N91-31513 Department of National Defence, Ottawa (Ontario).
RECONFIGURABLE PARAMETER FILTER Patent
Robert J. Inkol, inventor 27 Dec. 1989 11 p
(Patent-1-264-072; Int-Patent-Class-H03H-1702; CTN-91-60154)
Copyright Avail: Micromedia Ltd., Technical Information Centre, 165 Hotel de Ville, Place du Portage, Phase 2, Hull, Quebec J8X 3X2, Canada HC $4.00 CAN, MF $2.75 CAN

Filtering of radar signals consists of selecting signals for which the signal parameters (time and angle of arrival, pulse width, amplitude, and frequency) fall within preselected ranges. A technique is described whereby a single standardized integrated circuit module can be reconfigured to efficiently handle parameter data received as a binary number (BN). The module can process two low precision BN's separately or combine them as one high precision number. The filter is comprised of two sections, each of which can be supplied with a binary number. Each section contains upper and lower limit storage registers and upper and lower limit comparitors. The comparitors are coupled to an AND gate. The AND gate is enabled if the value of the signal lies within the range set in the registers. In addition, the system is equipped with a mode selecting circuit including an OR gate having as one input the output of the AND gate and as its other input a mode select signal. This circuit has a pair of AND gates, each having as one input the output of the upper and lower comparitors from one of the two sections described above and as the other input the mode selecting signal. The output of the AND gates is connected to the upper and lower limit comparitors from the other of the two sections. This arrangement enables the sections to operate independently or to be coupled to act as a unit. CISTI

N91-31514 Canadian Astronautics Ltd., Ottawa (Ontario).
COMPOSITE WAVEGUIDE COUPLING APERTURE HAVING A THICKNESS DIMENSION Patent
Peter J. Wood, inventor 12 Sep. 1989 48 p
(Patent-1-259-401; Int-Patent-Class-H01Q-1310; CTN-91-60161)
Copyright Avail: Micromedia Ltd., Technical Information Centre, 165 Hotel de Ville, Place du Portage, Phase 2, Hull, Quebec J8X 3X2, Canada HC $4.00 CAN, MF $2.75 CAN

The present invention relates to antennas in general, and to planar waveguide fed slot-antenna arrays suitable for terrain mapping side looking radar airborne antennas (SLAR) in particular. It provides a novel coupling aperture or slot which has a variable cross sectional area along the coupling path; thus, it has a significant dimension perpendicular to the slot plane. A new composite coupling aperture or slot having at least three significant dimensions is achieved. These dimensions are length, width and thickness. In its broadest aspect, the composite coupling aperture is characterized by having non-uniform cross sectional areas along its thickness dimension. In its narrowest aspect the cross sectional area changes abruptly between the opposite waveguide coupled ends of the aperture. This coupling aperture is designed for use with a side looking radar antenna which requires coupling between

two waveguides separated by a thin wall. It was devised to adjust the degree of coupling while accommodating the necessary mechanical restraints. CISTI

N91-31515 Department of National Defence, Ottawa (Ontario). Directorate Research and Development Air.
TECHNIQUES TO ASSESS THE STATE OF HEALTH OF SEALED LEAD ACID BATTERIES
G. Verville, P. Roberge, and J. Smit (Ottawa Univ., Ontario) 1988 42 p Presented at the 16th International Power Sources Symposium, Bournemouth, England, 26-29 Sep. 1988
(CTN-91-60214) Avail: NTIS HC A03

Internal defects and short-circuit formation are causes of failure in aircraft batteries. Non-destructive investigation techniques which are sensitive to the internal design must be employed to detect these defects. Three techniques, cell impedance measurements, voltage noise measurements and video infrared thermography, are evaluated for this purpose. Thermography was found to be a very cost effective tool. It can be used to detect manufacturing defects when time is of the essence and is helpful in the interpretation of data collected by existing techniques. The use of ac impedance measurements at 1 kHz has been well received by battery shop personnel and has been used to complement the standard voltage measurements in providing advanced warning of potential problems. However, impedance measurements are sensitive to any change in cell design parameters introduced by manufacturers and therefore must be correlated with a specific cell design if they are to be used as a pass/fail criterion. The noise measurement technique appears to be a promising new tool in the interpretation of cell behavior. CISTI

N91-31516 New Hampshire Univ., Durham.
THE ANALYSIS AND DESIGN OF BRUSHLESS DC MOTORS Ph.D. Thesis
Steven Ronald Prina 1990 493 p
Avail: Univ. Microfilms Order No. DA9119143

This work is concerned with the magnetic analysis of brushless DC motors, and with the development of a method of designing brushless DC motors which have symmetric windings and rotors without any iron saliency. A 2-D nonlinear finite element magnetic model is used to analyze the magnetic behavior of the motor. Methods of using the finite element solution(s) to predict motor characteristic performance parameters, such as the torque-angle curve, detent torque-angle curve, torque constant, back electromotive force constant, and inductance are discussed in detail. It is shown that 3-D effects can make significant contributions to the motor inductance, making inductance prediction difficult. It is also shown that the prediction of detent torque can be extremely sensitive to the permanent magnet model. A simple means of understanding the effects of rotor magnet arc width and winding distribution on the stator torque-angle curve shape is presented. In addition, methods of reducing detent torque by altering magnet arc width are discussed. Finally, simple lumped models that allow one to predict motor performance characteristics as a function of important dimensions, magnet residual flux density, and phase current are developed and checked against finite element results. These models are used as a basis for an approach to designing brushless DC motors. Dissert. Abstr.

N91-31517# Sandia National Labs., Albuquerque, NM.
ACCELERATED AGING AND DISCHARGE OF LITHIUM/THIONYL-CHLORIDE D CELLS
W. R. Cieslak 1991 2 p Presented at the 180th Meeting of the Electrochemical Society, Phoenix, AZ, 13-18 Oct. 1991
(Contract DE-AC04-76DP-00789)
(DE91-012649; SAND-91-1157C; CONF-911047-1) Avail: NTIS HC/MF A01

Lithium/Thionyl-Chloride spiral wound 'D' cells from a variety of suppliers have been evaluated. Abuse testing has been used to verify safety of the cells, and accelerated aging has been used to estimate their performance for long life projects. DOE

N91-31518# Sandia National Labs., Albuquerque, NM.
ELECTROPHORETIC DIELECTRIC COATINGS FOR MAGNETIC SWITCHES
H. C. Harjes, G. A. Mann, and D. J. Sharp 1991 4 p Presented at the 8th IEEE Pulsed Power Conference, San Diego, CA, 17-19 Jun. 1991
(Contract DE-AC04-76DP-00789)
(DE91-015337; SAND-91-0177C; CONF-910640-28) Avail: NTIS HC/MF A01

In high magnetization rate magnetic switches, the insulation requirements are severe and in high average power applications the thermal management of core losses is a serious design issue. We have been investigating the possibility of using electrophoretic (EP) coating techniques to provide a viable alternative to dielectric films for insulation in such switches. The EP process is analogous to electroplating and as such offers advantages over other coating techniques including: excellent edge coverage, thicker coatings in areas of higher electric field stress, and the possibility of detecting and repairing any coating flaws or weak points in a secondary processing step. A continuous foil EP coating machine which is capable of coating Metglas at a rate of several feet/minute with a 2-24 micron thick methyl methacrylate coating has been constructed. In order to determine the dielectric strength of the coating in a wound geometry, capacitors have been wound with coated Metglas conductors and DC breakdown distributions have been obtained. Mean breakdown strengths in excess of 1 MV/cm have been observed. Experiments to demonstrate the effect of the second coating step on the breakdown distributions have also been conducted. In addition, the magnetic properties of small scale coated magnetic switch cores have been measured. Experiments have also been conducted on coated material at elevated temperatures. The results of these experiments will be presented. DOE

N91-31519# Argonne National Lab., IL.
DEVELOPMENT OF PROTOTYPE SEALED BIPOLAR LITHIUM/SULFIDE CELLS
T. D. Kaun, M. J. Duoba, W. P. Johll, V. Luong, F. C. Mrazek, D. J. Palkon, and D. R. Simon 1991 7 p Presented at the 26th Intersociety Energy Conversion Engineering (IECE) Conference, Boston, MA, 3-9 Aug. 1991
(Contract W-31-109-eng-38)
(DE91-015721; ANL/CP-73352; CONF-910801-13) Avail: NTIS HC/MF A02

Development of a prototype bipolar battery containing 13-cm dia cells for electric-vehicle propulsion is underway at Argonne National Laboratory (ANL). Both Li/FeS and Li/FeS2 cells have been tested with LiCl-LiBr-KBr electrolyte and MgO powder separators for electrolyte-starved cell operation at 400 to 425 C. These cells achieved the high performance and stability needed for the intended application. An innovative feature of this bipolar battery is a metal/ceramic bonded peripheral seal for each cell. The development of corrosion-resistant sealant materials at ANL has let to metal/ceramic bonds about 100 times stronger that obtainable with commercially available sealants for service at over 300 C. This peripheral seal promotes long battery life by eliminating electrolyte loss and prohibiting transport of electrolyte from one cell to the next in a bipolar stack. Fabrication facilities have been recently constructed that enable development of 13-cm I.D. peripheral seals. The initial tests of prototype bipolar Li/FeS and Li/FeS2 cells indicate improved performance as a result of scale-up. The 7-mm thick, 13-cm dia cells have total weight of 0.25 kg (cell density 2.8 g/cu cm). These cells are operated at 425 C. The Li/FeS2 cell exhibits 180 Wh/kg at a 30 W/kg discharge rate and the Li/FeS cell delivered 130 Wh/kg at a 25 W/kg rate. The low internal impedance of these cells enables high peak specific power capability; 400 W/kg for Li/FeS2 and 24 W/kg for Li/FeS at 80 percent DOD. DOE

N91-31520# Lawrence Livermore National Lab., CA.
INTERNATIONAL MAGNETIC PULSE COMPRESSION
H. C. Kirbie, M. A. Newton, and P. D. Siemens Apr. 1991 60 p Presented at the International Workshop on Magnetic Pulse

Compression, Lake Tahoe, CA, 12-14 Feb. 1990
(Contracts W-7405-eng-48; DE-AC04-76DP-00789)
(DE91-015774; CONF-900280-Vol-1) Avail: NTIS HC/MF A04

Although pulsed-power engineering traditionally has been practiced by a fairly small, close community in the areas of defense and energy research, it is becoming more common in high-power, high-energy commercial pursuits such as material processing and lasers. This paper is a synopsis of the Feb. 12-14, 1990 workshop on magnetic switching as it applies primarily to pulse compression (power transformation). During the course of the Workshop at Granlibakken, a great deal of information was amassed and a keen insight into both the problems and opportunities as to the use of this switching approach was developed. The segmented workshop format proved ideal for identifying key aspects affecting optimum performance in a variety of applications. Individual groups of experts addressed network and system modeling, magnetic materials, power conditioning, core cooling and dielectrics, and finally circuits and application. At the end, they came together to consolidate their input and formulate the workshop's conclusions, identifying roadblocks or suggesting research projects, particularly as they apply to magnetic switching's trump card - its high-average-power-handling capability (at least on a burst-mode basis). The workshop was especially productive both in the quality and quantity of information transfer in an environment conducive to a free and open exchange of ideas. We will not delve into the organization proper of this meeting, rather we wish to commend to the interested reader this volume, which provides the definitive and most up-to-date compilation on the subject of magnetic pulse compression from underlying principles to current state of the art as well as the prognosis for the future of magnetic pulse compression as a consensus of the workshop's organizers and participants. DOE

N91-31521# Lawrence Livermore National Lab., CA.
PROCEEDINGS OF THE INTERNATIONAL MAGNETIC PULSE COMPRESSION WORKSHOP. VOLUME 2: TECHNICAL SUMMARY
H. C. Kirbie, M. A. Newton, and P. D. Siemens Apr. 1991 331 p Workshop held in Lake Tahoe, CA, 12-14 Feb. 1990
(Contracts W-7405-eng-48; DE-AC04-76DP-00789)
(DE91-015775; CONF-900280-Vol-2) Avail: NTIS HC/MF A15

A few individuals have tried to broaden the understanding of specific and salient pulsed-power topics. One such attempt is this documentation of a workshop on magnetic switching as it applies primarily to pulse compression (power transformation), affording a truly international perspective by its participants under the initiative and leadership of Hugh Kirbie and Mark Newton of the Lawrence Livermore National Laboratory (LLNL) and supported by other interested organizations. During the course of the Workshop at Granlibakken, a great deal of information was amassed and a keen insight into both the problems and opportunities as to the use of this switching approach was developed. The segmented workshop format proved ideal for identifying key aspects affecting optimum performance in a variety of applications. Individual groups of experts addressed network and system modeling, magnetic materials, power conditioning, core cooling and dielectrics, and finally circuits and application. At the end, they came together to consolidate their input and formulate the workshop's conclusions, identifying roadblocks or suggesting research projects, particularly as they apply to magnetic switching's trump card--its high average power handling capability (at least on a burst-mode basis). The workshop was especially productive both in the quality and quantity of information transfer in an environment conducive to a free and open exchange of ideas. We will not delve into the organization proper of this meeting, rather we wish to commend to the interested reader this volume, which provides the definitive and most up-to-date compilation on the subject of magnetic pulse compression from underlying principles to current state of the art as well as the prognosis for the future of magnetic pulse compression as a consensus of the workshop's organizers and participants. DOE

N91-31522# Sandia National Labs., Albuquerque, NM.
TECHNOLOGY ASSESSMENT OF AMBIENT TEMPERATURE RECHARGEABLE LITHIUM BATTERIES FOR ELECTRIC VEHICLE APPLICATIONS
N. Doddapaneni Jul. 1991 57 p
(Contract DE-AC04-76DP-00789)
(DE91-016500; SAND-91-0938) Avail: NTIS HC/MF A04

This report presents an assessment of ambient temperature rechargeable lithium batteries for electric vehicle applications. It was prepared for the Department of Energy, Office of Propulsion Systems. The status of development programs in industry and research laboratories was determined for several positive and negative electrode materials and for organic liquid and solid polymer electrolytes. Recommendations are suggested for future research and development activities. DOE

N91-31523# Sandia National Labs., Albuquerque, NM.
NUMERICAL SIMULATION OF A SPLIT CAVITY OSCILLATOR AND RF CONVERSION
R. W. Lemke Jul. 1991 23 p
(Contract DE-AC04-76DP-00789)
(DE91-016501; SAND-91-1220) Avail: NTIS HC/MF A03

We have conducted an extensive investigation of the split cavity oscillator (SCO) using particle-in-cell simulation. The goal of this work is to test and optimize an inverse diode rf convertor for use with a cylindrical SCO, while simultaneously determining factors that control rf extraction efficiency. We present results from simulations of several configurations including the SCO with inverse diode extractor, the SCO in conjunction with post-acceleration and inverse diode extraction, and the SCO, using electron beams with a variety of currents, voltages, and radii. DOE

N91-31524# Laboratoire d'Automatique et d'Analyse des Systemes, Toulouse (France).
ON THE STABILITY OF SATURATED STATE FEEDBACK REGULATORS Ph.D. Thesis - Toulouse Univ.
Sophie Tarbouriech 1991 242 p In FRENCH; ENGLISH summary
(LAAS-91047; ETN-91-99748) Avail: NTIS HC/MF A11

The stability of saturated state feedback regulators obtained from dynamical linear systems is discussed. A state feedback guaranteeing the global asymptotic stability of a standard regulator in a critically or asymptotically stable open loop system is determined. The notion of a norm or a Lyapunov function contracting along the trajectories of a system is used. The cases of one constrained control and of multiple constrained controls in a critically stable open loop system are studied. Dynamics of saturated regulator and open loop systems are compared. The results are used to obtain saturated locally and globally asymptotically stable regulators. ESA

N91-31525# Ecole Centrale de Lyon (France). Lab. d'Electronique, d'Automatique et de Mesures Electriques.
A THREE-DIMENSIONAL CODE TO SOLVE THE POISSON EQUATION: NUMERICAL SIMULATION OF THE BREAKDOWN IN P-N JUNCTION DEVICES Ph.D. Thesis
Rabea Menezla 1990 145 p In FRENCH; ENGLISH summary
(ECL-90-27; ETN-91-99920) Avail: NTIS HC/MF A07

A three dimensional code to determine the potential distribution and the breakdown voltage in planar semiconductor devices, which solves the Poisson equation and computes the ionization integrals, is developed. The spherical and cylindrical avalanche breakdown due to the junction curvature in the planar P-N junctions are particularly considered. The breakdown voltages obtained by simulation are consistent with experimental results. ESA

N91-31526# Ecole Centrale de Lyon (France).
CONTRIBUTION TO THE IMPLEMENTATION OF A COMPLETELY IN SITU DEVICE IN ULTRAHIGH VACUUM FOR THE DEVELOPMENT OF MIS ON InP STRUCTURES: Al2O3/InP INTERFACE OPTIMIZATION Ph.D. Thesis [CONTRIBUTION A LA MISE AU POINT D'UNE FILIERE TOUT IN SITU EN ULTRA-VIDE, POUR L'ELABORATION DE STRUCTURES MIS SUR INP: OPTIMISATION DE L'INTERFACE AL2O3/INP]
Claude Santinelli 1991 178 p In FRENCH
(ECL-91-04; ETN-91-99922) Avail: NTIS HC/MF A09

A study contributing to the development of an in situ device for developing MIS Al203/InP structures is presented. The basic idea was to use ultrahigh vacuum technologies to try to control the MIS structure realization, step by step, and in particular the crucial steps of surface preparation and dielectric deposition. Results relating to the dielectric optimization are described. The InP surface preparation, previous to the deposition of the insulating layer, is described. Results obtained using techniques of electric (C(V)), structural (RHEED) and chemical (Auger, XPS) characterization are given throughout. ESA

N91-31527# Ecole Centrale de Lyon (France). Lab. d'Electronique, d'Automatique et de Mesures Electriques.
DESIGN OF A SPECIFIC INTEGRATED CIRCUIT FOR SOLVING THE THREE DIMENSIONAL POISSON EQUATION Ph.D. Thesis [CONCEPTION D'UN CIRCUIT INTEGRE SPECIFIQUE POUR LA RESOLUTION DE L'EQUATION DE POISSON A 3 DIMENSIONS]
Philippe Pagano 1990 134 p In FRENCH Original contains color illustrations
(ECL-90-24; ETN-91-99923) Avail: NTIS HC/MF A07

Application Specific Integrated Ciruits (ASIC's) are used in digital simulation for solving the Poisson equation. An algorithm of the CLAC3D program, which is a three dimensional simulator to study potential distribution in semiconductor components, is used as a starting point. An MIMD architecture is chosen for the cabled computer. The speed gain of the cabled system over the software simulator is evaluated. The specific circuit structure, its integration in CMOS technology, and its programming are addressed. An automatic generation program of simulation stimuli or a test coupled with a behavioral model of the circuit is presented. ESA

N91-31528* National Aeronautics and Space Administration. Pasadena Office, CA.
A UNIVERSAL COMPUTER CONTROL SYSTEM FOR MOTORS Patent
Zoltan F. Szakaly, inventor (to NASA) 10 Sep. 1991 17 p Filed 23 Mar. 1988 Supersedes N88-24864 (26 - 18, p 2506)
(NASA-Case-NPO-17134-1-CU; US-Patent-5,047,700;
US-Patent-Appl-SN-172105; US-Patent-Class-318-568.1;
US-Patent-Class-318-568.2; US-Patent-Class-318-573;
US-Patent-Class-364-513; US-Patent-Class-901-19;
Int-Patent-Class-G05B-19/42) Avail: US Patent and Trademark Office CSCL 09A

A control system for a multi-motor system such as a space telerobot, having a remote computational node and a local computational node interconnected with one another by a high speed data link is described. A Universal Computer Control System (UCCS) for the telerobot is located at each node. Each node is provided with a multibus computer system which is characterized by a plurality of processors with all processors being connected to a common bus, and including at least one command processor. The command processor communicates over the bus with a plurality of joint controller cards. A plurality of direct current torque motors, of the type used in telerobot joints and telerobot hand-held controllers, are connected to the controller cards and responds to digital control signals from the command processor. Essential motor operating parameters are sensed by analog sensing circuits and the sensed analog signals are converted to digital signals for storage at the controller cards where such signals can be read during an address read/write cycle of the command processing processor.
Official Gazette of the U.S. Patent and Trademark Office

N91-31529* National Aeronautics and Space Administration. Lewis Research Center, Cleveland, OH.
LOW COST, FORMABLE, HIGH T(SUB c) SUPERCONDUCTING WIRE Patent
James L. Smialek, inventor (to NASA) 17 Sep. 1991 5 p Filed 31 Jan. 1989
(NASA-Case-LEW-14676-1; US-Patent-5,049,539;
US-Patent-Appl-SN-305675; US-Patent-Class-505-1;
US-Patent-Class-505-701; US-Patent-Class-505-702;
US-Patent-Class-505-703; US-Patent-Class-505-704;
US-Patent-Class-421-209; US-Patent-Class-421-457) Avail: US Patent and Trademark Office CSCL 09A

A ceramic superconductivity part such as a wire is produced through the partial oxidation of a specially formulated copper alloy in the core. The alloys contain low level quantities of rare earth and alkaline earth dopant elements. Upon oxidation at high temperature, superconducting oxide phases are formed as a thin film. Official Gazette of the U.S. Patent and Trademark Office

N91-31530* National Aeronautics and Space Administration. Goddard Space Flight Center, Greenbelt, MD.
EMERGENCY LOCATING TRANSMITTER Patent
Paul E. Wren, inventor (to NASA) 7 May 1991 12 p Filed 9 Sep. 1988 Division of US-Patent-Appl-SN-921576, filed 21 Oct. 1986
(NASA-Case-GSC-12821-2; US-Patent-5,014,340;
US-Patent-Appl-SN-242254; US-Patent-Appl-SN-921576;
US-Patent-Class-455-1; US-Patent-Class-455-99;
US-Patent-Class-455-102; Int-Patent-Class-H04K-3/00) Avail: US Patent and Trademark Office CSCL 09A

A transmitter generates three signals for sequential transmission. These signal are an unmodulated r.f. carrier, a r.f. carrier amplitude modulated by a first audio frequency waveform and a r.f. carrier amplitude modulated by a second audio frequency waveform which is distinguishable from the first and which may be employed as a means for identifying a particular transmitter. The composite, sequentially transmitted signal may be varied in terms of the individual signal transmission sequence, the duration of the individual signals, overall composite signal repetition rate and the frequency of the second audio waveform. Various combinations of signal variations may be employed to transmit different information.
Official Gazette of the U.S. Patent and Trademark Office

N91-31531*# National Aeronautics and Space Administration. Langley Research Center, Hampton, VA.
A CASE STUDY FOR THE REAL-TIME EXPERIMENTAL EVALUATION OF THE VIPER MICROPROCESSOR
Victor A. Carreno and Rob K. Angellatta (Lockheed Engineering and Sciences Co., Hampton, VA.) Sep. 1991 45 p
(NASA-TM-104098; NAS 1.15:104098) Avail: NTIS HC/MF A03 CSCL 09A

An experiment to evaluate the applicability of the Verifiable Integrated Processor for Enhanced Reliability (VIPER) microprocessor to real time control is described. The VIPER microprocessor was invented by the Royal Signals and Radar Establishment (RSRE), U.K., and is an example of the use of formal mathematical methods for developing electronic digital systems with a high degree of assurance on the system design and implementation correctness. The experiment consisted of selecting a control law, writing the control law algorithm for the VIPER processor, and providing real time, dynamic inputs into the processor and monitoring the outputs. The control law selected and coded for the VIPER processor was the yaw damper function of an automatic landing program for a 737 aircraft. The mechanisms for interfacing the VIPER Single Board Computer to the VAX host are described. Results include run time experiences, performance evaluation, and comparison of VIPER and FORTRAN yaw damper algorithm output for accuracy estimation. Author

N91-31532# Oak Ridge National Lab., TN.
EFFECTIVE IONIZATION COEFFICIENTS, ELECTRON DRIFT VELOCITIES, AND LIMITING BREAKDOWN FIELDS FOR GAS MIXTURES OF POSSIBLE INTEREST TO PARTICLE DETECTORS
P. G. Datskos (Tennessee Univ., Knoxville.), L. G. Christophorou, and J. G. Carter 1991 8 p Presented at the Electrical Insulation and Dielectric Phenomena Conference, Knoxville, TN, 20-24 Oct. 1991
(Contract DE-AC05-84OR-21400)
(DE91-015921; CONF-911087-1) Avail: NTIS HC/MF A02

We have measured the gas-density, N, normalized effective ionization coefficient, bar-alpha/N, and the electron drift velocity, w, as a function of the density-reduced electric field, E/N, and obtained the limiting, (E/N)(sub lim), value of E/N for the unitary gases Ar, CO2, and CF4, the binary gas mixtures CO2:Ar (20:80), CO2:CH4 (20:80), and CF4:Ar (20:80), and the ternary gas mixtures CO2:CF4:Ar (10:10:80) and H2O:CF4:Ar (2:18:80). Addition of the strongly electron thermalizing gas CO2 or H2O to the binary mixture CF4:Ar (1)'cools' the mixture (i.e., lowers the electron energies), (2) has only a small effect on the magnitude of w(E/N) in the E/N range employed in the particle detectors, and (3) increases bar-alpha/N for E/N greater than or equal to 50 x 10(exp -17) V sq cm. The increase in bar-alpha/N, even though the electron energies are lower in the ternary mixture, is due to the Penning ionization of CO2 (or H2O) in collisions with excited Ar* atoms. The ternary mixtures - being fast, cool, and efficient - have potential for advanced gas-filled particle detectors such as those for the SCC muon chambers. DOE

N91-31533# Sandia National Labs., Albuquerque, NM.
THE DEVELOPMENT OF ALUMINUM-AIR BATTERIES FOR APPLICATION IN ELECTRIC VEHICLES
E. J. Rudd and S. Lott Dec. 1990 242 p Prepared in cooperation with Eltech Systems, Inc., Fairport Harbor, OH
(Contract DE-AC04-76DP-00789)
(DE91-016863; SAND-91-7066) Avail: NTIS HC/MF A11

The recently concluded program, jointly funded by ELTECH Research Corporation and the Department of Energy, focused upon the development of an aluminum-air battery system for electric vehicle applications. The operation of the aluminum-air battery involves the dissolution of aluminum to produce a current and aluminate. Initially the objectives were to evaluate and optimize the battery design that was developed prior to this program (designated as the B300 cell) and to design and evaluate the components of the auxiliary system. During the program, three additional tasks were undertaken, addressing needs identified by ELTECH and by Sandia National Laboratories. First, the capability to produce aluminum alloys as relatively large ingots (100 to 150 lbs), with the required electrochemical performance, was considered essential to the development of the battery. The second additional task was the adoption of an advanced cell (designated as the AT400 cell), designed by ELTECH in a different program. Finally, it was recognized that a system model would allow evaluation of the interactions of the several unit operations involved in the battery. Therefore, the development of a mathematical model, based upon material and energy balances for the battery, was undertaken. At a systems level, sufficient information was obtained in the completion of this program to support the design, fabrication and operation of a batch or solids-free battery system. For the first time, the components of the auxiliary system, i.e., a heat exchanger, carbon dioxide scrubber and hydrogen disposal technology, have been defined for a vehicle battery. Progress on each component or system is summarized in the following sections. DOE

N91-31534# Air Force Inst. of Tech., Wright-Patterson AFB, OH.
HARDWARE MODELING AND TOP-DOWN DESIGN USING VHDL M.S. Thesis
Dennis P. Morton Jun. 1991 231 p
(AD-A239356; AFIT/CI/CIA-91-055) Avail: NTIS HC/MF A11 CSCL 12/5

As digital designs grow more and more complex, some method of controlling this complexity must be used in order to reduce the number of errors and the time spent on a design. VHDL(Very High Speed Integrated Circuit Hardware Description Language) promises to ease the design and verification of complex digital circuits by encouraging the use of top-down design. It is demonstrated how VHDL, combined with a top-down design methodology, enables the designer to specify and verify a digital design faster and with fewer errors. The scoreboard, a section of hardware in the Charles Stark Draper Laboratory's Fault Tolerant Parallel Processor, is used as an example to demonstrate the utility of VHDL. The scoreboard is responsible for message processing within the FTPP and thus has a critical effect on performance. It also represents the most significant risk of any component in the FTPP. The use of VHDL has the potential for ensuring an optimal scoreboard design with minimal errors and an improved design time. GRA

N91-31535# TRW Space Technology Labs., Redondo Beach, CA.
PHASED ARRAY COMPONENTS FOR THE HIGH TEMPERATURE SUPERCONDUCTING SPACE EXPERIMENT (HTSSE) Final Report
7 Jun. 1991 26 p
(Contract N00014-91-C-2057)
(AD-A239361) Avail: NTIS HC/MF A03 CSCL 09/1

A new class of X-band phase shifters using the distributed Josephson inductance (DJI) effect were delivered to NRL for the HTS Space Experiment project. Phase shifts were observed above 77 K, and large phase shifts were observed at 65 K and below. This narrow-band device was developed as a first step to a broadband device. A total of 40 HTS SQUIDs were successfully integrated into a monolithic circuit. Measurement of the temperature dependence of the Q of a resonator in June 1990 and in February 1991 showed no significant change due to aging. A total of seven X-band phase shifters were fabricated, and five were delivered to Naval Research Laboratory. The HTS phase shifter consists of a low loss YBa2Cu3O7 microstrip resonator with 40 SQUID devices monolithically imbedded into the transmission line. This narrow-band device was developed as a first step to a broadband device. GRA

N91-31536# Illinois Univ., Urbana-Champaign. Coordinated Science Lab.
JOINT SERVICES ELECTRONICS PROGRAM Annual Progress Report No. 2, 1 Apr. 1990 - 31 Mar. 1991
W. K. Jenkins 30 Jun. 1991 106 p
(Contract N00014-90-J-1270)
(AD-A239459) Avail: NTIS HC/MF A06 CSCL 09/1

This is the second annual progress report of the research conducted at the Coordinated Science Laboratory, University of Illinois at Urbana-Champaign, under the sponsorship of the Joint Services Electronics Program from 1 April 1990 through 31 March 1991. The research areas include: (1) Physical Electronics, (2) VLSI Circuits and Computer Systems, (3) Electronic Systems, and (4) Management Initiatives (discretionary Director's unit). This report summarizes the areas of research, identifies the most significant results, and lists the publications sponsored by JSEP as well as other sponsoring agencies. GRA

N91-31537# Naval Postgraduate School, Monterey, CA.
A METHODOLOGY FOR PRODUCING AND TESTING A GENESIL SILICON COMPILER DESIGNED VLSI CHIP WHICH INCORPORATES DESIGN FOR TESTABILITY M.S. Thesis
Brian L. Pooler Sep. 1990 168 p
(AD-A239465) Avail: NTIS HC/MF A08 CSCL 12/5

Testability issues concerning the need for including Design for Testability (DFT) techniques in VLSI (Very Large Scale Integration) designs are discussed. Types of fault models, the use of fault simulation and the DFT techniques of Scan Path and Built in Test are described. An engineering methodology that uses the Genesil Silicon Compiler to produce a VLSI design, DFT-CHIP, which utilizes the DFT Scan Path technique is presented. Included

are the procedures for using Genesil's simulation, timing analysis and automatic test generation features. The steps taken to fabricate the DFT-CHIP design through MOSIS are discussed. The methodology used to test the fabricated DFT-CHIP design on the Tektronix DAS 9100 tester is described. Appendix A and Appendix B provide copies of the Genesil check functions written for use during simulation on the DFT-CHIP design. Appendix C specifies the Genesil timing information for the DFT-CHIP design. Appendix D lists the conversion program which translates Genesil produced test vector files to the file format used during testing on the Tektronix tester. GRA

N91-31538# Colorado Univ., Boulder. Dept. of Electrical and Computer Engineering.
AN INVESTIGATION OF OPTICALLY CONTROLLED, INTEGRATED MILLIMETER WAVE RECEIVING PHASED ARRAYS Final Progress Report, Aug. 1988 - Jan. 1991
Alan R. Mickelson and David C. Chang Jan. 1991 5 p
Sponsored by ONR
(AD-A239504) Avail: NTIS HC/MF A01 CSCL 09/1

The principal objective of this project is to determine the most efficient means of encoding a microwave/millimeter wave signal from a patch antenna onto an optical carrier in an electro-optical substrate for subsequent optical processing of the microwave/millimeter wave signal. Our approach was to develop design models that would relate the performance of integrated electro-optic devices to the fabrication parameters used in making them and then experimentally verify their performance. Where lack of agreement was observed, the models were rethought and modified to improve their predictive behavior. Such performance characteristics included modal field distributions, propagation constants, coupling coefficients of channel waveguides and coupling lengths of proton exchanged directional couplers. This information was then used to design patch antennas and integrated optical modulators using various fabrication techniques and substrates. Similar design methods were used to determine the depth of modulation of electro-optic modulators. GRA

N91-31539# Naval Research Lab., Washington, DC.
CONVERGENCE PERFORMANCE OF ADAPTIVE DETECTORS, PART 1 Interim Report, 1 Oct. 1990 - 30 Sep. 1991
Karl Gerlach 30 Jul. 1991 23 p
(AD-A239507; NRL-9311-Pt-1) Avail: NTIS HC/MF A03 CSCL 12/1

Convergence results for a mean level adaptive detector (MLAD) are presented. The MLAD consists of an adaptive matched filter (for spatially correlated inputs) followed by a mean level detector (MLD). The optimal weights of the adaptive matched filter are estimated from one batch of ata and applied to a statistically independent batch of nonconcurrent data. The threshold of the MLD is determined from the resultant data. Thereafter, a candidate cell is compared against this threshold. Probabilities of false alarm and detection are derived as functions of the threshold factor, the order of the matched filter, the number of independent samples per channel used to calculate the adaptive matched filter weights, the number of samples used to set the MLD threshold, and the output signal-to-noise power ratio of the optimal matched filter. A number of performance curves are shown and discussed. GRA

N91-31540# Naval Research Lab., Washington, DC.
CONVERGENCE PERFORMANCE OF ADAPTIVE DETECTORS, PART 2 Interim Report
Karl Gerlach 7 Aug. 1991 28 p
(AD-A239532; NRL-9337) Avail: NTIS HC/MF A03 CSCL 12/1

Two schemes for adaptive detection are compared: Kelly's generalized likelihood ratio test (GLRT) and the mean level adaptive detector (MLAD). Detection performance P(D) is predicted for the two schemes under the assumptions that the input noises are zero-mean Gaussian random variables that are temporally independent but spatially correlated; and the desired signal is Rayleigh distributed. P(D) is computed as a function of the false alarm probability, the number of input channels, the number of independent samples-per-channel, and the matched filtered output signal-to-noise (S/N) power ratio. In this analysis, the GLRT is shown to have better detection performance than the MLAD. The difference in detection performance increases as one uses fewer input samples. However, the required number of samples necessary to have only a 3 dB detection loss for both detection schemes is approximately the same. This is significant since, for the present, the MLAD is considerably less complex to implement than the GLRT. GRA

N91-31541# Defence and Civil Inst. of Environmental Medicine, Downsview (Ontario).
METHODOLOGY FOR CALIBRATION AND USE OF HEAT FLUX TRANSDUCERS
Michel B. Ducharme and John Frim May 1991 57 p
(AD-A239552; DCIEM-91-45) Avail: NTIS HC/MF A04 CSCL 09/1

The direct assessment of heat flux from the body is a basic measurement in thermal physiology. Heat flux transducers (HFTs) are being used increasingly for that purpose under different environmental conditions. However, questions have been raised regarding the accuracy of the manufacturer's constant of calibration, and also about the effect of the thermal resistance of the device on the true thermal flux from the skin. Two different types of waterproofed HFTs were checked for their calibration using the Rapid-k thermal conductivity instrument. A detailed description of the methodology used during the calibration is given. A model capable of simulating a large range of tissue insulation was used to study the effect of the underlying tissue insulation on the relative error in thermal flux due to the thermal resistance of the HFTs. The data show that the deviation from the true value of thermal flux increases with the reciprocal of the underlying tissue insulation ($r = 0.99$, p less than 0.001). The underestimation of the heat flux through the skin measured by an HFT is minimal when the device is used on vasoconstricted skin in cool subjects (3 to 13 pct. error), but becomes important when used on warm vasodilated subjects (29 to 35 pct. error), and even more important on metallic skin mannequins (greater than 60 pct. error). In order to optimize the accuracy of the heat flux measurements by HFTs, it is important to recalibrate the HFTs and to correct the heat flux values for the thermal resistance of the HFT when used on vasodilated tissues. GRA

N91-31542# Pittsburgh Univ., PA. Learning Research and Development Center.
QUICK DEVELOPMENT MICROCOMPUTER SYSTEM: TRAINING AUTOMATIC COMPONENTS FOR ELECTRONIC TROUBLESHOOTING Final Report, Aug. 1986 - Aug. 1989
Walter Schneider Jun. 1991 17 p
(Contract MDA903-86-C-0149)
(AD-A239573; ARI-RN-91-76) Avail: NTIS HC/MF A03 CSCL 12/5

How practice aids development of diagnostic troubleshooting skill and how to speed the skill acquisition process using desktop simulation techniques is examined. Experiments show how practice can build up automatic component skills so they can be executed quickly, reliably, with little effort, and be incorporated into more complex skills. The researchers developed objective criteria that can be used in microcomputer software to specify when to promote a student from practicing a component skill to practicing the aggregate skill level. GRA

N91-31543# General Electric Co., Schenectady, NY. Research and Development Div.
DEVELOPMENT OF ELEMENTS OF A HIGH T(SUB c) SUPERCONDUCTING CABLE Annual Report, 1 Jul. 1990 - 30 Jun. 1991
Kenneth W. Lay 30 Jun. 1991 10 p
(Contract N00014-88-C-0681)
(AD-A239766) Avail: NTIS HC/MF A02 CSCL 09/1

The program is aimed at the development of long lengths of silver-clad BSCCO ($Bi_2Sr_2CaCu_2O_8$). The material of choice is BSCCO-2223 with 20 K the operating temperature goal. Such a

tape conductor ultimately could be used in a coil for a magnet, motor or generator. The program is designed to tackle several key problems with parallel tasks. A large variety of BSCCO powders are under investigation. Silver tubes are packed with superconductor powder and deformed to form tape conductors. An alternate method of making silver-encapsulated superconducting tape is being pursued. Variations in the powders and processing parameters are used to optimize the tape Jc.
GRA

N91-32028# Technische Univ., Eindhoven (Netherlands). Faculty of Electrical Engineering.
MEASUREMENTS OF INCEPTION TIME LAGS OF REPETITIVELY PULSED CORONA IN AIR
E. M. vanVeldhuizen, W. R. Rutgers, and R. P. Dahiya (Indian Inst. of Tech., New Delhi.) *In* Keuring van Electrotechnische Materialen N.V., KEMA Scientific Reports, Volume 8, Number 2, 1990 Apr. 1990 p 121-129 Sponsored by Keuring van Electrotechnische Materialen N.V. (For primary document see N91-32023 23-99)
Avail: NTIS HC/MF A04

34 FLUID MECHANICS AND HEAT TRANSFER

Includes boundary layers; hydrodynamics; fluidics; mass transfer; and ablation cooling.

For related information see also *02 Aerodynamics* and *77 Thermodynamics and Statistical Physics.*

N91-31544 University Coll. of Wales, Aberystwyth.
COMPUTATIONAL FLUID DYNAMICS Ph.D. Thesis
Muhammad Imtiaz Hussain 1988 233 p
Avail: Univ. Microfilms Order No. BRDX92602

The rheological behavior of a viscoelastic fluid in a complex flow situation involving an abrupt change in geometry is discussed. An implicit differential model is chosen to characterize the complex behavior of the fluid. The model retains the simplicity necessary to solve the complicated flow problems of the sort considered. Both planar and axisymmetric flows are considered. Standard numerical finite difference methods are applied to a number of related flow problems. In the method, the physical variables are determined numerically at grid points, Also, the method of upwind differencing is used. Dissert. Abstr.

N91-31545 Ohio State Univ., Columbus.
LINEAR AND NONLINEAR STABILITY OF BOUNDARY LAYERS WITH STREAMWISE VARYING PROPERTIES Ph.D. Thesis
Fabio Paolo Bertolotti 1991 262 p
Avail: Univ. Microfilms Order No. DA9120631

A new technique is presented for the study of transition in convectively unstable flows that uses nonlinear partial differential equations of parabolic type based on the slow change of the mean flow, disturbance velocity profiles, wavelength, and growth rate in the streamwise direction. Solutions comparable in accuracy to direct Navier-Stokes simulations can be obtained with a marching procedure using a small fraction of the computational cost. The development of Tollmien-Schlichting waves in the Blasius boundary layer is studied. The results are compared with previous work and the effects of nonparallelism and nonlinearity are clarified. The linearized Parabolic Stability Equation are extended to compressible flow. Results up to a Mach number of 1.6 indicate that compressibility does not alter greatly the findings obtained in the incompressible case. The incompressible analysis is extended to a variety of wave-wave and wave-vortex interactions. The initial conditions simulate those present in experiments using a vibrating ribbon, and consist of a TS wave of dominant amplitude, and small amplitude 3-D disturbances. Dissert. Abstr.

N91-31546 Virginia Polytechnic Inst. and State Univ., Blacksburg.
GENERALIZED SPATIAL DISCRETIZATION TECHNIQUES FOR SPACE-MARCHING ALGORITHMS Ph.D. Thesis
William Dandridge McGrory 1991 122 p
Avail: Univ. Microfilms Order No. DA9120400

Two unique spatial discretizations using generalized indexing strategies suitable for use with space marching algorithms are presented for the numerical solution of the equations of fluid dynamics. Both discretizations attempt to improve geometric flexibility as compared to structured indexing strategies and were formulated while considering the current and future availability of unstructured grid generation techniques. The first discretization uses a generalized indexing strategy using triangular elements in the two dimensions normal to the streamwise direction. The second discretization subdivides the domain into a collection of computational blocks. Each block has inflow and outflow boundaries suitable for space marching. A completely generalized indexing strategy using tetrahedra is used within each computational block. The solution to the flow in each block is found independently in a fashion similar to the cross flow planes of a structured discretization. Numerical algorithms were developed for the solution of the governing equations on each of the two proposed discretizations. Dissert. Abstr.

N91-31547 Texas A&M Univ., College Station.
A THREE-DIMENSIONAL VISCOUS FLOW MODEL OF STATOR/ROTOR INTERACTION IN TURBOMACHINES Ph.D. Thesis
John Donald MacGregor, III 1990 125 p
Avail: Univ. Microfilms Order No. DA9118269

The current numerical model takes into account the full three dimensionality and cyclic fluctuations of the flow variables in a turbomachinery stage. The cyclic fluctuations are the result of circumferential irregularities in the flow pattern generated by blade rows upstream of the airfoil cascade under consideration. The flow irregularities in the current model result from such flow zones as the viscous wakes produced by the preceding blade row. The model is based on the use of the finite element method to solve the time dependent Navier-Stokes equations in a generally rotating blade-to-blade, hub-to-tip flow passage. Use of the finite element technique greatly simplifies the modeling of this highly complicated flow domain. The equations governing the relative flow through rotating blade rows are cast in cylindrical coordinates, enabling the model to be used for both rotor and stator blade rows. Real flow effects, such as separation and recirculation, are rigorously simulated as the flow ellipticity is retained throughout the flow domain. Retention of all the viscous terms is an upgrade of virtually all existing models which use such approximations as a totally or partially parabolic flow field. Dissert. Abstr.

N91-31548 Stanford Univ., CA.
THE INTERACTION OF PARTICLES WITH HOMOGENEOUS TURBULENCE Ph.D. Thesis
Kyle David Squires 1990 298 p
Avail: Univ. Microfilms Order No. DA9108906

The interaction of particles with homogeneous turbulence was investigated using Direct Numerical Simulation of the incompressible Navier-Stokes equations. Lagrangian statistics of fluid material points and small, spherical particles were obtained in simulations of decaying and forced isotropic turbulence as well as homogeneous shear flow. The effect of turbulence on particle concentration fields and turbulence modification by particles was investigated using simulation of stationary isotropic turbulence.
Dissert. Abstr.

N91-31549 State Univ. of New York, Buffalo.
PREDICTION OF ROTOR SURFACE UNSTEADY PRESSURE AND HEAT TRANSFER FROM WAKE PASSING Ph.D. Thesis
Le Trong Tran 1991 176 p
Avail: Univ. Microfilms Order No. DA9121073

A numerical investigation of the effects of unsteady flow on gas turbine heat transfer, particularly on the rotor blade surface,

is described. Unsteady flow in a rotor blade passage and the unsteady heat transfer on the blade surface as a result of wake/rotor interaction are modeled by the inviscid flow/boundary layer approach. Euler equations which govern the inviscid flow are solved using a time accurate marching scheme. Unsteady flow in the blade passage is induced by periodically moving a wake model across the passage inlet. Unsteady flow solutions in the passage provide pressure gradients and boundary conditions for boundary layer equations which govern the viscous flow adjacent to the blade surface. Turbulent flow which is transported from upstream and created within the wake is modeled by a turbulent kinetic energy/dissipation model. Numerical solutions of the unsteady turbulent boundary layer yield surface heat flux values which then can be compared to experimental data.
Dissert. Abstr.

N91-31550 Notre Dame Univ., IN.
LINEAR AND NONLINEAR RESPONSES OF THE FLOW AND TEMPERATURE FIELDS TO IMPOSED WALL TEMPERATURE OSCILLATIONS IN DIFFERENTIALLY HEATED VERTICAL RECTANGULAR ENCLOSURES Ph.D. Thesis
Qiong Xia 1991 189 p
Avail: Univ. Microfilms Order No. DA9119800

A 2-D numerical study, based on finite difference control volume method, was carried out to study the linear and nonlinear responses of flow and temperature fields to imposed wall temperature oscillations in differentially heated vertical rectangular enclosures. The results were obtained for tall cavities with varying Rayleigh number, Prandtl number, and frequency both numerically and analytically; also for the square cavities filled with air covering the complete ranges of small, large, and intermediate frequencies, Rayleigh numbers and amplitudes of the imposed temperature oscillations both in linear and nonlinear regimes. The numerical results obtained are in good agreement with analytical results known for some of the limiting cases. When the amplitude of the imposed forcing oscillation is sufficiently small, the heat transfer and flow field oscillations are directly proportional to the perturbation amplitude and this is defined as the linear response. For the nonlinear responses, flow undergoes two bifurcations prior to reaching chaos as Rayleigh number increases. The imposed forcing oscillation does destabilize the flow and each bifurcation is achieved at lower Rayleigh number. Dissert. Abstr.

N91-31551# Von Karman Inst. for Fluid Dynamics, Rhode-Saint-Genese (Belgium).
INTRODUCTION TO THE MODELING OF TURBULENCE
1991 453 p Lecture series held in Rhode-Saint-Genese, Belgium, 18-21 Mar. 1991
(VKI-LS-1991-02; ISSN-0377-8312; ETN-91-99903) Copyright Avail: NTIS HC/MF A20

An introduction to the fundamental physical and mathematical principles of turbulence modeling and a survey of the models currently available of their domain of application were given. Emphasis was put on those models which can be considered ready for application to a range of problems of practical interest and, in particular, to recent advances in second moment closures. A basic introduction to the field of advanced turbulence modeling through large eddy simulation was provided. For individual titles, see N91-31552 through N91-31564.

N91-31552# Manchester Univ. (England). Dept. of Mechanical Engineering.
INTRODUCTION TO THE MODELING OF TURBULENCE: INTRODUCTION
B. E. Launder *In* VKI, Introduction to the Modeling of Turbulence 1991 17 p (For primary document see N91-31551 23-34)
Copyright Avail: NTIS HC/MF A20

It is shown that Direct Numerical Simulation (DNS) of turbulent shear flows are beginning to appear. The DNS are based on the full time dependent Navier Stokes equations. It is important that models be invariant to the coordinate system. A turbulence model should have a great width of applicability, be mathematically simple, computationally stable, and based on a small number of basic concepts. Velocity distribution is examined. Logarithmic velocity laws are obtained by assuming instantaneous changeover from purely viscous to purely turbulent transport mechanism at edge of viscous layer.
ESA

N91-31553# Manchester Univ. (England). Dept. of Mechanical Engineering.
TWO-EQUATION MODELS FOR HIGH-REYNOLDS-NUMBER FLOW
M. A. Leschziner *In* VKI, Introduction to the Modeling of Turbulence 1991 16 p (For primary document see N91-31551 23-34)
Copyright Avail: NTIS HC/MF A20

It is shown that two equation models allow much wider range of turbulent flows to be predicted than one equation variants. The k epsilon turbulence model forms a good compromise between generality and economy of use for many engineering problems. The k epsilon model has a number of weaknesses related to curvature, adverse pressure gradient and flow geometry. Corrections were proposed, which are not generally applicable.
ESA

N91-31554# Manchester Univ. (England). Dept. of Mechanical Engineering.
TWO-EQUATION MODELS FOR LOW-REYNOLDS NUMBER FLOW
M. A. Leschziner *In* VKI, Introduction to the Modeling of Turbulence 1991 13 p (For primary document see N91-31551 23-34)
Copyright Avail: NTIS HC/MF A20

Low Reynolds number conditions were defined. The essential physics of turbulent flow in the near wall sublayer is dealt with. Representative forms of low Reynolds number two equation models are presented. Applications of the models to strongly nonequilibrium flows are shown. Weaknesses and approaches to their cure are indicated. It is concluded that the growth of computer power makes it possible to use Reynolds two equation models in many engineering flows.
ESA

N91-31555# Manchester Univ. (England). Dept. of Mechanical Engineering.
AN INTRODUCTION TO SECOND MOMENT CLOSURE
B. E. Launder *In* VKI, Introduction to the Modeling of Turbulence 1991 13 p (For primary document see N91-31551 23-34)
Copyright Avail: NTIS HC/MF A20

It is shown that second moment closures of either differential or algebraic type are becoming widely used for flows of direct industrial interest, and that they nearly always give accurate solutions. The Algebraic Stress Model (ASM) is not recommended for swirling flows, where a differential version is needed. Refinements to epsilon equation and phi(sub I,J) models are undergoing extensive testing before being incorporated into more general purpose software.
ESA

N91-31556# Manchester Univ. (England). Dept. of Mechanical Engineering.
INCLUSION OF SECOND-MOMENT CLOSURES INTO FINITE-VOLUME SOLVERS
M. A. Leschziner *In* VKI, Introduction to the Modeling of Turbulence 1991 11 p (For primary document see N91-31551 23-34)
Copyright Avail: NTIS HC/MF A20

Second moment closure equations are summarized. Main steps in finite volume discretization are indicated. Destabilizing mechanisms are identified. Commonly used algorithmic techniques enhancing numerical stability for algebraic and differential closure forms, are outlined. Near wall treatment of second moment equations are described. It is concluded that special stabilization practices are needed in order to use second moment closure for complex flows.
ESA

N91-31557# Manchester Univ. (England). Dept. of Mechanical Engineering.
NUMERICAL IMPLEMENTATION AND PERFORMANCE OF REYNOLDS STRESS CLOSURES IN FINITE-VOLUME COMPUTATIONS OF RECIRCULATING AND STRONGLY SWIRLING FLOWS
M. A. Leschziner *In* VKI, Introduction to the Modeling of Turbulence 1991 69 p Sponsored in part by United Kingdom Science and Engineering Research Council; Rolls Royce; United Kingdom Ministry of Defence; British Aerospace; and Nielsen Engineering and Research Inc. (For primary document see N91-31551 23-34)
Copyright Avail: NTIS HC/MF A20

The nature, basic properties and rationale of stress closures are reported. A statement of the complete turbulence models under consideration is made. Aspects of discretization are considered. A series of generally applicable numerical measures are introduced, which were specifically developed to promote stability when stress closures are used in conjuction with nondiffusive discretization within the finite volume framework. The performance of the stress closures is illustrated through comparisons between computed and measured results for twelve flow geometries. ESA

N91-31558# Manchester Univ. (England). Dept. of Mechanical Engineering.
BODY FORCE EFFECTS ON TURBULENCE
B. E. Launder *In* VKI, Introduction to the Modeling of Turbulence 1991 13 p (For primary document see N91-31551 23-34)
Copyright Avail: NTIS HC/MF A20

Indirect effects and direct effects of body forces in second moment equations are examined. Buoyancy effects on the epsilon equations are reported. Secondary generation effects in plumes are studied. A new second moment closure and its application in buoyant flows are outlined. It is shown that second moment closure is needed to capture effects, when force fields modify turbulence structure directly. ESA

N91-31559# Manchester Univ. (England). Dept. of Mechanical Engineering.
APPLICATION OF SECOND-MOMENT CLOSURE IN COMPLEX FLOWS
M. A. Leschziner *In* VKI, Introduction to the Modeling of Turbulence 1991 23 p (For primary document see N91-31551 23-34)
Copyright Avail: NTIS HC/MF A20

Differential and algebraic forms of second moment closure were used. Boundary conditions at fluid inlet and outlet, walls and symmetry lines were examined. The main features of a range of flow geometries computed hitherto were summarized. Application examples were given. It was concluded that stress closures do not perform well consistently, but are virtually always superior to viscosity models. ESA

N91-31560# Manchester Univ. (England).
A NEW FORM OF SECOND-MOMENT CLOSURE
B. E. Launder *In* VKI, Introduction to the Modeling of Turbulence 1991 15 p (For primary document see N91-31551 23-34)
Copyright Avail: NTIS HC/MF A20

The stress invariants and their characteristics are introduced. The new models of pressure interactions for phi(sub I,J) and phi(sub I,theta) are discussed. New forms of dissipation rate equations are considered. The wrong dependence of effective turbulent Prandtl number on strain rate is shown. It is concluded that computing advances are rapidly popularizing the use of low Reynolds second moment closures in two dimensional boundary layer computations. ESA

N91-31561# Manchester Univ. (England). Dept. of Mechanical Engineering.
AN INTRODUCTION TO SINGLE-POINT CLOSURE METHODOLOGY
B. E. Launder *In* VKI, Introduction to the Modeling of Turbulence 1991 90 p (For primary document see N91-31551 23-34)
Copyright Avail: NTIS HC/MF A20

It is shown that there is a wide range of modeling methodology within the single point framework. The exact second moment equations are examined. The WET model is presented, based on the simple economic idea that Wealth is proportional to Earnings multiplied by Time. A considerable simplification to the task of turbulence modeling results from applying the high Reynolds number hypothesis. An account of turbulent transport in the viscosity modified sublayer is given. Low Reynolds number treatments are discussed. Wall functions are considered. Though some flows are unsuitable for prediction by wall functions, a wide range of flows phenomena seems amenable to successful treatment. ESA

N91-31562# Deutsche Forschungsanstalt fuer Luft- und Raumfahrt, Oberpfaffenhofen (Germany, F.R.). Inst. fuer Physik der Atmosphere.
DIRECT AND LARGE EDDY SIMULATION OF TURBULENCE: SUMMARY OF THE STATE-OF-THE-ART 1991
U. Schumann *In* VKI, Introduction to the Modeling of Turbulence 1991 30 p (For primary document see N91-31551 23-34)
Copyright Avail: NTIS HC/MF A20

The basic approach used to simulated turbulence either directly or in terms of the large eddies, is described. Direct Numerical Simulation (DNS) of turbulence and Large Eddy Simulation (LES) of turbulence are successfully examined. Applications for which DNS and LES can be used are given. It is concluded that DNS and LES are tools for basic turbulence research which are a complement of other approaches to turbulence. ESA

N91-31563# Karlsruhe Univ. (Germany, F.R.). Inst. fuer Hydromechnik.
EXAMPLES OF TURBULENCE MODEL APPLICATIONS
W. Rodi *In* VKI, Introduction to the Modeling of Turbulence 1991 53 p (For primary document see N91-31551 23-34)
Copyright Avail: NTIS HC/MF A20

It is shown how commonly used turbulence models describe flow situations of practical relevance. Examples of model calculations are presented for a wide range of flows from different areas of engineering. The results are compared with experimental data. Attention is focused on the application of eddy viscosity models. Among these, the k epsilon model has greater potential for universality than the simpler eddy viscosity models. Results obtained with other models are included for comparison. The relative performance of the different models is discussed. ESA

N91-31564# Institut National des Sciences Appliquees, Routen (France). Faculte des Sciences et Techniques.
TURBULENCE MODELING FOR COMPRESSIBLE FLOWS AND IMPLEMENTATION IN NAVIER-STOKES SOLVERS
D. Vandromme *In* VKI, Introduction to the Modeling of Turbulence 1991 65 p (For primary document see N91-31551 23-34)
Copyright Avail: NTIS HC/MF A20

The basic features for compressible flows are given. Algebraic turbulence models are presented. Field equations after used to globally describe one or more characteristic turbulence scales. A two equation model is presented, with a more formal equation for the determination of the length scale. All models are based on the use of the constitutive relationship between the turbulent stress and the mean strain tensor. Second order closure is considered through the problem of the Reynolds stress modeling. Difficulties associated with transport equations for turbulence models are focused. ESA

N91-31565# Von Karman Inst. for Fluid Dynamics, Rhode-Saint-Genese (Belgium).
NEW APPROACHES IN THE DESCRIPTION AND MODELING OF TURBULENCE
1991 445 p Lecture series held in Rhode-Saint-Genese, Belgium, 6-8 May 1991
(VKI-LS-1991-03; ISSN-0377-8312; ETN-91-99904) Copyright Avail: NTIS HC/MF A19

Subjects covered were direct and large eddy simulations of transition in the compressible boundary layer, spectral large eddy simulation of isotropic and stably stratified turbulence, large eddy simulation of the turbulent flow in the downstream region of a backward facing step, spatiotemporal intermittency, RNG (Renormalizing Group) and turbulence modeling, finite dimensional dynamics and chaos in fluid flows. For individual titles, see N91-31566 through N91-31571.

N91-31566# Institut de Mecanique de Grenoble (France).
DIRECT AND LARGE-EDDY SIMULATIONS OF TRANSITION IN THE COMPRESSIBLE BOUNDARY LAYER
X. Normand and M. Lesieur *In* VKI, New Approaches in the Description and Modeling of Turbulence 1991 47 p Sponsored in part by CNRS (For primary document see N91-31565 23-34)
(Contracts RDMF3-86; DRET-87-808-11; DRET-88-150)
Copyright Avail: NTIS HC/MF A19

The transition to turbulence in the three dimensional compressible boundary layer over a semi-infinite insulated flat plate is studied by means of direct and large eddy simulations. Results are presented in the quasi-incompressible and high supersonic cases, both in temporal and spatial configurations. Simulations of controlled transition allow study of the secondary instability of the flow. The complete transition process is examined, with emphasis put on vortex filament dynamics. It is shown that the development to turbulence is well simulated, at least for the prediction of average quantities of the flow. In the high Mach number case, a subgrid scale model is used, in order to perform a large eddy simulation of the transition. ESA

N91-31567# Institut de Mecanique de Grenoble (France).
SPECTRAL LARGE-EDDY SIMULATION OF ISOTROPIC AND STABLY-STRATIFIED TURBULENCES
O. Metais and M. Lesieur *In* VKI, New Approaches in the Description and Modeling of Turbulence 1991 67 p Sponsored in part by CNRS (For primary document see N91-31565 23-34)
(Contract DRET-87-238)
Copyright Avail: NTIS HC/MF A19

The case of a spectrum which does not decrease as k to the -5/3 power at the cutoff is studied. A spectral large eddy simulation of decaying isotropic turbulence convecting a passive temperature is performed, at a resolution of 128 cubed collocation points. When self similar spectra have developed, the temperature variance and kinetic energy decay. The spectral eddy viscosity and diffusivity are recalculated explicitly from the large eddy simulation. The pressure distribution is exponential in the lows and Gaussian in the highs. A generalization of the spectral eddy viscosity to highly intermittent situations in physical space is proposed. ESA

N91-31568# Commissariat a l'Energie Atomique, Grenoble (France).
LARGE-EDDY SIMULATION OF THE TURBULENT FLOW IN THE DOWNSTREAM REGION OF A BACKWARD FACING STEP
A. SilveiraNeto, D. Grand, O. Metais, and M. Lesieur (Institut de Mecanique de Grenoble, France) *In* VKI, New Approaches in the Description and Modeling of Turbulence 1991 16 p Sponsored in part by Conselho Nacional de Pesquisas (For primary document see N91-31565 23-34)
Copyright Avail: NTIS HC/MF A19

A numerical simulation of a complex turbulent shear flow using large eddy simulation techniques is carried out. The filtered Navier-Stokes equations are solved with a finite volume method. The subgrid model is a local adaptation to the physical space of the spectral eddy viscosity concept. The statistics of the mean field are in good agreement with experimental data, corresponding to an aspect ratio of 2.4. It is shown that calculations at a lower aspect ratio outline that the eddy structure of the flow presents striking analogies with the plane shear layers, with large billows shed behind the step, and longitudinal vortices strained between these billows. ESA

N91-31569# Commissariat a l'Energie Atomique, Saclay (France). Direction des Sciences de la Matiere.
SPATIOTEMPORAL INTERMITTENCY
H. Chate and F. Daviaud *In* VKI, New Approaches in the Description and Modeling of Turbulence 1991 75 p (For primary document see N91-31565 23-34)
Copyright Avail: NTIS HC/MF A19

Spatiotemporal intermittency designates all situations where a spatially extended system presents intermittency both in its spatial structure and during its temporal evolution. The recent development of the theory of chaos is reviewed. Rayleigh-Bernard convection is at the center of laboratory experiment description, showing spatiotemporal intermittency. A stochastic model of contamination processes is presented. A detailed account of the transition to spatiotemporal intermittency is given. The general methodology involved is introduced. Theoretical issues concerning the transition to spatiotemporal intermittency are reported. ESA

N91-31570# Stanford Univ., CA.
RNG AND TURBULENCE MODELING
Leslie A. Smith *In* VKI, New Approaches in the Description and Modeling of Turbulence 1991 68 p (For primary document see N91-31565 23-34)
Copyright Avail: NTIS HC/MF A19

The ReNormalization Group (RNG) theory involves approximations which neglect much of the complexity of turbulent flow. The Yakhot and Orszag method is explained in detail. The strengths and weaknesses of RNG turbulence models are outlined. The basic RNG theory of the forced Navier-Stokes equations and the calculation of the Kolmogorov constant are studied. The derivation of the RNG kappa epsilon equations, which should serve as a guide for the derivation of other turbulence models is examined. The asymptotic theory of infinite Reynolds number turbulence is described. Extensions of RNG models to finite Reynolds number flows are dealt with. The practical application of RNG results is given. ESA

N91-31571# Oxford Univ. (England). Clarendon Lab.
FINITE-DIMENSIONAL DYNAMICS AND CHAOS IN FLUID FLOWS
Tom Mullin *In* VKI, New Approaches in the Description and Modeling of Turbulence 1991 59 p Sponsored in part by United Kingdom Science and Engineering Research Council (For primary document see N91-31565 23-34)
Copyright Avail: NTIS HC/MF A19

The role of finite dimensional dynamics and chaos in interpreting nonlinear fluid mechanical motion is discussed. The emphasis is put on the practicalities of applying the abstract concepts of finite dimensional dynamics to the experimental study of fluid flows. A detailed overview is given of the essential features of the underpinning bifurcation structure of the equations. Finite dimensional chaos is demonstrated. It is shown that finite dimensional chaos is uncovered, when the same combination of experiment and theory is applied to a more general flow problem. ESA

N91-31572# Lawrence Livermore National Lab., CA.
PHOTOGRAPHY OF SHOCK WAVES IN EXPLOSIVE CRYSTALS
A. M. Frank and W. C. Tao 11 Jul. 1991 7 p Presented at the Society of Photo-Optical Instrumentation Engineers (SPIE) Meeting, San Diego, CA, 21-26 Jul. 1991
(Contract W-7405-eng-48)
(DE91-015772; UCRL-JC-107195; CONF-9107115-14) Avail: NTIS HC/MF A02

Recent advances in high-speed microscopy allow successful streak photography of nonreactive shock waves passing through individual explosive crystals. Measurement of the shock velocity both in the crystal and in the water surrounding the crystal allows us to determine the shock pressures. These diagnostic tools have the required temporal and spatial resolutions to enable us to study the microscopic processes in nonreactive and possibly reactive shock environments. DOE

N91-31573# Sandia National Labs., Albuquerque, NM.
A BOUNDARY INTEGRAL EQUATION METHOD FOR STEADY TWO-DIMENSIONAL FLOW IN PARTIALLY SATURATED MEDIA
M. J. Martinez and D. F. McTigue Jul. 1991 58 p
(Contract DE-AC04-76DP-00789)
(DE91-016056; SAND-90-0253) Avail: NTIS HC/MF A04

The governing equation for steady flow in a partially saturated, porous medium can be written in a linear form if one adopts a hydraulic conductivity function that is exponential in the capillary-pressure head. The resulting linear field equation is well suited to numerical solution by the boundary integral equation method (BIEM). The exponential conductivity function is compared to a more complex form often assumed for tuffs, and is found to be a reasonable approximation over limited ranges of pressure head. A computer code based on the BIEM is described and tested. The BIEM is found to exhibit quadratic convergence with element size reduction on smooth solutions and on singular problems, if mesh grading is used. Agreement between results from the BIEM code an a finite-element code that solves the fully nonlinear problem is excellent, and is achieved at a substantial advantage in computer processing time. DOE

N91-31574# Sandia National Labs., Albuquerque, NM.
APPROXIMATE TREATMENT OF A STRONG EXPLOSION AND EXPANSION IN A NEAR VACUUM
A. L. Thornton Jul. 1991 30 p
(Contract DE-AC04-76DP-00789)
(DE91-016063; SAND-91-1578) Avail: NTIS HC/MF A03

The hydrodynamic blast created by the initiation of a 1 keV X-ray source from an arc-induced ionized gas column, involves density and temperature ratios of such magnitude that the strong shock theory of propagation from continuum fluid mechanics does not apply. Because these simulations occurs in a near vacuum, the continuum equations of motion break down and become invalid during the expansion process as the wavefront density decreases. This report summarizes an approximate treatment of the hydrodynamics of a strong explosion followed by an expanding wavefront in a near vacuum. The analysis was performed in support of the Saturn program to assist the test engineers in the design of a shroud which is optimized to receive the maximum cold X-ray radiation through its aperture while minimizing the hydrodynamic damage to the rest specimens. The analytical treatment uses mass conversion and the assumption of a liner velocity profile to assess the dynamic behavior of the developing wavefront. This technique provides a first estimate of the gas motion and pressure pulse and indicates some general trends of the hydrodynamic phenomenon. DOE

N91-31575# Oregon State Univ., Corvallis. Dept. of Nuclear Engineering.
THE EFFECTS OF FLUID PARTICLE INTERACTIONS ON INTERFACIAL TRANSFER AND FLOW STRUCTURE
J. N. Reyes, Jr. and A. Lafi 1991 31 p
(Contract DE-FG07-90ER-13034)
(DE91-016409; DOE/ER-13034/T1) Avail: NTIS HC/MF A03

Advancements in computer technology may permit the next generation of reactor thermal hydraulic analysis codes to implement highly detailed statistical approaches for the treatment of fluid particle distributions. This may significantly improve the code's ability to predict interfacial transfer processes. On September 30, 1990 a program was initiated at Oregon State University to compile a set of fundamental models for fluid particle coalescence and breakage frequencies for incorporation into a statistically based (Population Balance Approach or Statistical Monte Carlo Approach) two-phase thermal hydraulics code. This report describes the progress achieved during the first seven months of the project. This report briefly describes the general framework into which the fluid particle interaction models can be incorporated. Also presented is an overview of the types of phenomenological models that have been identified as the result of a literature survey. The project objectives complement a research program at INEL aimed at developing an advanced two-phase flow computer code. The project overview presented at the annual DOE-OER review meeting at Savannah River Laboratory on April 22-24, 1991 is included. DOE

N91-31576*# Institute for Computer Applications in Science and Engineering, Hampton, VA.
CONTROL OF OSCILLATORY FORCES ON A CIRCULAR CYLINDER BY ROTATION Final Report
Yuh-Roung Ou Aug. 1991 18 p Submitted for publication
(Contract NAS1-18605; AF-AFOSR-0079-89)
(NASA-CR-187619; NAS 1.26:187619; ICASE-91-67) Avail: NTIS HC/MF A03 CSCL 20D

The temporal development of forces acting on a rotating cylinder is investigated numerically in response to a variety of of time-dependent rotation rates. Solutions are presented for several types of rotation that illustrate signific nt effects of the rotation rate on lift, drag, and lift/drag coefficients. Of special interest is the formulation of an optimal control problem for the case of constant speed of rotation. Researchers found an optimal rate that achieves the maximum value of time-averaged lift/drag ratio. Author

N91-31577# Groningen Rijksuniv. (Netherlands). Dept. of Mathematics.
ARTIFICIAL DIFFUSION METHODS IN CONVECTION DOMINATED FLOWS
Marc I. Gerritsma Dec. 1990 109 p
(W-9016; TNO-BOUW-BI-90-209; ETN-91-99577) Avail: NTIS HC/MF A06

A stationary scalar linear convection-diffusion equation is considered. For the one dimensional equation a standard Galerkin formulation, which serves at the same time as an introduction to the Finite Element Method (FEM) is deduced. The eigenvalues of the resulting stiffness matrices are examined. For the two dimensional problem, the oblique shock, the same equation is formulated with suppression of the 'crosswind diffusion'. The diffusion resulting from specific time integration techniques is examined, using space-time FEM and discontinuous Galerkin method. Navier-Stokes equations are derived and results of an implementation of the Streamline Upwind Petrov Galerkin (SUPG) method for the flow over a step and the backward facing step are given. The Galerkin/least squares method is discussed. ESA

N91-31578# National Aerospace Lab., Amsterdam (Netherlands). Space Div.
DEVELOPMENT OF A SENSOR FOR HIGH-QUALITY TWO-PHASE FLOW
A. A. M. Delil and J. F. Heemskerk 7 Sep. 1988 14 p Presented at the 3rd European Symposium on Space Thermal Control and Life Support Systems, Noordwijk, Netherlands, 3-6 Oct. 1988 Previously announced as N89-28230 Sponsored by Netherlands Agency for Aerospace Programs
(NLR-MP-88059-U; ETN-91-99657) Avail: NTIS HC/MF A03

The monitoring of the quality of the two phase mixture at various locations in the system is a valuable, possibly indispensable, part of the control system needed to properly operate a two phase heat transport system for large spacecraft. Based on tradeoff of various quality monitoring concepts, a dedicated quality sensor of the axial capacitance principle was developed. Its theoretically demonstrated feasibility as a quality and wetting sensor was experimentally confirmed by preliminary experiments using liquid layer simulating plastic sheets and annular air/liquid flow. Experiments in a two phase freon test loop show the sensor to be an accurate, fastly responding, sensitive instrument. Recently, it was accepted for further development as a critical component of the two phase heat transport system developed by ESA. A review of the development is presented. Performance figures, obtained by calibrations in a new freon 114 loop, are given. Recommendations for future work and applications foreseen are indicated. ESA

N91-31579# National Aerospace Lab., Amsterdam (Netherlands). Fluid Dynamics Dept.

DEVELOPMENT OF AN ADVANCED PANEL METHOD FOR COMPLEX CONFIGURATIONS IN SUBSONIC COMPRESSIBLE FLOW; APPLICATION TO THE COMPUTATION OF THE POTENTIAL FLOW THROUGH DUCTS

C. M. vanBeek 19 Jan. 1987 48 p
(Contract NIVR-RB-3111-01201N)
(NLR-TR-88001-U; ETN-91-99658) Avail: NTIS HC/MF A03

The application of a boundary integral or panel method to duct flows is desribed. The method is capable of computing the three dimensional, steady state, subsonic, linearized (Prandtl-Glauert) potential flow about general configurations. The method is characterized by the application of a Dirichlet boundary condition and of compressible source and doublet distributions which are directly applied in the physical space. The geometry of the nonbranching duct (one inflow and one outflow cross section) may be arbitrary as long as the requirements for using the Prandtl-Glauert equation are met. A description of the method is given and three examples of application are presented with emphasis on the investigation of the conservation of mass flow through the ducts. ESA

N91-31580# Universiteit Twente, Enschede (Netherlands). Dept. of Applied Mathematics.

ACCELERATION TECHNIQUES FOR A SPECTRAL MULTI-GRID METHOD

R. W. deVries and P. J. Zandbergen 12 Dec. 1990 22 p
(MEMO-914; ISSN-0169-2690; ETN-91-99716) Avail: NTIS HC/MF A03

A symmetric preconditioning matrix is constructed in order that acceleration techniques such as FFT (Fast Fourier Transform) and ICCG (Incomplete Cholesky Conjugate Gradient) can be used. The method is used to solve the biharmonic equation as it appears in the stream function vorticity formulation of the Navier-Stokes equations. The driven cavity problem is solved numerically. Two dimensional flow problems are formulated in terms of stream function and vorticity. This formulation leads to a biharmonic equation for the streamfunction. This equation is split into two Poisson problems, one for the vorticity by means of Green's identity. ESA

N91-31581# Max-Planck-Inst. fuer Stroemungsforschung, Goettingen (Germany, F.R.).

EXAMINATION OF MOLECULAR EVAPORATION, COOLING, AND CLUSTER DISSOCIATION OF VERY THIN LIQUID JETS IN A HIGH VACUUM Thesis [UNTERSUCHUNGEN ZU MOLEKULARER VERDAMPFUNG, KUEHLUNG UND CLUSTERZERFALL VON SEHR DUENNEN FLUESSIGKEITSSTRAHLEN IM HOCHVAKUUM]

Bjoern Steiner Aug. 1990 140 p In GERMAN; ENGLISH summary
(MPIS-12/1990; ISSN-0436-1199; ETN-91-99739) Avail: NTIS HC/MF A07

A microscopic study of the evaporation of liquids with high vapor pressures is presented. It is shown that the injection of a pure water jet in a vacuum causes freezing, and that with a very thin liquid jet, this point can be undergone. With a very small jet diameter, the Kundsen conditions can be fulfilled. By introducing a skimmer near the jet, it is shown that the free molecular Maxwell velocity distribution of the molecules originating from the surface can be extracted. The cooling of the thin jet as a function of the nozzle skimmer distance is measured. The angular distribution of the evaporation could be evaluated by introducing a new designed skimmer with rectangular dimensions. By measuring the angular distributions and the surface temperatures, the heat of evaporation can be calculated with a simple Clausins Clapeyron equation. The evaporation coefficient of water is estimated to be near unity. ESA

N91-31582# Max-Planck-Inst. fuer Stroemungsforschung, Goettingen (Germany, F.R.).

LASER DOPPLER VELOCIMETER MEASUREMENTS OF THE STREAMWISE VELOCITY COMPONENT IN THE VISCOUS SUBLAYER OF A TURBULENT CHANNEL FLOW

Eduard Bawirzanski 1990 118 p In GERMAN; ENGLISH summary
(MPIS-Mitt-97; ISSN-0374-1257; ETN-91-99740) Avail: NTIS HC/MF A06

Measurements of mean velocity, mean square, skewness and flatness of velocity fluctuations, as a function of the wall distance were carried out. The correlation between the instantaneous velocity and the instantaneous data rate was eliminated. The analysis of the velocity fluctuation spectra, which also takes the velocity bias into account, allows estimates of the typical turbulent time scales to be made. The measured distribution of the mean velocity as a function of the wall distance in the viscous sublayer, which was obtained at twelve different positions, is almost exactly linear. The measured distribution of the mean square velocity, normalized with the local mean velocity, as a function of the wall distance in the wall vicinity confirms the results of the numerical simulations. ESA

N91-31583# Paris-Sud Univ., Orsay (France). Lab. d'Analyse Numerique.

THREE DIMENSIONAL EULER EQUATION SOLVING ON PARALLEL MACHINES Final Summary Report [RESOLUTION SUR MACHINE PARALLELE DES EQUATIONS D'EULER EN DIMENSION TROIS]

Charles-Henri Bruneau, Jacques Lamine, and Roger Teman 23 Jun. 1990 43 p In FRENCH; ENGLISH summary
(Contract DRET-87-229)
(ETN-91-99913) Avail: NTIS HC/MF A03

An attempt to specify and test a set of synchronizing functions for parallel programming is presented. Their main characteristic is that they use a queue to store tasks. Every active task inserts new tasks into the list; an available processor finds its next work in the list. The resolution of Euler problem around a three dimensional stationary body, and the resolution of two dimensional Stokes problem are given as examples of application. The tests are made on CEDAR, CRAY 2, and IBM 3090 machines. ESA

N91-31584# Centre d'Etudes et de Recherches, Toulouse (France). Dept. d'Etudes et de Recherches en Aerothermodynamique.

THREE DIMENSIONAL SHEAR FLOW: FLOW VISUALISATION AROUND A HIGHLY SWEPT BACK AND HIGH INCIDENCE WING Final Report [ECOULEMENTS CISAILLES TRIDIMENSIONNELS: VISUALISATION DE L'ECOULEMENT AUTOUR D'UNE AILE A FORTE FLECHE ET FORTE INCIDENCE]

G. Pailhas Mar. 1990 20 p In FRENCH
(Contract STPA-85-95-004/46)
(ONERA-RT-35/5025-28; ETN-91-99914) Avail: NTIS HC/MF A03

A study to find a geometric profile position (sweep 60 degrees fixed, variable incidence) such that the vincinity of the wing body junction becomes a likely field for a horseshoe type turbulent motion, as found in the classical case of the straight wing, is presented. Cavitation flow visualizations by viscous coatings were carried out at incidences of 15, 20, 25, and 30 degrees. Results showed differences in the flows at the wing-body vicinity of differing swept back wings and straight wings. ESA

N91-31585# Office National d'Etudes et de Recherches Aerospatiales, Paris (France). Direction de l'Aerodynamique.

DEVELOPMENT OF A COMPUTATION CODE FOR NONEQUILIBRIUM GAS AXISYMMETRIC HYPERSONIC LAMINAR FLOW Summary Report [DEVELOPPEMENT D'UN CODE DE CALCUL D'ECOULEMENT AXISYMETRIQUE HYPERSONIQUE LAMINAIRE DE GAZ HORS D'EQUILIBRE. RAPPORT DE SYNTHESE]

C. Flament, F. Coquel, and H. Hollanders May 1990 53 p In

FRENCH
(Contract DRET-89-34-001)
(ONERA-RS-14/3637-AY; ETN-91-99928) Avail: NTIS HC/MF A04

The complex structure of hypersonic flows around reentry bodies is discussed. Equations ruling the nonequilibrium axisymmetric two dimensional flow are focused on. A discretization scheme solving these equations is described. Results of applications to the flow around a sphere-cylinder configuration obtained in chemical nonequilibrium hypothesis (vibration energies being computed at equilibrium) are presented and discussed. Annexes detail the physical and numerical approaches in the code. ESA

N91-31586# Office National d'Etudes et de Recherches Aerospatiales, Paris (France). Direction Scientifique de la Resistance des Structures.
COMPRESSIBLE TWO DIMENSIONAL BOUNDARY LAYER STRONG PERFECT FLUID COUPLING IN THE CASE OF SHARP LEADING EDGE PROFILES. STATIONARY CASE [COUPLAGE FORT FLUIDE PARFAIT COUCHE LIMITE 2D COMPRESSIBLE DANS LE CAS DES PROFILS A BORD D'ATTAQUE AIGU. CAS STATIONNAIRE]
C. Soize May 1990 61 p In FRENCH
(ONERA-RT-42/1621-RY-093-R; ETN-91-99935) Avail: NTIS HC/MF A04

Developments in studies of aeroelasticity of blade grids are presented. The final objective is the development of a compressible steady and unsteady two dimensional code for isolated profiles and blade grids. Validation of the steady part and the isolated profile of this code is presented based on mathematical models and numerical analysis. The approach is based on a perfect fluid strong coupling boundary layer method. The resolution method is made in nonstructured finite element mesh with an implicit time scheme. ESA

N91-31587# Association Aeronautique et Astronautique de France, Paris.
BOUNDARY LAYER TURBULENCE APPEARANCE MECHANISMS STUDIED BY PLANE LASER VISUALIZATIONS [ETUDE DES MECANISMES D'APPARITION DE LA TURBULENCE DANS UNE COUCHE LIMITE A L'AIDE DE VISUALISATIONS PAR PLANS LASER]
F. Ladhari, R. Morel, and E. Alcaraz (Ecole Centrale de Lyon, France) 1989 8 p In FRENCH Presented at 26th Colloque d'Aerodynamique Appliquee, Toulouse, France, 23-25 Oct. 1990
(AAAF-NT-89-10; ISBN-2-7170-0943-4; ISSN-0243-0177;
ETN-91-99951) Avail: NTIS HC/MF A02; CEDOCAR, Section des Diffusions, 26 Blvd Victor, 75996 Paris Armees, France, HC 15 francs

Boundary layer turbulence study by plane laser visualization is described. Conditional techniques of effective signal processing in a turbulent boundary layer can quantify the contributions to Reynolds stress of organized structure type events. The technique used can be extended to three components of the instantaneously measured velocity either using a three wire probe or four wire probe to measure the vorticity component. ESA

N91-31588# Association Aeronautique et Astronautique de France, Paris.
USE OF 4-HOT-WIRE PROBES TO STUDY TURBULENT FLOW [UTILISATION DE SONDES A 4 FILS CHAUDS POUR L'ETUDE D'ECOULEMENTS TURBULENTS]
L. Jacquin, O. Leuchter, and P. Geffroy (Office National d'Etudes et de Recherches Aerospatiales, Paris, France) 1989 39 p In FRENCH; ENGLISH summary Presented at the 26th Colloque d'Aerodynamique Appliquee, Toulouse, France, 23-25 Oct. 1990 Original language document was announced in IAA as A90-22441
(AAAF-NT-89-15; ISBN-2-7170-0948-5; ISSN-0243-0177;
ETN-91-99956) Avail: NTIS HC/MF A03; CEDOCAR, Section des Diffusions, 26 Blvd Victor, 75996 Paris Armees, France, HC 30 francs

A four wire probe turbulent flow measurement method is described. The principles are based on the decomposition of the four wire probe into two crossed wire probes in order to perform two modes of processing: a normal four wire mode and a reduced two wire mode. Examples relative to homogenous turbulent fields and jet mixing layers are presented. Limitations concerning the spatial resolution problem and the angular limitation encountered in flows of high turbulent intensity are discussed. ESA

N91-31589# Association Aeronautique et Astronautique de France, Paris.
CHOICE REPRESENTATION MODES AND COLOR PALETTES [CHOIX DES MODES DE REPRESENTATION ET DES PALETTES DE COULEUR]
Marie Farge (Ecole Normale Superieure, Paris, France) 1989 8 p In FRENCH Presented at the 26th Colloque d'Aerodynamique Appliquee, Toulouse, France, 23-25 Oct. 1990 Previously announced in IAA as A91-19590
(AAAF-NT-89-17; ISBN-2-7170-0950-7; ISSN-0243-0177;
ETN-91-99958) Avail: NTIS HC/MF A02; CEDOCAR, Section des Diffusions, 26 Blvd Victor, 75996 Paris Armees, France, HC 15 francs

Characteristics of visualized fields are described. The fields to be visualized are acquired either by satellite observations or numerical simulations and represent complex but identifiable morphological structures, for example clouds, vortices or waves not known for sure a priori. Representation mode choice to analyze a given field by posing questions as to its structure and as to how one representation mode corresponds more adequately than the others to each one, is discussed. The choice of color palette to better distinguish different fields to identify structures at the heart of the same field is discussed. ESA

N91-31590# Association Aeronautique et Astronautique de France, Paris.
FLOW VISUALIZATION AND SIMULATION [VISUALISATION ET SIMULATIONS D'ECOULEMENTS]
A. Naim, T. Pre, and T. Chevalier (Avions Marcel Dassault-Breguet Aviation, Saint-Cloud, France) 1989 23 p In FRENCH Presented at the 26th Colloque d'Aerodynamique Appliquee, Toulouse, France, 23-25 Oct. 1990 Previously announced in IAA as A91-19589
(AAAF-NT-89-18; ISBN-2-7170-0951-5; ISSN-0243-0177;
ETN-91-99959) Avail: NTIS HC/MF A03; CEDOCAR, Section des Diffusions, 26 Blvd Victor, 75996 Paris Armees, France, HC 15 francs

The development of interactive visualization tools for the study of aircraft models is examined. The philosophy underlying the development of interactive hardware is elaborated, and attention is given to types of available visualizations and visualization limits. Features of the image analysis and animation techniques in this domain are discussed. ESA

N91-31591# Association Aeronautique et Astronautique de France, Paris.
POSTPROCESSING OF TEST AND COMPUTATION RESULTS BY THE WAVELET METHOD [POST-TRAITEMENT DE RESULTATS D'ESSAIS ET DE CALCUL PAR LA METHODE DES ONDELETTES]
R. Schlegel 28 Sep. 1989 38 p In FRENCH Presented at the 26th Colloque d'Aerodynamique Appliquee, Toulouse, France, 23-25 Oct. 1990 Previously announced in IAA as A91-19586
(AAAF-NT-89-24; ISBN-2-7170-0957-4; ISSN-0243-0177;
ETN-91-99965) Avail: NTIS HC/MF A03; CEDOCAR, Section des Diffusions, 26 Blvd Victor, 75996 Paris Armees, France, HC 30 francs

Wavelet transformation analysis is described and some examples of analysis studies in aerodynamics are given. Signal analysis by Fourier transform is recalled. Cavitation and compressor outflow during pumping are analyzed. The benefits of wavelet transformation, analysis and interpretation are underlined. ESA

N91-31592# Association Aeronautique et Astronautique de France, Paris.
POSTPROCESSING OF EXPERIMENTAL AND NUMERICAL RESULTS IN THE CASE OF TWO AND THREE DIMENSIONAL FLOWS [POST-TRAITEMENT DES RESULTATS EXPERIMENTAUX ET NUMERIQUES DANS LE CAS DES ECOULEMENTS BI ET TRIDIMENSIONNELS]
C. Gleyzes and G. Pailhas (Centre d'Etudes et de Recherches, Toulouse, France) 1989 32 p In FRENCH Presented at the 26th Colloque d'Aerodynamique Appliquee, Toulouse, France, 23-25 Oct. 1990 Previously announced in IAA as A91-19585
(AAAF-NT-89-25; ISBN-2-7170-0958-2; ISSN-0243-0177;
ETN-91-99966) Avail: NTIS HC/MF A03; CEDOCAR, Section des Diffusions, 26 Blvd Victor, 75996 Paris Armees, France, HC 30 francs

Solutions for representation of experimental and numerical results in the study of 2-D and 3-D shear flows are presented: local scale level lines (pressure, mean velocities, Reynolds stresses); wall flow lines from 3-D body boundary layers; global quantity lines (friction coefficient, integral thicknesses, wall pressure coefficients, etc.) in 3-D; secondary 3-D vortex wake flow representation. ESA

N91-31593# Association Aeronautique et Astronautique de France, Paris.
THE DEVELOPMENT OF A SPECIFIC IMAGE ANALYSIS TECHNIQUE FOR EXPLOITING FLOW VISUALIZATION NEGATIVES [SUR LA MISE AU POINT D'UNE TECHNIQUE SPECIFIQUE D'ANALYSE D'IMAGE POUR L'EXPLOITATION DE CLICHES DE VISUALISATION D'ECOULEMENTS]
Alain Texier, M. F. Collin, and Madelaine Coutanceau (Poitiers Univ., France) 1989 23 p In FRENCH Presented at the 26th Colloque d'Aerodynamique Appliquee, Toulouse, France, 23-25 Oct. 1990 Previously announced in IAA as A91-19583
(AAAF-NT-89-26; ISBN-2-7170-0959-0; ISSN-0243-0177;
ETN-91-99967) Avail: NTIS HC/MF A03; CEDOCAR, Section des Diffusions, 26 Blvd Victor, 75996 Paris Armees, France, HC 15 francs

An automatic flow visualization analysis chain was developed with the aim of providing sufficient experimental data indispensable for new numerical models. The chain consists of an image reading component and a processing system for the read data. Algorithms for the analysis chain are described and applied to unsteady nonviscous flow visualizations of a NACA 0012 airfoil at 30 degree high incidence and Reynolds number 3000. The recognition, interpretation and data segmentation algorithms are operational and give good results. ESA

N91-31594# Laboratoire d'Informatique pour la Mecanique et les Sciences de l'Ingenieur, Paris (France).
NUMERICAL SIMULATION OF THREE DIMENSIONAL UNSTEADY FLOW BY MULTIPROCESSOR SOLVING OF THE NAVIER-STOKES EQUATIONS Final Summary Report [SIMULATION NUMERIQUE D'ECOULEMENTS INSTATIONNAIRES TRIDIMENSIONNELS PAR RESOLUTION DES EQUATIONS DE NAVIER-STOKES SUR UN SYSTEME MULTIPROCESSEUR]
TaPhuoc Loc, W. Labidi, Annie Dulieu, Madelaine Coutanceau, G. Pineau, and Alain Texier (Poitiers Univ., France) Sep. 1990 163 p In FRENCH
(Contract DRET/LIMSI-88-047)
(ETN-91-99974) Avail: NTIS HC/MF A08

Results obtained in numerical and experimental studies of the unsteady flows of an incompressible viscous fluid around an infinite span circular cylinder or profile (2-D problem) and around finite span circular cylinder between two walls (3-D problem) are presented. The Cray2 and VP200 vector computers were used for numerical simulation, the LIMSI software for image processing and a fluid mechanics laboratory for visualization experiments. The algorithm is adapted to external and internal flows and uses the velocity-vortex vector. ESA

N91-31595*# National Aeronautics and Space Administration. Langley Research Center, Hampton, VA.
A RELATIVE-INTENSITY TWO-COLOR PHOSPHOR THERMOGRAPHY SYSTEM
N. Ronald Merski Sep. 1991 32 p
(NASA-TM-104123; NAS 1.15:104123) Avail: NTIS HC/MF A03 CSCL 20D

The NASA LaRC has developed a relative-intensity two-color phosphor thermography system. This system has become a standard technique for acquiring aerothermodynamic data in LaRC Hypersonic Facilities Complex (HFC). The relative intensity theory and its application to the LaRC phosphor thermography system is discussed along with the investment casting technique which is critical to the utilization of the phosphor method for aerothermodynamic studies. Various approaches to obtaining quantitative heat transfer data using thermographic phosphors are addressed and comparisons between thin-film data and thermographic phosphor data on an orbiter-like configuration are presented. In general, data from these two techniques are in good agreement. A discussion is given on the application of phosphors to integration heat transfer data reduction techniques (the thin film method) and preliminary heat transfer data obtained on a calibration sphere using thin-film equations are presented. Finally, plans for a new phosphor system which uses target recognition software are discussed. Author

N91-31596* National Aeronautics and Space Administration. Langley Research Center, Hampton, VA.
METHOD AND APPARATUS FOR DETECTING LAMINAR FLOW SEPARATION AND REATTACHMENT Patent
John P. Stack, inventor (to NASA) and Sivaramakrishnan M. Mangalam, inventor (to NASA) (Analytical Services and Materials, Inc., Hampton, VA.) 26 Jun. 1990 13 p Filed 4 May 1989 Supersedes N91-21472 (29 - 13, p 2082) Division of US-Patent-Appl-SN-203178, filed 7 Jun. 1988
(NASA-Case-LAR-13952-2-SB; US-Patent-4,936,146;
US-Patent-Appl-SN-348223; US-Patent-Appl-SN-203178;
US-Patent-Class-73-432.1; Int-Patent-Class-G01F-1/00) Avail: US Patent and Trademark Office CSCL 20D

The invention is a method and apparatus for simultaneously detecting laminar separation and reattachment of a fluid stream such as an airstream from and to the upper surface of an airfoil by simultaneously sensing and comparing a plurality of output signals. Each signal represents the dynamic shear stress at one of an equal number of sensors spaced along a straight line on the surface of the airfoil that extends parallel to the airstream. The output signals are simultaneously compared to detect the sensors across which a reversal in phase of said output signal occurs, said detected sensors being in the region of laminar separation or reattachment.
Official Gazette of the U.S. Patent and Trademark Office

N91-31597*# National Aeronautics and Space Administration. Lewis Research Center, Cleveland, OH.
A CRITICAL COMPARISON OF TWO-EQUATION TURBULENCE MODELS
N. J. Lang and T. H. Shih Sep. 1991 35 p
(NASA Order C-99066-G)
(NASA-TM-105237; ICOMP-91-15; E-6562; NAS 1.15:105237;
CMOTT-91-05) Avail: NTIS HC/MF A03 CSCL 20D

Several two-equation models were proposed and tested against benchmark flows by various researchers. For each study, different numerical methods or codes were used to obtain the results which were reported to be an improvement over other models. However, these comparisons may be overshadowed by the different numerical schemes used to obtain the results. With this in mind, several existing two-equation turbulence models, including k-epsilon, k-tau, k-omega, and q-omega models, are implemented into a common flow solver code for near wall turbulent flows. The quality of each model is based on several criteria, including robustness and accuracy of predicting the turbulent quantities.
Author

N91-31322# Fraunhofer-Gesellschaft e.V., Stuttgart (Germany, F.R.). Inst. fuer Grenzflaechen und Bioverfahrenstechnik.
LIQUID MOTION IN CAPILLARY TUBES (TEXUS 3)
P. J. Sell, E. Maisch, and J. Siekmann (Essen Univ., Germany, F.R.) *In* ESA, Summary Review of Sounding Rocket Experiments in Fluid Science and Materials Sciences: TEXUS 1 to 20; MASER 1 and 2 Feb. 1991 p 20-21 (For primary document see N91-31321 23-29)
Copyright Avail: NTIS HC/MF A15; EPD, ESTEC, Noordwijk, Netherlands, HC 75 Dutch guilders

N91-31323# Fraunhofer-Gesellschaft e.V., Stuttgart (Germany, F.R.). Inst. fuer Grenzflaechen und Bioverfahrenstechnik.
LIQUID MOTION IN CAPILLARY TUBES (TEXUS 5)
P. J. Sell, D. Renzow, and E. Maisch *In* ESA, Summary Review of Sounding Rocket Experiments in Fluid Science and Materials Sciences: TEXUS 1 to 20; MASER 1 and 2 Feb. 1991 p 22-23 (For primary document see N91-31321 23-29)
Copyright Avail: NTIS HC/MF A15; EPD, ESTEC, Noordwijk, Netherlands, HC 75 Dutch guilders

N91-31324# Fraunhofer-Gesellschaft e.V., Stuttgart (Germany, F.R.). Inst. fuer Grenzflaechen und Bioverfahrenstechnik.
BUBBLES AND FOAMS (TEXUS 10) ESA
P. J. Sell, D. Renzow, and K. F. Gebhardt *In* ESA, Summary Review of Sounding Rocket Experiments in Fluid Science and Materials Sciences: TEXUS 1 to 20; MASER 1 and 2 Feb. 1991 p 24 (For primary document see N91-31321 23-29)
Copyright Avail: NTIS HC/MF A15; EPD, ESTEC, Noordwijk, Netherlands, HC 75 Dutch guilders

N91-31629# Florida State Univ., Tallahassee. Coll. of Engineering.
UNSTEADY FLOW PAST AN AIRFOIL PITCHING AT A CONSTANT RATE
C. Shih, L. M. Lourenco, L. VanDommelen, and A. Krothapalli *In* VKI, Laser Velocimetry, Volume 2 1991 25 p Sponsored by AFOSR (For primary document see N91-31625 23-36)
Copyright Avail: NTIS HC/MF A10

N91-31630# Florida State Univ., Tallahassee. Coll. of Engineering.
VORTEX INTERACTIONS IN THE TRANSITION REGION OF A RECTANGULAR JET
L. M. Lourenco, A. Krothapalli, and C. Shih *In* VKI, Laser Velocimetry, Volume 2 1991 10 p (For primary document see N91-31625 23-36)
Copyright Avail: NTIS HC/MF A10

N91-31631# Institut Franco-Allemand de Recherches, Saint-Louis (France).
REVIEW OF TYPICAL APPLICATIONS. PART 1: MEASUREMENTS IN LIQUID FLOWS, FREE JETS, COMBUSTION, AND IN THE ATMOSPHERE
Hans-Joachim Pfeifer *In* VKI, Laser Velocimetry, Volume 2 1991 14 p (For primary document see N91-31625 23-36)
Copyright Avail: NTIS HC/MF A10

N91-31633# Institut Franco-Allemand de Recherches, Saint-Louis (France).
POST-PROCESSING OF DATA
Hans-Joachim Pfeifer *In* VKI, Laser Velocimetry, Volume 2 1991 24 p (For primary document see N91-31625 23-36)
Copyright Avail: NTIS HC/MF A10

35 INSTRUMENTATION AND PHOTOGRAPHY

Includes remote sensors; measuring instruments and gages; detectors; cameras and photographic supplies; and holography.

For aerial photography see *43 Earth Resources and Remote Sensing.* For related information see also *06 Aircraft Instrumentation,* and *19 Spacecraft Instrumentation.*

N91-31598 Pratt and Whitney Aircraft of Canada Ltd., Longueuil (Quebec).
CAPACITIVE BRIDGE-TYPE PROBE AND CONVERSION CIRCUITRY Patent
Kevin A. Dooley, inventor 28 Nov. 1989 12 p
(Patent-1-263-444; Int-Patent-Class-G01R-2726; CTN-91-60155)
Copyright Avail: Micromedia Ltd., Technical Information Centre, 165 Hotel de Ville, Place du Portage, Phase 2, Hull, Quebec J8X 3X2, Canada HC $4.00 CAN, MF $2.75 CAN

This invention relates to a structure for a capacitive bridge-type probe which is suitable for measuring the clearance between a fixed surface, such as the inner surface of the turbine shroud, and a member movable in relation to the fixed surface, such as the tip of a movable turbine blade. The system is comprised of a capacitance to voltage conversion circuit for converting changes in capacitance in the probe to voltage. The probe has a bridge with a sensitive arm and excitation means for providing an excitation signal to the capacitive bridge and a detector capable of detecting changes in the excitation signal across the sensitive arm due to changes in capacitance. An advantage of the system is the extremely high sensitivity which can be maintained while maintaining stability and wide bandwidth. Lab tests show sensitivity to changes of less than 10(exp -16) farad at bandwidths of 1 megahertz. This enables the use of a very small sensitive plate which reduces the overall size of the probe and improves the accuracy. CISTI

N91-31599 Pratt and Whitney Aircraft of Canada Ltd., Longueuil (Quebec).
CAPACITIVE BRIDGE-TYPE PROBE AND CONVERSION CIRCUITRY Patent
Kevin A. Dooley, inventor 28 Nov. 1989 27 p
(Patent-1-263-443; Int-Patent-Class-G01R-2726; CTN-91-60156)
Copyright Avail: Micromedia Ltd., Technical Information Centre, 165 Hotel de Ville, Place du Portage, Phase 2, Hull, Quebec J8X 3X2, Canada HC $4.00 CAN, MF $2.75 CAN

A structure for a capacitive bridge-type probe which is suitable for measuring the clearance between a fixed surface, such as the inner surface of the turbine shroud, and a member movable in relation to the fixed surface, such as the tip of a movable turbine blade, is described. The probe is comprised of a capacitance to voltage conversion circuit for converting changes in capacitance of the probe to a voltage. The conversion circuit uses offset means for providing a predetermined imbalance to the bridge thus providing automatic calibration of the circuit. The probe includes an elongated conductive casing filled with a dielectric material in which are embedded four arms, including at least one of which is a sensitive variable capacitance arm. The probe is mounted in the fixed surface such that the plate member of the sensitive arm faces the movable member. The character and magnitude of the dielectric medium between the plate member and the casing is sensitive to a change in clearance between the fixed surface and the movable member. An advantage of the system is the extremely high sensitivity which can be maintained while maintaining stability and wide bandwidth. Lab tests show sensitivity to changes of less than 10(exp -16) farad at bandwidths of 1 megahertz. This enables the use of a very small sensitive plate which reduces the overall size of the probe and improves the accuracy. CISTI

N91-31600 Grumman Aerospace Corp., Bethpage, NY.
SYSTEM AND METHOD FOR AUTOMATICALLY FABRICATING MULTIPLE MEMORY HOLOGRAPHIC ELEMENTS Patent
Kenneth G. Leib, inventor, Alexander N. Peck, II, inventor, and

Suey Jue, inventor 9 May 1989 40 p
(Patent-1-253-724; Int-Patent-Class-G03H-126; CTN-91-60175)
Copyright Avail: Micromedia Ltd., Technical Information Centre, 165 Hotel de Ville, Place du Portage, Phase 2, Hull, Quebec J8X 3X2, Canada HC $4.00 CAN, MF $2.75 CAN

A method is described for recording multiple holograms on an individual recording medium. The recording signal beam is passed through a gate to expose a plurality of beams to the signal beam to spatially modulate the beam. A matrix of beams is generated from the spatially modulated signal beam, each of the matrix beams converging on a different area on the recording medium. The matrix beam is passed through a mask and onto the recording medium to record a plurality of diffraction patterns on different areas of the recording medium. This system may be used in a number of other ways. A plurality of views of a single object may be exposed one at a time to the signal beams, without moving the mask, to form a plurality of non-coherent holograms on a particular area of the recording medium. The procedure may be repeated a number of times moving the mask so that an array of such non-coherent holograms are formed on the recording medium. Also, a different hologram may be made on a different area of the recording medium for each object presented to the signal beam. This system can be used to construct an array of many holograms, which may represent many targets or many views of the same target. A matched filter memory having a library of holograms can form the basis of an optical memory system for robot vision systems. CISTI

N91-31601 Maryland Univ., College Park.
ANALYSIS AND DEVELOPMENT OF A WIDE-BANDWIDTH GRAVITATIONAL WAVE DETECTOR Ph.D. Thesis
Yi Pang 1990 217 p
Avail: Univ. Microfilms Order No. DA9121402

The theory and design of multi-mode bar detectors of gravitational waves and the construction and test of a five-mode system are discussed. The theory includes the calculation of the energy absorbed from a pulse of gravitational radiation, the calculation of the energy transfer from the bar antenna to the electromechanical transducer, the detector noise analysis, and an algorithm for the design of the optimum filter for gravitational signal retrieval. Design and construction efforts were focussed on a five-mode system. The use of finite element methods (FEM's), computer-aided design (CAD), and results from tests on a 10 g niobium resonator in the design of multi-mode systems and in the construction of a specific five-mode system. The results of tests of that five-mode system carried at room temperature are given. The energy transfer from the bar to the fifth resonator is determined to be high (67 percent) and completed within 4.6 ms, which leads to an effective detector bandwidth of approximately 500 Hz. Dissert. Abstr.

N91-31602# Los Alamos National Lab., NM.
HIGH-SPEED TV CAMERAS FOR STREAK TUBE READOUT
G. J. Yates, R. A. Gallegos, V. H. Holmes, and B. T. Turko (California Univ., Berkeley. Lawrence Berkeley Lab.) 1991 15 p Presented at the Society of Photo-Optical Instrumentation Engineers (SPIE) Meeting, San Diego, CA, 21-26 Jul. 1991
(Contract W-7405-eng-36)
(DE91-016081; LA-UR-91-2144; CONF-9107115-16) Avail: NTIS HC/MF A03

Two fast framing TV cameras have been characterized and compared as readout media for imaging of 40 mm diameter streak tube (P-11) phosphor screens. One camera is based upon a Focus-Projection-Scan (FPS) high-speed electrostatic deflected vidicon with 30-mm-diameter PbO target. The other uses an interline transfer charge-coupled device (CCD) with 8.8 x 11.4 mm rectangular Si target. The field-of-view (FOV), resolution, responsivity, and dynamic range provided by both cameras when exposed to short duration (approximately 10 microns full width at half maximum) transient illumination followed by a single field readout period of less than 3 ms are presented. DOE

N91-31603# Poitiers Univ. (France). Lab. de Mecanique des Fluides.
AUTOMATIC ANALYSIS OF VISUALIZATION NEGATIVES Summary Report [ANALYSE AUTOMATISEE DE CLICHES DE VISUALISATIONS D'ECOULEMENTS]
Marie-France Collin, Madelaine Coutanceau, Alain Texier, Annie Dulieu, and TaPhuoc Loc (Laboratoire d'Informatique pour la Mecanique et les Sciences de l'Ingenieur, Paris, France) Mar. 1990 60 p In FRENCH
(Contract DRET-87-212)
(ETN-91-99971) Avail: NTIS HC/MF A04

An automatic system to quantatively exploit flow visualization negatives obtained with individualized solid tracers with a view to unsteady inviscid flow analysis is proposed. The system is tested on the flow around a NACA 012 airfoil at 30 degree incidence submitted to an impulsive start. The analysis chain consists of an image reader and processing system. The possibility of analyzing three dimensional flow is considered. ESA

N91-31604# Institut de Mecanique des Fluides de Lille (France). Groupe Mecanique des Fluides Appliquee.
SPECIAL DESIGN AND GAUGING OF ANEMOCLINOMETRIC SONDES [CONCEPTION ET ETALONNAGE SPECIAUX DE SONDES ANEMOCLINOMETRIQUES]
O. Desreumaux, P. Bailleux, and J. P. Bourez 14 Mar. 1990 56 p In FRENCH
(Contract DRET-89-003)
(IMFL-90/03; ETN-91-99977) Avail: NTIS HC/MF A04

A gauging method for anemoclinometry sondes is presented. The method is based on the combined use and balancing of several pressure detectors for the definition of kinetic pressure provided by the sonde, as well as over an overlay in several angular field regions, thus the gauging scale, for the bipolynomial smoothing. Using the method, gauging and anemoclinometry sonde utilization are possible up to angle of at least 50 degree incidence and drag and eliminate the precision problems and scale creasing observed from about 30 degrees with the classical method. The method is implemented on classical sondes as well as on miniaturized sondes specially designed for this application. ESA

N91-31605*# National Aeronautics and Space Administration. Lewis Research Center, Cleveland, OH.
LASER INTERFEROMETRIC MEASUREMENT OF ION ELECTRODE SHAPE AND CHARGE EXCHANGE EROSION
Gregory S. MacRae and Carolyn R. Mercer 1991 17 p Presented at the 27th Joint Propulsion Conference, Sacramento, CA, 24-27 Jun. 1991; cosponsored by AIAA, SAE, ASME, and ASEE Previously announced in IAA as A91-45786
(NASA-TM-105165; E-6454; NAS 1.15:105165; AIAA-91-2121)
Avail: NTIS HC/MF A03 CSCL 14B

A projected fringe profilometry system was applied to surface contour measurements of an accelerator electrode from an ion thrustor. The system permitted noncontact, nondestructive evaluation of the fine and gross structure of the electrode. A 3-D surface map of a dished electrode was generated without altering the electrode surface. The same system was used to examine charge exchange erosion pits near the periphery of the electrode to determine the depth, location, and volume of material lost. This electro-optical measurement system allowed rapid, nondestructive, digital data acquisition coupled with automated computer data processing. In addition, variable sensitivity allowed both coarse and fine measurements of objects having various surface finishes. Author

N91-31606*# National Aeronautics and Space Administration. Marshall Space Flight Center, Huntsville, AL.
MULTIPLEXING READOUT CHANNELS IN PROPORTIONAL COUNTERS
James Caristi Aug. 1991 25 p
(NASA-TM-103552; NAS 1.15:103552) Avail: NTIS HC/MF A03 CSCL 14B

Proportional counters are important instruments used in sensing hard x-rays. The possibility is described of doubling the number

of readout channels in the detector without increasing the electronics needed to amplify channel signals. This suggests that it should be possible, conversely, to reduce the number of amplifiers, thereby reducing the weight and energy budget of the instrument. Various numerical multiplexing schemes are analyzed, and a computer program is presented that can reconstruct multiplexed channel outputs with very good accuracy. Author

N91-31607*# Alabama Univ., Birmingham. Dept. of Physics.
DESIGN AND ANALYSIS OF MULTILAYER X RAY/XUV MICROSCOPE Final Report, 1 May 1989 - 31 Jan. 1990
David L. Shealy 1 Apr. 1990 79 p
(NASA Order H-80589-B)
(NASA-CR-184197; NAS 1.26:184197) Avail: NTIS HC/MF A05 CSCL 14B

The design and analysis of a large number of normal incidence multilayer x ray microscopes based on the spherical mirror Schwarzschild configuration is examined. Design equations for the spherical mirror Schwarzschild microscopes are summarized and used to evaluate mirror parameters for microscopes with magnifications ranging from 2 to 50x. Ray tracing and diffraction analyses are carried out for many microscope configurations to determine image resolution as a function of system parameters. The results are summarized in three publication included herein. A preliminary study of advanced reflecting microscope configurations, where aspherics are used in place of the spherical microscope mirror elements, has indicated that the aspherical elements will improve off-axis image resolution and increase the effective field of view. Author

N91-31608* National Aeronautics and Space Administration. Lewis Research Center, Cleveland, OH.
PLUG-TYPE HEAT FLUX GAUGE Patent
Curt H. Liebert, inventor (to NASA) and John Koch, Jr., inventor (to NASA) 17 Sep. 1991 7 p Filed 31 May 1990 Supersedes N91-13685 (29 -5, p 663)
(NASA-Case-LEW-14967-1; US-Patent-5,048,973;
US-Patent-Appl-SN-531433; US-Patent-Class-374-29;
US-Patent-Class-374-180; US-Patent-Class-374-208;
US-Patent-Class-250-356.1; US-Patent-Class-136-200;
Int-Patent-Class-G01K-17/16; Int-Patent-Class-G01K-17/06)
Avail: US Patent and Trademark Office CSCL 14B

A plug-type heat flux gauge formed in a material specimen and having a thermoplug integrally formed in the material specimen, and a method for making the same are disclosed. The thermoplug is surrounded by a concentric annulus, through which thermocouple wires are routed. The end of each thermocouple wire is welded to the thermoplug, with each thermocouple wire welded at a different location along the length of the thermoplug. The thermoplug and concentric annulus may be formed in the material specimen by electrical discharge machining and trepanning procedures.
Official Gazette of the U.S. Patent and Trademark Office

N91-31609*# Photon Research Associates, Inc., Cambridge, MA. Research Div.
ADVANCED OPTICAL SENSING AND PROCESSING TECHNOLOGIES FOR THE DISTRIBUTED CONTROL OF LARGE FLEXIBLE SPACECRAFT Final Report
G. M. Williams and J. C. Fraser Washington NASA Oct. 1991 131 p Prepared in cooperation with McDonnell-Douglas Space Systems Co., Huntsville, Al
(Contract NAS1-18763)
(NASA-CR-4399; NAS 1.26:4399) Avail: NTIS HC/MF A07 CSCL 20F

The objective was to examine state-of-the-art optical sensing and processing technology applied to control the motion of flexible spacecraft. Proposed large flexible space systems, such an optical telescopes and antennas, will require control over vast surfaces. Most likely distributed control will be necessary involving many sensors to accurately measure the surface. A similarly large number of actuators must act upon the system. The used technical approach included reviewing proposed NASA missions to assess system needs and requirements. A candidate mission was chosen as a baseline study spacecraft for comparison of conventional and optical control components. Control system requirements of the baseline system were used for designing both a control system containing current off-the-shelf components and a system utilizing electro-optical devices for sensing and processing. State-of-the-art surveys of conventional sensor, actuator, and processor technologies were performed. A technology development plan is presented that presents a logical, effective way to develop and integrate advancing technologies. Author

N91-31610# Los Alamos National Lab., NM.
CIRCULAR FORMAT ZIG-ZAG SCANNING OF VIDICON TUBES
C. G. Peterson and C. M. Simmons 1991 6 p Presented at the Society of Photo-Optical Instrumentation Engineers (SPIE) Meeting, San Diego, CA, 21-26 Jul. 1991
(Contract W-7405-eng-36)
(DE91-016084; LA-UR-91-2129; CONF-9107115-20) Avail: NTIS HC/MF A02

In an effort to increase camera readout speed, we have developed a nonconventional vidicon tube scanning technique. Because all vidicon targets are round, acquiring a full view requires overscanning with a conventional square format scan, resulting in 22 pct. of the video field time wasted. Furthermore, conventional scanning employs horizontal flyback, which for high frame rates can be more than 10 pct. of the total field time. Our nonconventional scanning technique eliminates flyback time by utilizing a triangular waveform rather than a sawtooth for horizontal deflection. This triangle wave is amplitude modulated in order to scan only the (circular) area of interest. The vertical deflection is a staircase ramp, with a step occurring at the end of each horizontal line. This maintains even spacing and a parallel relationship between horizontal lines, as opposed to skewed lines with conventional scans. To display the video ouput, the X-Y monitor must also be driven with these waveforms in order to maintain the correct temporal and spatial position of the video data. Sweep rates of 400 lines in a 1 ms field have been demonstrated. Test results using this technique show a frame time reduction of approx. 30 pct., with no loss of resolution or dynamic range, and no increased video bandwidth requirements. DOE

N91-31611# California Univ., Berkeley. Lawrence Berkeley Lab.
HIGH-T(SUB c) BOLOMETERS
P. L. Richards, J. Clarke, Q. Hu, R. Leoni, Ph. Lerch, M. Nahum, S. Verghese, M. R. Beasley, T. H. Geballe, and R. H. Hammond (Stanford Univ., CA.) et al Jun. 1991 3 p Presented at the International Superconductive Electronics Conference (ISEC '91), Glasgow, Scotland, 25-27 Jun. 1991
(Contract DE-AC03-76SF-00098)
(DE91-017009; LBL-30950; CONF-910623-2) Avail: NTIS HC/MF A01

High T sub c superconducting bolometers were studied for infrared and millimeter wavelengths. Measurements are described of the thermal boundary resistance between YBCO films and various substrates. This resistance is much larger than expected from the acoustic impedance mismatch model and a thermal time constant is given in the nanosecond range for typical YBCO films. Then, the design and experimental performance is discussed of two different types of high T sub c bolometric detectors. One is a conventional bolometer with a gold-black absorber. The other is an antenna-coupled microbolometer. Finally, there is a description of the ultimate performance expected from high T sub c bolometers on Si and Si3N4 membrane substrates, with comparisons to other detectors used for thermal imaging. DOE

N91-31612# Aerospace Corp., El Segundo, CA. Lab. Operations.
SENSITIVITY OF IMAGING MATERIALS TO ELECTRON BEAM IRRADIATION
Thomas W. Giants 1 Apr. 1991 44 p
(Contract F04701-88-C-0089)

(AD-A239365; TR-0090(5935-03)-5; SSD-TR-91-13) Avail: NTIS HC/MF A03 CSCL 20/5

A literature review was conducted in order to assess what approaches could be taken to enhance the sensitivity of PERM (processless electron recording media) film to electron beam irradiation. It was implied that the process for producing the film had been optimized with the current imaging component and that a different imaging component would be required. Among the few imaging compounds capable of being converted from a colorless to a colored product directly upon exposure to an electron beam without further processing are the substituted diacetylenes. The surveyed diacetylene literature revealed little previous work with regard to the electron beam imaging process. Much of the early work involved thermal, UV, and gamma radiation induced polymerization, primarily in the solid state. Only in the late 70s were soluble diacetylene polymers synthesized, creating the opportunity to study the solution chemistry of diacetylene polymerization. This result produced a wide variety of studies directed toward a better understanding of the structural changes that give rise to the observed chromic effects. GRA

N91-32024# Keuring van Electrotechnische Materialen N.V., Arnhem (Netherlands). Dept. of Physical Research.
EXPERIMENTS ON ULTRASONIC THERMOMETRY FOR WET-ASH COAL GASIFICATION
K. Schoonderwoerd and R. Hunik *In its* KEMA Scientific Reports, Volume 8, Number 2, 1990 Apr. 1990 p 81-96 (For primary document see N91-32023 23-99)
Avail: NTIS HC/MF A04

36 LASERS AND MASERS

Includes parametric amplifiers.
For related information see also *76 Solid-State Physics.*

N91-31613 Texas A&M Univ., College Station.
DYNAMICS OF 1.3 MICRON SEMICONDUCTOR LASERS AND NONLINEAR GAIN Ph.D. Thesis
Jinseob Eom 1990 94 p
Avail: Univ. Microfilms Order No. DA9118220

Optical modulation is used for the first time to determine the intrinsic frequency response of a laser diode. The measured frequency response does not have the undesirable signal rolloff caused by diode parasitics that occurs with direct RF current modulation. The ability to obtain parasitic-free data creates new opportunities for studying the dynamics of semiconductor lasers. Using the optical modulation technique, the origin of nonlinear gain in 1.3 micron InGaAsP semiconductor diode lasers was studied by measuring the magnitude and phase of the laser's intrinsic frequency response. The measured results indicate that a dielectric grating induced by stimulated emission in the laser cavity is important in determining the nonlinear gain. Since physical processes such as spectral hole burning, hot carriers, etc. are all induced by stimulated emission, it is not possible by this experiment alone to determine the process which is responsible for the dielectric grating. However, by comparison of the measured modulation K-factors of distributed feedback and Fabry-Perot lasers, it was found that the relaxation time associated with nonlinear gain for 1.3 micron InGaAsP semiconductor laser is about 0.1 ps. This short time constant indicates that spectral hole burning is the dominant process responsible for the stimulated emission induced dielectric grating, which causes the nonlinear gain. Using this technique, the rate of spontaneous emission into the guided modes, the nonlinear gain coefficient, and the carrier lifetime at lasing threshold are measured to unprecedented accuracy. These results are used in other work for understanding the noise properties of diode lasers. In addition, the modulation K-factor is shown for the first time to depend on the doping level for semiconductor lasers. This finding has important implication with regard to the issue of the upper modulation bandwidth of semiconductor lasers. Dissert. Abstr.

N91-31614# Von Karman Inst. for Fluid Dynamics, Rhode-Saint-Genese (Belgium).
LASER VELOCIMETRY, VOLUME 1
A. Boutier 1991 345p Lecture series held in Rhode-Sainte-Genese, Belgium, 10-14 Jun. 1991
(VKI-1991-05-Vol-1; ISSN-0377-8312; ETN-91-99905) Copyright Avail: NTIS HC/MF A15

A lecture series providing an opportunity for scientists to become acquainted with the state of the art of laser velocimetry is presented. A large part of the course was also devoted to fundamentals. The main focus was on laser Doppler and laser transit velocimetry. The recent methods of particle image velocimetry and particle size measurement methods were also presented. The main lecturers discussed most of the practical problems associated with these measurement techniques. Seeding methods were presented as well as the latest Doppler signal processing techniques which were compared to conventional techniques. Biasing of data and overall accuracy of the measurements were also the subject of several lectures. The very recent methods of image capture and processing used in particle image velocimetry were described and examples of applications of all the laser velocimetry techniques are discussed. For individual titles, see N91-31615 through N91-31624.

N91-31615# Office National d'Etudes et de Recherches Aerospatiales, Paris (France).
INTRODUCTION TO LASER VELOCIMETER TECHNIQUES
A. Boutier *In* VKI, Laser Velocimetry, Volume 1 1991 9 p (For primary document see N91-31614 23-36)
Copyright Avail: NTIS HC/MF A15

Laser velocimetry is an optical technique which locally measures instantaneous flow velocities. The various ways to determine this velocity parameter, which have led to various concepts for optical schemes are introduced. The vocabulary associated to the different setups is given; advantages and problems related to this measurement technique are listed. ESA

N91-31616# Office National d'Etudes et de Recherches Aerospatiales, Paris (France).
BASIC LDV1 COMPONENT SYSTEM
A. Boutier *In* VKI, Laser Velocimetry, Volume 1 1991 39 p (For primary document see N91-31614 23-36)
Copyright Avail: NTIS HC/MF A15

To measure one velocity component, the four different optical setups deduced from the theory of the Doppler effect are described; the most widely used 'fringe' LDV (Laser Doppler Velocimetry) is more detailed: signal to noise ratio evaluation, velocity sign determination, general structure of the emitting and receiving optics. ESA

N91-31617# Institut Franco-Allemand de Recherches, Saint-Louis (France).
FUNDAMENTALS OF SIGNAL PROCESSING
Hans-Joachim Pfeifer *In* VKI, Laser Velocimetry, Volume 1 1991 15 p (For primary document see N91-31614 23-36)
Copyright Avail: NTIS HC/MF A15

An introduction to data acquisition in laser Doppler anemometry is presented. Single particle systems are described, such as they are if the particles are well separated in time. Nowadays, this situation is the most frequent one in laser Doppler anemometry, at least as far as gaseous flows are considered. Special emphasis is devoted to possible source causes of imperfect signal shape. Multiple particle systems are addressed, as they are observed in many liquid flows and in heavily seeded gaseous flows. ESA

N91-31618*# National Aeronautics and Space Administration. Langley Research Center, Hampton, VA.
GENERATION OF PARTICLES AND SEEDING
James F. Meyers *In* VKI, Laser Velocimetry, Volume 1 1991 43 p (For primary document see N91-31614 23-36)
Copyright Avail: NTIS HC/MF A15 CSCL 20E

One of the most important elements in laser velocimetry, yet the most neglected, is the small particle embedded in the flow

field that scatters the light necessary to make velocity measurements. An attempt to remove the confusion in choosing a seeding method by assessing many of the techniques currently used is presented. Their characteristics and typical limitations imposed by various applications are outlined. The ramifications of these methods on measurement accuracy are addressed. ESA

N91-31619# Office National d'Etudes et de Recherches Aerospatiales, Paris (France).
ADVANCED SYSTEMS: MULTICOMPONENT LDV
A. Boutier *In* VKI, Laser Velocimetry, Volume 1 1991 21 p (For primary document see N91-31614 23-36)
Copyright Avail: NTIS HC/MF A15

In its earlier stage of development, Laser Doppler Velocimetry (LDV) gave only one component of the local velocity; progressively two velocity components were simultaneously measured (for two dimensional flow investigations), and nowadays the local velocity vector can be obtained, which is of particular interest in three dimensional complex flows. The great variety of systems able to provide three velocity components simultaneously is reviewed; among these setups, the most operational three dimensional LV is based on a probe volume formed by three fringe patterns, with different directions in space and with three colors. Nevertheless, this optimal concept of a three dimensional LV may lead to several mechanical and optical structurers, the merits of which are discussed. ESA

N91-31620# Institut Franco-Allemand de Recherches, Saint-Louis (France).
SIGNAL PROCESSING: TIME DOMAIN AND FREQUENCY DOMAIN
Hans-Joachim Pfeifer *In* VKI, Laser Velocimetry, Volume 1 1991 30 p (For primary document see N91-31614 23-36)
Copyright Avail: NTIS HC/MF A15

A review of currently existing signal acquisition techniques in Laser Doppler Anemometry (LDA) is presented. It relies on the foregoing lectures on fundamentals of LDA and on fundamentals of signal processing. Emphasis is put on counter processors which are still the most frequently used instruments and on recently developed fast Fourier transform processors. However, other instruments such as frequency trackers, photon correlators, filter banks, and transient recorders are mentioned. ESA

N91-31621*# National Aeronautics and Space Administration. Langley Research Center, Hampton, VA.
BIASING ERRORS AND CORRECTIONS
James F. Meyers *In* VKI, Laser Velocimetry, Volume 1 1991 36 p (For primary document see N91-31614 23-36)
Copyright Avail: NTIS HC/MF A15 CSCL 20E

The dependence of laser velocimeter measurement rate on flow velocity is discussed. Investigations outlining that any dependence is purely statistical, and is nonstationary both spatially and temporally, are described. Main conclusions drawn are that the times between successive particle arrivals should be routinely measured and the calculation of the velocity data rate correlation coefficient should be performed to determine if a dependency exists. If none is found, accept the data ensemble as an independent sample of the flow. If a dependency is found, the data should be modified to obtain an independent sample. Universal correcting procedures should never be applied because their underlying assumptions are not valid. ESA

N91-31622# Office National d'Etudes et de Recherches Aerospatiales, Paris (France).
ACCURACY OF LASER VELOCIMETRY
A. Boutier *In* VKI, Laser Velocimetry, Volume 1 1991 31 p (For primary document see N91-31614 23-36)
Copyright Avail: NTIS HC/MF A15

A great number of parameters must be taken into account in order to ensure a good confidence in laser velocimetry measurements; the accuracy is not given only by the resolution of the electronics; the influence of other parameters such as the calibration, the probe volume location and characteristics, and the particle behavior are discussed in addition to the way of making the statistics. ESA

N91-31623# Deutsche Forschungsanstalt fuer Luft- und Raumfahrt, Cologne (Germany, F.R.).
LASER TRANSIT VELOCIMETRY
Richard Schodl *In* VKI, Laser Velocimetry, Volume 1 1991 96 p (For primary document see N91-31614 23-36)
Copyright Avail: NTIS HC/MF A15

A description of the development and a review of various publications of the Laser Two Focus (L2F) velocimetry are presented. The capability of the L2F system at close to wall measurements could be further improved. Results of measurements in a very small flow channel and in a small turbocharger compressor rotor are presented. The influence of beam diameter-beam separation ratio on the measuring accuracy and on the measuring time is treated. A multicolor two dimensional system with selectable beam separation is presented, which enables a considerable measuring time reduction particularly in flows of high turbulence intensities. Two different three dimensional L2F methods are introduced, the crossed beam method and the method which is based on an axial displacement between start and stop beam centers. The optical setups and the signal processing are described and some first experimental results are shown and compared with theoretical data from a computer simulation of the measuring procedure. L2F systems based on optical fibers are discussed. ESA

N91-31624# Deutsche Forschungsanstalt fuer Luft- und Raumfahrt, Cologne (Germany, F.R.). Inst. fuer Antriebstechnik.
LASER TRANSIT VELOCIMETRY: RECENT PUBLICATIONS
Wolfgang Foerster, Richard Schodl, Manfred Beversdorff, Anton Klemmer, and Elza Rijmenants *In* VKI, Laser Velocimetry, Volume 1 1991 7 p (For primary document see N91-31614 23-36)
Copyright Avail: NTIS HC/MF A15

Two improved methods to extend the Laser 2 Focus technique to three dimensional flow measurements in turbomachines are presented. The first one uses the method of inclined beams with a rather small coupling angle. The second one takes advantage of the on axis sensitivity of axially displaced measurement volumes. The principle design of both systems is shown as well as basic and critical tests to verify the system performance in three dimensional flow. Results of a comparison measurement of both systems in a propfan test rig are presented and discussed. ESA

N91-31625# Von Karman Inst. for Fluid Dynamics, Rhode-Saint-Genese (Belgium).
LASER VELOCIMETRY, VOLUME 2
A. Boutier 1991 216p Lecture series held in Rhode-Sainte-Genese, Belgium, 10-14 Jun. 1991
(VKI-1991-05-Vol-2; ISSN-0377-8312; ETN-91-99906) Copyright Avail: NTIS HC/MF A10

A lecture series providing an opportunity for scientists to become acquainted with state of the art laser velocimetry is presented. A large part of the course was also devoted to fundamentals. The main focus being on laser Doppler and laser transit velocimetry, the recent methods of particle image velocimetry and particle size measurement methods were also presented. The lecturers discussed most of the practical problems associated with these measurement techniques. Seeding methods were presented as well as the latest Doppler signal processing techniques which were compared to conventional techniques. Biasing of data and overall accuracy of the measurements were also the subject of several lectures. The very recent methods of image capture and processing used in particle image velocimetry were described and examples of applications of all the laser velocimetry techniques were discussed. For individual titles, see N91-31626 through N91-31633.

N91-31626# Office National d'Etudes et de Recherches Aerospatiales, Paris (France).
ADVANCED AND NON-CONVENTIONAL OPTICAL SCHEMES

A. Boutier *In* VKI, Laser Velocimetry, Volume 2 1991 37 p (For primary document see N91-31625 23-36)
Copyright Avail: NTIS HC/MF A10

If most of LV (Laser Velocimetry) setups are based on a fringe pattern configuration in the probe volume, new trends appear in the technology, making use of fiber optics and aiming at building miniature equipments. The optical spectrum analysis of the Doppler shifted laser light gives rise to new set ups, either for local measurements or for planar velocity pictures of the flow. Several other specific instruments are described which allow measurements in special difficult situations. The ways to overcome practical problems in large facilities are evoked and some useful recommendations concerning the security to be applied around a LV are given. ESA

N91-31627# Institut National des Sciences Appliquees, Routen (France). Lab. d'Energetique des Systemes et Procedes.
QUASI-ELASTIC LIGHT SCATTERING AND APPLICATIONS TO OPTICAL SIZING
G. Gousbet *In* VKI, Laser Velocimetry, Volume 2 1991 15 p (For primary document see N91-31625 23-36)
Copyright Avail: NTIS HC/MF A10

Advances in quasi elastic light scattering theory (generalized Lorenz-Mie theory) and applications to optical sizing and diagnosis are addressed. Three measurement techniques are discussed: top hat beam technique, visible infrared double extinction technique, and quasi elastic light scattering spectroscopy. ESA

N91-31628# Florida State Univ., Tallahassee. Coll. of Engineering.
PARTICLE IMAGE VELOCIMETRY: PHOTOGRAPHIC AND VIDEO TECHNIQUES
L. M. Lourenco *In* VKI, Laser Velocimetry, Volume 2 1991 44 p (For primary document see N91-31625 23-36)
Copyright Avail: NTIS HC/MF A10

The basic principles behind LSV (Laser Speckle Velocimetry) and PIV (Particle Image Velocimetry) techniques are described. The various methods of data acquisition and reduction are addressed and some parameters that affect its utilization and some examples of its use are presented. ESA

N91-31629# Florida State Univ., Tallahassee. Coll. of Engineering.
UNSTEADY FLOW PAST AN AIRFOIL PITCHING AT A CONSTANT RATE **c34**
C. Shih, L. M. Lourenco, L. VanDommelen, and A. Krothapalli *In* VKI, Laser Velocimetry, Volume 2 1991 25 p Sponsored by AFOSR (For primary document see N91-31625 23-36)
Copyright Avail: NTIS HC/MF A10

The unsteady flow past a NACA 0012 airfoil in pitching up motion is experimentally investigated in a water towing tank using the Particle Image Displacement Velocimetry (PIDV) technique. The Reynolds number, based on the airfoil chord and the freestream velocity, is 5000. The airfoil pitching motion is from 0 to 30 degrees angle of attack at a dimensionless pitch rate alpha of 0.131. Instantaneous velocity fields at different times were acquired over the entire flow field. Using the whole field data, the out of plane component of vorticity is computed. The following features are observed. Boundary layer separation near the airfoil leading edge leads to the formation of a vortical structure. The evolution of this vortex along the upper surface dominates the aerodynamic performance of the airfoil. Complete stall emerges when the boundary layer near the leading edge detaches from the airfoil, under the influence of the vortex. The vortex further triggers the shedding of a counter rotating vortex near the trailing edge. A parallel computational study using the discrete vortex, random walk approximation was conducted. In general, the computational results agree very well. ESA

N91-31630# Florida State Univ., Tallahassee. Coll. of Engineering.
VORTEX INTERACTIONS IN THE TRANSITION REGION OF A RECTANGULAR JET **c34**
L. M. Lourenco, A. Krothapalli, and C. Shih *In* VKI, Laser Velocimetry, Volume 2 1991 10 p (For primary document see N91-31625 23-36)
Copyright Avail: NTIS HC/MF A10

An experimental investigation of the large scale vortical structures in the transition region of a rectangular jet of aspect ratio 4 at a Reynolds number, based on the equivalent diameter, of 4500 is described. The instanteous 2-D flow for the first 4 equivalent diameters in the jet was measured using the Particle Image Displacement Velocimetry (PIDV) technique. This technique provides an instantaneous velocity field measurement capability with good spatial resolution, from which the vorticity field can be computed accurately. The kinematics of the vortex interaction process are described in terms of the formation and evolution of coherent vorticity distributions. An important observation is that the interaction process of cylindrical vortices is not unique and consists of several different events. Two such processes which are typical of rectangular jets are described. ESA

N91-31631# Institut Franco-Allemand de Recherches, Saint-Louis (France).
REVIEW OF TYPICAL APPLICATIONS. PART 1: MEASUREMENTS IN LIQUID FLOWS, FREE JETS, COMBUSTION, AND IN THE ATMOSPHERE **c34**
Hans-Joachim Pfeifer *In* VKI, Laser Velocimetry, Volume 2 1991 14 p (For primary document see N91-31625 23-36)
Copyright Avail: NTIS HC/MF A10

Some highlights on the application of fringe type laser Doppler anemometers to fluid flow research are presented. The examples selected are applications to liquid flows with some reference to two phase flows and phase Doppler anemometry followed by studies in gaseous free jets and in combustion. Some information on wind velocity measurements in the atmosphere is given. ESA

N91-31632*# National Aeronautics and Space Administration. Langley Research Center, Hampton, VA.
REVIEW OF TYPICAL APPLICATIONS: WIND TUNNELS **c09**
James F. Meyers *In* VKI, Laser Velocimetry, Volume 2 1991 43 p (For primary document see N91-31625 23-36)
Copyright Avail: NTIS HC/MF A10 CSCL 14B

Laser velocimetry applications to wind tunnels are highlighted. The following are covered: investigation of the flow within a metalorganic chemical vapor deposition reactor; helicopter flow investigations in the 4 by 7 m low speed wind tunnel; boundary layer measurements in a supersonic flow using a laser transit anemometer; basic aerodynamic research tunnel. The future of wind tunnel testing with laser velocimetry. ESA

N91-31633# Institut Franco-Allemand de Recherches, Saint-Louis (France).
POST-PROCESSING OF DATA **c34**
Hans-Joachim Pfeifer *In* VKI, Laser Velocimetry, Volume 2 1991 24 p (For primary document see N91-31625 23-36)
Copyright Avail: NTIS HC/MF A10

The post processing of Laser Doppler Anemometer (LDA) data has comparable influence on the final results, e.g. reliability, accuracy etc., as well as all the other aspects of LDA instruments. This is due to the fact that signal statistics in LDA are completely different from signal statistics well known in other measuring procedures where the continuous time history of the physical quantity under consideration is available. Four topics are presented: statistical quantities such as mean velocity, turbulence intensity, and histograms; filter control for both counter processors and FFT processors; auto and cross correlation and their Fourier transform; post processing of photon correlograms. ESA

N91-31634# Sandia National Labs., Albuquerque, NM.
A SIMPLE MODEL FOR THE MOTION OF PULSED-LASER-DRIVEN THIN FLYERS
R. J. Lawrence and W. M. Trott 1991 7 p Presented at the 3rd International Conference on Mechanical and Physical Behavior of Materials Under Dynamic Loading, Strasbourg, France, 14-18 Oct. 1991

(Contract DE-AC04-76DP-00789)
(DE91-011325; SAND-91-0946C; CONF-911069-2) Avail: NTIS HC/MF A02

A model that predicts the final velocity of high-power, pulsed-laser-driven thin flyers is described. The required input parameters can either be obtained from standard handbooks or simply extracted from one set of data. The model yields a number of features and scaling laws that are well verified by experiment. Specific comparisons of model predictions with experimental results illustrate excellent agreement for variations of laser fluence and pulse width as well as flyer diameter and thickness. DOE

N91-31635# Messerschmitt-Boelkow-Blohm G.m.b.H., Ottobrunn (Germany, F.R.). Zentralbereich Technik.
THE MICROCRYSTAL LASER: A FIRST STEP ON THE WAY TO A LASER MICROSYSTEM [MIKROKRISTALL-LASER: EIN ERSTER SCHRITT AUF DEM WEG ZUM MIKROSYSTEM-LASER]
Peter Peuser, Stefan Heinemann, Walter Kroy, Axel Mehnert, and Nikolaus-P. Schmitt 1990 6 p In GERMAN Presented at the Symposium 'Stand und Perspektive des Festkoerperlasers', Berlin, Fed. Republic of Germany, 26 Apr. 1990
(MBB-Z-0336-90-PUB; OTN-030852; ETN-91-99758) Avail: NTIS HC/MF A02

It is shown that the concept of a microcrystal laser for the production of monomode frequency stable radiation proved very successful. Laser stimulated semiconductors and submillimeter monolithic lasers were experimentally examined. The experiments showed that the polarization direction of the pump radiation is of importance in obtaining maximum efficiency. They also showed that a diode laser pumped solid state laser can be extremely miniaturized, and that additional, completely new, interesting laser properties could accrue from miniaturization. ESA

N91-31636# Bertin et Cie., Aix-les-Milles (France).
REAL TIME ACTUATING OF LASER POWER AND SCANNING VELOCITY FOR THERMAL REGULATION DURING LASER HARDENING
F. Bataille, D. Kechemair, and R. Houdjal (Etablissement Technique Central de l'Armement, Arcueil, France) 1991 5 p Presented at ECO4: The International Congress on Optical Science and Engineering, The Hague, Netherlands, 11-15 Mar. 1991
(ETN-91-99908) Avail: NTIS HC/MF A01

Real time control during multikilowatt CO2 laser surface treatments is required to improve reproducibility, to simplify applications to complex geometry workpieces and to deal with a very kind of unsteady situation. A strategy involving automation was chosen, using linearization around some working points to solve nonlinear problems. Surface temperature was measured by a scanning pyrometer and a real time temperature calculation allowed estimation of maximum temperatures at the chosen treatment depth. In the second step, maximum temperatures both at the surface and in the volume could be regulated simultaneously, by actuating the laser power and the scanning velocity. Applications to laser self quenching is detailed. The experimental set up and the complete closed loop automatic system are described. The experimental results of the closed loop system are displayed. Improvements of the regularity of the treatments are developed for complex geometry pieces. Another regulator was considered to ensure temperature cycles for 10 by 10 by 1 cu mm samples at a standstill in a controlled atmosphere chamber during titanium nitriding. ESA

N91-31637# Association Aeronautique et Astronautique de France, Paris.
LASER DOPPLER ANEMOMETER MINIATURIZED WITH DIODE LASER [ANEMOMETRIE LASER A EFFECT DOPPLER MINIATURISE A DIODE LASER]
S. Damp and Hans-Joachim Pfeifer (Institut Franco-Allemand de Recherches, Saint-Louis, France) 1989 16 p In FRENCH Presented at 26th Colloque d'Aerodynamique Appliquee, Toulouse, France, 23-25 Oct. 1990
(AAAF-NT-89-06; ISL-CO-224/878; ISBN-2-7170-0939-6; ISSN-0243-0177; ETN-91-99947) Avail: NTIS HC/MF A03; CEDOCAR, Section des Diffusions, 26 Blvd Victor, 75996 Paris Armees, France, HC 15 francs

An 11 by 4 by 4 cm miniaturized laser Doppler anemometer system using laser diodes is described. The system was tested with a velocity profile of a free jet. The use of synthetic resin optics would improve the miniaturization and reduce the cost of this type of system. ESA

N91-31638# Naval Research Lab., Washington, DC.
HYDRODYNAMIC TARGET RESPONSE TO AN INDUCED SPATIAL INCOHERENCE-SMOOTHED LASER BEAM
M. H. Emery, J. H. Gardner, R. H. Lehmberg, and S. P. Obenschain 23 Jul. 1991 43 p
(DE91-015757; NRL-MR-6853) Avail: NTIS HC/MF A03

One of the critical elements for high gain target designs is the high degree of symmetry that must be maintained in the implosion process. The induced spatial incoherence (ISI) concept has some promise for reducing ablation pressure nonuniformities to approximately 1 percent. The ISI method produces a spatial irradiance profile that undergoes large random fluctuations on picosecond time scales but is smooth on long time scales. The ability of the ISI method to produce a nearly uniform ablation pressure is contingent on both temporal smoothing and thermal diffusion. In the startup phase of a shaped reactor-like laser pulse, the target is directly illuminated by the laser light and thermal diffusion is not effective a smoothing residual nonuniformities in the laser beam. During this period in the laser pulse, the target response is dominated by the initial shock generated by the laser pulse and the results indicate that this first shock can be the determining factor in the success or failure of the implosion process. The results of numerical simulations of several target/laser pulse designs which were investigated in an attempt to mitigate the impact of the initial shock structure stemming from the early temporal phase of an ISI-smoothed laser beam are presented. It is shown that foam-like layers, multiple laser wavelengths and shallow angles of incidence can sharply reduce the perturbation level stemming from the first shock. DOE

N91-31639# Los Alamos National Lab., NM.
COMPARISON OF INTEGRATED NUMERICAL EXPERIMENTS WITH ACCELERATOR AND FEL EXPERIMENTS
L. E. Thode, B. E. Carlsten, K. C. D. Chan, R. K. Cooper, J. C. Elliott, S. J. Gitomer, J. C. Goldstein, M. E. Jones, B. D. McVey, and M. J. Schmitt et al 1991 20 p Presented at the Society of Photo-Optical Instrumentation Engineers (SPIE) Meeting, San Diego, CA, 21-26 Jul. 1991
(Contract W-7405-eng-36)
(DE91-016071; LA-UR-91-2248; CONF-9107115-23) Avail: NTIS HC/MF A03

Even at the conceptual level, the strong coupling between the laser subsystem elements, such as the accelerator, wiggler, optics, and control, greatly complicates the understanding and design of an FEL. Given the requirements for a high performance FEL, the coupling between the laser subsystems must be included in the design approach. To address the subsystem coupling the concept of an integrated numerical experiment (INEX) has been implemented. Unique features of the INEX approach are consistency and numerical equivalence of experimental diagnostic. The equivalent numerical diagnostics mitigates the major problem of misinterpretation that often occurs when theoretical and experimental data are compared. A complete INEX model has been applied to the 10 micron high-extraction-efficiency experiment at Los Alamos and the 0.6 micron Burst Mode experiment at Boeing Aerospace. In addition, various subsets of the INEX model have been compared with a number of other experiments. Overall, the agreement between INEX and the experiments is very good. With the INEX approach, it now appears possible to design high performance FELS for numerous applications. The first full scale test of the INEX approach is the Los Alamos HIBAF experiment. The INEX concept, implementation, and validation with experiments are discussed. DOE

N91-31640# Los Alamos National Lab., NM.
COMPACT FREE-ELECTRON LASER AT THE LOS ALAMOS NATIONAL LABORATORY
K. C. D. Chan, K. L. Meier, D. Nguyen, R. L. Sheffield, Tai-Sen F. Wang, R. W. Warren, W. L. Wilson, and L. M. Young 1991 11 p Presented at the Society of Photo-Optical Instrumentation Engineers (SPIE) Meeting, San Diego, CA, 21-26 Jul. 1991
(Contract W-7405-eng-36)
(DE91-016079; LA-UR-91-2170; CONF-9107115-25) Avail: NTIS HC/MF A03

The design and construction of second-generation free electron laser (FEL) system at Los Alamos will be described. Comprised of state of the art components, this FEL system will be sufficiently compact, robust and user friendly for application in industry, medicine, and research. DOE

N91-31641# City Coll. of the City Univ. of New York, NY. Dept. of Physics.
ELECTRONIC TRANSPORT AND LASING IN MICROSTRUCTURES
M. Lax 25 Jul. 1991 6 p
(Contract DE-FG02-84ER-45058)
(DE91-016751; DOE/ER-45058/7) Avail: NTIS HC/MF A02

We consider the interaction of hot carriers with hot phonons in a quantum well. Transport is considered in the transverse direction and tunneling through the well barriers. Time dependent transport effects down to the femto-second regime are included, as are strong and/or microwave fields, with negative resistance effects. Resonant tunneling assisted by phonon relaxation and infrared radiation are explored. Partition noise in semiconductor lasers has been considered. DOE

N91-31642# Lawrence Livermore National Lab., CA.
LASER ABLATION MECHANISMS AND OPTICAL SURFACE DAMAGE
L. L. Chase, A. V. Hamza, and H. W. H. Lee May 1991 11 p Presented at the HASRD Workshop on Laser Ablation: Mechanisms and Application, Oak Ridge, TN, 8-10 Apr. 1991
(Contract W-7405-eng-48)
(DE91-016928; UCRL-JC-106370; CONF-9104192-14) Avail: NTIS HC/MF A03

Laser ablation usually accompanies optical surface damage to bare surfaces and coatings. Investigations of optical damage mechanisms by observation of ablation processes at laser fluences very close to the optical damage threshold are described. Several promising surface characterization methods for investigating damage mechanisms are also described. The possible role of laser ablation in initiating or promoting optical surface damage is discussed. DOE

N91-31643# Air Force Inst. of Tech., Wright-Patterson AFB, OH.
APPLICATION OF MULTIVARIABLE CONTROL SYSTEM DESIGN METHODOLOGIES TO ROBUST BEAM CONTROL OF A SPACE-BASED LASER M.S. Thesis
Kelly D. Hammett Jun. 1991 179 p
(AD-A239460; AFIT/CI/CIA-91-058) Avail: NTIS HC/MF A09 CSCL 09/3

The complexity of large-scale dynamic systems provides a challenging proving ground for modern control system analysis and design techniques. High plant dimensionality inherent in large-scale systems can lead to breakdowns in numerics of state-space algorithms or intolerably long computational times, necessitating use of model reduction techniques. Reducing plant order consequently introduces unmodeled dynamics into the system, which must then be accounted for via stability and performance robustness considerations. A design framework is adopted herein which allows stability robustness to be guaranteed via unstructured uncertainty representation and the Small Gain Theorem, and performance robustness to be independently verified. The applicability of modern multivariable controller design techniques to large-scale systems is demonstrated by synthesis of robustly stable H2 optimal, H at infinity optimal, and H2/H at infinity loop-shaped compensators for a space-based laser forebody using reduced order models. Performance goals are expressed in terms of both allowable 2-norms and root-mean-square values of line-of-sight and segment phasing errors, and an evolutionary process leads to a final controller design. First, ideally performing but non-robust unconstrained bandwidth H2 and H at infinity designs are presented which illustrate the danger of ignoring unmodeled high-frequency dynamics. GRA

N91-31644# Massachusetts Inst. of Tech., Lexington. Lincoln Lab.
AN ADAPTIVE COHERENT OPTICAL RECEIVER ARRAY
L. B. Mercer 18 Jun. 1991 16 p
(Contract F19628-90-C-0002)
(AD-A239672; TR-921; ESD-TR-91-062) Avail: NTIS HC/MF A03 CSCL 20/6

A linear, four-element, adaptive heterodyne optical receiver array employing semiconductor lasers is described. The array adaptively adjusts the phase of each subaperture Intermediate Frequency signal to correct for wavefront tilt and distortion and nonuniform optical and Radio Frequency path delays across the array by phase locking each channel to a reference channel. Author (GRA)

37 MECHANICAL ENGINEERING

Includes auxiliary systems (nonpower); machine elements and processes; and mechanical equipment.

N91-31645# Computational Systems, Inc., Knoxville, TN.
DIAGNOSTIC TOOLS FOR RECIPROCATING ENGINE SYSTEMS Annual Report, 1990
J. F. Kirkpatrick Jan. 1991 65 p
(Contract GRI-5089-294-1795)
(PB91-184960; GRI-91/0041) Avail: NTIS HC/MF A04 CSCL 13I

The testing of used engine oils is described. The tests were conducted to verify the utility of on-line engine oil quality sensors being developed as part of a comprehensive microprocessor-based engine monitoring package. The test results compare the candidate on-line sensors with standard laboratory instruments used to measure lube oil condition. GRA

N91-31646 Ohio State Univ., Columbus.
ANALYSIS AND DEVELOPMENT OF A REAL-TIME CONTROL METHODOLOGY IN RESISTANCE SPOT WELDING Ph.D. Thesis
Wen-Long Dai 1991 169 p
Avail: Univ. Microfilms Order No. DA9120649

Presented here is a systematic approach to develop the expansion based control algorithm for resistance spot welding. The finite element method was used to simulate the welding process and to determine the physical response of the joint material to the various welding conditions. Direct correlations between nugget formation and expansion displacement between electrodes were obtained. By systematic computer simulations, a weldability characteristic curve for spot welding was developed. This weldability curve shows inadequate welding conditions which could cause nugget eupulsion current shunting. A welding duration curve, which shows the appropriate time for squeeze, weld, and hold cycles, was developed and used as a basis for in-process resistance spot welding control. Dissert. Abstr.

N91-31647 Rensselaer Polytechnic Inst., Troy, NY.
MODELING AND SIMULATION OF MULTIPLE COOPERATING MANIPULATORS ON A MOBILE PLATFORM Ph.D. Thesis
Stephen Henry Murphy 1990 190 p
Avail: Univ. Microfilms Order No. DA9120236

The problem is examined of modeling and simulation of multiple cooperating manipulators on a mobile platform. The system of cooperating robot manipulators forms a closed kinematic chain where the forces of interaction must be included in the formulation of robot and platform dynamics. The formulation includes the full

dynamic interactions from arms-to-platform and arm-tip to arm-tip and the possible translation and rotation of the platform. The structure of the closed chain dynamics allows the use of any solution for the open topological tree of base and manipulator links. A simulation of two cooperating manipulators on a mobile platform is presented and the motion is graphically displays. Additional dynamic model accuracy is achieved through the development of Newton-Euler modeling techniques for geared manipulators and manipulators with nonnegligible joint flexibility. The resulting Newton-Euler models of flexibly jointed manipulators and geared manipulators have many advantages over the traditional Lagrange-Euler methods; the complete effects of the gear rations and the gyroscopic effects of the spinning motor/gear are included in the recursive formulation. Dissert. Abstr.

N91-31648*# National Aeronautics and Space Administration. Lewis Research Center, Cleveland, OH.
SPUR-GEAR OPTIMIZATION USING SPUROPT COMPUTER PROGRAM
Harold H. Coe Sep. 1991 19 p
(DA Proj. 1L1-62211-A-47A)
(NASA-TM-104394; E-6210; NAS 1.15:104394;
AVSCOM-TR-90-C-014) Avail: NTIS HC/MF A03 CSCL 13I

A computer program developed for optimizing spur gear designs, SPUROPT, was updated by installing a new subroutine that uses AGMA 908-B89 standards to calculate the J-factor for determining tooth-bending stress. The updated SPUROPT program was then used to optimize a spur gear set for maximum fatigue life, minimum dynamic load, or minimum weight. All calculations were made with constraints on as many as 13 parameters by using three design variables: the number of teeth, diametral pitch, and tooth-face width. Results depended largely on constraints values. When the limiting bending stress was set at a high value, the optimal solution was the highest allowable number of teeth. When the allowable bending stress was lowered, the optimal solution moved toward the fewest number of teeth permitted. Final results were also affected by the amount of transmission error. A lower error permitted a higher number of teeth. Author

N91-31649# Oak Ridge National Lab., TN.
EFFECT OF CONVECTION ON WELD POOL DEVELOPMENT
T. Zacharia, S. A. David, and J. M. Vitek 1991 7 p Presented at the Fall Meeting of the Minerals, Metals and Materials Society of AIME and Materials Week of the American Society of Metals, Cincinnati, OH, 20-24 Oct. 1991
(Contract DE-AC05-84OR-21400)
(DE91-014213; CONF-911003-3) Avail: NTIS HC/MF A02

A computational study of the transient convective phenomena in the weld pool during gas tungsten arc (GTA) welding of Type 304 stainless steel is presented. The solution of the transport equations is based on a control volume approach that directly utilizes the integral form of the governing equations. The computational model considers buoyancy and electromagnetic and surface tension forces in the solution of convective heat transfer in the weld pool. In addition, the model includes weld metal vaporization and temperature-dependent thermophysical properties. The results confirm that the development of the weld pool is very sensitive to the convective flow in the weld pool. Theoretical predictions of the weld pool surface temperature distributions and the cross-sectional weld pool size and shape were compared with corresponding experimental measurements with good agreement. DOE

N91-31650# Oak Ridge National Lab., TN.
WELD POOL SOLIDIFICATION AND MICROSTRUCTURES
S. A. David and J. M. Vitek 1991 26 p Presented at the Fall Meeting of the Minerals, Metals and Materials Society of AIME and Materials Week of the American Society of Metals, Cincinnati, OH, 20-24 Oct. 1991
(Contract DE-AC05-84OR-21400)
(DE91-014263; CONF-911003-2) Avail: NTIS HC/MF A03

Solidification behavior controls the size and shape of grains, the rate and extent of segregation, the distribution of inclusions, the extent of defects such as porosity and hot-cracking, and, ultimately, the properties of weld metal. In the past, theories related to single crystal growth technology and castings have been extrapolated to describe weld metal solidification. However within the last two decades there have been several new developments in solidification theory. The paper will address the solidification behavior of a weld pool, incorporating recent advances in solidification theories. Basic principles from ingot, single crystal, and rapid solidification processes will be used to understand and explain observed weld metal microstructures. Finally, and most importantly, solidification parameters that control weld pool solidification such as temperature gradient and growth rate and the resultant undercooling have been correlated with weld metal microstructure. DOE

N91-31651# Oak Ridge National Lab., TN.
BES WELDING SCIENCE
S. A. David, comp. 1990 26 p
(Contract DE-AC05-84OR-21400)
(DE91-015625; ORNL/M-1276) Avail: NTIS HC/MF A03

The purpose of this report is to present work by the Oak Ridge National Laboratory, Massachusetts Institute of Technology, Pennsylvania State University, and the Colorado School of Mines in the BES Welding Science Program. The topics covered include: the fundamentals of welding; mass transfer during laser welding; the modelling of transport phenomena in weld pools; and the role of compositional and microstructural gradients on weld metal properties and behavior. DOE

N91-31652# Allied-Signal Corp., Kansas City, MO.
MICROWAVE MODULE YAG LASER WELD DEVELOPMENT
J. P. Dereskiewicz Jul. 1991 63 p
(Contract DE-AC04-76DP-00613)
(DE91-015750; KCP-613-4385) Avail: NTIS HC/MF A04

Advance microwave products require low weld heat input, hermetically sealed, lightweight metal packages with low thermal coefficients of expansion and high thermal conductivity. Large quantities of these microwave packages are required. Use of the Nd:YAG laser with high silicon aluminum alloys is presently the best solution for the stated design criteria. Studies were conducted on seven aluminum-silicon (Al-Si) alloy combinations: 4047 Al to 1100 Al, 4047 Al to 6061-T6 Al, 4047 Al to 4047 Al, A40 to 1100 Al, A40 to 6061-T6 Al, A40 to 4047 Al, and A40 to A40. Weldability and leak rate were evaluated. A minimum leak rate of 10(exp -6) atm cu cm/s of He was desirable. Weld metal hot-cracking was the major factor limiting the ability to achieve the low He leak rate. Si content and weld metal ductility have the greatest influence on hot-cracking. Electron probe microanalysis (EMP) determined that a hermetic weld with leak rates of better than 10(exp -6) atm cu cm/s of He could be obtained if silicon content in the weld metal was 7-26 weight percent silicon. Al-Si alloy combinations that would produce silicon contents in the desired range are 4047 to 4047, A40 to 1100, A40 to 6061-T6, and A40 to 4047. The recommended alloy combination is A40 to 1100 Al because the 1100 Al lid adds the most ductility to the weld metal when the preferred A40 housing is used. This added ductility absorbs more thermally induced stresses and reduces the likelihood of weld metal hot-cracking. Studies are planned to evaluate the effects of gold and nickel plating on weldability of Al-Si alloys. Other planned studies would evaluate temperature exposures around glass-to-metal connector seals during welding and the inclusion of purge tubes to the housing package for purge, backfill, and leak testing. DOE

N91-31653# Allied-Signal Aerospace Co., Kansas City, MO.
ECONOMIC ANALYSIS OF ROBOTIC TORQUE MEASUREMENT SYSTEM
J. R. Lembke Jul. 1991 13 p
(Contract DE-AC04-76DP-00613)
(DE91-016480; KCP-613-4368) Avail: NTIS HC/MF A03

A cleanroom robot is being used to measure the torque characteristic of rotary solenoids, replacing a manual measurement procedure. The system can test two different part numbers and

can distinguish between these parts without operator assistance. To make the system more cost-effective, several tests have been added to sequence. Bearing drag and coil resistance are measured, and the change in resistance due to coil heating is monitored. The insulation resistance between coil and housing is measured at 250 volts. The bar-coded serial number of each unit is read by passing the housing over a bar code wand. All information is used to generate a report for each unit tested, showing part number, serial number, measured data, and pass-fail notification. The system saves 0.114 standard hours per part compared to manual testing and generates a return on investment of over 20 percent. DOE

N91-31654*# National Aeronautics and Space Administration. Lewis Research Center, Cleveland, OH.
RECENT MANUFACTURING ADVANCES FOR SPIRAL BEVEL GEARS
Robert F. Handschuh and Robert C. Bill (Army Aviation Systems Command, Cleveland, OH.) 1991 14 p Presented at the Aerotech 1991, Long Beach, CA, 23-26 Sep. 1991; sponsored by SAE
(DA Proj. 1L1-62211-A-47A)
(NASA-TM-104479; E-6326; NAS 1.15:104479;
AVSCOM-TR-91-C-022) Avail: NTIS HC/MF A03 CSCL 13I

The U.S. Army Aviation Systems Command (AVSCOM), through the Propulsion Directorate at NASA LRC, has recently sponsored projects to advance the manufacturing process for spiral bevel gears. This type of gear is a critical component in rotary-wing propulsion systems. Two successfully completed contracted projects are described. The first project addresses the automated inspection of spiral bevel gears through the use of coordinate measuring machines. The second project entails the computer-numerical-control (CNC) conversion of a spiral bevel gear grinding machine that is used for all aerospace spiral bevel gears. The results of these projects are described with regard to the savings effected in manufacturing time. Author

N91-31655* National Aeronautics and Space Administration. Lyndon B. Johnson Space Center, Houston, TX.
POWER SAW Patent
Jimmy D. Bradley, inventor (to NASA) 13 Aug. 1991 10 p Filed 28 Feb. 1990 Supersedes N90-26340 (28 - 20, p 2872)
(NASA-Case-MSC-21469-1; US-Patent-5,038,473;
US-Patent-Appl-SN-486458; US-Patent-Class-30-92;
US-Patent-Class-30-388; Int-Patent-Class-B23D-21/06;
Int-Patent-Class-B26B-27/00; Int-Patent-Class-B26D-3/16) Avail: US Patent and Trademark Office CSCL 13I

A power saw is disclosed for space or robotic operations with jaw members for clamping to a work piece by an operation of a lever arm. The saw assembly is slidably mounted on the jaw assembly and fed into the work piece by a hand operated feed screw. The saw assembly includes a motor and gear belt. A current sensing circuit provides a current signal which actuates colored lights to visually depict the load on the saw blade during the cutting operations.
Official Gazette of the U.S. Patent and Trademark Office

N91-31656* National Aeronautics and Space Administration. Goddard Space Flight Center, Greenbelt, MD.
ROBOTIC TOOL CHANGE MECHANISM Patent
George M. Voellmer, inventor (to NASA) 3 Sep. 1991 9 p Filed 2 Nov. 1990 Supersedes N91-15556 (29 - 7, p 1012)
(NASA-Case-GSC-13239-1; US-Patent-5,044,063;
US-Patent-Appl-SN-608657; US-Patent-Class-29-568;
US-Patent-Class-294-86.4; US-Patent-Class-901-30;
Int-Patent-Class-B23Q-3/155) Avail: US Patent and Trademark Office CSCL 13I

An assembly of three major components is disclosed which included a wrist interface plate which is secured to the wrist joint of a robotic arm, a tool interface plate which is secured to each tool intended for use by the robotic arm, and a tool holster for each tool attached to the interface plate. The wrist interface plate and a selected tool interface plate are mutually connectable together through an opening or recess in the upper face of the interface plate by means of a notched tongue protruding from the front face of the wrist interface plate which engages a pair of spring-biased rotatable notched wheels located within the body of the tool interface plate. The tool holster captures and locks onto the tool interface plate by means of a pair of actuation claws including a locking tab and an unlocking wedge which operate respective actuation bosses on each of the notched wheels in response to a forward and backward motion of the tool interface plate as a result of motion of the robotic arm to either park the tool or use the tool.
Official Gazette of the U.S. Patent and Trademark Office

N91-31657# Allied-Signal Aerospace Co., Kansas City, MO.
EVALUATION OF THE INTERMITTENT GTA COLD WIRE FEED WELD SYSTEM
J. P. Dereskiewicz Aug. 1991 101 p
(Contract DE-AC04-76DP-00613)
(DE91-016477; KCP-613-4396) Avail: NTIS HC/MF A06

An intermittent gas tungsten arc cold wire feed process was statistically evaluated to determine the feasibility of applying this process to meet the 0.030-inch weld penetration and peak temperature requirements when unfavorable joint tolerances exist on a subassembly weld. The wire feed system was determined to only slightly benefit the welding process over normal pulsed gas tungsten arc welding using traditional wire feeding capabilities. However, the complexity of this process and extensive welding operator training and qualification does not outweigh the benefits of incorporating this synchronized pulse wire feed system in production. DOE

N91-31658# Lawrence Livermore National Lab., CA.
TECHNICAL ABSTRACTS: MECHANICAL ENGINEERING, 1990 Abstracts Only
J. Y. Broesius, comp. 1 Mar. 1991 86 p
(Contract W-7405-eng-48)
(DE91-016502; UCRL-ID-103495-90) Avail: NTIS HC/MF A05

This document is a compilation of the published, unclassified abstracts produced by mechanical engineers at Lawrence Livermore National Laboratory (LLNL) during the calendar year 1990. Many abstracts summarize work completed and published in report form. These are UCRL-JC series documents, which include the full text of articles to be published in journals and of papers to be presented at meetings, and UCID reports, which are informal documents. Not all UCIDs contain abstracts: short summaries were generated when abstracts were not included. Technical Abstracts also provides descriptions of those documents assigned to the UCRL-MI (miscellaneous) category. These are generally viewgraphs or photographs presented at meetings. An author index is provided at the back of this volume for cross referencing. DOE

N91-31659# Cornell Univ., Ithaca, NY.
A PROGRAM OF CONTINUING RESEARCH ON REPRESENTING, MANIPULATING, AND REASONING ABOUT PHYSICAL OBJECTS Quarterly Status Report, Apr. - Jun. 1991
John E. Hopcroft Jun. 1991 102 p
(Contract N00014-89-J-1946)
(AD-A239596) Avail: NTIS HC/MF A06 CSCL 13/9

One of the great deficiencies of today's robots is their lack of flexibility. Most industrial robots are capable only of simple and repetitive tasks, such as spot welding or spray painting. There are two main reasons for this deficiency. First, typical end-effectors use a very simple two stick structure. Second, dexterous manipulation (manipulation by grippers with independently moving fingers) is not well understood. Effective techniques for dexterous manipulation would have application within a wide range of areas, including industrial assembly, decontamination of nuclear plants, and exploration of remote environments (e.g., ocean bottoms or space). We are developing a new strategy, finger tracking for the autonomous manipulation of objects by multifinger robot hands. Most of the earlier efforts devoted to understanding dexterous manipulation have been devoted to grasping or to manipulation for task-specific problems. The finger tracking paradigm reorients

an object with a series of rotations effected by fine finger motions, in which the hand maintains contact with the object at all times. It is common for humans to reorient an object using extra fingers - those not needed for grasping. Finger tracking captures and formalizes these ideas. Our notion of manipulation refers to the reorientation of an object by a mechanical hand. The reorientation is accomplished by fine finger motions, with the object held in the hand through the entire process. GRA

38 QUALITY ASSURANCE AND RELIABILITY

Includes product sampling procedures and techniques; and quality control.

N91-31660 General Electric Co., Fairfield, CT.
X-RAY INSPECTION SYSTEM Patent
Douglas S. Steele, inventor, Larry C. Howington, inventor, James W. Schuler, inventor, Joseph J. Sostarich, inventor, Charles R. Wojciechowski, inventor, Theodore W. Sippel, inventor, Joseph M. Portaz, inventor, and Ralph G. Isaacs, inventor 29 Aug. 1989 162 p
(Patent-1-258-924; Int-Patent-Class-G01N-2318; Int-Patent-Class-G06F-1562; CTN-91-60162) Copyright Avail: Micromedia Ltd., Technical Information Centre, 165 Hotel de Ville, Place du Portage, Phase 2, Hull, Quebec J8X 3X2, Canada HC $4.00 CAN, MF $2.75 CAN

This invention presents an automated digital X-ray inspection system for evaluating aircraft engine gas turbine blades. An X-ray inspection system, comprised of the X-ray machine and the image system is described. The system may be operated manually or automatically. The manual mode allows the operator to image the blade, display the image, and repeat if necessary. The automatic system performs automatic flaw detection, flaw analysis, and blade disposition. The system has the following capabilities: it quickly identifies the location of flaws in a single turbine engine; it can make, accept, or reject decisions; or it can automatically position the blade at an inspection site for performing digital fluoroscopy and computed tomography inspections. Data for the latter two inspections are collected at a maximum view rate of 60 views per second and the images obtained are displayed for an operator in real time. It can also initiate analysis of X-ray data during the data acquisition time of the next blade to be inspected. Digital fluoroscopy and computed tomography images are archived for future reference. Inspections information is conveyed in a manner which permits its use in subsequent statistical analysis and as feedback for quality control and repair. CISTI

N91-31661 Ohio State Univ., Columbus.
THE DEVELOPMENT OF AN INTELLIGENT DIMENSIONAL INSPECTION ENVIRONMENT USING COORDINATE MEASURING MACHINES Ph.D. Thesis
Hong-Tzong Yau 1991 191 p
Avail: Univ. Microfilms Order No. DA9120741

Computer aided dimensional inspection has emerged as one of the key components in the modern manufacturing environment. Current development in Computer Integrated Manufacturing (CIM) systems has shown a continuous trend of achieving higher automation levels in dimensional inspection. The development is described of an intelligent dimensional inspection environment in manufacturing. The objective is to develop and advance the related knowledge and automation technologies in dimensional inspection for the implementation of a highly automated dimensional inspection system. CATIA of the IBM CAD/CAM system and a Sheffield CORDAX RS-30 Coordinate Measuring Machine (CMM) are used as the primary tools for system implementation. The basic structure of the intelligent inspection environment is examined. Five interrelated modules of the system, namely, inspection specification, automatic planning, inspection verification, CMM execution, and comparative analysis are developed and implemented. The proposed system can bridge the missing link between inspection and design and feed back measurement information for manufacturing compensation. Dissert. Abstr.

N91-31662# Laboratoire d'Automatique et d'Analyse des Systemes, Toulouse (France).
INTRUSION AND FAULT TOLERANCE COMPATIBILITY. PART 1: FAULT PROTECTION, CODING AND TOLERANCE STATE OF THE ART [COMPATIBILITE ENTRE TOLERANCE AUX INTRUSIONS ET TOLERANCE AUX FAUTES. PARTIE 1: SUR L'ETAT DE L'ART EN PROTECTION, CHIFFREMENT ET TOLERANCE AUX FAUTES]
Gilles Trouessin, Jean-Charles Fabre, and Yves Deswarte Nov. 1989 165 p In FRENCH
(Contract DRET/LAAS-CNRS-83-34-051-00-47)
(LAAS-89-395; ETN-91-99972) Avail: NTIS HC/MF A08

Basic concepts and definitions of the compatibility between fault and intrusion tolerance are reviewed. The antagonism engendered in the development of a high security system for both accidental (relating to reliability) and intentional (relating to the confidential and integrity security) faults is described. A solution to remedy this, by providing intrusion tolerance mechanisms using protection and coding techniques and by providing (accidental) fault tolerant mechanisms using recovery, autocheck components and masking techniques, is proposed. A fault and intrusion tolerant architecture, based on the Delta-4 project, is proposed. A totally different technique, fragmented data processing during information processing, is also considered. ESA

N91-31663# Allied-Signal Aerospace Co., Columbia, MD.
RELIABILITY MODELING OF DEPENDABLE DISTRIBUTED SYSTEMS Report, 1 May - 31 Jul. 1991
C. J. Walter and M. C. McElvany 31 Jul. 1991 11 p
(Contract N00014-91-C-0014)
(AD-A239734) Avail: NTIS HC/MF A03 CSCL 12/7

The overall goal of this project is to develop theory for improved reliability modeling of systems with mixed fault types. This also provides the basis for formal methods to be used in the specification design, construction and verification of ultra-reliable multiprocessor systems. We assume that a fault is an anomalous physical condition, the identified or hypothesized cause of an error, which may eventually lead to a failure, a loss of service. In the initial project phase, our goal is to develop a hybrid fault and static reliability model that addresses mixed fault types. An in depth study of faults, including their sources, their manifestations, and the techniques needed to reduce malicious fault effects, will then provide accurate inputs to the hybrid model. We partitioned our work into three tasks: analysis of static reliability models, investigation of faults, and evaluation of the impact of fault containment on fault effects and on system reliability. GRA

N91-31664# Allied-Signal Aerospace Co., Columbia, MD.
THE POTENTIAL IMPACT OF VHDL ON DEPENDABLE DISTRIBUTED SYSTEM DESIGN
M. C. McElvany 1991 6 p
(Contract N00014-91-C-0014)
(AD-A239769) Avail: NTIS HC/MF A02 CSCL 12/5

The goal of dependable systems and components is to provide proper service in the presence of faults. One design approach is to develop extremely dependable building blocks, using fault avoidance techniques to decrease generic or design faults. Then, the reliable system components are combined using fault tolerance to create a dependable distributed system. The adoption and implementation of a standard hardware description language in VHDL (VHSIC hardware description language) promotes the use of fault avoidance techniques throughout the system design cycle. Descriptive languages such as VHDL also provide a basis for tools which can aid in the specification, design, and validation of both dependable systems and their component building blocks. However, integration of VHDL and existing high-level system evaluation tools remains a research problem. Author (GRA)

N91-31665# Massachusetts Inst. of Tech., Cambridge. Research Lab. of Electronics.
DISTORTION-FREE X RAY MASK TECHNOLOGY Final Technical Report, 12 Jun. 1990 - 10 Jun. 1991
Henry I. Smith 16 Aug. 1991 10 p
(Contract N00014-90-K-2018)
(AD-A239770) Avail: NTIS HC/MF A02 CSCL 20/12

The objective is to develop a closed loop, feedback controlled, robust system for reliably achieving zero stress in tungsten (W) films sputtered onto various x ray mask membranes, and to transfer the technology to the National x ray mask shop. The system for controlling stress in sputtered W films is based on the measurement of resonant frequency. Since resonant frequency depends on both the thickness and the stress of the W films, if the thickness is known, the stress is easily calculated. GRA

39 STRUCTURAL MECHANICS

Includes structural element design and weight analysis; fatigue; and thermal stress.

For applications see *05 Aircraft Design, Testing and Performance* and *18 Spacecraft Design, Testing and Performance.*

N91-31666# International Centre for Theoretical Physics, Trieste (Italy).
STRESS RELAXATION IN BENDING OF TYPE AISI 304 STAINLESS STEEL AT 773K AND 823K
F. Povolo, R. J. Tinivella, J. F. Reggiardo, and G. B. Botteri (Universidad Technologica Nacional, San Nicolas, Argentina) Aug. 1990 31 p
(DE91-618657; IC-90/201) Avail: NTIS HC/MF A03

Stress relaxation measurements at 773 and 823 K, in bending and for different initial stresses in Type AISI 304 stainless steel are reported. Several thermal treatments were given to the specimens prior to the relaxation testing. The data are fitted to a general equation that describes thermally activated dislocation motion and it is shown that, in some cases, the internal stress changes with the applied stress. No substantial differences were found in the stress relaxation behavior on changing the thermal treatment. This is attributed to the influence of dynamic strain aging and an equation which can be used to describe experimental log stress against log strain rate curves is presented. DOE

N91-31667 Massachusetts Univ., Amherst.
INVESTIGATION OF TWO-DIMENSIONAL CRACKS AT AN ANGLE TO AN INTERFACE Ph.D. Thesis
Borliang Chen 1991 221 p
Avail: Univ. Microfilms Order No. DA9120860

Models using a dislocation density to characterize a crack are presented to investigate the behavior of a straight crack approaching the interface of a bimaterial system. Three cases of the crack approaching the interface of a bimaterial system are considered: a semi-infinite crack under concentrated loading, a finite crack under concentrating loading, and a finite crack under uniform pressure. The formulation of the model for investigating these cases lead to a system of singular integral equations. A collocation method is used to solve this system. The effects of the orientation of the crack, the distance between the crack and the interface, and the material properties of the constituents of the systems are investigated. Dissert. Abstr.

N91-31668 Virginia Polytechnic Inst. and State Univ., Blacksburg.
NONLINEAR PROBABILISTIC FINITE ELEMENT MODELING OF COMPOSITE SHELLS Ph.D. Thesis
Stephen Phillip Engelstad 1990 212 p
Avail: Univ. Microfilms Order No. DA9118792

A probabilistic finite element analysis procedure for laminated composite shells was developed. A total Lagrangian finite element formulation, employing a degenerated 3-D laminated composite shell element with the full Green-Lagrange strains and first-order shear deformable kinematics, forms the modeling foundation. The first-order second-moment technique for probabilistic finite element analysis of random fields is employed and results are presented in the form of mean and variance of the structural response. The effects of material nonlinearity are included through the use of a rate-independent anisotropic plasticity formulation with the macroscopic point of view. A number of sample problems are solved to verify the accuracy of the procedures developed and to quantify the variability of certain material type/structure combinations. Dissert. Abstr.

N91-31669 Wisconsin Univ., Madison.
ASYMPTOTIC FINITE STRAIN ANALYSIS OF PROPAGATING CRACKS IN ELASTIC-PLASTIC MATERIALS Ph.D. Thesis
Carl R. Reid 1991 152 p
Avail: Univ. Microfilms Order No. DA9111400

The near tip solutions for the stress and velocity fields of a plane strain, Mode I, quasistatically propagating crack in an elastic perfectly plastic material are derived. The formulation includes a rigorous, finite strain generalization of the Prandtl-Reuss constitutive equations for a homogeneous, isotropic, incompressible material obeying the Huber-Mises yield condition. Finite geometric effects are also incorporated in the analysis by specifying boundary conditions appropriate for the propagation of an invariant crack tip profile. The solutions for the stress and velocity components are expressed as singular asymptotic perturbation series with the perturbation parameter, mu, being proportional to (yield stress)/(elastic modulus). The singularity in the perturbation expansion is quantified by integer powers of ((mu)lnr), where r is a nondimensional radius. The solution process requires the use of strained coordinates to eliminate difficulties encountered near a singular surface between the leading constant stress and centered fan plastic sectors of the modified Prandtl field derived previously using small strain formulations. Dissert. Abstr.

N91-31670 Utah Univ., Salt Lake City.
IN SITU SHORT FATIGUE CRACK CHARACTERIZATION OF A NICKEL-BASE SUPERALLOY AT AMBIENT AND ELEVATED TEMPERATURE Ph.D. Thesis
Robert Ralph Stephens 1991 325 p
Avail: Univ. Microfilma Order No. DA9121791

Fatigue experiments were performed using a nickel-base superalloy at various temperatures in a load frame attached to a scanning electron microscope. An elevated temperature stage was designed, constructed, and coupled to the apparatus, allowing temperatures in excess of 700 C. Experiments on Waspaloy at 25, 500, and 700 C showed similar crack nucleation characteristics. The dominant mechanism of fatigue crack growth for the short cracks at 25 and 500 C was one of mixed mode 1 and 2 by slip band cracking. At 700 C, crack growth proceeded by a stage II cracking process showing very little signs of crystallographic growth. Discontinuous crack growth rates at 25 and 500 C were attributed to microstructural barriers such as grain boundaries, twin boundaries, and carbides. Dissert. Abstr.

N91-31671 Virginia Polytechnic Inst. and State Univ., Blacksburg.
THE CONTROL OF FLEXIBLE STRUCTURE VIBRATIONS USING A CANTILEVERED ADAPTIVE TRUSS Ph.D. Thesis
Robert H. Wynn, Jr. 1991 131 p
Avail: Univ. Microfilms Order No. DA9118816

Analytical and experimental procedures and design tools are presented for control of flexible structure vibrations using a cantilevered adaptive truss. A specific six-actuator, octa-/octra-hedral truss effects the control of different flexible structures. These structures could represent space structures or robotic manipulators or a variety of other flexible structures where unwanted structural vibration could reduce the performance of the system. Three of these structures; a slender beam, a single curved beam, and two curved beams are controlled both in simulation and with an experimental test article. The test article, comprised of the flexible structure, the adaptive truss, and the actuators shows excellent agreement between simulated and

experimental responses to initial conditions in both open loop and (LQR) closed loop control. As an example of the ability of the truss to control the slender beam, a first mode simulated frequency of 3.11 Hz and damping ratio of 0.0044 are controlled to produce a 3.20 Hz fre quency and a damping ratio of 0.2876. This 600 pct. increase in damping without a great change in the modal frequency shows the potential of the adaptive truss in vibration control. Dissert. Abstr.

N91-31672# Los Alamos National Lab., NM.
ANELASTIC RELEASE FROM THE SHOCK-COMPRESSED STATE
J. N. Johnson and P. S. Lomdahl 1991 7 p Presented at the 3rd International Conference on Mechanical and Physical Behavior of Materials Under Dynamic Loading, Strasbourg, France, 14-18 Oct. 1991
(Contract W-7405-eng-36)
(DE91-009961; LA-UR-91-941; CONF-911069-1) Avail: NTIS HC/MF A02

Anelastic release from the shock-compressed state is analyzed in terms of internal self stresses acting on dislocation pile-ups and pinned dislocation loops. Reverse anelastic deformation occurs immediately upon release due to these internal stresses and is responsible for departure from ideal elastic-plastic unloading wave behavior: anelastic release is commonly observed in all shock-loaded metals. The rate at which this readjustment of internal stress occurs is determined by the viscous drag coefficient in the shock-compressed state and has important consequences regarding determination of elastic moduli from unloading wave data. Author

N91-31673# Los Alamos National Lab., NM.
PRESSURE-STRAIN-TEMPERATURE RELATIONSHIP IN SHOCK LOADED CYLINDRICAL SAMPLES OF 304 STAINLESS STEEL
K. P. Staudhammer 1991 9 p Presented at the 3rd International Conference on Mechanical and Physical Behavior of Materials Under Dynamic Loading, Strasbourg, France, 14-18 Oct. 1991
(Contract W-7405-eng-36)
(DE91-013379; LA-UR-91-1777; CONF-911069-5) Avail: NTIS HC/MF A02

The residual temperature resulting from pressure-strain relationships in an axisymmetric cylindrical sample of 304 stainless steel is described. Axisymmetric implosions result in nonuniform pressure-strain-temperature combinations that need to be better understood. This paper describes each temperature contribution and the net effect on the sample. DOE

N91-31674# Argonne National Lab., IL.
RESPONSE OF SEISMIC-ISOLATED STRUCTURES UNDER LONG-PERIOD MOTIONS
D. C. Ma 1991 7 p Presented at the 11th International Conference on Structural Mechanics in Reactor Technology, Tokyo, Japan, 18-23 Aug. 1991
(Contract W-31-109-eng-38)
(DE91-015673; ANL/CP-72765; CONF-910817-22) Avail: NTIS HC/MF A02

In the past decade, considerable progress has been made on reducing the seismic response of structures through seismic isolation. Application of seismic-isolation techniques to nuclear power facilities is currently being investigated. This paper presents an analysis of the effect of long period motions on a seismic-isolated nuclear structure. Preliminary analysis indicates that long-period earthquake motions increase structural accelerations and relative displacements between the upper and lower mats. Relative displacement between the mats can be represented by spectral displacement at the frequency of the structure, and can be effectively reduced by increasing viscous damping in the isolator. The isolated structure behaves as a system with one degree of freedom. Future analysis of seismic effects on seismic-isolated structures should include the linear and nonlinear effects of soil-structure interactions. DOE

N91-31675# Lawrence Livermore National Lab., CA.
DYNA3D: A NONLINEAR, EXPLICIT, THREE-DIMENSIONAL FINITE ELEMENT CODE FOR SOLID AND STRUCTURAL MECHANICS
R. G. Whirley May 1991 301 p
(Contract W-7405-eng-48)
(DE91-015735; UCRL-MA-107254) Avail: NTIS HC/MF A14

This report is the User Manual for the 1991 version of DYNA3D, and also serves as an interim User Guide. DYNA3D is a nonlinear, explicit, finite element code for analyzing the transient dynamic response of three-dimensional solids and structures. The code is fully vectorized and is available on several computer platforms. DYNA3D includes solid, shell, beam, and truss elements to allow maximum flexibility in modeling physical problems. Many material models are available to represent a wide range of material behavior, including elasticity, plasticity, composites, thermal effects, and rate dependence. In addition, DYNA3D has a sophisticated contact interface capability, including frictional sliding and single surface contact. Rigid materials provide added modeling flexibility. A material model driver with interactive graphics display is incorporated into DYNA3D to permit accurate modeling of complex material response based on experimental data. Along with the DYNA3D Example Problem Manual, this document provides the information necessary to apply DYNA3D to solve a wide range of engineering analysis problems. DOE

N91-31676# Aeronautical Research Labs., Melbourne (Australia).
VARIATIONS IN THE STATIC PROPERTIES, UNNOTCHED AND NOTCHED FATIGUE LIFE BEHAVIOUR OF 13 BATCHES OF 2L.65 ALUMINIUM ALLOY EXTRUDED BAR
J. Y. Mann and F. G. Haris Jul. 1987 118 p
(ARL-Struc-R-427; AR-004-540) Copyright Avail: NTIS HC/MF A06

Static tensile tests and rotating cantilever fatigue tests were carried out on both unnotched and notched specimens taken from 13 batches of B.S.2L.65 aluminium alloy extrusions. The extrusions, representing the products of at least five different manufacturers, were manufactured to the same specification and ranged in size from 16 to 25 mm in diameter. The various batches exhibitied significant difference in their average static strength properties, unnotched fatigue lives, and also in the variability in static strengths and fatigue lives. No correlation was found between the variability of static strengths and fatigue lives suggesting that different structural features may be responsible for scatter in properties under these two loading conditions. Author

N91-31677*# National Aeronautics and Space Administration. Langley Research Center, Hampton, VA.
ANALYSIS OF THERMOMECHANICAL FATIGUE OF UNIDIRECTIONAL TITANIUM METAL MATRIX COMPOSITES
M. Mirdamadi, W. S. Johnson, Y. A. Bahei-El-Din, and M. G. Castelli (Sverdrup Technology, Inc., Cleveland, OH.) Jul. 1991 34 p Presented at ASTM Symposium on Composites Materials: Fatigue and Fracture IV, Indianapolis, IN, 6-9 May 1991
(NASA-TM-104105; NAS 1.15:104105) Avail: NTIS HC/MF A03 CSCL 20K

Thermomechanical fatigue (TMF) data was generated for a Ti-15V-3Cr-3Al-3Sn (Ti-15-3) material reinforced with SCS-6 silicon carbide fibers for both in-phase and out-of-phase thermomechanical cycling. Significant differences in failure mechanisms and fatigue life were noted for in-phase and out-of-phase testing. The purpose of the research is to apply a micromechanical model to the analysis of the data. The analysis predicts the stresses in the fiber and the matrix during the thermal and mechanical cycling by calculating both the thermal and mechanical stresses and their rate-dependent behavior. The rate-dependent behavior of the matrix was characterized and was used to calculate the constituent stresses in the composite. The predicted 0 degree fiber stress range was used to explain the composite failure. It was found that for a given condition, temperature, loading frequency, and time at temperature, the 0 degree fiber stress range may control the fatigue life of the unidirectional composite. Author

N91-31678*# Florida Atlantic Univ., Boca Raton. Dept. of Ocean Engineering.
MOBILITY POWER FLOW ANALYSIS OF COUPLED PLATE STRUCTURE SUBJECTED TO MECHANICAL AND ACOUSTICS EXCITATION Final Report, Sep. 1988 - Jan. 1991
J. M. Cuschieri 1991 42 p
(Grants NAG1-685; NAG1-1077)
(NASA-CR-188791; NAS 1.26:188791) Avail: NTIS HC/MF A03 CSCL 20K

. The mobility power flow approach is generalized, previously applied in the derivation of expressions for the vibrational power flow between coupled plate substructures forming an L configuration and subjected to mechanical loading. Using the generalized expressions, both point and distributed mechanical loads on one or both of the plates can be considered. The generalized approach is extended to deal with acoustic excitation of one of the plate substructures. In the case of the L-shaped plate, acoustic interaction exists between the two plates substructures due to the generation of the acoustic waves by each of the substructures. An approach to deal with this phenomena is described. Author

N91-31679*# Rensselaer Polytechnic Inst., Troy, NY. Dept. of Mechanical Engineering, Aeronautical Engineering and Mechanics.
STATIC STRAIN AND VIBRATION CHARACTERISTICS OF A METAL SEMIMONOCOQUE HELICOPTER TAIL CONE OF MODERATE SIZE Final Report
Richard L. Bielawa, Rachel E. Hefner, and Andre Castagna Jun. 1991 128 p
(Contract NAG1-807; DAAG29-82-K-0093; NSF MSM-88-06257)
(NASA-CR-187576; NAS 1.26:187576) Avail: NTIS HC/MF A07 CSCL 20K

The results are presented of an analytic and experimental research program involving a Sikorsky S-55 helicopter tail cone directed ultimately to the improved structural analysis of airframe substructures typical of moderate sized helicopters of metal semimonocoque construction. Experimental static strain and dynamic shake-testing measurements are presented. Correlation studies of each of these tests with a PC-based finite element analysis (COSMOS/M) are described. The tests included static loadings at the end of the tail cone supported in the cantilever configuration as well as vibrational shake-testing in both the cantilever and free-free configurations. Author

N91-31680# Ecole Centrale de Lyon (France). Lab. de Mecanique des Solides.
IDENTIFYING BEHAVIOR CHARACTERISTICS USING PRESSUREMETER TESTS Ph.D. Thesis [IDENTIFICATION DE PARAMETRES DE COMPORTEMENT A PARTIR DE L'ESSAI PRESSIONMETRIQUE]
Antoine Boubanga 1990 194 p In FRENCH
(ETN-91-99917) Avail: NTIS HC/MF A09

A method to interpret pressuremeter data, by which characteristics intrinsic to a soil are determined, is presented. A code to simulate a pressuremeter test and determine the characteristics of a behavior model using the pressuremeter curve data and an inverse optimization method was developed. The software is IBM compatible and was used to identify three models: nonlinear elastic law and two elastoplastic laws. Real examples are analyzed and compared to classical theoretical methods. The representativity of these characteristics is tested for the calculation of the preloading embankment foundations of a nuclear power station atmospheric cooler. The results are compared to foundations measured on the terrain. ESA

N91-31681# Ecole Centrale de Lyon (France). Lab. de Mecanique des Solides.
BEHAVIOR OF NONLINEAR MECHANICAL STRUCTURES SUBJECTED TO STATIONARY EXCITATIONS Ph.D. Thesis [COMPORTEMENT DES STRUCTURES MECANIQUES NON-LINEAIRES SOUMISES A DES EXCITATIONS STATIONNAIRES]
Sangriyadi Setio 1991 234 p In FRENCH; ENGLISH summary
(ECL-91-01; ETN-91-99924) Avail: NTIS HC/MF A11

Experimental and theoretical studies of multidegree of freedom systems possessing elastic nonlinear behavior subjected to harmonic excitation are presented. A procedure to identify frequencies and nonlinear modes from experimental testing is proposed. A procedure of sensitivity to estimate the forced responses of a perturbed nonlinear structure in mass or in stiffness from known nonlinear modal parameters is proposed. Numerical simulations of discrete and continuous systems subjected to stationary excitation are presented. An experimental study on the steady state response of a beam with local nonlinear stiffness is reported to justify the methods. ESA

N91-31682# Office National d'Etudes et de Recherches Aerospatiales, Paris (France). Direction Scientifique de la Resistance des Structures.
UPDATING OF FINITE ELEMENT MODELS USING EXPERIMENTAL VIBRATORY TYPE DATA. PROCESS OF STATIC SUBSTRUCTURING [RECALAGE DE MODELE ELEMENTS FINIS A PARTIR DE DONNEES EXPERIMENTALES DE TYPE VIBRATOIRE. PROCESSUS DE SOUS-STRUCTURATION STATIQUE]
H. Berger, L. Barthe, and R. Ohayon Mar. 1990 27 p In FRENCH
(Contract DRET-89-34-001)
(ONERA-RT-10/3313-RY-090-R; ETN-91-99933) Avail: NTIS HC/MF A03

Starting from the updating method of finite element models, it is shown how, by using the error function, the initial problem can be divided into independent subproblems of reduced size. A numerical application illustrates this static substructuring process. A possible updating of a repetitive structure is presented: the idea is to localize the errors on a simpler equivalent structure, the actual updating being carried out on the cell(s) thus detected. It is shown that in treating the unknowns, unmeasured degrees of freedom and simultaneous corrector parameters, the complete displacement computation is enormously simplified at each iteration except the first. This approach could be adapted to the case where measurements are spoilt by errors. ESA

N91-31683# Direction des Recherches, Etudes et Techniques, Paris (France). Centres des Materiaux Pierre Marie Fourt.
CRACK PROPAGATION IN HEAT RESISTANT DISK ALLOYS. SHORT CRACK PROPAGATION IN ALLOYS FOR HIGH CHARACTERISTIC TURBOMACHINE DISKS Final Summary Report [PROPAGATION DES FISSURES COURTES DANS LES ALLIAGES POUR DISQUES DE TURBOMACHINE A HAUTES CARACTERISTIQUES]
P. Bernede and L. Remy Mar. 1990 56 p In FRENCH
(Contract DRET/ARMINES-87-193)
(ETN-91-99981) Avail: NTIS HC/MF A04

The characterization of cast-forged Astroloy (trademark) high temperature fatigue crack propagation was addressed for small cracks and more particularly for the study of environment influence. Tests were carried on test specimens on disks. The experimental methods are outlined and different steps in the research are reviewed. An analysis of the results is given. ESA

N91-31684*# Comtek Co., Grafton, VA.
LARGE ANGLE TRANSIENT DYNAMICS (LATDYN) DEMONSTRATION PROBLEM MANUAL Final Report
Shih-Chin Wu Washington NASA Oct. 1991 62 p
(Contract NAS1-18478)
(NASA-CR-4400; NAS 1.26:4400) Avail: NTIS HC/MF A04 CSCL 20K

LATDYN is a computer code for modeling the Large Angle Transient Dynamics of structures. The objective in developing the code was to investigate new techniques for analyzing flexible deformation and control/structure interaction problems associated with large angular motions of spacecraft. Such motions may consist of pointing the entire spacecraft or articulation of individual

components, events which occur frequently during construction, operation, and maintenance of large spacecraft. This type of analysis is beyond the routine capability of conventional analytical tools without simplifying assumptions. In some instances, the motion may be sufficiently slow and the spacecraft (or component) sufficiently rigid to simplify the analysis of dynamics and controls by making pseudo-static and/or rigid body assumptions. LATDYN introduces a new approach to the problem by combining finite element structural analysis, multi-body dynamics, and control system analysis in a single tool. It includes a new type of finite element that can deform and rotate through large angles at the same time, and which can be connected to other finite elements either rigidly or through mechanical joints. LATDYN also provides symbolic capabilities for modeling control systems which are interfaced directly with the finite element structural model. Thus, the nonlinear equations representing the structural model are integrated along with the equations representing sensors, processing, and controls as a coupled system. Author

N91-31685*# Comtek Co., Grafton, VA.
LARGE ANGLE TRANSIENT DYNAMICS (LATDYN) USER'S MANUAL Final Report
A. Louis Abrahamson, Che-Wei Chang, Michael G. Powell, Shih-Chin Wu, Bradford D. Bingel, and Paula M. Theophilos (Computer Sciences Corp., Hampton, VA.) Washington NASA Oct. 1991 129 p
(Contract NAS1-18478)
(NASA-CR-4401; NAS 1.26:4401) Avail: NTIS HC/MF A07 CSCL 20K

A computer code for modeling the large angle transient dynamics (LATDYN) of structures was developed to investigate techniques for analyzing flexible deformation and control/structure interaction problems associated with large angular motions of spacecraft. This type of analysis is beyond the routine capability of conventional analytical tools without simplifying assumptions. In some instances, the motion may be sufficiently slow and the spacecraft (or component) sufficiently rigid to simplify analyses of dynamics and controls by making pseudo-static and/or rigid body assumptions. The LATDYN introduces a new approach to the problem by combining finite element structural analysis, multi-body dynamics, and control system analysis in a single tool. It includes a type of finite element that can deform and rotate through large angles at the same time, and which can be connected to other finite elements either rigidly or through mechanical joints. The LATDYN also provides symbolic capabilities for modeling control systems which are interfaced directly with the finite element structural model. Thus, the nonlinear equations representing the structural model are integrated along with the equations representing sensors, processing, and controls as a coupled system. Author

N91-31686*# Comtek Co., Grafton, VA.
A FINITE ELEMENT APPROACH FOR THE DYNAMIC ANALYSIS OF JOINT-DOMINATED STRUCTURES
Che-Wei Chang and Shih-Chin Wu Oct. 1991 39 p
(Contract NAS1-18478)
(NASA-CR-4402; NAS 1.26:4402) Avail: NTIS HC/MF A03 CSCL 20K

A finite element method to model dynamic structural systems undergoing large rotations is presented. The dynamic systems are composed of rigid joint bodies and flexible beam elements. The configurations of these systems are subject to change due to the relative motion in the joints among interconnected elastic beams. A body fixed reference is defined for each joint body to describe the joint body's displacements. Using the finite element method and the kinematic relations between each flexible element and its corotational reference, the total displacement field of an element, which contains gross rigid as well as elastic effects, can be derived in terms of the translational and rotational displacements of the two end nodes. If one end of an element is hinged to a joint body, the joint body's displacements and the hinge degree of freedom at the end are used to represent the nodal displacements. This results in a highly coupled system of differential equations written in terms of hinge degrees of freedom as well as the rotational and translational displacements of joint bodies and element nodes. Author

N91-31687*# National Aeronautics and Space Administration. Langley Research Center, Hampton, VA.
IMPROVED FINITE-ELEMENT METHODS FOR ROTORCRAFT STRUCTURES
Howard E. Hinnant Aug. 1991 27 p
(DA Proj. 1L1-61102-AH-45C)
(NASA-TM-104104; NAS 1.15:104104; AVSCOM-TR-91-B-006)
Avail: NTIS HC/MF A03 CSCL 20K

An overview of the research directed at improving finite-element methods for rotorcraft airframes is presented. The development of a modification to the finite element method which eliminates interelement discontinuities is covered. The following subject areas are discussed: geometric entities, interelement continuity, dependent rotational degrees of freedom, and adaptive numerical integration. This new methodology is being implemented as an anisotropic, curvilinear, p-version, beam, shell, and brick finite element program. Author

N91-31688# Ames Lab., IA.
ULTRASONIC CHARACTERIZATION OF FATIGUE CRACK CLOSURE
R. B. Thompson, O. Buck, and D. K. Rehbein 1991 26 p
Presented at the 23rd National Symposium on Fracture Mechanics, College Station, TX, 18-20 Jun. 1991
(Contract W-7405-eng-82)
(DE91-015161; IS-M-670; CONF-910624-4) Avail: NTIS HC/MF A03

The characterization of fatigue crack closure is an important objective because of its influence on fatigue crack propagation, particularly under conditions of variable amplitude loading. A nontraditional technique is described for characterizing closure, in which ultrasonic scattering measurements are used to obtain estimates of the number density and size of asperities bridging the crack faces, with subsequent estimates of the crack tip shielding being based on those geometrical parameters. The experimental configuration is first reviewed along with the basic elasto-dynamic theory underlying the technique. Recent results are then presented which were obtained in studies of the influence of block overloads and load shedding on the growth of fatigue cracks in aluminum alloys. In both cases, the change in the closure state after the overload can be unambiguously seen even in the raw data. Moreover, data analysis suggests that it may be possible to predict when the crack will reinitiate based on more subtle changes in the ultrasonically inferred closure state. In the case of load shedding, a massive closure region is observed, whose characteristics appear consistent with the notion that threshold phenomena can be explained in terms of crack closure. DOE

N91-31689# Sandia National Labs., Albuquerque, NM.
FORCE RECONSTRUCTION USING THE INVERSE OF THE MODE-SHAPE MATRIX
T. G. Carne, V. I. Bateman, and C. R. Dohrman 1991 8 p
Presented at the 13th Biennial American Society of Mechanical Engineers (ASME) Mechanical Vibration and Noise Conference, Miami, FL, 22-25 Sep. 1991
(Contract DE-AC04-76DP-00789)
(DE91-016407; SAND-90-2281C; CONF-910957-2) Avail: NTIS HC/MF A02

Force reconstruction is a process in which response signals from a dynamic event are used to infer what the applied force must have been to produce these responses. Force reconstruction is of interest when the input force cannot be directly measured, while the response signals are easily obtained using transducers such as accelerometers or strain gages. In many evaluation tests of a structure, the dynamic response is not sufficient information; one may really need a description of the input force. A new technique for force reconstruction is developed. To estimate the externally applied force, this technique sums the weight-scaled acceleration signals, and is referred to as the Sum of Weighted

Accelerations Technique (SWAT). To obtain the scalar weights the inverse of the mode shape matrix is used. Application of this technique is illustrated with both numerical calculations using a mass-spring model and experimental data from a structure impacting a rigid barrier. DOE

N91-31690# Los Alamos National Lab., NM.
A WEIBULL BRITTLE MATERIAL FAILURE MODEL FOR THE ABAQUS COMPUTER PROGRAM
J. Bennett Aug. 1991 29 p
(Contract W-7405-eng-36)
(DE91-016813; LA-12152-MS) Avail: NTIS HC/MF A03

A statistical failure theory for brittle materials that traces its origins to the Weibull distribution function is developed for use in the general purpose ABAQUS finite element computer program. One of the fundamental assumptions for this development is that Mode 1 microfractures perpendicular to the direction of the principal stress contribute independently to the fast fracture. The theory is implemented by a user subroutine for ABAQUS. Example problems illustrating the capability and accuracy of the model are given. DOE

N91-31691# Maryland Univ., College Park. Inst. for Physical Science and Technology.
RELIABILITY OF COMPUTATIONAL ANALYSIS OF PLASTICITY PROBLEMS Final Report
Ivo Babuska, Y. Li, and K. L. Jerina Mar. 1991 27 p
(Contracts N00014-90-J-1030; N00014-87-K-0429)
(AD-A239646; BN-1123) Avail: NTIS HC/MF A03 CSCL 20/11

The reliability is addressed of computational analysis of plastically problems in light of the experimental work and its mathematical formulation. Also addressed are some basic constitutive laws used in engineering and one is proposed which leads to a well posed mathematical problem and agrees well with the experimental data. The data of the experimental project for 5454 aluminum alloy in the H32 condition for periodic and random strains are presented. Various constitutive laws are assessed in light of the experimental data. Outstanding problems related to the reliability of the analysis are mentioned. GRA

N91-31692*# Analytical Services and Materials, Inc., Hampton, VA.
AN EQUIVALENT DOMAIN INTEGRAL METHOD FOR THREE-DIMENSIONAL MIXED-MODE FRACTURE PROBLEMS
K. N. Shivakumar and I. S. Raju Aug. 1991 60 p
(Contract NAS1-18599)
(NASA-CR-182021; NAS 1.26:182021) Avail: NTIS HC/MF A04 CSCL 20K

A general formulation of the equivalent domain integral (EDI) method for mixed mode fracture problems in cracked solids is presented. The method is discussed in the context of a 3-D finite element analysis. The J integral consists of two parts: the volume integral of the crack front potential over a torus enclosing the crack front and the crack surface integral due to the crack front potential plus the crack face loading. In mixed mode crack problems the total J integral is split into J sub I, J sub II, and J sub III representing the severity of the crack front in three modes of deformations. The direct and decomposition methods are used to separate the modes. These two methods were applied to several mixed mode fracture problems, were analyzed, and results were found to agree well with those available in the literature. The method lends itself to be used as a post-processing subroutine in a general purpose finite element program. Author

42 GEOSCIENCES (GENERAL)

No abstracts in this category.

43 EARTH RESOURCES AND REMOTE SENSING

Includes remote sensing of earth resources by aircraft and spacecraft; photogrammetry; and aerial photography.

For instrumentation see *35 Instrumentation and Photography.*

N91-31693 Messerschmitt-Boelkow-Blohm G.m.b.H., Munich (Germany, F.R.).
STEREOPHOTOGRAMMETRIC SURVEYING AND INTERPRETING METHOD, AND INTERPRETING APPARATUS Patent
Otto Hofmann, inventor 23 May 1989 25 p
(Patent-1-254-651; Int-Patent-Class-H04N-718; CTN-91-60170)
Copyright Avail: Micromedia Ltd., Technical Information Centre, 165 Hotel de Ville, Place du Portage, Phase 2, Hull, Quebec J8X 3X2, Canada HC $4.00 CAN, MF $2.75 CAN

This invention relates to an aerial stereo photogrammetric surveying method to obtain orientation data from a camera and to construct a digital elevation model (DEM) of the terrain overflown using three sensor lines, A, B, and C, which are arranged transversely or obliquely to the flight direction for continuous line by line scanning of the terrain. The three scanners develop overlapping strip images taken from different perspectives. A mesh-like array of points, corresponding to points in the DEM, is developed on one of the line strip images and the corresponding points in the other images are identified. By means of spatial intersection, the digital elevation model coordinates x, y, and z are determined using approximately known flight movements for each of the model points, the approximate orientation parameters and the image point coordinates establishing intersection conditions for image point beams belonging to each DEM point. All image points within the DEM mesh are mathematically transformed into the ground plane. The corresponding points in the image plane are projected onto the ground plane. In this manner orthophotos and stereopartners are produced. CISTI

N91-31694# Los Alamos National Lab., NM.
SMALL SATELLITE RADIOMETRIC MEASUREMENTS
P. G. Weber 1991 7 p Presented at the 5th Annual AIAA/Utah State University (USU) Conference on Small Satellites, Logan, UT, 27 Aug. 1991
(Contract W-7405-eng-36)
(DE91-016308; LA-UR-91-2541; CONF-9108117-1) Avail: NTIS HC/MF A02

A critical need for the Mission to Planet Earth is to provide continuous, well-calibrated radiometric data for the radiation budget. This paper describes a new, compact, flexible radiometer which will provide both spectrally integrated data and data in selected spectral bands. The radiometer design is suitable for use on small satellites, aircraft, or remotely piloted vehicles (RPVs). DOE

N91-31695# Technische Univ., Delft (Netherlands). Faculteit der Geodesie.
THE IMPLEMENTATION OF A QUALITY SYSTEM IN AN AERIAL MAPPING COMPANY Thesis [HET OPZETTEN VAN EEN KWALITEITSSYSTEEM VOOR EEN LUCHTKAARTERINGSBEDRIJF]
R. M. F. Helmer Feb. 1990 169 p In DUTCH; ENGLISH summary
(ETN-91-99424) Avail: NTIS HC/MF A08

The geodetic and management problems involved in the implementation of a quality system for the photogrammetric production process for aerial mapping are investigated. The procedures and schemes of the production process are described in the quality handbook, in which the ideas of quality assurance and prequalification are also outlined. A quality team was installed in order to involve employees and management in quality improvement. A method to solve pratical quality problems as well as different types of costs is presented. A check of all the materials used during the production and a final check before the delivery

of the product are necessary. During the process of digitizing, a feedback to the person performing the photogrammetry is recommended. ESA

N91-31696# Deutsche Forschungsanstalt fuer Luft- und Raumfahrt, Oberpfaffenhofen (Germany, F.R.).
EXAMINATION AND MAPPING OF FOREST DAMAGE, USING REMOTE SENSING METHODS Final Report [UNTERSUCHUNG UND KARTIERUNG VON WALDSCHAEDEN MIT METHODEN DER FERNERKUNDUNG, ABSCHLUSSDOKUMENTATION]
M. Keil, ed. and H.-H. Voss, ed. Sep. 1990 216 p In GEORGIAN
(Contract BMFT-FK-037459)
(ETN-91-99741) Avail: NTIS HC/MF A10

Computer aided evaluation was performed using aircraft scanner data. It was shown that the behavior of spectral signatures of healthy and damaged trees in aircraft scanner data and the signatures of leaves and needles from laboratory and ground measurements were simular. A digital ground model bound to a three dimensional compensation is necessary for the realization of a classification. The radiometric compensation is to be reduced along the scanning line. Statistics were calculated by blending classification results with digitized cards. The classification costs depend on the number of classes and the classification accuracy. Results showed that satellite remote sensing can bring a contribution to the treatment of forest maps in scale 1:200,000 or also 1:100,000. ESA

N91-31697# Army Engineer Topographic Labs., Fort Belvoir, VA.
HYPERSPECTRAL SIGNATURES (400 TO 2500 NM) OF VEGETATION, MINERALS, SOILS, ROCKS, AND CULTURAL FEATURES: LABORATORY AND FIELD MEASUREMENTS Technical Report, Jan. 1985 - Jan. 1989
Melvin B. Satterwhite and J. P. Henley Dec. 1990 487 p
(DA Proj. 4A1-61102-B-52-C)
(AD-A239496; ETL-0573) Avail: NTIS HC/MF A21 CSCL 20/5

The objective of this catalog was to document the visible near-infrared reflectance spectra (400-2500 nm) of vegetation, soils, rocks, and man-made materials, and to provide information about their unique physical and chemical properties. Spectra were taken of representative samples of a particular plant species or soil type and selected conditions so that a specific feature could be evaluated. Seasonal differences in vegetation spectra were measured for tree, shrub, herbaceous, and grass species. Soils having different textures and moisture potentials were measured. These spectra summarize results of ongoing research in different environments, although many of the field spectra were taken in semiarid and arid environments. GRA

44 ENERGY PRODUCTION AND CONVERSION

Includes specific energy conversion systems, e.g., fuel cells; global sources of energy; geophysical conversion; and windpower.

For related information see also *07 Aircraft Propulsion and Power, 20 Spacecraft Propulsion and Power,* and *28 Propellants and Fuels.*

N91-31698# Lawrence Livermore National Lab., CA.
THE STATUS OF LIGHTWEIGHT PHOTOVOLTAIC SPACE ARRAY TECHNOLOGY BASED ON AMORPHOUS SILICON SOLAR CELLS
J. J. Hanak (Hanak, Joseph J., Birmingham, MI) and J. L. Kaschmitter 1 May 1991 10 p Presented at the 11th Space Photovoltaic Research and Technology Conference, Cleveland, OH, 7-9 May 1991
(Contract W-7405-eng-48)
(DE91-014985; UCRL-JC-106588; CONF-9105232-1) Avail: NTIS HC/MF A02

An ultralight, flexible photovoltaic (PV) array of amorphous silicon (a-Si) has been identified as a potential low-cost power source for small satellites. We have conducted a survey of the status of the a-Si PV array technology with respect to present and future performance, availability, cost and risks. For existing, experimental array 'blankets' made of commercial cell material, utilizing metal foil substrates, the BOL performance at AM0 and 35 C includes total power up to 200 W, power per area of 64 W/sq m and power per weight of 258 W/kg. Doubling of power per weight occurs when polyimide substrates are used. Estimated EOL power output after 10 years in a nominal low-earth orbit would be 80 percent of BOL, the degradation being due to largely light-induced effects (minus 10 to minus 15 percent) and in part (minus 5 percent) to space radiation. Predictions for the year 1995 for flexible PV arrays, made on the basis of published results for rigid a-Si modules, indicate EOL power output per area and per weight of 105 W/sq m and 400 W/kg, respectively, while predictions for the late 1990s based on existing US national PV program goals indicate EOL values of 157 W/sq m and 600 W/kg. cost estimates by vendors for 200 W ultralight arrays in volume of over 1000 units range from $100/watt to $125/watt. Identified risks include the lack of flexible, space compatible encapsulant, the lack of space qualification effort, recent partial or full acquisitions of US manufacturers of a-Si cells by foreign firms, and the absence of a national commitment for a long-range development program toward developing of this important power source for space. One new US developer has emerged as a future potential supplier of a-Si PV devices on thin, polyimide substrates. DOE

N91-31699# Sandia National Labs., Albuquerque, NM.
ONE-SUN, SINGLE-CRYSTALLINE SILICON SOLAR CELL RESEARCH
R. R. King, R. A. Sinton, and R. M. Swanson (Stanford Univ., CA.) Jun. 1991 86 p
(Contract DE-AC04-76DP-00789)
(DE91-015646; SAND-91-7003) Avail: NTIS HC/MF A05

The point-contact solar cell design, the most efficient silicon concentrator solar cell design to date, is explored for use in one-sun applications. The necessary modifications to backside-contact concentrator cell design for operation at one-sun are explored and implemented. Large-area, point-contact solar cells were fabricated on n- and p-type substrates in low-level injection (LLI). The characteristics of these LLI cells were compared to those of four different architectures of cells with substrates in high-level injection (HLI). Both types of cell achieved open-circuit voltages over 700 mV at one-sun, LLI cells had higher fill factors, and HLI cells had substantially higher short-circuit currents. The mechanisms responsible for these observations are discussed. The high V(sub oc) and J(sub sc) of the HLI cells combine to make them more efficient than the LLI cells, with efficiencies measured at Sandia up to 22.7 percent for a 37.5 sq cm cell at one sun. This is the highest one-sun efficiency for a silicon cell larger than 4 sq cm. Simplified, backside-contact solar cell processes were also developed, which have nearly 100 percent yield. Over 80 such cells, each with a 35-sq cm area or greater, were delivered to Sandia. Cells made with these simplified processes had efficiencies up to 21.3 percent for a 37.5-sq cm cell. The recombination properties of Si3N4b layers over SiO2 were characterized, since Si3N4 is an excellent antireflection coating for cells laminated under glass. Several prototype flat-plate modules of backside-contact cells were built, with up to 24 cells and efficiencies up to 19 percent. DOE

N91-31700# Massachusetts Inst. of Tech., Cambridge.
INTERFACIAL SYSTEMS FOR PHOTOCHEMICAL ENERGY CONVERSION
M. S. Wrighton 1991 29 p
(Contract DE-FG02-88ER-13914)
(DE91-015743; DOE/ER-13914/14) Avail: NTIS HC/MF A03

Progress in several areas related to photoelectrochemical energy conversion is summarized, including work on selective modification of 2-6 semiconductors, inter- and intramolecular

excited state electron transfer, pH-dependent molecular rectification, new surface modification reagents, enzyme-catalyzed redox processes, and synthesis of new rigid rod molecules for light absorption and charge separation. DOE

N91-31701# Argonne National Lab., IL.
PROCEEDINGS OF THE NINTH SYMPOSIUM ON ENERGY ENGINEERING SCIENCES: FLUID AND DYNAMICAL SYSTEMS
1991 340 p Symposium held in Argonne, IL, 13-15 May 1991
(Contract W-31-109-eng-38)
(DE91-015974; CONF-9105116) Avail: NTIS HC/MF A15

The Ninth Symposium on Energy Engineering Sciences was held on May 13-14, 1991, at the Argonne National Laboratory. These proceedings include the program, list of participants, and the papers that were presented during the nine technical sessions held at this meeting. The central theme of this year's meeting was fluid and dynamical systems and related topics. Each year a group of selected researchers in the DOE/BES Engineering Research Program are invited to present their research findings in such an open forum. By organizing around a central theme, principal investigators, their associates, and other interested parties are able to engage in discussions and share thoughts on subjects of common interests. This Symposium was organized into nine technical sessions: multi-phase flow, dynamical systems, porous media and transport, robotic systems, fluid systems, nonequilibrium systems, combustions and thermo/fluid systems, heat and mass transfer, and measurement of thermophysical properties. DOE

N91-31702# Sandia National Labs., Albuquerque, NM.
THE FEASIBILITY OF TESTING NASA'S SCAD CONCENTR[illegible] EARTH
T. R. Mancini, C. P. Cameron, and V. R. Goldberg (WG Associates, Dallas, TX.) Jul. 1991 113 p
(Contract DE-AC04-76DP-00789)
(DE91-016055; SAND-89-1724) Avail: NTIS HC/MF A06

NASA has proposed that the solar concentrator for the manned space station, referred to as the Solar Concentrator Advanced Development (SCAD) dish, undergo terrestrial testing prior to being deployed in space. Because reliable flight concentrator performance is so important, independent tests of the SCAD concentrator are needed to demonstrate the offset parabolic concept and validate the computer codes needed for predicting concentrator flux profile and power generating capability. This report documents the first phase of a three-phase project to test the SCAD concentrator on sun. The three phases of the project are: (1) feasibility of on-sun testing; (2) detailed design and fabrication of test fixtures; and (3) testing and analysis of results. The objectives of Phase 1 are to evaluate the feasibility of testing the concentrator on sun in a terrestrial environment and to determine the potential for accurately predicting its performance in space. The feasibility study includes: an evaluation of terrestrial structures to support and track the concentrator; an assessment of methods for protecting the concentrator from the environment when it is not on test; the selection of the most feasible support structure and protection system; an evaluation of the effects of terrestrial solar power levels and sunshapes on the verification of computer codes for predicting the on-orbit performance of the concentrator; the development of a preliminary test plan complete with procedures and instrumentation; and the development of schedule and cost estimates for Phases 2 and 3 of the project. DOE

N91-31703# Sandia National Labs., Albuquerque, NM.
THE 1991 DOE/SANDIA CRYSTALLINE PHOTOVOLTAIC TECHNOLOGY PROJECT REVIEW MEETING
M. L. Whipple, ed. Jul. 1991 129 p Meeting held in Albuquerque, NM, 30-31 Jul. 1991
(Contract DE-AC04-76DP-00789)
(DE91-016062; SAND-91-1467; CONF-9107149) Avail: NTIS HC/MF A07

This document serves as the proceedings for the manual project review meeting held by Sandia's Photovoltaic Technology Research Division. It contains information supplied by each organization making a presentation at the meeting, which was held July 30 through 31, 1991 at the Sheraton Hotel in Albuquerque, New Mexico. Sessions were held to discuss national photovoltaic programs, one-sun crystalline silicon cell research, concentrator silicon cell research, and concentrating collector development. DOE

N91-31704# Stanford Univ., CA. Dept. of Chemistry.
ENERGY TRANSFER PROCESSES IN SOLAR ENERGY CONVERSION
M. D. Fayer 1991 11 p
(Contract DE-FG03-84ER-13251)
(DE91-016102; DOE/ER-13251/T1) Avail: NTIS HC/MF A03

During the past year, we have made substantial progress in both theoretical and experimental aspects of the program. The program involves the investigation of excitation transport and electron transfer in complex molecular systems. In the area of electron transfer, we have been studying the influences of solvent relaxation and molecular diffusion in liquids on photoinduced forward and back electron transfer. Studies of excitation transport have focused on clustered chromophore systems including theory and experiments on intercluster transport in systems such as micelles and polymers and on dispersive excitation transport in liquids. DOE

N91-31705# Messerschmitt-Boelkow-Blohm G.m.b.H., Munich (Germany, F.R.). Unternehmensnereich Energie- und Industrietechnik.
DEVELOPMENT OF SINGLE BLADE ROTOR WIND ENERGY CONVERTERS: FROM M400 PROTOTYPE TO MON 50 PRESERIES [ENTWICKLUNG VON EINBLATTROTOR-WINDENERGIEKONVERTERN: VON PROTOTYP (M 400) ZUR VORSERIE (MON 50)]
Horst Stemme, Siegfried Mickeler, and Andreas Preiss 1990 10 p In GERMAN
(MBB-UE-0015-90-PUB; OTN-030861; ETN-91-99761) Avail: NTIS HC/MF A02

The project and the working program are presented. A comparison is made between M400 and MON 50 converters. Examples are given for the analytical system comparison. The rotor diameter is examined with regard to performance. The relationship between wind behavior in position and the favorable design of a pitch controlled single blade wind turbine is analyzed. A six month installation is examined. ESA

N91-31706# Messerschmitt-Boelkow-Blohm G.m.b.H., Ottobrunn (Germany, F.R.). Unternehmensbereich Energie- und Industrietechnik.
FUEL CELLS FOR COMMERCIAL ENERGY [BRENNSTOFFZELENN FUER DIE ENERGIEWIRTSCHAFT]
Gerhard Huppmann, Eckart Weisse, and Manfred Bischoff 1990 6 p In GERMAN
(MBB-UE-0018-90-PUB; OTN-028386; ETN-91-99762) Avail: NTIS HC/MF A02

The development of various types of fuel cells is described. Advantges and drawbacks are considered for alkaline fuel cells, phosphoric acid fuel cells, and molten carbonate fuel cells. It is shown that their modular construction is particularly adapted to power heat systems. A comparison which is largely in favor of fuel cells, is made between coal, oil, natural gas power stations, and fuel cells. Safety risks in operation are also compared with those of conventional power stations. Fuel cells are particularly suited for dwellings, shopping centers, swimming pools, other sporting installations, and research facilities, whose high current and heat requirements can be covered by power heat coupling. ESA

N91-31707 Academy of Sciences of the Ukrainian SSR, Kiev. Inst. of Physics.
THE PHOTOVOLTAIC EFFECT ON PYROELECTICS [FOTOVALTAICHESKII EFFECT V PIROELEKTRIKE]
M. A. Itskovskii 1990 20 p In RUSSIAN
Copyright Avail: Issuing Activity

The mechanism that causes the onset of photoelectromagnetic

force and photocurrent during a uniform exposure to pyroelectronics is proposed and investigated. The mechanism is based on the screening of spontaneous polarization by unequal current carriers in a pyroelectric-semiconductor model with donor and acceptor levels. Author

N91-31708*# National Aeronautics and Space Administration. Lewis Research Center, Cleveland, OH.
NICKEL-HYDROGEN CELL LOW-EARTH LIFE TEST UPDATE
David T. Frate 1991 8 p Presented at the 26th Intersociety Energy Conversion Engineering Conference, Boston, MA, 4-9 Aug. 1991; cosponsored by ANS, SAE, ACS, AIAA, ASME, IEEE, and AIChE
(NASA-TM-105229; E-6552; NAS 1.15:105229) Avail: NTIS HC/MF A02 CSCL 10A

When individual pressure vessel (IPV) nickel-hydrogen (Ni/H2) cells were selected as the energy storage system for the Space Station Freedom in March of 1986, a limited database existed on life and performance characteristics of these cells in a low earth orbit (LEO) regime. Therefore, NASA LeRC initiated a Ni/H2 cell test program with the primary objectives of building a test facility, procuring cells from existing NASA contracts, and screening several cell designs by life testing in a LEO 35 percent depth of discharge (DOD) scenario. A total of 40 cells incorporating 13 designs were purchased from Yardney, Hughes, and Eagle-Picher. Thirty-two of the cells purchased were 65 A-hr nameplate capacity and eight cells were 50 A-hr. Yardney and Eagle-Picher cells were built with both the Air Force recirculating and the advanced back-to-back electrode stack configurations and incorporated 31 and 26 percent KOH. Acceptance testing of the first delivered cells began in March of 1988, with life testing following in September of that year. Performance comparisons of these cells are made here while specifically addressing life test data relative to the design differences. Author

N91-31709# Argonne National Lab., IL. Energy Systems Div.
OPEN-CYCLE OCEAN THERMAL ENERGY CONVERSION SURFACE-CONDENSER DESIGN ANALYSIS AND COMPUTER PROGRAM
C. B. Panchal and T. J. Rabas May 1991 53 p
(Contract W-31-109-eng-38)
(DE91-015973; ANL/ESD/TM-15) Avail: NTIS HC/MF A04

This report documents a computer program for designing a surface condenser that condenses low-pressure steam in an ocean thermal energy conversion (OTEC) power plant. The primary emphasis is on the open-cycle (OC) OTEC power system, although the same condenser design can be used for conventional and hybrid cycles because of their highly similar operating conditions. In an OC-OTEC system, the pressure level is very low (deep vacuums), temperature differences are small, and the inlet noncondensable gas concentrations are high. Because current condenser designs, such as the shell-and-tube, are not adequate for such conditions, a plate-fin configuration is selected. This design can be implemented in aluminum, which makes it very cost-effective when compared with other state-of-the-art vacuum steam condenser designs. Support for selecting a plate-fin heat exchanger for OC-OTEC steam condensation can be found in the sizing (geometric details) and rating (heat transfer and pressure drop) calculations presented. These calculations are then used in a computer program to obtain all the necessary thermal performance details for developing design specifications for a plate-fin steam condenser. DOE

N91-31710# Los Alamos National Lab., NM.
PSEUDOHOMOGENEOUS CATALYST LAYER MODEL FOR POLYMER ELECTROLYTE FUEL CELL
T. E. Springer and S. Gottesfeld 1991 11 p Presented at the 180th Meeting of the Electrochemical Society, Phoenix, AZ, 13-18 Oct. 1991
(Contract W-7405-eng-36)
(DE91-016014; LA-UR-91-2390; CONF-911047-4) Avail: NTIS HC/MF A03

We have developed a relatively simple one-dimensional model for the cathode catalyst layer. This model explains certain observed polarization curve features at higher current densities. These features include a change in linear slope, instead of a sharp limiting current feature, and a lower than expected ratio of current density measured using O2 relative to air. Diffusional paths, ionic resistance, and catalyst sites are intimately coupled in a pseudohomogeneous layer using 'effective' parameters. DOE

N91-31711# Los Alamos National Lab., NM.
ELECTROCHEMICAL ENERGY STORAGE USING PEM SYSTEMS
N. E. Vanderborgh, J. C. Hedstrom, and J. R. Huff 1991 6 p Presented at the 2nd European Space Power Conference, Florence, Italy, 2-6 Sep. 1991
(Contract W-7405-eng-36)
(DE91-016020; LA-UR-91-2377; CONF-9109201-1) Avail: NTIS HC/MF A02

This paper gives the results of an engineering assessment for future, long-lived space power systems for extraterrestrial applications. Solar based, regenerative fuel cell power plants formed from either alkaline or proton exchange membrane (PEM) components are the focus. Test results on advanced PEM fuel cell stack components are presented. DOE

N91-31712# CBY Associates, Inc., Washington, DC.
SOLAR ENERGY AND CONSERVATION TECHNOLOGIES FOR CARIBBEAN TOURIST FACILITIES (CTF)
1991 29 p
(Contract DE-FG02-89CH-10418)
(DE91-016451; DOE/CH-10418/1) Avail: NTIS HC/MF A03

The primary objectives of the Caribbean Tourist Facilities (CTF) project were to develop and publish materials and conduct workshops on solar energy and conservation technologies that would directly address the needs and interests of tourist facilities in the Caribbean basin. Past contacts with the Caribbean and US tourist industries indicated that decision-makers remained unconvinced that renewable technologies could have a significant impact on development and operation costs or that renewable energy products and services suited their needs. In order to assure that the materials and programs developed were responsive to the Caribbean tourist industry and U.S. conservation and renewable energy industries, marketing research with potential end users and the organizations and associations that serve those users was included as an underlying task in the project. The tasks outlined in the CTF Statement of Work included conference planning, gathering of field data, development of educational materials, and conduct of workshop(s). In addition to providing a chronicle of the fulfillment of those tasks, this final report includes suggestions for distributing the documents developed during the project, venues for future workshops, and other technology transfer and market influence strategies. DOE

N91-31713# Sandia National Labs., Albuquerque, NM.
FACET DEVELOPMENT FOR A FACETED STRETCHED-MEMBRANE DISH BY SOLAR KINETICS, INC.
P. T. Schertz, D. C. Brown, and A. Konnerth, III Jul. 1991 88 p Prepared in cooperation with Solar Kinetics, Inc., Dallas, TX
(Contract DE-AC04-76DP-00789)
(DE91-016866; SAND-91-7009) Avail: NTIS HC/MF A05

A 3.6-meter diameter stretched-membrane optical facet for a parabolic dish has been successfully designed and demonstrated under contract with Sandia National Laboratories. Twelve facets identical to them will be used to make the lightweight reflector of the dish. The project goal of 2.5-mrad surface accuracy was met with each of the two full-sized prototypes, and accuracies of as low as 1.1 mrad were achieved. The facet weight is 11.7 kg/sq m (2.4 lbs/sq ft). The facet is similar in construction to the successful stretched-membrane heliostat; it has two thin metal membranes attached to a ring. However, the front membrane for this facet is plastically formed at the factor in order to achieve a shorter facet f/D (approximately 3.0). A passive tether restrains the front membrane when not in operation, that is, when the

stabilizing vacuum is off. The optical surface is achieved with a silvered-acrylic film laminated to the metal membrane. The facet is expected to cost $55.40/sq m at a production rate of 10,000 facets per year and $115,000/sq m at a production rate of 500 facets a year. Several key issues have been resolved. Stress concentrations due to seams in the reflective laminate did not cause membrane rupture during forming as they have for dishes with lower focal length-to-diameter ratios. The laminate survived the forming process and simulated operation without deterioration. The optical effect of the tether on the membrane was tested and found to be very small. Most important, highly accurate shapes were obtained using a simple forming procedure. Additional tests are needed to demonstrate process repeatability and facet performance in typical operating conditions. DOE

N91-31714# Sandia National Labs., Albuquerque, NM.
PARABOLIC DISH PHOTOVOLTAIC CONCENTRATOR DEVELOPMENT
K. Beninga, R. Davenport, M. Featherby, J. Sandubrae, and K. Walcott May 1991 280 p Prepared in cooperation with Science Applications International Corp., San Diego, CA
(Contract DE-AC04-76DP-00789)
(DE91-016868; SAND-91-7004) Avail: NTIS HC/MF A13

Science Applications International Corporation (SAIC) and Tactical Fabs, Inc. (TFI) have fabricated a prototype parabolic dish photovoltaic (PV) concentrator system to demonstrate the functionality of this approach. A 1.5 m diameter parabolic dish was fabricated of a polyester/fiberglass composite, with a silvered polymer reflective surface. An innovative receiver cooling system used outward radial flow of cooling water in a narrow passage. This configuration matches the heat transfer capability of the cooling system to the flux profile on the PV receiver, minimizing temperature variations across the receiver. The photovoltaic cells used in the system were a new, TFI-proprietary design. Interleaved contacts form a bi-polar, rear-contact cell configuration. Because the electrical contacts are made on the rear of the cells, cells can be close-packed to form receiver arrays of arbitrary shape and size. Optical testing of the dish concentrator was performed by SAIC, SERI, and Sandia National Labs. The dish concentrator, designed for solar thermal applications, had a tight focal spot but exhibited flux non-uniformities away from the focal plane. Thermal testing of the receiver cooling system was performed with excellent success. Single PV cells, 4-cell blocks, and 144-cell receiver modules were built and tested. The cells successfully demonstrated the TFI design concept, but due to cell processing problems their efficiency was very low. Sources of the processing problems were identified and solutions were proposed, but funding limitations precluded further cell production. Operation of the complete PV dish system was conducted, and the functionality of the system was demonstrated. However, low cell efficiencies and receiver plane flux non-uniformities caused the system performance to be very low. These problems are not generic to the concept, and solutions to them proposed. DOE

N91-31715# Sandia National Labs., Albuquerque, NM.
DESIGN AND COST OF THE FIRST COMMERCIAL STRETCHED-MEMBRANE HELIOSTAT
D. Brown, A. Konnerth, III, P. T. Schertz, and D. White Jul. 1991 146 p Prepared in cooperation with Solar Kinetics, Inc., Dallas, TX
(Contract DE-AC04-76DP-00789)
(DE91-016870; SAND-90-7038) Avail: NTIS HC/MF A07

A complete design of an 50 sq m stretched-membrane heliostat was developed specifically for the early stages of manufacturing. The design included mirror-module refinements, drive selection, pylon and foundation design, and detailing and tracking control design. The mirror module and rear structure are highly similar to the Mark II prototype erected at Sandia National Laboratories, Albuquerque, 1989. The pylon and foundation consist of a single pipe set in a cast-in-place pier as successfully developed at Sandia. The unique tracking control uses only commercially available industrial control components. Also, all real-time communication requirements have been eliminated to assure against the most common source of malfunctions in previous central receiver fields. Control commands are calculated internally to the local controller using a polynomial approximation curve fitted to actual sun position and adjusted for individual heliostat requirements. Direct material costs, in 1990 dollars were obtained for several different production volumes from material and component manufacturers and subassembly subcontractors. Manufacturing costs for a low-volume production company are projected to be competitive with glass/metal heliostats. DOE

45 ENVIRONMENT POLLUTION

Includes atmospheric, noise, thermal, and water pollution.

N91-31716# Pacific Northwest Lab., Richland, WA.
A REVIEW OF ACCELERATED RESPONSE ACTIONS AVAILABLE TO THE ENVIRONMENTAL RESTORATION PROGRAM: SELECTED CASE HISTORIES AND ASSOCIATED ISSUES
J. D. Smyth, R. D. Quinn, and S. J. Gianti (CH2M/Hill, Inc., Reston, VA.) May 1991 38 p
(Contract DE-AC06-76RL-01830)
(DE91-013608; PNL-7715) Avail: NTIS HC/MF A03

Accelerated actions were developed by the Environmental Protection Agency (EPA) within the regulatory framework for initiating early cleanup action or accelerating ongoing cleanup action to abate, mitigate, or reduce risk to human health or the environment at a contaminated waste site. The purposes of this report are to review the regulatory frameworks available to initiate accelerated actions at sites on the National Priorities List (NPL) and to provide case histories of sites where accelerated actions have been implemented. The findings of this report are applicable to non-NPL waste sites also. Accelerated actions are of interest to the Department of Energy (DOE) for two primary reasons: they are methods available to demonstrate progress in environmental restoration at DOE waste sites; and a subset of accelerated actions, termed interim remedial actions, may be required in place of final actions to avoid violating National Environmental Policy Act (NEPA) guidelines during the development of DOE Office of Environmental Restoration and Waste Management's (DOE- EM's) Programmatic Environmental Impact Statement (PEIS). To provide the case histories, interviews with staff and reviews of compliance documents were conducted for sites in EPA Regions 3, 4, and 7. DOE

N91-31717# Lawrence Livermore National Lab., CA.
TEMPORAL SAMPLING CONSIDERATIONS IN GLOBAL CLIMATE MODELING
T. J. Phillips, W. L. Gates, and K. Arpe Jun. 1991 6 p Presented at the 5th Conference on Climate Variations, Denver, CO, 14-18 Oct. 1991
(Contract W-7405-eng-48)
(DE91-015695; UCRL-JC-105259; CONF-9110161-2) Avail: NTIS HC/MF A02

The effect of sampling frequency on the climate statistics of atmospheric models has received comparatively little attention. The sampling problem is complicated by the typical computer storage practices followed in global climate modeling: many variables are updated at every time step, but the simulation history usually is saved no more frequently than every 6 hours. We investigated the effects of different sampling schemes on climate statistics by analyzing selected variables from an experiment using the European Centre for Medium Range Weather Forecasts (ECMWF) general circulation model (GCM). Three interrelated questions were considered: (1) What are minimum appropriate sampling frequencies for accurate estimation of the climate statistics of selected model variables?; (2) What are the relative contributions of intradiurnal versus lower-frequency fluctuations to these climate statistics?; and (3) How are these climate statistics impacted by sampling at the same time, versus different times, each day? DOE

N91-31718# Lawrence Livermore National Lab., CA.
TIME SCALES OF VARIABILITY ASSOCIATED WITH NORDESTE PRECIPITATION
K. R. Sperber and S. Hameed (State Univ. of New York, Stony Brook.) Jun. 1991 6 p Presented at the 5th Conference on Climate Variations, Denver, CO, 14-18 Oct. 1991
(Contracts W-7405-eng-48; DE-FG02-85ER-60314)
(DE91-015696; UCRL-JC-106445; CONF-9110161-3) Avail: NTIS HC/MF A02

The Northeast section of Brazil, called the Nordeste, experiences flood and drought regimes as the norm rather than the exception. This region receives its principal dose of precipitation during March-April, subsequent to regions to the west and north due to its proximity to the southern Atlantic subtropical high. A weakening of this anticyclone and strengthening of its counterpart in the northern Atlantic during this season results in the farthest southward penetration of the ITCZ and the Nordeste rainy season. Fluctuations in the large-scale circulation of the atmosphere, such as ENSO, modulate the track of the ITCZ causing the interannual drought or flood conditions that plague this region. Empirical studies have shown that Nordeste rainfall is related to the sea-surface temperature (SST) in the tropical Atlantic Ocean. DOE

N91-31719# Lawrence Livermore National Lab., CA.
GLOBAL MODEL SIMULATIONS OF THE LONG RANGE TRANSPORT OF SOOT AND SULFUR FROM THE KUWAIT OIL FIRES
J. E. Penner Jun. 1991 16 p Presented at the Expert Meeting on the Atmospheric Part of the Emergency Response To the Kuwait Oilfield Fires, Geneva, Switzerland, 27-30 Apr. 1991
(Contract W-7405-eng-48)
(DE91-015771; UCRL-JC-107737; CONF-9104282-1) Avail: NTIS HC/MF A03

It has been reported that up to 6 million barrels of oil per day may be on fire in Kuwait. If 5 percent of the oil becomes soot and the emissions continue for a year, the total amount injected into the atmosphere would be 18 Tg. If less oil is on fire, but the emission factor is actually 10 to 15 percent, a similarly large total amount of soot may be injected over the coarse of a year. The potential emissions of soot from the Kuwait oil fires are large relative to the global emissions of this substance. The spread of soot may reach as far as Mauna Loa in some seasons. In other seasons, the loading of soot within a large area centered about the fires may more than double. This soot will certainly have regional implications for climate, but its global consequences should be investigated. Enhancements to existing monitoring stations throughout the region should be pursued in order to quantify the amount and spread of the soot. The sulfur emissions from the fires are a large source relative to other sources in the area. The monitoring of SO2 and SO4(=) throughout the region could help quantify the spread of this pollutant as well. DOE

N91-31720# Brookhaven National Lab., Upton, NY.
CHEMICAL CHARACTERIZATION OF AEROSOL PARTICLES BY RAMAN SPECTROSCOPY
I. N. Tang and K. H. Fung Jun. 1991 5 p Presented at the 7th International Conference on Surfaces and Colloids, Compiegne (France), 7-12 Jul. 1991
(Contract DE-AC02-76CH-00016)
(DE91-015836; BNL-46378; CONF-910742-1) Avail: NTIS HC/MF A01

Microparticles play a very important role in areas of atmospheric chemistry, combustion, interfacial science and others. Of particular importance is a knowledge of the chemical composition of these airborne particles. Until recently, much of the chemical information could only be obtained by analyzing sufficient quantities of particles collected on some substrate surfaces. In this paper, some of our work on chemical characterization of single particles by Raman spectroscopy is described. DOE

N91-31721# Argonne National Lab., IL.
COAL UTILIZATION AND CO2 EMISSIONS: WHAT ARE THE CONTROL OPTIONS?
D. W. South, A. F. Fish, and R. Kane (Energy Research and Development Administration, Washington, DC.) 1991 32 p Presented at the 4th International Conference on Processing and Utilization of High Sulfur Coals, Idaho Falls, ID, 26-30 Aug. 1991
(Contract W-31-109-eng-38)
(DE91-015988; ANL/CP-72014; CONF-910819-1) Avail: NTIS HC/MF A03

Concerns about global climate change have focused on coal utilization and the associated carbon dioxide (CO2) emissions. To minimize CO2 emissions from coal utilization requires the use of more efficient technologies. Clean coal technologies (CCTs), under development and demonstration by the US Department of Energy, have the capability through improved conversion efficiencies to reduce CO2 emission at new power plants by up to 20 percent, relative to conventional technologies. This paper will examine coal utilization worldwide and the options that exist to reduce CO2 emissions with continued coal use, should such reductions be mandated. It will be shown that if it is determined that CO2 emissions should be reduced, coal and coal-based technologies can, and must, play a role. DOE

N91-31722# Missouri Univ., Columbia. Cooperative Inst. for Applied Meteorology.
SIMULATED EFFECTS OF A DOUBLING OF CARBON DIOXIDE ON CORN PRODUCTION IN PORTIONS OF THE CENTRAL US
W. L. Decker, V. R. Achutuni, and G. Dhakhwa 1 Mar. 1991 37 p
(Contract DE-FG02-86ER-60444)
(DE91-016843; DOE/ER-60444/2) Avail: NTIS HC/MF A03

One aspect of global change with consequence for agriculture is the greenhouse effect. In recent years many of the greenhouse gases have been increasing in concentration. The trace gas most often identified as a major contributor to the increased concentration of the greenhouse gases is carbon dioxide. Water vapor, although not a pollutant, remains as the most important greenhouse gas in the atmosphere. Global warming will result in increased evaporization and consequently, the concentration of atmospheric water vapor. Carbon dioxide, in addition to its importance as a greenhouse gas, also supplies the carbon for the photosynthetic reaction in plant growth. There are many reports in the literature which demonstrate that as the concentration of carbon dioxide increases the amount of photosynthate produced at a given light level will be increased. Thus, carbon dioxide acts as a fertilizer enhancing the growth process and the levels of grain and forage production. To simulate the effects of increases in carbon dioxide, it is necessary to develop a model of how plants respond to both these changes and any interactions between the two effects. The model must consider the effects of climate change on the water balance and crop development (rates of growth and phenological stages). It must consider how these factors will interact with the changes induced in the plant by the increased carbon dioxide to either increased or decreased carbohydrate production. DOE

N91-31724*# Harvard-Smithsonian Center for Astrophysics, Cambridge, MA.
RETRIEVAL AND MOLECULE SENSITIVITY STUDIES FOR THE GLOBAL OZONE MONITORING EXPERIMENT AND THE SCANNING IMAGING ABSORPTION SPECTROMETER FOR ATMOSPHERIC CHARTOGRAPHY
Kelly V. Chance, John P. Burrows, and Wolfgang Schneider (Deutsche Forschungs- und Versuchsanstalt fuer Luft- und Raumfahrt, Oberpfaffenhofen, Germany, F.R.) *In* NASA. Langley Research Center, Tunable Far Infrared Studies of Molecular Parameters in Support of Stratospheric Measurements Aug. 1991 16 p (For primary document see N91-31723 23-46)
Avail: NTIS HC/MF A03 CSCL 13B

46 GEOPHYSICS

Includes aeronomy; upper and lower atmosphere studies; ionospheric and magnetospheric physics; and geomagnetism.

For space radiation see *93 Space Radiation.*

N91-31723*# National Aeronautics and Space Administration. Langley Research Center, Hampton, VA.
TUNABLE FAR INFRARED STUDIES OF MOLECULAR PARAMETERS IN SUPPORT OF STRATOSPHERIC MEASUREMENTS Semiannual Progress Report, 1 Jun. 1989 - 31 May 1991
Kelly V. Chance, K. M. Evenson, K. Park, J. V. Radostitz (Oregon Univ., Eugene.), D. A. Jennings, I. G. Nolt, and M. D. Vanek Aug. 1991 33 p
(Grant NAGw-1292)
(NASA-CR-188774; NAS 1.26:188774; SAR-3; SAR-4; SAR-5; SAR-6) Avail: NTIS HC/MF A03 CSCL 04A

Lab studies were made in support of far infrared spectroscopy of the stratosphere using the Tunable Far InfraRed (TuFIR) method of ultrahigh resolution spectroscopy and, more recently, spectroscopic and retrieval calculations performed in support of satellite-based atmospheric measurement programs: the Global Ozone Monitoring Experiment (GOME), and the SCanning Imaging Absorption spectroMeter for Atmospheric CHartographY (SCIAMACHY). For individual titles, see N91-31724 through N91-31725.

N91-31724*# Harvard-Smithsonian Center for Astrophysics, Cambridge, MA.
RETRIEVAL AND MOLECULE SENSITIVITY STUDIES FOR THE GLOBAL OZONE MONITORING EXPERIMENT AND THE SCANNING IMAGING ABSORPTION SPECTROMETER FOR ATMOSPHERIC CHARTOGRAPHY c45
Kelly V. Chance, John P. Burrows, and Wolfgang Schneider (Deutsche Forschungs- und Versuchsanstalt fuer Luft- und Raumfahrt, Oberpfaffenhofen, Germany, F.R.) *In* NASA. Langley Research Center, Tunable Far Infrared Studies of Molecular Parameters in Support of Stratospheric Measurements Aug. 1991 16 p (For primary document see N91-31723 23-46)
Avail: NTIS HC/MF A03 CSCL 13B

The Global Ozone Monitoring Experiment (GOME) and the SCanning Imaging Absorption spectroMeter for Atmospheric CHartographY (SCIAMACHY) are diode based spectrometers that will make atmospheric constituent and aerosol measurements from European satellite platforms beginning in the mid 1990's. GOME measures the atmosphere in the UV and visible in nadir scanning, while SCIAMACHY performs a combination of nadir, limb, and occultation measurements in the UV, visible, and infrared. A summary is presented of the sensitivity studies that were performed for SCIAMACHY measurements. As the GOME measurement capability is a subset of the SCIAMACHY measurement capability, the nadir, UV, and visible portion of the studies is shown to apply to GOME as well. Author

N91-31725*# Max-Planck-Inst. fuer Chemie, Mainz (Germany, F.R.).
SCANNING IMAGING ABSORPTION SPECTROMETER FOR ATMOSPHERIC CHARTOGRAPHY
John P. Burrows and Kelly V. Chance (Harvard-Smithsonian Center for Astrophysics, Cambridge, MA.) *In* NASA. Langley Research Center, Tunable Far Infrared Studies of Molecular Parameters in Support of Stratospheric Measurements Aug. 1991 10 p (For primary document see N91-31723 23-46)
Avail: NTIS HC/MF A03 CSCL 04A

The SCanning Imaging Absorption SpectroMeter for Atmospheric CHartographY is an instrument which measures backscattered, reflected, and transmitted light from the earth's atmosphere and surface. SCIAMACHY has eight spectral channels which observe simultaneously the spectral region between 240 and 1700 nm and selected windows between 1940 and 2400 nm. Each spectral channel contains a grating and linear diode array detector. SCIAMACHY observes the atmosphere in nadir, limb, and solar and lunar occultation viewing geometries. Author

N91-31726 Columbia Univ., New York, NY.
THE TIME-DOMAIN EARTH TIDES Ph.D. Thesis
Yuanchong Zhang 1990 204 p
Avail: Univ. Microfilms Order No. DA9118669

Based upon the theories of general harmonic analysis and statistical modeling, principles and methods for analyzing the observed earth-tide time series were developed. With these principles and methods of time-domain tidal analysis, and the calculated Time-Domain Earth Tide (TDET) time series, the time lag and the resultant amplitude of an observed tital series can be determined so that the earth-tide time series at any given time and any locality can be more precisely predicted. Using synthetic tidal gravity time series, numerical experiments show that the time lag can be determined to a precision of the sampling time interval of the observed series in most of the continents, and that the resultant amplitude to a precision of the order of the perturbations of the ocean tides. Dissert. Abstr.

N91-31727 Washington Univ., Seattle.
ON THE RESPONSE OF THE SPECIAL SENSOR MICROWAVE/IMAGER TO THE MARINE ENVIRONMENT: IMPLICATIONS FOR ATMOSPHERIC PARAMETER RETRIEVALS Ph.D. Thesis
Grant William Petty 1990 305 p
Avail: Univ. Microfilms Order No. DA9117976

The objective is to provide a reasonably rigorous basis for understanding and extracting the physical information content of Special Sensor Microwave/Imager (SSM/I) satellite images of the maritime environment. To this end, a comprehensive algebraic parameterization was developed for the response of the SSM/I to a set of nine atmospheric and ocean surface parameters. The brightness temperature model includes a closed-form approximation to microwave radiative transfer in a non-scattering atmosphere and fitted models for surface emission and scattering based on geometric optics calculations for the roughened sea surface. The combined model is empirically tuned using suitable sets of SSM/I data and coincident surface observations. The brightness temperature model is then used to examine the sensitivity of the SSM/I to realistic variations in the scene being observed and to evaluate the theoretical maximum precision of global SSM/I retrievals of integrated water vapor, integrated cloud liquid water, and surface wind speed. A unified set of efficient statistical and semi-physical algorithms is presented for obtaining fields of surface wind speed, integrated water vapor, cloud liquid water, and precipitation from SSM/I brightness temperature data.
Dissert. Abstr.

N91-31728 New Hampshire Univ., Durham.
A STUDY OF ION ACCELERATION AT ROCKET ALTITUDES AND DEVELOPMENT AND CALIBRATION OF PITCH ANGLE IMAGING CHARGED PARTICLE DETECTORS Ph.D. Thesis
Gregory Paul Garbe 1990 231 p
Avail: Univ. Microfilms Order No. DA9119139

Data obtained from the Jan. 1988 flight of the Topaz 2 sounding rocket is presented. It was found that four types of ion populations were observed during this flight. During the early portions of the upleg and late portions of the downleg numerical fits of the plasma was compared with in-situ data to show the Maxwellian behavior and derived plasma parameters. Throughout the middle portion of the flight superthermal tails (ion conics) were observed and are modeled using a bi-Maxwellian distribution function from which T sub perp and T sub par can be derived. Two other ion populations were observed in the most intense auroral arcs. Transverse accelerated ions (TAI) were observed continuously in these arcs. The second ion population found in the arcs of high energy electron precipitation is a cold downflowing population. Preparation and calibration of the instruments for NASA flight 35.020 is also presented. A procedure for the coating of electrostatic charged particle analyzers with metal blacks were devised and is presented.

The results of the calibration tests of the instruments flow on flight 35.020 is shown. Dissert. Abstr.

N91-31729 British Aerospace Public Ltd. Co., Preston (England). Military Aircraft.
BAe UNIVERSITY ROUND TABLE ON GRAVITATIONAL RESEARCH
R. A. Evans Nov. 1990 122 p Meeting held in Preston, England, 26-27 Mar. 1990
(BAe-FBS-007; ETN-91-99836) Copyright Avail: British Aerospace (Military Aircraft) Ltd., Warton Aerodrome, Preston, Lancashire PR4 1AX, England

A report on a round table on gravitational research held 26 to 27 Mar. 1990 is presented. The objective of this meeting was to learn, to identify any potential areas of breakthrough that could have a dramatic effect on BAe (British Aerospace) Military Aircraft Limited (MAL) future business, and to single out any business opportunities. Current research projects were discussed, including gravitational wave astronomy, gravity gradiometry and fifth force experiments. Speculative ideas about gravitation were presented, including microgravity research, the Heavisidian field, a relativistic wave model of the electron and an experiment which might detect a link between the gravitational constant G, the permittivity, and the permeability, of free space. For individual titles, see N91-31730 through N91-31738.

N91-31730 British Aerospace Public Ltd. Co., Bristol (England). Sowerby Research Center.
THE SOWERBY RESEARCH CENTRE AND UNIVERSITY LIAISON **c09**
J. Ackroyd *In its* BAe University Round Table on Gravitational Research Nov. 1990 3 p (For primary document see N91-31729 23-46)
Copyright Avail: British Aerospace (Military Aircraft) Ltd., Warton Aerodrome, Preston, Lancashire PR4 1AX, England

An introduction to the Sowerby Research Centre and its links with universities is presented. Although in some cases universities are an alternative resource to BAe (Bristish Aerospace) facilities there are others where they are clearly the most appropriate choice: fundamental studies to elicit basic understanding is one such case and speculative studies may be another less obvious one. ESA

N91-31731 British Aerospace Public Ltd. Co., Preston (England).
BAe OVERVIEW OF CURRENT GRAVITATIONAL PHYSICS RESEARCH
R. A. Evans *In its* BAe University Round Table on Gravitational Research Nov. 1990 11 p (For primary document see N91-31729 23-46)
Copyright Avail: British Aerospace (Military Aircraft) Ltd., Warton Aerodrome, Preston, Lancashire PR4 1AX, England

The interest of BAe (British Aerospace) in gravitation is discussed. An overview of gravitational physics research, including gravitational wave telescopes, research on a fifth force in nature, the Higgs particle, the extraction of energy from a vacuum by the molecular Van der Waals, or Casimir, force, inertial drive machines and gravity satellite probes, is given. ESA

N91-31732 Glasgow Univ. (Scotland).
GRAVITATIONAL WAVE RESEARCH
A. Carmichael and E. Morrison *In its* BAe University Round Table on Gravitational Research Nov. 1990 18 p (For primary document see N91-31729 23-46)
Copyright Avail: British Aerospace (Military Aircraft) Ltd., Warton Aerodrome, Preston, Lancashire PR4 1AX, England

A summary of the proposal for a joint German British interferometric gravitational wave detector is presented. An optical delay line and a Fabry-Perot arrangement are employed to increase the optical path length in the two arms of the interferometer. A 10 m prototype Fabry-Perot detector is summarized. The project is expected to make significant contributions to scientific knowledge in providing test of gravitational wave polarization, wave propagation speed, and tests of strong field gravity. Astrophysics will benefit from additional data on the early Universe, cosmological mass distribution, Hubbles constant, compact object, statistics, equations of State for neutron stars, and the morphology of supernova cores. ESA

N91-31733 Newcastle-upon-Tyne Univ. (England). Dept. of Physics.
FIFTH FORCE EXPERIMENTS
M. Gross and M. Hill *In its* BAe University Round Table on Gravitational Research Nov. 1990 20 p (For primary document see N91-31729 23-46)
Copyright Avail: British Aerospace (Military Aircraft) Ltd., Warton Aerodrome, Preston, Lancashire PR4 1AX, England

A series of preliminary experiments to investigate methods which might feasibly be employed to check claims of the existence of a fifth force of nature is reported. To overcome problems associated with poor knowledge of the density distribution of test masses, large controlled volumes of water with uniform density (docks, reservoirs, sea tides) were used as gravitational test masses. Unsuccessful dock experiments showed the need for a very accurate modeling of the body water geometry, with a low error bounds, in order to isolate any non Newtonian fifth force. A gravitational 'panel method' for a reservoir is described. A computer program was developed to predict the gravitational field of any solid body. Gravimetric measurements are being made at a reservoir with a less porous boundary and results are awaited. Over the range measured, it is felt that results indicate the non existence of the fifth force but research is not complete. ESA

N91-31734 Strathclyde Univ., Glasgow (Scotland). Dept. of Applied Physics.
THE SUPERCONDUCTING GRAVITY GRADIOMETER
M. Hosey *In its* BAe University Round Table on Gravitational Research Nov. 1990 23 p (For primary document see N91-31729 23-46)
Copyright Avail: British Aerospace (Military Aircraft) Ltd., Warton Aerodrome, Preston, Lancashire PR4 1AX, England

An insight into the use of a one dimensional gradiometer is reported. The device is limited by the noise introduced by a SQUID amplifier, which causes troublesome resonances near 100 Hz. Present work is aimed at increasing the operating bandwidth by employing electronic methods to overcome the resonances. The sensitivity of the device is expected to be 0.1 E and 1 E. The aim is to build a three dimensional gradiometer. ESA

N91-31735 British Aerospace Public Ltd. Co., Preston (England).
A REMINDER OF FARADAY'S GRAVITATIONAL EXPERIMENTS
R. A. Evans *In its* BAe University Round Table on Gravitational Research Nov. 1990 10 p (For primary document see N91-31729 23-46)
Copyright Avail: British Aerospace (Military Aircraft) Ltd., Warton Aerodrome, Preston, Lancashire PR4 1AX, England

With a view to demonstrating a link between gravity and electromagnetism, a reminder of Faraday's original gravitational research is presented. Since Faraday's time, two further fundamental forces have been discovered: strong and weak nuclear forces which operate over microscopic ranges within the atom. Unification between electromagnetism and the weak nuclear force has already been demonstrated and the search for a link between electromagnetism and gravity continues. ESA

N91-31736 Commercial Space Technologies Ltd., London (England).
REVIEW OF MICROGRAVITY **c29**
Per Anders Hansson *In its* BAe University Round Table on Gravitational Research Nov. 1990 10 p (For primary document see N91-31729 23-46)
Copyright Avail: British Aerospace (Military Aircraft) Ltd., Warton Aerodrome, Preston, Lancashire PR4 1AX, England

A review of microgavity which included gravity sensing with plants and a disussion of Puthoff's interpretation of Sakharov's idea that gravity might be due to an induced effect brought about by quantum fluctuations of the vacuum (the Ether?) due to the

prescence of matter, rather than as an inherent property of the matter itself, is reported. An observable feature arising from fluctuations of the vacuum, the Casimir or Van der Waals force, is discussed. The theory of quantum electrodynamics, which treats the interactions between all charged particles in terms of the exchange of virtual photons, is discussed. ESA

N91-31737 British Aerospace Public Ltd. Co., Preston (England).
HEAVISIDE'S LINEARISED GRAVITATIONAL THEORY
R. A. Evans *In its* BAe University Round Table on Gravitational Research Nov. 1990 9 p (For primary document see N91-31729 23-46)
Copyright Avail: British Aerospace (Military Aircraft) Ltd., Warton Aerodrome, Preston, Lancashire PR4 1AX, England

The development by Heaviside of an electromagnetic analogy of Maxwell, where he tried to extend the Newtonian potential theory of gravitation to incorporate dynamic effects, is discussed. Heaviside introduced a dual of the gravitational field. For weak gravitational fields Heaviside's method is seen to be a linearized, flat space-time, approximation to general relativity, although there are some unexplained scale factor differences. Heaviside's method shows that the Lense-Thirring precession is related to the Coriolis force, and is directly analogous to Larmor precession in electromagnetic theory. ESA

N91-31738 Kent Univ., Canterbury (England).
A NEW MODEL OF THE ELECTRON: A SUGGESTED EXPERIMENT TO SEARCH FOR A LINK BETWEEN ELECTROMAGNETISM AND GRAVITY **c72**
Roger C. Jennison *In its* BAe University Round Table on Gravitational Research Nov. 1990 7 p (For primary document see N91-31729 23-46)
Copyright Avail: British Aerospace (Military Aircraft) Ltd., Warton Aerodrome, Preston, Lancashire PR4 1AX, England

An electromagnetic model of the electron is derived from the application of rotational relativity to the trapping of an electromagnetic wave at the Compton frequency. An experiment to investigate the possibility of a link between electromagnetism and gravity by a connection between the gravitational constant G, the permittivity, and permeability, is outlined. The apparatus is described. Many orders of magnitude are claimed to be recoverable by use of the gradient due to altitude of the Earth's gravitational potential. ESA

N91-31739# Range Commanders Council, White Sands Missile Range, NM. Meteorology Group.
RANGE REFERENCE ATMOSPHERE, FAIRBANKS, ALASKA
Aug. 1990 161 p
(AD-A239520; RCC-378-91) Avail: NTIS HC/MF A08 CSCL 04/2

A reference atmosphere is a statistical model of the earth's atmosphere, derived from upper air observations over a specific location. The individual RRA is the authoritative source for upper-atmosphere climatology over the launch and recovery site for which it has been prepared. The RRAs are used to plan, evaluate, and establish environmental launch constraints for aerospace vehicles launched from a particular location. GRA

N91-31740# Range Commanders Council, White Sands Missile Range, NM.
RANGE REFERENCE ATMOSPHERE WAKE ISLAND, NORTH PACIFIC
Aug. 1991 158 p
(AD-A239602; RCC-376-91) Avail: NTIS HC/MF A08 CSCL 09/2

A reference atmosphere is a statistical model of the earth's atmosphere, derived from upper air observations over a specific location. The individual RRA is the authoritative source for upper atmosphere climatology over the launch and recovery site for which it has been prepared. The RRA's are used to plan, evaluate, and establish environmental launch constraints for aerospace vehicles launch from a particular location. GRA

N91-31741# Range Commanders Council, White Sands Missile Range, NM.
RANGE REFERENCE ATMOSPHERE SHEMYA, ALASKA
Aug. 1991 170 p
(AD-A239603; RCC-380-91) Avail: NTIS HC/MF A08 CSCL 04/2

A reference atmosphere is a statistical model of the earth's atmosphere, derived from upper air observations over a specific location. The individual RRA is the authoritative source for upper atmosphere climatology over the launch and recovery site for which it has been prepared. The RRA's are used to plan, evaluate, and establish environmental launch constraints for aerospace vehicles launched from a particular location. GRA

N91-31742# Range Commanders Council, White Sands Missile Range, NM.
RANGE REFERENCE ATMOSPHERE: THULE, GREENLAND
Aug. 1991 90 p
(AD-A239659; RCC-379-91) Avail: NTIS HC/MF A05 CSCL 04/2

A reference atmosphere is a statistical model of the earth's atmosphere, derived from upper-air observations over a specific location. The individual RRA is the authoritative source for upper atmosphere climatology over the launch and recovery site for which it has been prepared. The RRA's are used to plan, evaluate, and establish environmental launch constraints for aerospace vehicles launched from a particular location. GRA

N91-31743# Massachusetts Inst. of Tech., Lexington. Lincoln Lab.
ARTIFICIAL NEURAL NETWORKS FOR SEISMIC DATA INTERPRETATION Semiannual Technical Summary Report No. 1, 1 May - 30 Nov. 1990
Richard T. Lacoss, Robert K. Cunningham, Susan R. Curtis, and Michael C. Seibert 30 Nov. 1990 40 p
(Contract F19628-90-C-0002)
(AD-A239673; S/A-ANN-12-30-90; ESD-TR-91-058) Avail: NTIS HC/MF A03 CSCL 12/7

Seismic surveillance applications were reviewed and data interpretation tasks were selected for initial neural network experimentation. The selected tasks are estimation of signal arrival time (time picking), labeling of seismic phases, and recognition of typical and atypical events on a regional basis. Basic seismology and surveillance techniques are reviewed and preliminary experimental results are summarized. Two types of data are used. Seismic waveform data with associated parametric information are being provided by SAIC in San Diego, CA. Parametric data for a much larger data set are being obtained by remote access to an on-line data base at the Center for Seismic Studies (CSS) in Arlington, VA. All the data are from NORESS and ARCESS arrays in Scandinavia and were processed by the IMS (Intelligent Monitoring System) regional seismic surveillance system. At the start of the contract SAIC provided an initial waveform data set for exploratory experimentation. While using it, the waveform data requirements and formats were worked out with SAIC and the first installment of waveforms for 50 events was received. GRA

N91-31172# Deutsche Forschungsanstalt fuer Luft- und Raumfahrt, Oberpfaffenhofen (Germany, F.R.). Inst. for Atmospheric Physics.
A DOCUMENTATION OF VERTICAL AND HORIZONTAL AIRCRAFT SOUNDINGS OF ICING RELEVANT CLOUDPHYSICAL PARAMETERS
H.-E. Hoffmann *In* AGARD, Low Temperature Environment Operations of Turboengines (Design and User's Problems) 1990 14 p (For primary document see N91-31144 23-07)
Copyright Avail: NTIS HC/MF A16; Non-NATO Nationals requests available only from AGARD/Scientific Publications Executive

47 METEOROLOGY AND CLIMATOLOGY

Includes weather forecasting and modification.

N91-31744# National Weather Service, Fort Worth, TX. Scientific Services Div.
ESTIMATING THE STRENGTH OF THE CAPPING INVERSION AND THE PROBABILITY OF STRONG CONVECTION
Michael Emlaw (National Weather Service, Norman, OK.) May 1991 27 p
(PB91-176685; NOAA-TM-NWS-SR-134) Avail: NTIS HC/MF A03 CSCL 04B

Two different techniques are introduced to aid the operational forecaster in determining the strength of the capping inversion and the possibility of strong convection. In both techniques, the forecaster must predict the maximum afternoon surface wet-bulb potential temperature and determine the strength of the forcing. The first technique requires use of the 12 hour Nested Grid Model (NGM) 850-700 mb thickness forecast, while the second technique requires use of the 12 hour 9000 ft. temperature forecast from the FD wind product. GRA

N91-31745# National Weather Service, Fort Worth, TX.
A QUANTITATIVE ANALYSIS OF QUASI-GEOSTROPHIC FORCING DURING RECENT SEVERE WEATHER OUTBREAKS ACROSS THE SOUTHERN GREAT PLAINS
David Andra (National Weather Service, Norman, OK.) May 1991 88 p Sponsored in part by Oklahoma Univ. and Oklahoma climatology Survey
(PB91-176693; NOAA-TM-NWS-SR-135) Avail: NTIS HC/MF A05 CSCL 04B

Numerous authors have proposed and discussed severe thunderstorm forecasting techniques based upon synoptic scale data. Although traditional techniques play an important role in forecasting, they are somehow unsatisfying in the sense that they sometimes do not provide quantitative guidance information, and frequently provide little insight and understanding into the physical processes responsible for the ensuing weather. In contrast, objective analyses of quasi-geostropic quantities, developed recently for the operational environment, show promise for forecasters on both of these points. It is important to learn more about the applications of these new tools toward severe storms forecasting, especially since major new technologies and training initiatives are scheduled for deployment into the operation forecast environment during the decade of the 1990's. To meet these goals, an objective analysis of upper air data was performed for 25 percent severe weather events in the Southern Great Plains. Results indicate that the analysis routines were useful in the quantitative assessment of certain aspects of the convective environment, particularly moisture and mid tropospheric static stability. Furthermore, the analysis of differential thickness advection, moisture advection, and Q-vector divergence provided insight into large-scale physical mechanisms acting to modify static stability and moisture (and hence buoyant energy). The results suggest large scale or quasigeostrophic motions have their primary role in the creation of an environment favorable for severe convection, rather than its initiation. GRA

N91-31746# World Meteorological Organization, Geneva (Switzerland).
REPORT OF THE WORKSHOP ON A CLICOM-HOMS INTERFACE World Climate Applications Programme
Jan. 1991 57 p Workshop held in Reading, England, 6-15 Mar. 1990
(WCAP-16; WMO/TD-409) Avail: NTIS HC/MF A04; print copy available at WMO, Geneva

The workshop was seen as having four purposes. They are summarized as follow. (1) to review the need for hydrological and water resource applications software in conjunction with CLICON. (2) to identify Hydrological Operational Multipurpose Subroutines (HOMS) components that might serve in this capacity. (3) to work with examples of these components, by adapting them or compiling appropriate interfaces, so that they can be used as applications software linked to CLICON. And (4) to draw conclusions from the above work with regard to the wider question of the relationship between HOMS and CLICOM, as well as to the need for further development of software, tutorials and/or manuals relating to interfacing applications software to CLICON. Author

N91-31747# Stockholm Univ. (Sweden). Dept. of Meteorology.
INITIALIZATION OF THE HIRLAM MODEL USING A DIGITAL FILTER
Peter Lynch (Meteorological Service, Dublin, Ireland) and Xiang-Lu Huang May 1991 38 p Prepared in cooperation with International Meteorological Inst., Stockholm, Sweden
(Contracts NFR-E-DG-2923-300; NFR-G-GU-1705-311)
(DM-57; ISSN-0349-0467; ETN-91-99785) Avail: NTIS HC/MF A03

Spurious high frequency oscillations occur in forecasts made with the primitive equations if the initial fields of mass and wind are not in an appropriate state of balance. These oscillations are due to gravity inertia waves of unrealistically large amplitude; the primary purpose of initialization is the removal or reduction of this high frequency noise by a delicate adjustment of the analyzed data. A simple method of eliminating spurious oscillations is presented. The method uses a digital filter applied to time series of the model variables generated by short-range forward and backward integrations from the initial time. The digital filtering technique is applied to initialize data for the HIRLAM model. The method is shown to have the three characteristics essential to any satisfactory initialization scheme. High frequency noise is effectively removed from the forecast, changes made to the analyzed fields are acceptably small, and the forecast is not degraded by application of the initialization. The Digital Filtering Initialization (DFI) technique is compared to the standard nonlinear Normal Mode Initialization (NMI) used with the HIRLAM model. ESA

N91-31748# Lawrence Livermore National Lab., CA.
THE USE OF DISTRIBUTIONAL AND POINTWISE STATISTICAL MEASURES IN GCM INTERCOMPARISONS
S. L. Grotch Jun. 1991 5 p Presented at the 5th Conference on Climate Variations, Denver, CO, 14-18 Oct. 1991
(Contract W-7405-eng-48)
(DE91-015697; UCRL-JC-106260; CONF-9110161-4) Avail: NTIS HC/MF A01

In climate research there is an increasing need to intercompare models and datasets over a variety of spatial scales. Distributional (non-parametric) statistics provide useful tools for such intercomparisons. Several illustrations of these methods will be presented using five global precipitation datasets as examples. DOE

N91-31749# Lawrence Livermore National Lab., CA.
IMPACT OF THE ICE PHASE ON A MESOSCALE CONVECTIVE SYSTEM: CLOUD ENSEMBLE FEATURES AND CLOUD RADIATIVE PROPERTIES
Hung-Neng S. Chin, M. M. Bradley, and C. R. Molenkamp Jun. 1991 16 p Presented at the 5th Conference on Climate Variations, Denver, CO, 14-18 Oct. 1991
(Contract W-7405-eng-48)
(DE91-015769; UCRL-JC-107526; CONF-9110161-5) Avail: NTIS HC/MF A03

This study attempts to provide further understanding of the effect of the ice phase on cloud ensemble features which are useful for improving GCM cumulus parameterization. In addition, cloud model results are also used to diagnose the radiative properties of anvils, and to assess cloud feedback on the larger-scale climate. The heat, moisture and mass budget analyses of a simulated squall line system indicate that, at least for this type of system, the inclusion of the ice phase in the microphysics does not considerably change the net cloud heating and drying effects and the feedback on the large-scale motion. Nonetheless, its impact on the radiative properties of clouds significantly influences not only the squall line system itself, but also the larger-scale circulation due to the favorable stratification for long-lasting anvil clouds. The finding of this study suggests that

more scientific effort should be focused on the effect of the ice phase to further explore cloud feedback on the large-scale climate through the radiative process. The inclusion of the ice phase can, however, be ignored in the cumulus parameterization in order to save significant amounts of computational resources. DOE

N91-31750*# Kansas Univ. Center for Research, Inc., Lawrence. Radar Systems and Remote Sensing Lab.
A SATELLITE-BASED RADAR WIND SENSOR
Weizhuang Xin Jun. 1991 168 p
(Grant NAG8-796)
(NASA-CR-188805; NAS 1.26:188805; RSL-TR-8760-2) Avail: NTIS HC/MF A08 CSCL 04B

The objective is to investigate the application of Doppler radar systems for global wind measurement. A model of the satellite-based radar wind sounder (RAWS) is discussed, and many critical problems in the designing process, such as the antenna scan pattern, tracking the Doppler shift caused by satellite motion, and backscattering of radar signals from different types of clouds, are discussed along with their computer simulations. In addition, algorithms for measuring mean frequency of radar echoes, such as the Fast Fourier Transform (FFT) estimator, the covariance estimator, and the estimators based on autoregressive models, are discussed. Monte Carlo computer simulations were used to compare the performance of these algorithms. Anti-alias methods are discussed for the FFT and the autoregressive methods. Several algorithms for reducing radar ambiguity were studied, such as random phase coding methods and staggered pulse repitition frequncy (PRF) methods. Computer simulations showed that these methods are not applicable to the RAWS because of the broad spectral widths of the radar echoes from clouds. A waveform modulation method using the concept of spread spectrum and correlation detection was developed to solve the radar ambiguity. Radar ambiguity functions were used to analyze the effective signal-to-noise ratios for the waveform modulation method. The results showed that, with suitable bandwidth product and modulation of the waveform, this method can achieve the desired maximum range and maximum frequency of the radar system. Author

N91-31751*# National Aeronautics and Space Administration, Washington, DC.
NASA AERODYNAMICS PROGRAM Annual Report, 1990
Louis J. Williams, Kristin A. Hessenius, Michael Dudley, Pamela F. Richardson, George Unger, and Steve Wander Aug. 1991 216 p
(Contract NASw-4430)
(NASA-TM-4312; NAS 1.15:4312) Avail: NTIS HC/MF A10 CSCL 04B

A review of the NASA Aerodynamics Division for FY 1990 is given. The program includes both fundamental and applied research directed at the full spectrum of aerospace vehicles, from rotorcraft to planetary entry probes. Computational methods and applications, computational fluid dynamics validation, transition and turbulence physics, numerical aerodynamic instrumentation, configuration aerodynamics, aeroacoustics, aerothermodynmics, hypersonics, subsonics, fighter aircraft, and rotorcraft are discussed. Author

N91-31752 Royal Netherlands Meteorological Inst., De Bilt.
DESCRIPTION OF CRAU DATA SET: METEOSAT DATA, RADIOSONDE DATA, SEA SURFACE TEMPERATURES: COMPARISON OF METEOSAT AND HEIMANN DATA
Sara H. Muller, Han The, Wim Kohsiek, and Wim A. A. Monna 1990 59 p
(KNMI-WR-90-03; ISSN-0169-1615; ETN-91-90009) Copyright Avail: Royal Netherlands Meteorological Inst., P.O. Box 201, 3730 AE De Bilt, Wilhelminalaan 10, Netherlands

In June 1987 the Crau experiment took place in the south of France. The purpose of this experiment was to study the exchange of heat and moisture between the Earth's surface and the atmosphere over homogeneous and nonhomogeneous terrain in relation to satellite observations of surface temperature; and to investigate the behavior of the atmospheric surface layer if dry warm air is advected over a wet cool surface. The Meteosat PDUS data which was recorded during the same period is described. Some related data sets which have not been described elsewhere are summarized. These include sea surface temperatures and radiosonde data. Comparisons between Meteosat and Heimann data are made. The comparison between raw Meteosat and Heimann data aims at an accurate localization of the Meteosat data. Data for all available days are compared after the application of atmospheric corrections. ESA

48 OCEANOGRAPHY

Includes biological, dynamic, and physical oceanography; and marine resources.

For related information see also *43 Earth Resources and Remote Sensing.*

N91-31753# Minerals Management Service, Camarillo, CA.
A SUMMARY OF THE PHYSICAL OCEANOGRAPHY OF THE PACIFIC NORTHWEST COAST
David F. Purdy 1990 51 p
(PB91-164434; MMS-91/0003) Avail: NTIS HC/MF A04 CSCL 08C

Current information on the physical oceanography of the Pacific Coast of Washington and Oregon, including information on currents, water mass characteristics, vertical stratification and mixing, upwelling, and waves is summarized. A general outline of the California current system is given, including the California and Davidson surface currents, the California and Washington undercurrents, and shelf currents. Conditions affecting local and nearshore currents, considered important in the event of an oil spill, are discussed. A summary of wave data is included from several sources including the Corps of Engineers Wave Information Study, based on meteorological information, and the Minerals Management Service's Coastal Wave Statistical Data Base (CWSDB), based on high quality data from a system of buoys. GRA

N91-31754# Naval Oceanographic Office, Bay Saint Louis, MS.
NORTH PACIFIC GUYOTS
N. C. Smoot May 1991 100 p
(AD-A239388; NOO-TN-01-91) Avail: NTIS HC/MF A05 CSCL 08/3

A bathymetric atlas of North Pacific guyots is presented as a series of chartlets along with a description, the derivation of names, and a history of guyots and associated geomorphology. The features were surveyed by swath bathymetric systems that provide total coverage and permit a comprehensive study of guyot geomorphology. A description of navigation and sonar equipment is included. GRA

51 LIFE SCIENCES (GENERAL)

N91-31755* National Aeronautics and Space Administration. Lyndon B. Johnson Space Center, Houston, TX.
BIOFILM MONITORING COUPON SYSTEM AND METHOD OF USE Patent
Richard L. Sauer, inventor (to NASA) and David T. Flanagan, inventor (to NASA) 17 Sep. 1991 10 p Filed 14 Mar. 1990 supersedes N91-13857 (29 - 5, p 693)
(NASA-Case-MSC-21585-1; US-Patent-5,049,492; US-Patent-Appl-SN-493529; US-Patent-Class-435-30; US-Patent-Class-73-863.85; US-Patent-Class-73-863.86; US-Patent-Class-73-863.41; US-Patent-Class-73-863.22; US-Patent-Class-422-99; US-Patent-Class-422-101) Avail: US Patent and Trademark Office CSCL 06C

An apparatus and method is disclosed for biofilm monitoring of a water distribution system which includes the mounting of at least one fitting in a wall port of a manifold in the water distribution

system with a passage through the fitting in communication. The insertion of a biofilm sampling member is through the fitting with planar sampling surfaces of different surface treatment provided on linearly arrayed sample coupons of the sampling member disposed in the flow stream in edge-on parallel relation to the direction of the flow stream of the manifold under fluid-tight sealed conditions. The sampling member is adapted to be aseptically removed from or inserted in the fitting and manifold under a positive pressure condition and the fitting passage sealed immediately thereafter by appropriate closure means so as to preclude contamination of the water distribution system through the fitting. The apparatus includes means for clamping the sampling member and for establishing electrical continuity between the sampling surfaces and the system for minimizing electropotential effects. The apparatus may also include a plurality of fittings and sampling members mounted on the manifold to permit extraction of the sampling members in a timed sequence throughout the monitoring period. Official Gazette of the U.S. Patent and Trademark Office

N91-31756# Brookhaven National Lab., Upton, NY.
PYRIMIDINE DIMER FORMATION BY UVA RADIATION: IMPLICATIONS FOR PHOTOREACTIVATION
B. M. Sutherland, H. Hacham, J. C. Sutherland, and R. W. Gange (Harvard Medical School, Boston, MA.) 1991 12 p Presented at the 2nd International Conference on the Biological Effects of UVA Radiation, San Antonio, TX, 27-28 Jun. 1991
(Contract DE-AC02-76CH-00016)
(DE91-015837; BNL-46391; CONF-9106254-1) Avail: NTIS HC/MF A03

The duality of biological and biochemical effects mediated by UVA radiation complicates evaluation of its biological role. On the one hand, UVA can drive photoreactivation and prevent inactivation of a UV-irradiated organism; on the other hand, UVA clearly kills cells. We have investigated the ability of UVA to induce pyrimidine dimers in human skin in situ. Results of these studies indicate that UVA induces easily quantifiable levels of pyrimidine dimers in the DNA of human skin exposed in situ; and significant levels of dimers are induced in skin exposed to biologically relevant UVA doses (e.g. 0-1 minimal erythemal dose (MED)). Also, UVA doses appropriate for photorepair may induce sufficient dimer frequencies to mask photoreactivation in biological systems, including human skin. Therefore, careful design of photoreactivation experiments is essential. The UV lamp used must not reverse or convert photodamage, nor induce additional lesions in the DNA. DOE

N91-31757# Air Force Inst. of Tech., Wright-Patterson AFB, OH.
THE EFFECT OF EXERCISE TRAINING ON SKELETAL MUSCLE GLUCOSE TRANSORTER ISOFORM GLUT4 CONCENTRATION IN THE OBESE ZUCKER RAT M.S. Thesis
Eric A. Banks May 1991 110 p
(AD-A239461; AFIT/CI/CIA-91-054) Avail: NTIS HC/MF A06 CSCL 06/1

Exercise training has been demonstrated to improve skeletal muscle insulin resistance. However, the mechanisms for this improvement have not been fully chararcterized. The effects of high (HT) and low (LT) intensity exercise training were therefore examined on insulin-stimulated 3-O-methyl-D-glucose (3-OMG) transport and the concentration of glucose transporter isoform GLUT4 in the red (fast-twitch oxidative) and white (fast-twitch glycolytic) guadriceps of the obese Zucker rat. Sedentary obese (SED) and lean (LN) rats served as controls. 3-OMG transport was determined during hindlimb HT and LT rats displayed greater red quadriceps 3-OMG transport rates and GLUT4 concentrations than SED rats. Citrate synthase activity, which is an oxidative enzyme marker for skeletal muscle exercise training, highly correlated with GLUT4 concentration. The 3-OMG transport rate of LN rats was two-fold greater than SED rats despite similar GLUT4 concentration. These results suggest muscle insulin resistance in the obese Zucker rat is not due to a reduced GLUT4 concentration. However, the improved insulin resistance seen with exercise training appears to be due in part to an increased GLUT4 concentration which is only observed in muscle fibers recruited during training. GRA

N91-31758# Case Western Reserve Univ., Cleveland, OH. Inst. of Pathology.
ELECTRON MICROSCOPY TO CORRELATE CELL STRUCTURES AND BIOCHEMICAL ACTIVITY Midterm Report, 15 Nov. 1989 - 14 May 1991
Masamichi Aikawa 15 Jun. 1991 27 p
(Contract DAMD17-90-C-0010; DA Proj. 3M1-61102-BS-13)
(AD-A239640) Avail: NTIS HC/MF A03 CSCL 06/5

Electron microscopy showed that desferrioxamine (DFO) appears to act specifically during the late trophzoite and early schizont stages of P. falciparum by preventing nuclear division. This finding is consistent with inhibition of the iron-dependent enzyme ribonucleotide reductase induced by DFO. Inhibition of this enzyme appears to contribute to the antimalarial effect of iron chelate. Immuno-electron microscopy showed liposome-encapsulated malarial antigen that is phagocytosed by macrophages can enter an intracellular compartment in which some of the antigenic epitopes are not degraded by lysosomal enzymes. This indicates the possible existence of a pathway in which liposomal contents can bypass lysosomal degradation. PRBC sequestration and cytoadherence of knobs on PRBC to endothelial cells in cerebral vessels were shown in rhesus monkeys infected with P. coatneyi. This indicates that rhesus monkeys infected with P. coatneyi can be used as a primate model for human cerebral malaria. GRA

N91-31776*# Utah State Univ., Logan.
EXPLORING THE LIMITS OF CROP PRODUCTIVITY: A MODEL TO EVALUATE PROGRESS
Bruce Bugbee *In* NASA. Ames Research Center, Controlled Ecological Life Support Systems: CELSS '89 Workshop Mar. 1990 p 1-2 (For primary document see N91-31775 23-54)
Avail: NTIS HC/MF A19 CSCL 06K

N91-31779*# Wisconsin Univ., Madison.
ENVIRONMENTAL AND CULTURAL CONSIDERATIONS FOR GROWTH OF POTATOES IN CELSS
Theodore W. Tibbitts, Susan M. Bennett, and Robert C. Morrow *In* NASA. Ames Research Center, Controlled Ecological Life Support Systems: CELSS '89 Workshop Mar. 1990 p 77-92 (For primary document see N91-31775 23-54)
Avail: NTIS HC/MF A19 CSCL 02C

N91-32027# Keuring van Electrotechnische Materialen N.V., Arnhem (Netherlands). Dept. of Environment Research.
A SYSTEM TO DETERMINE WHOLE-PLANT EXCHANGE RATES OF OZONE, CARBON DIOXIDE AND WATER VAPOUR
J. M. M. Aben *In its* KEMA Scientific Reports, Volume 8, Number 2, 1990 Apr. 1990 p 109-120 (For primary document see N91-32023 23-99)
Avail: NTIS HC/MF A04

52 AEROSPACE MEDICINE

Includes physiological factors; biological effects of radiation; and effects of weightlessness on man and animals.

N91-31759# Chicago Univ., IL.
NUCLEAR MEDICINE AND IMAGING RESEARCH: QUANTITATIVE STUDIES IN RADIOPHARMACEUTICAL SCIENCE
M. Copper and R. N. Beck Jun. 1991 83 p
(Contract DE-FG02-86ER-60438)
(DE91-015447; DOE/ER-60438/T3) Avail: NTIS HC/MF A05

During the past three years, the program has undergone a substantial revitalization. There has been no significant change in the scientific direction of this grant, in which emphasis continues to be placed on developing new or improved methods of obtaining quantitative data from radiotracer imaging studies. However, considerable scientific progress has been made in the three areas

of interest: radiochemistry, quantitative methodologies, and experimental methods and feasibility studies, resulting in a sharper focus of perspective and improved integration of the overall scientific effort. Changes in faculty and staff, including development of new collaborations, have contributed to this, as has acquisition of additional and new equipment and renovations and expansion of the core facilities. DOE

N91-31760* National Aeronautics and Space Administration, Washington, DC.
AEROSPACE MEDICINE AND BIOLOGY: A CONTINUING BIBLIOGRAPHY WITH INDEXES (SUPPLEMENT 353)
Feb. 1989 84 p
(NASA-SP-7011(353); NAS 1.21:7011(353)) Avail: NTIS HC A03; NTIS standing order as PB91-912300, $10.50 domestic, $21.00 foreign CSCL 06E

This bibliography lists 238 reports, articles, and other documents introduced into the NASA Scientific and Technical Information System in August 1991. Subject coverage includes: aerospace medicine and psychology, life support systems and controlled environments, safety equipment, exobiology and extraterrestrial life, biotechnology, human factors engineering, and flight crew behavior and performance. Author

N91-31761# Hopital d'Instruction des Armees, Versailles (France). Service de Medecine Aerospatiale.
CONTINUOUS 24 HOUR ECG STUDY, ON GROUND AND IN FLIGHT, OF 19 MIRAGE 2000 PILOTS STATIONED AT THE DIJON AIRBASE (FRANCE). COMPARISON WITH SIMILAR RECORDINGS TAKEN ON OTHER TYPES OF FIGHTER AIRCRAFT OR IN OPERATIONALLY DIFFERENT CONDITIONS [ETUDE DE L'ECG CONTINU DE 24 HEURES, AU SOL ET EN VOL CHEZ 19 PILOTES DE MIRAGE 2000 STATIONNES SUR LA B.A. DE DIJON. COMPARAISON AVEC LES ENREGISTREMENTS SIMILAIRES EFFECTUES SUR D'AUTRES TYPES D'AVIONS DE COMBAT OU DANS DES CONDITIONS OPERATIONELLE]
A. Seigneuric and J. P. Burlaton 1990 26 p In FRENCH
(Contract DRET-87-1027)
(ETN-91-99973) Avail: NTIS HC/MF A03

Electrocardiograph (ECG) studies of fighter pilots in different Mirage types are presented and compared. Recordings covered several different types of operational missions, as well as the sleep phase and a diurnal activity which had not been standardized. The results relating to the diurnal, nocturnal and in-flight sinusal frequency, the variations of auricular-ventricular conduction, supraventricular and ventricular excitability troubles, and repolarization modifications, were compared for Mirage 2000 and Mirage 3 and F1 pilots. ESA

N91-31762# Manchester Univ. (England). School of Management.
DEVELOPMENTS IN MEDICAL AUDIT IN HOSPITALS IN THE NATIONAL HEALTH SERVICE M.S. Thesis
M. Djumic 1990 214 p
(ETN-91-99984) Copyright Avail: NTIS HC/MF A10

The current work on establishing comprehensive medical audit, focusing in particular on the role of information systems in the development of medical audit, the problems with outcome measurement, the perceived implications of medical audit for clinical freedom and the relationship of the activity to other reforms affecting the NHS (National Health Service, United Kingdom), is reviewed. In addition to a comprehensive review of the literature on medical audit, the study involved interviews with clinicians and management staffs. ESA

N91-31763# Lawrence Livermore National Lab., CA.
BIOLOGICAL DOSIMETRY AND MECHANISMS OF CARCINOGENESIS
M. L. Mendelsohn 14 Jun. 1991 13 p Presented at the Symposium on Chemical Carcinogenesis: the Relevance of Mechanistic Understanding in Toxicological Evaluation, Berlin, Federal Rep. of Germany, 29-30 Apr. 1991
(Contract W-7405-eng-48)
(DE91-015689; UCRL-JC-107755; CONF-9104280-1) Avail: NTIS HC/MF A03

Biological dosimetry has been given new meaning in recent years by advancing methodologies which provide increasingly sensitive and detailed cellular and biochemical information on the exposed subject. One mode of dosimetry is the toxicological mode; this involves the study of cause and effect relationships across subjects, doses, agents and species. The primary purpose of this mode is to understand and generalize the underlying mechanisms of biological damage, and to help predict or prevent ultimate toxic effects. The other mode of dosimetry described is the epidemiological mode. The emphasis is on using the biological response to reconstruct the dose received by occupationally, environmentally or medically exposed populations. The use is described of these two modes of dosimetry in unraveling the mechanisms and risks of carcinogenesis in human populations. DOE

N91-31764# Tennessee Univ., Knoxville. Dept. of Chemistry.
BORON IN NUCLEAR MEDICINE: NEW SYNTHETIC APPROACHES TO PET, SPECT, AND BNCT AGENTS
G. W. Kabalka Sep. 1991 25 p
(Contract DE-FG05-86ER-60434)
(DE91-016488; DOE/ER-60434/6) Avail: NTIS HC/MF A03

The primary objective of the DOE Nuclear Medicine Program at The University of Tennessee is the creation of new methods for introducing short-lived isotopes into agents for use in computerized tomography. A portion of the research effort is directed toward the development of new synthetic methods for the preparation of boron-containing neutron therapy agents. The uniqueness of the UT program is its focus on the design of new chemistry and technology as opposed to the application of known reactions to the synthesis of specific radiopharmaceuticals. The versatile organic boron reagents are utilized in most of the new chemistry. This new technology is then used in nuclear medicine research at the UT Biomedical Imaging Center and in collaborative research programs with colleagues at other DOE facilities. An important goal of the DOE Nuclear Medicine Program at UT is to provide training for students (predoctoral and postdoctoral) in the scientific aspects of nuclear medicine. DOE

N91-31765# Naval Medical Research and Development Command, Bethesda, MD.
NAVAL MEDICAL RESEARCH AND DEVELOPMENT COMMAND Annual Report, 1990
1990 55 p
(AD-A239393) Avail: NTIS HC/MF A04 CSCL 06/5

Cold-induced amnesia was initiated in the Naval Medical Research and Development Command's (NMRDC) FY90 Independent Research Program to elucidate the neurochemical and physiological mechanisms underlying the decrements to working memory that are induced by exposure to moderate or severe cold (here termed cold-induced amnesia). Such memory impairment has been reported by Navy personnel who are commonly exposed to cold temperatures, yet clearly must be able to function effectively in increasingly complex and high tech operational environments. Cold-induced amnesia proposed to determine the effects of temperature on specific neurotransmitters and neurohormones in vivo, in brain regions whose physiological integrity is known to be critical for normal memory function, and to relate observed neurophysiological changes to alterations in working memory and behavioral performance. The ultimate transition goal of this study is to provide advanced biomedical therapies for the prevention and treatment of cold-induced memory impairment in Navy personnel. GRA

N91-31766# Tennessee Univ., Memphis.
MURAMYL PEPTIDE-ENHANCED SLEEP: PHARMACOLOGICAL OPTIMIZATION OF PERFORMANCE Annual Report, 1 Jun. 1990 - 31 May 1991
James M. Krueger 1 Jun. 1991 110 p

(Contract DAMD17-86-C-6194; DA Proj. 3M1-61102-BS-15)
(AD-A239442) Avail: NTIS HC/MF A06 CSCL 06/5

It is now recognized that sleep results from neuronal activity which is regulated by the interactions of neurons with substances produced by neurons and other cellular components of the brain. Over the past 30 years, the technical abilities to identify and synthesize biochemicals has greatly improved; these advances have led to the identification of several endogenous sleep factors (SFs) (substances that promote sleep). Over the past five years, several new SFs were identified and analogs were synthesized which may be developed into new, more effective, and safer somnogenic agents. The broad goal of this work was to develop the information needed to determine if it is reasonable to propose either endogenous SFs or synthetic analogs as potential sleep inducing agents for military use. GRA

N91-31767# Army Research Inst. of Environmental Medicine, Natick, MA.
COLD-INDUCED CHANGES IN ARTERIAL SENSITIVITY Final Report
Stephen P. Bruttig and Donald E. Roberts May 1991 33 p
(AD-A239493; USARIEM-T11-91) Avail: NTIS HC/MF A03 CSCL 06/10

We studied the effects of cold on rabbits and pigs: (1) to determine how cold affects the smooth muscle sensitivity to receptor-mediated (NEPI--Norepinephrine) or nonreceptor-mediated (KCL) (pigs only) agonist induction of in vitro vascular contraction; (2) to determine whether cold-induced vascular sensitivity to catecholamines exists in an intact hypothermic pig model; and (3) to determine the effect of cortisol on the arterial smooth muscle contraction. The in vitro exposure of femoral arteries from rabbits and pigs to cold resulted in a progressive loss of sensitivity to agonist. Femoral arteries isolated from hypothermic pigs (core temp = 25 C for 2 hours) were no more sensitive to NEPI in vitro than arteries from normothermic animals. However, the in situ hind limb arterial bed of the hypothermic pig was ten times more sensitive to arterial injection of NEPI than the arterial bed of the normothermic pig. The sensitivity of porcine vascular smooth muscle to NEPI does not appear to be affected by cortisol. These data suggest that cold evokes an extravascular control (mechanisms not intrinsic to vascular tissue) over NEPI sensitivity. Moreover, these data suggest that the mechanism for control of cold-induced sensitivity to sympathetic neurotransmitter in the pig is different from the mechanism which operates in the rabbit. GRA

N91-31768# Naval Air Development Center, Warminster, PA. Air Vehicle and Crew Systems Technology Dept.
THE G-LOC SYNDROME Final Report
James E. Whinnery 31 Oct. 1990 15 p
(AD-A239561; NADC-91042-60) Avail: NTIS HC/MF A03 CSCL 06/5

Acceleration (+GZ)-induced loss of consciousness (G LOC) is but one isolated symptom that results when central nervous system (CNS) function is altered by G-stress. Other symptoms and changes also result when reduction of oxygenated blood flow to the CNS occurs. The complex of symptoms and changes that result from G-stress occur in close temporal relationship and therefore form a G-LOC syndrome. Recognition of the G-LOC syndrome serves to include the associated symptoms as part of the normal response to CNS ischemia/hypoxia. This recognition is important in reducing the potential for unnecessary aeromedical evaluation or disqualification of normal aircrew who have an uncomplicated G-LOC episode. It also serves to ensure that abnormal responses can be more clearly identified. Recognition of the G-LOC syndrome also serves to enhance the understanding that G-LOC is a primary neurologic disturbance induced by G-stress. The existing situation is clarified by recognizing the G-LOC syndrome as including all of the +GZ-induced CNS symptoms, either alone or in combination, as a normal response to +GZ stress in normal human beings. GRA

N91-31769# Naval Medical Research Inst., Bethesda, MD.
BASIC OPERATION AND PRELIMINARY TRIALS OF A DETECTOR FOR STATIONARY GAS BUBBLES Technical Report, Sep. 1988 - May 1989
Gary Albin, Paul Massell, and Edward Thalmann Jul. 1991 46 p
(AD-A239710; NMRI-91-39) Avail: NTIS HC/MF A03 CSCL 06/10

Symptoms of decompression sickness (DCS) typically are assumed to result from the formation of gas bubbles in blood or extravascular tissue. Information on extravascular bubbles has been severely limited by the lack of any nondestructive testing method of observing them. A system has been developed to detect stationary gas bubbles 1 to 20 microns in diameter by using ultrasonic interrogation. We describe the system and propose a protocol for using it to identify the sizes and numbers of bubbles. A mathematical model of a vibrating bubble in liquid has been coded into a computer program, and currently we are developing an analogous model to simulate a bubble in an elastic solid. A technique is described for preparing calibration standards by trapping bubbles in a transparent hydrogel, which can be assayed using light microscopy. Crude preliminary trials with the bubble detector demonstrate that it can detect sufficiently large populations of bubbles, although its signal/noise ratio appears too low for detecting individual bubbles. Quantitative assay of bubbles is not possible until the system has been modified to provide a way to capture and store the output signal. GRA

N91-31770# Naval Health Research Center, San Diego, CA.
SLEEP LOGS: MEASUREMENT OF INDIVIDUAL AND OPERATIONAL EFFICIENCY Interim Report, period ending Oct. 1988
P. Naitoh, G. Banta, T. Kelly, J. Bower, and R. Burr May 1991 24 p Sponsored by Navy Medical Research and Development Command
(AD-A239774; NHRC-90-29) Avail: NTIS HC/MF A03 CSCL 06/10

Sleep logistics are based on scientific knowledge of how sleep loss influences human performance, and provides techniques to assure that every member of a group receives sufficient sleep at appropriate times so that serious sleep loss does not interfere with mission completion. Sleep logistics require careful measurement of the amount and pattern of sleep each group member can obtain during a given mission scenario. There are many tools for measuring amounts and patterns of sleep. The most economical and preferred method to study sleep, especially in a large group of individuals, has been the sleep log (diary). Two to four days of sleep log data were collected from 39 Navy and Marine Corps personnel during an at-sea Naval operation in the Persian Gulf. For the overall group, the average sleep episode duration was 6.8 hours per 24-hours without serious sleep fragmentation. An exception was a group of four boiler technicians. These boiler technicians accumulated a sleep debt which might interfere with maintaining sustained attention and situational awareness. Various techniques for analyzing sleep log data are discussed. Advantages and disadvantages of sleep log techniques are compared to those of other methods of collecting sleep data. GRA

53 BEHAVIORAL SCIENCES

Includes psychological factors; individual and group behavior; crew training and evaluation; and psychiatric research.

N91-31771# Illinois Univ., Chicago. State Psychiatric Inst.
FULL-INFORMATION ITEM BI-FACTOR ANALYSIS Report, 31 Jul. 1989 - 31 Jul. 1990
Robert D. Gibbons, Donald R. Hedeker, and R. D. Bock Jul. 1990 20 p
(Contract N00014-89-J-1104; NR Proj. RR0-42046)
(AD-A229346) Avail: NTIS HC/MF A03 CSCL 05/8

A plausible s-factor solution for many types of psychological and educational tests is one in which there is one general factor and s-1 group or method related factors. The bi-factor solution results from the constraint that each item has a non-zero loading on the primary dimension alpha j 1 and at most one of the s-1 group factors. This structure has been termed the bi-factor solution by Holzinger & Swineford but it also appears in the work of Tucker and Joreskog. All attempts at estimating the parameters of this model have been restricted to continuously measured variables; it has not been previously considered in the context of item-response theory (IRT). It is conceivable, however, that the bi-factor structure might arise in IRT related problems. The purpose of this paper is to derive a bi-factor item-response model for binary response data, and to develop a corresponding method of parameter estimation. This restriction leads to a major simplification of the likelihood equations that (1) permits the statistical evaluation of problems of unlimited dimensionality; (2) permits conditional dependence among discrete and previously identified subsets of items, and (3) in some cases provides more parsimonious factor solutions than an unrestricted full-information item factor analysis might provide (e.g. Bock and Aitkin, 1981). GRA

N91-31772# Colorado Univ., Boulder. Center for Research on Judgment and Policy.
EFFECTS OF STRESS ON JUDGMENT AND DECISION MAKING IN DYNAMIC TASKS Interim Report, 1 Sep. 1988 - 31 Dec. 1989
Kenneth R. Hammond and Cynthia M. Lusk Jun. 1991 183 p
(Contract MDA903-86-C-0142)
(AD-A239452; ARI-RN-91-82) Avail: NTIS HC/MF A09 CSCL 05/8

Three empirical studies on judgment and decision making in dynamic tasks were carried out during the period 1 September 1988 to 31 December 1989. Subjects were expert research meteorologists. Topics were forecasting (a) hail, (b) microbursts, and (c) convection initiation (thunderstorms) at an airport approach. Primary findings were as follows: in the hail study, meteorologists' forecasts were closely approximated by a weighted-sum model; in the microburst study, experts who worked together for years, when tested in work conditions, did not agree on the judgments of principal cues; in the convection study, more accurate forecasts were made on high stress than low stress days, thus contradicting the conventional wisdom. Two annotated bibliographies were produced: the effects of stress on judgment and decision making, and the effects of variation of display formats on judgment and decision making. GRA

N91-31773# Colorado Univ., Boulder.
OPTIMIZING THE LONG-TERM RETENTION OF SKILLS: STRUCTURAL AND ANALYTIC APPROACHES TO SKILL MAINTENANCE 3 Interim Report, Aug. 1988 - Aug. 1989
Alice F. Healy, K. A. Ericsson, and Lyle E. Bourne, Jr. Jun. 1991 13 p
(Contract MDA903-86-K-0155)
(AD-A239574; CU-153-0638; ARI-RN-91-81) Avail: NTIS HC/MF A03 CSCL 05/8

This research program identifies the characteristics of knowledge and skill most resistant to decay because of disuse. The program is divided into analytic and structural approaches. Two lines of research are used to investigate skill retention and maintenance using the analytic approach. The first investigates different laboratory analogues of component military skills, and the second investigates parallel natural skills learned by the college population during prior education. We have developed five laboratory methodologies and completed experimental studies involving each of them, and have identified four natural skills and gathered long-term retention data for each of these skills. For the structural approach, we designed an experimental paradigm to assess the detailed encoding of new knowledge at presentation and at delay using verbal report techniques and chronometric measurement of retrieval components. We completed several studies of retention of vocabulary items with this paradigm. In addition, we formulated a theoretical framework, on the notion of procedural reinstatement, and have used this framework to account for findings from many different facets of our research program, both analytic and structural. GRA

N91-31774# Decision Science Consortium, Inc., Reston, VA.
EXAMINING THE EFFECT OF INFORMATION ORDER ON EXPERT JUDGMENT Interim Report, May 1989 - May 1990
Leonard Adelman, Martin A. Tolcott, and Terry A. Bresnick Jun. 1991 27 p
(Contract MDA903-89-C-0134)
(AD-A239708; Rept-90-6; ARI-RN-91-78) Avail: NTIS HC/MF A03 CSCL 05/8

Research indicates that humans use heuristics to make inferences and that, depending on task characteristics, these heuristics can lead to inconsistencies and errors in judgment - that is, cognitive biases. Most of this research has been performed with university students performing tasks, requiring logical thinking but not expertise in a particular substantive area. Our concern is in determining whether heuristics can lead to cognitive biases among experienced personnel performing their substantive task. In particular, we examined whether information order and response mode could affect the judgements of Army air defense operators. A within-subject factorial experiment was performed in December, 1989, with 63 Army air defense operators. Information order and response mode interacted to affect the Army air defense operators' judgments. When information was presented sequentially and a probability estimate was obtained after each piece of information, participants gave different probability estimates of whether an unknown aircraft was friendly or hostile, depending on the order with which the same information was presented. These results support the predictions of the Hogarth-Einhorn belief updating model. GRA

54 MAN/SYSTEM TECHNOLOGY AND LIFE SUPPORT

Includes human engineering; biotechnology; and space suits and protective clothing.

For related information see also *16 Space Transportation.*

N91-31775*# National Aeronautics and Space Administration. Ames Research Center, Moffett Field, CA.
CONTROLLED ECOLOGICAL LIFE SUPPORT SYSTEMS: CELSS '89 WORKSHOP
Robert D. MacElroy, ed. Mar. 1990 433 p Workshop held in Orlando, FL, Feb. 1989
(NASA-TM-102277; A-90059; NAS 1.15:102277) Avail: NTIS HC/MF A19 CSCL 06K

Topics discussed at NASA's Controlled Ecological Life Support Systems (CELSS) workshop concerned the production of edible biomass. Specific areas of interest ranged from the efficiency of plant growth, to the conversion of inedible plant material to edible food, to the use of plant culture techniques. Models of plant growth and whole CELSS systems are included. The use of algae to supplement and improve dietary requirements is addressed. Flight experimentation is covered in topics ranging from a Salad Machine for use on the Space Station Freedom to conceptual designs for a lunar base CELSS. For individual titles, see N91-31776 through N91-31800.

N91-31776*# Utah State Univ., Logan.
EXPLORING THE LIMITS OF CROP PRODUCTIVITY: A MODEL TO EVALUATE PROGRESS **c51**
Bruce Bugbee *In* NASA. Ames Research Center, Controlled Ecological Life Support Systems: CELSS '89 Workshop Mar. 1990 p 1-2 (For primary document see N91-31775 23-54)
Avail: NTIS HC/MF A19 CSCL 06K

The goal was to determine the limits of crop productivity when all environmental constraints were removed. Researchers define productivity as food output per unit of input. Researchers evaluated cultivars of wheat with reduced leaf size and number to decrease

the leaf area index at high plant densities. These cultivars may also have an improved harvest index. Hydroponic studies indicate that 1 mM nitrate in solution is adequate to support maximum growth in these systems, provided iron nutrition is adequate. Wheat does not accumulate nitrate in leaves even when the solution nitrate concentration is 15 mM. Long-term photosynthetic efficiency (g mol (exp -1) of photons) and harvest index were not altered by photoperiod (16, 20, or 24 hours). Wheat does not need, nor benefit from, a diurnal dark period. Author

N91-31777*# National Aeronautics and Space Administration. Ames Research Center, Moffett Field, CA.
ENVIRONMENTAL MODIFICATION OF YIELD AND FOOD COMPOSITION OF COWPEA AND LEAF LETTUCE
Cary A. Mitchell, Suzanne S. Nielsen (Purdue Univ., West Lafayette, IN.), and David L. Bubenheim *In its* Controlled Ecological Life Support Systems: CELSS '89 Workshop Mar. 1990 p 25-53 (For primary document see N91-31775 23-54)
(Contract NCC2-100)
Avail: NTIS HC/MF A19 CSCL 06K

Cowpea (Vigna unguiculata (L.) Walp.) and leaf lettuce (Lactuca sativa L.) are candidate species to provide ligume protein and starch or serve as a salad base for a nutritionally balanced and psychologically satisfying vegetarian diet in the Controlled Ecology Life Support System (CELSS). Various nutritional parameters are reported. Hydroponic leaf lettuce grew best under CO2 enrichment and photosynthetic photon flux (PPF) enhancement. Leaf protein content reached 36 percent with NH4(+) + NO3 nutrition; starch and free sugar content was as high as 7 or 8.4 percent of DW, respectively, for high PPF/CO2 enriched environments. Author

N91-31778*# California Univ., Davis.
EFFICIENCY OF N USE BY WHEAT AS A FUNCTION OF INFLUX AND EFFLUX OF NO3
R. C. Huffaker, M. Aslam, and M. R. Ward *In* NASA. Ames Research Center, Controlled Ecological Life Support Systems: CELSS '89 Workshop Mar. 1990 p 55-76 (For primary document see N91-31775 23-54)
Avail: NTIS HC/MF A19 CSCL 06K

Since N assimilation is one of the most costly functions of a plant, its efflux before assimilation results in a serious energy cost and loss in efficiency which could decrease yields. Efficient crop production is critical to the Closed Ecology Life Support System (CELSS). The objective is to determine the extent of efflux of the N species NO3(-), NH4(+), NO2(-), and urea after uptake, and possible means of regulation. Researchers found that NO3 efflux became serious as its substrate level increased. Efflux/Influx (E/I) of NO3(-) was greater in darkness (35 percent) than in light (14 percent), and the ratio greatly increased with substrate NO3 (-), (up to 45 percent at 10 mM). It seems advantageous to use the lowest possible nutrient concentration of NO3(-). The feasibility of using ClO3(-) was assessed and its toxicity determined.
Author

N91-31779*# Wisconsin Univ., Madison.
ENVIRONMENTAL AND CULTURAL CONSIDERATIONS FOR GROWTH OF POTATOES IN CELSS **c51**
Theodore W. Tibbitts, Susan M. Bennett, and Robert C. Morrow *In* NASA. Ames Research Center, Controlled Ecological Life Support Systems: CELSS '89 Workshop Mar. 1990 p 77-92 (For primary document see N91-31775 23-54)
Avail: NTIS HC/MF A19 CSCL 02C

The white potato (Solanum tuberosum) was evaluated for use in the Closed Ecology Life Support System (CELSS) because of its high ratio of edible to inedible biomass and highly nutritious tuber that consists of readily digestible carbohydrates and proteins. Results are given for conditions that will produce the highest yields. The results, given in tabluar form, indicate the optimum temperatures, irradiance, carbon dioxide concentration, root environment, plant spacing, root and stolen containment, and harvesting times. Author

N91-31780*# National Aeronautics and Space Administration. John F. Kennedy Space Center, Cocoa Beach, FL.
EFFECTS OF ATMOSPHERIC CO2 ON PHOTOSYNTHETIC CHARACTERISTICS OF SOYBEAN LEAVES
R. M. Wheeler, C. L. Mackowiak (Bionetics Corp., Cocoa Beach, FL.), J. C. Sager, and W. M. Knott *In* NASA. Ames Research Center, Controlled Ecological Life Support Systems: CELSS '89 Workshop Mar. 1990 p 93-105 (For primary document see N91-31775 23-54)
Avail: NTIS HC/MF A19 CSCL 06K

Soybean (Glycine max. cv. McCall) plants were grown at 500, 1000, and 2000 umol mol (exp -1) CO2 for 35 days with a photosynthetic photon flux of 300 umol m (exp -2) s (-1). Individual leaves were exposed to step changes of photosynthetic photon flux to study CO2 assimilation rates (CAR), i.e., leaf net photosynthesis. In general, CAR increased when CO2 increased from 500 to 1000 umol mol (exp -1), but not from 1000 to 2000 umol mol (exp -1). Regardless of the CO2 level, all leaves showed similar CAR at similar CO2 and PPF. This observation contrasts with reports that plants tend to become 'lazy' at elevated CO2 levels over time. Although leaf stomatal conductance (to water vapor) showed diurnal rhythms entrained to the photoperiod, leaf CAR did not show these rhythms and remained constant across the light period, indicating that stomatal conductance had little effect on CAR. Such measurements suggest that short-term changes in CO2 exchange dynamics for a controlled ecological life support system can be closely predicted for an actively growing soybean crop. Author

N91-31781*# National Aeronautics and Space Administration. John F. Kennedy Space Center, Cocoa Beach, FL.
EFFECTS OF ELEVATED ATMOSPHERIC CARBON DIOXIDE CONCENTRATIONS ON WATER AND ACID REQUIREMENTS OF SOYBEANS GROWN IN A RECIRCULATING HYDROPONIC SYSTEM
C. L. Mackowiak, R. M. Wheeler, W. Lowery (Bionetics Corp., Cocoa Beach, FL.), and J. C. Sager *In* NASA. Ames Research Center, Controlled Ecological Life Support Systems: CELSS '89 Workshop Mar. 1990 p 107-118 (For primary document see N91-31775 23-54)
Avail: NTIS HC/MF A19 CSCL 06K

Establishing mass budgets of various crop needs, i.e. water and nutrients, in different environments is essential for the Controlled Ecological Life Support System (CELSS). The effects of CO2 (500 and 1000 umol mol (exp -1)) on water and acid use (for pH control) by soybeans in a recirculating hydroponic system were examined. Plants of cvs. McCall and Pixie were grown for 90 days using the nutrient film technique (NFT) and a nitrate based nutrient solution. System acid use for both CO2 levels peaked near 4 weeks during a phase of rapid vegetative growth, but acid use decreased more rapidly under 500 compared to 1000 umol mol (exp GR) CO2. Total system water use by 500 and 1000 umol mol (exp -1) plants was similar, leaving off at 5 weeks and declining as plants senesced (ca. 9 weeks). However, single leaf transpiration rates were consistently lower at 1000 umol mol (exp -1). The data suggest that high CO2 concentrations increase system acid (and nutrient) use because of increased vegetative growth, which in turn negates the benefit of reduced water use (lower transpiration rates) per unit leaf area. Author

N91-31782*# Tuskegee Inst., AL. Agricultural Experiment Station.
SWEET POTATO FOR CLOSED ECOLOGICAL LIFE SUPPORT SYSTEMS USING THE NUTRIENT FILM TECHNIQUE
P. A. Loretan, W. A. Hill, C. K. Bonsi, C. E. Morris, J. Y. Lu, C. R. A. Ogbuehi, and D. G. Mortley *In* NASA. Ames Research Center, Controlled Ecological Life Support Systems: CELSS '89 Workshop Mar. 1990 p 119-126 Sponsored in part by Department of Agriculture (For primary document see N91-31775 23-54)
(Grant NAG10-24)
Avail: NTIS HC/MF A19 CSCL 06K

Sweet potatoes were grown hydroponically using the nutrient

film technique (NFT) in support of the Closed Ecological Life Support System (CELSS) program. Experiments in the greenhouse with the TI-155 sweet potato cultivar produced up to 1790 g/plant of fresh storage roots. Studies with both TI-155 and Georgia Jet cultivars resulted in an edible biomass index of approximately 60 percent, with edible biomass linear growth rates of 12.1 to 66.0 g m(exp -2)d(exp -1) in 0.05 to 0.13 sq meters in 105 to 130 days. Additional experimental results are given. All studies indicate good potential for sweet potatoes in CELSS. Author

N91-31783*# Utah State Univ., Logan. Dept. of Plant Science.
CLONING CROPS IN A CELSS VIA TISSUE CULTURE: PROSPECTS AND PROBLEMS
John G. Carman and J. Richard Hess *In* NASA. Ames Research Center, Controlled Ecological Life Support Systems: CELSS '89 Workshop Mar. 1990 p 127-146 (For primary document see N91-31775 23-54)
Avail: NTIS HC/MF A19 CSCL 06K

Micropropagation is currently used to clone fruits, nuts, and vegetables and involves controlling the outgrowth in vitro of basal, axillary, or adventitious buds. Following clonal multiplication, shoots are divided and rooted. This process has greatly reduced space and energy requirements in greenhouses and field nurseries and has increased multiplication rates by greater than 20 fold for some vegetatively propagated crops and breeding lines. Cereal and legume crops can also be cloned by tissue culture through somatic embryogenesis. Somatic embryos can be used to produce 'synthetic seed', which can tolerate desiccation and germinate upon rehydration. Synthetic seed of hybrid wheat, rice, soybean and other crops could be produced in a controlled ecological life support system. Thus, yield advantages of hybreds over inbreds (10 to 20 percent) could be exploited without having to provide additional facilities and energy for parental-line and hybrid seed nurseries. Author

N91-31784*# Jet Propulsion Lab., California Inst. of Tech., Pasadena.
THE CONVERSION OF LIGNOCELLULOSICS TO FERMENTABLE SUGARS: A SURVEY OF CURRENT RESEARCH AND APPLICATION TO CELSS
Gene R. Petersen and Larry Baresi *In* NASA. Ames Research Center, Controlled Ecological Life Support Systems: CELSS '89 Workshop Mar. 1990 p 147-183 (For primary document see N91-31775 23-54)
Avail: NTIS HC/MF A19 CSCL 06K

An overview of the options for converting lignocellulosics into fermentable sugars as applied to the Closed Ecological Life Support System (CELSS) is given. A requirement for pretreatment is shown as well as the many available options. At present, physical/chemical methods are the simplest and best characterized options, but enzymatic processes will likely be the method of choice in the future. The use of pentose sugars by microorganisms to produce edibles at levels comparable to conventional plants is shown. The possible use of mycelial food production on pretreated but not hydrolyzed lignocelluloscis is also presented. Simple tradeoff analysis among some of the many possible biological pathways to regeneration of waste lignocellulosics was undertaken. Comparisons with complete oxidation processes were made. It is suggested that the NASA Life Sciences CELSS program maintain relationships with other government agencies involved in lignocellulosic conversions and use their expertise when the actual need for such conversion technology arises rather than develop this expertise within NASA. Author

N91-31785*# Bionetics Corp., Cocoa Beach, FL.
USE OF INEDIBLE WHEAT RESIDUES FROM THE KSC-CELSS BREADBOARD FACILITY FOR PRODUCTION OF FUNGAL CELLULASE
R. F. Strayer, M. A. Brannon, and J. L. Garland *In* NASA. Ames Research Center, Controlled Ecological Life Support Systems: CELSS '89 Workshop Mar. 1990 p 185-202 (For primary document see N91-31775 23-54)
Avail: NTIS HC/MF A19 CSCL 06K

Cellulose and xylan (a hemicellulose) comprise 50 percent of inedible wheat residue (which is 60 percent of total wheat biomass) produced in the Kennedy Space Center Closed Ecological Life Support System (CELSS) Breadboard Biomass Production Chamber (BPC). These polysaccharides can be converted by enzymatic hydrolysis into useful monosaccharides, thus maximizing the use of BPC volume and energy, and minimizing waste material to be treated. The evaluation of CELSS-derived wheat residues for production for cellulase enzyme complex by Trichoderma reesei and supplemental beta-glucosidase by Aspergillus phoenicis is in progress. Results to date are given. Author

N91-31786*# California Univ., Berkeley. Lawrence Berkeley Lab.
CYANOBACTERIA IN CELSS: GROWTH STRATEGIES FOR NUTRITIONAL VARIATION AND NITROGEN CYCLING
I. V. Fry and L. Packer *In* NASA. Ames Research Center, Controlled Ecological Life Support Systems: CELSS '89 Workshop Mar. 1990 p 203-216 (For primary document see N91-31775 23-54)
Avail: NTIS HC/MF A19 CSCL 06K

Cyanobacteria (blue-green algae) are versatile organisms which are capable of adjusting their cellular levels of carbohydrate, protein, and lipid in response to changes in the environment. Under stress conditions there is an imbalance between nitrogen metabolism and carbohydrate/lipid synthesis. The lesion in nitrogen assimilation is at the level of transport: the stress condition diverts energy from the active accumulation of nitrate to the extrusion of salt, and probably inhibits a cold-labile ATP'ace in the case of cold shock. Both situations affect the bioenergetic status of the cell such that the nitrogenous precursors for protein synthesis are depleted. Dispite the inhibition of protein synthesis and growth, photosynthetic reductant generation is relatively unaffected. The high O2 reductant would normally lead to photo-oxidative damage of cellular components; however, the organism copes by channeling the 'excess' reductant into carbon storage products. The increase in glycogen (28 to 35 percent dry weight increase) and the elongation of lipid fatty acid side chains (2 to 5 percent dry weight increase) at the expense of protein synthesis (25 to 34 percent dry weight decrease) results in carbohydrate, lipid and protein ratios that are closer to those required in the human diet. In addition, the selection of nitrogen fixing mutants which excrete ammonium ions present an opportunity to tailor these micro-organisms to meet the specific need for a sub-system to reverse potential loss of fixed nitrogen material. Author

N91-31787*# Alabama A & M Univ., Normal. Dept. of Biology.
ALGAE FOR CONTROLLED ECOLOGICAL LIFE SUPPORT SYSTEM DIET CHARACTERIZATION OF CYANOBACTERIA 'SPIRULINA' IN BATCH CULTURES
M. G. Tadros *In* NASA. Ames Research Center, Controlled Ecological Life Support Systems: CELSS '89 Workshop Mar. 1990 p 217-243 (For primary document see N91-31775 23-54)
Avail: NTIS HC/MF A19 CSCL 06K

Spirulina sp. is a bioregenerative photosynthetic and edible alga for space craft crews in a Closed Ecological Life Support System (CLESS). It was characterized for growth rate and biomass yield in batch cultures, under various environmental conditions. The cell characteristics were identified for one strain of Spirulina: S. maxima. Fast growth rate and high yield were obtained. The partitioning of the assimulatory products (proteins, carbohydrates, lipids) were manipulated by varying the environmental conditions. Experiments with Spirulina demonstrated that under stress conditions carbohydrate increased at the expense of protein. In other experiments, where the growth media were sufficient in nutrients and incubated under optimum growth conditions, the total proteins were increased up to almost 70 percent of the organic weight. In other words, the nutritional quality of the alga could be manipulated by growth conditions. These results support the feasibility of considering Spirulina as a subsystem in CELSS because of the ease with which its nutrient content can be manipulated. Author

N91-31788*# New Mexico State Univ., Las Cruces. Dept. of Civil Engineering.
PRELIMINARY EVALUATION OF WASTE PROCESSING IN A CELSS
Ricardo B. Jacquez *In* NASA. Ames Research Center, Controlled Ecological Life Support Systems: CELSS '89 Workshop Mar. 1990 p 245-263 (For primary document see N91-31775 23-54)
Avail: NTIS HC/MF A19 CSCL 06K

Physical/chemical, biological, and hybrid methods can be used in a space environment for processing wastes generated by a Closed Ecological Life Support System (CELSS). Two recycling scenarios are presented. They reflect differing emphases on and responses to the waste system formation rates and their composition, as well as indicate the required products from waste treatment that are needed in a life support system. Author

N91-31789*# Bionetics Corp., Cocoa Beach, FL.
BIOMASS PRODUCTION AND NITROGEN DYNAMICS IN AN INTEGRATED AQUACULTURE/AGRICULTURE SYSTEM
L. P. Owens and C. R. Hall *In* NASA. Ames Research Center, Controlled Ecological Life Support Systems: CELSS '89 Workshop Mar. 1990 p 265-277 (For primary document see N91-31775 23-54)
Avail: NTIS HC/MF A19 CSCL 06K

A combined aquaculture/agriculture system that brings together the three major components of a Controlled Ecological Life Support System (CELSS) - biomass production, biomass processing, and waste recycling - was developed to evaluate ecological processes and hardware requirements necessary to assess the feasibility of and define design criteria for integration into the Kennedy Space Center (KSC) Breadboard Project. The system consists of a 1 square meter plant growth area, a 500 liter fish culture tank, and computerized monitoring and control hardware. Nutrients in the hydrophonic solution were derived from fish metabolites and fish food leachate. In five months of continuous operation, 27.0 kg of lettuce tops, 39.9 kg of roots and biofilm, and 6.6 kg of fish (wet weights) were produced with 12.7 kg of fish food input. Based on dry weights, a biomass conversion index of 0.52 was achieved. A nitrogen budget was derived to determine partitioning of nitrogen within various compartments of the system. Accumulating nitrogen in the hypoponic solution indicated a need to enlarge the plant growth area, potentially increasing the biomass production and improving the biomass conversion index. Author

N91-31790*# Colorado Univ., Boulder. Bioserve Space Technologies.
SEED SPROUT PRODUCTION: CONSUMABLES AND A FOUNDATION FOR HIGHER PLANT GROWTH IN SPACE
Michelle Day, Terri Thomas, Steve Johnson, and Marvin Luttges *In* NASA. Ames Research Center, Controlled Ecological Life Support Systems: CELSS '89 Workshop Mar. 1990 p 279-293 (For primary document see N91-31775 23-54)
Avail: NTIS HC/MF A19 CSCL 06K

Seed sprouts can be produced as a source of fresh vegetable materials and as higher plant seedlings in space. Sprout production was undertaken to evaluate the mass accumulations possible, the technologies needed, and the reliability of the overall process. Baseline experiments corroborated the utility of sprout production protocols for a variety of seed types. The automated delivery of saturated humidity effectively supplants labor intensive manual soaking techniques. Automated humidification also lend itself to modest centrifugal sprout growth environments. A small amount of ultraviolet radiation effectively suppressed bacterial and fungal contamination, and the sprouts were suitable for consumption. Author

N91-31791*# National Aeronautics and Space Administration. John F. Kennedy Space Center, Cocoa Beach, FL.
CONTROLLED ECOLOGICAL LIFE SUPPORT SYSTEM BREADBOARD PROJECT, 1988
W. M. Knott *In* NASA. Ames Research Center, Controlled Ecological Life Support Systems: CELSS '89 Workshop Mar. 1990 p 295-302 Previously announced in IAA as A90-24803 (For primary document see N91-31775 23-54)
Avail: NTIS HC/MF A19 CSCL 06K

The Closed Ecological Life Support System (CELSS) Breadboard Project, NASA's effort to develop the technology required to produce a functioning bioregenerative system, is discussed. The different phases of the project and its current status are described. The relationship between the project components are shown, and major project activities for fiscal years 1989 to 1993 are listed. The Biomass Production Chamber (BPC) became operational and tests of wheat as a single crop are nearing completion. Author

N91-31792*# National Aeronautics and Space Administration. Ames Research Center, Moffett Field, CA.
THE CROP GROWTH RESEARCH CHAMBER: A GROUND-BASED FACILITY FOR CELSS RESEARCH
David L. Bubenheim *In its* Controlled Ecological Life Support Systems: CELSS '89 Workshop Mar. 1990 p 303-317 (For primary document see N91-31775 23-54)
Avail: NTIS HC/MF A19 CSCL 06K

A ground based facility for the study of plant growth and development under stringently controlled environments is being developed by the Closed Ecological Life Support System (CELSS) program at the Ames Research Center. Several Crop Growth Research Chambers (CGRC) and laboratory support equipment provide the core of this facility. The CGRC is a closed (sealed) system with a separate recirculating atmosphere and nutrient delivery systems. The atmospheric environment, hydroponic environment, systems controls, and data acquisition are discussed. Author

N91-31793*# National Aeronautics and Space Administration. Lyndon B. Johnson Space Center, Houston, TX.
DEVELOPMENT OF THE CELSS EMULATOR AT NASA. JOHNSON SPACE CENTER
Hatice S. Cullingford *In* NASA. Ames Research Center, Controlled Ecological Life Support Systems: CELSS '89 Workshop Mar. 1990 p 319-325 Previously announced in IAA as A90-27445 Prepared in cooperation with Lockheed Engineering and Sciences Co., Houston, TX (For primary document see N91-31775 23-54)
(Contract NAS9-17900)
Avail: NTIS HC/MF A19 CSCL 06K

The Closed Ecological Life Support System (CELSS) Emulator is under development. It will be used to investigate computer simulations of integrated CELSS operations involving humans, plants, and process machinery. Described here is Version 1.0 of the CELSS Emulator that was initiated in 1988 on the Johnson Space Center (JSC) Multi Purpose Applications Console Test Bed as the simulation framework. The run model of the simulation system now contains a CELSS model called BLSS. The CELSS simulator empowers us to generate model data sets, store libraries of results for further analysis, and also display plots of model variables as a function of time. The progress of the project is presented with sample test runs and simulation display pages. Author

N91-31794*# Texas Univ., Arlington. Center for Dynamic Systems Control Studies.
A PERSPECTIVE ON CELSS CONTROL ISSUES
Ann L. Blackwell *In* NASA. Ames Research Center, Controlled Ecological Life Support Systems: CELSS '89 Workshop Mar. 1990 p 327-353 (For primary document see N91-31775 23-54)
Avail: NTIS HC/MF A19 CSCL 06K

Some issues of Closed Ecological Life Support System (CELSS) analysis and design are effectively addressed from a systems control perspective. CELSS system properties that may be elucidated using control theory in conjunction with mathematical and simulation modeling are enumerated. The approach that is being taken to the design of a control strategy for the Crop Growth

Research Chamber (CGRC) and the relationship of that approach to CELSS plant growth unit subsystems control is described. Author

N91-31795*# National Aeronautics and Space Administration, Washington, DC.
TRANSPIRATION DURING LIFE CYCLE IN CONTROLLED WHEAT GROWTH
Tyler Volk (New York Univ., New York.) and John D. Rummel *In* NASA. Ames Research Center, Controlled Ecological Life Support Systems: CELSS '89 Workshop Mar. 1990 p 355-358 Previously announced in IAA as A90-15432 (For primary document see N91-31775 23-54)
(Contract NCA2-101)
Avail: NTIS HC/MF A19 CSCL 06K

A previously developed model of wheat growth, designed for convenient incorporation into system level models of advanced space life support systems is described. The model is applied to data from an experiment that grew wheat under controlled conditions and measured fresh biomass and cumulated transpiration as a function of time. The adequacy of modeling the transpiration as proportional to the inedible biomass and an age factor that varies during the life cycle are discussed. Author

N91-31796*# Utah State Univ., Logan. Dept. of Plant Science.
PREPARATORY SPACE EXPERIMENTS FOR DEVELOPMENT OF A CELSS
Frank B. Salisbury *In* NASA. Ames Research Center, Controlled Ecological Life Support Systems: CELSS '89 Workshop Mar. 1990 p 359-372 (For primary document see N91-31775 23-54)
Avail: NTIS HC/MF A19 CSCL 06K

The goal of Closed Ecological Life Support System (CELSS) studies is to examine the effects of microgravity on yield and quality of plant products and on the interactions between irradiance and crop area. Measuring yield and quality of crops as a function of irradiance in microgravity is virtually unique to the CELSS program, as is the emphasis on canopies rather than individual plants. The first step for space experiments is to develop a relatively stress free environment for plant growth, something that has so far never been achieved. High light levels are essential, and there must be time enough to complete a significant portion of the life cycle. Optimal atmosphere and nutrients must be provided. Such responses as germination, orientation of roots and shoots, photosynthesis and respiration, floral initiation and development, and seed maturation and viability will be studied. Author

N91-31797*# National Aeronautics and Space Administration. John F. Kennedy Space Center, Cocoa Beach, FL.
FACTORS AFFECTING PLANT GROWTH IN MEMBRANE NUTRIENT DELIVERY
T. W. Dreschel, R. M. Wheeler (Bionetics Corp., Cocoa Beach, FL.), J. C. Sager, and W. M. Knott *In* NASA. Ames Research Center, Controlled Ecological Life Support Systems: CELSS '89 Workshop Mar. 1990 p 373-382 (For primary document see N91-31775 23-54)
Avail: NTIS HC/MF A19 CSCL 06K

The development of the tubular membrane plant growth unit for the delivery of water and nutrients to roots in microgravity has recently focused on measuring the effects of changes in physical variables controlling solution availability to the plants. Significant effects of membrane pore size and the negative pressure used to contain the solution were demonstrated. Generally, wheat grew better in units with a larger pore size but equal negative pressure and in units with the same pore size but less negative pressure. Lettuce also exhibited better plant growth at less negative pressure. Author

N91-31798*# National Aeronautics and Space Administration. Lyndon B. Johnson Space Center, Houston, TX.
CONCEPTUAL DESIGN OF A CLOSED LOOP NUTRIENT SOLUTION DELIVERY SYSTEM FOR CELSS IMPLEMENTATION IN A MICRO-GRAVITY ENVIRONMENT
Steven H. Schwartzkopf, Mel W. Oleson (Boeing Aerospace Co., Seattle, WA.), and Hatice S. Cullingford *In* NASA. Ames Research Center, Controlled Ecological Life Support Systems: CELSS '89 Workshop Mar. 1990 p 383-390 Previously announced in IAA as A90-27545 (For primary document see N91-31775 23-54)
(Contract NAS9-17981)
Avail: NTIS HC/MF A19 CSCL 06K

Described here are the results of a study to develop a conceptual design for an experimental closed loop fluid handling system capable of monitoring, controlling, and supplying nutrient solution to higher plants. The Plant Feeder Experiment (PFE) is designed to be flight tested in a microgravity environment. When flown, the PFX will provide information on both the generic problems of microgravity fluid handling and the specific problems associated with the delivery of the nutrient solution in a microgravity environment. The experimental hardware is designed to fit into two middeck lockers on the Space Shuttle, and incorporates several components that have previously been flight tested. Author

N91-31799*# Wisconsin Univ., Madison.
TECHNOLOGY FOR SUBSYSTEMS OF SPACE-BASED PLANT GROWTH FACILITIES
R. J. Bula, R. C. Morrow, T. W. Tibbitts, and R. B. Corey *In* NASA. Ames Research Center, Controlled Ecological Life Support Systems: CELSS '89 Workshop Mar. 1990 p 391-408 (For primary document see N91-31775 23-54)
Avail: NTIS HC/MF A19 CSCL 06K

Technologies for different subsystems of space-based plant growth facilities are being developed at the Wisconsin Center for Space Automation and Robotics, a NASA Center for the Commercial Development of Space. The technologies include concepts for water and nutrient delivery, for nutrient composition control, and for irradiation. Effort is being concentrated on these subsystems because available technologies cannot be effectively utilized for space applications. Author

N91-31800*# National Aeronautics and Space Administration. Lyndon B. Johnson Space Center, Houston, TX.
SOLID-SUPPORT SUBSTRATES FOR PLANT GROWTH AT A LUNAR BASE
D. W. Ming and C. Galindo (Lockheed Engineering and Sciences Co., Houston, TX.) *In* NASA. Ames Research Center, Controlled Ecological Life Support Systems: CELSS '89 Workshop Mar. 1990 p 409-437 (For primary document see N91-31775 23-54)
Avail: NTIS HC/MF A19 CSCL 06K

Zeoponics is only in its developmental stages at the Johnson Space Center and is defined as the cultivation of plants in zeolite substrates that contain several essential plant growth cations on their exchange sites, and have minor amounts of mineral phases and/or anion-exchange resins that supply essential plant growth anions. Zeolites are hydrated aluminosilicates of alkali and alkaline earth cations with the ability to exchange most of their constituent exchange cations as well as hydrate/dehydrate without change to their structural framework. Because zeolites have extremely high cation exchange capabilities, they are very attractive media for plant growth. It is possible to partially or fully saturate plant-essential cations on zeolites. Zeoponic systems will probably have their greatest applications at planetary bases (e.g., lunar bases). Lunar raw materials will have to be located that are suited for the synthesis of zeolites and other exchange resings. Lunar 'soil' simulants have been or are being prepared for zeolite/smectite synthesis and 'soil' dissolution studies. Author

N91-31801 Defence and Civil Inst. of Environmental Medicine, Downsview (Ontario).
FEMALE AIRCREW: THE CANADIAN FORCES EXPERIENCE, 1979-1989
R. J. Hicks Apr. 1990 15 p Previously announced as N91-11367
(DCIEM-90-P-14; CTN-91-60197) Avail: NTIS HC A03

Data collected since females first started aircrew training in

Canada in 1979 is reviewed. Selection test data over a 10 year period indicates that females score significantly lower in quantitative and spatial / psychomotor skills; as long as the pilot job task emphasizes these skills, proportionately fewer females will be selected for training. Medical assessment data does indicate that a greater number of females will fail to meet the medical standard for pilot. The only reason for the difference is in the area of anthropometry. Again, as long as military cockpits are designed primarily with male indices, a greater number of females will continue to be excluded. Experience over the period has demonstrated that appropriately selected female aircrew, that is, using the same standards as for males, can perform equally with their male peers during training and in operational flying in the Air Force. CISTI

N91-31802# Sandia National Labs., Albuquerque, NM.
HUMAN FACTORS ENGINEERING DESIGN GUIDELINES FOR THE SOFTWARE USER INTERFACE
H. W. Allen and D. L. Campbell Jul. 1991 57 p
(Contract DE-AC04-76DP-00789)
(DE91-016061; SAND-91-0872) Avail: NTIS HC/MF A04

This report provides system designers with basic human factors information and guidelines for designing and developing the software user interface. A brief discussion of the user interface design philosophy is presented, followed by an overview of the user interface options available (such as color and highlighting), candidate approaches, and discussion of general display concepts and user interface features. We have presented information to facilitate discussions of user interface options, to aid in making final user interface design decisions, and to further the refinement of the user interface. We provide a candidate questionnaire for evaluating your software user interface. DOE

N91-31803*# National Aeronautics and Space Administration. Lyndon B. Johnson Space Center, Houston, TX.
METHOD AND APPARATUS FOR BIO-REGENERATIVE LIFE SUPPORT SYSTEM Patent
Hatice S. Cullingford, inventor (to NASA) 9 Apr. 1991 13 p
Filed 11 Jul. 1989 Supersedes N89-29027 (27 - 23, p 3335)
(NASA-Case-MSC-21629-1; US-Patent-5,005,787;
US-Patent-Appl-SN-378548; US-Patent-Class-244-163;
US-Patent-Class-244-159; US-Patent-Class-47-1.4;
US-Patent-Class-47-62; US-Patent-Class-55-75;
US-Patent-Class-210-748; Int-Patent-Class-B64G-1/46) Avail: US Patent and Trademark Office CSCL 06K

A life support system is disclosed for human habitation (cabin) which has a bioregenerative capability through the use of a plant habitat (greenhouse) whereby oxygen-rich air from the greenhouse is processed and used in the cabin and carbon dioxide-rich air from the cabin is used in the greenhouse. Moisture from the air of both cabin and greenhouse is processed and reused in both. Wash water from the cabin is processed and reused in the cabin as hygiene water, and urine from the cabin is processed and used in the greenhouse. Spent water from the greenhouse is processed and reused in the greenhouse. Portions of the processing cycles are separated between cabin and greenhouse in order to reduce to a minimum cross contamination of the two habitat systems. Other portions of the processing cycles are common to both cabin and greenhouse. The use of bioregenerative techniques permits a substantial reduction of the total consumables used by the life support system.
Official Gazette of the U.S. Patent and Trademark Office

N91-31804# Air Force Inst. of Tech., Wright-Patterson AFB, OH.
COCKPIT RESOURCE MANAGEMENT: EFFECTS ON BEHAVIORAL INTERACTIONS ACROSS AIRLINES AND AIRCRAFT TYPES M.S. Thesis
Cathy C. Clothier May 1991 111 p
(AD-A239467; AFIT/CI/CIA-91-028) Avail: NTIS HC/MF A06 CSCL 05/9

Due to the growing concern over human errors playing an instrumental role in aircraft accidents, the Federal Aviation Administration encouraged airlines to develop Cockpit Resource Management (CRM) training programs to address that issue. Baseline data measured crew interaction before pilots were exposed to seminars and simulators. Longitudinal data described behavioral changes wrought by the intervention. Within airline and within fleet data clearly showed that crews were more effective after CRM training. Within airline and across fleet data verified fleet differences discovered by the first method. Technology level seemed to be a cause of the fleet differences for crews performing in simulators. Crew size affected performance both on the line and in the simulator. Finally, the across airline and across fleet data, in addition to describing fleet differences, highlighted differences between the behavioral effectiveness of crews in different airlines. GRA

N91-31805# Aerospace Corp., El Segundo, CA. Lab. Operations.
GARMENT SELECTION FOR CLEANROOMS AND CONTROLLED ENVIRONMENTS FOR SPACECRAFT
Ethel J. Watts 1 Apr. 1991 44 p
(Contract F04701-88-C-0089)
(AD-A239512; TR-0090(5530-02)-1; SSD-TR-91-26) Avail: NTIS HC/MF A03 CSCL 06/11

Strict contamination control practices are exercised throughout the lifetime of a spacecraft in order to satisfy the performance requirements of the system. Spacecraft materials are carefully selected to have low outgassing values and particulate deposition. Parts are cleaned, and the vehicle is assembled in cleanrooms and work stations having controlled environments. Specifications are examined which govern the selection of special items of clothing designed to protect spacecraft from contaminants released by personnel and by garments. Special clothing includes coveralls, footwear, and head/face covers. Garments appropriate for both hazardous (meltproof as well as flame resistant), and nonhazardous operations are described. GRA

N91-31806# Naval Submarine Medical Research Lab., Groton, CT.
THE MEDICAL HAZARDS OF FLAME-SUPPRESSANT ATMOSPHERES
Douglas R. Knight 19 Apr. 1991 24 p
(AD-A239618; NSMRL-1167) Avail: NTIS HC/MF A03 CSCL 06/5

Flames are a potential hazard to the occupants of sealed chambers. Four modifications of air are described that will suppress or extinguish flames. They are: (1) SUPPLEMENTATION - the addition of an appropriate foreign gas to air; (2) N2 PRESSURIZATION - the addition of compressed N2 to air; (3) DEPRESSURIZATION - the partial evacuation of air from the chamber; and (4) N2 DILUTION - the exchange of N2 for O2. The primary medical hazards of flame suppressant atmospheres are barotrauma, N2 narcosis, decompression sickness, hypoxia and inhalation toxicity. Experimental evidence supports the use of N2 DILUTION to suppress flames aboard patrolling submarines. One or more of the following adjuncts may enhance the use of N2 DILUTION without impairing human health: Physiological adaptation to hypoxia, addition of CO2 to the atmosphere and N2 PRESSURIZATION. GRA

N91-31807# School of Aerospace Medicine, Brooks AFB, TX.
TESTING AND EVALUATION OF THE CATALYST RESEARCH MINIOX 3 OXYGEN MONITOR Final Report, Oct. 1988 - Mar. 1989
Thomas E. Philbeck, Jr., Rebecca B. Schultz, and Ernest G. Roy Dec. 1990 24 p
(AF Proj. 7930)
(AD-A239665; USAFSAM-TR-90-25) Avail: NTIS HC/MF A03 CSCL 15/6

The Military Airlift Command (MAC) directs and controls aeromedical evacuation missions for the United States Air Force (USAF) and most of the Department of Defense (DOD). There is often a need to monitor and control the percentage of therapeutic oxygen being administered to patients. The Catalyst Research

MiniOX III oxygen monitor was selected by MAC as its primary oxygen monitoring device. The Aeromedical Research Function tested and evaluated the MiniOX III, and found it to be a safe and reliable device and acceptable for worldwide aeromedical evacuation use. GRA

N91-31808# Naval Air Development Center, Warminster, PA. Air Vehicle and Crew Systems Technology Dept.
ADAPTIVE FUNCTION ALLOCATION FOR INTELLIGENT COCKPITS Final Report, Oct. 1989 - Oct. 1991
Jeffrey Morrison, Jonathan Gluckman, and John Deaton 1 Jan. 1991 67 p
(NADC Proj. RS-3-4-H20)
(AD-A239714; NADC-91028-60) Avail: NTIS HC/MF A04
CSCL 23/2

The demands associated with flying modern tactical, strategic and commercial aircraft have made the cockpit a prime arena for the development of technology designed to aid human operators. The development of ever more powerful computers, expert systems, and artificial intelligence technology has led researchers and system designers to propose that decision making be aided dynamically using this technology. The implementation of this technology may modify the tasks normally performed by pilots in any of a number of ways, in order to facilitate the best performance of man machine systems. A series of Cockpit Automation Studies are being performed as part of the Adaptive Function Allocation for Intelligent Cockpits program. The goal of the program is to develop a prospective set of human performance based principles and guidelines for the application of adaptive automation technology. As the first study this research developed a basic set of tasks in which automation concepts could later be applied. Derivatives of two common laboratory tasks were used: one task was a pursuit tracking task while the other task was a tactical assessment task (TAT). Subject's response time and accuracy were measured on the TAT while root mean square errors were obtained on the tracking task. Simple and complex task performance was measured as a function of task difficulty. Simple task results generally supported a resource view of human performance. GRA

N91-31809# Naval Air Development Center, Warminster, PA. Air Vehicle and Crew Systems Technology Dept.
AIRCREW CRITIQUE OF HIGH-G CENTRIFUGE TRAINING. PART 1: WHAT WAS THE BEST PART OF THE PROGRAM? Final Report, Oct. 1988 - May 1991
James E. Whinnery and Richard J. Hamilton 1 May 1991 55 p
(AD-A239781; NADC-91054-60-Pt-1) Avail: NTIS HC/MF A04
CSCL 15/1

A fighter attack aviator high-G centrifuge training program was initated at NADC. The critiques are review of 515 of 525 aircrew who participated in the centrifuge training. No negative overall critiques were received from USN, USMC, or USAF aircrew. Of particular note was the favorable aircrew attitude toward the 'HOOK maneuver' as the preferred method for teaching and performing the anti-G straining maneuver, and aircrew agreement that a G-LOC exposure would be a very beneficial part of the training program. A multitude of additional suggestions by the fighter aircrews offer the potential for further enhancement of successful program. The centrifuge training program has the potential for making the most significant enhancement of the interface between the fighter aviation medicine/aerospace physiology programs and fighter-attack operations that has yet to exist. The centrifuge training program not only enhances flight safety it also can immediately improve the combat readiness and capability of fighter-attack aircrew. GRA

55 SPACE BIOLOGY

Includes exobiology; planetary biology; and extraterrestrial life.

No abstracts in this category.

59 MATHEMATICAL AND COMPUTER SCIENCES (GENERAL)

No abstracts in this category.

60 COMPUTER OPERATIONS AND HARDWARE

Includes hardware for computer graphics, firmware, and data processing.

For components see *33 Electronics and Electrical Engineering.*

N91-31810* National Aeronautics and Space Administration. Pasadena Office, CA.
ASYMMETRIC SOFT-ERROR RESISTANT MEMORY Patent
Martin G. Buehler, inventor (to NASA) and Marvin Perlman, inventor (to NASA) (Jet Propulsion Lab., California Inst. of Tech., Pasadena.) 10 Sep. 1991 7 p Filed, 16 Feb. 1989
(NASA-Case-NPO-17394-1-CU; US-Patent-5,048,023; US-Patent-Appl-SN-311024; US-Patent-Class-371-40.1; US-Patent-Class-365-156; US-Patent-Class-365-200; Int-Patent-Class-G11C-29/00; Int-Patent-Class-H03M-13/00)
Avail: US Patent and Trademark Office CSCL 09B

A memory system is provided, of the type that includes an error-correcting circuit that detects and corrects, that more efficiently utilizes the capacity of a memory formed of groups of binary cells whose states can be inadvertently switched by ionizing radiation. Each memory cell has an asymmetric geometry, so that ionizing radiation causes a significantly greater probability of errors in one state than in the opposite state (e.g., an erroneous switch from '1' to '0' is far more likely than a switch from '0' to'1'. An asymmetric error correcting coding circuit can be used with the asymmetric memory cells, which requires fewer bits than an efficient symmetric error correcting code.
Official Gazette of the U.S. Patent and Trademark Office

N91-31811# Massachusetts Inst. of Tech., Cambridge. Lab. for Computer Science.
A FAST MULTIPORT MEMORY BASED ON SINGLE-PORT MEMORY CELLS
Ronald L. Rivest and Lance A. Glasser 10 Jul. 1991 15 p
(Contract N00014-89-J-1988)
(AD-A239455; MIT/LCS/TM-455) Avail: NTIS HC/MF A03
CSCL 12/6

We present a new design for dual-port memories that uses single-port memory cells but guarantees fast deterministic read/write access. The basic unit of storage is the word, rather than the bit, and addressing conflicts results in bit errors that are removed by correction circuitry. The addressing scheme uses Galois field arithmetic to guarantee that the maximum number of bit errors in any word accessed is one. These errors can be corrected every time with a simple correction scheme. The scheme can be generalized to an arbitrary number of ports. GRA

N91-31812# California Univ., Irvine. Dept. of Electrical and Computer Engineering.
DESIGN AND ANALYSIS OF FAULT-TOLERANT DISTRIBUTED REAL-TIME COMPUTER SYSTEMS Final Report, 1 Mar. 1987 - 31 Dec. 1989
K. H. Kim 25 Jul. 1991 195 p
(Contract N00014-87-K-0231)
(AD-A239521) Avail: NTIS HC/MF A09 CSCL 12/7

The objective was to contribute to the establishment of the scientific foundation for designing fault tolerant distributed computer systems. Main results obtained are as follows: (1) identification of critical research issues and some promising research directions in real time fault tolerant distributed computing; (2) a skeleton of the foundation for realizing system level fault tolerance, which includes among others the DRB (distributed recovery block) scheme, the DCONV (distributed conversation) scheme, the PTC (programmer-transparent coordination) scheme, a TB (temporary blackout) handling scheme, and the complementary relationship among the schemes; These schemes enable the computer system to detect and recover from both hardware and software faults without missing the deadlines for processing important data and delivering outputs to the controlled object/environment; (3) a preliminary structure of a model of real time distributed computation; (4) a theoretical investigation into the efficiency and diagnostic power of basic processor-level diagnosis approaches in diagnosing hypercubes conducted; and (5) an enhancement of three of the real time computer network testbeds established in the UCI DREAM (Distributed Real time Ever Available Microcomputing) Laboratory. GRA

61 COMPUTER PROGRAMMING AND SOFTWARE

Includes computer programs, routines, alogorithms, and specific applications, e.g., CAD/CAM.

N91-31813*# National Aeronautics and Space Administration. Goddard Space Flight Center, Greenbelt, MD.
ULDA USER'S GUIDE
Charleen Perry, Cornelius Driessen, and Fabio Pasian (Osservatorio Astronomico, Trieste, Italy) Dec. 1989 36 p
(NASA-TM-105074; NAS 1.15:105074;
NSSDC-WDC-A-R/S-89-27) Avail: NTIS HC/MF A03 CSCL 09B

The Uniform Low Dispersion Archive (ULDA) is a software system which, in one sitting, allows one to obtain copies on one's personal computer of those International Ultraviolet Explorer (IUE) low dispersion spectra that are of interest to the user. Overviews and use instructions are given for two programs, one to search for and select spectra, and the other to convert those spectra into a form suitable for the user's image processing system. Author

N91-31814# Computer Resource Management, Inc., Pleasantville, NJ.
SOFTWARE QUALITY METRICS Final Report
N. VanSuetendael and D. Elwell Jul. 1991 267 p
(Contract DTFA03-86-C-00042)
(DOT/FAA/CT-91/1) Avail: NTIS HC/MF A12

When digital technology is employed to perform some function aboard aircraft, the designer documents the technology and the applicant presents a package to the Certification Engineer (CE). Typically, the package might include design and test specifications, test plans, and test results for the system. This package assures the CE that the designer has properly developed and validated the system. Software Quality Metrics (SQM) may be used during the software (SW) development and testing. The SQM technology attempts to quantify various quality-oriented factors, such as reliability and maintainability. The SW developer determines the quality factors that are important to the application. The SW metrics that correlate to these factors are used on the code to determine to what extent these factors were reached. Based on the results, the developer determines whether the SW meets the requirements set for it and how well the SW will perform. This technical report documents the results of a study conducted to analyze SQM as they apply to the code contained in avionic equipment and systems. This report is intended to provide an indepth explanation of how SQM may be applied and interpreted. Author

N91-31815# Lawrence Livermore National Lab., CA.
A SCIENTIFIC VISUALIZATION SYNTHESIZER
R. A. Crawfis and M. J. Allison 14 May 1991 11 p Presented at the Visual '91, San Diego, CA, 22-25 Oct. 1991
(Contract W-7405-eng-48)
(DE91-012877; UCRL-JC-107230; CONF-9110123-1) Avail: NTIS HC/MF A03

We describe methods for displaying scientific data using textures and raster operations. A large class of the images produced using geometric techniques can be generated using raster operations and, the flexibility and simplicity of raster operations allow a greater choice of visualization techniques with only a small set of basic operations. Texture mapping techniques will be shown that allow the representation of several variables simultaneously, without a high degree of clutter. The combination of traditional geometric techniques, image composition techniques and image rendering techniques can be integrated into a single framework for the display of scientific data. This paper will present a system for generating and operating on textures and images for the purposes of scientific visualization. The advantages of using such a system will be demonstrated through the use of examples. DOE

N91-31816# Florida State Univ., Tallahassee. Supercomputer Computations Research Inst.
ABSORBING CAD SYSTEM GEOMETRIES INTO GEANT
J. Womersley, P. Dragovitsch, S. Youssef, W. L. Dunn, J. D. Simpkins, and A. M. Yacout 1991 8 p Presented at the Workshop on Detector and Event Simulation in High Energy Physics, Amsterdam, Netherlands, 8-12 Apr. 1991
(Contract DE-FG05-87ER-40319)
(DE91-015707; CONF-9104249-2) Avail: NTIS HC/MF A02

The simulation community has for many years discussed the possibility of direct conversion of geometrical detector models from computer-aided design and engineering systems (CAD systems) to the simulation packages (which we shall assume means GEANT). This would allow fast and simultaneous optimization of the physics performance and structural integrity of detector designs. The benefit that this would offer is the avoidance of such problems as the late discovery of the rather thick cryostats in the D-Zero detector. Recent progress in the absorption of CAD geometries into GEANT models is reviewed, including descriptions of the additions to the I-DEAS solid modeller package developed for the EMPACT SSC proposal, the COGENT CAD-to-GEANT interpreter developed by Quantum Research Services, and the OCTAGON package for representing arbitrary shapes in GEANT. Likely future directions of development are described. DOE

N91-31817# Superconducting Super Collider Lab., Dallas, TX.
SHOWTIME.C: A C-LANGUAGE PROGRAM FOR DATA ACQUISITION AND DISPLAY USER'S GUIDE
A. D. Justice, III Jun. 1991 12 p
(Contract DE-AC35-89ER-40486)
(DE91-016241; SSCL-MAN-0012) Avail: NTIS HC/MF A03

The program is invoked by entering SHOWTIME at the command line prompt while in the directory containing SHOWTIME.EXE and its associated files. The main menu and SHOWTIME command prompt will appear, with the following menu options: book histogram; bin contents; clear histogram; delete histogram; edit text file; histogram as text data; toggle input mode; list booked histogram; toggle log/linear display; menu display; and notes to screen; print screen; profile plot; run/resume; record on/off; scatter plot for two channels; statistics for booked histograms; view histogram; exit program; and reset data acquisition system. The action of each of these menu selections will be described. DOE

N91-31818# Los Alamos National Lab., NM.
DEVELOPING DATAFLOW ALGORITHMS
R. E. Hiromoto and A. P. W. Bohm (Colorado State Univ., Fort Collins.) 1991 4 p Presented at the 13th IMACS World Congress on Computation and Applied Mathematics, Dublin (Ireland), 22-26 Jul. 1991
(Contract W-7405-eng-36)
(DE91-016300; LA-UR-91-2440; CONF-910771-3) Avail: NTIS HC/MF A01

Our goal is to study the performance of a collection of numerical algorithms written in Id which is available to users of Motorola's dataflow machine Monsoon. We will study the dataflow performance of these implementations first under the parallel profiling simulator Id World, and second in comparison with actual dataflow execution on the Motorola Monsoon. This approach will allow us to follow the computational and structural details of the parallel algorithms as implemented on dataflow systems. When running our programs on the Id World simulator we will examine the behaviour of algorithms at dataflow graph level, where each instruction takes one timestep and data becomes available at the next. This implies that important machine level phenomena such as the effect that global communication time may have on the computation are not addressed. These phenomena will be addressed when we run our programs on the Monsoon hardware. Potential ramifications for compilation techniques, functional programming style, and program efficiency are significant to this study. In a later stage of our research we will compare the efficiency of Id programs to programs written in other languages. This comparison will be of a rather qualitative nature as there are too many degrees of freedom in a language implementation for a quantitative comparison to be of interest. We begin our study by examining one routine that exhibit different computational characteristics. This routine and its corresponding characteristics is Fast Fourier Transforms; computational parallelism and data dependences between the butterfly shuffles. DOE

N91-31819# Allied-Signal Aerospace Co., Kansas City, MO.
ATOMATIC FEATURE (AFEAT) IDENTIFICATION FOR COMPUTER-AIDED PROCESS PLANNING (CAPP)
N. C. Christensen Jul. 1991 43 p
(Contract DE-AC04-76DP-00613)
(DE91-016478; KCP-613-4372) Avail: NTIS HC/MF A03

A prototype system of computer programs was created to demonstrate the feasibility of automatic conversion from Boundary Representation solid models to Constructive Solid Geometry (CSG) solid models. The prototype is an implementation of the now-patented PHOENIX method, which is not an algorithm, but which uses expert system technology to find a 'good' CSG representation. 'Good' was defined as using fewest CSG primitives. Efforts to extend 'good' representation to include manufacturing form features were begun but not completed. Work is continuing under another project. DOE

N91-31820*# Mississippi State Univ., Mississippi State. NSF Engineering Research Center for Computational Field Simulation.
ENHANCEMENT OF SURFACE DEFINITION AND GRIDDING IN THE EAGLE CODE Semiannual Progress Report 1 Oct. 1990 - 31 Mar. 1991
1991 17 p
(Grant NAG1-1061)
(NASA-CR-188796; NAS 1.26:188796) Avail: NTIS HC/MF A03 CSCL 09B

A method for locally fairing uniform cubic B-spline curves and surfaces is presented. The algorithm uses an automated technique which detects undesirable geometric characteristics by using a local fairness criterion. The geometric entity is then smoothed using a method based on the repeated removal and insertion of the spline knots in the vicinity of the geometric irregularity.
Author

N91-31821# Groningen Rijksuniv. (Netherlands). Dept. of Computing Science.
OMISSION OF SYMBOLS
Wim H. Hesselink Feb. 1991 11 p
(CS-9101; WHH-114-0; ETN-91-99579) Avail: NTIS HC/MF A03

A problem inspired by the preprocessing phase of an LR(k) parser is addressed. An omission relation on strings, which allows for the omission of a productive symbol at the end of the string or of a nullable symbol that is not the head of the string, is considered. Recurrence equations for the omission relation are sought and one of the recurrence equations found is converted easily into an iterative algorithm. The generalization is concluded to be highly satisfactory. ESA

N91-31822# Groningen Rijksuniv. (Netherlands). Dept. of Computing Science.
A SIMPLIFICATION OF EARLEY'S ALGORITHM
Henk Doornbos 22 Feb. 1991 26 p
(CS-9102; ETN-91-99580) Avail: NTIS HC/MF A03

A parsing algorithm, essentially Earley's algorithm without a predictor, is presented and proved. The algorithm is constructed by successive refinement of statements, using a notation based on Caroll Morgan's refinement calculus. This method turns out to allow a complete, concise, and elegant proof. ESA

N91-31823# Groningen Rijksuniv. (Netherlands). Dept. of Computer Sciences.
LR-PARSING DERIVED
Wim H. Hesselink Mar. 1991 32 p Revised
(CS-9105; CS-8906; ETN-91-99583) Avail: NTIS HC/MF A03

The LR(k) parsing algorithm is derived, i.e., presented and proved as an interplay between program development and parsing theory. The program development uses invariants and the new concept of weakest angelic precondition. The parsing theory involved relates rightmost derivability to three other transitive relations on strings. The usual stack of item sets and the finite automation appear in an optimization of the abstract algorithm.
ESA

N91-31824# Nijmegen Univ. (Netherlands). Dept. of Informatics.
THE ABC-MACHINE: A SEQUENTIAL STACK-BASED ABSTRACT MACHINE FOR GRAPH REWRITING
P. W. M. Koopman, M. C. J. D. vanEekelen, E. G. J. M. H. Noecker, J. E. W. Smetsers, and M. J. Plasmeijer Dec. 1990 88 p
(TR-90-22; ETN-91-99585) Avail: NTIS HC/MF A05

An abstract machine to describe graph reduction in an imperative way, but abstracting from the details of a specific concrete machine, is introduced. This machine is designed to describe the implementation of CLEAN on stack based imperative machines. A functional program is first translated to an equivalent CLEAN program. It is justified why an abstract machine is introduced between CLEAN and the concrete machine level. This abstract machine and the associated compilation schemes are described. A functional programming language is used with success for the descriptions. Functional languages appear to be very well suited as description formalism; the specifications obtained are concise descriptions and useful prototypes. The specifications shown emerged to be valuable in the construction of the associated products. These products provide a very efficient implementation of functional programming languages. ESA

N91-31825# Nijmegen Univ. (Netherlands). Dept. of Informatics.
ON A TERNARY BRACKETING PROBLEM FROM THE THEORY OF FORMAL LANGUAGES
D. C. vanLeijenhorst Dec. 1990 6 p
(TR-90-24; ETN-91-99586) Avail: NTIS HC/MF A02

Whether or not there exists a sizable number of permutations that can not be generated in the following way is addressed: put the numbers 1 to n in a row, and take two adjacent nonempty 'segments', interchange the two segments, keeping order inside each of them; then proceed in the same way independently within each segment or within the set of (as yet) unused elements, and do this as far as one likes. The permutations that can be obtained

in this way are called k permutations. The number of these k permutations is not actually derived, but an upper bound is given instead by studying a generalization, of Catalan numbers. ESA

N91-31826# Nijmegen Univ. (Netherlands). Dept. of Informatics.
PARTIAL EVALUATION GRAMMARS
Mark-Jan Nederhof and Janos Sarbo Jan. 1991 12 p
(TR-91-01; ETN-91-99589) Avail: NTIS HC/MF A03

A new formalism called PEG (Partial Evaluation Grammar) which allows the integration of syntactic and semantic aspects of a programming language into one clear specification, is introduced. A specification of a language in our formalism can be considered an interpreter. The process of compiler generation is made possible by including in the specification language the concept of goal delay known from PROLOG. This brings about a natural separation of compile time and run time calculations by means of partial evaluation. An essential new construct in the formalism is a particular kind of dynamic definition of predicates, which eliminates the need for an intermediate language. Partial evaluation plays an important role here as well. The compilation of a PEG into machine code for an abstract machine called PEWAM which is an extension of the Warren Abstract Machine, is discussed. ESA

N91-31827# Utrecht State Univ. (Netherlands). Dept. of Computer Science.
THE DERIVATION OF DISTRIBUTED TERMINATION DETECTION ALGORITHMS FROM GARBAGE DETECTION SCHEMES
Gerard Tel and Friedmann Mattern (Kaiserslautern Univ., Germany, F.R.) Jul. 1990 34 p
(Contract EC-3075)
(RUU-CS-90-24; ISSN-0924-3275; ETN-91-99590) Avail: NTIS HC/MF A03

It is shown that the termination detection problem for distributed computations can be modeled as an instance of the garbage collection problem. Consequently, algorithms for the termination detection problem are obtained by applying transformations to garbage collection algorithms. The transformation can be applied to collectors of the mark and sweep type as well as to reference counting garbage collectors. As examples, the scheme is used to transform the weighted reference counting protocol, the distributed reference counting protocol of Lermen and Maurer, and Ben-Ari's mark and sweep collector into termination detection algorithms. Known termination detection algorithms as well as new variants are obtained. ESA

N91-31828# Utrecht State Univ. (Netherlands). Dept. of Computer Science.
DISTRIBUTED INCREMENTAL MAXIMUM FINDING IN HIERARCHICALLY DIVIDED GRAPHS
P. J. A. Lentfert, S. D. Swierstra, and A. H. Uittenbogaard (HCS Industrial Automation B.V., Apeldoorn, Netherlands) Sep. 1990 18 p
(RUU-CS-90-30; ISSN-0924-3275; ETN-91-99594) Avail: NTIS HC/MF A03

A distributed algorithm on a hierarchically divided network is derived. Every node in the network has an associated input value and a variable in which it keeps the maximum of all inputs. The inputs may change spontaneously. Within finite time after a change, every node has updated its maximum value of the inputs. The algorithm is developed in stages. After the problem description, an abstract algorithm on a (virtual) division tree is given. Next, the algorithm is tranformed in the distributed algorithm that operates on a hierarchically divided network. The stages are described informally as well as in UNITY. This combination appeared to be an ideal combination to design distributed and concurrent algorithms. It is hoped that the derivation and techniques used in the algorithm will be helpful in the future to design more distributed algorithms on hierarchically divided networks. ESA

N91-31829# Utrecht State Univ. (Netherlands). Dept. of Computer Science.
THE ON-LINE D-DIMENSIONAL DICTIONARY PROBLEM
Teofilo F. Gonzalez (California Univ., Santa Barbara.) Oct. 1990 18 p
(RUU-CS-90-31; ISSN-0924-3275; ETN-91-99595) Avail: NTIS HC/MF A03

The on-line d dimensional dictionary problem is studied. This problem consists of executing on-line any sequence of operations of the form: INERT(p), DELETE(p) and MEMBERSHIP(p), where p is any point in d space. To represent the set of points a new generalization of balanced binary search trees, called d dimensional balanced binary search trees is used. It is shown that any of the above operations can be implemented to take O(d + log n) time, where n is the current number of points in the set, and each INSERT and DELETE operation requires no more than a constant number of rotations. The procedures are almost identical to the ones for balanced binary search trees. The main difference is in the way an element is searched for. The search strategy is based on the principle Assume, Verify and Conquer (AVC). This principle is applied as follows. To avoid multiple verifications it is assumed that some prefixes of strings match. At the end of the search whether or not these assumptions were valid must be determined. This can be done by performing one simple verification step that takes O(d) time. The elimination of multiple verifications is important because in the worst case there are Omega(log n) verifications, each taking O(d) time. ESA

N91-31830# Utrecht State Univ. (Netherlands). Dept. of Computer Science.
LINEAR LOGIC, DOMAIN THEORY, AND SEMI-FUNCTORS
R. Hoofman 19 Nov. 1990 25 p
(RUU-CS-90-34; ISSN-0924-3275; ETN-91-99598) Avail: NTIS HC/MF A03

Girard Categories (GCs) have been defined as categorical models for linear logic. It was shown that the Kleisli category of a GC is Cartesian closed. It is shown that the category of sets and relations Rel nearly is a GC, but not quite. This situation is studied in more abstract terms using semi-category theoretical notions, and weak GCs are defined. It is shown that the semi-Kleisli category of a weak GC is weak Cartesian closed. The Karoubi envelope construction can be used to transform various semi-notions. It is shown that the Karoubi envelope of Rel is a simple example of a cancellative GC, and that the Karoubi envelope of the Kleisli category of Rel is equivalent to the category of continuous lattices and continuous functions. It is considered that semi-notions are perhaps more important in domain theory than is usually realized. Linear type theory is to be considered as being a decomposition of the usual theory belonging to the typed lambda calculus. ESA

N91-31831# Utrecht State Univ. (Netherlands). Dept. of Computer Science.
PERFECT COLORINGS
Erwin M. Bakker, Jan vanLeeuwen, and Richard B. Tan (Oklahoma Coll. of Liberal Arts, Chickasha.) Nov. 1990 29 p
(Contract EC-3075)
(RUU-CS-90-35; ISSN-0924-3275; ETN-91-99599) Avail: NTIS HC/MF A03

A problem that arises when the segmentation of a file in a network is considered without redundancy is studied. This problem translates to a graph coloring problem: k colorability. Several basic results for perfectly k colorable graphs are proved. It is shown how to generate all perfectly k colorable graphs, and some simple classes of perfectly k colorable graphs are characterized. On the other hand, it is proved that the problem of deciding whether a given (k - 1) regular graph is perfectly k colorable is NP complete for every fixed k greater than or equal to 4. ESA

N91-31832# Utrecht State Univ. (Netherlands). Dept. of Computer Science.
ON THE EFFICIENT INCREMENTAL EVALUATION OF HIGHER ORDER ATTRIBUTE GRAMMARS
Harald Vogt, Doaitse Swierstra, and Matthijs Kuiper 3 Dec. 1990

14 p
(RUU-CS-90-36; ISSN-0924-3275; ETN-91-99600) Avail: NTIS HC/MF A03

A new algorithm for the incremental evaluation of Ordered Attribute Grammars (OAGs), which also solves the problem of the incremental evaluation of Ordered Higher order Attribute Grammars (OHAGs) is presented. Two new approaches are used in the algorithm. First, instead of caching all results of semantic functions in the grammar, all results of visits to trees are caught. There are no attributed trees, because all attributes are stored in the cache. Trees are built using hash consing, thus sharing multiple instances of the same tree and avoiding repeated attributions of the same tree with the same inherited attributes. Second, each visit computes not only synthesized attributes but also bindings for subsequent visits. Bindings, which contain attribute values computed in one visit and used in subsequent visits, are also stored in the cache. As a result, second and further visits get a subtree containing only all necessary earlier computer values (the bindings) as a parameter. The algorithm runs in O((Affected) + (paths-to-roots)) steps after modifying subtrees, where paths-to-roots is the sum of the lengths of all paths from the root to all modified subtrees. ESA

N91-31833# Utrecht State Univ. (Netherlands). Dept. of Computer Science.
CATEGORICAL SEMANTICS AS A BASIS FOR PROGRAM TRANSFORMATION
Nico Verwer Dec. 1990 21 p
(RUU-CS-90-38; ISSN-0924-3275; ETN-91-99602) Avail: NTIS HC/MF A03

Program transformation in the Bird-Meertens formalism is based on so called laws, which are equalitities between expressions. It is shown how these laws can be derived in a very general way, starting from equations which hold in a particular semantics, namely cartesian closed categories. It is argued that datatypes correspond to 'strong' functors, which means that their action on functions can be expressed as a program. By proving that functors defined by initial algebras are strong, the validity of this approach for deriving laws about abstract data types is established. Very general formulations of the factorization and promotion laws for homomorphisms are derived. ESA

N91-31834# Utrecht State Univ. (Netherlands). Dept. of Computer Science.
ON LOGIC PROGRAMMING AND THE REFINEMENT CALCULUS: SEMANTICS BASED PROGRAM TRANSFORMATIONS
Joost N. Kok Dec. 1990 20 p Sponsored by Commission of the European Communities
(RUU-CS-90-39; ISSN-0924-3275; ETN-91-99603) Avail: NTIS HC/MF A03

An attempt to bridge the gap between logic programming and a refinement calculus for imperative programs is made. In order to make an embedding of logic progamming possible, the refinement calculus is extended in several ways. The result is a notion of stepwise refinement for logic programs and the advantages of the refinement calculus become available for logic programing. For example, program transformation rules for logic programming in the calculus can be justified. ESA

N91-31835# Utrecht State Univ. (Netherlands). Dept. of Computer Science.
THE FAILURE OF FAILURES: TOWARDS A PARADIGM FOR A SYNCHRONOUS COMMUNICATION
F. S. deBoer, J. N. Kok, C. Palamidessi, and J. J. M. M. Rutten (Center for Mathematics and Computer Science, Amsterdam, Netherlands) Dec. 1990 27 p Sponsored in part by Commission of the European Communities and Netherlands Research and Education in Concurrent Systems
(RUU-CS-90-40; ISSN-0924-3275; ETN-91-99604) Avail: NTIS HC/MF A03

A general framework to study the variety of concurrent languages based on asynchronous communication, like data flow, concurrent logic, concurrent constraint languages, and communications sequential processes with asynchronous channels is developed. The main characteristics of these languages is that the process interacts by reading and modifying the state of some common data structure. The study abstracts from the specific features of the various communication mechanisms by means of a uniform language where actions are interpreted as partial transformations on an abstract set of states. Suspension is modeled by an action being undefined in a state. The languages listed above can be seen as instances of the paradigm, obtained by fixing a specific set of states and interpretation of the actions. The computational model of the paradigm is described by a transition system. It is shown that the traces generated by it already constitute a compositional semantics. This sharply contrasts with the synchronous case, where some additional branching information (like failure sets) is needed to describe deadlock. The specific features of a particular language come to surface when the problem of full abstraction is considered. These features are reflected by closure conditions on the set of states. Finally, by means of a formal method for language comparison (embedding) the expressive power of the paradigm was investigated; it is shown that under certain reasonable restrictions, it is not possible to embed CCS. ESA

N91-31836# Utrecht State Univ. (Netherlands). Dept. of Computer Science.
APPROXIMATING TREEWIDTH, PATHWIDTH, AND MINIMUM ELIMINATION TREE HEIGHT
Hans L. Bodlaender, John R. Gilbert, Hjalmtyr Hafsteinsson (Iceland Univ., Reykjavik.), and Ton Kloks Jan. 1991 17 p Sponsored in part by Netherlands Foundation for Computer Science (Contract EC-3075)
(RUU-CS-91-01; ISSN-0924-3275; ETN-91-99608) Avail: NTIS HC/MF A03

It is shown how the value of various parameters of graphs connected to sparse matrix factorization and other applications can be approximated using an algorithm that finds vertex separators of graphs. The approximate values of the parameters, which include minimum front size, treewidth, pathwidth, and minimum elimination tree height, are no more than O(log n) (minimum front size and treewidth) and O(squared logarithm of n) (pathwidth and minimum elimination tree height) times the optimal values. In addition, the existence of bounded approximation algorithms for the parameters are examined, and it is shown that unless P = NP, there are no absolute approximation algorithms for them. ESA

N91-31837# Utrecht State Univ. (Netherlands). Dept. of Computer Science.
SYNCHRONOUS LINK-LEVEL PROTOCOLS
Anneke A. Schoone Feb. 1991 16 p
(Contract EC-3075)
(RUU-CS-91-02; ISSN-0924-3275; ETN-91-99609) Avail: NTIS HC/MF A03

Aho et al gave several protocols for sending a sequence of bits over an error prone link an a synchronous environment. How the Krogdahl-Knuth technique of system wide invariants can be used for proving the protocols correct is investigated. ESA

N91-31838# Utrecht State Univ. (Netherlands). Dept. of Computer Science.
THE COMPLEXITY OF COLORING GAMES ON PERFECT GRAPHS
Hans L. Bodlaender and Dieter Kratsch (Universitaets-Sternwarte, Jena, German D.R.) Feb. 1991 17 p
(Contract EC-3075)
(RUU-CS-91-03; ISSN-0924-3275; ETN-91-99610) Avail: NTIS HC/MF A03

Consideration is given to the following type of game: two players must color the vertices of a given graph G (V,E), in a predescribed order, such that no two adjacent vertices are colored with the same color. In one variant, the first player which is unable to move loses the game. In another variant, player 1 wins the game, if and only if the game ends with all vertices colored. Several

results on the complexity of the problem to decide whether there is a winning strategy for player 1 in a given game instance, when G is restricted to split graphs, interval graphs, or bipartite graphs is obtained. ESA

N91-31839# Utrecht State Univ. (Netherlands). Dept. of Computer Science.
DYNAMIC OUTPUT-SENSITIVE HIDDEN SURFACE REMOVAL FOR C-ORIENTED POLYHEDRA
Mark deBerg Feb. 1990 24 p Sponsored in part by Netherlands Organization for Applied Scientific Research TNO and Commission of the European Communities
(RUU-CS-91-06; ISSN-0924-3275; ETN-91-99613) Avail: NTIS HC/MF A03

An output sensitive algorithm to maintain the view of a set of c oriented polyhedra under insertions into or deletions from the set is presented. (A set of polyhedra is c oriented if the number of different orientation of its edges is bounded by some constant c.) Cyclic overlap in the scene is allowed and the polyhedra may even instersect. The time needed for an update is O((K + 1) cubed logarithm of n), where n is the total number of vertices of all polyhedra and k is the number of changes in the visibility map. The solution is based on new dynamic data structures for ray shooting and range searching problems for c oriented objects. ESA

N91-31840# Universiteit Twente, Enschede (Netherlands). Dept. of Computer Science.
THE HIERARCHY OF LR-ATTRIBUTED GRAMMARS
Rieks opdenAkker, Borivoj Melichar, and Jorma Tarhio (Helsinki Univ. of Technology, Espoo, Finland) Apr. 1991 19 p Revised
(MEMO-INF-91-26; ISSN-0923-1714; ETN-91-99706) Avail: NTIS HC/MF A03

Attribute evaluation during LR parsing is considered. Several definitions of LR attributed grammars are presented. Relations of corresponding classes of attribute grammars are discussed. The relations between LR attributed grammars and LL attributed grammars and between LR attributed grammars and a class of one pass attributed grammars based on left corner grammars are considered. ESA

N91-31841# Universiteit Twente, Enschede (Netherlands). Dept. of Computer Science.
ATTRIBUTE EVALUATION AND PARSING
Rieks opdenAkker, Borivoj Melichar, and Jorma Tarhio (Helsinki Univ. of Technology, Espoo, Finland) Apr. 1991 32 p
(MEMO-INF-91-31; ISSN-0923-1714; ETN-91-99710) Avail: NTIS HC/MF A03

Attribute evaluation during top down, bottom up and left corner parsing strategies is considered. For each of these parsing strategies, restrictions are given for left attributed grammars that allow deterministic non backtracking, one pass evaluators to be used. Left corner parsing is treated in detail, and it is shown how a one pass left corner compiler can be constructed by means of techniques used in the top down and the bottom up evaluators. ESA

N91-31842# Universiteit Twente, Enschede (Netherlands). Dept. of Applied Mathematics.
AN ALGORITHM FOR SPECTRAL FACTORIZATION OF POLYNOMIAL MATRICES WITH ANY SIGNATURE
Michael Sebek (Ceskoslovenska Akademie Ved, Prague.) Dec. 1990 110 p Original contains floppy disk
(MEMO-912; ISSN-0169-2690; ETN-91-99714) Avail: NTIS HC/MF A06

An algorithm for spectral factorization of polynomial matrices with any signature on the stability boundary (non-positive, non-negative definite, indefinite, singular, etc.) is described. Conditions for the existence of a spectral factor are given and its uniqueness is discussed. A package of MATLAB programs to computer the spectral factor is documented in the appendix and included on a diskette. ESA

N91-31843# Universiteit Twente, Enschede (Netherlands). Dept. of Applied Mathematics.
DYNAMIC DISTURBANCE DECOUPLING FOR DISCRETE-TIME NONLINEAR SYSTEMS
U. Kotta (Academy of Sciences of the Estonian SSR, Tallinn.) and H. Nijmeijer 5 Dec. 1990 29 p In RUSSIAN; ENGLISH summary Submitted for publication
(MEMO-913; ISSN-0169-2690; ETN-91-99715) Avail: NTIS HC/MF A03

The inversion (structure) algorithm for discrete time nonlinear systems around an equilibrium point is given in a more general and simple form and the new structural parameters of the system called invertibility indices, are introduced. Using an approach based on the inversion algorithm, the Dynamic Disturbance Decoupling Problem (DDDP) for discrete time nonlinear systems is investigated. Necessary and sufficient conditions for the local solvability of the DDDP as well as the equations of the dynamic compensator are found under the assumption that the system is invertible. Both the cases of measurable and unmeasurable disturbances are considered. The approach and results obtained are close to earlier results for continuous time nonlinear systems. The theory developed is illustrated by means of an example of a closed economy. ESA

N91-31844# Universiteit Twente, Enschede (Netherlands). Faculty of Applied Mathematics.
AN ALGORITHM FOR THE ONE-TO-ALL SHORTEST PATH PROBLEM WITH ARBITRARY ARC LENGTHS
B. Dorhout Dec. 1990 14 p
(MEMO-919; ISSN-0169-2690; ETN-91-99721) Avail: NTIS HC/MF A03

One of the most successful methods for the one to all shortest path problem in a directed graph, Dijkstra's method, is discussed. If m is the number of arcs of the graph, its worst case complexity is O(m). A drawback of this method is that it can only be applied on graphs with nonnegative arc lengths. A method is described for graphs with arbitrary arc lengths. It can be considered as an extension of Dijkstra's method. It uses Dijkstra's method in two ways: for the transformation of the problem into a problem with only non negative arc lengths and for the solution of this new problem. The transformation is made through the solution of a linear assignment problem. If r is the number of nodes which are tails of one or more arcs with negative length, this assignment problem is solved by applying Dijsktra's method at most r times on small subproblems. So the worst case complexity of the method is O((r + 1) m). ESA

N91-31845# Universiteit Twente, Enschede (Netherlands). Faculty of Applied Mathematics.
ALGORITHMS FOR FINDING AN OPTIMAL MATCHING BETWEEN A GIVEN STRING AND A STRING GENERATED BY A REGULAR GRAMMAR
S. M. Baas and P. vanSchaik Dec. 1990 25 p
(MEMO-921; ISSN-0169-2690; ETN-91-99723) Avail: NTIS HC/MF A03

The application of a boundary integral or panel method to duct flows is described. The method is capable of computing the 3-D, steady state, subsonic, linearized (Prandtl-Glauert) potential flow about general configurations. The method is characterized by the application of the Dirichlet boundary condition and of compressible source and doublet distributions which are directly applied in the physical space. The geometry of the non branching duct (one inflow and one outflow cross section) may be arbitrary as long as the requirements for using the Prandtl-Glauert equation are met. A description of the method is given and three examples of application are presented with emphasis on the investigation of the conservation of mass flow through the ducts. ESA

N91-31846 Politecnico di Milano (Italy). Dipt. di Elettronica.
ON THE APPLICATION OF TEMPORAL LOGIC IN REAL TIME TO SPECIFY TELECOMMUNICATION PROTOCOLS [APPPLICAZIONE DI LOGGICA TEMPORALE IN TEMPO ESPLICITO PER LA SPECIFICA DI PROTOCOLLI PER TELECOMUNICAZIONI]
L. Favalli 1990 26 p In ITALIAN
(Rept-90-071; ETN-91-99926) Avail: Politecnico di Milano, Piazza Leonardo da Vinci 32, 20133 Milan, Italy

The problem of formally specifying network protocols is addressed. Languages derived from mathematical logic to determine data transmission behavior have received much attention. The application of the formal logic TRIO to the specification of ISO802.3 standard, as well as improper terms, like Ethernet, is presented. ESA

N91-31847# Association Aeronautique et Astronautique de France, Paris.
INTERACTIVE TOOL VISUALIZATION OF THREE DIMENSIONAL 3D RESULTS [VISUALISATION PAR UN OUTIL INTERACTIF DE RESULTATS TRIDIMENSIONNELS 3D]
P. Guillen and A. M. Vuillot (Office National d'Etudes et de Recherches Aerospatiales, Paris, France) 1989 20 p In FRENCH Presented at 26th Colloque d'Aerodynamique Appliquee, Toulouse, France, 23-25 Oct. 1990
(AAAF-NT-89-19; ISBN-2-7170-0952-3; ISSN-0243-0177; ETN-91-99960) Avail: NTIS HC/MF A03; CEDOCAR, Section des Diffusions, 26 Blvd Victor, 75996 Paris Armees, France, HC 15 francs

Computer graphics requirements and user and fluid mechanics software developer constraints are described, and the VOIR3D (French acronym for interactive tool visualization of three dimensional results) is presented. This software unifies two preceding kinds of software by the macrocommand concept. A number of general considerations on desired features are described and constraints to be respected are examined. VOIR3D three dimensional object creation algorithms are described and the software in-processing mode utilization is outlined. ESA

N91-31848# Association Aeronautique et Astronautique de France, Paris.
POST PROCESSING OF THREE DIMENSIONAL AEROTHERMAL COMPUTATION [POST-TRAITEMENT DE CALCUL AEROTHERMIQUES TRIDIMENSIONNELS]
A. Luc-Bouhali, D. DevezeauxdeLavergne, V. Kurg, and Y. Lecointe (Ecole Nationale Superieure de Mecanique, Nantes, France) 1989 13 p In FRENCH Presented at the 26th Colloque d'Aerodynamique Appliquee, Toulouse, France, 23-25 Oct. 1990 Previously announced in IAA as A90-21050
(AAAF-NT-89-21; ISBN-2-7170-0954-X; ISSN-0243-0177; ETN-91-99962) Avail: NTIS HC/MF A03; CEDOCAR, Section des Diffusions, 26 Blvd Victor, 75996 Paris Armees, France, HC 15 francs

Graphics software programs which visualize static and dynamic 3-D aerodynamic computation results are described. The BLUNT code, which solves 3-D unsteady Euler equations, and the STEIN super/hypersonic Euler code are discussed. Post processing of 3-D results and visualization of 3-D surfaces are discussed. The ASCETE (French acronym for aid to simulation and comprehension of 3-D external flows) and its two derivatives, COUPE3D and ANIM3D are discussed. ESA

N91-31849# Association Aeronautique et Astronautique de France, Paris.
USE OF THE ANIMATED IMAGES FOR THE VISUALIZATION OF COMPUTATIONAL RESULTS [UTILISATION DE L'IMAGE ANIMEE POUR LA VISUALISATION DE RESULTATS DE CALCULS]
Pierre Herchuelz and Ulrich Rist (Centre Europeen Recherche et de Formation Advance en Calcul Scientific, Toulouse, France) 1989 6 p Presented at the 26th Colloque d'Aerodynamique Appliquee, Toulouse, France, 23-25 Oct. 1990 Previously announced in IAA as A91-19587
(AAAF-NT-89-22; ISBN-2-7170-0955-8; ISSN-0243-0177; ETN-91-99963) Avail: NTIS HC/MF A02; CEDOCAR, Section des Diffusions, 26 Blvd Victor, 75996 Paris Armees, France, HC 15 francs

Techniques, terms, hardware and experience relating to the animation of computational results by frame recording of single images with the help of a video recorder or directly on the computer terminal are discussed. Examples to emphasize the general aspects and advantages of animation in scientific computation are given: where animation is used to understand flow physics, to view three dimensional data, to explore the influence of computational parameters, to explore numerical stability, and to debug a code. ESA

N91-31850# Association Aeronautique et Astronautique de France, Paris.
VISUALIZATION OF THREE DIMENSIONAL UNSTEADY COMPUTATION RESULTS [VISUALISATION DE RESULTATS DE CALCULS TRIDIMENSIONNELS ET INSTATIONNAIRES]
Alain Lesain and Antoine Fourmaux 1989 20 p In FRENCH Presented at the 26th Colloque d'Aerodynamique Appliquee, Toulouse, France, 23-25 Oct. 1990 Previously announced in IAA as A90-21040
(AAAF-NT-89-23; ISBN-2-7170-0956-6; ISSN-0243-0177; ETN-91-99964) Avail: NTIS HC/MF A03; CEDOCAR, Section des Diffusions, 26 Blvd Victor, 75996 Paris Armees, France, HC 15 francs

Software for developing numerical matrix-images representing 3-D objects (for example turbomachine blades) was developed with the aim of creating graphical images of computation results. The design principles and performance of the software is presented. Two techniques for making animated films are shown. ESA

N91-31851# Association Aeronautique et Astronautique de France, Paris.
APPLICATION OF AN ACQUISITION IMAGE PROCESSING SYSTEM TO THE QUANTITATIVE ANALYSIS OF FLOWS [APPLICATION D'UN SYSTEME D'ACQUISITION ET DE TRAITEMENT D'IMAGES A L'ANALYSE QUANTITATIVE D'ECOULEMENTS]
P. Berthoumieu, C. Lempereur, and J. M. Mathe (Centre d'Etudes et de Recherches, Toulouse, France) 1989 13 p In FRENCH Presented at the 26th Colloque d'Aerodynamique Appliquee, Toulouse, France, 23-25 Oct. 1990 Previously announced in IAA as A91-19584
(AAAF-NT-89-27; ISBN-2-7170-0960-4; ISSN-0243-0177; ETN-91-99968) Avail: NTIS HC/MF A03; CEDOCAR, Section des Diffusions, 26 Blvd Victor, 75996 Paris Armees, France, HC 15 francs

A real time data acquisition image processing system which uses a Motorola computer and Datacube cards is presented. High speed digital data exchange is achieved with an assembly of specific buses (VME and MAXbus). Two kinds of processing (mean and histogram) give information on the nozzle outlet fuel concentrations. A second study analyzes images to produce geometric information (size, surface, convection speed, etc.) on vortex cores. A third study involves the implementation of a three dimensional trajectory system. ESA

N91-31852# Wales Univ. Inst. of Science and Technology, Cardiff. School of Electrical, Electronic and Systems Engineering.
GENETIC ALGORITHMS M.S. Thesis
R. A. Mansfield 1990 145 p
(ETN-91-99985) Copyright Avail: NTIS HC/MF A07

The origins of genetic algorithms are examined and the concepts and terminology used by their exponents are explained. An overview of their current application is given and areas for the possible future application of adaptive evolutionary based systems are discussed. The performance of genetic algorithms is compared with that of other similar optimization techniques such as hill climbing and simulated annealing. The use of metalevel genetic algorithms to optimize the parameters of a particular genetic algorithm is analyzed. Three programs demonstrating specific

applications of genetic algorithms in TURBO PASCAL 5.0 are explained and their results are analyzed. The examples are a simple genetic algorithm to find the maximum value of the sine function, the metalevel optimization of the first example and the optimization of gait parameters for a bipedal walking robot. Areas for future work are identified. ESA

N91-31853*# Remtech, Inc., Huntsville, AL.
AERO/FLUIDS DATABASE SYSTEM Final Report
John E. Reardon and Duane L. Violett, Jr. May 1991 91 p
(Contract NAS8-37463)
(NASA-CR-184208; NAS 1.26:184208; RTR-193-04) Avail: NTIS HC/MF A05 CSCL 09B

The AFAS Database System was developed to provide the basic structure of a comprehensive database system for the Marshall Space Flight Center (MSFC) Structures and Dynamics Laboratory Aerophysics Division. The system is intended to handle all of the Aerophysics Division Test Facilities as well as data from other sources. The system was written for the DEC VAX family of computers in FORTRAN-77 and utilizes the VMS indexed file system and screen management routines. Various aspects of the system are covered, including a description of the user interface, lists of all code structure elements, descriptions of the file structures, a description of the security system operation, a detailed description of the data retrieval tasks, a description of the session log, and a description of the archival system. Author

N91-31854# Sandia National Labs., Albuquerque, NM.
APPLICATION OF DIGITAL COMPRESSION TECHNIQUES TO OPTICAL SURVEILLANCE SYSTEMS
C. S. Johnson 1991 5 p Presented at the 32nd Institute of Nuclear Materials Management (INMM) Annual Meeting, New Orleans, LA, 28-31 Jul. 1991
(Contract DE-AC04-76DP-00789)
(DE91-016404; SAND-91-1731C; CONF-910774-63) Avail: NTIS HC/MF A01

There are many benefits to handling video images electronically. However, the amount of digital data in a normal video image is a major obstacle. The solution is to remove the high frequency and redundant information in a process that is referred to as compression. Compression allows the number of digital bits required for a given image to be reduced for more efficient storage or transmission of images. The next question is how much compression can be done without impairing the image quality beyond its usefulness for a given application. This paper will discuss image compression that might be applied to provide useful images in unattended surveillance applications. DOE

N91-31855# Oak Ridge National Lab., TN.
A USERS' GUIDE TO PVM (PARALLEL VIRTUAL MACHINE)
A. Beguelin, J. Dongarra, A. Geist, R. Manchek, and V. S. Sunderam (Emory Univ., Atlanta, GA.) Jul. 1991 21 p
(Contract DE-AC05-84OR-21400)
(DE91-016934; ORNL/TM-11826) Avail: NTIS HC/MF A03

The PVM version 2.3 users' guide is presented. It contains an overview of PVM and how it is installed and used. Example programs in C and Fortran are included. PVM stands for Parallel Virtual Machine. It is a software package that allows the utilization of a heterogeneous network of parallel and serial computers as a single computational resource. PVM consists of two parts: a daemon process that any user can install on a machine, and a user library that contains routines for initiating process on other machines, for communicating between processes, and synchronizing process. DOE

N91-31856# Air Force Inst. of Tech., Wright-Patterson AFB, OH.
INTERACTIVE CONSTRAINT-BASED SOLID MODELING AS A DESIGN TOOL M.S. Thesis
Kenneth L. Toblin 1991 150 p
(AD-A239358; AFIT/CI/CIA-91-046) Avail: NTIS HC/MF A07 CSCL 12/5

Architectural design knowledge which may take the form of constraints and how it can be incorporated into the solid modeling process is explored and discussed. This theoretical exploration leads to an illustration of a functional general purpose 3-D solid modeler which utilizes design knowledge as constraints upon the interactive solid modeling process. From this illustration, it is shown that the incorporation of constraints into Computer-Aided Architectural Design can effectively assist in the early stages of the design process. A prototypical application is presented which provides an example in which the definition and implementation of specific design knowledge constraints or characterizes the generative and interactive behavior of user definable 3-D entities. The basis of the thesis lies in the ability to create a design space, or building envelope, and to allow the interactive modeling of conceptual elements within, and constrained to, that design space, including the realistic interaction between the entities themselves. GRA

N91-31857# Stanford Univ., CA. Dept. of Computer Science.
OPEN ARCHITECTURE FOR FORMAL REASONING Final Report, 1-30 Sep. 1990
John McCarthy Aug. 1991 5 p
(Contract N00039-84-C-0211)
(AD-A239395) Avail: NTIS HC/MF A01 CSCL 23/2

This task represents an initial part of a long term project aimed at making both theoretical and practical advances in the field of formal reasoning. The main goal is to provide a framework for designing and experimenting with symbol manipulation programs, and in particular, to provide a general software architecture for implementing formal reasoning systems and interfaces to existing software components including special purpose theorem provers, program transformers, and databases. The kernel will be a computation system that supports a rich collection of data structures for formal reasoning, a wide spectrum of programming paradigms including both high-level constructs, and objects as self contained entities that may be used uniformly and independently of internal representation. GRA

N91-31858# Stanford Univ., CA. Systems Optimization Lab.
PRACTICAL ASPECTS OF AN INTERIOR-POINT METHOD FOR CONVEX PROGRAMMING
Florian Jarre and Michael A. Saunders Jul. 1991 22 p
(Contract N00014-89-J-1659)
(AD-A239457; SU-SOL-91-9) Avail: NTIS HC/MF A03 CSCL 12/4

We present an algorithm for solving convex programs with nonlinear constraints. The algorithm works in the primal space only and uses a predictor-corrector strategy to follow a smooth path that leads to an optimal solution. The algorithm simultaneously iterates towards feasibility and optimality. The matrices occurring in the algorithm can be kept sparse if the nonlinear functions are separable or depend on few variables only. Some promising numerical examples obtained from a preliminary implementation are included. GRA

N91-31859# Naval Postgraduate School, Monterey, CA.
APPLICATION OF THE CONSTRAINED IMPLICANTS SET CONCEPT TO THE MINIMIZATION OF BINARY FUNCTIONS M.S. Thesis
Ugur Ozkan Sep. 1990 87 p
(AD-A239470) Avail: NTIS HC/MF A05 CSCL 12/6

Several heuristics and algorithms have been developed to find minimal sum-of-products expressions in binary logic. Most of them use prime implicants during minimization process. An efficient search strategy has been developed for finding minimal sum-of-products expressions for multiple-valued logic (MVL) functions by using the constrained implicants set concept. The search space can be considerably reduced over the only other known exact minimization technique and exhaustive search. The primary goals of this research are to: (1) examine whether the constrained implicant set concept can be efficiently used in binary logic, and; (2) develop a heuristic called the constrained implicant set heuristic (CISH). The general idea of the CISH is to select the minterm with the least implicant cover size and find the implicant

with the largest minterm coverage that covers a selected minterm. In this research, the implementation of the CISH is presented, the performance analysis of the CISH is shown by comparing with other heuristics (Maximum Implicant Heuristic, Espresso II) with respect to the average number of the product terms, the average computation time, and the average memory usage. GRA

N91-31860# Delta Information Systems, Inc., Horsham, PA.
INVESTIGATION OF THE PROGRESSIVE BI-LEVEL CODING TECHNIQUE FOR THE HIGH-RESOLUTION BI-LEVEL DATA COMPRESSION STANDARD Final Report
Jul. 1990 108 p
(AD-A239597; NCS-TIB-90-12) Avail: NTIS HC/MF A06 CSCL 25/5

The purpose of this study was to investigate the Progressive Bi-Level Coding Technique for the High Resolution Bi-Level Data Compression Standard. At the present time, the Consultative Committee for International Telephone and Telegraph (CCITT) Recommendations for Group 4 permit the transmission of only sequentially transmitted black and white imagery. In addition, coding efficiency of Group 4 machines suffers for input pages containing half-time information. As a result of much increased commercial interest from major computer and telecommunications companies, there has been intense effort in the international standards bodies to select a bi-level image compression technique for future image storage and communications applications. The focal point of this activity has been the Joint Bi-level Image Group (JBIG) of ISO/IEC and CCITT. GRA

N91-31861# Air Force Academy, CO.
METHODS OF ASTRODYNAMICS, A COMPUTER APPROACH Final Report, May 1988 - Feb. 1991
David A. Vallado 14 Feb. 1991 369 p
(AD-A239662; USAFA-TR-91-6; AD-M000073) Avail: NTIS HC/MF A16 CSCL 03/2

A library PASCAL and FORTRAN computer routines to solve various Astrodynamic problems is presented. Diagrams and equations are given for each routine. Rigorous documentation and coding discipline was used during development of these routines. The code contains extensive information for each routine defining Input/Output variables, local variables, constants, coupling, and references. Finally, test cases and answers are presented. References are given, therefore formulas are not derived. THe code presented will run under TURBO PASCAL Ver5.0 +, MICROSOFT FORTRAN Ver 4.0 +, and VAX FORTRAN Ver 4.6. Both langauges have two files, astrodynamic and mathematical. The PASCAL mathematical code includes a number of mathematical operations not inherent to language. The FORTRAN code was developed in LAHEY FORTRAN Ver 3.0 and uses several features of FORTRAN 90. Driver programs are not included since these routines are designed to be a library which one may attach to a main program. These routines were developed for academic use and as such, may not match operational data. Information concerning the latest software version may be obtained from the author. GRA

N91-31862# Institute for Defense Analyses, Alexandria, VA.
REPORT ON THE SOFTWARE TECHNOLOGY FOR ADAPTABLE, RELIABLE SYSTEMS (STARS) CONFERENCE ON FRAMEWORKS CONVERGENCE Final Report
David J. Carney and Frank Belz Jun. 1991 85 p Conference held in Gaithersburg, MD, 22-23 Jan. 1991
(Contract MDA903-89-C-0003)
(AD-A239691; IDA-D-972; IDA/HQ-91-038002; AD-E501420)
Avail: NTIS HC/MF A05 CSCL 12/8

This paper reports on a conference sponsored by DARPA to address technical approaches and barriers to the convergence of Software Engineering Environment (SEE) frameworks. Several efforts currently specifying, designing, and/or implementing SEEs or SEE frameworks are proposing standards for tool interfaces and object management services. Potential conflicts have been thought to exist between some of these proposed standards. However, there is an emerging hypothesis that some approaches previously considered in conflict may in fact be complementary. It may be possible to develop standards that are convergent rather than competitive, in that they operate in conjunction with each other, or may be merged into single standards. Successful convergence would result in the simultaneous satisfaction of a broader range of tool and environment developer needs that can be satisfied by the standards individually, and thereby would broaden the applicability of these standards. This paper reports on the technical discussions of the conference as well as the agreements and conclusions reached by the participants. GRA

62 COMPUTER SYSTEMS

Includes computer networks and special application computer systems.

N91-31863# Universiteit Twente, Enschede (Netherlands). Faculty of Computer Science.
STUDY DAY ON THE DESIGN OF A NETWORK DATABASE IN FOUR LANGUAGES [ONTWERPEN VAN EEN NETWERKDATABASE IN VIER TALEN]
N. M. vanDiepen, H. Grunefeld, and W. A. Vervoort Mar. 1991 89 p Partly in DUTCH and ENGLISH Held in Enschede, Netherlands, 13 Nov. 1990
(Memo-INF-91-22; ISSN-0923-1714; ETN-91-99702) Avail: NTIS HC A05/MF A01

Four experienced designers/programmers demonstrate how they realized a network data base, each in their own programming style. The four different programming approaches are imperative, object oriented, logical, and functional, respectively. For individual titles, see N91-31864 through N91-31867.

N91-31864# Groningen Rijksuniv. (Netherlands). Vakgroep Informatica.
A SOLUTION FOR THE NETWORK DATABASE PROBLEM IN AN IMPERATIVE LANGUAGE [EEN OPLOSSING VAN HET NETWERK DATA BASE PROBLEEM IN EEN IMPERATIEVE TAAL]
C. Bron *In* Univ. Twente, Study Day on the Design of a Network Database in Four Languages Mar. 1991 7 p In DUTCH (For primary document see N91-31863 23-62)
Avail: NTIS HC/MF A02

A network data base was imperatively programmed in modular PASCAL. All the names of nodes and relations occurring in the data base are stored in a string store and identified with a number. The program shows two limitations: the first in the declared space of the node administration and in the space claimed by the dynamic data structures of the leap; and the second in the space occupied by the different names (of nodes and relations) in the data bases. ESA

N91-31865# Universiteit Twente, Enschede (Netherlands).
AN OBJECT-ORIENTED ANALYSIS, DESIGN, AND IMPLEMENTATION OF A NETWORK DATABASE
Mehmet Aksit, Lodewijk Bergmans, and Enis Yucesoy *In its* Study Day on the Design of a Network Database in Four Languages Mar. 1991 27 p (For primary document see N91-31863 23-62)
Avail: NTIS HC/MF A03

A network data base is realized in an object oriented way using the SMALLTALK code. This object oriented approach comprises a complete development methodology, starting from analysis through design, down to implementation. The major ideas of this specific development are explained. The three steps of the development analysis, design, and implementation, are outlined and demonstrated for this particular example. The SMALLTALK code for the network data base is presented. ESA

N91-31866# Enschede Univ. (Netherlands). Hoger Informatica Onderwijs.
NETWORK DATABASE IN PROLOG [NETWERK DATABASE IN PROLOG]

Jan Stroet *In* Univ. Twente, Study Day on the Design of a Network Database in Four Languages Mar. 1991 32 p In DUTCH (For primary document see N91-31863 23-62)
Avail: NTIS HC/MF A03

The network data base problem is solved using a logical program written in PROLOG. The different aspects of PROLOG programming are outlined. The problem of the network data base is formalized. A NIAM (Nyssens Information Analysis Method) is deduced from the information analysis, resulting in a mapping on the PROLOG data structures and finally in a program. Input/output routines for the network data base problem are presented. ESA

N91-31867# Universiteit Twente, Enschede (Netherlands).
A NETWORK DATABASE: A CASE STUDY IN FUNCTIONAL PROGRAMMING
S. Joosten *In its* Study Day on the Design of a Network Database in Four Languages Mar. 1991 14 p (For primary document see N91-31863 23-62)
Avail: NTIS HC/MF A03

A prototype of a network data base system is built according to a given (informal) specification using functional programming in MIRANDA. The problem is divided into subproblems. The system is built using the concept of directed graph. The data base is a state based system, where every command changes the current state. The starting point of the system is a certain graph in which one node is identified as root node. Rapid prototyping in a functional language is shown to be flexible. ESA

N91-31868# Sandia National Labs., Albuquerque, NM.
BENCHMARKING A NETWORK STORAGE SERVICE
S. M. Kelly, R. A. Haynes, and M. J. Ernest 1991 6 p Presented at the 11th IEEE Symposium on Mass Storage Systems, Monterey, CA, 7-10 Oct. 1991
(Contract DE-AC04-76DP-00789)
(DE91-013510; SAND-91-0210C; CONF-9110125-1) Avail: NTIS HC/MF A02

Benchmarking a network file server introduces some unique considerations over traditional benchmarking scenarios. Since the user is executing on a client system interconnected to the file server, the client and network must be provided for during benchmarking. During a recent procurement action, Sandia National Laboratories was challenged to develop a benchmark suite that would accurately test the network requirements. This paper describes the benchmark design and summarizes the experience gained from the benchmark executions. DOE

N91-31869# Los Alamos National Lab., NM.
LOCAL AREA GIGABIT NETWORKING
D. E. Tolmie 1991 7 p Presented at the 11th IEEE Symposium on Mass Storage Systems, Monterey, CA, 7-10 Oct. 1991
(Contract W-7405-eng-36)
(DE91-014780; LA-UR-91-1722; CONF-9110125-2) Avail: NTIS HC/MF A02

Computer networks must become faster as the equipment that is being interconnected increases in power and performance. Ethernet, with a 10 Mbit/s speed, seemed awesome a few years ago, but is beginning to show its age as more machines are tied together, and workstations attain the power of yesterdays mainframes. Networks using gigabit speeds are just starting to become available and offer a whole new set of problems and potential. This paper addresses what the higher speeds are being used for, the standards efforts specifying the higher speed channels, the network architectures being proposed, and some of the open problems requiring extensive further work. DOE

N91-31870# Oak Ridge National Lab., TN.
THE PVM SYSTEM: SUPERCOMPUTER LEVEL CONCURRENT COMPUTATION ON A HETEROGENEOUS NETWORK OF WORKSTATIONS
G. A. Geist and V. S. Sunderam (Emory Univ., Atlanta, GA.) 1991 5 p Presented at the 6th Distributed Memory Computing Conference, Portland, OR, 28 Apr. -2 May 1991
(Contract DE-AC05-84OR-21400)
(DE91-016276; CONF-9104158-6) Avail: NTIS HC/MF A01

The Parallel Virtual Machine (PVM) system enables supercomputer level concurrent computations to be performed on interconnected networks of heterogeneous computer systems. Specifically, a network of 13 IBM RS/6000 powerstations has been used to run superconductor modeling codes at more than 250 Mflops. This paper describes the PVM system and two example applications running on it. DOE

N91-31871# Messerschmitt-Boelkow-Blohm G.m.b.H., Ottobrunn (Germany, F.R.). Unternehmensbereich Verteidigungssysteme.
CONSTRUCTION AND REALIZATION OF DISTRIBUTED MULTIPROCESSOR SYSTEMS FOR REAL TIME TASKS [AUFBAU UND REALISIERUNG VERTEILTER MEHRPROZESSORSYSTEME FUER ECHTZEITAUFGABEN]
Dieter Flemming 1990 6 p In GERMAN Presented at the Tagung 'Echtzeit 1990', Sindelfingen, Fed. Republic of Germany, 19-21 Jun. 1990
(MBB-UA-1189-90-PUB; OTN-032761; ETN-91-99750) Avail: NTIS HC/MF A02

The software and hardware transparent project of integrated computer systems for real time critical and complex automatization tasks, is assisted by the Ada programming language. Distributed multiprocessor architecture is used. It presupposes that the communication concept of the architecture is flexible, efficient, and in harmony with Ads. The designed project shows that the distributed architectures for real time automatization tasks can be programmed and implementated with syntax restrictions, a semantic determination (still to be prescribed), and additional tools for the Ada programming environment. ESA

N91-31872 Physics and Electronics Lab. TNO, The Hague (Netherlands).
OSI-SECURITY AND RELATIONS WITH OTHER SECURITY STANDARDS Final Report
P. L. Overbeek Mar. 1991 36 p
(FEL-91-B099; TD-91-2008; ETN-91-90004) Copyright Avail: Physics and Electronics Lab. TNO, P.O. Box 96864, 2509 JG, The Hague, Netherlands

Within NATO it is acknowledged that it is an advantage if standard civil information technology products can be used for military purposes. For this, military security requirements should be met. The Open System Interconnection (OSI) security architecture addresses only one of the relevant security issues. Other relevant issues are: security in (open) systems, security in distributed applications and secure information technology products. The relations of the open system interconnection security architecture with other areas of security and other standards in thse areas are described. An emphasis is put on civil standards for the evaluation of security in information technology products. This project is aimed at a better understanding of and contribution to security in distributed information systems. ESA

N91-31873 Physics and Electronics Lab. TNO, The Hague (Netherlands).
INFORMATION SECURITY: PAST, PRESENT AND FUTURE Final Report
P. L. Overbeek Mar. 1991 44 p
(FEL-91-B100; TD-91-2007; ETN-91-90005) Copyright Avail: Physics and Electronics Lab. TNO, P.O. Box 96864, 2509 JG, The Hague, Netherlands

The development of information security in relation to the development of information technology is addressed. The leading question is: how has information security developed itself so far, and how should it progress to address tomorrow's security needs. This project aims at a better understanding of and contribution to security in distributed information systems. ESA

N91-31874*# National Aeronautics and Space Administration. Hugh L. Dryden Flight Research Facility, Edwards, CA.
A KNOWLEDGE BASED APPLICATION OF THE EXTENDED AIRCRAFT INTERROGATION AND DISPLAY SYSTEM

Richard D. Glover and Richard R. Larson Washington Oct. 1991 39 p
(NASA-TM-4327; H-1706; NAS 1.15:4327) Avail: NTIS HC/MF A03 CSCL 09B

A family of multiple-processor ground support test equipment was used to test digital flight-control systems on high-performance research aircraft. A unit recently built for the F-18 high alpha research vehicle project is the latest model in a series called the extended aircraft interrogation and display system. The primary feature emphasized monitors the aircraft MIL-STD-1553B data buses and provides real-time engineering units displays of flight-control parameters. A customized software package was developed to provide real-time data interpretation based on rules embodied in a highly structured knowledge database. The configuration of this extended aircraft interrogation and display system is briefly described, and the evolution of the rule based package and its application to failure modes and effects testing on the F-18 high alpha research vehicle is discussed. Author

N91-31875# University of South Florida, Tampa. Dept. of Computer Science and Engineering.
DESIGN AND ANALYSIS OF FAULT-TOLERANT DISTRIBUTED REAL-TIME COMPUTER SYSTEMS Final Report, 1 Jun. 1986 - 30 Jun. 1987
K. H. Kim 23 Jul. 1991 17 p
(Contract N00014-86-K-0392)
(AD-A239382) Avail: NTIS HC/MF A03 CSCL 12/7

The objective of this project was to contribute to the establishment of the scientific foundation for designing fault-tolerant distributed computer systems. The results obtained from the Phase I of this research project are summarized. Main results are as follows: (1) a preliminary approach to specification of timing constraints during distributed computer system design and to validation of the temporal behavior of the system; (2) a scheme for coordinated execution of independently designed recoverable distributed processes; and (3) establishment of initial versions of three of the real time computer network testbeds and a testbed-based evaluation of the distributed recovery block (DRB) scheme. GRA

63 CYBERNETICS

Includes feedback and control theory, artificial intelligence, robotics and expert systems.

For related information see also *54 Man/System Technology and Life Support.*

N91-31876*# National Aeronautics and Space Administration. Lewis Research Center, Cleveland, OH.
TUNING MAPS FOR SETPOINT CHANGES AND LOAD DISTURBANCE UPSETS IN A THREE CAPACITY PROCESS UNDER MULTIVARIABLE CONTROL
Jonathan S. Litt and Ira C. Smith (Westlake High School, OH.) Aug. 1991 19 p
(DA Proj. 1L1-61102-AH-45)
(NASA-TM-104419; E-6253; NAS 1.15:104419; AVSCOM-TM-90-C-011) Avail: NTIS HC/MF A03 CSCL 09B

Tuning maps are an aid in the controller tuning process because they provide a convenient way for the plant operator to determine the consequences of adjusting different controller parameters. In this application the maps provide a graphical representation of the effect of varying the gains in the state feedback matrix on startup and load disturbance transients for a three capacity process. Nominally, the three tank system, represented in diagonal form, has a Proportional-Integral control on each loop. Cross coupling is then introduced between the loops by using non-zero off-diagonal proportional parameters. Changes in transient behavior due to setpoint and load changes are examined by varying the gains of the cross coupling terms. Author

N91-31877 Washington Univ., Seattle.
NEURAL NETWORK BASED MODEL REFERENCE ADAPTIVE CONTROL Ph.D. Thesis
Douglas Alan Hoskins 1990 258 p
Avail: Univ. Microfilms Order No. DA9117954

The principal aim was to develop a control architecture for the analysis of closed loop stability in the controlled system. The controller described here was applied to the adaptive control of a single degree of freedom system and to the control of the cart/inverted pendulum problem. The addition of a dither signal to the calculated control input was shown to enhance the ability of error back propagation to improve the artificial neural network model online. Dissert. Abstr.

N91-31878# National Aerospace Lab., Amsterdam (Netherlands). Informatics Div.
INVESTIGATION INTO THE APPLICABILITY OF KNOWLEDGE ENGINEERING
P. J. Kat and S. R. v.d.Brink (APT Nederland B.V., Hilversum.) 14 Feb. 1989 26 p In DUTCH; ENGLISH summary Presented at the CAPE 1989, Amsterdam, Netherlands, May 1989
(NLR-TP-89031-U; ETN-91-99637) Avail: NTIS HC/MF A03

The feasibility of knowledge engineering technology is assessed, with relation to a number of knowledge based systems. Use was made of the development environment of knowledge based systems shell NEXT (NLR engineering X-pert system Toolkit). NEXT consists of a knowledge editing, and a knowledge validation and a consultation subsystems. These subsystems communicate via a knowledge base which uses a knowledge representation method. This method consists of object descriptions, production rules, and program components. There exists no generally applicable development environment for knowledge systems. The applicability of knowledge technology depends on the application domain and can be industry specific. ESA

N91-31879*# National Aeronautics and Space Administration. Langley Research Center, Hampton, VA.
KINEMATICS OF THE SIX-DEGREE-OF-FREEDOM FORCE-REFLECTING KRAFT MASTER
Robert L. Williams, II Jul. 1991 24 p
(NASA-TM-104124; NAS 1.15:104124) Avail: NTIS HC/MF A03 CSCL 09B

Presented here are kinematic equations for a six degree of freedom force-reflecting hand controller. The forward kinematics solution is developed and shown in simplified form. The Jacobian matrix, which uses terms from the forward kinematics solution, is derived. Both of these kinematic solutions require joint angle inputs. A calibration method is presented to determine the hand controller joint angles given the respective potentiometer readings. The kinematic relationship describing the mechanical coupling between the hand and controller shoulder and elbow joints is given. These kinematic equations may be used in an algorithm to control the hand controller as a telerobotic system component. The purpose of the hand controller is two-fold: operator commands to the telerobotic system are entered using the hand controller, and contact forces and moments from the task are reflected to the operator via the hand controller. Author

N91-31880# Nijmegen Univ. (Netherlands). Dept. of Informatics.
INVENTORY AND FUNCTIONAL PROTOTYPES OF NEURAL NETWORKS
L. M. W. J. Rutten, P. W. M. Koopman, M. C. J. D. vanEekelen, and M. J. Plasmeijer Oct. 1990 49 p
(TR-90-15; ETN-91-99584) Avail: NTIS HC/MF A03

An inventory of some well known neural network models is presented. The learning categories of each model are indicated. Informal and formal descriptions are given for each model. The formal descriptions are written in the purely functional programming language MIRANDA. As a consequence, these formal descriptions are also prototype implementations. A small pattern recognition or optimization task is expressed in each model. Neural model descriptions written in MIRANDA are short and readable. They

bear quite a large resemblance with the original network specifications, written in mathematical language. Usually, translating an original specification to MIRANDA is a simple task. While translating specifications, a number of network similarities emerge. The functions associated with these similarities can be shared between the descriptions. This leads to unusually short descriptions, each clearly exhibiting a network's particular characteristics.
ESA

N91-31881# Universiteit Twente, Enschede (Netherlands). Faculty of Applied Mathematics.
CLASSES OF FEEDFORWARD NEURAL NETWORKS AND THEIR CIRCUIT COMPLEXITY
John Shawe-Taylor, Martin Anthony (London Univ., England), and Walter Kern 13 Dec. 1990 16 p
(MEMO-920; ISSN-0169-2690; ETN-91-99722) Avail: NTIS HC/MF A03

Classes of neural networks with specified fan in accuracy of computation and depth are introduced. These classes are shown to fit into a well studied hierarchy of boolean circuits classes. The neural network class introduced has two significant limitations. The number of bits used to represent the real numbers involved is one limitation. Fan into the nodes is the second limitation. The limitation on the fan in is sublinear, but significantly larger than logarithmic. This appears to be a critical limitation on the computational power of the network.
ESA

N91-31882# Laboratoire d'Automatique et d'Analyse des Systemes, Toulouse (France).
PATH PLANNING FOR NON-HOLONOMIC MOBILE ROBOTS Ph.D. Thesis - Toulouse Univ.
Michel Taix 1991 132 p In FRENCH; ENGLISH summary
(LAAS-91135; ETN-91-99749) Avail: NTIS HC/MF A07

The kinematic constraint which makes it such that the direction of robot motion is always tangent to the trajectory is taken into account in path planning for a car like robot. This constraint is called a nonholonomic constraint. A solution is found for the nonholonomic system if a collision free trajectory without contact exists. Particular curves which give shortest paths for a point with a curvature of bounded radios are presented. A topological property that allows such curves to be used in building a feasible trajectory for a car like robot from any holonomic trajectory without contact and collision is proved. The general algorithm requires a holonomic motion planner. The iterative non holonomic motion planner is described. An obstacle avoidance method which takes the kinematic constraints of the robot and sensing information into account is presented.
ESA

N91-31883# Ecole Centrale de Lyon (France).
SMALL TIME STEP ADAPTIVE CONTROL: THEORY AND APPLICATION TO AN ELECTRIC FURNACE Ph.D. Thesis [COMMANDE ADAPTATIVE A PETIT PAS DE TEMPS: THEORIE ET APPLICATION SUR UN FOUR ELECTRIQUE]
Marie-Agnes Garnero 1990 301 p In FRENCH
(ECL-90-17; ETN-91-99921) Avail: NTIS HC/MF A14

Process adaptive control is studied with the focus on system identification. Simple control laws of the pole placement type can be used, assuming a robust estimation of process model parameters. Standard estimation algorithms such as least squares recursion are used. A stability study of adaptive control schemes is carried out. The results of the methods are applied to a laboratory furnace.
ESA

N91-31884 Politecnico di Milano (Italy). Dipt. di Elettronica.
THE PROBLEM OF NETWORK MANAGEMENT: AN APPROACH USING AI TECHNIQUES
L. Favalli 1990 23 p
(Rept-90-072; ETN-91-99927) Avail: Politecnico di Milano, Piazza Leonardo da Vinci 32, 20133 Milan, Italy

The number of problems that may occur in communication networks is growing with their size and complexity. Many of these problems have also special characteristics which make tham hard to detect. It may happen that symptoms of an upcoming problem are hidden by other factors or by the overwhelming amount of information going around. The use of expert systems in support of a network manager is seen as a promising approach to troubleshooting, and several prototypes are being developed by different research labs and companies. A system called DIXIE which uses artificial intelligence techniques to monitor and intelligently report on the status of a DECNET environment is introduced.
ESA

N91-31885* National Aeronautics and Space Administration. Pasadena Office, CA.
SYNCHRONIZED COMPUTATIONAL ARCHITECTURE FOR GENERALIZED BILATERAL CONTROL OF ROBOT ARMS Patent
Zoltan F. Szakaly, inventor (to NASA) (Jet Propulsion Lab., California Inst. of Tech., Pasadena.) 6 Aug. 1991 19 p Filed 28 Oct. 1988 Continuation-in-part of abandoned US-Patent-Appl-SN-172105, filed 23 Mar. 1988
(NASA-Case-NPO-17401-1-CU; US-Patent-5,038,089; US-Patent-Appl-SN-264326; US-Patent-Appl-SN-172105; US-Patent-Class-318-568.11; US-Patent-Class-318-573; US-Patent-Class-364-513; Int-Patent-Class-G05B-19/24; Int-Patent-Class-G06F-15/46) Avail: US Patent and Trademark Office CSCL 09B

A master six degree of freedom Force Reflecting Hand Controller (FRHC) is available at a master site where a received image displays, in essentially real time, a remote robotic manipulator which is being controlled in the corresponding six degree freedom by command signals which are transmitted to the remote site in accordance with the movement of the FRHC at the master site. Software is user-initiated at the master site in order to establish the basic system conditions, and then a physical movement of the FRHC in Cartesean space is reflected at the master site by six absolute numbers that are sensed, translated and computed as a difference signal relative to the earlier position. The change in position is then transmitted in that differential signal form over a high speed synchronized bilateral communication channel which simultaneously returns robot-sensed response information to the master site as forces applied to the FRHC so that the FRHC reflects the feel of what is taking place at the remote site. A system wide clock rate is selected at a sufficiently high rate that the operator at the master site experiences the Force Reflecting operation in real time.
Official Gazette of the U.S. Patent and Trademark Office

N91-31886# Los Alamos National Lab., NM.
AN APPLICATION OF NEURAL NETWORKS TO PROCESS AND MATERIALS CONTROL
J. A. Howell and R. Whiteson 1991 12 p Presented at the 32nd Institute of Nuclear Materials Management (INMM) Annual Meeting, New Orleans, LA, 28-31 Jul. 1991
(Contract W-7405-eng-36)
(DE91-016016; LA-UR-91-2386; CONF-910774-62) Avail: NTIS HC/MF A03

Process control consists of two basic elements: a model of the process and knowledge of the desired control algorithm. In some cases the level of the control algorithm is merely supervisory, as in an alarm-reporting or anomaly-detection system. If the model of the process is known, then a set of equations may often be solved explicitly to provide the control algorithm. Otherwise, the model has to be discovered through empirical studies. Neural networks have properties that make them useful in this application. They can learn (make internal models from experience or observations). The problem of anomaly detection in materials control systems fits well into this general control framework. To successfully model a process with a neutral network, a good set of observables must be chosen. These observables must in some sense adequately span the space of representable events, so that a signature metric can be built for normal operation. In this way, a non-normal event, one that does not fit within the signature, can be detected. In this paper, we discuss the issues involved in applying a neural network model to anomaly detection in materials

control systems. These issues include data selection and representation, network architecture, prediction of events, the use of simulated data, and software tools. DOE

64 NUMERICAL ANALYSIS

Includes iteration, difference equations, and numerical approximation.

N91-31887# Universiteit Twente, Enschede (Netherlands). Tele-Informatics and Open Systems Group.
ON THE EXPRESSIVENESS OF EQUATIONAL TYPE LOGIC
Vincenzo Manca, Antonino Salibra (Pisa Univ., Italy), and Giuseppe Scollo Mar. 1991 18 p Repr. from the Institute of Mathematics and its Apstry Session, Sapporo, Japan, 22-27 May 1988, M.S. Thesis Presented at IMA Conference on the Unified Computation Laboratory, Stirling, Scotland, 3-6 Jul. 1990 Revised
(Memo-INF-90-39-Rev; TIOS-91/006; ETN-91-99659) Avail: NTIS HC/MF A03

Equational type logic is an extension of (conditional) equational logic, that widens 'equational reasoning' towards 'reasoning with equations and type assignments'. A comparison is made with other extensions of equational logic, such as (conditional) equational order sorted logic, logics of partial algebras, and Horn clausal logic. Translations of these logics into equational type logic are formulated, that endow these logics with sound and complete derivation systems. The study of equational type logic as a formal system for category theory is proposed as a topic for further investigation. ESA

N91-31888*# Institute for Computer Applications in Science and Engineering, Hampton, VA.
A DYNAMICALLY ADAPTIVE MULTIGRID ALGORITHM FOR THE INCOMPRESSIBLE NAVIER-STOKES EQUATIONS: VALIDATION AND MODEL PROBLEMS Final Report
C. P. Thompson, G. K. Leaf (Argonne National Lab., IL.), and J. VanRosendale Jun. 1991 33 p Submitted for publication
(Contracts NAS1-18605; W-31-109-eng-38)
(NASA-CR-187595; NAS 1.26:187595; ICASE-91-36) Avail: NTIS HC/MF A03 CSCL 12A

An algorithm is described for the solution of the laminar, incompressible Navier-Stokes equations. The basic algorithm is a multigrid based on a robust, box-based smoothing step. Its most important feature is the incorporation of automatic, dynamic mesh refinement. This algorithm supports generalized simple domains. The program is based on a standard staggered-grid formulation of the Navier-Stokes equations for robustness and efficiency. Special grid transfer operators were introduced at grid interfaces in the multigrid algorithm to ensure discrete mass conservation. Results are presented for three models: the driven-cavity, a backward-facing step, and a sudden expansion/contraction. Author

N91-31889*# Institute for Computer Applications in Science and Engineering, Hampton, VA.
A COMPARISON OF TIME DOMAIN BOUNDARY CONDITIONS FOR ACOUSTIC WAVES IN WAVE GUIDES Final Report
H. T. Banks, G. Propst, and R. J. Silcox (National Aeronautics and Space Administration. Langley Research Center, Hampton, VA.) Aug. 1991 26 p Submitted for publication
(Contract NAS1-18605; AF-AFOSR-0091-90)
(NASA-CR-187618; NAS 1.26:187618; ICASE-91-27) Avail: NTIS HC/MF A03 CSCL 12A

Researchers consider several types of boundary conditions in the context of time domain models for acoustic waves. Experiments with four different duct terminations (hard wall, free radiation, foam, and wedge) were carried out in a wave duct from which reflection coefficients over a wide frequency range were measured. These reflection coefficients were used to estimate parameters in the time domain boundary conditions. A comparison of the relative merits of the models in describing the data is presented. Boundary conditions which yield a good fit of the model to the experimental data were found for all duct terminations except the wedge. Author

N91-31890*# McDonnell-Douglas Space Systems Co., Houston, TX.
ON THE OPTIMAL USE OF FICTITIOUS TIME IN VARIATION OF PARAMETERS METHODS WITH APPLICATION TO BG14
Robert G. Gottlieb Jul. 1991 25 p
(Contract NAS9-17885)
(NASA-CR-185650; NAS 1.26:185650) Avail: NTIS HC/MF A03 CSCL 12A

The optimal way to use fictitious time in variation of parameter methods is presented. Setting fictitious time to zero at the end of each step is shown to cure the instability associated with some types of problems. Only some parameters are reinitialized, thereby retaining redundant information. Author

N91-31891# Amsterdam Univ. (Netherlands). Dept. of Mathematics and Computer Science.
WEAK EQUIVALENCE
Sieger vanDenneheuvel and Karen Kwast Mar. 1991 17 p
(ITLI-CT-91-04; ISSN-0924-8374; ETN-91-99574) Avail: NTIS HC/MF A03

A generalization of equivalence between constraint sets, called 'weak equivalence' is described. This equivalence relation takes into account that not all variables have the same function in a constraint set and therefore distinguishes between 'restriction variables' and 'intermediate variables'. The properties of weak equivalence and its underlying notion of weak implication with an axiomatic approach are explore and a complete set of axioms for weak implication is presented. As an application of the axiomatization, a general tool for constraint set simplification is derived. Two constraint solving strategies are described in terms of weak equivalence. The notion of weak equivalence is compared with equivalence of substitution with respect to a set of variables as used in unification theory. A detailed proof of the soundness of the axioms inferred for weak implication is given. ESA

N91-31892# Groningen Rijksuniv. (Netherlands). Dept. of Mathematics.
BIFURCATIONS OF PARAMETRICALLY FORCED OSCILLATORS
Henk Broer 1990 8 p
(W-9007; ETN-91-99576) Avail: NTIS HC/MF A02

A parametrically forced oscillator, i.e. an oscillator with periodically varying coefficients, near resonance, is addressed. There exists a vast amount of literature on this subject, especially on the linear case which involves differential equations of Mathieu type. The nonlinear problem, localized near a central equilibrium solution of the free oscillator, is addressed. In particular, the branching off of certain subharmonic periodic solutions is studied, and more general bifurcational aspects of this. . ESA

N91-31893# Groningen Rijksuniv. (Netherlands). Dept. of Mathematics and Computing Science.
AN EXTENSION OF THE POTENTIAL METHOD TO HIGHER-ORDER BLENDINGS
Menno T. Kosters 1991 14 p Presented at the ACM Conference on Solid Modelling Foundations and CAD/CAM, Austin, TX, 1991
(CS-9103; ETN-91-99581) Avail: NTIS HC/MF A03

The problem of blending d hyperplanes in d dimensional space meeting at a single point (a so called corner), where the blending hypersurfaces are implicity defined, is considered. In the case of C sup 1 blendings, a solution to this problem is known which constructs blendings consisting of piecewise quadric hypersurfaces. The same problem for the case of c sup m blendings (m greater than or equal to 1) is considered. The following result is obtained: for every corner it is possible to construct a one parameter family of C sup m blendings using patches of degree (2 sup d - 1) m only. This means that for a given corner the degree increases only linearly with m. The constant of proportionality 2 sup (d - 1) increases very rapidly with d, but in practical applications in

computer aided geometric design d is usually not higher than 5 or 6, which means that the construction probably is of more than only theoretical interest. The construction relies heavily on some concepts from multilinear algebra, in particular polarizations and tensors, which have proved to be useful in other areas of computer aided geometric design also. ESA

N91-31894# Groningen Rijksuniv. (Netherlands). Dept. of Mathematics and Computing Science.
ON A THEOREM OF MACMAHON
Menno T. Kosters Jan. 1991 13 p
(CS-9104; ETN-91-99582) Avail: NTIS HC/MF A03

A simple proof of MacMahon's theorem that the number of permutations of n elements having k equals the number of permutations of n elements having k inversions is given. The proof relies on a construction of a so called index table for a permutation, a construction similar to that of the well knwon inversion table of a permutation. ESA

N91-31895# Nijmegen Univ. (Netherlands). Dept. of Informatics.
A FORMAL POWER SERIES EQUATION FROM FORMULA COMPLEXITY THEORY
D. C. vanLeijenhorst Dec. 1990 6 p
(TR-90-25; ETN-91-99587) Avail: NTIS HC/MF A02

An explicit solution of a certain type of functional equation in the field of formal Laurent series is given. An application to a recursion from Boolean complexity theory is made. ESA

N91-31896# Utrecht State Univ. (Netherlands). Dept. of Computer Science.
LONGEST SEGMENT PROBLEMS
H. Zantema Aug. 1990 41 p
(RUU-CS-90-28; ISSN-0924-3275; ETN-91-99592) Avail: NTIS HC/MF A03

The following problem is considered: given a predicate p on strings, determine the longest segment of a given string that satisfies p. An investigation of algorithms solving this problem for various predicates is performed. The predicates considered are expressed in simple functions like the size, the minimum, the maximum, the leftmost and the rightmost element of the segment. The algorithms are linear in the length of the string. ESA

N91-31897# Utrecht State Univ. (Netherlands). Dept. of Computer Science.
ON DISJOINT CYCLES
Hans L. Bodlaender Aug. 1990 14 p
(Contract EC-3075)
(RUU-CS-90-29; ISSN-0924-3275; ETN-91-99593) Avail: NTIS HC/MF A03

It is shown, that for each constant k is greater than equal to 1, the following problems can be solved in O(n) time: given a graph G, determine whether G has K vertex disjoint cycles, determine whether G has k edge disjoint cycles, determine whether G has a feedback vertex set of size less than or equal to k. Also, every class G, that is closed under minor taking, or that is closed under immersion taking, and that does not contain the graph formed by taking the disjoint union of k copies of K(3), has an O(n) membership test algorithm. ESA

N91-31898# Utrecht State Univ. (Netherlands). Dept. of Computer Science.
COVERING A SET OF POINTS WITH FIXED SIZE HYPERSQUARES AND RELATED PROBLEMS
Teofilo F. Gonzalez (California Univ., Santa Barbara.) Oct. 1990 20 p
(RUU-CS-90-32; ISSN-0924-3275; ETN-91-99596) Avail: NTIS HC/MF A03

Let the set P p1, p2, ...pn be a set of points in d space. The problem of covering with the minimum number of fixed size orthogonal hypersquares (CS(d) for short) all points in P are studied. An improved polynomial time approximation scheme and fast algorithm that generates probably good solutions to these problems quickly is presented. A variation of the CS(d) problem is the CR(d), covering by fixed size orthogonal hyperrectangles, where the covering of the points is by hyperrectangles with dimensions D1, D2,..., Dd instead of hypersquares of size D. Another variation is the CD(d) problem in which the set of points with hyperdiscs of diamater D is covered. The algorithms can also be generalized to handle these two problems. ESA

N91-31899# Utrecht State Univ. (Netherlands). Dept. of Computer Science.
HIDDEN SURFACE REMOVAL FOR C-ORIENTED POLYHEDRA
Mark deBerg and Mark H. Overmars Nov. 1990 24 p Sponsored in part by Commission of the European Communities and Netherlands Organization for Applied Scientific Research TNO
(RUU-CS-90-33; ISSN-0924-3275; ETN-91-99597) Avail: NTIS HC/MF A03

A new, efficient, output sensitive method for computing the visibility map of a set of c oriented polyhedra (polyhedra with their faces and edges in c orientations, for some constant c) as seen from a given viewpoint is presented. For non intersecting polyhedra with n edges in total, the algorithms runs in time O((n + k) log n), where k is the complexity of the visibility map. The method can handle cyclic overlap of the polyedra and perspective views without any problem. The method can even deal with intersecting polyhedra. In the latter case the algorithm runs in time O((n + k) squared logarithm of n). ESA

N91-31900# Utrecht State Univ. (Netherlands). Dept. of Computer Science.
COMPUTING MINIMUM LENGTH PATHS OF A GIVEN HOMOTOPY CLASS
John Hershberger and Jack Snoeyink (British Columbia Univ., Vancouver.) 21 Dec. 1990 31 p Sponsored by Commission of the European Communities and Digital Equipment Corp.
(RUU-CS-90-37; ISSN-0924-3275; ETN-91-99601) Avail: NTIS HC/MF A03

The universal covering space of a surface is used to generalize previous results on computing paths in a simple polygon. Optimizing paths among obstacles in the plane are looked at under the Euclidean and link metrics and polygonal convex distance functions. The universal cover is a unifying framework that reveals connections between minimum paths under these three distance functions, as well as yielding simpler linear time algorithms for shortest path trees and minimum link paths in simple polygons. ESA

N91-31901# Utrecht State Univ. (Netherlands). Dept. of Computer Science.
A NOTE ON SEMI-ADJUNCTIONS
R. Hoofman 17 Dec. 1990 14 p
(RUU-CS-90-41; ISSN-0924-3275; ETN-91-99605) Avail: NTIS HC/MF A03

Two methods to generalize categorical notions involving functors to semi-functors are considered. It turns out that the two methods give in general the same results. In particular, the notion of semi-adjunction is studied. Semi-adjunctions in our sense prove to be exactly the normal semi-adjunctions of Hayashi. ESA

N91-31902# Utrecht State Univ. (Netherlands). Dept. of Computer Science.
THE LINEAR DECOMPOSITION OF DELTA-SQUARED MODELS
R. Hoofman 7 Feb. 1991 18 p
(RUU-CS-91-04; ISSN-0924-3275; ETN-91-99611) Avail: NTIS HC/MF A03

It is shown that the category of sets and relations gives rise to a model of weak second order linear type theory. To describe the structure of this model, categorical notions based on the concept of semi functor are used. It is easy to transform the model into a lambda squared algebra, i.e., a categorical model of the non extensional lambda squared calculus. A slight extension of this lambda squared algebra yields a 'non stable' version of

the 'coherence space model' of the lambda squared calculus. ESA

N91-31903# Utrecht State Univ. (Netherlands). Dept. of Computer Science.

UNION-COPY STRUCTURES AND DYNAMIC SEGMENT TREES

Marc J. vanKreveld and Mark H. Overmars 13 Feb. 1991 22 p Sponsored in part by Commission of the European Communities
(RUU-CS-91-05; ISSN-0924-3275; ETN-91-99612) Avail: NTIS HC/MF A03

A new data structure, the union copy structure, is introduced, which generalizes the well known union find structure. Besides the usual union and find operations, the new structure also supports a copy operation, that generates a duplicate of a given set. The structure can enumerate a given set, find all sets that contain a given element, insert and delete elements, etc. All these operations can be performed very efficiently. The structure can be tuned as to obtain different tradeoffs in the efficiency of the different operations. As an application of the union copy structure, a dynamic version of the segment tree is introduced. Contrary to the classical semi dynamic segment trees, the dynamic segment tree is not restricted to a fixed universe, from which the endpoints of the segments must be chosen. The tree allows for insertions, splits and concatenations in O(log n) time each. Deletions can be performed in slightly more time. ESA

N91-31904# Universiteit Twente, Enschede (Netherlands). Faculty of Applied Mathematics.

FITTING SCATTERED DATA ON SPHERELIKE SURFACES USING TENSOR PRODUCTS OF TRIGONOMETRIC AND POLYNOMIAL SPLINES

Larry L. Schumaker (Vanderbilt Univ., Nashville, TN.) and Cornelis Traas Nov. 1990 18 p Sponsored in part by Alexander von Humboldt Foundation
(Grant NSF DMS-89-02331)
(MEMO-909; ISSN-0169-2690; ETN-91-99711) Avail: NTIS HC/MF A03

A method is presented for fitting a function defined on a general smooth spherelike surface S, given measurements on the function at a set of scattered points lying on S. The approximating surface is constructed by mapping the surface onto a rectangle, and using a tensor product of polynomial splines with periodic trigonometric splines. The use of trigonometric splines allows a convenient solution of the problem of assuring that the resulting surface is continuous and has continuous tangent planes at all points on S. Two alternative algorithms for computing the coefficients of the tensor fit are presented; one based on global least squares, and the other on the use of local quasi-interpolators. The approximation order of the method is established, and the numerical performance of the two algorithms is compared. ESA

N91-31905# Universiteit Twente, Enschede (Netherlands). Dept. of Applied Mathematics.

A NOTE ON 'THE MATCHING POLYNOMIAL OF A POLYGRAPH'

H. J. Broersma and Li Xueliang (Xinjiang Univ., Urumqi, China) Dec. 1990 12 p
(MEMO-910; ISSN-0169-2690; ETN-91-99712) Avail: NTIS HC/MF A03

Two phenomena mentioned in the concluding remarks on 'the matching polynomials of a polygraph' by Babic et al are explained. The following results are obtained: although three matrices for given polygraphs defined in the above article in general have different orders, they determine the same recurrence relations for the matching polynomial of these polygraphs; and under certain symmetry conditions, the order of the recurrence relations can be reduced by almost a half. The method can be used in the computation of Hosoya's index which in turn can be used in the fields of physical chemistry, statistical physics, and thermodynamics. ESA

N91-31906# Universiteit Twente, Enschede (Netherlands). Faculty of Applied Mathematics.

MULTIGRID AND RUNGE-KUTTA TIME STEPPING APPLIED TO THE UNIFORMLY NON-OSCILLATORY SCHEME FOR CONSERVATION LAWS

J. W. vanderBurg, J. G. M. Kuerten, and P. J. Zandbergen 20 Dec. 1990 36 p
(MEMO-911; ISSN-0169-2690; ETN-91-99713) Avail: NTIS HC/MF A03

It is known that Harten's uniformly nonoscillatory scheme is a second order accurate scheme for discretizing conservation laws. It is shown that a multigrid technique and Runge-Kutta time stepping with frozen dissipation applied to this scheme lead to a better convergence to the steady state solution of a first order conservation law when the same techniques are applied to Jameson's scheme. It is concluded that the first order Roe scheme performs best in combination with multigrid and Runge-Kutta time stepping. Extension of Harten's dissipation model to multidimensional calculations is considered more efficient and accurate than Jameson's dissipation model if multigrid with Runge-Kutta timestepping and frozen dissipation is applied. ESA

N91-31907# Universiteit Twente, Enschede (Netherlands). Dept. of Applied Mathematics.

EXTENSIVE COVERINGS AND EXACT CORE BOUNDS

O. N. Bondareva (Leningrad State Univ., USSR) and T. S. H. Driessen Dec. 1990 21 p
(MEMO-915; ISSN-0169-2690; ETN-91-99717) Avail: NTIS HC/MF A03

The exact bounds for the nonempty core of a cooperative game in characteristic function form are determined. The exact lower and upper core bounds are determined in terms of the external excesses with respect to reduced upper and lower coverings. An efficient compromise between the upper and lower extremal excess vectors or in the other case, the upper and lower weighted average excess vectors is constructed. Specific relationships of such an efficient compromise with the Shapley value and the pi value are treated. ESA

N91-31908# Universiteit Twente, Enschede (Netherlands). Dept. of Applied Mathematics.

CYCLES CONTAINING MANY VERTICES OF LARGE DEGREE

H. J. Veldman Dec. 1990 13 p
(MEMO-916; ISSN-0169-2690; ETN-91-99718) Avail: NTIS HC/MF A03

Let G be a 2 connected graph of order n, r a real number and V(sub r) = v member of the set V(G) over d(v) greater than or equal to r. It is shown that G contains a cycle missing at most max (0, n - 2r) vertices V(sub r), yielding a common generalization of a result of Dirac and one of Shi Ronghua. A stronger conclusion holds if r is greater or less than 1/3(n+2): G contains a cycle C such that either V(C) is part of or equal to the set V(sub r). This theorem extends a result of Haggskvist and Jackson and is proved by first showing that if r is greater than or equal to 1/3(n+2), then G contains a cycle C. ESA

N91-31909# Universiteit Twente, Enschede (Netherlands). Dept. of Applied Mathematics.

PARAMETER IDENTIFICATION FOR TWO-POINT BOUNDARY VALUE PROCESSES

Shin Ichi Aihara (Science Univ. of Tokyo, Japan) and Arunabha Bagchi 18 Dec. 1990 19 p
(MEMO-917; ISSN-0169-2690; ETN-91-99719) Avail: NTIS HC/MF A03

The problem of identifying unknown parameters in Two Point Boundary Value Processes (TPBVP) is studied. Using the explicit form of the likelihhod function, the consistency property of the maximum likelihood estimate is analyzed through a number of independent experiments. The remaining problem for parameter identification for TPBVP is that of deriving the practical algorithm for generating the optimal Maximum Likelihood Estimates (MLE). It is possible to show the explicit form of the necessary conditions

for the optimal MLE and from these construct an algorithm for generating the optimal MLE. ESA

N91-31910# Universiteit Twente, Enschede (Netherlands). Faculty of Applied Mathematics.
LEARNING CONVEX BODIES UNDER UNIFORM DISTRIBUTION
Walter Kern Dec. 1990 12 p
(MEMO-918; ISSN-0169-2690; ETN-91-99720) Avail: NTIS HC/MF A03

It is proved that the class of convex bodies contained in a fixed (prescribed) bounded region is PAC learnable, if the positive examples are drawn uniform. Distributions are D(+) on the target concept (the distribution d(-) on the negative examples may be arbitrary). The results extend previous works by E. Baum. ESA

N91-31911*# National Aeronautics and Space Administration. Lewis Research Center, Cleveland, OH.
LEAST-SQUARES SOLUTION OF INCOMPRESSIBLE NAVIER-STOKES EQUATIONS WITH THE P-VERSION OF FINITE ELEMENTS
Bo-Nan Jiang and Vijay Sonnad (International Business Machines Corp., Austin, TX.) Sep. 1991 15 p
(NASA Order C-99066-G)
(NASA-TM-105203; ICOMP-91-14; E-6506; NAS 1.15:105203)
Avail: NTIS HC/MF A03 CSCL 12A

A p-version of the least squares finite element method, based on the velocity-pressure-vorticity formulation, is developed for solving steady state incompressible viscous flow problems. The resulting system of symmetric and positive definite linear equations can be solved satisfactorily with the conjugate gradient method. In conjunction with the use of rapid operator application which avoids the formation of either element of global matrices, it is possible to achieve a highly compact and efficient solution scheme for the incompressible Navier-Stokes equations. Numerical results are presented for two-dimensional flow over a backward facing step. The effectiveness of simple outflow boundary conditions is also demonstrated. Author

N91-31912# Stanford Univ., CA. Dept. of Computer Science.
MATHEMATICAL THEORY OF COMPUTATION Final Report, 30 Aug. 1988 - 28 Sep. 1990
John McCarthy Aug. 1991 8 p
(Contract N00039-84-C-0211)
(AD-A239419) Avail: NTIS HC/MF A02 CSCL 12/5

This project was concerned with the development of correct and reusable software through the use of higher order abstractions (function, control, assignment, process) and reflection. A semantic framework for these notions will be the basis of an experimental system for manipulating and reasoning about programs. The goals were the development of logical formalisms for reasoning about programs that use abstractions and reflection, and the application of these theoretical results to selected software problems. Example applications include (1) clarification of existing programming paradigms, (2) analysis of existing and proposed languages used in the DARPA community for specifying, writing, and transforming programs, and (3) development and implementation of tools for computer aided reasoning about and operating on programs. The accomplishments of this project fit into four categories: (1) logics for reasoning about function and control abstractions; (2) logics for reasoning about data mutation; (3) logics for reasoning about function and control abstractions in the presence of mutable data; and (4) applying methodology for reasoning about programs to the mechanical verification of hardware. GRA

N91-31913# Army Armament Research, Development and Engineering Center, Watervliet, NY.
AN EXTENSION OF MESH EQUIDISTRIBUTION TO TIME-DEPENDENT PARTIAL DIFFERENTIAL EQUATIONS Final Report
J. M. Coyle Jul. 1991 17 p
(AD-A239579; ARCCB-TR-91024) Avail: NTIS HC/MF A03 CSCL 12/1

Mesh equidistribution for static approximation problems is extended to a domain that admits time dependency. Instead of some quantity being equidistributed over a static mesh, the change in this quantity is equidistributed over a dynamic, moving mesh. Applications are for utilization in numerical methods to solve time-dependent partial differential equations. This mesh moving scheme is incorporated into a finite element code which already refines adaptively. Comparisons are made for stationary and moving meshes. GRA

N91-31914# Maryland Univ., College Park. Inst. for Physical Science and Technology.
LOCKING EFFECTS IN THE FINITE ELEMENT APPROXIMATION OF ELASTICITY PROBLEMS Final Report
Ivo Babuska and Manil Suri Dec. 1990 44 p
(AD-A239645; BN-1119; TR90-56) Avail: NTIS HC/MF A03 CSCL 12/1

The phenomenon is analyzed of Poisson Locking. This is said to occur when the approximations obtained using the finite element method for elasticity problems deteriorate as a result of the Poisson ratio being close to 0.5. Using the general theory developed in an earlier paper on locking, precise mathematical definitions are given of locking and robustness and some abstract theorems are applied to analyze the locking of various h, p and h-p finite element schemes. In particular, two types of rectangular elements are analyzed for the h-version. Extensions to the 3-D case are also discussed. GRA

N91-31915# Maryland Univ., College Park. Inst. for Physical Science and Technology.
ANALYSIS OF THE EFFICIENCY OF AN A-POSTERIORI ERROR ESTIMATOR FOR LINEAR TRIANGULAR FINITE ELEMENTS Final Report
Ivo Babuska, Ricardo Duran, and Rodolfo Rodriguez Jun. 1991 25 p
(Contract N00014-90-J-1030)
(AD-A239647; BN-1125) Avail: NTIS HC/MF A03 CSCL 12/1

The problem is addressed of determining upper and lower bounds for the effectivity index on the a-posteriori estimate of the error in the finite element method. These bounds are given explicitly for a certain concrete estimator for linear elements and unstructured triangular meshes. They depend strongly on the geometry of the triangles and (relatively weakly) on the smoothness of the solution. An example shows that the bounds are not over pessimistic. GRA

65 STATISTICS AND PROBABILITY

Includes data sampling and smoothing; Monte Carlo method; and stochastic processes.

N91-31916# Groningen Rijksuniv. (Netherlands). Dept. of Mathematics.
STRONG APPROXIMATION ON LOG DENSE SETS
I. Berkes and H. Dehling 1991 24 p
(Grant HNFSR-1808)
(W-9101; ETN-91-99578) Avail: NTIS HC/MF A03

Extensions of classical probability limit theorems involving log average and log density are considered. The purpose is to extend Fisher's approximation theorem to i.i.d. sequences the set X(n) with EX (upper bound 2, lower bound 1) + infinity belonging to the domain of attraction of the normal law or of an alpha stable law, 0 less than alpha less than 2. As a byproduct of the proof, the analog of the a.s. central limit theorem for a large class of independent sequences is obtained and necessary and sufficient criteria for the a.s. central limit theorem and the log density version of the strong law of large numbers are given. ESA

N91-31917# Utrecht State Univ. (Netherlands). Dept. of Computer Science.
A PRAGMATICAL VIEW ON THE CERTAINTY FACTOR MODEL

Linda vanderGaag Dec. 1990 10 p
(RUU-CS-90-42; ISSN-0924-3275; ETN-91-99606) Avail: NTIS HC/MF A02

Since its introduction in the 1970s, the certainty factor model has enjoyed widespread use in rule based expert systems. Many present day, commercially available expert system shells offer the model for modeling and reasoning with uncertainty information. Among researchers in the field of plausible reasoning, it is widely known that the model is mathematically incorrect: many have investigated the probabilistic foundation of the model. The detailed results of these theoretical analyses of the model, however, are relatively unknown to engineers interested in applying or developing an expert system. A pragmatical look at the theoretical results is taken and they are used to formulate some guidelines for the representation of expert knowledge in production rules which, if adhered to, allow the certainty factor model to behave satisfactorily from a probabilistic point of view. ESA

N91-31918# Leiden Univ. (Netherlands). Div. of Applied Mathematics.
ON THE RELATION BETWEEN RECURRENCE AND ERGODICITY PROPERTIES IN DENUMERABLE MARKOV DECISION CHAINS
R. Dekker, A. Hordijk, and F. Spieksma 1991 35 p Sponsored in part by Netherlands Organization for Applied Scientific Research, TNO
(TW-91-02; ETN-91-99629) Avail: NTIS HC/MF A03

Two properties of the set of Markov chains induced by the deterministic policies in a Markov decision chain are studied. These properties are called mu uniform geometric ergodicity and mu uniform geometric reccurrence. Mu uniform ergodicity generalizes a quasi compactness condition. It can be interpreted as a strong version of stability, as it implies that the Markov chains generated by the deterministic stationary policies are uniformly stable. Mu uniform geometric recurrence can be shown to be equivalent to the simultaneous Doeblin condition, if mu is bounded. Both properties imply the existence of deterministic sensitive optimal policies. The second Key theorem shows the equivalence of mu uniform geometric ergodicity and weak mu uniform geometric recurrence under appropriate conditions. The first key theorem derives the relation between several of these conditions, which turn out to be equivalent in most cases. It appears that often a slightly stronger condition, mu uniform geometric recurrence, can be verified. This is illustrated by an overview of queueing networks that satisfy our conditions. These include the two centre open Jackson network with controllable server, the K competing queues model, the generalized random walk in N sub o, a symmetric ALOHA-type system, and a coupled processors model. The verification of the mu-uniform geometric recurrence property for these models implies strong stability and the existence of average and sensitive optimal policies. ESA

N91-31919# Stanford Univ., CA. Dept. of Statistics.
BAYES THEOREM FROM A SAMPLING-RESAMPLING PERSPECTIVE
A. F. Smith and A. E. Gelfand 31 Jul. 1991 7 p
(Contract N00014-89-J-1627)
(AD-A239515; TR-445) Avail: NTIS HC/MF A02 CSCL 12/3

Even to the initiated, statistical calculations based on Bayes theorem can be daunting because of the numerical integrations required in all but the simplest applications. Moreover, from a teaching perspective, introductions to Bayesian statistics (if they are given at all) are circumscribed by these apparent calculational difficulties. Here we offer a straightforward sampling-resampling perspective on Bayesian inference, which has both pedagogic appeal and suggests easily implemented calculation strategies. GRA

N91-31920# Stanford Univ., CA. Dept. of Physics.
ON COMBINING INDEPENDENT SIGNIFICANCE TESTS
F. J. OReilly and Michael A. Stephens 24 Jul. 1991 21 p
(Contract N00014-89-J-1627)
(AD-A239660; SU-TR-444) Avail: NTIS HC/MF A03 CSCL 12/3

How to combine the results of k independent tests of significance has long been an important problem in statistics. The problem can arise, for example, in such diverse situations as when tests on the mean survival time after diagnosis of a terminal disease are made on k groups of patients in different hospitals, or when the sets of observations in k cells of an ANOVA table are separately tested for normality. An important feature of such tests is that often the individual sample sizes will be small, so that asymptotic results will not necessarily be valid. It is suggested that they might even be misleading in some situations. GRA

66 SYSTEMS ANALYSIS

Includes mathematical modeling; network analysis; and operations research.

N91-31921# Utrecht State Univ. (Netherlands). Dept. of Computer Science.
FROM GAME TREES TO GAME GRAPHS
W. T. M. Kars Dec. 1990 18 p
(RUU-CS-90-43; ISSN-0924-3275; ETN-91-99607) Avail: NTIS HC/MF A03

The definition of the score of a game tree is extended using the minimax rule to game graphs containing cycles. This is accomplished by taking the limit of a sequence of scores of game trees that in some sense approximate the game graph. It is shown that this score is well defined for all game graphs, and algorithms for its evaluation are given, including one that uses memorization. ESA

67 THEORETICAL MATHEMATICS

Includes topology and number theory.

No abstracts in this category.

70 PHYSICS (GENERAL)

For precision time and time interval (PTTI) see *35 Instrumentation and Photography;* for geophysics, astrophysics or solar physics see *46 Geophysics, 90 Astrophysics,* or *92 Solar Physics.*

No abstracts in this category.

71 ACOUSTICS

Includes sound generation, transmission and attenuation. For noise pollution see *45 Environmental Pollution.*

N91-31922 Defence and Civil Inst. of Environmental Medicine, Downsview (Ontario).
ASSESSING THE EFFICACY OF ACTIVE NOISE REDUCTION
Julia M. Rylands 1990 6 p Presented at the Defence Science Symposium, Ottawa, Ontario, 1990
(CTN-91-60200) Avail: NTIS HC A02

Active noise reduction (ANR) is an electronic technique, based on reverse phase cancellation, for reducing low frequency noise reaching an operators ears. This report discussed the basic concept, its capabilities and some approaches to assessing its efficacy. The technique provides a great enhancement to hearing protection and also enhances signal detection and communications

capabilities. Tests of detectibility of pure tones at frequencies ranging up to 1750 Hz using ANR systems which had maximum noise attenuation between 300 and 600 Hz and masking noise typical of the SeaKing helicopter showed that improvements in detection performance extend up to 1000 Hz. ANR systems also offer improved speech intelligibility in high noise environments by reducing the upward spread of masking and adding speech pre-emphasis. CISTI

N91-31923*# Lockheed Engineering and Sciences Co., Hampton, VA.
USER'S MANUAL FOR THE LANGLEY BOUNDARY LAYER NOISE PROPAGATION PROGRAM (MRS-BLP)
Peter L. Spence Aug. 1991 38 p
(Contract NAS1-19000)
(NASA-CR-187559; NAS 1.26:187559) Avail: NTIS HC/MF A03 CSCL 20A

A computer program, McAninch-Rawls-Spence Boundary Layer Propagation (MRS-BLP), is described. This program models the refractive and scattering effects on acoustic pressure waves propagating through a boundary layer encompassing an aircraft's fuselage. The noise source is assumed known and generated by a propeller. The fuselage is represented by an infinitely long cylinder embedded in a longitudinal flow. By matching a numerical solution inside the boundary layer with an analytical solution outside the boundary layer, the program calculates the acoustic pressure at the surface of the cylinder given the incident field at the top of the boundary layer. The boundary layer flow velocity and sound speed profiles, as well as the boundary layer thickness may be specified by the user. A detailed description of the input parameters and how to execute the program is given. Example executions of MRS-BLP showing results are also included. Author

N91-31924# Office National d'Etudes et de Recherches Aerospatiales, Paris (France). Direction de la Physique Generale.
THREE DIMENSIONAL ACOUSTIC PROPAGATION AT LOW TEMPERATURE ALTITUDE [PROPAGATION ACOUSTIQUE TRIDIMENSIONNELLE A BASSE ALTITUDE]
Y. Dalrieux Apr. 1990 67 p In FRENCH
(Contract DRET-89-001-46)
(ONERA-RT-13/3641-PY; ETN-91-99934) Avail: NTIS HC/MF A04

Different computation methods of submarine propagation are described and the effects of marine currents and thermal variations are analyzed. A beam tracing software is developed to show meteorological and topographical three dimensional effects on aerial propagation. Relief is taken into account in the two dimensional parabolic approximation method. A Fresnel integral is used to validate a medium at rest. The presence of wind causes a tendency for the shaded region created by a slope to disappear but the results can be different according to frequency since the wind causes new interference regions to appear. The three dimensional parabolic equation and an alternate direction method allowing use of the Roach algorithm are described. ESA

N91-31925# Office National d'Etudes et de Recherches Aerospatiales, Paris (France). Direction de la Physique Generale.
USE OF AN ARMA MODEL IN TURBULENT MEDIUM ACOUSTIC PROPAGATION Final Report [UTILISATION D'UN MODELE ARMA DANS LE CADRE DE LA PROPAGATION ACOUSTIQUE EN MILIEU TURBULENT]
P. Malbequi Apr. 1990 25 p In FRENCH
(Contract DRET-89-001-46)
(ONERA-RF-14/3641-PY; ETN-91-99938) Avail: NTIS HC/MF A03

Possibilities offered by the Auto Regressive and Moving Average (ARMA) models in reproducing a gaussian form turbulence spectra are analyzed. Using the MA model, it is quite simple to get an isotropic spectra at fast decrease, but this model requires a relatively high order, which takes quite a major computation time. The AR model gets a satisfactory spectra with a weak order, while the isotropy is not strictly respected. Using the AR model, a computation of problematical medium turbulence is carried out to generate the turbulence field. The result, on the pressure field, agrees well with that where the turbulence spectra is computed by filtering Fourier transformation of a spatial white noise. The suppression of interferences is once again found between the direct and reflected fields, due to turbulence. ESA

N91-31926*# Douglas Aircraft Co., Inc., Long Beach, CA.
FUSELAGE SHELL AND CAVITY RESPONSE MEASUREMENTS ON A DC-9 TEST SECTION Final Report
M. A. Simpson, G. P. Mathur, M. R. Cannon, B. N. Tran, and P. L. Burge Aug. 1991 55 p
(Contract NAS1-18037)
(NASA-CR-187557; NAS 1.26:187557) Avail: NTIS HC/MF A04 CSCL 20A

A series of fuselage shell and cavity response measurements conducted on a DC-9 aircraft test section are described. The objectives of these measurements were to define the shell and cavity model characteristics of the fuselage, understand the structural-acoustic coupling characteristics of the fuselage, and measure the response of the fuselage to different types of acoustic and vibration excitation. The fuselage was excited with several combinations of acoustic and mechanical sources using interior and exterior loudspeakers and shakers, and the response to these inputs was measured with arrays of microphones and accelerometers. The data were analyzed to generate spatial plots of the shell acceleration and cabin acoustic pressure field, and corresponding acceleration and pressure wavenumber maps. Analysis and interpretation of the spatial plots and wavenumber maps provided the required information on modal characteristics, structural-acoustic coupling, and fuselage response. Author

N91-31927*# Douglas Aircraft Co., Inc., Long Beach, CA.
ANALYSIS OF INTERIOR NOISE GROUND AND FLIGHT TEST DATA FOR ADVANCED TURBOPROP AIRCRAFT APPLICATIONS Final Report
M. A. Simpson and B. N. Tran Aug. 1991 66 p
(Contract NAS1-18037)
(NASA-CR-187558; NAS 1.26:187558) Avail: NTIS HC/MF A04 CSCL 20A

Interior noise ground tests conducted on a DC-9 aircraft test section are described. The objectives were to study ground test and analysis techniques for evaluating the effectiveness of interior noise control treatments for advanced turboprop aircraft, and to study the sensitivity of the ground test results to changes in various test conditions. Noise and vibration measurements were conducted under simulated advanced turboprop excitation, for two interior noise control treatment configurations. These ground measurement results were compared with results of earlier UHB (Ultra High Bypass) Demonstrator flight tests with comparable interior treatment configurations. The Demonstrator is an MD-80 test aircraft with the left JT8D engine replaced with a prototype UHB advanced turboprop engine. Author

N91-31928*# Minnesota Univ., Minneapolis. Dept. of Aerospace Engineering and Mechanics.
A PARAMETRIC STUDY OF TRANSONIC BLADE-VORTEX INTERACTION NOISE Final Technical Report, 1 Jul. 1990 - 30 Jun. 1991
A. S. Lyrintzis 30 Jun. 1991 59 p
(Grant NAG6-626)
(NASA-CR-188811; NAS 1.26:188811) Avail: NTIS HC/MF A04 CSCL 20A

Several parameters of transonic blade-vortex interactions (BVI) are being studied and some ideas for noise reduction are introduced and tested using numerical simulation. The model used is the two-dimensional high frequency transonic small disturbance equation with regions of distributed vorticity (VTRAN2 code). The far-field noise signals are obtained by using the Kirchhoff method with extends the numerical 2-D near-field aerodynamic results to the linear acoustic 3-D far-field. The BVI noise mechanisms are explained and the effects of vortex type and strength, and angle of attack are studied. Particularly, airfoil shape modifications which

lead to noise reduction are investigated. The results presented are expected to be helpful for better understanding of the nature of the BVI noise and better blade design. Author

N91-31929# Los Alamos National Lab., NM.
COMPARISON OF NOISE REDUCTION SYSTEMS
S. D. Noel and R. W. Whitaker Jun. 1991 20 p
(Contract W-7405-eng-36)
(DE91-015318; LA-12008-MS) Avail: NTIS HC/MF A03

When using infrasound as a tool for verification, the most important measurement to determine yield has been the peak-to-peak pressure amplitude of the signal. Therefore, there is a need to operate at the most favorable signal-to-noise ratio (SNR) possible. Winds near the ground can degrade the SNR, thereby making accurate signal amplitude measurement difficult. Wind noise reduction techniques were developed to help alleviate this problem; however, a noise reducing system should reduce the noise, and should not introduce distortion of coherent signals. An experiment is described to study system response for a variety of noise reducing configurations to a signal generated by an underground test (UGT) at the Nevada Test Site (NTS). In addition to the signal, background noise reduction is examined through measurements of variance. Sensors using two particular geometries of noise reducing equipment, the spider and the cross appear to deliver the best SNR. Because the spider configuration is easier to deploy, it is now the most commonly used. DOE

72 ATOMIC AND MOLECULAR PHYSICS

Includes atomic structure, electron properties, and molecular spectra.

N91-31930# Wisconsin Univ., Madison. Dept. of Physics.
SEARCHING FOR THE HIGGS IN EP COLLISIONS AT LEP/LHC
G. Grindhammer, D. Haidt, J. Ohnemus, and J. Vermaseren Nov. 1990 20 p Presented at the Large Hadron Collider (LHC) Workshop: Physics and Instrumentation, Aachen (Fed. Republic of Germany, 4-9 Oct. 1990
(Contracts DE-FG05-87ER-40319; DE-AC02-76ER-00881)
(DE91-015701; CONF-9010291-2; MAD/PH-618) Avail: NTIS HC/MF A03

We investigate the possibility to observe an intermediate mass Higgs in ep collisions at LEP/LHC. We find that such a particle can be observed once a reasonable level of flavor identification is available to separate efficiently the b bar-b decay mode of the Higgs from most of the background. DOE

N91-31931# Oak Ridge National Lab., TN.
PARTICLE PRODUCTION THROUGH TWO-PHOTON PROCESSES IN RELATIVISTIC HEAVY-ION COLLIDERS
J.-S. Wu, C. Bottcher, M. R. Strayer, and C. M. Shakin (City Univ. of New York, Brooklyn.) 1991 12 p Presented at the Conference on Computational Quantum Physics, Nashville, TN, 22-25 May 1991
(Contract DE-AC05-84OR-21400)
(DE91-016221; CONF-9105238-2) Avail: NTIS HC/MF A03

Particle production via two-photon processes in relativistic heavy-ion colliders is discussed. We consider the coherent production, including its impact parameter dependence, and incoherent production. Particular attention is given to Higgs boson production in the energy regime of the LHC and the SSC. DOE

N91-31932# Los Alamos National Lab., NM.
OPTICALLY PUMPED POLARIZED ION SOURCES
O. B. vanDyck 1991 7 p Presented at the Conference on the Intersections Between Particle and Nuclear Physics, Tucson, AZ, 23-29 May 1991
(Contract W-7405-eng-36)
(DE91-016086; LA-UR-91-2119; CONF-9105106-24) Avail: NTIS HC/MF A02

Recent development and operating experience of the Optically Pumped Polarized Ion Source (OPPIS) projects at LAMPF and other laboratories is reviewed. DOE

N91-31933# Los Alamos National Lab., NM.
INTRINSIC NEUTRON SOURCE STRENGTHS IN URANIUM SOLUTIONS
R. E. Anderson, A. A. Robba, R. L. Seale, D. A. Rutherford, K. B. Butterfield, and G. S. Brunson 1991 11 p Presented at the International Conference on Nuclear Criticality (ICNC) Safety, Oxford, England, 9-13 Sep. 1991
(Contract W-7405-eng-36)
(DE91-016091; LA-UR-91-2081; CONF-910993-11) Avail: NTIS HC/MF A03

Neutron production rates for 5 pct. enriched uranyl fluoride and 93 pct. uranyl nitrate solutions have been measured using a high efficiency neutron well counter. Measurements were made for both solution types as a function of sample volume. These results were extrapolated to zero sample volume to eliminate sample size effects, such as multiplication and absorption. For the 5 pct. enriched uranyl fluoride solution, a neutron production rate of 0.0414 (+ or -) 0.0041 n/s/ml was measured; for the 93 pct. enriched uranyl nitrate solution, a neutron production rate of 0.0232 (+ or -) 0.0023 n/s/ml was measured. The biggest uncertainty is in measuring the detector efficiency, and further work on this aspect of the experiment is planned. Calculations for the neutron production rates based on measured thick-target (alpha, n) production rates and the known alpha stopping powers are in reasonable agreement with the data for the uranyl nitrate solution, but are in poor agreement with the data for the uranyl fluoride solution. DOE

N91-31934# Northwestern Univ., Evanston, IL. Dept. of Materials Science and Engineering.
ATOMIC STRUCTURES AND COMPOSITIONS OF INTERNAL INTERFACES
D. N. Seidman and K. L. Merkle (Argonne National Lab., IL.) 1991 11 p
(Contract DE-FG02-89ER-45403)
(DE91-016095; DOE/ER-45403/2) Avail: NTIS HC/MF A03

The emphasis during the past year has been on reproducibly obtaining metal/metal oxide interfaces in a number of binary alloy systems that are suitable for combined transmission electron and atom probe field-ion microscopy, as well as analytical electron microscopy. This requires obtaining a high number density (N sub D) (greater than 5 x 10(exp 16)/cu cm) of a small metal oxide precipitates (1 to 20 nm diam) in wire specimens. These requirements are essential, as the primary goal of our initial research to study the chemical compositions of metal/metal oxide interfaces on an atomic scale using the atom-probe technique. The basic approach we are employing is to prepare binary metal alloys, for which the solute species has a greater affinity for oxygen than the solvent, and where the permeability of the oxygen c sub O D sub O is greater than c sub s D sub s for the solute (s) elements. The specific systems presently being investigated are: (1) Pt-4 at. pct. W and Pt-8.5 at. pct. W; (2) Cu-0.1 wt. pct. and Cu-1.3 at. pct. Mg; (3) Cu-2.7 at. pct. Co; (4) Pt-9.15 wt. pct. Co; and (5) Ni-20 wt. pct. Cr. Internal oxide precipitates of MgO and CoO (in Cu(Mg) and Cu(Co) alloys) have been obtained at values of N sub d and precipitate diameter that are suitable for combined transmission electron microscope and atom probe studies. Also results have been obtained which indicate that internal oxides of Cr2O3 in a Ni(Cr) alloy and CoO in a Pt(Co) alloy should be suitable for experimental programs. DOE

N91-31935# Argonne National Lab., IL.
A NEW METHOD TO DO TIME RESOLVED, X RAY DIFFRACTION STUDIES: THE ROTATING CRYSTAL LAUE METHOD
G. S. Knapp and M. A. Beno Jul. 1991 13 p Presented at the 4th International Conference on Synchrotron Radiation Instrumentation, Manchester, England, 15-19 Jul. 1991

(Contract W-31-109-eng-38)
(DE91-016527; ANL/CP-72869; CONF-910730-2) Avail: NTIS HC/MF A03

In order to achieve the ultimate time resolution of a synchrotron source we propose a new experimental technique by which time dependent structural changes can be monitored on the time scale of synchrotron pulse widths. Samples will be studied by a rotating crystal Laue diffraction technique where we rapidly spin the sample and observe the diffraction pattern from a broad band of incident x-rays. A computer simulation is presented of the diffraction pattern time evolution using the parameters for an APS undulator of a phase change in the YBa2Cu3O(7-x) superconductor. We will discuss the application of this and closely related techniques at other synchrotron sources including bending magnets and insertion devices. DOE

N91-31936# Rochester Univ., NY.
THEORETICAL NUCLEAR PHYSICS
J. B. French and D. S. Koltun Jun. 1991 13 p
(Contract DE-FG02-88ER-40425)
(DE91-016745; DOE/ER-40425/253) Avail: NTIS HC/MF A03

This report summarizes progress during the past year in the following areas of research: (1) pion double charge exchange, including studies of the contribution of meson exchange currents and the roles of chiral symmetry and of vector mesons; (2) the possibility of bound states of two hyperons and the H dibaryon; (3) many body theory, including studies of nuclear scattering in a quark cluster model, nuclear structure calculations, and a one-dimensional model with charged bosons; and (4) statistical nuclear spectroscopy, including formalism and programs for state densities and partition functions, single-state occupancies and spin-cut off factors, measures for symmetry breaking, and the relationship between statistical and shell-model spectroscopy. DOE

N91-31937# Kent State Univ., OH. Dept. of Physics.
NUCLEUS-NUCLEUS COLLISIONS AND THE NUCLEAR EQUATION OF STATE
D. Keane 1991 19 p
(Contract DE-FG02-89ER-40531)
(DE91-016747; DOE/ER-40531/2) Avail: NTIS HC/MF A03

Activities during the period of support included: (1) the analysis of existing experimental data from the Bevalac streamer chamber and from the Kent State neutron flow experiment 848H; (2) work at the interface between theory and experiment, including transport model comparisons with the above data and with published results from other experiments, a new model to probe the possible use of spectator recoil to measure properties of the equation of state, and new methodologies for study of flow and HBT correlations; and (3) development of future Bevalac experiments, with particular emphasis on the EOS TPC. DOE

N91-31738 Kent Univ., Canterbury (England).
A NEW MODEL OF THE ELECTRON: A SUGGESTED EXPERIMENT TO SEARCH FOR A LINK BETWEEN ELECTROMAGNETISM AND GRAVITY
Roger C. Jennison *In its* BAe University Round Table on Gravitational Research Nov. 1990 7 p (For primary document see N91-31729 23-46)
Copyright Avail: British Aerospace (Military Aircraft) Ltd., Warton Aerodrome, Preston, Lancashire PR4 1AX, England

73 NUCLEAR AND HIGH-ENERGY PHYSICS

Includes elementary and nuclear particles; and reactor theory.

For space radiation see *93 Space Radiation.*

N91-31938# Florida State Univ., Tallahassee. Dept. of Physics.
HIGH ENERGY PHYSICS PROGRAM. TASK A: EXPERIMENT AND THEORY. TASK B: NUMERICAL SIMULATION OF QUANTUM FIELD THEORIES
J. E. Lannutti 1991 88 p
(Contract DE-FG05-87ER-40319)
(DE91-015652; DOE/ER-40319/4) Avail: NTIS HC/MF A05

This report discusses the following research: fixed target experiments; collider experiments; computing, networking and VAX upgrade; SSC preparation, detector development and detector construction; solid argon calorimetry; absorption of CAD system geometries into GEANT for SSC; and particle theory programs. DOE

N91-31939# Duke Univ., Durham, NC. High Energy Physics Group.
HIGH ENERGY PHYSICS
L. R. Fortney, A. T. Goshaw, and W. D. Walker 12 Jun. 1991 95 p
(Contract DE-AS05-76ER-03065)
(DE91-015796; DOE/ER-03065/T9) Avail: NTIS HC/MF A05

This progress report presents a review of research done over the past five years by the Duke High Energy Physics Group. This research has been centered at Fermilab where we have had a continuing involvement with both the Tevatron collider and fixed-target programs. In 1988 we began extensive detector R and D for the SSC through its Major Subsystem Program. Duke has been an active member of the Solenoidal Detector Collaboration (SDC) since its formation. These last five years has also been used to finish the analysis of data from a series of hybrid bubble chamber experiments which formed the core of Duke's research program in the early 1980's. DOE

N91-31940# Los Alamos National Lab., NM.
PROGRESS IN THE SP-100 FSQ REACTOR DEVELOPMENT
M. B. Parker 1991 5 p Presented at the AIAA/NASA/OAI Conference on Advanced SEI Technologies, Cleveland, OH, 3-4 Sep. 1991
(Contract W-7405-eng-36)
(DE91-016033; LA-UR-91-2314; CONF-9109226-4) Avail: NTIS HC/MF A01

The reactor for the SP-100 Space Power Supply System is described in this paper. The various components that make up the reactor are discussed and the testing programs to assure that the design will meet the SP-100 requirements are described. DOE

N91-31941# Brown Univ., Providence, RI. Dept. of Physics.
A RESEARCH PROGRAM IN EXPERIMENTAL HIGH ENERGY PHYSICS Progress Report
M. Widgoff 1 Jul. 1991 45 p
(Contract DE-AC02-76ER-03130)
(DE91-016208; DOE/ER-03130/270) Avail: NTIS HC/MF A03

The Large Volume Detector (LVD) Collaboration has made major progress during the past year in constructing the basic modules of the detector and installing them in five-tower LVD structure. Each of these modules consists of a portatank containing eight liquid scintillation counters (each 1.0m times 1.0m times 1.5m, viewed by three photomultipliers) totalling 9.6 tons of liquid scintillator and 6.7 tons of steel. Each portatank is covered on its bottom and one side by two layers of limited streamer tubes which form the tracking system of the detector. About half of the first tower has now been installed and initial data-taking with the entire tower is expected to being during the Fall of 1991. Data acquisition hardware and software are in place for this. The data-taking run of FNAL Experiment E782, a study of the interactions of 200 GeV

muons in a hybrid system with the Tohoku Freon bubble chamber as visible target, was completed in August 1990. Film analysis is now in progress. The results will be readily comparable to those obtained in FNAL Experiment E745, a study of the interactions of muon neutrinos in a similar system. The film analysis of E745 has been completed, and some preliminary results are presented on the production of strange particles, based on the combined data of both the 1985 and 1987 runs of this experiment. DOE

N91-31942# Brookhaven National Lab., Upton, NY.
ACCELERATION USING TOTAL INTERNAL REFLECTION
R. C. Fernow Jun. 1991 18 p
(Contract DE-AC02-76CH-00016)
(DE91-016612; BNL-52290) Avail: NTIS HC/MF A03

This report considers the use of a dielectric slab undergoing total internal reflection as an accelerating structure for charged particle beams. We examine the functional dependence of the electromagnetic fields above the surface of the dielectric for polarized incident waves. We present an experimental arrangement for testing the performance of the method, using apparatus under construction for the Grating Acceleration experiment at Brookhaven National Laboratory. DOE

N91-31943# Nationaal Inst. voor Kernfysica en Hoge Energiefysica, Amsterdam (Netherlands).
THE TIMING OF INJECTION KICKERS [TIMING INJECTIEKICKERS]
R. Maas Jan. 1991 7 p In DUTCH
(NIKHEF-K/AmPS/91-04; ETN-91-99525) Avail: NTIS HC/MF A02

The manipulation of the Closed Orbit (CO) injector using two electrostatic injection kickers was studied. The action of the kickers K1 and K2 is the creation of a local CO perturbation in the vertical plane. The minimum of the displaced CO touches the injection channel plane. The second kicker K2 prevents the returning bundle being deviated in case of multiple turn injection. In the case of single-turn injection, the relative increase of vertical emittance due to the action of K1 was calculated. In the case of three turn injection, timing errors and/or the difference between K1 and K2 lead to an increase in emittance. No bundle losses occurs in the kickers. ESA

N91-31944 Academy of Sciences of the Ukrainian SSR, Kiev. Inst. of Physics.
NEAR-WALL CONDUCTIVITY [PRISTENOCHNAIA PROVODIMOST]
A. I. Bugrova, A. A. Kurochkina, A. I. Morozov, and A. P. Shubin 1990 20 p In RUSSIAN
Copyright Avail: Issuing Activity

Theoretical and experimental research on near-wall conductivity is examined. The mechanism of the onset of near-wall conductivity and its fundamental characteristics are analyzed. It is shown that this mechanism of current transfer is manifested in accelerators with closed loop drift electrons. Author

N91-31945# Los Alamos National Lab., NM.
CARBIDE FUELS FOR NUCLEAR THERMAL PROPULSION
R. B. Matthews, H. T. Blair, K. M. Chidester, K. V. Davidson, W. E. Stark, and E. K. Storms 1991 11 p Presented at the AIAA/NASA/OAI Conference on Advanced SEI Technologies, Cleveland, OH, 3-4 Sep. 1991
(Contract W-7405-eng-36)
(DE91-016032; LA-UR-91-2317; CONF-9109226-3) Avail: NTIS HC/MF A03

A renewed interest in manned exploration of space has revitalized interest in the potential for advancing nuclear rocket technology developed during the 1960's. Carbide fuel performance, melting point, stability, fabricability and compatibility are key technology issues for advanced Nuclear Thermal Propulsion reactors. The Rover fuels development ended with proven carbide fuel forms with demonstrated operating temperatures up to 2700 K for over 100 minutes. The next generation of nuclear rockets will start where the Rover technology ended, but with a more rigorous set of operating requirements including operating lifetime to 10 hours, operating temperatures greater that 3000 K, low fission product release, and compatibility. A brief overview of Rover/NERVA carbide fuel development is presented. A new fuel form with the highest potential combination of operating temperature and lifetime is proposed that consists of a coated uranium carbide fuel sphere with built-in porosity to contain fission products. The particles are dispersed in a fiber reinforced ZrC matrix to increase thermal shock resistance. DOE

74 OPTICS

Includes light phenomena; and optical devices.
For lasers see *36 Lasers and Masers.*

N91-31946 Grumman Aerospace Corp., Bethpage, NY.
AVIOPTIC PLUG-IN INTERCONNECTION Patent
Anthony L. Caserta, inventor and Bruno Lijoi, inventor 23 May 1989 15 p
(Patent-1-254-415; Int-Patent-Class-G02B-624; CTN-91-60172)
Copyright Avail: Micromedia Ltd., Technical Information Centre, 165 Hotel de Ville, Place du Portage, Phase 2, Hull, Quebec J8X 3X2, Canada HC $4.00 CAN, MF $2.75 CAN

A secure interconnection is claimed for optical and avioptic cables located in exposed positions, which often occur on aircraft communications circuits, for connecting those cables into equipment such as circuit boards. In this invention the interconnection for optical fiber cables comprises a connector which is engaged in a receptacle in a mother board provided with optical circuitry. The connector comprises a cuplike body or plug containing a metal sleeve which encases the optical fiber cable such that the cable end is exposed. The mating receptacle comprises a cylindrical shell having its lower end embedded in the mother board. A hole in the receptacle shell wall receives the end of an optical fiber on the optical circuitry of the mother board. The end of the sleeve of the connector fits over the end of the receptacle shell protruding from the mother board. Beam deflection means in the receptacle or on the connector directs light between the fiber optic cable and the optical circuit element of the mother board. Electrical coupling can be incorporated into the interconnection such that the termination can accommodate electrical as well as optical functions. CISTI

N91-31947*# Alabama Univ., Huntsville. Dept. of Computer Science.
A GRAPH THEORETIC APPROACH TO SCENE MATCHING Final Progress Report, period ending 1 Aug. 1991
Heggere S. Ranganath and Laure J. Chipman 1 Aug. 1991 155 p
(Contract NCC8-16)
(NASA-CR-187817; NAS 1.26:187817) Avail: NTIS HC/MF A08 CSCL 20F

The ability to match two scenes is a fundamental requirement in a variety of computer vision tasks. A graph theoretic approach to inexact scene matching is presented which is useful in dealing with problems due to imperfect image segmentation. A scene is described by a set of graphs, with nodes representing objects and arcs representing relationships between objects. Each node has a set of values representing the relations between pairs of objects, such as angle, adjacency, or distance. With this method of scene representation, the task in scene matching is to match two sets of graphs. Because of segmentation errors, variations in camera angle, illumination, and other conditions, an exact match between the sets of observed and stored graphs is usually not possible. In the developed approach, the problem is represented as an association graph, in which each node represents a possible mapping of an observed region to a stored object, and each arc represents the compatibility of two mappings. Nodes and arcs have weights indicating the merit or a region-object mapping and the degree of compatibility between two mappings. A match between the two graphs corresponds to a clique, or fully connected subgraph, in the association graph. The task is to find the clique

that represents the best match. Fuzzy relaxation is used to update the node weights using the contextual information contained in the arcs and neighboring nodes. This simplifies the evaluation of cliques. A method of handling oversegmentation and undersegmentation problems is also presented. The approach is tested with a set of realistic images which exhibit many types of sementation errors. Author

N91-31948# California Univ., Berkeley. Lawrence Berkeley Lab.
RECENT ADVANCES IN FIBER OPTICS COMPONENTS FOR HIGH SPEED DATA TRANSMISSION
B. Leskovar 23 Apr. 1991 13 p Presented at the Lasers 1991, Munich (Germany), 12-14 Jun. 1991
(Contract DE-AC03-76SF-00098)
(DE91-016252; LBL-30677; CONF-9106231-2) Avail: NTIS HC/MF A03

The concept of guided lightwave communication along optical fibers has stimulated a major new technology over the past two decades. This technology profoundly impacts communication and instrumentation systems as well as computer interconnections and systems architecture. In this paper, the state of the art of optical transmitters, low loss fiber waveguides, receivers, and associated electronics components are reviewed and summarized for optical data transmission systems operating between 100 Mbit/s and 2.5 Gbit/s. Emphasis is placed on high speed data transmission subassemblies, such as time division multiplexers and demultiplexers, clock and data recovery circuits, as well as optical transmitters and receivers. In addition, the performance of candidate components of the wide band digital transmission systems intended for deployment in large detection systems for particle physics is discussed. DOE

N91-31949# Messerschmitt-Boelkow-Blohm G.m.b.H., Munich (Germany, F.R.). Central Area for Research Applied Physics.
MICROMECHANICAL CONCEPTS IN OPTICS AND OPTOELECTRONICS
Peter P. Deimel 1990 9 p
(MBB-Z-0339-90-PUB; OTN-028392; ETN-91-99760) Avail: NTIS HC/MF A02

A selection of various micromechanical components and devices is presented. With the ever increasing drive for smaller dimensions and integration of various components, micromechanical principles play an increasing role in production processes. Production of mirrors, optical gratings, lenses, waveguides, airbridges for electrical interconnents, and alignment aids, involves micromechanical principles. A wide range of possibilities to manufacture the various components and especially to batch produce and integrate them on a wafer are discussed. Micromechanical principles can be applied both in silicon and semiconductor technology. New capabilities of micromechanics in combination with microoptics and optoelectronics are reviewed. ESA

N91-31950* National Aeronautics and Space Administration. Langley Research Center, Hampton, VA.
SINGLE LAYER MULTI-COLOR LUMINESCENT DISPLAY Patent
James B. Robertson, inventor (to NASA) 10 Sep. 1991 8 p Filed 31 Dec. 1987
(NASA-Case-LAR-13616-1; US-Patent-5,047,686; US-Patent-Appl-SN-140185; US-Patent-Class-313-503; US-Patent-Class-313-506; US-Patent-Class-313-509; US-Patent-Class-313-502; Int-Patent-Class-H05B-33/14) Avail: US Patent and Trademark Office CSCL 20F

The invention is a multi-color luminescent display comprising an insulator substrate and a single layer of host material which may be a phosphor deposited thereon that hosts one or more differential impurities, therein forming a pattern of selected and distinctly colored phosphors such as blue, green, and red phosphors in a single layer of host material. Transparent electrical conductor means may be provided for subjecting selected portions of the pattern of colored phosphors to an electric field thereby forming a multi-color, single layer electroluminescent display.
Official Gazette of the U.S. Patent and Trademark Office

N91-31951# Cornell Univ., Ithaca, NY.
INNOVATIVE OPTOELECTRONIC MATERIALS AND STRUCTURES USING OMVPE Final Technical Report, Apr. 1986 - Dec. 1988
James R. Shealy 9 Sep. 1991 5 p
(Contract N00014-86-K-0531)
(AD-A239518) Avail: NTIS HC/MF A01 CSCL 20/12

The materials investigations in this program have contributed to extending the wavelength range of high power diode lasers and to the development of improved Organometallic Vapor Phase Epitaxy (OMVPE) processes. The main research thrusts are OMVPE growth of wide bandgap alloys, and in-situ processes during OMVPE. Growth of large bandgap III-V phosphide alloys was developed for optoelectronic applications including red semiconductor lasers. The lattice matched materials system Aluminum Gallium Indium Phosphide/Gallium Arsenide resulted in high power, low threshold single quantum well lasers (wavelength = 655 nm). A materials investigation of a potentially shorter wavelength system, pseudomorphic Gallium Indium Phosphide/Aluminum Gallium Phosphide-Gallium Phosphide, was initiated. Conventional growth was unsuccessful as the In containing alloys do not remain stable during high temperature growth of Aluminum Gallium Phosphide. A multichamber OMVPE process employing flow modulation techniques was planned to overcome this problem. The phonon frequency shifts due to lattice expansion were measured and a temperature-tuned resonance was observed on GaAs at 600 C. GRA

N91-31952# Naval Research Lab., Washington, DC.
EXACT RESULT FOR THE GRAZING ANGLE OF SPECULAR REFLECTION FROM A SPHERE Memorandum Report, Jan. - May 1991
Allen R. Miller and Emanuel Vegh 9 Aug. 1991 15 p
(AD-A239578; NRL-MR-6867) Avail: NTIS HC/MF A03 CSCL 20/6

The present paper shows that it is possible to exhibit the grazing angle of specular reflection as one of four angles derived from the zeros of a certain self-inversive quartic polynomial whose coefficients are complex. Thus the grazing angle may now be found deterministically, whereas heretofore it had to be computed either by approximations or numerical procedures. The preceeding analysis shows further that factoring, in a useful way, a quartic polynomial whose complex coefficients depend on even a small number of parameters, is not always a trivial matter, even though the methods of Cardan and Ferrari have been known for centuries. GRA

N91-31953# Carnegie-Mellon Univ., Pittsburgh, PA. Center for Excellence in Optical Data Processing.
MULTITARGET TRACKING USING OPTICAL PROCESSING Final Report, Aug. 1990 - Aug. 1991
David Casasent Aug. 1991 123 p Sponsored by ONR
(AD-A239656) Avail: NTIS HC/MF A06 CSCL 20/6

The SDIO multitarget tracking optical system is described. It involves point target detection and localization of sub-pixel targets below the noise level (using an optical correlator), track initiation (using an optical Hough transform), data association (using an optical neural net), a simple estimator (alpha, beta, gamma tracker), and inherent error correction (in the full modular system). New algorithms and optical architectures were devised, and real ISTEF data was processed on real-time optical laboratory systems. Author (GRA)

N91-31954# Massachusetts Inst. of Tech., Lexington. Lincoln Lab.
PARAMETRIC STUDY OF DIFFUSION-ENHANCEMENT NETWORKS FOR SPATIOTEMPORAL GROUPING IN REAL-TIME ARTIFICIAL VISION Annual Technical Summary Report No. 1, Oct. 1989 - Mar. 1991

Robert K. Cunningham and Allen M. Waxman 4 Jun. 1991 41 p
(Contract F19628-90-C-0002)
(AD-A239674; ESD-TR-91-108) Avail: NTIS HC/MF A03 CSCL 07/4

This is the first Annual Technical Summary of the MIT Lincoln Laboratory effort into the parametric study of diffusion-enhancement networks for spatiotemporal grouping in real-time artificial vision. Spatiotemporal grouping phenomena are examined in the context of static and time-varying imagery. Dynamics that exhibit static feature grouping on multiple scales as a function of time and long-range apparent motion between time-varying inputs are developed for a biologically plausible diffusion-enhancement bilayer. The architecture consists of a diffusion and a contrast-enhancement layer coupled by feedforward and feedback connections: input is provided by a separate feature extracting layer. The model is cast as an analog circuit that is realizable in VLSI, the parameters of which are selected to satisfy a psychophysical database on apparent motion. Specific topics include: neural networks, astrocyte glial networks, diffusion enhancement, long-range apparent motion, spatiotemporal grouping dynamics, and interference suppression. GRA

75 PLASMA PHYSICS

Includes magnetohydrodynamics and plasma fusion.
For ionospheric plasmas see *46 Geophysics*. For space plasmas see *90 Astrophysics*.

N91-31955# Los Alamos National Lab., NM.
COMPUTATIONAL MODEL FOR DETERMINISTIC CHAOS IN A MAGNETICALLY CONFINED PLASMA
E. L. Vold 1991 9 p Presented at the 14th Conference on Numerical Simulation of Plasmas, Annapolis, MD, 4-6 Sep. 1991
(Contract W-7405-eng-36)
(DE91-016022; LA-UR-91-2346; CONF-9109108-5) Avail: NTIS HC/MF A02

Deterministic chaos, originally seen in the Lorentz equations, designates the concept that turbulent behavior arises from systems of non-linear equations, including the fluid moment or Navier-Stokes equations, and specifically the fluid approximation to a magnetized plasma. Consistent computations capable of reproducing 'anomalous' transport observed in tokamaks are assumed to rely upon the correct computational treatment of the dominant macroscopic nonlinearities in the tokamak. These non-linear effects include: the divergence of the momentum flux tensor in magnetic flux surface coordinates, the core and edge plasma treated as a single region coupled to the sheath and edge physics boundary conditions including neutral particle recycling, and the plasma potential, (Phi), calculated in non-ambipolar conditions. Unresolved subgrid transport and plasma kinetic effects can be added in the momentum viscosity tensor. An iterative and time dependent solution for the coupled quantities: n, u, T(sub i), and (Phi) j, T(sub e) with B and diffusive neutrals and impurity species is described for the toroidally symmetric case in ((theta), (psi), (phi)) coordinates. An inner iteration solves the transport problem in an estimated flux surface geometry assuming E (approx) - (del)(theta)(Phi) - (del)(Psi)(Phi) + E(sub i)(phi), and an outer iteration couples the plasma transport to consistent MHD surfaces. The control volume form of the momentum flux tensor in magnetic surface geometry, an elliptic equation for (Phi), and algorithm sweep considerations for the magnetic surface topology are emphasized. DOE

N91-31956 Academy of Sciences of the Ukrainian SSR, Kiev. Inst. of Physics.
PLASMA-OPTICS SYSTEMS FOR THE FORMATION AND FOCUSING OF ION BEAMS [PLAZMOOTICHESKIE SISTEMY FORMIROVANNIIA I FOKUSIROVKI IONNYKH PUCHKOV]
I. S. Gasanov, A. A. Goncharov, and I. M. Protsenko 1990 41 p In RUSSIAN
Copyright Avail: Issuing Activity

Given here is an all-encompassing 10-year summary of the development of plasma-optics systems for the formation, direction, and focusing of balanced ion beams. Two systems are analyzed in detail: the plasma lens and the magnetoinsulatory diode interval (path) in the plasma-optical regime. Author

N91-31957* Max-Planck-Inst. fuer Physik und Astrophysik, Garching (Germany, F.R.).
PLASMA DIFFUSION AT THE MAGNETOPAUSE? THE CASE OF LOWER HYBRID DRIFT WAVES
R. A. Treumann, J. LaBelle, R. Pottelette, and S. P. Gary (Los Alamos National Lab., NM.) Nov. 1990 29 p Submitted for publication Sponsored in cooperation with DOE
(Grant NAGw-1540)
(NASA-CR-188913; NAS 1.26:188913; MPE-Preprint-196; ISSN-0178-0719; ETN-91-90017) Copyright Avail: Fachinformationszentrum Karlsruhe, 7514 Eggenstein-Leopoldshafen 2, Fed. Republic of Germany CSCL 20I

The diffusion expected from the quasilinear theory of the lower hybrid drift instability at the Earth's magnetopause is recalculated. The resulting diffusion coefficient is in principle just marginally large enough to explain the thickness of the boundary layer under quiet conditions, based on observational upper limits for the wave intensities. Thus, one possible model for the boundary layer could involve equilibrium between the diffusion arising from lower hybrid waves and various low processes. However, some recent data and simulations seems to indicate that the magnetopause is not consistent with such a soft diffusive equilibrium model. Furthermore, investigation of the nonlinear equations for the lower hybrid waves for magnetopause parameters indicates that the quasilinear state may never arise because coalescence to large wavelengths, followed by collapse once a critical wavelengths is reached, occur on a time scale faster than the quasilinear diffusion. In this case, an inhomogeneous boundary layer is to be expected. More simulations are required over longer time periods to explore whether this nonlinear evolution really takes place at the magnetopause. ESA

N91-31958# Los Alamos National Lab., NM.
AN INTERPARTICLE COLLISION MODEL FOR ELECTROMAGNETIC HYBRID SIMULATIONS OF HIGH DENSITY PLASMAS
M. E. Jones, V. A. Thomas, and D. Winske 1991 5 p Presented at the 14th Conference on Numerical Simulation of Plasmas, Annapolis, MD, 4-6 Sep. 1991
(Contract W-7405-eng-36)
(DE91-016025; LA-UR-91-2342; CONF-9109108-4) Avail: NTIS HC/MF A01

Particle-in-cell methods have long been used to model collisionless plasma phenomena. At the other extreme, fluid methods have been used to model highly collisional plasmas. Hybrid models in which ions are treated by the particle-in-cell method and electrons are treated as a massless fluid allow one to ignore phenomena on the electron plasma frequency time scale and thus have proven to be useful for modeling certain aspects high density plasmas. Until now particle collisions in PIC or hybrid models have been limited to scattering of the particles off a fixed background. The key ingredient in developing plasma simulation methods that allow one to study the transitional region between collisionless and collisional plasmas has been the development of an adequate interparticle collision model that takes into account the self-consistent reaction of the colliding species. We have developed and incorporated one type of interparticle collision model into the hybrid version of our particle-in-cell code, ISIS. The method is highly efficient and ensures local conservation of momentum and energy. DOE

N91-31959# Naval Research Lab., Washington, DC.
ADVANCED CONCEPTS THEORY Annual Report, 1990
16 Aug. 1991 168 p Sponsored by DNA
(AD-A239780; NRL-MR-6870) Avail: NTIS HC/MF A08 CSCL 20/9

Several critical problems concerning the design of z-pinch implosions and the optimization of their radiative output are examined. Separate sections describe progress in the analysis of z-pinch experiments, the development of atomic, electron, plasma and MHD dynamical models to describe z-pinch implosions, and the analysis of atomic number scaling of z-pinch K-shell emission. GRA

76 SOLID-STATE PHYSICS

Includes superconductivity.

For related information, see also *33 Electronics and Electrical Engineering* and *36 Lasers and Masers.*

N91-31960# Montpellier-2 Univ. (France)
ADVANCED RESEARCH WORKSHOP ON WIDE GAP II-VI SEMICONDUCTORS
18 Jan. 1991 49 p Workshop held in Montpellier, France, 16-18 Jan. 1991
(AD-A233796; R/D-6646-EE-02) Avail: NTIS HC/MF A03 CSCL 20/12

The following subject areas are covered: physics of wide-gap II-VI heterostructures and super-lattices; growth of ZnSe layers by MBE; epitaxial growth of ZnSe for bulk emission (current research in Japan); growth of bulk ZnSe crystals for epitaxial substrates; p-type ZnSe and Blue LEDs; theoretical study of electron transport in ZnSe (application to material quality assessment); growth of ZnSe and other wide-bandgap II-VI semiconductors by MOCVD; new precursors for wide-gap II-VI semiconductors; optical and electro-optical properties of II-VI quantum dots; optical properties of II-VI epitaxial layers; incorporation of impurities and photo-excitation effects in wide-bandgap II-VI semiconductors; and ZnSe switching and logic devices and their application to information processing. GRA

N91-31961*# Ohio State Univ., Columbus. Dept. of Materials Science and Engineering.
CRYSTALLIZATION OF THE GLASSY GRAIN BOUNDARY PHASE IN SILICON NITRIDE CERAMICS Final Report
Charles H. Drummond, III Aug. 1991 77 p
(Grant NAG3-824)
(NASA-CR-188717; NAS 1.26:188717) Avail: NTIS HC/MF A05 CSCL 20B

The role was studied of the intergranular glassy phase in silicon nitride as-processed with yttria as a sintering aid. The microstructure, crystallization, and viscosity of the glassy phase were areas studied. Crystallization of the intergranular glassy phase to more refractory crystalline phases should improve the high temperature mechanical properties of the silicon nitride. The addition of a nucleating agent will increase the rate of crystallization. The measurement of the viscosity of the glassy phase will permit the estimation of the high temperature deformation of the silicon nitride. For individual titles, see N91-31962 through N91-31965.

N91-31962*# National Aeronautics and Space Administration. Lewis Research Center, Cleveland, OH.
CRYSTALLIZATION AND CHARACTERIZATION OF Y2O3-SiO2 GLASSES
Charles H. Drummond, III, William E. Lee (Ohio State Univ., Columbus.), W. A. Sanders, and J. D. Kiser *In* Ohio State Univ., Crystallization of the GlassyGrain Boundary Phase in Silicon Nitride Ceramics Aug. 1991 18 p Repr. from Ceram. Eng. Sci. Proc., 9(9-10) 1988 p 1343-1354 Previously announced in IAA as A89-19486 (For primary document see N91-31961 23-76)
Avail: NTIS HC/MF A05 CSCL 20B

Glasses in the yttria-silica system with 20 to 40 mol pct Y2O3 were subjected to recrystallization studies after melting at 1900 to 2100 C in W crucibles in 1 and 50 atm N2. The TEM and XRD results obtained indicate the presence of the delta, gamma, gamma prime, and beta-Y2Si2O7 crystalline phases, depending on melting and quenching conditions. Heat treatment in air at 1100 to 1600 C increased the amount of crystallization, and led to the formation of Y2SiO5, cristabalite, and polymorphs of Y2Si2O7. Also investigated were the effects of 5 and 10 wt pct zirconia additions. Author

N91-31963*# Ohio State Univ., Columbus. Dept. of Materials Science and Engineering.
MICROSTRUCTURAL CHANGES IN BETA-SILICON NITRIDE GRAINS UPON CRYSTALLIZING THE GRAIN-BOUNDARY GLASS
William E. Lee, Gregory E. Hilmas, and F. F. Lange, ed. *In its* Crystallization of the Glassy Grain Boundary Phase in Silicon Nitride Ceramics Aug. 1991 12 p Repr. from J. Am. Ceram. Soc., 72(10) 1989 p 1931-1937 (For primary document see N91-31961 23-76)
(Grant NAG3-824)
Avail: NTIS HC/MF A05 CSCL 20B

Crystallizing the grain boundary glass of a liquid phase sintered Si3N4 ceramic for 2 h or less at 1500 C led to formation of gamma Y2Si2O7. After 5 h at 1500 C, the gamma Y2Si2O7 had transformed to beta Y2Si2O7 with a concurrent dramatic increase in dislocation density within beta Si3N4 grains. Reasons for the increased dislocation density is discussed. Annealing for 20 h at 1500 C reduced dislocation densities to the levels found in as-sintered materials. Author

N91-31964*# Ohio State Univ., Columbus. Dept. of Materials Science and Engineering.
GLASS FORMATION AND CRYSTALLIZATION IN HIGH-TEMPERATURE GLASS-CERAMICS AND Si3N4
Charles H. Drummond, III *In its* Crystallization of the Glassy Grain Boundary Phase in Silicon Nitride Ceramics Aug. 1991 15 p Repr. from J. of Non-Crystalline Solids 123, 1990 p 114-128 North-Holland (For primary document see N91-31961 23-76)
Avail: NTIS HC/MF A05 CSCL 20B

The softening of glassy grain boundaries in ceramic matrix composites and Si3N4 at high temperatures reduces mechanical strength and the upper-use temperature. By crystallizing this glass to a more refractory crystalline phase, a material which performs at higher temperatures may result. Three systems were examined: a cordierite composition with ZrO2 as a nucleating agent; celsian compositions; and yttrium silicate glasses both in bulk and intergranular in Si3N4. For the cordierite compositions, a series of metastable phases was obtained. The crystallization of these compositions was summarized in terms of metastable ternary isothermal sections. Zircon formed at the expense of ZrO2 and spinel. In SiC composites, the transformations were slower. In celsian, two polymorphs were crystallized. One phase, hexacelsian, which always crystallized, even when metastable, had an undesirable volume change. The other phase, celsian, was very difficult to crystallize. In yttrium silicate bulk glasses, similar in composition to the intergranular glass in Si3N4, a number of polymorphs of Y2Si2O7 were crystallized. The conditions under which these polymorphs formed are compared with crystallization in Si3N4. Author

N91-31965*# Ohio State Univ., Columbus. Dept. of Materials Science and Engineering.
INDIRECT MEASUREMENT OF THE VISCOSITY OF THE INTERGRANULAR GLASS PHASE IN YTTRIA-SINTERED SILICON NITRIDE
Mark B. Dittmar and Charles H. Drummond, III *In its* Crystallization of the Glassy Grain Boundary Phase in Silicon Nitride Ceramics Aug. 1991 16 p Submitted for publication (For primary document see N91-31961 23-76)
Avail: NTIS HC/MF A05 CSCL 20B

Dense, sintered Si3N4 possesses a residual intergranular glass phase which softens at high temperatures, resulting in degradation of the ceramic's mechanical properties at high temperatures. An important parameter in the determination of the high temperature mechanical properties of sintered Si3N4 is the temperature-viscosity relationship of the intergranular glass. A method for indirectly measuring the intergranular glass viscosity at a given temperature using physical modelling of a two phase

glass crystal microstructure and beam bending viscometry measurements of Si3N4 is described. Intergranular glass viscosities obtained by this method are presented for a yttria sintered Si3N4.
Author

N91-31966# EG and G Energy Measurements, Inc., Las Vegas, NV.
PHOTOPHYSICS AND CHEMISTRY OF ULTRA-FAST ZnO AND CdS PHOSPHORS
J. Gleason, W. D. Turley, and W. Lehmann 1991 2 p Presented at the 180th Meeting of the Electrochemical Society, Phoenix, AZ, 13-18 Oct. 1991
(Contract DE-AC08-88NV-10617)
(DE91-013106; EGG-10617-2096; CONF-911047-2) Avail: NTIS HC/MF A01

Powder and vapor deposited samples of the strongly n-type doped II-VI semiconductors, zinc oxide doped with gallium (ZnO:Ga) and cadmium sulfide doped with indium (CdS:In), were synthesized. The relationship between the emission spectrum and the unusually fast decay constant, and the material composition and crystalline structure was studied. Our efforts concentrated primarily on the high speed green (500 to 530 nm) CdS:In emission. The green emission is shown by control experiments to be intrinsic to CdS. However, indium doping followed by reduction in high temperature hydrogen gas is required to generate sufficient luminescent yield. The green emission is believed to result from electronic transitions between the conduction band and centers close to the valence band edge and the improved efficiency from an increased concentration of free electrons. A model linking the short decay constant to the concentration of free electrons is proposed.
DOE

N91-31967# Argonne National Lab., IL.
INTRINSIC STABILITY AND RECOVERY ANALYSIS FOR TAPE/FILM TYPE SUPERCONDUCTORS
A. Uenal, M. C. Chyu (Texas Technological Univ., Lubbock.), and T. M. Kuzay 1991 6 p Presented at the 26th Intersociety Energy Conversion Engineering (IECE) Conference, Boston, MA, 3-9 Aug. 1991
(Contract W-31-109-eng-38)
(DE91-015568; ANL/CP-73336; CONF-910801-9) Avail: NTIS HC/MF A02

This work presents an analysis for a tape/film superconductor subjected to the thermal disturbance from a line heat source. The behavior of the superconductor is studied by considering its intrinsic stability and recoverability of superconductivity. The temperature field for intrinsic stability analysis is solved analytically. The mechanism is studied based on the data of instability parameter, cryogenic cooling rate, and joule heating rate during the heat diffusion process for both low- and high-(Tc) superconductors.
DOE

N91-31968# Argonne National Lab., IL.
MEAN FIELD ANALYSIS OF THE CuO2 LATTICE: COMPARISON TO MONTE CARLO SIMULATIONS
A. J. Fedro, Yu Zhou, T. C. Leung, and B. N. Harmon (Ames Lab., IA.) May 1991 9 p Presented at the International Workshop on Electronic Properties and Mechanisms in High-Tc Superconductors, Tsukuba (Japan), 29-31 Jul. 1991 Prepared in cooperation with University of Northern Illinois, De Kalb
(Contracts W-31-109-eng-38; W-7405-eng-82)
(DE91-015570; ANL/CP-73398; CONF-9107143-1) Avail: NTIS HC/MF A02

In this short paper we outline a mean field (MF) calculation of the multi-band Hubbard model of the CuO2 lattice based on a projection operator scheme. We then make a detailed comparison of our MF results to the above-mentioned MC simulations which we will regard as exact. In this approach, the two usual Hubbard projection operators are defined (involving creation/destruction of a fermion at site j with spin (sigma) either in the presence or absence of the fermion at the same site j with spin -(sigma)), and the model is solved with an equation of motion method for these operators using a well-defined truncation procedure which treats the complicated statistics of these operators properly and reduces to well-established decoupling in the case of pure fermions. In this way we generate an exact Dyson-like equation for the Green's functions where the self energy is found to contain both static and dynamic contributions. We will ignore the effects due to the dynamic terms (in this context termed memory functions) in this paper thus defining a MF set of equations for the needed Green's functions. These equations are then solved self-consistently for all band fillings and for possible antiferromagnetic (AF) order.
DOE

N91-31969# Oak Ridge National Lab., TN.
PROPERTIES OF LOW TEMPERATURE, LOW OXYGEN PRESSURE POST-ANNEALED YBa2Cu3O(SUB 7-x) THIN FILMS
R. Feenstra, D. K. Christen, J. D. Budai, S. J. Pennycook, D. P. Norton, D. H. Lowndes, C. E. Klabunde, and M. D. Galloway 1991 13 p Presented at the International Conference on Advanced Materials (ICAM 91), Strasbourg, France, 27-31 May 1991
(Contract DE-AC05-84OR-21400)
(DE91-015632; CONF-910580-2) Avail: NTIS HC/MF A03

The application and effects of low oxygen pressures for the growth of YBa2Cu3O(7-x) films by post deposition annealing are reviewed and related to available thermodynamic data at subatmospheric oxygen pressures. Special emphasis is given to the correlation between epitaxial growth properties and high temperature annealing conditions and the effect of variable low temperature oxidation. The application of low oxygen pressures is extended to the recrystallization of ion implanted, amorphized YBa2Cu3O(7-x) layers for comparison with epitaxial growth properties during initial post deposition annealing. DOE

N91-31970# Oak Ridge National Lab., TN.
STUDIES OF NON-IDEAL SUPERCONDUCTORS USING DC MAGNETIC METHODS
J. R. Thompson (Oak Ridge National Lab., TN.), D. K. Christen, H. R. Kerchner, L. A. Boatner, B. C. Sales, B. C. Chakoumakos, H. Hsu, J. Brynestad, D. M. Kroeger, and R. Williams 1991 19 p Presented at the Three-day International Workshop on AC Susceptibility, Coolfont, WV, 20-22 May 1991
(Contract DE-AC05-84OR-21400)
(DE91-015642; CONF-9105147-2) Avail: NTIS HC/MF A03

Among the most informative and facile methods for investigations of a superconductor are measurements of its static magnetization. The objective of this paper is to analyze some experimental features frequently observed in static (dc) magnetization studies of conventional and high-(Tc) superconductors. We shall discuss investigations employing measurement protocols in which the sample is cooled through the superconductive transition temperature in a finite magnetic field ('field cooled') and compare this with zero-field-cooled studies. Also considered are reversible and irreversible materials; particle size effects; some effects of granular and multiply-connected materials; penetration depth studies of type 2 materials in the vortex state; and fine scale 'multi-connected' materials produced by heavy ion irradiation that produces very significant enhancements of the critical current density J(sub c) in the high temperature superconductor YBa2Cu3O7. Many of these superconductors are 'non-ideal' in that they may contain defects and inhomogeneities or may have small dimensions comparable with microscopic superconductive lengths. Practically speaking, however, such materials are often encountered experimentally and can have very desirable physical properties, such as high J(sub c) values in the ion-irradiated crystal. DOE

N91-31971# Sandia National Labs., Albuquerque, NM.
DEPTH PROFILES FOR HYDROGEN-ASSISTED THERMAL DONOR FORMATION IN SILICON
H. J. Stein, P. M. Richards, and S. Hahn (Stanford Univ., CA.) 1991 6 p Presented at the 16th International Conference on Defects in Semiconductors, Bethlehem, PA, 22-26 Jul. 1991

(Contract DE-AC04-76DP-00789)
(DE91-015719; SAND-91-0589C; CONF-9107146-1) Avail: NTIS HC/MF A02

Concentration and depth profiles for thermal donor formation in Si under hydrogen plasma exposure have been investigated by infrared, IR absorption and spreading resistance probe, SEP measurements. Donors measured by SRP are shown to correlate with oxygen-related thermal donors, TD's detected by IR. Hydrogen-independent precursor nuclei formation at the hydrogenation temperature, and continued hydrogen activity in TD formation after hydrogenation are inferred from effects of extended pre and post heating on TD concentrations and profiles. A model wherein diffusing hydrogen activates precursor sites is presented to explain concentrations and profiles for TD's formed in a hydrogen plasma. DOE

N91-31972# Brookhaven National Lab., Upton, NY.
MODELS OF FLUX DIFFUSION AND FLUX CREEP IN HIGH-TEMPERATURE SUPERCONDUCTORS
D. O. Welch 31 Jul. 1991 4 p Presented at the 6th International Workshop on Critical Currents in Superconductors (IWCCVI), Cambridge, England, 7-12 Jul. 1991
(Contract DE-AC02-76CH-00016)
(DE91-015838; BNL-46400; CONF-910710-1) Avail: NTIS HC/MF A01

Some aspects of the phenomenological modelling of the kinetics of magnetic flux diffusion and creep in high-temperature superconductors in the low-temperature flux-creep regime are discussed with emphasis on the effects of the current-dependence of the activation energy. Flux creep by quantum tunneling is also discussed. DOE

N91-31973# Cornell Univ., Ithaca, NY.
STUDIES OF THE III-V COMPOUNDS IN THE MEGABAR REGIME
A. L. Ruoff 1991 13 p
(Contract DE-FG02-87ER-45320)
(DE91-015911; DOE/ER-45320/4) Avail: NTIS HC/MF A03

In this project we make systematic studies of the crystal structure of III-V compounds as a function of pressure along with developing the techniques for making these studies. The broad objective of the proposed research its to provide experimental data over a broad range of coordination number and interatomic spacing which can play a leading role in the testing and development of theoretical models of binding. In a monumental breakthrough we reached pressures greater than that of the center of the earth (361 GPa) for the first time by doing x-ray diffraction to 416 GPa. We analyzed the effect of nonhydrostaticity on pressure measurement. We showed how the decreasing band gap of diamond placed an upper limit on the use of the ruby pressure gauge. We carried out optical studies on GaAs to 115 GPa and found that it was amorphous when we decreased the pressure to atmospheric indicating that in the high pressure metallic state the Ga and As atoms are random. We made x-ray studies at pressure on AlAs to 42 GPa and extended our studies on InAs to 70 GPa; both sets of data are being analyzed now. A chapter was written on High Pressure Phase Transitions. DOE

N91-31974# California Univ., Berkeley. Lawrence Berkeley Lab.
MACROSCOPIC QUANTUM TUNNELING IN JOSEPHSON TUNNEL JUNCTIONS AND COULOMB BLOCKADE IN SINGLE SMALL TUNNEL JUNCTIONS Ph.D. Thesis
A. N. Cleland Apr. 1991 171 p
(Contract DE-AC03-76SF-00098)
(DE91-016258; LBL-30563) Avail: NTIS HC/MF A08

Experiments investigating the process of macroscopic quantum tunneling in a moderately-damped, resistively shunted, Josephson junction are described, followed by a discussion of experiments performed on very small capacitance normal-metal tunnel junctions. The experiments on the resistively-shunted Josephson junction were designed to investigate a quantum process, that of the tunneling of the Josephson phase variable under a potential barrier, in a system in which dissipation plays a major role in the dynamics of motion. All the parameters of the junction were measured using the classical phenomena of thermal activation and resonant activation. Theoretical predictions are compared with the experimental results, showing good agreement with no adjustable parameters; the tunneling rate in the moderately damped (Q approximately 1) junction is seen to be reduced by a factor of 300 from that predicted for an undamped junction. The phase is seen to be a good quantum-mechanical variable. The experiments on small capacitance tunnel junctions extend the measurements on the larger-area Josephson junctions from the region in which the phase variable has a fairly well-defined value, i.e. its wavefunction has a narrow width, to the region where its value is almost completely unknown. The charge on the junction becomes well-defined and is predicted to quantize the current through the junction, giving rise to the Coulomb blockade at low bias. I present the first clear observation of the Coulomb blockade in single junctions. The electrical environment of the tunnel junction, however, strongly affects the behavior of the junction: higher resistance leads are observed to greatly sharpen the Coulomb blockade over that seen with lower resistance leads. I present theoretical descriptions of how the environment influences the junctions; comparisons with the experimental results are in reasonable agreement. DOE

N91-31975# California Univ., Berkeley. Lawrence Berkeley Lab.
TEM ANALYSIS OF CRYSTALLINE INTERFACE STRUCTURE: THE STATE OF THE ART
U. Dahmen May 1991 2 p Presented at the 25th Annual Microbeam Analysis Society Meeting, San Jose, CA, 4-9 Aug. 1991
(Contract DE-AC03-76SF-00098)
(DE91-016427; LBL-30917; CONF-910872-7) Avail: NTIS HC/MF A01

The characterization of the structure and chemistry of solid/solid interfaces is becoming increasingly important in materials science. Although electron microscopy has contributed a great deal to our present understanding of interfaces, many problems remain to be solved. A recent workshop, held at the National Center for Electron Microscopy in Berkeley examined the field in some detail with the goal of pinpointing the most important problems, present limitations, and future developments. This paper will present a selective illustrated summary of the field on the basis of this workshop. DOE

N91-31976# Argonne National Lab., IL.
Cu-O CHARGE FLUCTUATIONS AND ELECTRON-PHONON COUPLING IN THE EFFECTIVE SINGLE-BAND HUBBARD THEORY FOR CUPRATE SUPERCONDUCTORS
A. J. Fedro and H. B. Schuettler (Georgia Univ., Athens.) 1991 3 p Presented at the International Conference on Materials and Mechanisms of Superconductivity, Kanazawa (Japan), 22-26 Jul. 1991
(Contract W-31-109-eng-38)
(DE91-016526; ANL/CP-72997; CONF-910736-12) Avail: NTIS HC/MF A01

We present results for the effective electronic and breathing mode electron-phonon coupling parameters in an effective single band model for the cuprate materials which explicitly incorporates the lowest energy Cu-O charge excitations of the more complicated multi-band models. We point out the possibility that the cuprates may be close to a phonon-driven charge instability. DOE

N91-31977*# National Aeronautics and Space Administration. Lewis Research Center, Cleveland, OH.
NEAR-EDGE STUDY OF GOLD-SUBSTITUTED YBa2Cu3O(7-DELTA)
Mark W. Ruckman (Brookhaven National Lab., Upton, NY.) and Aloysius F. Hepp Sep. 1991 11 p
(Contracts DE-AC02-76CH-00016; DE-AC05-80ER-10742)
(NASA-TM-105220; E-6509; NAS 1.15:105220) Avail: NTIS HC/MF A03 CSCL 20L

The valence of Cu and Au in YBa2Au0.3Cu2.7O7-delta was investigated using x-ray absorption near edge structure (XANES). X-ray and neutron diffraction studies indicate that Au goes on the Cu(1) site and Cu K-edge XANES shows that this has little effect on the oxidation state of the remaining copper. The Au L3 edge develops a white line feature whose position lies between that of trivalent gold oxide and monovalent potassium gold cyanide, and whose height relative to the edge step is smaller than in the two reference compounds. The appearance of the Au L3 edge suggests that fewer Au 3d states are involved in forming the Au-O bond in YBa2Au0.3Cu2.7O7-delta than in trivalent gold oxide. Author

N91-31978# Sandia National Labs., Albuquerque, NM.
RAPID THERMAL ANNEALING EFFECTS IN In(X)Ga(1-X)As/GaAs STRAINED-LAYER SUPERLATTICES
J. A. Olsen, E. L. Hu, D. R. Myers, J. F. Klem, and A. Skumanich (IBM Research Lab., San Jose, CA.) 1991 6 p Presented at the Spring Meeting of the Materials Research Society (MRS), Anaheim, CA, 19 Apr. - 3 May 1991
(Contract DE-AC04-76DP-00789)
(DE91-015901; SAND-90-3106C; CONF-910406-33) Avail: NTIS HC/MF A02

The effect of repetitive rapid thermal annealing (RTA) at 800 C was investigated in the strained-layer superlattices (SLC's) In(0.2)Ga(0.8)As/GaAs (80 A/80 A)) and In(0.3)Ga(0.7)As/GaAs (80 A/80 A) using photoluminescence (PL) and the highly sensitive absorption technique photothermal deflection spectroscopy (PDS). The samples were repetitively annealed at 800 C for 15 second intervals up to a total time of 45 seconds. Between each anneal, PL spectra were taken at 1.4 K. PL measurements show initial red shifts and subsequent blue shifts with increased annealing times. These shifts were accompanied by a decrease in the intensity of the PL peaks. PDS absorption data were measured at room temperature for the as-grown materials and for the 45 seconds RTA. The PDS data measured at room temperature for 0 and 45 seconds RTA were consistent with the PL data. The spectral shifts may indicate a competition between the effects of thermally driven strain relaxation and chemical interdiffusion. DOE

N91-31979# Los Alamos National Lab., NM.
WEAK LINKS WITHIN A Bi2Sr2Ca1Cu2O(x) SINGLE CRYSTAL BY MAGNETIZATION AND DIRECT OPTICAL OBSERVATIONS
J. O. Willis, N. Nakamura, S. Gotoh, K. Takamuku, N. Koshizuka, and S. Tanaka 1991 3 p Presented at the International Conference on Materials and Mechanisms of Superconductivity, Kanazawa, Japan, 22-26 Jul. 1991
(Contract W-7405-eng-36)
(DE91-016085; LA-UR-91-2120; CONF-910736-8) Avail: NTIS HC/MF A01

We have performed magnetic susceptibility and direct optical High Contrast Magnetic Flux (HICOM) observations on a single crystal of Bi2Sr2CaCu2O(x). Low temperature pinning and high temperature flux creep have been observed by HICOM. The results suggest that the breakdown of flux pinning may occur gradually with temperature and may exhibit spatial variation related to sample inhomogeneities. DOE

N91-31980# Sandia National Labs., Albuquerque, NM.
GROUND-STATE IN-PLANE LIGHT-HOLES IN GaAs/AlGaAs STRUCTURES
E. D. Jones, S. K. Lyo, J. F. Klem, J. E. Schirber, and S. K. Lin (Princeton Univ., NJ.) 1991 8 p Presented at the International Symposium on Gallium Arsenide and Related Compounds, Seattle, WA, 23-26 Sep. 1991
(Contract DE-AC04-76DP-00789)
(DE91-016408; SAND-91-0956C; CONF-9109208-1) Avail: NTIS HC/MF A02

We have performed low-temperature magnetoluminescence, far-infrared cyclotron resonance, and magneto-transport measurements on narrow (4.5 nm) GaAs/Al(0.25)Ga(0.75)As single quantum-wells. The ground state in-plane valence band was found to be light and very nonparabolic, i.e., at zone center, the valence band mass is m(sub v) approx. O(sub .1) and for E(sub f) approx. 10 meV, m(sub v) approx. 0.25. DOE

N91-31981# Brookhaven National Lab., Upton, NY.
SUPERCONDUCTING MAGNET PROGRAM FOR X RAY LITHOGRAPHY SOURCE AT BROOKHAVEN NATIONAL LABORATORY
H. Hsieh, R. Blumberg, R. Heese, J. Murphy, S. Pjerov, S. Sharma, E. M. W. Leung, S. Kalsi, and M. F. Reusch (Grumman Aerospace Corp., Bethpage, NY.) 1991 4 p Presented at the 1991 Institute of Electrical and Electronics Engineers (IEEE) Particle Accelerator Conference (PAC), San Francisco, CA, 6-9 May 1991
(Contract DE-AC02-76CH-00016)
(DE91-016995; BNL-46475; CONF-910505-394) Avail: NTIS HC/MF A01

Brookhaven National Laboratory is funded by DOD-DARPA to develop a compact electron storage ring to be used as a X Ray source for producing high density computer chips. The circumference of this machine is 8.5 meters, the machine lattice consists of four quadrupoles, two sextupoles and a pair of air-core combined function 3.87 Tesla superconducting dipoles. BNL is developing the superconducting dipoles in collaboration with its industrial partners GDSSD and GSED. The field characteristics and engineering realization of these magnets is described and the status of the program is presented. DOE

N91-31982# Brookhaven National Lab., Upton, NY.
REVIEW OF VACUUM SYSTEMS FOR X RAY LITHOGRAPHY LIGHT SOURCES
J. C. Schuchman 1990 14 p Presented at the 37th National American Vacuum Society Symposium, Toronto, Ontario, 8-12 Oct. 1990
(Contract DE-AC02-76CH-00016)
(DE91-017008; BNL-46470; CONF-901035-19) Avail: NTIS HC/MF A03

Vacuum systems for X-Ray lithography light sources are reviewed. Conventional machines and compact machines (machines using superconducting magnets) are included. The vacuum systems are described and compared with regard to basic machine parameters, pumping systems, types of pumps, chamber design and material, gauging and diagnostics, and machine performance. DOE

N91-31983# Stanford Univ., CA.
LIMITED REACTION PROCESSING FOR SEMICONDUCTOR MATERIALS PREPARATION Final Report, 1 Nov. 1987 - 31 May 1991
J. L. Hoyt 26 Jul. 1991 12 p
(Contracts DAAL03-88-K-0020; DAAL03-88-G-0001)
(AD-A239639; ARO-25611.1-EL) Avail: NTIS HC/MF A03 CSCL 20/2

Limited Reaction Processing (LRP) is a layer deposition technique based upon a combination of rapid thermal processing (RTP) and chemical vapor deposition. The versatility of LRP was shwon in research on epitaxial growth in three different materials systems. Research was spurred at several other laboratories in the area of epitaxial growth and applications involving RTP techniques, particularly in the Si(1-x)Ge(x) materials system. The first CVD grown Si/Si(1-x)Ge(x) heterojunction bipolar transistors were fabricated using this technique, with maximum oscillation frequencies on the order of 40 GHz. In the III-V area, arsine alternative sources were explored for GaAs expitaxy which greatly improve the safety of MOCVD. A new atomic layer growth technique was developed by combining LRP with an alternating gas pulse method. GRA

N91-31984# California Univ., Los Angeles.
EPITAXIAL GROWTH AND ELECTRO-OPTICAL PROPERTIES OF METAL GaAs SUPERLATTICES Report, 1 Jun. 1990 - 31 May 1991
Kang L. Wang and R. S. Williams 31 May 1991 12 p
(Contract N00014-90-J-1761)
(AD-A239719) Avail: NTIS HC/MF A03 CSCL 20/12

The following subject areas are covered: epitaxial growth and electro-optical properties of metal GaAs superlattices; electrical resistivity, magnetic susceptibility and thermoelectric power of PtGa2; electronic structure study of the Pt-Ga intermetallic thin films on GaAs (100) using X-ray photoemission spectroscopy; RHEED studies of epitaxial growth of CoGa on GaAs by MBE-determination of epitaxial phases and orientations; internal photoemission in CoGa/GaAs Schottky barriers, possible injection of electrons into the L valley; chemistry of metal/compound-semiconductor interfaces; phase stability versus the lattice mismatch of (100)Co(1-x)Ga(x) thin films on (100)GaAs; electrical resistivity of ultrathin, epitaxial CoGa on GaAs; and growth and annealing of Co(1-x)Ga(x) thin films on GaAs (100). GRA

77 THERMODYNAMICS AND STATISTICAL PHYSICS

Includes quantum mechanics; theoretical physics; and Bose and Fermi statistics.

For related information see also *25 Inorganic and Physical Chemistry* and *34 Fluid Mechanics and Heat Transfer.*

No abstracts in this category.

80 SOCIAL SCIENCES (GENERAL)

Includes educational matters.

No abstracts in this category.

81 ADMINISTRATION AND MANAGEMENT

Includes management planning and research.

N91-31985# Government-Univ.-Industry Research Roundtable, Washington, DC.

SURVEY TO ASSESS THE USEFULNESS OF TWO MODEL AGREEMENTS FOR UNIVERSITY-INDUSTRY COOPERATIVE RESEARCH

Aug. 1990 17 p Prepared in cooperation with Industrial Research Inst., Inc., New York, NY

(Contract DE-FG05-89ER-75498)

(DE91-013937; DOE/ER-75498/6) Avail: NTIS HC/MF A03

In 1988, the Government-University-Industry Research Roundtable together with the Industrial Research Institute (IRI) published Simplified and Standardized Model Agreements for University-Industry Cooperative Research. Designed to serve as starting points for negotiating the details of research agreements between universities and industry sponsors, the publication includes two model agreements: a research grant and a research agreement. Their purpose was to decrease the time and effort required for such negotiations and to provide companies and universities new to research alliances a sense of what is reasonable to consider in establishing an agreement. Over 14,000 copies of the Model Agreements document have been distributed. To assess the extent to which the two models have fulfilled their intended purpose, and to determine what additional steps, if any, the roundtable can take to clarify operating procedures and minimize administrative burdens and requirements for university-industry research partnerships, the roundtable staff conducted a telephone survey in the fall of 1989 of about 70 university and industry users of the model agreements document. In addition to assessing the usefulness of the model agreements, survey participants suggested potential follow-on activities for the roundtable on issues of intellectual property and licensing. This document summarizes the results of the survey. DOE

N91-31986# Government-Univ.-Industry Research Roundtable, Washington, DC.

WHAT IS THE FEDERAL DEMONSTRATION PROJECT?

1990 14 p

(Contract DE-FG05-89ER-75498)

(DE91-013936; DOE/ER-75498/5) Avail: NTIS HC/MF A03

The Federal Demonstration Project is a cooperative effort between a number of universities, a private research institute, and several federal agencies to increase research productivity by eliminating unnecessary administrative procedures and by streamlining and standardizing needed controls. The Project aims to locate responsibility for decision-making as close as possible to principal investigators while maintaining necessary institutional and agency oversight to ensure accountability. By freeing researchers from some of their paperwork burden, more efficient research administration systems will enable investigators to spend more of their time doing science and engineering. The Federal Demonstration Project is an outgrowth of an earlier activity sponsored by five major federal R&D agencies at the Florida State University System and the University of Miami. In Florida, the focus was on standardizing and streamlining procedures for administering research grants after the grants had been awarded to the universities. In May 1988, the most successful of the demonstrated procedures were approved by the US Office of Management and Budget for use in grants awarded by any federal agency to any research organization. The new procedures give agencies authority to waive requirements that grantees obtain federal approval prior to taking a number of administrative actions with respect to grant management. The FDP institutions together with the participating federal agencies are designing and demonstrating innovative research administration procedures and are assessing the impact of those new procedures. DOE

N91-31987# Manchester Univ. (England). School of Management.

A STUDY OF THE LOGISTICS FUNCTION WITHIN A MEDIUM SIZED, SALES ORIENTED CHEMICAL COMPANY M.S. Thesis

S. Oakley Oct. 1990 255 p

(ETN-91-99983) Copyright Avail: NTIS HC/MF A12

The extent to which logistics integration has been achieved in a medium sized, sales oriented chemical company which is committed to technical excellence and customer service as its principal competitive strategic tools is examined. Particular reference is made to the need to develop interdepartmental communications and to rationalize the way in which IT (Information Technology) is used within the firm. The relationships with outside third party service providers is examined and commented upon. The research finds that internal linkages within the company are not well developed, that an unusual line management organization leads to warehouse inefficiencies, that the computer system in use is hampered by an overdependence on manual interfacing and that a review of the transport/firm interface is necessary to release economies of scale and to prepare for the SEM. The lack of IT in one department is shown to be exacerbating an organizational anomaly, especially where the dispatch of samples is concerned. Suggestions for remedies are given and areas of related future research made. ESA

N91-31988# Sandia Labs., Albuquerque, NM.

IMPROVING MANAGERS' EFFECTIVENESS

M. R. James 1991 9 p Presented at the IEEE USA's Biennial Careers Conference, Denver, CO, 10 Oct. 1991

(Contract DE-AC04-76DP-00789)

(DE91-016405; SAND-91-1784C; CONF-9110171-1) Avail: NTIS HC/MF A02

Upward Feedback is a program that gives employees and opportunity to anonymously provide their manager with feedback concerning the manager's job performance. It is an opportunity for managers to receive confidential feedback evaluating their

implementation of corporate values and management behaviors as perceived by those who work for them. This feedback can come from employees who report directly to the manager, that is, one level below them (referred to as direct reports), or from those two reporting levels below them (referred to as skip-level reports). Managers then share information with their employees in feedback meetings and develop action plans to address areas of concern. Sandia National Laboratories has developed and implemented an Upward Feedback Pilot Program and follow up survey. This paper discussed the program and the lessons learned. DOE

82 DOCUMENTATION AND INFORMATION SCIENCE

Includes information management; information storage and retrieval technology; technical writing; graphic arts; and micrography.

For computer documentation see *61 Computer Programming and Software.*

N91-31989 Indiana Univ., Bloomington.
THE RELATIONSHIP BETWEEN THE USE OF US GOVERNMENT TECHNICAL REPORTS BY US AEROSPACE ENGINEERS AND SCIENTISTS AND SELECTED INSTITUTIONAL AND SOCIAMETRIC VARIABLES Ph.D. Thesis
Thomas Edward Pinelli 1990 354 p
Avail: Univ. Microfilms Order No. DA9119754

A study was undertaken that studied the relationship between the use of U.S. government technical reports by U.S. aerospace engineers and scientists and selected institutional and sociometric variables. Two sets of variables were studied. The first set, identified as institutional or structural variables, included the following six: level of education, academic preparation, year of professional aerospace work experience, type of organization, professional duty, and technical discipline. The second set, identified as sociometric or source selection variables, included the following seven: accessibility, ease of use, expense, familiarity or experience, technical quality or reliability, comprehensiveness, and relevance. The goal of the study was to determine which variables explain the use of U.S. government technical reports by U.S. aerospace engineers and scientists. The results indicate that the institutional variables best explain the use of U.S. government technical reports. Dissert. Abstr.

N91-31990 Rochester Univ., NY.
OPTIMAL CONFIGURATION OF DISTRIBUTED DATABASE SYSTEMS Ph.D. Thesis
Myung Whan Suh 1991 193 p
Avail: Univ. Microfilms Order No. DA9119486

The objective was to investigate the optimal configuration of distributed database systems. A series of mathematical models were formulated to determine the best configuration of data processing facilities as well as the best allocation of data and applications. Heuristics and branch and bound procedure are proposed to solve the limited models that were developed, and tested extensively on randomly generated data. By comparing different strategies of replicated primary database only vs. two-tiered with single primary database vs. two-tiered with replicated under various situations, some useful guidelines are obtained for efficient configuration of distributed databases in a general context. The functional design issues regarding concurrency and failure control and distributed query processing are also discussed in order to identify their effects on optimal configuration of distributed database systems. Author

N91-31991 University of Southwestern Louisiana, Lafayette.
CLUSTER-BASED ADAPTIVE INFORMATION RETRIEVAL Ph.D. Thesis
Jayanarayan Bhuyan 1990 194 p
Avail: Univ. Microfilms Order No. DA9119523

A complete Information Retrieval system is designed and evaluated in which the feedback from a number of users of the system, about its performance (global feedback), is stored in the form of clusters called user-oriented clusters. These clusters are used in answering a query in conjunction with feedback obtained about the system's performance after a partial retrieval for that query (local feedback). The classification schemes are developed in 2 stages. The first stage involves the accumulation of relevance judgement provided by users vis-a-vis past query instances. The second stage consists of the identification of clusters. Once the clusters are formed, two methods are developed for searching the clusters relevant to a user's query. In one method, called Retrieval without cluster characterization, a probabilistic model in which the information in the feedback accumulation stage is used to determine the probability of relevance of a query to a cluster is developed. In the other, the description of documents is taken into account in order to describe the clusters, and use traditional vector space model for retrieval purposes. Dissert. Abstr.

N91-31992 Arizona Univ., Tucson.
INTERACTIVE RETRIEVAL IN INFORMATION SPACES DISTRIBUTED ACROSS A WIDE-AREA NETWORK Ph.D. Thesis
Bruce Raymond Schatz 1991 152 p
Avail: Univ. Microfilms Order No. DA9121550

The potential to provide interactive data control across high speed nationwide networks is stimulating development of new data base technology. An information space is a data model that can support rapid browsing of large amounts of information contained in a digital library physically distributed across many disparate sources. Supporting interactive retrieval of objects inside an information space across the nationwide scientific network is discussed. Implementing such interactive retrieval requires designing caching policies that enable fetching requested objects into a local user workstation from a remote file server with sufficiently short response time to support effective browsing interaction. An adequate caching policy should use properties of user perception and data representation within an information space. A series of new techniques are described for caching objects within an information space and measurements are given of their performance across the NSFNET. A prototype, the Telesophy System, supports interactive retrieval for information spaces across local area networks and serves as a basis for identification of special features. Dissert. Abstr.

N91-31993 Massachusetts Univ., Amherst.
INFERENCE NETWORKS FOR DOCUMENT RETRIEVAL Ph.D. Thesis
Howard Robert Turtle 1991 211 p
Avail: Univ. Microfilms Order No. DA9120950

Information retrieval is concerned with selecting documents from a collection that will be of interest to a user with a stated information need or query. Research aimed at improving the performance or retrieval systems, that is, selecting those documents most likely to match the user's information need, remains an area of considerable theoretical and practical importance. A new formal retrieval model that uses probabilistic inference networks to represent documents and information needs. Retrieval is viewed as an evidential reasoning process in which multiple sources of evidence about document and query content are combined to estimate the probability that a given document matches a query. This model generalizes several current retrieval models and provides a framework within which disparate information retrieval research results can be integrated. To test the effectiveness of the inference network model, a retrieval system based on the model was implemented. Two test collections were built and used to compare retrieval performance with that of conventional retrieval models. The inference network model gives substantial improvements in retrieval performance with computational costs that are comparable to those associated conventional retrieval models and which are feasible for large collections. Dissert. Abstr.

N91-31994 Politecnico di Milano (Italy). Lab. di Calcolatori.
THE DESIGN OF AN INTEGRITY CONSISTENCY CHECKER (ICC) FOR AN OBJECT ORIENTED DATABASE SYSTEM
Christine Delcourt (GIP Altair, France) and Roberto Zicari 29 Nov. 1990 28 p
(Rept-91-021; ETN-91-99767) Avail: Politecnico di Milano, Piazzo Leonardo da Vinci 32, 20133 Milan, Italy

Schema evolution is an important facility in object oriented databases. Updates should not result in inconsistencies either in the schema or in the database. A tool called ICC, which ensures the structural consistency when updating an object oriented database system is presented. The tool is implemented to evaluate the correctness of schema updates for the O2 object oriented database system. ESA

N91-31995 Politecnico di Milano (Italy). Dipartimento di Elettronica.
HYPERTEXT DEVELOPMENT USING A MODEL-BASED APPROACH
Andrea Caloini, Franca Garzotto, Paolo Paolini, and Daniel Schwabe (Pontificia Univ. Catolica, Rio de Janeiro, Brazil) 1990 42 p Sponsored in part by Instituto de Pesquisas Espaciais
(Rept-90-074; ETN-91-99515) Avail: Politecnico di Milano, Piazza Leonardo da Vinci 32, 20133 Milan, Italy

Hypertext development is still for the most part at the handcrafting level, where each hypertext document must be hand designed. A compiler which takes hyperdocuments designed using a model based approach and generates stacks executable in HyperCard is presented. This compiler is implemented in standard SQL over a relational database representation of a hyperdocument designed using the Hypermedia Design Model (HDM). The compiling approach, even though illustrated with HDM, can be used with any structures design methodology. ESA

N91-31996# Nijmegen Univ. (Netherlands). Dept. of Informatics.
FORMALISATION OF TECHNIQUES: CHOPPING DOWN THE METHODOLOGY JUNGLE
T. P. vanderWeide and A. H. M. terHofstede 14 Dec. 1990 23 p Sponsored in part by Software Engineering Research Center
(TR-90-26; ETN-91-99588) Avail: NTIS HC/MF A03

Formalization of techniques in the context of information system development methodologies is discussed. When such methodologies are developed, the primary goal is applicability. After the methodology has proven itself in practice, the methodology will be applied in more sophisticated situations, pushing the methodology to its limits. In those cases, informal definitions are known to be inappropriate. Some typical problems are addressed and a procedure for proper formalization is described. The predicator model is presented as an extended example. Some experiences with this approach to formalization are described. ESA

N91-31997# Utrecht State Univ. (Netherlands). Dept. of Computer Science.
CONTINUOUS INFORMATIONS SYSTEMS
R. Hoofman 31 Jul. 1990 30 p
(RUU-CS-90-25; ISSN-0924-3275; ETN-91-99591) Avail: NTIS HC/MF A03

The motion of an algebraic information system is generalized to that of a continuous information system. Just as algebraic information systems are concrete representations of bounded complete algebraic dcpo's (Scott domains), continuous information systems are concrete representations of bounded complete continuous dcpo's. A certain subclass of information systems, consisting of the so called qualitative information systems, which corresponds to the class of qualitative domains, is basic in the sense that all other information systems are generated by this class. It follows that the category of bounded complete continuous dcpo's and continuous functions is equivalent to the Karoubi envelope of the category of qualitative domains and continuous functions. It is shown how certain constructions on qualitative information systems (such as product and function space) can be translated to constructions on continuous information systems. The category of qualitative domains and continuous functions is proved to be a semi Cartesian closed category. Two universal information systems are defined. ESA

N91-31998# Geological Survey, Denver, CO.
GEOTRANS: AN INTERFACE PROGRAM FROM GEOPROGRAM TO A GEOGRAPHIC INFORMATION SYSTEM
S. P. Schilling 1991 89 p
(Contract DE-AI08-78ET-44802)
(DE91-016111; USGS-OFR-90-615) Avail: NTIS HC/MF A05

The U.S. Geological Survey Plotter Lab., Denver, CO, has created a computer program to translate data from GEOPROGRAM recording files to a geographic information system (GIS) and a relational database. The program, GEOTRANS, takes files recorded on a Kern DSR 11 Analytical Plotter and translates the coordinate information into the KORK Geographic Information System (KGIS) and places the non-coordinate information into ORACLE, a relational database program. The advantage of linking the data collection capabilities of GEOPROGRAM with KGIS and ORACLE is to offer geologists a means of merging, editing, and querying coordinate and relational databases online. GEOTRANS is written in Pascal v.3.8 running under the DEC VMS operating system on a Microvax II computer. The program is structured in such a manner as to facilitate converting and restructuring of the program to translate 3-D coordinate and attribute data collected with an analytical plotter to either 3-D or other 2-D GIS. This report describes how files from GEOPROGRAM are read, how 2-D topology is created, and how GEOTRANS procedures and various calls to libraries transform and insert dat to the proper place. A user's manual is included to run GEOTRANS. DOE

N91-31999# General Accounting Office, Washington, DC. National Security and International Affairs Div.
ACQUISITION REFORM: IMPLEMENTING DEFENSE MANAGEMENT REVIEW INITIATIVES. REPORT TO THE CHAIRMAN AND RANKING MINORITY MEMBER, SUBCOMMITTEE ON DEFENSE INDUSTRY AND TECHNOLOGY, SENATE COMMITTEE ON ARMED SERVICES
Aug. 1991 14 p
(AD-A239423; GAO/NSIAD-91-269) Avail: NTIS HC/MF A03 CSCL 15/5

DOD has made several of the changes to its acquisition system that were recommended by the Packard Commission. DOD, for example, has streamlined the acquisition management structure, established the position of Under Secretary of Defense for Acquisition, and limited formal reporting requirements. The Packard Commission concluded that DOD's acquisition system had become an increasingly bureaucratic and overregulated process in which acquisition policy making and program management responsibility were fragmented and diluted. The Commission painted, in its words, a 'stark' picture of a highly competitive acquisition system in which program managers, buffeted by numerous internal and external pressures, become 'supplicants' for, rather than managers of, major new defense systems. These competitive pressures resulted in a huckster psychology that leads program managers to optimistically interpret information about a system's cost, schedule, and performance. GRA

N91-32000# Naval Postgraduate School, Monterey, CA.
EXPLOITING CAPTIONS FOR ACCESS TO MULTIMEDIA DATABASES Progress Report, Mar. 1990 - Mar. 1991
Neil C. Rowe and Eugene J. Guglielmo Apr. 1991 33 p
(AD-A239435; NPSCS-91-012) Avail: NTIS HC/MF A03 CSCL 05/7

Descriptive captions help organize noncompetitive media. But automated use of captions in retrieval from computerized multimedia databases has not been much examined because it would seem to require significant natural language processing. We argue that captions can be naturally expressed in a restricted language whose interpretation is easier than general natural-language understanding. We describe a multimedia

database system that stores interpreted captions in predicate calculus for each media datum; it then interprets restricted-language queries, and finds matching media objects. GRA

N91-32001# Harvard Univ., Cambridge, MA. Dept. of Statistics.
RESEARCH IN REGRESSION, INFORMATION RETRIEVAL, INVERSION OF NOISY TRANSFORMS, AND STOCHASTIC CONTROL Final Report, 1 Apr. 1986 - 31 Mar. 1991
Herman Chernoff 30 May 1991 7 p
(Contract N00014-86-K-0246)
(AD-A239490) Avail: NTIS HC/MF A02 CSCL 12/3

One of the first reports, directed at the study of movement of ice, attempted to measure a rigid body motion based on noisy observations at two distinct times of observable points on the rigid body. The noise makes the measured locations subject to the error and may lead to missing some of the points which are not distinguishable from one another. Computer intensive methods appeared in three reports. One involves resampling methods for time series. A second involves the use of simple programs which are computer intensive to provide useful, if not optimal, estimates of parameters of complex models by relatively simple means. A third involves the numerical solution of Bayes sequential decision problems applied to the bioequivalence problems. Some work was done and will soon be completed on an astronomical problem involving apparent superluminal motion. Recently a good deal of effort has been devoted to some problems from molecular biology. GRA

83 ECONOMICS AND COST ANALYSIS

Includes cost effectiveness studies.

No abstracts in this category.

84 LAW, POLITICAL SCIENCE AND SPACE POLICY

Includes NASA appropriation hearings; aviation law; space law and policy; international law; international cooperation; and patent policy.

No abstracts in this category.

85 URBAN TECHNOLOGY AND TRANSPORTATION

Includes applications of space technology to urban problems; technology transfer; technology assessment; and surface and mass transportation.

For related information see also *03 Air Transportation and Safety, 16 Space Transportation,* and *44 Energy Production and Conversion.*

No abstracts in this category.

88 SPACE SCIENCES (GENERAL)

N91-32002# Max-Planck-Inst. fuer Physik und Astrophysik, Garching (Germany, F.R.). Inst. fuer Extraterrestrische Physik.
[ACTIVITIES REPORT OF THE INSTITUTE OF EXTRATERRESTRIAL PHYSICS] Annual Report, 1990 [INSTITUT FUER EXTRATERRESTRISCHE PHYSIK, TAETIGKEITSBERICHT 1990]
Jan. 1991 166 p In GERMAN
(MPE-223; ISSN-0173-699X; ETN-91-99737) Copyright Avail: NTIS HC/MF A08

The scientific and technical activities of the Max Planck Institute are described. The progress achieved in 1990 in the five following experimental fields is reported: near earth space and solar system, e.g., plasma physics and energetic particles; infrared and submillimeter astronomy; X ray astronomy; gamma astronomy; and labor astrophysics. International cooperation and cooperation with other German institutes and with companies are outlined. The three main themes dealt with were protoplanetary discs, lunar X ray emissions, and active galactic nuclei. ESA

89 ASTRONOMY

Includes radio, gamma-ray, and infrared astronomy, and astrometry.

N91-32003*# National Aeronautics and Space Administration. Goddard Space Flight Center, Greenbelt, MD.
AN ATLAS OF STELLAR SPECTRA BETWEEN 2.00 AND 2.45 MICROMETERS (ARNAUD, GILMORE, AND COLLIER CAMERON 1989)
Wayne N. Warren, Jr. Jan. 1990 13 p Previous announced in IAA as A89-35191
(NASA-TM-105044; NAS 1.15:105044;
NSSDC-WDC-A-R/S-90-02) Avail: NTIS HC/MF A03 CSCL 03A

The machine-readable version of the atlas, as it is currently being distributed from the Astronomical Data Center, is described. The atlas represent a collection of spectra in the wavelength range 2.00 to 2.45 micros having a resolution of approximately 0.02 micron. The sample of 73 stars includes a supergiant, giants, dwarfs, and subdwarfs with a chemical abundance range of about -2 to +0.5 dex. Author

N91-32004 Catholic Univ. of America, Washington, DC.
ULTRAVIOLET MORPHOLOGY OF NGC 1068: THE STARBURST KNOTS AND THE EXTENDED EMISSION REGION Ph.D. Thesis
Khong Quang Truong 1991 145 p
Avail: Univ. Microfilms Order No. DA9119788

Observations of the inner 3 kpc region of NGC 1068 with the International Ultraviolet Explorer satellite indicate very bright starburst knots of early-type stellar population. These knots likely represent the most luminous H II regions yet studied at optical and ultraviolet wavelengths. Moreover, the total observed flux of the knots at 1350A exceed that of the nucleus of this galaxy. The UV spectra clearly show that the starburst knots have undergone recent intense star formation. The stellar population of the knots is dominated by luminous B0-B1 supergiants with ages less than 10(exp 7) yrs. The UV emission morphology of the inner disk of NGC 1068 also reveals extremely strong emission of the highly ionized species. The emission is also seen enhanced at positions corresponding to the knots. Dissert. Abstr.

N91-32005 Indiana Univ., Bloomington.
A SPECTROPHOTOMETRIC STUDY OF THE SECONDARIES OF ALGOL SYSTEMS Ph.D. Thesis
Tae Seog Yoon 1991 226 p
Avail: Univ. Microfilms Order No. DA9120517

Time resolved spectra of short time (P less than 6 days) Algol binary star systems obtained during total eclipse are used to study

the spectral types and the carbon abundance (from the G band feature of the CH molecule) of the mass losing secondary star. The spectral classifications used a new quantitative calibration of the strengths of absorption features in standard stars and in the program stars. IRAF software was used to obtain equivalent widths for numerous atomic lines and the CH molecular band near 4300A. Spectral types of Algol secondaries were obtained by comparing with both main sequence and giant stars. Carbon depletions are deduced from a calibration of G band strength and carbon abundance using abundance standard stars as well as synthetic spectra from model atmospheres. Most Algol secondaries are found to have carbon depletion compared with normal G, K-type giants. Dissert. Abstr.

N91-32006*# National Aeronautics and Space Administration. Marshall Space Flight Center, Huntsville, AL.
DEVELOPMENT OF THE BURST AND TRANSIENT SOURCE EXPERIMENT (BATSE)
J. M. Horack Sep. 1991 322 p
(NASA-RP-1268; M-668; NAS 1.61-1268) Avail: NTIS HC/MF A14 CSCL 03A

The Burst and Transient Source Experiment (BATSE), one of four instruments on the Gamma Ray Observatory, consists of eight identical detector modules mounted on the corners of the spacecraft. Developed at MSFC, BATSE is the most sensitive gamma ray burst detector flown to date. Details of the assembly and test phase of the flight hardware development are presented. Results and descriptions of calibrations performed at MSFC, TRW, and KSC are documented extensively. With the presentation of each calibration results, the reader is provided with the means to access raw calibration data for further review or analysis. Author

N91-32007*# Computer Sciences Corp., Laurel, MD.
THE IN-FLIGHT CALIBRATION OF THE HUBBLE SPACE TELESCOPE ATTITUDE SENSORS
Gary L. Welter 3 Jun. 1991 28 p Presented at the 3rd International Symposium on Spacecraft Flight Dynamics, Darmstadt, Federal Rep. of Germany, 30 Sep. - 4 Oct. 1991
(Contract NAS5-31500)
(NASA-CR-183485; NAS 1.26:183485) Avail: NTIS HC/MF A03 CSCL 03A

A detailed review of the in-flight calibration of the Hubble Space Telescope attitude sensors is given. The review, which covers the period from the April 24, 1990 launch of the spacecraft until April 1991, describes the calibrations required and accuracies achieved for the four principal attitude sensing systems on the spacecraft: the magnetometers, the fixed-head star trackers, the gyroscopes, and the fine guidance sensors. Author

N91-32008# Royal Observatory, Edinburgh (Scotland).
UKIRT OBSERVER'S MANUAL
J. K. Davies, ed. Apr. 1991 80 p
(ETN-91-99747) Avail: NTIS HC/MF A05

The United Kingdom 3.8 m Infrared Telescope (UKIRT) located at the summit of Mauna Kea on the big island of Hawaii is described. Summit sky conditions are photometric more than half the time and spectroscopic more than three quaters of the time. Photometry through all atmospheric windows in the 1 to 30 micrometer range and spectroscopy in the 1 to 5 micrometer range are possible. The telescope is equipped with a 1 to 5 micrometer infrared camera housing a 58 by 62 element detector array. Other individual instruments and aspects of operation at the telescope are described. ESA

N91-32009* Max-Planck-Inst. fuer Physik und Astrophysik, Garching (Germany, F.R.).
A SURVEY OF THE 158 MICRON CII FINE-STRUCTURE LINE IN THE CENTRAL 50 PC OF THE GALAXY
A. Poglitsch, G. J. Stacey, N. Geis, M. Haggerty, J. Jackson, M. Rumitz, R. Genzel, and C. H. Townes (California Univ., Berkeley.) Nov. 1990 20 p Submitted for publication
(Grant NAG2-208)
(NASA-CR-188912; NAS 1.26:188912; MPE-Preprint-197; ETN-91-90018) Copyright Avail: Fachinformationszentrum Karlsruhe, 7514 Eggenstein-Leopoldshafen 2, Fed. Republic of Germany CSCL 03A

An extensive velocity resolved survey at 1 minute resolution of 158 microns CII fine structure line emission in the central 50 pc of the Galaxy is reported. Spectra were taken toward about 625 positions with a new imaging far infrared spectrometer on board the NASA Kuiper Airborne Observatory. Observations and results are given and discussed under the following headings: mass and luminosity of CII in the central 50 pc; CII emission from the SgrA complex; the relationship between SgrA and the radio arc; CII emission and galactic center molecular clouds; and mass accretion into the circumnuclear region. ESA

N91-32010# California Univ., Berkeley. Lawrence Berkeley Lab.
THE BERKELEY SEARCH FOR DISTANT SUPERNOVAE TO MEASURE OMEGA Progress Report
C. Pennypacker, S. Perlmutter, G. Goldhaber, H. Marvin, R. Muller, and B. J. Boyle (Cambridge Univ., England) Mar. 1991 5 p Presented at the Distribution of Matter in the Universe Conference, Meudon (France), 6 Mar. 1991
(Contract DE-AC03-76SF-00098)
(DE91-016418; LBL-30946; CONF-9103196-1) Avail: NTIS HC/MF A01

Over the past two years, in collaboration with the Anglo-Australian Observatory, we have constructed a prototype version of the hardware and software needed to discover distant supernovae for a measurement of (Omega), the ratio of the average density of the universe to the critical density. To make this measurement, we will use Type Ia supernova, which are now thought to be adequate standard candles for this purpose. DOE

N91-32011# Air Force Inst. of Tech., Wright-Patterson AFB, OH.
A SEARCH FOR PERIODICITY IN THE X RAY SPECTRUM OF BLACK HOLE CANDIDATE A0620-00 M.S. Thesis
Kenneth Plaks Jun. 1991 77 p
(AD-A239488; AFIT/CI/CIA-91-063) Avail: NTIS HC/MF A05 CSCL 03/1

Using archival data from the MIT X-Ray Observatory on board the SAS-3 satellite, we have produced refined X-ray light curves of the X-ray nova A0620-00 during its initial outburst and subsequent decay. We use data from similar observations of the Crab Nebula to generate elevation dependent response functions for the SAS-3 detectors and to develop objective criteria for perfecting the A0620 data in the energy ranges 1.3 - 5 keV and 5 - 13 keV. We then analyzed the A0620 light curves and the hardness ratio for evidence of periodicity. In particular, we searched for evidence of the 7.75h orbital period found in optical observations by McClintock and Remillard (1986). Using a Monte Carlo simulation, we showed that the 3 sigma upper limit on the amplitude of oscillation in the harness ratio is 3.2 percent. We also searched for the 7.8d period reported by Matilsky et al. (1976). We found three cycles of a 7.8d oscillation in a 22 day section of the data with a approximately 40 percent amplitude. However, in the remainder of the data, in excess of 200 days, we were able to place 3 sigma upper limits on the intensity amplitude of 2.2 percent before the section and 7.3 percent after. We therefore find no evidence to substantiate a persistent 7.8 day period. We conclude that the system exhibits little to no persistent X-ray periodicity at any frequency. We also conclude that high inclination angle models of the system where the accretion disk is fed via Roche lobe overflow are not appropriate. GRA

90 ASTROPHYSICS

Includes cosmology; celestial mechanics; space plasmas; and interstellar and interplanetary gases and dust.
For related information see also *75 Plasma Physics.*

N91-32012*# Computer Sciences Corp., Calverton, MD. System Sciences Div.
RESEARCH STUDIES WITH THE INTERNATIONAL ULTRAVIOLET EXPLORER Final Report, 19 Jun. 1985 - 2 May 1991
2 May 1991 133 p
(Contract NAS5-28749)
(NASA-CR-183495; NAS 1.26:183495) Avail: NTIS HC/MF A07 CSCL 03B

The IUE research studies comprises 118 separate research programs involving observations, data analysis, and research conducted of the IUE satellite and the NASA Astrophysics Data Program. Herein are presented 92 programs. For each program there is a title, program ID, name of the investigator, statement of work, summary of results, and list of publications. Author

N91-32013 Princeton Univ., NJ.
HYDRODYNAMIC SIMULATIONS OF COSMOLOGY Ph.D. Thesis
Renyue Cen 1990 258 p
Avail: Univ. Microfilms Order No. DA9112948

A hydrodynamic code for evolving self-gravitating cosmological systems is described. The code may be coupled with a standard particle code, e.g., a particle-mesh code designed for engineering hydrodynamical applications. The resolution of the code is a few cells, giving accuracy of one to three percent. A standard PM particle code is also described. Researchers tracked six species, computing ionization and recombination processes, as well as line and continuum heating and cooling. The background radiation field is determined in the range 1eV to 100KeV, allowing for absorption, emission, and cosmological effects. Researchers show how the numerical inaccuracies can be estimated and to some extent overcome. Dissert. Abstr.

N91-32014 Maryland Univ., College Park.
A STUDY OF A 21-cm-SELECTED SAMPLE OF GALAXIES Ph.D. Thesis
Patricia A. Henning 1990 193 p
Avail: Univ. Microfilms Order No. DA9121350

Discussed here is a pilot survey for galaxies at 21 cm conducted with the National Radio Astronomy Observatory's 300 foot telescope. The survey was done to test the feasibility of finding unseen galaxies through the detection of the radiation emitted by neutral hydrogen. This blind search method is appropriate in optically obscured regions because the long wavelength radiation from neutral hydrogen is not blocked by interstellar dust in the Milky Way. As a control experiment, the same style of search was conducted in unobscured parts of the sky. Dissert. Abstr.

N91-32015 Rochester Univ., NY.
MAGNETIC FIELD DECAY IN NEUTRON STARS WITH SUPERCONDUCTING CORES Ph.D. Thesis
Charles Edward Wendell 1991 132 p
Avail: Univ. Microfilms Order No. DA9119491

Observations of pulsars suggest that the magnetic fields in neutron stars decay exponentially on time scales of approx. 10(exp 7) yr. The magnetic flux in the superconducting cores of neutron stars takes the form of quantized flux tubes, which are buoyant. The hypothesis is explored that these tubes float rapidly up to the crust of the star, where ohmic dissipation reduces the field at the observed rate. The various forces are calculated which were acting on a flux tube (buoyancy, drag, tension, and interaction pressure), and an equation of motion was derived for flux tubes. This equation is solved in realistic neutron star models, assuming that the ends of the tubes are fixed at the base of the crust. The tubes rise to the crust in roughly 10(exp 6) yr, forming a compressed mat of flux. Dissert. Abstr.

N91-32016# California Univ., Berkeley. Lawrence Berkeley Lab.
NUCLEAR AND PARTICLE ASTROPHYSICS
N. K. Glendenning 31 Oct. 1990 80 p Presented at the Conference on Structure of Hadrons and Hadronic Matter, Dronten (Netherlands), 14-17 Aug. 1990
(Contract DE-AC03-76SF-00098)
(DE91-016260; LBL-29415; CONF-9008166-2) Avail: NTIS HC/MF A05

We discuss the physics of matter that is relevant to the structure of compact stars. This includes nuclear, neutron star matter and quark matter and phase transitions between them. Many aspects of neutron star structure and its dependence on a number of physical assumptions about nuclear matter properties and hyperon couplings are investigated. We also discuss the prospects for obtaining constraints on the equation of state from astrophysical sources. Neutron star masses although few are known at present, provide a very direct constraint in as much as the connection to the equation of state involves only the assumption that Einstein's general theory of relativity is correct at the macroscopic scale. Supernovae simulations involve such a plethora of physical processes including those involved in the evolution of the precollapse configuration, not all of them known or understood, that they provide no constraint at the present time. Indeed the prompt explosion, from which a constraint had been thought to follow, is now believed not to be mechanism by which most, if any stars, explode. In any case the nuclear equation of state is but one of a multitude of uncertain factors, and possibly one of the least important. The rapid rotation of pulsars is also discussed. It is shown that for periods below a certain limit it becomes increasingly difficult to reconcile them with neutron stars. Strange stars are possible if strange matter is the absolute ground state. We discuss such stars and their compatibility with observation. DOE

N91-32017 Max-Planck-Inst. fuer Physik und Astrophysik, Garching (Germany, F.R.).
EVOLUTIONARY POPULATION SYNTHESIS IN STARBURST REGIONS
J. M. MasHesse and Daniel Kunth (Institut d'Astrophysique, Paris, France) Nov. 1990 122 p Submitted for publication
Sponsored by MEC and CAYCIT
(MPE-Preprint-198; ETN-91-90019) Copyright Avail: Fachinformationszentrum Karlsruhe, 7514
Eggenstein-Lepoldschafen 2, Fed. Republic of Germany

A set of evolutionary population synthesis models which are used to study the properties of the star formation episodes taking place in starburst regions are presented. The compilation of stellar parameters used are described and the way of evaluating the different observational parameters and their interest is discussed. The evolution with time of predicted parameters and their dependence on the star formation scanario is shown and their sensitivity to variations in the interplanetary magnetic field, star formation rate and metallicity is discussed. ESA

N91-32018# California Univ., Berkeley. Lawrence Berkeley Lab.
FAST PULSARS, VARIATIONAL BOUND, OTHER FACETS OF COMPACT STARS
N. K. Glendenning 1 May 1991 13 p Presented at the Workshop on Strange Quark Matter in Physics and Astrophysics, Aarhus (Denmark), 20-24 May 1991
(Contract DE-AC03-76SF-00098)
(DE91-016416; LBL-30878; CONF-9105243-1) Avail: NTIS HC/MF A03

We derive a limit on the rotation period of a gravitationally bound star that is analogous to Ruffini's mass limit for a neutron star. We discuss the impact of gravitational radiation-reaction instabilities. The condition that self-bound stars can rotate faster is derived. The present status of searches for fast pulsars is reviewed. The composition of neutron stars is discussed in the context of nuclear and hypernuclear constraints. The phase transition from hadron to quark phase in the interior of dense

neutron stars is discussed properly accounting for the fact that this first order phase transition involves two conserved charges. Hybrid stars are then described. DOE

91 LUNAR AND PLANETARY EXPLORATION

Includes planetology; and manned and unmanned flights.

For spacecraft design or space stations see *18 Spacecraft Design, Testing and Performance.*

N91-32019 Texas Univ., Austin.
THE MOTIONS OF MARS' POLE Ph.D. Thesis
James Lindsay Hilton 1990 264 p
Avail: Univ. Microfilms Order No. DA9116873

The change in the orientation of the planet Mars as a function of time is studied. This analysis includes corrections for the elasticity of the planet and the existence of a liquid core. The rate of precession is 7 sec 295 + or - 0.012 sec/yr; based on an inertia ratio of 0.3654. All nutations with an amplitude of 0.001 sec or larger are calculated. Although both of Mars' satellites are very small and have orbits nearly in the plane of Mars' equator, each satellite produces one nutation in both longitude and obliquity larger than 0.001 sec in amplitude. The nutations caused by the martian satellites are driven by the motions of the nodes of the satellite orbits. The uncertainty in Mars' inertia ratio is the primary source of uncertainty in the precession period and nutation amplitudes. The elastic planet models are more rigid than the Earth because of Mars' smaller mean radius. The rigidity and the greater oblateness of Mars combine to greatly reduce the effect of planetary structure on Mars' Chandler wobble. The Chandler wobble period is found to be 154.6 days for the rigid planet model and about 165 days for the elastic planet model. Dissert. Abstr.

92 SOLAR PHYSICS

Includes solar activity, solar flares, solar radiation and sunspots.

For related information see *93 Space Radiation.*

N91-32020*# National Aeronautics and Space Administration. Goddard Space Flight Center, Greenbelt, MD.
THE Li-7 AND Be-7 DEEXCITATION LINES: PROBES FOR ACCELERATED PARTICLE TRANSPORT MODELS IN SOLAR FLARES
Ronald J. Murphy, X-M, Hua, B. Kozlovsky (Tel-Aviv Univ., Israel), and R. Ramaty 25 Jul. 1989 20 p
(Contract NAS5-30534)
(NASA-CR-183490; NAS 1.26:183490) Avail: NTIS HC/MF A03 CSCL 03B

The photon energy spectrum of a spectral feature composed of the 429 and 478 keV gamma-ray lines from Li-7 and Be-7 (produced by interactions of flare-accelerated alpha particles with ambient He in the solar atmosphere) depends on the angular distribution of the interacting accelerated particles. This spectrum is calculated for limb and disc-centered flares using a loop model for the transport of the ions. In this model, the flux tube magnetic field is constant in the corona and converges in the chromosphere to the photosphere. Magnetic mirroring and MHD pitch-angle scattering are both taken into account. Comparison of these results with data from other experiments is presented. Author

N91-32021*# Hulburt (E. O.) Center for Space Research, Washington, DC.
GRO SOURCE CANDIDATES: (A) NEARBY MODEST-SIZE MOLECULAR CLOUDS; (B) PULSAR WITH WOLF-RAYET COMPANION THAT HAS LOST ITS H-ENVELOPE
R. Silberberg and Ronald J. Murphy (Universities Space Research Association, Washington, DC.) 1989 7 p
(Contract NAS5-30534)
(NASA-CR-183491; NAS 1.26:183491) Avail: NTIS HC/MF A02

Within 100 pc of the sun there are over a hundred cirrus clouds with masses of approx. 60 solar mass and dense molecular clouds with masses of approx. 4 solar mass. If the local interstellar density of cosmic rays is also present in these clouds, the flux of neutral pion from the decay of gamma rays from the core of a cloud at a distance of 20 pc is approx. 13 x 10(exp -8) photons/sq cm/s. The flux from the more extensive cirrus cloud is approx 4 x 10(exp -7) photons/sq cm/s. A relativistic beam of particles generated by a compact stellar object and incident upon a large, close companion can be a strong gamma ray line source if more of the beam energy is used in interactions with C and O and heavier nuclei and less with H and He. This would be the case if the companion has lost its hydrogen envelope and nucleosynthesized much of its He into C, O, and Ne. Such objects are Wolf-Rayet stars and it is believed that some Wolf-Rayet stars do, in fact, have compact companions. For a beam of protons of 10(exp 37) erg/s, the flux at 1 kpc of the 4.4 MeV C-12 line could be as high as 5 x 10(exp -6) photons/sq cm/s. The fluxes of the deexcitation lines from the spallation products of O-16 are also presented. Author

N91-32022*# Universities Space Research Association, Washington, DC.
ABUNDANCES FROM SOLAR FLARE LINE SPECTROSCOPY Final Report
Ronald J. Murphy 25 Jul. 1989 8 p
(Contract NAS5-30534)
(NASA-CR-183492; NAS 1.26:183492) Avail: NTIS HC/MF A02

Updating and improvement of computer codes used in the abundance analyses of solar-flare gamma-ray data are described. These modifications are itemized in detail. The abundance analysis technique was then applied to data obtained by the Gamma-Ray Spectrometer of the Solar Maximum Mission spacecraft for the 27 April 1981 solar flare to set constraints on the interacting-particle angular distribution. The results are presented. Research in several other areas was also performed and they are discussed. Author

93 SPACE RADIATION

Includes cosmic radiation; and inner and outer earth's radiation belts.

For biological effects of radiation see *52 Aerospace Medicine.* For theory see *73 Nuclear and High-Energy Physics.*

No abstracts in this category.

99 GENERAL

N91-32023# Keuring van Electrotechnische Materialen N.V., Arnhem (Netherlands).
KEMA SCIENTIFIC AND TECHNICAL REPORTS, VOLUME 8, NUMBER 2, 1990
A. J. vanLoon, ed. Apr. 1990 67 p
(ST-Rept-Vol-8-No-2; ISSN-0167-8590; ETN-91-90007) Avail: NTIS HC/MF A04

Reports on both pure and applied research carried out in the fields related to the generation and distribution of electricity are compiled. The following subject areas are covered: experiments on ultrasonic thermometry for wet-ash coal gasification; the critical temperature for drying-out of soils around power cables as a function of local conditions; the selective catalytic oxidation of ammonia to N2 and H2O over silica supported molybdena catalysts; a system to determine whole-plant exchange rates of ozone, carbon dioxide and water vapor; measurements of inception time lags of repetitively pulsed corona in air; some applications of X-ray photoelectron spectroscopy and secondary-ion spectrometry; and

adjustment of the mixing-rate constant in the eddy breakup model for a jet flame. For individual titles, see N91-32024 through N91-32030.

N91-32024# Keuring van Electrotechnische Materialen N.V., Arnhem (Netherlands). Dept. of Physical Research.
EXPERIMENTS ON ULTRASONIC THERMOMETRY FOR WET-ASH COAL GASIFICATION **c35**
K. Schoonderwoerd and R. Hunik *In its* KEMA Scientific Reports, Volume 8, Number 2, 1990 Apr. 1990 p 81-96 (For primary document see N91-32023 23-99)
Avail: NTIS HC/MF A04

Ultrasonic thermometry may be a solution for the problem of temperature monitoring of the reactor in a coal gasification plant. The technique offers fast determination of the temperature profile along a line by measurement of the propagation velocity of an ultrasonic signal through a thin massive rod with a number of reflecting nodges. The thermometer rod in a wet ash gasifier becomes covered with slag, which disturbs the calibration of the rod by hundreds of kelvins. This disturbance was modeled theoretically, and verified for coal slag in laboratory experiments at ambient temperature with simulation liquids. A correction mechanism for this disturbance is suggested that is based on the viscous and elastic properties of the coal slag. A method to measure these properties is demonstrated. ESA

N91-32025# Keuring van Electrotechnische Materialen N.V., Arnhem (Netherlands). Dept. of Physical Research.
THE CRITICAL TEMPERATURE FOR DRYING-OUT OF SOILS AROUND POWER CABLES AS A FUNCTION OF LOCAL CONDITIONS **c31**
G. Koopmans and J. Kuiper *In its* KEMA Scientific Reports, Volume 8, Number 2, 1990 Apr. 1990 p 97-103 (For primary document see N91-32023 23-99)
Avail: NTIS HC/MF A04

Approximate expressions are developed for the critical temperature at which drying out starts around power cables buried in sandy soils. This temperature is a key parameter in the two layer (Cox/Coates) model, accepted as a simplified calculation method for thermal rating of buried power cables. The expressions for the critical temperature were arrived at by fitting data obtained from calculations with a previously published model that is based on the equations of Philip and De Vries. One single and three equally loaded cables in flat formation were considered under various geometric and ambient conditions. The principle parameters in the expressions fitted are ambient thermal resistivity and ambient section tension. A practical method was developed for indicating how to obtain the highest values of these parameters from a soil survey along the cable route. ESA

N91-32026# Keuring van Electrotechnische Materialen N.V., Arnhem (Netherlands). Dept. of Chemical Research.
THE SELECTIVE CATALYTIC OXIDATION OF AMMONIA TO N2 AND H2O OVER SILICA-SUPPORTED MOLYBDENA CATALYSTS **c25**
F. J. J. G. Janssen and J. J. P. Biermann *In its* KEMA Scientific Reports, Volume 8, Number 2, 1990 Apr. 1990 p 105-108 (For primary document see N91-32023 23-99)
Avail: NTIS HC/MF A04

The behavior of molybdena catalysts was studied with respect to the oxidation of ammonia. The catalysts were prepared according to two techniques: homogeneous deposition precipitation, and incipient wetness precipitation. In both techniques, the materials were dried and calcinated. Mo(3+) was used as precursor in both types of preparation. Mo(3+) was obtained by electrochemical reduction of Mo(6+). Ammonia can be oxidized to nitrogen and water over MoO3 on SiO2 catalysts if the amount of MoO3 present in the catalyst is greater than 15 by weight. The reaction of NH3 and O2 was carried out in both the presence and the absence of NO. The presence of NO in the feed influenced neither the conversion of ammonia nor the selectivity for nitrogen. The yield (activity selectivity) of nitrogen was maximum when lead was present in the catalysts. ESA

N91-32027# Keuring van Electrotechnische Materialen N.V., Arnhem (Netherlands). Dept. of Environment Research.
A SYSTEM TO DETERMINE WHOLE-PLANT EXCHANGE RATES OF OZONE, CARBON DIOXIDE AND WATER VAPOUR **c51**
J. M. M. Aben *In its* KEMA Scientific Reports, Volume 8, Number 2, 1990 Apr. 1990 p 109-120 (For primary document see N91-32023 23-99)
Avail: NTIS HC/MF A04

A whole plant gas exchange system was developed for the determination of ozone uptake, photosynthesis, respiration and transpiration. Performance studies showed that the boundary layer resistance was sufficiently low to allow accurate determination of the influence of environmental conditions on gas exchange. Ozone degradation at the inner surfaces of the chamber depended on air humidity but was always sufficiently low to enable accurate determination of the ozone flux to the plant and the influence on it of environmental factors. Both short term and long term stability were very good, facilitating the detection of small changes in gas exchange and favoring the performance of long experiments. Applications of the system in air pollutant research are illustrated. ESA

N91-32028# Technische Univ., Eindhoven (Netherlands). Faculty of Electrical Engineering.
MEASUREMENTS OF INCEPTION TIME LAGS OF REPETITIVELY PULSED CORONA IN AIR **c33**
E. M. vanVeldhuizen, W. R. Rutgers, and R. P. Dahiya (Indian Inst. of Tech., New Delhi.) *In* Keuring van Electrotechnische Materialen N.V., KEMA Scientific Reports, Volume 8, Number 2, 1990 Apr. 1990 p 121-129 Sponsored by Keuring van Electrotechnische Materialen N.V. (For primary document see N91-32023 23-99)
Avail: NTIS HC/MF A04

An optical detection system was used to measure corona inception in a coaxial configuration in air at ambient conditions. The time lag for primary corona was determined for various forms of electrical energization. Electrical pulses of positive and negative polarity were used with a rise time of 3 micros, a decay time of 300 micros and a repetition frequency of 2 Hz. The amplitude of the pulses was varied from inception to breakdown, in combination with a DC bias. ESA

N91-32029# Keuring van Electrotechnische Materialen N.V., Arnhem (Netherlands). Dept. of Chemical Research.
SOME APPLICATIONS OF X-RAY PHOTOELECTRON SPECTROSCOPY AND SECONDARY-ION MASS SPECTROSCOPY **c25**
F. J. J. G. Janssen and H. M. Weijers *In its* KEMA Scientific Reports, Volume 8, Number 2, 1990 Apr. 1990 p 131-141 (For primary document see N91-32023 23-99)
Avail: NTIS HC/MF A04

The advantages that X-ray Photoelectron Spectroscopy (XPS), Auger electron spectroscopy and Secondary-Ion Mass Spectroscopy (SIMS) offer for the physicochemical characterization of materials used in the electrical industry are described. Applications of these techniques regard fly ash, gypsum from flue gas desulfurization plants, catalysts for the selective catalytic reduction of NOx in flue gas, corrosion studies and the consequences of adhesion. Examples are given of the use of the technique and some difficulties encountered during measurements are discussed. ESA

N91-32030# International Flame Research Foundation, Ijmuiden (Netherlands).
ADJUSTMENT OF THE MIXING-RATE CONSTANT IN THE EDDY BREAK-UP MODEL FOR A JET FLAME **c25**
B. M. Visser and G. Koopmans (Keuring van Electrotechnische Materialen N.V., Arnhem, Netherlands) *In* Keuring van Electrotechnische Materialen N.V., KEMA Scientific Reports, Volume 8, Number 2, 1990 Apr. 1990 p 143-147 (For primary document see N91-32023 23-99)
Avail: NTIS HC/MF A04

The eddy breakup model is widely used for the calculation of the gas phase combustion rate in flames. The value of the mixing rate constant in this model is verified by comparison of model based predictions with experimental data obtained for CO combustion in a small jet. It was recently observed that the model overpredicts combustion rates by a factor of about 7 for semi industrial swirling pulverized coal flames. The value obtained for the mixing rate constant for these flames was in the range 0.5 to 0.7, rather than the usually applied value of 4. It is now shown that accurate predictions for the CO combustion experiment can be obtained only with a mixing rate constant of 0.6. This value is consistent with the observed values. It thus seems that the lower value for the mixing rate constant should be applied more generally. ESA

N91-32031# Lawrence Livermore National Lab., CA.
ENERGY AND TECHNOLOGY REVIEW, FEBRUARY-MARCH L991
K. C. Johnson, ed., L. deVore, ed., K. Gleason, ed., N. M. Sanford, ed., and P. T. VanDyke, ed. Mar. 1991 45 p
(Contract W-7405-eng-48)
(DE91-015487; UCRL-52000-91-2/3) Avail: NTIS HC/MF A03

This review contains four articles: (1) The Chemical Kinetics of Engine Knock. Kinetic models were developed of hydrocarbon oxidation (combustion) that have revealed a great deal about engine knock. It was learned how and why such factors as molecular size and structure influence knock tendency and, therefore, octane rating. (2) Interface Science: The Next Frontier in Materials Research. Interface science has recently become established as a technical discipline within the realm of materials research. First principles models were developed of the properties of materials interfaces and comparing them to high resolution electron micrography images of bicrystals to test and validate predictions. Ultimately, it is hoped to develop these capabilities to the point that it will be possible to produce materials by design. (3) The Ultrahigh Vacuum Diffusion Bonding Machine: An ultrahigh vacuum diffusion bonding machine was designed and built for installation at LLNL with which will be produced a variety of bicrystals. (4) Laser Driven X Ray Lithography of Integrated Circuits: LLNL scientist were working cooperatively with Hampshire Instruments to develop a commercially viable laser driven x ray lithography system. DOE

Typical Subject Index Listing

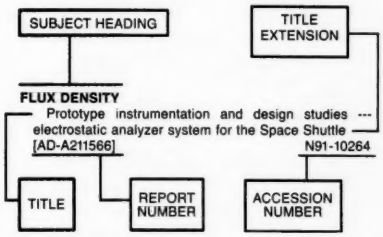

The subject heading is a key to the subject content of the document. Titles, report numbers, and accession numbers of pertinent documents are provided under each subject heading. When the title is insufficiently descriptive of the document content, a title extension has been added, separated from the title by three hyphens. The report number helps to indicate the type of document cited (e.g., NASA report, NASA translation, NASA contractor report). The accession number is the number by which the document abstracts are arranged in this journal and by which the document is sold or requested. The titles, with title extensions if present, are arranged under each subject heading in ascending accession number order. The subject headings have been selected from the latest revision of the *NASA Thesaurus*.

A

ABILITIES
Optimizing the long-term retention of skills: Structural and analytic approaches to skill maintenance 3
[AD-A239574] N91-31773
ABLATION
Laser deposition of cubic boron nitride on electronic materials
[AD-A238313] N91-31249
Laser ablation mechanisms and optical surface damage
[DE91-016928] N91-31642
ABSORPTION SPECTROSCOPY
Determination of aqueous processable photoresist in tin-lead plating solutions
[DE91-015575] N91-31251
Experimental determination of the temperature and density of opacity samples
[DE91-015686] N91-31252
X ray and gamma ray spectroscopy of solids under pressure
[DE91-016948] N91-31263
ABSTRACTS
Technical abstracts: Mechanical engineering, 1990
[DE91-016502] N91-31658
ABUNDANCE
An atlas of stellar spectra between 2.00 and 2.45 micrometers (Arnaud, Gilmore, and Collier Cameron 1989)
[NASA-TM-105044] N91-32003
A spectrophotometric study of the secondaries of Algol systems N91-32005
Abundances from solar flare line spectroscopy
[NASA-CR-183492] N91-32022
ACCELERATED LIFE TESTS
Accelerated aging and discharge of lithium/thionyl-chloride D cells
[DE91-012649] N91-31517
ACCELERATION (PHYSICS)
Vibration analysis of the SA349/2 helicopter
[NASA-TM-102794] N91-31078
A new model of the electron: A suggested experiment to search for a link between electromagnetism and gravity N91-31738
Acceleration using total internal reflection
[DE91-016612] N91-31942
ACCELERATION STRESSES (PHYSIOLOGY)
The G-LOC syndrome
[AD-A239561] N91-31768
ACCELERATION TOLERANCE
Aircrew critique of high-G centrifuge training. Part 1: What was the best part of the program?
[AD-A239781] N91-31809
ACCELEROMETERS
Measurement of six component efforts in transition flow
[AAAF-NT-89-01] N91-31097
Force reconstruction using the inverse of the mode-shape matrix
[DE91-016407] N91-31689
ACCEPTOR MATERIALS
The photovoltaic effect on pyroelectics N91-31707
ACCRETION DISKS
A search for periodicity in the x ray spectrum of black hole candidate A0620-00
[AD-A239488] N91-32011
ACCUMULATORS
The 1991 DOE/Sandia Crystalline Photovoltaic Technology Project Review Meeting
[DE91-016062] N91-31703
ACCURACY
Accuracy of laser velocimetry N91-31622
ACETYLENE
Sensitivity of imaging materials to electron beam irradiation
[AD-A239365] N91-31612
ACOUSTIC ATTENUATION
Assessing the efficacy of active noise reduction
[CTN-91-60200] N91-31922
ACOUSTIC EXCITATION
Mobility power flow analysis of coupled plate structure subjected to mechanical and acoustics excitation
[NASA-CR-188791] N91-31678
Fuselage shell and cavity response measurements on a DC-9 test section
[NASA-CR-187557] N91-31926
ACOUSTIC LEVITATION
Acoustic positioning of a molten alloy sample (TEXUS 1) N91-31464
Acoustic positioning (TEXUS 9) ESA N91-31465
Containerless solidification of a Pd-Cu-Si sample (TEXUS 9) ESA N91-31466
Acoustic positioning (TEXUS 14b) ESA N91-31467
Containerless undercooling of a Pd-Cu-Si alloy (TEXUS 14b) ESA N91-31468
ACOUSTIC PROPAGATION
Three dimensional acoustic propagation at low temperature altitude
[ONERA-RT-13/3641-PY] N91-31924
Use of an ARMA model in turbulent medium acoustic propagation
[ONERA-RF-14/3641-PY] N91-31925
ACOUSTIC VELOCITY
Elastic wave dispersion in high-strength ceramics
[DE91-016648] N91-31309
ACOUSTICS
Acoustic mixing (TEXUS 5) N91-31423
Solidification of immiscible alloys (TEXUS 8) N91-31424
Mobility power flow analysis of coupled plate structure subjected to mechanical and acoustics excitation
[NASA-CR-188791] N91-31678
A comparison of time domain boundary conditions for acoustic waves in wave guides
[NASA-CR-187618] N91-31889
ACOUSTO-OPTICS
Hybrid electro-optic processor
[AD-A239547] N91-31505
ACTINIDE SERIES
Summaries of FY 1991 research in the chemical sciences
[DE91-011221] N91-31222
ACTIVE CONTROL
Reusable rocket engine intelligent control system framework design, phase 2
[NASA-CR-187213] N91-31219
Advanced optical sensing and processing technologies for the distributed control of large flexible spacecraft
[NASA-CR-4399] N91-31609
ACTIVITY (BIOLOGY)
Electron microscopy to correlate cell structures and biochemical activity
[AD-A239640] N91-31758
ACTS
Interim Service ISDN Satellite (ISIS) network model for advanced satellite designs and experiments
[NASA-CR-186565] N91-31488
ACTUATION
Real time actuating of laser power and scanning velocity for thermal regulation during laser hardening
[ETN-91-99908] N91-31636
ACTUATORS
Robotic tool change mechanism
[NASA-CASE-GSC-13239-1] N91-31656
ADA (PROGRAMMING LANGUAGE)
Construction and realization of distributed multiprocessor systems for real time tasks
[MBB-UA-1189-90-PUB] N91-31871
ADAPTIVE CONTROL
Convergence performance of adaptive detectors, part 2
[AD-A239532] N91-31540
Adaptive function allocation for intelligent cockpits
[AD-A239714] N91-31808
Neural network based model reference adaptive control N91-31877
Small time step adaptive control: Theory and application to an electric furnace
[ECL-90-17] N91-31883
Cluster-based adaptive information retrieval N91-31991
ADAPTIVE FILTERS
High speed digital direct access filter for tracking or excision of parametric signal data
[PATENT-1-271-231] N91-31511
Convergence performance of adaptive detectors, part 1
[AD-A239507] N91-31539
ADAPTIVE OPTICS
An adaptive coherent optical receiver array
[AD-A239672] N91-31644
Small time step adaptive control: Theory and application to an electric furnace
[ECL-90-17] N91-31883
ADDITIVES
Rapidly solidified nickel aluminide of improved stoichiometry and ductilization
[PATENT-1-257-987] N91-31270
Method for imparting strength to intermetallic phases
[PATENT-1-255-929] N91-31271
Floating zone growth of GaAs crystals (TEXUS 20) N91-31386
ADHESION
Icing research related to engine icing characteristics N91-31168
Adhesion of thick layer systems on ceramic based precious metals in hybrid microelectronic circuits
[MBB-UA-1191-90-PUB] N91-31304
Ion beam enhanced adhesion of iron films to sapphire substrates
[DE91-015931] N91-31308
Adhesion of metals on ceramic substrates (MASER 2) ESA N91-31463
ADHESIVE BONDING
Effect of porcelain surface pretreatments on composite resin-porcelain shear bond strength
[AD-A239359] N91-31241
Influence of adhesive polymerization conditions on the durability of adhesive joints
[DCR/I-03357-90] N91-31305

ADHESIVES
Influence of adhesive polymerization conditions on the durability of adhesive joints
[DCR/I-03357-90] N91-31305
ADSORPTION
The chemistry of transition metal clusters
[DE91-015108] N91-31250
AERIAL EXPLOSIONS
Calculation of fragment ejection velocities on explosion of a launcher
[CNES-NT-128] N91-31195
AERIAL PHOTOGRAPHY
Stereophotogrammetric surveying and interpreting method, and interpreting apparatus
[PATENT-1-254-651] N91-31693
The implementation of a quality system in an aerial mapping company
[ETN-91-99424] N91-31695
Examination and mapping of forest damage, using remote sensing methods
[ETN-91-99741] N91-31696
AEROACOUSTICS
NASA Aerodynamics Program
[NASA-TM-4312] N91-31751
AERODYNAMIC CHARACTERISTICS
Conditional sampling
[AAAF-NT-89-04] N91-31099
AERODYNAMIC COEFFICIENTS
Measurement of six component efforts in transition flow
[AAAF-NT-89-01] N91-31097
Second generation supersonic transport aircraft: Low speed aerodynamics
[AAAF-NT-89-02] N91-31137
AERODYNAMIC CONFIGURATIONS
Computational analysis of hypersonic flows past elliptic-cone waveriders N91-31080
Aerothermodynamical project of hypersonic projectiles
[MBB-UA-1193-90-PUB] N91-31086
Activities report of the National Aerospace Laboratory
[ETN-91-99438] N91-31132
Development of an advanced panel method for complex configurations in subsonic compressible flow; application to the computation of the potential flow through ducts
[NLR-TR-88001-U] N91-31579
Algorithms for finding an optimal matching between a given string and a string generated by a regular grammar
[MEMO-921] N91-31845
AERODYNAMIC DRAG
Application of semianalytic satellite theory to maneuver planning
[AD-A239417] N91-31205
Control of oscillatory forces on a circular cylinder by rotation
[NASA-CR-187619] N91-31576
AERODYNAMIC FORCES
RADAC model deformation measurement system: First results at the F1 wind tunnel
[AAAF-NT-89-03] N91-31098
AERODYNAMIC HEATING
Predicted thermal response of a cryogenic fuel tank exposed to simulated aerodynamic heating profiles with different cryogens and fill levels
[NASA-CR-4395] N91-31470
AERODYNAMIC NOISE
User's manual for the Langley boundary layer noise propagation program (MRS-BLP)
[NASA-CR-187559] N91-31923
A parametric study of transonic blade-vortex interaction noise
[NASA-CR-188811] N91-31928
AERODYNAMIC STABILITY
Robustness and techniques of multivariable control for helicopter piloting. Dispatch 3: Inclusion regions technique on linear model
[RD/PA-14-227] N91-31184
AERODYNAMICS
Model of an aerospace plane based on an idealized cone-derived waverider forebody N91-31129
Activities report of the National Aerospace Laboratory
[ETN-91-99438] N91-31132
Flow visualization and simulation
[AAAF-NT-89-18] N91-31590
Postprocessing of test and computation results by the wavelet method
[AAAF-NT-89-24] N91-31591
Postprocessing of experimental and numerical results in the case of two and three dimensional flows
[AAAF-NT-89-25] N91-31592
NASA Aerodynamics Program
[NASA-TM-4312] N91-31751
AEROELASTICITY
User's guide to a system of finite-element supersonic panel flutter programs
[NASA-TM-104109] N91-31082
Compressible two dimensional boundary layer strong perfect fluid coupling in the case of sharp leading edge profiles. Stationary case
[ONERA-RT-42/1621-RY-093-R] N91-31586
AERONAUTICAL SATELLITES
Aeronautical Mobile Satellite Service (AMSS) test plan
[DOT/FAA/CT-TN91/20] N91-31495
AEROSOLS
Chemical characterization of aerosol particles by Raman spectroscopy
[DE91-015836] N91-31720
Retrieval and molecule sensitivity studies for the global ozone monitoring experiment and the scanning imaging absorption spectrometer for atmospheric chartography N91-31724
AEROSPACE ENGINEERING
Reliability of computational analysis of plasticity problems
[AD-A239646] N91-31691
AEROSPACE ENVIRONMENTS
Study of space qualification specifications
[CTN-91-60201] N91-31199
AEROSPACE MEDICINE
Aerospace medicine and biology: A continuing bibliography with indexes (supplement 353)
[NASA-SP-7011(353)] N91-31760
AEROSPACE PLANES
Model of an aerospace plane based on an idealized cone-derived waverider forebody N91-31129
AEROSPACE VEHICLES
An investigation of dual-mode operation of a nuclear-thermal rocket engine
[DE91-015977] N91-31210
Composite flexible blanket insulation
[NASA-CASE-NPO-11907-1-NP] N91-31236
Large Angle Transient Dynamics (LATDYN) demonstration problem manual
[NASA-CR-4400] N91-31684
Range reference atmosphere, Fairbanks, Alaska
[AD-A239520] N91-31739
Range reference atmosphere Wake Island, North Pacific
[AD-A239602] N91-31740
NASA Aerodynamics Program
[NASA-TM-4312] N91-31751
AEROTHERMODYNAMICS
Aerothermodynamical project of hypersonic projectiles
[MBB-UA-1193-90-PUB] N91-31086
Viscous effects
[MBB-FE202/S/PUB/441] N91-31088
A relative-intensity two-color phosphor thermography system
[NASA-TM-104123] N91-31595
Post processing of three dimensional aerothermal computation
[AAAF-NT-89-21] N91-31848
AGING (MATERIALS)
Accelerated aging and discharge of lithium/thionyl-chloride D cells
[DE91-012649] N91-31517
AGING (METALLURGY)
Fatigue-resistant nickel-base superalloys
[PATENT-1-253-363] N91-31268
AGRICULTURE
Simulated effects of a doubling of carbon dioxide on corn production in portions of the central US
[DE91-016843] N91-31722
Biomass production and nitrogen dynamics in an integrated aquaculture/agriculture system N91-31789
AIR FLOW
Icing test programmes and techniques N91-31171
AIR INTAKES
ATSF supersonic aircraft intake. Review of the analyses of some particular problems, technical summary
[ONERA-RTS-134/2149-AY-640-A] N91-31094
Vulnerability of a small powerplant to wet snow conditions N91-31148
Ice tolerant engine inlet screens for CH113/113A search and rescue helicopters N91-31149
AIR NAVIGATION
Development of a geographic navigational display device for general aviation aircraft
[PB91-170282] N91-31114
AIR POLLUTION
Global model simulations of the long range transport of soot and sulfur from the Kuwait oil fires
[DE91-015771] N91-31719
AIR TRAFFIC CONTROL
Bayesian multi-sensor tracking for advanced air-traffic control systems
[NLR-MP-88056-U] N91-31119
Flight tests with a data link used for air traffic control information exchange
[NASA-TP-3135] N91-31143
AIR TRANSPORTATION
Annual review of aircraft accident data. US air carrier operations, calendar year 1988
[PB91-176040] N91-31110
AIRBORNE EQUIPMENT
Airborne rescue system
[NASA-CASE-ARC-11909-1] N91-31113
Large scale CAESAR images using inertial navigation and pressure altitude measurement. Accuracy deformations and possibilities for a Global Positioning System (GPS)
[ETN-91-99418] N91-31117
Airborne ESM receivers: Techniques and technologies
[ETN-91-99988] N91-31498
Examination and mapping of forest damage, using remote sensing methods
[ETN-91-99741] N91-31696
AIRCRAFT ACCIDENT INVESTIGATION
Annual review of aircraft accident data. US air carrier operations, calendar year 1988
[PB91-176040] N91-31110
AIRCRAFT ACCIDENTS
Beacon activation device
[PATENT-1-256-916] N91-31108
Annual review of aircraft accident data. US air carrier operations, calendar year 1988
[PB91-176040] N91-31110
Cockpit resource management: Effects on behavioral interactions across airlines and aircraft types
[AD-A239467] N91-31804
AIRCRAFT CARRIERS
Effect of wind over deck conditions on aircraft approach speeds for carrier landings
[AD-A239511] N91-31141
AIRCRAFT COMPARTMENTS
Analysis of interior noise ground and flight test data for advanced turboprop aircraft applications
[NASA-CR-187558] N91-31927
AIRCRAFT CONFIGURATIONS
Noxious matter minimization as a project criterion for aircraft
[MBB-Z-0337-90-PUB] N91-31134
AIRCRAFT CONSTRUCTION MATERIALS
Enhanced fighter maneuverability aircraft (X-31A) wing and thrust vectoring vane design
[MBB-FE22/S/PUB/0433/A] N91-31135
Field evaluation of six protective coatings applied to T56 turbine blades after 500 hours of engine use
[ARL-MAT-TM-405] N91-31179
Fatigue-resistant nickel-base superalloys
[PATENT-1-253-363] N91-31268
Composite ingot casting
[PATENT-1-250-128] N91-31269
AIRCRAFT CONTROL
Rotatable non-circular forebody flow controller
[NASA-CASE-LAR-14212-1-CU] N91-31140
AIRCRAFT DESIGN
Laser velocimetry at the CEAT aerodynamic group: Application to unsteady measurements on a fluid flap profile
[AAAF-NT-89-05] N91-31100
Design and testing of a multiblock grid-generation procedure for aircraft design and research
[NLR-TP-89146-U] N91-31131
Activities report of the National Aerospace Laboratory
[ETN-91-99438] N91-31132
Enhanced fighter maneuverability aircraft (X-31A) wing and thrust vectoring vane design
[MBB-FE22/S/PUB/0433/A] N91-31135
AIRCRAFT ENGINES
Inlet edge funnel of a civil aircraft gondola engine
[ETN-91-99775] N91-31130
Low Temperature Environment Operations of Turboengines (Design and User's Problems)
[AGARD-CP-480] N91-31144
Cold starting small gas turbines: An overview N91-31150
Cold start optimization on a military jet engine N91-31151
Cold weather ignition characteristics of advanced small gas turbine combustion systems N91-31152
Control system design considerations for starting turbo-engines during cold weather operation N91-31155
Cold start development of modern small gas turbine engines at Pratt and Whitney Aircraft of Canada Ltd. N91-31156
Design considerations based upon low temperature starting tests on military aircraft turbo engines N91-31157
Climatic considerations in the life cycle management of the CF-18 engine N91-31158
Engine icing criticality assessment N91-31161
Fuels and oils as factors in the operation of aero gas turbine engines at low temperatures N91-31163

Icing test capabilities for aircraft propulsion systems at the Arnold Engineering Development Center N91-31170

Developments in icing test techniques for aerospace applications in the RAE Pyestock altitude test facility N91-31173

AIRCRAFT EQUIPMENT

Software quality metrics [DOT/FAA/CT-91/1] N91-31814

AIRCRAFT FUELS

Fuels and oils as factors in the operation of aero gas turbine engines at low temperatures N91-31163

AIRCRAFT ICING

A documentation of vertical and horizontal aircraft soundings of icing relevant cloudphysical parameters N91-31172

AIRCRAFT INSTRUMENTS

Process for detecting the likelihood of ice formation, ice warning system for carrying out the process, and utilization thereof [PATENT-1-250-926] N91-31107

Study of lightning strikes on an aircraft in flight. Electromagnetic measurements [ONERA-RF-25/7234-PY] N91-31111

Study of lightning strikes on an aircraft in flight. Electric measurements [ONERA-RF-98/7154-PY] N91-31112

Development of a geographic navigational display device for general aviation aircraft [PB91-170282] N91-31114

AIRCRAFT LANDING

Effect of wind over deck conditions on aircraft approach speeds for carrier landings [AD-A239511] N91-31141

AIRCRAFT MAINTENANCE

An integer programming model for Navy's maritime patrol aviation fleet [AD-A239464] N91-31079

Low temperature environment operations of turbo engines N91-31146

Climatic considerations in the life cycle management of the CF-18 engine N91-31158

AIRCRAFT MANEUVERS

Bayesian multi-sensor tracking for advanced air-traffic control systems [NLR-MP-88056-U] N91-31119

AIRCRAFT MODELS

The effect of jet bleed on base pressure distribution, shedding frequency, and mean velocity profiles in the wake behind a two-dimensional blunt model [MPIS-12/1990] N91-31085

AIRCRAFT NOISE

Analysis of interior noise ground and flight test data for advanced turboprop aircraft applications [NASA-CR-187558] N91-31927

AIRCRAFT PERFORMANCE

Airplane takeoff and landing performance monitoring system [NASA-CASE-LAR-13854-1-CU] N91-31120

Low temperature environment operations of turbo engines N91-31146

The development of a computational model to predict low temperature fuel flow phenomena N91-31166

A knowledge based application of the extended aircraft interrogation and display system [NASA-TM-4327] N91-31874

AIRCRAFT PILOTS

Aircrew critique of high-G centrifuge training. Part 1: What was the best part of the program? [AD-A239781] N91-31809

AIRCRAFT PRODUCTION

An integer programming model for Navy's maritime patrol aviation fleet [AD-A239464] N91-31079

AIRCRAFT SAFETY

Process for detecting the likelihood of ice formation, ice warning system for carrying out the process, and utilization thereof [PATENT-1-250-926] N91-31107

Annual review of aircraft accident data. US air carrier operations, calendar year 1988 [PB91-176040] N91-31110

Numerical model of evolution in supercooled cloud of water droplets in a case of icing N91-31169

AIRCRAFT STRUCTURES

Method for fastening aircraft frame elements to sandwich skin panels covering same using woven fiber connectors [PATENT-1-274-075] N91-31126

Torsion resistant grooved joint [PATENT-1-258-589] N91-31127

Activities report of the National Aerospace Laboratory [ETN-91-99436] N91-31132

AIRFOIL PROFILES

Exploitation of OAT15A profile tests in the T2 wind tunnel: Experimental determination of the wave drag [ONERA-RSF-88/1685-AY-158-A] N91-31092

Study of the flow around the GARTEUR AD/AG07 wing: First F2 test campaign results [ONERA/DERAT-37/5025-26] N91-31096

Laser velocimetry at the CEAT aerodynamic group: Application to unsteady measurements on a fluid flap profile [AAAF-NT-89-05] N91-31100

Compressible two dimensional boundary layer strong perfect fluid coupling in the case of sharp leading edge profiles. Stationary case [ONERA-RT-42/1621-RY-093-R] N91-31586

Numerical simulation of three dimensional unsteady flow by multiprocessor solving of the Navier-Stokes equations [ETN-91-99974] N91-31594

AIRFOILS

Airfoil-vortex interaction: Unsteady wall pressure measurement [AAAF-NT-89-13] N91-31104

AIRFRAMES

Vibration analysis of the SA349/2 helicopter [NASA-TM-102794] N91-31078

Icing research related to engine icing characteristics N91-31168

Static strain and vibration characteristics of a metal semimonocoque helicopter tail cone of moderate size [NASA-CR-187576] N91-31679

Improved finite-element methods for rotorcraft structures [NASA-TM-104104] N91-31687

AIRPORT PLANNING

The effects of different sequencing strategies on the capacity of airports [DLR-MITT-90-18] N91-31185

AIRPORTS

The effects of different sequencing strategies on the capacity of airports [DLR-MITT-90-18] N91-31185

A knowledge-base for rehabilitation of airfield concrete pavements [AD-A239354] N91-31191

Effects of stress on judgment and decision making in dynamic tasks [AD-A239452] N91-31772

ALGAE

Algae for controlled ecological life support system diet characterization of cyanobacteria 'spirulina' in batch cultures N91-31787

ALGEBRA

An introduction to second moment closure N91-31555

On the expressiveness of equational type logic [MEMO-INF-90-39-REV] N91-31887

ALGORITHMS

A shock-fitting algorithm for the simulation of inviscid flows in chemical non-equilibrium [MBB-UK-0131-90-PUB] N91-31087

Two alternative ways for solving the coordination problem in multilevel optimization [NASA-TM-104036] N91-31138

Inter-GEN: A hybrid approach to engineering design optimization N91-31471

Design of a specific integrated circuit for solving the three dimensional Poisson equation [ECL-90-24] N91-31527

Generalized spatial discretization techniques for space-marching algorithms N91-31546

Three dimensional Euler equation solving on parallel machines [ETN-91-99913] N91-31583

The development of a specific image analysis technique for exploiting flow visualization negatives [AAAF-NT-89-26] N91-31593

Analysis and development of a wide-bandwidth gravitational wave detector N91-31601

A satellite-based radar wind sensor [NASA-CR-188805] N91-31750

Developing dataflow algorithms [DE91-016300] N91-31818

Enhancement of surface definition and gridding in the Eagle code [NASA-CR-188796] N91-31820

The derivation of distributed termination detection algorithms from garbage detection schemes [RUU-CS-90-24] N91-31827

Distributed incremental maximum finding in hierarchically divided graphs [RUU-CS-90-30] N91-31828

The on-line d-dimensional dictionary problem [RUU-CS-90-31] N91-31829

On the efficient incremental evaluation of higher order attribute grammars [RUU-CS-90-36] N91-31832

Approximating treewidth, pathwidth, and minimum elimination tree height [RUU-CS-91-01] N91-31836

The complexity of coloring games on perfect graphs [RUU-CS-91-03] N91-31838

Dynamic output-sensitive hidden surface removal for c-oriented polyhedra [RUU-CS-91-06] N91-31839

An algorithm for spectral factorization of polynomial matrices with any signature [MEMO-912] N91-31842

An algorithm for the one-to-all shortest path problem with arbitrary arc lengths [MEMO-919] N91-31844

Genetic algorithms [ETN-91-99985] N91-31852

Practical aspects of an interior-point method for convex programming [AD-A239457] N91-31858

An application of neural networks to process and materials control [DE91-016016] N91-31886

A dynamically adaptive multigrid algorithm for the incompressible Navier-Stokes equations: Validation and model problems [NASA-CR-187595] N91-31888

Longest segment problems [RUU-CS-90-28] N91-31896

On disjoint cycles [RUU-CS-90-29] N91-31897

Covering a set of points with fixed size hypersquares and related problems [RUU-CS-90-32] N91-31898

Hidden surface removal for c-oriented polyhedra [RUU-CS-90-33] N91-31899

Computing minimum length paths of a given homotopy class [RUU-CS-90-37] N91-31900

Fitting scattered data on spherelike surfaces using tensor products of trigonometric and polynomial splines [MEMO-909] N91-31904

Cluster-based adaptive information retrieval N91-31991

ALKALI METALS

Defect diffusion in ion implanted glasses [DE91-016119] N91-31302

ALKALIES

Self- and interdiffusion in alkali-silicate melts (TEXUS 11 and 12) N91-31366

Self- and interdiffusion in alkali-silicate melts (TEXUS 13) N91-31367

Reaction kinetics in molten glasses: Self-diffusion in alkali-silicate melts (TEXUS 20) N91-31368

ALKALINE BATTERIES

Fuel cells for commercial energy [MBB-UE-0018-90-PUB] N91-31706

ALLOYING

Rapidly solidified nickel aluminide of improved stoichiometry and ductilization [PATENT-1-257-987] N91-31270

Method for imparting strength to intermetallic phases [PATENT-1-255-929] N91-31271

Alloy formation (TEXUS 5) N91-31398

ALLOYS

Alloy formation (TEXUS 5) N91-31398

ALTITUDE

A study of ion acceleration at rocket altitudes and development and calibration of pitch angle imaging charged particle detectors N91-31728

ALTITUDE CONTROL

Large scale CAESAR images using inertial navigation and pressure altitude measurement. Accuracy deformations and possibilities for a Global Positioning System (GPS) [ETN-91-99418] N91-31117

ALTITUDE TESTS

Icing test programmes and techniques N91-31171

Developments in icing test techniques for aerospace applications in the RAE Pyestock altitude test facility N91-31173

ALUMINATES

The development of aluminum-air batteries for application in electric vehicles [DE91-016863] N91-31533

ALUMINIDES

Field evaluation of six protective coatings applied to T56 turbine blades after 500 hours of engine use [ARL-MAT-TM-405] N91-31179

Weldability and hot ductility of iron aluminides [DE91-016343] N91-31280

ALUMINUM

Influence of adhesive polymerization conditions on the durability of adhesive joints [DCR/I-03357-90] N91-31305

Metal matrix composites (TEXUS 14b) N91-31439

Solidification of fine dispersions in microgravity (TEXUS 14b) N91-31441

Contribution to the implementation of a completely in situ device in ultrahigh vacuum for the development of MIS on InP structures: Al2O3/InP interface optimization [ECL-91-04] N91-31526
The development of aluminum-air batteries for application in electric vehicles [DE91-016863] N91-31533

ALUMINUM ALLOYS
Inlet edge funnel of a civil aircraft gondola engine [ETN-91-99775] N91-31130
Composite ingot casting [PATENT-1-250-128] N91-31269
Rapidly solidified nickel aluminide of improved stoichiometry and ductilization [PATENT-1-257-987] N91-31270
Method for imparting strength to intermetallic phases [PATENT-1-255-929] N91-31271
Creep deformation and fracture of a two-phase TiAl intermetallics [DE91-011963] N91-31274
Weldability and hot ductility of iron aluminides [DE91-016343] N91-31280
Theoretical studies of metallic alloys [DE91-016486] N91-31281
Corrosion fatigue crack arrest in aluminium alloys [NLR-MP-88050-U] N91-31282
Development and characterization of low temperature Cu-Al-Be shape memory alloys [ISAL-90-0093] N91-31284
Diffusion of Ni in Cu-Au and Cu-Al alloys (TEXUS 20) N91-31373
Solidification of alloys (TEXUS 2) N91-31401
Directional solidification of Al-Cu alloys (MASER 2) N91-31403
Directional solidification of eutectics (TEXUS 6) N91-31404
Dispersion alloys (TEXUS 7) N91-31412
Al-Pb bearing alloy (TEXUS 1) N91-31413
Immiscible alloy system Al-Pb (TEXUS 7) N91-31422
Demixing of a monotectic ternary alloy (TEXUS 20) N91-31429
Alloys with oxide inclusions (TEXUS 2) N91-31432
Pores in aluminium alloys (TEXUS 3) N91-31447
Preparation of aluminium foams (TEXUS 9) N91-31452
The development of aluminum-air batteries for application in electric vehicles [DE91-016863] N91-31533
Microwave module YAG laser weld development [DE91-015750] N91-31652
Variations in the static properties, unnotched and notched fatigue life behaviour of 13 batches of 2L.65 aluminium alloy extruded bar [ARL-STRUC-R-427] N91-31676

ALUMINUM ARSENIDES
Studies of the III-V compounds in the megabar regime [DE91-015911] N91-31973

ALUMINUM GALLIUM ARSENIDES
Innovative optoelectronic materials and structures using OMVPE [AD-A239518] N91-31951
Ground-state in-plane light-holes in GaAs/AlGaAs structures [DE91-016408] N91-31980

ALUMINUM OXIDES
Alumina reinforced tetragonal zirconia (TZP) composites [DE91-016748] N91-31239
Response of an alumina fiber reinforced aluminum composite to combined tension-torsion [AD-A239560] N91-31245
Ceramic composition [PATENT-1-249-609] N91-31294
Alloys with oxide inclusions (TEXUS 2) N91-31432
The behaviour of alumina-copper suspensions (TEXUS 3A and 3B) N91-31433
Copper-alumina suspensions (TEXUS 5) N91-31434
Solidification of fine dispersions in microgravity (TEXUS 14b) N91-31441
Gas bubbles in a copper-alumina suspension (TEXUS 11) N91-31453

ALUMINUM SILICATES
Solid-support substrates for plant growth at a lunar base N91-31800

ALUMINUM-LITHIUM ALLOYS
Stress corrosion cracking of 2091 ad 8090 aluminum-lithium alloys in chloride containing aqueous solutions. Influence of sulphate and nitrate additions [REPT-431/91] N91-31285

AMBIENT TEMPERATURE
Control system design considerations for starting turbo-engines during cold weather operation N91-31155
Experiments on ultrasonic thermometry for wet-ash coal gasification N91-32024

AMMONIA
The selective catalytic oxidation of ammonia to N2 and H2O over silica-supported molybdena catalysts N91-32026

AMORPHOUS SILICON
The status of lightweight photovoltaic space array technology based on amorphous silicon solar cells [DE91-014985] N91-31698

AMPLIFIERS
The superconducting gravity gradiometer N91-31734

AMPLITUDE MODULATION
Circular format zig-zag scanning of vidicon tubes [DE91-016084] N91-31610

ANALOG CIRCUITS
Parametric study of diffusion-enhancement networks for spatiotemporal grouping in real-time artificial vision [AD-A239674] N91-31954

ANALOG DATA
Theory and application of the wavelet transform to signal processing [AD-A239533] N91-31501

ANALOGIES
Genetic algorithms [ETN-91-99985] N91-31852

ANALYSIS (MATHEMATICS)
Computational analysis of hypersonic flows past elliptic-cone waveriders N91-31080
Reliability of computational analysis of plasticity problems [AD-A239646] N91-31691
Extensive coverings and exact core bounds [MEMO-915] N91-31907

ANELASTICITY
Anelastic release from the shock-compressed state [DE91-009961] N91-31672

ANEMOMETERS
Special design and gauging of anemoclinometric sondes [IMFL-90/03] N91-31604

ANGLES (GEOMETRY)
Exact result for the grazing angle of specular reflection from a sphere [AD-A239578] N91-31952

ANIMATION
Use of the animated images for the visualization of computational results [AAAF-NT-89-22] N91-31849

ANISOTROPY
The influence of plastic-strain-induced anisotropy on stress distributions in the finite deformation of ductile metals N91-31273

ANNEALING
Fatigue-resistant nickel-base superalloys [PATENT-1-253-363] N91-31268
Rapid thermal annealing effects in In(x)Ga(1-x)As/GaAs strained-layer superlattices [DE91-015901] N91-31978

ANTENNA ARRAYS
Performance of an angle-of-arrival estimator in the presence of a mainbeam interference source [AD-A239629] N91-31508
Adaptive arrays in packet radio networks [AD-A239636] N91-31509
An investigation of optically controlled, integrated millimeter wave receiving phased arrays [AD-A239504] N91-31538
An adaptive coherent optical receiver array [AD-A239672] N91-31644

ANTENNA DESIGN
Electromagnetically coupled microstrip antennas having feeding patches capacitively coupled to feedlines [PATENT-1-263-181] N91-31480
Antenna study for 60 GHz intersatellite link [CD-RPT-ITL-5043-003] N91-31482
Composite waveguide coupling aperture having a thickness dimension [PATENT-1-259-401] N91-31514

ANTENNAS
Radome-lens EHF antenna development [PATENT-1-262-571] N91-31481

ANTHROPOMETRY
Female aircrew: The Canadian Forces experience, 1979-1989 [DCIEM-90-P-14] N91-31801

ANTICYCLONES
Time scales of variability associated with Nordeste precipitation [DE91-015696] N91-31718

ANTIKNOCK ADDITIVES
The autoignition chemistry of paraffinic fuels and pro-knock and anti-knock additives: A detailed chemical kinetic study [DE91-014992] N91-31314

ANTIMONY ALLOYS
Solidification of a hypereutectic alloy (TEXUS 1) N91-31399
Directional solidification of eutectics InSb-NiSb (TEXUS 10) N91-31405

ANTITANK MISSILES
Procedure for steering a low-speed missile, weapon system, and missile for implementation of the procedure [PATENT-1-265-947] N91-31182

APERTURES
Electromagnetic penetration of slot apertures with depth and losses [DE91-016401] N91-31500
Composite waveguide coupling aperture having a thickness dimension [PATENT-1-259-401] N91-31514

APEXES
Cycles containing many vertices of large degree [MEMO-916] N91-31908

APPLICATION SPECIFIC INTEGRATED CIRCUITS
Design of a specific integrated circuit for solving the three dimensional Poisson equation [ECL-90-24] N91-31527

APPLICATIONS PROGRAMS (COMPUTERS)
User's guide to a system of finite-element supersonic panel flutter programs [NASA-TM-104109] N91-31082
A Weibull brittle material failure model for the ABAQUS computer program [DE91-016813] N91-31690
Report of the Workshop on a CLICOM-HOMS Interface [WCAP-16] N91-31746
A users' guide to PVM (parallel virtual machine) [DE91-016934] N91-31855
Methods of astrodynamics, a computer approach [AD-A239662] N91-31861
A knowledge based application of the extended aircraft interrogation and display system [NASA-TM-4327] N91-31874
User's manual for the Langley boundary layer noise propagation program (MRS-BLP) [NASA-CR-187559] N91-31923

APPROXIMATION
A numerical procedure for recovering true scattering coefficients from measurements with wide-beam antennas [NASA-CR-186042] N91-31492
RNG and turbulence modeling N91-31570
Approximating treewidth, pathwidth, and minimum elimination tree height [RUU-CS-91-01] N91-31836
Strong approximation on log dense sets [W-9101] N91-31916

AQUEOUS SOLUTIONS
Determination of aqueous processable photoresist in tin-lead plating solutions [DE91-015575] N91-31251
Stress corrosion cracking of 2091 ad 8090 aluminum-lithium alloys in chloride containing aqueous solutions. Influence of sulphate and nitrate additions [REPT-431/91] N91-31285
Ionic solutions near the critical point of water (TEXUS 10) ESA N91-31375
Ionic solutions near the critical point of water (TEXUS 12) ESA N91-31376

AQUICULTURE
Biomass production and nitrogen dynamics in an integrated aquaculture/agriculture system N91-31789

ARC JET ENGINES
Medium power hydrogen arcjet performance [NASA-TM-104533] N91-31216

ARCHITECTURE (COMPUTERS)
Interactive constraint-based solid modeling as a design tool [AD-A239358] N91-31856
Open architecture for formal reasoning [AD-A239395] N91-31857
Benchmarking a Network Storage Service [DE91-013510] N91-31868
Local area gigabit networking [DE91-014780] N91-31869
OSI-security and relations with other security standards [FEL-91-B099] N91-31872
Synchronized computational architecture for generalized bilateral control of robot arms [NASA-CASE-NPO-17401-1-CU] N91-31885

ARCTIC REGIONS
Cold start development of modern small gas turbine engines at Pratt and Whitney Aircraft of Canada Ltd. N91-31156
Arctic VLF/LF data acquisition [AD-A239704] N91-31510

ARGON
Effective ionization coefficients, electron drift velocities, and limiting breakdown fields for gas mixtures of possible interest to particle detectors [DE91-015921] N91-31532

ARIANE LAUNCH VEHICLE
Calculation of fragment ejection velocities on explosion of a launcher
[CNES-NT-128] N91-31195
ARID LANDS
Hyperspectral signatures (400 to 2500 nm) of vegetation, minerals, soils, rocks, and cultural features: Laboratory and field measurements
[AD-A239496] N91-31697
ARITHMETIC
A fast multiport memory based on single-port memory cells
[AD-A239455] N91-31811
ARRAYS
High speed digital direct access filter for tracking or excision of parametric signal data
[PATENT-1-271-231] N91-31511
ARSENIC COMPOUNDS
Epitaxial growth and electro-optical properties of metal GaAs superlattices
[AD-A239719] N91-31984
ARTERIES
Cold-induced changes in arterial sensitivity
[AD-A239493] N91-31767
ARTIFICIAL INTELLIGENCE
The development of an intelligent dimensional inspection environment using coordinate measuring machines N91-31661
Adaptive function allocation for intelligent cockpits
[AD-A239714] N91-31808
Open architecture for formal reasoning
[AD-A239395] N91-31857
The problem of network management: An approach using AI techniques
[REPT-90-072] N91-31884
ASHES
Experiments on ultrasonic thermometry for wet-ash coal gasification N91-32024
ASPERGILLUS
Use of inedible wheat residues from the KSC-CELSS breadboard facility for production of fungal cellulase N91-31785
ASSIMILATION
Efficiency of N use by wheat as a function of influx and efflux of NO3 N91-31778
ASTRODYNAMICS
Methods of astrodynamics, a computer approach
[AD-A239662] N91-31861
ASTROLOY (TRADEMARK)
Crack propagation in heat resistant disk alloys. Short crack propagation in alloys for high characteristic turbomachine disks
[ETN-91-99981] N91-31683
ASTRONOMICAL CATALOGS
An atlas of stellar spectra between 2.00 and 2.45 micrometers (Arnaud, Gilmore, and Collier Cameron 1989)
[NASA-TM-105044] N91-32003
ASTRONOMICAL SPECTROSCOPY
An atlas of stellar spectra between 2.00 and 2.45 micrometers (Arnaud, Gilmore, and Collier Cameron 1989)
[NASA-TM-105044] N91-32003
ASTRONOMY
BAe University Round Table on Gravitational Research
[BAE-FBS-007] N91-31729
ASTROPHYSICS
Activities report of the Institute of Extraterrestrial Physics
[MPE-223] N91-32002
Research studies with the International Ultraviolet Explorer
[NASA-CR-183495] N91-32012
Nuclear and particle astrophysics
[DE91-016260] N91-32016
ASYMMETRY
Asymmetric soft-error resistant memory
[NASA-CASE-NPO-17394-1-CU] N91-31810
ATMOSPHERIC CHEMISTRY
Chemical characterization of aerosol particles by Raman spectroscopy
[DE91-015836] N91-31720
ATMOSPHERIC CIRCULATION
A quantitative analysis of quasi-geostrophic forcing during recent severe weather outbreaks across the southern Great Plains
[PB91-176693] N91-31745
ATMOSPHERIC COMPOSITION
Simulated effects of a doubling of carbon dioxide on corn production in portions of the central US
[DE91-016843] N91-31722
Tunable far infrared studies of molecular parameters in support of stratospheric measurements
[NASA-CR-188774] N91-31723
Retrieval and molecule sensitivity studies for the global ozone monitoring experiment and the scanning imaging absorption spectrometer for atmospheric chartography N91-31724
Scanning imaging absorption spectrometer for atmospheric chartography N91-31725
ATMOSPHERIC ENTRY
NASA Aerodynamics Program
[NASA-TM-4312] N91-31751
ATMOSPHERIC GENERAL CIRCULATION MODELS
Temporal sampling considerations in global climate modeling
[DE91-015695] N91-31717
Time scales of variability associated with Nordeste precipitation
[DE91-015696] N91-31718
The use of distributional and pointwise statistical measures in GCM intercomparisons
[DE91-015697] N91-31748
ATMOSPHERIC MODELS
Global model simulations of the long range transport of soot and sulfur from the Kuwait oil fires
[DE91-015771] N91-31719
On the response of the special sensor microwave/imager to the marine environment: Implications for atmospheric parameter retrievals N91-31727
Estimating the strength of the capping inversion and the probability of strong convection
[PB91-176685] N91-31744
Impact of the ice phase on a mesoscale convective system: Cloud ensemble features and cloud radiative properties
[DE91-015769] N91-31749
ATMOSPHERIC PHYSICS
Aero/fluids database system
[NASA-CR-184208] N91-31853
ATMOSPHERIC RADIATION
Small satellite radiometric measurements
[DE91-016308] N91-31694
ATMOSPHERIC SOUNDING
Tunable far infrared studies of molecular parameters in support of stratospheric measurements
[NASA-CR-188774] N91-31723
A satellite-based radar wind sensor
[NASA-CR-188805] N91-31750
ATMOSPHERICS
Study of lightning strikes on an aircraft in flight. Electric measurements
[ONERA-RF-98/7154-PY] N91-31112
ATOMIC PHYSICS
Summaries of FY 1991 research in the chemical sciences
[DE91-011221] N91-31222
ATOMIC SPECTRA
A spectrophotometric study of the secondaries of Algol systems N91-32005
ATOMIC STRUCTURE
Atomic structures and compositions of internal interfaces
[DE91-016095] N91-31934
Cu-O charge fluctuations and electron-phonon coupling in the effective single-band Hubbard theory for cuprate superconductors
[DE91-016526] N91-31976
ATOMIZING
The effect of fuel properties and atomization on low temperature ignition in gas turbine combustors N91-31164
ATOMS
Atomic hydrogen driven halogen extraction from Si(100): Eley-Rideal surface kinetics
[AD-A239544] N91-31266
ATTITUDE CONTROL
The in-flight calibration of the Hubble space telescope attitude sensors
[NASA-CR-183485] N91-32007
ATTITUDE INDICATORS
The in-flight calibration of the Hubble space telescope attitude sensors
[NASA-CR-183485] N91-32007
AUDIO FREQUENCIES
Emergency locating transmitter
[NASA-CASE-GSC-12821-2] N91-31530
AUGER SPECTROSCOPY
Atomic hydrogen driven halogen extraction from Si(100): Eley-Rideal surface kinetics
[AD-A239544] N91-31266
Some applications of X-ray photoelectron spectroscopy and secondary-ion mass spectroscopy N91-32029
AUGMENTATION
Radome-lens EHF antenna development
[PATENT-1-262-571] N91-31481
AUSTENITE
Non-equilibrium solidification in austenitic stainless steel welds
[DE91-014279] N91-31277
Magnetic field-induced fracture changes in metastable austenites at 4.2 K
[DE91-016263] N91-31279
Metastable austenites in cryogenic high magnetic field environments
[DE91-016420] N91-31288
AUSTENITIC STAINLESS STEELS
Non-equilibrium solidification in austenitic stainless steel welds
[DE91-014279] N91-31277
Metastable austenites in cryogenic high magnetic field environments
[DE91-016420] N91-31288
AUTOMATIC CONTROL
Automatic satellite tracking system for the NASA Satellite Photometric Observatory
[NASA-TM-105037] N91-31194
System and method for automatically fabricating multiple memory holographic elements
[PATENT-1-253-724] N91-31600
Automatic analysis of visualization negatives
[ETN-91-99971] N91-31603
Analysis and development of a real-time control methodology in resistance spot welding N91-31646
Adaptive function allocation for intelligent cockpits
[AD-A239714] N91-31808
AUTOMATIC PILOTS
Robustness and techniques of multivariable control for helicopter piloting. Dispatch 3: Inclusion regions technique on linear model
[RD/PA-14-227] N91-31184
AUTOMATIC TEST EQUIPMENT
Recent manufacturing advances for spiral bevel gears
[NASA-TM-104479] N91-31654
AUTONOMY
A program of continuing research on representing, manipulating, and reasoning about physical objects
[AD-A239596] N91-31659
AUTOREGRESSIVE PROCESSES
Use of an ARMA model in turbulent medium acoustic propagation
[ONERA-RF-14/3641-PY] N91-31925
AUXILIARY POWER SOURCES
Cold starting small gas turbines: An overview N91-31150
Cold start investigation of an APU with annular combustor and fuel vaporizers N91-31154
AVIONICS
An integer programming model for Navy's maritime patrol aviation fleet
[AD-A239464] N91-31079
Software quality metrics
[DOT/FAA/CT-91/1] N91-31814
Avioptic plug-in interconnection
[PATENT-1-254-415] N91-31946
AXIAL LOADS
Response of an alumina fiber reinforced aluminum composite to combined tension-torsion
[AD-A239560] N91-31245
AXIAL STRAIN
Modelling the response of thick composite materials due to axisymmetric shock loading
[AD-A239531] N91-31243
AXIOMS
Weak equivalence
[ITLI-CT-91-04] N91-31891
AXISYMMETRIC FLOW
Computational fluid dynamics N91-31544
Development of a computation code for nonequilibrium gas axisymmetric hypersonic laminar flow
[ONERA-RS-14/3637-AY] N91-31585
AZIMUTH
Coordinate conversions for presenting and compositing weather radar data
[KNMI-TR-129] N91-31497

B

BACKGROUND NOISE
Behaviour of the SIR for space-based DPCA radar under various spatial clutter distributions
[CRC-W7714-7-5271] N91-31485
BACKGROUND RADIATION
Hydrodynamic simulations of cosmology N91-32013
BACKWARD FACING STEPS
Least-squares solution of incompressible Navier-Stokes equations with the p-version of finite elements
[NASA-TM-105203] N91-31911
BACTERIA
Cyanobacteria in CELSS: Growth strategies for nutritional variation and nitrogen cycling N91-31786
Algae for controlled ecological life support system diet characterization of cyanobacteria 'spirulina' in batch cultures N91-31787

BAND STRUCTURE OF SOLIDS
Theoretical studies of metallic alloys
[DE91-016486] N91-31281
BANDPASS FILTERS
Dielectric image-resonator multiplexer
[PATENT-1-252-835] N91-31479
BARIUM OXIDES
Near-edge study of gold-substituted YBa2Cu3O(7-delta)
[NASA-TM-105220] N91-31977
BAROTRAUMA
The medical hazards of flame-suppressant atmospheres
[AD-A239618] N91-31806
BATHYMETERS
North Pacific guyots
[AD-A239388] N91-31754
BAYES THEOREM
Bayesian multi-sensor tracking for advanced air-traffic control systems
[NLR-MP-88056-U] N91-31119
Bayes theorem from a sampling-resampling perspective
[AD-A239515] N91-31919
Research in regression, information retrieval, inversion of noisy transforms, and stochastic control
[AD-A239490] N91-32001
BEAM INTERACTIONS
Theoretical studies of metallic alloys
[DE91-016486] N91-31281
BEAMS (SUPPORTS)
A finite element approach for the dynamic analysis of joint-dominated structures
[NASA-CR-4402] N91-31686
BEARING (DIRECTION)
Passive ranging of an airborne emitter by a single non-maneuvering or stationary sensor
[PATENT-1-254-292] N91-31116
BEARING ALLOYS
Al-Pb bearing alloy (TEXUS 1) N91-31413
BEND TESTS
Dual ion implantation effects on fatigue properties of Fe-13Cr-15Ni alloys
[DE91-015930] N91-31286
Stress relaxation in bending of type AISI 304 stainless steel at 773K and 823K
[DE91-618657] N91-31666
BENDING
Stress relaxation in bending of type AISI 304 stainless steel at 773K and 823K
[DE91-618657] N91-31666
A new method to do time resolved, x ray diffraction studies: The rotating crystal Laue method
[DE91-016527] N91-31935
BENZENE
Mass resolved excitation spectroscopy of benzyl and phenylnitrene radicals
[AD-A239394] N91-31264
BERYLLIUM ALLOYS
Development and characterization of low temperature Cu-Al-Be shape memory alloys
[ISAL-90-0093] N91-31284
BERYLLIUM ISOTOPES
The Li-7 and Be-7 deexcitation lines: Probes for accelerated particle transport models in solar flares
[NASA-CR-183490] N91-32020
BIAS
Biasing errors and corrections N91-31621
BIBLIOGRAPHIES
Study of space qualification specifications
[CTN-91-60201] N91-31199
Aerospace medicine and biology: A continuing bibliography with indexes (supplement 353)
[NASA-SP-7011(353)] N91-31760
BINARY ALLOYS
Dispersion alloys (TEXUS 7) N91-31412
Atomic structures and compositions of internal interfaces
[DE91-016095] N91-31934
BINARY DATA
Reconfigurable parameter filter
[PATENT-1-264-072] N91-31513
Application of the constrained implicants set concept to the minimization of binary functions
[AD-A239470] N91-31859
BINARY DIGITS
Full-information item bi-factor analysis
[AD-A229346] N91-31771
BINARY FLUIDS
Phase separation of a binary fluid near its critical point (TEXUS 11) N91-31377
Phase separation in microgravity of binary fluids near the critical point (TEXUS 13) N91-31378
Spinoidal decomposition (TEXUS 17) N91-31379
BINARY SYSTEMS (MATERIALS)
Marangoni transport of droplets at a solidification front (TEXUS 9) N91-31426
Investigation of two-dimensional cracks at an angle to an interface N91-31667
BINDERS (MATERIALS)
Processing and characterization of continuous fiber-reinforced glass and glass-ceramic matrix composites N91-31227
BIOASTRONAUTICS
Aerospace medicine and biology: A continuing bibliography with indexes (supplement 353)
[NASA-SP-7011(353)] N91-31760
BIOCHEMISTRY
Summaries of FY 1991 research in the chemical sciences
[DE91-011221] N91-31222
Pyrimidine dimer formation by UVA radiation: Implications for photoreactivation
[DE91-015837] N91-31756
Electron microscopy to correlate cell structures and biochemical activity
[AD-A239640] N91-31758
BIOCONVERSION
Production of organic chemicals via bioconversion: A review of the potential
[DE91-015524] N91-31223
Biomass production and nitrogen dynamics in an integrated aquaculture/agriculture system N91-31789
BIOLOGICAL EFFECTS
Pyrimidine dimer formation by UVA radiation: Implications for photoreactivation
[DE91-015837] N91-31756
Aerospace medicine and biology: A continuing bibliography with indexes (supplement 353)
[NASA-SP-7011(353)] N91-31760
BIOMASS
Conversion of biomass and fossil fuels to methanol and its effect on CO2 emissions
[DE91-015846] N91-31320
Controlled Ecological Life Support Systems: CELSS '89 Workshop
[NASA-TM-102277] N91-31775
Environmental and cultural considerations for growth of potatoes in CELSS N91-31779
Sweet potato for closed ecological life support systems using the nutrient film technique N91-31782
Use of inedible wheat residues from the KSC-CELSS breadboard facility for production of fungal cellulase N91-31785
Biomass production and nitrogen dynamics in an integrated aquaculture/agriculture system N91-31789
Controlled ecological life support system breadboard project, 1988 N91-31791
Transpiration during life cycle in controlled wheat growth N91-31795
BIOMASS ENERGY PRODUCTION
Biomass production and nitrogen dynamics in an integrated aquaculture/agriculture system N91-31789
BIOPOLYMERS
Strategies for biopolymer engineering of PHB-like materials
[AD-A239690] N91-31313
BIOSYNTHESIS
Strategies for biopolymer engineering of PHB-like materials
[AD-A239690] N91-31313
BIPOLARITY
Development of prototype sealed bipolar lithium/sulfide cells
[DE91-015721] N91-31519
BISMUTH ALLOYS
Fundamental studies in the manganese-bismuth system (TEXUS 2) N91-31414
Solidification of immiscible alloys: ZnBi (TEXUS 2) N91-31415
The coalescence process in immiscible alloys (TEXUS 3) N91-31416
The coalescence process in immiscible alloys (TEXUS 5) N91-31417
Unidirectional solidification of immiscible alloys (TEXUS 7) N91-31419
Unidirectional solidification of Zn-Bi samples (TEXUS 14b) N91-31420
Demixing of a monotectic ternary alloy (TEXUS 20) N91-31429
BISMUTH OXIDES
Weak links within a Bi2Sr2Ca1Cu2O(x) single crystal by magnetization and direct optical observations
[DE91-016085] N91-31979
BLACK HOLES (ASTRONOMY)
A search for periodicity in the x ray spectrum of black hole candidate A0620-00
[AD-A239488] N91-32011
BLACKOUT
Aircrew critique of high-G centrifuge training. Part 1: What was the best part of the program?
[AD-A239781] N91-31809
BLACKOUT (PHYSIOLOGY)
The G-LOC syndrome
[AD-A239561] N91-31768
BLADE SLAP NOISE
Noxious matter minimization as a project criterion for aircraft
[MBB-Z-0337-90-PUB] N91-31134
BLADE-VORTEX INTERACTION
Vortex-blade interaction on a helicopter principal rotor. Validation of the S2DI computation program and study of vortex models
[ONERA-RT-92/5094-PY] N91-31136
A parametric study of transonic blade-vortex interaction noise
[NASA-CR-188811] N91-31928
BLOOD
Basic operation and preliminary trials of a detector for stationary gas bubbles
[AD-A239710] N91-31769
BLOOD FLOW
The G-LOC syndrome
[AD-A239561] N91-31768
BLUE GREEN ALGAE
Cyanobacteria in CELSS: Growth strategies for nutritional variation and nitrogen cycling N91-31786
BLUNT TRAILING EDGES
The effect of jet bleed on base pressure distribution, shedding frequency, and mean velocity profiles in the wake behind a two-dimensional blunt model
[MPIS-12/1990] N91-31085
BODY TEMPERATURE
Methodology for calibration and use of heat flux transducers
[AD-A239552] N91-31541
BODY-WING CONFIGURATIONS
Three dimensional shear flow: Flow visualisation around a highly swept back and high incidence wing
[ONERA-RT-35/5025-28] N91-31584
BOLOMETERS
High-T(sub c) bolometers
[DE91-017009] N91-31611
BOOLEAN ALGEBRA
Classes of feedforward neural networks and their circuit complexity
[MEMO-920] N91-31881
BORON
Rapidly solidified nickel aluminide of improved stoichiometry and ductilization
[PATENT-1-257-987] N91-31270
Method for imparting strength to intermetallic phases
[PATENT-1-255-929] N91-31271
Boron in nuclear medicine: New synthetic approaches to PET, SPECT, and BNCT agents
[DE91-016488] N91-31764
BORON NITRIDES
Laser deposition of cubic boron nitride on electronic materials
[AD-A238313] N91-31249
BOROSILICATE GLASS
Processing and characterization of continuous fiber-reinforced glass and glass-ceramic matrix composites N91-31227
Immiscibles, 2 (TEXUS 5) N91-31411
BOSONS
Particle production through two-photon processes in relativistic heavy-ion colliders
[DE91-016221] N91-31931
BOUNDARY CONDITIONS
Contributions to a space station for flights in the near field and towards geostationary Earth orbit
[ETN-91-99744] N91-31203
Application of second-moment closure in complex flows N91-31559
A comparison of time domain boundary conditions for acoustic waves in wave guides
[NASA-CR-187618] N91-31889
BOUNDARY INTEGRAL METHOD
A boundary integral equation method for steady two-dimensional flow in partially saturated media
[DE91-016056] N91-31573
Development of an advanced panel method for complex configurations in subsonic compressible flow; application to the computation of the potential flow through ducts
[NLR-TR-88001-U] N91-31579
BOUNDARY LAYER FLOW
Linear and nonlinear stability of boundary layers with streamwise varying properties N91-31545
Compressible two dimensional boundary layer strong perfect fluid coupling in the case of sharp leading edge profiles. Stationary case
[ONERA-RT-42/1621-RY-093-R] N91-31586

User's manual for the Langley boundary layer noise propagation program (MRS-BLP)
[NASA-CR-187559] N91-31923
BOUNDARY LAYER STABILITY
Interfacial convection (TEXUS 2) N91-31328
Diffusion-induced interfacial convection (TEXUS 3) N91-31329
Thermally induced interfacial convection (TEXUS 4) N91-31330
Diffusion-induced interfacial convection (TEXUS 11) N91-31332
BOUNDARY LAYER TRANSITION
Transition length determination in the F1 wind tunnel, test report
[ONERA-PV-1/8571-GY] N91-31089
Low level turbulence detection by a laser velocimetry technique: Application to transonic flows
[AAAF-NT-89-07] N91-31101
Boundary layer transition detection and measurement methods at CERT/DERAT
[AAAF-NT-89-14] N91-31105
Direct and large-eddy simulations of transition in the compressible boundary layer N91-31566
BOUNDARY LAYERS
Boundary layers in transparent melts (TEXUS 10) N91-31406
Laser Doppler velocimeter measurements of the streamwise velocity component in the viscous sublayer of a turbulent channel flow
[MPIS-MITT-97] N91-31582
BOUNDARY VALUE PROBLEMS
Development and validation of characteristic boundary conditions for cell-centered Euler flow calculations with a shock-free airfoil
[NLR-TP-89360-U] N91-31081
Parameter identification for two-point boundary value processes
[MEMO-917] N91-31909
BOW WAVES
A shock-fitting algorithm for the simulation of inviscid flows in chemical non-equilibrium
[MBB-UK-0131-90-PUB] N91-31087
BRAIN
Muramyl peptide-enhanced sleep: Pharmacological optimization of performance
[AD-A239442] N91-31766
BRANCHING (MATHEMATICS)
Bifurcations of parametrically forced oscillators
[W-9007] N91-31892
BRAZIL
Time scales of variability associated with Nordeste precipitation
[DE91-015696] N91-31718
BRAZING
Brazing of capillary gaps (TEXUS 2) N91-31461
Adhesion of metals on ceramic substrates (MASER 2) ESA N91-31463
BREEDING (REPRODUCTION)
Cloning crops in a CELSS via tissue culture: Prospects and problems N91-31783
BRIDGES
Long liquid bridges aboard sounding rockets (TEXUS 12) ESA N91-31325
BRIGHTNESS TEMPERATURE
On the response of the special sensor microwave/imager to the marine environment: Implications for atmospheric parameter retrievals N91-31727
BRITTLE MATERIALS
A Weibull brittle material failure model for the ABAQUS computer program
[DE91-016813] N91-31690
BROADBAND
Analysis and development of a wide-bandwidth gravitational wave detector N91-31601
BROWNIAN MOVEMENTS
Colloid chemistry (TEXUS 17) ESA N91-31362
BRUSH SEALS
Eccentricity effects on leakage of a brush seal at low speeds
[NASA-TM-105141] N91-31220
BUBBLE CHAMBERS
A research program in experimental high energy physics
[DE91-016208] N91-31941
BUBBLES
Bubbles and foams (TEXUS 10) ESA N91-31324
Three-dimensional Marangoni convection (MASER 2) ESA N91-31344
Electrolytic hydrogen formation (TEXUS 1) N91-31347
Electrolytically generated hydrogen bubbles (TEXUS 6) N91-31348
Bubble formation, 1 (TEXUS 5) N91-31355
Bubble formation, 2 (TEXUS 10) N91-31356
Bubble formation, 2. Microgravity measurements of the boiling heat transfer from flat heating surfaces (TEXUS 11) N91-31357
Inst. A fuer Thermodynamik. N91-31358
Preparation of aluminium foams (TEXUS 9) N91-31452
Gas bubbles in a copper-alumina suspension (TEXUS 11) N91-31453
Bubble formation, growth, and expansion during the liquid phase sintering of a WC-Co sample N91-31454
Basic operation and preliminary trials of a detector for stationary gas bubbles
[AD-A239710] N91-31769
BUCKLING
A method for the geometrically nonlinear analysis of compressively loaded prismatic composite structures N91-31229
BUFFER STORAGE
Filter system for radar applications
[PATENT-1-273-409] N91-31512
BUOYANCY
Composite materials, 1 (TEXUS 1) N91-31408
Body force effects on turbulence N91-31558
BUSHINGS
Eccentricity effects on leakage of a brush seal at low speeds
[NASA-TM-105141] N91-31220
BUTYRIC ACID
Strategies for biopolymer engineering of PHB-like materials
[AD-A239690] N91-31313
BYPASS RATIO
Engine icing criticality assessment N91-31161

C

C (PROGRAMMING LANGUAGE)
SHOWTIME.C: A C-language program for data acquisition and display user's guide
[DE91-016241] N91-31817
CADMIUM SULFIDES
Photophysics and chemistry of ultra-fast ZnO and CdS phosphors
[DE91-013106] N91-31966
CALCULUS
A simplification of Earley's algorithm
[CS-9102] N91-31822
On logic programming and the refinement calculus: Semantics based program transformations
[RUU-CS-90-39] N91-31834
The linear decomposition of delta-squared models
[RUU-CS-91-04] N91-31902
CALCULUS OF VARIATIONS
On the optimal use of fictitious time in variation of parameters methods with application to BG14
[NASA-CR-185650] N91-31890
CALIBRATING
Arctic VLF/LF data acquisition
[AD-A239704] N91-31510
Methodology for calibration and use of heat flux transducers
[AD-A239552] N91-31541
Special design and gauging of anemoclinometric sondes
[IMFL-90/03] N91-31604
Development of the Burst and Transient Source Experiment (BATSE)
[NASA-RP-1268] N91-32006
The in-flight calibration of the Hubble space telescope attitude sensors
[NASA-CR-183485] N91-32007
CANADA
Low temperature environment operations of turbo engines N91-31146
CAPACITANCE-VOLTAGE CHARACTERISTICS
Capacitive bridge-type probe and conversion circuitry
[PATENT-1-263-444] N91-31598
Capacitive bridge-type probe and conversion circuitry
[PATENT-1-263-443] N91-31599
CAPILLARY FLOW
Liquid motion in capillary tubes (TEXUS 3) N91-31322
Liquid motion in capillary tubes (TEXUS 5) N91-31323
Thermocapillary drop motion, 1 (MASER 1) ESA N91-31345
Thermocapillary drop motion, 2 (MASER 2) ESA N91-31346
Brazing of capillary gaps (TEXUS 2) N91-31461
Soldering in microgravity (TEXUS 5) N91-31462
Technology for subsystems of space-based plant growth facilities N91-31799
CAPILLARY TUBES
Liquid motion in capillary tubes (TEXUS 3) N91-31322
Liquid motion in capillary tubes (TEXUS 5) N91-31323
Brazing of capillary gaps (TEXUS 2) N91-31461
CARBOHYDRATES
Cyanobacteria in CELSS: Growth strategies for nutritional variation and nitrogen cycling N91-31786
Algae for controlled ecological life support system diet characterization of cyanobacteria 'spirulina' in batch cultures N91-31787
CARBON
A spectrophotometric study of the secondaries of Algol systems N91-32005
CARBON DIOXIDE
Conversion of biomass and fossil fuels to methanol and its effect on CO2 emissions
[DE91-015846] N91-31320
Effective ionization coefficients, electron drift velocities, and limiting breakdown fields for gas mixtures of possible interest to particle detectors
[DE91-015921] N91-31532
Coal utilization and CO2 emissions: What are the control options?
[DE91-015988] N91-31721
A system to determine whole-plant exchange rates of ozone, carbon dioxide and water vapour N91-32027
CARBON DIOXIDE CONCENTRATION
Simulated effects of a doubling of carbon dioxide on corn production in portions of the central US
[DE91-016843] N91-31722
Effects of atmospheric CO2 on photosynthetic characteristics of soybean leaves N91-31780
Effects of elevated atmospheric carbon dioxide concentrations on water and acid requirements of soybeans grown in a recirculating hydroponic system N91-31781
CARBON DIOXIDE LASERS
Real time actuating of laser power and scanning velocity for thermal regulation during laser hardening
[ETN-91-99908] N91-31636
CARBON DIOXIDE REMOVAL
Method and apparatus for bio-regenerative life support system
[NASA-CASE-MSC-21629-1] N91-31803
CARBON FIBERS
Method for stabilizing thick honeycomb core composite articles
[PATENT-1-253-424] N91-31224
Processing and characterization of continuous fiber-reinforced glass and glass-ceramic matrix composites N91-31227
Relation between fiber proportion and mechanical characteristics of carbon-resin composites
[RE-50-345/F] N91-31231
Field 3, theme 1: Structural materials. Post 2: Thermotropic liquid crystal polymers
[ETN-91-99982] N91-31306
CARCINOGENS
Biological dosimetry and mechanisms of carcinogenesis
[DE91-015689] N91-31763
CARDIOVASCULAR SYSTEM
Cold-induced changes in arterial sensitivity
[AD-A239493] N91-31767
Basic operation and preliminary trials of a detector for stationary gas bubbles
[AD-A239710] N91-31769
CASE HISTORIES
A review of accelerated response actions available to the environmental restoration program: Selected case histories and associated issues
[DE91-013608] N91-31716
CAST ALLOYS
Sulphur diffusion in liquid cast iron (TEXUS 6) ESA N91-31370
CASTING
Composite ingot casting
[PATENT-1-250-128] N91-31269
Skin technology (TEXUS 3) N91-31457
Skin technology (TEXUS 11 and 12) N91-31460
CATALOGS (PUBLICATIONS)
Hyperspectral signatures (400 to 2500 nm) of vegetation, minerals, soils, rocks, and cultural features: Laboratory and field measurements
[AD-A239496] N91-31697
CATALYSIS
Catalysis-by-design impacts assessment
[DE91-013280] N91-31247
High pressure catalytic reactions over single-crystal metal surfaces
[DE91-016475] N91-31256
Chemically modified electrodes and related solution studies
[DE91-016740] N91-31262

CATALYSTS
Correlations between surface structure and catalytic activity/selectivity
[DE91-016453] N91-31255
Catalyst dispersion and activity under conditions of temperature-staged liquefaction
[DE91-016602] N91-31261
Chemically modified electrodes and related solution studies
[DE91-016740] N91-31262
Pseudohomogeneous catalyst layer model for polymer electrolyte fuel cell
[DE91-016014] N91-31710
KEMA scientific and technical reports, volume 8, number 2, 1990
[ST-REPT-VOL-8-NO-2] N91-32023
The selective catalytic oxidation of ammonia to N2 and H2O over silica-supported molybdena catalysts
N91-32026

CATALYTIC ACTIVITY
Catalysis-by-design impacts assessment
[DE91-013280] N91-31247
Correlations between surface structure and catalytic activity/selectivity
[DE91-016453] N91-31255
The selective catalytic oxidation of ammonia to N2 and H2O over silica-supported molybdena catalysts
N91-32026

CATECHOLAMINE
Cold-induced changes in arterial sensitivity
[AD-A239493] N91-31767

CATEGORIES
Categorical semantics as a basis for program transformation
[RUU-CS-90-38] N91-31833
A note on semi-adjunctions
[RUU-CS-90-41] N91-31901

CATHODES
Pseudohomogeneous catalyst layer model for polymer electrolyte fuel cell
[DE91-016014] N91-31710

CATIONS
Solid-support substrates for plant growth at a lunar base N91-31800

CAVITATION FLOW
Three dimensional shear flow: Flow visualisation around a highly swept back and high incidence wing
[ONERA-RT-35/5025-28] N91-31584

CAVITIES
Application of microwave cavity perturbation techniques in conducting polymers
[AD-A239376] N91-31310
Fuselage shell and cavity response measurements on a DC-9 test section
[NASA-CR-187557] N91-31926

CAVITY RESONATORS
Numerical simulation of a split cavity oscillator and rf conversion
[DE91-016501] N91-31523

CELLULOSE
The conversion of lignocellulosics to fermentable sugars: A survey of current research and application to CELSS
N91-31784
Use of inedible wheat residues from the KSC-CELSS breadboard facility for production of fungal cellulase
N91-31785

CENTRAL NERVOUS SYSTEM
The G-LOC syndrome
[AD-A239561] N91-31768

CENTRIFUGAL FORCE
Aircrew critique of high-G centrifuge training. Part 1: What was the best part of the program?
[AD-A239781] N91-31809

CENTRIFUGAL PUMPS
Hydrogen test of a small, low specific speed centrifugal pump stage
[NASA-CR-187117] N91-31213

CERAMIC BONDING
Adhesion of metals on ceramic substrates (MASER 2) ESA N91-31463

CERAMIC COATINGS
Skin technology (TEXUS 3) N91-31457
Skin technology (TEXUS 11 and 12) N91-31460

CERAMIC MATRIX COMPOSITES
Processing and characterization of continuous fiber-reinforced glass and glass-ceramic matrix composites N91-31227
Ceramic composition
[PATENT-1-249-609] N91-31294
Glass formation and crystallization in high-temperature glass-ceramics and Si3N4 N91-31964

CERAMICS
Composite flexible blanket insulation
[NASA-CASE-NPO-11907-1-NP] N91-31236
Effects of trapped gases on ceramic-filled-glass composite densification
[DE91-015850] N91-31237
Alumina reinforced tetragonal zirconia (TZP) composites
[DE91-016748] N91-31239
Development of ceramic membranes for gas separation: FY 1990 development activities
[DE91-015915] N91-31300
Development of toughened ceramics for elevated temperatures
[DE91-015923] N91-31301
Adhesion of thick layer systems on ceramic based precious metals in hybrid microelectronic circuits
[MBB-UA-1191-90-PUB] N91-31304
Elastic wave dispersion in high-strength ceramics
[DE91-016648] N91-31309
Effect of thickness and brand of metal ceramic porcelain on color
[AD-A239398] N91-31312
Adhesion of metals on ceramic substrates (MASER 2) ESA N91-31463
Low cost, formable, high T(sub c) superconducting wire
[NASA-CASE-LEW-14676-1] N91-31529
Crystallization of the glassy grain boundary phase in silicon nitride ceramics
[NASA-CR-188717] N91-31961
Microstructural changes in Beta-silicon nitride grains upon crystallizing the grain-boundary glass N91-31963
Indirect measurement of the viscosity of the intergranular glass phase in yttria-sintered silicon nitride N91-31965

CERIUM COMPOUNDS
Single crystals of CeMg3 (TEXUS 7) ESA N91-31382
Growth of rare Earth-magnesium crystals (TEXUS 12)
N91-31383

CHAOS
Spatiotemporal intermittency N91-31569
Finite-dimensional dynamics and chaos in fluid flows
N91-31571
Computational model for deterministic chaos in a magnetically confined plasma
[DE91-016022] N91-31955

CHARGE COUPLED DEVICES
High-speed TV cameras for streak tube readout
[DE91-016081] N91-31602

CHARGE EFFICIENCY
Development of prototype sealed bipolar lithium/sulfide cells
[DE91-015721] N91-31519

CHARGE EXCHANGE
Laser interferometric measurement of ion electrode shape and charge exchange erosion
[NASA-TM-105165] N91-31605
Theoretical nuclear physics
[DE91-016745] N91-31936

CHARTS
North Pacific guyots
[AD-A239388] N91-31754

CHEMICAL ANALYSIS
Deformation induced microstructural and microchemical changes during thermomechanical treatment
[DE91-016949] N91-31290

CHEMICAL BONDS
Model description of transition metals using the rotated second moment approximation
[DE91-016043] N91-31287

CHEMICAL COMPOSITION
Ceramic composition
[PATENT-1-249-609] N91-31294
Influence of adhesive polymerization conditions on the durability of adhesive joints
[DCR/I-03357-90] N91-31305
Chemical characterization of aerosol particles by Raman spectroscopy
[DE91-015836] N91-31720
Retrieval and molecule sensitivity studies for the global ozone monitoring experiment and the scanning imaging absorption spectrometer for atmospheric chartography
N91-31724
Scanning imaging absorption spectrometer for atmospheric chartography N91-31725
Atomic structures and compositions of internal interfaces
[DE91-016095] N91-31934

CHEMICAL ENGINEERING
Catalysis-by-design impacts assessment
[DE91-013280] N91-31247

CHEMICAL EXPLOSIONS
Performance evaluation of insensitive explosives
[DE91-015767] N91-31315
Understanding composite explosive energetics
[DE91-015770] N91-31316

CHEMICAL PROPERTIES
TEM analysis of crystalline interface structure: The state of the art
[DE91-016427] N91-31975

CHEMICAL PROPULSION
Mass comparisons of electric propulsion systems for NSSK of geosynchronous spacecraft
[NASA-TM-105153] N91-31212
Hydrogen test of a small, low specific speed centrifugal pump stage
[NASA-CR-187117] N91-31213

CHEMICAL REACTIONS
Jet-A reaction mechanism study for combustion application
[NASA-TM-104441] N91-31181
Catalysis-by-design impacts assessment
[DE91-013280] N91-31247
The chemistry of transition metal clusters
[DE91-015108] N91-31250
Correlations between surface structure and catalytic activity/selectivity
[DE91-016453] N91-31255
Conversion of biomass and fossil fuels to methanol and its effect on CO2 emissions
[DE91-015846] N91-31320
KEMA scientific and technical reports, volume 8, number 2, 1990
[ST-REPT-VOL-8-NO-2] N91-32023

CHIPS (ELECTRONICS)
A methodology for producing and testing a genesil silicon compiler designed VLSI chip which incorporates design for testability
[AD-A239465] N91-31537
The microcrystal laser: A first step on the way to a laser microsystem
[MBB-Z-0336-90-PUB] N91-31635
Superconducting magnet program for x ray lithography source at Brookhaven National Laboratory
[DE91-016995] N91-31981

CHIRAL DYNAMICS
Theoretical nuclear physics
[DE91-016745] N91-31936

CHOLESKY FACTORIZATION
Acceleration techniques for a spectral multi-grid method
[MEMO-914] N91-31580

CHROMIUM ALLOYS
Dual ion implantation effects on fatigue properties of Fe-13Cr-15Ni alloys
[DE91-015930] N91-31286
Initial determination of the micromechanical properties of oxide scales
[DE90-012164] N91-31291

CHROMIUM OXIDES
Ceramic composition
[PATENT-1-249-609] N91-31294

CHROMIUM STEELS
Effect of convection on weld pool development
[DE91-014213] N91-31649
Pressure-strain-temperature relationship in shock loaded cylindrical samples of 304 stainless steel
[DE91-013379] N91-31673

CIRCUIT BOARDS
Soldering of complex multilayer printed boards
[CNES-NT-127] N91-31474
Avioptic plug-in interconnection
[PATENT-1-254-415] N91-31946

CIRCUIT DIAGRAMS
Hardware modeling and top-down design using VHDL
[AD-A239356] N91-31534

CIRCUITS
The physical properties of a pyrotechnical circuit element
[MBB-UA-1192-90-PUB] N91-31317
Capacitive bridge-type probe and conversion circuitry
[PATENT-1-263-444] N91-31598
Capacitive bridge-type probe and conversion circuitry
[PATENT-1-263-443] N91-31599
Asymmetric soft-error resistant memory
[NASA-CASE-NPO-17394-1-CU] N91-31810
Classes of feedforward neural networks and their circuit complexity
[MEMO-920] N91-31881

CIRCULAR CYLINDERS
Control of oscillatory forces on a circular cylinder by rotation
[NASA-CR-187619] N91-31576

CIVIL AVIATION
Flight tests with a data link used for air traffic control information exchange
[NASA-TP-3135] N91-31143
Solid-State Radar Beacon Decoder (SSRBD) Master Test Plan (MTP)
[DOT/FAA/CT-TN91/33] N91-31494
Aeronautical Mobile Satellite Service (AMSS) test plan
[DOT/FAA/CT-TN91/20] N91-31495

Cockpit resource management: Effects on behavioral interactions across airlines and aircraft types [AD-A239467] N91-31804

CL-41 AIRCRAFT
Photoelastic coating study of redesigned CT114 coupon joint test specimen for horizontal stabilizer rear attachment fitting to vertical stabilizer rear spar [NAE-LTR-ST-1701] N91-31125

CLADDING
Development of elements of a high T(sub c) superconducting cable [AD-A239766] N91-31543

CLAMPS
Power saw [NASA-CASE-MSC-21469-1] N91-31655

CLASSIFICATIONS
Examination and mapping of forest damage, using remote sensing methods [ETN-91-99741] N91-31696

CLEARANCES
Developments in icing test techniques for aerospace applications in the RAE Pyestock altitude test facility N91-31173
Capacitive bridge-type probe and conversion circuitry [PATENT-1-263-444] N91-31598
Capacitive bridge-type probe and conversion circuitry [PATENT-1-263-443] N91-31599

CLIMATE
Climatic considerations in the life cycle management of the CF-18 engine N91-31158
Temporal sampling considerations in global climate modeling [DE91-015695] N91-31717
The use of distributional and pointwise statistical measures in GCM intercomparisons [DE91-015697] N91-31748

CLIMATE CHANGE
Coal utilization and CO2 emissions: What are the control options? [DE91-015988] N91-31721

CLIMATOLOGY
Temporal sampling considerations in global climate modeling [DE91-015695] N91-31717
Coal utilization and CO2 emissions: What are the control options? [DE91-015988] N91-31721
Range reference atmosphere, Fairbanks, Alaska [AD-A239520] N91-31739
Range reference atmosphere Wake Island, North Pacific [AD-A239602] N91-31740
Range reference atmosphere Shemya, Alaska [AD-A239603] N91-31741
Range reference atmosphere: Thule, Greenland [AD-A239659] N91-31742
Report of the Workshop on a CLICOM-HOMS Interface [WCAP-16] N91-31746

CLIPS
Airborne rescue system [NASA-CASE-ARC-11909-1] N91-31113

CLOSED ECOLOGICAL SYSTEMS
Controlled Ecological Life Support Systems: CELSS '89 Workshop [NASA-TM-102277] N91-31775
Environmental modification of yield and food composition of cowpea and leaf lettuce N91-31777
Efficiency of N use by wheat as a function of influx and efflux of NO3 N91-31778
Environmental and cultural considerations for growth of potatoes in CELSS N91-31779
Effects of elevated atmospheric carbon dioxide concentrations on water and acid requirements of soybeans grown in a recirculating hydroponic system N91-31781
Sweet potato for closed ecological life support systems using the nutrient film technique N91-31782
Cloning crops in a CELSS via tissue culture: Prospects and problems N91-31783
The conversion of lignocellulosics to fermentable sugars: A survey of current research and application to CELSS N91-31784
Use of inedible wheat residues from the KSC-CELSS breadboard facility for production of fungal cellulase N91-31785
Cyanobacteria in CELSS: Growth strategies for nutritional variation and nitrogen cycling N91-31786
Algae for controlled ecological life support system diet characterization of cyanobacteria 'spirulina' in batch cultures N91-31787
Preliminary evaluation of waste processing in a CELSS N91-31788
Biomass production and nitrogen dynamics in an integrated aquaculture/agriculture system N91-31789
Controlled ecological life support system breadboard project, 1988 N91-31791
The crop growth research chamber: A ground-based facility for CELSS research N91-31792
Development of the CELSS emulator at NASA. Johnson Space Center N91-31793
A perspective on CELSS control issues N91-31794
Preparatory space experiments for development of a CELSS N91-31796
Conceptual design of a closed loop nutrient solution delivery system for CELSS implementation in a micro-gravity environment N91-31798
Method and apparatus for bio-regenerative life support system [NASA-CASE-MSC-21629-1] N91-31803

CLOSURE LAW
Introduction to the Modeling of Turbulence [VKI-LS-1991-02] N91-31551
An introduction to second moment closure N91-31555
Inclusion of second-moment closures into finite-volume solvers N91-31556
Numerical implementation and performance of Reynolds stress closures in finite-volume computations of recirculating and strongly swirling flows N91-31557
Body force effects on turbulence N91-31558
Application of second-moment closure in complex flows N91-31559
A new form of second-moment closure N91-31560
An introduction to single-point closure methodology N91-31561
Turbulence modeling for compressible flows and implementation in Navier-Stokes solvers N91-31564

CLOUD PHYSICS
Impact of the ice phase on a mesoscale convective system: Cloud ensemble features and cloud radiative properties [DE91-015769] N91-31749

CLOUDS
Numerical model of evolution in supercooled cloud of water droplets in a case of icing N91-31169
Developments in icing test techniques for aerospace applications in the RAE Pyestock altitude test facility N91-31173

CLOUDS (METEOROLOGY)
A documentation of vertical and horizontal aircraft soundings of icing relevant cloudphysical parameters N91-31172

CLUSTERS
The chemistry of transition metal clusters [DE91-015108] N91-31250

CLUTTER
Updates to the DREO airborne radar simulator [ASSGI-167] N91-31478
Behaviour of the SIR for space-based DPCA radar under various spatial clutter distributions [CRC-W7714-7-5271] N91-31485

CMOS
Design of a specific integrated circuit for solving the three dimensional Poisson equation [ECL-90-24] N91-31527

COAGULATION
Dispersion electrolysis (TEXUS 9) N91-31353
Colloid chemistry (TEXUS 17) ESA N91-31362

COAL
Electrostatic precipitation of condensed acid mist [DE91-016530] N91-31260
Experiments on ultrasonic thermometry for wet-ash coal gasification N91-32024

COAL GASIFICATION
Development of ceramic membranes for gas separation: FY 1990 development activities [DE91-015915] N91-31300
KEMA scientific and technical reports, volume 8, number 2, 1990 [ST-REPT-VOL-8-NO-2] N91-32023
Experiments on ultrasonic thermometry for wet-ash coal gasification N91-32024

COAL LIQUEFACTION
Catalyst dispersion and activity under conditions of temperature-staged liquefaction [DE91-016602] N91-31261

COAL UTILIZATION
Coal utilization and CO2 emissions: What are the control options? [DE91-015988] N91-31721

COALESCING
Bubbles and foams (TEXUS 10) ESA N91-31324
Electrolytic hydrogen formation (TEXUS 1) N91-31347
The coalescence process in immiscible alloys (TEXUS 3) N91-31416
The coalescence process in immiscible alloys (TEXUS 5) N91-31417
The effects of fluid particle interactions on interfacial transfer and flow structure [DE91-016409] N91-31575

COASTAL CURRENTS
A summary of the physical oceanography of the Pacific Northwest Coast [PB91-164434] N91-31753

COATING
HVOF: Particle, flame diagnostics, and coating characteristics [DE91-014654] N91-31248

COATINGS
Photoelastic coating study of redesigned CT114 coupon joint test specimen for horizontal stabilizer rear attachment fitting to vertical stabilizer rear spar [NAE-LTR-ST-1701] N91-31125
Skin technology (TEXUS 2) N91-31456

COBALT ALLOYS
Process for producing plasma sprayed carbide-based coatings with minimal decarburization and near theoretical density [DE91-012016] N91-31292

COBALT COMPOUNDS
Epitaxial growth and electro-optical properties of metal GaAs superlattices [AD-A239719] N91-31984

COCKPITS
Cockpit resource management: Effects on behavioral interactions across airlines and aircraft types [AD-A239467] N91-31804
Adaptive function allocation for intelligent cockpits [AD-A239714] N91-31808

CODING
A case study for the real-time experimental evaluation of the VIPER microprocessor [NASA-TM-104098] N91-31531
An investigation of optically controlled, integrated millimeter wave receiving phased arrays [AD-A239504] N91-31538
Full-information item bi-factor analysis [AD-A229346] N91-31771
Optimizing the long-term retention of skills: Structural and analytic approaches to skill maintenance 3 [AD-A239574] N91-31773
Investigation of the progressive bi-level coding technique for the high-resolution bi-level data compression standard [AD-A239597] N91-31860

COGENERATION
Fuel cells for commercial energy [MBB-UE-0018-90-PUB] N91-31706

COGNITION
Quick development microcomputer system: Training automatic components for electronic troubleshooting [AD-A239573] N91-31542
Optimizing the long-term retention of skills: Structural and analytic approaches to skill maintenance 3 [AD-A239574] N91-31773

COGNITIVE PSYCHOLOGY
Examining the effect of information order on expert judgment [AD-A239708] N91-31774

COHERENT RADAR
Updates to the DREO airborne radar simulator [ASSGI-167] N91-31478
Pulse Doppler radar simulation study [ASSGI-14SV-W7714-7-5353] N91-31486

COLD WEATHER
Low Temperature Environment Operations of Turboengines (Design and User's Problems) [AGARD-CP-480] N91-31144
Low temperature environment operations of turbo engines N91-31146
Analysis of starting problems in cold weather with ASTAZOU type turbine engines in helicopters N91-31147
Cold weather jet engine starting strategies made possible by engine digital control systems N91-31153
Cold start investigation of an APU with annular combustor and fuel vaporizers N91-31154

COLLISIONAL PLASMAS
An interparticle collision model for electromagnetic hybrid simulations of high density plasmas [DE91-016025] N91-31958

COLLISIONLESS PLASMAS
An interparticle collision model for electromagnetic hybrid simulations of high density plasmas [DE91-016025] N91-31958

COLLOIDING
Colloid chemistry (TEXUS 17) ESA N91-31362

COLLOIDS
Colloid chemistry (TEXUS 17) ESA N91-31362

COLOR
Effect of thickness and brand of metal ceramic porcelain on color [AD-A239398] N91-31312

Choice representation modes and color palettes [AAAF-NT-89-17] N91-31589
Sensitivity of imaging materials to electron beam irradiation [AD-A239365] N91-31612
Perfect colorings [RUU-CS-90-35] N91-31831
Single layer multi-color luminescent display [NASA-CASE-LAR-13616-1] N91-31950

COLUMNS (PROCESS ENGINEERING)
Freezing of a long liquid column (TEXUS 18) ESA N91-31326

COMBUSTION
Summaries of FY 1991 research in the chemical sciences [DE91-011221] N91-31222
Effects of oxidation and combustion environments on the properties of Nicalon/SiC composites [DE91-016778] N91-31240
Electrostatic precipitation of condensed acid mist [DE91-016530] N91-31260
Proceedings of the Ninth Symposium on Energy Engineering Sciences: Fluid and Dynamical Systems [DE91-015974] N91-31701

COMBUSTION CHAMBERS
Cold weather ignition characteristics of advanced small gas turbine combustion systems N91-31152
Cold start investigation of an APU with annular combustor and fuel vaporizers N91-31154
The effect of fuel properties and atomization on low temperature ignition in gas turbine combustors N91-31164

COMBUSTION CHEMISTRY
Jet-A reaction mechanism study for combustion application [NASA-TM-104441] N91-31181
The autoignition chemistry of paraffinic fuels and pro-knock and anti-knock additives: A detailed chemical kinetic study [DE91-014992] N91-31314

COMBUSTION PHYSICS
The influence of fuel characteristics on heterogeneous flame propagation N91-31165

COMBUSTION PRODUCTS
Performance evaluation of insensitive explosives [DE91-015767] N91-31315
Understanding composite explosive energetics [DE91-015770] N91-31316

COMBUSTION STABILITY
Nonlinear combustion instability model in two- to three-dimensions [NASA-TM-102381] N91-31208

COMBUSTION TEMPERATURE
Effects of oxidation and combustion environments on the properties of Nicalon/SiC composites [DE91-016778] N91-31240

COMMERCIAL AIRCRAFT
Adaptive function allocation for intelligent cockpits [AD-A239714] N91-31808

COMMERCIAL ENERGY
Fuel cells for commercial energy [MBB-UE-0018-90-PUB] N91-31706

COMMUNICATION
A study of the logistics function within a medium sized, sales oriented chemical company [ETN-91-99983] N91-31987

COMMUNICATION NETWORKS
Some order dimension bounds for communication complexity problems [MEMO-938] N91-31489
Refining interfaces of communicating systems [MEMO-INF-91-19] N91-31493
The data distribution satellite system [NASA-CR-187172] N91-31499
Adaptive arrays in packet radio networks [AD-A239636] N91-31509
The failure of failures: Towards a paradigm for a synchronous communication [RUU-CS-90-40] N91-31835
On the application of temporal logic in real time to specify telecommunication protocols [REPT-90-071] N91-31846
The problem of network management: An approach using AI techniques [REPT-90-072] N91-31884

COMMUNICATION SATELLITES
Traffic model for advanced satellite designs and experiments for ISDN services [NASA-CR-188802] N91-31200
Choice of a differential method for attitude restitution with dynamic imbalance [CNES-NT-126] N91-31202
Aeronautical Mobile Satellite Service (AMSS) test plan [DOT/FAA/CT-TN91/20] N91-31495
The data distribution satellite system [NASA-CR-187172] N91-31499

COMPARISON
Initialization of the HIRLAM model using a digital filter [DM-57] N91-31747

COMPATIBILITY
Intrusion and fault tolerance compatibility. Part 1: Fault protection, coding and tolerance state of the art [LAAS-89-395] N91-31662

COMPILERS
Partial evaluation grammars [TR-91-01] N91-31826
Hypertext development using a model-based approach [REPT-90-074] N91-31995

COMPLEX COMPOUNDS
Chemically modified electrodes and related solution studies [DE91-016740] N91-31262
Energy transfer processes in solar energy conversion [DE91-016102] N91-31704

COMPLEXITY
A formal power series equation from formula complexity theory [TR-90-25] N91-31895

COMPOSITE MATERIALS
Vaudreuil (France) large hydrodynamic tunnel: Acoustic chamber damping [METRAVIB-RDS-1-007-67] N91-31090
Composite ingot casting [PATENT-1-250-128] N91-31269
Composite materials, 1 (TEXUS 1) N91-31430
Composite materials, 2 (TEXUS 2) N91-31431
The behaviour of alumina-copper suspensions (TEXUS 3A and 3B) N91-31433
Copper-molybdenum suspension (TEXUS 9) N91-31435
Tungsten composites (TEXUS 19) ESA N91-31445
Liquid phase sintering (TEXUS 19) ESA N91-31446
Pores in aluminium alloys (TEXUS 3) N91-31447
Manufacture of steel foam (TEXUS 4) N91-31448
Manufacture of steel foam (TEXUS 6) N91-31449
Manufacture of iron foam (TEXUS 7) N91-31450
Metallic foams (TEXUS 5) N91-31451
Preparation of aluminium foams (TEXUS 9) N91-31452
Gas bubbles in a copper-alumina suspension (TEXUS 11) N91-31453
Bubble formation, growth, and expansion during the liquid phase sintering of a WC-Co sample N91-31454

COMPOSITE STRUCTURES
Method for fastening aircraft frame elements to sandwich skin panels covering same using woven fiber connectors [PATENT-1-274-075] N91-31126
Method for stabilizing thick honeycomb core composite articles [PATENT-1-253-424] N91-31224
A method for the geometrically nonlinear analysis of compressively loaded prismatic composite structures N91-31229
Nonlinear probabilistic finite element modeling of composite shells N91-31668

COMPOSITION (PROPERTY)
Rapidly solidified nickel aluminide of improved stoichiometry and ductilization [PATENT-1-257-987] N91-31270

COMPRESSED AIR
The medical hazards of flame-suppressant atmospheres [AD-A239618] N91-31806

COMPRESSIBILITY
Elastic wave dispersion in high-strength ceramics [DE91-016648] N91-31309

COMPRESSIBLE BOUNDARY LAYER
Direct and large-eddy simulations of transition in the compressible boundary layer N91-31566

COMPRESSIBLE FLOW
Linear and nonlinear stability of boundary layers with streamwise varying properties N91-31545
Turbulence modeling for compressible flows and implementation in Navier-Stokes solvers N91-31564
Algorithms for finding an optimal matching between a given string and a string generated by a regular grammar [MEMO-921] N91-31845

COMPRESSION LOADS
Anelastic release from the shock-compressed state [DE91-009961] N91-31672

COMPRESSOR BLADES
Ice ingestion experience on a small turboprop engine N91-31162

COMPUTATION
Mathematical theory of computation [AD-A239419] N91-31912
Computational model for deterministic chaos in a magnetically confined plasma [DE91-016022] N91-31955

COMPUTATIONAL FLUID DYNAMICS
Computational analysis of hypersonic flows past elliptic-cone waveriders N91-31080
A computational and experimental investigation of a three-dimensional hypersonic scramjet inlet flow field [NASA-CR-188788] N91-31083
A European collaborative investigation of the three-dimensional turbulent shear layers of a swept wing [NLR-MP-88054-U] N91-31084
Design and testing of a multiblock grid-generation procedure for aircraft design and research [NLR-TP-89146-U] N91-31131
The development of a computational model to predict low temperature fuel flow phenomena N91-31166
Two-equation models for low-Reynolds number flow N91-31554
Development of a computation code for nonequilibrium gas axisymmetric hypersonic laminar flow [ONERA-RS-14/3637-AY] N91-31585
Flow visualization and simulation [AAAF-NT-89-18] N91-31590
Postprocessing of test and computation results by the wavelet method [AAAF-NT-89-24] N91-31591
Review of typical applications: Wind tunnels N91-31632
NASA Aerodynamics Program [NASA-TM-4312] N91-31751
Post processing of three dimensional aerothermal computation [AAAF-NT-89-21] N91-31848
Use of the animated images for the visualization of computational results [AAAF-NT-89-22] N91-31849

COMPUTATIONAL GRIDS
Laser Fourier densitometry and laser induced photochemical anemometry in supersonic flow [AAAF-NT-89-09] N91-31103
Design and testing of a multiblock grid-generation procedure for aircraft design and research [NLR-TP-89146-U] N91-31131
Finite element modeling of orthogonal machining using an elastic-viscoplastic material model [DE91-016815] N91-31477
Acceleration techniques for a spectral multi-grid method [MEMO-914] N91-31580
Estimating the strength of the capping inversion and the probability of strong convection [PB91-176685] N91-31744
A dynamically adaptive multigrid algorithm for the incompressible Navier-Stokes equations: Validation and model problems [NASA-CR-187595] N91-31888
Multigrid and Runge-Kutta time stepping applied to the uniformly non-oscillatory scheme for conservation laws [MEMO-911] N91-31906
An extension of mesh equidistribution to time-dependent partial differential equations [AD-A239579] N91-31913
Analysis of the efficiency of an a-posteriori error estimator for linear triangular finite elements [AD-A239647] N91-31915

COMPUTER AIDED DESIGN
Application of a water droplet trajectory prediction code to the design of inlet particle separator anti-icing systems N91-31159
Inter-GEN: A hybrid approach to engineering design optimization N91-31471
Hardware modeling and top-down design using VHDL [AD-A239356] N91-31534
Analysis and development of a wide-bandwidth gravitational wave detector N91-31601
Spur-gear optimization using SPUROPT computer program [NASA-TM-104394] N91-31648
Absorbing CAD system geometries into GEANT [DE91-015707] N91-31816
Interactive constraint-based solid modeling as a design tool [AD-A239358] N91-31856
An extension of the potential method to higher-order blendings [CS-9103] N91-31893

COMPUTER AIDED MANUFACTURING
Recent manufacturing advances for spiral bevel gears [NASA-TM-104479] N91-31654
The development of an intelligent dimensional inspection environment using coordinate measuring machines N91-31661
Atomatic Feature (AFEAT) identification for Computer-Aided Process Planning (CAPP) [DE91-016478] N91-31819

COMPUTER AIDED MAPPING
Examination and mapping of forest damage, using remote sensing methods
[ETN-91-99741] N91-31696
COMPUTER AIDED TOMOGRAPHY
Boron in nuclear medicine: New synthetic approaches to PET, SPECT, and BNCT agents
[DE91-016488] N91-31764
COMPUTER ANIMATION
Flow visualization and simulation
[AAAF-NT-89-18] N91-31590
COMPUTER GRAPHICS
Airplane takeoff and landing performance monitoring system
[NASA-CASE-LAR-13854-1-CU] N91-31120
Flow visualization and simulation
[AAAF-NT-89-18] N91-31590
A scientific visualization synthesizer
[DE91-012877] N91-31815
Dynamic output-sensitive hidden surface removal for c-oriented polyhedra
[RUU-CS-91-06] N91-31839
Interactive tool visualization of three dimensional 3D results
[AAAF-NT-89-19] N91-31847
Post processing of three dimensional aerothermal computation
[AAAF-NT-89-21] N91-31848
Use of the animated images for the visualization of computational results
[AAAF-NT-89-22] N91-31849
COMPUTER INFORMATION SECURITY
Intrusion and fault tolerance compatibility. Part 1: Fault protection, coding and tolerance state of the art
[LAAS-89-395] N91-31662
OSI-security and relations with other security standards
[FEL-91-B099] N91-31872
Information security: Past, present and future
[FEL-91-B100] N91-31873
COMPUTER NETWORKS
Traffic model for advanced satellite designs and experiments for ISDN services
[NASA-CR-188802] N91-31200
Interim Service ISDN Satellite (ISIS) network model for advanced satellite designs and experiments
[NASA-CR-186565] N91-31488
The development of an intelligent dimensional inspection environment using coordinate measuring machines N91-31661
Design and analysis of fault-tolerant distributed real-time computer systems
[AD-A239521] N91-31812
Distributed incremental maximum finding in hierarchically divided graphs
[RUU-CS-90-30] N91-31828
The failure of failures: Towards a paradigm for a synchronous communication
[RUU-CS-90-40] N91-31835
A users' guide to PVM (parallel virtual machine)
[DE91-016934] N91-31855
Study day on the design of a network database in four languages
[MEMO-INF-91-22] N91-31863
A solution for the network database problem in an imperative language N91-31864
An object-oriented analysis, design, and implementation of a network database N91-31865
Network database in PROLOG N91-31866
A network database: A case study in functional programming N91-31867
Benchmarking a Network Storage Service
[DE91-013510] N91-31868
The PVM system: Supercomputer level concurrent computation on a heterogeneous network of workstations
[DE91-016276] N91-31870
Design and analysis of fault-tolerant distributed real-time computer systems
[AD-A239382] N91-31875
Inventory and functional prototypes of neural networks
[TR-90-15] N91-31880
COMPUTER PROGRAM INTEGRITY
Intrusion and fault tolerance compatibility. Part 1: Fault protection, coding and tolerance state of the art
[LAAS-89-395] N91-31662
COMPUTER PROGRAMMING
Improvements to programs for system studies of space-based radar
[DRE-179] N91-31484
LR-parsing derived
[CS-9105] N91-31823
Categorical semantics as a basis for program transformation
[RUU-CS-90-38] N91-31833
Study day on the design of a network database in four languages
[MEMO-INF-91-22] N91-31863
A network database: A case study in functional programming N91-31867
COMPUTER PROGRAMS
ATSF supersonic aircraft intake. Review of the analyses of some particular problems, technical summary
[ONERA-RTS-134/2149-AY-640-A] N91-31094
Vortex-blade interaction on a helicopter principal rotor. Validation of the S2DI computation program and study of vortex models
[ONERA-RT-92/5094-PY] N91-31136
Understanding composite explosive energetics
[DE91-015770] N91-31316
Finite element modeling of orthogonal machining using an elastic-viscoplastic material model
[DE91-016815] N91-31477
Updates to the DREO airborne radar simulator
[ASSGI-167] N91-31478
The automatic surveillance, tracking, and imaging program. User manual
[SK-1600-44-001-02-0] N91-31483
A boundary integral equation method for steady two-dimensional flow in partially saturated media
[DE91-016056] N91-31573
Development of a computation code for nonequilibrium gas axisymmetric hypersonic laminar flow
[ONERA-RS-14/3637-AY] N91-31585
Spur-gear optimization using SPUROPT computer program
[NASA-TM-104394] N91-31648
DYNA3D: A nonlinear, explicit, three-dimensional finite element code for solid and structural mechanics
[DE91-015735] N91-31675
Large Angle Transient Dynamics (LATDYN) demonstration problem manual
[NASA-CR-4400] N91-31684
Large Angle Transient Dynamics (LATDYN) user's manual
[NASA-CR-4401] N91-31685
Open-cycle ocean thermal energy conversion surface-condenser design analysis and computer program
[DE91-015973] N91-31709
Human factors engineering design guidelines for the software user interface
[DE91-016061] N91-31802
Design and analysis of fault-tolerant distributed real-time computer systems
[AD-A239521] N91-31812
Software quality metrics
[DOT/FAA/CT-91/1] N91-31814
Absorbing CAD system geometries into GEANT
[DE91-015707] N91-31816
SHOWTIME.C: A C-language program for data acquisition and display user's guide
[DE91-016241] N91-31817
Interactive tool visualization of three dimensional 3D results
[AAAF-NT-89-19] N91-31847
Visualization of three dimensional unsteady computation results
[AAAF-NT-89-23] N91-31850
Open architecture for formal reasoning
[AD-A239395] N91-31857
Practical aspects of an interior-point method for convex programming
[AD-A239457] N91-31858
Report on the Software Technology for Adaptable, Reliable Systems (STARS) Conference on Frameworks Convergence
[AD-A239691] N91-31862
On the optimal use of fictitious time in variation of parameters methods with application to BG14
[NASA-CR-185650] N91-31890
Mathematical theory of computation
[AD-A239419] N91-31912
Research in regression, information retrieval, inversion of noisy transforms, and stochastic control
[AD-A239490] N91-32001
Abundances from solar flare line spectroscopy
[NASA-CR-183492] N91-32022
COMPUTER STORAGE DEVICES
Temporal sampling considerations in global climate modeling
[DE91-015695] N91-31717
Asymmetric soft-error resistant memory
[NASA-CASE-NPO-17394-1-CU] N91-31810
A fast multiport memory based on single-port memory cells
[AD-A239455] N91-31811
COMPUTER SYSTEMS DESIGN
Hybrid electro-optic processor
[AD-A239547] N91-31505
Reliability modeling of dependable distributed systems
[AD-A239734] N91-31663
The potential impact of VHDL on dependable distributed system design
[AD-A239769] N91-31664
Design and analysis of fault-tolerant distributed real-time computer systems
[AD-A239521] N91-31812
Design and analysis of fault-tolerant distributed real-time computer systems
[AD-A239382] N91-31875
The problem of network management: An approach using AI techniques
[REPT-90-072] N91-31884
Hypertext development using a model-based approach
[REPT-90-074] N91-31995
COMPUTER SYSTEMS PERFORMANCE
Touch screen use on flight simulator instructor/operator stations
[AD-A239524] N91-31192
The potential impact of VHDL on dependable distributed system design
[AD-A239769] N91-31664
Interactive constraint-based solid modeling as a design tool
[AD-A239358] N91-31856
Methods of astrodynamics, a computer approach
[AD-A239662] N91-31861
COMPUTER TECHNIQUES
Human factors engineering design guidelines for the software user interface
[DE91-016061] N91-31802
Adaptive function allocation for intelligent cockpits
[AD-A239714] N91-31808
Atomatic Feature (AFEAT) identification for Computer-Aided Process Planning (CAPP)
[DE91-016478] N91-31819
The derivation of distributed termination detection algorithms from garbage detection schemes
[RUU-CS-90-24] N91-31827
The on-line d-dimensional dictionary problem
[RUU-CS-90-31] N91-31829
Synchronous link-level protocols
[RUU-CS-91-02] N91-31837
Covering a set of points with fixed size hypersquares and related problems
[RUU-CS-90-32] N91-31898
Mathematical theory of computation
[AD-A239419] N91-31912
Formalisation of techniques: Chopping down the methodology jungle
[TR-90-26] N91-31996
COMPUTER VISION
A graph theoretic approach to scene matching
[NASA-CR-187817] N91-31947
Parametric study of diffusion-enhancement networks for spatiotemporal grouping in real-time artificial vision
[AD-A239674] N91-31954
COMPUTERIZED SIMULATION
The effects of different sequencing strategies on the capacity of airports
[DLR-MITT-90-18] N91-31185
Understanding composite explosive energetics
[DE91-015770] N91-31316
Immiscibles, 2 (TEXUS 5) N91-31411
Inter-GEN: A hybrid approach to engineering design optimization N91-31471
Finite element modeling of orthogonal machining using an elastic-viscoplastic material model
[DE91-016815] N91-31477
Numerical simulation of a split cavity oscillator and rf conversion
[DE91-016501] N91-31523
The interaction of particles with homogeneous turbulence N91-31548
Introduction to the Modeling of Turbulence
[VKI-LS-1991-02] N91-31551
An introduction to second moment closure N91-31555
Inclusion of second-moment closures into finite-volume solvers N91-31556
A boundary integral equation method for steady two-dimensional flow in partially saturated media
[DE91-016056] N91-31573
Hydrodynamic target response to an induced spatial incoherence-smoothed laser beam
[DE91-015757] N91-31638
Modeling and simulation of multiple cooperating manipulators on a mobile platform N91-31647
A Weibull brittle material failure model for the ABAQUS computer program
[DE91-016813] N91-31690
Development of the CELSS emulator at NASA. Johnson Space Center N91-31793
Absorbing CAD system geometries into GEANT
[DE91-015707] N91-31816

Developing dataflow algorithms
[DE91-016300] N91-31818
High energy physics program. Task A: Experiment and Theory. Task B: Numerical simulation of quantum field theories
[DE91-015652] N91-31938

CONCENTRATION (COMPOSITION)
Growth of a Si crystal covered with a SiO2 skin (TEXUS 12) N91-31385

CONCENTRATORS
Thin film, concentrator and multijunction space solar cells: Status and potential
[NASA-TM-104505] N91-31218
Parabolic dish photovoltaic concentrator development
[DE91-016868] N91-31714

CONCORDE AIRCRAFT
Second generation supersonic transport aircraft: Low speed aerodynamics
[AAAF-NT-89-02] N91-31137

CONCRETES
A knowledge-base for rehabilitation of airfield concrete pavements
[AD-A239354] N91-31191

CONCURRENT PROCESSING
The failure of failures: Towards a paradigm for a synchronous communication
[RUU-CS-90-40] N91-31835
The PVM system: Supercomputer level concurrent computation on a heterogeneous network of workstations
[DE91-016276] N91-31870

CONDENSERS (LIQUEFIERS)
Open-cycle ocean thermal energy conversion surface-condenser design analysis and computer program
[DE91-015973] N91-31709

CONDENSING
Bubble formation, 1 (TEXUS 5) N91-31355

CONDUCTING POLYMERS
Chemically modified electrodes and related solution studies
[DE91-016740] N91-31262
Application of microwave cavity perturbation techniques in conducting polymers
[AD-A239376] N91-31310

CONDUCTIVITY
Application of microwave cavity perturbation techniques in conducting polymers
[AD-A239376] N91-31310

CONFERENCES
Abstracts of papers presented at the First Los Alamos Symposium on Ultra-Wideband Radar
[DE91-015976] N91-31491
Proceedings of the International Magnetic Pulse Compression Workshop. Volume 2: Technical summary
[DE91-015775] N91-31521
Proceedings of the Ninth Symposium on Energy Engineering Sciences: Fluid and Dynamical Systems
[DE91-015974] N91-31701
Controlled Ecological Life Support Systems: CELSS '89 Workshop
[NASA-TM-102277] N91-31775

CONJUGATE GRADIENT METHOD
Least-squares solution of incompressible Navier-Stokes equations with the p-version of finite elements
[NASA-TM-105203] N91-31911

CONSERVATION LAWS
Multigrid and Runge-Kutta time stepping applied to the uniformly non-oscillatory scheme for conservation laws
[MEMO-911] N91-31906

CONSTANTS
Radar-cross-section measurement errors caused by test object interaction with low-dielectric-constant supports
[DE91-015340] N91-31490

CONSUMABLES (SPACECRAFT)
Seed sprout production: Consumables and a foundation for higher plant growth in space N91-31790

CONTAINERLESS MELTS
Acoustic positioning of a molten alloy sample (TEXUS 1) N91-31464
Acoustic positioning (TEXUS 9) ESA N91-31465
Containerless solidification of a Pd-Cu-Si sample (TEXUS 9) ESA N91-31466
Acoustic positioning (TEXUS 14b) ESA N91-31467
Containerless undercooling of a Pd-Cu-Si alloy (TEXUS 14b) ESA N91-31468
Electrostatic positioning for containerless processing of a Li-silicate glass (TEXUS 10) ESA N91-31469

CONTAMINANTS
Noxious matter minimization as a project criterion for aircraft
[MBB-Z-0337-90-PUB] N91-31134

CONTAMINATION
Biofilm monitoring coupon system and method of use
[NASA-CASE-MSC-21585-1] N91-31755
Garment selection for cleanrooms and controlled environments for spacecraft
[AD-A239512] N91-31805

CONTINUITY (MATHEMATICS)
Continuous informations systems
[RUU-CS-90-25] N91-31997

CONTINUUM MECHANICS
An investigation into the effects of damage on the stresses in a composite laminate N91-31226

CONTRACT MANAGEMENT
What is the Federal Demonstration Project?
[DE91-013936] N91-31986

CONTRACTION
Cold-induced changes in arterial sensitivity
[AD-A239493] N91-31767

CONTRACTORS
Solid-State Radar Beacon Decoder (SSRBD) Master Test Plan (MTP)
[DOT/FAA/CT-TN91/33] N91-31494

CONTRACTS
Survey to assess the usefulness of two model agreements for university-industry cooperative research
[DE91-013937] N91-31985

CONTROL EQUIPMENT
Rotatable non-circular forebody flow controller
[NASA-CASE-LAR-14212-1-CU] N91-31140
Procedure for steering a low-speed missile, weapon system, and missile for implementation of the procedure
[PATENT-1-265-947] N91-31182

CONTROL STABILITY
On the stability of saturated state feedback regulators
[LAAS-91047] N91-31524

CONTROL SURFACES
Enhanced fighter maneuverability aircraft (X-31A) wing and thrust vectoring vane design
[MBB-FE22/S/PUB/0433/A] N91-31135
Rotatable non-circular forebody flow controller
[NASA-CASE-LAR-14212-1-CU] N91-31140

CONTROL SYSTEMS DESIGN
Rotatable non-circular forebody flow controller
[NASA-CASE-LAR-14212-1-CU] N91-31140
Cold weather jet engine starting strategies made possible by engine digital control systems N91-31153
Control system design considerations for starting turbo-engines during cold weather operation N91-31155
Reusable rocket engine intelligent control system framework design, phase 2
[NASA-CR-187213] N91-31219
Integrated control of thermally distorted large space antennas N91-31487
A universal computer control system for motors
[NASA-CASE-NPO-17134-1-CU] N91-31528
Advanced optical sensing and processing technologies for the distributed control of large flexible spacecraft
[NASA-CR-4399] N91-31609
Application of multivariable control system design methodologies to robust beam control of a space-based laser
[AD-A239460] N91-31643
Large Angle Transient Dynamics (LATDYN) demonstration problem manual
[NASA-CR-4400] N91-31684
Large Angle Transient Dynamics (LATDYN) user's manual
[NASA-CR-4401] N91-31685
Design and cost of the first commercial stretched-membrane heliostat
[DE91-016870] N91-31715
An application of neural networks to process and materials control
[DE91-016016] N91-31886
Analysis of interior noise ground and flight test data for advanced turboprop aircraft applications
[NASA-CR-187558] N91-31927

CONTROL THEORY
A case study for the real-time experimental evaluation of the VIPER microprocessor
[NASA-TM-104098] N91-31531
A perspective on CELSS control issues N91-31794
Small time step adaptive control: Theory and application to an electric furnace
[ECL-90-17] N91-31883

CONTROL VALVES
A high-frequency servosystem for fuel control in hypersonic engines
[NASA-TM-104333] N91-31178

CONTROLLABILITY
Restructured Freedom configuration characteristics
[NASA-TM-104057] N91-31201

CONTROLLED ATMOSPHERES
The crop growth research chamber: A ground-based facility for CELSS research N91-31792
Garment selection for cleanrooms and controlled environments for spacecraft
[AD-A239512] N91-31805

CONTROLLERS
Robust impedance control of robot manipulators N91-31297
A universal computer control system for motors
[NASA-CASE-NPO-17134-1-CU] N91-31528
Application of multivariable control system design methodologies to robust beam control of a space-based laser
[AD-A239460] N91-31643
Tuning maps for setpoint changes and load disturbance upsets in a three capacity process under multivariable control
[NASA-TM-104419] N91-31876
Neural network based model reference adaptive control N91-31877
Kinematics of the six-degree-of-freedom force-reflecting Kraft Master
[NASA-TM-104124] N91-31879
Synchronized computational architecture for generalized bilateral control of robot arms
[NASA-CASE-NPO-17401-1-CU] N91-31885

CONVECTION
Diffusion-induced interfacial convection (TEXUS 8) N91-31331
Diffusion-induced interfacial convection (TEXUS 11) N91-31332
Intermittent polarization (TEXUS 2) N91-31349
Solidification of alloys (TEXUS 1) N91-31400
Directional solidification of Al-Cu alloys (MASER 2) N91-31403
Directional solidification of eutectics InSb-NiSb (TEXUS 10) N91-31405
Effect of convection on weld pool development
[DE91-014213] N91-31649
Impact of the ice phase on a mesoscale convective system: Cloud ensemble features and cloud radiative properties
[DE91-015769] N91-31749

CONVECTIVE FLOW
Interfacial convection (TEXUS 1) N91-31327
Interfacial convection (TEXUS 2) N91-31328
Thermally induced interfacial convection (TEXUS 4) N91-31330
Diffusion-induced interfacial convection (TEXUS 8) N91-31331
Three-dimensional Marangoni convection (MASER 2) ESA N91-31344
Artificial diffusion methods in convection dominated flows
[W-9016] N91-31577
Estimating the strength of the capping inversion and the probability of strong convection
[PB91-176685] N91-31744

CONVERGENCE
Local mean mass volume measurement around a model with lateral jet in supersonic flow
[AAAF-NT-89-08] N91-31102
Convergence performance of adaptive detectors, part 1
[AD-A239507] N91-31539
Convergence performance of adaptive detectors, part 2
[AD-A239532] N91-31540

CONVERSION
Capacitive bridge-type probe and conversion circuitry
[PATENT-1-263-444] N91-31598
Capacitive bridge-type probe and conversion circuitry
[PATENT-1-263-443] N91-31599

CONVEXITY
Practical aspects of an interior-point method for convex programming
[AD-A239457] N91-31858
Learning convex bodies under uniform distribution
[MEMO-918] N91-31910

COOLING
Acoustic positioning (TEXUS 14b) ESA N91-31467
Containerless undercooling of a Pd-Cu-Si alloy (TEXUS 14b) ESA N91-31468
Examination of molecular evaporation, cooling, and cluster dissociation of very thin liquid jets in a high vacuum
[MPIS-12/1990] N91-31581

COOPERATION
Survey to assess the usefulness of two model agreements for university-industry cooperative research
[DE91-013937] N91-31985

COORDINATES
Coordinate conversions for presenting and compositing weather radar data
[KNMI-TR-129] N91-31497

COORDINATION
Two alternative ways for solving the coordination problem in multilevel optimization
[NASA-TM-104036] N91-31138

COPOLYMERS
Determination of aqueous processable photoresist in tin-lead plating solutions
[DE91-015575] N91-31251
COPPER
Influence of loading rate on the mechanical response and substructure evolution of shock-loaded copper
[DE91-013390] N91-31276
The behaviour of alumina-copper suspensions (TEXUS 3A and 3B) N91-31433
Copper-alumina suspensions (TEXUS 5) N91-31434
Copper-molybdenum suspension (TEXUS 9) N91-31435
Metallic composites with particles (TEXUS 6) N91-31436
Metallic composites with particles (TEXUS 7) N91-31437
Melting and solidification of metallic composites (TEXUS 9) N91-31438
Liquid phase sintering (TEXUS 8) N91-31443
Soldering in microgravity (TEXUS 5) N91-31462
Near-edge study of gold-substituted YBa2Cu3O(7-delta)
[NASA-TM-105220] N91-31977
COPPER ALLOYS
Theoretical studies of metallic alloys
[DE91-016486] N91-31281
Development and characterization of low temperature Cu-Al-Be shape memory alloys
[ISAL-90-0093] N91-31284
Diffusion of Ni in Cu-Au and Cu-Al alloys (TEXUS 20) N91-31373
Directional solidification of Al-Cu alloys (MASER 2) N91-31403
Directional solidification of eutectics (TEXUS 6) N91-31404
Unidirectional solidification of immiscible alloys (TEXUS 5) N91-31418
Alloys with oxide inclusions (TEXUS 2) N91-31432
Gas bubbles in a copper-alumina suspension (TEXUS 11) N91-31453
Low cost, formable, high T(sub c) superconducting wire
[NASA-CASE-LEW-14676-1] N91-31529
COPPER OXIDES
Mean field analysis of the CuO2 lattice: Comparison to Monte Carlo simulations
[DE91-015570] N91-31968
Cu-O charge fluctuations and electron-phonon coupling in the effective single-band Hubbard theory for cuprate superconductors
[DE91-016526] N91-31976
Near-edge study of gold-substituted YBa2Cu3O(7-delta)
[NASA-TM-105220] N91-31977
CORN
Simulated effects of a doubling of carbon dioxide on corn production in portions of the central US
[DE91-016843] N91-31722
CORROSION
Reaction kinetics in glass melts: Corrosion of SiO2 (TEXUS 4) N91-31364
CORROSION RESISTANCE
Field evaluation of six protective coatings applied to T56 turbine blades after 500 hours of engine use
[ARL-MAT-TM-405] N91-31179
Stress corrosion cracking of 2091 ad 8090 aluminum-lithium alloys in chloride containing aqueous solutions. Influence of sulphate and nitrate additions
[REPT-431/91] N91-31285
Initial determination of the micromechanical properties of oxide scales
[DE90-012164] N91-31291
CORROSION TESTS
Field evaluation of six protective coatings applied to T56 turbine blades after 500 hours of engine use
[ARL-MAT-TM-405] N91-31179
Corrosion fatigue crack arrest in aluminium alloys
[NLR-MP-88050-U] N91-31282
Stress corrosion cracking of 2091 ad 8090 aluminum-lithium alloys in chloride containing aqueous solutions. Influence of sulphate and nitrate additions
[REPT-431/91] N91-31285
COSMOLOGY
Hydrodynamic simulations of cosmology N91-32013
COST ANALYSIS
The question of an efficient space transportation system for extraterrestrial materials
[ILR-MITT-252(1990)] N91-31197
Assessment of costs and benefits of flexible and alternative fuel use in the US transportation sector
[DE91-015451] N91-31319
Economic analysis of robotic torque measurement system
[DE91-016480] N91-31653
Design and cost of the first commercial stretched-membrane heliostat
[DE91-016870] N91-31715
COST EFFECTIVENESS
The question of an efficient space transportation system for extraterrestrial materials
[ILR-MITT-252(1990)] N91-31197
COST ESTIMATES
Facet development for a faceted stretched-membrane dish by Solar Kinetics, Inc.
[DE91-016866] N91-31713
COULOMB POTENTIAL
Macroscopic quantum tunneling in Josephson tunnel junctions and Coulomb blockade in single small tunnel junctions
[DE91-016258] N91-31974
COUPLING
Composite waveguide coupling aperture having a thickness dimension
[PATENT-1-259-401] N91-31514
COVERALLS
Garment selection for cleanrooms and controlled environments for spacecraft
[AD-A239512] N91-31805
COVERINGS
Steerable windowed enclosures
[PATENT-1-262-653] N91-31142
Extensive coverings and exact core bounds
[MEMO-915] N91-31907
COWLINGS
Removable slider shoe for a translating sleeve used on a jet engine cowl and duct
[PATENT-1-247-868] N91-31177
CRAB NEBULA
A search for periodicity in the x ray spectrum of black hole candidate A0620-00
[AD-A239488] N91-32011
CRACK ARREST
Corrosion fatigue crack arrest in aluminium alloys
[NLR-MP-88050-U] N91-31282
CRACK CLOSURE
Ultrasonic characterization of fatigue crack closure
[DE91-015161] N91-31688
CRACK PROPAGATION
Relation between fiber proportion and mechanical characteristics of carbon-resin composites
[RE-50-345/F] N91-31231
Composite materials damage. Transverse cracking and delamination
[ONERA-RT-6/7256-RY-080-R] N91-31234
Alumina reinforced tetragonal zirconia (TZP) composites
[DE91-016748] N91-31239
Investigation of two-dimensional cracks at an angle to an interface N91-31667
Asymptotic finite strain analysis of propagating cracks in elastic-plastic materials N91-31669
In situ short fatigue crack characterization of a nickel-base superalloy at ambient and elevated temperature N91-31670
Crack propagation in heat resistant disk alloys. Short crack propagation in alloys for high characteristic turbomachine disks
[ETN-91-99981] N91-31683
Ultrasonic characterization of fatigue crack closure
[DE91-015161] N91-31688
An equivalent domain integral method for three-dimensional mixed-mode fracture problems
[NASA-CR-182021] N91-31692
CRACK TIPS
Alumina reinforced tetragonal zirconia (TZP) composites
[DE91-016748] N91-31239
Metastable austenites in cryogenic high magnetic field environments
[DE91-016420] N91-31288
Fracture toughness characterization of polymers N91-31296
Investigation of two-dimensional cracks at an angle to an interface N91-31667
Asymptotic finite strain analysis of propagating cracks in elastic-plastic materials N91-31669
CRACKING (FRACTURING)
An analytical prediction of matrix cracking in fibrous composite laminates N91-31225
Weldability and hot ductility of iron aluminides
[DE91-016343] N91-31280
Crack propagation in heat resistant disk alloys. Short crack propagation in alloys for high characteristic turbomachine disks
[ETN-91-99981] N91-31683
CRACKS
An investigation into the effects of damage on the stresses in a composite laminate N91-31226
Investigation of two-dimensional cracks at an angle to an interface N91-31667
In situ short fatigue crack characterization of a nickel-base superalloy at ambient and elevated temperature N91-31670
CRASH LANDING
Beacon activation device
[PATENT-1-256-916] N91-31108
CREEP PROPERTIES
Creep deformation and fracture of a two-phase TiAl intermetallics
[DE91-011963] N91-31274
Models of flux diffusion and flux creep in high-temperature superconductors
[DE91-015838] N91-31972
CRITICAL POINT
Phase transition (TEXUS 8) N91-31374
Ionic solutions near the critical point of water (TEXUS 10) ESA N91-31375
Ionic solutions near the critical point of water (TEXUS 12) ESA N91-31376
Phase separation of a binary fluid near its critical point (TEXUS 11) N91-31377
Phase separation in microgravity of binary fluids near the critical point (TEXUS 13) N91-31378
Spinoidal decomposition (TEXUS 17) N91-31379
CRITICAL TEMPERATURE
Segregation behaviour of rare earths under microgravity and normal gravity conditions (TEXUS 13) N91-31407
Studies of non-ideal superconductors using DC magnetic methods
[DE91-015642] N91-31970
The critical temperature for drying-out of soils around power cables as a function of local conditions N91-32025
CROP GROWTH
Simulated effects of a doubling of carbon dioxide on corn production in portions of the central US
[DE91-016843] N91-31722
Efficiency of N use by wheat as a function of influx and efflux of NO3 N91-31778
The crop growth research chamber: A ground-based facility for CELSS research N91-31792
A perspective on CELSS control issues N91-31794
CROSS CORRELATION
Post-processing of data N91-31633
CROSS COUPLING
Tuning maps for setpoint changes and load disturbance upsets in a three capacity process under multivariable control
[NASA-TM-104419] N91-31876
CRUCIBLES
Metallic composites with particles (TEXUS 7) N91-31437
Metal matrix composites (TEXUS 20) N91-31440
Tungsten composites (TEXUS 10) N91-31444
CRUDE OIL
Global model simulations of the long range transport of soot and sulfur from the Kuwait oil fires
[DE91-015771] N91-31719
CRUISE MISSILES
Environmental icing testing at the Naval Air Propulsion Center N91-31167
CRYOGENIC FLUID STORAGE
Predicted thermal response of a cryogenic fuel tank exposed to simulated aerodynamic heating profiles with different cryogens and fill levels
[NASA-CR-4395] N91-31470
CRYOGENIC FLUIDS
Predicted thermal response of a cryogenic fuel tank exposed to simulated aerodynamic heating profiles with different cryogens and fill levels
[NASA-CR-4395] N91-31470
CRYOGENIC TEMPERATURE
Magnetic field-induced fracture changes in metastable austenites at 4.2 K
[DE91-016263] N91-31279
CRYOGENICS
Metastable austenites in cryogenic high magnetic field environments
[DE91-016420] N91-31288
Predicted thermal response of a cryogenic fuel tank exposed to simulated aerodynamic heating profiles with different cryogens and fill levels
[NASA-CR-4395] N91-31470
CRYSTAL DEFECTS
Dynamic strength and strain rate effects on fracture behavior of tungsten and tungsten alloys
[DE91-013029] N91-31275
Influence of loading rate on the mechanical response and substructure evolution of shock-loaded copper
[DE91-013390] N91-31276
Formation of defect structures in metals during irradiation
[DE91-015548] N91-31278
Studies of non-ideal superconductors using DC magnetic methods
[DE91-015642] N91-31970

CRYSTAL GROWTH
Long liquid bridges aboard sounding rockets (TEXUS 12) ESA N91-31325
Freezing of a long liquid column (TEXUS 18) ESA N91-31326
Striations in germanium (TEXUS 6) ESA N91-31381
Single crystals of CeMg3 (TEXUS 7) ESA N91-31382
Growth of rare Earth-magnesium crystals (TEXUS 12) N91-31383
Floating-zone growth of a silicon single crystal (TEXUS 7) N91-31384
Growth of a Si crystal covered with a SiO2 skin (TEXUS 12) N91-31385
Floating zone growth of GaAs crystals (TEXUS 20) N91-31386
Floating zone crystal growth of Ga-doped germanium (TEXTUS 10) ESA N91-31387
Floating-zone experiments with germanium crystals (TEXUS 12) ESA N91-31388
Floating zone growth of germanium crystals (TEXUS 14b) ESA N91-31389
Semi-confined Bridgman growth of Ga-doped Ge (MASER 2) N91-31390
Semi-confined Bridgman growth of Ga-doped Ge (MASER 2) N91-31391
Crystallisation experiments with salts (TEXUS 13) N91-31392
Solution growth of GaAs single crystals (TEXUS 19) N91-31393
Vapour growth of an InP crystal (TEXUS 20) N91-31394
Diffusion-controlled growth of protein single crystals: B-galactosidase (TEXUS 3) N91-31395
Solidification of alloys (TEXUS 2) N91-31401
Macrosegregation in Ag-Sn alloys (MASER 1) N91-31402
Directional solidification of Al-Cu alloys (MASER 2) N91-31403
Epitaxial growth and electro-optical properties of metal GaAs superlattices
[AD-A239719] N91-31984

CRYSTAL LATTICES
Mean field analysis of the CuO2 lattice: Comparison to Monte Carlo simulations
[DE91-015570] N91-31968

CRYSTAL STRUCTURE
Method for imparting strength to intermetallic phases
[PATENT-1-255-929] N91-31271
Theoretical studies of metallic alloys
[DE91-016486] N91-31281
Influence of surface defects and local structure on oxygenate reaction pathways over metal oxide surfaces
[DE91-016600] N91-31289
Solution growth of GaAs single crystals (TEXUS 19) N91-31393
Solidification of a hypereutectic alloy (TEXUS 1) N91-31399
Solidification of alloys (TEXUS 2) N91-31401
Studies of the III-V compounds in the megabar regime
[DE91-015911] N91-31973
TEM analysis of crystalline interface structure: The state of the art
[DE91-016427] N91-31975

CRYSTALLINITY
Ion-implantation induced crystallization of glass
[DE91-016121] N91-31303
Structure property relationship of aliphatic polyurethane elastomers prepared from CHDI
[AD-A239397] N91-31311
Growth of rare Earth-magnesium crystals (TEXUS 12) N91-31383
The 1991 DOE/Sandia Crystalline Photovoltaic Technology Project Review Meeting
[DE91-016062] N91-31703

CRYSTALLITES
Diffusion-controlled growth of protein single crystals: B-galactosidase (TEXUS 3) N91-31395

CRYSTALLIZATION
Ion-implantation induced crystallization of glass
[DE91-016121] N91-31303
Crystallisation experiments with salts (TEXUS 13) N91-31392
Diffusion-controlled growth of protein single crystals: Investigation of B-galactosidase at low temperature (TEXUS 4) N91-31396
Crystallization of the glassy grain boundary phase in silicon nitride ceramics
[NASA-CR-188717] N91-31961
Microstructural changes in Beta-silicon nitride grains upon crystallizing the grain-boundary glass N91-31963
Glass formation and crystallization in high-temperature glass-ceramics and Si3N4 N91-31964

CRYSTALLOGRAPHY
TEM analysis of crystalline interface structure: The state of the art
[DE91-016427] N91-31975

CRYSTALS
Growth of rare Earth-magnesium crystals (TEXUS 12) N91-31383
Floating-zone growth of a silicon single crystal (TEXUS 7) N91-31384
Growth of a Si crystal covered with a SiO2 skin (TEXUS 12) N91-31385
Floating zone growth of GaAs crystals (TEXUS 20) N91-31386
Photography of shock waves in explosive crystals
[DE91-015772] N91-31572
A new method to do time resolved, x ray diffraction studies: The rotating crystal Laue method
[DE91-016527] N91-31935

CUES
Fighter agility metrics N91-31128

CULTIVATION
Solid-support substrates for plant growth at a lunar base N91-31800

CULTURE TECHNIQUES
Controlled Ecological Life Support Systems: CELSS '89 Workshop
[NASA-TM-102277] N91-31775
Environmental and cultural considerations for growth of potatoes in CELSS N91-31779
Cloning crops in a CELSS via tissue culture: Prospects and problems N91-31783

CURRENT REGULATORS
On the stability of saturated state feedback regulators
[LAAS-91047] N91-31524

CURVES
Enhancement of surface definition and gridding in the Eagle code
[NASA-CR-188796] N91-31820

CURVES (GEOMETRY)
An algorithm for the one-to-all shortest path problem with arbitrary arc lengths
[MEMO-919] N91-31844

CUTTING
Power saw
[NASA-CASE-MSC-21469-1] N91-31655

CYANO COMPOUNDS
Influence of adhesive polymerization conditions on the durability of adhesive joints
[DCR/I-03357-90] N91-31305

CYCLES
Cyanobacteria in CELSS: Growth strategies for nutritional variation and nitrogen cycling N91-31786
Cycles containing many vertices of large degree
[MEMO-916] N91-31908
A search for periodicity in the x ray spectrum of black hole candidate A0620-00
[AD-A239488] N91-32011

CYCLOHEXANE
Separation of transparent fluids due to Marangoni convection (TEXUS 7) N91-31425
Marangoni transport of droplets at a solidification front (TEXUS 9) N91-31426

CYCLOTRON RESONANCE
Ground-state in-plane light-holes in GaAs/AlGaAs structures
[DE91-016408] N91-31980

CYLINDRICAL BODIES
Interlaminar deformations on the cylindrical surface of a hole in laminated composites by moire interferometry
[DE91-015922] N91-31238
Pressure-strain-temperature relationship in shock loaded cylindrical samples of 304 stainless steel
[DE91-013379] N91-31673

CZOCHRALSKI METHOD
Directional solidification of doped germanium (TEXUS 4) ESA N91-31380

D

DAMAGE
Space engine safety system
[NASA-CR-187219] N91-31209

DAMAGE ASSESSMENT
Ice ingestion experience on a small turboprop engine N91-31162
Examination and mapping of forest damage, using remote sensing methods
[ETN-91-99741] N91-31696

DATA ACQUISITION
Arctic VLF/LF data acquisition
[AD-A239704] N91-31510
Laser Velocimetry, volume 1
[VKI-1991-05-VOL-1] N91-31614
Fundamentals of signal processing N91-31617
Signal processing: Time domain and frequency domain N91-31620
Description of Crau data set: Meteosat data, radiosonde data, sea surface temperatures: Comparison of Meteosat and Heimann data
[KNMI-WR-90-03] N91-31752
SHOWTIME.C: A C-language program for data acquisition and display user's guide
[DE91-016241] N91-31817
Application of an acquisition image processing system to the quantitative analysis of flows
[AAAF-NT-89-27] N91-31851
A research program in experimental high energy physics
[DE91-016208] N91-31941

DATA BASE MANAGEMENT SYSTEMS
Aero/fluids database system
[NASA-CR-184208] N91-31853
The design of an Integrity Consistency Checker (ICC) for an object oriented database system
[REPT-91-021] N91-31994

DATA BASES
Traffic model for advanced satellite designs and experiments for ISDN services
[NASA-CR-188802] N91-31200
ULDA user's guide
[NASA-TM-105074] N91-31813
Aero/fluids database system
[NASA-CR-184208] N91-31853
Study day on the design of a network database in four languages
[MEMO-INF-91-22] N91-31863
A solution for the network database problem in an imperative language N91-31864
An object-oriented analysis, design, and implementation of a network database N91-31865
Network database in PROLOG N91-31866
A network database: A case study in functional programming N91-31867
Parametric study of diffusion-enhancement networks for spatiotemporal grouping in real-time artificial vision
[AD-A239674] N91-31954
Optimal configuration of distributed database systems N91-31990
Interactive retrieval in information spaces distributed across a wide-area network N91-31992
The design of an Integrity Consistency Checker (ICC) for an object oriented database system
[REPT-91-021] N91-31994
Hypertext development using a model-based approach
[REPT-90-074] N91-31995
Exploiting captions for access to multimedia databases
[AD-A239435] N91-32000

DATA COMPRESSION
Investigation of the progressive bi-level coding technique for the high-resolution bi-level data compression standard
[AD-A239597] N91-31860

DATA CONVERSION ROUTINES
Coordinate conversions for presenting and compositing weather radar data
[KNMI-TR-129] N91-31497

DATA FLOW ANALYSIS
The failure of failures: Towards a paradigm for a synchronous communication
[RUU-CS-90-40] N91-31835

DATA LINKS
Flight tests with a data link used for air traffic control information exchange
[NASA-TP-3135] N91-31143
Antenna study for 60 GHz intersatellite link
[CD-RPT-ITL-5043-003] N91-31482
The data distribution satellite system
[NASA-CR-187172] N91-31499
A universal computer control system for motors
[NASA-CASE-NPO-17134-1-CU] N91-31528

DATA PROCESSING
Post-processing of data N91-31633
Developing dataflow algorithms
[DE91-016300] N91-31818
The design of an Integrity Consistency Checker (ICC) for an object oriented database system
[REPT-91-021] N91-31994

DATA REDUCTION
A scientific visualization synthesizer
[DE91-012877] N91-31815
Benchmarking a Network Storage Service
[DE91-013510] N91-31868
The design of an Integrity Consistency Checker (ICC) for an object oriented database system
[REPT-91-021] N91-31994

DATA RETRIEVAL
Aero/fluids database system
[NASA-CR-184208] N91-31853

DATA SAMPLING
Temporal sampling considerations in global climate modeling
[DE91-015695] N91-31717
DATA STORAGE
Filter system for radar applications
[PATENT-1-273-409] N91-31512
DATA STRUCTURES
Union-copy structures and dynamic segment trees
[RUU-CS-91-05] N91-31903
DATA SYSTEMS
The data distribution satellite system
[NASA-CR-187172] N91-31499
DATA TRANSMISSION
Recent advances in fiber optics components for high speed data transmission
[DE91-016252] N91-31948
The design of an Integrity Consistency Checker (ICC) for an object oriented database system
[REPT-91-021] N91-31994
DC 9 AIRCRAFT
Fuselage shell and cavity response measurements on a DC-9 test section
[NASA-CR-187557] N91-31926
DECARBURIZATION
Process for producing plasma sprayed carbide-based coatings with minimal decarburization and near theoretical density
[DE91-012016] N91-31292
DECISION MAKING
Effects of stress on judgment and decision making in dynamic tasks
[AD-A239452] N91-31772
On the relation between recurrence and ergodicity properties in denumerable Markov decision chains
[TW-91-02] N91-31918
DECODERS
Solid-State Radar Beacon Decoder (SSRBD) Master Test Plan (MTP)
[DOT/FAA/CT-TN91/33] N91-31494
DECODING
Filter system for radar applications
[PATENT-1-273-409] N91-31512
DECOMPOSITION
Two alternative ways for solving the coordination problem in multilevel optimization
[NASA-TM-104036] N91-31138
DECOMPRESSION SICKNESS
Basic operation and preliminary trials of a detector for stationary gas bubbles
[AD-A239710] N91-31769
DECOUPLING
Dynamic disturbance decoupling for discrete-time nonlinear systems
[MEMO-913] N91-31843
DEFECTS
X-ray inspection system
[PATENT-1-258-924] N91-31660
DEFENSE INDUSTRY
Acquisition reform: Implementing defense management review initiatives. Report to the Chairman and Ranking Minority Member, Subcommittee on Defense Industry and Technology, Senate Committee on Armed Services
[AD-A239423] N91-31999
DEFLECTORS
Segmented rotatable nozzles
[CA-PATENT-APPL-SN-2-009-634] N91-31174
Ventral segmented nozzles
[CA-PATENT-APPL-SN-2-009-636] N91-31176
DEFORMATION
RADAC model deformation measurement system: First results at the F1 wind tunnel
[AAAF-NT-89-03] N91-31098
The influence of interphase regions on local thermal stresses and deformations in composites N91-31228
Composite matrix deformation process in relation to molecular structure
[ETN-91-99915] N91-31232
Experimental and analytical analysis of stress-strain behavior in a (90/0 deg)2s, SiC/Ti-15-3 laminate
[NASA-TM-104470] N91-31235
Interlaminar deformations on the cylindrical surface of a hole in laminated composites by moire interferometry
[DE91-015922] N91-31238
The influence of plastic-strain-induced anisotropy on stress distributions in the finite deformation of ductile metals N91-31273
Deformation induced microstructural and microchemical changes during thermomechanical treatment
[DE91-016949] N91-31290
Fracture toughness characterization of polymers N91-31296
Skin technology (TEXUS 4) N91-31458
Pressure-strain-temperature relationship in shock loaded cylindrical samples of 304 stainless steel
[DE91-013379] N91-31673
DEGREES OF FREEDOM
Synchronized computational architecture for generalized bilateral control of robot arms
[NASA-CASE-NPO-17401-1-CU] N91-31885
DEICERS
Application of a water droplet trajectory prediction code to the design of inlet particle separator anti-icing systems N91-31159
Development of an anti-icing system for the T800-LHT-800 turboshaft engine N91-31160
DEICING
Low Temperature Environment Operations of Turboengines (Design and User's Problems)
[AGARD-CP-480] N91-31144
DELAMINATING
An investigation into the effects of damage on the stresses in a composite laminate N91-31226
Relation between fiber proportion and mechanical characteristics of carbon-resin composites
[RE-50-345/F] N91-31231
Composite materials damage. Transverse cracking and delamination
[ONERA-RT-6/7256-RY-080-R] N91-31234
DENDRITIC CRYSTALS
Boundary layers in transparent melts (TEXUS 10) N91-31406
DENSIFICATION
Effects of trapped gases on ceramic-filled-glass composite densification
[DE91-015850] N91-31237
DENSITOMETERS
Laser Fourier densitometry and laser induced photochemical anemometry in supersonic flow
[AAAF-NT-89-09] N91-31103
Development of an infrared Laser Fourier Densitometer (LFD) and first wind tunnel tests
[PMI-2335] N91-31189
DENSITY MEASUREMENT
Development of an infrared Laser Fourier Densitometer (LFD) and first wind tunnel tests
[PMI-2335] N91-31189
Experimental determination of the temperature and density of opacity samples
[DE91-015686] N91-31252
DENTISTRY
Effect of porcelain surface pretreatments on composite resin-porcelain shear bond strength
[AD-A239359] N91-31241
DEPLETION
Defect diffusion in ion implanted glasses
[DE91-016119] N91-31302
DEPOSITION
Laser deposition of cubic boron nitride on electronic materials
[AD-A238313] N91-31249
DESIGN ANALYSIS
OMEGA system Performance Assessment and Coverage Evaluation (PACE) workstation design and implementation, volume 2
[AD-A239724] N91-31123
A knowledge-base for rehabilitation of airfield concrete pavements
[AD-A239354] N91-31191
The analysis and design of brushless DC motors N91-31516
The development of aluminum-air batteries for application in electric vehicles
[DE91-016863] N91-31533
Open-cycle ocean thermal energy conversion surface-condenser design analysis and computer program
[DE91-015973] N91-31709
Design and cost of the first commercial stretched-membrane heliostat
[DE91-016870] N91-31715
DESORPTION
Atomic hydrogen driven halogen extraction from Si(100): Eley-Rideal surface kinetics
[AD-A239544] N91-31266
DESULFURIZING
Electrostatic precipitation of condensed acid mist
[DE91-016530] N91-31260
DETECTION
Boundary layer transition detection and measurement methods at CERT/DERAT
[AAAF-NT-89-14] N91-31105
A research program in experimental high energy physics
[DE91-016208] N91-31941
Multitarget tracking using optical processing
[AD-A239656] N91-31953
DETECTORS
Convergence performance of adaptive detectors, part 1
[AD-A239507] N91-31539
DETONATION
Performance evaluation of insensitive explosives
[DE91-015767] N91-31315
Understanding composite explosive energetics
[DE91-015770] N91-31316
DIAMONDS
Studies of the III-V compounds in the megabar regime
[DE91-015911] N91-31973
DICTIONARIES
The on-line d-dimensional dictionary problem
[RUU-CS-90-31] N91-31829
DIELECTRIC PROPERTIES
Radar-cross-section measurement errors caused by test object interaction with low-dielectric-constant supports
[DE91-015340] N91-31490
DIELECTRICS
Electrophoretic dielectric coatings for magnetic switches
[DE91-015337] N91-31518
Proceedings of the International Magnetic Pulse Compression Workshop. Volume 2: Technical summary
[DE91-015775] N91-31521
Capacitive bridge-type probe and conversion circuitry
[PATENT-1-263-443] N91-31599
DIETS
Environmental modification of yield and food composition of cowpea and leaf lettuce N91-31777
Cyanobacteria in CELSS: Growth strategies for nutritional variation and nitrogen cycling N91-31786
Algae for controlled ecological life support system diet characterization of cyanobacteria 'spirulina' in batch cultures N91-31787
DIFFERENTIAL EQUATIONS
Tuning maps for setpoint changes and load disturbance upsets in a three capacity process under multivariable control
[NASA-TM-104419] N91-31876
DIFFRACTION PATTERNS
Basic LDV1 component system N91-31616
Advanced systems: Multicomponent LDV N91-31619
Review of typical applications. Part 1: Measurements in liquid flows, free jets, combustion, and in the atmosphere N91-31631
A new method to do time resolved, x ray diffraction studies: The rotating crystal Laue method
[DE91-016527] N91-31935
DIFFUSION
Diffusion-induced interfacial convection (TEXUS 11) N91-31332
Reaction kinetics in glass melts (TEXUS 1) N91-31363
Reaction kinetics in glass melts: Corrosion of SiO2 (TEXUS 4) N91-31364
Reaction kinetics in glass melts: Sodium self-diffusion in alkali-silicate melts (TEXUS 6) N91-31365
Self- and interdiffusion in alkali-silicate melts (TEXUS 11 and 12) N91-31366
Self- and interdiffusion in alkali-silicate melts (TEXUS 13) N91-31367
Reaction kinetics in molten glasses: Self-diffusion in alkali-silicate melts (TEXUS 20) N91-31368
Special refractive index profiles in glasses obtained by ion exchange (TEXUS 19) ESA N91-31369
Sulphur diffusion in liquid cast iron (TEXUS 6) ESA N91-31370
Ventilation and filling of an optical diffusion cell (TEXUS 8) N91-31371
Solutal diffusion measurements in liquid PbSnTe under microgravity (TEXUS 19) N91-31372
Diffusion of Ni in Cu-Au and Cu-Al alloys (TEXUS 20) N91-31373
Diffusion-controlled growth of protein single crystals: B-galactosidase (TEXUS 3) N91-31395
Diffusion-controlled growth of single crystals of protein (TEXUS 5) N91-31397
Artificial diffusion methods in convection dominated flows
[W-9016] N91-31577
Models of flux diffusion and flux creep in high-temperature superconductors
[DE91-015838] N91-31972
DIFFUSION COEFFICIENT
Self- and interdiffusion in alkali-silicate melts (TEXUS 13) N91-31367
Reaction kinetics in molten glasses: Self-diffusion in alkali-silicate melts (TEXUS 20) N91-31368
Solutal diffusion measurements in liquid PbSnTe under microgravity (TEXUS 19) N91-31372
Plasma diffusion at the magnetopause? The case of lower hybrid drift waves
[NASA-CR-188913] N91-31957
DIFFUSION WELDING
Energy and Technology Review, February-March 1991
[DE91-015487] N91-32031

DIGITAL DATA
Application of an acquisition image processing system to the quantitative analysis of flows
[AAAF-NT-89-27] N91-31851
Application of digital compression techniques to optical surveillance systems
[DE91-016404] N91-31854
DIGITAL ELECTRONICS
Hardware modeling and top-down design using VHDL
[AD-A239356] N91-31534
DIGITAL FILTERS
High speed digital direct access filter for tracking or excision of parametric signal data
[PATENT-1-271-231] N91-31511
Initialization of the HIRLAM model using a digital filter
[DM-57] N91-31747
DIGITAL SIMULATION
A three-dimensional code to solve the Poisson equation: Numerical simulation of the breakdown in P-N junction devices
[ECL-90-27] N91-31525
Design of a specific integrated circuit for solving the three dimensional Poisson equation
[ECL-90-24] N91-31527
Direct and large eddy simulation of turbulence: Summary of the state-of-the-art 1991 N91-31562
DIGITAL SYSTEMS
Cold weather jet engine starting strategies made possible by engine digital control systems N91-31153
A case study for the real-time experimental evaluation of the VIPER microprocessor
[NASA-TM-104098] N91-31531
DIGITAL TECHNIQUES
Application of digital compression techniques to optical surveillance systems
[DE91-016404] N91-31854
DIISOCYANATES
Structure property relationship of aliphatic polyurethane elastomers prepared from CHDI
[AD-A239397] N91-31311
DIMENSIONAL ANALYSIS
Finite-dimensional dynamics and chaos in fluid flows N91-31571
DIMERS
Pyrimidine dimer formation by UVA radiation: Implications for photoreactivation
[DE91-015837] N91-31756
DIODES
Plasma-optics systems for the formation and focusing of ion beams N91-31956
DIOXIDES
Elastic wave dispersion in high-strength ceramics
[DE91-016648] N91-31309
DIPOLE MOMENTS
Electromagnetic penetration of slot apertures with depth and losses
[DE91-016401] N91-31500
DIRECT CURRENT
The analysis and design of brushless DC motors N91-31516
Studies of non-ideal superconductors using DC magnetic methods
[DE91-015642] N91-31970
DIRECTION FINDING
Spectrum monitoring procedures and techniques
[AD-A239567] N91-31507
DIRECTIONAL SOLIDIFICATION (CRYSTALS)
Solidification of a hypereutectic alloy (TEXUS 1) N91-31399
Solidification of alloys (TEXUS 2) N91-31401
Macrosegregation in Ag-Sn alloys (MASER 1) N91-31402
Directional solidification of Al-Cu alloys (MASER 2) N91-31403
Directional solidification of eutectics (TEXUS 6) N91-31404
Directional solidification of eutectics InSb-NiSb (TEXUS 10) N91-31405
Unidirectional solidification of immiscible alloys (TEXUS 5) N91-31418
Unidirectional solidification of immiscible alloys (TEXUS 7) N91-31419
Unidirectional solidification of Zn-Bi samples (TEXUS 14b) N91-31420
Directional solidification of immiscible alloys Zn-Pb (MASER 2) N91-31421
Acoustic mixing (TEXUS 5) N91-31423
Solidification of immiscible alloys (TEXUS 8) N91-31424
The behaviour of alumina-copper suspensions (TEXUS 3A and 3B) N91-31433
Copper-alumina suspensions (TEXUS 5) N91-31434
Metallic composites with particles (TEXUS 6) N91-31436
Melting and solidification of metallic composites (TEXUS 9) N91-31438
Metal matrix composites (TEXUS 14b) N91-31439
Solidification of fine dispersions in microgravity (TEXUS 14b) N91-31441
Dispersion alloys (TEXUS 19) N91-31442
Pores in aluminium alloys (TEXUS 3) N91-31447
Skin technology (TEXUS 1) N91-31455
Skin technology (TEXUS 2) N91-31456
Containerless solidification of a Pd-Cu-Si sample (TEXUS 9) ESA N91-31466
DISLOCATIONS (MATERIALS)
Anelastic release from the shock-compressed state
[DE91-009961] N91-31672
Microstructural changes in Beta-silicon nitride grains upon crystallizing the grain-boundary glass N91-31963
DISPERSIONS
Dispersion layers by electrodeposition (TEXUS 1) N91-31350
Dispersion electrolysis (TEXUS 4) N91-31351
Dispersion electrolysis (TEXUS 7) N91-31352
Dispersion electrolysis (TEXUS 9) N91-31353
Composite materials, 2 (TEXUS 2) N91-31409
Immiscibles, 2 (TEXUS 5) N91-31411
Dispersion alloys (TEXUS 7) N91-31412
Al-Pb bearing alloy (TEXUS 1) N91-31413
Immiscible alloy system Al-Pb (TEXUS 7) N91-31422
Acoustic mixing (TEXUS 5) N91-31423
Solidification of immiscible alloys (TEXUS 8) N91-31424
Copper-alumina suspensions (TEXUS 5) N91-31434
Metal matrix composites (TEXUS 20) N91-31440
Solidification of fine dispersions in microgravity (TEXUS 14b) N91-31441
Dispersion alloys (TEXUS 19) N91-31442
Pores in aluminium alloys (TEXUS 3) N91-31447
Gas bubbles in a copper-alumina suspension (TEXUS 11) N91-31453
DISPLACEMENT
The influence of interphase regions on local thermal stresses and deformations in composites N91-31228
Fracture toughness characterization of polymers N91-31296
DISPLAY DEVICES
Development of a geographic navigational display device for general aviation aircraft
[PB91-170282] N91-31114
Airplane takeoff and landing performance monitoring system
[NASA-CASE-LAR-13854-1-CU] N91-31120
Fighter agility metrics N91-31128
Touch screen use on flight simulator instructor/operator stations
[AD-A239524] N91-31192
Theory and application of the wavelet transform to signal processing
[AD-A239533] N91-31501
Interactive tool visualization of three dimensional 3D results
[AAAF-NT-89-19] N91-31847
A knowledge based application of the extended aircraft interrogation and display system
[NASA-TM-4327] N91-31874
Synchronized computational architecture for generalized bilateral control of robot arms
[NASA-CASE-NPO-17401-1-CU] N91-31885
Single layer multi-color luminescent display
[NASA-CASE-LAR-13616-1] N91-31950
DISSOCIATION
Examination of molecular evaporation, cooling, and cluster dissociation of very thin liquid jets in a high vacuum
[MPIS-12/1990] N91-31581
DISTANCE
Computing minimum length paths of a given homotopy class
[RUU-CS-90-37] N91-31900
DISTANCE MEASURING EQUIPMENT
Capacitive bridge-type probe and conversion circuitry
[PATENT-1-263-444] N91-31598
Capacitive bridge-type probe and conversion circuitry
[PATENT-1-263-443] N91-31599
DISTORTION
Integrated control of thermally distorted large space antennas N91-31487
Distortion-free x ray mask technology
[AD-A239770] N91-31665
DISTRIBUTED PARAMETER SYSTEMS
Advanced optical sensing and processing technologies for the distributed control of large flexible spacecraft
[NASA-CR-4399] N91-31609
DISTRIBUTED PROCESSING
Reliability modeling of dependable distributed systems
[AD-A239734] N91-31663
The potential impact of VHDL on dependable distributed system design
[AD-A239769] N91-31664
The derivation of distributed termination detection algorithms from garbage detection schemes
[RUU-CS-90-24] N91-31827
Distributed incremental maximum finding in hierarchically divided graphs
[RUU-CS-90-30] N91-31828
Construction and realization of distributed multiprocessor systems for real time tasks
[MBB-UA-1189-90-PUB] N91-31871
OSI-security and relations with other security standards
[FEL-91-B099] N91-31872
Information security: Past, present and future
[FEL-91-B100] N91-31873
Design and analysis of fault-tolerant distributed real-time computer systems
[AD-A239382] N91-31875
Optimal configuration of distributed database systems N91-31990
DISTRIBUTION (PROPERTY)
Reaction kinetics in glass melts (TEXUS 1) N91-31363
Reaction kinetics in glass melts: Corrosion of SiO2 (TEXUS 4) N91-31364
Self- and interdiffusion in alkali-silicate melts (TEXUS 11 and 12) N91-31366
Special refractive index profiles in glasses obtained by ion exchange (TEXUS 19) ESA N91-31369
Diffusion of Ni in Cu-Au and Cu-Al alloys (TEXUS 20) N91-31373
DISTRIBUTION FUNCTIONS
A Weibull brittle material failure model for the ABAQUS computer program
[DE91-016813] N91-31690
Learning convex bodies under uniform distribution
[MEMO-918] N91-31910
DOCUMENTATION
Hypertext development using a model-based approach
[REPT-90-074] N91-31995
DONOR MATERIALS
Depth profiles for hydrogen-assisted thermal donor formation in silicon
[DE91-015719] N91-31971
DOPED CRYSTALS
Directional solidification of doped germanium (TEXUS 4) ESA N91-31380
Striations in germanium (TEXUS 6) ESA N91-31381
Floating zone crystal growth of Ga-doped germanium (TEXTUS 10) ESA N91-31387
Floating-zone experiments with germanium crystals (TEXUS 12) ESA N91-31388
Floating zone growth of germanium crystals (TEXUS 14b) ESA N91-31389
Semi-confined Bridgman growth of Ga-doped Ge (MASER 2) N91-31390
Semi-confined Bridgman growth of Ga-doped Ge (MASER 2) N91-31391
Vapour growth of an InP crystal (TEXUS 20) N91-31394
DOPPLER EFFECT
Basic LDV1 component system N91-31616
DOPPLER RADAR
A satellite-based radar wind sensor
[NASA-CR-188805] N91-31750
DOSAGE
Biological dosimetry and mechanisms of carcinogenesis
[DE91-015689] N91-31763
DOSIMETERS
Biological dosimetry and mechanisms of carcinogenesis
[DE91-015689] N91-31763
DRAG
Validation of two dimensional drag prediction methods
[ONERA-RSF-85/1685-AY] N91-31093
DRAG REDUCTION
Cold starting small gas turbines: An overview N91-31150
DROP TRANSFER
Thermocapillary drop motion, 1 (MASER 1) ESA N91-31345
Thermocapillary drop motion, 2 (MASER 2) ESA N91-31346
DROPS (LIQUIDS)
Numerical model of evolution in supercooled cloud of water droplets in a case of icing N91-31169
Icing test capabilities for aircraft propulsion systems at the Arnold Engineering Development Center N91-31170
Developments in icing test techniques for aerospace applications in the RAE Pyestock altitude test facility N91-31173
Unidirectional solidification of immiscible alloys (TEXUS 5) N91-31418
Unidirectional solidification of immiscible alloys (TEXUS 7) N91-31419

Separation of transparent fluids due to Marangoni convection (TEXUS 7) N91-31425
Marangoni transport of droplets at a solidification front (TEXUS 9) N91-31426
Demixing of a monotectic ternary alloy (TEXUS 20) N91-31429

DROUGHT
Time scales of variability associated with Nordeste precipitation
[DE91-015696] N91-31718

DRYING
The critical temperature for drying-out of soils around power cables as a function of local conditions N91-32025

DUAL SPIN SPACECRAFT
Choice of a differential method for attitude restitution with dynamic imbalance
[CNES-NT-126] N91-31202

DUCT GEOMETRY
Experimental investigation of turbulent flow through a circular-to-rectangular transition duct
[NASA-TM-105210] N91-31106

DUCTED FLOW
Experimental investigation of turbulent flow through a circular-to-rectangular transition duct
[NASA-TM-105210] N91-31106
Development of an advanced panel method for complex configurations in subsonic compressible flow; application to the computation of the potential flow through ducts
[NLR-TR-88001-U] N91-31579

DUCTILITY
The influence of plastic-strain-induced anisotropy on stress distributions in the finite deformation of ductile metals N91-31273
Weldability and hot ductility of iron aluminides
[DE91-016343] N91-31280

DUCTS
Environmental icing testing at the Naval Air Propulsion Center N91-31167
Removable slider shoe for a translating sleeve used on a jet engine cowl and duct
[PATENT-1-247-868] N91-31177
A comparison of time domain boundary conditions for acoustic waves in wave guides
[NASA-CR-187618] N91-31889

DURABILITY
Corrosion fatigue crack arrest in aluminium alloys
[NLR-MP-88050-U] N91-31282

DYES
Tropical tests of a seawater marker
[MRL-TR-90-19] N91-31109

DYNAMIC CHARACTERISTICS
Dynamic yield strength of a palladium alloy metallic glass
[DE91-015111] N91-31298

DYNAMIC CONTROL
Large Angle Transient Dynamics (LATDYN) demonstration problem manual
[NASA-CR-4400] N91-31684

DYNAMIC LOADS
Vibration analysis of the SA349/2 helicopter
[NASA-TM-102794] N91-31078
Method and apparatus for detecting laminar flow separation and reattachment
[NASA-CASE-LAR-13952-2-SB] N91-31596

DYNAMIC MODELS
A new model of the electron: A suggested experiment to search for a link between electromagnetism and gravity N91-31738

DYNAMIC PROGRAMMING
Dynamic disturbance decoupling for discrete-time nonlinear systems
[MEMO-913] N91-31843

DYNAMIC RESPONSE
Dynamics of 1.3 micron semiconductor lasers and nonlinear gain N91-31613
Behavior of nonlinear mechanical structures subjected to stationary excitations
[ECL-91-01] N91-31681
Force reconstruction using the inverse of the mode-shape matrix
[DE91-016407] N91-31689

DYNAMIC STRUCTURAL ANALYSIS
Vibration analysis of the SA349/2 helicopter
[NASA-TM-102794] N91-31078
Mobility power flow analysis of coupled plate structure subjected to mechanical and acoustics excitation
[NASA-CR-188791] N91-31678
Updating of finite element models using experimental vibratory type data. Process of static substructuring
[ONERA-RT-10/3313-RY-090-R] N91-31682
Large Angle Transient Dynamics (LATDYN) demonstration problem manual
[NASA-CR-4400] N91-31684
Large Angle Transient Dynamics (LATDYN) user's manual
[NASA-CR-4401] N91-31685
A finite element approach for the dynamic analysis of joint-dominated structures
[NASA-CR-4402] N91-31686
Improved finite-element methods for rotorcraft structures
[NASA-TM-104104] N91-31687

DYNAMICAL SYSTEMS
Proceedings of the Ninth Symposium on Energy Engineering Sciences: Fluid and Dynamical Systems
[DE91-015974] N91-31701

E

EARTH OBSERVING SYSTEM (EOS)
Advanced power systems for EOS
[NASA-TM-105222] N91-31217

EARTH ORBITAL ENVIRONMENTS
Contributions to a space station for flights in the near field and towards geostationary Earth orbit
[ETN-91-99744] N91-31203
Nickel-hydrogen cell low-Earth life test update
[NASA-TM-105229] N91-31708

EARTH RADIATION BUDGET
Small satellite radiometric measurements
[DE91-016308] N91-31694

EARTH TIDES
The time-domain earth tides N91-31726

EARTHQUAKES
Response of seismic-isolated structures under long-period motions
[DE91-015673] N91-31674

ECCENTRICITY
Eccentricity effects on leakage of a brush seal at low speeds
[NASA-TM-105141] N91-31220

ECLIPSING BINARY STARS
A spectrophotometric study of the secondaries of Algol systems N91-32005

ECONOMIC ANALYSIS
Assessment of costs and benefits of flexible and alternative fuel use in the US transportation sector
[DE91-015451] N91-31319
Economic analysis of robotic torque measurement system
[DE91-016480] N91-31653

ECOSYSTEMS
Controlled Ecological Life Support Systems: CELSS '89 Workshop
[NASA-TM-102277] N91-31775

EDDY VISCOSITY
Examples of turbulence model applications N91-31563

EDGE DISLOCATIONS
Dual ion implantation effects on fatigue properties of Fe-13Cr-15Ni alloys
[DE91-015930] N91-31286

EDITING ROUTINES (COMPUTERS)
GEOTRANS: An interface program from GEOPROGRAM to a geographic information system
[DE91-016111] N91-31998

EDUCATION
Quick development microcomputer system: Training automatic components for electronic troubleshooting
[AD-A239573] N91-31542
Solar energy and conservation technologies for Caribbean Tourist Facilities (CTF)
[DE91-016451] N91-31712
Boron in nuclear medicine: New synthetic approaches to PET, SPECT, and BNCT agents
[DE91-016488] N91-31764
Optimizing the long-term retention of skills: Structural and analytic approaches to skill maintenance 3
[AD-A239574] N91-31773

EFFECTIVENESS
Improving managers' effectiveness
[DE91-016405] N91-31988

EFFLUX
Efficiency of N use by wheat as a function of influx and efflux of NO3 N91-31778

EJECTION
Low altitude ejection release (total mass between 1,660 and 5,600 kg)
[REPT-90/05] N91-31475

ELASTIC DEFORMATION
Plastic deformation processes in relation to molecular structure
[ETN-91-99916] N91-31233

ELASTIC PROPERTIES
Finite element modeling of orthogonal machining using an elastic-viscoplastic material model
[DE91-016815] N91-31477
Identifying behavior characteristics using pressuremeter tests
[ETN-91-99917] N91-31680
Behavior of nonlinear mechanical structures subjected to stationary excitations
[ECL-91-01] N91-31681
Locking effects in the finite element approximation of elasticity problems
[AD-A239645] N91-31914

ELASTIC SCATTERING
Quasi-elastic light scattering and applications to optical sizing N91-31627

ELASTIC WAVES
Elastic wave dispersion in high-strength ceramics
[DE91-016648] N91-31309

ELASTOMERS
Mechanical characterization of seismic base isolation elastomers
[DE91-015680] N91-31299
Structure property relationship of aliphatic polyurethane elastomers prepared from CHDI
[AD-A239397] N91-31311

ELASTOPLASTICITY
Inlet edge funnel of a civil aircraft gondola engine
[ETN-91-99775] N91-31130
Asymptotic finite strain analysis of propagating cracks in elastic-plastic materials N91-31669
Identifying behavior characteristics using pressuremeter tests
[ETN-91-99917] N91-31680

ELECTRIC BATTERIES
Accelerated aging and discharge of lithium/thionyl-chloride D cells
[DE91-012649] N91-31517
Technology assessment of ambient temperature rechargeable lithium batteries for electric vehicle applications
[DE91-016500] N91-31522

ELECTRIC CHARGE
Cu-O charge fluctuations and electron-phonon coupling in the effective single-band Hubbard theory for cuprate superconductors
[DE91-016526] N91-31976

ELECTRIC CONTACTS
One-sun, single-crystalline silicon solar cell research
[DE91-015646] N91-31699

ELECTRIC CONTROL
A high-frequency servosystem for fuel control in hypersonic engines
[NASA-TM-104333] N91-31178

ELECTRIC CORONA
Measurements of inception time lags of repetitively pulsed corona in air N91-32028

ELECTRIC CURRENT
The photovoltaic effect on pyroelectics N91-31707
Near-wall conductivity N91-31944
Models of flux diffusion and flux creep in high-temperature superconductors
[DE91-015838] N91-31972

ELECTRIC DISCHARGES
Study of lightning strikes on an aircraft in flight. Electric measurements
[ONERA-RF-98/7154-PY] N91-31112

ELECTRIC ENERGY STORAGE
Electrochemical energy storage using PEM systems
[DE91-016020] N91-31711

ELECTRIC FIELDS
Study of lightning strikes on an aircraft in flight. Electromagnetic measurements
[ONERA-RF-25/7234-PY] N91-31111
Study of lightning strikes on an aircraft in flight. Electric measurements
[ONERA-RF-98/7154-PY] N91-31112
The timing of injection kickers
[NIKHEF-K/AMPS/91-04] N91-31943

ELECTRIC FURNACES
Small time step adaptive control: Theory and application to an electric furnace
[ECL-90-17] N91-31883

ELECTRIC GENERATORS
An investigation of dual-mode operation of a nuclear-thermal rocket engine
[DE91-015977] N91-31210

ELECTRIC MOTOR VEHICLES
Technology assessment of ambient temperature rechargeable lithium batteries for electric vehicle applications
[DE91-016500] N91-31522
The development of aluminum-air batteries for application in electric vehicles
[DE91-016863] N91-31533

ELECTRIC POTENTIAL
Electromagnetic penetration of slot apertures with depth and losses
[DE91-016401] N91-31500

A three-dimensional code to solve the Poisson equation: Numerical simulation of the breakdown in P-N junction devices
[ECL-90-27] N91-31525
ELECTRIC PROPULSION
Mass comparisons of electric propulsion systems for NSSK of geosynchronous spacecraft
[NASA-TM-105153] N91-31212
ELECTRIC PULSES
Measurements of inception time lags of repetitively pulsed corona in air N91-32028
ELECTRIC SWITCHES
Beacon activation device
[PATENT-1-256-916] N91-31108
ELECTRICAL ENGINEERING
Contribution to the implementation of a completely in situ device in ultrahigh vacuum for the development of MIS on InP structures: Al2O3/InP interface optimization
[ECL-91-04] N91-31526
The superconducting gravity gradiometer N91-31734
ELECTRICAL FAULTS
Electrophoretic dielectric coatings for magnetic switches
[DE91-015337] N91-31518
A three-dimensional code to solve the Poisson equation: Numerical simulation of the breakdown in P-N junction devices
[ECL-90-27] N91-31525
ELECTRICAL IMPEDANCE
Chemical reduction of intermodulation interference caused by metal-oxide-metal junctions aboard ship
[AD-A239530] N91-31265
Techniques to assess the state of health of sealed lead acid batteries
[CTN-91-60214] N91-31515
ELECTRICAL MEASUREMENT
Application of microwave cavity perturbation techniques in conducting polymers
[AD-A239376] N91-31310
ELECTRICAL RESISTIVITY
Near-wall conductivity N91-31944
ELECTRICITY
KEMA scientific and technical reports, volume 8, number 2, 1990
[ST-REPT-VOL-8-NO-2] N91-32023
ELECTRO-OPTICS
Automatic satellite tracking system for the NASA Satellite Photometric Observatory
[NASA-TM-105037] N91-31194
Hybrid electro-optic processor
[AD-A239547] N91-31505
An investigation of optically controlled, integrated millimeter wave receiving phased arrays
[AD-A239504] N91-31538
Laser interferometric measurement of ion electrode shape and charge exchange erosion
[NASA-TM-105165] N91-31605
Advanced research workshop on Wide Gap II-VI Semiconductors
[AD-A233796] N91-31960
Epitaxial growth and electro-optical properties of metal GaAs superlattices
[AD-A239719] N91-31984
ELECTROCARDIOGRAPHY
Continuous 24 hour ECG study, on ground and in flight, of 19 Mirage 2000 pilots stationed at the Dijon airbase (France). Comparison with similar recordings taken on other types of fighter aircraft or in operationally different conditions
[ETN-91-99973] N91-31761
ELECTROCHEMICAL CELLS
Interfacial systems for photochemical energy conversion
[DE91-015743] N91-31700
ELECTROCHEMICAL CORROSION
Intermittent polarization (TEXUS 2) N91-31349
ELECTROCHEMICAL MACHINING
Silicon micromachining based on porous silicon formation
[DE91-013744] N91-31472
ELECTROCHEMISTRY
Water transport properties of fuel cell ionomers
[DE91-016015] N91-31259
ELECTRODE MATERIALS
Chemically modified electrodes and related solution studies
[DE91-016740] N91-31262
ELECTRODEPOSITION
Dispersion layers by electrodeposition (TEXUS 1) N91-31350
ELECTRODES
Silicon micromachining based on porous silicon formation
[DE91-013744] N91-31472
Technology assessment of ambient temperature rechargeable lithium batteries for electric vehicle applications
[DE91-016500] N91-31522
Laser interferometric measurement of ion electrode shape and charge exchange erosion
[NASA-TM-105165] N91-31605
ELECTROLUMINESCENCE
Single layer multi-color luminescent display
[NASA-CASE-LAR-13616-1] N91-31950
ELECTROLYSIS
Summaries of FY 1991 research in the chemical sciences
[DE91-011221] N91-31222
Electrolytic hydrogen formation (TEXUS 1) N91-31347
Electrolytically generated hydrogen bubbles (TEXUS 6) N91-31348
Dispersion electrolysis (TEXUS 4) N91-31351
Dispersion electrolysis (TEXUS 7) N91-31352
Dispersion electrolysis (TEXUS 9) N91-31353
Electrochemical energy storage using PEM systems
[DE91-016020] N91-31711
ELECTROLYTES
Silicon micromachining based on porous silicon formation
[DE91-013744] N91-31472
Development of prototype sealed bipolar lithium/sulfide cells
[DE91-015721] N91-31519
Technology assessment of ambient temperature rechargeable lithium batteries for electric vehicle applications
[DE91-016500] N91-31522
ELECTROLYTIC POLARIZATION
Intermittent polarization (TEXUS 2) N91-31349
ELECTROMAGNETIC COUPLING
Comparison of integrated numerical experiments with accelerator and FEL experiments
[DE91-016071] N91-31639
ELECTROMAGNETIC FIELDS
Abstracts of papers presented at the First Los Alamos Symposium on Ultra-Wideband Radar
[DE91-015976] N91-31491
Acceleration using total internal reflection
[DE91-016612] N91-31942
Mean field analysis of the CuO2 lattice: Comparison to Monte Carlo simulations
[DE91-015570] N91-31968
ELECTROMAGNETIC INTERACTIONS
Particle production through two-photon processes in relativistic heavy-ion colliders
[DE91-016221] N91-31931
ELECTROMAGNETIC INTERFERENCE
Chemical reduction of intermodulation interference caused by metal-oxide-metal junctions aboard ship
[AD-A239530] N91-31265
Performance of an angle-of-arrival estimator in the presence of a mainbeam interference source
[AD-A239629] N91-31508
ELECTROMAGNETIC MEASUREMENT
Study of lightning strikes on an aircraft in flight. Electromagnetic measurements
[ONERA-RF-25/7234-PY] N91-31111
ELECTROMAGNETIC NOISE
Techniques to assess the state of health of sealed lead acid batteries
[CTN-91-60214] N91-31515
Initialization of the HIRLAM model using a digital filter
[DM-57] N91-31747
ELECTROMAGNETIC PULSES
Abstracts of papers presented at the First Los Alamos Symposium on Ultra-Wideband Radar
[DE91-015976] N91-31491
ELECTROMAGNETIC RADIATION
Electromagnetic penetration of slot apertures with depth and losses
[DE91-016401] N91-31500
Time domain electromagnetic waves in multilayered media
[AD-A239545] N91-31504
ELECTROMAGNETIC WAVE FILTERS
Filter system for radar applications
[PATENT-1-273-409] N91-31512
ELECTROMAGNETIC WAVE TRANSMISSION
Time domain electromagnetic waves in multilayered media
[AD-A239545] N91-31504
ELECTROMAGNETISM
A reminder of Faraday's gravitational experiments N91-31735
Heaviside's linearised gravitational theory N91-31737
A new model of the electron: A suggested experiment to search for a link between electromagnetism and gravity N91-31738
ELECTRON BEAM WELDING
Weldability and hot ductility of iron aluminides
[DE91-016343] N91-31280
ELECTRON BEAMS
Electron-beam-pinch experiment at Harry Diamond Laboratories: Providing for a high-dose-rate flash x ray facility for Transient Radiation Effects on Electronics (TREE) testing of piecepartS
[AD-A239558] N91-31193
Numerical simulation of a split cavity oscillator and rf conversion
[DE91-016501] N91-31523
Effective ionization coefficients, electron drift velocities, and limiting breakdown fields for gas mixtures of possible interest to particle detectors
[DE91-015921] N91-31532
Sensitivity of imaging materials to electron beam irradiation
[AD-A239365] N91-31612
Comparison of integrated numerical experiments with accelerator and FEL experiments
[DE91-016071] N91-31639
Compact free-electron laser at the Los Alamos National Laboratory
[DE91-016079] N91-31640
ELECTRON DISTRIBUTION
Comparison of integrated numerical experiments with accelerator and FEL experiments
[DE91-016071] N91-31639
ELECTRON MICROSCOPY
A jet polishing technique for thinning two phase materials
[DE91-016422] N91-31473
Electron microscopy to correlate cell structures and biochemical activity
[AD-A239640] N91-31758
TEM analysis of crystalline interface structure: The state of the art
[DE91-016427] N91-31975
ELECTRON ORBITALS
Model description of transition metals using the rotated second moment approximation
[DE91-016043] N91-31287
ELECTRON PLASMA
An interparticle collision model for electromagnetic hybrid simulations of high density plasmas
[DE91-016025] N91-31958
Advanced concepts theory
[AD-A239780] N91-31959
ELECTRON SPECTROSCOPY
Some applications of X-ray photoelectron spectroscopy and secondary-ion mass spectroscopy N91-32029
ELECTRON STATES
Mass resolved excitation spectroscopy of benzyl and phenylnitrene radicals
[AD-A239394] N91-31264
ELECTRON TRANSFER
Energy transfer processes in solar energy conversion
[DE91-016102] N91-31704
ELECTRON TUNNELING
Macroscopic quantum tunneling in Josephson tunnel junctions and Coulomb blockade in single small tunnel junctions
[DE91-016258] N91-31974
ELECTRON-POSITRON PAIRS
Searching for the Higgs in ep collisions at LEP/LHC
[DE91-015701] N91-31930
ELECTRONIC COUNTERMEASURES
Airborne ESM receivers: Techniques and technologies
[ETN-91-99988] N91-31498
ELECTRONIC EQUIPMENT
Assessing the efficacy of active noise reduction
[CTN-91-60200] N91-31922
ELECTRONIC MODULES
Reconfigurable parameter filter
[PATENT-1-264-072] N91-31513
ELECTRONIC WARFARE
Electronic warfare: Faulty test equipment impairs Navy readiness
[AD-A239562] N91-31506
ELECTRONS
A new model of the electron: A suggested experiment to search for a link between electromagnetism and gravity N91-31738
Near-wall conductivity N91-31944
Cu-O charge fluctuations and electron-phonon coupling in the effective single-band Hubbard theory for cuprate superconductors
[DE91-016526] N91-31976
ELECTROPHORESIS
Dispersion electrolysis (TEXUS 7) N91-31352
Electrophoretic dielectric coatings for magnetic switches
[DE91-015337] N91-31518

ELECTROPLATING
Determination of aqueous processable photoresist in tin-lead plating solutions
[DE91-015575] N91-31251
ELECTROPOLISHING
A jet polishing technique for thinning two phase materials
[DE91-016422] N91-31473
ELECTROSTATIC PRECIPITATORS
Electrostatic precipitation of condensed acid mist
[DE91-016530] N91-31260
ELECTROSTATICS
Electrostatic positioning for containerless processing of a Li-silicate glass (TEXUS 10) ESA N91-31469
ELEMENTARY EXCITATIONS
Proceedings of the Ninth Symposium on Energy Engineering Sciences: Fluid and Dynamical Systems
[DE91-015974] N91-31701
ELEMENTARY PARTICLE INTERACTIONS
Searching for the Higgs in ep collisions at LEP/LHC
[DE91-015701] N91-31930
ELEMENTARY PARTICLES
High energy physics
[DE91-015796] N91-31939
EMBRYOLOGY
Cloning crops in a CELSS via tissue culture: Prospects and problems N91-31783
EMERGENCIES
Emergency locating transmitter
[NASA-CASE-GSC-12821-2] N91-31530
EMISSION SPECTRA
Photophysics and chemistry of ultra-fast ZnO and CdS phosphors
[DE91-013106] N91-31966
Ultraviolet morphology of NGC 1068: The starburst knots and the extended emission region N91-32004
EMITTANCE
A study of a 21-cm-selected sample of galaxies N91-32014
EMITTERS
Spectrum monitoring procedures and techniques
[AD-A239567] N91-31507
END EFFECTORS
Robust impedance control of robot manipulators N91-31297
A program of continuing research on representing, manipulating, and reasoning about physical objects
[AD-A239596] N91-31659
ENERGETIC PARTICLES
Activities report of the Institute of Extraterrestrial Physics
[MPE-223] N91-32002
ENERGY ABSORPTION
A simple model for the motion of pulsed-laser-driven thin flyers
[DE91-011325] N91-31634
ENERGY CONSERVATION
One-sun, single-crystalline silicon solar cell research
[DE91-015646] N91-31699
Solar energy and conservation technologies for Caribbean Tourist Facilities (CTF)
[DE91-016451] N91-31712
ENERGY CONVERSION
Interfacial systems for photochemical energy conversion
[DE91-015743] N91-31700
ENERGY DISSIPATION
A simple model for the motion of pulsed-laser-driven thin flyers
[DE91-011325] N91-31634
Efficiency of N use by wheat as a function of influx and efflux of NO3 N91-31778
Macroscopic quantum tunneling in Josephson tunnel junctions and Coulomb blockade in single small tunnel junctions
[DE91-016258] N91-31974
ENERGY DISTRIBUTION
Vaudreuil (France) large hydrodynamic tunnel: Acoustic chamber damping
[METRAVIB-RDS-1-007-67] N91-31090
ENERGY GAPS (SOLID STATE)
Advanced research workshop on Wide Gap II-VI Semiconductors
[AD-A233796] N91-31960
ENERGY POLICY
Assessment of costs and benefits of flexible and alternative fuel use in the US transportation sector
[DE91-015451] N91-31319
ENERGY SPECTRA
The Li-7 and Be-7 deexcitation lines: Probes for accelerated particle transport models in solar flares
[NASA-CR-183490] N91-32020
ENERGY TECHNOLOGY
International magnetic pulse compression
[DE91-015774] N91-31520
Technical abstracts: Mechanical engineering, 1990
[DE91-016502] N91-31658
Solar energy and conservation technologies for Caribbean Tourist Facilities (CTF)
[DE91-016451] N91-31712
Energy and Technology Review, February-March 1991
[DE91-015487] N91-32031
ENERGY TRANSFER
A simple model for the motion of pulsed-laser-driven thin flyers
[DE91-011325] N91-31634
Energy transfer processes in solar energy conversion
[DE91-016102] N91-31704
ENGINE CONTROL
Cold weather jet engine starting strategies made possible by engine digital control systems N91-31153
ENGINE DESIGN
Ice tolerant engine inlet screens for CH113/113A search and rescue helicopters N91-31149
Control system design considerations for starting turbo-engines during cold weather operation N91-31155
Cold start development of modern small gas turbine engines at Pratt and Whitney Aircraft of Canada Ltd. N91-31156
Design considerations based upon low temperature starting tests on military aircraft turbo engines N91-31157
Application of a water droplet trajectory prediction code to the design of inlet particle separator anti-icing systems N91-31159
Development of an anti-icing system for the T800-LHT-800 turboshaft engine N91-31160
Engine icing criticality assessment N91-31161
Ice ingestion experience on a small turboprop engine N91-31162
Evaluation of undeveloped rocket engine cycle applications to advanced transportation
[NASA-CR-184205] N91-31215
Medium power hydrogen arcjet performance
[NASA-TM-104533] N91-31216
ENGINE FAILURE
Space engine safety system
[NASA-CR-187219] N91-31209
ENGINE INLETS
Ice tolerant engine inlet screens for CH113/113A search and rescue helicopters N91-31149
Application of a water droplet trajectory prediction code to the design of inlet particle separator anti-icing systems N91-31159
Development of an anti-icing system for the T800-LHT-800 turboshaft engine N91-31160
Environmental icing testing at the Naval Air Propulsion Center N91-31167
Icing test programmes and techniques N91-31171
ENGINE MONITORING INSTRUMENTS
Climatic considerations in the life cycle management of the CF-18 engine N91-31158
Diagnostic tools for reciprocating engine systems
[PB91-184960] N91-31645
ENGINE NOISE
Analysis of interior noise ground and flight test data for advanced turboprop aircraft applications
[NASA-CR-187558] N91-31927
ENGINE PARTS
Cold start optimization on a military jet engine N91-31151
A high-frequency servosystem for fuel control in hypersonic engines
[NASA-TM-104333] N91-31178
Hydrogen test of a small, low specific speed centrifugal pump stage
[NASA-CR-187117] N91-31213
ENGINE STARTERS
Low Temperature Environment Operations of Turboengines (Design and User's Problems)
[AGARD-CP-480] N91-31144
Analysis of starting problems in cold weather with ASTAZOU type turbine engines in helicopters N91-31147
Cold starting small gas turbines: An overview N91-31150
Cold weather ignition characteristics of advanced small gas turbine combustion systems N91-31152
Cold weather jet engine starting strategies made possible by engine digital control systems N91-31153
Cold start investigation of an APU with annular combustor and fuel vaporizers N91-31154
ENGINE TESTS
Cold start optimization on a military jet engine N91-31151
Design considerations based upon low temperature starting tests on military aircraft turbo engines N91-31157
Ice ingestion experience on a small turboprop engine N91-31162
Icing test capabilities for aircraft propulsion systems at the Arnold Engineering Development Center N91-31170
Space engine safety system
[NASA-CR-187219] N91-31209
Hydrogen test of a small, low specific speed centrifugal pump stage
[NASA-CR-187117] N91-31213
Medium power hydrogen arcjet performance
[NASA-TM-104533] N91-31216
ENRICHMENT
Environmental modification of yield and food composition of cowpea and leaf lettuce N91-31777
ENTHALPY
Alloy formation (TEXUS 5) N91-31398
ENVIRONMENT EFFECTS
A review of accelerated response actions available to the environmental restoration program: Selected case histories and associated issues
[DE91-013608] N91-31716
ENVIRONMENT POLLUTION
Noxious matter minimization as a project criterion for aircraft
[MBB-Z-0337-90-PUB] N91-31134
ENVIRONMENT PROTECTION
A review of accelerated response actions available to the environmental restoration program: Selected case histories and associated issues
[DE91-013608] N91-31716
ENVIRONMENT SIMULATION
Environmental icing testing at the Naval Air Propulsion Center N91-31167
ENVIRONMENTAL TESTS
Nickel-hydrogen cell low-Earth life test update
[NASA-TM-105229] N91-31708
ENZYMES
Use of inedible wheat residues from the KSC-CELSS breadboard facility for production of fungal cellulase N91-31785
ENZYMOLOGY
Strategies for biopolymer engineering of PHB-like materials
[AD-A239690] N91-31313
EPITAXY
Properties of low temperature, low oxygen pressure post-annealed YBa2Cu3O(sub 7-x) thin films
[DE91-015632] N91-31969
Limited reaction processing for semiconductor materials preparation
[AD-A239639] N91-31983
Epitaxial growth and electro-optical properties of metal GaAs superlattices
[AD-A239719] N91-31984
EPOXY COMPOUNDS
Enhanced fighter maneuverability aircraft (X-31A) wing and thrust vectoring vane design
[MBB-FE22/S/PUB/0433/A] N91-31135
EPOXY MATRIX COMPOSITES
Composite matrix deformation process in relation to molecular structure
[ETN-91-99915] N91-31232
Plastic deformation processes in relation to molecular structure
[ETN-91-99916] N91-31233
EPOXY RESINS
Composite matrix deformation process in relation to molecular structure
[ETN-91-99915] N91-31232
EQUATIONS OF MOTION
On the optimal use of fictitious time in variation of parameters methods with application to BG14
[NASA-CR-185650] N91-31890
EQUATIONS OF STATE
Virial coefficients and equations of state for mixed fluids; application to CH4-H2O
[DE91-016248] N91-31254
Nucleus-nucleus collisions and the nuclear equation of state
[DE91-016747] N91-31937
EQUILIBRIUM FLOW
Least-squares solution of incompressible Navier-Stokes equations with the p-version of finite elements
[NASA-TM-105203] N91-31911
EQUIPMENT SPECIFICATIONS
Study of space qualification specifications
[CTN-91-60201] N91-31199
EQUIVALENCE
Weak equivalence
[ITLI-CT-91-04] N91-31891
On the relation between recurrence and ergodicity properties in denumerable Markov decision chains
[TW-91-02] N91-31918
EROSION
Laser interferometric measurement of ion electrode shape and charge exchange erosion
[NASA-TM-105165] N91-31605

ERROR ANALYSIS
Radar-cross-section measurement errors caused by test object interaction with low-dielectric-constant supports
[DE91-015340] N91-31490
A numerical procedure for recovering true scattering coefficients from measurements with wide-beam antennas
[NASA-CR-186042] N91-31492
Neural network based model reference adaptive control N91-31677
Analysis of the efficiency of an a-posteriori error estimator for linear triangular finite elements
[AD-A239647] N91-31915
ERROR CORRECTING DEVICES
Choice of a differential method for attitude restitution with dynamic imbalance
[CNES-NT-126] N91-31202
ERROR DETECTION CODES
Intrusion and fault tolerance compatibility. Part 1: Fault protection, coding and tolerance state of the art
[LAAS-89-395] N91-31662
ERRORS
Radar-cross-section measurement errors caused by test object interaction with low-dielectric-constant supports
[DE91-015340] N91-31490
Updating of finite element models using experimental vibratory type data. Process of static substructuring
[ONERA-RT-10/3313-RY-090-R] N91-31682
Cockpit resource management: Effects on behavioral interactions across airlines and aircraft types
[AD-A239467] N91-31804
Asymmetric soft-error resistant memory
[NASA-CASE-NPO-17394-1-CU] N91-31810
ETCHING
Etching method for photoresists or polymers
[NASA-CASE-ARC-11873-2] N91-31258
Defect diffusion in ion implanted glasses
[DE91-016119] N91-31302
Silicon micromachining based on porous silicon formation
[DE91-013744] N91-31472
ETHERS
Ethynyl terminated imidothioethers and resins therefrom
[NASA-CASE-LAR-13910-2-CU] N91-31307
ETHYL ALCOHOL
Thermal conductivity of liquids (MASER 1) ESA N91-31361
Boundary layers in transparent melts (TEXUS 10) N91-31406
EUCLIDEAN GEOMETRY
Computing minimum length paths of a given homotopy class
[RUU-CS-90-37] N91-31900
EULER EQUATIONS OF MOTION
Development and validation of characteristic boundary conditions for cell-centered Euler flow calculations with a shock-free airfoil
[NLR-TP-89360-U] N91-31081
A shock-fitting algorithm for the simulation of inviscid flows in chemical non-equilibrium
[MBB-UK-0131-90-PUB] N91-31087
Three dimensional extension of a numerical method for resolving small transonic perturbations in unstructured mesh
[ONERA-RT-50/3064-RY-093-R] N91-31095
Design and testing of a multiblock grid-generation procedure for aircraft design and research
[NLR-TP-89146-U] N91-31131
Calculating the flow in a turbomachine with Clebsch variables and a finite element method
[ETN-91-99918] N91-31180
Generalized spatial discretization techniques for space-marching algorithms N91-31546
Prediction of rotor surface unsteady pressure and heat transfer from wake passing N91-31549
Three dimensional Euler equation solving on parallel machines
[ETN-91-99913] N91-31583
EUTECTIC ALLOYS
Solidification of a hypereutectic alloy (TEXUS 1) N91-31399
Solidification of alloys (TEXUS 1) N91-31400
Solidification of alloys (TEXUS 2) N91-31401
Macrosegregation in Ag-Sn alloys (MASER 1) N91-31402
Directional solidification of eutectics (TEXUS 6) N91-31404
Directional solidification of eutectics InSb-NiSb (TEXUS 10) N91-31405
Alloys with oxide inclusions (TEXUS 2) N91-31432
Brazing of capillary gaps (TEXUS 2) N91-31461
Acoustic positioning of a molten alloy sample (TEXUS 1) N91-31464
Acoustic positioning (TEXUS 9) ESA N91-31465
Containerless solidification of a Pd-Cu-Si sample (TEXUS 9) ESA N91-31466
Acoustic positioning (TEXUS 14b) ESA N91-31467
Containerless undercooling of a Pd-Cu-Si alloy (TEXUS 14b) ESA N91-31468
EVACUATING (TRANSPORTATION)
Testing and evaluation of the catalyst research MiniOX 3 oxygen monitor
[AD-A239665] N91-31807
EVALUATION
Performance Assessment and Coverage Evaluation (PACE) workstation (user manual)
[AD-A239723] N91-31122
OMEGA system Performance Assessment and Coverage Evaluation (PACE) workstation design and implementation, volume 2
[AD-A239724] N91-31123
Analysis of production solutions by polarography
[DE91-016479] N91-31257
Assessing the efficacy of active noise reduction
[CTN-91-60200] N91-31922
EVAPORATION
Predicted thermal response of a cryogenic fuel tank exposed to simulated aerodynamic heating profiles with different cryogens and fill levels
[NASA-CR-4395] N91-31470
Examination of molecular evaporation, cooling, and cluster dissociation of very thin liquid jets in a high vacuum
[MPIS-12/1990] N91-31581
EVOLUTION (DEVELOPMENT)
Genetic algorithms
[ETN-91-99985] N91-31852
EXCITATION
Atomic hydrogen driven halogen extraction from Si(100): Eley-Rideal surface kinetics
[AD-A239544] N91-31266
EXERCISE PHYSIOLOGY
The effect of exercise training on skeletal muscle glucose transorter isoform GLUT4 concentration in the obese Zucker rat
[AD-A239461] N91-31757
EXOBIOLOGY
The International Space University's variable gravity research facility design
[NASA-TM-105224] N91-31196
Aerospace medicine and biology: A continuing bibliography with indexes (supplement 353)
[NASA-SP-7011(353)] N91-31760
EXPERIMENT DESIGN
Comparison of integrated numerical experiments with accelerator and FEL experiments
[DE91-016071] N91-31639
Fifth force experiments N91-31733
A reminder of Faraday's gravitational experiments N91-31735
EXPERIMENTATION
Contribution of low wave numbers to the wall pressure field in a two dimensional turbulent boundary layer: Comparison of different experimental techniques
[ECL-90-15] N91-31091
Liquid phase sintering (TEXUS 19) ESA N91-31446
EXPERT SYSTEMS
A knowledge-base for rehabilitation of airfield concrete pavements
[AD-A239354] N91-31191
An expert system for the identification of silicon impurities using FTIR spectroscopy
[AD-A236504] N91-31246
Inter-GEN: A hybrid approach to engineering design optimization N91-31471
Adaptive function allocation for intelligent cockpits
[AD-A239714] N91-31808
Atomatic Feature (AFEAT) identification for Computer-Aided Process Planning (CAPP)
[DE91-016478] N91-31819
Investigation into the applicability of knowledge engineering
[NLR-TP-89031-U] N91-31878
The problem of network management: An approach using AI techniques
[REPT-90-072] N91-31884
A pragmatical view on the certainty factor model
[RUU-CS-90-42] N91-31917
EXPLOSIONS
Approximate treatment of a strong explosion and expansion in a near vacuum
[DE91-016063] N91-31574
EXPLOSIVE DEVICES
Apparatus and method for explosive bonding to edge of flyer plate
[NASA-CASE-LAR-14096-1] N91-31476
EXPLOSIVE WELDING
Apparatus and method for explosive bonding to edge of flyer plate
[NASA-CASE-LAR-14096-1] N91-31476
EXPLOSIVES
Performance evaluation of insensitive explosives
[DE91-015767] N91-31315
Understanding composite explosive energetics
[DE91-015770] N91-31316
Photography of shock waves in explosive crystals
[DE91-015772] N91-31572
EXPOSURE
Cold-induced changes in arterial sensitivity
[AD-A239493] N91-31767
EXTERNALLY BLOWN FLAPS
Segmented vectoring cruise nozzles
[CA-PATENT-APPL-SN-2-009-635] N91-31175
EXTRACTION
Atomic hydrogen driven halogen extraction from Si(100): Eley-Rideal surface kinetics
[AD-A239544] N91-31266
Development of ceramic membranes for gas separation: FY 1990 development activities
[DE91-015915] N91-31300
EXTRATERRESTRIAL ENVIRONMENTS
Activities report of the Institute of Extraterrestrial Physics
[MPE-223] N91-32002
EXTRATERRESTRIAL RESOURCES
Technical prospects for utilizing extraterrestrial propellants for space exploration
[NASA-TM-105263] N91-31318
EXTREME ULTRAVIOLET RADIATION
Design and analysis of multilayer x ray/XUV microscope
[NASA-CR-184197] N91-31607
EXTRUDING
Variations in the static properties, unnotched and notched fatigue life behaviour of 13 batches of 2L.65 aluminium alloy extruded bar
[ARL-STRUC-R-427] N91-31676

F

F-18 AIRCRAFT
Climatic considerations in the life cycle management of the CF-18 engine N91-31158
A knowledge based application of the extended aircraft interrogation and display system
[NASA-TM-4327] N91-31874
FABRICATION
Processing and characterization of continuous fiber-reinforced glass and glass-ceramic matrix composites N91-31227
A methodology for producing and testing a genesil silicon compiler designed VLSI chip which incorporates design for testability
[AD-A239465] N91-31537
System and method for automatically fabricating multiple memory holographic elements
[PATENT-1-253-724] N91-31600
FABRICS
The mechanical response of woven Kevlar fabric
[DE91-010581] N91-31230
Composite flexible blanket insulation
[NASA-CASE-NPO-11907-1-NP] N91-31236
FACTOR ANALYSIS
Full-information item bi-factor analysis
[AD-A229346] N91-31771
FACTORIZATION
An algorithm for spectral factorization of polynomial matrices with any signature
[MEMO-912] N91-31842
FAILURE ANALYSIS
An analytical prediction of matrix cracking in fibrous composite laminates N91-31225
Analysis of thermomechanical fatigue of unidirectional titanium metal matrix composites
[NASA-TM-104105] N91-31677
The failure of failures: Towards a paradigm for a synchronous communication
[RUU-CS-90-40] N91-31835
FAILURE MODES
A Weibull brittle material failure model for the ABAQUS computer program
[DE91-016813] N91-31690
FAR INFRARED RADIATION
Tunable far infrared studies of molecular parameters in support of stratospheric measurements
[NASA-CR-188774] N91-31723
FARADAY EFFECT
A reminder of Faraday's gravitational experiments N91-31735
FARM CROPS
Production of organic chemicals via bioconversion: A review of the potential
[DE91-015524] N91-31223
Cloning crops in a CELSS via tissue culture: Prospects and problems N91-31783

Preparatory space experiments for development of a CELSS N91-31796

FAST FOURIER TRANSFORMATIONS
Acceleration techniques for a spectral multi-grid method
[MEMO-914] N91-31580

FASTENERS
Photoelastic coating study of redesigned CT114 coupon joint test specimen for horizontal stabilizer rear attachment fitting to vertical stabilizer rear spar
[NAE-LTR-ST-1701] N91-31125
Method for fastening aircraft frame elements to sandwich skin panels covering same using woven fiber connectors
[PATENT-1-274-075] N91-31126

FATIGUE (MATERIALS)
Corrosion fatigue crack arrest in aluminium alloys
[NLR-MP-88050-U] N91-31282
Ultrasonic characterization of fatigue crack closure
[DE91-015161] N91-31688

FATIGUE LIFE
Variations in the static properties, unnotched and notched fatigue life behaviour of 13 batches of 2L.65 aluminium alloy extruded bar
[ARL-STRUC-R-427] N91-31676
Analysis of thermomechanical fatigue of unidirectional titanium metal matrix composites
[NASA-TM-104105] N91-31677

FATIGUE TESTS
Dual ion implantation effects on fatigue properties of Fe-13Cr-15Ni alloys
[DE91-015930] N91-31286
In situ short fatigue crack characterization of a nickel-base superalloy at ambient and elevated temperature N91-31670
Variations in the static properties, unnotched and notched fatigue life behaviour of 13 batches of 2L.65 aluminium alloy extruded bar
[ARL-STRUC-R-427] N91-31676

FAULT TOLERANCE
Electronic warfare: Faulty test equipment impairs Navy readiness
[AD-A239562] N91-31506
Intrusion and fault tolerance compatibility. Part 1: Fault protection, coding and tolerance state of the art
[LAAS-89-395] N91-31662
The potential impact of VHDL on dependable distributed system design
[AD-A239769] N91-31664
Design and analysis of fault-tolerant distributed real-time computer systems
[AD-A239521] N91-31812
Design and analysis of fault-tolerant distributed real-time computer systems
[AD-A239382] N91-31875

FEASIBILITY ANALYSIS
An investigation of dual-mode operation of a nuclear-thermal rocket engine
[DE91-015977] N91-31210
Investigation into the applicability of knowledge engineering
[NLR-TP-89031-U] N91-31878

FEED SYSTEMS
Evaluation of the intermittent GTA cold wire feed weld system
[DE91-016477] N91-31657

FEEDBACK CONTROL
On the stability of saturated state feedback regulators
[LAAS-91047] N91-31524
The control of flexible structure vibrations using a cantilevered adaptive truss N91-31671
Conceptual design of a closed loop nutrient solution delivery system for CELSS implementation in a micro-gravity environment N91-31798
Neural network based model reference adaptive control N91-31877
Near-wall conductivity N91-31944

FEEDERS
Factors affecting plant growth in membrane nutrient delivery N91-31797
Conceptual design of a closed loop nutrient solution delivery system for CELSS implementation in a micro-gravity environment N91-31798
Technology for subsystems of space-based plant growth facilities N91-31799

FEEDFORWARD CONTROL
Classes of feedforward neural networks and their circuit complexity
[MEMO-920] N91-31881
Parametric study of diffusion-enhancement networks for spatiotemporal grouping in real-time artificial vision
[AD-A239674] N91-31954

FEMALES
Female aircrew: The Canadian Forces experience, 1979-1989
[DCIEM-90-P-14] N91-31801

FERMENTATION
The conversion of lignocellulosics to fermentable sugars: A survey of current research and application to CELSS N91-31784

FERROMAGNETIC MATERIALS
X ray and gamma ray spectroscopy of solids under pressure
[DE91-016948] N91-31263
Fundamental studies in the manganese-bismuth system (TEXUS 2) N91-31414

FIBER COMPOSITES
Method for stabilizing thick honeycomb core composite articles
[PATENT-1-253-424] N91-31224
An analytical prediction of matrix cracking in fibrous composite laminates N91-31225
Processing and characterization of continuous fiber-reinforced glass and glass-ceramic matrix composites N91-31227
Relation between fiber proportion and mechanical characteristics of carbon-resin composites
[RE-50-345/F] N91-31231
Response of an alumina fiber reinforced aluminum composite to combined tension-torsion
[AD-A239560] N91-31245
Field 3, theme 1: Structural materials. Post 2: Thermotropic liquid crystal polymers
[ETN-91-99982] N91-31306
Analysis of thermomechanical fatigue of unidirectional titanium metal matrix composites
[NASA-TM-104105] N91-31677

FIBER OPTICS
Advanced and non-conventional optical schemes N91-31626
Recent advances in fiber optics components for high speed data transmission
[DE91-016252] N91-31948

FIELD OF VIEW
Radome-lens EHF antenna development
[PATENT-1-262-571] N91-31481

FIELD STRENGTH
Arctic VLF/LF data acquisition
[AD-A239704] N91-31510

FIELD THEORY (PHYSICS)
High energy physics program. Task A: Experiment and Theory. Task B: Numerical simulation of quantum field theories
[DE91-015652] N91-31938

FIGHTER AIRCRAFT
Fighter agility metrics N91-31128
Enhanced fighter maneuverability aircraft (X-31A) wing and thrust vectoring vane design
[MBB-FE22/S/PUB/0433/A] N91-31135

FILLING
Ventilation and filling of an optical diffusion cell (TEXUS 8) N91-31371

FINE STRUCTURE
A survey of the 158 micron CII fine-structure line in the central 50 pc of the galaxy
[NASA-CR-188912] N91-32009

FINGERS
A program of continuing research on representing, manipulating, and reasoning about physical objects
[AD-A239596] N91-31659

FINITE DIFFERENCE THEORY
A shock-fitting algorithm for the simulation of inviscid flows in chemical non-equilibrium
[MBB-UK-0131-90-PUB] N91-31087
Three dimensional acoustic propagation at low temperature altitude
[ONERA-RT-13/3641-PY] N91-31924

FINITE ELEMENT METHOD
User's guide to a system of finite-element supersonic panel flutter programs
[NASA-TM-104109] N91-31082
Three dimensional extension of a numerical method for resolving small transonic perturbations in unstructured mesh
[ONERA-RT-50/3064-RY-093-R] N91-31095
Inlet edge funnel of a civil aircraft gondola engine
[ETN-91-99775] N91-31130
Calculating the flow in a turbomachine with Clebsch variables and a finite element method
[ETN-91-99918] N91-31180
A method for the geometrically nonlinear analysis of compressively loaded prismatic composite structures N91-31229
Finite element modeling of orthogonal machining using an elastic-viscoplastic material model
[DE91-016815] N91-31477
The analysis and design of brushless DC motors N91-31516
Artificial diffusion methods in convection dominated flows
[W-9016] N91-31577
Compressible two dimensional boundary layer strong perfect fluid coupling in the case of sharp leading edge profiles. Stationary case
[ONERA-RT-42/1621-RY-093-R] N91-31586
Analysis and development of a wide-bandwidth gravitational wave detector N91-31601
Analysis and development of a real-time control methodology in resistance spot welding N91-31646
Nonlinear probabilistic finite element modeling of composite shells N91-31668
DYNA3D: A nonlinear, explicit, three-dimensional finite element code for solid and structural mechanics
[DE91-015735] N91-31675
Updating of finite element models using experimental vibratory type data. Process of static substructuring
[ONERA-RT-10/3313-RY-090-R] N91-31682
Large Angle Transient Dynamics (LATDYN) demonstration problem manual
[NASA-CR-4400] N91-31684
Large Angle Transient Dynamics (LATDYN) user's manual
[NASA-CR-4401] N91-31685
A finite element approach for the dynamic analysis of joint-dominated structures
[NASA-CR-4402] N91-31686
Improved finite-element methods for rotorcraft structures
[NASA-TM-104104] N91-31687
A Weibull brittle material failure model for the ABAQUS computer program
[DE91-016813] N91-31690
Least-squares solution of incompressible Navier-Stokes equations with the p-version of finite elements
[NASA-TM-105203] N91-31911
An extension of mesh equidistribution to time-dependent partial differential equations
[AD-A239579] N91-31913
Locking effects in the finite element approximation of elasticity problems
[AD-A239645] N91-31914
Analysis of the efficiency of an a-posteriori error estimator for linear triangular finite elements
[AD-A239647] N91-31915

FINITE VOLUME METHOD
Inclusion of second-moment closures into finite-volume solvers N91-31556
Numerical implementation and performance of Reynolds stress closures in finite-volume computations of recirculating and strongly swirling flows N91-31557

FIRES
Global model simulations of the long range transport of soot and sulfur from the Kuwait oil fires
[DE91-015771] N91-31719

FIRING (IGNITING)
The physical properties of a pyrotechnical circuit element
[MBB-UA-1192-90-PUB] N91-31317

FISHES
Biomass production and nitrogen dynamics in an integrated aquaculture/agriculture system N91-31789

FLAME PROPAGATION
The influence of fuel characteristics on heterogeneous flame propagation N91-31165
A comparison of several theories which use jet scaling to predict liftoff heights of turbulent-jet flames
[AD-A239717] N91-31267

FLAME RETARDANTS
Characterization of fire resistant GRP's by mechanical properties determination
[DREA-CR-88-421] N91-31295
The medical hazards of flame-suppressant atmospheres
[AD-A239618] N91-31806

FLAMES
HVOF: Particle, flame diagnostics, and coating characteristics
[DE91-014654] N91-31248
Adjustment of the mixing-rate constant in the eddy break-up model for a jet flame N91-32030

FLAMMABILITY
Characterization of fire resistant GRP's by mechanical properties determination
[DREA-CR-88-421] N91-31295

FLAT SURFACES
Facet development for a faceted stretched-membrane dish by Solar Kinetics, Inc.
[DE91-016866] N91-31713

FLEXIBILITY
A program of continuing research on representing, manipulating, and reasoning about physical objects
[AD-A239596] N91-31659

FLEXIBLE BODIES
The control of flexible structure vibrations using a cantilevered adaptive truss N91-31671

A finite element approach for the dynamic analysis of joint-dominated structures
[NASA-CR-4402] N91-31686
FLEXIBLE SPACECRAFT
Advanced optical sensing and processing technologies for the distributed control of large flexible spacecraft
[NASA-CR-4399] N91-31609
FLIGHT CONTROL
Airplane takeoff and landing performance monitoring system
[NASA-CASE-LAR-13854-1-CU] N91-31120
Rotatable non-circular forebody flow controller
[NASA-CASE-LAR-14212-1-CU] N91-31140
Rocket boosted target
[PATENT-1-254-289] N91-31207
FLIGHT CREWS
Female aircrew: The Canadian Forces experience, 1979-1989
[DCIEM-90-P-14] N91-31801
Aircrew critique of high-G centrifuge training. Part 1: What was the best part of the program?
[AD-A239781] N91-31809
FLIGHT HAZARDS
Engine icing criticality assessment N91-31161
FLIGHT MECHANICS
Activities report of the National Aerospace Laboratory
[ETN-91-99438] N91-31132
FLIGHT OPERATIONS
Flight tests with a data link used for air traffic control information exchange
[NASA-TP-3135] N91-31143
Low Temperature Environment Operations of Turboengines (Design and User's Problems)
[AGARD-CP-480] N91-31144
FLIGHT PLANS
Aeronautical Mobile Satellite Service (AMSS) test plan
[DOT/FAA/CT-TN91/20] N91-31495
FLIGHT SIMULATORS
Simulation of distance-dependent functions in visual systems for training simulators using the z-buffer technique
[MBB-UA-1190-90-PUB] N91-31186
Touch screen use on flight simulator instructor/operator stations
[AD-A239524] N91-31192
FLIGHT TEST INSTRUMENTS
Flight testing in the Netherlands: An overview
[NLR-MP-88053-U] N91-31133
FLIGHT TESTS
Fighter agility metrics N91-31128
Activities report of the National Aerospace Laboratory
[ETN-91-99438] N91-31132
Flight testing in the Netherlands: An overview
[NLR-MP-88053-U] N91-31133
Flight tests with a data link used for air traffic control information exchange
[NASA-TP-3135] N91-31143
Low altitude ejection release (total mass between 1,660 and 5,600 kg)
[REPT-90/05] N91-31475
Flight test digitized/compressed video spectrum allocation
[AD-A239535] N91-31503
FLOAT ZONES
Oscillatory Marangoni convection (TEXUS 3A and 3B) N91-31333
Critical Marangoni number (TEXUS 5) N91-31334
Critical Marangoni number (TEXUS 8) N91-31335
Thermal Marangoni convection in a floating zone (TEXUS 3) N91-31336
Oscillatory and turbulent flow regimes due to Marangoni convection (TEXUS 7) N91-31337
Thermal Marangoni convection in a floating zone (TEXUS 9) ESA N91-31341
Floating-zone growth of a silicon single crystal (TEXUS 7) N91-31384
Floating zone growth of GaAs crystals (TEXUS 20) N91-31386
Floating zone crystal growth of Ga-doped germanium (TEXTUS 10) ESA N91-31387
Floating-zone experiments with germanium crystals (TEXUS 12) ESA N91-31388
Floating zone growth of germanium crystals (TEXUS 14b) ESA N91-31389
Semi-confined Bridgman growth of Ga-doped Ge (MASER 2) N91-31391
FLOODS
Time scales of variability associated with Nordeste precipitation
[DE91-015696] N91-31718
FLOW CHARACTERISTICS
The effect of jet bleed on base pressure distribution, shedding frequency, and mean velocity profiles in the wake behind a two-dimensional blunt model
[MPIS-12/1990] N91-31085
Direct and large eddy simulation of turbulence: Summary of the state-of-the-art 1991 N91-31562
Examples of turbulence model applications N91-31563
Application of an acquisition image processing system to the quantitative analysis of flows
[AAAF-NT-89-27] N91-31851
FLOW DISTRIBUTION
Computational analysis of hypersonic flows past elliptic-cone waveriders N91-31080
A computational and experimental investigation of a three-dimensional hypersonic scramjet inlet flow field
[NASA-CR-188788] N91-31083
Study of the flow around the GARTEUR AD/AG07 wing: First F2 test campaign results
[ONERA/DERAT-37/5025-26] N91-31096
Model of an aerospace plane based on an idealized cone-derived waverider forebody N91-31129
Vortex-blade interaction on a helicopter principal rotor. Validation of the S2DI computation program and study of vortex models
[ONERA-RT-92/5094-PY] N91-31136
Second generation supersonic transport aircraft: Low speed aerodynamics
[AAAF-NT-89-02] N91-31137
A first hot wire scanner
[AAAF-NT-89-16] N91-31188
Flow induced vibrations in the SSME injector heads
[NASA-CR-184209] N91-31214
Field 3, theme 1: Structural materials. Post 2: Thermotropic liquid crystal polymers
[ETN-91-99982] N91-31306
Colloid chemistry (TEXUS 17) ESA N91-31362
Spinoidal decomposition (TEXUS 17) N91-31379
Generalized spatial discretization techniques for space-marching algorithms N91-31546
A three-dimensional viscous flow model of stator/rotor interaction in turbomachines N91-31547
Linear and nonlinear responses of the flow and temperature fields to imposed wall temperature oscillations in differentially heated vertical rectangular enclosures N91-31550
Three dimensional shear flow: Flow visualisation around a highly swept back and high incidence wing
[ONERA-RT-35/5025-28] N91-31584
Use of 4-hot-wire probes to study turbulent flow
[AAAF-NT-89-15] N91-31588
Choice representation modes and color palettes
[AAAF-NT-89-17] N91-31589
Method and apparatus for detecting laminar flow separation and reattachment
[NASA-CASE-LAR-13952-2-SB] N91-31596
Basic LDV1 component system N91-31616
Generation of particles and seeding N91-31618
Unsteady flow past an airfoil pitching at a constant rate N91-31629
Vortex interactions in the transition region of a rectangular jet N91-31630
Review of typical applications. Part 1: Measurements in liquid flows, free jets, combustion, and in the atmosphere N91-31631
FLOW EQUATIONS
Two-equation models for low-Reynolds number flow N91-31554
Artificial diffusion methods in convection dominated flows
[W-9016] N91-31577
FLOW GEOMETRY
Numerical implementation and performance of Reynolds stress closures in finite-volume computations of recirculating and strongly swirling flows N91-31557
Application of second-moment closure in complex flows N91-31559
Choice representation modes and color palettes
[AAAF-NT-89-17] N91-31589
FLOW MEASUREMENT
Contribution of low wave numbers to the wall pressure field in a two dimensional turbulent boundary layer: Comparison of different experimental techniques
[ECL-90-15] N91-31091
Measurement of six component efforts in transition flow
[AAAF-NT-89-01] N91-31097
Airfoil-vortex interaction: Unsteady wall pressure measurement
[AAAF-NT-89-13] N91-31104
Boundary layer transition detection and measurement methods at CERT/DERAT
[AAAF-NT-89-14] N91-31105
Experimental investigation of turbulent flow through a circular-to-rectangular transition duct
[NASA-TM-105210] N91-31106
Instrumentation under development for the ONERA F4 wind tunnel
[AAAF-NT-89-11] N91-31187
Development of a sensor for high-quality two-phase flow
[NLR-MP-88059-U] N91-31578
Introduction to laser velocimeter techniques N91-31615
Accuracy of laser velocimetry N91-31622
Laser transit velocimetry N91-31623
Laser transit velocimetry: Recent publications N91-31624
FLOW STABILITY
Linear and nonlinear stability of boundary layers with streamwise varying properties N91-31545
Linear and nonlinear responses of the flow and temperature fields to imposed wall temperature oscillations in differentially heated vertical rectangular enclosures N91-31550
FLOW VELOCITY
HVOF: Particle, flame diagnostics, and coating characteristics
[DE91-014654] N91-31248
Linear and nonlinear stability of boundary layers with streamwise varying properties N91-31545
Laser Doppler velocimeter measurements of the streamwise velocity component in the viscous sublayer of a turbulent channel flow
[MPIS-MITT-97] N91-31582
Laser Velocimetry, volume 1
[VKI-1991-05-VOL-1] N91-31614
Introduction to laser velocimeter techniques N91-31615
Generation of particles and seeding N91-31618
Advanced systems: Multicomponent LDV N91-31619
Biasing errors and corrections N91-31621
Laser Velocimetry, volume 2
[VKI-1991-05-VOL-2] N91-31625
FLOW VISUALIZATION
Laser Fourier densitometry and laser induced photochemical anemometry in supersonic flow
[AAAF-NT-89-09] N91-31103
Boundary layer transition detection and measurement methods at CERT/DERAT
[AAAF-NT-89-14] N91-31105
Three dimensional shear flow: Flow visualisation around a highly swept back and high incidence wing
[ONERA-RT-35/5025-28] N91-31584
Boundary layer turbulence appearance mechanisms studied by plane laser visualizations
[AAAF-NT-89-10] N91-31587
Flow visualization and simulation
[AAAF-NT-89-18] N91-31590
Postprocessing of experimental and numerical results in the case of two and three dimensional flows
[AAAF-NT-89-25] N91-31592
The development of a specific image analysis technique for exploiting flow visualization negatives
[AAAF-NT-89-26] N91-31593
Automatic analysis of visualization negatives
[ETN-91-99971] N91-31603
Interactive tool visualization of three dimensional 3D results
[AAAF-NT-89-19] N91-31847
Post processing of three dimensional aerothermal computation
[AAAF-NT-89-21] N91-31848
Use of the animated images for the visualization of computational results
[AAAF-NT-89-22] N91-31849
Visualization of three dimensional unsteady computation results
[AAAF-NT-89-23] N91-31850
FLOWMETERS
Development of a sensor for high-quality two-phase flow
[NLR-MP-88059-U] N91-31578
FLUE GASES
Electrostatic precipitation of condensed acid mist
[DE91-016530] N91-31260
FLUID DYNAMICS
Summary review of sounding rocket experiments in fluid science and material sciences: TEXUS 1 to 20; MASER 1 and 2
[ESA-SP-1132] N91-31321
Liquid motion in capillary tubes (TEXUS 3) N91-31322
Liquid motion in capillary tubes (TEXUS 5) N91-31323
Interfacial convection (TEXUS 1) N91-31327
Interfacial convection (TEXUS 2) N91-31328
Diffusion-induced interfacial convection (TEXUS 3) N91-31329
Thermally induced interfacial convection (TEXUS 4) N91-31330
Diffusion-induced interfacial convection (TEXUS 8) N91-31331
Diffusion-induced interfacial convection (TEXUS 11) N91-31332

Oscillatory Marangoni convection (TEXUS 3A and 3B) N91-31333
Critical Marangoni number (TEXUS 5) N91-31334
Critical Marangoni number (TEXUS 8) N91-31335
Thermal Marangoni convection in a floating zone (TEXUS 3) N91-31336
Oscillatory and turbulent flow regimes due to Marangoni convection (TEXUS 7) N91-31337
Influence of a surface tension minimum on the Marangoni effect (TEXUS 8) ESA N91-31338
Influence of a surface tension minimum on the Marangoni effect (TEXUS 9) ESA N91-31339
Influence of a surface tension minimum on the Marangoni effect (TEXUS 19) ESA N91-31340
Thermal Marangoni convection in a floating zone (TEXUS 9) ESA N91-31341
Experimental results on microgravitational fluid dynamics (TEXUS 14b) ESA N91-31342
Three-dimensional Marangoni convection (MASER 1) ESA N91-31343
Three-dimensional Marangoni convection (MASER 2) ESA N91-31344
Thermocapillary drop motion, 1 (MASER 1) ESA N91-31345
Thermocapillary drop motion, 2 (MASER 2) ESA N91-31346
Phase separation of a binary fluid near its critical point (TEXUS 11) N91-31377
Phase separation in microgravity of binary fluids near the critical point (TEXUS 13) N91-31378
Spinoidal decomposition (TEXUS 17) N91-31379
New Approaches in the Description and Modeling of Turbulence
[VKI-LS-1991-03] N91-31565
Direct and large-eddy simulations of transition in the compressible boundary layer N91-31566
Spectral large-eddy simulation of isotropic and stably-stratified turbulences N91-31567
Large-eddy simulation of the turbulent flow in the downstream region of a backward facing step N91-31568
Spatiotemporal intermittency N91-31569
RNG and turbulence modeling N91-31570
Finite-dimensional dynamics and chaos in fluid flows N91-31571
A critical comparison of two-equation turbulence models
[NASA-TM-105237] N91-31597

FLUID FLOW
Metal matrix composites (TEXUS 20) N91-31440
Computational fluid dynamics N91-31544
The interaction of particles with homogeneous turbulence N91-31548
New Approaches in the Description and Modeling of Turbulence
[VKI-LS-1991-03] N91-31565
Finite-dimensional dynamics and chaos in fluid flows N91-31571
A boundary integral equation method for steady two-dimensional flow in partially saturated media
[DE91-016056] N91-31573
Review of typical applications. Part 1: Measurements in liquid flows, free jets, combustion, and in the atmosphere N91-31631

FLUID JETS
Examination of molecular evaporation, cooling, and cluster dissociation of very thin liquid jets in a high vacuum
[MPIS-12/1990] N91-31581
Vortex interactions in the transition region of a rectangular jet N91-31630

FLUID MECHANICS
Proceedings of the Ninth Symposium on Energy Engineering Sciences: Fluid and Dynamical Systems
[DE91-015974] N91-31701
Interactive tool visualization of three dimensional 3D results
[AAAF-NT-89-19] N91-31847

FLUORESCENCE
Tropical tests of a seawater marker
[MRL-TR-90-19] N91-31109

FLUOROCARBONS
Effective ionization coefficients, electron drift velocities, and limiting breakdown fields for gas mixtures of possible interest to particle detectors
[DE91-015921] N91-31532

FLUTTER ANALYSIS
User's guide to a system of finite-element supersonic panel flutter programs
[NASA-TM-104109] N91-31082

FLUX PINNING
Weak links within a Bi2Sr2Ca1Cu2O(x) single crystal by magnetization and direct optical observations
[DE91-016085] N91-31979

FLUX QUANTIZATION
Methodology for calibration and use of heat flux transducers
[AD-A239552] N91-31541

FLY ASH
Electrostatic precipitation of condensed acid mist
[DE91-016530] N91-31260

FOAMS
Bubbles and foams (TEXUS 10) ESA N91-31324

FOCUSING
Laser transit velocimetry N91-31623
Laser transit velocimetry: Recent publications N91-31624

FOKKER AIRCRAFT
Activities report of the National Aerospace Laboratory
[ETN-91-99438] N91-31132

FOOD PRODUCTION (IN SPACE)
Controlled Ecological Life Support Systems: CELSS '89 Workshop
[NASA-TM-102277] N91-31775
Exploring the limits of crop productivity: A model to evaluate progress N91-31776
Environmental modification of yield and food composition of cowpea and leaf lettuce N91-31777
Efficiency of N use by wheat as a function of influx and efflux of NO3 N91-31778
Environmental and cultural considerations for growth of potatoes in CELSS N91-31779
Effects of atmospheric CO2 on photosynthetic characteristics of soybean leaves N91-31780
Effects of elevated atmospheric carbon dioxide concentrations on water and acid requirements of soybeans grown in a recirculating hydroponic system N91-31781
Sweet potato for closed ecological life support systems using the nutrient film technique N91-31782
Seed sprout production: Consumables and a foundation for higher plant growth in space N91-31790
Controlled ecological life support system breadboard project, 1988 N91-31791
The crop growth research chamber: A ground-based facility for CELSS research N91-31792
Development of the CELSS emulator at NASA. Johnson Space Center N91-31793
A perspective on CELSS control issues N91-31794
Transpiration during life cycle in controlled wheat growth N91-31795
Preparatory space experiments for development of a CELSS N91-31796
Factors affecting plant growth in membrane nutrient delivery N91-31797
Conceptual design of a closed loop nutrient solution delivery system for CELSS implementation in a micro-gravity environment N91-31798
Technology for subsystems of space-based plant growth facilities N91-31799
Solid-support substrates for plant growth at a lunar base N91-31800

FOREBODIES
Model of an aerospace plane based on an idealized cone-derived waverider forebody N91-31129

FORECASTING
Effects of stress on judgment and decision making in dynamic tasks
[AD-A239452] N91-31772

FORESTS
Examination and mapping of forest damage, using remote sensing methods
[ETN-91-99741] N91-31696

FORGING
Fatigue-resistant nickel-base superalloys
[PATENT-1-253-363] N91-31268

FORMALDEHYDE
Influence of surface defects and local structure on oxygenate reaction pathways over metal oxide surfaces
[DE91-016600] N91-31289

FORMALISM
The ABC-machine: A sequential stack-based abstract machine for graph rewriting
[TR-90-22] N91-31824
On a ternary bracketing problem from the theory of formal languages
[TR-90-24] N91-31825
Partial evaluation grammars
[TR-91-01] N91-31826
Mathematical theory of computation
[AD-A239419] N91-31912
Formalisation of techniques: Chopping down the methodology jungle
[TR-90-26] N91-31996

FORMIC ACID
Influence of surface defects and local structure on oxygenate reaction pathways over metal oxide surfaces
[DE91-016600] N91-31289

FORMULAS (MATHEMATICS)
On the expressiveness of equational type logic
[MEMO-INF-90-39-REV] N91-31887
A formal power series equation from formula complexity theory
[TR-90-25] N91-31895

FORTRAN
A case study for the real-time experimental evaluation of the VIPER microprocessor
[NASA-TM-104098] N91-31531
Methods of astrodynamics, a computer approach
[AD-A239662] N91-31861

FOSSIL FUELS
Conversion of biomass and fossil fuels to methanol and its effect on CO2 emissions
[DE91-015846] N91-31320

FOURIER ANALYSIS
Development of an infrared Laser Fourier Densitometer (LFD) and first wind tunnel tests
[PMI-2335] N91-31189

FOURIER TRANSFORMATION
An expert system for the identification of silicon impurities using FTIR spectroscopy
[AD-A236504] N91-31246
Postprocessing of test and computation results by the wavelet method
[AAAF-NT-89-24] N91-31591
Developing dataflow algorithms
[DE91-016300] N91-31818

FRACTURE MECHANICS
An investigation into the effects of damage on the stresses in a composite laminate N91-31226
Dynamic strength and strain rate effects on fracture behavior of tungsten and tungsten alloys
[DE91-013029] N91-31275
Metastable austenites in cryogenic high magnetic field environments
[DE91-016420] N91-31288
Fracture toughness characterization of polymers N91-31296
An equivalent domain integral method for three-dimensional mixed-mode fracture problems
[NASA-CR-182021] N91-31692

FRACTURE STRENGTH
Alumina reinforced tetragonal zirconia (TZP) composites
[DE91-016748] N91-31239
Metastable austenites in cryogenic high magnetic field environments
[DE91-016420] N91-31288
Fracture toughness characterization of polymers N91-31296
Development of toughened ceramics for elevated temperatures
[DE91-015923] N91-31301

FRACTURING
Creep deformation and fracture of a two-phase TiAl intermetallics
[DE91-011963] N91-31274
Magnetic field-induced fracture changes in metastable austenites at 4.2 K
[DE91-016263] N91-31279
Metastable austenites in cryogenic high magnetic field environments
[DE91-016420] N91-31288

FRAGMENTATION
Calculation of fragment ejection velocities on explosion of a launcher
[CNES-NT-128] N91-31195

FRAMES
Method for fastening aircraft frame elements to sandwich skin panels covering same using woven fiber connectors
[PATENT-1-274-075] N91-31126

FRAMING CAMERAS
High-speed TV cameras for streak tube readout
[DE91-016081] N91-31602

FREE CONVECTION
Thermally induced interfacial convection (TEXUS 4) N91-31330
Thermal Marangoni convection in a floating zone (TEXUS 3) N91-31336
Influence of a surface tension minimum on the Marangoni effect (TEXUS 8) ESA N91-31338
Influence of a surface tension minimum on the Marangoni effect (TEXUS 9) ESA N91-31339
Thermal Marangoni convection in a floating zone (TEXUS 9) ESA N91-31341
Nucleate pool boiling (TEXUS 3) N91-31354
Solidification of a hypereutectic alloy (TEXUS 1) N91-31399

FREE ELECTRON LASERS
Comparison of integrated numerical experiments with accelerator and FEL experiments
[DE91-016071] N91-31639

Compact free-electron laser at the Los Alamos National Laboratory
[DE91-016079] N91-31640

FREE FLOW
Environmental icing testing at the Naval Air Propulsion Center N91-31167

FREE JETS
Icing test capabilities for aircraft propulsion systems at the Arnold Engineering Development Center N91-31170
HVOF: Particle, flame diagnostics, and coating characteristics
[DE91-014654] N91-31248

FREEZING
The development of a computational model to predict low temperature fuel flow phenomena N91-31166
Freezing of a long liquid column (TEXUS 18) ESA N91-31326
Examination of molecular evaporation, cooling, and cluster dissociation of very thin liquid jets in a high vacuum
[MPIS-12/1990] N91-31581

FREQUENCIES
Signal processing: Time domain and frequency domain N91-31620

FREQUENCY MEASUREMENT
Arctic VLF/LF data acquisition
[AD-A239704] N91-31510

FREQUENCY RESPONSE
Dynamics of 1.3 micron semiconductor lasers and nonlinear gain N91-31613

FRUITS
Cloning crops in a CELSS via tissue culture: Prospects and problems N91-31783

FUEL CELLS
Water transport properties of fuel cell ionomers
[DE91-016015] N91-31259
Fuel cells for commercial energy
[MBB-UE-0018-90-PUB] N91-31706
Pseudohomogeneous catalyst layer model for polymer electrolyte fuel cell
[DE91-016014] N91-31710

FUEL COMBUSTION
The effect of fuel properties and atomization on low temperature ignition in gas turbine combustors N91-31164
The influence of fuel characteristics on heterogeneous flame propagation N91-31165
Nonlinear combustion instability model in two- to three-dimensions
[NASA-TM-102381] N91-31208
The autoignition chemistry of paraffinic fuels and pro-knock and anti-knock additives: A detailed chemical kinetic study
[DE91-014992] N91-31314

FUEL CONTROL
A high-frequency servosystem for fuel control in hypersonic engines
[NASA-TM-104333] N91-31178

FUEL FLOW
The development of a computational model to predict low temperature fuel flow phenomena N91-31166

FUEL PRODUCTION
Technical prospects for utilizing extraterrestrial propellants for space exploration
[NASA-TM-105263] N91-31318

FUEL SPRAYS
HVOF: Particle, flame diagnostics, and coating characteristics
[DE91-014654] N91-31248

FUEL SYSTEMS
Cold start investigation of an APU with annular combustor and fuel vaporizers N91-31154

FUEL TANKS
Predicted thermal response of a cryogenic fuel tank exposed to simulated aerodynamic heating profiles with different cryogens and fill levels
[NASA-CR-4395] N91-31470

FUNCTIONS (MATHEMATICS)
A technique for locating function roots and for satisfying equality constraints in optimization
[NASA-TM-104037] N91-31139
Linear logic, domain theory, and semi-functors
[RUU-CS-90-34] N91-31830
Categorical semantics as a basis for program transformation
[RUU-CS-90-38] N91-31833
A formal power series equation from formula complexity theory
[TR-90-25] N91-31895
A note on semi-adjunctions
[RUU-CS-90-41] N91-31901

FUNNELS
Inlet edge funnel of a civil aircraft gondola engine
[ETN-91-99775] N91-31130

FURNACES
Solidification of alloys (TEXUS 1) N91-31400

FUSELAGES
Fuselage shell and cavity response measurements on a DC-9 test section
[NASA-CR-187557] N91-31926

G

GALACTIC RADIATION
A survey of the 158 micron CII fine-structure line in the central 50 pc of the galaxy
[NASA-CR-188912] N91-32009

GALACTOSE
Diffusion-controlled growth of protein single crystals: B-galactosidase (TEXUS 3) N91-31395
Diffusion-controlled growth of protein single crystals: Investigation of B-galactosidase at low temperature (TEXUS 4) N91-31396
Diffusion-controlled growth of single crystals of protein (TEXUS 5) N91-31397

GALAXIES
A study of a 21-cm-selected sample of galaxies N91-32014

GALERKIN METHOD
Artificial diffusion methods in convection dominated flows
[W-9016] N91-31577

GALLIUM
Semi-confined Bridgman growth of Ga-doped Ge (MASER 2) N91-31390
Semi-confined Bridgman growth of Ga-doped Ge (MASER 2) N91-31391

GALLIUM ALLOYS
Photophysics and chemistry of ultra-fast ZnO and CdS phosphors
[DE91-013106] N91-31966

GALLIUM ARSENIDES
Floating zone growth of GaAs crystals (TEXUS 20) N91-31386
Solution growth of GaAs single crystals (TEXUS 19) N91-31393
Innovative optoelectronic materials and structures using OMVPE
[AD-A239518] N91-31951
Studies of the III-V compounds in the megabar regime
[DE91-015911] N91-31973
Rapid thermal annealing effects in In(x)Ga(1-x)As/GaAs strained-layer superlattices
[DE91-015901] N91-31978
Epitaxial growth and electro-optical properties of metal GaAs superlattices
[AD-A239719] N91-31984

GALLIUM COMPOUNDS
Epitaxial growth and electro-optical properties of metal GaAs superlattices
[AD-A239719] N91-31984

GALLIUM PHOSPHIDES
Innovative optoelectronic materials and structures using OMVPE
[AD-A239518] N91-31951

GAME THEORY
The complexity of coloring games on perfect graphs
[RUU-CS-91-03] N91-31838
Extensive coverings and exact core bounds
[MEMO-915] N91-31907
From game trees to game graphs
[RUU-CS-90-43] N91-31921

GAMMA RAY BURSTS
Development of the Burst and Transient Source Experiment (BATSE)
[NASA-RP-1268] N91-32006

GAMMA RAY OBSERVATORY
Development of the Burst and Transient Source Experiment (BATSE)
[NASA-RP-1268] N91-32006

GAMMA RAYS
Development of the Burst and Transient Source Experiment (BATSE)
[NASA-RP-1268] N91-32006
The Li-7 and Be-7 deexcitation lines: Probes for accelerated particle transport models in solar flares
[NASA-CR-183490] N91-32020
GRO source candidates: (A) Nearby modest-size molecular clouds; (B) Pulsar with Wolf-Rayet companion that has lost its H-envelope
[NASA-CR-183491] N91-32021
Abundances from solar flare line spectroscopy
[NASA-CR-183492] N91-32022

GAPS
Brazing of capillary gaps (TEXUS 2) N91-31461

GARMENTS
Garment selection for cleanrooms and controlled environments for spacecraft
[AD-A239512] N91-31805

GAS DENSITY
Effective ionization coefficients, electron drift velocities, and limiting breakdown fields for gas mixtures of possible interest to particle detectors
[DE91-015921] N91-31532

GAS DETECTORS
Basic operation and preliminary trials of a detector for stationary gas bubbles
[AD-A239710] N91-31769
Testing and evaluation of the catalyst research MiniOX 3 oxygen monitor
[AD-A239665] N91-31807

GAS DISCHARGES
Etching method for photoresists or polymers
[NASA-CASE-ARC-11873-2] N91-31258

GAS EXCHANGE
A system to determine whole-plant exchange rates of ozone, carbon dioxide and water vapour N91-32027

GAS FLOW
HVOF: Particle, flame diagnostics, and coating characteristics
[DE91-014654] N91-31248

GAS MIXTURES
Effective ionization coefficients, electron drift velocities, and limiting breakdown fields for gas mixtures of possible interest to particle detectors
[DE91-015921] N91-31532

GAS PRESSURE
Effects of trapped gases on ceramic-filled-glass composite densification
[DE91-015850] N91-31237
Properties of low temperature, low oxygen pressure post-annealed YBa2Cu3O(sub 7-x) thin films
[DE91-015632] N91-31969

GAS STREAMS
HVOF: Particle, flame diagnostics, and coating characteristics
[DE91-014654] N91-31248

GAS TUNGSTEN ARC WELDING
Weldability and hot ductility of iron aluminides
[DE91-016343] N91-31280
Effect of convection on weld pool development
[DE91-014213] N91-31649
Evaluation of the intermittent GTA cold wire feed weld system
[DE91-016477] N91-31657

GAS TURBINE ENGINES
Ice tolerant engine inlet screens for CH113/113A search and rescue helicopters N91-31149
Cold starting small gas turbines: An overview N91-31150
Cold weather ignition characteristics of advanced small gas turbine combustion systems N91-31152
Cold start development of modern small gas turbine engines at Pratt and Whitney Aircraft of Canada Ltd. N91-31156
Fuels and oils as factors in the operation of aero gas turbine engines at low temperatures N91-31163
The effect of fuel properties and atomization on low temperature ignition in gas turbine combustors N91-31164
Field evaluation of six protective coatings applied to T56 turbine blades after 500 hours of engine use
[ARL-MAT-TM-405] N91-31179

GAS TURBINES
Cold weather ignition characteristics of advanced small gas turbine combustion systems N91-31152
Prediction of rotor surface unsteady pressure and heat transfer from wake passing N91-31549

GATES (CIRCUITS)
Reconfigurable parameter filter
[PATENT-1-264-072] N91-31513

GEAR TEETH
Spur-gear optimization using SPUROPT computer program
[NASA-TM-104394] N91-31648

GEARS
Spur-gear optimization using SPUROPT computer program
[NASA-TM-104394] N91-31648
Recent manufacturing advances for spiral bevel gears
[NASA-TM-104479] N91-31654

GENERAL AVIATION AIRCRAFT
Development of a geographic navigational display device for general aviation aircraft
[PB91-170282] N91-31114

GENETICS
Strategies for biopolymer engineering of PHB-like materials
[AD-A239690] N91-31313
Genetic algorithms
[ETN-91-99985] N91-31852

GEODESY
Origins of GPS surveying
[AD-A239676] N91-31121

Coordinate conversions for presenting and compositing weather radar data
[KNMI-TR-129] N91-31497

GEODETIC SATELLITES
Investigations on the use of GPS for geodetic and orbit determination applications
[LR-649] N91-31118

GEOGRAPHIC INFORMATION SYSTEMS
GEOTRANS: An interface program from GEOPROGRAM to a geographic information system
[DE91-016111] N91-31998

GEOLOGICAL SURVEYS
GEOTRANS: An interface program from GEOPROGRAM to a geographic information system
[DE91-016111] N91-31998

GEOMAGNETIC TAIL
A study of ion acceleration at rocket altitudes and development and calibration of pitch angle imaging charged particle detectors N91-31728

GEOMETRIC ACCURACY
Large scale CAESAR images using inertial navigation and pressure altitude measurement. Accuracy deformations and possibilities for a Global Positioning System (GPS)
[ETN-91-99418] N91-31117

GEOMETRICAL OPTICS
On the response of the special sensor microwave/imager to the marine environment: Implications for atmospheric parameter retrievals N91-31727

GEOMETRY
Atomatic Feature (AFEAT) identification for Computer-Aided Process Planning (CAPP)
[DE91-016478] N91-31819
Enhancement of surface definition and gridding in the Eagle code
[NASA-CR-188796] N91-31820
An extension of the potential method to higher-order blendings
[CS-9103] N91-31893

GEOMORPHOLOGY
North Pacific guyots
[AD-A239388] N91-31754

GEOSTROPHIC WIND
A quantitative analysis of quasi-geostrophic forcing during recent severe weather outbreaks across the southern Great Plains
[PB91-176693] N91-31745

GEOTECHNICAL ENGINEERING
Identifying behavior characteristics using pressuremeter tests
[ETN-91-99917] N91-31680

GERMAN SPACE PROGRAM
Summary review of sounding rocket experiments in fluid science and material sciences: TEXUS 1 to 20; MASER 1 and 2
[ESA-SP-1132] N91-31321

GERMANIUM
Directional solidification of doped germanium (TEXUS 4) ESA N91-31380
Striations in germanium (TEXUS 6) ESA N91-31381
Floating zone crystal growth of Ga-doped germanium (TEXTUS 10) ESA N91-31387
Floating-zone experiments with germanium crystals (TEXUS 12) ESA N91-31388
Floating zone growth of germanium crystals (TEXUS 14b) ESA N91-31389
Semi-confined Bridgman growth of Ga-doped Ge (MASER 2) N91-31390
Semi-confined Bridgman growth of Ga-doped Ge (MASER 2) N91-31391

GERMINATION
Preparatory space experiments for development of a CELSS N91-31796

GLASS
Effects of trapped gases on ceramic-filled-glass composite densification
[DE91-015850] N91-31237
Fracture toughness characterization of polymers N91-31296
Defect diffusion in ion implanted glasses
[DE91-016119] N91-31302
Reaction kinetics in molten glasses: Self-diffusion in alkali-silicate melts (TEXUS 20) N91-31368
Special refractive index profiles in glasses obtained by ion exchange (TEXUS 19) ESA N91-31369
Composite materials, 1 (TEXUS 1) N91-31408
Composite materials, 2 (TEXUS 2) N91-31409
Immiscibles, 1 (TEXUS 3) N91-31410
Crystallization of the glassy grain boundary phase in silicon nitride ceramics
[NASA-CR-188717] N91-31961
Glass formation and crystallization in high-temperature glass-ceramics and Si3N4 N91-31964
Indirect measurement of the viscosity of the intergranular glass phase in yttria-sintered silicon nitride N91-31965

GLASS FIBER REINFORCED PLASTICS
The influence of moisture and pressure on the mechanical properties of a glass-epoxy matrix composite and a graphite-epoxy matrix composite
[AD-A239509] N91-31242
Characterization of fire resistant GRP's by mechanical properties determination
[DREA-CR-88-421] N91-31295
Parabolic dish photovoltaic concentrator development
[DE91-016868] N91-31714

GLASS FIBERS
Processing and characterization of continuous fiber-reinforced glass and glass-ceramic matrix composites N91-31227

GLOBAL POSITIONING SYSTEM
Enhanced global positioning system delta-range processing
[PATENT-1-254-637] N91-31115
Large scale CAESAR images using inertial navigation and pressure altitude measurement. Accuracy deformations and possibilities for a Global Positioning System (GPS)
[ETN-91-99418] N91-31117
Investigations on the use of GPS for geodetic and orbit determination applications
[LR-649] N91-31118
Origins of GPS surveying
[AD-A239676] N91-31121

GLUCOSE
The effect of exercise training on skeletal muscle glucose transorter isoform GLUT4 concentration in the obese Zucker rat
[AD-A239461] N91-31757

GOLD ALLOYS
Diffusion of Ni in Cu-Au and Cu-Al alloys (TEXUS 20) N91-31373

GOVERNMENT PROCUREMENT
Acquisition reform: Implementing defense management review initiatives. Report to the Chairman and Ranking Minority Member, Subcommittee on Defense Industry and Technology, Senate Committee on Armed Services
[AD-A239423] N91-31999

GOVERNMENTS
What is the Federal Demonstration Project?
[DE91-013936] N91-31986

GRAIN BOUNDARIES
Deformation induced microstructural and microchemical changes during thermomechanical treatment
[DE91-016949] N91-31290
Microstructural changes in Beta-silicon nitride grains upon crystallizing the grain-boundary glass N91-31963
Glass formation and crystallization in high-temperature glass-ceramics and Si3N4 N91-31964

GRAIN SIZE
Mechanical behavior of a nickel based alloy UDIMET 700 fabricated by powder metallurgy
[JUEL-2414] N91-31283

GRAINS (FOOD)
Cloning crops in a CELSS via tissue culture: Prospects and problems N91-31783

GRAMMARS
LR-parsing derived
[CS-9105] N91-31823
On a ternary bracketing problem from the theory of formal languages
[TR-90-24] N91-31825
Partial evaluation grammars
[TR-91-01] N91-31826
On the efficient incremental evaluation of higher order attribute grammars
[RUU-CS-90-36] N91-31832
The hierarchy of LR-attributed grammars
[MEMO-INF-91-26] N91-31840
Attribute evaluation and parsing
[MEMO-INF-91-31] N91-31841

GRANTS
Survey to assess the usefulness of two model agreements for university-industry cooperative research
[DE91-013937] N91-31985
What is the Federal Demonstration Project?
[DE91-013936] N91-31986

GRANULAR MATERIALS
Studies of non-ideal superconductors using DC magnetic methods
[DE91-015642] N91-31970

GRAPH THEORY
Perfect colorings
[RUU-CS-90-35] N91-31831
Approximating treewidth, pathwidth, and minimum elimination tree height
[RUU-CS-91-01] N91-31836
On disjoint cycles
[RUU-CS-90-29] N91-31897
Cycles containing many vertices of large degree
[MEMO-916] N91-31908
A graph theoretic approach to scene matching
[NASA-CR-187817] N91-31947

GRAPHITE-EPOXY COMPOSITES
The influence of moisture and pressure on the mechanical properties of a glass-epoxy matrix composite and a graphite-epoxy matrix composite
[AD-A239509] N91-31242
Modelling the response of thick composite materials due to axisymmetric shock loading
[AD-A239531] N91-31243

GRAPHS (CHARTS)
The ABC-machine: A sequential stack-based abstract machine for graph rewriting
[TR-90-22] N91-31824
Distributed incremental maximum finding in hierarchically divided graphs
[RUU-CS-90-30] N91-31828
Perfect colorings
[RUU-CS-90-35] N91-31831
The complexity of coloring games on perfect graphs
[RUU-CS-91-03] N91-31838
An algorithm for the one-to-all shortest path problem with arbitrary arc lengths
[MEMO-919] N91-31844
On disjoint cycles
[RUU-CS-90-29] N91-31897
From game trees to game graphs
[RUU-CS-90-43] N91-31921

GRAVITATION
The time-domain earth tides N91-31726
BAe University Round Table on Gravitational Research
[BAE-FBS-007] N91-31729
The Sowerby Research Centre and university liaison N91-31730
BAe overview of current gravitational physics research N91-31731
Gravitational wave research N91-31732
Fifth force experiments N91-31733
A reminder of Faraday's gravitational experiments N91-31735

GRAVITATION THEORY
A reminder of Faraday's gravitational experiments N91-31735
Review of microgravity N91-31736
Heaviside's linearised gravitational theory N91-31737
A new model of the electron: A suggested experiment to search for a link between electromagnetism and gravity N91-31738

GRAVITATIONAL EFFECTS
Directional solidification of Al-Cu alloys (MASER 2) N91-31403

GRAVITATIONAL FIELDS
BAe University Round Table on Gravitational Research
[BAE-FBS-007] N91-31729
Gravitational wave research N91-31732
Fifth force experiments N91-31733
Heaviside's linearised gravitational theory N91-31737

GRAVITATIONAL PHYSIOLOGY
The International Space University's variable gravity research facility design
[NASA-TM-105224] N91-31196

GRAVITATIONAL WAVES
Analysis and development of a wide-bandwidth gravitational wave detector N91-31601
BAe overview of current gravitational physics research N91-31731
Gravitational wave research N91-31732

GRAVITY GRADIOMETERS
The superconducting gravity gradiometer N91-31734
Review of microgravity N91-31736

GRAZING
Exact result for the grazing angle of specular reflection from a sphere
[AD-A239578] N91-31952

GREAT PLAINS CORRIDOR (NORTH AMERICA)
A quantitative analysis of quasi-geostrophic forcing during recent severe weather outbreaks across the southern Great Plains
[PB91-176693] N91-31745

GREENHOUSE EFFECT
Simulated effects of a doubling of carbon dioxide on corn production in portions of the central US
[DE91-016843] N91-31722

GREENHOUSES
Method and apparatus for bio-regenerative life support system
[NASA-CASE-MSC-21629-1] N91-31803

GRID GENERATION (MATHEMATICS)
Three dimensional extension of a numerical method for resolving small transonic perturbations in unstructured mesh
[ONERA-RT-50/3064-RY-093-R] N91-31095

Laser Fourier densitometry and laser induced photochemical anemometry in supersonic flow
[AAAF-NT-89-09] N91-31103
Design and testing of a multiblock grid-generation procedure for aircraft design and research
[NLR-TP-89146-U] N91-31131
Generalized spatial discretization techniques for space-marching algorithms N91-31546
Compressible two dimensional boundary layer strong perfect fluid coupling in the case of sharp leading edge profiles. Stationary case
[ONERA-RT-42/1621-RY-093-R] N91-31586
Enhancement of surface definition and gridding in the Eagle code
[NASA-CR-188796] N91-31820
A dynamically adaptive multigrid algorithm for the incompressible Navier-Stokes equations: Validation and model problems
[NASA-CR-187595] N91-31888

GRINDING MACHINES
Recent manufacturing advances for spiral bevel gears
[NASA-TM-104479] N91-31654

GROUND STATE
Ground-state in-plane light-holes in GaAs/AlGaAs structures
[DE91-016408] N91-31980

GROUND SUPPORT EQUIPMENT
A knowledge based application of the extended aircraft interrogation and display system
[NASA-TM-4327] N91-31874

GROUND TESTS
Vulnerability of a small powerplant to wet snow conditions N91-31148
Analysis of interior noise ground and flight test data for advanced turboprop aircraft applications
[NASA-CR-187558] N91-31927

GUIDANCE (MOTION)
Possibilities of simulation and optimization for guided missile systems
[MBB-UA-1201-90-PUB] N91-31183
Path planning for non-holonomic mobile robots
[LAAS-91135] N91-31882

GUIDANCE SENSORS
The in-flight calibration of the Hubble space telescope attitude sensors
[NASA-CR-183485] N91-32007

GYROSCOPES
The in-flight calibration of the Hubble space telescope attitude sensors
[NASA-CR-183485] N91-32007

GYROSTABILIZERS
Steerable windowed enclosures
[PATENT-1-262-653] N91-31142

H

H II REGIONS
Ultraviolet morphology of NGC 1068: The starburst knots and the extended emission region N91-32004

HABITATS
Method and apparatus for bio-regenerative life support system
[NASA-CASE-MSC-21629-1] N91-31803

HADRONS
Fast pulsars, variational bound, other facets of compact stars
[DE91-016416] N91-32018

HAFNIUM OXIDES
Ceramic composition
[PATENT-1-249-609] N91-31294

HALOGENS
Atomic hydrogen driven halogen extraction from Si(100): Eley-Rideal surface kinetics
[AD-A239544] N91-31266

HARDENING (MATERIALS)
Dynamic strength and strain rate effects on fracture behavior of tungsten and tungsten alloys
[DE91-013029] N91-31275

HARMONIC ANALYSIS
The time-domain earth tides N91-31726

HARMONIC EXCITATION
Behavior of nonlinear mechanical structures subjected to stationary excitations
[ECL-91-01] N91-31681

HAWAII
UKIRT observer's manual
[ETN-91-99747] N91-32008

HEART FUNCTION
Continuous 24 hour ECG study, on ground and in flight, of 19 Mirage 2000 pilots stationed at the Dijon airbase (France). Comparison with similar recordings taken on other types of fighter aircraft or in operationally different conditions
[ETN-91-99973] N91-31761

HEAT FLUX
Predicted thermal response of a cryogenic fuel tank exposed to simulated aerodynamic heating profiles with different cryogens and fill levels
[NASA-CR-4395] N91-31470
Methodology for calibration and use of heat flux transducers
[AD-A239552] N91-31541
Plug-type heat flux gauge
[NASA-CASE-LEW-14967-1] N91-31608

HEAT MEASUREMENT
Description of Crau data set: Meteosat data, radiosonde data, sea surface temperatures: Comparison of Meteosat and Heimann data
[KNMI-WR-90-03] N91-31752

HEAT OF VAPORIZATION
Examination of molecular evaporation, cooling, and cluster dissociation of very thin liquid jets in a high vacuum
[MPIS-12/1990] N91-31581

HEAT RESISTANT ALLOYS
Fatigue-resistant nickel-base superalloys
[PATENT-1-253-363] N91-31268
Skin technology (TEXUS 1) N91-31455
Skin technology (TEXUS 2) N91-31456
Skin technology (TEXUS 3) N91-31457
Skin technology (TEXUS 4) N91-31458
Skin technology (TEXUS 9) N91-31459
Skin technology (TEXUS 11 and 12) N91-31460
In situ short fatigue crack characterization of a nickel-base superalloy at ambient and elevated temperature N91-31670
Crack propagation in heat resistant disk alloys. Short crack propagation in alloys for high characteristic turbomachine disks
[ETN-91-99981] N91-31683

HEAT TRANSFER
Nucleate pool boiling (TEXUS 3) N91-31354
Bubble formation, 1 (TEXUS 5) N91-31355
Bubble formation, 2 (TEXUS 10) N91-31356
Bubble formation, 2. Microgravity measurements of the boiling heat transfer from flat heating surfaces (TEXUS 11) N91-31357
Inst. A fuer Thermodynamik. N91-31358
Prediction of rotor surface unsteady pressure and heat transfer from wake passing N91-31549
Linear and nonlinear responses of the flow and temperature fields to imposed wall temperature oscillations in differentially heated vertical rectangular enclosures N91-31550
The effects of fluid particle interactions on interfacial transfer and flow structure
[DE91-016409] N91-31575
A relative-intensity two-color phosphor thermography system
[NASA-TM-104123] N91-31595
Proceedings of the Ninth Symposium on Energy Engineering Sciences: Fluid and Dynamical Systems
[DE91-015974] N91-31701
Open-cycle ocean thermal energy conversion surface-condenser design analysis and computer program
[DE91-015973] N91-31709

HEAT TREATMENT
Beneficial effects of austemper post-treatment on tungsten carbide based wear coatings
[DE91-013260] N91-31293
Stress relaxation in bending of type AISI 304 stainless steel at 773K and 823K
[DE91-618657] N91-31666
Depth profiles for hydrogen-assisted thermal donor formation in silicon
[DE91-015719] N91-31971

HEAVY IONS
Particle production through two-photon processes in relativistic heavy-ion colliders
[DE91-016221] N91-31931

HELICOPTER CONTROL
Robustness and techniques of multivariable control for helicopter piloting. Dispatch 3: Inclusion regions technique on linear model
[RD/PA-14-227] N91-31184

HELICOPTER ENGINES
Low temperature environment operation of turbo engines: A military operator's experience and requirements N91-31145
Analysis of starting problems in cold weather with ASTAZOU type turbine engines in helicopters N91-31147
Development of an anti-icing system for the T800-LHT-800 turboshaft engine N91-31160
Icing test programmes and techniques N91-31171

HELICOPTER PERFORMANCE
Low temperature environment operation of turbo engines: A military operator's experience and requirements N91-31145

HELICOPTERS
Vibration analysis of the SA349/2 helicopter
[NASA-TM-102794] N91-31078
Airborne rescue system
[NASA-CASE-ARC-11909-1] N91-31113
Flight testing in the Netherlands: An overview
[NLR-MP-88053-U] N91-31133
Static strain and vibration characteristics of a metal semimonocoque helicopter tail cone of moderate size
[NASA-CR-187576] N91-31679

HELIOSTATS
Facet development for a faceted stretched-membrane dish by Solar Kinetics, Inc.
[DE91-016866] N91-31713
Design and cost of the first commercial stretched-membrane heliostat
[DE91-016870] N91-31715

HERMES MANNED SPACEPLANE
Measurement of six component efforts in transition flow
[AAAF-NT-89-01] N91-31097

HETERODYNING
An adaptive coherent optical receiver array
[AD-A239672] N91-31644

HETEROGENEITY
The influence of fuel characteristics on heterogeneous flame propagation N91-31165
Composite materials, 2 (TEXUS 2) N91-31409
Composite materials, 2 (TEXUS 2) N91-31431

HEURISTIC METHODS
Examining the effect of information order on expert judgment
[AD-A239708] N91-31774
Application of the constrained implicants set concept to the minimization of binary functions
[AD-A239470] N91-31859
Optimal configuration of distributed database systems N91-31990

HIERARCHIES
Distributed incremental maximum finding in hierarchically divided graphs
[RUU-CS-90-30] N91-31828
The hierarchy of LR-attributed grammars
[MEMO-INF-91-26] N91-31840

HIGH ENERGY INTERACTIONS
High energy physics program. Task A: Experiment and Theory. Task B: Numerical simulation of quantum field theories
[DE91-015652] N91-31938
High energy physics
[DE91-015796] N91-31939
A research program in experimental high energy physics
[DE91-016208] N91-31941

HIGH FREQUENCIES
A parametric study of transonic blade-vortex interaction noise
[NASA-CR-188811] N91-31928

HIGH GAIN
Hydrodynamic target response to an induced spatial incoherence-smoothed laser beam
[DE91-015757] N91-31638

HIGH POWER LASERS
Innovative optoelectronic materials and structures using OMVPE
[AD-A239518] N91-31951

HIGH PRESSURE
High pressure catalytic reactions over single-crystal metal surfaces
[DE91-016475] N91-31256

HIGH SPEED
Recent advances in fiber optics components for high speed data transmission
[DE91-016252] N91-31948

HIGH SPEED CAMERAS
Photography of shock waves in explosive crystals
[DE91-015772] N91-31572
High-speed TV cameras for streak tube readout
[DE91-016081] N91-31602

HIGH STRENGTH ALLOYS
Corrosion fatigue crack arrest in aluminium alloys
[NLR-MP-88050-U] N91-31282

HIGH TEMPERATURE ENVIRONMENTS
Characterization of fire resistant GRP's by mechanical properties determination
[DREA-CR-88-421] N91-31295

HIGH TEMPERATURE GASES
Development of ceramic membranes for gas separation: FY 1990 development activities
[DE91-015915] N91-31300

HIGH TEMPERATURE RESEARCH
Effects of oxidation and combustion environments on the properties of Nicalon/SiC composites
[DE91-016778] N91-31240

HIGH TEMPERATURE SUPERCONDUCTORS
Phased array components for the High Temperature Superconducting Space Experiment (HTSSE)
[AD-A239361] N91-31535
Development of elements of a high T(sub c) superconducting cable
[AD-A239766] N91-31543
High-T(sub c) bolometers
[DE91-017009] N91-31611
Intrinsic stability and recovery analysis for tape/film type superconductors
[DE91-015568] N91-31967
Studies of non-ideal superconductors using DC magnetic methods
[DE91-015642] N91-31970
Models of flux diffusion and flux creep in high-temperature superconductors
[DE91-015838] N91-31972
Weak links within a Bi2Sr2Ca1Cu2O(x) single crystal by magnetization and direct optical observations
[DE91-016085] N91-31979
HIGH TEMPERATURE TESTS
Mechanical behavior of a nickel based alloy UDIMET 700 fabricated by powder metallurgy
[JUEL-2414] N91-31283
In situ short fatigue crack characterization of a nickel-base superalloy at ambient and elevated temperature N91-31670
HIGH VACUUM
Examination of molecular evaporation, cooling, and cluster dissociation of very thin liquid jets in a high vacuum
[MPIS-12/1990] N91-31581
HIGH VOLTAGES
International magnetic pulse compression
[DE91-015774] N91-31520
Proceedings of the International Magnetic Pulse Compression Workshop. Volume 2: Technical summary
[DE91-015775] N91-31521
HOLES (MECHANICS)
Interlaminar deformations on the cylindrical surface of a hole in laminated composites by moire interferometry
[DE91-015922] N91-31238
HOLOGRAPHY
System and method for automatically fabricating multiple memory holographic elements
[PATENT-1-253-724] N91-31600
HOMOGENEITY
Pseudohomogeneous catalyst layer model for polymer electrolyte fuel cell
[DE91-016014] N91-31710
HOMOGENEOUS TURBULENCE
The interaction of particles with homogeneous turbulence N91-31548
HOMOGENIZING
Colloid chemistry (TEXUS 17) ESA N91-31362
HOMOTOPY THEORY
Computing minimum length paths of a given homotopy class
[RUU-CS-90-37] N91-31900
HONEYCOMB STRUCTURES
Method for stabilizing thick honeycomb core composite articles
[PATENT-1-253-424] N91-31224
HOSPITALS
Developments in medical audit in hospitals in the National Health Service
[ETN-91-99984] N91-31762
HOT CORROSION
Field evaluation of six protective coatings applied to T56 turbine blades after 500 hours of engine use
[ARL-MAT-TM-405] N91-31179
HOT ISOSTATIC PRESSING
Tungsten composites (TEXUS 19) ESA N91-31445
HOT PRESSING
Processing and characterization of continuous fiber-reinforced glass and glass-ceramic matrix composites N91-31227
HOT-WIRE ANEMOMETERS
Experimental investigation of turbulent flow through a circular-to-rectangular transition duct
[NASA-TM-105210] N91-31106
HOT-WIRE FLOWMETERS
A first hot wire scanner
[AAAF-NT-89-16] N91-31188
Boundary layer turbulence appearance mechanisms studied by plane laser visualizations
[AAAF-NT-89-10] N91-31587
Use of 4-hot-wire probes to study turbulent flow
[AAAF-NT-89-15] N91-31588
HUBBLE SPACE TELESCOPE
The in-flight calibration of the Hubble space telescope attitude sensors
[NASA-CR-183485] N91-32007
HUMAN FACTORS ENGINEERING
Possibilities of simulation and optimization for guided missile systems
[MBB-UA-1201-90-PUB] N91-31183
Human factors engineering design guidelines for the software user interface
[DE91-016061] N91-31802
HUMAN PERFORMANCE
Sleep logs: Measurement of individual and operational efficiency
[AD-A239774] N91-31770
Effects of stress on judgment and decision making in dynamic tasks
[AD-A239452] N91-31772
Examining the effect of information order on expert judgment
[AD-A239708] N91-31774
Improving managers' effectiveness
[DE91-016405] N91-31988
HYBRID CIRCUITS
Adhesion of thick layer systems on ceramic based precious metals in hybrid microelectronic circuits
[MBB-UA-1191-90-PUB] N91-31304
HYDRAULIC CONTROL
A high-frequency servosystem for fuel control in hypersonic engines
[NASA-TM-104333] N91-31178
HYDRAULIC JETS
Examination of molecular evaporation, cooling, and cluster dissociation of very thin liquid jets in a high vacuum
[MPIS-12/1990] N91-31581
HYDROCARBON COMBUSTION
Energy and Technology Review, February-March l991
[DE91-015487] N91-32031
HYDROCARBON FUELS
The autoignition chemistry of paraffinic fuels and pro-knock and anti-knock additives: A detailed chemical kinetic study
[DE91-014992] N91-31314
HYDRODYNAMICS
Approximate treatment of a strong explosion and expansion in a near vacuum
[DE91-016063] N91-31574
The effects of fluid particle interactions on interfacial transfer and flow structure
[DE91-016409] N91-31575
Hydrodynamic target response to an induced spatial incoherence-smoothed laser beam
[DE91-015757] N91-31638
Hydrodynamic simulations of cosmology N91-32013
HYDROGEN
Atomic hydrogen driven halogen extraction from Si(100): Eley-Rideal surface kinetics
[AD-A239544] N91-31266
Development of ceramic membranes for gas separation: FY 1990 development activities
[DE91-015915] N91-31300
A study of a 21-cm-selected sample of galaxies N91-32014
HYDROGEN EMBRITTLEMENT
Corrosion fatigue crack arrest in aluminium alloys
[NLR-MP-88050-U] N91-31282
HYDROGEN ENGINES
Noxious matter minimization as a project criterion for aircraft
[MBB-Z-0337-90-PUB] N91-31134
Medium power hydrogen arcjet performance
[NASA-TM-104533] N91-31216
HYDROGEN IONS
Optically pumped polarized ion sources
[DE91-016086] N91-31932
HYDROGEN PLASMA
Depth profiles for hydrogen-assisted thermal donor formation in silicon
[DE91-015719] N91-31971
HYDROGEN PRODUCTION
Electrolytic hydrogen formation (TEXUS 1) N91-31347
Electrolytically generated hydrogen bubbles (TEXUS 6) N91-31348
HYDROGENATION
High pressure catalytic reactions over single-crystal metal surfaces
[DE91-016475] N91-31256
Catalyst dispersion and activity under conditions of temperature-staged liquefaction
[DE91-016602] N91-31261
Depth profiles for hydrogen-assisted thermal donor formation in silicon
[DE91-015719] N91-31971
HYDROLOGICAL CYCLE
Report of the Workshop on a CLICOM-HOMS Interface
[WCAP-16] N91-31746
HYDROPONICS
Exploring the limits of crop productivity: A model to evaluate progress N91-31776
Environmental modification of yield and food composition of cowpea and leaf lettuce N91-31777
Effects of elevated atmospheric carbon dioxide concentrations on water and acid requirements of soybeans grown in a recirculating hydroponic system N91-31781
Sweet potato for closed ecological life support systems using the nutrient film technique N91-31782
Controlled ecological life support system breadboard project, 1988 N91-31791
The crop growth research chamber: A ground-based facility for CELSS research N91-31792
HYPERPLANES
An extension of the potential method to higher-order blendings
[CS-9103] N91-31893
HYPERSONIC FLIGHT
Viscous effects
[MBB-FE202/S/PUB/441] N91-31088
HYPERSONIC FLOW
Computational analysis of hypersonic flows past elliptic-cone waveriders N91-31080
Viscous effects
[MBB-FE202/S/PUB/441] N91-31088
Measurement of six component efforts in transition flow
[AAAF-NT-89-01] N91-31097
Development of a computation code for nonequilibrium gas axisymmetric hypersonic laminar flow
[ONERA-RS-14/3637-AY] N91-31585
A relative-intensity two-color phosphor thermography system
[NASA-TM-104123] N91-31595
HYPERSONIC INLETS
A computational and experimental investigation of a three-dimensional hypersonic scramjet inlet flow field
[NASA-CR-188788] N91-31083
HYPERSONIC REENTRY
Development of a computation code for nonequilibrium gas axisymmetric hypersonic laminar flow
[ONERA-RS-14/3637-AY] N91-31585
HYPERSONIC VEHICLES
Computational analysis of hypersonic flows past elliptic-cone waveriders N91-31080
A high-frequency servosystem for fuel control in hypersonic engines
[NASA-TM-104333] N91-31178
The SAENGER concept and the German hypersonic technology program
[MBB-UK-0132-91-PUB] N91-31198
HYPERSONIC WAKES
A shock-fitting algorithm for the simulation of inviscid flows in chemical non-equilibrium
[MBB-UK-0131-90-PUB] N91-31087
HYPERSONIC WIND TUNNELS
A relative-intensity two-color phosphor thermography system
[NASA-TM-104123] N91-31595
HYPERSONICS
Computational analysis of hypersonic flows past elliptic-cone waveriders N91-31080
Aerothermodynamical project of hypersonic projectiles
[MBB-UA-1193-90-PUB] N91-31086
Model of an aerospace plane based on an idealized cone-derived waverider forebody N91-31129
HYPERSPACES
An extension of the potential method to higher-order blendings
[CS-9103] N91-31893
Covering a set of points with fixed size hypersquares and related problems
[RUU-CS-90-32] N91-31898
HYPERVELOCITY GUNS
Aerothermodynamical project of hypersonic projectiles
[MBB-UA-1193-90-PUB] N91-31086
HYPERVELOCITY IMPACT
Optimization techniques applied to passive measures for in-orbit spacecraft survivability
[NASA-CR-184198] N91-31204
HYPERVELOCITY PROJECTILES
Aerothermodynamical project of hypersonic projectiles
[MBB-UA-1193-90-PUB] N91-31086
HYPOTHERMIA
Cold-induced changes in arterial sensitivity
[AD-A239493] N91-31767
HYSTERESIS
Eccentricity effects on leakage of a brush seal at low speeds
[NASA-TM-105141] N91-31220

I

ICE
Ice ingestion experience on a small turboprop engine N91-31162
Icing research related to engine icing characteristics N91-31168
Impact of the ice phase on a mesoscale convective system: Cloud ensemble features and cloud radiative properties
[DE91-015769] N91-31749
Research in regression, information retrieval, inversion of noisy transforms, and stochastic control
[AD-A239490] N91-32001

ICE CLOUDS
Impact of the ice phase on a mesoscale convective system: Cloud ensemble features and cloud radiative properties
[DE91-015769] N91-31749

ICE FORMATION
Process for detecting the likelihood of ice formation, ice warning system for carrying out the process, and utilization thereof
[PATENT-1-250-926] N91-31107
Low Temperature Environment Operations of Turboengines (Design and User's Problems)
[AGARD-CP-480] N91-31144
Vulnerability of a small powerplant to wet snow conditions N91-31148
Ice tolerant engine inlet screens for CH113/113A search and rescue helicopters N91-31149
Engine icing criticality assessment N91-31161
Ice ingestion experience on a small turboprop engine N91-31162
Environmental icing testing at the Naval Air Propulsion Center N91-31167
Icing research related to engine icing characteristics N91-31168
Numerical model of evolution in supercooled cloud of water droplets in a case of icing N91-31169
Icing test capabilities for aircraft propulsion systems at the Arnold Engineering Development Center N91-31170
Icing test programmes and techniques N91-31171
Developments in icing test techniques for aerospace applications in the RAE Pyestock altitude test facility N91-31173

ICE PREVENTION
Low Temperature Environment Operations of Turboengines (Design and User's Problems)
[AGARD-CP-480] N91-31144
Vulnerability of a small powerplant to wet snow conditions N91-31148
Application of a water droplet trajectory prediction code to the design of inlet particle separator anti-icing systems N91-31159
Development of an anti-icing system for the T800-LHT-800 turboshaft engine N91-31160

IGNITION
The effect of fuel properties and atomization on low temperature ignition in gas turbine combustors N91-31164
The physical properties of a pyrotechnical circuit element
[MBB-UA-1192-90-PUB] N91-31317

IGNITION LIMITS
Control system design considerations for starting turbo-engines during cold weather operation N91-31155

IGNITION SYSTEMS
Cold weather ignition characteristics of advanced small gas turbine combustion systems N91-31152
Cold start investigation of an APU with annular combustor and fuel vaporizers N91-31154
Control system design considerations for starting turbo-engines during cold weather operation N91-31155
Cold start development of modern small gas turbine engines at Pratt and Whitney Aircraft of Canada Ltd. N91-31156

IMAGE ANALYSIS
The development of a specific image analysis technique for exploiting flow visualization negatives
[AAAF-NT-89-26] N91-31593
Stereophotogrammetric surveying and interpreting method, and interpreting apparatus
[PATENT-1-254-651] N91-31693

IMAGE PROCESSING
Abstracts of papers presented at the First Los Alamos Symposium on Ultra-Wideband Radar
[DE91-015976] N91-31491
Flow visualization and simulation
[AAAF-NT-89-18] N91-31590
System and method for automatically fabricating multiple memory holographic elements
[PATENT-1-253-724] N91-31600
Automatic analysis of visualization negatives
[ETN-91-99971] N91-31603
ULDA user's guide
[NASA-TM-105074] N91-31813
Application of an acquisition image processing system to the quantitative analysis of flows
[AAAF-NT-89-27] N91-31851
Application of digital compression techniques to optical surveillance systems
[DE91-016404] N91-31854
A graph theoretic approach to scene matching
[NASA-CR-187817] N91-31947
Multitarget tracking using optical processing
[AD-A239656] N91-31953

IMAGE RESOLUTION
Design and analysis of multilayer x ray/XUV microscope
[NASA-CR-184197] N91-31607

IMAGERY
Parametric study of diffusion-enhancement networks for spatiotemporal grouping in real-time artificial vision
[AD-A239674] N91-31954

IMAGES
System and method for automatically fabricating multiple memory holographic elements
[PATENT-1-253-724] N91-31600
A scientific visualization synthesizer
[DE91-012877] N91-31815

IMAGING SPECTROMETERS
Scanning imaging absorption spectrometer for atmospheric chartography N91-31725

IMAGING TECHNIQUES
Choice representation modes and color palettes
[AAAF-NT-89-17] N91-31589
High-speed TV cameras for streak tube readout
[DE91-016081] N91-31602
Sensitivity of imaging materials to electron beam irradiation
[AD-A239365] N91-31612
Laser Velocimetry, volume 1
[VKI-1991-05-VOL-1] N91-31614
Laser Velocimetry, volume 2
[VKI-1991-05-VOL-2] N91-31625
Particle image velocimetry: Photographic and video techniques N91-31628
Unsteady flow past an airfoil pitching at a constant rate N91-31629
Nuclear medicine and imaging research: Quantitative studies in radiopharmaceutical science
[DE91-015447] N91-31759
Boron in nuclear medicine: New synthetic approaches to PET, SPECT, and BNCT agents
[DE91-016488] N91-31764

IMMUNE SYSTEMS
Electron microscopy to correlate cell structures and biochemical activity
[AD-A239640] N91-31758

IMPACT TESTS
Optimization techniques applied to passive measures for in-orbit spacecraft survivability
[NASA-CR-184198] N91-31204
Dynamic yield strength of a palladium alloy metallic glass
[DE91-015111] N91-31298

IMPEDANCE
Robust impedance control of robot manipulators N91-31297

IMPLOSIONS
Hydrodynamic target response to an induced spatial incoherence-smoothed laser beam
[DE91-015757] N91-31638
Pressure-strain-temperature relationship in shock loaded cylindrical samples of 304 stainless steel
[DE91-013379] N91-31673
Advanced concepts theory
[AD-A239780] N91-31959

IMPURITIES
An expert system for the identification of silicon impurities using FTIR spectroscopy
[AD-A236504] N91-31246

IN-FLIGHT MONITORING
Climatic considerations in the life cycle management of the CF-18 engine N91-31158

INCLUSIONS
Alloys with oxide inclusions (TEXUS 2) N91-31432

INCOHERENCE
Hydrodynamic target response to an induced spatial incoherence-smoothed laser beam
[DE91-015757] N91-31638

INCOMPRESSIBLE FLOW
Experimental investigation of turbulent flow through a circular-to-rectangular transition duct
[NASA-TM-105210] N91-31106
The interaction of particles with homogeneous turbulence N91-31548
A dynamically adaptive multigrid algorithm for the incompressible Navier-Stokes equations: Validation and model problems
[NASA-CR-187595] N91-31888
Least-squares solution of incompressible Navier-Stokes equations with the p-version of finite elements
[NASA-TM-105203] N91-31911

INDEPENDENT VARIABLES
On the optimal use of fictitious time in variation of parameters methods with application to BG14
[NASA-CR-185650] N91-31890

INDEXES (DOCUMENTATION)
Aerospace medicine and biology: A continuing bibliography with indexes (supplement 353)
[NASA-SP-7011(353)] N91-31760

INDICATING INSTRUMENTS
Process for detecting the likelihood of ice formation, ice warning system for carrying out the process, and utilization thereof
[PATENT-1-250-926] N91-31107

INDIUM ALLOYS
Directional solidification of eutectics InSb-NiSb (TEXUS 10) N91-31405

INDIUM ARSENIDES
Innovative optoelectronic materials and structures using OMVPE
[AD-A239518] N91-31951
Studies of the III-V compounds in the megabar regime
[DE91-015911] N91-31973

INDIUM GALLIUM ARSENIDES
Rapid thermal annealing effects in In(x)Ga(1-x)As/GaAs strained-layer superlattices
[DE91-015901] N91-31978

INDIUM PHOSPHATES
Vapour growth of an InP crystal (TEXUS 20) N91-31394
Contribution to the implementation of a completely in situ device in ultrahigh vacuum for the development of MIS on InP structures: Al2O3/InP interface optimization
[ECL-91-04] N91-31526

INDIUM PHOSPHIDES
Advanced power systems for EOS
[NASA-TM-105222] N91-31217
Innovative optoelectronic materials and structures using OMVPE
[AD-A239518] N91-31951

INDUCTANCE
Phased array components for the High Temperature Superconducting Space Experiment (HTSSE)
[AD-A239361] N91-31535

INDUCTION MOTORS
The analysis and design of brushless DC motors N91-31516

INDUSTRIAL WASTES
A review of accelerated response actions available to the environmental restoration program: Selected case histories and associated issues
[DE91-013608] N91-31716

INDUSTRIES
Production of organic chemicals via bioconversion: A review of the potential
[DE91-015524] N91-31223
Survey to assess the usefulness of two model agreements for university-industry cooperative research
[DE91-013937] N91-31985
What is the Federal Demonstration Project?
[DE91-013936] N91-31986
Some applications of X-ray photoelectron spectroscopy and secondary-ion mass spectroscopy N91-32029

INERTIAL NAVIGATION
Large scale CAESAR images using inertial navigation and pressure altitude measurement. Accuracy deformations and possibilities for a Global Positioning System (GPS)
[ETN-91-99418] N91-31117

INFERENCE
Inference networks for document retrieval N91-31993

INFILTRATION
Processing and characterization of continuous fiber-reinforced glass and glass-ceramic matrix composites N91-31227

INFORMATION
A study of the logistics function within a medium sized, sales oriented chemical company
[ETN-91-99983] N91-31987

INFORMATION DISSEMINATION
Information security: Past, present and future
[FEL-91-B100] N91-31873
The relationship between the use of US government technical reports by US aerospace engineers and scientists and selected institutional and sociametric variables N91-31989

INFORMATION MANAGEMENT
Hypertext development using a model-based approach
[REPT-90-074] N91-31995
INFORMATION PROCESSING (BIOLOGY)
Quick development microcomputer system: Training automatic components for electronic troubleshooting
[AD-A239573] N91-31542
Examining the effect of information order on expert judgment
[AD-A239708] N91-31774
INFORMATION RETRIEVAL
Cluster-based adaptive information retrieval
N91-31991
Interactive retrieval in information spaces distributed across a wide-area network N91-31992
Inference networks for document retrieval
N91-31993
Research in regression, information retrieval, inversion of noisy transforms, and stochastic control
[AD-A239490] N91-32001
INFORMATION SYSTEMS
Developments in medical audit in hospitals in the National Health Service
[ETN-91-99984] N91-31762
OSI-security and relations with other security standards
[FEL-91-B099] N91-31872
Information security: Past, present and future
[FEL-91-B100] N91-31873
A study of the logistics function within a medium sized, sales oriented chemical company
[ETN-91-99983] N91-31987
Inference networks for document retrieval
N91-31993
Formalisation of techniques: Chopping down the methodology jungle
[TR-90-26] N91-31996
Continuous informations systems
[RUU-CS-90-25] N91-31997
INFORMATION THEORY
The relationship between the use of US government technical reports by US aerospace engineers and scientists and selected institutional and sociametric variables
N91-31989
INFRARED ABSORPTION
Depth profiles for hydrogen-assisted thermal donor formation in silicon
[DE91-015719] N91-31971
INFRARED IMAGERY
Development of an infrared Laser Fourier Densitometer (LFD) and first wind tunnel tests
[PMI-2335] N91-31189
INFRARED LASERS
Development of an infrared Laser Fourier Densitometer (LFD) and first wind tunnel tests
[PMI-2335] N91-31189
INFRARED SOURCES (ASTRONOMY)
UKIRT observer's manual
[ETN-91-99747] N91-32008
A survey of the 158 micron CII fine-structure line in the central 50 pc of the galaxy
[NASA-CR-188912] N91-32009
INFRARED SPECTRA
An expert system for the identification of silicon impurities using FTIR spectroscopy
[AD-A236504] N91-31246
High-T(sub c) bolometers
[DE91-017009] N91-31611
Hyperspectral signatures (400 to 2500 nm) of vegetation, minerals, soils, rocks, and cultural features: Laboratory and field measurements
[AD-A239496] N91-31697
A survey of the 158 micron CII fine-structure line in the central 50 pc of the galaxy
[NASA-CR-188912] N91-32009
INFRARED SPECTROSCOPY
An expert system for the identification of silicon impurities using FTIR spectroscopy
[AD-A236504] N91-31246
Tunable far infrared studies of molecular parameters in support of stratospheric measurements
[NASA-CR-188774] N91-31723
INFRARED TELESCOPES
UKIRT observer's manual
[ETN-91-99747] N91-32008
INGESTION (ENGINES)
Ice ingestion experience on a small turboprop engine
N91-31162
INGOTS
Composite ingot casting
[PATENT-1-250-128] N91-31269
INJECTION
Icing test capabilities for aircraft propulsion systems at the Arnold Engineering Development Center
N91-31170
INJECTORS
Flow induced vibrations in the SSME injector heads
[NASA-CR-184209] N91-31214
INLET AIRFRAME CONFIGURATIONS
Inlet edge funnel of a civil aircraft gondola engine
[ETN-91-99775] N91-31130
INLET FLOW
A computational and experimental investigation of a three-dimensional hypersonic scramjet inlet flow field
[NASA-CR-188788] N91-31083
INLET NOZZLES
Model of an aerospace plane based on an idealized cone-derived waverider forebody N91-31129
INSPECTION
The development of an intelligent dimensional inspection environment using coordinate measuring machines
N91-31661
INSULIN
The effect of exercise training on skeletal muscle glucose transorter isoform GLUT4 concentration in the obese Zucker rat
[AD-A239461] N91-31757
INTEGERS
An integer programming model for Navy's maritime patrol aviation fleet
[AD-A239464] N91-31079
INTEGRAL EQUATIONS
Electromagnetic penetration of slot apertures with depth and losses
[DE91-016401] N91-31500
A boundary integral equation method for steady two-dimensional flow in partially saturated media
[DE91-016056] N91-31573
INTEGRATED CIRCUITS
Reconfigurable parameter filter
[PATENT-1-264-072] N91-31513
Hardware modeling and top-down design using VHDL
[AD-A239356] N91-31534
Joint Services Electronics Program
[AD-A239459] N91-31536
INTEGRATED OPTICS
Micromechanical concepts in optics and optoelectronics
[MBB-Z-0339-90-PUB] N91-31949
INTERACTIONAL AERODYNAMICS
Airfoil-vortex interaction: Unsteady wall pressure measurement
[AAAF-NT-89-13] N91-31104
A three-dimensional viscous flow model of stator/rotor interaction in turbomachines N91-31547
Modeling and simulation of multiple cooperating manipulators on a mobile platform N91-31647
INTERATOMIC FORCES
Model description of transition metals using the rotated second moment approximation
[DE91-016043] N91-31287
INTERFACES
Refining interfaces of communicating systems
[MEMO-INF-91-19] N91-31493
INTERFACIAL ENERGY
Interfacial systems for photochemical energy conversion
[DE91-015743] N91-31700
INTERFACIAL TENSION
Interfacial convection (TEXUS 1) N91-31327
Interfacial convection (TEXUS 2) N91-31328
Diffusion-induced interfacial convection (TEXUS 8)
N91-31331
Influence of a surface tension minimum on the Marangoni effect (TEXUS 8) ESA N91-31338
Influence of a surface tension minimum on the Marangoni effect (TEXUS 9) ESA N91-31339
Influence of a surface tension minimum on the Marangoni effect (TEXUS 19) ESA N91-31340
Thermocapillary drop motion, 1 (MASER 1) ESA
N91-31345
Thermocapillary drop motion, 2 (MASER 2) ESA
N91-31346
Composite materials, 1 (TEXUS 1) N91-31408
Directional solidification of immiscible alloys Zn-Pb (MASER 2) N91-31421
INTERMETALLICS
Rapidly solidified nickel aluminide of improved stoichiometry and ductilization
[PATENT-1-257-987] N91-31270
Method for imparting strength to intermetallic phases
[PATENT-1-255-929] N91-31271
Fundamental studies in the manganese-bismuth system (TEXUS 2) N91-31414
INTERMITTENCY
Intermittent polarization (TEXUS 2) N91-31349
Spatiotemporal intermittency N91-31569
INTERMODULATION
Chemical reduction of intermodulation interference caused by metal-oxide-metal junctions aboard ship
[AD-A239530] N91-31265
INTERMOLECULAR FORCES
Fifth force experiments N91-31733
INTERNAL COMBUSTION ENGINES
The autoignition chemistry of paraffinic fuels and pro-knock and anti-knock additives: A detailed chemical kinetic study
[DE91-014992] N91-31314
INTERNATIONAL COOPERATION
Activities report of the Institute of Extraterrestrial Physics
[MPE-223] N91-32002
INTRUSION
Intrusion and fault tolerance compatibility. Part 1: Fault protection, coding and tolerance state of the art
[LAAS-89-395] N91-31662
INVARIANCE
A new form of second-moment closure N91-31560
INVENTIONS
Single layer multi-color luminescent display
[NASA-CASE-LAR-13616-1] N91-31950
INVENTORIES
An integer programming model for Navy's maritime patrol aviation fleet
[AD-A239464] N91-31079
Inventory and functional prototypes of neural networks
[TR-90-15] N91-31880
INVERSIONS
Dynamic disturbance decoupling for discrete-time nonlinear systems
[MEMO-913] N91-31843
INVISCID FLOW
Calculating the flow in a turbomachine with Clebsch variables and a finite element method
[ETN-91-99918] N91-31180
Prediction of rotor surface unsteady pressure and heat transfer from wake passing N91-31549
The development of a specific image analysis technique for exploiting flow visualization negatives
[AAAF-NT-89-26] N91-31593
Automatic analysis of visualization negatives
[ETN-91-99971] N91-31603
ION ACCELERATORS
A study of ion acceleration at rocket altitudes and development and calibration of pitch angle imaging charged particle detectors N91-31728
ION BEAMS
A multifunction ion-irradiation/surface modification ultrahigh vacuum chamber system
[DE91-016819] N91-31190
Ion beam enhanced adhesion of iron films to sapphire substrates
[DE91-015931] N91-31308
Acceleration using total internal reflection
[DE91-016612] N91-31942
Plasma-optics systems for the formation and focusing of ion beams N91-31956
ION DISTRIBUTION
A study of ion acceleration at rocket altitudes and development and calibration of pitch angle imaging charged particle detectors N91-31728
ION ENGINES
Laser interferometric measurement of ion electrode shape and charge exchange erosion
[NASA-TM-105165] N91-31605
ION EXCHANGE RESINS
Water transport properties of fuel cell ionomers
[DE91-016015] N91-31259
ION EXCHANGING
Special refractive index profiles in glasses obtained by ion exchange (TEXUS 19) ESA N91-31369
ION IMPLANTATION
Dual ion implantation effects on fatigue properties of Fe-13Cr-15Ni alloys
[DE91-015930] N91-31286
Defect diffusion in ion implanted glasses
[DE91-016119] N91-31302
Ion-implantation induced crystallization of glass
[DE91-016121] N91-31303
Ion beam enhanced adhesion of iron films to sapphire substrates
[DE91-015931] N91-31308
ION IRRADIATION
A multifunction ion-irradiation/surface modification ultrahigh vacuum chamber system
[DE91-016819] N91-31190
ION SOURCES
A study of ion acceleration at rocket altitudes and development and calibration of pitch angle imaging charged particle detectors N91-31728
Optically pumped polarized ion sources
[DE91-016086] N91-31932
IONIC MOBILITY
Ionic solutions near the critical point of water (TEXUS 10) ESA N91-31375
Ionic solutions near the critical point of water (TEXUS 12) ESA N91-31376

IONIZATION COEFFICIENTS
Effective ionization coefficients, electron drift velocities, and limiting breakdown fields for gas mixtures of possible interest to particle detectors
[DE91-015921] N91-31532
IONIZED GASES
Approximate treatment of a strong explosion and expansion in a near vacuum
[DE91-016063] N91-31574
IONOSPHERIC PROPAGATION
Integration losses and clutter-Doppler spread for a space based radar caused by ionospheric scintillation during a solar maximum
[AD-A239534] N91-31502
IRON
Ion beam enhanced adhesion of iron films to sapphire substrates
[DE91-015931] N91-31308
Sulphur diffusion in liquid cast iron (TEXUS 6) ESA N91-31370
Tungsten composites (TEXUS 19) ESA N91-31445
Manufacture of iron foam (TEXUS 7) N91-31450
IRON ALLOYS
Weldability and hot ductility of iron aluminides
[DE91-016343] N91-31280
Dual ion implantation effects on fatigue properties of Fe-13Cr-15Ni alloys
[DE91-015930] N91-31286
Tungsten composites (TEXUS 10) N91-31444
IRRADIANCE
Preparatory space experiments for development of a CELSS N91-31796
IRRADIATION
Electron-beam-pinch experiment at Harry Diamond Laboratories: Providing for a high-dose-rate flash x ray facility for Transient Radiation Effects on Electronics (TREE) testing of pieceparts
[AD-A239558] N91-31193
Formation of defect structures in metals during irradiation
[DE91-015548] N91-31278
Sensitivity of imaging materials to electron beam irradiation
[AD-A239365] N91-31612
ISCHEMIA
The G-LOC syndrome
[AD-A239561] N91-31768
ISOCHORIC PROCESSES
Phase transition (TEXUS 8) N91-31374
ISOMORPHISM
The linear decomposition of delta-squared models
[RUU-CS-91-04] N91-31902
ISOTOPES
Boron in nuclear medicine: New synthetic approaches to PET, SPECT, and BNCT agents
[DE91-016488] N91-31764
ISOTROPIC TURBULENCE
The interaction of particles with homogeneous turbulence N91-31548
Spectral large-eddy simulation of isotropic and stably-stratified turbulences N91-31567
ITERATION
Practical aspects of an interior-point method for convex programming
[AD-A239457] N91-31858
IUE
ULDA user's guide
[NASA-TM-105074] N91-31813
Research studies with the International Ultraviolet Explorer
[NASA-CR-183495] N91-32012

J

J INTEGRAL
An equivalent domain integral method for three-dimensional mixed-mode fracture problems
[NASA-CR-182021] N91-31692
JAMMERS
Electronic warfare: Faulty test equipment impairs Navy readiness
[AD-A239562] N91-31506
JET ENGINE FUELS
The development of a computational model to predict low temperature fuel flow phenomena N91-31166
Jet-A reaction mechanism study for combustion application
[NASA-TM-104441] N91-31181
JET ENGINES
Cold start optimization on a military jet engine N91-31151
Cold weather jet engine starting strategies made possible by engine digital control systems N91-31153
Removable slider shoe for a translating sleeve used on a jet engine cowl and duct
[PATENT-1-247-868] N91-31177
JET FLAPS
Segmented vectoring cruise nozzles
[CA-PATENT-APPL-SN-2-009-635] N91-31175
JET FLOW
Vortex interactions in the transition region of a rectangular jet N91-31630
Adjustment of the mixing-rate constant in the eddy break-up model for a jet flame N91-32030
JET MIXING FLOW
Use of 4-hot-wire probes to study turbulent flow
[AAAF-NT-89-15] N91-31588
JOINTS (JUNCTIONS)
Torsion resistant grooved joint
[PATENT-1-258-589] N91-31127
Influence of adhesive polymerization conditions on the durability of adhesive joints
[DCR/I-03357-90] N91-31305
A finite element approach for the dynamic analysis of joint-dominated structures
[NASA-CR-4402] N91-31686
JOSEPHSON JUNCTIONS
Phased array components for the High Temperature Superconducting Space Experiment (HTSSE)
[AD-A239361] N91-31535
Macroscopic quantum tunneling in Josephson tunnel junctions and Coulomb blockade in single small tunnel junctions
[DE91-016258] N91-31974
JP-4 JET FUEL
The influence of fuel characteristics on heterogeneous flame propagation N91-31165
JUDGMENTS
Effects of stress on judgment and decision making in dynamic tasks
[AD-A239452] N91-31772
Examining the effect of information order on expert judgment
[AD-A239708] N91-31774

K

K-EPSILON TURBULENCE MODEL
Two-equation models for high-Reynolds-number flow N91-31553
Examples of turbulence model applications N91-31563
A critical comparison of two-equation turbulence models
[NASA-TM-105237] N91-31597
KEVLAR (TRADEMARK)
The mechanical response of woven Kevlar fabric
[DE91-010581] N91-31230
KINEMATIC EQUATIONS
Kinematics of the six-degree-of-freedom force-reflecting Kraft Master
[NASA-TM-104124] N91-31879
KINEMATICS
Kinematics of the six-degree-of-freedom force-reflecting Kraft Master
[NASA-TM-104124] N91-31879
KINETIC ENERGY
A simple model for the motion of pulsed-laser-driven thin flyers
[DE91-011325] N91-31634
KINETICS
Atomic hydrogen driven halogen extraction from Si(100): Eley-Rideal surface kinetics
[AD-A239544] N91-31266
KNOWLEDGE
Optimizing the long-term retention of skills: Structural and analytic approaches to skill maintenance 3
[AD-A239574] N91-31773
KNOWLEDGE BASES (ARTIFICIAL INTELLIGENCE)
Interactive constraint-based solid modeling as a design tool
[AD-A239358] N91-31856
A knowledge based application of the extended aircraft interrogation and display system
[NASA-TM-4327] N91-31874
Hypertext development using a model-based approach
[REPT-90-074] N91-31995
KNOWLEDGE REPRESENTATION
Open architecture for formal reasoning
[AD-A239395] N91-31857
Investigation into the applicability of knowledge engineering
[NLR-TP-89031-U] N91-31878
KNUDSEN FLOW
Development of ceramic membranes for gas separation: FY 1990 development activities
[DE91-015915] N91-31300
KUWAIT
Global model simulations of the long range transport of soot and sulfur from the Kuwait oil fires
[DE91-015771] N91-31719

L

LABORATORIES
Improving managers' effectiveness
[DE91-016405] N91-31988
LABYRINTH SEALS
Eccentricity effects on leakage of a brush seal at low speeds
[NASA-TM-105141] N91-31220
LAMELLA (METALLURGY)
Preparation of aluminium foams (TEXUS 9) N91-31452
LAMINAR BOUNDARY LAYER
User's manual for the Langley boundary layer noise propagation program (MRS-BLP)
[NASA-CR-187559] N91-31923
LAMINAR FLOW
Development of a computation code for nonequilibrium gas axisymmetric hypersonic laminar flow
[ONERA-RS-14/3637-AY] N91-31585
Method and apparatus for detecting laminar flow separation and reattachment
[NASA-CASE-LAR-13952-2-SB] N91-31596
LAMINATES
An analytical prediction of matrix cracking in fibrous composite laminates N91-31225
An investigation into the effects of damage on the stresses in a composite laminate N91-31226
Relation between fiber proportion and mechanical characteristics of carbon-resin composites
[RE-50-345/F] N91-31231
Composite materials damage. Transverse cracking and delamination
[ONERA-RT-6/7256-RY-080-R] N91-31234
Experimental and analytical analysis of stress-strain behavior in a (90/0 deg)2s, SiC/Ti-15-3 laminate
[NASA-TM-104470] N91-31235
Interlaminar deformations on the cylindrical surface of a hole in laminated composites by moire interferometry
[DE91-015922] N91-31238
Mechanical characterization of seismic base isolation elastomers
[DE91-015680] N91-31299
Adhesion of thick layer systems on ceramic based precious metals in hybrid microelectronic circuits
[MBB-UA-1191-90-PUB] N91-31304
Nonlinear probabilistic finite element modeling of composite shells N91-31668
LARGE SPACE STRUCTURES
Advanced power systems for EOS
[NASA-TM-105222] N91-31217
Integrated control of thermally distorted large space antennas N91-31487
Advanced optical sensing and processing technologies for the distributed control of large flexible spacecraft
[NASA-CR-4399] N91-31609
The control of flexible structure vibrations using a cantilevered adaptive truss N91-31671
Large Angle Transient Dynamics (LATDYN) demonstration problem manual
[NASA-CR-4400] N91-31684
LASER APPLICATIONS
Laser Fourier densitometry and laser induced photochemical anemometry in supersonic flow
[AAAF-NT-89-09] N91-31103
Development of an infrared Laser Fourier Densitometer (LFD) and first wind tunnel tests
[PMI-2335] N91-31189
Boundary layer turbulence appearance mechanisms studied by plane laser visualizations
[AAAF-NT-89-10] N91-31587
Laser interferometric measurement of ion electrode shape and charge exchange erosion
[NASA-TM-105165] N91-31605
Real time actuating of laser power and scanning velocity for thermal regulation during laser hardening
[ETN-91-99908] N91-31636
Compact free-electron laser at the Los Alamos National Laboratory
[DE91-016079] N91-31640
Laser ablation mechanisms and optical surface damage
[DE91-016928] N91-31642
Energy and Technology Review, February-March 1991
[DE91-015487] N91-32031
LASER BEAMS
Laser transit velocimetry N91-31623
Hydrodynamic target response to an induced spatial incoherence-smoothed laser beam
[DE91-015757] N91-31638

Compact free-electron laser at the Los Alamos National Laboratory
[DE91-016079] N91-31640
Optically pumped polarized ion sources
[DE91-016086] N91-31932

LASER DOPPLER VELOCIMETERS
Exploitation of OAT15A profile tests in the T2 wind tunnel: Experimental determination of the wave drag
[ONERA-RSF-88/1685-AY-158-A] N91-31092
Laser velocimetry at the CEAT aerodynamic group: Application to unsteady measurements on a fluid flap profile
[AAAF-NT-89-05] N91-31100
Low level turbulence detection by a laser velocimetry technique: Application to transonic flows
[AAAF-NT-89-07] N91-31101
HVOF: Particle, flame diagnostics, and coating characteristics
[DE91-014654] N91-31248
Laser Doppler velocimeter measurements of the streamwise velocity component in the viscous sublayer of a turbulent channel flow
[MPIS-MITT-97] N91-31582
Laser Velocimetry, volume 1
[VKI-1991-05-VOL-1] N91-31614
Introduction to laser velocimeter techniques N91-31615
Basic LDV1 component system N91-31616
Fundamentals of signal processing N91-31617
Generation of particles and seeding N91-31618
Advanced systems: Multicomponent LDV N91-31619
Signal processing: Time domain and frequency domain N91-31620
Biasing errors and corrections N91-31621
Accuracy of laser velocimetry N91-31622
Laser transit velocimetry N91-31623
Laser transit velocimetry: Recent publications N91-31624
Laser Velocimetry, volume 2
[VKI-1991-05-VOL-2] N91-31625
Advanced and non-conventional optical schemes N91-31626
Quasi-elastic light scattering and applications to optical sizing N91-31627
Particle image velocimetry: Photographic and video techniques N91-31628
Unsteady flow past an airfoil pitching at a constant rate N91-31629
Vortex interactions in the transition region of a rectangular jet N91-31630
Review of typical applications. Part 1: Measurements in liquid flows, free jets, combustion, and in the atmosphere N91-31631
Review of typical applications: Wind tunnels N91-31632
Post-processing of data N91-31633
Laser Doppler anemometer miniaturized with diode laser
[AAAF-NT-89-06] N91-31637

LASER INTERFEROMETRY
Laser interferometric measurement of ion electrode shape and charge exchange erosion
[NASA-TM-105165] N91-31605

LASER MATERIALS
Laser deposition of cubic boron nitride on electronic materials
[AD-A238313] N91-31249

LASER MODES
The microcrystal laser: A first step on the way to a laser microsystem
[MBB-Z-0336-90-PUB] N91-31635

LASER OUTPUTS
Advanced and non-conventional optical schemes N91-31626
Quasi-elastic light scattering and applications to optical sizing N91-31627

LASER PUMPING
Optically pumped polarized ion sources
[DE91-016086] N91-31932

LASER SPECTROSCOPY
Chemical characterization of aerosol particles by Raman spectroscopy
[DE91-015836] N91-31720

LASER TARGETS
A simple model for the motion of pulsed-laser-driven thin flyers
[DE91-011325] N91-31634
Hydrodynamic target response to an induced spatial incoherence-smoothed laser beam
[DE91-015757] N91-31638

LASER WELDING
BES welding science
[DE91-015625] N91-31651
Microwave module YAG laser weld development
[DE91-015750] N91-31652

LASERS
Laser deposition of cubic boron nitride on electronic materials
[AD-A238313] N91-31249
International magnetic pulse compression
[DE91-015774] N91-31520
The microcrystal laser: A first step on the way to a laser microsystem
[MBB-Z-0336-90-PUB] N91-31635
Application of multivariable control system design methodologies to robust beam control of a space-based laser
[AD-A239460] N91-31643

LASING
Electronic transport and lasing in microstructures
[DE91-016751] N91-31641

LATTICES (MATHEMATICS)
Some order dimension bounds for communication complexity problems
[MEMO-938] N91-31489
Linear logic, domain theory, and semi-functors
[RUU-CS-90-34] N91-31830

LAUE METHOD
A new method to do time resolved, x ray diffraction studies: The rotating crystal Laue method
[DE91-016527] N91-31935

LAUNCH VEHICLES
Range reference atmosphere, Fairbanks, Alaska
[AD-A239520] N91-31739

LAUNCHERS
Calculation of fragment ejection velocities on explosion of a launcher
[CNES-NT-128] N91-31195

LAUNCHING SITES
Range reference atmosphere Wake Island, North Pacific
[AD-A239602] N91-31740
Range reference atmosphere Shemya, Alaska
[AD-A239603] N91-31741
Range reference atmosphere: Thule, Greenland
[AD-A239659] N91-31742

LAY-UP
Method for stabilizing thick honeycomb core composite articles
[PATENT-1-253-424] N91-31224

LEACHING
Defect diffusion in ion implanted glasses
[DE91-016119] N91-31302

LEAD (METAL)
Determination of aqueous processable photoresist in tin-lead plating solutions
[DE91-015575] N91-31251

LEAD ACID BATTERIES
Techniques to assess the state of health of sealed lead acid batteries
[CTN-91-60214] N91-31515

LEAD ALLOYS
Al-Pb bearing alloy (TEXUS 1) N91-31413
Unidirectional solidification of immiscible alloys (TEXUS 5) N91-31418
Directional solidification of immiscible alloys Zn-Pb (MASER 2) N91-31421
Immiscible alloy system Al-Pb (TEXUS 7) N91-31422
Acoustic mixing (TEXUS 5) N91-31423
Solidification of immiscible alloys (TEXUS 8) N91-31424

LEAD COMPOUNDS
Solutal diffusion measurements in liquid PbSnTe under microgravity (TEXUS 19) N91-31372

LEADING EDGES
Compressible two dimensional boundary layer strong perfect fluid coupling in the case of sharp leading edge profiles. Stationary case
[ONERA-RT-42/1621-RY-093-R] N91-31586

LEAF AREA INDEX
Exploring the limits of crop productivity: A model to evaluate progress N91-31776

LEAKAGE
Eccentricity effects on leakage of a brush seal at low speeds
[NASA-TM-105141] N91-31220

LEAST SQUARES METHOD
Artificial diffusion methods in convection dominated flows
[W-9016] N91-31577
Least-squares solution of incompressible Navier-Stokes equations with the p-version of finite elements
[NASA-TM-105203] N91-31911

LEAVES
Effects of atmospheric CO2 on photosynthetic characteristics of soybean leaves N91-31780

LENGTH
Transition length determination in the F1 wind tunnel, test report
[ONERA-PV-1/8571-GY] N91-31089

LENSES
Plasma-optics systems for the formation and focusing of ion beams N91-31956

LEVITATION MELTING
Acoustic positioning of a molten alloy sample (TEXUS 1) N91-31464
Acoustic positioning (TEXUS 9) ESA N91-31465
Containerless solidification of a Pd-Cu-Si sample (TEXUS 9) ESA N91-31466
Acoustic positioning (TEXUS 14b) ESA N91-31467
Containerless undercooling of a Pd-Cu-Si alloy (TEXUS 14b) ESA N91-31468
Electrostatic positioning for containerless processing of a Li-silicate glass (TEXUS 10) ESA N91-31469

LIAPUNOV FUNCTIONS
On the stability of saturated state feedback regulators
[LAAS-91047] N91-31524

LIFE (DURABILITY)
Climatic considerations in the life cycle management of the CF-18 engine N91-31158
Nickel-hydrogen cell low-Earth life test update
[NASA-TM-105229] N91-31708

LIFE SUPPORT SYSTEMS
Effects of atmospheric CO2 on photosynthetic characteristics of soybean leaves N91-31780
The crop growth research chamber: A ground-based facility for CELSS research N91-31792
Transpiration during life cycle in controlled wheat growth N91-31795
Method and apparatus for bio-regenerative life support system
[NASA-CASE-MSC-21629-1] N91-31803

LIGANDS
Chemically modified electrodes and related solution studies
[DE91-016740] N91-31262

LIGHT EMISSION
Introduction to laser velocimeter techniques N91-31615
Advanced and non-conventional optical schemes N91-31626

LIGHT MODULATION
Dynamics of 1.3 micron semiconductor lasers and nonlinear gain N91-31613

LIGHT SCATTERING
Generation of particles and seeding N91-31618
Quasi-elastic light scattering and applications to optical sizing N91-31627
Retrieval and molecule sensitivity studies for the global ozone monitoring experiment and the scanning imaging absorption spectrometer for atmospheric chartography N91-31724
Scanning imaging absorption spectrometer for atmospheric chartography N91-31725

LIGHT SOURCES
Review of vacuum systems for x ray lithography light sources
[DE91-017008] N91-31982

LIGHTNING
Study of lightning strikes on an aircraft in flight. Electromagnetic measurements
[ONERA-RF-25/7234-PY] N91-31111
Study of lightning strikes on an aircraft in flight. Electric measurements
[ONERA-RF-98/7154-PY] N91-31112

LIKELIHOOD RATIO
Convergence performance of adaptive detectors, part 2
[AD-A239532] N91-31540

LIMITS (MATHEMATICS)
Strong approximation on log dense sets
[W-9101] N91-31916

LINE SPECTRA
A spectrophotometric study of the secondaries of Algol systems N91-32005
A survey of the 158 micron CII fine-structure line in the central 50 pc of the galaxy
[NASA-CR-188912] N91-32009
Abundances from solar flare line spectroscopy
[NASA-CR-183492] N91-32022

LINEAR ACCELERATORS
Proceedings of the International Magnetic Pulse Compression Workshop. Volume 2: Technical summary
[DE91-015775] N91-31521

LINEAR EQUATIONS
An extension of the potential method to higher-order blendings
[CS-9103] N91-31893

LINEAR OPERATORS
Linear logic, domain theory, and semi-functors
[RUU-CS-90-34] N91-31830

LINEAR SYSTEMS
Heaviside's linearised gravitational theory N91-31737

LINEAR TRANSFORMATIONS
The linear decomposition of delta-squared models
[RUU-CS-91-04] N91-31902

LINES (GEOMETRY)
Longest segment problems
[RUU-CS-90-28] N91-31896
LIPIDS
Cyanobacteria in CELSS: Growth strategies for nutritional variation and nitrogen cycling N91-31786
LIQUID CHROMATOGRAPHY
Determination of aqueous processable photoresist in tin-lead plating solutions
[DE91-015575] N91-31251
LIQUID CRYSTALS
Field 3, theme 1: Structural materials. Post 2: Thermotropic liquid crystal polymers
[ETN-91-99982] N91-31306
LIQUID HYDROGEN
Hydrogen test of a small, low specific speed centrifugal pump stage
[NASA-CR-187117] N91-31213
LIQUID METAL FAST BREEDER REACTORS
Progress in the SP-100 FSQ reactor development
[DE91-016033] N91-31940
LIQUID METALS
Meniscus stability in immiscible metals (MASER 1) N91-31428
LIQUID OXYGEN
Flow induced vibrations in the SSME injector heads
[NASA-CR-184209] N91-31214
LIQUID PHASE SINTERING
Effects of trapped gases on ceramic-filled-glass composite densification
[DE91-015850] N91-31237
Liquid phase sintering (TEXUS 8) N91-31443
LIQUID PHASES
Composite materials, 1 (TEXUS 1) N91-31408
Composite materials, 2 (TEXUS 2) N91-31409
Immiscibles, 1 (TEXUS 3) N91-31410
Immiscibles, 2 (TEXUS 5) N91-31411
Fundamental studies in the manganese-bismuth system (TEXUS 2) N91-31414
Solidification of immiscible alloys: ZnBi (TEXUS 2) N91-31415
Composite materials, 1 (TEXUS 1) N91-31430
Composite materials, 2 (TEXUS 2) N91-31431
Liquid phase sintering (TEXUS 19) ESA N91-31446
Bubble formation, growth, and expansion during the liquid phase sintering of a WC-Co sample N91-31454
LIQUID PROPELLANT ROCKET ENGINES
Hydrogen test of a small, low specific speed centrifugal pump stage
[NASA-CR-187117] N91-31213
Evaluation of undeveloped rocket engine cycle applications to advanced transportation
[NASA-CR-184205] N91-31215
LIQUID SURFACES
Freezing of a long liquid column (TEXUS 18) ESA N91-31326
LIQUID-GAS MIXTURES
Virial coefficients and equations of state for mixed fluids; application to CH4-H2O
[DE91-016248] N91-31254
Three-dimensional Marangoni convection (MASER 1) ESA N91-31343
Manufacture of iron foam (TEXUS 7) N91-31450
LIQUID-LIQUID INTERFACES
Interfacial convection (TEXUS 1) N91-31327
Interfacial convection (TEXUS 2) N91-31328
Diffusion-induced interfacial convection (TEXUS 3) N91-31329
Thermally induced interfacial convection (TEXUS 4) N91-31330
Diffusion-induced interfacial convection (TEXUS 8) N91-31331
Diffusion-induced interfacial convection (TEXUS 11) N91-31332
Immiscibles, 1 (TEXUS 3) N91-31410
Dispersion alloys (TEXUS 7) N91-31412
Al-Pb bearing alloy (TEXUS 1) N91-31413
Unidirectional solidification of immiscible alloys (TEXUS 5) N91-31418
Meniscus stability in immiscible metals (MASER 1) N91-31428
LIQUID-SOLID INTERFACES
Freezing of a long liquid column (TEXUS 18) ESA N91-31326
Metallic composites with particles (TEXUS 6) N91-31436
Melting and solidification of metallic composites (TEXUS 9) N91-31438
Metal matrix composites (TEXUS 20) N91-31440
LIQUIDS
Long liquid bridges aboard sounding rockets (TEXUS 12) ESA N91-31325
Thermal conductivity of liquids (MASER 1) ESA N91-31361
LITHIUM
Accelerated aging and discharge of lithium/thionyl-chloride D cells
[DE91-012649] N91-31517
LITHIUM ALLOYS
Composite ingot casting
[PATENT-1-250-128] N91-31269
LITHIUM COMPOUNDS
Electrostatic positioning for containerless processing of a Li-silicate glass (TEXUS 10) ESA N91-31469
Technology assessment of ambient temperature rechargeable lithium batteries for electric vehicle applications
[DE91-016500] N91-31522
LITHIUM ISOTOPES
The Li-7 and Be-7 deexcitation lines: Probes for accelerated particle transport models in solar flares
[NASA-CR-183490] N91-32020
LITHIUM OXIDES
Ion-implantation induced crystallization of glass
[DE91-016121] N91-31303
LITHIUM SULFUR BATTERIES
Development of prototype sealed bipolar lithium/sulfide cells
[DE91-015721] N91-31519
LITHOGRAPHY
Superconducting magnet program for x ray lithography source at Brookhaven National Laboratory
[DE91-016995] N91-31981
Review of vacuum systems for x ray lithography light sources
[DE91-017008] N91-31982
LOADING RATE
Influence of loading rate on the mechanical response and substructure evolution of shock-loaded copper
[DE91-013390] N91-31276
LOADS (FORCES)
Power saw
[NASA-CASE-MSC-21469-1] N91-31655
Tuning maps for setpoint changes and load disturbance upsets in a three capacity process under multivariable control
[NASA-TM-104419] N91-31876
LOCAL AREA NETWORKS
Local area gigabit networking
[DE91-014780] N91-31869
Interactive retrieval in information spaces distributed across a wide-area network N91-31992
LOGARITHMS
Strong approximation on log dense sets
[W-9101] N91-31916
LOGIC CIRCUITS
Reconfigurable parameter filter
[PATENT-1-264-072] N91-31513
Hardware modeling and top-down design using VHDL
[AD-A239356] N91-31534
LOGIC PROGRAMMING
On logic programming and the refinement calculus: Semantics based program transformations
[RUU-CS-90-39] N91-31834
On the application of temporal logic in real time to specify telecommunication protocols
[REPT-90-071] N91-31846
Network database in PROLOG N91-31866
LOGISTICS
A study of the logistics function within a medium sized, sales oriented chemical company
[ETN-91-99983] N91-31987
LOGISTICS MANAGEMENT
A study of the logistics function within a medium sized, sales oriented chemical company
[ETN-91-99983] N91-31987
LONGITUDINAL CONTROL
Robustness and techniques of multivariable control for helicopter piloting. Dispatch 3: Inclusion regions technique on linear model
[RD/PA-14-227] N91-31184
LOOPS
Tuning maps for setpoint changes and load disturbance upsets in a three capacity process under multivariable control
[NASA-TM-104419] N91-31876
LORAN
Development of a geographic navigational display device for general aviation aircraft
[PB91-170282] N91-31114
LOW ALTITUDE
Low altitude ejection release (total mass between 1,660 and 5,600 kg)
[REPT-90/05] N91-31475
LOW GRAVITY MANUFACTURING
Diffusion-controlled growth of single crystals of protein (TEXUS 5) N91-31397
Alloy formation (TEXUS 5) N91-31398
Solidification of a hypereutectic alloy (TEXUS 1) N91-31399
Solidification of alloys (TEXUS 1) N91-31400
Solidification of alloys (TEXUS 2) N91-31401
Macrosegregation in Ag-Sn alloys (MASER 1) N91-31402
Directional solidification of eutectics (TEXUS 6) N91-31404
LOW PRESSURE
Properties of low temperature, low oxygen pressure post-annealed YBa2Cu3O(sub 7-x) thin films
[DE91-015632] N91-31969
LOW TEMPERATURE
Control system design considerations for starting turbo-engines during cold weather operation N91-31155
Fuels and oils as factors in the operation of aero gas turbine engines at low temperatures N91-31163
The effect of fuel properties and atomization on low temperature ignition in gas turbine combustors N91-31164
The development of a computational model to predict low temperature fuel flow phenomena N91-31166
Naval medical research and development command
[AD-A239393] N91-31765
Properties of low temperature, low oxygen pressure post-annealed YBa2Cu3O(sub 7-x) thin films
[DE91-015632] N91-31969
LOW TEMPERATURE ENVIRONMENTS
Low Temperature Environment Operations of Turboengines (Design and User's Problems)
[AGARD-CP-480] N91-31144
Low temperature environment operation of turbo engines: A military operator's experience and requirements N91-31145
Low temperature environment operations of turbo engines N91-31146
Analysis of starting problems in cold weather with ASTAZOU type turbine engines in helicopters N91-31147
Cold starting small gas turbines: An overview N91-31150
Cold start optimization on a military jet engine N91-31151
Cold weather ignition characteristics of advanced small gas turbine combustion systems N91-31152
Cold start development of modern small gas turbine engines at Pratt and Whitney Aircraft of Canada Ltd. N91-31156
The effect of fuel properties and atomization on low temperature ignition in gas turbine combustors N91-31164
LOW TEMPERATURE TESTS
Design considerations based upon low temperature starting tests on military aircraft turbo engines N91-31157
LUBRICANT TESTS
Diagnostic tools for reciprocating engine systems
[PB91-184960] N91-31645
LUBRICATING OILS
Fuels and oils as factors in the operation of aero gas turbine engines at low temperatures N91-31163
Diagnostic tools for reciprocating engine systems
[PB91-184960] N91-31645
LUMINESCENCE
Single layer multi-color luminescent display
[NASA-CASE-LAR-13616-1] N91-31950
Photophysics and chemistry of ultra-fast ZnO and CdS phosphors
[DE91-013106] N91-31966
LUNAR BASES
Solid-support substrates for plant growth at a lunar base N91-31800
LUNAR EXPLORATION
Technical prospects for utilizing extraterrestrial propellants for space exploration
[NASA-TM-105263] N91-31318
LUNAR RADIATION
Activities report of the Institute of Extraterrestrial Physics
[MPE-223] N91-32002
LUNAR RESOURCES
Technical prospects for utilizing extraterrestrial propellants for space exploration
[NASA-TM-105263] N91-31318
LUNAR SOIL
Solid-support substrates for plant growth at a lunar base N91-31800

M

MACHINE LEARNING
An application of neural networks to process and materials control
[DE91-016016] N91-31886

MACHINING
Finite element modeling of orthogonal machining using an elastic-viscoplastic material model
[DE91-016815] N91-31477
Plug-type heat flux gauge
[NASA-CASE-LEW-14967-1] N91-31608
MAGNESIUM COMPOUNDS
Single crystals of CeMg3 (TEXUS 7) ESA N91-31382
Growth of rare Earth-magnesium crystals (TEXUS 12) N91-31383
MAGNETIC COMPRESSION
International magnetic pulse compression
[DE91-015774] N91-31520
Proceedings of the International Magnetic Pulse Compression Workshop. Volume 2: Technical summary
[DE91-015775] N91-31521
MAGNETIC CORES
International magnetic pulse compression
[DE91-015774] N91-31520
Proceedings of the International Magnetic Pulse Compression Workshop. Volume 2: Technical summary
[DE91-015775] N91-31521
MAGNETIC FIELDS
Study of lightning strikes on an aircraft in flight. Electromagnetic measurements
[ONERA-RF-25/7234-PY] N91-31111
Magnetic field-induced fracture changes in metastable austenites at 4.2 K
[DE91-016263] N91-31279
Metastable austenites in cryogenic high magnetic field environments
[DE91-016420] N91-31288
Studies of non-ideal superconductors using DC magnetic methods
[DE91-015642] N91-31970
MAGNETIC FLUX
Models of flux diffusion and flux creep in high-temperature superconductors
[DE91-015838] N91-31972
Weak links within a Bi2Sr2Ca1Cu2O(x) single crystal by magnetization and direct optical observations
[DE91-016085] N91-31979
Magnetic field decay in neutron stars with superconducting cores N91-32015
MAGNETIC MATERIALS
Proceedings of the International Magnetic Pulse Compression Workshop. Volume 2: Technical summary
[DE91-015775] N91-31521
MAGNETIC PERMEABILITY
Weak links within a Bi2Sr2Ca1Cu2O(x) single crystal by magnetization and direct optical observations
[DE91-016085] N91-31979
MAGNETIC PROPERTIES
The analysis and design of brushless DC motors N91-31516
Models of flux diffusion and flux creep in high-temperature superconductors
[DE91-015838] N91-31972
MAGNETIC SWITCHING
International magnetic pulse compression
[DE91-015774] N91-31520
MAGNETIZATION
Studies of non-ideal superconductors using DC magnetic methods
[DE91-015642] N91-31970
MAGNETOHYDRODYNAMICS
Advanced concepts theory
[AD-A239780] N91-31959
MAGNETOMETERS
The in-flight calibration of the Hubble space telescope attitude sensors
[NASA-CR-183485] N91-32007
MAGNETOPAUSE
Plasma diffusion at the magnetopause? The case of lower hybrid drift waves
[NASA-CR-188913] N91-31957
MAGNETS
A new method to do time resolved, x ray diffraction studies: The rotating crystal Laue method
[DE91-016527] N91-31935
MALFUNCTIONS
Design and cost of the first commercial stretched-membrane heliostat
[DE91-016870] N91-31715
MAN MACHINE SYSTEMS
Possibilities of simulation and optimization for guided missile systems
[MBB-UA-1201-90-PUB] N91-31183
Tuning maps for setpoint changes and load disturbance upsets in a three capacity process under multivariable control
[NASA-TM-104419] N91-31876
MAN-COMPUTER INTERFACE
Human factors engineering design guidelines for the software user interface
[DE91-016061] N91-31802
MANAGEMENT
Improving managers' effectiveness
[DE91-016405] N91-31988
MANAGEMENT INFORMATION SYSTEMS
The design of an Integrity Consistency Checker (ICC) for an object oriented database system
[REPT-91-021] N91-31994
MANAGEMENT METHODS
What is the Federal Demonstration Project?
[DE91-013936] N91-31986
MANAGEMENT PLANNING
Climatic considerations in the life cycle management of the CF-18 engine N91-31158
MANEUVERABILITY
Fighter agility metrics N91-31128
MANGANESE ALLOYS
Fundamental studies in the manganese-bismuth system (TEXUS 2) N91-31414
MANIPULATORS
Robust impedance control of robot manipulators N91-31297
Kinematics of the six-degree-of-freedom force-reflecting Kraft Master
[NASA-TM-104124] N91-31879
Synchronized computational architecture for generalized bilateral control of robot arms
[NASA-CASE-NPO-17401-1-CU] N91-31885
MANNED MARS MISSIONS
Technical prospects for utilizing extraterrestrial propellants for space exploration
[NASA-TM-105263] N91-31318
MANNED SPACE FLIGHT
The feasibility of testing NASA's SCAD concentrator on Earth
[DE91-016055] N91-31702
MANUALS
UKIRT observer's manual
[ETN-91-99747] N91-32008
MANUFACTURING
The development of an intelligent dimensional inspection environment using coordinate measuring machines N91-31661
Design and cost of the first commercial stretched-membrane heliostat
[DE91-016870] N91-31715
Micromechanical concepts in optics and optoelectronics
[MBB-Z-0339-90-PUB] N91-31949
MAPS
North Pacific guyots
[AD-A239388] N91-31754
MARANGONI CONVECTION
Diffusion-induced interfacial convection (TEXUS 3) N91-31329
Oscillatory Marangoni convection (TEXUS 3A and 3B) N91-31333
Critical Marangoni number (TEXUS 5) N91-31334
Critical Marangoni number (TEXUS 8) N91-31335
Thermal Marangoni convection in a floating zone (TEXUS 3) N91-31336
Oscillatory and turbulent flow regimes due to Marangoni convection (TEXUS 7) N91-31337
Influence of a surface tension minimum on the Marangoni effect (TEXUS 8) ESA N91-31338
Influence of a surface tension minimum on the Marangoni effect (TEXUS 9) ESA N91-31339
Influence of a surface tension minimum on the Marangoni effect (TEXUS 19) ESA N91-31340
Thermal Marangoni convection in a floating zone (TEXUS 9) ESA N91-31341
Experimental results on microgravitational fluid dynamics (TEXUS 14b) ESA N91-31342
Three-dimensional Marangoni convection (MASER 1) ESA N91-31343
Three-dimensional Marangoni convection (MASER 2) ESA N91-31344
Thermocapillary drop motion, 1 (MASER 1) ESA N91-31345
Thermocapillary drop motion, 2 (MASER 2) ESA N91-31346
Floating-zone growth of a silicon single crystal (TEXUS 7) N91-31384
Growth of a Si crystal covered with a SiO2 skin (TEXUS 12) N91-31385
Semi-confined Bridgman growth of Ga-doped Ge (MASER 2) N91-31390
Solidification of immiscible alloys: ZnBi (TEXUS 2) N91-31415
Separation of transparent fluids due to Marangoni convection (TEXUS 7) N91-31425
Marangoni transport of droplets at a solidification front (TEXUS 9) N91-31426
MARINE ENVIRONMENTS
On the response of the special sensor microwave/imager to the marine environment: Implications for atmospheric parameter retrievals N91-31727
MARKERS
Tropical tests of a seawater marker
[MRL-TR-90-19] N91-31109
MARKET RESEARCH
Solar energy and conservation technologies for Caribbean Tourist Facilities (CTF)
[DE91-016451] N91-31712
MARKOV CHAINS
On the relation between recurrence and ergodicity properties in denumerable Markov decision chains
[TW-91-02] N91-31918
MARTENSITIC TRANSFORMATION
Metastable austenites in cryogenic high magnetic field environments
[DE91-016420] N91-31288
MASKS
Distortion-free x ray mask technology
[AD-A239770] N91-31665
MASS FLOW
Local mean mass volume measurement around a model with lateral jet in supersonic flow
[AAAF-NT-89-08] N91-31102
MASS SPECTROSCOPY
Atomic hydrogen driven halogen extraction from Si(100): Eley-Rideal surface kinetics
[AD-A239544] N91-31266
Some applications of X-ray photoelectron spectroscopy and secondary-ion mass spectroscopy N91-32029
MASS TRANSFER
Interfacial convection (TEXUS 1) N91-31327
Three-dimensional Marangoni convection (MASER 1) ESA N91-31343
Three-dimensional Marangoni convection (MASER 2) ESA N91-31344
Low altitude ejection release (total mass between 1,660 and 5,600 kg)
[REPT-90/05] N91-31475
BES welding science
[DE91-015625] N91-31651
Proceedings of the Ninth Symposium on Energy Engineering Sciences: Fluid and Dynamical Systems
[DE91-015974] N91-31701
MATCHED FILTERS
Convergence performance of adaptive detectors, part 1
[AD-A239507] N91-31539
MATHEMATICAL LOGIC
Linear logic, domain theory, and semi-functors
[RUU-CS-90-34] N91-31830
On the application of temporal logic in real time to specify telecommunication protocols
[REPT-90-071] N91-31846
On the expressiveness of equational type logic
[MEMO-INF-90-39-REV] N91-31887
MATHEMATICAL MODELS
Validation of two dimensional drag prediction methods
[ONERA-RSF-85/1685-AY] N91-31093
Low level turbulence detection by a laser velocimetry technique: Application to transonic flows
[AAAF-NT-89-07] N91-31101
The development of a computational model to predict low temperature fuel flow phenomena N91-31166
Numerical model of evolution in supercooled cloud of water droplets in a case of icing N91-31169
Calculation of fragment ejection velocities on explosion of a launcher
[CNES-NT-128] N91-31195
Nonlinear combustion instability model in two- to three-dimensions
[NASA-TM-102381] N91-31208
The influence of interphase regions on local thermal stresses and deformations in composites N91-31228
Modelling the response of thick composite materials due to axisymmetric shock loading
[AD-A239531] N91-31243
Model description of transition metals using the rotated second moment approximation
[DE91-016043] N91-31287
Finite element modeling of orthogonal machining using an elastic-viscoplastic material model
[DE91-016815] N91-31477
Behaviour of the SIR for space-based DPCA radar under various spatial clutter distributions
[CRC-W7714-7-5271] N91-31485
The development of aluminum-air batteries for application in electric vehicles
[DE91-016863] N91-31533
Computational fluid dynamics N91-31544
A three-dimensional viscous flow model of stator/rotor interaction in turbomachines N91-31547
Prediction of rotor surface unsteady pressure and heat transfer from wake passing N91-31549
A new form of second-moment closure N91-31560
New Approaches in the Description and Modeling of Turbulence
[VKI-LS-1991-03] N91-31565

Direct and large-eddy simulations of transition in the compressible boundary layer N91-31566
Spectral large-eddy simulation of isotropic and stably-stratified turbulences N91-31567
RNG and turbulence modeling N91-31570
The development of a specific image analysis technique for exploiting flow visualization negatives [AAAF-NT-89-26] N91-31593
Comparison of integrated numerical experiments with accelerator and FEL experiments [DE91-016071] N91-31639
Reliability modeling of dependable distributed systems [AD-A239734] N91-31663
Nonlinear probabilistic finite element modeling of composite shells N91-31668
Updating of finite element models using experimental vibratory type data. Process of static substructuring [ONERA-RT-10/3313-RY-090-R] N91-31682
Large Angle Transient Dynamics (LATDYN) user's manual [NASA-CR-4401] N91-31685
A finite element approach for the dynamic analysis of joint-dominated structures [NASA-CR-4402] N91-31686
Improved finite-element methods for rotorcraft structures [NASA-TM-104104] N91-31687
Energy transfer processes in solar energy conversion [DE91-016102] N91-31704
Pseudohomogeneous catalyst layer model for polymer electrolyte fuel cell [DE91-016014] N91-31710
Simulated effects of a doubling of carbon dioxide on corn production in portions of the central US [DE91-016843] N91-31722
The time-domain earth tides N91-31726
The use of distributional and pointwise statistical measures in GCM intercomparisons [DE91-015697] N91-31748
Absorbing CAD system geometries into GEANT [DE91-015707] N91-31816
An application of neural networks to process and materials control [DE91-016016] N91-31886
A dynamically adaptive multigrid algorithm for the incompressible Navier-Stokes equations: Validation and model problems [NASA-CR-187595] N91-31888
A note on 'the matching polynomial of a polygraph' [MEMO-910] N91-31905
Multigrid and Runge-Kutta time stepping applied to the uniformly non-oscillatory scheme for conservation laws [MEMO-911] N91-31906
A pragmatical view on the certainty factor model [RUU-CS-90-42] N91-31917
Use of an ARMA model in turbulent medium acoustic propagation [ONERA-RF-14/3641-PY] N91-31925
A parametric study of transonic blade-vortex interaction noise [NASA-CR-188811] N91-31928
Theoretical nuclear physics [DE91-016745] N91-31936
Computational model for deterministic chaos in a magnetically confined plasma [DE91-016022] N91-31955
Adjustment of the mixing-rate constant in the eddy break-up model for a jet flame N91-32030

MATRICES (MATHEMATICS)
Some order dimension bounds for communication complexity problems [MEMO-938] N91-31489
Acceleration techniques for a spectral multi-grid method [MEMO-914] N91-31580
Force reconstruction using the inverse of the mode-shape matrix [DE91-016407] N91-31689
An algorithm for spectral factorization of polynomial matrices with any signature [MEMO-912] N91-31842

MATRIX MATERIALS
An analytical prediction of matrix cracking in fibrous composite laminates N91-31225
Ceramic composition [PATENT-1-249-609] N91-31294

MATRIX METHODS
Approximating treewidth, pathwidth, and minimum elimination tree height [RUU-CS-91-01] N91-31836

MATTER (PHYSICS)
Nuclear and particle astrophysics [DE91-016260] N91-32016

MAXIMUM LIKELIHOOD ESTIMATES
Parameter identification for two-point boundary value processes [MEMO-917] N91-31909

MEASURING INSTRUMENTS
Experimental determination of the temperature and density of opacity samples [DE91-015686] N91-31252
Plug-type heat flux gauge [NASA-CASE-LEW-14967-1] N91-31608

MECHANICAL ENGINEERING
Technical abstracts: Mechanical engineering, 1990 [DE91-016502] N91-31658

MECHANICAL PROPERTIES
The mechanical response of woven Kevlar fabric [DE91-010581] N91-31230
Relation between fiber proportion and mechanical characteristics of carbon-resin composites [RE-50-345/F] N91-31231
Plastic deformation processes in relation to molecular structure [ETN-91-99916] N91-31233
Creep deformation and fracture of a two-phase TiAl intermetallics [DE91-011963] N91-31274
Mechanical behavior of a nickel based alloy UDIMET 700 fabricated by powder metallurgy [JUEL-2414] N91-31283
Behavior of nonlinear mechanical structures subjected to stationary excitations [ECL-91-01] N91-31681

MEDICAL SCIENCE
Developments in medical audit in hospitals in the National Health Service [ETN-91-99984] N91-31762

MELTING
Unidirectional solidification of immiscible alloys (TEXUS 7) N91-31419
Composite materials, 2 (TEXUS 2) N91-31431
Alloys with oxide inclusions (TEXUS 2) N91-31432

MELTS (CRYSTAL GROWTH)
Reaction kinetics in glass melts (TEXUS 1) N91-31363
Reaction kinetics in glass melts: Corrosion of SiO2 (TEXUS 4) N91-31364
Reaction kinetics in glass melts: Sodium self-diffusion in alkali-silicate melts (TEXUS 6) N91-31365
Self- and interdiffusion in alkali-silicate melts (TEXUS 11 and 12) N91-31366
Self- and interdiffusion in alkali-silicate melts (TEXUS 13) N91-31367
Reaction kinetics in molten glasses: Self-diffusion in alkali-silicate melts (TEXUS 20) N91-31368
Ventilation and filling of an optical diffusion cell (TEXUS 8) N91-31371
Directional solidification of doped germanium (TEXUS 4) ESA N91-31380
Semi-confined Bridgman growth of Ga-doped Ge (MASER 2) N91-31391
Immiscibles, 1 (TEXUS 3) N91-31410
Unidirectional solidification of Zn-Bi samples (TEXUS 14b) N91-31420
Composite materials, 2 (TEXUS 2) N91-31431
Copper-alumina suspensions (TEXUS 5) N91-31434
Metallic composites with particles (TEXUS 6) N91-31436
Metal matrix composites (TEXUS 14b) N91-31439
Solidification of fine dispersions in microgravity (TEXUS 14b) N91-31441
Dispersion alloys (TEXUS 19) N91-31442
Liquid phase sintering (TEXUS 8) N91-31443
Manufacture of iron foam (TEXUS 7) N91-31450
Skin technology (TEXUS 1) N91-31455
Skin technology (TEXUS 2) N91-31456
Skin technology (TEXUS 3) N91-31457
Skin technology (TEXUS 4) N91-31458
Skin technology (TEXUS 9) N91-31459
Skin technology (TEXUS 11 and 12) N91-31460

MEMBRANES
Water transport properties of fuel cell ionomers [DE91-016015] N91-31259
Development of ceramic membranes for gas separation: FY 1990 development activities [DE91-015915] N91-31300
Facet development for a faceted stretched-membrane dish by Solar Kinetics, Inc. [DE91-016866] N91-31713
Factors affecting plant growth in membrane nutrient delivery N91-31797

MEMORY
Naval medical research and development command [AD-A239393] N91-31765

MEMORY (COMPUTERS)
Asymmetric soft-error resistant memory [NASA-CASE-NPO-17394-1-CU] N91-31810
A fast multiport memory based on single-port memory cells [AD-A239455] N91-31811

MENISCI
Meniscus stability in immiscible metals (MASER 1) N91-31428
Liquid phase sintering (TEXUS 8) N91-31443

MERCURY COMPOUNDS
Crystallisation experiments with salts (TEXUS 13) N91-31392

MERGING ROUTINES
GEOTRANS: An interface program from GEOPROGRAM to a geographic information system [DE91-016111] N91-31998

MESOSCALE PHENOMENA
Impact of the ice phase on a mesoscale convective system: Cloud ensemble features and cloud radiative properties [DE91-015769] N91-31749

METAL AIR BATTERIES
The development of aluminum-air batteries for application in electric vehicles [DE91-016863] N91-31533

METAL BONDING
Apparatus and method for explosive bonding to edge of flyer plate [NASA-CASE-LAR-14096-1] N91-31476
Energy and Technology Review, February-March l991 [DE91-015487] N91-32031

METAL CRYSTALS
Alloy formation (TEXUS 5) N91-31398

METAL FATIGUE
Dual ion implantation effects on fatigue properties of Fe-13Cr-15Ni alloys [DE91-015930] N91-31286
Crack propagation in heat resistant disk alloys. Short crack propagation in alloys for high characteristic turbomachine disks [ETN-91-99981] N91-31683
Ultrasonic characterization of fatigue crack closure [DE91-015161] N91-31688

METAL FILMS
Composite flexible blanket insulation [NASA-CASE-NPO-11907-1-NP] N91-31236
Ion beam enhanced adhesion of iron films to sapphire substrates [DE91-015931] N91-31308
Distortion-free x ray mask technology [AD-A239770] N91-31665

METAL FOAMS
Manufacture of steel foam (TEXUS 4) N91-31448
Manufacture of steel foam (TEXUS 6) N91-31449
Manufacture of iron foam (TEXUS 7) N91-31450
Metallic foams (TEXUS 5) N91-31451
Preparation of aluminium foams (TEXUS 9) N91-31452

METAL FOILS
Composite flexible blanket insulation [NASA-CASE-NPO-11907-1-NP] N91-31236
A jet polishing technique for thinning two phase materials [DE91-016422] N91-31473

METAL JOINTS
Adhesion of metals on ceramic substrates (MASER 2) ESA N91-31463

METAL MATRIX COMPOSITES
Experimental and analytical analysis of stress-strain behavior in a (90/0 deg)2s, SiC/Ti-15-3 laminate [NASA-TM-104470] N91-31235
Response of an alumina fiber reinforced aluminum composite to combined tension-torsion [AD-A239560] N91-31245
Composite materials, 1 (TEXUS 1) N91-31408
Immiscibles, 2 (TEXUS 5) N91-31411
Metallic composites with particles (TEXUS 6) N91-31436
Metallic composites with particles (TEXUS 7) N91-31437
Melting and solidification of metallic composites (TEXUS 9) N91-31438
Metal matrix composites (TEXUS 14b) N91-31439
Metal matrix composites (TEXUS 20) N91-31440
Solidification of fine dispersions in microgravity (TEXUS 14b) N91-31441
Dispersion alloys (TEXUS 19) N91-31442
Liquid phase sintering (TEXUS 8) N91-31443
Tungsten composites (TEXUS 10) N91-31444
Analysis of thermomechanical fatigue of unidirectional titanium metal matrix composites [NASA-TM-104105] N91-31677

METAL OXIDES
Influence of surface defects and local structure on oxygenate reaction pathways over metal oxide surfaces [DE91-016600] N91-31289

Atomic structures and compositions of internal interfaces
[DE91-016095] N91-31934
METAL PARTICLES
Understanding composite explosive energetics
[DE91-015770] N91-31316
Dispersion alloys (TEXUS 19) N91-31442
Liquid phase sintering (TEXUS 8) N91-31443
METAL PLATES
Modelling the response of thick composite materials due to axisymmetric shock loading
[AD-A239531] N91-31243
Apparatus and method for explosive bonding to edge of flyer plate
[NASA-CASE-LAR-14096-1] N91-31476
METAL SURFACES
High pressure catalytic reactions over single-crystal metal surfaces
[DE91-016475] N91-31256
Macroscopic quantum tunneling in Josephson tunnel junctions and Coulomb blockade in single small tunnel junctions
[DE91-016258] N91-31974
METAL VAPORS
A multifunction ion-irradiation/surface modification ultrahigh vacuum chamber system
[DE91-016819] N91-31190
METALLIC GLASSES
Dynamic yield strength of a palladium alloy metallic glass
[DE91-015111] N91-31298
METALLOGRAPHY
Experimental and analytical analysis of stress-strain behavior in a (90/0 deg)2s, SiC/Ti-15-3 laminate
[NASA-TM-104470] N91-31235
A comparison of techniques for the metallographic preparation of thermal sprayed samples
[DE91-014704] N91-31272
Directional solidification of immiscible alloys Zn-Pb (MASER 2) N91-31421
METALS
Summaries of FY 1991 research in the chemical sciences
[DE91-011221] N91-31222
Correlations between surface structure and catalytic activity/selectivity
[DE91-016453] N91-31255
The influence of plastic-strain-induced anisotropy on stress distributions in the finite deformation of ductile metals N91-31273
Formation of defect structures in metals during irradiation
[DE91-015548] N91-31278
Anelastic release from the shock-compressed state
[DE91-009961] N91-31672
METASTABLE STATE
Magnetic field-induced fracture changes in metastable austenites at 4.2 K
[DE91-016263] N91-31279
METEOROID CONCENTRATION
Optimization techniques applied to passive measures for in-orbit spacecraft survivability
[NASA-CR-184198] N91-31204
METEOROID HAZARDS
Optimization techniques applied to passive measures for in-orbit spacecraft survivability
[NASA-CR-184198] N91-31204
METEOROID PROTECTION
Optimization techniques applied to passive measures for in-orbit spacecraft survivability
[NASA-CR-184198] N91-31204
METEOROLOGICAL RADAR
Coordinate conversions for presenting and compositing weather radar data
[KNMI-TR-129] N91-31497
A satellite-based radar wind sensor
[NASA-CR-188805] N91-31750
METEOSAT SATELLITE
Description of Crau data set: Meteosat data, radiosonde data, sea surface temperatures: Comparison of Meteosat and Heimann data
[KNMI-WR-90-03] N91-31752
METHANE
Virial coefficients and equations of state for mixed fluids; application to CH4-H2O
[DE91-016248] N91-31254
Effective ionization coefficients, electron drift velocities, and limiting breakdown fields for gas mixtures of possible interest to particle detectors
[DE91-015921] N91-31532
METHYL ALCOHOL
Influence of surface defects and local structure on oxygenate reaction pathways over metal oxide surfaces
[DE91-016600] N91-31289
Assessment of costs and benefits of flexible and alternative fuel use in the US transportation sector
[DE91-015451] N91-31319
Conversion of biomass and fossil fuels to methanol and its effect on CO2 emissions
[DE91-015846] N91-31320
Separation of transparent fluids due to Marangoni convection (TEXUS 7) N91-31425
Marangoni transport of droplets at a solidification front (TEXUS 9) N91-31426
METROLOGY
Fighter agility metrics N91-31128
MICROCOMPUTERS
Quick development microcomputer system: Training automatic components for electronic troubleshooting
[AD-A239573] N91-31542
MICROCRYSTALS
The microcrystal laser: A first step on the way to a laser microsystem
[MBB-Z-0336-90-PUB] N91-31635
MICROELECTRONICS
Adhesion of thick layer systems on ceramic based precious metals in hybrid microelectronic circuits
[MBB-UA-1191-90-PUB] N91-31304
Silicon micromachining based on porous silicon formation
[DE91-013744] N91-31472
MICROGRAVITY APPLICATIONS
Summary review of sounding rocket experiments in fluid science and material sciences: TEXUS 1 to 20; MASER 1 and 2
[ESA-SP-1132] N91-31321
Segregation behaviour of rare earths under microgravity and normal gravity conditions (TEXUS 13) N91-31407
Composite materials, 1 (TEXUS 1) N91-31408
Composite materials, 2 (TEXUS 2) N91-31409
Immiscibles, 1 (TEXUS 3) N91-31410
Immiscibles, 2 (TEXUS 5) N91-31411
Meniscus stability in immiscible metals (MASER 1) N91-31428
Composite materials, 1 (TEXUS 1) N91-31430
Composite materials, 2 (TEXUS 2) N91-31431
MICROHARDNESS
Dual ion implantation effects on fatigue properties of Fe-13Cr-15Ni alloys
[DE91-015930] N91-31286
MICROMECHANICS
Initial determination of the micromechanical properties of oxide scales
[DE90-012164] N91-31291
Analysis of thermomechanical fatigue of unidirectional titanium metal matrix composites
[NASA-TM-104105] N91-31677
Micromechanical concepts in optics and optoelectronics
[MBB-Z-0339-90-PUB] N91-31949
MICROORGANISMS
Biofilm monitoring coupon system and method of use
[NASA-CASE-MSC-21585-1] N91-31755
The conversion of lignocellulosics to fermentable sugars: A survey of current research and application to CELSS N91-31784
MICROPROCESSORS
Hybrid electro-optic processor
[AD-A239547] N91-31505
A case study for the real-time experimental evaluation of the VIPER microprocessor
[NASA-TM-104098] N91-31531
MICROSCOPY
Photography of shock waves in explosive crystals
[DE91-015772] N91-31572
MICROSTRIP ANTENNAS
Electromagnetically coupled microstrip antennas having feeding patches capacitively coupled to feedlines
[PATENT-1-263-181] N91-31480
MICROSTRIP DEVICES
Phased array components for the High Temperature Superconducting Space Experiment (HTSSE)
[AD-A239361] N91-31535
MICROSTRUCTURE
The mechanical response of woven Kevlar fabric
[DE91-010581] N91-31230
Experimental and analytical analysis of stress-strain behavior in a (90/0 deg)2s, SiC/Ti-15-3 laminate
[NASA-TM-104470] N91-31235
A comparison of techniques for the metallographic preparation of thermal sprayed samples
[DE91-014704] N91-31272
Deformation induced microstructural and microchemical changes during thermomechanical treatment
[DE91-016949] N91-31290
Al-Pb bearing alloy (TEXUS 1) N91-31413
Soldering in microgravity (TEXUS 5) N91-31462
Electronic transport and lasing in microstructures
[DE91-016751] N91-31641
Weld pool solidification and microstructures
[DE91-014263] N91-31650
BES welding science
[DE91-015625] N91-31651
Crystallization of the glassy grain boundary phase in silicon nitride ceramics
[NASA-CR-188717] N91-31961
Microstructural changes in Beta-silicon nitride grains upon crystallizing the grain-boundary glass N91-31963
Indirect measurement of the viscosity of the intergranular glass phase in yttria-sintered silicon nitride N91-31965
MICROWAVE ANTENNAS
Antenna study for 60 GHz intersatellite link
[CD-RPT-ITL-5043-003] N91-31482
An investigation of optically controlled, integrated millimeter wave receiving phased arrays
[AD-A239504] N91-31538
MICROWAVE EQUIPMENT
Microwave module YAG laser weld development
[DE91-015750] N91-31652
MICROWAVE FILTERS
Dielectric image-resonator multiplexer
[PATENT-1-252-835] N91-31479
MICROWAVE FREQUENCIES
Electromagnetically coupled microstrip antennas having feeding patches capacitively coupled to feedlines
[PATENT-1-263-181] N91-31480
Airborne ESM receivers: Techniques and technologies
[ETN-91-99988] N91-31498
MICROWAVE IMAGERY
On the response of the special sensor microwave/imager to the marine environment: Implications for atmospheric parameter retrievals N91-31727
MICROWAVES
Application of microwave cavity perturbation techniques in conducting polymers
[AD-A239376] N91-31310
MIE SCATTERING
Quasi-elastic light scattering and applications to optical sizing N91-31627
MIGRATION
Composite materials, 2 (TEXUS 2) N91-31409
MILITARY HELICOPTERS
Low temperature environment operation of turbo engines: A military operator's experience and requirements N91-31145
MILITARY OPERATIONS
Low temperature environment operation of turbo engines: A military operator's experience and requirements N91-31145
Low temperature environment operations of turbo engines N91-31146
MILKY WAY GALAXY
A survey of the 158 micron CII fine-structure line in the central 50 pc of the galaxy
[NASA-CR-188912] N91-32009
MILLIMETER WAVES
An investigation of optically controlled, integrated millimeter wave receiving phased arrays
[AD-A239504] N91-31538
High-T(sub c) bolometers
[DE91-017009] N91-31611
MIMD (COMPUTERS)
Design of a specific integrated circuit for solving the three dimensional Poisson equation
[ECL-90-24] N91-31527
MINERALOGY
Solid-support substrates for plant growth at a lunar base N91-31800
MINERALS
Hyperspectral signatures (400 to 2500 nm) of vegetation, minerals, soils, rocks, and cultural features: Laboratory and field measurements
[AD-A239496] N91-31697
MINIATURIZATION
The microcrystal laser: A first step on the way to a laser microsystem
[MBB-Z-0336-90-PUB] N91-31635
Laser Doppler anemometer miniaturized with diode laser
[AAAF-NT-89-06] N91-31637
MINIMAX TECHNIQUE
From game trees to game graphs
[RUU-CS-90-43] N91-31921
MIRRORS
Design and analysis of multilayer x ray/XUV microscope
[NASA-CR-184197] N91-31607
MIS (SEMICONDUCTORS)
Contribution to the implementation of a completely in situ device in ultrahigh vacuum for the development of MIS on InP structures: Al2O3/InP interface optimization
[ECL-91-04] N91-31526
MISCIBILITY GAP
Segregation behaviour of rare earths under microgravity and normal gravity conditions (TEXUS 13) N91-31407

Dispersion alloys (TEXUS 7) N91-31412
Fundamental studies in the manganese-bismuth system (TEXUS 2) N91-31414
Solidification of immiscible alloys: ZnBi (TEXUS 2) N91-31415
The coalescence process in immiscible alloys (TEXUS 3) N91-31416
The coalescence process in immiscible alloys (TEXUS 5) N91-31417
Unidirectional solidification of immiscible alloys (TEXUS 5) N91-31418
Unidirectional solidification of immiscible alloys (TEXUS 7) N91-31419
Unidirectional solidification of Zn-Bi samples (TEXUS 14b) N91-31420
Directional solidification of immiscible alloys Zn-Pb (MASER 2) N91-31421
Immiscible alloy system Al-Pb (TEXUS 7) N91-31422
Separation of transparent fluids due to Marangoni convection (TEXUS 7) N91-31425
Marangoni transport of droplets at a solidification front (TEXUS 9) N91-31426
Solidification of an Al-Pb-Bi alloy under microgravity (TEXUS 13) N91-31427
Meniscus stability in immiscible metals (MASER 1) N91-31428

MISSILE CONTROL
Rotatable non-circular forebody flow controller [NASA-CASE-LAR-14212-1-CU] N91-31140
Procedure for steering a low-speed missile, weapon system, and missile for implementation of the procedure [PATENT-1-265-947] N91-31182

MISSILES
Possibilities of simulation and optimization for guided missile systems [MBB-UA-1201-90-PUB] N91-31183

MISSION PLANNING
Contributions to a space station for flights in the near field and towards geostationary Earth orbit [ETN-91-99744] N91-31203
Thin film, concentrator and multijunction space solar cells: Status and potential [NASA-TM-104505] N91-31218

MIST
Electrostatic precipitation of condensed acid mist [DE91-016530] N91-31260

MIXED OXIDES
Development of elements of a high T(sub c) superconducting cable [AD-A239766] N91-31543

MIXING
Solutal diffusion measurements in liquid PbSnTe under microgravity (TEXUS 19) N91-31372
Acoustic mixing (TEXUS 5) N91-31423
Solidification of immiscible alloys (TEXUS 8) N91-31424
Adjustment of the mixing-rate constant in the eddy break-up model for a jet flame N91-32030

MIXTURES
Ethynyl terminated imidothioethers and resins therefrom [NASA-CASE-LAR-13910-2-CU] N91-31307

MOBILITY
Mobility power flow analysis of coupled plate structure subjected to mechanical and acoustics excitation [NASA-CR-188791] N91-31678

MODAL RESPONSE
Fuselage shell and cavity response measurements on a DC-9 test section [NASA-CR-187557] N91-31926

MODEL REFERENCE ADAPTIVE CONTROL
Neural network based model reference adaptive control N91-31677

MODELS
Survey to assess the usefulness of two model agreements for university-industry cooperative research [DE91-013937] N91-31985

MODULARITY
Parabolic dish photovoltaic concentrator development [DE91-016868] N91-31714

MODULATION
An investigation of optically controlled, integrated millimeter wave receiving phased arrays [AD-A239504] N91-31538

MODULATORS
An investigation of optically controlled, integrated millimeter wave receiving phased arrays [AD-A239504] N91-31538

MODULES
Fuel cells for commercial energy [MBB-UE-0018-90-PUB] N91-31706

MOIRE FRINGES
Advanced and non-conventional optical schemes N91-31626

MOIRE INTERFEROMETRY
Interlaminar deformations on the cylindrical surface of a hole in laminated composites by moire interferometry [DE91-015922] N91-31238

MOISTURE
The influence of moisture and pressure on the mechanical properties of a glass-epoxy matrix composite and a graphite-epoxy matrix composite [AD-A239509] N91-31242

MOISTURE CONTENT
A documentation of vertical and horizontal aircraft soundings of icing relevant cloudphysical parameters N91-31172
Description of Crau data set: Meteosat data, radiosonde data, sea surface temperatures: Comparison of Meteosat and Heimann data [KNMI-WR-90-03] N91-31752

MOLDS
Composite ingot casting [PATENT-1-250-128] N91-31269

MOLECULAR BEAM EPITAXY
Advanced research workshop on Wide Gap II-VI Semiconductors [AD-A233796] N91-31960

MOLECULAR CLOUDS
GRO source candidates: (A) Nearby modest-size molecular clouds; (B) Pulsar with Wolf-Rayet companion that has lost its H-envelope [NASA-CR-183491] N91-32021

MOLECULAR DIFFUSION
Examination of molecular evaporation, cooling, and cluster dissociation of very thin liquid jets in a high vacuum [MPIS-12/1990] N91-31581

MOLECULAR ENERGY LEVELS
Interfacial systems for photochemical energy conversion [DE91-015743] N91-31700

MOLECULAR EXCITATION
Mass resolved excitation spectroscopy of benzyl and phenylnitrene radicals [AD-A239394] N91-31264
Energy transfer processes in solar energy conversion [DE91-016102] N91-31704

MOLECULAR SPECTRA
Mass resolved excitation spectroscopy of benzyl and phenylnitrene radicals [AD-A239394] N91-31264
Tunable far infrared studies of molecular parameters in support of stratospheric measurements [NASA-CR-186774] N91-31723
Scanning imaging absorption spectrometer for atmospheric chartography N91-31725

MOLECULAR STRUCTURE
Composite matrix deformation process in relation to molecular structure [ETN-91-99915] N91-31232
Plastic deformation processes in relation to molecular structure [ETN-91-99916] N91-31233
Energy and Technology Review, February-March l991 [DE91-015487] N91-32031

MOLECULES
The chemistry of transition metal clusters [DE91-015108] N91-31250

MOLTEN SALTS
Ultrasound absorption in molten salts (TEXUS 14b) N91-31359
Ultrasound absorption in molten salts (TEXUS 17) ESA N91-31360
Ventilation and filling of an optical diffusion cell (TEXUS 8) N91-31371
Fuel cells for commercial energy [MBB-UE-0018-90-PUB] N91-31706

MOLYBDENUM
The behaviour of alumina-copper suspensions (TEXUS 3A and 3B) N91-31433
Copper-molybdenum suspension (TEXUS 9) N91-31435

MOLYBDENUM OXIDES
The selective catalytic oxidation of ammonia to N2 and H2O over silica-supported molybdena catalysts N91-32026

MOM (SEMICONDUCTORS)
Chemical reduction of intermodulation interference caused by metal-oxide-metal junctions aboard ship [AD-A239530] N91-31265

MOMENTS
An introduction to second moment closure N91-31555
Inclusion of second-moment closures into finite-volume solvers N91-31556
Body force effects on turbulence N91-31558
Application of second-moment closure in complex flows N91-31559
A new form of second-moment closure N91-31560
An introduction to single-point closure methodology N91-31561

MONITORS
Airplane takeoff and landing performance monitoring system [NASA-CASE-LAR-13854-1-CU] N91-31120
Biofilm monitoring coupon system and method of use [NASA-CASE-MSC-21585-1] N91-31755
Testing and evaluation of the catalyst research MiniOX 3 oxygen monitor [AD-A239665] N91-31807

MONOCOQUE STRUCTURES
Static strain and vibration characteristics of a metal semimonocoque helicopter tail cone of moderate size [NASA-CR-187576] N91-31679

MONOTECTIC ALLOYS
Segregation behaviour of rare earths under microgravity and normal gravity conditions (TEXUS 13) N91-31407
Demixing of a monotectic ternary alloy (TEXUS 20) N91-31429

MONTE CARLO METHOD
The effects of fluid particle interactions on interfacial transfer and flow structure [DE91-016409] N91-31575
Mean field analysis of the CuO2 lattice: Comparison to Monte Carlo simulations [DE91-015570] N91-31968

MOON-EARTH TRAJECTORIES
The question of an efficient space transportation system for extraterrestrial materials [ILR-MITT-252(1990)] N91-31197

MORPHOLOGY
Solution growth of GaAs single crystals (TEXUS 19) N91-31393
Ultraviolet morphology of NGC 1068: The starburst knots and the extended emission region N91-32004

MOUNTING
Ventral segmented nozzles [CA-PATENT-APPL-SN-2-009-636] N91-31176
Biofilm monitoring coupon system and method of use [NASA-CASE-MSC-21585-1] N91-31755

MULTIGRID METHODS
Design and testing of a multiblock grid-generation procedure for aircraft design and research [NLR-TP-89146-U] N91-31131

MULTILAYER INSULATION
Composite flexible blanket insulation [NASA-CASE-NPO-11907-1-NP] N91-31236

MULTIPATH TRANSMISSION
Hybrid electro-optic processor [AD-A239547] N91-31505

MULTIPHOTON ABSORPTION
Particle production through two-photon processes in relativistic heavy-ion colliders [DE91-016221] N91-31931

MULTIPLEXING
Dielectric image-resonator multiplexer [PATENT-1-252-835] N91-31479
Multiplexing readout channels in proportional counters [NASA-TM-103552] N91-31606

MULTIPROCESSING (COMPUTERS)
A universal computer control system for motors [NASA-CASE-NPO-17134-1-CU] N91-31528
Reliability modeling of dependable distributed systems [AD-A239734] N91-31663
Construction and realization of distributed multiprocessor systems for real time tasks [MBB-UA-1189-90-PUB] N91-31871
A knowledge based application of the extended aircraft interrogation and display system [NASA-TM-4327] N91-31874

MULTISENSOR APPLICATIONS
Bayesian multi-sensor tracking for advanced air-traffic control systems [NLR-MP-88056-U] N91-31119

MULTISPECTRAL BAND SCANNERS
Scanning imaging absorption spectrometer for atmospheric chartography N91-31725

MULTIVARIABLE CONTROL
Application of multivariable control system design methodologies to robust beam control of a space-based laser [AD-A239460] N91-31643
Tuning maps for setpoint changes and load disturbance upsets in a three capacity process under multivariable control [NASA-TM-104419] N91-31876

MUONS
A research program in experimental high energy physics [DE91-016208] N91-31941

MUSCLES
The effect of exercise training on skeletal muscle glucose transorter isoform GLUT4 concentration in the obese Zucker rat [AD-A239461] N91-31757

Cold-induced changes in arterial sensitivity
[AD-A239493] N91-31767

N

NARCOSIS
The medical hazards of flame-suppressant atmospheres
[AD-A239618] N91-31806
NASA PROGRAMS
NASA Aerodynamics Program
[NASA-TM-4312] N91-31751
NATURAL LANGUAGE (COMPUTERS)
Exploiting captions for access to multimedia databases
[AD-A239435] N91-32000
NAVIER-STOKES EQUATION
The interaction of particles with homogeneous turbulence N91-31548
Introduction to the Modeling of Turbulence: Introduction N91-31552
Turbulence modeling for compressible flows and implementation in Navier-Stokes solvers N91-31564
Artificial diffusion methods in convection dominated flows
[W-9016] N91-31577
Numerical simulation of three dimensional unsteady flow by multiprocessor solving of the Navier-Stokes equations
[ETN-91-99974] N91-31594
A dynamically adaptive multigrid algorithm for the incompressible Navier-Stokes equations: Validation and model problems
[NASA-CR-187595] N91-31888
Least-squares solution of incompressible Navier-Stokes equations with the p-version of finite elements
[NASA-TM-105203] N91-31911
NAVIGATION AIDS
Development of a geographic navigational display device for general aviation aircraft
[PB91-170282] N91-31114
Simulation of distance-dependent functions in visual systems for training simulators using the z-buffer technique
[MBB-UA-1190-90-PUB] N91-31186
NAVSTAR SATELLITES
Investigations on the use of GPS for geodetic and orbit determination applications
[LR-649] N91-31118
NAVY
An integer programming model for Navy's maritime patrol aviation fleet
[AD-A239464] N91-31079
NEAR FIELDS
Contributions to a space station for flights in the near field and towards geostationary Earth orbit
[ETN-91-99744] N91-31203
Arctic VLF/LF data acquisition
[AD-A239704] N91-31510
NEAR WAKES
A European collaborative investigation of the three-dimensional turbulent shear layers of a swept wing
[NLR-MP-88054-U] N91-31084
NEODYMIUM LASERS
Microwave module YAG laser weld development
[DE91-015750] N91-31652
NETWORK ANALYSIS
Inventory and functional prototypes of neural networks
[TR-90-15] N91-31880
NETWORK CONTROL
The problem of network management: An approach using AI techniques
[REPT-90-072] N91-31884
NETWORKS
inference networks for document retrieval N91-31993
NEURAL NETS
Artificial neural networks for seismic data interpretation
[AD-A239673] N91-31743
Neural network based model reference adaptive control N91-31877
Inventory and functional prototypes of neural networks
[TR-90-15] N91-31880
Classes of feedforward neural networks and their circuit complexity
[MEMO-920] N91-31881
An application of neural networks to process and materials control
[DE91-016016] N91-31886
Parametric study of diffusion-enhancement networks for spatiotemporal grouping in real-time artificial vision
[AD-A239674] N91-31954
NEURONS
Muramyl peptide-enhanced sleep: Pharmacological optimization of performance
[AD-A239442] N91-31766
NEUROPHYSIOLOGY
Naval medical research and development command
[AD-A239393] N91-31765
NEUROTRANSMITTERS
Naval medical research and development command
[AD-A239393] N91-31765
Cold-induced changes in arterial sensitivity
[AD-A239493] N91-31767
NEUTRAL GASES
A study of a 21-cm-selected sample of galaxies N91-32014
NEUTRINOS
A research program in experimental high energy physics
[DE91-016208] N91-31941
NEUTRON COUNTERS
Intrinsic neutron source strengths in uranium solutions
[DE91-016091] N91-31933
NEUTRON DIFFRACTION
Near-edge study of gold-substituted YBa2Cu3O(7-delta)
[NASA-TM-105220] N91-31977
NEUTRON SOURCES
Intrinsic neutron source strengths in uranium solutions
[DE91-016091] N91-31933
NEUTRON STARS
Nuclear and particle astrophysics
[DE91-016260] N91-32016
Fast pulsars, variational bound, other facets of compact stars
[DE91-016416] N91-32018
NICKEL
Diffusion of Ni in Cu-Au and Cu-Al alloys (TEXUS 20) N91-31373
Tungsten composites (TEXUS 19) ESA N91-31445
NICKEL ALLOYS
Fatigue-resistant nickel-base superalloys
[PATENT-1-253-363] N91-31268
Rapidly solidified nickel aluminide of improved stoichiometry and ductilization
[PATENT-1-257-987] N91-31270
Method for imparting strength to intermetallic phases
[PATENT-1-255-929] N91-31271
Theoretical studies of metallic alloys
[DE91-016486] N91-31281
Mechanical behavior of a nickel based alloy UDIMET 700 fabricated by powder metallurgy
[JUEL-2414] N91-31283
Dual ion implantation effects on fatigue properties of Fe-13Cr-15Ni alloys
[DE91-015930] N91-31286
Process for producing plasma sprayed carbide-based coatings with minimal decarburization and near theoretical density
[DE91-012016] N91-31292
Directional solidification of eutectics InSb-NiSb (TEXUS 10) N91-31405
Tungsten composites (TEXUS 10) N91-31444
In situ short fatigue crack characterization of a nickel-base superalloy at ambient and elevated temperature N91-31670
NICKEL HYDROGEN BATTERIES
Nickel-hydrogen cell low-Earth life test update
[NASA-TM-105229] N91-31708
NITRILES
Boundary layers in transparent melts (TEXUS 10) N91-31406
NITROGEN
Cyanobacteria in CELSS: Growth strategies for nutritional variation and nitrogen cycling N91-31786
Biomass production and nitrogen dynamics in an integrated aquaculture/agriculture system N91-31789
The medical hazards of flame-suppressant atmospheres
[AD-A239618] N91-31806
Crystallization and characterization of Y2O3-SiO2 glasses N91-31962
NITROGEN METABOLISM
Cyanobacteria in CELSS: Growth strategies for nutritional variation and nitrogen cycling N91-31786
NITROGEN OXIDES
Efficiency of N use by wheat as a function of influx and efflux of NO3 N91-31778
NITROGENATION
Cyanobacteria in CELSS: Growth strategies for nutritional variation and nitrogen cycling N91-31786
NOBLE METALS
Adhesion of thick layer systems on ceramic based precious metals in hybrid microelectronic circuits
[MBB-UA-1191-90-PUB] N91-31304
NOISE INTENSITY
Multitarget tracking using optical processing
[AD-A239656] N91-31953
NOISE PREDICTION (AIRCRAFT)
User's manual for the Langley boundary layer noise propagation program (MRS-BLP)
[NASA-CR-187559] N91-31923
NOISE PROPAGATION
User's manual for the Langley boundary layer noise propagation program (MRS-BLP)
[NASA-CR-187559] N91-31923
NOISE REDUCTION
Noxious matter minimization as a project criterion for aircraft
[MBB-Z-0337-90-PUB] N91-31134
Initialization of the HIRLAM model using a digital filter
[DM-57] N91-31747
Assessing the efficacy of active noise reduction
[CTN-91-60200] N91-31922
Analysis of interior noise ground and flight test data for advanced turboprop aircraft applications
[NASA-CR-187558] N91-31927
A parametric study of transonic blade-vortex interaction noise
[NASA-CR-188811] N91-31928
Comparison of noise reduction systems
[DE91-015318] N91-31929
NONDESTRUCTIVE TESTS
Composite materials damage. Transverse cracking and delamination
[ONERA-RT-6/7256-RY-080-R] N91-31234
Techniques to assess the state of health of sealed lead acid batteries
[CTN-91-60214] N91-31515
X-ray inspection system
[PATENT-1-258-924] N91-31660
NONEQUILIBRIUM FLOW
Development of a computation code for nonequilibrium gas axisymmetric hypersonic laminar flow
[ONERA-RS-14/3637-AY] N91-31585
NONFLAMMABLE MATERIALS
Characterization of fire resistant GRP's by mechanical properties determination
[DREA-CR-88-421] N91-31295
NONLINEAR EQUATIONS
Nonlinear combustion instability model in two- to three-dimensions
[NASA-TM-102381] N91-31208
Linear and nonlinear stability of boundary layers with streamwise varying properties N91-31545
NONLINEAR OPTICS
Dynamics of 1.3 micron semiconductor lasers and nonlinear gain N91-31613
NONLINEAR PROGRAMMING
A technique for locating function roots and for satisfying equality constraints in optimization
[NASA-TM-104037] N91-31139
Optimal configuration of distributed database systems N91-31990
NONLINEAR SYSTEMS
DYNA3D: A nonlinear, explicit, three-dimensional finite element code for solid and structural mechanics
[DE91-015735] N91-31675
Behavior of nonlinear mechanical structures subjected to stationary excitations
[ECL-91-01] N91-31681
Dynamic disturbance decoupling for discrete-time nonlinear systems
[MEMO-913] N91-31843
NONLINEARITY
A method for the geometrically nonlinear analysis of compressively loaded prismatic composite structures N91-31229
Nonlinear probabilistic finite element modeling of composite shells N91-31668
Practical aspects of an interior-point method for convex programming
[AD-A239457] N91-31858
Bifurcations of parametrically forced oscillators
[W-9007] N91-31892
NONOSCILLATORY ACTION
Multigrid and Runge-Kutta time stepping applied to the uniformly non-oscillatory scheme for conservation laws
[MEMO-911] N91-31906
NOREPINEPHRINE
Cold-induced changes in arterial sensitivity
[AD-A239493] N91-31767
NOSES (FOREBODIES)
Rotatable non-circular forebody flow controller
[NASA-CASE-LAR-14212-1-CU] N91-31140
NOTCH TESTS
Variations in the static properties, unnotched and notched fatigue life behaviour of 13 batches of 2L.65 aluminium alloy extruded bar
[ARL-STRUC-R-427] N91-31676

NOZZLE DESIGN
Segmented rotatable nozzles
[CA-PATENT-APPL-SN-2-009-634] N91-31174
Segmented vectoring cruise nozzles
[CA-PATENT-APPL-SN-2-009-635] N91-31175
Ventral segmented nozzles
[CA-PATENT-APPL-SN-2-009-636] N91-31176
NOZZLE GEOMETRY
Medium power hydrogen arcjet performance
[NASA-TM-104533] N91-31216
NUCLEAR BINDING ENERGY
The chemistry of transition metal clusters
[DE91-015108] N91-31250
NUCLEAR ENERGY
Defect diffusion in ion implanted glasses
[DE91-016119] N91-31302
NUCLEAR ENGINE FOR ROCKET VEHICLES
Nuclear thermal rockets: A systems study
[DE91-017066] N91-31221
NUCLEAR FISSION
Intrinsic neutron source strengths in uranium solutions
[DE91-016091] N91-31933
NUCLEAR FUEL ELEMENTS
A review of the Los Alamos effort in the development of nuclear rocket propulsion
[DE91-016036] N91-31211
NUCLEAR FUELS
An investigation of dual-mode operation of a nuclear-thermal rocket engine
[DE91-015977] N91-31210
Intrinsic neutron source strengths in uranium solutions
[DE91-016091] N91-31933
Carbide fuels for nuclear thermal propulsion
[DE91-016032] N91-31945
NUCLEAR INTERACTIONS
Nucleus-nucleus collisions and the nuclear equation of state
[DE91-016747] N91-31937
NUCLEAR MEDICINE
Nuclear medicine and imaging research: Quantitative studies in radiopharmaceutical science
[DE91-015447] N91-31759
Boron in nuclear medicine: New synthetic approaches to PET, SPECT, and BNCT agents
[DE91-016488] N91-31764
NUCLEAR PHYSICS
Theoretical nuclear physics
[DE91-016745] N91-31936
Nucleus-nucleus collisions and the nuclear equation of state
[DE91-016747] N91-31937
Nuclear and particle astrophysics
[DE91-016260] N91-32016
NUCLEAR POWER PLANTS
Response of seismic-isolated structures under long-period motions
[DE91-015673] N91-31674
NUCLEAR PROPULSION
An investigation of dual-mode operation of a nuclear-thermal rocket engine
[DE91-015977] N91-31210
A review of the Los Alamos effort in the development of nuclear rocket propulsion
[DE91-016036] N91-31211
Nuclear thermal rockets: A systems study
[DE91-017066] N91-31221
Carbide fuels for nuclear thermal propulsion
[DE91-016032] N91-31945
NUCLEAR REACTOR CONTROL
Progress in the SP-100 FSQ reactor development
[DE91-016033] N91-31940
NUCLEAR REACTORS
Mechanical characterization of seismic base isolation elastomers
[DE91-015680] N91-31299
The effects of fluid particle interactions on interfacial transfer and flow structure
[DE91-016409] N91-31575
NUCLEAR ROCKET ENGINES
A review of the Los Alamos effort in the development of nuclear rocket propulsion
[DE91-016036] N91-31211
NUCLEAR SCATTERING
Theoretical nuclear physics
[DE91-016745] N91-31936
Nucleus-nucleus collisions and the nuclear equation of state
[DE91-016747] N91-31937
NUCLEAR STRUCTURE
Theoretical nuclear physics
[DE91-016745] N91-31936
NUCLEATE BOILING
Nucleate pool boiling (TEXUS 3) N91-31354
Bubble formation, 1 (TEXUS 5) N91-31355
Bubble formation, 2 (TEXUS 10) N91-31356
Bubble formation, 2. Microgravity measurements of the boiling heat transfer from flat heating surfaces (TEXUS 11) N91-31357
Inst. A fuer Thermodynamik. N91-31358
NUCLEATION
Electrolytically generated hydrogen bubbles (TEXUS 6) N91-31348
In situ short fatigue crack characterization of a nickel-base superalloy at ambient and elevated temperature N91-31670
NUCLEONS
A research program in experimental high energy physics
[DE91-016208] N91-31941
Nuclear and particle astrophysics
[DE91-016260] N91-32016
NUMERICAL ANALYSIS
Application of semianalytic satellite theory to maneuver planning
[AD-A239417] N91-31205
Postprocessing of experimental and numerical results in the case of two and three dimensional flows
[AAAF-NT-89-25] N91-31592
A critical comparison of two-equation turbulence models
[NASA-TM-105237] N91-31597
Application of an acquisition image processing system to the quantitative analysis of flows
[AAAF-NT-89-27] N91-31851
NUMERICAL CONTROL
A universal computer control system for motors
[NASA-CASE-NPO-17134-1-CU] N91-31528
NUMERICAL FLOW VISUALIZATION
Design and testing of a multiblock grid-generation procedure for aircraft design and research
[NLR-TP-89146-U] N91-31131
Flow visualization and simulation
[AAAF-NT-89-18] N91-31590
NUMERICAL WEATHER FORECASTING
Estimating the strength of the capping inversion and the probability of strong convection
[PB91-176685] N91-31744
NUTATION
The motions of Mars' pole N91-32019
NUTRIENTS
Factors affecting plant growth in membrane nutrient delivery N91-31797
Conceptual design of a closed loop nutrient solution delivery system for CELSS implementation in a micro-gravity environment N91-31798
Technology for subsystems of space-based plant growth facilities N91-31799
NUTRITION
Exploring the limits of crop productivity: A model to evaluate progress N91-31776
Environmental modification of yield and food composition of cowpea and leaf lettuce N91-31777

O

OBJECT PROGRAMS
An object-oriented analysis, design, and implementation of a network database N91-31865
OBSERVATORIES
The Berkeley search for distant supernovae to measure omega
[DE91-016418] N91-32010
OCEAN BOTTOM
North Pacific guyots
[AD-A239388] N91-31754
OCEAN CURRENTS
A summary of the physical oceanography of the Pacific Northwest Coast
[PB91-164434] N91-31753
OCEAN DYNAMICS
A summary of the physical oceanography of the Pacific Northwest Coast
[PB91-164434] N91-31753
OCEAN SURFACE
On the response of the special sensor microwave/imager to the marine environment: Implications for atmospheric parameter retrievals N91-31727
OCEAN THERMAL ENERGY CONVERSION
Open-cycle ocean thermal energy conversion surface-condenser design analysis and computer program
[DE91-015973] N91-31709
OCEANOGRAPHY
A summary of the physical oceanography of the Pacific Northwest Coast
[PB91-164434] N91-31753
OMEGA NAVIGATION SYSTEM
Performance Assessment and Coverage Evaluation (PACE) workstation (user manual)
[AD-A239723] N91-31122
OMEGA system Performance Assessment and Coverage Evaluation (PACE) workstation design and implementation, volume 2
[AD-A239724] N91-31123
Analysis and evaluation of selected PACE applications
[AD-A239726] N91-31124
ON-LINE SYSTEMS
Artificial neural networks for seismic data interpretation
[AD-A239673] N91-31743
The on-line d-dimensional dictionary problem
[RUU-CS-90-31] N91-31829
Interactive retrieval in information spaces distributed across a wide-area network N91-31992
OPACITY
Experimental determination of the temperature and density of opacity samples
[DE91-015686] N91-31252
OPERATING SYSTEMS (COMPUTERS)
GEOTRANS: An interface program from GEOPROGRAM to a geographic information system
[DE91-016111] N91-31998
OPERATING TEMPERATURE
Effects of oxidation and combustion environments on the properties of Nicalon/SiC composites
[DE91-016778] N91-31240
Development of elements of a high T(sub c) superconducting cable
[AD-A239766] N91-31543
Carbide fuels for nuclear thermal propulsion
[DE91-016032] N91-31945
OPERATIONS RESEARCH
Investigations on the use of GPS for geodetic and orbit determination applications
[LR-649] N91-31118
OPERATOR PERFORMANCE
Low temperature environment operation of turbo engines: A military operator's experience and requirements N91-31145
OPERATORS (PERSONNEL)
Tuning maps for setpoint changes and load disturbance upsets in a three capacity process under multivariable control
[NASA-TM-104419] N91-31876
OPTICAL COMMUNICATION
Recent advances in fiber optics components for high speed data transmission
[DE91-016252] N91-31948
OPTICAL CORRELATORS
Multitarget tracking using optical processing
[AD-A239656] N91-31953
OPTICAL COUPLING
Avioptic plug-in interconnection
[PATENT-1-254-415] N91-31946
OPTICAL DATA PROCESSING
Hybrid electro-optic processor
[AD-A239547] N91-31505
Advanced optical sensing and processing technologies for the distributed control of large flexible spacecraft
[NASA-CR-4399] N91-31609
Multitarget tracking using optical processing
[AD-A239656] N91-31953
OPTICAL EQUIPMENT
Hybrid electro-optic processor
[AD-A239547] N91-31505
Facet development for a faceted stretched-membrane dish by Solar Kinetics, Inc.
[DE91-016866] N91-31713
Recent advances in fiber optics components for high speed data transmission
[DE91-016252] N91-31948
Plasma-optics systems for the formation and focusing of ion beams N91-31956
OPTICAL FIBERS
A simple model for the motion of pulsed-laser-driven thin flyers
[DE91-011325] N91-31634
Avioptic plug-in interconnection
[PATENT-1-254-415] N91-31946
OPTICAL MEASUREMENT
Experimental determination of the temperature and density of opacity samples
[DE91-015686] N91-31252
Advanced and non-conventional optical schemes N91-31626
Quasi-elastic light scattering and applications to optical sizing N91-31627
Measurements of inception time lags of repetitively pulsed corona in air N91-32028
OPTICAL MEMORY (DATA STORAGE)
System and method for automatically fabricating multiple memory holographic elements
[PATENT-1-253-724] N91-31600

OPTICAL MICROSCOPES
Design and analysis of multilayer x ray/XUV microscope
[NASA-CR-184197] N91-31607
OPTICAL RADAR
An adaptive coherent optical receiver array
[AD-A239672] N91-31644
OPTICAL REFLECTION
Acceleration using total internal reflection
[DE91-016612] N91-31942
OPTIMAL CONTROL
Control of oscillatory forces on a circular cylinder by rotation
[NASA-CR-187619] N91-31576
OPTIMIZATION
Enhanced global positioning system delta-range processing
[PATENT-1-254-637] N91-31115
Two alternative ways for solving the coordination problem in multilevel optimization
[NASA-TM-104036] N91-31138
A technique for locating function roots and for satisfying equality constraints in optimization
[NASA-TM-104037] N91-31139
Cold start optimization on a military jet engine N91-31151
Possibilities of simulation and optimization for guided missile systems
[MBB-UA-1201-90-PUB] N91-31183
Optimization techniques applied to passive measures for in-orbit spacecraft survivability
[NASA-CR-184198] N91-31204
Inter-GEN: A hybrid approach to engineering design optimization N91-31471
Improvements to programs for system studies of space-based radar
[DRE-179] N91-31484
Application of the constrained implicants set concept to the minimization of binary functions
[AD-A239470] N91-31859
OPTOELECTRONIC DEVICES
An investigation of optically controlled, integrated millimeter wave receiving phased arrays
[AD-A239504] N91-31538
Advanced optical sensing and processing technologies for the distributed control of large flexible spacecraft
[NASA-CR-4399] N91-31609
Micromechanical concepts in optics and optoelectronics
[MBB-Z-0339-90-PUB] N91-31949
ORBIT CALCULATION
On the optimal use of fictitious time in variation of parameters methods with application to BG14
[NASA-CR-185650] N91-31890
ORBIT TRANSFER VEHICLES
Contributions to a space station for flights in the near field and towards geostationary Earth orbit
[ETN-91-99744] N91-31203
ORBITAL VELOCITY
Automatic satellite tracking system for the NASA Satellite Photometric Observatory
[NASA-TM-105037] N91-31194
ORGANIC COMPOUNDS
Production of organic chemicals via bioconversion: A review of the potential
[DE91-015524] N91-31223
ORGANOMETALLIC COMPOUNDS
Innovative optoelectronic materials and structures using OMVPE
[AD-A239518] N91-31951
Advanced research workshop on Wide Gap II-VI Semiconductors
[AD-A233796] N91-31960
ORIGINS
Origins of GPS surveying
[AD-A239676] N91-31121
OSCILLATING FLOW
Oscillatory Marangoni convection (TEXUS 3A and 3B) N91-31333
Critical Marangoni number (TEXUS 5) N91-31334
Critical Marangoni number (TEXUS 8) N91-31335
Oscillatory and turbulent flow regimes due to Marangoni convection (TEXUS 7) N91-31337
Experimental results on microgravitational fluid dynamics (TEXUS 14b) ESA N91-31342
OSCILLATIONS
Control of oscillatory forces on a circular cylinder by rotation
[NASA-CR-187619] N91-31576
A search for periodicity in the x ray spectrum of black hole candidate A0620-00
[AD-A239488] N91-32011
OSCILLATORS
Numerical simulation of a split cavity oscillator and rf conversion
[DE91-016501] N91-31523
Bifurcations of parametrically forced oscillators
[W-9007] N91-31892
OXIDATION
Effects of oxidation and combustion environments on the properties of Nicalon/SiC composites
[DE91-016778] N91-31240
High pressure catalytic reactions over single-crystal metal surfaces
[DE91-016475] N91-31256
Chemically modified electrodes and related solution studies
[DE91-016740] N91-31262
Initial determination of the micromechanical properties of oxide scales
[DE90-012164] N91-31291
Low cost, formable, high T(sub c) superconducting wire
[NASA-CASE-LEW-14676-1] N91-31529
Near-edge study of gold-substituted YBa2Cu3O(7-delta)
[NASA-TM-105220] N91-31977
Limited reaction processing for semiconductor materials preparation
[AD-A239639] N91-31983
The selective catalytic oxidation of ammonia to N2 and H2O over silica-supported molybdena catalysts N91-32026
OXIDATION RESISTANCE
Skin technology (TEXUS 9) N91-31459
Skin technology (TEXUS 11 and 12) N91-31460
OXIDATION-REDUCTION REACTIONS
Interfacial systems for photochemical energy conversion
[DE91-015743] N91-31700
OXIDES
Initial determination of the micromechanical properties of oxide scales
[DE90-012164] N91-31291
OXYGEN
Copper-alumina suspensions (TEXUS 5) N91-31434
The medical hazards of flame-suppressant atmospheres
[AD-A239618] N91-31806
Testing and evaluation of the catalyst research MiniOX 3 oxygen monitor
[AD-A239665] N91-31807
Properties of low temperature, low oxygen pressure post-annealed YBa2Cu3O(sub 7-x) thin films
[DE91-015632] N91-31969
The selective catalytic oxidation of ammonia to N2 and H2O over silica-supported molybdena catalysts N91-32026
OZONE
Retrieval and molecule sensitivity studies for the global ozone monitoring experiment and the scanning imaging absorption spectrometer for atmospheric chartography N91-31724
A system to determine whole-plant exchange rates of ozone, carbon dioxide and water vapour N91-32027

P

P-N JUNCTIONS
A three-dimensional code to solve the Poisson equation: Numerical simulation of the breakdown in P-N junction devices
[ECL-90-27] N91-31525
PACIFIC OCEAN
A summary of the physical oceanography of the Pacific Northwest Coast
[PB91-164434] N91-31753
North Pacific guyots
[AD-A239388] N91-31754
PACKETS (COMMUNICATION)
Adaptive arrays in packet radio networks
[AD-A239636] N91-31509
PALLADIUM ALLOYS
Theoretical studies of metallic alloys
[DE91-016486] N91-31281
Dynamic yield strength of a palladium alloy metallic glass
[DE91-015111] N91-31298
PANEL FLUTTER
User's guide to a system of finite-element supersonic panel flutter programs
[NASA-TM-104109] N91-31082
PANEL METHOD (FLUID DYNAMICS)
Development of an advanced panel method for complex configurations in subsonic compressible flow; application to the computation of the potential flow through ducts
[NLR-TR-88001-U] N91-31579
Algorithms for finding an optimal matching between a given string and a string generated by a regular grammar
[MEMO-921] N91-31845
PANELS
Method for fastening aircraft frame elements to sandwich skin panels covering same using woven fiber connectors
[PATENT-1-274-075] N91-31126
PARABOLIC DIFFERENTIAL EQUATIONS
Three dimensional acoustic propagation at low temperature attitude
[ONERA-RT-13/3641-PY] N91-31924
Use of an ARMA model in turbulent medium acoustic propagation
[ONERA-RF-14/3641-PY] N91-31925
PARABOLIC REFLECTORS
Facet development for a faceted stretched-membrane dish by Solar Kinetics, Inc.
[DE91-016866] N91-31713
Parabolic dish photovoltaic concentrator development
[DE91-016868] N91-31714
PARAFFINS
The autoignition chemistry of paraffinic fuels and pro-knock and anti-knock additives: A detailed chemical kinetic study
[DE91-014992] N91-31314
PARALLEL COMPUTERS
Three dimensional Euler equation solving on parallel machines
[ETN-91-99913] N91-31583
A users' guide to PVM (parallel virtual machine)
[DE91-016934] N91-31855
PARALLEL PROCESSING (COMPUTERS)
Local area gigabit networking
[DE91-014780] N91-31869
The PVM system: Supercomputer level concurrent computation on a heterogeneous network of workstations
[DE91-016276] N91-31870
PARALLEL PROGRAMMING
Three dimensional Euler equation solving on parallel machines
[ETN-91-99913] N91-31583
PARAMETER IDENTIFICATION
Identifying behavior characteristics using pressuremeter tests
[ETN-91-99917] N91-31680
Parameter identification for two-point boundary value processes
[MEMO-917] N91-31909
PARAMETERIZATION
Impact of the ice phase on a mesoscale convective system: Cloud ensemble features and cloud radiative properties
[DE91-015769] N91-31749
PARSING ALGORITHMS
Omission of symbols
[CS-9101] N91-31821
A simplification of Earley's algorithm
[CS-9102] N91-31822
LR-parsing derived
[CS-9105] N91-31823
The hierarchy of LR-attributed grammars
[MEMO-INF-91-26] N91-31840
Attribute evaluation and parsing
[MEMO-INF-91-31] N91-31841
PARTIAL DIFFERENTIAL EQUATIONS
An extension of mesh equidistribution to time-dependent partial differential equations
[AD-A239579] N91-31913
PARTICLE ACCELERATION
A study of ion acceleration at rocket altitudes and development and calibration of pitch angle imaging charged particle detectors N91-31728
The Li-7 and Be-7 deexcitation lines: Probes for accelerated particle transport models in solar flares
[NASA-CR-183490] N91-32020
PARTICLE ACCELERATOR TARGETS
High energy physics
[DE91-015796] N91-31939
PARTICLE ACCELERATORS
The timing of injection kickers
[NIKHEF-K/AMPS/91-04] N91-31943
PARTICLE COLLISIONS
Searching for the Higgs in ep collisions at LEP/LHC
[DE91-015701] N91-31930
Particle production through two-photon processes in relativistic heavy-ion colliders
[DE91-016221] N91-31931
An interparticle collision model for electromagnetic hybrid simulations of high density plasmas
[DE91-016025] N91-31958
PARTICLE INTERACTIONS
The interaction of particles with homogeneous turbulence N91-31548
The effects of fluid particle interactions on interfacial transfer and flow structure
[DE91-016409] N91-31575

A research program in experimental high energy physics
[DE91-016208] N91-31941
The Li-7 and Be-7 deexcitation lines: Probes for accelerated particle transport models in solar flares
[NASA-CR-183490] N91-32020

PARTICLE MOTION
Particle image velocimetry: Photographic and video techniques N91-31628
Unsteady flow past an airfoil pitching at a constant rate N91-31629
Proceedings of the Ninth Symposium on Energy Engineering Sciences: Fluid and Dynamical Systems
[DE91-015974] N91-31701

PARTICLE PRODUCTION
Searching for the Higgs in ep collisions at LEP/LHC
[DE91-015701] N91-31930
Particle production through two-photon processes in relativistic heavy-ion colliders
[DE91-016221] N91-31931
Intrinsic neutron source strengths in uranium solutions
[DE91-016091] N91-31933
High energy physics
[DE91-015796] N91-31939
A research program in experimental high energy physics
[DE91-016208] N91-31941

PARTICLE SIZE DISTRIBUTION
The effects of fluid particle interactions on interfacial transfer and flow structure
[DE91-016409] N91-31575

PARTICLE THEORY
BAe overview of current gravitational physics research N91-31731
High energy physics program. Task A: Experiment and Theory. Task B: Numerical simulation of quantum field theories
[DE91-015652] N91-31938
Nuclear and particle astrophysics
[DE91-016260] N91-32016

PARTICLE TRAJECTORIES
Application of a water droplet trajectory prediction code to the design of inlet particle separator anti-icing systems N91-31159

PARTICLES
Dispersion electrolysis (TEXUS 4) N91-31351
Dispersion electrolysis (TEXUS 7) N91-31352
Dispersion electrolysis (TEXUS 9) N91-31353
Generation of particles and seeding N91-31618

PARTICULATES
Electrostatic precipitation of condensed acid mist
[DE91-016530] N91-31260

PASCAL (PROGRAMMING LANGUAGE)
Methods of astrodynamics, a computer approach
[AD-A239662] N91-31861
A solution for the network database problem in an imperative language N91-31864

PASSIVITY
Stress corrosion cracking of 2091 ad 8090 aluminum-lithium alloys in chloride containing aqueous solutions. Influence of sulphate and nitrate additions
[REPT-431/91] N91-31285

PATTERN RECOGNITION
Atomatic Feature (AFEAT) identification for Computer-Aided Process Planning (CAPP)
[DE91-016478] N91-31819
A graph theoretic approach to scene matching
[NASA-CR-187817] N91-31947
Multitarget tracking using optical processing
[AD-A239656] N91-31953

PAVEMENTS
A knowledge-base for rehabilitation of airfield concrete pavements
[AD-A239354] N91-31191

PAYLOAD DELIVERY (STS)
The question of an efficient space transportation system for extraterrestrial materials
[ILR-MITT-252(1990)] N91-31197

PENETRATION
Electromagnetic penetration of slot apertures with depth and losses
[DE91-016401] N91-31500
Evaluation of the intermittent GTA cold wire feed weld system
[DE91-016477] N91-31657

PENTOSE
The conversion of lignocellulosics to fermentable sugars: A survey of current research and application to CELSS N91-31784

PEPTIDES
Muramyl peptide-enhanced sleep: Pharmacological optimization of performance
[AD-A239442] N91-31766

PERFORMANCE PREDICTION
Pulse Doppler radar simulation study
[ASSGI-14SV-W7714-7-5353] N91-31486
The analysis and design of brushless DC motors N91-31516

PERFORMANCE TESTS
Performance Assessment and Coverage Evaluation (PACE) workstation (user manual)
[AD-A239723] N91-31122
OMEGA system Performance Assessment and Coverage Evaluation (PACE) workstation design and implementation, volume 2
[AD-A239724] N91-31123
Performance evaluation of insensitive explosives
[DE91-015767] N91-31315
Updates to the DREO airborne radar simulator
[ASSGI-167] N91-31478
Aeronautical Mobile Satellite Service (AMSS) test plan
[DOT/FAA/CT-TN91/20] N91-31495
A methodology for producing and testing a genesil silicon compiler designed VLSI chip which incorporates design for testability
[AD-A239465] N91-31537
Analysis and development of a wide-bandwidth gravitational wave detector N91-31601
Identifying behavior characteristics using pressuremeter tests
[ETN-91-99917] N91-31680
The feasibility of testing NASA's SCAD concentrator on Earth
[DE91-016055] N91-31702
Controlled ecological life support system breadboard project, 1988 N91-31791
Female aircrew: The Canadian Forces experience, 1979-1989
[DCIEM-90-P-14] N91-31801

PERIODIC VARIATIONS
Bifurcations of parametrically forced oscillators
[W-9007] N91-31892
A search for periodicity in the x ray spectrum of black hole candidate A0620-00
[AD-A239488] N91-32011

PERMUTATIONS
On a ternary bracketing problem from the theory of formal languages
[TR-90-24] N91-31825
On a theorem of MacMahon
[CS-9104] N91-31894

PERSONNEL
Developments in medical audit in hospitals in the National Health Service
[ETN-91-99984] N91-31762
Improving managers' effectiveness
[DE91-016405] N91-31988

PERSONNEL SELECTION
Female aircrew: The Canadian Forces experience, 1979-1989
[DCIEM-90-P-14] N91-31801

PERTURBATION
Three dimensional extension of a numerical method for resolving small transonic perturbations in unstructured mesh
[ONERA-RT-50/3064-RY-093-R] N91-31095
Robustness and techniques of multivariable control for helicopter piloting. Dispatch 3: Inclusion regions technique on linear model
[RD/PA-14-227] N91-31184
Application of microwave cavity perturbation techniques in conducting polymers
[AD-A239376] N91-31310

PERTURBATION THEORY
Computational analysis of hypersonic flows past elliptic-cone waveriders N91-31080
Dynamic disturbance decoupling for discrete-time nonlinear systems
[MEMO-913] N91-31843

PHARMACOLOGY
Nuclear medicine and imaging research: Quantitative studies in radiopharmaceutical science
[DE91-015447] N91-31759
Muramyl peptide-enhanced sleep: Pharmacological optimization of performance
[AD-A239442] N91-31766

PHASE DIAGRAMS
Segregation behaviour of rare earths under microgravity and normal gravity conditions (TEXUS 13) N91-31407

PHASE SHIFT
Phased array components for the High Temperature Superconducting Space Experiment (HTSSE)
[AD-A239361] N91-31535

PHASE TRANSFORMATIONS
Oscillatory Marangoni convection (TEXUS 3A and 3B) N91-31333
Critical Marangoni number (TEXUS 5) N91-31334
Critical Marangoni number (TEXUS 8) N91-31335
Experimental results on microgravitational fluid dynamics (TEXUS 14b) ESA N91-31342
Phase transition (TEXUS 8) N91-31374
Ionic solutions near the critical point of water (TEXUS 10) ESA N91-31375
Ionic solutions near the critical point of water (TEXUS 12) ESA N91-31376
Phase separation of a binary fluid near its critical point (TEXUS 11) N91-31377
Phase separation in microgravity of binary fluids near the critical point (TEXUS 13) N91-31378
Spinoidal decomposition (TEXUS 17) N91-31379
Composite materials, 1 (TEXUS 1) N91-31408
Composite materials, 2 (TEXUS 2) N91-31409
Fundamental studies in the manganese-bismuth system (TEXUS 2) N91-31414
Crystallization and characterization of Y2O3-SiO2 glasses N91-31962
Microstructural changes in Beta-silicon nitride grains upon crystallizing the grain-boundary glass N91-31963

PHASED ARRAYS
Phased array components for the High Temperature Superconducting Space Experiment (HTSSE)
[AD-A239361] N91-31535
An investigation of optically controlled, integrated millimeter wave receiving phased arrays
[AD-A239504] N91-31538

PHENYLS
Mass resolved excitation spectroscopy of benzyl and phenyinitrene radicals
[AD-A239394] N91-31264

PHONONS
Cu-O charge fluctuations and electron-phonon coupling in the effective single-band Hubbard theory for cuprate superconductors
[DE91-016526] N91-31976

PHOSPHIDES
Innovative optoelectronic materials and structures using OMVPE
[AD-A239518] N91-31951

PHOSPHORIC ACID FUEL CELLS
Fuel cells for commercial energy
[MBB-UE-0018-90-PUB] N91-31706

PHOSPHORS
A relative-intensity two-color phosphor thermography system
[NASA-TM-104123] N91-31595
Single layer multi-color luminescent display
[NASA-CASE-LAR-13616-1] N91-31950
Photophysics and chemistry of ultra-fast ZnO and CdS phosphors
[DE91-013106] N91-31966

PHOTOCHEMICAL REACTIONS
Laser Fourier densitometry and laser induced photochemical anemometry in supersonic flow
[AAAF-NT-89-09] N91-31103
Summaries of FY 1991 research in the chemical sciences
[DE91-011221] N91-31222
Interfacial systems for photochemical energy conversion
[DE91-015743] N91-31700
Pyrimidine dimer formation by UVA radiation: Implications for photoreactivation
[DE91-015837] N91-31756
Photophysics and chemistry of ultra-fast ZnO and CdS phosphors
[DE91-013106] N91-31966

PHOTOCONDUCTORS
Etching method for photoresists or polymers
[NASA-CASE-ARC-11873-2] N91-31258

PHOTOELASTIC ANALYSIS
Photoelastic coating study of redesigned CT114 coupon joint test specimen for horizontal stabilizer rear attachment fitting to vertical stabilizer rear spar
[NAE-LTR-ST-1701] N91-31125

PHOTOELASTIC MATERIALS
Photoelastic coating study of redesigned CT114 coupon joint test specimen for horizontal stabilizer rear attachment fitting to vertical stabilizer rear spar
[NAE-LTR-ST-1701] N91-31125

PHOTOELECTROCHEMISTRY
Summaries of FY 1991 research in the chemical sciences
[DE91-011221] N91-31222
Interfacial systems for photochemical energy conversion
[DE91-015743] N91-31700

PHOTOELECTRON SPECTROSCOPY
KEMA scientific and technical reports, volume 8, number 2, 1990
[ST-REPT-VOL-8-NO-2] N91-32023
Some applications of X-ray photoelectron spectroscopy and secondary-ion mass spectroscopy N91-32029

PHOTOGRAMMETRY
Stereophotogrammetric surveying and interpreting method, and interpreting apparatus
[PATENT-1-254-651] N91-31693

The implementation of a quality system in an aerial mapping company
[ETN-91-99424] N91-31695

PHOTOGRAPHY
Particle image velocimetry: Photographic and video techniques N91-31628

PHOTOLUMINESCENCE
Rapid thermal annealing effects in In(x)Ga(1-x)As/GaAs strained-layer superlattices
[DE91-015901] N91-31978

PHOTOMAPPING
The implementation of a quality system in an aerial mapping company
[ETN-91-99424] N91-31695

PHOTOMETRY
Automatic satellite tracking system for the NASA Satellite Photometric Observatory
[NASA-TM-105037] N91-31194

PHOTONS
Effects of atmospheric CO2 on photosynthetic characteristics of soybean leaves N91-31780
The Li-7 and Be-7 deexcitation lines: Probes for accelerated particle transport models in solar flares
[NASA-CR-183490] N91-32020

PHOTOSYNTHESIS
Exploring the limits of crop productivity: A model to evaluate progress N91-31776
Environmental modification of yield and food composition of cowpea and leaf lettuce N91-31777
Effects of atmospheric CO2 on photosynthetic characteristics of soybean leaves N91-31780
Preparatory space experiments for development of a CELSS N91-31796
A system to determine whole-plant exchange rates of ozone, carbon dioxide and water vapour N91-32027

PHOTOVOLTAIC CELLS
Parabolic dish photovoltaic concentrator development
[DE91-016868] N91-31714

PHOTOVOLTAIC CONVERSION
The status of lightweight photovoltaic space array technology based on amorphous silicon solar cells
[DE91-014985] N91-31698
One-sun, single-crystalline silicon solar cell research
[DE91-015646] N91-31699
The 1991 DOE/Sandia Crystalline Photovoltaic Technology Project Review Meeting
[DE91-016062] N91-31703

PHOTOVOLTAIC EFFECT
The status of lightweight photovoltaic space array technology based on amorphous silicon solar cells
[DE91-014985] N91-31698
The photovoltaic effect on pyroelectics N91-31707

PHYSICAL CHEMISTRY
Electrolytic hydrogen formation (TEXUS 1) N91-31347
Electrolytically generated hydrogen bubbles (TEXUS 6) N91-31348
Intermittent polarization (TEXUS 2) N91-31349
Dispersion layers by electrodeposition (TEXUS 1) N91-31350
Dispersion electrolysis (TEXUS 4) N91-31351
Dispersion electrolysis (TEXUS 7) N91-31352
Dispersion electrolysis (TEXUS 9) N91-31353
Nucleate pool boiling (TEXUS 3) N91-31354
Bubble formation, 1 (TEXUS 5) N91-31355
Bubble formation, 2 (TEXUS 10) N91-31356
Bubble formation, 2. Microgravity measurements of the boiling heat transfer from flat heating surfaces (TEXUS 11) N91-31357
Inst. A fuer Thermodynamik. N91-31358
Ultrasound absorption in molten salts (TEXUS 14b) N91-31359
Ultrasound absorption in molten salts (TEXUS 17) ESA N91-31360
Thermal conductivity of liquids (MASER 1) ESA N91-31361
Colloid chemistry (TEXUS 17) ESA N91-31362
A note on 'the matching polynomial of a polygraph'
[MEMO-910] N91-31905

PHYSICAL EXERCISE
The effect of exercise training on skeletal muscle glucose transorter isoform GLUT4 concentration in the obese Zucker rat
[AD-A239461] N91-31757

PHYSIOLOGICAL EFFECTS
The effect of exercise training on skeletal muscle glucose transorter isoform GLUT4 concentration in the obese Zucker rat
[AD-A239461] N91-31757
Naval medical research and development command
[AD-A239393] N91-31765

PHYSIOLOGICAL RESPONSES
The G-LOC syndrome
[AD-A239561] N91-31768
The medical hazards of flame-suppressant atmospheres
[AD-A239618] N91-31806

PHYSIOLOGICAL TESTS
Continuous 24 hour ECG study, on ground and in flight, of 19 Mirage 2000 pilots stationed at the Dijon airbase (France). Comparison with similar recordings taken on other types of fighter aircraft or in operationally different conditions
[ETN-91-99973] N91-31761

PHYTOTRONS
The crop growth research chamber: A ground-based facility for CELSS research N91-31792
A perspective on CELSS control issues N91-31794

PILOT PERFORMANCE
Continuous 24 hour ECG study, on ground and in flight, of 19 Mirage 2000 pilots stationed at the Dijon airbase (France). Comparison with similar recordings taken on other types of fighter aircraft or in operationally different conditions
[ETN-91-99973] N91-31761
Female aircrew: The Canadian Forces experience, 1979-1989
[DCIEM-90-P-14] N91-31801
Cockpit resource management: Effects on behavioral interactions across airlines and aircraft types
[AD-A239467] N91-31804

PILOT TRAINING
Cockpit resource management: Effects on behavioral interactions across airlines and aircraft types
[AD-A239467] N91-31804

PINCH EFFECT
Electron-beam-pinch experiment at Harry Diamond Laboratories: Providing for a high-dose-rate flash x ray facility for Transient Radiation Effects on Electronics (TREE) testing of pieceparts
[AD-A239558] N91-31193

PIPES (TUBES)
Torsion resistant grooved joint
[PATENT-1-258-589] N91-31127
Factors affecting plant growth in membrane nutrient delivery N91-31797
Technology for subsystems of space-based plant growth facilities N91-31799

PISTON ENGINES
Diagnostic tools for reciprocating engine systems
[PB91-184960] N91-31645

PLANE WAVES
Modelling the response of thick composite materials due to axisymmetric shock loading
[AD-A239531] N91-31243

PLANETARY BOUNDARY LAYER
Plasma diffusion at the magnetopause? The case of lower hybrid drift waves
[NASA-CR-188913] N91-31957

PLANTS (BOTANY)
Review of microgravity N91-31736
Method and apparatus for bio-regenerative life support system
[NASA-CASE-MSC-21629-1] N91-31803

PLASMA CONTROL
Computational model for deterministic chaos in a magnetically confined plasma
[DE91-016022] N91-31955
An interparticle collision model for electromagnetic hybrid simulations of high density plasmas
[DE91-016025] N91-31958

PLASMA DENSITY
An interparticle collision model for electromagnetic hybrid simulations of high density plasmas
[DE91-016025] N91-31958

PLASMA DIFFUSION
Plasma diffusion at the magnetopause? The case of lower hybrid drift waves
[NASA-CR-188913] N91-31957

PLASMA DRIFT
Plasma diffusion at the magnetopause? The case of lower hybrid drift waves
[NASA-CR-188913] N91-31957

PLASMA JET WIND TUNNELS
Vaudreuil (France) large hydrodynamic tunnel: Acoustic chamber damping
[METRAVIB-RDS-1-007-67] N91-31090

PLASMA JETS
Etching method for photoresists or polymers
[NASA-CASE-ARC-11873-2] N91-31258

PLASMA PHYSICS
Activities report of the Institute of Extraterrestrial Physics
[MPE-223] N91-32002

PLASMA SPRAYING
Process for producing plasma sprayed carbide-based coatings with minimal decarburization and near theoretical density
[DE91-012016] N91-31292
Beneficial effects of austemper post-treatment on tungsten carbide based wear coatings
[DE91-013260] N91-31293

PLASMA WAVES
Plasma diffusion at the magnetopause? The case of lower hybrid drift waves
[NASA-CR-188913] N91-31957

PLASMAS (PHYSICS)
Computational model for deterministic chaos in a magnetically confined plasma
[DE91-016022] N91-31955
Plasma-optics systems for the formation and focusing of ion beams N91-31956

PLASTIC DEFORMATION
Plastic deformation processes in relation to molecular structure
[ETN-91-99916] N91-31233
Fracture toughness characterization of polymers N91-31296

PLASTIC FLOW
The influence of plastic-strain-induced anisotropy on stress distributions in the finite deformation of ductile metals N91-31273

PLASTIC PROPERTIES
Experimental and analytical analysis of stress-strain behavior in a (90/0 deg)2s, SiC/Ti-15-3 laminate
[NASA-TM-104470] N91-31235
Reliability of computational analysis of plasticity problems
[AD-A239646] N91-31691

PLASTICS
Fracture toughness characterization of polymers N91-31296

PLATES (STRUCTURAL MEMBERS)
Mobility power flow analysis of coupled plate structure subjected to mechanical and acoustics excitation
[NASA-CR-188791] N91-31678

PLATING
Determination of aqueous processable photoresist in tin-lead plating solutions
[DE91-015575] N91-31251

PLY ORIENTATION
Field 3, theme 1: Structural materials. Post 2: Thermotropic liquid crystal polymers
[ETN-91-99982] N91-31306

POINT DEFECTS
Atomic structures and compositions of internal interfaces
[DE91-016095] N91-31934

POISSON EQUATION
A three-dimensional code to solve the Poisson equation: Numerical simulation of the breakdown in P-N junction devices
[ECL-90-27] N91-31525
Design of a specific integrated circuit for solving the three dimensional Poisson equation
[ECL-90-24] N91-31527

POISSON RATIO
Locking effects in the finite element approximation of elasticity problems
[AD-A239645] N91-31914

POLAR CAPS
The motions of Mars' pole N91-32019

POLAR WANDERING (GEOLOGY)
The motions of Mars' pole N91-32019

POLARIMETRY
Introduction to radar polarimetry
[FEL-91-B122] N91-31496

POLARIZATION (WAVES)
Introduction to radar polarimetry
[FEL-91-B122] N91-31496

POLARIZED RADIATION
Introduction to radar polarimetry
[FEL-91-B122] N91-31496

POLAROGRAPHY
Analysis of production solutions by polarography
[DE91-016479] N91-31257

POLISHING
A comparison of techniques for the metallographic preparation of thermal sprayed samples
[DE91-014704] N91-31272

POLLUTION CONTROL
Electrostatic precipitation of condensed acid mist
[DE91-016530] N91-31260
A review of accelerated response actions available to the environmental restoration program: Selected case histories and associated issues
[DE91-013608] N91-31716

POLYESTER RESINS
Parabolic dish photovoltaic concentrator development
[DE91-016868] N91-31714

POLYGONS
Computing minimum length paths of a given homotopy class
[RUU-CS-90-37] N91-31900

POLYHEDRONS
Dynamic output-sensitive hidden surface removal for c-oriented polyhedra
[RUU-CS-91-06] N91-31839
Hidden surface removal for c-oriented polyhedra
[RUU-CS-90-33] N91-31899
POLYMER BLENDS
The formation of novel thermoplastic composites from liquid crystalline polymers and their blends
[AD-A239546] N91-31244
POLYMER MATRIX COMPOSITES
The influence of interphase regions on local thermal stresses and deformations in composites N91-31228
The formation of novel thermoplastic composites from liquid crystalline polymers and their blends
[AD-A239546] N91-31244
Field 3, theme 1: Structural materials. Post 2: Thermotropic liquid crystal polymers
[ETN-91-99982] N91-31306
POLYMERIC FILMS
Composite flexible blanket insulation
[NASA-CASE-NPO-11907-1-NP] N91-31236
Chemically modified electrodes and related solution studies
[DE91-016740] N91-31262
POLYMERIZATION
The formation of novel thermoplastic composites from liquid crystalline polymers and their blends
[AD-A239546] N91-31244
Influence of adhesive polymerization conditions on the durability of adhesive joints
[DCR/I-03357-90] N91-31305
Sensitivity of imaging materials to electron beam irradiation
[AD-A239365] N91-31612
POLYMERS
Etching method for photoresists or polymers
[NASA-CASE-ARC-11873-2] N91-31258
Pseudohomogeneous catalyst layer model for polymer electrolyte fuel cell
[DE91-016014] N91-31710
POLYNOMIALS
An algorithm for spectral factorization of polynomial matrices with any signature
[MEMO-912] N91-31842
An extension of the potential method to higher-order blendings
[CS-9103] N91-31893
Covering a set of points with fixed size hypersquares and related problems
[RUU-CS-90-32] N91-31898
Fitting scattered data on spherelike surfaces using tensor products of trigonometric and polynomial splines
[MEMO-909] N91-31904
A note on 'the matching polynomial of a polygraph'
[MEMO-910] N91-31905
POLYPROPYLENE
The formation of novel thermoplastic composites from liquid crystalline polymers and their blends
[AD-A239546] N91-31244
POLYSACCHARIDES
Use of inedible wheat residues from the KSC-CELSS breadboard facility for production of fungal cellulase N91-31785
POLYURETHANE RESINS
Structure property relationship of aliphatic polyurethane elastomers prepared from CHDI
[AD-A239397] N91-31311
PORCELAIN
Effect of porcelain surface pretreatments on composite resin-porcelain shear bond strength
[AD-A239359] N91-31241
Effect of thickness and brand of metal ceramic porcelain on color
[AD-A239398] N91-31312
POROSITY
Effects of trapped gases on ceramic-filled-glass composite densification
[DE91-015850] N91-31237
Composite materials, 1 (TEXUS 1) N91-31430
Pores in aluminium alloys (TEXUS 3) N91-31447
Preparation of aluminium foams (TEXUS 9) N91-31452
Silicon micromachining based on porous silicon formation
[DE91-013744] N91-31472
POROUS MATERIALS
A boundary integral equation method for steady two-dimensional flow in partially saturated media
[DE91-016056] N91-31573
Proceedings of the Ninth Symposium on Energy Engineering Sciences: Fluid and Dynamical Systems
[DE91-015974] N91-31701
PORTABLE EQUIPMENT
Procedure for steering a low-speed missile, weapon system, and missile for implementation of the procedure
[PATENT-1-265-947] N91-31182
POSITION (LOCATION)
Investigations on the use of GPS for geodetic and orbit determination applications
[LR-649] N91-31118
A technique for locating function roots and for satisfying equality constraints in optimization
[NASA-TM-104037] N91-31139
Emergency locating transmitter
[NASA-CASE-GSC-12821-2] N91-31530
POSITION INDICATORS
Beacon activation device
[PATENT-1-256-916] N91-31108
POSITION SENSING
Passive ranging of an airborne emitter by a single non-maneuvering or stationary sensor
[PATENT-1-254-292] N91-31116
POTATOES
Environmental and cultural considerations for growth of potatoes in CELSS N91-31779
Sweet potato for closed ecological life support systems using the nutrient film technique N91-31782
POTENTIAL ENERGY
Model description of transition metals using the rotated second moment approximation
[DE91-016043] N91-31287
POTENTIAL FLOW
Development of an advanced panel method for complex configurations in subsonic compressible flow; application to the computation of the potential flow through ducts
[NLR-TR-88001-U] N91-31579
Algorithms for finding an optimal matching between a given string and a string generated by a regular grammar
[MEMO-921] N91-31845
POWDER (PARTICLES)
Mechanical behavior of a nickel based alloy UDIMET 700 fabricated by powder metallurgy
[JUEL-2414] N91-31283
Tungsten composites (TEXUS 19) ESA N91-31445
POWDER METALLURGY
Mechanical behavior of a nickel based alloy UDIMET 700 fabricated by powder metallurgy
[JUEL-2414] N91-31283
Dispersion alloys (TEXUS 7) N91-31412
Al-Pb bearing alloy (TEXUS 1) N91-31413
Tungsten composites (TEXUS 10) N91-31444
Gas bubbles in a copper-alumina suspension (TEXUS 11) N91-31453
POWDERED ALUMINUM
Understanding composite explosive energetics
[DE91-015770] N91-31316
POWER CONDITIONING
Proceedings of the International Magnetic Pulse Compression Workshop. Volume 2: Technical summary
[DE91-015775] N91-31521
POWER CONVERTERS
Development of single blade rotor wind energy converters: From M400 prototype to MON 50 preseries
[MBB-UE-0015-90-PUB] N91-31705
POWER GAIN
Dynamics of 1.3 micron semiconductor lasers and nonlinear gain N91-31613
POWER LINES
Development of elements of a high T(sub c) superconducting cable
[AD-A239766] N91-31543
KEMA scientific and technical reports, volume 8, number 2, 1990
[ST-REPT-VOL-8-NO-2] N91-32023
The critical temperature for drying-out of soils around power cables as a function of local conditions N91-32025
POWER SERIES
A formal power series equation from formula complexity theory
[TR-90-25] N91-31895
PRECESSION
The motions of Mars' pole N91-32019
PRECIPITATES
A jet polishing technique for thinning two phase materials
[DE91-016422] N91-31473
PRECIPITATION (CHEMISTRY)
The coalescence process in immiscible alloys (TEXUS 5) N91-31417
Unidirectional solidification of immiscible alloys (TEXUS 5) N91-31418
Unidirectional solidification of Zn-Bi samples (TEXUS 14b) N91-31420
PRECIPITATION (METEOROLOGY)
The use of distributional and pointwise statistical measures in GCM intercomparisons
[DE91-015697] N91-31748
PRECIPITATION HARDENING
Stress relaxation in bending of type AISI 304 stainless steel at 773K and 823K
[DE91-618657] N91-31666
PREDICTION ANALYSIS TECHNIQUES
User's guide to a system of finite-element supersonic panel flutter programs
[NASA-TM-104109] N91-31082
Application of a water droplet trajectory prediction code to the design of inlet particle separator anti-icing systems N91-31159
An analytical prediction of matrix cracking in fibrous composite laminates N91-31225
Catalysis-by-design impacts assessment
[DE91-013280] N91-31247
The analysis and design of brushless DC motors N91-31516
Fifth force experiments N91-31733
PREDICTIONS
A comparison of several theories which use jet scaling to predict liftoff heights of turbulent-jet flames
[AD-A239717] N91-31267
PREDICTOR-CORRECTOR METHODS
Practical aspects of an interior-point method for convex programming
[AD-A239457] N91-31858
PRESSURE DISTRIBUTION
Development and validation of characteristic boundary conditions for cell-centered Euler flow calculations with a shock-free airfoil
[NLR-TP-89360-U] N91-31081
Contribution of low wave numbers to the wall pressure field in a two dimensional turbulent boundary layer: Comparison of different experimental techniques
[ECL-90-15] N91-31091
Conditional sampling
[AAAF-NT-89-04] N91-31099
Vortex-blade interaction on a helicopter principal rotor. Validation of the S2DI computation program and study of vortex models
[ONERA-RT-92/5094-PY] N91-31136
Prediction of rotor surface unsteady pressure and heat transfer from wake passing N91-31549
Postprocessing of experimental and numerical results in the case of two and three dimensional flows
[AAAF-NT-89-25] N91-31592
Fuselage shell and cavity response measurements on a DC-9 test section
[NASA-CR-187557] N91-31926
PRESSURE EFFECTS
The influence of moisture and pressure on the mechanical properties of a glass-epoxy matrix composite and a graphite-epoxy matrix composite
[AD-A239509] N91-31242
X ray and gamma ray spectroscopy of solids under pressure
[DE91-016948] N91-31263
Influence of loading rate on the mechanical response and substructure evolution of shock-loaded copper
[DE91-013390] N91-31276
Pressure-strain-temperature relationship in shock loaded cylindrical samples of 304 stainless steel
[DE91-013379] N91-31673
Properties of low temperature, low oxygen pressure post-annealed YBa2Cu3O(sub 7-x) thin films
[DE91-015632] N91-31969
Studies of the III-V compounds in the megabar regime
[DE91-015911] N91-31973
PRESSURE MEASUREMENT
Conditional sampling
[AAAF-NT-89-04] N91-31099
Airfoil-vortex interaction: Unsteady wall pressure measurement
[AAAF-NT-89-13] N91-31104
HVOF: Particle, flame diagnostics, and coating characteristics
[DE91-014654] N91-31248
Identifying behavior characteristics using pressuremeter tests
[ETN-91-99917] N91-31680
PRESSURE SENSORS
Special design and gauging of anemoclinometric sondes
[IMFL-90/03] N91-31604
PRESSURE VESSELS
Nickel-hydrogen cell low-Earth life test update
[NASA-TM-105229] N91-31708
PRETREATMENT
Effect of porcelain surface pretreatments on composite resin-porcelain shear bond strength
[AD-A239359] N91-31241

PREVAPORIZATION
The influence of fuel characteristics on heterogeneous flame propagation N91-31165
PRINCIPAL COMPONENTS ANALYSIS
Integrated control of thermally distorted large space antennas N91-31487
PRINTED CIRCUITS
Determination of aqueous processable photoresist in tin-lead plating solutions
[DE91-015575] N91-31251
Soldering of complex multilayer printed boards
[CNES-NT-127] N91-31474
PROBABILITY THEORY
Performance Assessment and Coverage Evaluation (PACE) workstation (user manual)
[AD-A239723] N91-31122
Convergence performance of adaptive detectors, part 1
[AD-A239507] N91-31539
Nonlinear probabilistic finite element modeling of composite shells N91-31668
Estimating the strength of the capping inversion and the probability of strong convection
[PB91-176685] N91-31744
Asymmetric soft-error resistant memory
[NASA-CASE-NPO-17394-1-CU] N91-31810
Strong approximation on log dense sets
[W-9101] N91-31916
A pragmatical view on the certainty factor model
[RUU-CS-90-42] N91-31917
Inference networks for document retrieval N91-31993
PROBLEM SOLVING
A technique for locating function roots and for satisfying equality constraints in optimization
[NASA-TM-104037] N91-31139
Three dimensional Euler equation solving on parallel machines
[ETN-91-99913] N91-31583
The derivation of distributed termination detection algorithms from garbage detection schemes
[RUU-CS-90-24] N91-31827
An algorithm for the one-to-all shortest path problem with arbitrary arc lengths
[MEMO-919] N91-31844
Longest segment problems
[RUU-CS-90-28] N91-31896
Extensive coverings and exact core bounds
[MEMO-915] N91-31907
Learning convex bodies under uniform distribution
[MEMO-918] N91-31910
PROCUREMENT
An integer programming model for Navy's maritime patrol aviation fleet
[AD-A239464] N91-31079
PROCUREMENT MANAGEMENT
Acquisition reform: Implementing defense management review initiatives. Report to the Chairman and Ranking Minority Member, Subcommittee on Defense Industry and Technology, Senate Committee on Armed Services
[AD-A239423] N91-31999
PROCUREMENT POLICY
Acquisition reform: Implementing defense management review initiatives. Report to the Chairman and Ranking Minority Member, Subcommittee on Defense Industry and Technology, Senate Committee on Armed Services
[AD-A239423] N91-31999
PRODUCTIVITY
Exploring the limits of crop productivity: A model to evaluate progress N91-31776
PROFILOMETERS
Laser interferometric measurement of ion electrode shape and charge exchange erosion
[NASA-TM-105165] N91-31605
PROGRAM VERIFICATION (COMPUTERS)
Software quality metrics
[DOT/FAA/CT-91/1] N91-31814
PROGRAMMING LANGUAGES
Hardware modeling and top-down design using VHDL
[AD-A239356] N91-31534
LR-parsing derived
[CS-9105] N91-31823
The ABC-machine: A sequential stack-based abstract machine for graph rewriting
[TR-90-22] N91-31824
On a ternary bracketing problem from the theory of formal languages
[TR-90-24] N91-31825
Partial evaluation grammars
[TR-91-01] N91-31826
Categorical semantics as a basis for program transformation
[RUU-CS-90-38] N91-31833
The failure of failures: Towards a paradigm for a synchronous communication
[RUU-CS-90-40] N91-31835
On the application of temporal logic in real time to specify telecommunication protocols
[REPT-90-071] N91-31846
PROJECT MANAGEMENT
Solid-State Radar Beacon Decoder (SSRBD) Master Test Plan (MTP)
[DOT/FAA/CT-TN91/33] N91-31494
The feasibility of testing NASA's SCAD concentrator on Earth
[DE91-016055] N91-31702
What is the Federal Demonstration Project?
[DE91-013936] N91-31986
Acquisition reform: Implementing defense management review initiatives. Report to the Chairman and Ranking Minority Member, Subcommittee on Defense Industry and Technology, Senate Committee on Armed Services
[AD-A239423] N91-31999
Research studies with the International Ultraviolet Explorer
[NASA-CR-183495] N91-32012
PROJECT PLANNING
Aeronautical Mobile Satellite Service (AMSS) test plan
[DOT/FAA/CT-TN91/20] N91-31495
PROJECTILES
Aerothermodynamical project of hypersonic projectiles
[MBB-UA-1193-90-PUB] N91-31086
Dynamic yield strength of a palladium alloy metallic glass
[DE91-015111] N91-31298
PROPELLANT PROPERTIES
The physical properties of a pyrotechnical circuit element
[MBB-UA-1192-90-PUB] N91-31317
PROPELLER NOISE
User's manual for the Langley boundary layer noise propagation program (MRS-BLP)
[NASA-CR-187559] N91-31923
PROPORTIONAL COUNTERS
Multiplexing readout channels in proportional counters
[NASA-TM-103552] N91-31606
PROPULSION
Model of an aerospace plane based on an idealized cone-derived waverider forebody N91-31129
PROPULSION SYSTEM CONFIGURATIONS
Mass comparisons of electric propulsion systems for NSSK of geosynchronous spacecraft
[NASA-TM-105153] N91-31212
Hydrogen test of a small, low specific speed centrifugal pump stage
[NASA-CR-187117] N91-31213
Evaluation of undeveloped rocket engine cycle applications to advanced transportation
[NASA-CR-184205] N91-31215
Medium power hydrogen arcjet performance
[NASA-TM-104533] N91-31216
PROPULSION SYSTEM PERFORMANCE
Fuels and oils as factors in the operation of aero gas turbine engines at low temperatures N91-31163
Icing test capabilities for aircraft propulsion systems at the Arnold Engineering Development Center N91-31170
Mass comparisons of electric propulsion systems for NSSK of geosynchronous spacecraft
[NASA-TM-105153] N91-31212
Hydrogen test of a small, low specific speed centrifugal pump stage
[NASA-CR-187117] N91-31213
Evaluation of undeveloped rocket engine cycle applications to advanced transportation
[NASA-CR-184205] N91-31215
Medium power hydrogen arcjet performance
[NASA-TM-104533] N91-31216
PROTECTIVE COATINGS
Field evaluation of six protective coatings applied to T56 turbine blades after 500 hours of engine use
[ARL-MAT-TM-405] N91-31179
A comparison of techniques for the metallographic preparation of thermal sprayed samples
[DE91-014704] N91-31272
Process for producing plasma sprayed carbide-based coatings with minimal decarburization and near theoretical density
[DE91-012016] N91-31292
Beneficial effects of austemper post-treatment on tungsten carbide based wear coatings
[DE91-013260] N91-31293
Skin technology (TEXUS 3) N91-31457
Skin technology (TEXUS 4) N91-31458
Skin technology (TEXUS 9) N91-31459
Skin technology (TEXUS 11 and 12) N91-31460
Electrophoretic dielectric coatings for magnetic switches
[DE91-015337] N91-31518
PROTEIN CRYSTAL GROWTH
Diffusion-controlled growth of protein single crystals: Investigation of B-galactosidase at low temperature (TEXUS 4) N91-31396
Diffusion-controlled growth of single crystals of protein (TEXUS 5) N91-31397
PROTEIN SYNTHESIS
Cyanobacteria in CELSS: Growth strategies for nutritional variation and nitrogen cycling N91-31786
PROTEINS
Diffusion-controlled growth of protein single crystals: B-galactosidase (TEXUS 3) N91-31395
Diffusion-controlled growth of protein single crystals: Investigation of B-galactosidase at low temperature (TEXUS 4) N91-31396
Environmental modification of yield and food composition of cowpea and leaf lettuce N91-31777
Cyanobacteria in CELSS: Growth strategies for nutritional variation and nitrogen cycling N91-31786
Algae for controlled ecological life support system diet characterization of cyanobacteria 'spirulina' in batch cultures N91-31787
PROTOCOL (COMPUTERS)
Synchronous link-level protocols
[RUU-CS-91-02] N91-31837
On the application of temporal logic in real time to specify telecommunication protocols
[REPT-90-071] N91-31846
PROTONS
Electrochemical energy storage using PEM systems
[DE91-016020] N91-31711
PROTOTYPES
Development of prototype sealed bipolar lithium/sulfide cells
[DE91-015721] N91-31519
Development of single blade rotor wind energy converters: From M400 prototype to MON 50 preseries
[MBB-UE-0015-90-PUB] N91-31705
Inventory and functional prototypes of neural networks
[TR-90-15] N91-31880
PSYCHOLOGICAL EFFECTS
Naval medical research and development command
[AD-A239393] N91-31765
PSYCHOLOGICAL TESTS
Full-information item bi-factor analysis
[AD-A229346] N91-31771
PSYCHOMETRICS
Full-information item bi-factor analysis
[AD-A229346] N91-31771
PSYCHOMOTOR PERFORMANCE
Female aircrew: The Canadian Forces experience, 1979-1989
[DCIEM-90-P-14] N91-31801
PUBLIC HEALTH
Biological dosimetry and mechanisms of carcinogenesis
[DE91-015689] N91-31763
PULSARS
Magnetic field decay in neutron stars with superconducting cores N91-32015
Nuclear and particle astrophysics
[DE91-016260] N91-32016
Fast pulsars, variational bound, other facets of compact stars
[DE91-016416] N91-32018
GRO source candidates: (A) Nearby modest-size molecular clouds; (B) Pulsar with Wolf-Rayet companion that has lost its H-envelope
[NASA-CR-183491] N91-32021
PULSE COMPRESSION
International magnetic pulse compression
[DE91-015774] N91-31520
PULSE DOPPLER RADAR
Improvements to programs for system studies of space-based radar
[DRE-179] N91-31484
PULSE GENERATORS
Proceedings of the International Magnetic Pulse Compression Workshop. Volume 2: Technical summary
[DE91-015775] N91-31521
PULSE RADAR
Updates to the DREO airborne radar simulator
[ASSGI-167] N91-31478
Pulse Doppler radar simulation study
[ASSGI-14SV-W7714-7-5353] N91-31486
PYRIMIDINES
Pyrimidine dimer formation by UVA radiation: Implications for photoreactivation
[DE91-015837] N91-31756
PYROTECHNICS
The physical properties of a pyrotechnical circuit element
[MBB-UA-1192-90-PUB] N91-31317

Q

Q FACTORS
Electromagnetic penetration of slot apertures with depth and losses
[DE91-016401] N91-31500

QUALITY CONTROL
The implementation of a quality system in an aerial mapping company
[ETN-91-99424] N91-31695
Software quality metrics
[DOT/FAA/CT-91/1] N91-31814

QUANTITATIVE ANALYSIS
Determination of aqueous processable photoresist in tin-lead plating solutions
[DE91-015575] N91-31251
Analysis of production solutions by polarography
[DE91-016479] N91-31257

QUANTUM MECHANICS
Macroscopic quantum tunneling in Josephson tunnel junctions and Coulomb blockade in single small tunnel junctions
[DE91-016258] N91-31974

QUANTUM THEORY
High energy physics program. Task A: Experiment and Theory. Task B: Numerical simulation of quantum field theories
[DE91-015652] N91-31938
Advanced research workshop on Wide Gap II-VI Semiconductors
[AD-A233796] N91-31960

QUANTUM WELLS
Electronic transport and lasing in microstructures
[DE91-016751] N91-31641
Innovative optoelectronic materials and structures using OMVPE
[AD-A239518] N91-31951
Ground-state in-plane light-holes in GaAs/AlGaAs structures
[DE91-016408] N91-31980

QUARKS
Fast pulsars, variational bound, other facets of compact stars
[DE91-016416] N91-32018

QUARTZ
Ion-implantation induced crystallization of glass
[DE91-016121] N91-31303

QUEUEING THEORY
Three dimensional Euler equation solving on parallel machines
[ETN-91-99913] N91-31583

R

RABBITS
Cold-induced changes in arterial sensitivity
[AD-A239493] N91-31767

RADAR
Introduction to radar polarimetry
[FEL-91-B122] N91-31496

RADAR ANTENNAS
Behaviour of the SIR for space-based DPCA radar under various spatial clutter distributions
[CRC-W7714-7-5271] N91-31485
A numerical procedure for recovering true scattering coefficients from measurements with wide-beam antennas
[NASA-CR-186042] N91-31492
Airborne ESM receivers: Techniques and technologies
[ETN-91-99988] N91-31498

RADAR BEACONS
Solid-State Radar Beacon Decoder (SSRBD) Master Test Plan (MTP)
[DOT/FAA/CT-TN91/33] N91-31494

RADAR CROSS SECTIONS
Radar-cross-section measurement errors caused by test object interaction with low-dielectric-constant supports
[DE91-015340] N91-31490

RADAR FILTERS
Reconfigurable parameter filter
[PATENT-1-264-072] N91-31513

RADAR IMAGERY
The automatic surveillance, tracking, and imaging program. User manual
[SK-1600-44-001-02-0] N91-31483

RADAR MEASUREMENT
Radar-cross-section measurement errors caused by test object interaction with low-dielectric-constant supports
[DE91-015340] N91-31490
A numerical procedure for recovering true scattering coefficients from measurements with wide-beam antennas
[NASA-CR-186042] N91-31492

RADAR RECEIVERS
Airborne ESM receivers: Techniques and technologies
[ETN-91-99988] N91-31498
Electronic warfare: Faulty test equipment impairs Navy readiness
[AD-A239562] N91-31506
Filter system for radar applications
[PATENT-1-273-409] N91-31512
An adaptive coherent optical receiver array
[AD-A239672] N91-31644

RADAR SCATTERING
A numerical procedure for recovering true scattering coefficients from measurements with wide-beam antennas
[NASA-CR-186042] N91-31492
Introduction to radar polarimetry
[FEL-91-B122] N91-31496

RADAR TRACKING
Bayesian multi-sensor tracking for advanced air-traffic control systems
[NLR-MP-88056-U] N91-31119
The automatic surveillance, tracking, and imaging program. User manual
[SK-1600-44-001-02-0] N91-31483

RADIATION COUNTERS
A study of ion acceleration at rocket altitudes and development and calibration of pitch angle imaging charged particle detectors N91-31728
High energy physics
[DE91-015796] N91-31939
Development of the Burst and Transient Source Experiment (BATSE)
[NASA-RP-1268] N91-32006

RADIATION DETECTORS
Analysis and development of a wide-bandwidth gravitational wave detector N91-31601
Multiplexing readout channels in proportional counters
[NASA-TM-103552] N91-31606
Gravitational wave research N91-31732

RADIATION DISTRIBUTION
Hydrodynamic simulations of cosmology N91-32013

RADIATION DOSAGE
Electron-beam-pinch experiment at Harry Diamond Laboratories: Providing for a high-dose-rate flash x ray facility for Transient Radiation Effects on Electronics (TREE) testing of pieceparts
[AD-A239558] N91-31193
Pyrimidine dimer formation by UVA radiation: Implications for photoreactivation
[DE91-015837] N91-31756

RADIATION EFFECTS
Electron-beam-pinch experiment at Harry Diamond Laboratories: Providing for a high-dose-rate flash x ray facility for Transient Radiation Effects on Electronics (TREE) testing of pieceparts
[AD-A239558] N91-31193
Formation of defect structures in metals during irradiation
[DE91-015548] N91-31278
Impact of the ice phase on a mesoscale convective system: Cloud ensemble features and cloud radiative properties
[DE91-015769] N91-31749
Pyrimidine dimer formation by UVA radiation: Implications for photoreactivation
[DE91-015837] N91-31756
Fast pulsars, variational bound, other facets of compact stars
[DE91-016416] N91-32018

RADIATION HARDENING
Real time actuating of laser power and scanning velocity for thermal regulation during laser hardening
[ETN-91-99908] N91-31636

RADIATION MEASUREMENT
Small satellite radiometric measurements
[DE91-016308] N91-31694
A research program in experimental high energy physics
[DE91-016208] N91-31941

RADIATION SOURCES
Advanced concepts theory
[AD-A239780] N91-31959
GRO source candidates: (A) Nearby modest-size molecular clouds; (B) Pulsar with Wolf-Rayet companion that has lost its H-envelope
[NASA-CR-183491] N91-32021

RADIATION SPECTRA
Retrieval and molecule sensitivity studies for the global ozone monitoring experiment and the scanning imaging absorption spectrometer for atmospheric chartography N91-31724

RADIATION TOLERANCE
Advanced power systems for EOS
[NASA-TM-105222] N91-31217

RADIATION TRANSPORT
A simple model for the motion of pulsed-laser-driven thin flyers
[DE91-011325] N91-31634

RADIATIVE TRANSFER
On the response of the special sensor microwave/imager to the marine environment: Implications for atmospheric parameter retrievals N91-31727

RADICALS
Mass resolved excitation spectroscopy of benzyl and phenylnitrene radicals
[AD-A239394] N91-31264

RADIO ASTRONOMY
A study of a 21-cm-selected sample of galaxies N91-32014

RADIO BEACONS
Beacon activation device
[PATENT-1-256-916] N91-31108

RADIO COMMUNICATION
Antenna study for 60 GHz intersatellite link
[CD-RPT-ITL-5043-003] N91-31482

RADIO FREQUENCIES
Flight tests with a data link used for air traffic control information exchange
[NASA-TP-3135] N91-31143
Spectrum monitoring procedures and techniques
[AD-A239567] N91-31507
Numerical simulation of a split cavity oscillator and rf conversion
[DE91-016501] N91-31523

RADIO RECEIVERS
Adaptive arrays in packet radio networks
[AD-A239636] N91-31509

RADIO TRANSMISSION
Adaptive arrays in packet radio networks
[AD-A239636] N91-31509

RADIOACTIVE DECAY
Magnetic field decay in neutron stars with superconducting cores N91-32015

RADIOCHEMISTRY
Nuclear medicine and imaging research: Quantitative studies in radiopharmaceutical science
[DE91-015447] N91-31759

RADIOMETERS
Small satellite radiometric measurements
[DE91-016308] N91-31694

RADIOSONDES
Description of Crau data set: Meteosat data, radiosonde data, sea surface temperatures: Comparison of Meteosat and Heimann data
[KNMI-WR-90-03] N91-31752

RADOMES
Radome-lens EHF antenna development
[PATENT-1-262-571] N91-31481

RAMAN SPECTRA
Local mean mass volume measurement around a model with lateral jet in supersonic flow
[AAAF-NT-89-08] N91-31102
Chemical characterization of aerosol particles by Raman spectroscopy
[DE91-015836] N91-31720

RAMAN SPECTROSCOPY
Chemical characterization of aerosol particles by Raman spectroscopy
[DE91-015836] N91-31720

RANDOM ACCESS MEMORY
High speed digital direct access filter for tracking or excision of parametric signal data
[PATENT-1-271-231] N91-31511

RANDOM NOISE
Behaviour of the SIR for space-based DPCA radar under various spatial clutter distributions
[CRC-W7714-7-5271] N91-31485

RANDOM PROCESSES
Genetic algorithms
[ETN-91-99985] N91-31852
Computational model for deterministic chaos in a magnetically confined plasma
[DE91-016022] N91-31955

RANDOM VARIABLES
Convergence performance of adaptive detectors, part 2
[AD-A239532] N91-31540

RANDOM WALK
On the relation between recurrence and ergodicity properties in denumerable Markov decision chains
[TW-91-02] N91-31918

RANGE FINDERS
Passive ranging of an airborne emitter by a single non-maneuvering or stationary sensor
[PATENT-1-254-292] N91-31116

RARE EARTH ELEMENTS
Segregation behaviour of rare earths under microgravity and normal gravity conditions (TEXUS 13) N91-31407

REACTION KINETICS
Jet-A reaction mechanism study for combustion application
[NASA-TM-104441] N91-31181
Summaries of FY 1991 research in the chemical sciences
[DE91-011221] N91-31222
Catalysis-by-design impacts assessment
[DE91-013280] N91-31247
The chemistry of transition metal clusters
[DE91-015108] N91-31250
Determination of solvation kinetics in supercritical fluids
[DE91-016096] N91-31253
Correlations between surface structure and catalytic activity/selectivity
[DE91-016453] N91-31255
Atomic hydrogen driven halogen extraction from Si(100): Eley-Rideal surface kinetics
[AD-A239544] N91-31266
The autoignition chemistry of paraffinic fuels and pro-knock and anti-knock additives: A detailed chemical kinetic study
[DE91-014992] N91-31314
Reaction kinetics in glass melts (TEXUS 1) N91-31363
Reaction kinetics in glass melts: Corrosion of SiO2 (TEXUS 4) N91-31364
Reaction kinetics in glass melts: Sodium self-diffusion in alkali-silicate melts (TEXUS 6) N91-31365
Reaction kinetics in molten glasses: Self-diffusion in alkali-silicate melts (TEXUS 20) N91-31368
Sulphur diffusion in liquid cast iron (TEXUS 6) ESA N91-31370
Phase transition (TEXUS 8) N91-31374
KEMA scientific and technical reports, volume 8, number 2, 1990
[ST-REPT-VOL-8-NO-2] N91-32023
Energy and Technology Review, February-March 1991
[DE91-015487] N91-32031

REACTIVITY
Catalyst dispersion and activity under conditions of temperature-staged liquefaction
[DE91-016602] N91-31261

REACTOR DESIGN
An investigation of dual-mode operation of a nuclear-thermal rocket engine
[DE91-015977] N91-31210
A review of the Los Alamos effort in the development of nuclear rocket propulsion
[DE91-016036] N91-31211

REACTOR SAFETY
Mechanical characterization of seismic base isolation elastomers
[DE91-015680] N91-31299

REACTOR TECHNOLOGY
Experiments on ultrasonic thermometry for wet-ash coal gasification N91-32024

READOUT
High-speed TV cameras for streak tube readout
[DE91-016081] N91-31602
Multiplexing readout channels in proportional counters
[NASA-TM-103552] N91-31606

REAL TIME OPERATION
A case study for the real-time experimental evaluation of the VIPER microprocessor
[NASA-TM-104098] N91-31531
Real time actuating of laser power and scanning velocity for thermal regulation during laser hardening
[ETN-91-99908] N91-31636
Analysis and development of a real-time control methodology in resistance spot welding N91-31646
Design and cost of the first commercial stretched-membrane heliostat
[DE91-016870] N91-31715
Design and analysis of fault-tolerant distributed real-time computer systems
[AD-A239521] N91-31812
On the application of temporal logic in real time to specify telecommunication protocols
[REPT-90-071] N91-31846
Application of an acquisition image processing system to the quantitative analysis of flows
[AAAF-NT-89-27] N91-31851
Construction and realization of distributed multiprocessor systems for real time tasks
[MBB-UA-1189-90-PUB] N91-31871
Design and analysis of fault-tolerant distributed real-time computer systems
[AD-A239382] N91-31875
Synchronized computational architecture for generalized bilateral control of robot arms
[NASA-CASE-NPO-17401-1-CU] N91-31885
Parametric study of diffusion-enhancement networks for spatiotemporal grouping in real-time artificial vision
[AD-A239674] N91-31954

REATTACHED FLOW
Method and apparatus for detecting laminar flow separation and reattachment
[NASA-CASE-LAR-13952-2-SB] N91-31596

RECIRCULATIVE FLUID FLOW
Numerical implementation and performance of Reynolds stress closures in finite-volume computations of recirculating and strongly swirling flows N91-31557

RECOVERABILITY
Intrinsic stability and recovery analysis for tape/film type superconductors
[DE91-015568] N91-31967

RECRYSTALLIZATION
Crystallization and characterization of Y2O3-SiO2 glasses N91-31962

RECYCLING
Preliminary evaluation of waste processing in a CELSS N91-31788
Biomass production and nitrogen dynamics in an integrated aquaculture/agriculture system N91-31789

REDUCED GRAVITY
The International Space University's variable gravity research facility design
[NASA-TM-105224] N91-31196
Summary review of sounding rocket experiments in fluid science and material sciences: TEXUS 1 to 20; MASER 1 and 2
[ESA-SP-1132] N91-31321
Liquid motion in capillary tubes (TEXUS 3) N91-31322
Liquid motion in capillary tubes (TEXUS 5) N91-31323
Bubbles and foams (TEXUS 10) ESA N91-31324
Long liquid bridges aboard sounding rockets (TEXUS 12) ESA N91-31325
Freezing of a long liquid column (TEXUS 18) ESA N91-31326
Interfacial convection (TEXUS 1) N91-31327
Interfacial convection (TEXUS 2) N91-31328
Diffusion-induced interfacial convection (TEXUS 3) N91-31329
Thermally induced interfacial convection (TEXUS 4) N91-31330
Diffusion-induced interfacial convection (TEXUS 8) N91-31331
Diffusion-induced interfacial convection (TEXUS 11) N91-31332
Oscillatory Marangoni convection (TEXUS 3A and 3B) N91-31333
Critical Marangoni number (TEXUS 5) N91-31334
Critical Marangoni number (TEXUS 8) N91-31335
Thermal Marangoni convection in a floating zone (TEXUS 3) N91-31336
Oscillatory and turbulent flow regimes due to Marangoni convection (TEXUS 7) N91-31337
Influence of a surface tension minimum on the Marangoni effect (TEXUS 8) ESA N91-31338
Influence of a surface tension minimum on the Marangoni effect (TEXUS 9) ESA N91-31339
Influence of a surface tension minimum on the Marangoni effect (TEXUS 19) ESA N91-31340
Thermal Marangoni convection in a floating zone (TEXUS 9) ESA N91-31341
Experimental results on microgravitational fluid dynamics (TEXUS 14b) ESA N91-31342
Three-dimensional Marangoni convection (MASER 1) ESA N91-31343
Three-dimensional Marangoni convection (MASER 2) ESA N91-31344
Thermocapillary drop motion, 1 (MASER 1) ESA N91-31345
Thermocapillary drop motion, 2 (MASER 2) ESA N91-31346
Electrolytic hydrogen formation (TEXUS 1) N91-31347
Electrolytically generated hydrogen bubbles (TEXUS 6) N91-31348
Intermittent polarization (TEXUS 2) N91-31349
Dispersion layers by electrodeposition (TEXUS 1) N91-31350
Dispersion electrolysis (TEXUS 4) N91-31351
Dispersion electrolysis (TEXUS 7) N91-31352
Dispersion electrolysis (TEXUS 9) N91-31353
Nucleate pool boiling (TEXUS 3) N91-31354
Bubble formation, 1 (TEXUS 5) N91-31355
Bubble formation, 2 (TEXUS 10) N91-31356
Bubble formation, 2. Microgravity measurements of the boiling heat transfer from flat heating surfaces (TEXUS 11) N91-31357
Inst. A fuer Thermodynamik. N91-31358
Ultrasound absorption in molten salts (TEXUS 14b) N91-31359
Ultrasound absorption in molten salts (TEXUS 17) ESA N91-31360
Thermal conductivity of liquids (MASER 1) ESA N91-31361
Colloid chemistry (TEXUS 17) ESA N91-31362
Reaction kinetics in glass melts (TEXUS 1) N91-31363
Reaction kinetics in glass melts: Corrosion of SiO2 (TEXUS 4) N91-31364
Reaction kinetics in glass melts: Sodium self-diffusion in alkali-silicate melts (TEXUS 6) N91-31365
Self- and interdiffusion in alkali-silicate melts (TEXUS 11 and 12) N91-31366
Self- and interdiffusion in alkali-silicate melts (TEXUS 13) N91-31367
Reaction kinetics in molten glasses: Self-diffusion in alkali-silicate melts (TEXUS 20) N91-31368
Special refractive index profiles in glasses obtained by ion exchange (TEXUS 19) ESA N91-31369
Sulphur diffusion in liquid cast iron (TEXUS 6) ESA N91-31370
Ventilation and filling of an optical diffusion cell (TEXUS 8) N91-31371
Solutal diffusion measurements in liquid PbSnTe under microgravity (TEXUS 19) N91-31372
Diffusion of Ni in Cu-Au and Cu-Al alloys (TEXUS 20) N91-31373
Phase transition (TEXUS 8) N91-31374
Ionic solutions near the critical point of water (TEXUS 10) ESA N91-31375
Ionic solutions near the critical point of water (TEXUS 12) ESA N91-31376
Phase separation of a binary fluid near its critical point (TEXUS 11) N91-31377
Phase separation in microgravity of binary fluids near the critical point (TEXUS 13) N91-31378
Spinoidal decomposition (TEXUS 17) N91-31379
Directional solidification of doped germanium (TEXUS 4) ESA N91-31380
Striations in germanium (TEXUS 6) ESA N91-31381
Single crystals of CeMg3 (TEXUS 7) ESA N91-31382
Growth of rare Earth-magnesium crystals (TEXUS 12) N91-31383
Floating-zone growth of a silicon single crystal (TEXUS 7) N91-31384
Growth of a Si crystal covered with a SiO2 skin (TEXUS 12) N91-31385
Floating zone growth of GaAs crystals (TEXUS 20) N91-31386
Floating zone crystal growth of Ga-doped germanium (TEXTUS 10) ESA N91-31387
Floating-zone experiments with germanium crystals (TEXUS 12) ESA N91-31388
Floating zone growth of germanium crystals (TEXUS 14b) ESA N91-31389
Semi-confined Bridgman growth of Ga-doped Ge (MASER 2) N91-31390
Semi-confined Bridgman growth of Ga-doped Ge (MASER 2) N91-31391
Crystallisation experiments with salts (TEXUS 13) N91-31392
Solution growth of GaAs single crystals (TEXUS 19) N91-31393
Vapour growth of an InP crystal (TEXUS 20) N91-31394
Diffusion-controlled growth of protein single crystals: B-galactosidase (TEXUS 3) N91-31395
Diffusion-controlled growth of protein single crystals: Investigation of B-galactosidase at low temperature (TEXUS 4) N91-31396
Diffusion-controlled growth of single crystals of protein (TEXUS 5) N91-31397
Alloy formation (TEXUS 5) N91-31398
Macrosegregation in Ag-Sn alloys (MASER 1) N91-31402
Directional solidification of eutectics (TEXUS 6) N91-31404
Directional solidification of eutectics InSb-NiSb (TEXUS 10) N91-31405
Boundary layers in transparent melts (TEXUS 10) N91-31406
Segregation behaviour of rare earths under microgravity and normal gravity conditions (TEXUS 13) N91-31407
Composite materials, 1 (TEXUS 1) N91-31408
Immiscibles, 1 (TEXUS 3) N91-31410
Immiscibles, 2 (TEXUS 5) N91-31411
Dispersion alloys (TEXUS 7) N91-31412
Al-Pb bearing alloy (TEXUS 1) N91-31413
Fundamental studies in the manganese-bismuth system (TEXUS 2) N91-31414
Solidification of immiscible alloys: ZnBi (TEXUS 2) N91-31415
The coalescence process in immiscible alloys (TEXUS 3) N91-31416
The coalescence process in immiscible alloys (TEXUS 5) N91-31417
Unidirectional solidification of immiscible alloys (TEXUS 5) N91-31418
Unidirectional solidification of immiscible alloys (TEXUS 7) N91-31419

Unidirectional solidification of Zn-Bi samples (TEXUS 14b) N91-31420
Directional solidification of immiscible alloys Zn-Pb (MASER 2) N91-31421
Immiscible alloy system Al-Pb (TEXUS 7) N91-31422
Acoustic mixing (TEXUS 5) N91-31423
Solidification of immiscible alloys (TEXUS 8) N91-31424
Separation of transparent fluids due to Marangoni convection (TEXUS 7) N91-31425
Marangoni transport of droplets at a solidification front (TEXUS 9) N91-31426
Solidification of an Al-Pb-Bi alloy under microgravity (TEXUS 13) N91-31427
Meniscus stability in immiscible metals (MASER 1) N91-31428
Demixing of a monotectic ternary alloy (TEXUS 20) N91-31429
Composite materials, 1 (TEXUS 1) N91-31430
Composite materials, 2 (TEXUS 2) N91-31431
Alloys with oxide inclusions (TEXUS 2) N91-31432
The behaviour of alumina-copper suspensions (TEXUS 3A and 3B) N91-31433
Copper-alumina suspensions (TEXUS 5) N91-31434
Copper-molybdenum suspension (TEXUS 9) N91-31435
Metallic composites with particles (TEXUS 6) N91-31436
Metallic composites with particles (TEXUS 7) N91-31437
Melting and solidification of metallic composites (TEXUS 9) N91-31438
Metal matrix composites (TEXUS 14b) N91-31439
Metal matrix composites (TEXUS 20) N91-31440
Solidification of fine dispersions in microgravity (TEXUS 14b) N91-31441
Dispersion alloys (TEXUS 19) N91-31442
Liquid phase sintering (TEXUS 8) N91-31443
Tungsten composites (TEXUS 10) N91-31444
Liquid phase sintering (TEXUS 19) ESA N91-31446
Pores in aluminium alloys (TEXUS 3) N91-31447
Manufacture of steel foam (TEXUS 4) N91-31448
Manufacture of steel foam (TEXUS 6) N91-31449
Manufacture of iron foam (TEXUS 7) N91-31450
Metallic foams (TEXUS 5) N91-31451
Preparation of aluminium foams (TEXUS 9) N91-31452
Gas bubbles in a copper-alumina suspension (TEXUS 11) N91-31453
Bubble formation, growth, and expansion during the liquid phase sintering of a WC-Co sample N91-31454
Skin technology (TEXUS 1) N91-31455
Skin technology (TEXUS 2) N91-31456
Skin technology (TEXUS 3) N91-31457
Skin technology (TEXUS 4) N91-31458
Skin technology (TEXUS 9) N91-31459
Skin technology (TEXUS 11 and 12) N91-31460
Brazing of capillary gaps (TEXUS 2) N91-31461
Soldering in microgravity (TEXUS 5) N91-31462
Adhesion of metals on ceramic substrates (MASER 2) ESA N91-31463
Acoustic positioning of a molten alloy sample (TEXUS 1) N91-31464
Acoustic positioning (TEXUS 9) ESA N91-31465
Containerless solidification of a Pd-Cu-Si sample (TEXUS 9) ESA N91-31466
Acoustic positioning (TEXUS 14b) ESA N91-31467
Containerless undercooling of a Pd-Cu-Si alloy (TEXUS 14b) ESA N91-31468
Electrostatic positioning for containerless processing of a Li-silicate glass (TEXUS 10) ESA N91-31469
Review of microgravity N91-31736
Preparatory space experiments for development of a CELSS N91-31796
Conceptual design of a closed loop nutrient solution delivery system for CELSS implementation in a micro-gravity environment N91-31798
Technology for subsystems of space-based plant growth facilities N91-31799

REDUCTION (CHEMISTRY)
Chemical reduction of intermodulation interference caused by metal-oxide-metal junctions aboard ship
[AD-A239530] N91-31265

REFERENCE ATMOSPHERES
Range reference atmosphere, Fairbanks, Alaska
[AD-A239520] N91-31739
Range reference atmosphere Wake Island, North Pacific
[AD-A239602] N91-31740
Range reference atmosphere Shemya, Alaska
[AD-A239603] N91-31741
Range reference atmosphere: Thule, Greenland
[AD-A239659] N91-31742

REFLECTANCE
A comparison of time domain boundary conditions for acoustic waves in wave guides
[NASA-CR-187618] N91-31889

REFRACTIVITY
Special refractive index profiles in glasses obtained by ion exchange (TEXUS 19) ESA N91-31369

REFRACTORY MATERIALS
Ceramic composition
[PATENT-1-249-609] N91-31294

REGENERATION (PHYSIOLOGY)
Algae for controlled ecological life support system diet characterization of cyanobacteria 'spirulina' in batch cultures N91-31787
Controlled ecological life support system breadboard project, 1988 N91-31791
Method and apparatus for bio-regenerative life support system
[NASA-CASE-MSC-21629-1] N91-31803

REGENERATIVE FUEL CELLS
Electrochemical energy storage using PEM systems
[DE91-016020] N91-31711

REINFORCING FIBERS
Asbestos-free insulant for rocket motors
[PATENT-1-263-227] N91-31206
The influence of interphase regions on local thermal stresses and deformations in composites N91-31228

REINFORCING MATERIALS
Method for stabilizing thick honeycomb core composite articles
[PATENT-1-253-424] N91-31224

RELATIVISTIC VELOCITY
Particle production through two-photon processes in relativistic heavy-ion colliders
[DE91-016221] N91-31931

RELATIVITY
Heaviside's linearised gravitational theory N91-31737
Nuclear and particle astrophysics
[DE91-016260] N91-32016

RELEASING
Low altitude ejection release (total mass between 1,660 and 5,600 kg)
[REPT-90/05] N91-31475
Anelastic release from the shock-compressed state
[DE91-009961] N91-31672

RELIABILITY
Reliability of computational analysis of plasticity problems
[AD-A239646] N91-31691

RELIABILITY ANALYSIS
Analysis and evaluation of selected PACE applications
[AD-A239726] N91-31124
Reliability modeling of dependable distributed systems
[AD-A239734] N91-31663

RELIABILITY ENGINEERING
Soldering of complex multilayer printed boards
[CNES-NT-127] N91-31474

REMOTE MANIPULATOR SYSTEM
Modeling and simulation of multiple cooperating manipulators on a mobile platform N91-31647
Synchronized computational architecture for generalized bilateral control of robot arms
[NASA-CASE-NPO-17401-1-CU] N91-31885

REMOTE SENSING
Large scale CAESAR images using inertial navigation and pressure altitude measurement. Accuracy deformations and possibilities for a Global Positioning System (GPS)
[ETN-91-99418] N91-31117
Examination and mapping of forest damage, using remote sensing methods
[ETN-91-99741] N91-31696

REPORTS
The relationship between the use of US government technical reports by US aerospace engineers and scientists and selected institutional and sociametric variables N91-31989

REPRODUCTION (BIOLOGY)
Cloning crops in a CELSS via tissue culture: Prospects and problems N91-31783

RESCUE OPERATIONS
Airborne rescue system
[NASA-CASE-ARC-11909-1] N91-31113
Ice tolerant engine inlet screens for CH113/113A search and rescue helicopters N91-31149

RESEARCH AIRCRAFT
Flight testing in the Netherlands: An overview
[NLR-MP-88053-U] N91-31133
A knowledge based application of the extended aircraft interrogation and display system
[NASA-TM-4327] N91-31874

RESEARCH AND DEVELOPMENT
Catalysis-by-design impacts assessment
[DE91-013280] N91-31247

RESEARCH FACILITIES
The International Space University's variable gravity research facility design
[NASA-TM-105224] N91-31196
The Sowerby Research Centre and university liaison N91-31730

RESEARCH MANAGEMENT
A review of the Los Alamos effort in the development of nuclear rocket propulsion
[DE91-016036] N91-31211
The 1991 DOE/Sandia Crystalline Photovoltaic Technology Project Review Meeting
[DE91-016062] N91-31703
BAe University Round Table on Gravitational Research
[BAE-FBS-007] N91-31729
The Sowerby Research Centre and university liaison N91-31730
BAe overview of current gravitational physics research N91-31731
High energy physics program. Task A: Experiment and Theory. Task B: Numerical simulation of quantum field theories
[DE91-015652] N91-31938

RESEARCH PROJECTS
The 1991 DOE/Sandia Crystalline Photovoltaic Technology Project Review Meeting
[DE91-016062] N91-31703
BAe University Round Table on Gravitational Research
[BAE-FBS-007] N91-31729
The Sowerby Research Centre and university liaison N91-31730
Gravitational wave research N91-31732
Review of microgravity N91-31736
Heaviside's linearised gravitational theory N91-31737
High energy physics program. Task A: Experiment and Theory. Task B: Numerical simulation of quantum field theories
[DE91-015652] N91-31938
Survey to assess the usefulness of two model agreements for university-industry cooperative research
[DE91-013937] N91-31985
What is the Federal Demonstration Project?
[DE91-013936] N91-31986

RESIDUAL STRESS
Anelastic release from the shock-compressed state
[DE91-009961] N91-31672

RESIDUES
Use of inedible wheat residues from the KSC-CELSS breadboard facility for production of fungal cellulase N91-31785

RESIN MATRIX COMPOSITES
Method for stabilizing thick honeycomb core composite articles
[PATENT-1-253-424] N91-31224
Relation between fiber proportion and mechanical characteristics of carbon-resin composites
[RE-50-345/F] N91-31231

RESINS
Effect of porcelain surface pretreatments on composite resin-porcelain shear bond strength
[AD-A239359] N91-31241
Ethynyl terminated imidothioethers and resins therefrom
[NASA-CASE-LAR-13910-2-CU] N91-31307

RESONANCE
Electromagnetic penetration of slot apertures with depth and losses
[DE91-016401] N91-31500

RESONANT TUNNELING
Electronic transport and lasing in microstructures
[DE91-016751] N91-31641

RESOURCES MANAGEMENT
Cockpit resource management: Effects on behavioral interactions across airlines and aircraft types
[AD-A239467] N91-31804

RESTORATION
Theory and application of the wavelet transform to signal processing
[AD-A239533] N91-31501
A review of accelerated response actions available to the environmental restoration program: Selected case histories and associated issues
[DE91-013608] N91-31716

RETENTION (PSYCHOLOGY)
Naval medical research and development command
[AD-A239393] N91-31765

REUSABLE ROCKET ENGINES
Reusable rocket engine intelligent control system framework design, phase 2
[NASA-CR-187213] N91-31219

REUSABLE SPACECRAFT
The SAENGER concept and the German hypersonic technology program
[MBB-UK-0132-91-PUB] N91-31198

REYNOLDS NUMBER
Transition length determination in the F1 wind tunnel, test report
[ONERA-PV-1/8571-GY] N91-31089
Thermocapillary drop motion, 1 (MASER 1) ESA N91-31345
Thermocapillary drop motion, 2 (MASER 2) ESA N91-31346
Two-equation models for high-Reynolds-number flow N91-31553
Two-equation models for low-Reynolds number flow N91-31554
An introduction to single-point closure methodology N91-31561

REYNOLDS STRESS
Experimental investigation of turbulent flow through a circular-to-rectangular transition duct
[NASA-TM-105210] N91-31106
Numerical implementation and performance of Reynolds stress closures in finite-volume computations of recirculating and strongly swirling flows N91-31557

RHEOLOGY
Computational fluid dynamics N91-31544

RIGID STRUCTURES
A method for the geometrically nonlinear analysis of compressively loaded prismatic composite structures N91-31229
Large Angle Transient Dynamics (LATDYN) demonstration problem manual
[NASA-CR-4400] N91-31684
A finite element approach for the dynamic analysis of joint-dominated structures
[NASA-CR-4402] N91-31686
Research in regression, information retrieval, inversion of noisy transforms, and stochastic control
[AD-A239490] N91-32001

ROBOT ARMS
Robust impedance control of robot manipulators N91-31297
Modeling and simulation of multiple cooperating manipulators on a mobile platform N91-31647
Robotic tool change mechanism
[NASA-CASE-GSC-13239-1] N91-31656
A program of continuing research on representing, manipulating, and reasoning about physical objects
[AD-A239596] N91-31659
Synchronized computational architecture for generalized bilateral control of robot arms
[NASA-CASE-NPO-17401-1-CU] N91-31885

ROBOT CONTROL
Robust impedance control of robot manipulators N91-31297
A universal computer control system for motors
[NASA-CASE-NPO-17134-1-CU] N91-31528

ROBOT DYNAMICS
Robust impedance control of robot manipulators N91-31297
Modeling and simulation of multiple cooperating manipulators on a mobile platform N91-31647
Robotic tool change mechanism
[NASA-CASE-GSC-13239-1] N91-31656

ROBOTICS
Economic analysis of robotic torque measurement system
[DE91-016480] N91-31653
Power saw
[NASA-CASE-MSC-21469-1] N91-31655
A program of continuing research on representing, manipulating, and reasoning about physical objects
[AD-A239596] N91-31659
Technology for subsystems of space-based plant growth facilities N91-31799
Genetic algorithms
[ETN-91-99985] N91-31852
Path planning for non-holonomic mobile robots
[LAAS-91135] N91-31882

ROBOTS
Economic analysis of robotic torque measurement system
[DE91-016480] N91-31653
A program of continuing research on representing, manipulating, and reasoning about physical objects
[AD-A239596] N91-31659
Proceedings of the Ninth Symposium on Energy Engineering Sciences: Fluid and Dynamical Systems
[DE91-015974] N91-31701
Kinematics of the six-degree-of-freedom force-reflecting Kraft Master
[NASA-TM-104124] N91-31879
Path planning for non-holonomic mobile robots
[LAAS-91135] N91-31882

ROBUSTNESS (MATHEMATICS)
Robustness and techniques of multivariable control for helicopter piloting. Dispatch 3: Inclusion regions technique on linear model
[RD/PA-14-227] N91-31184
Robust impedance control of robot manipulators N91-31297
A dynamically adaptive multigrid algorithm for the incompressible Navier-Stokes equations: Validation and model problems
[NASA-CR-187595] N91-31888
Locking effects in the finite element approximation of elasticity problems
[AD-A239645] N91-31914

ROCKET ENGINE CASES
Asbestos-free insulant for rocket motors
[PATENT-1-263-227] N91-31206

ROCKET ENGINE CONTROL
Reusable rocket engine intelligent control system framework design, phase 2
[NASA-CR-187213] N91-31219

ROCKET ENGINES
An investigation of dual-mode operation of a nuclear-thermal rocket engine
[DE91-015977] N91-31210

ROCKET FIRING
Rocket boosted target
[PATENT-1-254-289] N91-31207

ROCKET NOZZLES
Segmented rotatable nozzles
[CA-PATENT-APPL-SN-2-009-634] N91-31174

ROCKET PROPELLANTS
Technical prospects for utilizing extraterrestrial propellants for space exploration
[NASA-TM-105263] N91-31318

ROCKET VEHICLES
Rocket boosted target
[PATENT-1-254-289] N91-31207

ROCKS
Hyperspectral signatures (400 to 2500 nm) of vegetation, minerals, soils, rocks, and cultural features: Laboratory and field measurements
[AD-A239496] N91-31697

ROTARY WING AIRCRAFT
Vibration analysis of the SA349/2 helicopter
[NASA-TM-102794] N91-31078
Improved finite-element methods for rotorcraft structures
[NASA-TM-104104] N91-31687
NASA Aerodynamics Program
[NASA-TM-4312] N91-31751

ROTARY WINGS
Vortex-blade interaction on a helicopter principal rotor. Validation of the S2DI computation program and study of vortex models
[ONERA-RT-92/5094-PY] N91-31136
Developments in icing test techniques for aerospace applications in the RAE Pyestock altitude test facility N91-31173
Recent manufacturing advances for spiral bevel gears
[NASA-TM-104479] N91-31654

ROTATING CYLINDERS
Control of oscillatory forces on a circular cylinder by rotation
[NASA-CR-187619] N91-31576

ROTATING SHAFTS
Eccentricity effects on leakage of a brush seal at low speeds
[NASA-TM-105141] N91-31220

ROTATION
Control of oscillatory forces on a circular cylinder by rotation
[NASA-CR-187619] N91-31576
A program of continuing research on representing, manipulating, and reasoning about physical objects
[AD-A239596] N91-31659
A new method to do time resolved, x ray diffraction studies: The rotating crystal Laue method
[DE91-016527] N91-31935
Fast pulsars, variational bound, other facets of compact stars
[DE91-016416] N91-32018

ROTOR BLADES
Prediction of rotor surface unsteady pressure and heat transfer from wake passing N91-31549

ROTOR BLADES (TURBOMACHINERY)
Ice ingestion experience on a small turboprop engine N91-31162
A three-dimensional viscous flow model of stator/rotor interaction in turbomachines N91-31547
Development of single blade rotor wind energy converters: From M400 prototype to MON 50 preseries
[MBB-UE-0015-90-PUB] N91-31705

ROTORS
Eccentricity effects on leakage of a brush seal at low speeds
[NASA-TM-105141] N91-31220

RUBIDIUM 86
Reaction kinetics in molten glasses: Self-diffusion in alkali-silicate melts (TEXUS 20) N91-31368

RUNGE-KUTTA METHOD
Multigrid and Runge-Kutta time stepping applied to the uniformly non-oscillatory scheme for conservation laws
[MEMO-911] N91-31906

RUNWAYS
Airplane takeoff and landing performance monitoring system
[NASA-CASE-LAR-13854-1-CU] N91-31120
A knowledge-base for rehabilitation of airfield concrete pavements
[AD-A239354] N91-31191

S

S MATRIX THEORY
Introduction to radar polarimetry
[FEL-91-B122] N91-31496

SAFETY
Space engine safety system
[NASA-CR-187219] N91-31209

SAFETY DEVICES
Process for detecting the likelihood of ice formation, ice warning system for carrying out the process, and utilization thereof
[PATENT-1-250-926] N91-31107

SAFETY FACTORS
Airborne rescue system
[NASA-CASE-ARC-11909-1] N91-31113
Flight tests with a data link used for air traffic control information exchange
[NASA-TP-3135] N91-31143

SAMPLING
Conditional sampling
[AAAF-NT-89-04] N91-31099
Biofilm monitoring coupon system and method of use
[NASA-CASE-MSC-21585-1] N91-31755
Bayes theorem from a sampling-resampling perspective
[AD-A239515] N91-31919

SANDWICH STRUCTURES
Vaudreuil (France) large hydrodynamic tunnel: Acoustic chamber damping
[METRAVIB-RDS-1-007-67] N91-31090
Method for fastening aircraft frame elements to sandwich skin panels covering same using woven fiber connectors
[PATENT-1-274-075] N91-31126

SAPPHIRE
Ion beam enhanced adhesion of iron films to sapphire substrates
[DE91-015931] N91-31308

SAS-3
A search for periodicity in the x ray spectrum of black hole candidate A0620-00
[AD-A239488] N91-32011

SATELLITE ATTITUDE CONTROL
Choice of a differential method for attitude restitution with dynamic imbalance
[CNES-NT-126] N91-31202

SATELLITE COMMUNICATION
Traffic model for advanced satellite designs and experiments for ISDN services
[NASA-CR-188802] N91-31200
Dielectric image-resonator multiplexer
[PATENT-1-252-835] N91-31479
Antenna study for 60 GHz intersatellite link
[CD-RPT-ITL-5043-003] N91-31482
Interim Service ISDN Satellite (ISIS) network model for advanced satellite designs and experiments
[NASA-CR-186565] N91-31488
The data distribution satellite system
[NASA-CR-187172] N91-31499

SATELLITE CONTROL
Application of semianalytic satellite theory to maneuver planning
[AD-A239417] N91-31205

SATELLITE DESIGN
Traffic model for advanced satellite designs and experiments for ISDN services
[NASA-CR-188802] N91-31200
Interim Service ISDN Satellite (ISIS) network model for advanced satellite designs and experiments
[NASA-CR-186565] N91-31488

SATELLITE DOPPLER POSITIONING
Origins of GPS surveying
[AD-A239676] N91-31121

SATELLITE IMAGERY
On the response of the special sensor microwave/imager to the marine environment: Implications for atmospheric parameter retrievals N91-31727

SATELLITE NETWORKS
Interim Service ISDN Satellite (ISIS) network model for advanced satellite designs and experiments
[NASA-CR-186565] N91-31488
The data distribution satellite system
[NASA-CR-187172] N91-31499

SATELLITE OBSERVATION
Small satellite radiometric measurements
[DE91-016308] N91-31694
SATELLITE ORBITS
The motions of Mars' pole N91-32019
SATELLITE ORIENTATION
Choice of a differential method for attitude restitution with dynamic imbalance
[CNES-NT-126] N91-31202
SATELLITE ROTATION
Choice of a differential method for attitude restitution with dynamic imbalance
[CNES-NT-126] N91-31202
SATELLITE TRACKING
Automatic satellite tracking system for the NASA Satellite Photometric Observatory
[NASA-TM-105037] N91-31194
SATELLITE-BORNE INSTRUMENTS
Small satellite radiometric measurements
[DE91-016308] N91-31694
SATELLITE-BORNE RADAR
Improvements to programs for system studies of space-based radar
[DRE-179] N91-31484
A satellite-based radar wind sensor
[NASA-CR-188805] N91-31750
SAWS
Power saw
[NASA-CASE-MSC-21469-1] N91-31655
SCALE (CORROSION)
Initial determination of the micromechanical properties of oxide scales
[DE90-012164] N91-31291
SCANNERS
A first hot wire scanner
[AAAF-NT-89-16] N91-31188
A methodology for producing and testing a genesil silicon compiler designed VLSI chip which incorporates design for testability
[AD-A239465] N91-31537
Circular format zig-zag scanning of vidicon tubes
[DE91-016084] N91-31610
SCATTERING
Abstracts of papers presented at the First Los Alamos Symposium on Ultra-Wideband Radar
[DE91-015976] N91-31491
On the response of the special sensor microwave/imager to the marine environment: Implications for atmospheric parameter retrievals N91-31727
SCATTERING COEFFICIENTS
A numerical procedure for recovering true scattering coefficients from measurements with wide-beam antennas
[NASA-CR-186042] N91-31492
SCATTERING CROSS SECTIONS
Searching for the Higgs in ep collisions at LEP/LHC
[DE91-015701] N91-31930
SCENE ANALYSIS
A graph theoretic approach to scene matching
[NASA-CR-187817] N91-31947
SCHEDULES
An integer programming model for Navy's maritime patrol aviation fleet
[AD-A239464] N91-31079
SCHEDULING
Spectrum monitoring procedures and techniques
[AD-A239567] N91-31507
SCIENTIFIC SATELLITES
The International Space University's variable gravity research facility design
[NASA-TM-105224] N91-31196
SCINTILLATION
Integration losses and clutter-Doppler spread for a space based radar caused by ionospheric scintillation during a solar maximum
[AD-A239534] N91-31502
SCRUBBERS
Electrostatic precipitation of condensed acid mist
[DE91-016530] N91-31260
SEA SURFACE TEMPERATURE
Time scales of variability associated with Nordeste precipitation
[DE91-015696] N91-31718
Description of Crau data set: Meteosat data, radiosonde data, sea surface temperatures: Comparison of Meteosat and Heimann data
[KNMI-WR-90-03] N91-31752
SEA WATER
Tropical tests of a seawater marker
[MRL-TR-90-19] N91-31109
SEALERS
Development of prototype sealed bipolar lithium/sulfide cells
[DE91-015721] N91-31519
SEALING
Vulnerability of a small powerplant to wet snow conditions N91-31148
Development of prototype sealed bipolar lithium/sulfide cells
[DE91-015721] N91-31519
SEAMOUNTS
North Pacific guyots
[AD-A239388] N91-31754
SEDIMENTS
Composite materials, 1 (TEXUS 1) N91-31408
Composite materials, 2 (TEXUS 2) N91-31409
Metal matrix composites (TEXUS 14b) N91-31439
SEEDS
Cloning crops in a CELSS via tissue culture: Prospects and problems N91-31783
Seed sprout production: Consumables and a foundation for higher plant growth in space N91-31790
Preparatory space experiments for development of a CELSS N91-31796
SEGMENTS
Longest segment problems
[RUU-CS-90-28] N91-31896
Union-copy structures and dynamic segment trees
[RUU-CS-91-05] N91-31903
SEISMIC WAVES
Mechanical characterization of seismic base isolation elastomers
[DE91-015680] N91-31299
Response of seismic-isolated structures under long-period motions
[DE91-015673] N91-31674
SEISMOLOGY
Artificial neural networks for seismic data interpretation
[AD-A239673] N91-31743
SELECTIVITY
Correlations between surface structure and catalytic activity/selectivity
[DE91-016453] N91-31255
SELF ALIGNMENT
Steerable windowed enclosures
[PATENT-1-262-653] N91-31142
SEMANTICS
On the efficient incremental evaluation of higher order attribute grammars
[RUU-CS-90-36] N91-31832
Categorical semantics as a basis for program transformation
[RUU-CS-90-38] N91-31833
On logic programming and the refinement calculus: Semantics based program transformations
[RUU-CS-90-39] N91-31834
Mathematical theory of computation
[AD-A239419] N91-31912
SEMICONDUCTING FILMS
Intrinsic stability and recovery analysis for tape/film type superconductors
[DE91-015568] N91-31967
SEMICONDUCTOR DIODES
Dynamics of 1.3 micron semiconductor lasers and nonlinear gain N91-31613
Laser Doppler anemometer miniaturized with diode laser
[AAAF-NT-89-06] N91-31637
SEMICONDUCTOR JUNCTIONS
Chemical reduction of intermodulation interference caused by metal-oxide-metal junctions aboard ship
[AD-A239530] N91-31265
SEMICONDUCTOR LASERS
Dynamics of 1.3 micron semiconductor lasers and nonlinear gain N91-31613
Laser Doppler anemometer miniaturized with diode laser
[AAAF-NT-89-06] N91-31637
Electronic transport and lasing in microstructures
[DE91-016751] N91-31641
An adaptive coherent optical receiver array
[AD-A239672] N91-31644
Innovative optoelectronic materials and structures using OMVPE
[AD-A239518] N91-31951
SEMICONDUCTORS (MATERIALS)
Interfacial systems for photochemical energy conversion
[DE91-015743] N91-31700
The photovoltaic effect on pyroelectics N91-31707
Advanced research workshop on Wide Gap II-VI Semiconductors
[AD-A233796] N91-31960
Photophysics and chemistry of ultra-fast ZnO and CdS phosphors
[DE91-013106] N91-31966
Depth profiles for hydrogen-assisted thermal donor formation in silicon
[DE91-015719] N91-31971
Ground-state in-plane light-holes in GaAs/AlGaAs structures
[DE91-016408] N91-31980
Limited reaction processing for semiconductor materials preparation
[AD-A239639] N91-31983
SENSORS
Diagnostic tools for reciprocating engine systems
[PB91-184960] N91-31645
SEPARATED FLOW
Method and apparatus for detecting laminar flow separation and reattachment
[NASA-CASE-LAR-13952-2-SB] N91-31596
SEQUENCING
The effects of different sequencing strategies on the capacity of airports
[DLR-MITT-90-18] N91-31185
Rocket boosted target
[PATENT-1-254-289] N91-31207
The complexity of coloring games on perfect graphs
[RUU-CS-91-03] N91-31838
SEQUENTIAL COMPUTERS
The ABC-machine: A sequential stack-based abstract machine for graph rewriting
[TR-90-22] N91-31824
SERVICE LIFE
An integer programming model for Navy's maritime patrol aviation fleet
[AD-A239464] N91-31079
Mass comparisons of electric propulsion systems for NSSK of geosynchronous spacecraft
[NASA-TM-105153] N91-31212
SERVOCONTROL
A high-frequency servosystem for fuel control in hypersonic engines
[NASA-TM-104333] N91-31178
SERVOMECHANISMS
A high-frequency servosystem for fuel control in hypersonic engines
[NASA-TM-104333] N91-31178
SET THEORY
Some order dimension bounds for communication complexity problems
[MEMO-938] N91-31489
Application of the constrained implicants set concept to the minimization of binary functions
[AD-A239470] N91-31859
On a theorem of MacMahon
[CS-9104] N91-31894
The linear decomposition of delta-squared models
[RUU-CS-91-04] N91-31902
Strong approximation on log dense sets
[W-9101] N91-31916
Continuous informations systems
[RUU-CS-90-25] N91-31997
SHAPE CONTROL
Skin technology (TEXUS 3) N91-31457
Skin technology (TEXUS 9) N91-31459
SHAPE MEMORY ALLOYS
Development and characterization of low temperature Cu-Al-Be shape memory alloys
[ISAL-90-0093] N91-31284
SHEAR FLOW
Study of the flow around the GARTEUR AD/AG07 wing: First F2 test campaign results
[ONERA/DERAT-37/5025-26] N91-31096
The interaction of particles with homogeneous turbulence N91-31548
Introduction to the Modeling of Turbulence: Introduction N91-31552
Large-eddy simulation of the turbulent flow in the downstream region of a backward facing step N91-31568
Three dimensional shear flow: Flow visualisation around a highly swept back and high incidence wing
[ONERA-RT-35/5025-28] N91-31584
Postprocessing of experimental and numerical results in the case of two and three dimensional flows
[AAAF-NT-89-25] N91-31592
SHEAR LAYERS
A European collaborative investigation of the three-dimensional turbulent shear layers of a swept wing
[NLR-MP-88054-U] N91-31084
Composite matrix deformation process in relation to molecular structure
[ETN-91-99915] N91-31232
SHEAR STRAIN
Response of an alumina fiber reinforced aluminum composite to combined tension-torsion
[AD-A239560] N91-31245
SHEAR STRENGTH
Effect of porcelain surface pretreatments on composite resin-porcelain shear bond strength
[AD-A239359] N91-31241

SHEAR STRESS
Relation between fiber proportion and mechanical characteristics of carbon-resin composites
[RE-50-345/F] N91-31231
SHELLS (STRUCTURAL FORMS)
Steerable windowed enclosures
[PATENT-1-262-653] N91-31142
Nonlinear probabilistic finite element modeling of composite shells N91-31668
SHOCK ABSORBERS
Response of seismic-isolated structures under long-period motions
[DE91-015673] N91-31674
SHOCK LOADS
Anelastic release from the shock-compressed state
[DE91-009961] N91-31672
SHOCK TESTS
Modelling the response of thick composite materials due to axisymmetric shock loading
[AD-A239531] N91-31243
SHOCK WAVE PROPAGATION
Approximate treatment of a strong explosion and expansion in a near vacuum
[DE91-016063] N91-31574
SHOCK WAVES
Model of an aerospace plane based on an idealized cone-derived waverider forebody N91-31129
Modelling the response of thick composite materials due to axisymmetric shock loading
[AD-A239531] N91-31243
Influence of loading rate on the mechanical response and substructure evolution of shock-loaded copper
[DE91-013390] N91-31276
Photography of shock waves in explosive crystals
[DE91-015772] N91-31572
Pressure-strain-temperature relationship in shock loaded cylindrical samples of 304 stainless steel
[DE91-013379] N91-31673
Response of seismic-isolated structures under long-period motions
[DE91-015673] N91-31674
SHORT CIRCUIT CURRENTS
One-sun, single-crystalline silicon solar cell research
[DE91-015646] N91-31699
SHORT CRACKS
In situ short fatigue crack characterization of a nickel-base superalloy at ambient and elevated temperature N91-31670
SHROUDS
Capacitive bridge-type probe and conversion circuitry
[PATENT-1-263-444] N91-31598
Capacitive bridge-type probe and conversion circuitry
[PATENT-1-263-443] N91-31599
SIDE-LOOKING RADAR
Composite waveguide coupling aperture having a thickness dimension
[PATENT-1-259-401] N91-31514
SIGNAL DETECTION
Convergence performance of adaptive detectors, part 2
[AD-A239532] N91-31540
SIGNAL DISTORTION
Time domain electromagnetic waves in multilayered media
[AD-A239545] N91-31504
Comparison of noise reduction systems
[DE91-015318] N91-31929
SIGNAL GENERATORS
Passive ranging of an airborne emitter by a single non-maneuvering or stationary sensor
[PATENT-1-254-292] N91-31116
SIGNAL MEASUREMENT
Comparison of noise reduction systems
[DE91-015318] N91-31929
SIGNAL PROCESSING
Enhanced global positioning system delta-range processing
[PATENT-1-254-637] N91-31115
Updates to the DREO airborne radar simulator
[ASSGI-167] N91-31478
Theory and application of the wavelet transform to signal processing
[AD-A239533] N91-31501
Performance of an angle-of-arrival estimator in the presence of a mainbeam interference source
[AD-A239629] N91-31508
High speed digital direct access filter for tracking or excision of parametric signal data
[PATENT-1-271-231] N91-31511
Filter system for radar applications
[PATENT-1-273-409] N91-31512
Reconfigurable parameter filter
[PATENT-1-264-072] N91-31513
Boundary layer turbulence appearance mechanisms studied by plane laser visualizations
[AAAF-NT-89-10] N91-31587
Postprocessing of test and computation results by the wavelet method
[AAAF-NT-89-24] N91-31591
Fundamentals of signal processing N91-31617
Signal processing: Time domain and frequency domain N91-31620
Post-processing of data N91-31633
SIGNAL TO NOISE RATIOS
Behaviour of the SIR for space-based DPCA radar under various spatial clutter distributions
[CRC-W7714-7-5271] N91-31485
Convergence performance of adaptive detectors, part 1
[AD-A239507] N91-31539
The superconducting gravity gradiometer N91-31734
Comparison of noise reduction systems
[DE91-015318] N91-31929
SIGNAL TRANSMISSION
Analysis and evaluation of selected PACE applications
[AD-A239726] N91-31124
Emergency locating transmitter
[NASA-CASE-GSC-12821-2] N91-31530
SIGNATURE ANALYSIS
An algorithm for spectral factorization of polynomial matrices with any signature
[MEMO-912] N91-31842
SIGNATURES
Hyperspectral signatures (400 to 2500 nm) of vegetation, minerals, soils, rocks, and cultural features: Laboratory and field measurements
[AD-A239496] N91-31697
SIGNIFICANCE
On combining independent significance tests
[AD-A239660] N91-31920
SIGNS AND SYMPTOMS
Basic operation and preliminary trials of a detector for stationary gas bubbles
[AD-A239710] N91-31769
SILICA GLASS
Ion-implantation induced crystallization of glass
[DE91-016121] N91-31303
Crystallization and characterization of Y2O3-SiO2 glasses N91-31962
SILICATES
Self- and interdiffusion in alkali-silicate melts (TEXUS 11 and 12) N91-31366
Self- and interdiffusion in alkali-silicate melts (TEXUS 13) N91-31367
Reaction kinetics in molten glasses: Self-diffusion in alkali-silicate melts (TEXUS 20) N91-31368
Electrostatic positioning for containerless processing of a Li-silicate glass (TEXUS 10) ESA N91-31469
SILICON
An expert system for the identification of silicon impurities using FTIR spectroscopy
[AD-A236504] N91-31246
Floating-zone growth of a silicon single crystal (TEXUS 7) N91-31384
Growth of a Si crystal covered with a SiO2 skin (TEXUS 12) N91-31385
Silicon micromachining based on porous silicon formation
[DE91-013744] N91-31472
A methodology for producing and testing a genesil silicon compiler designed VLSI chip which incorporates design for testability
[AD-A239465] N91-31537
Depth profiles for hydrogen-assisted thermal donor formation in silicon
[DE91-015719] N91-31971
SILICON ALLOYS
Method for imparting strength to intermetallic phases
[PATENT-1-255-929] N91-31271
Solidification of alloys (TEXUS 2) N91-31401
Demixing of a monotectic ternary alloy (TEXUS 20) N91-31429
Microwave module YAG laser weld development
[DE91-015750] N91-31652
SILICON CARBIDES
Composite flexible blanket insulation
[NASA-CASE-NPO-11907-1-NP] N91-31236
Effects of oxidation and combustion environments on the properties of Nicalon/SiC composites
[DE91-016778] N91-31240
Metallic composites with particles (TEXUS 6) N91-31436
Metal matrix composites (TEXUS 14b) N91-31439
Analysis of thermomechanical fatigue of unidirectional titanium metal matrix composites
[NASA-TM-104105] N91-31677
SILICON DIOXIDE
Metallic composites with particles (TEXUS 7) N91-31437
The selective catalytic oxidation of ammonia to N2 and H2O over silica-supported molybdena catalysts N91-32026
SILICON NITRIDES
Crystallization of the glassy grain boundary phase in silicon nitride ceramics
[NASA-CR-188717] N91-31961
Microstructural changes in Beta-silicon nitride grains upon crystallizing the grain-boundary glass N91-31963
Glass formation and crystallization in high-temperature glass-ceramics and Si3N4 N91-31964
Indirect measurement of the viscosity of the intergranular glass phase in yttria-sintered silicon nitride N91-31965
SILICON OXIDES
Ceramic composition
[PATENT-1-249-609] N91-31294
SILVER
Composite materials, 1 (TEXUS 1) N91-31408
Composite materials, 2 (TEXUS 2) N91-31409
Immiscibles, 1 (TEXUS 3) N91-31410
Immiscibles, 2 (TEXUS 5) N91-31411
Composite materials, 1 (TEXUS 1) N91-31430
Metal matrix composites (TEXUS 20) N91-31440
Dispersion alloys (TEXUS 19) N91-31442
Liquid phase sintering (TEXUS 8) N91-31443
Development of elements of a high T(sub c) superconducting cable
[AD-A239766] N91-31543
SILVER ALLOYS
Solidification of a hypereutectic alloy (TEXUS 1) N91-31399
Macrosegregation in Ag-Sn alloys (MASER 1) N91-31402
Composite materials, 2 (TEXUS 2) N91-31431
SILVER NITRATES
Special refractive index profiles in glasses obtained by ion exchange (TEXUS 19) ESA N91-31369
Ventilation and filling of an optical diffusion cell (TEXUS 8) N91-31371
SIMPLIFICATION
Weak equivalence
[ITLI-CT-91-04] N91-31891
SIMULATION
Icing test programmes and techniques N91-31171
Developments in icing test techniques for aerospace applications in the RAE Pyestock altitude test facility N91-31173
Possibilities of simulation and optimization for guided missile systems
[MBB-UA-1201-90-PUB] N91-31183
A methodology for producing and testing a genesil silicon compiler designed VLSI chip which incorporates design for testability
[AD-A239465] N91-31537
Large-eddy simulation of the turbulent flow in the downstream region of a backward facing step N91-31568
A perspective on CELSS control issues N91-31794
Mean field analysis of the CuO2 lattice: Comparison to Monte Carlo simulations
[DE91-015570] N91-31968
Hydrodynamic simulations of cosmology N91-32013
SIMULATORS
The development of a computational model to predict low temperature fuel flow phenomena N91-31166
Improvements to programs for system studies of space-based radar
[DRE-179] N91-31484
Development of the CELSS emulator at NASA. Johnson Space Center N91-31793
Cockpit resource management: Effects on behavioral interactions across airlines and aircraft types
[AD-A239467] N91-31804
SINGLE CRYSTALS
High pressure catalytic reactions over single-crystal metal surfaces
[DE91-016475] N91-31256
Diffusion-controlled growth of protein single crystals: Investigation of B-galactosidase at low temperature (TEXUS 4) N91-31396
Diffusion-controlled growth of single crystals of protein (TEXUS 5) N91-31397
One-sun, single-crystalline silicon solar cell research
[DE91-015646] N91-31699
SINTERING
Tungsten composites (TEXUS 19) ESA N91-31445
Liquid phase sintering (TEXUS 19) ESA N91-31446
Bubble formation, growth, and expansion during the liquid phase sintering of a WC-Co sample N91-31454
Indirect measurement of the viscosity of the intergranular glass phase in yttria-sintered silicon nitride N91-31965
SKIN (STRUCTURAL MEMBER)
Method for fastening aircraft frame elements to sandwich skin panels covering same using woven fiber connectors
[PATENT-1-274-075] N91-31126
SLEEP
Muramyl peptide-enhanced sleep: Pharmacological optimization of performance
[AD-A239442] N91-31766

Sleep logs: Measurement of individual and operational efficiency
[AD-A239774] N91-31770
SLEEP DEPRIVATION
Sleep logs: Measurement of individual and operational efficiency
[AD-A239774] N91-31770
SLEEVES
Removable slider shoe for a translating sleeve used on a jet engine cowl and duct
[PATENT-1-247-868] N91-31177
SLOT ANTENNAS
Composite waveguide coupling aperture having a thickness dimension
[PATENT-1-259-401] N91-31514
SLOTS
Electromagnetic penetration of slot apertures with depth and losses
[DE91-016401] N91-31500
SLURRIES
Processing and characterization of continuous fiber-reinforced glass and glass-ceramic matrix composites N91-31227
SMOOTHING
Hydrodynamic target response to an induced spatial incoherence-smoothed laser beam
[DE91-015757] N91-31638
SNOW
Vulnerability of a small powerplant to wet snow conditions N91-31148
SODIUM CHLORIDES
Stress corrosion cracking of 2091 ad 8090 aluminum-lithium alloys in chloride containing aqueous solutions. Influence of sulphate and nitrate additions
[REPT-431/91] N91-31285
SODIUM NITRATES
Ventilation and filling of an optical diffusion cell (TEXUS 8) N91-31371
SODIUM SILICATES
Reaction kinetics in glass melts (TEXUS 1) N91-31363
Reaction kinetics in glass melts: Sodium self-diffusion in alkali-silicate melts (TEXUS 6) N91-31365
SOFTWARE ENGINEERING
Software quality metrics
[DOT/FAA/CT-91/1] N91-31814
Report on the Software Technology for Adaptable, Reliable Systems (STARS) Conference on Frameworks Convergence
[AD-A239691] N91-31862
SOFTWARE TOOLS
Flow visualization and simulation
[AAAF-NT-89-18] N91-31590
The potential impact of VHDL on dependable distributed system design
[AD-A239769] N91-31664
Software quality metrics
[DOT/FAA/CT-91/1] N91-31814
Post processing of three dimensional aerothermal computation
[AAAF-NT-89-21] N91-31848
Open architecture for formal reasoning
[AD-A239395] N91-31857
Investigation into the applicability of knowledge engineering
[NLR-TP-89031-U] N91-31878
An application of neural networks to process and materials control
[DE91-016016] N91-31886
SOIL SCIENCE
Solid-support substrates for plant growth at a lunar base N91-31800
SOILS
Hyperspectral signatures (400 to 2500 nm) of vegetation, minerals, soils, rocks, and cultural features: Laboratory and field measurements
[AD-A239496] N91-31697
The critical temperature for drying-out of soils around power cables as a function of local conditions N91-32025
SOLAR ACTIVITY
Integration losses and clutter-Doppler spread for a space based radar caused by ionospheric scintillation during a solar maximum
[AD-A239534] N91-31502
SOLAR ACTIVITY EFFECTS
Integration losses and clutter-Doppler spread for a space based radar caused by ionospheric scintillation during a solar maximum
[AD-A239534] N91-31502
SOLAR ARRAYS
Restructured Freedom configuration characteristics
[NASA-TM-104057] N91-31201
Advanced power systems for EOS
[NASA-TM-105222] N91-31217
Thin film, concentrator and multijunction space solar cells: Status and potential
[NASA-TM-104505] N91-31218
The status of lightweight photovoltaic space array technology based on amorphous silicon solar cells
[DE91-014985] N91-31698
Parabolic dish photovoltaic concentrator development
[DE91-016868] N91-31714
SOLAR CELLS
Thin film, concentrator and multijunction space solar cells: Status and potential
[NASA-TM-104505] N91-31218
One-sun, single-crystalline silicon solar cell research
[DE91-015646] N91-31699
The 1991 DOE/Sandia Crystalline Photovoltaic Technology Project Review Meeting
[DE91-016062] N91-31703
SOLAR COLLECTORS
Thin film, concentrator and multijunction space solar cells: Status and potential
[NASA-TM-104505] N91-31218
One-sun, single-crystalline silicon solar cell research
[DE91-015646] N91-31699
The feasibility of testing NASA's SCAD concentrator on Earth
[DE91-016055] N91-31702
Facet development for a faceted stretched-membrane dish by Solar Kinetics, Inc.
[DE91-016866] N91-31713
Parabolic dish photovoltaic concentrator development
[DE91-016868] N91-31714
Design and cost of the first commercial stretched-membrane heliostat
[DE91-016870] N91-31715
SOLAR ENERGY
Solar energy and conservation technologies for Caribbean Tourist Facilities (CTF)
[DE91-016451] N91-31712
SOLAR ENERGY CONVERSION
Summaries of FY 1991 research in the chemical sciences
[DE91-011221] N91-31222
The feasibility of testing NASA's SCAD concentrator on Earth
[DE91-016055] N91-31702
Energy transfer processes in solar energy conversion
[DE91-016102] N91-31704
SOLAR FLARES
The Li-7 and Be-7 deexcitation lines: Probes for accelerated particle transport models in solar flares
[NASA-CR-183490] N91-32020
Abundances from solar flare line spectroscopy
[NASA-CR-183492] N91-32022
SOLAR GENERATORS
The status of lightweight photovoltaic space array technology based on amorphous silicon solar cells
[DE91-014985] N91-31698
The feasibility of testing NASA's SCAD concentrator on Earth
[DE91-016055] N91-31702
SOLAR RADIATION
Impact of the ice phase on a mesoscale convective system: Cloud ensemble features and cloud radiative properties
[DE91-015769] N91-31749
SOLAR SYSTEM
Activities report of the Institute of Extraterrestrial Physics
[MPE-223] N91-32002
SOLDERING
Soldering in microgravity (TEXUS 5) N91-31462
Soldering of complex multilayer printed boards
[CNES-NT-127] N91-31474
SOLDERS
Soldering in microgravity (TEXUS 5) N91-31462
SOLID ELECTROLYTES
Pseudohomogeneous catalyst layer model for polymer electrolyte fuel cell
[DE91-016014] N91-31710
SOLID MECHANICS
DYNA3D: A nonlinear, explicit, three-dimensional finite element code for solid and structural mechanics
[DE91-015735] N91-31675
SOLID PROPELLANT ROCKET ENGINES
Asbestos-free insulant for rocket motors
[PATENT-1-263-227] N91-31206
SOLID STATE
Solid-State Radar Beacon Decoder (SSRBD) Master Test Plan (MTP)
[DOT/FAA/CT-TN91/33] N91-31494
SOLID-SOLID INTERFACES
The influence of interphase regions on local thermal stresses and deformations in composites N91-31228
Atomic structures and compositions of internal interfaces
[DE91-016095] N91-31934
TEM analysis of crystalline interface structure: The state of the art
[DE91-016427] N91-31975
Epitaxial growth and electro-optical properties of metal GaAs superlattices
[AD-A239719] N91-31984
SOLIDIFICATION
Non-equilibrium solidification in austenitic stainless steel welds
[DE91-014279] N91-31277
Solutal diffusion measurements in liquid PbSnTe under microgravity (TEXUS 19) N91-31372
Directional solidification of doped germanium (TEXUS 4) ESA N91-31380
Striations in germanium (TEXUS 6) ESA N91-31381
Solidification of alloys (TEXUS 1) N91-31400
Boundary layers in transparent melts (TEXUS 10) N91-31406
Solidification of immiscible alloys: ZnBi (TEXUS 2) N91-31415
Immiscible alloy system Al-Pb (TEXUS 7) N91-31422
Marangoni transport of droplets at a solidification front (TEXUS 9) N91-31426
Solidification of an Al-Pb-Bi alloy under microgravity (TEXUS 13) N91-31427
Copper-molybdenum suspension (TEXUS 9) N91-31435
Weld pool solidification and microstructures
[DE91-014263] N91-31650
SOLIDS
X ray and gamma ray spectroscopy of solids under pressure
[DE91-016948] N91-31263
An equivalent domain integral method for three-dimensional mixed-mode fracture problems
[NASA-CR-182021] N91-31692
Interactive constraint-based solid modeling as a design tool
[AD-A239358] N91-31856
SOLUBILITY
The formation of novel thermoplastic composites from liquid crystalline polymers and their blends
[AD-A239546] N91-31244
SOLUTES
Determination of solvation kinetics in supercritical fluids
[DE91-016096] N91-31253
SOLUTIONS
Solutal diffusion measurements in liquid PbSnTe under microgravity (TEXUS 19) N91-31372
SOLVATION
Determination of solvation kinetics in supercritical fluids
[DE91-016096] N91-31253
SOLVENTS
Ethynyl terminated imidothioethers and resins therefrom
[NASA-CASE-LAR-13910-2-CU] N91-31307
SONDES
Special design and gauging of anemoclinometric sondes
[IMFL-90/03] N91-31604
SOOT
Global model simulations of the long range transport of soot and sulfur from the Kuwait oil fires
[DE91-015771] N91-31719
SOUND PRESSURE
Fuselage shell and cavity response measurements on a DC-9 test section
[NASA-CR-187557] N91-31926
SOUND WAVES
A comparison of time domain boundary conditions for acoustic waves in wave guides
[NASA-CR-187618] N91-31889
SOUNDING
A documentation of vertical and horizontal aircraft soundings of icing relevant cloudphysical parameters N91-31172
SOUNDING ROCKETS
Directional solidification of doped germanium (TEXUS 4) ESA N91-31380
SOYBEANS
Effects of atmospheric CO2 on photosynthetic characteristics of soybean leaves N91-31780
Effects of elevated atmospheric carbon dioxide concentrations on water and acid requirements of soybeans grown in a recirculating hydroponic system N91-31781
SPACE BASED RADAR
Integration losses and clutter-Doppler spread for a space based radar caused by ionospheric scintillation during a solar maximum
[AD-A239534] N91-31502

SPACE EXPLORATION
A review of the Los Alamos effort in the development of nuclear rocket propulsion
[DE91-016036] N91-31211
SPACE FLIGHT
Contributions to a space station for flights in the near field and towards geostationary Earth orbit
[ETN-91-99744] N91-31203
SPACE FLIGHT FEEDING
Controlled Ecological Life Support Systems: CELSS '89 Workshop
[NASA-TM-102277] N91-31775
Exploring the limits of crop productivity: A model to evaluate progress N91-31776
Environmental modification of yield and food composition of cowpea and leaf lettuce N91-31777
Efficiency of N use by wheat as a function of influx and efflux of NO3 N91-31778
Environmental and cultural considerations for growth of potatoes in CELSS N91-31779
Effects of atmospheric CO2 on photosynthetic characteristics of soybean leaves N91-31780
Effects of elevated atmospheric carbon dioxide concentrations on water and acid requirements of soybeans grown in a recirculating hydroponic system N91-31781
Sweet potato for closed ecological life support systems using the nutrient film technique N91-31782
Seed sprout production: Consumables and a foundation for higher plant growth in space N91-31790
Controlled ecological life support system breadboard project, 1988 N91-31791
The crop growth research chamber: A ground-based facility for CELSS research N91-31792
Development of the CELSS emulator at NASA. Johnson Space Center N91-31793
A perspective on CELSS control issues N91-31794
Transpiration during life cycle in controlled wheat growth N91-31795
Preparatory space experiments for development of a CELSS N91-31796
Factors affecting plant growth in membrane nutrient delivery N91-31797
Conceptual design of a closed loop nutrient solution delivery system for CELSS implementation in a micro-gravity environment N91-31798
Technology for subsystems of space-based plant growth facilities N91-31799
SPACE MISSIONS
Contributions to a space station for flights in the near field and towards geostationary Earth orbit
[ETN-91-99744] N91-31203
SPACE PLASMAS
Plasma diffusion at the magnetopause? The case of lower hybrid drift waves
[NASA-CR-188913] N91-31957
SPACE PLATFORMS
Advanced power systems for EOS
[NASA-TM-105222] N91-31217
Modeling and simulation of multiple cooperating manipulators on a mobile platform N91-31647
SPACE POWER REACTORS
An investigation of dual-mode operation of a nuclear-thermal rocket engine
[DE91-015977] N91-31210
Nuclear thermal rockets: A systems study
[DE91-017066] N91-31221
Progress in the SP-100 FSQ reactor development
[DE91-016033] N91-31940
SPACE PROCESSING
Summary review of sounding rocket experiments in fluid science and material sciences: TEXUS 1 to 20; MASER 1 and 2
[ESA-SP-1132] N91-31321
Ultrasound absorption in molten salts (TEXUS 14b) N91-31359
Thermal conductivity of liquids (MASER 1) ESA N91-31361
Colloid chemistry (TEXUS 17) ESA N91-31362
Reaction kinetics in glass melts (TEXUS 1) N91-31363
Reaction kinetics in glass melts: Corrosion of SiO2 (TEXUS 4) N91-31364
Reaction kinetics in glass melts: Sodium self-diffusion in alkali-silicate melts (TEXUS 6) N91-31365
Self- and interdiffusion in alkali-silicate melts (TEXUS 11 and 12) N91-31366
Self- and interdiffusion in alkali-silicate melts (TEXUS 13) N91-31367
Reaction kinetics in molten glasses: Self-diffusion in alkali-silicate melts (TEXUS 20) N91-31368
Special refractive index profiles in glasses obtained by ion exchange (TEXUS 19) ESA N91-31369
Sulphur diffusion in liquid cast iron (TEXUS 6) ESA N91-31370
Ventilation and filling of an optical diffusion cell (TEXUS 8) N91-31371
Solutal diffusion measurements in liquid PbSnTe under microgravity (TEXUS 19) N91-31372
Diffusion of Ni in Cu-Au and Cu-Al alloys (TEXUS 20) N91-31373
Phase transition (TEXUS 8) N91-31374
Ionic solutions near the critical point of water (TEXUS 10) ESA N91-31375
Ionic solutions near the critical point of water (TEXUS 12) ESA N91-31376
Phase separation of a binary fluid near its critical point (TEXUS 11) N91-31377
Phase separation in microgravity of binary fluids near the critical point (TEXUS 13) N91-31378
Spinoidal decomposition (TEXUS 17) N91-31379
Directional solidification of doped germanium (TEXUS 4) ESA N91-31380
Striations in germanium (TEXUS 6) ESA N91-31381
Single crystals of CeMg3 (TEXUS 7) ESA N91-31382
Growth of rare Earth-magnesium crystals (TEXUS 12) N91-31383
Floating-zone growth of a silicon single crystal (TEXUS 7) N91-31384
Growth of a Si crystal covered with a SiO2 skin (TEXUS 12) N91-31385
Floating zone growth of GaAs crystals (TEXUS 20) N91-31386
Floating zone crystal growth of Ga-doped germanium (TEXTUS 10) ESA N91-31387
Floating-zone experiments with germanium crystals (TEXUS 12) ESA N91-31388
Floating zone growth of germanium crystals (TEXUS 14b) ESA N91-31389
Semi-confined Bridgman growth of Ga-doped Ge (MASER 2) N91-31390
Crystallisation experiments with salts (TEXUS 13) N91-31392
Vapour growth of an InP crystal (TEXUS 20) N91-31394
Diffusion-controlled growth of protein single crystals: B-galactosidase (TEXUS 3) N91-31395
Solidification of immiscible alloys: ZnBi (TEXUS 2) N91-31415
The coalescence process in immiscible alloys (TEXUS 5) N91-31417
Unidirectional solidification of Zn-Bi samples (TEXUS 14b) N91-31420
Directional solidification of immiscible alloys Zn-Pb (MASER 2) N91-31421
Immiscible alloy system Al-Pb (TEXUS 7) N91-31422
Acoustic mixing (TEXUS 5) N91-31423
Solidification of an Al-Pb-Bi alloy under microgravity (TEXUS 13) N91-31427
Alloys with oxide inclusions (TEXUS 2) N91-31432
Pores in aluminium alloys (TEXUS 3) N91-31447
Manufacture of steel foam (TEXUS 4) N91-31448
Manufacture of steel foam (TEXUS 6) N91-31449
Manufacture of iron foam (TEXUS 7) N91-31450
Metallic foams (TEXUS 5) N91-31451
Preparation of aluminium foams (TEXUS 9) N91-31452
Gas bubbles in a copper-alumina suspension (TEXUS 11) N91-31453
Bubble formation, growth, and expansion during the liquid phase sintering of a WC-Co sample N91-31454
Skin technology (TEXUS 1) N91-31455
Skin technology (TEXUS 2) N91-31456
SPACE SHUTTLE MAIN ENGINE
Space engine safety system
[NASA-CR-187219] N91-31209
Flow induced vibrations in the SSME injector heads
[NASA-CR-184209] N91-31214
Reusable rocket engine intelligent control system framework design, phase 2
[NASA-CR-187213] N91-31219
SPACE SHUTTLES
The SAENGER concept and the German hypersonic technology program
[MBB-UK-0132-91-PUB] N91-31198
SPACE STATION FREEDOM
Restructured Freedom configuration characteristics
[NASA-TM-104057] N91-31201
Nickel-hydrogen cell low-Earth life test update
[NASA-TM-105229] N91-31708
SPACE STATION POWER SUPPLIES
Nickel-hydrogen cell low-Earth life test update
[NASA-TM-105229] N91-31708
SPACE STATIONS
Contributions to a space station for flights in the near field and towards geostationary Earth orbit
[ETN-91-99744] N91-31203
The feasibility of testing NASA's SCAD concentrator on Earth
[DE91-016055] N91-31702
SPACE TRANSPORTATION SYSTEM
The question of an efficient space transportation system for extraterrestrial materials
[ILR-MITT-252(1990)] N91-31197
The SAENGER concept and the German hypersonic technology program
[MBB-UK-0132-91-PUB] N91-31198
SPACEBORNE EXPERIMENTS
Summary review of sounding rocket experiments in fluid science and material sciences: TEXUS 1 to 20; MASER 1 and 2
[ESA-SP-1132] N91-31321
Liquid motion in capillary tubes (TEXUS 3) N91-31322
Liquid motion in capillary tubes (TEXUS 5) N91-31323
Bubbles and foams (TEXUS 10) ESA N91-31324
Long liquid bridges aboard sounding rockets (TEXUS 12) ESA N91-31325
Freezing of a long liquid column (TEXUS 18) ESA N91-31326
Interfacial convection (TEXUS 1) N91-31327
Interfacial convection (TEXUS 2) N91-31328
Diffusion-induced interfacial convection (TEXUS 3) N91-31329
Thermally induced interfacial convection (TEXUS 4) N91-31330
Diffusion-induced interfacial convection (TEXUS 8) N91-31331
Diffusion-induced interfacial convection (TEXUS 11) N91-31332
Oscillatory Marangoni convection (TEXUS 3A and 3B) N91-31333
Critical Marangoni number (TEXUS 5) N91-31334
Critical Marangoni number (TEXUS 8) N91-31335
Thermal Marangoni convection in a floating zone (TEXUS 3) N91-31336
Oscillatory and turbulent flow regimes due to Marangoni convection (TEXUS 7) N91-31337
Influence of a surface tension minimum on the Marangoni effect (TEXUS 8) ESA N91-31338
Influence of a surface tension minimum on the Marangoni effect (TEXUS 9) ESA N91-31339
Influence of a surface tension minimum on the Marangoni effect (TEXUS 19) ESA N91-31340
Thermal Marangoni convection in a floating zone (TEXUS 9) ESA N91-31341
Experimental results on microgravitational fluid dynamics (TEXUS 14b) ESA N91-31342
Three-dimensional Marangoni convection (MASER 1) ESA N91-31343
Three-dimensional Marangoni convection (MASER 2) ESA N91-31344
Thermocapillary drop motion, 1 (MASER 1) ESA N91-31345
Thermocapillary drop motion, 2 (MASER 2) ESA N91-31346
Electrolytic hydrogen formation (TEXUS 1) N91-31347
Electrolytically generated hydrogen bubbles (TEXUS 6) N91-31348
Intermittent polarization (TEXUS 2) N91-31349
Dispersion layers by electrodeposition (TEXUS 1) N91-31350
Dispersion electrolysis (TEXUS 4) N91-31351
Dispersion electrolysis (TEXUS 7) N91-31352
Dispersion electrolysis (TEXUS 9) N91-31353
Nucleate pool boiling (TEXUS 3) N91-31354
Bubble formation, 1 (TEXUS 5) N91-31355
Bubble formation, 2 (TEXUS 10) N91-31356
Bubble formation, 2. Microgravity measurements of the boiling heat transfer from flat heating surfaces (TEXUS 11) N91-31357
Inst. A fuer Thermodynamik. N91-31358
Solution growth of GaAs single crystals (TEXUS 19) N91-31393
Solidification of alloys (TEXUS 1) N91-31400
Tungsten composites (TEXUS 19) ESA N91-31445
Skin technology (TEXUS 3) N91-31457
Skin technology (TEXUS 4) N91-31458
Skin technology (TEXUS 9) N91-31459
Skin technology (TEXUS 11 and 12) N91-31460
Brazing of capillary gaps (TEXUS 2) N91-31461
Soldering in microgravity (TEXUS 5) N91-31462
Adhesion of metals on ceramic substrates (MASER 2) ESA N91-31463
Acoustic positioning of a molten alloy sample (TEXUS 1) N91-31464
Acoustic positioning (TEXUS 9) ESA N91-31465
Containerless solidification of a Pd-Cu-Si sample (TEXUS 9) ESA N91-31466
Acoustic positioning (TEXUS 14b) ESA N91-31467
Containerless undercooling of a Pd-Cu-Si alloy (TEXUS 14b) ESA N91-31468
Electrostatic positioning for containerless processing of a Li-silicate glass (TEXUS 10) ESA N91-31469

Phased array components for the High Temperature Superconducting Space Experiment (HTSSE)
[AD-A239361] N91-31535
Preparatory space experiments for development of a CELSS N91-31796
Development of the Burst and Transient Source Experiment (BATSE)
[NASA-RP-1268] N91-32006

SPACECRAFT COMPONENTS
Large Angle Transient Dynamics (LATDYN) demonstration problem manual
[NASA-CR-4400] N91-31684

SPACECRAFT CONFIGURATIONS
Restructured Freedom configuration characteristics
[NASA-TM-104057] N91-31201

SPACECRAFT CONTROL
Restructured Freedom configuration characteristics
[NASA-TM-104057] N91-31201
Large Angle Transient Dynamics (LATDYN) user's manual
[NASA-CR-4401] N91-31685

SPACECRAFT DESIGN
The International Space University's variable gravity research facility design
[NASA-TM-105224] N91-31196
Interim Service ISDN Satellite (ISIS) network model for advanced satellite designs and experiments
[NASA CR-186565] N91-31488

SPACECRAFT EQUIPMENT
Application of multivariable control system design methodologies to robust beam control of a space-based laser
[AD-A239460] N91-31643

SPACECRAFT MANEUVERS
Application of semianalytic satellite theory to maneuver planning
[AD-A239417] N91-31205

SPACECRAFT POWER SUPPLIES
Advanced power systems for EOS
[NASA-TM-105222] N91-31217
The feasibility of testing NASA's SCAD concentrator on Earth
[DE91-016055] N91-31702
Electrochemical energy storage using PEM systems
[DE91-016020] N91-31711
Progress in the SP-100 FSQ reactor development
[DE91-016033] N91-31940

SPACECRAFT PROPULSION
Hydrogen test of a small, low specific speed centrifugal pump stage
[NASA-CR-187117] N91-31213
Reusable rocket engine intelligent control system framework design, phase 2
[NASA-CR-187213] N91-31219
Technical prospects for utilizing extraterrestrial propellants for space exploration
[NASA-TM-105263] N91-31318

SPACECRAFT SHIELDING
Optimization techniques applied to passive measures for in-orbit spacecraft survivability
[NASA-CR-184198] N91-31204

SPACECRAFT TEMPERATURE
Development of a sensor for high-quality two-phase flow
[NLR-MP-88059-U] N91-31578

SPACECREWS
Sleep logs: Measurement of individual and operational efficiency
[AD-A239774] N91-31770

SPACETENNAS
Integrated control of thermally distorted large space antennas N91-31487

SPARK IGNITION
The autoignition chemistry of paraffinic fuels and pro-knock and anti-knock additives: A detailed chemical kinetic study
[DE91-014992] N91-31314

SPATIAL DISTRIBUTION
Spatiotemporal intermittency N91-31569

SPATIAL MARCHING
Generalized spatial discretization techniques for space-marching algorithms N91-31546

SPECIFIC IMPULSE
Nuclear thermal rockets: A systems study
[DE91-017066] N91-31221

SPECKLE PATTERNS
Particle image velocimatry: Photographic and video techniques N91-31628

SPECTRA
Flight test digitized/compressed video spectrum allocation
[AD-A239535] N91-31503
Spectral large-eddy simulation of isotropic and stably-stratified turbulences N91-31567
ULDA user's guide
[NASA-TM-105074] N91-31813

SPECTRAL BANDS
Scanning imaging absorption spectrometer for atmospheric chartography N91-31725

SPECTRAL REFLECTANCE
Hyperspectral signatures (400 to 2500 nm) of vegetation, minerals, soils, rocks, and cultural features: Laboratory and field measurements
[AD-A239496] N91-31697

SPECTROSCOPY
Abundances from solar flare line spectroscopy
[NASA-CR-183492] N91-32022

SPECTRUM ANALYSIS
An expert system for the identification of silicon impurities using FTIR spectroscopy
[AD-A236504] N91-31246
Spectrum monitoring procedures and techniques
[AD-A239567] N91-31507
An algorithm for spectral factorization of polynomial matrices with any signature
[MEMO-912] N91-31842
An atlas of stellar spectra between 2.00 and 2.45 micrometers (Arnaud, Gilmore, and Collier Cameron 1989)
[NASA-TM-105044] N91-32003
Research studies with the International Ultraviolet Explorer
[NASA-CR-183495] N91-32012

SPECULAR REFLECTION
Exact result for the grazing angle of specular reflection from a sphere
[AD-A239578] N91-31952

SPHERES
Exact result for the grazing angle of specular reflection from a sphere
[AD-A239578] N91-31952

SPHERICAL WAVES
Modelling the response of thick composite materials due to axisymmetric shock loading
[AD-A239531] N91-31243

SPIN STABILIZATION
Choice of a differential method for attitude restitution with dynamic imbalance
[CNES-NT-126] N91-31202

SPLINE FUNCTIONS
Fitting scattered data on spherelike surfaces using tensor products of trigonometric and polynomial splines
[MEMO-909] N91-31904

SPLINES
Enhancement of surface definition and gridding in the Eagle code
[NASA-CR-188796] N91-31820

SPOT WELDS
Analysis and development of a real-time control methodology in resistance spot welding N91-31646

SPRAY NOZZLES
Icing test capabilities for aircraft propulsion systems at the Arnold Engineering Development Center N91-31170

SPRAYED COATINGS
A comparison of techniques for the metallographic preparation of thermal sprayed samples
[DE91-014704] N91-31272
Process for producing plasma sprayed carbide-based coatings with minimal decarburization and near theoretical density
[DE91-012016] N91-31292
Beneficial effects of austemper post-treatment on tungsten carbide based wear coatings
[DE91-013260] N91-31293

SPRAYERS
The influence of fuel characteristics on heterogeneous flame propagation N91-31165
Icing test capabilities for aircraft propulsion systems at the Arnold Engineering Development Center N91-31170
Developments in icing test techniques for aerospace applications in the RAE Pyestock altitude test facility N91-31173
HVOF: Particle, flame diagnostics, and coating characteristics
[DE91-014654] N91-31248
Electrostatic precipitation of condensed acid mist
[DE91-016530] N91-31260

STABILITY
Dispersion alloys (TEXUS 7) N91-31412
Neural network based model reference adaptive control N91-31877

STABILITY TESTS
Intrinsic stability and recovery analysis for tape/film type superconductors
[DE91-015568] N91-31967

STABILIZATION
Method for stabilizing thick honeycomb core composite articles
[PATENT-1-253-424] N91-31224

STABILIZERS
Photoelastic coating study of redesigned CT114 coupon joint test specimen for horizontal stabilizer rear attachment fitting to vertical stabilizer rear spar
[NAE-LTR-ST-1701] N91-31125

STAINLESS STEELS
Effect of convection on weld pool development
[DE91-014213] N91-31649
Stress relaxation in bending of type AISI 304 stainless steel at 773K and 823K
[DE91-618657] N91-31666
Pressure-strain-temperature relationship in shock loaded cylindrical samples of 304 stainless steel
[DE91-013379] N91-31673

STANDARDS
Benchmarking a Network Storage Service
[DE91-013510] N91-31868
Local area gigabit networking
[DE91-014780] N91-31869

STAR FORMATION
Ultraviolet morphology of NGC 1068: The starburst knots and the extended emission region N91-32004
Evolutionary population synthesis in starburst regions
[MPE-PREPRINT-198] N91-32017

STAR TRACKERS
The in-flight calibration of the Hubble space telescope attitude sensors
[NASA-CR-183485] N91-32007

STARBURST GALAXIES
Evolutionary population synthesis in starburst regions
[MPE-PREPRINT-198] N91-32017

STARCHES
Environmental modification of yield and food composition of cowpea and leaf lettuce N91-31777

STARTERS
Cold start development of modern small gas turbine engines at Pratt and Whitney Aircraft of Canada Ltd. N91-31156

STARTING
Design considerations based upon low temperature starting tests on military aircraft turbo engines N91-31157

STATIC CHARACTERISTICS
Static strain and vibration characteristics of a metal semimonocoque helicopter tail cone of moderate size
[NASA-CR-187576] N91-31679

STATIC TESTS
Variations in the static properties, unnotched and notched fatigue life behaviour of 13 batches of 2L.65 aluminium alloy extruded bar
[ARL-STRUC-R-427] N91-31676

STATIONKEEPING
Mass comparisons of electric propulsion systems for NSSK of geosynchronous spacecraft
[NASA-TM-105153] N91-31212

STATISTICAL ANALYSIS
Behaviour of the SIR for space-based DPCA radar under various spatial clutter distributions
[CRC-W7714-7-5271] N91-31485
The effects of fluid particle interactions on interfacial transfer and flow structure
[DE91-016409] N91-31575
Post-processing of data N91-31633
The time-domain earth tides N91-31726
Report of the Workshop on a CLICOM-HOMS Interface
[WCAP-16] N91-31746
Full-information item bi-factor analysis
[AD-A229346] N91-31771
Analysis of the efficiency of an a-posteriori error estimator for linear triangular finite elements
[AD-A239647] N91-31915
Bayes theorem from a sampling-resampling perspective
[AD-A239515] N91-31919
Theoretical nuclear physics
[DE91-016745] N91-31936

STATISTICAL CORRELATION
Biasing errors and corrections N91-31621

STATISTICAL DISTRIBUTIONS
The use of distributional and pointwise statistical measures in GCM intercomparisons
[DE91-015697] N91-31748
Learning convex bodies under uniform distribution
[MEMO-918] N91-31910

STATISTICAL MECHANICS
Virial coefficients and equations of state for mixed fluids; application to CH4-H2O
[DE91-016248] N91-31254

STATISTICAL TESTS
On combining independent significance tests
[AD-A239660] N91-31920

STATOR BLADES
A three-dimensional viscous flow model of stator/rotor interaction in turbomachines N91-31547

STEADY FLOW
Experimental investigation of turbulent flow through a circular-to-rectangular transition duct
[NASA-TM-105210] N91-31106
Vortex-blade interaction on a helicopter principal rotor. Validation of the S2DI computation program and study of vortex models
[ONERA-RT-92/5094-PY] N91-31136
A boundary integral equation method for steady two-dimensional flow in partially saturated media
[DE91-016056] N91-31573

STEAM
Open-cycle ocean thermal energy conversion surface-condenser design analysis and computer program
[DE91-015973] N91-31709

STEELS
A comparison of techniques for the metallographic preparation of thermal sprayed samples
[DE91-014704] N91-31272
Beneficial effects of austemper post-treatment on tungsten carbide based wear coatings
[DE91-013260] N91-31293
Manufacture of steel foam (TEXUS 4) N91-31448
Manufacture of steel foam (TEXUS 6) N91-31449

STEERING
Steerable windowed enclosures
[PATENT-1-262-653] N91-31142
Procedure for steering a low-speed missile, weapon system, and missile for implementation of the procedure
[PATENT-1-265-947] N91-31182

STELLAR COMPOSITION
A spectrophotometric study of the secondaries of Algol systems N91-32005
Evolutionary population synthesis in starburst regions
[MPE-PREPRINT-198] N91-32017

STELLAR ENVELOPES
GRO source candidates: (A) Nearby modest-size molecular clouds; (B) Pulsar with Wolf-Rayet companion that has lost its H-envelope
[NASA-CR-183491] N91-32021

STELLAR EVOLUTION
Ultraviolet morphology of NGC 1068: The starburst knots and the extended emission region N91-32004

STELLAR MAGNETIC FIELDS
Magnetic field decay in neutron stars with superconducting cores N91-32015

STELLAR MODELS
Magnetic field decay in neutron stars with superconducting cores N91-32015
Evolutionary population synthesis in starburst regions
[MPE-PREPRINT-198] N91-32017

STELLAR SPECTRA
An atlas of stellar spectra between 2.00 and 2.45 micrometers (Arnaud, Gilmore, and Collier Cameron 1989)
[NASA-TM-105044] N91-32003

STELLAR SPECTROPHOTOMETRY
A spectrophotometric study of the secondaries of Algol systems N91-32005

STEP FUNCTIONS
Electromagnetic penetration of slot apertures with depth and losses
[DE91-016401] N91-31500

STEREOPHOTOGRAPHY
RADAC model deformation measurement system: First results at the F1 wind tunnel
[AAAF-NT-89-03] N91-31098
Coordinate conversions for presenting and compositing weather radar data
[KNMI-TR-129] N91-31497

STEROIDS
Cold-induced changes in arterial sensitivity
[AD-A239493] N91-31767

STOCHASTIC PROCESSES
Research in regression, information retrieval, inversion of noisy transforms, and stochastic control
[AD-A239490] N91-32001

STRAIN GAGES
Force reconstruction using the inverse of the mode-shape matrix
[DE91-016407] N91-31689

STRAIN MEASUREMENT
Photoelastic coating study of redesigned CT114 coupon joint test specimen for horizontal stabilizer rear attachment fitting to vertical stabilizer rear spar
[NAE-LTR-ST-1701] N91-31125

STRAIN RATE
A comparison of several theories which use jet scaling to predict liftoff heights of turbulent-jet flames
[AD-A239717] N91-31267
Dynamic strength and strain rate effects on fracture behavior of tungsten and tungsten alloys
[DE91-013029] N91-31275
Influence of loading rate on the mechanical response and substructure evolution of shock-loaded copper
[DE91-013390] N91-31276

STRAPS
Method for fastening aircraft frame elements to sandwich skin panels covering same using woven fiber connectors
[PATENT-1-274-075] N91-31126

STRATIFIED FLOW
Spectral large-eddy simulation of isotropic and stably-stratified turbulences N91-31567

STRATOSPHERE
Tunable far infrared studies of molecular parameters in support of stratospheric measurements
[NASA-CR-188774] N91-31723

STREAK CAMERAS
High-speed TV cameras for streak tube readout
[DE91-016081] N91-31602

STREAK PHOTOGRAPHY
Photography of shock waves in explosive crystals
[DE91-015772] N91-31572

STRESS (PHYSIOLOGY)
Effects of stress on judgment and decision making in dynamic tasks
[AD-A239452] N91-31772

STRESS (PSYCHOLOGY)
Effects of stress on judgment and decision making in dynamic tasks
[AD-A239452] N91-31772

STRESS ANALYSIS
An investigation into the effects of damage on the stresses in a composite laminate N91-31226
Stress relaxation in bending of type AISI 304 stainless steel at 773K and 823K
[DE91-618657] N91-31666
An equivalent domain integral method for three-dimensional mixed-mode fracture problems
[NASA-CR-182021] N91-31692

STRESS CONCENTRATION
Response of an alumina fiber reinforced aluminum composite to combined tension-torsion
[AD-A239560] N91-31245

STRESS CORROSION CRACKING
Corrosion fatigue crack arrest in aluminium alloys
[NLR-MP-88050-U] N91-31282
Stress corrosion cracking of 2091 ad 8090 aluminum-lithium alloys in chloride containing aqueous solutions. Influence of sulphate and nitrate additions
[REPT-431/91] N91-31285

STRESS DISTRIBUTION
The influence of plastic-strain-induced anisotropy on stress distributions in the finite deformation of ductile metals N91-31273
Asymptotic finite strain analysis of propagating cracks in elastic-plastic materials N91-31669

STRESS RELAXATION
Stress relaxation in bending of type AISI 304 stainless steel at 773K and 823K
[DE91-618657] N91-31666

STRESS-STRAIN RELATIONSHIPS
Experimental and analytical analysis of stress-strain behavior in a (90/0 deg)2s, SiC/Ti-15-3 laminate
[NASA-TM-104470] N91-31235

STRESSES
Dynamic strength and strain rate effects on fracture behavior of tungsten and tungsten alloys
[DE91-013029] N91-31275

STRIATION
Striations in germanium (TEXUS 6) ESA N91-31381
Floating-zone growth of a silicon single crystal (TEXUS 7) N91-31384
Floating zone growth of GaAs crystals (TEXUS 20) N91-31386

STRINGS
Omission of symbols
[CS-9101] N91-31821

STRUCTURAL ANALYSIS
Two alternative ways for solving the coordination problem in multilevel optimization
[NASA-TM-104036] N91-31138
A method for the geometrically nonlinear analysis of compressively loaded prismatic composite structures N91-31229
Nonlinear probabilistic finite element modeling of composite shells N91-31668
DYNA3D: A nonlinear, explicit, three-dimensional finite element code for solid and structural mechanics
[DE91-015735] N91-31675
Static strain and vibration characteristics of a metal semimonocoque helicopter tail cone of moderate size
[NASA-CR-187576] N91-31679
Behavior of nonlinear mechanical structures subjected to stationary excitations
[ECL-91-01] N91-31681

STRUCTURAL DESIGN
Two alternative ways for solving the coordination problem in multilevel optimization
[NASA-TM-104036] N91-31138
Robotic tool change mechanism
[NASA-CASE-GSC-13239-1] N91-31656
Design and cost of the first commercial stretched-membrane heliostat
[DE91-016870] N91-31715

STRUCTURAL MEMBERS
Torsion resistant grooved joint
[PATENT-1-258-589] N91-31127

STRUCTURAL VIBRATION
Vibration analysis of the SA349/2 helicopter
[NASA-TM-102794] N91-31078
The control of flexible structure vibrations using a cantilevered adaptive truss N91-31671
Mobility power flow analysis of coupled plate structure subjected to mechanical and acoustics excitation
[NASA-CR-188791] N91-31678
Static strain and vibration characteristics of a metal semimonocoque helicopter tail cone of moderate size
[NASA-CR-187576] N91-31679

STUDENTS
Examining the effect of information order on expert judgment
[AD-A239708] N91-31774

SUBHARMONIC GENERATORS
Bifurcations of parametrically forced oscillators
[W-9007] N91-31892

SUBROUTINES
Spur-gear optimization using SPUROPT computer program
[NASA-TM-104394] N91-31648

SUBSONIC FLOW
Second generation supersonic transport aircraft: Low speed aerodynamics
[AAAF-NT-89-02] N91-31137
Development of an advanced panel method for complex configurations in subsonic compressible flow; application to the computation of the potential flow through ducts
[NLR-TR-88001-U] N91-31579
Algorithms for finding an optimal matching between a given string and a string generated by a regular grammar
[MEMO-921] N91-31845

SUBSTRATES
Etching method for photoresists or polymers
[NASA-CASE-ARC-11873-2] N91-31258
Atomic hydrogen driven halogen extraction from Si(100): Eley-Rideal surface kinetics
[AD-A239544] N91-31266
A comparison of techniques for the metallographic preparation of thermal sprayed samples
[DE91-014704] N91-31272
Beneficial effects of austemper post-treatment on tungsten carbide based wear coatings
[DE91-013260] N91-31293
Ion beam enhanced adhesion of iron films to sapphire substrates
[DE91-015931] N91-31308
Adhesion of metals on ceramic substrates (MASER 2) ESA N91-31463
Solid-support substrates for plant growth at a lunar base N91-31800

SUBSTRUCTURES
Mobility power flow analysis of coupled plate structure subjected to mechanical and acoustics excitation
[NASA-CR-188791] N91-31678
Static strain and vibration characteristics of a metal semimonocoque helicopter tail cone of moderate size
[NASA-CR-187576] N91-31679

SUGARS
The conversion of lignocellulosics to fermentable sugars: A survey of current research and application to CELSS N91-31784

SULFONES
Ethynyl terminated imidothicethers and resins therefrom
[NASA-CASE-LAR-13910-2-CU] N91-31307

SULFUR
Sulphur diffusion in liquid cast iron (TEXUS 6) ESA N91-31370
Global model simulations of the long range transport of soot and sulfur from the Kuwait oil fires
[DE91-015771] N91-31719

SULFUR FLUORIDES
Phase transition (TEXUS 8) N91-31374

SUPERCOMPUTERS
Local area gigabit networking
[DE91-014780] N91-31869
The PVM system: Supercomputer level concurrent computation on a heterogeneous network of workstations
[DE91-016276] N91-31870

SUPERCONDUCTING FILMS
High-T(sub c) bolometers
[DE91-017009] N91-31611
Properties of low temperature, low oxygen pressure post-annealed YBa2Cu3O(sub 7-x) thin films
[DE91-015632] N91-31969
SUPERCONDUCTING MAGNETS
Superconducting magnet program for x ray lithography source at Brookhaven National Laboratory
[DE91-016995] N91-31981
SUPERCONDUCTING SUPER COLLIDER
High energy physics
[DE91-015796] N91-31939
SUPERCONDUCTIVITY
Low cost, formable, high T(sub c) superconducting wire
[NASA-CASE-LEW-14676-1] N91-31529
Development of elements of a high T(sub c) superconducting cable
[AD-A239766] N91-31543
Intrinsic stability and recovery analysis for tape/film type superconductors
[DE91-015568] N91-31967
Cu-O charge fluctuations and electron-phonon coupling in the effective single-band Hubbard theory for cuprate superconductors
[DE91-016526] N91-31976
Magnetic field decay in neutron stars with superconducting cores N91-32015
SUPERCONDUCTORS
Solidification of an Al-Pb-Bi alloy under microgravity (TEXUS 13) N91-31427
Low cost, formable, high T(sub c) superconducting wire
[NASA-CASE-LEW-14676-1] N91-31529
The superconducting gravity gradiometer N91-31734
A new method to do time resolved, x ray diffraction studies: The rotating crystal Laue method
[DE91-016527] N91-31935
Intrinsic stability and recovery analysis for tape/film type superconductors
[DE91-015568] N91-31967
Properties of low temperature, low oxygen pressure post-annealed YBa2Cu3O(sub 7-x) thin films
[DE91-015632] N91-31969
Cu-O charge fluctuations and electron-phonon coupling in the effective single-band Hubbard theory for cuprate superconductors
[DE91-016526] N91-31976
Near-edge study of gold-substituted YBa2Cu3O(7-delta)
[NASA-TM-105220] N91-31977
SUPERCRITICAL AIRFOILS
Development and validation of characteristic boundary conditions for cell-centered Euler flow calculations with a shock-free airfoil
[NLR-TP-89360-U] N91-31081
SUPERCRITICAL FLUIDS
Determination of solvation kinetics in supercritical fluids
[DE91-016096] N91-31253
SUPERLATTICES
Rapid thermal annealing effects in In(x)Ga(1-x)As/GaAs strained-layer superlattices
[DE91-015901] N91-31978
Epitaxial growth and electro-optical properties of metal GaAs superlattices
[AD-A239719] N91-31984
SUPERNOVAE
The Berkeley search for distant supernovae to measure omega
[DE91-016418] N91-32010
Nuclear and particle astrophysics
[DE91-016260] N91-32016
SUPERSONIC AIRCRAFT
ATSF supersonic aircraft intake. Review of the analyses of some particular problems, technical summary
[ONERA-RTS-134/2149-AY-640-A] N91-31094
SUPERSONIC COMBUSTION RAMJET ENGINES
A computational and experimental investigation of a three-dimensional hypersonic scramjet inlet flow field
[NASA-CR-188788] N91-31083
SUPERSONIC FLOW
ATSF supersonic aircraft intake. Review of the analyses of some particular problems, technical summary
[ONERA-RTS-134/2149-AY-640-A] N91-31094
Local mean mass volume measurement around a model with lateral jet in supersonic flow
[AAAF-NT-89-08] N91-31102
SUPERSONIC FLUTTER
User's guide to a system of finite-element supersonic panel flutter programs
[NASA-TM-104109] N91-31082
SUPERSONIC INLETS
ATSF supersonic aircraft intake. Review of the analyses of some particular problems, technical summary
[ONERA-RTS-134/2149-AY-640-A] N91-31094
SUPPORT SYSTEMS
The feasibility of testing NASA's SCAD concentrator on Earth
[DE91-016055] N91-31702
SUPPORTS
Removable slider shoe for a translating sleeve used on a jet engine cowl and duct
[PATENT-1-247-868] N91-31177
Radar-cross-section measurement errors caused by test object interaction with low-dielectric-constant supports
[DE91-015340] N91-31490
SUPPRESSORS
Initialization of the HIRLAM model using a digital filter
[DM-57] N91-31747
SURFACE DEFECTS
Influence of surface defects and local structure on oxygenate reaction pathways over metal oxide surfaces
[DE91-016600] N91-31289
SURFACE LAYERS
Laser ablation mechanisms and optical surface damage
[DE91-016928] N91-31642
SURFACE PROPERTIES
A multifunction ion-irradiation/surface modification ultrahigh vacuum chamber system
[DE91-016819] N91-31190
Correlations between surface structure and catalytic activity/selectivity
[DE91-016453] N91-31255
Influence of adhesive polymerization conditions on the durability of adhesive joints
[DCR/I-03357-90] N91-31305
SURFACE REACTIONS
Correlations between surface structure and catalytic activity/selectivity
[DE91-016453] N91-31255
Etching method for photoresists or polymers
[NASA-CASE-ARC-11873-2] N91-31258
Atomic hydrogen driven halogen extraction from Si(100): Eley-Rideal surface kinetics
[AD-A239544] N91-31266
Influence of surface defects and local structure on oxygenate reaction pathways over metal oxide surfaces
[DE91-016600] N91-31289
SURVEILLANCE
Abstracts of papers presented at the First Los Alamos Symposium on Ultra-Wideband Radar
[DE91-015976] N91-31491
Application of digital compression techniques to optical surveillance systems
[DE91-016404] N91-31854
SURVEILLANCE RADAR
The automatic surveillance, tracking, and imaging program. User manual
[SK-1600-44-001-02-0] N91-31483
Improvements to programs for system studies of space-based radar
[DRE-179] N91-31484
SURVEYS
Origins of GPS surveying
[AD-A239676] N91-31121
Survey to assess the usefulness of two model agreements for university-industry cooperative research
[DE91-013937] N91-31985
A study of a 21-cm-selected sample of galaxies N91-32014
SUSPENSIONS
The behaviour of alumina-copper suspensions (TEXUS 3A and 3B) N91-31433
SWEDISH SPACE PROGRAM
Summary review of sounding rocket experiments in fluid science and material sciences: TEXUS 1 to 20; MASER 1 and 2
[ESA-SP-1132] N91-31321
SWEPT FORWARD WINGS
Study of the flow around the GARTEUR AD/AG07 wing: First F2 test campaign results
[ONERA/DERAT-37/5025-26] N91-31096
SWEPT WINGS
A European collaborative investigation of the three-dimensional turbulent shear layers of a swept wing
[NLR-MP-88054-U] N91-31084
SWEPTBACK WINGS
Three dimensional shear flow: Flow visualisation around a highly swept back and high incidence wing
[ONERA-RT-35/5025-28] N91-31584
SWITCHES
Electrophoretic dielectric coatings for magnetic switches
[DE91-015337] N91-31518
Asymmetric soft-error resistant memory
[NASA-CASE-NPO-17394-1-CU] N91-31810
SWITCHING
Asymmetric soft-error resistant memory
[NASA-CASE-NPO-17394-1-CU] N91-31810
SWITCHING CIRCUITS
Proceedings of the International Magnetic Pulse Compression Workshop. Volume 2: Technical summary
[DE91-015775] N91-31521
SYMBOLS
Omission of symbols
[CS-9101] N91-31821
Open architecture for formal reasoning
[AD-A239395] N91-31857
SYMMETRY
Model of an aerospace plane based on an idealized cone-derived waverider forebody N91-31129
Hydrodynamic target response to an induced spatial incoherence-smoothed laser beam
[DE91-015757] N91-31638
Theoretical nuclear physics
[DE91-016745] N91-31936
SYNCHRONISM
The failure of failures: Towards a paradigm for a synchronous communication
[RUU-CS-90-40] N91-31835
Synchronous link-level protocols
[RUU-CS-91-02] N91-31837
Synchronized computational architecture for generalized bilateral control of robot arms
[NASA-CASE-NPO-17401-1-CU] N91-31885
SYNCHRONOUS SATELLITES
Antenna study for 60 GHz intersatellite link
[CD-RPT-ITL-5043-003] N91-31482
SYNCHROTRONS
Summaries of FY 1991 research in the chemical sciences
[DE91-011221] N91-31222
A new method to do time resolved, x ray diffraction studies: The rotating crystal Laue method
[DE91-016527] N91-31935
SYNOPTIC METEOROLOGY
A quantitative analysis of quasi-geostrophic forcing during recent severe weather outbreaks across the southern Great Plains
[PB91-176693] N91-31745
SYNTAX
Attribute evaluation and parsing
[MEMO-INF-91-31] N91-31841
SYNTHESIS (CHEMISTRY)
High pressure catalytic reactions over single-crystal metal surfaces
[DE91-016475] N91-31256
SYNTHESIZERS
A scientific visualization synthesizer
[DE91-012877] N91-31815
SYNTHETIC APERTURE RADAR
Abstracts of papers presented at the First Los Alamos Symposium on Ultra-Wideband Radar
[DE91-015976] N91-31491
SYNTHETIC FUELS
Assessment of costs and benefits of flexible and alternative fuel use in the US transportation sector
[DE91-015451] N91-31319
SYNTHETIC RUBBERS
Mechanical characterization of seismic base isolation elastomers
[DE91-015680] N91-31299
SYSTEM EFFECTIVENESS
Assessing the efficacy of active noise reduction
[CTN-91-60200] N91-31922
SYSTEM FAILURES
The failure of failures: Towards a paradigm for a synchronous communication
[RUU-CS-90-40] N91-31835
SYSTEM IDENTIFICATION
Behavior of nonlinear mechanical structures subjected to stationary excitations
[ECL-91-01] N91-31681
Small time step adaptive control: Theory and application to an electric furnace
[ECL-90-17] N91-31883
SYSTEMS ANALYSIS
Application of multivariable control system design methodologies to robust beam control of a space-based laser
[AD-A239460] N91-31643
Large Angle Transient Dynamics (LATDYN) demonstration problem manual
[NASA-CR-4400] N91-31684
A perspective on CELSS control issues N91-31794
SYSTEMS ENGINEERING
Analysis and evaluation of selected PACE applications
[AD-A239726] N91-31124
Flight tests with a data link used for air traffic control information exchange
[NASA-TP-3135] N91-31143

Flight test digitized/compressed video spectrum allocation
[AD-A239535] N91-31503
Laser Velocimetry, volume 1
[VKI-1991-05-VOL-1] N91-31614
Laser transit velocimetry N91-31623
Laser transit velocimetry: Recent publications N91-31624
Laser Velocimetry, volume 2
[VKI-1991-05-VOL-2] N91-31625
DYNA3D: A nonlinear, explicit, three-dimensional finite element code for solid and structural mechanics
[DE91-015735] N91-31675
A system to determine whole-plant exchange rates of ozone, carbon dioxide and water vapour N91-32027

SYSTEMS MANAGEMENT
Joint Services Electronics Program
[AD-A239459] N91-31536

SYSTEMS SIMULATION
Possibilities of simulation and optimization for guided missile systems
[MBB-UA-1201-90-PUB] N91-31183
Absorbing CAD system geometries into GEANT
[DE91-015707] N91-31816

SYSTEMS STABILITY
Small time step adaptive control: Theory and application to an electric furnace
[ECL-90-17] N91-31883

T

TABLES (DATA)
Annual review of aircraft accident data. US air carrier operations, calendar year 1988
[PB91-176040] N91-31110

TABS (CONTROL SURFACES)
Robotic tool change mechanism
[NASA-CASE-GSC-13239-1] N91-31656

TAIL ASSEMBLIES
Photoelastic coating study of redesigned CT114 coupon joint test specimen for horizontal stabilizer rear attachment fitting to vertical stabilizer rear spar
[NAE-LTR-ST-1701] N91-31125

TANK GEOMETRY
The development of a computational model to predict low temperature fuel flow phenomena N91-31166

TARGET ACQUISITION
Performance of an angle-of-arrival estimator in the presence of a mainbeam interference source
[AD-A239629] N91-31508
Multitarget tracking using optical processing
[AD-A239656] N91-31953

TARGET RECOGNITION
The automatic surveillance, tracking, and imaging program. User manual
[SK-1600-44-001-02-0] N91-31483

TARGETS
Passive ranging of an airborne emitter by a single non-maneuvering or stationary sensor
[PATENT-1-254-292] N91-31116
Rocket boosted target
[PATENT-1-254-289] N91-31207
Coordinate conversions for presenting and compositing weather radar data
[KNMI-TR-129] N91-31497

TECHNOLOGY ASSESSMENT
Evaluation of undeveloped rocket engine cycle applications to advanced transportation
[NASA-CR-184205] N91-31215
Airborne ESM receivers: Techniques and technologies
[ETN-91-99988] N91-31498
Laser Velocimetry, volume 1
[VKI-1991-05-VOL-1] N91-31614
Laser Velocimetry, volume 2
[VKI-1991-05-VOL-2] N91-31625
Review of typical applications: Wind tunnels N91-31632
The status of lightweight photovoltaic space array technology based on amorphous silicon solar cells
[DE91-014985] N91-31698
Genetic algorithms
[ETN-91-99985] N91-31852
Investigation into the applicability of knowledge engineering
[NLR-TP-89031-U] N91-31878
Assessing the efficacy of active noise reduction
[CTN-91-60200] N91-31922

TECHNOLOGY TRANSFER
Solar energy and conservation technologies for Caribbean Tourist Facilities (CTF)
[DE91-016451] N91-31712

TECHNOLOGY UTILIZATION
Thin film, concentrator and multijunction space solar cells: Status and potential
[NASA-TM-104505] N91-31218

TEETH
Effect of thickness and brand of metal ceramic porcelain on color
[AD-A239398] N91-31312

TELECOMMUNICATION
Investigation of the progressive bi-level coding technique for the high-resolution bi-level data compression standard
[AD-A239597] N91-31860

TELEMETRY
Spectrum monitoring procedures and techniques
[AD-A239567] N91-31507

TELEROBOTICS
Kinematics of the six-degree-of-freedom force-reflecting Kraft Master
[NASA-TM-104124] N91-31879

TELEVISION CAMERAS
High-speed TV cameras for streak tube readout
[DE91-016081] N91-31602

TELEVISION SYSTEMS
Automatic satellite tracking system for the NASA Satellite Photometric Observatory
[NASA-TM-105037] N91-31194

TELLURIUM COMPOUNDS
Solutal diffusion measurements in liquid PbSnTe under microgravity (TEXUS 19) N91-31372

TEMPER (METALLURGY)
Beneficial effects of austemper post-treatment on tungsten carbide based wear coatings
[DE91-013260] N91-31293

TEMPERATURE CONTROL
Integrated control of thermally distorted large space antennas N91-31487
Development of a sensor for high-quality two-phase flow
[NLR-MP-88059-U] N91-31578
Real time actuating of laser power and scanning velocity for thermal regulation during laser hardening
[ETN-91-99908] N91-31636

TEMPERATURE DISTRIBUTION
Linear and nonlinear responses of the flow and temperature fields to imposed wall temperature oscillations in differentially heated vertical rectangular enclosures N91-31550

TEMPERATURE EFFECTS
Cold start development of modern small gas turbine engines at Pratt and Whitney Aircraft of Canada Ltd. N91-31156
Design considerations based upon low temperature starting tests on military aircraft turbo engines N91-31157
Fuels and oils as factors in the operation of aero gas turbine engines at low temperatures N91-31163
The effect of fuel properties and atomization on low temperature ignition in gas turbine combustors N91-31164
Catalyst dispersion and activity under conditions of temperature-staged liquefaction
[DE91-016602] N91-31261
Characterization of fire resistant GRP's by mechanical properties determination
[DREA-CR-88-421] N91-31295
Development of toughened ceramics for elevated temperatures
[DE91-015923] N91-31301
Predicted thermal response of a cryogenic fuel tank exposed to simulated aerodynamic heating profiles with different cryogens and fill levels
[NASA-CR-4395] N91-31470
Pressure-strain-temperature relationship in shock loaded cylindrical samples of 304 stainless steel
[DE91-013379] N91-31673
Naval medical research and development command
[AD-A239393] N91-31765
Rapid thermal annealing effects in In(x)Ga(1-x)As/GaAs strained-layer superlattices
[DE91-015901] N91-31978

TEMPERATURE GRADIENTS
Acoustic positioning (TEXUS 14b) ESA N91-31467
Linear and nonlinear responses of the flow and temperature fields to imposed wall temperature oscillations in differentially heated vertical rectangular enclosures N91-31550

TEMPERATURE MEASUREMENT
Experimental determination of the temperature and density of opacity samples
[DE91-015686] N91-31252
Plug-type heat flux gauge
[NASA-CASE-LEW-14967-1] N91-31608
KEMA scientific and technical reports, volume 8, number 2, 1990
[ST-REPT-VOL-8-NO-2] N91-32023
Experiments on ultrasonic thermometry for wet-ash coal gasification N91-32024

TEMPERATURE PROFILES
Icing research related to engine icing characteristics N91-31168
Influence of a surface tension minimum on the Marangoni effect (TEXUS 19) ESA N91-31340
Phase separation of a binary fluid near its critical point (TEXUS 11) N91-31377
Phase separation in microgravity of binary fluids near the critical point (TEXUS 13) N91-31378
Containerless undercooling of a Pd-Cu-Si alloy (TEXUS 14b) ESA N91-31468
Experiments on ultrasonic thermometry for wet-ash coal gasification N91-32024

TEMPORAL DISTRIBUTION
Spatiotemporal intermittency N91-31569

TENSILE PROPERTIES
Magnetic field-induced fracture changes in metastable austenites at 4.2 K
[DE91-016263] N91-31279

TENSILE STRENGTH
Method for imparting strength to intermetallic phases
[PATENT-1-255-929] N91-31271

TENSILE TESTS
Experimental and analytical analysis of stress-strain behavior in a (90/0 deg)2s, SiC/Ti-15-3 laminate
[NASA-TM-104470] N91-31235
Variations in the static properties, unnotched and notched fatigue life behaviour of 13 batches of 2L.65 aluminium alloy extruded bar
[ARL-STRUC-R-427] N91-31676

TENSION
Response of an alumina fiber reinforced aluminum composite to combined tension-torsion
[AD-A239560] N91-31245

TERMINOLOGY
Formalisation of techniques: Chopping down the methodology jungle
[TR-90-26] N91-31996

TERNARY ALLOYS
Solidification of an Al-Pb-Bi alloy under microgravity (TEXUS 13) N91-31427
Demixing of a monotectic ternary alloy (TEXUS 20) N91-31429

TEST CHAMBERS
Environmental icing testing at the Naval Air Propulsion Center N91-31167

TEST EQUIPMENT
Electron-beam-pinch experiment at Harry Diamond Laboratories: Providing for a high-dose-rate flash x ray facility for Transient Radiation Effects on Electronics (TREE) testing of piecepartsa
[AD-A239558] N91-31193
Electronic warfare: Faulty test equipment impairs Navy readiness
[AD-A239562] N91-31506
A knowledge based application of the extended aircraft interrogation and display system
[NASA-TM-4327] N91-31874

TEST FACILITIES
Cold start optimization on a military jet engine N91-31151
Icing test capabilities for aircraft propulsion systems at the Arnold Engineering Development Center N91-31170
Developments in icing test techniques for aerospace applications in the RAE Pyestock altitude test facility N91-31173
The International Space University's variable gravity research facility design
[NASA-TM-105224] N91-31196
Aeronautical Mobile Satellite Service (AMSS) test plan
[DOT/FAA/CT-TN91/20] N91-31495

TEST RANGES
Range reference atmosphere Shemya, Alaska
[AD-A239603] N91-31741

TEXTURES
Hyperspectral signatures (400 to 2500 nm) of vegetation, minerals, soils, rocks, and cultural features: Laboratory and field measurements
[AD-A239496] N91-31697

THEMATIC MAPPING
Examination and mapping of forest damage, using remote sensing methods
[ETN-91-99741] N91-31696

THEOREM PROVING
Open architecture for formal reasoning
[AD-A239395] N91-31857

THEOREMS
Perfect colorings
[RUU-CS-90-35] N91-31831
On a theorem of MacMahon
[CS-9104] N91-31894
On the relation between recurrence and ergodicity properties in denumerable Markov decision chains
[TW-91-02] N91-31918

THEORETICAL PHYSICS
Theoretical nuclear physics
[DE91-016745] N91-31936
THERAPY
Boron in nuclear medicine: New synthetic approaches to PET, SPECT, and BNCT agents
[DE91-016488] N91-31764
THERMAL ANALYSIS
Structure property relationship of aliphatic polyurethane elastomers prepared from CHDI
[AD-A239397] N91-31311
THERMAL CONDUCTIVITY
Thermal conductivity of liquids (MASER 1) ESA N91-31361
Methodology for calibration and use of heat flux transducers
[AD-A239552] N91-31541
Microwave module YAG laser weld development
[DE91-015750] N91-31652
THERMAL ENERGY
Open-cycle ocean thermal energy conversion surface-condenser design analysis and computer program
[DE91-015973] N91-31709
THERMAL EXPANSION
Microwave module YAG laser weld development
[DE91-015750] N91-31652
THERMAL INSULATION
Asbestos-free insulant for rocket motors
[PATENT-1-263-227] N91-31206
THERMAL REACTORS
Carbide fuels for nuclear thermal propulsion
[DE91-016032] N91-31945
THERMAL RESISTANCE
Characterization of fire resistant GRP's by mechanical properties determination
[DREA-CR-88-421] N91-31295
Methodology for calibration and use of heat flux transducers
[AD-A239552] N91-31541
THERMAL STABILITY
Effects of oxidation and combustion environments on the properties of Nicalon/SiC composites
[DE91-016778] N91-31240
Intrinsic stability and recovery analysis for tape/film type superconductors
[DE91-015568] N91-31967
THERMAL STRESSES
The influence of interphase regions on local thermal stresses and deformations in composites N91-31228
THERMOCHEMISTRY
Performance evaluation of insensitive explosives
[DE91-015767] N91-31315
THERMOCOUPLES
Plug-type heat flux gauge
[NASA-CASE-LEW-14967-1] N91-31608
THERMODYNAMIC CYCLES
Evaluation of undeveloped rocket engine cycle applications to advanced transportation
[NASA-CR-184205] N91-31215
THERMODYNAMICS
An investigation into the effects of damage on the stresses in a composite laminate N91-31226
A note on 'the matching polynomial of a polygraph'
[MEMO-910] N91-31905
THERMOELECTRIC GENERATORS
Progress in the SP-100 FSQ reactor development
[DE91-016033] N91-31940
THERMOGRAPHY
Transition length determination in the F1 wind tunnel, test report
[ONERA-PV-1/8571-GY] N91-31089
Techniques to assess the state of health of sealed lead acid batteries
[CTN-91-60214] N91-31515
A relative-intensity two-color phosphor thermography system
[NASA-TM-104123] N91-31595
THERMOMECHANICAL TREATMENT
Deformation induced microstructural and microchemical changes during thermomechanical treatment
[DE91-016949] N91-31290
Analysis of thermomechanical fatigue of unidirectional titanium metal matrix composites
[NASA-TM-104105] N91-31677
THERMOPLASTICITY
The formation of novel thermoplastic composites from liquid crystalline polymers and their blends
[AD-A239546] N91-31244
THICK PLATES
Modelling the response of thick composite materials due to axisymmetric shock loading
[AD-A239531] N91-31243
THIN FILMS
Thin film, concentrator and multijunction space solar cells: Status and potential
[NASA-TM-104505] N91-31218
Low cost, formable, high T(sub c) superconducting wire
[NASA-CASE-LEW-14676-1] N91-31529
A relative-intensity two-color phosphor thermography system
[NASA-TM-104123] N91-31595
Biofilm monitoring coupon system and method of use
[NASA-CASE-MSC-21585-1] N91-31755
THIN WALLS
A method for the geometrically nonlinear analysis of compressively loaded prismatic composite structures N91-31229
THREE DIMENSIONAL BOUNDARY LAYER
A European collaborative investigation of the three-dimensional turbulent shear layers of a swept wing
[NLR-MP-88054-U] N91-31084
THREE DIMENSIONAL FLOW
A computational and experimental investigation of a three-dimensional hypersonic scramjet inlet flow field
[NASA-CR-188788] N91-31083
Study of the flow around the GARTEUR AD/AG07 wing: First F2 test campaign results
[ONERA/DERAT-37/5025-26] N91-31096
Calculating the flow in a turbomachine with Clebsch variables and a finite element method
[ETN-91-99918] N91-31180
Nonlinear combustion instability model in two- to three-dimensions
[NASA-TM-102381] N91-31208
Three-dimensional Marangoni convection (MASER 1) ESA N91-31343
Three-dimensional Marangoni convection (MASER 2) ESA N91-31344
A three-dimensional viscous flow model of stator/rotor interaction in turbomachines N91-31547
Three dimensional shear flow: Flow visualisation around a highly swept back and high incidence wing
[ONERA-RT-35/5025-28] N91-31584
Postprocessing of experimental and numerical results in the case of two and three dimensional flows
[AAAF-NT-89-25] N91-31592
Numerical simulation of three dimensional unsteady flow by multiprocessor solving of the Navier-Stokes equations
[ETN-91-99974] N91-31594
Laser transit velocimetry N91-31623
Laser transit velocimetry: Recent publications N91-31624
Post processing of three dimensional aerothermal computation
[AAAF-NT-89-21] N91-31848
Visualization of three dimensional unsteady computation results
[AAAF-NT-89-23] N91-31850
THREE DIMENSIONAL MODELS
Design of a specific integrated circuit for solving the three dimensional Poisson equation
[ECL-90-24] N91-31527
DYNA3D: A nonlinear, explicit, three-dimensional finite element code for solid and structural mechanics
[DE91-015735] N91-31675
THRUST DISTRIBUTION
Segmented rotatable nozzles
[CA-PATENT-APPL-SN-2-009-634] N91-31174
Segmented vectoring cruise nozzles
[CA-PATENT-APPL-SN-2-009-635] N91-31175
Ventral segmented nozzles
[CA-PATENT-APPL-SN-2-009-636] N91-31176
THRUST VECTOR CONTROL
Enhanced fighter maneuverability aircraft (X-31A) wing and thrust vectoring vane design
[MBB-FE22/S/PUB/0433/A] N91-31135
Segmented rotatable nozzles
[CA-PATENT-APPL-SN-2-009-634] N91-31174
Segmented vectoring cruise nozzles
[CA-PATENT-APPL-SN-2-009-635] N91-31175
Procedure for steering a low-speed missile, weapon system, and missile for implementation of the procedure
[PATENT-1-265-947] N91-31182
THRUST-WEIGHT RATIO
Nuclear thermal rockets: A systems study
[DE91-017066] N91-31221
THUNDERSTORMS
A quantitative analysis of quasi-geostrophic forcing during recent severe weather outbreaks across the southern Great Plains
[PB91-176693] N91-31745
TIME
Signal processing: Time domain and frequency domain N91-31620
TIME DEPENDENCE
Phase transition (TEXUS 8) N91-31374
Phase separation of a binary fluid near its critical point (TEXUS 11) N91-31377
Phase separation in microgravity of binary fluids near the critical point (TEXUS 13) N91-31378
Integrated control of thermally distorted large space antennas N91-31467
An extension of mesh equidistribution to time-dependent partial differential equations
[AD-A239579] N91-31913
Parametric study of diffusion-enhancement networks for spatiotemporal grouping in real-time artificial vision
[AD-A239674] N91-31954
The motions of Mars' pole N91-32019
TIME LAG
Enhanced global positioning system delta-range processing
[PATENT-1-254-637] N91-31115
The time-domain earth tides N91-31726
The timing of injection kickers
[NIKHEF-K/AMPS/91-04] N91-31943
Measurements of inception time lags of repetitively pulsed corona in air N91-32028
TIME MARCHING
Multigrid and Runge-Kutta time stepping applied to the uniformly non-oscillatory scheme for conservation laws
[MEMO-911] N91-31906
TIME MEASUREMENT
KEMA scientific and technical reports, volume 8, number 2, 1990
[ST-REPT-VOL-8-NO-2] N91-32023
Measurements of inception time lags of repetitively pulsed corona in air N91-32028
TIME SERIES ANALYSIS
The time-domain earth tides N91-31726
Research in regression, information retrieval, inversion of noisy transforms, and stochastic control
[AD-A239490] N91-32001
TIMING DEVICES
The timing of injection kickers
[NIKHEF-K/AMPS/91-04] N91-31943
TIN ALLOYS
Macrosegregation in Ag-Sn alloys (MASER 1) N91-31402
TISSUES (BIOLOGY)
Cloning crops in a CELSS via tissue culture: Prospects and problems N91-31783
TITANIUM
Analysis of thermomechanical fatigue of unidirectional titanium metal matrix composites
[NASA-TM-104105] N91-31677
TITANIUM ALLOYS
Creep deformation and fracture of a two-phase TiAl intermetallics
[DE91-011963] N91-31274
TOKAMAK DEVICES
Computational model for deterministic chaos in a magnetically confined plasma
[DE91-016022] N91-31955
TOMAHAWK MISSILES
Environmental icing testing at the Naval Air Propulsion Center N91-31167
TOPOGRAPHY
Three dimensional acoustic propagation at low temperature altitude
[ONERA-RT-13/3641-PY] N91-31924
TORQUE
Torsion resistant grooved joint
[PATENT-1-258-589] N91-31127
Economic analysis of robotic torque measurement system
[DE91-016480] N91-31653
TORQUE MOTORS
A universal computer control system for motors
[NASA-CASE-NPO-17134-1-CU] N91-31528
TORSION
Torsion resistant grooved joint
[PATENT-1-258-589] N91-31127
Response of an alumina fiber reinforced aluminum composite to combined tension-torsion
[AD-A239560] N91-31245
TOUCH
Touch screen use on flight simulator instructor/operator stations
[AD-A239524] N91-31192
TOUGHNESS
Development of toughened ceramics for elevated temperatures
[DE91-015923] N91-31301
TOXICITY
Biological dosimetry and mechanisms of carcinogenesis
[DE91-015689] N91-31763
The medical hazards of flame-suppressant atmospheres
[AD-A239618] N91-31806

TRACKING (POSITION)
Passive ranging of an airborne emitter by a single non-maneuvering or stationary sensor
[PATENT-1-254-292] N91-31116
TRACKING FILTERS
Bayesian multi-sensor tracking for advanced air-traffic control systems
[NLR-MP-88056-U] N91-31119
High speed digital direct access filter for tracking or excision of parametric signal data
[PATENT-1-271-231] N91-31511
TRACKING PROBLEM
Performance of an angle-of-arrival estimator in the presence of a mainbeam interference source
[AD-A239629] N91-31508
TRAFFIC
Traffic model for advanced satellite designs and experiments for ISDN services
[NASA-CR-188802] N91-31200
TRAINING DEVICES
Simulation of distance-dependent functions in visual systems for training simulators using the z-buffer technique
[MBB-UA-1190-90-PUB] N91-31186
TRAINING EVALUATION
Aircrew critique of high-G centrifuge training. Part 1: What was the best part of the program?
[AD-A239781] N91-31809
TRAJECTORY ANALYSIS
Application of a water droplet trajectory prediction code to the design of inlet particle separator anti-icing systems N91-31159
TRAJECTORY CONTROL
Path planning for non-holonomic mobile robots
[LAAS-91135] N91-31882
TRAJECTORY PLANNING
Path planning for non-holonomic mobile robots
[LAAS-91135] N91-31882
Computing minimum length paths of a given homotopy class
[RUU-CS-90-37] N91-31900
TRANSDUCERS
Methodology for calibration and use of heat flux transducers
[AD-A239552] N91-31541
Force reconstruction using the inverse of the mode-shape matrix
[DE91-016407] N91-31689
TRANSFER ORBITS
Mass comparisons of electric propulsion systems for NSSK of geosynchronous spacecraft
[NASA-TM-105153] N91-31212
TRANSFORMATIONS (MATHEMATICS)
A note on semi-adjunctions
[RUU-CS-90-41] N91-31901
Research in regression, information retrieval, inversion of noisy transforms, and stochastic control
[AD-A239490] N91-32001
TRANSITION FLOW
Measurement of six component efforts in transition flow
[AAAF-NT-89-01] N91-31097
Linear and nonlinear stability of boundary layers with streamwise varying properties N91-31545
Vortex interactions in the transition region of a rectangular jet N91-31630
TRANSITION METALS
The chemistry of transition metal clusters
[DE91-015108] N91-31250
Model description of transition metals using the rotated second moment approximation
[DE91-016043] N91-31287
TRANSLATING
The ABC-machine: A sequential stack-based abstract machine for graph rewriting
[TR-90-22] N91-31824
TRANSMISSION LINES
Electromagnetic penetration of slot apertures with depth and losses
[DE91-016401] N91-31500
Phased array components for the High Temperature Superconducting Space Experiment (HTSSE)
[AD-A239361] N91-31535
TRANSMISSIONS (MACHINE ELEMENTS)
Recent manufacturing advances for spiral bevel gears
[NASA-TM-104479] N91-31654
TRANSMITTERS
Emergency locating transmitter
[NASA-CASE-GSC-12821-2] N91-31530
TRANSONIC FLOW
Development and validation of characteristic boundary conditions for cell-centered Euler flow calculations with a shock-free airfoil
[NLR-TP-89360-U] N91-31081
Three dimensional extension of a numerical method for resolving small transonic perturbations in unstructured mesh
[ONERA-RT-50/3064-RY-093-R] N91-31095
Low level turbulence detection by a laser velocimetry technique: Application to transonic flows
[AAAF-NT-89-07] N91-31101
Boundary layer transition detection and measurement methods at CERT/DERAT
[AAAF-NT-89-14] N91-31105
A parametric study of transonic blade-vortex interaction noise
[NASA-CR-188811] N91-31928
TRANSONIC WIND TUNNELS
Validation of two dimensional drag prediction methods
[ONERA-RSF-85/1685-AY] N91-31093
TRANSPARENCE
Boundary layers in transparent melts (TEXUS 10) N91-31406
Separation of transparent fluids due to Marangoni convection (TEXUS 7) N91-31425
Single layer multi-color luminescent display
[NASA-CASE-LAR-13616-1] N91-31950
TRANSPIRATION
Transpiration during life cycle in controlled wheat growth N91-31795
TRANSPORT PROPERTIES
Water transport properties of fuel cell ionomers
[DE91-016015] N91-31259
Composite materials, 2 (TEXUS 2) N91-31431
BES welding science
[DE91-015625] N91-31651
Global model simulations of the long range transport of soot and sulfur from the Kuwait oil fires
[DE91-015771] N91-31719
Nucleus-nucleus collisions and the nuclear equation of state
[DE91-016747] N91-31937
The Li-7 and Be-7 deexcitation lines: Probes for accelerated particle transport models in solar flares
[NASA-CR-183490] N91-32020
TRAPPED PARTICLES
Effects of trapped gases on ceramic-filled-glass composite densification
[DE91-015850] N91-31237
TREES (MATHEMATICS)
Distributed incremental maximum finding in hierarchically divided graphs
[RUU-CS-90-30] N91-31828
The on-line d-dimensional dictionary problem
[RUU-CS-90-31] N91-31829
Approximating treewidth, pathwidth, and minimum elimination tree height
[RUU-CS-91-01] N91-31836
Union-copy structures and dynamic segment trees
[RUU-CS-91-05] N91-31903
From game trees to game graphs
[RUU-CS-90-43] N91-31921
TRIGONOMETRIC FUNCTIONS
Fitting scattered data on spherelike surfaces using tensor products of trigonometric and polynomial splines
[MEMO-909] N91-31904
TROPICAL REGIONS
Tropical tests of a seawater marker
[MRL-TR-90-19] N91-31109
TRUSSES
The control of flexible structure vibrations using a cantilevered adaptive truss N91-31671
TUNGSTEN
Metallic composites with particles (TEXUS 7) N91-31437
Metal matrix composites (TEXUS 20) N91-31440
Dispersion alloys (TEXUS 19) N91-31442
Liquid phase sintering (TEXUS 8) N91-31443
Tungsten composites (TEXUS 10) N91-31444
Tungsten composites (TEXUS 19) ESA N91-31445
Liquid phase sintering (TEXUS 19) ESA N91-31446
Distortion-free x ray mask technology
[AD-A239770] N91-31665
TUNGSTEN ALLOYS
Dynamic strength and strain rate effects on fracture behavior of tungsten and tungsten alloys
[DE91-013029] N91-31275
Bubble formation, growth, and expansion during the liquid phase sintering of a WC-Co sample N91-31454
TUNGSTEN CARBIDES
Process for producing plasma sprayed carbide-based coatings with minimal decarburization and near theoretical density
[DE91-012016] N91-31292
Beneficial effects of austemper post-treatment on tungsten carbide based wear coatings
[DE91-013260] N91-31293
Dispersion alloys (TEXUS 19) N91-31442
TUNING
Tuning maps for setpoint changes and load disturbance upsets in a three capacity process under multivariable control
[NASA-TM-104419] N91-31876
TURBINE BLADES
Field evaluation of six protective coatings applied to T56 turbine blades after 500 hours of engine use
[ARL-MAT-TM-405] N91-31179
Capacitive bridge-type probe and conversion circuitry
[PATENT-1-263-444] N91-31598
Capacitive bridge-type probe and conversion circuitry
[PATENT-1-263-443] N91-31599
X-ray inspection system
[PATENT-1-258-924] N91-31660
TURBINE ENGINES
Control system design considerations for starting turbo-engines during cold weather operation N91-31155
Design considerations based upon low temperature starting tests on military aircraft turbo engines N91-31157
Development of an anti-icing system for the T800-LHT-800 turboshaft engine N91-31160
Environmental icing testing at the Naval Air Propulsion Center N91-31167
Icing test capabilities for aircraft propulsion systems at the Arnold Engineering Development Center N91-31170
TURBINE WHEELS
Fatigue-resistant nickel-base superalloys
[PATENT-1-253-363] N91-31268
Crack propagation in heat resistant disk alloys. Short crack propagation in alloys for high characteristic turbomachine disks
[ETN-91-99981] N91-31683
TURBOFAN ENGINES
Low temperature environment operations of turbo engines N91-31146
Analysis of starting problems in cold weather with ASTAZOU type turbine engines in helicopters N91-31147
Engine icing criticality assessment N91-31161
Icing research related to engine icing characteristics N91-31168
TURBOMACHINERY
Calculating the flow in a turbomachine with Clebsch variables and a finite element method
[ETN-91-99918] N91-31180
TURBOPROP AIRCRAFT
Analysis of interior noise ground and flight test data for advanced turboprop aircraft applications
[NASA-CR-187558] N91-31927
TURBOPROP ENGINES
Vulnerability of a small powerplant to wet snow conditions N91-31148
Ice ingestion experience on a small turboprop engine N91-31162
Analysis of interior noise ground and flight test data for advanced turboprop aircraft applications
[NASA-CR-187558] N91-31927
TURBOSHAFTS
Development of an anti-icing system for the T800-LHT-800 turboshaft engine N91-31160
TURBULENCE
A comparison of several theories which use jet scaling to predict liftoff heights of turbulent-jet flames
[AD-A239717] N91-31267
Introduction to the Modeling of Turbulence
[VKI-LS-1991-02] N91-31551
Body force effects on turbulence N91-31558
New Approaches in the Description and Modeling of Turbulence
[VKI-LS-1991-03] N91-31565
RNG and turbulence modeling N91-31570
TURBULENCE EFFECTS
Use of an ARMA model in turbulent medium acoustic propagation
[ONERA-RF-14/3641-PY] N91-31925
TURBULENCE MODELS
Introduction to the Modeling of Turbulence
[VKI-LS-1991-02] N91-31551
Introduction to the Modeling of Turbulence: Introduction N91-31552
Two-equation models for low-Reynolds number flow N91-31554
An introduction to second moment closure N91-31555
Inclusion of second-moment closures into finite-volume solvers N91-31556
Body force effects on turbulence N91-31558
An introduction to single-point closure methodology N91-31561
Direct and large eddy simulation of turbulence: Summary of the state-of-the-art 1991 N91-31562

Turbulence modeling for compressible flows and implementation in Navier-Stokes solvers N91-31564
TURBULENT BOUNDARY LAYER
A European collaborative investigation of the three-dimensional turbulent shear layers of a swept wing [NLR-MP-88054-U] N91-31084
Contribution of low wave numbers to the wall pressure field in a two dimensional turbulent boundary layer: Comparison of different experimental techniques [ECL-90-15] N91-31091
Development of an infrared Laser Fourier Densitometer (LFD) and first wind tunnel tests [PMI-2335] N91-31189
Boundary layer turbulence appearance mechanisms studied by plane laser visualizations [AAAF-NT-89-10] N91-31587
User's manual for the Langley boundary layer noise propagation program (MRS-BLP) [NASA-CR-187559] N91-31923
TURBULENT FLOW
Experimental investigation of turbulent flow through a circular-to-rectangular transition duct [NASA-TM-105210] N91-31106
Vortex-blade interaction on a helicopter principal rotor. Validation of the S2DI computation program and study of vortex models [ONERA-RT-92/5094-PY] N91-31136
Second generation supersonic transport aircraft: Low speed aerodynamics [AAAF-NT-89-02] N91-31137
Oscillatory and turbulent flow regimes due to Marangoni convection (TEXUS 7) N91-31337
Two-equation models for high-Reynolds-number flow N91-31553
Large-eddy simulation of the turbulent flow in the downstream region of a backward facing step N91-31568
RNG and turbulence modeling N91-31570
Use of 4-hot-wire probes to study turbulent flow [AAAF-NT-89-15] N91-31588
TURBULENT HEAT TRANSFER
Prediction of rotor surface unsteady pressure and heat transfer from wake passing N91-31549
TURBULENT JETS
A comparison of several theories which use jet scaling to predict liftoff heights of turbulent-jet flames [AD-A239717] N91-31267
Use of 4-hot-wire probes to study turbulent flow [AAAF-NT-89-15] N91-31588
TWO DIMENSIONAL FLOW
Contribution of low wave numbers to the wall pressure field in a two dimensional turbulent boundary layer: Comparison of different experimental techniques [ECL-90-15] N91-31091
Validation of two dimensional drag prediction methods [ONERA-RSF-85/1685-AY] N91-31093
ATSF supersonic aircraft intake. Review of the analyses of some particular problems, technical summary [ONERA-RTS-134/2149-AY-640-A] N91-31094
Vortex-blade interaction on a helicopter principal rotor. Validation of the S2DI computation program and study of vortex models [ONERA-RT-92/5094-PY] N91-31136
Computational fluid dynamics N91-31544
A boundary integral equation method for steady two-dimensional flow in partially saturated media [DE91-016056] N91-31573
Acceleration techniques for a spectral multi-grid method [MEMO-914] N91-31580
Compressible two dimensional boundary layer strong perfect fluid coupling in the case of sharp leading edge profiles. Stationary case [ONERA-RT-42/1621-RY-093-R] N91-31586
Postprocessing of experimental and numerical results in the case of two and three dimensional flows [AAAF-NT-89-25] N91-31592
Laser transit velocimetry N91-31623
Vortex interactions in the transition region of a rectangular jet N91-31630
Least-squares solution of incompressible Navier-Stokes equations with the p-version of finite elements [NASA-TM-105203] N91-31911
TWO DIMENSIONAL MODELS
The effect of jet bleed on base pressure distribution, shedding frequency, and mean velocity profiles in the wake behind a two-dimensional blunt model [MPIS-12/1990] N91-31085
TWO PHASE FLOW
The effects of fluid particle interactions on interfacial transfer and flow structure [DE91-016409] N91-31575
Development of a sensor for high-quality two-phase flow [NLR-MP-88059-U] N91-31578

U

ULTRAHIGH VACUUM
A multifunction ion-irradiation/surface modification ultrahigh vacuum chamber system [DE91-016819] N91-31190
Contribution to the implementation of a completely in situ device in ultrahigh vacuum for the development of MIS on InP structures: Al2O3/InP interface optimization [ECL-91-04] N91-31526
ULTRASONIC RADIATION
Ultrasound absorption in molten salts (TEXUS 14b) N91-31359
Ultrasound absorption in molten salts (TEXUS 17) ESA N91-31360
ULTRASONICS
Experiments on ultrasonic thermometry for wet-ash coal gasification N91-32024
ULTRAVIOLET ASTRONOMY
Research studies with the International Ultraviolet Explorer [NASA-CR-183495] N91-32012
ULTRAVIOLET MICROSCOPY
Design and analysis of multilayer x ray/XUV microscope [NASA-CR-184197] N91-31607
ULTRAVIOLET RADIATION
Pyrimidine dimer formation by UVA radiation: Implications for photoreactivation [DE91-015837] N91-31756
ULTRAVIOLET SPECTRA
Ultraviolet morphology of NGC 1068: The starburst knots and the extended emission region N91-32004
Research studies with the International Ultraviolet Explorer [NASA-CR-183495] N91-32012
UNDERWATER EXPLOSIONS
Modelling the response of thick composite materials due to axisymmetric shock loading [AD-A239531] N91-31243
UNIONS (CONNECTORS)
Avioptic plug-in interconnection [PATENT-1-254-415] N91-31946
UNITED KINGDOM
Low temperature environment operation of turbo engines: A military operator's experience and requirements N91-31145
UNIVERSE
The Berkeley search for distant supernovae to measure omega [DE91-016418] N91-32010
UNIVERSITIES
Optimizing the long-term retention of skills: Structural and analytic approaches to skill maintenance 3 [AD-A239574] N91-31773
Survey to assess the usefulness of two model agreements for university-industry cooperative research [DE91-013937] N91-31985
UNIVERSITY PROGRAM
The International Space University's variable gravity research facility design [NASA-TM-105224] N91-31196
What is the Federal Demonstration Project? [DE91-013936] N91-31986
UNLOADING WAVES
Anelastic release from the shock-compressed state [DE91-009961] N91-31672
UNSTEADY AERODYNAMICS
User's guide to a system of finite-element supersonic panel flutter programs [NASA-TM-104109] N91-31082
Visualization of three dimensional unsteady computation results [AAAF-NT-89-23] N91-31850
UNSTEADY FLOW
Measurement of six component efforts in transition flow [AAAF-NT-89-01] N91-31097
Airfoil-vortex interaction: Unsteady wall pressure measurement [AAAF-NT-89-13] N91-31104
Prediction of rotor surface unsteady pressure and heat transfer from wake passing N91-31549
Postprocessing of test and computation results by the wavelet method [AAAF-NT-89-24] N91-31591
The development of a specific image analysis technique for exploiting flow visualization negatives [AAAF-NT-89-26] N91-31593
Numerical simulation of three dimensional unsteady flow by multiprocessor solving of the Navier-Stokes equations [ETN-91-99974] N91-31594
Automatic analysis of visualization negatives [ETN-91-99971] N91-31603
Unsteady flow past an airfoil pitching at a constant rate N91-31629
Visualization of three dimensional unsteady computation results [AAAF-NT-89-23] N91-31850
UPPER ATMOSPHERE
Range reference atmosphere, Fairbanks, Alaska [AD-A239520] N91-31739
Range reference atmosphere Wake Island, North Pacific [AD-A239602] N91-31740
Range reference atmosphere Shemya, Alaska [AD-A239603] N91-31741
Range reference atmosphere: Thule, Greenland [AD-A239659] N91-31742
UPPER SURFACE BLOWING
Method and apparatus for detecting laminar flow separation and reattachment [NASA-CASE-LAR-13952-2-SB] N91-31596
URANIUM CARBIDES
Carbide fuels for nuclear thermal propulsion [DE91-016032] N91-31945
URANIUM COMPOUNDS
Intrinsic neutron source strengths in uranium solutions [DE91-016091] N91-31933
URANIUM 235
Progress in the SP-100 FSQ reactor development [DE91-016033] N91-31940
USER MANUALS (COMPUTER PROGRAMS)
Performance Assessment and Coverage Evaluation (PACE) workstation (user manual) [AD-A239723] N91-31122
OMEGA system Performance Assessment and Coverage Evaluation (PACE) workstation design and implementation, volume 2 [AD-A239724] N91-31123
The automatic surveillance, tracking, and imaging program. User manual [SK-1600-44-001-02-0] N91-31483
DYNA3D: A nonlinear, explicit, three-dimensional finite element code for solid and structural mechanics [DE91-015735] N91-31675
Large Angle Transient Dynamics (LATDYN) user's manual [NASA-CR-4401] N91-31685
ULDA user's guide [NASA-TM-105074] N91-31813
SHOWTIME.C: A C-language program for data acquisition and display user's guide [DE91-016241] N91-31817
A users' guide to PVM (parallel virtual machine) [DE91-016934] N91-31855
User's manual for the Langley boundary layer noise propagation program (MRS-BLP) [NASA-CR-187559] N91-31923
GEOTRANS: An interface program from GEOPROGRAM to a geographic information system [DE91-016111] N91-31998
USER REQUIREMENTS
Cluster-based adaptive information retrieval N91-31991

V

V/STOL AIRCRAFT
Segmented rotatable nozzles [CA-PATENT-APPL-SN-2-009-634] N91-31174
Segmented vectoring cruise nozzles [CA-PATENT-APPL-SN-2-009-635] N91-31175
VACUUM
Approximate treatment of a strong explosion and expansion in a near vacuum [DE91-016063] N91-31574
VACUUM CHAMBERS
A multifunction ion-irradiation/surface modification ultrahigh vacuum chamber system [DE91-016819] N91-31190
VACUUM SYSTEMS
Review of vacuum systems for x ray lithography light sources [DE91-017008] N91-31982
VALENCE
Near-edge study of gold-substituted YBa2Cu3O(7-delta) [NASA-TM-105220] N91-31977

VAN DER WAALS FORCES
BAe overview of current gravitational physics research N91-31731
Review of microgravity N91-31736
VANADIUM ALLOYS
Method for imparting strength to intermetallic phases [PATENT-1-255-929] N91-31271
VANES
Enhanced fighter maneuverability aircraft (X-31A) wing and thrust vectoring vane design [MBB-FE22/S/PUB/0433/A] N91-31135
VAPOR DEPOSITION
A multifunction ion-irradiation/surface modification ultrahigh vacuum chamber system [DE91-016819] N91-31190
Advanced research workshop on Wide Gap II-VI Semiconductors [AD-A233796] N91-31960
Photophysics and chemistry of ultra-fast ZnO and CdS phosphors [DE91-013106] N91-31966
Limited reaction processing for semiconductor materials preparation [AD-A239639] N91-31983
VAPOR PHASE EPITAXY
Vapour growth of an InP crystal (TEXUS 20) N91-31394
Innovative optoelectronic materials and structures using OMVPE [AD-A239518] N91-31951
VAPOR PHASES
The chemistry of transition metal clusters [DE91-015108] N91-31250
Adjustment of the mixing-rate constant in the eddy break-up model for a jet flame N91-32030
VAPORIZING
Cold start investigation of an APU with annular combustor and fuel vaporizers N91-31154
VARIABILITY
Calculating the flow in a turbomachine with Clebsch variables and a finite element method [ETN-91-99918] N91-31180
Time scales of variability associated with Nordeste precipitation [DE91-015696] N91-31718
VARIATIONS
Transition length determination in the F1 wind tunnel, test report [ONERA-PV-1/8571-GY] N91-31089
VAX COMPUTERS
A case study for the real-time experimental evaluation of the VIPER microprocessor [NASA-TM-104098] N91-31531
VECTORS (MATHEMATICS)
A scientific visualization synthesizer [DE91-012877] N91-31815
VEGETABLES
Environmental modification of yield and food composition of cowpea and leaf lettuce N91-31777
Cloning crops in a CELSS via tissue culture: Prospects and problems N91-31783
Biomass production and nitrogen dynamics in an integrated aquaculture/agriculture system N91-31789
Seed sprout production: Consumables and a foundation for higher plant growth in space N91-31790
VEGETATION
Hyperspectral signatures (400 to 2500 nm) of vegetation, minerals, soils, rocks, and cultural features: Laboratory and field measurements [AD-A239496] N91-31697
VEGETATION GROWTH
Controlled Ecological Life Support Systems: CELSS '89 Workshop [NASA-TM-102277] N91-31775
Biomass production and nitrogen dynamics in an integrated aquaculture/agriculture system N91-31789
Seed sprout production: Consumables and a foundation for higher plant growth in space N91-31790
The crop growth research chamber: A ground-based facility for CELSS research N91-31792
Preparatory space experiments for development of a CELSS N91-31796
Factors affecting plant growth in membrane nutrient delivery N91-31797
Technology for subsystems of space-based plant growth facilities N91-31799
Solid-support substrates for plant growth at a lunar base N91-31800
VELOCITY
Passive ranging of an airborne emitter by a single non-maneuvering or stationary sensor [PATENT-1-254-292] N91-31116
VELOCITY DISTRIBUTION
Laser velocimetry at the CEAT aerodynamic group: Application to unsteady measurements on a fluid flap profile [AAAF-NT-89-05] N91-31100
Calculation of fragment ejection velocities on explosion of a launcher [CNES-NT-128] N91-31195
Influence of a surface tension minimum on the Marangoni effect (TEXUS 8) ESA N91-31338
Influence of a surface tension minimum on the Marangoni effect (TEXUS 9) ESA N91-31339
Influence of a surface tension minimum on the Marangoni effect (TEXUS 19) ESA N91-31340
Linear and nonlinear stability of boundary layers with streamwise varying properties N91-31545
Laser Doppler velocimeter measurements of the streamwise velocity component in the viscous sublayer of a turbulent channel flow [MPIS-MITT-97] N91-31582
Postprocessing of experimental and numerical results in the case of two and three dimensional flows [AAAF-NT-89-25] N91-31592
Numerical simulation of three dimensional unsteady flow by multiprocessor solving of the Navier-Stokes equations [ETN-91-99974] N91-31594
Unsteady flow past an airfoil pitching at a constant rate N91-31629
Vortex interactions in the transition region of a rectangular jet N91-31630
Laser Doppler anemometer miniaturized with diode laser [AAAF-NT-89-06] N91-31637
Asymptotic finite strain analysis of propagating cracks in elastic-plastic materials N91-31669
VELOCITY ERRORS
Biasing errors and corrections N91-31621
VELOCITY MEASUREMENT
Exploitation of OAT15A profile tests in the T2 wind tunnel: Experimental determination of the wave drag [ONERA-RSF-88/1685-AY-158-A] N91-31092
Low level turbulence detection by a laser velocimetry technique: Application to transonic flows [AAAF-NT-89-07] N91-31101
Laser Fourier densitometry and laser induced photochemical anemometry in supersonic flow [AAAF-NT-89-09] N91-31103
Understanding composite explosive energetics [DE91-015770] N91-31316
Laser Doppler velocimeter measurements of the streamwise velocity component in the viscous sublayer of a turbulent channel flow [MPIS-MITT-97] N91-31582
Special design and gauging of anemoclinometric sondes [IMFL-90/03] N91-31604
Laser Velocimetry, volume 1 [VKI-1991-05-VOL-1] N91-31614
Basic LDV1 component system N91-31616
Fundamentals of signal processing N91-31617
Advanced systems: Multicomponent LDV N91-31619
Accuracy of laser velocimetry N91-31622
Laser Velocimetry, volume 2 [VKI-1991-05-VOL-2] N91-31625
Particle image velocimetry: Photographic and video techniques N91-31628
Review of typical applications. Part 1: Measurements in liquid flows, free jets, combustion, and in the atmosphere N91-31631
Laser Doppler anemometer miniaturized with diode laser [AAAF-NT-89-06] N91-31637
VENTILATION
Ventilation and filling of an optical diffusion cell (TEXUS 8) N91-31371
VENTING
Predicted thermal response of a cryogenic fuel tank exposed to simulated aerodynamic heating profiles with different cryogens and fill levels [NASA-CR-4395] N91-31470
VERBAL COMMUNICATION
Optimizing the long-term retention of skills: Structural and analytic approaches to skill maintenance 3 [AD-A239574] N91-31773
VERY LARGE SCALE INTEGRATION
Joint Services Electronics Program [AD-A239459] N91-31536
A methodology for producing and testing a genesil silicon compiler designed VLSI chip which incorporates design for testability [AD-A239465] N91-31537
Parametric study of diffusion-enhancement networks for spatiotemporal grouping in real-time artificial vision [AD-A239674] N91-31954
VERY LOW FREQUENCIES
Arctic VLF/LF data acquisition [AD-A239704] N91-31510
VHSIC (CIRCUITS)
Time domain electromagnetic waves in multilayered media [AD-A239545] N91-31504
VIBRATION
Flow induced vibrations in the SSME injector heads [NASA-CR-184209] N91-31214
VIBRATION DAMPING
Vibration analysis of the SA349/2 helicopter [NASA-TM-102794] N91-31078
Mechanical characterization of seismic base isolation elastomers [DE91-015680] N91-31299
The control of flexible structure vibrations using a cantilevered adaptive truss N91-31671
Response of seismic-isolated structures under long-period motions [DE91-015673] N91-31674
VIBRATION ISOLATORS
Mechanical characterization of seismic base isolation elastomers [DE91-015680] N91-31299
Response of seismic-isolated structures under long-period motions [DE91-015673] N91-31674
VIBRATION MODE
Force reconstruction using the inverse of the mode-shape matrix [DE91-016407] N91-31689
Fuselage shell and cavity response measurements on a DC-9 test section [NASA-CR-187557] N91-31926
VIBRATION TESTS
Static strain and vibration characteristics of a metal semimonocoque helicopter tail cone of moderate size [NASA-CR-187576] N91-31679
VIBRATIONAL SPECTRA
Mass resolved excitation spectroscopy of benzyl and phenylnitrene radicals [AD-A239394] N91-31264
VIDEO DATA
Circular format zig-zag scanning of vidicon tubes [DE91-016084] N91-31610
VIDEO EQUIPMENT
Particle image velocimetry: Photographic and video techniques N91-31628
VIDEO SIGNALS
Flight test digitized/compressed video spectrum allocation [AD-A239535] N91-31503
VIDICONS
Circular format zig-zag scanning of vidicon tubes [DE91-016084] N91-31610
VIRIAL COEFFICIENTS
Virial coefficients and equations of state for mixed fluids; application to CH4-H2O [DE91-016248] N91-31254
VIRTUAL MEMORY SYSTEMS
The potential impact of VHDL on dependable distributed system design [AD-A239769] N91-31664
A users' guide to PVM (parallel virtual machine) [DE91-016934] N91-31855
VISCOELASTIC DAMPING
Vaudreuil (France) large hydrodynamic tunnel: Acoustic chamber damping [METRAVIB-RDS-1-007-67] N91-31090
VISCOELASTICITY
Composite matrix deformation process in relation to molecular structure [ETN-91-99915] N91-31232
Computational fluid dynamics N91-31544
VISCOPLASTICITY
Finite element modeling of orthogonal machining using an elastic-viscoplastic material model [DE91-016815] N91-31477
VISCOSITY
Application of second-moment closure in complex flows N91-31559
Crystallization of the glassy grain boundary phase in silicon nitride ceramics [NASA-CR-188717] N91-31961
Indirect measurement of the viscosity of the intergranular glass phase in yttria-sintered silicon nitride N91-31965
VISCOUS DRAG
Viscous effects [MBB-FE202/S/PUB/441] N91-31088
VISCOUS FLOW
A European collaborative investigation of the three-dimensional turbulent shear layers of a swept wing [NLR-MP-88054-U] N91-31084
Viscous effects [MBB-FE202/S/PUB/441] N91-31088

Exploitation of OAT15A profile tests in the T2 wind tunnel: Experimental determination of the wave drag
[ONERA-RSF-88/1685-AY-158-A] N91-31092
A three-dimensional viscous flow model of stator/rotor interaction in turbomachines N91-31547
Laser Doppler velocimeter measurements of the streamwise velocity component in the viscous sublayer of a turbulent channel flow
[MPIS-MITT-97] N91-31582
Numerical simulation of three dimensional unsteady flow by multiprocessor solving of the Navier-Stokes equations
[ETN-91-99974] N91-31594
Least-squares solution of incompressible Navier-Stokes equations with the p-version of finite elements
[NASA-TM-105203] N91-31911

VISUAL FLIGHT
Simulation of distance-dependent functions in visual systems for training simulators using the z-buffer technique
[MBB-UA-1190-90-PUB] N91-31186

VISUAL OBSERVATION
Laser ablation mechanisms and optical surface damage
[DE91-016928] N91-31642

VISUAL TASKS
A graph theoretic approach to scene matching
[NASA-CR-187817] N91-31947

VITREOUS MATERIALS
Crystallization and characterization of Y2O3-SiO2 glasses N91-31962

VOICE COMMUNICATION
Flight tests with a data link used for air traffic control information exchange
[NASA-TP-3135] N91-31143

VOID RATIO
On the relation between recurrence and ergodicity properties in denumerable Markov decision chains
[TW-91-02] N91-31918

VOIDS
Solidification of an Al-Pb-Bi alloy under microgravity (TEXUS 13) N91-31427

VORTEX BREAKDOWN
Adjustment of the mixing-rate constant in the eddy break-up model for a jet flame N91-32030

VORTICES
Airfoil-vortex interaction: Unsteady wall pressure measurement
[AAAF-NT-89-13] N91-31104
Introduction to the Modeling of Turbulence
[VKI-LS-1991-02] N91-31551
Direct and large eddy simulation of turbulence: Summary of the state-of-the-art 1991 N91-31562
Direct and large-eddy simulations of transition in the compressible boundary layer N91-31566
Spectral large-eddy simulation of isotropic and stably-stratified turbulences N91-31567
Large-eddy simulation of the turbulent flow in the downstream region of a backward facing step N91-31568
Numerical simulation of three dimensional unsteady flow by multiprocessor solving of the Navier-Stokes equations
[ETN-91-99974] N91-31594
Vortex interactions in the transition region of a rectangular jet N91-31630
A parametric study of transonic blade-vortex interaction noise
[NASA-CR-188811] N91-31928

VORTICITY
Unsteady flow past an airfoil pitching at a constant rate N91-31629

W

WAKES
The effect of jet bleed on base pressure distribution, shedding frequency, and mean velocity profiles in the wake behind a two-dimensional blunt model
[MPIS-12/1990] N91-31085
A three-dimensional viscous flow model of stator/rotor interaction in turbomachines N91-31547
Prediction of rotor surface unsteady pressure and heat transfer from wake passing N91-31549

WALL FLOW
Contribution of low wave numbers to the wall pressure field in a two dimensional turbulent boundary layer: Comparison of different experimental techniques
[ECL-90-15] N91-31091
Laser Doppler velocimeter measurements of the streamwise velocity component in the viscous sublayer of a turbulent channel flow
[MPIS-MITT-97] N91-31582
A critical comparison of two-equation turbulence models
[NASA-TM-105237] N91-31597

WALL PRESSURE
Airfoil-vortex interaction: Unsteady wall pressure measurement
[AAAF-NT-89-13] N91-31104

WALL TEMPERATURE
Linear and nonlinear responses of the flow and temperature fields to imposed wall temperature oscillations in differentially heated vertical rectangular enclosures N91-31550

WALLS
A comparison of time domain boundary conditions for acoustic waves in wave guides
[NASA-CR-187618] N91-31889

WARNING SYSTEMS
Process for detecting the likelihood of ice formation, ice warning system for carrying out the process, and utilization thereof
[PATENT-1-250-926] N91-31107

WASTE TREATMENT
A review of accelerated response actions available to the environmental restoration program: Selected case histories and associated issues
[DE91-013608] N91-31716
Preliminary evaluation of waste processing in a CELSS N91-31788

WATER
Virial coefficients and equations of state for mixed fluids; application to CH4-H2O
[DE91-016248] N91-31254
Water transport properties of fuel cell ionomers
[DE91-016015] N91-31259
Ionic solutions near the critical point of water (TEXUS 10) ESA N91-31375
Ionic solutions near the critical point of water (TEXUS 12) ESA N91-31376
Photography of shock waves in explosive crystals
[DE91-015772] N91-31572
Fifth force experiments N91-31733
Biofilm monitoring coupon system and method of use
[NASA-CASE-MSC-21585-1] N91-31755
Effects of elevated atmospheric carbon dioxide concentrations on water and acid requirements of soybeans grown in a recirculating hydroponic system N91-31781

WATER RESOURCES
Report of the Workshop on a CLICOM-HOMS Interface
[WCAP-16] N91-31746

WATER VAPOR
Simulated effects of a doubling of carbon dioxide on corn production in portions of the central US
[DE91-016843] N91-31722
A system to determine whole-plant exchange rates of ozone, carbon dioxide and water vapour N91-32027

WAVE ATTENUATION
Ultrasound absorption in molten salts (TEXUS 14b) N91-31359
Ultrasound absorption in molten salts (TEXUS 17) ESA N91-31360

WAVE DIFFRACTION
Three dimensional acoustic propagation at low temperature altitude
[ONERA-RT-13/3641-PY] N91-31924

WAVE DISPERSION
Elastic wave dispersion in high-strength ceramics
[DE91-016648] N91-31309

WAVE DRAG
Exploitation of OAT15A profile tests in the T2 wind tunnel: Experimental determination of the wave drag
[ONERA-RSF-88/1685-AY-158-A] N91-31092

WAVE EQUATIONS
Nonlinear combustion instability model in two- to three-dimensions
[NASA-TM-102381] N91-31208

WAVE FRONTS
Approximate treatment of a strong explosion and expansion in a near vacuum
[DE91-016063] N91-31574

WAVE PROPAGATION
Abstracts of papers presented at the First Los Alamos Symposium on Ultra-Wideband Radar
[DE91-015976] N91-31491
Gravitational wave research N91-31732
Artificial neural networks for seismic data interpretation
[AD-A239673] N91-31743

WAVE REFLECTION
Postprocessing of test and computation results by the wavelet method
[AAAF-NT-89-24] N91-31591

WAVEFORMS
Integration losses and clutter-Doppler spread for a space based radar caused by ionospheric scintillation during a solar maximum
[AD-A239534] N91-31502

WAVEGUIDE ANTENNAS
Composite waveguide coupling aperture having a thickness dimension
[PATENT-1-259-401] N91-31514

WAVERIDERS
Computational analysis of hypersonic flows past elliptic-cone waveriders N91-31080
Model of an aerospace plane based on an idealized cone-derived waverider forebody N91-31129

WEAPON SYSTEMS
Design considerations based upon low temperature starting tests on military aircraft turbo engines N91-31157
Procedure for steering a low-speed missile, weapon system, and missile for implementation of the procedure
[PATENT-1-265-947] N91-31182

WEAR
Eccentricity effects on leakage of a brush seal at low speeds
[NASA-TM-105141] N91-31220
A comparison of techniques for the metallographic preparation of thermal sprayed samples
[DE91-014704] N91-31272

WEAR INHIBITORS
Beneficial effects of austemper post-treatment on tungsten carbide based wear coatings
[DE91-013260] N91-31293

WEATHER FORECASTING
Temporal sampling considerations in global climate modeling
[DE91-015695] N91-31717
A quantitative analysis of quasi-geostrophic forcing during recent severe weather outbreaks across the southern Great Plains
[PB91-176693] N91-31745

WEAVING
The mechanical response of woven Kevlar fabric
[DE91-010581] N91-31230

WEDGES
A comparison of time domain boundary conditions for acoustic waves in wave guides
[NASA-CR-187618] N91-31889

WEIBULL DENSITY FUNCTIONS
A Weibull brittle material failure model for the ABAQUS computer program
[DE91-016813] N91-31690

WEIGHTLESSNESS
The International Space University's variable gravity research facility design
[NASA-TM-105224] N91-31196
Summary review of sounding rocket experiments in fluid science and material sciences: TEXUS 1 to 20; MASER 1 and 2
[ESA-SP-1132] N91-31321
Liquid motion in capillary tubes (TEXUS 3) N91-31322
Liquid motion in capillary tubes (TEXUS 5) N91-31323
Bubbles and foams (TEXUS 10) ESA N91-31324
Long liquid bridges aboard sounding rockets (TEXUS 12) ESA N91-31325
Freezing of a long liquid column (TEXUS 18) ESA N91-31326
Interfacial convection (TEXUS 1) N91-31327
Interfacial convection (TEXUS 2) N91-31328
Diffusion-induced interfacial convection (TEXUS 3) N91-31329
Thermally induced interfacial convection (TEXUS 4) N91-31330
Diffusion-induced interfacial convection (TEXUS 8) N91-31331
Diffusion-induced interfacial convection (TEXUS 11) N91-31332
Oscillatory Marangoni convection (TEXUS 3A and 3B) N91-31333
Critical Marangoni number (TEXUS 5) N91-31334
Critical Marangoni number (TEXUS 8) N91-31335
Thermal Marangoni convection in a floating zone (TEXUS 3) N91-31336
Oscillatory and turbulent flow regimes due to Marangoni convection (TEXUS 7) N91-31337
Influence of a surface tension minimum on the Marangoni effect (TEXUS 8) ESA N91-31338
Influence of a surface tension minimum on the Marangoni effect (TEXUS 9) ESA N91-31339
Influence of a surface tension minimum on the Marangoni effect (TEXUS 19) ESA N91-31340
Thermal Marangoni convection in a floating zone (TEXUS 9) ESA N91-31341
Experimental results on microgravitational fluid dynamics (TEXUS 14b) ESA N91-31342
Three-dimensional Marangoni convection (MASER 1) ESA N91-31343
Electrolytic hydrogen formation (TEXUS 1) N91-31347

Electrolytically generated hydrogen bubbles (TEXUS 6) N91-31348
Intermittent polarization (TEXUS 2) N91-31349
Dispersion layers by electrodeposition (TEXUS 1) N91-31350
Dispersion electrolysis (TEXUS 4) N91-31351
Dispersion electrolysis (TEXUS 7) N91-31352
Dispersion electrolysis (TEXUS 9) N91-31353
Nucleate pool boiling (TEXUS 3) N91-31354
Bubble formation, 1 (TEXUS 5) N91-31355
Bubble formation, 2 (TEXUS 10) N91-31356
Bubble formation, 2. Microgravity measurements of the boiling heat transfer from flat heating surfaces (TEXUS 11) N91-31357
Inst. A fuer Thermodynamik. N91-31358
Ultrasound absorption in molten salts (TEXUS 14b) N91-31359
Ultrasound absorption in molten salts (TEXUS 17) ESA N91-31360
Thermal conductivity of liquids (MASER 1) ESA N91-31361
Colloid chemistry (TEXUS 17) ESA N91-31362
Reaction kinetics in glass melts (TEXUS 1) N91-31363
Reaction kinetics in glass melts: Corrosion of SiO2 (TEXUS 4) N91-31364
Reaction kinetics in glass melts: Sodium self-diffusion in alkali-silicate melts (TEXUS 6) N91-31365
Self- and interdiffusion in alkali-silicate melts (TEXUS 11 and 12) N91-31366
Self- and interdiffusion in alkali-silicate melts (TEXUS 13) N91-31367
Reaction kinetics in molten glasses: Self-diffusion in alkali-silicate melts (TEXUS 20) N91-31368
Special refractive index profiles in glasses obtained by ion exchange (TEXUS 19) ESA N91-31369
Sulphur diffusion in liquid cast iron (TEXUS 6) ESA N91-31370
Ventilation and filling of an optical diffusion cell (TEXUS 8) N91-31371
Solutal diffusion measurements in liquid PbSnTe under microgravity (TEXUS 19) N91-31372
Diffusion of Ni in Cu-Au and Cu-Al alloys (TEXUS 20) N91-31373
Phase transition (TEXUS 8) N91-31374
Ionic solutions near the critical point of water (TEXUS 10) ESA N91-31375
Ionic solutions near the critical point of water (TEXUS 12) ESA N91-31376
Phase separation of a binary fluid near its critical point (TEXUS 11) N91-31377
Solution growth of GaAs single crystals (TEXUS 19) N91-31393
Pores in aluminium alloys (TEXUS 3) N91-31447
Manufacture of steel foam (TEXUS 4) N91-31448
Manufacture of steel foam (TEXUS 6) N91-31449
Manufacture of iron foam (TEXUS 7) N91-31450
Metallic foams (TEXUS 5) N91-31451
Preparation of aluminium foams (TEXUS 9) N91-31452
Gas bubbles in a copper-alumina suspension (TEXUS 11) N91-31453
Bubble formation, growth, and expansion during the liquid phase sintering of a WC-Co sample N91-31454
Skin technology (TEXUS 1) N91-31455
Skin technology (TEXUS 2) N91-31456
Skin technology (TEXUS 4) N91-31458
Skin technology (TEXUS 9) N91-31459
Brazing of capillary gaps (TEXUS 2) N91-31461

WELDABILITY
Weldability and hot ductility of iron aluminides [DE91-016343] N91-31280
Analysis and development of a real-time control methodology in resistance spot welding N91-31646
Microwave module YAG laser weld development [DE91-015750] N91-31652

WELDED JOINTS
Apparatus and method for explosive bonding to edge of flyer plate [NASA-CASE-LAR-14096-1] N91-31476
Effect of convection on weld pool development [DE91-014213] N91-31649
Weld pool solidification and microstructures [DE91-014263] N91-31650
BES welding science [DE91-015625] N91-31651

WELDING
Analysis and development of a real-time control methodology in resistance spot welding N91-31646
Weld pool solidification and microstructures [DE91-014263] N91-31650
BES welding science [DE91-015625] N91-31651

WETTABILITY
Adhesion of metals on ceramic substrates (MASER 2) ESA N91-31463

WETTING
Meniscus stability in immiscible metals (MASER 1) N91-31428
Composite materials, 1 (TEXUS 1) N91-31430
Metallic composites with particles (TEXUS 6) N91-31436
Metallic composites with particles (TEXUS 7) N91-31437
Melting and solidification of metallic composites (TEXUS 9) N91-31438
Metal matrix composites (TEXUS 20) N91-31440

WHEAT
Exploring the limits of crop productivity: A model to evaluate progress N91-31776
Efficiency of N use by wheat as a function of influx and efflux of NO3 N91-31778
Use of inedible wheat residues from the KSC-CELSS breadboard facility for production of fungal cellulase N91-31785
Transpiration during life cycle in controlled wheat growth N91-31795
Factors affecting plant growth in membrane nutrient delivery N91-31797

WHISKERS (CRYSTALS)
Development of toughened ceramics for elevated temperatures [DE91-015923] N91-31301

WIND DIRECTION
Effect of wind over deck conditions on aircraft approach speeds for carrier landings [AD-A239511] N91-31141

WIND EFFECTS
Effect of wind over deck conditions on aircraft approach speeds for carrier landings [AD-A239511] N91-31141
Three dimensional acoustic propagation at low temperature altitude [ONERA-RT-13/3641-PY] N91-31924

WIND MEASUREMENT
A satellite-based radar wind sensor [NASA-CR-188805] N91-31750

WIND PRESSURE
Development of single blade rotor wind energy converters: From M400 prototype to MON 50 preseries [MBB-UE-0015-90-PUB] N91-31705

WIND TUNNEL APPARATUS
Instrumentation under development for the ONERA F4 wind tunnel [AAAF-NT-89-11] N91-31187
A relative-intensity two-color phosphor thermography system [NASA-TM-104123] N91-31595

WIND TUNNEL MODELS
The effect of jet bleed on base pressure distribution, shedding frequency, and mean velocity profiles in the wake behind a two-dimensional blunt model [MPIS-12/1990] N91-31085
RADAC model deformation measurement system: First results at the F1 wind tunnel [AAAF-NT-89-03] N91-31098
Local mean mass volume measurement around a model with lateral jet in supersonic flow [AAAF-NT-89-08] N91-31102

WIND TUNNEL STABILITY TESTS
The effect of jet bleed on base pressure distribution, shedding frequency, and mean velocity profiles in the wake behind a two-dimensional blunt model [MPIS-12/1990] N91-31085

WIND TUNNEL TESTS
A European collaborative investigation of the three-dimensional turbulent shear layers of a swept wing [NLR-MP-88054-U] N91-31084
Transition length determination in the F1 wind tunnel, test report [ONERA-PV-1/8571-GY] N91-31089
Contribution of low wave numbers to the wall pressure field in a two dimensional turbulent boundary layer: Comparison of different experimental techniques [ECL-90-15] N91-31091
Exploitation of OAT15A profile tests in the T2 wind tunnel: Experimental determination of the wave drag [ONERA-RSF-88/1685-AY-158-A] N91-31092
Validation of two dimensional drag prediction methods [ONERA-RSF-85/1685-AY] N91-31093
Study of the flow around the GARTEUR AD/AG07 wing: First F2 test campaign results [ONERA/DERAT-37/5025-26] N91-31096
RADAC model deformation measurement system: First results at the F1 wind tunnel [AAAF-NT-89-03] N91-31098
Conditional sampling [AAAF-NT-89-04] N91-31099
Airfoil-vortex interaction: Unsteady wall pressure measurement [AAAF-NT-89-13] N91-31104
Second generation supersonic transport aircraft: Low speed aerodynamics [AAAF-NT-89-02] N91-31137
Instrumentation under development for the ONERA F4 wind tunnel [AAAF-NT-89-11] N91-31187
A first hot wire scanner [AAAF-NT-89-16] N91-31188
Development of an infrared Laser Fourier Densitometer (LFD) and first wind tunnel tests [PMI-2335] N91-31189
Review of typical applications: Wind tunnels N91-31632

WIND TUNNEL WALLS
Vaudreuil (France) large hydrodynamic tunnel: Acoustic chamber damping [METRAVIB-RDS-1-007-67] N91-31090

WIND TUNNELS
Numerical model of evolution in supercooled cloud of water droplets in a case of icing N91-31169
Instrumentation under development for the ONERA F4 wind tunnel [AAAF-NT-89-11] N91-31187
A first hot wire scanner [AAAF-NT-89-16] N91-31188
Review of typical applications: Wind tunnels N91-31632

WIND TURBINES
Development of single blade rotor wind energy converters: From M400 prototype to MON 50 preseries [MBB-UE-0015-90-PUB] N91-31705

WIND VELOCITY
Effect of wind over deck conditions on aircraft approach speeds for carrier landings [AD-A239511] N91-31141

WINDOWS (APERTURES)
Steerable windowed enclosures [PATENT-1-262-653] N91-31142

WINDPOWER UTILIZATION
Development of single blade rotor wind energy converters: From M400 prototype to MON 50 preseries [MBB-UE-0015-90-PUB] N91-31705

WING FLAPS
Laser velocimetry at the CEAT aerodynamic group: Application to unsteady measurements on a fluid flap profile [AAAF-NT-89-05] N91-31100

WINGS
Enhanced fighter maneuverability aircraft (X-31A) wing and thrust vectoring vane design [MBB-FE22/S/PUB/0433/A] N91-31135

WIRE
Low cost, formable, high T(sub c) superconducting wire [NASA-CASE-LEW-14676-1] N91-31529
Evaluation of the intermittent GTA cold wire feed weld system [DE91-016477] N91-31657

WOLF-RAYET STARS
GRO source candidates: (A) Nearby modest-size molecular clouds; (B) Pulsar with Wolf-Rayet companion that has lost its H-envelope [NASA-CR-183491] N91-32021

WORDS (LANGUAGE)
A fast multiport memory based on single-port memory cells [AD-A239455] N91-31811

WORK-REST CYCLE
Sleep logs: Measurement of individual and operational efficiency [AD-A239774] N91-31770

WORKSTATIONS
Performance Assessment and Coverage Evaluation (PACE) workstation (user manual) [AD-A239723] N91-31122
OMEGA system Performance Assessment and Coverage Evaluation (PACE) workstation design and implementation, volume 2 [AD-A239724] N91-31123
Analysis and evaluation of selected PACE applications [AD-A239726] N91-31124
Touch screen use on flight simulator instructor/operator stations [AD-A239524] N91-31192

X

X RAY ABSORPTION
X ray and gamma ray spectroscopy of solids under pressure [DE91-016948] N91-31263
Near-edge study of gold-substituted YBa2Cu3O(7-delta) [NASA-TM-105220] N91-31977

X RAY ASTRONOMY
Multiplexing readout channels in proportional counters [NASA-TM-103552] N91-31606
X RAY DIFFRACTION
A new method to do time resolved, x ray diffraction studies: The rotating crystal Laue method [DE91-016527] N91-31935
Photophysics and chemistry of ultra-fast ZnO and CdS phosphors [DE91-013106] N91-31966
X RAY INSPECTION
X-ray inspection system [PATENT-1-258-924] N91-31660
X RAY SOURCES
Approximate treatment of a strong explosion and expansion in a near vacuum [DE91-016063] N91-31574
Superconducting magnet program for x ray lithography source at Brookhaven National Laboratory [DE91-016995] N91-31981
Review of vacuum systems for x ray lithography light sources [DE91-017008] N91-31982
X RAY SPECTROSCOPY
KEMA scientific and technical reports, volume 8, number 2, 1990 [ST-REPT-VOL-8-NO-2] N91-32023
Some applications of X-ray photoelectron spectroscopy and secondary-ion mass spectroscopy N91-32029
X RAYS
Electron-beam-pinch experiment at Harry Diamond Laboratories: Providing for a high-dose-rate flash x ray facility for Transient Radiation Effects on Electronics (TREE) testing of pieceparts [AD-A239558] N91-31193
Multiplexing readout channels in proportional counters [NASA-TM-103552] N91-31606
Design and analysis of multilayer x ray/XUV microscope [NASA-CR-184197] N91-31607
Distortion-free x ray mask technology [AD-A239770] N91-31665
Near-edge study of gold-substituted YBa2Cu3O(7-delta) [NASA-TM-105220] N91-31977
A search for periodicity in the x ray spectrum of black hole candidate A0620-00 [AD-A239488] N91-32011

Y

YAG LASERS
Microwave module YAG laser weld development [DE91-015750] N91-31652
YARNS
The mechanical response of woven Kevlar fabric [DE91-010581] N91-31230
YIELD STRENGTH
The influence of moisture and pressure on the mechanical properties of a glass-epoxy matrix composite and a graphite-epoxy matrix composite [AD-A239509] N91-31242
Method for imparting strength to intermetallic phases [PATENT-1-255-929] N91-31271
Dynamic yield strength of a palladium alloy metallic glass [DE91-015111] N91-31298
YTTRIUM OXIDES
Crystallization and characterization of Y2O3-SiO2 glasses N91-31962
Indirect measurement of the viscosity of the intergranular glass phase in yttria-sintered silicon nitride N91-31965
Near-edge study of gold-substituted YBa2Cu3O(7-delta) [NASA-TM-105220] N91-31977

Z

ZEOLITES
Solid-support substrates for plant growth at a lunar base N91-31800
ZETA PINCH
Advanced concepts theory [AD-A239780] N91-31959
ZINC ALLOYS
Solidification of immiscible alloys: ZnBi (TEXUS 2) N91-31415
The coalescence process in immiscible alloys (TEXUS 3) N91-31416
The coalescence process in immiscible alloys (TEXUS 5) N91-31417
Unidirectional solidification of immiscible alloys (TEXUS 7) N91-31419
Unidirectional solidification of Zn-Bi samples (TEXUS 14b) N91-31420
Directional solidification of immiscible alloys Zn-Pb (MASER 2) N91-31421
Acoustic mixing (TEXUS 5) N91-31423
Solidification of immiscible alloys (TEXUS 8) N91-31424
ZINC OXIDES
Photophysics and chemistry of ultra-fast ZnO and CdS phosphors [DE91-013106] N91-31966
ZINC SELENIDES
Advanced research workshop on Wide Gap II-VI Semiconductors [AD-A233796] N91-31960
ZIRCONIUM OXIDES
Alumina reinforced tetragonal zirconia (TZP) composites [DE91-016748] N91-31239
Ceramic composition [PATENT-1-249-609] N91-31294

Typical Personal Author Index Listing

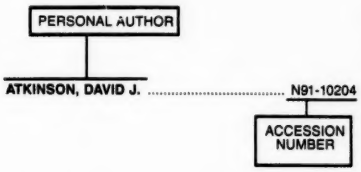

Listings in this index are arranged alphabetically by personal author. The accession number denotes the number by which the citation is identified.

A

AALTO, S. N91-31361
ABEN, J. M. M. N91-32027
ABRAHAMSON, A. LOUIS N91-31685
ACHUTUNI, V. R. N91-31722
ACKROYD, J. N91-31730
ACOSTA, WALDO N91-31181
ADELMAN, LEONARD N91-31774
ADKINS, N. J. E. N91-31441
AHLBORN, H. N91-31399
AIHARA, SHIN ICHI N91-31909
AIKAWA, MASAMICHI N91-31758
AKSIT, MEHMET N91-31865
ALBIN, GARY N91-31769
ALCARAZ, E. N91-31587
ALEXANDER, K. B. N91-31301
ALLEN, H. W. N91-31802
ALLISON, M. J. N91-31815
AMENDE, W. N91-31442
AMENDOLA, A. N91-31131
ANDERKO, A. N91-31254
ANDERSON, C. A. N91-31477
ANDERSON, R. E. N91-31933
ANDERSON, RON N91-31219
ANDRA, DAVID N91-31745
ANDREWS, G. F. N91-31223
ANGELLATTA, ROB K. N91-31531
ANSALDI, JEAN N91-31182
ANTHONY, MARTIN N91-31881
ARENA, ALDO N91-31127
ARMAND, C. N91-31099
ARNAL, D. N91-31105
ARNOLD, G. W. N91-31302
N91-31303
ARPE, K. N91-31717
ARTOK, L. N91-31261
ASH, D. I. N91-31280
ASLAM, M. N91-31778
ATTERIDGE, D. G. N91-31290

B

BAAS, S. M. N91-31845
BABUSKA, IVO N91-31691
N91-31914
N91-31915
BACH, D. N91-31252
BACH, H. N91-31407
BAE, GUN-WOONG N91-31297
BAGCHI, ARUNABHA N91-31909
BAHEI-EL-DIN, Y. A. N91-31677
BAILEY, SHEILA G. N91-31196
N91-31217
BAILLEUX, P. N91-31604
BAIRD, D. G. N91-31244
BAKER, LEONARD H. N91-31494
BAKKER, ERWIN M. N91-31831
BANGUI, F. N91-31095
BANKS, ERIC A. N91-31757
BANKS, H. T. N91-31889
BANTA, G. N91-31770
BARDON, M. F. N91-31165
BARESI, LARRY N91-31784
BARTHE, L. N91-31682
BARTLETT, C. SCOTT N91-31170
BARUCHEL, J. N91-31382
BASS, R. GERALD N91-31307
BATAILLE, F. N91-31636
BATCHELOR, G. L. N91-31163
BATEMAN, V. I. N91-31689
BATHKE, W. N91-31461
BATINA, JOHN T. N91-31082
BATTAGLIN, G. N91-31302
BAWIRZANSKI, EDUARD N91-31582
BAZIN, M. N91-31098
BEASLEY, M. R. N91-31611
BECHER, P. F. N91-31301
BECK, R. N. N91-31759
BEGIN, F. N91-31137
BEGUELIN, A. N91-31855
BEIER, W. N91-31364
N91-31369
BELKAHLA, SOLIMAN N91-31284
BELZ, FRANK N91-31862
BEMENT, LAURENCE J. N91-31476
BENINGA, K. N91-31714
BENNETT, J. N91-31690
BENNETT, SUSAN M. N91-31779
BENO, M. A. N91-31935
BENOIT, ROBERT L. N91-31127
BERGER, H. N91-31682
BERGMAN, A. N91-31416
N91-31417
N91-31418
N91-31421
BERGMANS, LODEWIJK N91-31865
BERKES, I. N91-31916
BERNEDE, P. N91-31683
BERNSTEIN, E. R. N91-31264
BERTHOUMIEU, P. N91-31851
BERTOLOTTI, FABIO PAOLO N91-31545
BETANCOURT, T. N91-31295
BEVERSDORFF, MANFRED N91-31624
BEYSENS, D. N91-31377
N91-31378
BEZARD, H. N91-31092
BHUYAN, JAYANARAYAN N91-31991
BIANCHINI, GARY V. N91-31160
BICKEL, J. E. N91-31510
BIELAWA, RICHARD L. N91-31679
BIERMANN, J. J. P. N91-32026
BILL, ROBERT C. N91-31654
BINCZEWSKI, GEORGE J. N91-31269
BINGEL, BRADFORD D. N91-31685
BISCHOFF, MANFRED N91-31706
BLACKBURN, JAMES C. N91-31193
BLACKWELL, ANN L. N91-31794
BLAIR, H. T. N91-31945
BLAIR, L. W. N91-31162
BLANCHET, P. N91-31112
BLOM, H. A. P. N91-31119
BLOMQUIST, STEVEN M. N91-31193
BLUMBERG, R. N91-31981
BOATNER, L. A. N91-31970
BOBIN, L. N91-31102
BOCK, R. D. N91-31771
BODLAENDER, HANS L. N91-31836
N91-31838
N91-31897
BOEMAN, RAYMOND G. N91-31238
BOERSTOEL, J. W. N91-31081
N91-31131
BOHL, R. J. N91-31211
BOHM, A. P. W. N91-31818
BONDAREVA, O. N. N91-31907
BONNET, J. P. N91-31103
N91-31189
BONSI, C. K. N91-31782
BOSCOLO-BOSCOLETTO, A. N91-31302
BOTTCHER, C. N91-31931
BOTTERI, G. B. N91-31666
BOUBANGA, ANTOINE N91-31680
BOUREZ, J. P. N91-31604
BOURNE, LYLE E., JR. N91-31773
BOUTIER, A. N91-31187
N91-31614
N91-31615
N91-31616
N91-31619
N91-31622
N91-31625
N91-31626
BOWER, J. N91-31770
BOYLE, B. J. N91-32010
BRADLEY, JIMMY D. N91-31655
BRADLEY, M. M. N91-31749
BRAEDT, M. N91-31364
N91-31365
BRAETSCH, V. N91-31366
N91-31367
BRANNON, M. A. N91-31785
BRATTON, THOMAS D. N91-31494
BRAUN, JEAN-FRANCOIS N91-31474
BRECKNER, HARVEY H., III N91-31241
BREISACHER, KEVIN J. N91-31208
BREITHAUPT, D. R. N91-31316
BREITHAUPT, R. D. N91-31315
BREITMAN, D. S. N91-31156
BRESNICK, TERRY A. N91-31774
BRIGHT, F. V. N91-31253
BRINKSMA, ED N91-31493
BROCK, B. C. N91-31490
BROER, HENK N91-31892
BROERSMA, H. J. N91-31905
BROESIUS, J. Y. N91-31658
BRON, C. N91-31864
BRONSON, M. J. N91-31257
BROOK, E. N91-31161
BROWN, ALISON N91-31115
BROWN, D. N91-31715
BROWN, D. C. N91-31713
BRUECKNER, R. N91-31327
N91-31328
N91-31329
N91-31330
N91-31331
N91-31332
BRUEMMER, S. M. N91-31290
BRUNE, GERHARD N91-31186
BRUNEAU, CHARLES-HENRI N91-31583
BRUNO, RONALD C. N91-31499
BRUNSON, G. S. N91-31933
BRUTTIG, STEPHEN P. N91-31767
BRYANT, DAVID M. T. N91-31479
BRYNESTAD, J. N91-31970
BUBENHEIM, DAVID L. N91-31777
N91-31792
BUCK, O. N91-31688
BUCKINGHAM, RONALD N91-31199
BUDAI, J. D. N91-31969
BUEHLER, MARTIN G. N91-31810
BUGBEE, BRUCE N91-31776
BUGROVA, A. I. N91-31944
BUHL, R. A. N91-31190
BUKSA, J. J. N91-31210
BULA, R. J. N91-31799
BULLOCK, S. RAY N91-31216
BURGE, P. L. N91-31926
BURLATON, J. P. N91-31761
BURR, R. N91-31770
BURROWS, JOHN P. N91-31724
N91-31725
BURTON, STANLEY K. N91-31207
BUTTERFIELD, K. B. N91-31933
BYRNE, CATHERINE A. N91-31311

C

CABRIT, B. N91-31103
N91-31189
CACCAVALE, F. N91-31302
CALOINI, ANDREA N91-31995
CAMEL, D. N91-31391
CAMERON, C. P. N91-31702
CAMERON, RICHARD J. N91-31479

CAMPBELL, D. L. N91-31802
CANNON, M. R. N91-31926
CAPPIELLO, M. W. N91-31210
CARHART, HOMER W. N91-31265
CARIGNAN, PIERRE J. N91-31206
CARISTI, JAMES N91-31606
CARLBERG, T. N91-31387
N91-31388
N91-31389
N91-31390
N91-31400
N91-31401
N91-31415
N91-31462
CARLIER, P. N91-31137
CARLSTEN, B. E. N91-31639
CARMAN, JOHN G. N91-31783
CARMICHAEL, A. N91-31732
CARNE, T. G. N91-31689
CARNEY, DAVID J. N91-31862
CARR, E. N91-31171
CARRENO, VICTOR A. N91-31531
CARTER, J. G. N91-31532
CASASENT, DAVID N91-31953
CASERTA, ANTHONY L. N91-31946
CASTAGNA, ANDRE N91-31679
CASTAN, C. N91-31098
CASTELLI, M. G. N91-31677
CATON, P. D. N91-31422
CAVEDON, A. N91-31305
CAYARD, MICHAEL SCOTT N91-31296
CAZALA-HOURCADE, E. N91-31202
CEN, RENYUE N91-32013
CHABOCHE, J. L. N91-31234
CHAKOUMAKOS, B. C. N91-31970
CHAN, JIN WAH N91-31279
N91-31288
CHAN, K. C. D. N91-31639
N91-31640
CHANCE, KELLY V. N91-31723
N91-31724
N91-31725
CHANG, CHE-WEI N91-31685
N91-31686
CHANG, DAVID C. N91-31538
CHANG, KEH-MINN N91-31268
N91-31270
N91-31271
CHASE, L. L. N91-31642
CHATE, H. N91-31569
CHAUDHURI, SUJEET K. N91-31481
CHEN, BORLIANG N91-31667
CHEN, K. C. N91-31500
CHENG, C. C. N91-31266
CHERNOFF, HERMAN N91-32001
CHEVALIER, T. N91-31590
CHEVALLIER, J. P. N91-31187
CHIARAMONTE, FRANCIS P. N91-31196
CHIDESTER, K. M. N91-31945
CHIN, B. A. N91-31286
CHIN, HUNG-NENG S. N91-31749
CHIPMAN, LAURE J. N91-31947
CHOW, YUNG L. N91-31481
CHOYKE, W. J. N91-31266
CHRIST, H. N91-31331
N91-31332
CHRISTEN, D. K. N91-31969
N91-31970
CHRISTENSEN, N. C. N91-31819
CHRISTOPHOROU, L. G. N91-31532
CHU, D. N91-31288
CHUN, C.-H. N91-31336
N91-31337
CHYU, M. C. N91-31967
CIESLAK, W. R. N91-31517
CLARKE, J. N91-31611
CLELAND, A. N. N91-31974
CLINE, C. F. N91-31298
CLOTHIER, CATHY C. N91-31804
COE, HAROLD H. N91-31648
COFFEY, CLAYTON G. N91-31207
COLLIN, K. H. N91-31154
COLLIN, M. F. N91-31593
COLLIN, MARIE-FRANCE N91-31603
COMPTON, R. T. N91-31509
CONNELL, JOHN W. N91-31307
CONNELL, L. W. N91-31221
COOPER, JOHN C. N91-31265
COOPER, R. K. N91-31639
COPPER, M. N91-31759
COQUEL, F. N91-31585
COREY, R. B. N91-31799
COUNSELMAN, C. C. N91-31121
COURQUET, JOEL N91-31169
COUTANCEAU, MADELAINE N91-31593
N91-31594
N91-31603
COUTURE, GUY J. E. N91-31206
COX, D. F. N91-31289
COYLE, J. M. N91-31913
CRAWFIS, R. A. N91-31815
CRAWFORD, P. C. N91-31315
CREISMEAS, PAUL N91-31169
CRITCHLEY, I. N91-31152
CROELL, A. N91-31385
CUE, R. W. N91-31158
CUKIERMAN, SERGE N91-31232
CULLINGFORD, HATICE S. N91-31793
N91-31798
N91-31803
CUNNINGHAM, ROBERT K. N91-31743
N91-31954
CUNTZ, J. M. N91-31305
CURRAN, FRANCIS M. N91-31216
CURTIS, SUSAN R. N91-31743
CUSCHIERI, J. M. N91-31678

D

DAHIYA, R. P. N91-32028
DAHLIN, R. S. N91-31260
DAHMEN, U. N91-31473
N91-31975
DAI, WEN-LONG N91-31646
DALRIEUX, Y. N91-31924
DAMP, S. N91-31637
DANIELS, FREDERICK N91-31199
DATSKOS, P. G. N91-31532
DATTA, A. N91-31244
DAVENPORT, R. N91-31714
DAVEY, J. N91-31259
DAVIAUD, F. N91-31569
DAVID, S. A. N91-31277
N91-31280
N91-31649
N91-31650
N91-31651
DAVIDIAN, KENNETH J. N91-31196
DAVIDSON, K. V. N91-31945
DAVIDSON, S. J. N91-31252
DAVIES, J. K. N91-32008
DAVIS, A. N91-31261
DAVIS, DAVID O. N91-31106
DAY, MICHELLE N91-31790
DEATON, JOHN N91-31808
DEBERG, MARK N91-31839
N91-31899
DEBOER, F. S. N91-31835
DECKER, W. L. N91-31722
DECUYPERE, R. N91-31101
DEGOER, J. N91-31404
DEHLING, H. N91-31916
DEIMEL, PETER P. N91-31949
DEKKER, R. N91-31918
DELAAT, MICHEL N91-31117
DELANNOY, A. N91-31112
DELCOURT, CHRISTINE N91-31994
DELIL, A. A. M. N91-31578
DEMARCHI, G. N91-31302
DERESKIEWICZ, J. P. N91-31652
N91-31657
DERUYTTERE, A. N91-31436
N91-31437
N91-31438
N91-31439
N91-31440
DESCLAUX, FRANCOIS N91-31195
DESPER, C. H. N91-31311
DESREUMAUX, O. N91-31604
DESROCHERS, GEORGE R. N91-31122
N91-31123
DESWARTE, YVES N91-31662
DEUERLER, F. N91-31446
DEVEZEAUXDELAVERGNE, D. N91-31848
DEVORE, L. N91-32031
DEVRIES, R. W. N91-31580
DHAKHWA, G. N91-31722
DIJKSTRA, H. A. N91-31343
DITTMAR, MARK B. N91-31965
DJUMIC, M. N91-31762
DOBBS, GEOFFREY N91-31108
DODDAPANENI, N. N91-31522
DODGE, L. G. N91-31164
DOHRMAN, C. R. N91-31689
DONGARRA, J. N91-31855
DOOLEY, KEVIN A. N91-31598
N91-31599
DOORNBOS, HENK N91-31822
DORHOUT, B. N91-31844
DRAGE, R. G. T. N91-31173
DRAGOVITSCH, P. N91-31816
DRASH, ROBERT W. N91-31079
DRESCHEL, T. W. N91-31797
DRIESSEN, CORNELIUS N91-31813
DRIESSEN, T. S. H. N91-31907
DRUMHELLER, DAVID M. N91-31501
DRUMMOND, CHARLES H., III N91-31961
N91-31962
N91-31964
N91-31965
DUCHARME, MICHEL B. N91-31541
DUDLEY, MICHAEL N91-31751
DUFOUR, P. N91-31100
DULIEU, ANNIE N91-31594
N91-31603
DUNN, W. L. N91-31816
DUOBA, M. J. N91-31519
DURAN, RICARDO N91-31915
DURHAM, F. P. N91-31211

E

ECKELMANN, H. N91-31085
ECKER, A. N91-31406
EDWARDS, G. R. N91-31280
EHRHARDT, J. N91-31350
N91-31351
N91-31352
N91-31353
EKBOM, L. B. N91-31444
N91-31445
ELGHAZZANI, EL MOSTAFA N91-31180
ELIASSON, A. N91-31421
ELLIOTT, C. M. N91-31262
ELLIOTT, J. C. N91-31639
ELWELL, D. N91-31814
EMERY, M. H. N91-31638
EMLAW, MICHAEL N91-31744
ENGELSTAD, STEPHEN PHILLIP N91-31668
EOM, JINSEOB N91-31613
EPSTEIN, A. J. N91-31310
ERICSSON, K. A. N91-31773
ERNEST, M. J. N91-31868
ESCAIG, B. N91-31233
ESCALANTE, E. N91-31242
EUSTACHE, RENE-PAUL N91-31232
EVANS, R. A. N91-31729
N91-31731
N91-31735
N91-31737
EVENSON, K. M. N91-31723
EWSUK, K. G. N91-31237
EYER, A. N91-31384

F

FABRE, JEAN-CHARLES N91-31662
FAIGLE, U. N91-31489
FAIN, D. E. N91-31300
FAIRCHILD, STEVEN B. N91-31246
FALCO, R. E. N91-31103
FARBRIDGE, JOSEPH E. N91-31175
N91-31176
FARGE, MARIE N91-31589
FASSBENDER, L. L. N91-31247
FAULKNER, J. S. N91-31281
FAVALLI, L. N91-31846
N91-31884
FAVIER, J. J. N91-31404
FAYER, M. D. N91-31704
FEATHERBY, M. N91-31714
FECKER, K. N91-31469
FEDRO, A. J. N91-31968
N91-31976
FEENSTRA, R. N91-31969
FEIG, H.-F. N91-31157
FERNAGUT, F. N91-31233
FERNOW, R. C. N91-31942
FERRET, B. N91-31104
FISH, A. F. N91-31721
FLAMENT, C. N91-31585
FLANAGAN, DAVID T. N91-31755
FLEMMING, DIETER N91-31871
FLOOD, DENNIS J. N91-31217
N91-31218
FOERSTER, WOLFGANG N91-31624
FORMISANO, A. N91-31130
FORTEZZA, R. N91-31342
FORTNEY, L. R. N91-31939
FOSTER, J. N91-31252
FOURMAUX, ANTOINE N91-31850
FRANCOIS, G. N91-31187
FRANK, A. M. N91-31572
FRASER, J. C. N91-31609
FRATE, DAVID T. N91-31708
FREDRIKSSON, H. N91-31400
N91-31401

N91-31402
N91-31403
N91-31415
N91-31416
N91-31417
N91-31418
N91-31419
N91-31420
N91-31421
N91-31444
N91-31445

FRENCH, J. B. N91-31936
FRIELER, K. N91-31461
FRIM, JOHN N91-31541
FRISCHAT, G. H. N91-31363
N91-31364
N91-31365
N91-31366
N91-31367
N91-31368
N91-31369
N91-31469
FROYEN, L. N91-31436
N91-31437
N91-31438
N91-31439
N91-31440
FRY, I. V. N91-31786
FUNG, K. H. N91-31720

G

GABARD, S. N91-31104
GALINDO, C. N91-31800
GALLEGOS, R. A. N91-31602
GALLOWAY, M. D. N91-31969
GANGE, R. W. N91-31756
GARBE, GREGORY PAUL N91-31728
GARDNER, J. H. N91-3*638
GARLAND, DOUGLAS N91-31174
N91-31175
N91-31176
GARLAND, J. L. N91-31785
GARNERO, MARIE-AGNES N91-31883
GARRATT, V. E. W. N91-31173
GARRETSON, TED D. N91-31170
GARRIGUE, JEAN-MARIE N91-31474
GARY, S. P. N91-31957
GARZOTTO, FRANCA N91-31995
GASANOV, I. S. N91-31956
GATES, W. L. N91-31717
GAUTHIER, J. E. D. N91-31165
GAUTIER, L. N91-31111
GEBALLE, T. H. N91-31611
GEBHARDT, K. F. N91-31324
GEFFROY, P. N91-31588
GEIS, N. N91-32009
GEIST, A. N91-31855
GEIST, G. A. N91-31870
GELFAND, A. E. N91-31919
GELLERT, E. N91-31109
GEMAUX, G. N91-31103
N91-31189
GENZEL, R. N91-32009
GERDES, INGRID N91-31185
GERLACH, KARL N91-31539
N91-31540
GERRITSMA, MARC I. N91-31577
GHOSH, SUBIR N91-31482
GIANTI, S. J. N91-31716
GIANTS, THOMAS W. N91-31612
GIBB, MURRAY N91-31486
GIBBONS, ROBERT D. N91-31771
GILBERT, JOHN R. N91-31836
GILLESSEN, F. N91-31468
GIRARD, A. N91-31187
GITOMER, S. J. N91-31639
GLASSER, LANCE A. N91-31811
GLEASON, J. N91-31966
GLEASON, K. N91-32031
GLENDENNING, N. K. N91-32016
N91-32018
GLEYZES, C. N91-31096
N91-31592
GLOVER, RICHARD D. N91-31874
GLUCKMAN, JONATHAN N91-31808
GOGINENI, S. P. N91-31492
GOLDBERG, V. R. N91-31702
GOLDHABER, G. N91-32010
GOLDSTEIN, HOWARD E. N91-31236
GOLDSTEIN, J. C. N91-31639
GOLINSKY, MARTIN N91-31116
GONCHAROV, A. A. N91-31956
GONZALEZ, TEOFILO F. N91-31829
N91-31898

GOODHEW, P. J. N91-31441
GOODMAN, D. W. N91-31255
N91-31256
GOSHAW, A. T. N91-31939
GOTOH, S. N91-31979
GOTTESFELD, S. N91-31259
N91-31710
GOTTLIEB, ROBERT G. N91-31890
GOUSBET, G. N91-31627
GRADY, D. E. N91-31309
GRAF, W. N91-31446
N91-31454
GRAND, D. N91-31568
GRAY, G. T., III N91-31275
N91-31276
GREIERT, ALFRED H. N91-31177
GRESILLON, D. N91-31103
N91-31189
GRINDHAMMER, G. N91-31930
GROOT, J. S. N91-31496
GROSS, M. N91-31733
GROSSBACH, R. N91-31465
N91-31467
N91-31469
GROTCH, S. L. N91-31748
GRUBER, H. N91-31151
GRUNEFELD, H. N91-31863
GUEDRA, D. N91-31231
GUENOUN, P. N91-31377
N91-31378
GUENTHER, G. N91-31135
GUGLIELMO, EUGENE J. N91-32000
GUILINGER, T. R. N91-31472
GUILLEN, P. N91-31847
GUILLOT, JEAN N91-31182
GUTLEBEN, H. N91-31266

H

HAAG, THOMAS W. N91-31216
HACHAM, H. N91-31756
HAESSNER, F. N91-31398
HAFSTEINSSON, HJALMTYR N91-31836
HAGER, E. PAUL N91-31200
N91-31488
HAGGERTY, M. N91-32009
HAHN, S. N91-31971
HAIDT, D. N91-31930
HALARY, JEAN-LOUIS N91-31232
HALL, C. R. N91-31789
HAMEED, S. N91-31718
HAMILTON, RICHARD J. N91-31809
HAMMER, JAY A. N91-31267
HAMMETT, KELLY D. N91-31643
HAMMOND, KENNETH R. N91-31772
HAMMOND, R. H. N91-31611
HAMZA, A. V. N91-31642
HANAK, J. J. N91-31698
HANDSCHUH, ROBERT F. N91-31654
HANNA, GREGORY J. N91-31470
HANSON, D. L. N91-31210
HANSSON, PER ANDERS N91-31736
HARIS, F. G. N91-31676
HARJES, H. C. N91-31518
HARMON, B. N. N91-31968
HASLIM, LEONARD A. N91-31113
HAYNES, R. A. N91-31868
HEALY, ALICE F. N91-31773
HECK, MICHAEL L. N91-31201
HEDEKER, DONALD R. N91-31771
HEDSTROM, J. C. N91-31210
N91-31711
HEEMSKERK, J. F. N91-31578
HEESE, R. N91-31981
HEFFERNAN, RUTH N91-31078
HEFNER, RACHEL E. N91-31679
HEHENKAMP, T. N91-31373
HEIDE, H. N91-31423
HEIDE, W. N91-31424
N91-31425
N91-31426
HEINEMANN, STEFAN N91-31635
HELMER, R. M. F. N91-31695
HENDRICKS, ROBERT C. N91-31220
HENFLING, J. A. N91-31272
N91-31292
N91-31293
HENLEY, J. P. N91-31697
HENNING, PATRICIA A. N91-32014
HEPNER, T. N91-31510
HEPP, ALOYSIUS F. N91-31977
HERCHUELZ, PIERRE N91-31849
HERGENROTHER, PAUL M. N91-31307
HERLACH, D. M. N91-31466
N91-31468

HERMANNS, J. N91-31371
HERSHBERGER, JOHN N91-31900
HESPER, E. T. N91-31118
HESS, J. RICHARD N91-31783
HESSELINK, WIM H. N91-31821
N91-31823
HESSENIUS, KRISTIN A. N91-31751
HICKS, R. J. N91-31801
HILL, M. N91-31733
HILL, W. A. N91-31782
HILMAS, GREGORY E. N91-31963
HILTON, JAMES LINDSAY N91-32019
HINNANT, HOWARD E. N91-31687
HIROMOTO, R. E. N91-31818
HIRSCHEL, E. H. N91-31088
HODES, E. N91-31413
HOEFSLOOT, H. C. J. N91-31344
HOFFMANN, H.-E. N91-31172
HOFFMEISTER, H. N91-31447
HOFMANN, OTTO N91-31693
HOGENDOORN, R. A. N91-31119
HOHENSTEIN, K. N91-31433
HOLLAND, SCOTT DOUGLAS N91-31083
HOLLANDERS, H. N91-31585
HOLMES, M. N91-31173
HOLMES, V. H. N91-31602
HOOFMAN, R. N91-31830
N91-31901
N91-31902
N91-31997
HOPCROFT, JOHN E. N91-31659
HOPKINS, W. G. N91-31422
HORACK, J. M. N91-32006
HORDIJK, A. N91-31918
HORST, U. N91-31369
HOSEY, M. N91-31734
HOSKINS, DOUGLAS ALAN N91-31877
HOUDJAL, R. N91-31636
HOWELL, J. A. N91-31886
HOWINGTON, LARRY C. N91-31660
HOYT, J. L. N91-31983
HSIEH, H. N91-31981
HSU, H. N91-31970
HU, E. L. N91-31978
HU, Q. N91-31611
HUA, X.-M. N91-32020
HUANG, J. S. N91-31274
HUANG, SHYH-CHIN N91-31270
N91-31271
HUANG, XIANG-LU N91-31747
HUCH, RUEDIGER N91-31304
HUDEMA, HENRY P. N91-31207
HUFF, J. R. N91-31711
HUFFAKER, R. C. N91-31778
HUGHES, T. H. N91-31299
HUMBERTCLAUDE, J. N91-31100
HUNIK, R. N91-32024
HUPPMANN, GERHARD N91-31706
HUSSAIN, MUHAMMAD IMTIAZ N91-31544
HYNES, ROBERT N91-31265

I

IBARS, PHILIPPE N91-31091
ILG, KARL-HEINZ N91-31317
IM, H. S. N91-31264
INGALLS, R. L. N91-31263
INKOL, ROBERT J. N91-31512
N91-31513
ISAACS, RALPH G. N91-31660
ITSKOVSKII, M. A. N91-31707

J

JABLONSKI, CAROLE A. N91-31205
JACARUSO, GARY J. N91-31224
JACKSON, J. N91-32009
JACOBS, J. M. J. W. N91-31131
JACQUEZ, RICARDO B. N91-31788
JACQUIN, L. N91-31588
JAMES, M. R. N91-31988
JAMES, R. D. N91-31240
JANSSEN, F. J. J. G. N91-32026
N91-32029
JANSSEN, L. P. B. M. N91-31344
JARRE, FLORIAN N91-31858
JAVADI, H. H. N91-31310
JENKINS, W. K. N91-31536
JENNINGS, D. A. N91-31723
JENNISON, ROGER C. N91-31738
JERINA, K. L. N91-31691
JIANG, BO-NAN N91-31911
JOHLL, W. P. N91-31519
JOHNSON, C. S. N91-31854

JOHNSON, J. N. N91-31672
JOHNSON, K. C. N91-32031
JOHNSON, STEVE N91-31790
JOHNSON, W. S. N91-31677
JOHNSON, WAYNE N91-31078
JONAS, PAUL J. N91-31126
JONES, E. D. N91-31980
JONES, M. E. N91-31639
N91-31958
JONES, R. B. N91-31149
JONSSON, BENGT N91-31493
JOOSTEN, S. N91-31867
JOSSE, M. N91-31475
JUE, SUEY N91-31600
JUILLEN, J. C. N91-31105
JUSTICE, A. D., III N91-31817

K

KABALKA, G. W. N91-31764
KALDEICH, BRIGITTE N91-31321
KALSI, S. N91-31981
KAMIN, R. A. N91-31166
KANE, R. N91-31721
KANEKO, M. N91-31372
KARS, W. T. M. N91-31921
KASCHMITTER, J. L. N91-31698
KASSIES, A. N91-31131
KAT, P. J. N91-31878
KATAYAMA, M. N91-31372
KAUN, T. D. N91-31519
KEANE, D. N91-31937
KECHEMAIR, D. N91-31636
KEIL, M. N91-31696
KEISER, J. R. N91-31291
KELLY, M. J. N91-31472
KELLY, S. M. N91-31868
KELLY, T. N91-31770
KERCHNER, H. R. N91-31970
KERN, WALTER N91-31489
N91-31881
N91-31910
KILKENNY, J. N91-31252
KIM, K. H. N91-31812
N91-31875
KIM, YOUNG-WON N91-31274
KIMURA, T. N91-31394
KING, R. R. N91-31699
KIPP, M. E. N91-31309
KIRBIE, H. C. N91-31520
N91-31521
KIRK, W. L. N91-31210
N91-31211
KIRKPATRICK, J. F. N91-31645
KIRSCHBAUM, E. N91-31359
N91-31360
KIRSCHNER, MICHAEL N91-31203
KISER, J. D. N91-31962
KLABUNDE, C. E. N91-31969
KLEIN, H. N91-31379
KLEM, J. F. N91-31978
N91-31980
KLEMMER, ANTON N91-31624
KLOKS, TON N91-31836
KNAPP, G. S. N91-31935
KNIGHT, DOUGLAS R. N91-31806
KNOTT, W. M. N91-31780
N91-31791
N91-31797
KNOX, CHARLES E. N91-31143
KOCH, JOHN, JR. N91-31608
KODAMA, S. N91-31393
KOESTLER, C. N91-31373
KOHSIEK, WIM N91-31752
KOK, J. N. N91-31835
KOK, JOOST N. N91-31834
KOLTUN, D. S. N91-31936
KOMOROWSKI, J. P. N91-31125
KONG, J. A. N91-31504
KONNERTH, A., III N91-31713
N91-31715
KOOPMAN, P. W. M. N91-31824
N91-31880
KOOPMANS, G. N91-32025
N91-32030
KOSHIZUKA, N. N91-31979
KOSTERS, MENNO T. N91-31893
N91-31894
KOTTA, U. N91-31843
KOURTIDES, DEMETRIUS A. N91-31236
KOWALSKY, K. A. N91-31248
KOZLOVSKY, B. N91-32020
KOZMA, L. N91-31463
KRATSCH, DIETER N91-31838
KRESS, J. D. N91-31287
KRETSCHMER, FRANK F., JR. N91-31508
KROEGER, D. M. N91-31970
KROTHAPALLI, A. N91-31629
N91-31630
KROY, WALTER N91-31635
KRUEGER, JAMES M. N91-31766
KUCZERA, HERIBERT N91-31198
KUERTEN, J. G. M. N91-31906
KUIPER, J. N91-32025
KUIPER, MATTHIJS N91-31832
KULAK, R. F. N91-31299
KUMAR, RENJITH R. N91-31201
KUNDU, KRISHNA N91-31181
KUNTH, DANIEL N91-32017
KURG, V. N91-31848
KUROCHKINA, A. A. N91-31944
KURY, J. W. N91-31315
KUSHNICK, ANNE C. N91-31476
KUZAY, T. M. N91-31967
KWAST, KAREN N91-31891
KYR, P. N91-31405

L

LAAKE, B. A. N91-31477
LABELLE, J. N91-31957
LABIDI, W. N91-31594
LACOSS, RICHARD T. N91-31743
LADHARI, F. N91-31587
LAFI, A. N91-31575
LAMINE, JACQUES N91-31583
LAMISCARRE, B. N91-31098
LANG, N. J. N91-31597
LANGBEIN, D. N91-31423
N91-31424
N91-31425
N91-31426
LANGE, F. F. N91-31963
LANGE, R. N91-31374
LANNUTTI, J. E. N91-31938
LAROCHE, P. N91-31112
LARSON, RICHARD R. N91-31874
LAUNDER, B. E. N91-31552
N91-31555
N91-31558
N91-31560
N91-31561
LAUPRETRE, FRANCOISE N91-31232
LAWRENCE, R. J. N91-31634
LAX, M. N91-31641
LAY, KENNETH W. N91-31543
LEAF, G. K. N91-31888
LEAVITT, JOHN N. N91-31142
LEBLANC, R. N91-31101
LECOINTE, Y. N91-31848
LEE, CHI-MING N91-31181
LEE, E. H. N91-31286
LEE, H. W. H. N91-31642
LEE, JONG-WON N91-31225
LEE, R. N91-31252
LEE, WILLIAM E. N91-31962
N91-31963
LEEPER, S. A. N91-31223
LEFEBVRE, J. M. N91-31233
LEGROS, J. C. N91-31338
N91-31339
N91-31340
LEHMANN, W. N91-31966
LEHMBERG, R. H. N91-31638
LEIB, KENNETH G. N91-31600
LEISTE, H. N91-31384
LEMBKE, J. R. N91-31653
LEMKE, R. W. N91-31523
LEMPEREUR, C. N91-31851
LENLING, W. J. N91-31272
N91-31292
N91-31293
LENTFERT, P. J. A. N91-31828
LEONI, R. N91-31611
LEPORE, FRANK A. N91-31214
LEPPARD, W. R. N91-31314
LERCH, BRADLEY A. N91-31235
LERCH, PH. N91-31611
LERNER, NARCINDA R. N91-31258
LESAIN, ALAIN N91-31850
LESCHZINER, M. A. N91-31553
N91-31554
N91-31556
N91-31557
N91-31559
LESIEUR, M. N91-31566
N91-31567
N91-31568
LESKOVAR, B. N91-31948
LEUCHTER, O. N91-31588
LEUNG, E. M. W. N91-31981
LEUNG, T. C. N91-31968
LEVRIER, J. N91-31231
LI, Y. N91-31691
LICHTENBELT, J. H. N91-31343
LIEBERT, CURT H. N91-31608
LIEFER, RANDALL KEITH N91-31128
LIERKE, E. G. N91-31464
N91-31465
N91-31467
N91-31469
LIGHTSTONE, LEONARD N91-31485
N91-31486
LIJOI, BRUNO N91-31946
LILJENDAHL, M. N91-31462
LIMBOURG-FONTAINE, M. C. N91-31338
N91-31339
N91-31340
LIN, FENG-LING C. N91-31508
LIN, H. T. N91-31301
LIN, S. K. N91-31980
LINNE, DIANE L. N91-31318
LITT, JONATHAN S. N91-31876
LITTKE, W. N91-31395
N91-31396
N91-31397
LITZ, MARC S. N91-31193
LOC, TAPHUOC N91-31594
N91-31603
LOMDAHL, P. S. N91-31672
LONSINGER, H. N91-31135
LORETAN, P. A. N91-31782
LOTT, S. N91-31533
LOURENCO, L. M. N91-31628
N91-31629
N91-31630
LOWDEN, R. A. N91-31240
LOWERY, W. N91-31781
LOWNDES, D. H. N91-31969
LU, J. Y. N91-31782
LUC-BOUHALI, A. N91-31848
LUCAS, S. R. N91-31266
LUCIER, W. A. N91-31149
LUONG, V. N91-31519
LUSK, CYNTHIA M. N91-31772
LUSTENBERGER, MARTIN N91-31107
LUTTGES, MARVIN N91-31790
LUYENDIJK, T. N91-31370
LYNCH, PETER N91-31747
LYO, S. K. N91-31980
LYRINTZIS, A. S. N91-31928

M

MA, D. C. N91-31674
MAAS, R. N91-31943
MACELROY, ROBERT D. N91-31775
MACGREGOR, JOHN DONALD, III N91-31547
MACKOWIAK, C. L. N91-31780
N91-31781
MACRAE, GREGORY S. N91-31605
MAISCH, E. N91-31322
N91-31323
MAJCHER, GREGORY A. N91-31212
MALBEQUI, P. N91-31925
MANCA, VINCENZO N91-31887
MANCHEK, R. N91-31855
MANCINI, T. R. N91-31702
MANGALAM, SIVARAMAKRISHNAN M. N91-31596
MANN, D. L. N91-31159
MANN, G. A. N91-31518
MANN, J. Y. N91-31676
MANNARA, G. N91-31341
MANSFIELD, R. A. N91-31852
MARANTZ, D. R. N91-31248
MAREE, MICHEL N91-31182
MARKOV, ALEXANDER B. N91-31207
MARSAC, SYLVIE N91-31285
MARTINEZ, I. N91-31325
N91-31326
MARTINEZ, M. J. N91-31573
MARVIN, H. N91-32010
MASHESSE, J. M. N91-32017
MASSELL, PAUL N91-31769
MATHE, J. M. N91-31851
MATHUR, G. P. N91-31926
MATTERN, FRIEDMANN N91-31827
MATTHEWS, R. B. N91-31945
MAUL, WILLIAM A. N91-31209
MAZANEK, DANIEL D. N91-31201
MAZZOLDI, P. N91-31302
MCCARTHY, JOHN N91-31857
N91-31912
MCELVANY, M. C. N91-31663
N91-31664

MCFARLAND, R. D. N91-31210
MCGRORY, WILLIAM DANDRIDGE N91-31546
MCGUFFIN, D. T. N91-31272
MCHARGUE, C. J. N91-31308
MCTIGUE, D. F. N91-31573
MCVEY, B. D. N91-31639
MEAD, JOEY L. N91-31311
MEHNERT, AXEL N91-31635
MEIER, K. L. N91-31640
MEIER, M. N91-31366
N91-31367
N91-31368
MEIJN, R. N91-31148
MELICHAR, BORIVOJ N91-31840
N91-31841
MELIS, MATTHEW E. N91-31235
MENDELSOHN, M. L. N91-31763
MENEZLA, RABEA N91-31525
MERCER, CAROLYN R. N91-31605
MERCER, L. B. N91-31644
MERCER, P. R. N91-31498
MERCIER, V. N91-31101
MERKENS, W. N91-31371
MERKLE, K. L. N91-31934
MERRIGAN, M. A. N91-31210
MERSKI, N. RONALD N91-31595
METAIS, O. N91-31567
N91-31568
METHFESSEL, S. N91-31407
METZE, WOLFGANG N91-31186
MEYER, BRIAN E. N91-31176
MEYER, CLAUDIA M. N91-31209
MEYER, MICHAEL L. N91-31318
MEYERS, JAMES F. N91-31618
N91-31621
N91-31632
MICKEAL, JAMES F. N91-31511
MICKELER, SIEGFRIED N91-31705
MICKELSON, ALAN R. N91-31538
MICKLOS, RICHARD P. N91-31141
MIDDLETON, DAVID B. N91-31120
MILLER, ALLEN R. N91-31952
MILLER, R. L. N91-31162
MING, D. W. N91-31800
MINSTER, OLIVIER N91-31321
MIOTELLO, A. N91-31302
MIRDAMADI, M. N91-31677
MITCHELL, CARY A. N91-31777
MITCHELL, G. D. N91-31261
MIX, G. N91-31349
MIZUGUCHI, K. N91-31394
MOELLER, WERNER N91-31304
MOG, ROBERT A. N91-31204
MOKOLE, ERIC L. N91-31502
MOLENKAMP, C. R. N91-31749
MOLIAN, ARUL N91-31249
MOLIAN, P. N91-31249
MONNA, WIM A. A. N91-31752
MONNERIE, LUCIEN N91-31232
MONTI, R. N91-31341
N91-31342
MOORE, J. RICHARD N91-31170
MOORE, S. W. N91-31210
MOREAU, J. P. N91-31111
MOREL, R. N91-31587
MOROZOV, A. I. N91-31944
MORRIS, C. E. N91-31276
N91-31782
MORRIS, J. W., JR. N91-31288
MORRIS, P. B. N91-31124
MORRISON, E. N91-31732
MORRISON, JEFFREY N91-31808
MORROW, R. C. N91-31799
MORROW, ROBERT C. N91-31779
MORTLEY, D. G. N91-31782
MORTON, DENNIS P. N91-31534
MOSES, C. A. N91-31164
MOSKOVITZ, CARY A. N91-31140
MOULATSIOTIS, DIMITRIOS N91-31283
MRAZEK, F. C. N91-31519
MUCKLOW, GLENN H. N91-31194
MUELLER, G. N91-31386
N91-31405
MUELLER, W. N91-31385
MUIR, D. E. N91-31158
MULLER, R. N91-32010
MULLER, SARA H. N91-31752
MULLIN, TOM N91-31571
MUROTANI, T. N91-31394
MURPHY, J. N91-31981
MURPHY, RONALD J. N91-32020
N91-32021
N91-32022
MURPHY, STEPHEN HENRY N91-31647
MURR, L. E. N91-31290
MYERS, D. R. N91-31978

N

NAEGELI, D. W. N91-31164
NAHUM, M. N91-31611
NAIM, A. N91-31590
NAITOH, P. N91-31770
NAKAMURA, N. N91-31979
NAPOLITANO, L. G. N91-31341
NAUNDORF, V. N91-31278
NAVARD, PATRICK N91-31306
NAYROLES, B. N91-31188
NEDERHOF, MARK-JAN N91-31826
NEMES, J. A. N91-31243
NEMETH, ED N91-31219
NEUSCHUETZ, D. N91-31432
NEWTON, M. A. N91-31520
N91-31521
NGUYEN, D. N91-31640
NICHOLS, A. L., III N91-31315
NIELSEN, SUZANNE S. N91-31777
NIESWAAG, H. N91-31370
NII, K. N91-31427
NIJMEIJER, H. N91-31843
NISHIMURA, T. N91-31394
NITSCHE, K. N91-31374
NITSCHE, R. N91-31385
NOECKER, E. G. J. M. H. N91-31824
NOEL, B. W. N91-31491
NOEL, S. D. N91-31929
NOLT, I. G. N91-31723
NORMAND, X. N91-31566
NORTON, D. P. N91-31969
NOTTORF, ERIC WALTER N91-31226
NOWACK, C. J. N91-31166

O

OAKLEY, S. N91-31987
OBENSCHAIN, S. P. N91-31638
OBERKAMPF, W. L. N91-31248
ODONNELL, H. N91-31244
OGBUEHI, C. R. A. N91-31782
OHAYON, R. N91-31682
OHNEMUS, J. N91-31930
OLESON, MEL W. N91-31798
OLIVER, W. C. N91-31291
OLMSTEAD, B. A. N91-31166
OLS, JOE N91-31219
OLSASKY, MARK N91-31219
OLSEN, J. A. N91-31978
OMELLAS, D. L. N91-31316
OPDENAKKER, RIEKS N91-31840
N91-31841
ORAVA, FREDRIK N91-31493
OREILLY, F. J. N91-31920
OU, YUH-ROUNG N91-31576
OUELLETTE, CHRISTIAN N91-31146
OVERBEEK, P. L. N91-31872
N91-31873
OVERMARS, MARK H. N91-31899
N91-31903
OVREBO, GREGORY K. N91-31193
OWENS, L. P. N91-31789
OZKAN, UGUR N91-31859

P

PACKER, L. N91-31786
PAGANO, PHILIPPE N91-31527
PAILHAS, G. N91-31584
N91-31592
PALAMIDESSI, C. N91-31835
PALKON, D. J. N91-31519
PANCHAL, C. B. N91-31709
PANG, YI N91-31601
PANT, P. N91-31414
N91-31435
N91-31448
N91-31449
N91-31450
PAOLINI, PAOLO N91-31995
PARK, HYUNG-KOO N91-31129
PARK, K. N91-31723
PARKER, M. B. N91-31940
PASIAN, FABIO N91-31813
PASSERONE, A. N91-31428
PATITZ, W. E. N91-31490
PAWEL, J. E. N91-31308
PAYNE, WILLIAM N91-31199
PECK, ALEXANDER N., II N91-31600
PELISSIER, CHRISTIAN N91-31089
PELLETIER, GARY P. N91-31245
PENNER, J. E. N91-31719
PENNYCOOK, S. J. N91-31969
PENNYPACKER, C. N91-32010
PEOPLES, OLIVER P. N91-31313
PEPI, MARC S. N91-31245
PEPIN, GERARD R. N91-31200
N91-31488
PERLMAN, MARVIN N91-31810
PERLMUTTER, S. N91-32010
PERRIN, RONALD E. N91-31246
PERROT, F. N91-31377
N91-31378
PERRY, CHARLEEN N91-31813
PERRY, T. S. N91-31252
PERSON, LEE H., JR. N91-31120
PETERSEN, GENE R. N91-31784
PETERSON, C. G. N91-31610
PETRE, G. N91-31338
N91-31339
N91-31340
PETTY, GRANT WILLIAM N91-31727
PEUBE, J. L. N91-31104
N91-31188
PEUSER, PETER N91-31635
PEUVREL, EDITH N91-31306
PFEIFER, HANS-JOACHIM N91-31617
N91-31620
N91-31631
N91-31633
N91-31637
PFITZNER, M. N91-31087
PHILBECK, THOMAS E., JR. N91-31807
PHILIPPOVICH, N. N91-31461
PHILLIPS, T. J. N91-31717
PIERRE, J. N91-31382
N91-31383
PIETERS, W. N91-31147
PINEAU, G. N91-31594
PINELLI, THOMAS EDWARD N91-31989
PITTS, WILLIAM C. N91-31236
PITZ, W. J. N91-31314
PITZER, K. S. N91-31254
PJEROV, S. N91-31981
PLAKS, KENNETH N91-32011
PLASMEIJER, M. J. N91-31824
N91-31880
POETSCHKE, J. N91-31432
N91-31433
N91-31434
N91-31435
N91-31446
N91-31448
N91-31449
N91-31450
N91-31453
POGLITSCH, A. N91-32009
POLLAK, ROBERT R. N91-31155
POOLER, BRIAN L. N91-31537
PORTAZ, JOSEPH M. N91-31660
POTTELETTE, R. N91-31957
POVOLO, F. N91-31666
POWELL, DAVID JOHN N91-31471
POWELL, MICHAEL G. N91-31685
PRE, T. N91-31590
PRECETTI, DOMINIQUE N91-31078
PREISS, ANDREAS N91-31705
PREM, HORST N91-31134
PRICE, D. MARVIN N91-31204
PRIEM, RICHARD J. N91-31208
PRINA, STEVEN RONALD N91-31516
PRINZ, B. N91-31429
PROCTOR, MARGARET P. N91-31220
PROPST, G. N91-31889
PROTSENKO, I. M. N91-31956
PUJOL, C. N91-31137
PURDY, DAVID F. N91-31753

Q

QUINN, R. D. N91-31716

R

RABAS, T. J. N91-31709
RADOSTITZ, J. V. N91-31723
RAFFETO, G. L. N91-31130
RAHIER, G. N91-31136
RAJU, I. S. N91-31692
RAMATY, R. N91-32020
RANDLES, P. W. N91-31243
RANGANATH, HEGGERE S. N91-31947
RAO, G. R. N91-31286
RAO, MADHAV N91-31249
RAO, V. K. N91-31165
RAUB, C. J. N91-31347
N91-31348

RAWLIN, VINCENT K. N91-31212
RAYNAUD, JACQUES N91-31182
REARDON, JOHN E. N91-31853
REARDON, WILLIAM H. N91-31167
REAUGH, J. E. N91-31298
REGGIARDO, J. F. N91-31666
REHBEIN, D. K. N91-31688
REICHERT, MICHAEL N91-31197
REID, CARL R. N91-31669
REMY, L. N91-31683
RENZOW, D. N91-31323
N91-31324
REUSCH, M. F. N91-31981
REYES, J. N., JR. N91-31575
RHA, CHOKYUN N91-31313
RICHARDS, P. L. N91-31611
RICHARDS, P. M. N91-31971
RICHARDSON, PAMELA F. N91-31751
RICHTER, J. N91-31359
N91-31360
N91-31371
RICKER, R. E. N91-31242
RIETHMULLER, M. N91-31101
RIJMENANTS, ELZA N91-31624
RILEY, S. J. N91-31168
N91-31250
RIST, ULRICH N91-31849
RITCHIE, CHARLES F. N91-31176
RIVEST, RONALD L. N91-31611
ROBBA, A. A. N91-31933
ROBERGE, P. N91-31515
ROBERTS, DONALD E. N91-31767
ROBERTSON, DALE N. N91-31193
ROBERTSON, JAMES B. N91-31950
ROBICHEAU, M. N91-31295
RODDE, A. M. N91-31093
RODGERS, C. N91-31150
RODI, W. N91-31563
RODRIGUEZ, J. A. N91-31256
RODRIGUEZ, RODOLFO N91-31915
ROETTGER, G. E. N91-31300
ROGGE, V. N91-31446
ROMANA, L. J. N91-31308
ROSSITO, F. N91-31428
ROSSITTO, F. N91-31443
ROWE, NEIL C. N91-32000
ROY, ERNEST G. N91-31807
RUCKMAN, MARK W. N91-31977
RUDD, E. J. N91-31533
RUEDIGER, J. N91-31447
RUMITZ, M. N91-32009
RUMMEL, JOHN D. N91-31795
RUOFF, A. L. N91-31973
RUPP, R. N91-31386
RUSSO, S. G. N91-31179
RUTGERS, W. R. N91-32028
RUTHERFORD, D. A. N91-31933
RUTTEN, J. J. M. M. N91-31835
RUTTEN, L. M. W. J. N91-31880
RYLANDS, JULIA M. N91-31922

S

SAGER, J. C. N91-31780
N91-31781
N91-31797
SAHM, P. R. N91-31406
SALES, B. C. N91-31970
SALIBRA, ANTONINO N91-31887
SALISBURY, FRANK B. N91-31796
SALVIA, M. N91-31090
SAMPATH, P. N91-31152
SANDERS, W. A. N91-31962
SANDLIN, SEAN M. N91-31495
SANDUBRAE, J. N91-31714
SANFORD, N. M. N91-32031
SANGIORGI, R. N91-31428
SANKOVIC, JOHN M. N91-31216
SANS, C. N91-31094
SANSCHAGRIN, DENIS J. N91-31206
SANTINELLI, CLAUDE N91-31526
SANZ, A. N91-31325
N91-31326
SAPER, RONALD H. N91-31478
N91-31484
N91-31486
SARBO, JANOS N91-31826
SARMIENTO, CHARLES J. N91-31216
SATO, J. N91-31372
SATTERWHITE, MELVIN B. N91-31697
SAUER, RICHARD L. N91-31755
SAUNDERS, MICHAEL A. N91-31858
SAWKO, PAUL M. N91-31236
SCANLON, CHARLES H. N91-31143
SCHAEFER, W. N91-31451
N91-31452
SCHARFENBERG, GOTTFRIED N91-31183
SCHARMANN, A. N91-31333
N91-31334
N91-31335
SCHATZ, BRUCE RAYMOND N91-31992
SCHERTZ, P. T. N91-31713
N91-31715
SCHEXNAYDER, A. R. N91-31176
SCHILLING, S. P. N91-31998
SCHIRBER, J. E. N91-31980
SCHLEGEL, R. N91-31591
SCHLENKER, M. N91-31382
SCHLUMBERGER, JULIE A. N91-31220
SCHMITT, M. J. N91-31639
SCHMITT, NIKOLAUS-P. N91-31635
SCHMITZ, G. N91-31379
SCHNEIDER, HORST N91-31086
SCHNEIDER, WALTER N91-31542
SCHNEIDER, WOLFGANG N91-31724
SCHOBERT, H. H. N91-31261
SCHODL, RICHARD N91-31623
N91-31624
SCHOONDERWOERD, K. N91-32024
SCHOONE, ANNEKE A. N91-31837
SCHRA, L. N91-31282
SCHUCHMAN, J. C. N91-31982
SCHUETTLER, H. B. N91-31976
SCHULER, JAMES W. N91-31660
SCHULTZ, REBECCA B. N91-31807
SCHUMAKER, LARRY L. N91-31904
SCHUMANN, U. N91-31562
SCHWABE, D. N91-31333
N91-31334
N91-31335
SCHWABE, DANIEL N91-31995
SCHWARTZKOPF, STEVEN H. N91-31798
SCHWEIGER, J. N91-31135
SCHWEITZER, K. N91-31455
N91-31456
N91-31457
N91-31458
SCOLLO, GIUSEPPE N91-31887
SEALE, R. L. N91-31933
SEBEK, MICHAEL N91-31842
SEIBERT, MICHAEL C. N91-31743
SEIDMAN, D. N. N91-31934
SEIGNEURIC, A. N91-31761
SEILER, WAYNE J. N91-31191
SELL, P. J. N91-31322
N91-31323
N91-31324
SELVAGGINI, R. N91-31099
SEN, R. K. N91-31247
SERDUKE, F. N91-31252
SETIO, SANGRIYADI N91-31681
SHAHANI, H. N91-31402
N91-31403
N91-31421
SHAKIN, C. M. N91-31931
SHARMA, S. N91-31981
SHARP, D. J. N91-31518
SHAWE-TAYLOR, JOHN N91-31881
SHEALY, DAVID L. N91-31607
SHEALY, JAMES R. N91-31951
SHEFFIELD, R. L. N91-31640
SHETTY, D. K. N91-31239
SHIH, C. N91-31629
N91-31630
SHIH, T. H. N91-31597
SHIVAKUMAR, K. N. N91-31692
SHUBIN, A. P. N91-31944
SHUM, F. N91-31152
SIAUD, E. N91-31382
N91-31383
SIDORUK, B. N91-31098
SIEKMANN, J. N91-31322
N91-31345
N91-31346
SIEMENS, P. D. N91-31520
N91-31521
SILBERBERG, R. N91-32021
SILCOX, R. J. N91-31889
SILVEIRANETO, A. N91-31568
SIMMONS, C. M. N91-31610
SIMON, D. R. N91-31519
SIMON, DONALD L. N91-31178
SIMPKINS, J. D. N91-31816
SIMPSON, M. A. N91-31926
N91-31927
SIMPSON, R. L. N91-31315
SINSKEY, ANTHONY J. N91-31313
SINTON, R. A. N91-31699
SIPPEL, THEODORE W. N91-31660
SKUMANICH, A. N91-31978
SMETSERS, J. E. W. N91-31824
SMIALEK, JAMES L. N91-31529
SMIT, J. N91-31515
SMITH, A. F. N91-31919
SMITH, C. C. N91-31252
SMITH, HENRY I. N91-31665
SMITH, IRA C. N91-31876
SMITH, LESLIE A. N91-31570
SMITH, M. F. N91-31248
N91-31272
N91-31292
N91-31293
SMITH, R. E. N91-31251
SMITH, R. W. N91-31402
SMOOT, N. C. N91-31754
SMYTH, J. D. N91-31716
SNOEYINK, JACK N91-31900
SOBIESZCZANSKI-SOBIESKI, JAROSLAW N91-31138
N91-31139
SOIZE, C. N91-31586
SONNAD, VIJAY N91-31911
SORENSEN, K. W. N91-31490
SOSTARICH, JOSEPH J. N91-31660
SOTTOS, NANCY R. N91-31228
SOUTH, D. W. N91-31721
SPENCE, PETER L. N91-31923
SPERBER, K. R. N91-31718
SPIEKSMA, F. N91-31918
SPRENGER, H. N91-31455
N91-31456
N91-31457
N91-31458
N91-31459
N91-31460
SPRENGER, S. N91-31407
SPRINGER, T. E. N91-31259
N91-31710
SQUIRES, KYLE DAVID N91-31548
SQUIRES, M. P. N91-31114
SRIVATSAN, RAGHAVACHARI N91-31120
STACEY, G. J. N91-32009
STACK, JOHN P. N91-31596
STARK, W. E. N91-31945
STAUDHAMMER, K. P. N91-31673
STEEG, M. N91-31413
STEELE, DOUGLAS S. N91-31660
STEIN, H. J. N91-31971
STEIN, H. N. N91-31362
STEINBERG, M. N91-31320
STEINER, BJOERN N91-31581
STEMME, HORST N91-31705
STEPHENS, CRAIG A. N91-31470
STEPHENS, MICHAEL A. N91-31920
STEPHENS, ROBERT RALPH N91-31670
STERNER, S. M. N91-31254
STEVENSON, J. O. N91-31472
STEWART, R. E. N91-31252
STICKLER, R. N91-31461
STOJANOWSKI, MARC N91-31097
STOLL, FREDERICK N91-31229
STORMS, E. K. N91-31945
STOUDT, M. R. N91-31242
STRAUB, J. N91-31354
N91-31355
N91-31356
N91-31357
N91-31358
N91-31374
STRAYER, M. R. N91-31931
STRAYER, R. F. N91-31785
STROET, JAN N91-31866
SUH, MYUNG WHAN N91-31990
SUH, YEONG SUNG N91-31273
SUKHADIA, A. M. N91-31244
SUMMERTON, M. N91-31145
SUN, T. N91-31244
SUNDERAM, V. S. N91-31855
N91-31870
SUNWOO, A. J. N91-31288
SURI, MANIL N91-31914
SUTHERLAND, B. M. N91-31756
SUTHERLAND, J. C. N91-31756
SUZUKI, Y. N91-31393
SWANSON, R. M. N91-31699
SWIERSTRA, DOAITSE N91-31832
SWIERSTRA, S. D. N91-31828
SWINTON, R. J. N91-31109
SZAKALY, ZOLTAN F. N91-31528
N91-31885
SZEGER, P. N91-31101
SZOZDA, JOE A. N91-31483

T

TACHIKAWA, K. N91-31427
TADROS, M. G. N91-31787
TAIX, MICHEL N91-31882

TAKAMUKU, K. N91-31979
TAN, RICHARD B. N91-31831
TAN, S. C. N91-31159
TANAKA, S. N91-31979
TANG, I. N. N91-31720
TANG, WAI-CHEUNG N91-31479
TAO, W. C. N91-31316
N91-31572
TAPPARO, D. J. N91-31162
TARBOURIECH, SOPHIE N91-31524
TARHIO, JORMA N91-31840
N91-31841
TARVER, C. M. N91-31316
TAUB, ALAN I. N91-31270
N91-31271
TEL, GERARD N91-31827
TEMAN, ROGER N91-31583
TERHOFSTEDE, A. H. M. N91-31996
TEXIER, ALAIN N91-31593
N91-31594
N91-31603
THALMANN, EDWARD N91-31769
THE, HAN N91-31752
THEOPHILOS, PAULA M. N91-31685
THODE, L. E. N91-31639
THOMAS, TERRI N91-31790
THOMAS, V. A. N91-31958
THOMPSON, C. P. N91-31888
THOMPSON, J. R. N91-31970
THOMPSON, R. B. N91-31688
THORNTON, A. L. N91-31574
TIBBITTS, T. W. N91-31799
TIBBITTS, THEODORE W. N91-31779
TIEN, TSENG-YING N91-31294
TILLBERG, E. N91-31389
N91-31390
TINIVELLA, R. J. N91-31666
TISON, P. N91-31391
TOBLIN, KENNETH L. N91-31856
TOGANO, K. N91-31427
TOGNACCINI, R. N91-31131
TOLCOTT, MARTIN A. N91-31774
TOLMIE, D. E. N91-31869
TOLSON, ROBERT HEATH N91-31487
TONG, MIKE N91-31235
TORTORELLI, P. F. N91-31291
TOWNES, C. H. N91-32009
TOWNSEND, PETER E. N91-31199
TRAAS, CORNELIS N91-31904
TRAN, B. N. N91-31926
N91-31927
TRAN, LE TRONG N91-31549
TREUMANN, R. A. N91-31957
TROTT, W. M. N91-31634
TROUESSIN, GILLES N91-31662
TROUTMAN, PATRICK A. N91-31201
TRUGLIO, VITO J. N91-31167
TRUONG, KHONG QUANG N91-32004
TSANGARAKIS, NIKOS N91-31245
TURKO, B. T. N91-31602
TURLEY, W. D. N91-31966
TURNER, D. J. N91-31375
N91-31376
TURTLE, HOWARD ROBERT N91-31993

U

UENAL, A. N91-31967
UITTENBOGAARD, A. H. N91-31828
UNGER, GEORGE N91-31751
URBANEK, J. N91-31373

V

V.D.BRINK, S. R. N91-31878
V.LUDWIGER, ILLOBRAND N91-31183
VAEL, G. N91-31442
VAILLANT, ROBERT N91-31182
VALERIO, J. N91-31259
VALLADO, DAVID A. N91-31861
VANBEEK, C. M. N91-31579
VANDENBERG, B. N91-31084
VANDENBERG, J. I. N91-31081
VANDENNEHEUVEL, SIEGER N91-31891
VANDERBORGH, N. E. N91-31711
VANDERBURG, J. W. N91-31906
VANDERGAAG, LINDA N91-31917
VANDERVELDE, R. L. N91-31133
VANDERWEIDE, T. P. N91-31996
VANDIEPEN, N. M. N91-31863
VANDOMMELEN, L. N91-31629
VANDOORN, J. T. M. N91-31133
VANDROMME, D. N91-31564
VANDYCK, O. B. N91-31932
VANDYKE, P. T. N91-32031
VANEEKELEN, M. C. J. D. N91-31824
N91-31880
VANEK, M. D. N91-31723
VANKREVELD, MARC J. N91-31903
VANLEEUWEN, JAN N91-31831
VANLEIJENHORST, D. C. N91-31825
N91-31895
VANLOON, A. J. N91-32023
VANROSENDALE, J. N91-31888
VANSCHAIK, F. J. N91-31119
VANSCHAIK, P. N91-31845
VANSUETENDAEL, N. N91-31814
VANVELDHUIZEN, E. M. N91-32028
VAZQUEZ, ALAN A. N91-31192
VEGH, EMANUEL N91-31952
VELDMAN, H. J. N91-31908
VERGHESE, S. N91-31611
VERMASEREN, J. N91-31930
VERVILLE, G. N91-31515
VERVOORT, W. A. N91-31863
VERWER, NICO N91-31833
VILLATTE, P. P. N91-31305
VINEBERG, KAREN A. N91-31478
VIOLETT, DUANE L., JR. N91-31853
VISSER, B. M. N91-32030
VITAGLIANO, P. L. N91-31131
VITEK, J. M. N91-31277
N91-31649
N91-31650
VOCHTEN, R. N91-31392
VOELLMER, GEORGE M. N91-31656
VOGT, HARALD N91-31832
VOLD, E. L. N91-31955
VOLK, TYLER N91-31795
VOSS, H.-H. N91-31696
VOTER, A. F. N91-31287
VUILLOT, A. M. N91-31847

W

WALCOTT, K. N91-31714
WALKER, W. D. N91-31939
WALLACE, R. N91-31252
WALTER, C. J. N91-31663
WALTER, G. N91-31352
WALTER, H. U. N91-31380
N91-31381
N91-31408
N91-31409
N91-31410
N91-31411
N91-31412
N91-31430
N91-31431
WANDER, STEVE N91-31751
WANG, KANG L. N91-31984
WANG, QINGLIN N91-31492
WANG, SHAIO-WEN N91-31227
WANG, TAI-SEN F. N91-31640
WANG, Z. H. N91-31310
WANHILL, R. J. H. N91-31282
WARD, M. R. N91-31778
WARD, MICHEL J. N91-31505
WARD, T. E. N91-31223
WARNE, L. K. N91-31500
WARREN, R. N91-31463
WARREN, R. W. N91-31640
WARREN, W. E. N91-31230
WARREN, WAYNE N., JR. N91-32003
WASSON, DOUGLAS J. N91-31312
WATTS, ETHEL J. N91-31805
WAXMAN, ALLEN M. N91-31954
WEBER, P. G. N91-31694
WEHR, P. N91-31398
WEIJERS, H. M. N91-32029
WEINBERG, AARON N91-31499
WEINBERG, IRVING N91-31217
WEINBERG, NORMAN S. N91-31170
WEINZIERL, A. N91-31354
N91-31355
WEISSE, ECKART N91-31706
WELCH, D. O. N91-31972
WELSTEAD, STEPHEN T. N91-31505
WELTER, GARY L. N91-32007
WENDELL, CHARLES EDWARD N91-32015
WERT, J. J. N91-31308
WESSELS, H. R. A. N91-31497
WESTBROOK, C. K. N91-31314
WHEELER, R. M. N91-31780
N91-31781
N91-31797
WHINNERY, JAMES E. N91-31768
N91-31809
WHIPPLE, M. L. N91-31703
WHIRLEY, R. G. N91-31675
WHITAKER, R. W. N91-31929
WHITE, D. N91-31715
WHITE, D. E. N91-31300
WHITESON, R. N91-31886
WIBBELSMAN, R. C. N91-31153
WIDGOFF, M. N91-31941
WIEDERSICH, H. N91-31278
WILLE, L. T. N91-31281
WILLIAMS, G. M. N91-31609
WILLIAMS, LOUIS J. N91-31751
WILLIAMS, R. N91-31970
WILLIAMS, R. S. N91-31984
WILLIAMS, ROBERT L., II N91-31879
WILLIS, J. O. N91-31979
WILLSON, K. R. N91-31291
WILNECKER, R. N91-31466
N91-31468
WILSON, W. L. N91-31640
WINSKE, D. N91-31958
WITCOMB, M. J. N91-31473
WOERMANN, D. N91-31379
WOJCIECHOWSKI, CHARLES R. N91-31660
WOLOSHUN, K. A. N91-31210
WOMERSLEY, J. N91-31816
WOOD, PETER J. N91-31514
WOOD, W. E. N91-31290
WOODHOUSE, D. N91-31171
WOOLLEY, CHRISTINE L. N91-31082
WOSPERNOV, W. N91-31347
WOZNIAK, G. N91-31345
N91-31346
WREN, PAUL E. N91-31530
WRIGHTON, M. S. N91-31700
WU, J.-S. N91-31931
WU, SHIH-CHIN N91-31684
N91-31685
N91-31686
WUEST, W. N91-31336
WYDEVEN, THEODORE J., JR. N91-31258
WYNN, ROBERT H., JR. N91-31671

X

XIA, QIONG N91-31550
XIN, WEIZHUANG N91-31750
XUELIANG, LI N91-31905

Y

YACOUT, A. M. N91-31816
YATES, G. J. N91-31602
YATES, J. T., JR. N91-31266
YAU, HONG-TZONG N91-31661
YEUNG, F. K. N91-31156
YOON, BOK-HYUN N91-31080
YOON, TAE SEOG N91-32005
YOSHIDA, Y. N91-31427
YOUNG, J. K. N91-31247
YOUNG, L. M. N91-31640
YOUSSEF, S. N91-31816
YUCESOY, ENIS N91-31865
YUKIMOTO, Y. N91-31394

Z

ZACHARIA, T. N91-31649
ZAGHLOUL, AMIR I. N91-31480
ZANDBERGEN, P. J. N91-31580
N91-31906
ZANTEMA, H. N91-31896
ZAWODZINSKI, T. A., JR. N91-31259
ZELL, M. N91-31356
N91-31357
N91-31358
ZHANG, YUANCHONG N91-31726
ZHDANOV, V. L. N91-31085
ZHOU, YU N91-31968
ZICARI, ROBERTO N91-31994
ZIEGLER, G. N91-31408
N91-31409
N91-31430
N91-31431
ZITTEL, D. H. N91-31490
ZUREK, A. K. N91-31275

Typical Corporate Source Index Listing

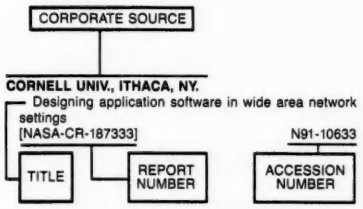

Listings in this index are arranged alphabetically by corporate source. The title of the document provides the user with a brief description of the subject matter. The report number helps to indicate the type of document cited (e.g., NASA report, translation, NASA contractor report). The accession number denotes the number by which the citation is identified. The titles are arranged under each corporate source in ascending accession number order.

A

ACADEMY OF SCIENCES OF THE UKRAINIAN SSR, KIEV.
The photovoltaic effect on pyroelectics N91-31707
Near-wall conductivity N91-31944
Plasma-optics systems for the formation and focusing of ion beams N91-31956

ADVISORY GROUP FOR AEROSPACE RESEARCH AND DEVELOPMENT, NEUILLY-SUR-SEINE (FRANCE).
Low Temperature Environment Operations of Turboengines (Design and User's Problems) [AGARD-CP-480] N91-31144

AERITALIA S.P.A., TURIN (ITALY).
Inlet edge funnel of a civil aircraft gondola engine [ETN-91-99775] N91-31130

AERO AND INDUSTRIAL TECHNOLOGY LTD., BURNLEY (ENGLAND).
Icing test programmes and techniques N91-31171

AERONAUTICAL RESEARCH LABS., MELBOURNE (AUSTRALIA).
Field evaluation of six protective coatings applied to T56 turbine blades after 500 hours of engine use [ARL-MAT-TM-405] N91-31179
Variations in the static properties, unnotched and notched fatigue life behaviour of 13 batches of 2L.65 aluminium alloy extruded bar [ARL-STRUC-R-427] N91-31676

AEROSPACE CORP., EL SEGUNDO, CA.
Sensitivity of imaging materials to electron beam irradiation [AD-A239365] N91-31612
Garment selection for cleanrooms and controlled environments for spacecraft [AD-A239512] N91-31805

AEROSPATIALE, SURESNES (FRANCE).
Relation between fiber proportion and mechanical characteristics of carbon-resin composites [RE-50-345/F] N91-31231
Influence of adhesive polymerization conditions on the durability of adhesive joints [DCR/I-03357-90] N91-31305

AIR FORCE ACADEMY, CO.
Methods of astrodynamics, a computer approach [AD-A239662] N91-31861

AIR FORCE INST. OF TECH., WRIGHT-PATTERSON AFB, OH.
A knowledge-base for rehabilitation of airfield concrete pavements [AD-A239354] N91-31191
Application of semianalytic satellite theory to maneuver planning [AD-A239417] N91-31205
Effect of porcelain surface pretreatments on composite resin-porcelain shear bond strength [AD-A239359] N91-31241
Effect of thickness and brand of metal ceramic porcelain on color [AD-A239398] N91-31312
Hardware modeling and top-down design using VHDL [AD-A239356] N91-31534
Application of multivariable control system design methodologies to robust beam control of a space-based laser [AD-A239460] N91-31643
The effect of exercise training on skeletal muscle glucose transorter isoform GLUT4 concentration in the obese Zucker rat [AD-A239461] N91-31757
Cockpit resource management: Effects on behavioral interactions across airlines and aircraft types [AD-A239467] N91-31804
Interactive constraint-based solid modeling as a design tool [AD-A239358] N91-31856
A search for periodicity in the x ray spectrum of black hole candidate A0620-00 [AD-A239488] N91-32011

ALABAMA A & M UNIV., NORMAL.
Algae for controlled ecological life support system diet characterization of cyanobacteria 'spirulina' in batch cultures N91-31787

ALABAMA UNIV., BIRMINGHAM.
Design and analysis of multilayer x ray/XUV microscope [NASA-CR-184197] N91-31607

ALABAMA UNIV., HUNTSVILLE.
A graph theoretic approach to scene matching [NASA-CR-187817] N91-31947

ALLIED-SIGNAL AEROSPACE CO., COLUMBIA, MD.
Reliability modeling of dependable distributed systems [AD-A239734] N91-31663
The potential impact of VHDL on dependable distributed system design [AD-A239769] N91-31664

ALLIED-SIGNAL AEROSPACE CO., KANSAS CITY, MO.
Determination of aqueous processable photoresist in tin-lead plating solutions [DE91-015575] N91-31251
Analysis of production solutions by polarography [DE91-016479] N91-31257
Economic analysis of robotic torque measurement system [DE91-016480] N91-31653
Evaluation of the intermittent GTA cold wire feed weld system [DE91-016477] N91-31657
Atomatic Feature (AFEAT) identification for Computer-Aided Process Planning (CAPP) [DE91-016478] N91-31819

ALLIED-SIGNAL CORP., KANSAS CITY, MO.
Microwave module YAG laser weld development [DE91-015750] N91-31652

AMES LAB., IA.
Ultrasonic characterization of fatigue crack closure [DE91-015161] N91-31688

AMSTERDAM UNIV. (NETHERLANDS).
Weak equivalence [ITLI-CT-91-04] N91-31891

ANALYTIC SCIENCES CORP., READING, MA.
Performance Assessment and Coverage Evaluation (PACE) workstation (user manual) [AD-A239723] N91-31122
OMEGA system Performance Assessment and Coverage Evaluation (PACE) workstation design and implementation, volume 2 [AD-A239724] N91-31123
Analysis and evaluation of selected PACE applications [AD-A239726] N91-31124

ANALYTICAL SERVICES AND MATERIALS, INC., HAMPTON, VA.
An equivalent domain integral method for three-dimensional mixed-mode fracture problems [NASA-CR-182021] N91-31692

ANTWERP UNIV. (BELGIUM).
Crystallisation experiments with salts (TEXUS 13) N91-31392

ARGONNE NATIONAL LAB., IL.
The chemistry of transition metal clusters [DE91-015108] N91-31250
Formation of defect structures in metals during irradiation [DE91-015548] N91-31278
Mechanical characterization of seismic base isolation elastomers [DE91-015680] N91-31299
Development of prototype sealed bipolar lithium/sulfide cells [DE91-015721] N91-31519
Response of seismic-isolated structures under long-period motions [DE91-015673] N91-31674
Proceedings of the Ninth Symposium on Energy Engineering Sciences: Fluid and Dynamical Systems [DE91-015974] N91-31701
Open-cycle ocean thermal energy conversion surface-condenser design analysis and computer program [DE91-015973] N91-31709
Coal utilization and CO2 emissions: What are the control options? [DE91-015988] N91-31721
A new method to do time resolved, x ray diffraction studies: The rotating crystal Laue method [DE91-016527] N91-31935
Intrinsic stability and recovery analysis for tape/film type superconductors [DE91-015568] N91-31967
Mean field analysis of the CuO2 lattice: Comparison to Monte Carlo simulations [DE91-015570] N91-31968
Cu-O charge fluctuations and electron-phonon coupling in the effective single-band Hubbard theory for cuprate superconductors [DE91-016526] N91-31976

ARIZONA UNIV., TUCSON.
Interactive retrieval in information spaces distributed across a wide-area network N91-31992

ARMY AIR CORPS, STOCKBRIDGE (ENGLAND).
Low temperature environment operation of turbo engines: A military operator's experience and requirements N91-31145

ARMY ARMAMENT RESEARCH, DEVELOPMENT AND ENGINEERING CENTER, WATERVLIET, NY.
An extension of mesh equidistribution to time-dependent partial differential equations [AD-A239579] N91-31913

ARMY ENGINEER TOPOGRAPHIC LABS., FORT BELVOIR, VA.
Hyperspectral signatures (400 to 2500 nm) of vegetation, minerals, soils, rocks, and cultural features: Laboratory and field measurements [AD-A239496] N91-31697

ARMY LAB. COMMAND, WATERTOWN, MA.
Response of an alumina fiber reinforced aluminum composite to combined tension-torsion [AD-A239560] N91-31245
Structure property relationship of aliphatic polyurethane elastomers prepared from CHDI [AD-A239397] N91-31311

ARMY RESEARCH INST. OF ENVIRONMENTAL MEDICINE, NATICK, MA.
Cold-induced changes in arterial sensitivity [AD-A239493] N91-31767

ASSOCIATION AERONAUTIQUE ET ASTRONAUTIQUE DE FRANCE, PARIS.
Measurement of six component efforts in transition flow [AAAF-NT-89-01] N91-31097
RADAC model deformation measurement system: First results at the F1 wind tunnel [AAAF-NT-89-03] N91-31098
Conditional sampling [AAAF-NT-89-04] N91-31099

Laser velocimetry at the CEAT aerodynamic group: Application to unsteady measurements on a fluid flap profile
[AAAF-NT-89-05] N91-31100
Low level turbulence detection by a laser velocimetry technique: Application to transonic flows
[AAAF-NT-89-07] N91-31101
Local mean mass volume measurement around a model with lateral jet in supersonic flow
[AAAF-NT-89-08] N91-31102
Laser Fourier densitometry and laser induced photochemical anemometry in supersonic flow
[AAAF-NT-89-09] N91-31103
Airfoil-vortex interaction: Unsteady wall pressure measurement
[AAAF-NT-89-13] N91-31104
Boundary layer transition detection and measurement methods at CERT/DERAT
[AAAF-NT-89-14] N91-31105
Second generation supersonic transport aircraft: Low speed aerodynamics
[AAAF-NT-89-02] N91-31137
Instrumentation under development for the ONERA F4 wind tunnel
[AAAF-NT-89-11] N91-31187
A first hot wire scanner
[AAAF-NT-89-16] N91-31188
Boundary layer turbulence appearance mechanisms studied by plane laser visualizations
[AAAF-NT-89-10] N91-31587
Use of 4-hot-wire probes to study turbulent flow
[AAAF-NT-89-15] N91-31588
Choice representation modes and color palettes
[AAAF-NT-89-17] N91-31589
Flow visualization and simulation
[AAAF-NT-89-18] N91-31590
Postprocessing of test and computation results by the wavelet method
[AAAF-NT-89-24] N91-31591
Postprocessing of experimental and numerical results in the case of two and three dimensional flows
[AAAF-NT-89-25] N91-31592
The development of a specific image analysis technique for exploiting flow visualization negatives
[AAAF-NT-89-26] N91-31593
Laser Doppler anemometer miniaturized with diode laser
[AAAF-NT-89-06] N91-31637
Interactive tool visualization of three dimensional 3D results
[AAAF-NT-89-19] N91-31847
Post processing of three dimensional aerothermal computation
[AAAF-NT-89-21] N91-31848
Use of the animated images for the visualization of computational results
[AAAF-NT-89-22] N91-31849
Visualization of three dimensional unsteady computation results
[AAAF-NT-89-23] N91-31850
Application of an acquisition image processing system to the quantitative analysis of flows
[AAAF-NT-89-27] N91-31851

ATLANTIS SCIENTIFIC SYSTEMS GROUP, INC., OTTAWA (ONTARIO).
Updates to the DREO airborne radar simulator
[ASSGI-167] N91-31478
Improvements to programs for system studies of space-based radar
[DRE-179] N91-31484
Behaviour of the SIR for space-based DPCA radar under various spatial clutter distributions
[CRC-W7714-7-5271] N91-31485
Pulse Doppler radar simulation study
[ASSGI-14SV-W7714-7-5353] N91-31486

B

BATTELLE INST., FRANKFURT AM MAIN (GERMANY, F.R.).
Dispersion layers by electrodeposition (TEXUS 1) N91-31350
Dispersion electrolysis (TEXUS 4) N91-31351
Dispersion electrolysis (TEXUS 7) N91-31352
Dispersion electrolysis (TEXUS 9) N91-31353
Acoustic mixing (TEXUS 5) N91-31423
Solidification of immiscible alloys (TEXUS 8) N91-31424
Separation of transparent fluids due to Marangoni convection (TEXUS 7) N91-31425
Marangoni transport of droplets at a solidification front (TEXUS 9) N91-31426
Acoustic positioning of a molten alloy sample (TEXUS 1) N91-31464
Acoustic positioning (TEXUS 9) ESA N91-31465
Acoustic positioning (TEXUS 14b) ESA N91-31467
Electrostatic positioning for containerless processing of a Li-silicate glass (TEXUS 10) ESA N91-31469

BEECH AIRCRAFT CORP., BOULDER, CO.
Method for fastening aircraft frame elements to sandwich skin panels covering same using woven fiber connectors
[PATENT-1-274-075] N91-31126

BERTIN ET CIE., AIX-LES-MILLES (FRANCE).
Real time actuating of laser power and scanning velocity for thermal regulation during laser hardening
[ETN-91-99908] N91-31636

BIONETICS CORP., COCOA BEACH, FL.
Use of inedible wheat residues from the KSC-CELSS breadboard facility for production of fungal cellulase N91-31785
Biomass production and nitrogen dynamics in an integrated aquaculture/agriculture system N91-31789

BOEING CANADA, TORONTO (ONTARIO).
Ice tolerant engine inlet screens for CH113/113A search and rescue helicopters N91-31149
Segmented rotatable nozzles
[CA-PATENT-APPL-SN-2-009-634] N91-31174
Segmented vectoring cruise nozzles
[CA-PATENT-APPL-SN-2-009-635] N91-31175
Ventral segmented nozzles
[CA-PATENT-APPL-SN-2-009-636] N91-31176

BOEING CO., SEATTLE, WA.
Removable slider shoe for a translating sleeve used on a jet engine cowl and duct
[PATENT-1-247-868] N91-31177

BRITISH AEROSPACE PUBLIC LTD. CO., BRISTOL (ENGLAND).
The Sowerby Research Centre and university liaison N91-31730

BRITISH AEROSPACE PUBLIC LTD. CO., PRESTON (ENGLAND).
BAe University Round Table on Gravitational Research
[BAE-FBS-007] N91-31729
BAe overview of current gravitational physics research N91-31731
A reminder of Faraday's gravitational experiments N91-31735
Heaviside's linearised gravitational theory N91-31737

BROOKHAVEN NATIONAL LAB., UPTON, NY.
Conversion of biomass and fossil fuels to methanol and its effect on CO2 emissions
[DE91-015846] N91-31320
Chemical characterization of aerosol particles by Raman spectroscopy
[DE91-015836] N91-31720
Pyrimidine dimer formation by UVA radiation: Implications for photoreactivation
[DE91-015837] N91-31756
Acceleration using total internal reflection
[DE91-016612] N91-31942
Models of flux diffusion and flux creep in high-temperature superconductors
[DE91-015838] N91-31972
Superconducting magnet program for x ray lithography source at Brookhaven National Laboratory
[DE91-016995] N91-31981
Review of vacuum systems for x ray lithography light sources
[DE91-017008] N91-31982

BROWN UNIV., PROVIDENCE, RI.
A research program in experimental high energy physics
[DE91-016208] N91-31941

BRUSSELS UNIV. (BELGIUM).
Influence of a surface tension minimum on the Marangoni effect (TEXUS 8) ESA N91-31338
Influence of a surface tension minimum on the Marangoni effect (TEXUS 9) ESA N91-31339
Influence of a surface tension minimum on the Marangoni effect (TEXUS 19) ESA N91-31340

BUNDESANSTALT FUER MATERIALPRUEFUNG, BERLIN (GERMANY, F.R.).
Brazing of capillary gaps (TEXUS 2) N91-31461

C

CALIFORNIA INST. OF TECH., PASADENA.
A comparison of several theories which use jet scaling to predict liftoff heights of turbulent-jet flames
[AD-A239717] N91-31267

CALIFORNIA UNIV., BERKELEY. LAWRENCE BERKELEY LAB.
Virial coefficients and equations of state for mixed fluids; application to CH4-H2O
[DE91-016248] N91-31254
Magnetic field-induced fracture changes in metastable austenites at 4.2 K
[DE91-016263] N91-31279
Metastable austenites in cryogenic high magnetic field environments
[DE91-016420] N91-31288
A jet polishing technique for thinning two phase materials
[DE91-016422] N91-31473
High-T(sub c) bolometers
[DE91-017009] N91-31611
Cyanobacteria in CELSS: Growth strategies for nutritional variation and nitrogen cycling N91-31786
Recent advances in fiber optic components for high speed data transmission
[DE91-016252] N91-31948
Macroscopic quantum tunneling in Josephson tunnel junctions and Coulomb blockade in single small tunnel junctions
[DE91-016258] N91-31974
TEM analysis of crystalline interface structure: The state of the art
[DE91-016427] N91-31975
The Berkeley search for distant supernovae to measure omega
[DE91-016418] N91-32010
Nuclear and particle astrophysics
[DE91-016260] N91-32016
Fast pulsars, variational bound, other facets of compact stars
[DE91-016416] N91-32018

CALIFORNIA UNIV., DAVIS.
Efficiency of N use by wheat as a function of influx and efflux of NO3 N91-31778

CALIFORNIA UNIV., IRVINE.
Design and analysis of fault-tolerant distributed real-time computer systems
[AD-A239521] N91-31812

CALIFORNIA UNIV., LOS ANGELES.
Epitaxial growth and electro-optical properties of metal GaAs superlattices
[AD-A239719] N91-31984

CANADIAN ASTRONAUTICS LTD., OTTAWA (ONTARIO).
Composite waveguide coupling aperture having a thickness dimension
[PATENT-1-259-401] N91-31514

CANADIAN FORCES BASE COLD LAKE, MEDLEY (ALBERTA).
Low temperature environment operations of turbo engines N91-31146

CANADIAN FORCES HEADQUARTERS, OTTAWA (ONTARIO).
Climatic considerations in the life cycle management of the CF-18 engine N91-31158

CANADIAN GENERAL ELECTRIC CO. LTD., TORONTO (ONTARIO).
Ventral segmented nozzles
[CA-PATENT-APPL-SN-2-009-636] N91-31176

CARNEGIE-MELLON UNIV., PITTSBURGH, PA.
Multitarget tracking using optical processing
[AD-A239656] N91-31953

CASE WESTERN RESERVE UNIV., CLEVELAND, OH.
Electron microscopy to correlate cell structures and biochemical activity
[AD-A239640] N91-31758

CATHOLIC UNIV. OF AMERICA, WASHINGTON, DC.
Ultraviolet morphology of NGC 1068: The starburst knots and the extended emission region N91-32004

CBY ASSOCIATES, INC., WASHINGTON, DC.
Solar energy and conservation technologies for Caribbean Tourist Facilities (CTF)
[DE91-016451] N91-31712

CENTRAL ELECTRICITY RESEARCH LABS., LEATHERHEAD (ENGLAND).
Ionic solutions near the critical point of water (TEXUS 10) ESA N91-31375
Ionic solutions near the critical point of water (TEXUS 12) ESA N91-31376

CENTRE AEROPORTE DE TOULOUSE (FRANCE).
Low altitude ejection release (total mass between 1,660 and 5,600 kg)
[REPT-90/05] N91-31475

CENTRE D'ESSAIS DES PROPULSEURS, ORSAY (FRANCE).
Numerical model of evolution in supercooled cloud of water droplets in a case of icing N91-31169

CENTRE D'ETUDES ET DE RECHERCHES, TOULOUSE (FRANCE).
Three dimensional shear flow: Flow visualisation around a highly swept back and high incidence wing
[ONERA-RT-35/5025-28] N91-31584

CENTRE NATIONAL D'ETUDES SPATIALES, TOULOUSE (FRANCE).
Calculation of fragment ejection velocities on explosion of a launcher
[CNES-NT-128] N91-31195

Choice of a differential method for attitude restitution with dynamic imbalance
[CNES-NT-126] N91-31202
Soldering of complex multilayer printed boards
[CNES-NT-127] N91-31474

CENTRE NATIONAL DE LA RECHERCHE SCIENTIFIQUE, GRENOBLE (FRANCE).
Single crystals of CeMg3 (TEXUS 7) ESA N91-31382
Growth of rare Earth-magnesium crystals (TEXUS 12) N91-31383

CHALMERS UNIV. OF TECHNOLOGY, GOETEBORG (SWEDEN).
Thermal conductivity of liquids (MASER 1) ESA N91-31361
Adhesion of metals on ceramic substrates (MASER 2) ESA N91-31463

CHICAGO UNIV., IL.
Nuclear medicine and imaging research: Quantitative studies in radiopharmaceutical science
[DE91-015447] N91-31759

CITY COLL. OF THE CITY UNIV. OF NEW YORK, NY.
Electronic transport and lasing in microstructures
[DE91-016751] N91-31641

COLORADO SCHOOL OF MINES, GOLDEN.
Weldability and hot ductility of iron aluminides
[DE91-016343] N91-31280

COLORADO STATE UNIV., FORT COLLINS.
Chemically modified electrodes and related solution studies
[DE91-016740] N91-31262
Mass resolved excitation spectroscopy of benzyl and phenylnitrene radicals
[AD-A239394] N91-31264

COLORADO UNIV., BOULDER.
An investigation of optically controlled, integrated millimeter wave receiving phased arrays
[AD-A239504] N91-31538
Effects of stress on judgment and decision making in dynamic tasks
[AD-A239452] N91-31772
Optimizing the long-term retention of skills: Structural and analytic approaches to skill maintenance 3
[AD-A239574] N91-31773
Seed sprout production: Consumables and a foundation for higher plant growth in space N91-31790

COLSA, INC., HUNTSVILLE, AL.
Hybrid electro-optic processor
[AD-A239547] N91-31505

COLUMBIA UNIV., NEW YORK, NY.
The time-domain earth tides N91-31726

COM DEV LTD., CAMBRIDGE (ONTARIO).
Dielectric image-resonator multiplexer
[PATENT-1-252-835] N91-31479
Antenna study for 60 GHz intersatellite link
[CD-RPT-ITL-5043-003] N91-31482

COMMERCIAL SPACE TECHNOLOGIES LTD., LONDON (ENGLAND).
Review of microgravity N91-31736

COMMISSARIAT A L'ENERGIE ATOMIQUE, GIF-SUR-YVETTE (FRANCE).
Phase separation in microgravity of binary fluids near the critical point (TEXUS 13) N91-31378

COMMISSARIAT A L'ENERGIE ATOMIQUE, GRENOBLE (FRANCE).
Semi-confined Bridgman growth of Ga-doped Ge (MASER 2) N91-31391
Directional solidification of eutectics (TEXUS 6) N91-31404
Large-eddy simulation of the turbulent flow in the downstream region of a backward facing step N91-31568

COMMISSARIAT A L'ENERGIE ATOMIQUE, SACLAY (FRANCE).
Phase separation of a binary fluid near its critical point (TEXUS 11) N91-31377
Spatiotemporal intermittency N91-31569

COMMUNICATIONS SATELLITE CORP., WASHINGTON, DC.
Electromagnetically coupled microstrip antennas having feeding patches capacitively coupled to feedlines
[PATENT-1-263-181] N91-31480

COMPUTATIONAL SYSTEMS, INC., KNOXVILLE, TN.
Diagnostic tools for reciprocating engine systems
[PB91-184960] N91-31645

COMPUTER RESOURCE MANAGEMENT, INC., PLEASANTVILLE, NJ.
Software quality metrics
[DOT/FAA/CT-91/1] N91-31814

COMPUTER SCIENCES CORP., CALVERTON, MD.
Research studies with the International Ultraviolet Explorer
[NASA-CR-183495] N91-32012

COMPUTER SCIENCES CORP., LAUREL, MD.
The in-flight calibration of the Hubble space telescope attitude sensors
[NASA-CR-183485] N91-32007

COMTEK CO., GRAFTON, VA.
Large Angle Transient Dynamics (LATDYN) demonstration problem manual
[NASA-CR-4400] N91-31684
Large Angle Transient Dynamics (LATDYN) user's manual
[NASA-CR-4401] N91-31685
A finite element approach for the dynamic analysis of joint-dominated structures
[NASA-CR-4402] N91-31686

CONSIGLIO NAZIONALE DELLE RICERCHE, GENOA (ITALY).
Meniscus stability in immiscible metals (MASER 1) N91-31428

CONTEL FEDERAL SYSTEMS, INC., CHANTILLY, VA.
Traffic model for advanced satellite designs and experiments for ISDN services
[NASA-CR-188802] N91-31200
Interim Service ISDN Satellite (ISiS) network model for advanced satellite designs and experiments
[NASA-CR-186565] N91-31488

CORNELL UNIV., ITHACA, NY.
A program of continuing research on representing, manipulating, and reasoning about physical objects
[AD-A239596] N91-31659
Innovative optoelectronic materials and structures using OMVPE
[AD-A239518] N91-31951
Studies of the III-V compounds in the megabar regime
[DE91-015911] N91-31973

D

DAELEN UND LOOS G.M.B.H., WIESBADEN-SCHIERSTEIN (GERMANY, F.R.).
Al-Pb bearing alloy (TEXUS 1) N91-31413

DECISION SCIENCE CONSORTIUM, INC., RESTON, VA.
Examining the effect of information order on expert judgment
[AD-A239708] N91-31774

DEFENCE AND CIVIL INST. OF ENVIRONMENTAL MEDICINE, DOWNSVIEW (ONTARIO).
Methodology for calibration and use of heat flux transducers
[AD-A239552] N91-31541
Female aircrew: The Canadian Forces experience, 1979-1989
[DCIEM-90-P-14] N91-31801
Assessing the efficacy of active noise reduction
[CTN-91-60200] N91-31922

DELAWARE UNIV., NEWARK.
Processing and characterization of continuous fiber-reinforced glass and glass-ceramic matrix composites N91-31227
The influence of interphase regions on local thermal stresses and deformations in composites N91-31228

DELTA INFORMATION SYSTEMS, INC., HORSHAM, PA.
Investigation of the progressive bi-level coding technique for the high-resolution bi-level data compression standard
[AD-A239597] N91-31860

DEPARTMENT OF ENERGY, OAK RIDGE, TN.
Summaries of FY 1991 research in the chemical sciences
[DE91-011221] N91-31222

DEPARTMENT OF ENERGY, WASHINGTON, DC.
Summaries of FY 1991 research in the chemical sciences
[DE91-011221] N91-31222
Assessment of costs and benefits of flexible and alternative fuel use in the US transportation sector
[DE91-015451] N91-31319

DEPARTMENT OF NATIONAL DEFENCE, OTTAWA (ONTARIO).
Asbestos-free insulant for rocket motors
[PATENT-1-263-227] N91-31206
Rocket boosted target
[PATENT-1-254-289] N91-31207
Radome-lens EHF antenna development
[PATENT-1-262-571] N91-31481
High speed digital direct access filter for tracking or excision of parametric signal data
[PATENT-1-271-231] N91-31511
Filter system for radar applications
[PATENT-1-273-409] N91-31512
Reconfigurable parameter filter
[PATENT-1-264-072] N91-31513
Techniques to assess the state of health of sealed lead acid batteries
[CTN-91-60214] N91-31515

DEUTSCHE FORSCHUNGS- UND VERSUCHSANSTALT FUER LUFT- UND RAUMFAHRT, COLOGNE (GERMANY, F.R.).
Composite materials, 1 (TEXUS 1) N91-31408
Composite materials, 2 (TEXUS 2) N91-31409
Immiscibles, 1 (TEXUS 3) N91-31410
Immiscibles, 2 (TEXUS 5) N91-31411
Dispersion alloys (TEXUS 7) N91-31412
Composite materials, 1 (TEXUS 1) N91-31430
Composite materials, 2 (TEXUS 2) N91-31431
Containerless solidification of a Pd-Cu-Si sample (TEXUS 9) ESA N91-31466
Containerless undercooling of a Pd-Cu-Si alloy (TEXUS 14b) ESA N91-31468

DEUTSCHE FORSCHUNGS- UND VERSUCHSANSTALT FUER LUFT- UND RAUMFAHRT, GOETTINGEN (GERMANY, F.R.).
Thermal Marangoni convection in a floating zone (TEXUS 3) N91-31336
Oscillatory and turbulent flow regimes due to Marangoni convection (TEXUS 7) N91-31337

DEUTSCHE FORSCHUNGSANSTALT FUER LUFT- UND RAUMFAHRT, BRUNSWICK (GERMANY, F.R.).
The effects of different sequencing strategies on the capacity of airports
[DLR-MITT-90-18] N91-31185

DEUTSCHE FORSCHUNGSANSTALT FUER LUFT- UND RAUMFAHRT, COLOGNE (GERMANY, F.R.).
Spinoidal decomposition (TEXUS 17) N91-31379
Directional solidification of doped germanium (TEXUS 4) ESA N91-31380
Striations in germanium (TEXUS 6) ESA N91-31381
Laser transit velocimetry N91-31623
Laser transit velocimetry: Recent publications N91-31624

DEUTSCHE FORSCHUNGSANSTALT FUER LUFT- UND RAUMFAHRT, OBERPFAFFENHOFEN (GERMANY, F.R.).
A documentation of vertical and horizontal aircraft soundings of icing relevant cloudphysical parameters N91-31172
Direct and large eddy simulation of turbulence: Summary of the state-of-the-art 1991 N91-31562
Examination and mapping of forest damage, using remote sensing methods
[ETN-91-99741] N91-31696

DIRECTION DES RECHERCHES, ETUDES ET TECHNIQUES, PARIS (FRANCE).
Crack propagation in heat resistant disk alloys. Short crack propagation in alloys for high characteristic turbomachine disks
[ETN-91-99981] N91-31683

DORNIER SYSTEM G.M.B.H., FRIEDRICHSHAFEN (GERMANY, F.R.).
Metallic foams (TEXUS 5) N91-31451
Preparation of aluminium foams (TEXUS 9) N91-31452

DOUGLAS AIRCRAFT CO., INC., LONG BEACH, CA.
Fuselage shell and cavity response measurements on a DC-9 test section
[NASA-CR-187557] N91-31926
Analysis of interior noise ground and flight test data for advanced turboprop aircraft applications
[NASA-CR-187558] N91-31927

DUKE UNIV., DURHAM, NC.
High energy physics
[DE91-015796] N91-31939

E

ECOLE CENTRALE DE LYON (FRANCE).
Contribution of low wave numbers to the wall pressure field in a two dimensional turbulent boundary layer: Comparison of different experimental techniques
[ECL-90-15] N91-31091
Calculating the flow in a turbomachine with Clebsch variables and a finite element method
[ETN-91-99918] N91-31180
A three-dimensional code to solve the Poisson equation: Numerical simulation of the breakdown in P-N junction devices
[ECL-90-27] N91-31525
Contribution to the implementation of a completely in situ device in ultrahigh vacuum for the development of MIS on InP structures: Al2O3/InP interface optimization
[ECL-91-04] N91-31526
Design of a specific integrated circuit for solving the three dimensional Poisson equation
[ECL-90-24] N91-31527
Identifying behavior characteristics using pressuremeter tests
[ETN-91-99917] N91-31680
Behavior of nonlinear mechanical structures subjected to stationary excitations
[ECL-91-01] N91-31681
Small time step adaptive control: Theory and application to an electric furnace
[ECL-90-17] N91-31883

ECOLE NATIONALE SUPERIEURE DES MINES, VALBONNE (FRANCE).
Field 3, theme 1: Structural materials. Post 2: Thermotropic liquid crystal polymers
[ETN-91-99982] N91-31306
ECOLE POLYTECHNIQUE, PALAISEAU (FRANCE).
Development of an infrared Laser Fourier Densitometer (LFD) and first wind tunnel tests
[PMI-2335] N91-31189
ECOLE SUPERIEURE DE PHYSIQUE ET DE CHIMIE INDUSTRIELLES, PARIS (FRANCE).
Composite matrix deformation process in relation to molecular structure
[ETN-91-99915] N91-31232
EDGERTON, GERMESHAUSEN AND GRIER, INC., IDAHO FALLS, ID.
Production of organic chemicals via bioconversion: A review of the potential
[DE91-015524] N91-31223
EG AND G ENERGY MEASUREMENTS, INC., LAS VEGAS, NV.
Photophysics and chemistry of ultra-fast ZnO and CdS phosphors
[DE91-013106] N91-31966
ELORET CORP., PALO ALTO, CA.
Composite flexible blanket insulation
[NASA-CASE-NPO-11907-1-NP] N91-31236
ELTECH SYSTEMS, INC., FAIRPORT HARBOR, OH.
The development of aluminum-air batteries for application in electric vehicles
[DE91-016863] N91-31533
ENSCHEDE UNIV. (NETHERLANDS).
Network database in PROLOG N91-31866
ERLANGEN-NUREMBERG UNIV. (GERMANY, F.R.).
Floating zone growth of GaAs crystals (TEXUS 20) N91-31386
Directional solidification of eutectics InSb-NiSb (TEXUS 10) N91-31405
ESCUELA TECNICA SUPERIOR DE INGENIEROS AERONAUTICOS, MADRID (SPAIN).
Long liquid bridges aboard sounding rockets (TEXUS 12) ESA N91-31325
Freezing of a long liquid column (TEXUS 18) ESA N91-31326
ESSEN UNIV. (GERMANY, F.R.).
Thermocapillary drop motion, 1 (MASER 1) ESA N91-31345
Thermocapillary drop motion, 2 (MASER 2) ESA N91-31346
EUROPEAN SPACE AGENCY, PARIS (FRANCE).
Summary review of sounding rocket experiments in fluid science and material sciences: TEXUS 1 to 20; MASER 1 and 2
[ESA-SP-1132] N91-31321

F

FEDERAL AVIATION ADMINISTRATION, ATLANTIC CITY, NJ.
Solid-State Radar Beacon Decoder (SSRBD) Master Test Plan (MTP)
[DOT/FAA/CT-TN91/33] N91-31494
Aeronautical Mobile Satellite Service (AMSS) test plan
[DOT/FAA/CT-TN91/20] N91-31495
FLIGHT DIGITAL CO., LAS CRUCES, NM.
Development of a geographic navigational display device for general aviation aircraft
[PB91-170282] N91-31114
FLORIDA ATLANTIC UNIV., BOCA RATON.
Theoretical studies of metallic alloys
[DE91-016486] N91-31281
Mobility power flow analysis of coupled plate structure subjected to mechanical and acoustics excitation
[NASA-CR-188791] N91-31678
FLORIDA STATE UNIV., TALLAHASSEE.
Particle image velocimetry: Photographic and video techniques N91-31628
Unsteady flow past an airfoil pitching at a constant rate N91-31629
Vortex interactions in the transition region of a rectangular jet N91-31630
Absorbing CAD system geometries into GEANT
[DE91-015707] N91-31816
High energy physics program. Task A: Experiment and Theory. Task B: Numerical simulation of quantum field theories
[DE91-015652] N91-31938
FLUGPLATZ BUTZWEILERHOF, COLOGNE (GERMANY, F.R.).
Analysis of starting problems in cold weather with ASTAZOU type turbine engines in helicopters N91-31147
FOKKER B.V., SCHIPOL-OOST (NETHERLANDS).
Vulnerability of a small powerplant to wet snow conditions N91-31148
FORSCHUNGSINSTITUT FUER EDELMETALLE UND METALLCHEMIE, SCHWAEBISCH GMUEND (GERMANY, F.R.).
Electrolytic hydrogen formation (TEXUS 1) N91-31347
Electrolytically generated hydrogen bubbles (TEXUS 6) N91-31348
FORSCHUNGSZENTRUM JUELICH G.M.B.H. (GERMANY, F.R.).
Mechanical behavior of a nickel based alloy UDIMET 700 fabricated by powder metallurgy
[JUEL-2414] N91-31283
FRAUNHOFER-GESELLSCHAFT E.V., STUTTGART (GERMANY, F.R.).
Liquid motion in capillary tubes (TEXUS 3) N91-31322
Liquid motion in capillary tubes (TEXUS 5) N91-31323
Bubbles and foams (TEXUS 10) ESA N91-31324
FREIBURG UNIV. (GERMANY, F.R.).
Floating-zone growth of a silicon single crystal (TEXUS 7) N91-31384
Growth of a Si crystal covered with a SiO2 skin (TEXUS 12) N91-31385
Diffusion-controlled growth of protein single crystals: B-galactosidase (TEXUS 3) N91-31395
Diffusion-controlled growth of protein single crystals: Investigation of B-galactosidase at low temperature (TEXUS 4) N91-31396
Diffusion-controlled growth of single crystals of protein (TEXUS 5) N91-31397
FULMER RESEARCH INST. LTD., STOKE POGES (ENGLAND).
Immiscible alloy system Al-Pb (TEXUS 7) N91-31422

G

GENERAL ACCOUNTING OFFICE, WASHINGTON, DC.
Electronic warfare: Faulty test equipment impairs Navy readiness
[AD-A239562] N91-31506
Acquisition reform: Implementing defense management review initiatives. Report to the Chairman and Ranking Minority Member, Subcommittee on Defense Industry and Technology, Senate Committee on Armed Services
[AD-A239423] N91-31999
GENERAL ELECTRIC CO., FAIRFIELD, CT.
Fatigue-resistant nickel-base superalloys
[PATENT-1-253-363] N91-31268
Rapidly solidified nickel aluminide of improved stoichiometry and ductilization
[PATENT-1-257-987] N91-31270
Method for imparting strength to intermetallic phases
[PATENT-1-255-929] N91-31271
X-ray inspection system
[PATENT-1-258-924] N91-31660
GENERAL ELECTRIC CO., PEEBLES, OH.
Cold weather jet engine starting strategies made possible by engine digital control systems N91-31153
GENERAL ELECTRIC CO., SCHENECTADY, NY.
Development of elements of a high T(sub c) superconducting cable
[AD-A239766] N91-31543
GENERAL ELECTRIC CO., WEST LYNN, MA.
Ice ingestion experience on a small turboprop engine N91-31162
GENERAL MOTORS CORP., INDIANAPOLIS, IN.
Development of an anti-icing system for the T800-LHT-800 turboshaft engine N91-31160
GEOLOGICAL SURVEY, DENVER, CO.
GEOTRANS: An interface program from GEOPROGRAM to a geographic information system
[DE91-016111] N91-31998
GLASGOW UNIV. (SCOTLAND).
Gravitational wave research N91-31732
GOETTINGEN UNIV. (GERMANY, F.R.).
Diffusion of Ni in Cu-Au and Cu-Al alloys (TEXUS 20) N91-31373
GOVERNMENT-UNIV.-INDUSTRY RESEARCH ROUNDTABLE, WASHINGTON, DC.
Survey to assess the usefulness of two model agreements for university-industry cooperative research
[DE91-013937] N91-31985
What is the Federal Demonstration Project?
[DE91-013936] N91-31986
GRONINGEN RIJKSUNIV. (NETHERLANDS).
Three-dimensional Marangoni convection (MASER 1) ESA N91-31343
Three-dimensional Marangoni convection (MASER 2) ESA N91-31344
Artificial diffusion methods in convection dominated flows
[W-9016] N91-31577
Omission of symbols
[CS-9101] N91-31821
A simplification of Earley's algorithm
[CS-9102] N91-31822
LR-parsing derived
[CS-9105] N91-31823
A solution for the network database problem in an imperative language N91-31864
Bifurcations of parametrically forced oscillators
[W-9007] N91-31892
An extension of the potential method to higher-order blendings
[CS-9103] N91-31893
On a theorem of MacMahon
[CS-9104] N91-31894
Strong approximation on log dense sets
[W-9101] N91-31916
GRUMMAN AEROSPACE CORP., BETHPAGE, NY.
Passive ranging of an airborne emitter by a single non-maneuvering or stationary sensor
[PATENT-1-254-292] N91-31116
Torsion resistant grooved joint
[PATENT-1-258-589] N91-31127
System and method for automatically fabricating multiple memory holographic elements
[PATENT-1-253-724] N91-31600
Avioptic plug-in interconnection
[PATENT-1-254-415] N91-31946

H

HAMBURG UNIV. (GERMANY, F.R.).
Solidification of a hypereutectic alloy (TEXUS 1) N91-31399
HANS-SACHS-STR., GROEBENZELL (GERMANY, F.R.).
Cold start optimization on a military jet engine N91-31151
HARRY DIAMOND LABS., ADELPHI, MD.
Electron-beam-pinch experiment at Harry Diamond Laboratories: Providing for a high-dose-rate flash x ray facility for Transient Radiation Effects on Electronics (TREE) testing of pieceparts
[AD-A239558] N91-31193
HARVARD-SMITHSONIAN CENTER FOR ASTROPHYSICS, CAMBRIDGE, MA.
Retrieval and molecule sensitivity studies for the global ozone monitoring experiment and the scanning imaging absorption spectrometer for atmospheric chartography N91-31724
HARVARD UNIV., CAMBRIDGE, MA.
Research in regression, information retrieval, inversion of noisy transforms, and stochastic control
[AD-A239490] N91-32001
HOCHSCHULE DER BUNDESWEHR, HAMBURG (GERMANY, F.R.).
Pores in aluminium alloys (TEXUS 3) N91-31447
HOPITAL D'INSTRUCTION DES ARMEES, VERSAILLES (FRANCE).
Continuous 24 hour ECG study, on ground and in flight, of 19 Mirage 2000 pilots stationed at the Dijon airbase (France). Comparison with similar recordings taken on other types of fighter aircraft or in operationally different conditions
[ETN-91-99973] N91-31761
HULBURT (E. O.) CENTER FOR SPACE RESEARCH, WASHINGTON, DC.
GRO source candidates: (A) Nearby modest-size molecular clouds; (B) Pulsar with Wolf-Rayet companion that has lost its H-envelope
[NASA-CR-183491] N91-32021

I

ILLINOIS UNIV., CHICAGO.
Full-information item bi-factor analysis
[AD-A229346] N91-31771
ILLINOIS UNIV., URBANA-CHAMPAIGN.
Joint Services Electronics Program
[AD-A239459] N91-31536
INDIANA UNIV., BLOOMINGTON.
The relationship between the use of US government technical reports by US aerospace engineers and scientists and selected institutional and sociametric variables N91-31989
A spectrophotometric study of the secondaries of Algol systems N91-32005
INDUSTRIAL RESEARCH INST., INC., NEW YORK, NY.
Survey to assess the usefulness of two model agreements for university-industry cooperative research
[DE91-013937] N91-31985
INSTITUT DE MECANIQUE DE GRENOBLE (FRANCE).
Direct and large-eddy simulations of transition in the compressible boundary layer N91-31566
Spectral large-eddy simulation of isotropic and stably-stratified turbulences N91-31567

INSTITUT DE MECANIQUE DES FLUIDES DE LILLE (FRANCE).
Special design and gauging of anemoclinometric sondes
[IMFL-90/03] N91-31604

INSTITUT FRANCO-ALLEMAND DE RECHERCHES, SAINT-LOUIS (FRANCE).
Fundamentals of signal processing N91-31617
Signal processing: Time domain and frequency domain N91-31620
Review of typical applications. Part 1: Measurements in liquid flows, free jets, combustion, and in the atmosphere N91-31631
Post-processing of data N91-31633

INSTITUT NATIONAL DES SCIENCES APPLIQUEES, LYON (FRANCE).
Development and characterization of low temperature Cu-Al-Be shape memory alloys
[ISAL-90-0093] N91-31284

INSTITUT NATIONAL DES SCIENCES APPLIQUEES, ROUTEN (FRANCE).
Turbulence modeling for compressible flows and implementation in Navier-Stokes solvers N91-31564
Quasi-elastic light scattering and applications to optical sizing N91-31627

INSTITUT NATIONAL POLYTECHNIQUE, TOULOUSE (FRANCE).
Stress corrosion cracking of 2091 ad 8090 aluminum-lithium alloys in chloride containing aqueous solutions. Influence of sulphate and nitrate additions
[REPT-431/91] N91-31285

INSTITUTE FOR COMPUTER APPLICATIONS IN SCIENCE AND ENGINEERING, HAMPTON, VA.
Control of oscillatory forces on a circular cylinder by rotation
[NASA-CR-187619] N91-31576
A dynamically adaptive multigrid algorithm for the incompressible Navier-Stokes equations: Validation and model problems
[NASA-CR-187595] N91-31888
A comparison of time domain boundary conditions for acoustic waves in wave guides
[NASA-CR-187618] N91-31889

INSTITUTE FOR DEFENSE ANALYSES, ALEXANDRIA, VA.
Report on the Software Technology for Adaptable, Reliable Systems (STARS) Conference on Frameworks Convergence
[AD-A239691] N91-31862

INTERNATIONAL CENTRE FOR THEORETICAL PHYSICS, TRIESTE (ITALY).
Stress relaxation in bending of type AISI 304 stainless steel at 773K and 823K
[DE91-618657] N91-31666

INTERNATIONAL FLAME RESEARCH FOUNDATION, IJMUIDEN (NETHERLANDS).
Adjustment of the mixing-rate constant in the eddy break-up model for a jet flame N91-32030

INTERNATIONAL METEOROLOGICAL INST., STOCKHOLM (SWEDEN).
Initialization of the HIRLAM model using a digital filter
[DM-57] N91-31747

INTERNATIONAL SUPERCONDUCTIVITY TECHNOLOGY CENTER, TOKYO (JAPAN).
Steerable windowed enclosures
[PATENT-1-262-653] N91-31142

J

JET PROPULSION LAB., CALIFORNIA INST. OF TECH., PASADENA.
Composite flexible blanket insulation
[NASA-CASE-NPO-11907-1-NP] N91-31236
A universal computer control system for motors
[NASA-CASE-NPO-17134-1-CU] N91-31528
The conversion of lignocellulosics to fermentable sugars: A survey of current research and application to CELSS N91-31784
Asymmetric soft-error resistant memory
[NASA-CASE-NPO-17394-1-CU] N91-31810
Synchronized computational architecture for generalized bilateral control of robot arms
[NASA-CASE-NPO-17401-1-CU] N91-31885

JUSTUS LIEBIG-UNIV., GIESSEN (GERMANY, F.R.).
Oscillatory Marangoni convection (TEXUS 3A and 3B) N91-31333
Critical Marangoni number (TEXUS 5) N91-31334
Critical Marangoni number (TEXUS 8) N91-31335

K

KAISER ALUMINUM AND CHEMICAL CORP., OAKLAND, CA.
Composite ingot casting
[PATENT-1-250-128] N91-31269

KANSAS UNIV., LAWRENCE.
Fighter agility metrics N91-31128

KANSAS UNIV. CENTER FOR RESEARCH, INC., LAWRENCE.
A numerical procedure for recovering true scattering coefficients from measurements with wide-beam antennas
[NASA-CR-186042] N91-31492
A satellite-based radar wind sensor
[NASA-CR-188805] N91-31750

KARLSRUHE UNIV. (GERMANY, F.R.).
Examples of turbulence model applications N91-31563

KATHOLIEKE UNIV. TE LEUVEN (BELGIUM).
Metallic composites with particles (TEXUS 6) N91-31436
Metallic composites with particles (TEXUS 7) N91-31437
Melting and solidification of metallic composites (TEXUS 9) N91-31438
Metal matrix composites (TEXUS 14b) N91-31439
Metal matrix composites (TEXUS 20) N91-31440

KENT STATE UNIV., OH.
Nucleus-nucleus collisions and the nuclear equation of state
[DE91-016747] N91-31937

KENT UNIV., CANTERBURY (ENGLAND).
A new model of the electron: A suggested experiment to search for a link between electromagnetism and gravity N91-31738

KEURING VAN ELECTROTECHNISCHE MATERIALEN N.V., ARNHEM (NETHERLANDS).
KEMA scientific and technical reports, volume 8, number 2, 1990
[ST-REPT-VOL-8-NO-2] N91-32023
Experiments on ultrasonic thermometry for wet-ash coal gasification N91-32024
The critical temperature for drying-out of soils around power cables as a function of local conditions N91-32025
The selective catalytic oxidation of ammonia to N2 and H2O over silica-supported molybdena catalysts N91-32026
A system to determine whole-plant exchange rates of ozone, carbon dioxide and water vapour N91-32027
Some applications of X-ray photoelectron spectroscopy and secondary-ion mass spectroscopy N91-32029

KHD LUFTFAHRTTECHNIK G.M.B.H., OBERURSEL (GERMANY, F.R.).
Cold start investigation of an APU with annular combustor and fuel vaporizers N91-31154

KIEL UNIV. (GERMANY, F.R.).
Intermittent polarization (TEXUS 2) N91-31349

KRUPP (FRIED.) G.M.B.H., ESSEN (GERMANY, F.R.).
Fundamental studies in the manganese-bismuth system (TEXUS 2) N91-31414
Alloys with oxide inclusions (TEXUS 2) N91-31432
The behaviour of alumina-copper suspensions (TEXUS 3A and 3B) N91-31433
Copper-alumina suspensions (TEXUS 5) N91-31434
Copper-molybdenum suspension (TEXUS 9) N91-31435
Liquid phase sintering (TEXUS 19) ESA N91-31446
Manufacture of steel foam (TEXUS 4) N91-31448
Manufacture of steel foam (TEXUS 6) N91-31449
Manufacture of iron foam (TEXUS 7) N91-31450
Gas bubbles in a copper-alumina suspension (TEXUS 11) N91-31453
Bubble formation, growth, and expansion during the liquid phase sintering of a WC-Co sample N91-31454

L

LABORATOIRE D'AUTOMATIQUE ET D'ANALYSE DES SYSTEMES, TOULOUSE (FRANCE).
On the stability of saturated state feedback regulators
[LAAS-91047] N91-31524
Intrusion and fault tolerance compatibility. Part 1: Fault protection, coding and tolerance state of the art
[LAAS-89-395] N91-31662
Path planning for non-holonomic mobile robots
[LAAS-91135] N91-31882

LABORATOIRE D'INFORMATIQUE POUR LA MECANIQUE ET LES SCIENCES DE L'INGENIEUR, PARIS (FRANCE).
Numerical simulation of three dimensional unsteady flow by multiprocessor solving of the Navier-Stokes equations
[ETN-91-99974] N91-31594

LASER SCIENCE, INC., AMES, IA.
Laser deposition of cubic boron nitride on electronic materials
[AD-A238313] N91-31249

LAWRENCE LIVERMORE NATIONAL LAB., CA.
Experimental determination of the temperature and density of opacity samples
[DE91-015686] N91-31252
Creep deformation and fracture of a two-phase TiAl intermetallics
[DE91-011963] N91-31274
Dynamic yield strength of a palladium alloy metallic glass
[DE91-015111] N91-31298
The autoignition chemistry of paraffinic fuels and pro-knock and anti-knock additives: A detailed chemical kinetic study
[DE91-014992] N91-31314
Performance evaluation of insensitive explosives
[DE91-015767] N91-31315
Understanding composite explosive energetics
[DE91-015770] N91-31316
International magnetic pulse compression
[DE91-015774] N91-31520
Proceedings of the International Magnetic Pulse Compression Workshop. Volume 2: Technical summary
[DE91-015775] N91-31521
Photography of shock waves in explosive crystals
[DE91-015772] N91-31572
Laser ablation mechanisms and optical surface damage
[DE91-016928] N91-31642
Technical abstracts: Mechanical engineering, 1990
[DE91-016502] N91-31658
DYNA3D: A nonlinear, explicit, three-dimensional finite element code for solid and structural mechanics
[DE91-015735] N91-31675
The status of lightweight photovoltaic space array technology based on amorphous silicon solar cells
[DE91-014985] N91-31698
Temporal sampling considerations in global climate modeling
[DE91-015695] N91-31717
Time scales of variability associated with Nordeste precipitation
[DE91-015696] N91-31718
Global model simulations of the long range transport of soot and sulfur from the Kuwait oil fires
[DE91-015771] N91-31719
The use of distributional and pointwise statistical measures in GCM intercomparisons
[DE91-015697] N91-31748
Impact of the ice phase on a mesoscale convective system: Cloud ensemble features and cloud radiative properties
[DE91-015769] N91-31749
Biological dosimetry and mechanisms of carcinogenesis
[DE91-015689] N91-31763
A scientific visualization synthesizer
[DE91-012877] N91-31815
Energy and Technology Review, February-March 1991
[DE91-015487] N91-32031

LEIDEN UNIV. (NETHERLANDS).
On the relation between recurrence and ergodicity properties in denumerable Markov decision chains
[TW-91-02] N91-31918

LEIGH INSTRUMENTS LTD., OTTAWA (ONTARIO).
Beacon activation device
[PATENT-1-256-916] N91-31108

LILLE UNIV. (FRANCE).
Plastic deformation processes in relation to molecular structure
[ETN-91-99916] N91-31233

LITTON SYSTEMS, INC., BEVERLY HILLS, CA.
Enhanced global positioning system delta-range processing
[PATENT-1-254-637] N91-31115

LOCKHEED ENGINEERING AND SCIENCES CO., HAMPTON, VA.
User's manual for the Langley boundary layer noise propagation program (MRS-BLP)
[NASA-CR-187559] N91-31923

LOCKHEED ENGINEERING AND SCIENCES CO., HOUSTON, TX.
Development of the CELSS emulator at NASA. Johnson Space Center N91-31793

LOS ALAMOS NATIONAL LAB., NM.
An investigation of dual-mode operation of a nuclear-thermal rocket engine
[DE91-015977] N91-31210
A review of the Los Alamos effort in the development of nuclear rocket propulsion
[DE91-016036] N91-31211
Water transport properties of fuel cell ionomers
[DE91-016015] N91-31259

Dynamic strength and strain rate effects on fracture behavior of tungsten and tungsten alloys
[DE91-013029] N91-31275
Influence of loading rate on the mechanical response and substructure evolution of shock-loaded copper
[DE91-013390] N91-31276
Model description of transition metals using the rotated second moment approximation
[DE91-016043] N91-31287
Finite element modeling of orthogonal machining using an elastic-viscoplastic material model
[DE91-016815] N91-31477
Abstracts of papers presented at the First Los Alamos Symposium on Ultra-Wideband Radar
[DE91-015976] N91-31491
High-speed TV cameras for streak tube readout
[DE91-016081] N91-31602
Circular format zig-zag scanning of vidicon tubes
[DE91-016084] N91-31610
Comparison of integrated numerical experiments with accelerator and FEL experiments
[DE91-016071] N91-31639
Compact free-electron laser at the Los Alamos National Laboratory
[DE91-016079] N91-31640
Anelastic release from the shock-compressed state
[DE91-009961] N91-31672
Pressure-strain-temperature relationship in shock loaded cylindrical samples of 304 stainless steel
[DE91-013379] N91-31673
A Weibull brittle material failure model for the ABAQUS computer program
[DE91-016813] N91-31690
Small satellite radiometric measurements
[DE91-016308] N91-31694
Pseudohomogeneous catalyst layer model for polymer electrolyte fuel cell
[DE91-016014] N91-31710
Electrochemical energy storage using PEM systems
[DE91-016020] N91-31711
Developing dataflow algorithms
[DE91-016300] N91-31818
Local area gigabit networking
[DE91-014780] N91-31869
An application of neural networks to process and materials control
[DE91-016016] N91-31886
Comparison of noise reduction systems
[DE91-015318] N91-31929
Optically pumped polarized ion sources
[DE91-016086] N91-31932
Intrinsic neutron source strengths in uranium solutions
[DE91-016091] N91-31933
Progress in the SP-100 FSQ reactor development
[DE91-016033] N91-31940
Carbide fuels for nuclear thermal propulsion
[DE91-016032] N91-31945
Computational model for deterministic chaos in a magnetically confined plasma
[DE91-016022] N91-31955
An interparticle collision model for electromagnetic hybrid simulations of high density plasmas
[DE91-016025] N91-31958
Weak links within a Bi2Sr2Ca1Cu2O(x) single crystal by magnetization and direct optical observations
[DE91-016085] N91-31979

LOUGHBOROUGH UNIV. OF TECHNOLOGY (ENGLAND).
Airborne ESM receivers: Techniques and technologies
[ETN-91-99988] N91-31498

M

MANCHESTER UNIV. (ENGLAND).
Introduction to the Modeling of Turbulence: Introduction N91-31552
Two-equation models for high-Reynolds-number flow N91-31553
Two-equation models for low-Reynolds number flow N91-31554
An introduction to second moment closure N91-31555
Inclusion of second-moment closures into finite-volume solvers N91-31556
Numerical implementation and performance of Reynolds stress closures in finite-volume computations of recirculating and strongly swirling flows N91-31557
Body force effects on turbulence N91-31558
Application of second-moment closure in complex flows N91-31559
A new form of second-moment closure N91-31560
An introduction to single-point closure methodology N91-31561
Developments in medical audit in hospitals in the National Health Service
[ETN-91-99984] N91-31762
A study of the logistics function within a medium sized, sales oriented chemical company
[ETN-91-99983] N91-31987

MARYLAND UNIV., COLLEGE PARK.
Analysis and development of a wide-bandwidth gravitational wave detector N91-31601
Reliability of computational analysis of plasticity problems
[AD-A239646] N91-31691
Locking effects in the finite element approximation of elasticity problems
[AD-A239645] N91-31914
Analysis of the efficiency of an a-posteriori error estimator for linear triangular finite elements
[AD-A239647] N91-31915
A study of a 21-cm-selected sample of galaxies N91-32014

MASCHINENFABRIK AUGSBURG-NUERNBERG A.G., MUNICH (GERMANY, F.R.).
Dispersion alloys (TEXUS 19) N91-31442
Skin technology (TEXUS 1) N91-31455
Skin technology (TEXUS 2) N91-31456
Skin technology (TEXUS 3) N91-31457
Skin technology (TEXUS 4) N91-31458
Skin technology (TEXUS 9) N91-31459
Skin technology (TEXUS 11 and 12) N91-31460

MASSACHUSETTS INST. OF TECH., CAMBRIDGE.
Origins of GPS surveying
[AD-A239676] N91-31121
Strategies for biopolymer engineering of PHB-like materials
[AD-A239690] N91-31313
Time domain electromagnetic waves in multilayered media
[AD-A239545] N91-31504
Distortion-free x ray mask technology
[AD-A239770] N91-31665
Interfacial systems for photochemical energy conversion
[DE91-015743] N91-31700
A fast multiport memory based on single-port memory cells
[AD-A239455] N91-31811

MASSACHUSETTS INST. OF TECH., LEXINGTON.
An adaptive coherent optical receiver array
[AD-A239672] N91-31644
Artificial neural networks for seismic data interpretation
[AD-A239673] N91-31743
Parametric study of diffusion-enhancement networks for spatiotemporal grouping in real-time artificial vision
[AD-A239674] N91-31954

MASSACHUSETTS UNIV., AMHERST.
Investigation of two-dimensional cracks at an angle to an interface N91-31667
Inference networks for document retrieval N91-31993

MATERIALS RESEARCH LABS., ASCOT VALE (AUSTRALIA).
Tropical tests of a seawater marker
[MRL-TR-90-19] N91-31109

MAX-PLANCK-INST. FUER CHEMIE, MAINZ (GERMANY, F.R.).
Scanning imaging absorption spectrometer for atmospheric chartography N91-31725

MAX-PLANCK-INST. FUER PHYSIK UND ASTROPHYSIK, GARCHING (GERMANY, F.R.).
Plasma diffusion at the magnetopause? The case of lower hybrid drift waves
[NASA-CR-188913] N91-31957
Activities report of the Institute of Extraterrestrial Physics
[MPE-223] N91-32002
A survey of the 158 micron CII fine-structure line in the central 50 pc of the galaxy
[NASA-CR-188912] N91-32009
Evolutionary population synthesis in starburst regions
[MPE-PREPRINT-198] N91-32017

MAX-PLANCK-INST. FUER STROEMUNGSFORSCHUNG, GOETTINGEN (GERMANY, F.R.).
The effect of jet bleed on base pressure distribution, shedding frequency, and mean velocity profiles in the wake behind a two-dimensional blunt model
[MPIS-12/1990] N91-31085
Examination of molecular evaporation, cooling, and cluster dissociation of very thin liquid jets in a high vacuum
[MPIS-12/1990] N91-31581
Laser Doppler velocimeter measurements of the streamwise velocity component in the viscous sublayer of a turbulent channel flow
[MPIS-MITT-97] N91-31582

MCDONNELL-DOUGLAS SPACE SYSTEMS CO., HOUSTON, TX.
On the optimal use of fictitious time in variation of parameters methods with application to BG14
[NASA-CR-185650] N91-31890

MCDONNELL-DOUGLAS SPACE SYSTEMS CO., HUNTSVILLE, AL.
Advanced optical sensing and processing technologies for the distributed control of large flexible spacecraft
[NASA-CR-4399] N91-31609

MESSERSCHMITT-BOELKOW-BLOHM G.M.B.H., MUNICH (GERMANY, F.R.).
A shock-fitting algorithm for the simulation of inviscid flows in chemical non-equilibrium
[MBB-UK-0131-90-PUB] N91-31087
Viscous effects
[MBB-FE202/S/PUB/441] N91-31088
Noxious matter minimization as a project criterion for aircraft
[MBB-Z-0337-90-PUB] N91-31134
Enhanced fighter maneuverability aircraft (X-31A) wing and thrust vectoring vane design
[MBB-FE22/S/PUB/0433/A] N91-31135
Simulation of distance-dependent functions in visual systems for training simulators using the z-buffer technique
[MBB-UA-1190-90-PUB] N91-31186
Adhesion of thick layer systems on ceramic based precious metals in hybrid microelectronic circuits
[MBB-UA-1191-90-PUB] N91-31304
Stereophotogrammetric surveying and interpreting method, and interpreting apparatus
[PATENT-1-254-651] N91-31693
Development of single blade rotor wind energy converters: From M400 prototype to MON 50 preseries
[MBB-UE-0015-90-PUB] N91-31705
Micromechanical concepts in optics and optoelectronics
[MBB-Z-0339-90-PUB] N91-31949

MESSERSCHMITT-BOELKOW-BLOHM G.M.B.H., OTTOBRUNN (GERMANY, F.R.).
Aerothermodynamical project of hypersonic projectiles
[MBB-UA-1193-90-PUB] N91-31086
Possibilities of simulation and optimization for guided missile systems
[MBB-UA-1201-90-PUB] N91-31183
The SAENGER concept and the German hypersonic technology program
[MBB-UK-0132-91-PUB] N91-31198
The physical properties of a pyrotechnical circuit element
[MBB-UA-1192-90-PUB] N91-31317
The microcrystal laser: A first step on the way to a laser microsystem
[MBB-Z-0336-90-PUB] N91-31635
Fuel cells for commercial energy
[MBB-UE-0018-90-PUB] N91-31706
Construction and realization of distributed multiprocessor systems for real time tasks
[MBB-UA-1189-90-PUB] N91-31871

METALLGESELLSCHAFT, A.G., FRANKFURT AM MAIN (GERMANY, F.R.).
Demixing of a monotectic ternary alloy (TEXUS 20) N91-31429

METRAVIB, LYON (FRANCE).
Vaudreuil (France) large hydrodynamic tunnel: Acoustic chamber damping
[METRAVIB-RDS-1-007-67] N91-31090

MICHIGAN TECHNOLOGICAL UNIV., HOUGHTON.
Ceramic composition
[PATENT-1-249-609] N91-31294

MINERALS MANAGEMENT SERVICE, CAMARILLO, CA.
A summary of the physical oceanography of the Pacific Northwest Coast
[PB91-164434] N91-31753

MINISTRY OF DEFENCE, LONDON (ENGLAND).
Fuels and oils as factors in the operation of aero gas turbine engines at low temperatures N91-31163

MINNESOTA UNIV., MINNEAPOLIS.
A parametric study of transonic blade-vortex interaction noise
[NASA-CR-188811] N91-31928

MISSISSIPPI STATE UNIV., MISSISSIPPI STATE.
Enhancement of surface definition and gridding in the Eagle code
[NASA-CR-188796] N91-31820

MISSOURI UNIV., COLUMBIA.
Simulated effects of a doubling of carbon dioxide on corn production in portions of the central US
[DE91-016843] N91-31722

MONTPELLIER-2 UNIV. (FRANCE)
Advanced research workshop on Wide Gap II-VI Semiconductors
[AD-A233796] N91-31960

N

NAPLES UNIV. (ITALY).
Thermal Marangoni convection in a floating zone (TEXUS 9) ESA N91-31341
Experimental results on microgravitational fluid dynamics (TEXUS 14b) ESA N91-31342

NATIONAAL INST. VOOR KERNFYSICA EN HOGE ENERGIEFYSICA, AMSTERDAM (NETHERLANDS).
The timing of injection kickers
[NIKHEF-K/AMPS/91-04] N91-31943

NATIONAL AERONAUTICAL ESTABLISHMENT, OTTAWA (ONTARIO).
Photoelastic coating study of redesigned CT114 coupon joint test specimen for horizontal stabilizer rear attachment fitting to vertical stabilizer rear spar
[NAE-LTR-ST-1701] N91-31125

NATIONAL AERONAUTICS AND SPACE ADMINISTRATION, WASHINGTON, DC.
NASA Aerodynamics Program
[NASA-TM-4312] N91-31751
Aerospace medicine and biology: A continuing bibliography with indexes (supplement 353)
[NASA-SP-7011(353)] N91-31760
Transpiration during life cycle in controlled wheat growth N91-31795

NATIONAL AERONAUTICS AND SPACE ADMINISTRATION. AMES RESEARCH CENTER, MOFFETT FIELD, CA.
Vibration analysis of the SA349/2 helicopter
[NASA-TM-102794] N91-31078
Airborne rescue system
[NASA-CASE-ARC-11909-1] N91-31113
Etching method for photoresists or polymers
[NASA-CASE-ARC-11873-2] N91-31258
Controlled Ecological Life Support Systems: CELSS '89 Workshop
[NASA-TM-102277] N91-31775
Environmental modification of yield and food composition of cowpea and leaf lettuce N91-31777
The crop growth research chamber: A ground-based facility for CELSS research N91-31792

NATIONAL AERONAUTICS AND SPACE ADMINISTRATION. GODDARD SPACE FLIGHT CENTER, GREENBELT, MD.
Emergency locating transmitter
[NASA-CASE-GSC-12821-2] N91-31530
Robotic tool change mechanism
[NASA-CASE-GSC-13239-1] N91-31656
ULDA user's guide
[NASA-TM-105074] N91-31813
An atlas of stellar spectra between 2.00 and 2.45 micrometers (Arnaud, Gilmore, and Collier Cameron 1989)
[NASA-TM-105044] N91-32003
The Li-7 and Be-7 deexcitation lines: Probes for accelerated particle transport models in solar flares
[NASA-CR-183490] N91-32020

NATIONAL AERONAUTICS AND SPACE ADMINISTRATION. HUGH L. DRYDEN FLIGHT RESEARCH FACILITY, EDWARDS, CA.
A knowledge based application of the extended aircraft interrogation and display system
[NASA-TM-4327] N91-31874

NATIONAL AERONAUTICS AND SPACE ADMINISTRATION. JOHN F. KENNEDY SPACE CENTER, COCOA BEACH, FL.
Effects of atmospheric CO2 on photosynthetic characteristics of soybean leaves N91-31780
Effects of elevated atmospheric carbon dioxide concentrations on water and acid requirements of soybeans grown in a recirculating hydroponic system N91-31781
Controlled ecological life support system breadboard project, 1988 N91-31791
Factors affecting plant growth in membrane nutrient delivery N91-31797

NATIONAL AERONAUTICS AND SPACE ADMINISTRATION. LYNDON B. JOHNSON SPACE CENTER, HOUSTON, TX.
Power saw
[NASA-CASE-MSC-21469-1] N91-31655
Biofilm monitoring coupon system and method of use
[NASA-CASE-MSC-21585-1] N91-31755
Development of the CELSS emulator at NASA. Johnson Space Center N91-31793
Conceptual design of a closed loop nutrient solution delivery system for CELSS implementation in a micro-gravity environment N91-31798
Solid-support substrates for plant growth at a lunar base N91-31800
Method and apparatus for bio-regenerative life support system
[NASA-CASE-MSC-21629-1] N91-31803

NATIONAL AERONAUTICS AND SPACE ADMINISTRATION. LANGLEY RESEARCH CENTER, HAMPTON, VA.
User's guide to a system of finite-element supersonic panel flutter programs
[NASA-TM-104109] N91-31082
Airplane takeoff and landing performance monitoring system
[NASA-CASE-LAR-13854-1-CU] N91-31120
Two alternative ways for solving the coordination problem in multilevel optimization
[NASA-TM-104036] N91-31138
A technique for locating function roots and for satisfying equality constraints in optimization
[NASA-TM-104037] N91-31139
Rotatable non-circular forebody flow controller
[NASA-CASE-LAR-14212-1-CU] N91-31140
Flight tests with a data link used for air traffic control information exchange
[NASA-TP-3135] N91-31143
Automatic satellite tracking system for the NASA Satellite Photometric Observatory
[NASA-TM-105037] N91-31194
Restructured Freedom configuration characteristics
[NASA-TM-104057] N91-31201
Ethynyl terminated imidothioethers and resins therefrom
[NASA-CASE-LAR-13910-2-CU] N91-31307
Apparatus and method for explosive bonding to edge of flyer plate
[NASA-CASE-LAR-14096-1] N91-31476
A case study for the real-time experimental evaluation of the VIPER microprocessor
[NASA-TM-104098] N91-31531
A relative-intensity two-color phosphor thermography system
[NASA-TM-104123] N91-31595
Method and apparatus for detecting laminar flow separation and reattachment
[NASA-CASE-LAR-13952-2-SB] N91-31596
Generation of particles and seeding N91-31618
Biasing errors and corrections N91-31621
Review of typical applications: Wind tunnels N91-31632
Analysis of thermomechanical fatigue of unidirectional titanium metal matrix composites
[NASA-TM-104105] N91-31677
Improved finite-element methods for rotorcraft structures
[NASA-TM-104104] N91-31687
Tunable far infrared studies of molecular parameters in support of stratospheric measurements
[NASA-CR-188774] N91-31723
Kinematics of the six-degree-of-freedom force-reflecting Kraft Master
[NASA-TM-104124] N91-31879
Single layer multi-color luminescent display
[NASA-CASE-LAR-13616-1] N91-31950

NATIONAL AERONAUTICS AND SPACE ADMINISTRATION. LEWIS RESEARCH CENTER, CLEVELAND, OH.
Experimental investigation of turbulent flow through a circular-to-rectangular transition duct
[NASA-TM-105210] N91-31106
A high-frequency servosystem for fuel control in hypersonic engines
[NASA-TM-104333] N91-31178
Jet-A reaction mechanism study for combustion application
[NASA-TM-104441] N91-31181
The International Space University's variable gravity research facility design
[NASA-TM-105224] N91-31196
Nonlinear combustion instability model in two- to three-dimensions
[NASA-TM-102381] N91-31208
Mass comparisons of electric propulsion systems for NSSK of geosynchronous spacecraft
[NASA-TM-105153] N91-31212
Medium power hydrogen arcjet performance
[NASA-TM-104533] N91-31216
Advanced power systems for EOS
[NASA-TM-105222] N91-31217
Thin film, concentrator and multijunction space solar cells: Status and potential
[NASA-TM-104505] N91-31218
Eccentricity effects on leakage of a brush seal at low speeds
[NASA-TM-105141] N91-31220
Experimental and analytical analysis of stress-strain behavior in a (90/0 deg)2s, SiC/Ti-15-3 laminate
[NASA-TM-104470] N91-31235
Technical prospects for utilizing extraterrestrial propellants for space exploration
[NASA-TM-105263] N91-31318
Low cost, formable, high T(sub c) superconducting wire
[NASA-CASE-LEW-14676-1] N91-31529
A critical comparison of two-equation turbulence models
[NASA-TM-105237] N91-31597
Laser interferometric measurement of ion electrode shape and charge exchange erosion
[NASA-TM-105165] N91-31605
Plug-type heat flux gauge
[NASA-CASE-LEW-14967-1] N91-31608
Spur-gear optimization using SPUROPT computer program
[NASA-TM-104394] N91-31648
Recent manufacturing advances for spiral bevel gears
[NASA-TM-104479] N91-31654
Nickel-hydrogen cell low-Earth life test update
[NASA-TM-105229] N91-31708
Tuning maps for setpoint changes and load disturbance upsets in a three capacity process under multivariable control
[NASA-TM-104419] N91-31876
Least-squares solution of incompressible Navier-Stokes equations with the p-version of finite elements
[NASA-TM-105203] N91-31911
Crystallization and characterization of Y2O3-SiO2 glasses N91-31962
Near-edge study of gold-substituted YBa2Cu3O(7-delta)
[NASA-TM-105220] N91-31977

NATIONAL AERONAUTICS AND SPACE ADMINISTRATION. MARSHALL SPACE FLIGHT CENTER, HUNTSVILLE, AL.
Multiplexing readout channels in proportional counters
[NASA-TM-103552] N91-31606
Development of the Burst and Transient Source Experiment (BATSE)
[NASA-RP-1268] N91-32006

NATIONAL AERONAUTICS AND SPACE ADMINISTRATION. PASADENA OFFICE, CA.
Composite flexible blanket insulation
[NASA-CASE-NPO-11907-1-NP] N91-31236
A universal computer control system for motors
[NASA-CASE-NPO-17134-1-CU] N91-31528
Asymmetric soft-error resistant memory
[NASA-CASE-NPO-17394-1-CU] N91-31810
Synchronized computational architecture for generalized bilateral control of robot arms
[NASA-CASE-NPO-17401-1-CU] N91-31885

NATIONAL AEROSPACE LAB., AMSTERDAM (NETHERLANDS).
Development and validation of characteristic boundary conditions for cell-centered Euler flow calculations with a shock-free airfoil
[NLR-TP-89360-U] N91-31081
A European collaborative investigation of the three-dimensional turbulent shear layers of a swept wing
[NLR-MP-88054-U] N91-31084
Bayesian multi-sensor tracking for advanced air-traffic control systems
[NLR-MP-88056-U] N91-31119
Design and testing of a multiblock grid-generation procedure for aircraft design and research
[NLR-TP-89146-U] N91-31131
Activities report of the National Aerospace Laboratory
[ETN-91-99438] N91-31132
Flight testing in the Netherlands: An overview
[NLR-MP-88053-U] N91-31133
Corrosion fatigue crack arrest in aluminium alloys
[NLR-MP-88050-U] N91-31282
Development of a sensor for high-quality two-phase flow
[NLR-MP-88059-U] N91-31578
Development of an advanced panel method for complex configurations in subsonic compressible flow; application to the computation of the potential flow through ducts
[NLR-TR-88001-U] N91-31579
Investigation into the applicability of knowledge engineering
[NLR-TP-89031-U] N91-31878

NATIONAL DEFENCE RESEARCH ESTABLISHMENT, STOCKHOLM (SWEDEN).
Tungsten composites (TEXUS 10) N91-31444
Tungsten composites (TEXUS 19) ESA N91-31445

NATIONAL INST. OF STANDARDS AND TECHNOLOGY, GAITHERSBURG, MD.
The influence of moisture and pressure on the mechanical properties of a glass-epoxy matrix composite and a graphite-epoxy matrix composite
[AD-A239509] N91-31242

NATIONAL RESEARCH INST. FOR METALS, IBARAKI (JAPAN).
Solidification of an Al-Pb-Bi alloy under microgravity (TEXUS 13) N91-31427

NATIONAL TRANSPORTATION SAFETY BOARD, WASHINGTON, DC.
Annual review of aircraft accident data. US air carrier operations, calendar year 1988
[PB91-176040] N91-31110
NATIONAL WEATHER SERVICE, FORT WORTH, TX.
Estimating the strength of the capping inversion and the probability of strong convection
[PB91-176685] N91-31744
A quantitative analysis of quasi-geostrophic forcing during recent severe weather outbreaks across the southern Great Plains
[PB91-176693] N91-31745
NAVAL AIR DEVELOPMENT CENTER, WARMINSTER, PA.
Effect of wind over deck conditions on aircraft approach speeds for carrier landings
[AD-A239511] N91-31141
The G-LOC syndrome
[AD-A239561] N91-31768
Adaptive function allocation for intelligent cockpits
[AD-A239714] N91-31808
Aircrew critique of high-G centrifuge training. Part 1: What was the best part of the program?
[AD-A239781] N91-31809
NAVAL AIR PROPULSION TEST CENTER, TRENTON, NJ.
The development of a computational model to predict low temperature fuel flow phenomena N91-31166
Environmental icing testing at the Naval Air Propulsion Center N91-31167
NAVAL HEALTH RESEARCH CENTER, SAN DIEGO, CA.
Sleep logs: Measurement of individual and operational efficiency
[AD-A239774] N91-31770
NAVAL MEDICAL RESEARCH AND DEVELOPMENT COMMAND, BETHESDA, MD.
Naval medical research and development command
[AD-A239393] N91-31765
NAVAL MEDICAL RESEARCH INST., BETHESDA, MD.
Basic operation and preliminary trials of a detector for stationary gas bubbles
[AD-A239710] N91-31769
NAVAL OCEAN SYSTEMS CENTER, SAN DIEGO, CA.
Arctic VLF/LF data acquisition
[AD-A239704] N91-31510
NAVAL OCEANOGRAPHIC OFFICE, BAY SAINT LOUIS, MS.
North Pacific guyots
[AD-A239388] N91-31754
NAVAL POSTGRADUATE SCHOOL, MONTEREY, CA.
An integer programming model for Navy's maritime patrol aviation fleet
[AD-A239464] N91-31079
Touch screen use on flight simulator instructor/operator stations
[AD-A239524] N91-31192
A methodology for producing and testing a genesil silicon compiler designed VLSI chip which incorporates design for testability
[AD-A239465] N91-31537
Application of the constrained implicants set concept to the minimization of binary functions
[AD-A239470] N91-31859
Exploiting captions for access to multimedia databases
[AD-A239435] N91-32000
NAVAL RESEARCH LAB., WASHINGTON, DC.
Modelling the response of thick composite materials due to axisymmetric shock loading
[AD-A239531] N91-31243
Chemical reduction of intermodulation interference caused by metal-oxide-metal junctions aboard ship
[AD-A239530] N91-31265
Theory and application of the wavelet transform to signal processing
[AD-A239533] N91-31501
Integration losses and clutter-Doppler spread for a space based radar caused by ionospheric scintillation during a solar maximum
[AD-A239534] N91-31502
Performance of an angle-of-arrival estimator in the presence of a mainbeam interference source
[AD-A239629] N91-31508
Convergence performance of adaptive detectors, part 1
[AD-A239507] N91-31539
Convergence performance of adaptive detectors, part 2
[AD-A239532] N91-31540
Hydrodynamic target response to an induced spatial incoherence-smoothed laser beam
[DE91-015757] N91-31638
Exact result for the grazing angle of specular reflection from a sphere
[AD-A239578] N91-31952
Advanced concepts theory
[AD-A239780] N91-31959
NAVAL SUBMARINE MEDICAL RESEARCH LAB., GROTON, CT.
The medical hazards of flame-suppressant atmospheres
[AD-A239618] N91-31806
NEW HAMPSHIRE UNIV., DURHAM.
The analysis and design of brushless DC motors N91-31516
A study of ion acceleration at rocket altitudes and development and calibration of pitch angle imaging charged particle detectors N91-31728
NEW MEXICO STATE UNIV., LAS CRUCES.
Preliminary evaluation of waste processing in a CELSS N91-31788
NEWCASTLE-UPON-TYNE UNIV. (ENGLAND).
Fifth force experiments N91-31733
NIJMEGEN UNIV. (NETHERLANDS).
The ABC-machine: A sequential stack-based abstract machine for graph rewriting
[TR-90-22] N91-31824
On a ternary bracketing problem from the theory of formal languages
[TR-90-24] N91-31825
Partial evaluation grammars
[TR-91-01] N91-31826
Inventory and functional prototypes of neural networks
[TR-90-15] N91-31880
A formal power series equation from formula complexity theory
[TR-90-25] N91-31895
Formalisation of techniques: Chopping down the methodology jungle
[TR-90-26] N91-31996
NORTH CAROLINA STATE UNIV., RALEIGH.
A computational and experimental investigation of a three-dimensional hypersonic scramjet inlet flow field
[NASA-CR-186788] N91-31083
NORTHWESTERN UNIV., EVANSTON, IL.
Atomic structures and compositions of internal interfaces
[DE91-016095] N91-31934
NOTRE DAME UNIV., IN.
Linear and nonlinear responses of the flow and temperature fields to imposed wall temperature oscillations in differentially heated vertical rectangular enclosures N91-31550
NOVA SCOTIA RESEARCH FOUNDATION CORP., DARTMOUTH.
Characterization of fire resistant GRP's by mechanical properties determination
[DREA-CR-88-421] N91-31295

O

OAK RIDGE K-25 SITE, TN.
Development of ceramic membranes for gas separation: FY 1990 development activities
[DE91-015915] N91-31300
OAK RIDGE NATIONAL LAB., TN.
A multifunction ion-irradiation/surface modification ultrahigh vacuum chamber system
[DE91-016819] N91-31190
Interlaminar deformations on the cylindrical surface of a hole in laminated composites by moire interferometry
[DE91-015922] N91-31238
Effects of oxidation and combustion environments on the properties of Nicalon/SiC composites
[DE91-016778] N91-31240
Non-equilibrium solidification in austenitic stainless steel welds
[DE91-014279] N91-31277
Weldability and hot ductility of iron aluminides
[DE91-016343] N91-31280
Dual ion implantation effects on fatigue properties of Fe-13Cr-15Ni alloys
[DE91-015930] N91-31286
Initial determination of the micromechanical properties of oxide scales
[DE90-012164] N91-31291
Development of toughened ceramics for elevated temperatures
[DE91-015923] N91-31301
Ion beam enhanced adhesion of iron films to sapphire substrates
[DE91-015931] N91-31308
Effective ionization coefficients, electron drift velocities, and limiting breakdown fields for gas mixtures of possible interest to particle detectors
[DE91-015921] N91-31532
Effect of convection on weld pool development
[DE91-014213] N91-31649
Weld pool solidification and microstructures
[DE91-014263] N91-31650
BES welding science
[DE91-015625] N91-31651
A users' guide to PVM (parallel virtual machine)
[DE91-016934] N91-31655
The PVM system: Supercomputer level concurrent computation on a heterogeneous network of workstations
[DE91-016276] N91-31870
Particle production through two-photon processes in relativistic heavy-ion colliders
[DE91-016221] N91-31931
Properties of low temperature, low oxygen pressure post-annealed YBa2Cu3O(sub 7-x) thin films
[DE91-015632] N91-31969
Studies of non-ideal superconductors using DC magnetic methods
[DE91-015642] N91-31970
OFFICE NATIONAL D'ETUDES ET DE RECHERCHES AEROSPATIALES, PARIS (FRANCE).
Transition length determination in the F1 wind tunnel, test report
[ONERA-PV-1/8571-GY] N91-31089
Exploitation of OAT15A profile tests in the T2 wind tunnel: Experimental determination of the wave drag
[ONERA-RSF-88/1685-AY-158-A] N91-31092
Validation of two dimensional drag prediction methods
[ONERA-RSF-85/1685-AY] N91-31093
ATSF supersonic aircraft intake. Review of the analyses of some particular problems, technical summary
[ONERA-RTS-134/2149-AY-640-A] N91-31094
Three dimensional extension of a numerical method for resolving small transonic perturbations in unstructured mesh
[ONERA-RT-50/3064-RY-093-R] N91-31095
Study of lightning strikes on an aircraft in flight. Electromagnetic measurements
[ONERA-RF-25/7234-PY] N91-31111
Study of lightning strikes on an aircraft in flight. Electric measurements
[ONERA-RF-98/7154-PY] N91-31112
Vortex-blade interaction on a helicopter principal rotor. Validation of the S2DI computation program and study of vortex models
[ONERA-RT-92/5094-PY] N91-31136
Composite materials damage. Transverse cracking and delamination
[ONERA-RT-6/7256-RY-080-R] N91-31234
Development of a computation code for nonequilibrium gas axisymmetric hypersonic laminar flow
[ONERA-RS-14/3637-AY] N91-31585
Compressible two dimensional boundary layer strong perfect fluid coupling in the case of sharp leading edge profiles. Stationary case
[ONERA-RT-42/1621-RY-093-R] N91-31586
Introduction to laser velocimeter techniques N91-31615
Basic LDV1 component system N91-31616
Advanced systems: Multicomponent LDV N91-31619
Accuracy of laser velocimetry N91-31622
Advanced and non-conventional optical schemes N91-31626
Updating of finite element models using experimental vibratory type data. Process of static substructuring
[ONERA-RT-10/3313-RY-090-R] N91-31682
Three dimensional acoustic propagation at low temperature altitude
[ONERA-RT-13/3641-PY] N91-31924
Use of an ARMA model in turbulent medium acoustic propagation
[ONERA-RF-14/3641-PY] N91-31925
OFFICE NATIONAL D'ETUDES ET DE RECHERCHES AEROSPATIALES, TOULOUSE (FRANCE).
Study of the flow around the GARTEUR AD/AG07 wing: First F2 test campaign results
[ONERA/DERAT-37/5025-26] N91-31096
OHIO STATE UNIV., COLUMBUS.
Adaptive arrays in packet radio networks
[AD-A239636] N91-31509
Linear and nonlinear stability of boundary layers with streamwise varying properties N91-31545
Analysis and development of a real-time control methodology in resistance spot welding N91-31646
The development of an intelligent dimensional inspection environment using coordinate measuring machines N91-31661
Crystallization of the glassy grain boundary phase in silicon nitride ceramics
[NASA-CR-188717] N91-31961
Microstructural changes in Beta-silicon nitride grains upon crystallizing the grain-boundary glass N91-31963
Glass formation and crystallization in high-temperature glass-ceramics and Si3N4 N91-31964
Indirect measurement of the viscosity of the intergranular glass phase in yttria-sintered silicon nitride N91-31965

OKLAHOMA UNIV., NORMAN.
Computational analysis of hypersonic flows past elliptic-cone waveriders N91-31080
Model of an aerospace plane based on an idealized cone-derived waverider forebody N91-31129
OLD DOMINION UNIV., NORFOLK, VA.
Integrated control of thermally distorted large space antennas N91-31487
OREGON GRADUATE CENTER FOR STUDY AND RESEARCH, BEAVERTON.
Deformation induced microstructural and microchemical changes during thermomechanical treatment [DE91-016949] N91-31290
OREGON STATE UNIV., CORVALLIS.
The effects of fluid particle interactions on interfacial transfer and flow structure [DE91-016409] N91-31575
OXFORD UNIV. (ENGLAND).
Finite-dimensional dynamics and chaos in fluid flows N91-31571

P

PACIFIC NORTHWEST LAB., RICHLAND, WA.
Catalysis-by-design impacts assessment [DE91-013280] N91-31247
A review of accelerated response actions available to the environmental restoration program: Selected case histories and associated issues [DE91-013608] N91-31716
PARIS-SUD UNIV., ORSAY (FRANCE).
Three dimensional Euler equation solving on parallel machines [ETN-91-99913] N91-31583
PENNSYLVANIA STATE UNIV., UNIVERSITY PARK.
Catalyst dispersion and activity under conditions of temperature-staged liquefaction [DE91-016602] N91-31261
PENNSYLVANIA UNIV., PHILADELPHIA.
Application of microwave cavity perturbation techniques in conducting polymers [AD-A239376] N91-31310
PHOTON RESEARCH ASSOCIATES, INC., CAMBRIDGE, MA.
Advanced optical sensing and processing technologies for the distributed control of large flexible spacecraft [NASA-CR-4399] N91-31609
PHYSICS AND ELECTRONICS LAB. TNO, THE HAGUE (NETHERLANDS).
Introduction to radar polarimetry [FEL-91-B122] N91-31496
OSI-security and relations with other security standards [FEL-91-B099] N91-31872
Information security: Past, present and future [FEL-91-B100] N91-31873
PITTSBURGH UNIV., PA.
Atomic hydrogen driven halogen extraction from Si(100): Eley-Rideal surface kinetics [AD-A239544] N91-31266
Quick development microcomputer system: Training automatic components for electronic troubleshooting [AD-A239573] N91-31542
PLANNING RESEARCH CORP., EDWARDS, CA.
Predicted thermal response of a cryogenic fuel tank exposed to simulated aerodynamic heating profiles with different cryogens and fill levels [NASA-CR-4395] N91-31470
POITIERS UNIV. (FRANCE).
Automatic analysis of visualization negatives [ETN-91-99971] N91-31603
POLITECNICO DI MILANO (ITALY).
Liquid phase sintering (TEXUS 8) N91-31443
On the application of temporal logic in real time to specify telecommunication protocols [REPT-90-071] N91-31846
The problem of network management: An approach using AI techniques [REPT-90-072] N91-31884
The design of an Integrity Consistency Checker (ICC) for an object oriented database system [REPT-91-021] N91-31994
Hypertext development using a model-based approach [REPT-90-074] N91-31995
PRATT AND WHITNEY AIRCRAFT, WEST PALM BEACH, FL.
Control system design considerations for starting turbo-engines during cold weather operation N91-31155
PRATT AND WHITNEY AIRCRAFT OF CANADA LTD., LONGUEUIL (QUEBEC).
Capacitive bridge-type probe and conversion circuitry [PATENT-1-263-444] N91-31598
Capacitive bridge-type probe and conversion circuitry [PATENT-1-263-443] N91-31599
PRATT AND WHITNEY AIRCRAFT OF CANADA LTD., MISSISSAUGA (ONTARIO).
Cold weather ignition characteristics of advanced small gas turbine combustion systems N91-31152
Cold start development of modern small gas turbine engines at Pratt and Whitney Aircraft of Canada Ltd. N91-31156
PRINCETON UNIV., NJ.
Hydrodynamic simulations of cosmology N91-32013

R

RANGE COMMANDERS COUNCIL, WHITE SANDS MISSILE RANGE, NM.
Flight test digitized/compressed video spectrum allocation [AD-A239535] N91-31503
Spectrum monitoring procedures and techniques [AD-A239567] N91-31507
Range reference atmosphere, Fairbanks, Alaska [AD-A239520] N91-31739
Range reference atmosphere Wake Island, North Pacific [AD-A239602] N91-31740
Range reference atmosphere Shemya, Alaska [AD-A239603] N91-31741
Range reference atmosphere: Thule, Greenland [AD-A239659] N91-31742
REMTECH, INC., HUNTSVILLE, AL.
Aero/fluids database system [NASA-CR-184208] N91-31853
RENSSELAER POLYTECHNIC INST., TROY, NY.
The influence of plastic-strain-induced anisotropy on stress distributions in the finite deformation of ductile metals N91-31273
Inter-GEN: A hybrid approach to engineering design optimization N91-31471
Modeling and simulation of multiple cooperating manipulators on a mobile platform N91-31647
Static strain and vibration characteristics of a metal semimonocoque helicopter tail cone of moderate size [NASA-CR-187576] N91-31679
ROCHESTER UNIV., NY.
Theoretical nuclear physics [DE91-016745] N91-31936
Optimal configuration of distributed database systems N91-31990
Magnetic field decay in neutron stars with superconducting cores N91-32015
ROCKWELL INTERNATIONAL CORP., CANOGA PARK, CA.
Hydrogen test of a small, low specific speed centrifugal pump stage [NASA-CR-187117] N91-31213
Flow induced vibrations in the SSME injector heads [NASA-CR-184209] N91-31214
Reusable rocket engine intelligent control system framework design, phase 2 [NASA-CR-187213] N91-31219
ROLLS-ROYCE LTD., DERBY (ENGLAND).
Engine icing criticality assessment N91-31161
Icing research related to engine icing characteristics N91-31168
ROLLS-ROYCE LTD., LEAVESDEN (ENGLAND).
Application of a water droplet trajectory prediction code to the design of inlet particle separator anti-icing systems N91-31159
ROUTES, INC., KANATA (ONTARIO).
Study of space qualification specifications [CTN-91-60201] N91-31199
ROYAL AEROSPACE ESTABLISHMENT, FARNBOROUGH (ENGLAND).
Developments in icing test techniques for aerospace applications in the RAE Pyestock altitude test facility N91-31173
ROYAL INST. OF TECH., STOCKHOLM (SWEDEN).
Floating zone crystal growth of Ga-doped germanium (TEXTUS 10) ESA N91-31387
Floating-zone experiments with germanium crystals (TEXUS 12) ESA N91-31388
Floating zone growth of germanium crystals (TEXUS 14b) ESA N91-31389
Semi-confined Bridgman growth of Ga-doped Ge (MASER 2) N91-31390
Solidification of alloys (TEXUS 1) N91-31400
Solidification of alloys (TEXUS 2) N91-31401
Macrosegregation in Ag-Sn alloys (MASER 1) N91-31402
Directional solidification of Al-Cu alloys (MASER 2) N91-31403
Solidification of immiscible alloys: ZnBi (TEXUS 2) N91-31415
The coalescence process in immiscible alloys (TEXUS 3) N91-31416
The coalescence process in immiscible alloys (TEXUS 5) N91-31417
Unidirectional solidification of immiscible alloys (TEXUS 5) N91-31418
Unidirectional solidification of immiscible alloys (TEXUS 7) N91-31419
Unidirectional solidification of Zn-Bi samples (TEXUS 14b) N91-31420
Directional solidification of immiscible alloys Zn-Pb (MASER 2) N91-31421
Soldering in microgravity (TEXUS 5) N91-31462
ROYAL MILITARY COLL. OF CANADA, KINGSTON (ONTARIO).
The influence of fuel characteristics on heterogeneous flame propagation N91-31165
ROYAL NETHERLANDS METEOROLOGICAL INST., DE BILT.
Coordinate conversions for presenting and compositing weather radar data [KNMI-TR-129] N91-31497
Description of Crau data set: Meteosat data, radiosonde data, sea surface temperatures: Comparison of Meteosat and Heimann data [KNMI-WR-90-03] N91-31752
ROYAL OBSERVATORY, EDINBURGH (SCOTLAND).
UKIRT observer's manual [ETN-91-99747] N91-32008
RUHR UNIV., BOCHUM (GERMANY, F.R.).
Segregation behaviour of rare earths under microgravity and normal gravity conditions (TEXUS 13) N91-31407

S

SANDIA LABS., ALBUQUERQUE, NM.
Improving managers' effectiveness [DE91-016405] N91-31988
SANDIA NATIONAL LABS., ALBUQUERQUE, NM.
Nuclear thermal rockets: A systems study [DE91-017066] N91-31221
The mechanical response of woven Kevlar fabric [DE91-010581] N91-31230
Effects of trapped gases on ceramic-filled-glass composite densification [DE91-015850] N91-31237
HVOF: Particle, flame diagnostics, and coating characteristics [DE91-014654] N91-31248
A comparison of techniques for the metallographic preparation of thermal sprayed samples [DE91-014704] N91-31272
Process for producing plasma sprayed carbide-based coatings with minimal decarburization and near theoretical density [DE91-012016] N91-31292
Beneficial effects of austemper post-treatment on tungsten carbide based wear coatings [DE91-013260] N91-31293
Defect diffusion in ion implanted glasses [DE91-016119] N91-31302
Ion-implantation induced crystallization of glass [DE91-016121] N91-31303
Elastic wave dispersion in high-strength ceramics [DE91-016648] N91-31309
Silicon micromachining based on porous silicon formation [DE91-013744] N91-31472
Radar-cross-section measurement errors caused by test object interaction with low-dielectric-constant supports [DE91-015340] N91-31490
Electromagnetic penetration of slot apertures with depth and losses [DE91-016401] N91-31500
Accelerated aging and discharge of lithium/thionyl-chloride D cells [DE91-012649] N91-31517
Electrophoretic dielectric coatings for magnetic switches [DE91-015337] N91-31518
Technology assessment of ambient temperature rechargeable lithium batteries for electric vehicle applications [DE91-016500] N91-31522
Numerical simulation of a split cavity oscillator and rf conversion [DE91-016501] N91-31523
The development of aluminum-air batteries for application in electric vehicles [DE91-016863] N91-31533
A boundary integral equation method for steady two-dimensional flow in partially saturated media [DE91-016056] N91-31573
Approximate treatment of a strong explosion and expansion in a near vacuum [DE91-016063] N91-31574

A simple model for the motion of pulsed-laser-driven thin flyers
[DE91-011325] N91-31634
Force reconstruction using the inverse of the mode-shape matrix
[DE91-016407] N91-31689
One-sun, single-crystalline silicon solar cell research
[DE91-015646] N91-31699
The feasibility of testing NASA's SCAD concentrator on Earth
[DE91-016055] N91-31702
The 1991 DOE/Sandia Crystalline Photovoltaic Technology Project Review Meeting
[DE91-016062] N91-31703
Facet development for a faceted stretched-membrane dish by Solar Kinetics, Inc.
[DE91-016866] N91-31713
Parabolic dish photovoltaic concentrator development
[DE91-016868] N91-31714
Design and cost of the first commercial stretched-membrane heliostat
[DE91-016870] N91-31715
Human factors engineering design guidelines for the software user interface
[DE91-016061] N91-31802
Application of digital compression techniques to optical surveillance systems
[DE91-016404] N91-31854
Benchmarking a Network Storage Service
[DE91-013510] N91-31868
Depth profiles for hydrogen-assisted thermal donor formation in silicon
[DE91-015719] N91-31971
Rapid thermal annealing effects in In(x)Ga(1-x)As/GaAs strained-layer superlattices
[DE91-015901] N91-31978
Ground-state in-plane light-holes in GaAs/AlGaAs structures
[DE91-016408] N91-31980

SCHOOL OF AEROSPACE MEDICINE, BROOKS AFB, TX.
Testing and evaluation of the catalyst research MiniOX 3 oxygen monitor
[AD-A239665] N91-31807

SCIENCE APPLICATIONS INTERNATIONAL CORP., HUNTSVILLE, AL.
Optimization techniques applied to passive measures for in-orbit spacecraft survivability
[NASA-CR-184198] N91-31204

SCIENCE APPLICATIONS INTERNATIONAL CORP., SAN DIEGO, CA.
Parabolic dish photovoltaic concentrator development
[DE91-016868] N91-31714

SOCIETE DE FABRICATION D'INSTRUMENTS DE MESURE, MASSY (FRANCE).
Robustness and techniques of multivariable control for helicopter piloting. Dispatch 3: Inclusion regions technique on linear model
[RD/PA-14-227] N91-31184

SOCIETE NATIONALE INDUSTRIELLE AEROSPATIALE, PARIS (FRANCE).
Procedure for steering a low-speed missile, weapon system, and missile for implementation of the procedure
[PATENT-1-265-947] N91-31182

SOFTWARE KINETICS LTD., STITTSVILLE (ONTARIO).
The automatic surveillance, tracking, and imaging program. User manual
[SK-1600-44-001-02-0] N91-31483

SOLAR KINETICS, INC., DALLAS, TX.
Facet development for a faceted stretched-membrane dish by Solar Kinetics, Inc.
[DE91-016866] N91-31713
Design and cost of the first commercial stretched-membrane heliostat
[DE91-016870] N91-31715

SOUTHERN RESEARCH INST., BIRMINGHAM, AL.
Electrostatic precipitation of condensed acid mist
[DE91-016530] N91-31260

SOUTHWEST RESEARCH INST., SAN ANTONIO, TX.
The effect of fuel properties and atomization on low temperature ignition in gas turbine combustors
N91-31164

SPACE TECHNOLOGY CORP., TOKYO (JAPAN).
Solutal diffusion measurements in liquid PbSnTe under microgravity (TEXUS 19) N91-31372
Solution growth of GaAs single crystals (TEXUS 19) N91-31393
Vapour growth of an InP crystal (TEXUS 20) N91-31394

SPECTRA RESEARCH SYSTEMS, INC., HUNTSVILLE, AL.
Evaluation of undeveloped rocket engine cycle applications to advanced transportation
[NASA-CR-184205] N91-31215

STANFORD TELECOMMUNICATIONS, INC., RESTON, VA.
The data distribution satellite system
[NASA-CR-187172] N91-31499

STANFORD UNIV., CA.
The interaction of particles with homogeneous turbulence N91-31548
RNG and turbulence modeling N91-31570
Energy transfer processes in solar energy conversion
[DE91-016102] N91-31704
Open architecture for formal reasoning
[AD-A239395] N91-31857
Practical aspects of an interior-point method for convex programming
[AD-A239457] N91-31858
Mathematical theory of computation
[AD-A239419] N91-31912
Bayes theorem from a sampling-resampling perspective
[AD-A239515] N91-31919
On combining independent significance tests
[AD-A239660] N91-31920
Limited reaction processing for semiconductor materials preparation
[AD-A239639] N91-31983

STATE UNIV. OF NEW YORK, BUFFALO.
Determination of solvation kinetics in supercritical fluids
[DE91-016096] N91-31253
Prediction of rotor surface unsteady pressure and heat transfer from wake passing N91-31549

STOCKHOLM UNIV. (SWEDEN).
Initialization of the HIRLAM model using a digital filter
[DM-57] N91-31747

STRATHCLYDE UNIV., GLASGOW (SCOTLAND).
The superconducting gravity gradiometer N91-31734

SUNDSTRAND TURBOMACH, SAN DIEGO, CA.
Cold starting small gas turbines: An overview
N91-31150

SUPERCONDUCTING SUPER COLLIDER LAB., DALLAS, TX.
SHOWTIME.C: A C-language program for data acquisition and display user's guide
[DE91-016241] N91-31817

SURREY UNIV., GUILDFORD (ENGLAND).
Solidification of fine dispersions in microgravity (TEXUS 14b) N91-31441

SVERDRUP TECHNOLOGY, INC., ARNOLD AFS, TN.
Icing test capabilities for aircraft propulsion systems at the Arnold Engineering Development Center
N91-31170

SVERDRUP TECHNOLOGY, INC., BROOK PARK, OH.
Space engine safety system
[NASA-CR-187219] N91-31209

T

TECHNISCHE HOCHSCHULE, AACHEN (GERMANY, F.R.).
Ultrasound absorption in molten salts (TEXUS 14b)
N91-31359
Ultrasound absorption in molten salts (TEXUS 17) ESA N91-31360
Ventilation and filling of an optical diffusion cell (TEXUS 8) N91-31371
Boundary layers in transparent melts (TEXUS 10)
N91-31406

TECHNISCHE UNIV., BERLIN (GERMANY, F.R.).
The question of an efficient space transportation system for extraterrestrial materials
[ILR-MITT-252(1990)] N91-31197
Interfacial convection (TEXUS 1) N91-31327
Interfacial convection (TEXUS 2) N91-31328
Diffusion-induced interfacial convection (TEXUS 3)
N91-31329
Thermally induced interfacial convection (TEXUS 4)
N91-31330
Diffusion-induced interfacial convection (TEXUS 8)
N91-31331
Diffusion-induced interfacial convection (TEXUS 11)
N91-31332

TECHNISCHE UNIV., BRUNSWICK (GERMANY, F.R.).
Alloy formation (TEXUS 5) N91-31398

TECHNISCHE UNIV., CLAUSTHAL-ZELLERFELD (GERMANY, F.R.).
Reaction kinetics in glass melts (TEXUS 1)
N91-31363
Reaction kinetics in glass melts: Corrosion of SiO2 (TEXUS 4) N91-31364
Reaction kinetics in glass melts: Sodium self-diffusion in alkali-silicate melts (TEXUS 6) N91-31365
Self- and interdiffusion in alkali-silicate melts (TEXUS 11 and 12) N91-31366
Self- and interdiffusion in alkali-silicate melts (TEXUS 13) N91-31367
Reaction kinetics in molten glasses: Self-diffusion in alkali-silicate melts (TEXUS 20) N91-31368
Special refractive index profiles in glasses obtained by ion exchange (TEXUS 19) ESA N91-31369

TECHNISCHE UNIV., DELFT (NETHERLANDS).
Large scale CAESAR images using inertial navigation and pressure altitude measurement. Accuracy deformations and possibilities for a Global Positioning System (GPS)
[ETN-91-99418] N91-31117
Investigations on the use of GPS for geodetic and orbit determination applications
[LR-649] N91-31118
Sulphur diffusion in liquid cast iron (TEXUS 6) ESA
N91-31370
The implementation of a quality system in an aerial mapping company
[ETN-91-99424] N91-31695

TECHNISCHE UNIV., EINDHOVEN (NETHERLANDS).
Colloid chemistry (TEXUS 17) ESA N91-31362
Measurements of inception time lags of repetitively pulsed corona in air N91-32028

TECHNISCHE UNIV., MUNICH (GERMANY, F.R.).
Contributions to a space station for flights in the near field and towards geostationary Earth orbit
[ETN-91-99744] N91-31203
Nucleate pool boiling (TEXUS 3) N91-31354
Bubble formation, 1 (TEXUS 5) N91-31355
Bubble formation, 2 (TEXUS 10) N91-31356
Bubble formation, 2. Microgravity measurements of the boiling heat transfer from flat heating surfaces (TEXUS 11) N91-31357
Inst. A fuer Thermodynamik. N91-31358
Phase transition (TEXUS 8) N91-31374

TENNESSEE UNIV., KNOXVILLE.
Boron in nuclear medicine: New synthetic approaches to PET, SPECT, and BNCT agents
[DE91-016488] N91-31764

TENNESSEE UNIV., MEMPHIS.
Muramyl peptide-enhanced sleep: Pharmacological optimization of performance
[AD-A239442] N91-31766

TEXAS A&M UNIV., COLLEGE STATION.
An analytical prediction of matrix cracking in fibrous composite laminates N91-31225
An investigation into the effects of damage on the stresses in a composite laminate N91-31226
Correlations between surface structure and catalytic activity/selectivity
[DE91-016453] N91-31255
High pressure catalytic reactions over single-crystal metal surfaces
[DE91-016475] N91-31256
Fracture toughness characterization of polymers
N91-31296
Robust impedance control of robot manipulators
N91-31297
A three-dimensional viscous flow model of stator/rotor interaction in turbomachines N91-31547
Dynamics of 1.3 micron semiconductor lasers and nonlinear gain N91-31613

TEXAS UNIV., ARLINGTON.
A perspective on CELSS control issues N91-31784

TEXAS UNIV., AUSTIN.
The motions of Mars' pole N91-32019

TRW SPACE TECHNOLOGY LABS., REDONDO BEACH, CA.
Phased array components for the High Temperature Superconducting Space Experiment (HTSSE)
[AD-A239361] N91-31535

TUSKEGEE INST., AL.
Sweet potato for closed ecological life support systems using the nutrient film technique N91-31782

U

UNITED TECHNOLOGIES CORP., EAST HARTFORD, CT.
Method for stabilizing thick honeycomb core composite articles
[PATENT-1-253-424] N91-31224

UNIVERSITEIT TWENTE, ENSCHEDE (NETHERLANDS).
Some order dimension bounds for communication complexity problems
[MEMO-938] N91-31489
Refining interfaces of communicating systems
[MEMO-INF-91-19] N91-31493
Acceleration techniques for a spectral multi-grid method
[MEMO-914] N91-31580
The hierarchy of LR-attributed grammars
[MEMO-INF-91-26] N91-31840
Attribute evaluation and parsing
[MEMO-INF-91-31] N91-31841

An algorithm for spectral factorization of polynomial matrices with any signature
[MEMO-912] N91-31842
Dynamic disturbance decoupling for discrete-time nonlinear systems
[MEMO-913] N91-31843
An algorithm for the one-to-all shortest path problem with arbitrary arc lengths
[MEMO-919] N91-31844
Algorithms for finding an optimal matching between a given string and a string generated by a regular grammar
[MEMO-921] N91-31845
Study day on the design of a network database in four languages
[MEMO-INF-91-22] N91-31863
An object-oriented analysis, design, and implementation of a network database N91-31865
A network database: A case study in functional programming N91-31867
Classes of feedforward neural networks and their circuit complexity
[MEMO-920] N91-31881
On the expressiveness of equational type logic
[MEMO-INF-90-39-REV] N91-31887
Fitting scattered data on spherelike surfaces using tensor products of trigonometric and polynomial splines
[MEMO-909] N91-31904
A note on 'the matching polynomial of a polygraph'
[MEMO-910] N91-31905
Multigrid and Runge-Kutta time stepping applied to the uniformly non-oscillatory scheme for conservation laws
[MEMO-911] N91-31906
Extensive coverings and exact core bounds
[MEMO-915] N91-31907
Cycles containing many vertices of large degree
[MEMO-916] N91-31908
Parameter identification for two-point boundary value processes
[MEMO-917] N91-31909
Learning convex bodies under uniform distribution
[MEMO-918] N91-31910

UNIVERSITIES SPACE RESEARCH ASSOCIATION, WASHINGTON, DC.
Abundances from solar flare line spectroscopy
[NASA-CR-183492] N91-32022

UNIVERSITY COLL. OF WALES, ABERYSTWYTH.
Computational fluid dynamics N91-31544

UNIVERSITY OF NORTHERN ILLINOIS, DE KALB.
Mean field analysis of the CuO2 lattice: Comparison to Monte Carlo simulations
[DE91-015570] N91-31968

UNIVERSITY OF SOUTH FLORIDA, TAMPA.
Design and analysis of fault-tolerant distributed real-time computer systems
[AD-A239382] N91-31875

UNIVERSITY OF SOUTHWESTERN LOUISIANA, LAFAYETTE.
Cluster-based adaptive information retrieval N91-31991

UTAH STATE UNIV., LOGAN.
Exploring the limits of crop productivity: A model to evaluate progress N91-31776
Cloning crops in a CELSS via tissue culture: Prospects and problems N91-31783
Preparatory space experiments for development of a CELSS N91-31796

UTAH UNIV., SALT LAKE CITY.
Alumina reinforced tetragonal zirconia (TZP) composites
[DE91-016748] N91-31239
In situ short fatigue crack characterization of a nickel-base superalloy at ambient and elevated temperature N91-31670

UTRECHT STATE UNIV. (NETHERLANDS).
The derivation of distributed termination detection algorithms from garbage detection schemes
[RUU-CS-90-24] N91-31827
Distributed incremental maximum finding in hierarchically divided graphs
[RUU-CS-90-30] N91-31828
The on-line d-dimensional dictionary problem
[RUU-CS-90-31] N91-31829
Linear logic, domain theory, and semi-functors
[RUU-CS-90-34] N91-31830
Perfect colorings
[RUU-CS-90-35] N91-31831
On the efficient incremental evaluation of higher order attribute grammars
[RUU-CS-90-36] N91-31832
Categorical semantics as a basis for program transformation
[RUU-CS-90-38] N91-31833
On logic programming and the refinement calculus: Semantics based program transformations
[RUU-CS-90-39] N91-31834
The failure of failures: Towards a paradigm for a synchronous communication
[RUU-CS-90-40] N91-31835
Approximating treewidth, pathwidth, and minimum elimination tree height
[RUU-CS-91-01] N91-31836
Synchronous link-level protocols
[RUU-CS-91-02] N91-31837
The complexity of coloring games on perfect graphs
[RUU-CS-91-03] N91-31838
Dynamic output-sensitive hidden surface removal for c-oriented polyhedra
[RUU-CS-91-06] N91-31839
Longest segment problems
[RUU-CS-90-28] N91-31896
On disjoint cycles
[RUU-CS-90-29] N91-31897
Covering a set of points with fixed size hypersquares and related problems
[RUU-CS-90-32] N91-31898
Hidden surface removal for c-oriented polyhedra
[RUU-CS-90-33] N91-31899
Computing minimum length paths of a given homotopy class
[RUU-CS-90-37] N91-31900
A note on semi-adjunctions
[RUU-CS-90-41] N91-31901
The linear decomposition of delta-squared models
[RUU-CS-91-04] N91-31902
Union-copy structures and dynamic segment trees
[RUU-CS-91-05] N91-31903
A pragmatical view on the certainty factor model
[RUU-CS-90-42] N91-31917
From game trees to game graphs
[RUU-CS-90-43] N91-31921
Continuous informations systems
[RUU-CS-90-25] N91-31997

V

VIBRO-METER S.A., FRIBOURG (SWITZERLAND).
Process for detecting the likelihood of ice formation, ice warning system for carrying out the process, and utilization thereof
[PATENT-1-250-926] N91-31107

VIRGINIA POLYTECHNIC INST. AND STATE UNIV., BLACKSBURG.
A method for the geometrically nonlinear analysis of compressively loaded prismatic composite structures N91-31229
The formation of novel thermoplastic composites from liquid crystalline polymers and their blends
[AD-A239546] N91-31244
Influence of surface defects and local structure on oxygenate reaction pathways over metal oxide surfaces
[DE91-016600] N91-31289
Generalized spatial discretization techniques for space-marching algorithms N91-31546
Nonlinear probabilistic finite element modeling of composite shells N91-31668
The control of flexible structure vibrations using a cantilevered adaptive truss N91-31671

VON KARMAN INST. FOR FLUID DYNAMICS, RHODE-SAINT-GENESE (BELGIUM).
Introduction to the Modeling of Turbulence
[VKI-LS-1991-02] N91-31551
New Approaches in the Description and Modeling of Turbulence
[VKI-LS-1991-03] N91-31565
Laser Velocimetry, volume 1
[VKI-1991-05-VOL-1] N91-31614
Laser Velocimetry, volume 2
[VKI-1991-05-VOL-2] N91-31625

W

WALES UNIV. INST. OF SCIENCE AND TECHNOLOGY, CARDIFF.
Genetic algorithms
[ETN-91-99985] N91-31852

WASHINGTON UNIV., SEATTLE.
X ray and gamma ray spectroscopy of solids under pressure
[DE91-016948] N91-31263
On the response of the special sensor microwave/imager to the marine environment: Implications for atmospheric parameter retrievals N91-31727
Neural network based model reference adaptive control N91-31877

WEHRTECHNISCHE DIENSTSTELLE FUER LUFTFAHRZEUGE, MANCHING (GERMANY, F.R.).
Design considerations based upon low temperature starting tests on military aircraft turbo engines N91-31157

WISCONSIN UNIV., MADISON.
Asymptotic finite strain analysis of propagating cracks in elastic-plastic materials N91-31669
Environmental and cultural considerations for growth of potatoes in CELSS N91-31779
Technology for subsystems of space-based plant growth facilities N91-31799
Searching for the Higgs in ep collisions at LEP/LHC
[DE91-015701] N91-31930

WORLD METEOROLOGICAL ORGANIZATION, GENEVA (SWITZERLAND).
Report of the Workshop on a CLICOM-HOMS Interface
[WCAP-16] N91-31746

WRIGHT LAB., WRIGHT-PATTERSON AFB, OH.
An expert system for the identification of silicon impurities using FTIR spectroscopy
[AD-A236504] N91-31246

Typical Contract Number Index Listing

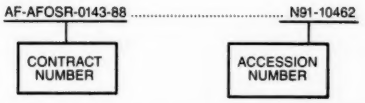

Listings in this index are arranged alphanumerically by contract number. Under each contract number the accession numbers denoting documents that have been produced as a result of research done under that contract are arranged in ascending order. The accession number denotes the number by which the citation is identified.

AF PROJ. 7930 ..... N91-31807
AF-AFOSR-0079-89 ..... N91-31576
AF-AFOSR-0091-90 ..... N91-31889
BMFT-FK-037459 ..... N91-31696
DA PROJ. 1L1-61102-AH-45 ..... N91-31178
N91-31876
DA PROJ. 1L1-61102-AH-45C N91-31687
DA PROJ. 1L1-62105-AH-42 ..... N91-31245
DA PROJ. 1L1-62211-A-47A N91-31181
N91-31648
N91-31654
DA PROJ. 3M1-61102-BS-13 ..... N91-31758
DA PROJ. 3M1-61102-BS-15 ..... N91-31766
DA PROJ. 4A1-61102-B-52-C N91-31697
DAAG29-82-K-0093 ..... N91-31679
DAAK70-85-C-0007 ..... N91-31164
DAAK70-87-C-0043 ..... N91-31164
DAAL03-88-G-0001 ..... N91-31983
DAAL03-88-K-0020 ..... N91-31983
DAAL03-88-K-0057 ..... N91-31504
DAAL03-88-K-0104 ..... N91-31244
DAAL03-89-K-0073 ..... N91-31509
DAMD17-86-C-6194 ..... N91-31766
DAMD17-90-C-0010 ..... N91-31758
DE-AC02-76CH-00016 ..... N91-31320
N91-31720
N91-31756
N91-31942
N91-31972
N91-31977
N91-31981
N91-31982
DE-AC02-76ER-00881 ..... N91-31930
DE-AC02-76ER-03130 ..... N91-31941
DE-AC03-76SF-00098 ..... N91-31254
N91-31279
N91-31288
N91-31473
N91-31611
N91-31948
N91-31974
N91-31975
N91-32010
N91-32016
N91-32018
DE-AC04-76DP-00613 ..... N91-31251
N91-31257
N91-31652
N91-31653
N91-31657
N91-31819
DE-AC04-76DP-00789 ..... N91-31221
N91-31230
N91-31237
N91-31248
N91-31272
N91-31292
N91-31293
N91-31302
N91-31303
N91-31309
N91-31472
N91-31490
N91-31500
N91-31517
N91-31518
N91-31520
N91-31521
N91-31522
N91-31523
N91-31533
N91-31573
N91-31574
N91-31634
N91-31689
N91-31699
N91-31702
N91-31703
N91-31713
N91-31714
N91-31715
N91-31802
N91-31854
N91-31868
N91-31971
N91-31978
N91-31980
N91-31988
DE-AC05-80ER-10742 ..... N91-31977
DE-AC05-84OR-21400 ..... N91-31190
N91-31238
N91-31240
N91-31277
N91-31280
N91-31286
N91-31291
N91-31301
N91-31308
N91-31532
N91-31649
N91-31650
N91-31651
N91-31855
N91-31870
N91-31931
N91-31969
N91-31970
DE-AC05-84OT-21400 ..... N91-31300
DE-AC06-76RL-01830 ..... N91-31247
N91-31716
DE-AC06-86NE-37963 ..... N91-31290
DE-AC07-76ID-01570 ..... N91-31223
DE-AC08-88NV-10617 ..... N91-31966
DE-AC22-88PC-88867 ..... N91-31260
DE-AC22-89PC-89877 ..... N91-31261
DE-AC35-89ER-40486 ..... N91-31817
DE-AI08-78ET-44802 ..... N91-31998
DE-AS05-76ER-03065 ..... N91-31939
DE-FG02-84ER-45058 ..... N91-31641
DE-FG02-85ER-60314 ..... N91-31718
DE-FG02-86ER-60438 ..... N91-31759
DE-FG02-86ER-60444 ..... N91-31722
DE-FG02-87ER-13666 ..... N91-31262
DE-FG02-87ER-45312 ..... N91-31239
DE-FG02-87ER-45320 ..... N91-31973
DE-FG02-88ER-13914 ..... N91-31700
DE-FG02-88ER-40425 ..... N91-31936
DE-FG02-89CH-10418 ..... N91-31712
DE-FG02-89ER-40531 ..... N91-31937
DE-FG02-89ER-45403 ..... N91-31934
DE-FG02-90ER-14143 ..... N91-31253
DE-FG03-84ER-13251 ..... N91-31704
DE-FG05-86ER-60434 ..... N91-31764
DE-FG05-87ER-40319 ..... N91-31816
N91-31930
N91-31938
DE-FG05-88ER-13954 ..... N91-31255
N91-31256
DE-FG05-89ER-45392 ..... N91-31281
DE-FG05-89ER-75498 ..... N91-31985
N91-31986
DE-FG05-90ER-14129 ..... N91-31289
DE-FG06-84ER-45163 ..... N91-31263
DE-FG07-90ER-13034 ..... N91-31575
DND-14SV-W7714-7-5353 ..... N91-31486
DRE-W7714-9-9272 ..... N91-31484
DREA-W7707-7-7935-01-OSC N91-31295
DREO-W7714-7-5271 ..... N91-31485
DREO-W7714-7-5353 ..... N91-31478
DREO-W7714-8-5734/01-ST N91-31482
DREO-66ER-7-0003/E2-ER N91-31483
DRET-DS/SSR-88-1441 ..... N91-31103
DRET-86-095 ..... N91-31103
N91-31189
DRET-87-140 ..... N91-31232
N91-31233
DRET-87-212 ..... N91-31603
DRET-87-229 ..... N91-31583
DRET-87-238 ..... N91-31567
DRET-87-808-11 ..... N91-31566
DRET-87-1027 ..... N91-31761
DRET-87-1187 ..... N91-31101
DRET-88-150 ..... N91-31566
DRET-88-509 ..... N91-31090
DRET-89-34-001 ..... N91-31092
N91-31095
N91-31136
N91-31585
N91-31682
DRET-89-001-19 ..... N91-31111
N91-31112
DRET-89-001-46 ..... N91-31924
N91-31925
DRET-89-003 ..... N91-31604
DRET-89-017-01 ..... N91-31306
DRET/ARMINES-87-193 ..... N91-31683
DRET/LAAS-CNRS-83-34-051-00-47 ..... N91-31662
DRET/LIMSI-88-047 ..... N91-31594
DTCG23-89-C-20008 ..... N91-31122
N91-31123
N91-31124
DTFA03-86-C-00042 ..... N91-31814
EC-3075 ..... N91-31827
N91-31831
N91-31836
N91-31837
N91-31838
N91-31897
F04701-88-C-0089 ..... N91-31612
N91-31805
F19628-86-K-0009 ..... N91-31121
F19628-90-C-0002 ..... N91-31644
N91-31743
N91-31954
F30602-88-D-0027 ..... N91-31505
GRI-5089-294-1795 ..... N91-31645
HNFSR-1808 ..... N91-31916
MDA903-86-C-0142 ..... N91-31772
MDA903-86-C-0149 ..... N91-31542
MDA903-86-K-0155 ..... N91-31773
MDA903-89-C-0003 ..... N91-31862
MDA903-89-C-0134 ..... N91-31774
NADC PROJ. RS-3-4-H20 ..... N91-31808
NAGW-1072 ..... N91-31083
NAGW-1292 ..... N91-31723
NAGW-1540 ..... N91-31957
NAGW-1984 ..... N91-31492
NAG1-685 ..... N91-31678
NAG1-807 ..... N91-31679
NAG1-1061 ..... N91-31820
NAG1-1077 ..... N91-31678
NAG2-208 ..... N91-32009
NAG3-376 ..... N91-31106
NAG3-824 ..... N91-31961
N91-31963
NAG6-626 ..... N91-31928
NAG8-796 ..... N91-31750
NAG10-24 ..... N91-31782
NASA ORDER C-99066-G N91-31597
N91-31911
NASA ORDER H-80589-B N91-31607
NASA ORDER T-0704-F N91-31495
NASW-4430 ..... N91-31751
NASW-4520 ..... N91-31200
N91-31488
NAS1-18037 ..... N91-31926
N91-31927

NAS1-18478 ..... N91-31684
N91-31685
N91-31686
NAS1-18599 ..... N91-31692
NAS1-18605 ..... N91-31576
N91-31888
N91-31889
NAS1-18763 ..... N91-31609
NAS1-19000 ..... N91-31923
NAS2-12722 ..... N91-31470
NAS3-23164 ..... N91-31213
NAS3-25091 ..... N91-31499
NAS3-25266 ..... N91-31209
NAS3-25557 ..... N91-31219
NAS5-28749 ..... N91-32012
NAS5-30534 ..... N91-32020
N91-32021
N91-32022
NAS5-31500 ..... N91-32007
NAS8-36195 ..... N91-31214
NAS8-36643 ..... N91-31215
NAS8-37378 ..... N91-31204
NAS8-37463 ..... N91-31853
NAS9-17885 ..... N91-31890
NAS9-17900 ..... N91-31793
NAS9-17981 ..... N91-31798
NCA2-101 ..... N91-31795
NCC2-100 ..... N91-31777
NCC8-16 ..... N91-31947
NDH-3600-1-9-3594-01-SV N91-31199
NFR-E-DG-2923-300 ..... N91-31747
NFR-G-GU-1705-311 ..... N91-31747
NIVR-RB-3111-01201N N91-31579
NIVR-1604N N91-31131
NR PROJ. RR0-42046 ..... N91-31771
NSF DMS-89-02331 ..... N91-31904
NSF MSM-88-06257 ..... N91-31679
N00014-82-K-0280 ..... N91-31266
N00014-86-K-0246 ..... N91-32001
N00014-86-K-0392 ..... N91-31875
N00014-86-K-0531 ..... N91-31951
N00014-87-K-0231 ..... N91-31812
N00014-87-K-0378 ..... N91-31313
N00014-87-K-0429 ..... N91-31691
N00014-88-C-0681 ..... N91-31543
N00014-89-F-0072 ..... N91-31242
N00014-89-J-1104 ..... N91-31771
N00014-89-J-1237 ..... N91-31264
N00014-89-J-1456 ..... N91-31492
N00014-89-J-1627 ..... N91-31919
N91-31920
N00014-89-J-1659 ..... N91-31858
N00014-89-J-1946 ..... N91-31659
N00014-89-J-1988 ..... N91-31811
N00014-89-J-1991 ..... N91-31267
N00014-90-J-1030 ..... N91-31691
N91-31915
N00014-90-J-1270 ..... N91-31536
N00014-90-J-1559 ..... N91-31310
N00014-90-J-1761 ..... N91-31984
N00014-90-K-2018 ..... N91-31665
N00014-91-C-0014 ..... N91-31663
N91-31664
N00014-91-C-0102 ..... N91-31249
N00014-91-C-2057 ..... N91-31535
N00039-84-C-0211 ..... N91-31857
N91-31912
RDMF3-86 ..... N91-31566
STPA-85-95-004/46 ..... N91-31584
STPA-87-96-008-00-471-75-81 ..... N91-31231
STPA-88-96-009 ..... N91-31305
STPA-89-95-004-52 ..... N91-31096
STPA-8595009 ..... N91-31089
W-31-109-ENG-38 ..... N91-31250
N91-31278
N91-31299
N91-31519
N91-31674
N91-31701
N91-31709
N91-31721
N91-31888
N91-31935
N91-31967
N91-31968
N91-31976
W-7405-ENG-36 ..... N91-31210
N91-31211
N91-31259
N91-31275
N91-31276
N91-31287
N91-31477
N91-31491
N91-31602
N91-31610
N91-31639
N91-31640
N91-31672
N91-31673
N91-31690
N91-31694
N91-31710
N91-31711
N91-31818
N91-31869
N91-31886
N91-31929
N91-31932
N91-31933
N91-31940
N91-31945
N91-31955
N91-31958
N91-31979
W-7405-ENG-48 ..... N91-31252
N91-31274
N91-31298
N91-31314
N91-31315
N91-31316
N91-31520
N91-31521
N91-31572
N91-31642
N91-31658
N91-31675
N91-31698
N91-31717
N91-31718
N91-31719
N91-31748
N91-31749
N91-31763
N91-31815
N91-32031
W-7405-ENG-82 ..... N91-31688
N91-31968
199-61-12 ..... N91-31775
474-46-10 ..... N91-31708
476-50-02-02 ..... N91-31201
505-61-51 ..... N91-31078
505-62-OK N91-31178
505-62-0U N91-31876
505-62-21 ..... N91-31597
N91-31911
505-62-52 ..... N91-31106
505-63-01-05 ..... N91-31677
505-63-36 ..... N91-31138
N91-31139
N91-31654
505-63-36-01 ..... N91-31679
N91-31687
505-63-40 ..... N91-31470
505-63-50-04 ..... N91-31692
505-63-51 ..... N91-31648
505-63-53 ..... N91-31685
N91-31686
505-64-10-05 ..... N91-31531
505-64-13-01 ..... N91-31143
505-90-52-01 ..... N91-31576
N91-31888
N91-31889
506-40-41-02 ..... N91-31595
506-41-11 ..... N91-31196
N91-31217
N91-31218
N91-31977
506-42-31 ..... N91-31212
N91-31216
N91-31605
506-42-72 ..... N91-31220
N91-31318
509-10-02-03 ..... N91-31082
510-01-50 ..... N91-31235
535-03-11-02 ..... N91-31923
535-03-11-03 ..... N91-31926
N91-31927
537-01-11 ..... N91-31181
582-01-21 ..... N91-31208
582-01-41 ..... N91-31219
590-11-22-01 ..... N91-31879
590-14-11-02 ..... N91-31609
590-21-41 ..... N91-31209
643-10-05 ..... N91-31499

Typical Report Number Index Listing

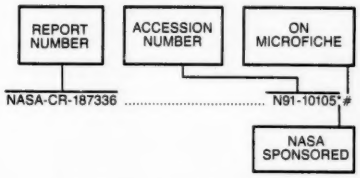

Listings in this index are arranged alphanumerically by report number. The accession number denotes the number by which the citation is identified. An asterisk (*) indicates that the item is a NASA report. A pound sign (#) indicates that the item is available on microfiche.

A-90059 ..... N91-31775* #
A-90083 ..... N91-31078* #

AAAF-NT-89-01 ..... N91-31097 #
AAAF-NT-89-02 ..... N91-31137 #
AAAF-NT-89-03 ..... N91-31098 #
AAAF-NT-89-04 ..... N91-31099 #
AAAF-NT-89-05 ..... N91-31100 #
AAAF-NT-89-06 ..... N91-31637 #
AAAF-NT-89-07 ..... N91-31101 #
AAAF-NT-89-08 ..... N91-31102 #
AAAF-NT-89-09 ..... N91-31103 #
AAAF-NT-89-10 ..... N91-31587 #
AAAF-NT-89-11 ..... N91-31187 #
AAAF-NT-89-13 ..... N91-31104 #
AAAF-NT-89-14 ..... N91-31105 #
AAAF-NT-89-15 ..... N91-31588 #
AAAF-NT-89-16 ..... N91-31188 #
AAAF-NT-89-17 ..... N91-31589 #
AAAF-NT-89-18 ..... N91-31590 #
AAAF-NT-89-19 ..... N91-31847 #
AAAF-NT-89-21 ..... N91-31848 #
AAAF-NT-89-22 ..... N91-31849 #
AAAF-NT-89-23 ..... N91-31850 #
AAAF-NT-89-24 ..... N91-31591 #
AAAF-NT-89-25 ..... N91-31592 #
AAAF-NT-89-26 ..... N91-31593 #
AAAF-NT-89-27 ..... N91-31851 #

AD-A229346 ..... N91-31771 #
AD-A233796 ..... N91-31960 #
AD-A236504 ..... N91-31246 #
AD-A238313 ..... N91-31249 #
AD-A239354 ..... N91-31191 #
AD-A239356 ..... N91-31534 #
AD-A239358 ..... N91-31856 #
AD-A239359 ..... N91-31241 #
AD-A239361 ..... N91-31535 #
AD-A239365 ..... N91-31612 #
AD-A239376 ..... N91-31310 #
AD-A239382 ..... N91-31875 #
AD-A239388 ..... N91-31754 #
AD-A239393 ..... N91-31765 #
AD-A239394 ..... N91-31264 #
AD-A239395 ..... N91-31857 #
AD-A239397 ..... N91-31311 #
AD-A239398 ..... N91-31312 #
AD-A239417 ..... N91-31205 #
AD-A239419 ..... N91-31912 #
AD-A239423 ..... N91-31999 #
AD-A239435 ..... N91-32000 #
AD-A239442 ..... N91-31766 #
AD-A239452 ..... N91-31772 #
AD-A239455 ..... N91-31811 #
AD-A239457 ..... N91-31858 #
AD-A239459 ..... N91-31536 #
AD-A239460 ..... N91-31643 #
AD-A239461 ..... N91-31757 #
AD-A239464 ..... N91-31079 #
AD-A239465 ..... N91-31537 #
AD-A239467 ..... N91-31804 #

AD-A239470 ..... N91-31859 #
AD-A239488 ..... N91-32011 #
AD-A239490 ..... N91-32001 #
AD-A239493 ..... N91-31767 #
AD-A239496 ..... N91-31697 #
AD-A239504 ..... N91-31538 #
AD-A239507 ..... N91-31539 #
AD-A239509 ..... N91-31242 #
AD-A239511 ..... N91-31141 #
AD-A239512 ..... N91-31805 #
AD-A239515 ..... N91-31919 #
AD-A239518 ..... N91-31951 #
AD-A239520 ..... N91-31739 #
AD-A239521 ..... N91-31812 #
AD-A239524 ..... N91-31192 #
AD-A239530 ..... N91-31265 #
AD-A239531 ..... N91-31243 #
AD-A239532 ..... N91-31540 #
AD-A239533 ..... N91-31501 #
AD-A239534 ..... N91-31502 #
AD-A239535 ..... N91-31503 #
AD-A239544 ..... N91-31266 #
AD-A239545 ..... N91-31504 #
AD-A239546 ..... N91-31244 #
AD-A239547 ..... N91-31505 #
AD-A239552 ..... N91-31541 #
AD-A239558 ..... N91-31193 #
AD-A239560 ..... N91-31245 #
AD-A239561 ..... N91-31768 #
AD-A239562 ..... N91-31506 #
AD-A239567 ..... N91-31507 #
AD-A239573 ..... N91-31542 #
AD-A239574 ..... N91-31773 #
AD-A239578 ..... N91-31952 #
AD-A239579 ..... N91-31913 #
AD-A239596 ..... N91-31659 #
AD-A239597 ..... N91-31860 #
AD-A239602 ..... N91-31740 #
AD-A239603 ..... N91-31741 #
AD-A239618 ..... N91-31806 #
AD-A239629 ..... N91-31508 #
AD-A239636 ..... N91-31509 #
AD-A239639 ..... N91-31983 #
AD-A239640 ..... N91-31758 #
AD-A239645 ..... N91-31914 #
AD-A239646 ..... N91-31691 #
AD-A239647 ..... N91-31915 #
AD-A239656 ..... N91-31953 #
AD-A239659 ..... N91-31742 #
AD-A239660 ..... N91-31920 #
AD-A239662 ..... N91-31861 #
AD-A239665 ..... N91-31807 #
AD-A239672 ..... N91-31644 #
AD-A239673 ..... N91-31743 #
AD-A239674 ..... N91-31954 #
AD-A239676 ..... N91-31121 #
AD-A239690 ..... N91-31313 #
AD-A239691 ..... N91-31862 #
AD-A239704 ..... N91-31510 #
AD-A239708 ..... N91-31774 #
AD-A239710 ..... N91-31769 #
AD-A239714 ..... N91-31808 #
AD-A239717 ..... N91-31267 #
AD-A239719 ..... N91-31984 #
AD-A239723 ..... N91-31122 #
AD-A239724 ..... N91-31123 #
AD-A239726 ..... N91-31124 #
AD-A239734 ..... N91-31663 #
AD-A239766 ..... N91-31543 #
AD-A239769 ..... N91-31664 #
AD-A239770 ..... N91-31665 #
AD-A239774 ..... N91-31770 #
AD-A239780 ..... N91-31959 #
AD-A239781 ..... N91-31809 #

AD-E501420 ..... N91-31862 #

AD-M000073 ..... N91-31861 #

AFIT/CI/CIA-91-004D ..... N91-31191 #
AFIT/CI/CIA-91-026 ..... N91-31312 #
AFIT/CI/CIA-91-028 ..... N91-31804 #
AFIT/CI/CIA-91-046 ..... N91-31856 #

AFIT/CI/CIA-91-049 ..... N91-31205 #
AFIT/CI/CIA-91-054 ..... N91-31757 #
AFIT/CI/CIA-91-055 ..... N91-31534 #
AFIT/CI/CIA-91-058 ..... N91-31643 #
AFIT/CI/CIA-91-062 ..... N91-31241 #
AFIT/CI/CIA-91-063 ..... N91-32011 #

AGARD-CP-480 ..... N91-31144 #

AIAA-91-2121 ..... N91-31605* #
AIAA-91-2227 ..... N91-31216* #
AIAA-91-2347 ..... N91-31212* #
AIAA-91-2355 ..... N91-31181* #
AIAA-91-3604 ..... N91-31209* #
AIAA-91-4007 ..... N91-31470* #

ANL/CP-72014 ..... N91-31721 #
ANL/CP-72558 ..... N91-31299 #
ANL/CP-72765 ..... N91-31674 #
ANL/CP-72869 ..... N91-31935 #
ANL/CP-72997 ..... N91-31976 #
ANL/CP-73328 ..... N91-31250 #
ANL/CP-73336 ..... N91-31967 #
ANL/CP-73352 ..... N91-31519 #
ANL/CP-73398 ..... N91-31968 #
ANL/CP-73552 ..... N91-31278 #

ANL/ESD/TM-15 ..... N91-31709 #

AR-004-540 ..... N91-31676 #
AR-006-615 ..... N91-31179 #

ARCCB-TR-91024 ..... N91-31913 #

ARI-RN-91-76 ..... N91-31542 #
ARI-RN-91-78 ..... N91-31774 #
ARI-RN-91-81 ..... N91-31773 #
ARI-RN-91-82 ..... N91-31772 #

ARL-MAT-TM-405 ..... N91-31179 #

ARL-STRUC-R-427 ..... N91-31676 #

ARO-25089.12-EL ..... N91-31504 #
ARO-25344.14-MS ..... N91-31244 #
ARO-25611.1-EL ..... N91-31983 #
ARO-26274.1-EL ..... N91-31509 #

ASSGI-TR-20 ..... N91-31486

ASSGI-14SV-W7714-7-5353 ..... N91-31486
ASSGI-167 ..... N91-31478 #

AVSCOM-TM-90-C-011 ..... N91-31876* #

AVSCOM-TR-90-C-014 ..... N91-31648* #
AVSCOM-TR-91-B-006 ..... N91-31687* #
AVSCOM-TR-91-C-016 ..... N91-31178* #
AVSCOM-TR-91-C-022 ..... N91-31654* #
AVSCOM-TR-91-C-029 ..... N91-31181* #

BAE-FBS-007 ..... N91-31729

BN-1119 ..... N91-31914 #
BN-1123 ..... N91-31691 #
BN-1125 ..... N91-31915 #

BNL-46300 ..... N91-31320 #
BNL-46378 ..... N91-31720 #
BNL-46391 ..... N91-31756 #
BNL-46400 ..... N91-31972 #
BNL-46470 ..... N91-31982 #
BNL-46475 ..... N91-31981 #
BNL-52290 ..... N91-31942 #

CA-PATENT-APPL-SN-2-009-634 ..... N91-31174
CA-PATENT-APPL-SN-2-009-635 ..... N91-31175
CA-PATENT-APPL-SN-2-009-636 ..... N91-31176

CD-RPT-ITL-5043-003 ..... N91-31482

CMOTT-91-05 ..... N91-31597* #

CNES-CT/DTI/MS/CM/290 ..... N91-31202 #

CNES-NT-126 ..... N91-31202 #
CNES-NT-127 ..... N91-31474 #
CNES-NT-128 ..... N91-31195 #

CONF-900280-VOL-1 ..... N91-31520 #
CONF-900280-VOL-2 ..... N91-31521 #
CONF-900397-ABSTS ..... N91-31491 #
CONF-900520-4 ..... N91-31292 #
CONF-900520-5 ..... N91-31293 #
CONF-900520-6 ..... N91-31248 #
CONF-900546-7 ..... N91-31291 #
CONF-901035-19 ..... N91-31982 #
CONF-910406-33 ..... N91-31978 #
CONF-910505-394 ..... N91-31981 #
CONF-910580-2 ..... N91-31969 #
CONF-910623-2 ..... N91-31611 #
CONF-910624-4 ..... N91-31688 #
CONF-910640-28 ..... N91-31518 #
CONF-910646-4 ..... N91-31302 #
CONF-910707-3 ..... N91-31286 #
CONF-910707-4 ..... N91-31308 #
CONF-910710-1 ..... N91-31972 #
CONF-910730-2 ..... N91-31935 #
CONF-910736-8 ..... N91-31979 #
CONF-910736-12 ..... N91-31976 #
CONF-910742-1 ..... N91-31720 #
CONF-910755-1 ..... N91-31237 #
CONF-910771-3 ..... N91-31818 #
CONF-910774-62 ..... N91-31886 #
CONF-910774-63 ..... N91-31854 #
CONF-910801-9 ..... N91-31967 #
CONF-910801-13 ..... N91-31519 #
CONF-910817-20 ..... N91-31299 #
CONF-910817-22 ..... N91-31674 #
CONF-910819-1 ..... N91-31721 #
CONF-910872-7 ..... N91-31975 #
CONF-910957-2 ..... N91-31689 #
CONF-910993-11 ..... N91-31933 #
CONF-911003-1 ..... N91-31277 #
CONF-911003-2 ..... N91-31650 #
CONF-911003-3 ..... N91-31649 #
CONF-911025-1 ..... N91-31314 #
CONF-911047-1 ..... N91-31517 #
CONF-911047-2 ..... N91-31966 #
CONF-911047-3 ..... N91-31472 #
CONF-911047-4 ..... N91-31710 #
CONF-911047-5 ..... N91-31259 #
CONF-911069-1 ..... N91-31672 #
CONF-911069-2 ..... N91-31634 #
CONF-911069-3 ..... N91-31275 #
CONF-911069-5 ..... N91-31673 #
CONF-911069-6 ..... N91-31276 #
CONF-911069-7 ..... N91-31298 #
CONF-911070-2 ..... N91-31230 #
CONF-911084-1 ..... N91-31301 #
CONF-911087-1 ..... N91-31532 #
CONF-9008166-2 ..... N91-32016 #
CONF-9010291-2 ..... N91-31930 #
CONF-9011119-5 ..... N91-31316 #
CONF-9012103-2 ..... N91-31473 #
CONF-9103196-1 ..... N91-32010 #
CONF-9104158-6 ..... N91-31870 #
CONF-9104192-14 ..... N91-31642 #
CONF-9104249-2 ..... N91-31816 #
CONF-9104280-1 ..... N91-31763 #
CONF-9104282-1 ..... N91-31719 #
CONF-9105106-24 ..... N91-31932 #
CONF-9105107-1 ..... N91-31272 #
CONF-9105116 ..... N91-31701 #
CONF-9105130-5 ..... N91-31278 #
CONF-9105147-2 ..... N91-31970 #
CONF-9105172-3 ..... N91-31287 #
CONF-9105184-12 ..... N91-31240 #
CONF-9105232-1 ..... N91-31698 #
CONF-9105238-2 ..... N91-31931 #
CONF-9105243-1 ..... N91-32018 #
CONF-9106176-4 ..... N91-31254 #
CONF-9106180-1 ..... N91-31250 #
CONF-9106231-2 ..... N91-31948 #
CONF-9106249-1 ..... N91-31252 #
CONF-9106253-1 ..... N91-31303 #
CONF-9106254-1 ..... N91-31756 #
CONF-9106255-1 ..... N91-31320 #
CONF-9107105-49 ..... N91-31309 #
CONF-9107115-14 ..... N91-31572 #
CONF-9107115-16 ..... N91-31602 #
CONF-9107115-20 ..... N91-31610 #
CONF-9107115-23 ..... N91-31639 #
CONF-9107115-25 ..... N91-31640 #
CONF-9107143-1 ..... N91-31968 #
CONF-9107146-1 ..... N91-31971 #
CONF-9107149 ..... N91-31703 #
CONF-9107157-1 ..... N91-31238 #
CONF-9108117-1 ..... N91-31694 #

CONF-9109108-4 ..... N91-31958 #
CONF-9109108-5 ..... N91-31955 #
CONF-9109201-1 ..... N91-31711 #
CONF-9109208-1 ..... N91-31980 #
CONF-9109226-1 ..... N91-31211 #
CONF-9109226-3 ..... N91-31945 #
CONF-9109226-4 ..... N91-31940 #
CONF-9109226-7 ..... N91-31221 #
CONF-9109228-1 ..... N91-31500 #
CONF-9110103-1 ..... N91-31274 #
CONF-9110123-1 ..... N91-31815 #
CONF-9110125-1 ..... N91-31868 #
CONF-9110125-2 ..... N91-31869 #
CONF-9110159-1 ..... N91-31490 #
CONF-9110161-2 ..... N91-31717 #
CONF-9110161-3 ..... N91-31718 #
CONF-9110161-4 ..... N91-31748 #
CONF-9110161-5 ..... N91-31749 #
CONF-9110164-1 ..... N91-31315 #
CONF-9110171-1 ..... N91-31988 #

CRC-W7714-7-5271 ..... N91-31485

CS-8906 ..... N91-31823 #
CS-9101 ..... N91-31821 #
CS-9102 ..... N91-31822 #
CS-9103 ..... N91-31893 #
CS-9104 ..... N91-31894 #
CS-9105 ..... N91-31823 #

CSDL-T-1086 ..... N91-31205 #

CTN-91-60026 ..... N91-31125 #
CTN-91-60129 ..... N91-31478 #
CTN-91-60131 ..... N91-31182
CTN-91-60133 ..... N91-31511
CTN-91-60134 ..... N91-31512
CTN-91-60135 ..... N91-31126
CTN-91-60136 ..... N91-31174
CTN-91-60137 ..... N91-31175
CTN-91-60138 ..... N91-31176
CTN-91-60139 ..... N91-31224
CTN-91-60140 ..... N91-31268
CTN-91-60143 ..... N91-31479
CTN-91-60144 ..... N91-31107
CTN-91-60145 ..... N91-31269
CTN-91-60147 ..... N91-31294
CTN-91-60151 ..... N91-31177
CTN-91-60153 ..... N91-31206
CTN-91-60154 ..... N91-31513
CTN-91-60155 ..... N91-31598
CTN-91-60156 ..... N91-31599
CTN-91-60158 ..... N91-31480
CTN-91-60159 ..... N91-31481
CTN-91-60160 ..... N91-31142
CTN-91-60161 ..... N91-31514
CTN-91-60162 ..... N91-31660
CTN-91-60164 ..... N91-31127
CTN-91-60165 ..... N91-31270
CTN-91-60168 ..... N91-31108
CTN-91-60169 ..... N91-31271
CTN-91-60170 ..... N91-31693
CTN-91-60171 ..... N91-31115
CTN-91-60172 ..... N91-31946
CTN-91-60173 ..... N91-31116
CTN-91-60174 ..... N91-31207
CTN-91-60175 ..... N91-31600
CTN-91-60178 ..... N91-31482
CTN-91-60179 ..... N91-31483
CTN-91-60197 ..... N91-31801
CTN-91-60199 ..... N91-31484
CTN-91-60200 ..... N91-31922
CTN-91-60201 ..... N91-31199
CTN-91-60203 ..... N91-31485
CTN-91-60204 ..... N91-31486
CTN-91-60214 ..... N91-31515
CTN-91-60216 ..... N91-31295

CU-153-0638 ..... N91-31773 #

DCIEM-90-P-14 ..... N91-31801
DCIEM-91-45 ..... N91-31541 #

DCR/I-03357-90 ..... N91-31305 #

DE90-012164 ..... N91-31291 #
DE91-009961 ..... N91-31672 #
DE91-010581 ..... N91-31230 #
DE91-011221 ..... N91-31222 #
DE91-011325 ..... N91-31634 #
DE91-011963 ..... N91-31274 #
DE91-012016 ..... N91-31292 #
DE91-012649 ..... N91-31517 #
DE91-012877 ..... N91-31615 #
DE91-013029 ..... N91-31275 #
DE91-013106 ..... N91-31966 #

DE91-013260 ..... N91-31293 #
DE91-013280 ..... N91-31247 #
DE91-013379 ..... N91-31673 #
DE91-013390 ..... N91-31276 #
DE91-013510 ..... N91-31868 #
DE91-013608 ..... N91-31716 #
DE91-013744 ..... N91-31472 #
DE91-013936 ..... N91-31986 #
DE91-013937 ..... N91-31985 #
DE91-014213 ..... N91-31649 #
DE91-014263 ..... N91-31650 #
DE91-014279 ..... N91-31277 #
DE91-014654 ..... N91-31248 #
DE91-014704 ..... N91-31272 #
DE91-014780 ..... N91-31869 #
DE91-014985 ..... N91-31698 #
DE91-014992 ..... N91-31314 #
DE91-015108 ..... N91-31250 #
DE91-015111 ..... N91-31298 #
DE91-015161 ..... N91-31688 #
DE91-015318 ..... N91-31929 #
DE91-015337 ..... N91-31518 #
DE91-015340 ..... N91-31490 #
DE91-015447 ..... N91-31759 #
DE91-015451 ..... N91-31319 #
DE91-015487 ..... N91-32031 #
DE91-015524 ..... N91-31223 #
DE91-015548 ..... N91-31278 #
DE91-015568 ..... N91-31967 #
DE91-015570 ..... N91-31968 #
DE91-015575 ..... N91-31251 #
DE91-015625 ..... N91-31651 #
DE91-015632 ..... N91-31969 #
DE91-015642 ..... N91-31970 #
DE91-015646 ..... N91-31699 #
DE91-015652 ..... N91-31938 #
DE91-015673 ..... N91-31674 #
DE91-015680 ..... N91-31299 #
DE91-015686 ..... N91-31252 #
DE91-015689 ..... N91-31763 #
DE91-015695 ..... N91-31717 #
DE91-015696 ..... N91-31718 #
DE91-015697 ..... N91-31748 #
DE91-015701 ..... N91-31930 #
DE91-015707 ..... N91-31816 #
DE91-015719 ..... N91-31971 #
DE91-015721 ..... N91-31519 #
DE91-015735 ..... N91-31675 #
DE91-015743 ..... N91-31700 #
DE91-015750 ..... N91-31652 #
DE91-015757 ..... N91-31638 #
DE91-015767 ..... N91-31315 #
DE91-015769 ..... N91-31749 #
DE91-015770 ..... N91-31316 #
DE91-015771 ..... N91-31719 #
DE91-015772 ..... N91-31572 #
DE91-015774 ..... N91-31520 #
DE91-015775 ..... N91-31521 #
DE91-015796 ..... N91-31939 #
DE91-015836 ..... N91-31720 #
DE91-015837 ..... N91-31756 #
DE91-015838 ..... N91-31972 #
DE91-015846 ..... N91-31320 #
DE91-015850 ..... N91-31237 #
DE91-015901 ..... N91-31978 #
DE91-015911 ..... N91-31973 #
DE91-015915 ..... N91-31300 #
DE91-015921 ..... N91-31532 #
DE91-015922 ..... N91-31238 #
DE91-015923 ..... N91-31301 #
DE91-015930 ..... N91-31286 #
DE91-015931 ..... N91-31308 #
DE91-015973 ..... N91-31709 #
DE91-015974 ..... N91-31701 #
DE91-015976 ..... N91-31491 #
DE91-015977 ..... N91-31210 #
DE91-015988 ..... N91-31721 #
DE91-016014 ..... N91-31710 #
DE91-016015 ..... N91-31259 #
DE91-016016 ..... N91-31886 #
DE91-016020 ..... N91-31711 #
DE91-016022 ..... N91-31955 #
DE91-016025 ..... N91-31958 #
DE91-016032 ..... N91-31945 #
DE91-016033 ..... N91-31940 #
DE91-016036 ..... N91-31211 #
DE91-016043 ..... N91-31287 #
DE91-016055 ..... N91-31702 #
DE91-016056 ..... N91-31573 #
DE91-016061 ..... N91-31602 #
DE91-016062 ..... N91-31703 #
DE91-016063 ..... N91-31574 #
DE91-016071 ..... N91-31639 #
DE91-016079 ..... N91-31640 #
DE91-016081 ..... N91-31602 #
DE91-016084 ..... N91-31610 #

DE91-016085 ..... N91-31979 #
DE91-016086 ..... N91-31932 #
DE91-016091 ..... N91-31933 #
DE91-016095 ..... N91-31934 #
DE91-016096 ..... N91-31253 #
DE91-016102 ..... N91-31704 #
DE91-016111 ..... N91-31998 #
DE91-016119 ..... N91-31302 #
DE91-016121 ..... N91-31303 #
DE91-016208 ..... N91-31941 #
DE91-016221 ..... N91-31931 #
DE91-016241 ..... N91-31817 #
DE91-016248 ..... N91-31254 #
DE91-016252 ..... N91-31948 #
DE91-016258 ..... N91-31974 #
DE91-016260 ..... N91-32016 #
DE91-016263 ..... N91-31279 #
DE91-016276 ..... N91-31870 #
DE91-016300 ..... N91-31818 #
DE91-016308 ..... N91-31694 #
DE91-016343 ..... N91-31280 #
DE91-016401 ..... N91-31500 #
DE91-016404 ..... N91-31854 #
DE91-016405 ..... N91-31988 #
DE91-016407 ..... N91-31689 #
DE91-016408 ..... N91-31980 #
DE91-016409 ..... N91-31575 #
DE91-016416 ..... N91-32018 #
DE91-016418 ..... N91-32010 #
DE91-016420 ..... N91-31288 #
DE91-016422 ..... N91-31473 #
DE91-016427 ..... N91-31975 #
DE91-016451 ..... N91-31712 #
DE91-016453 ..... N91-31255 #
DE91-016475 ..... N91-31256 #
DE91-016477 ..... N91-31657 #
DE91-016478 ..... N91-31819 #
DE91-016479 ..... N91-31257 #
DE91-016480 ..... N91-31652 #
DE91-016486 ..... N91-31281 #
DE91-016488 ..... N91-31764 #
DE91-016500 ..... N91-31522 #
DE91-016501 ..... N91-31523 #
DE91-016502 ..... N91-31658 #
DE91-016526 ..... N91-31976 #
DE91-016527 ..... N91-31935 #
DE91-016530 ..... N91-31260 #
DE91-016600 ..... N91-31289 #
DE91-016602 ..... N91-31261 #
DE91-016612 ..... N91-31942 #
DE91-016648 ..... N91-31309 #
DE91-016740 ..... N91-31262 #
DE91-016745 ..... N91-31936 #
DE91-016747 ..... N91-31937 #
DE91-016748 ..... N91-31239 #
DE91-016751 ..... N91-31641 #
DE91-016778 ..... N91-31240 #
DE91-016813 ..... N91-31690 #
DE91-016815 ..... N91-31477 #
DE91-016819 ..... N91-31190 #
DE91-016843 ..... N91-31722 #
DE91-016863 ..... N91-31533 #
DE91-016866 ..... N91-31713 #
DE91-016868 ..... N91-31714 #
DE91-016870 ..... N91-31715 #
DE91-016928 ..... N91-31642 #
DE91-016934 ..... N91-31855 #
DE91-016948 ..... N91-31263 #
DE91-016949 ..... N91-31290 #
DE91-016995 ..... N91-31981 #
DE91-017008 ..... N91-31982 #
DE91-017009 ..... N91-31611 #
DE91-017066 ..... N91-31221 #
DE91-618657 ..... N91-31666 #

DLR-MITT-90-18 ..... N91-31185 #

DM-57 ..... N91-31747 #

DOE/CH-10418/1 ..... N91-31712 #

DOE/ER-0144/9 ..... N91-31222 #
DOE/ER-03065/T9 ..... N91-31939 #
DOE/ER-03130/270 ..... N91-31941 #
DOE/ER-13034/T1 ..... N91-31575 #
DOE/ER-13251/T1 ..... N91-31704 #
DOE/ER-13666/T3 ..... N91-31262 #
DOE/ER-13914/14 ..... N91-31700 #
DOE/ER-13954/T1 ..... N91-31256 #
DOE/ER-13954/3 ..... N91-31255 #
DOE/ER-14129/1 ..... N91-31289 #
DOE/ER-14143/1 ..... N91-31253 #
DOE/ER-40319/4 ..... N91-31938 #
DOE/ER-40425/253 ..... N91-31936 #
DOE/ER-40531/2 ..... N91-31937 #
DOE/ER-45058/7 ..... N91-31641 #
DOE/ER-45163/26 ..... N91-31263 #
DOE/ER-45312/4 ..... N91-31239 #
DOE/ER-45320/4 ..... N91-31973 #
DOE/ER-45392/3 ..... N91-31281 #
DOE/ER-45403/2 ..... N91-31934 #
DOE/ER-60434/6 ..... N91-31764 #
DOE/ER-60438/T3 ..... N91-31759 #
DOE/ER-60444/2 ..... N91-31722 #
DOE/ER-75498/5 ..... N91-31986 #
DOE/ER-75498/6 ..... N91-31985 #

DOE/NE-37963/16 ..... N91-31290 #

DOE/PC-88867/T10 ..... N91-31260 #
DOE/PC-89877/6 ..... N91-31261 #

DOE/PE-0098P ..... N91-31319 #

DOT/FAA/CT-TN91/20 ..... N91-31495 #
DOT/FAA/CT-TN91/33 ..... N91-31494 #

DOT/FAA/CT-91/1 ..... N91-31814 #

DRE-179 ..... N91-31484

DREA-CR-88-421 ..... N91-31295

DREO-W7714-8-5620 ..... N91-31483

E-5097 ..... N91-31208* #
E-6098 ..... N91-31178* #
E-6210 ..... N91-31648* #
E-6253 ..... N91-31876* #
E-6279 ..... N91-31181* #
E-6319 ..... N91-31235* #
E-6326 ..... N91-31654* #
E-6366 ..... N91-31218* #
E-6409 ..... N91-31216* #
E-6414 ..... N91-31220* #
E-6438 ..... N91-31212* #
E-6454 ..... N91-31605* #
E-6506 ..... N91-31911* #
E-6509 ..... N91-31977* #
E-6522 ..... N91-31106* #
E-6536 ..... N91-31217* #
E-6541 ..... N91-31196* #
E-6552 ..... N91-31708* #
E-6562 ..... N91-31597* #
E-6565 ..... N91-31209* #
E-6594 ..... N91-31318* #

ECL-90-15 ..... N91-31091 #
ECL-90-17 ..... N91-31883 #
ECL-90-24 ..... N91-31527 #
ECL-90-27 ..... N91-31525 #
ECL-91-01 ..... N91-31681 #
ECL-91-04 ..... N91-31526 #

EGG-2645 ..... N91-31223 #
EGG-10617-2096 ..... N91-31966 #

ESA-SP-1132 ..... N91-31321 #

ESD-TR-91-058 ..... N91-31743 #
ESD-TR-91-062 ..... N91-31644 #
ESD-TR-91-108 ..... N91-31954 #

ETL-0573 ..... N91-31697 #

ETN-91-90004 ..... N91-31872
ETN-91-90005 ..... N91-31873
ETN-91-90006 ..... N91-31496
ETN-91-90007 ..... N91-32023 #
ETN-91-90008 ..... N91-31497
ETN-91-90009 ..... N91-31752
ETN-91-90017 ..... N91-31957*
ETN-91-90018 ..... N91-32009*
ETN-91-90019 ..... N91-32017
ETN-91-99418 ..... N91-31117 #
ETN-91-99424 ..... N91-31695 #
ETN-91-99438 ..... N91-31132 #
ETN-91-99515 ..... N91-31995
ETN-91-99525 ..... N91-31943 #
ETN-91-99531 ..... N91-31321 #
ETN-91-99533 ..... N91-31202 #
ETN-91-99534 ..... N91-31474 #
ETN-91-99535 ..... N91-31195 #
ETN-91-99561 ..... N91-31185 #
ETN-91-99574 ..... N91-31891 #
ETN-91-99576 ..... N91-31892 #
ETN-91-99577 ..... N91-31577 #
ETN-91-99578 ..... N91-31916 #
ETN-91-99579 ..... N91-31821 #
ETN-91-99580 ..... N91-31822 #
ETN-91-99581 ..... N91-31893 #
ETN-91-99582 ..... N91-31894 #
ETN-91-99583 ..... N91-31623 #
ETN-91-99584 ..... N91-31880 #
ETN-91-99585 ..... N91-31824 #
ETN-91-99586 ..... N91-31825 #
ETN-91-99587 ..... N91-31895 #
ETN-91-99588 ..... N91-31996 #
ETN-91-99589 ..... N91-31826 #
ETN-91-99590 ..... N91-31827 #
ETN-91-99591 ..... N91-31997 #
ETN-91-99592 ..... N91-31896 #
ETN-91-99593 ..... N91-31897 #
ETN-91-99594 ..... N91-31828 #
ETN-91-99595 ..... N91-31829 #
ETN-91-99596 ..... N91-31898 #
ETN-91-99597 ..... N91-31899 #
ETN-91-99598 ..... N91-31830 #
ETN-91-99599 ..... N91-31831 #
ETN-91-99600 ..... N91-31832 #
ETN-91-99601 ..... N91-31900 #
ETN-91-99602 ..... N91-31833 #
ETN-91-99603 ..... N91-31834 #
ETN-91-99604 ..... N91-31835 #
ETN-91-99605 ..... N91-31901 #
ETN-91-99606 ..... N91-31917 #
ETN-91-99607 ..... N91-31921 #
ETN-91-99608 ..... N91-31836 #
ETN-91-99609 ..... N91-31837 #
ETN-91-99610 ..... N91-31838 #
ETN-91-99611 ..... N91-31902 #
ETN-91-99612 ..... N91-31903 #
ETN-91-99613 ..... N91-31839 #
ETN-91-99614 ..... N91-31118 #
ETN-91-99629 ..... N91-31918 #
ETN-91-99637 ..... N91-31878 #
ETN-91-99643 ..... N91-31131 #
ETN-91-99647 ..... N91-31081 #
ETN-91-99652 ..... N91-31282 #
ETN-91-99654 ..... N91-31133 #
ETN-91-99655 ..... N91-31084 #
ETN-91-99656 ..... N91-31119 #
ETN-91-99657 ..... N91-31578 #
ETN-91-99658 ..... N91-31579 #
ETN-91-99659 ..... N91-31887 #
ETN-91-99700 ..... N91-31493 #
ETN-91-99702 ..... N91-31863 #
ETN-91-99706 ..... N91-31840 #
ETN-91-99710 ..... N91-31841 #
ETN-91-99711 ..... N91-31904 #
ETN-91-99712 ..... N91-31905 #
ETN-91-99713 ..... N91-31906 #
ETN-91-99714 ..... N91-31842 #
ETN-91-99715 ..... N91-31843 #
ETN-91-99716 ..... N91-31580 #
ETN-91-99717 ..... N91-31907 #
ETN-91-99718 ..... N91-31908 #
ETN-91-99719 ..... N91-31909 #
ETN-91-99720 ..... N91-31910 #
ETN-91-99721 ..... N91-31844 #
ETN-91-99722 ..... N91-31881 #
ETN-91-99723 ..... N91-31845 #
ETN-91-99736 ..... N91-31489 #
ETN-91-99737 ..... N91-32002 #
ETN-91-99738 ..... N91-31085 #
ETN-91-99739 ..... N91-31581 #
ETN-91-99740 ..... N91-31582 #
ETN-91-99741 ..... N91-31696 #
ETN-91-99742 ..... N91-31283 #
ETN-91-99743 ..... N91-31197 #
ETN-91-99744 ..... N91-31203 #
ETN-91-99746 ..... N91-31284 #
ETN-91-99747 ..... N91-32008 #
ETN-91-99748 ..... N91-31524 #
ETN-91-99749 ..... N91-31882 #
ETN-91-99750 ..... N91-31871 #
ETN-91-99751 ..... N91-31186 #
ETN-91-99752 ..... N91-31304 #
ETN-91-99753 ..... N91-31317 #
ETN-91-99754 ..... N91-31086 #
ETN-91-99755 ..... N91-31183 #
ETN-91-99756 ..... N91-31087 #
ETN-91-99757 ..... N91-31198 #
ETN-91-99758 ..... N91-31635 #
ETN-91-99759 ..... N91-31134 #
ETN-91-99760 ..... N91-31949 #
ETN-91-99761 ..... N91-31705 #
ETN-91-99762 ..... N91-31706 #
ETN-91-99763 ..... N91-31135 #
ETN-91-99764 ..... N91-31088 #
ETN-91-99767 ..... N91-31994
ETN-91-99775 ..... N91-31130 #
ETN-91-99785 ..... N91-31747 #
ETN-91-99836 ..... N91-31729
ETN-91-99903 ..... N91-31551 #
ETN-91-99904 ..... N91-31565 #
ETN-91-99905 ..... N91-31614 #
ETN-91-99906 ..... N91-31625 #

ETN-91-99907 ..... N91-31089 #
ETN-91-99908 ..... N91-31636 #
ETN-91-99910 ..... N91-31090 #
ETN-91-99911 ..... N91-31231 #
ETN-91-99912 ..... N91-31305 #
ETN-91-99913 ..... N91-31583 #
ETN-91-99914 ..... N91-31584 #
ETN-91-99915 ..... N91-31232 #
ETN-91-99916 ..... N91-31233 #
ETN-91-99917 ..... N91-31680 #
ETN-91-99918 ..... N91-31180 #
ETN-91-99919 ..... N91-31091 #
ETN-91-99920 ..... N91-31525 #
ETN-91-99921 ..... N91-31883 #
ETN-91-99922 ..... N91-31526 #
ETN-91-99923 ..... N91-31527 #
ETN-91-99924 ..... N91-31681 #
ETN-91-99925 ..... N91-31285 #
ETN-91-99926 ..... N91-31846
ETN-91-99927 ..... N91-31884
ETN-91-99928 ..... N91-31585 #
ETN-91-99929 ..... N91-31092 #
ETN-91-99930 ..... N91-31093 #
ETN-91-99931 ..... N91-31094 #
ETN-91-99932 ..... N91-31234 #
ETN-91-99933 ..... N91-31682 #
ETN-91-99934 ..... N91-31924 #
ETN-91-99935 ..... N91-31586 #
ETN-91-99936 ..... N91-31095 #
ETN-91-99937 ..... N91-31136 #
ETN-91-99938 ..... N91-31925 #
ETN-91-99939 ..... N91-31111 #
ETN-91-99940 ..... N91-31112 #
ETN-91-99941 ..... N91-31096 #
ETN-91-99942 ..... N91-31097 #
ETN-91-99943 ..... N91-31137 #
ETN-91-99944 ..... N91-31098 #
ETN-91-99945 ..... N91-31099 #
ETN-91-99946 ..... N91-31100 #
ETN-91-99947 ..... N91-31637 #
ETN-91-99948 ..... N91-31101 #
ETN-91-99949 ..... N91-31102 #
ETN-91-99950 ..... N91-31103 #
ETN-91-99951 ..... N91-31587 #
ETN-91-99952 ..... N91-31187 #
ETN-91-99954 ..... N91-31104 #
ETN-91-99955 ..... N91-31105 #
ETN-91-99956 ..... N91-31588 #
ETN-91-99957 ..... N91-31188 #
ETN-91-99958 ..... N91-31589 #
ETN-91-99959 ..... N91-31590 #
ETN-91-99960 ..... N91-31847 #
ETN-91-99962 ..... N91-31848 #
ETN-91-99963 ..... N91-31849 #
ETN-91-99964 ..... N91-31850 #
ETN-91-99965 ..... N91-31591 #
ETN-91-99966 ..... N91-31592 #
ETN-91-99967 ..... N91-31593 #
ETN-91-99968 ..... N91-31851 #
ETN-91-99971 ..... N91-31603 #
ETN-91-99972 ..... N91-31662 #
ETN-91-99973 ..... N91-31761 #
ETN-91-99974 ..... N91-31594 #
ETN-91-99975 ..... N91-31184 #
ETN-91-99976 ..... N91-31189 #
ETN-91-99977 ..... N91-31604 #
ETN-91-99980 ..... N91-31475 #
ETN-91-99981 ..... N91-31683 #
ETN-91-99982 ..... N91-31306 #
ETN-91-99983 ..... N91-31987 #
ETN-91-99984 ..... N91-31762 #
ETN-91-99985 ..... N91-31852 #
ETN-91-99988 ..... N91-31498 #

FEL-91-B099 ..... N91-31872
FEL-91-B100 ..... N91-31873
FEL-91-B122 ..... N91-31496

GALCIT-FM-90-3 ..... N91-31267 #

GAO/NSIAD-91-205 ..... N91-31506 #
GAO/NSIAD-91-269 ..... N91-31999 #

GARTEUR-AD(AG07)-TP048 ..... N91-31084 #

GRI-91/0041 ..... N91-31645 #

H-1706 ..... N91-31874* #
H-1738 ..... N91-31470* #

HDL-TM-91-11 ..... N91-31193 #

IC-90/201 ..... N91-31666 #

ICASE-91-27 ..... N91-31889* #
ICASE-91-36 ..... N91-31888* #
ICASE-91-67 ..... N91-31576* #

ICOMP-91-14 ..... N91-31911* #
ICOMP-91-15 ..... N91-31597* #

IDA-D-972 ..... N91-31862 #

IDA/HQ-91-038002 ..... N91-31862 #

ILR-MITT-252(1990) ..... N91-31197 #

IMFL-90/03 ..... N91-31604 #

INT-PATENT-CLASS-B22D-1100 ..... N91-31269
INT-PATENT-CLASS-B23D-21/06 ..... N91-31655*
INT-PATENT-CLASS-B23K-20/08 ..... N91-31476*
INT-PATENT-CLASS-B23Q-3/155 ..... N91-31656*
INT-PATENT-CLASS-B26B-27/00 ..... N91-31655*
INT-PATENT-CLASS-B26D-3/16 ..... N91-31655*
INT-PATENT-CLASS-B32B-7/08 ..... N91-31236*
INT-PATENT-CLASS-B32B-312 ..... N91-31224
INT-PATENT-CLASS-B63C-9/01 ..... N91-31113*
INT-PATENT-CLASS-B64C-1/22 ..... N91-31113*
INT-PATENT-CLASS-B64C-19/00 ..... N91-31140*
INT-PATENT-CLASS-B64C-318 ..... N91-31126
INT-PATENT-CLASS-B64C-2900 ..... N91-31174
INT-PATENT-CLASS-B64C-2900 ..... N91-31176
INT-PATENT-CLASS-B64D-1/08 ..... N91-31113*
INT-PATENT-CLASS-B64D-9/00 ..... N91-31113*
INT-PATENT-CLASS-B64G-1/46 ..... N91-31803* #

INT-PATENT-CLASS-C04B-3510 ..... N91-31294
INT-PATENT-CLASS-C08F-283/00 ..... N91-31307*
INT-PATENT-CLASS-C08F-283/04 ..... N91-31307*
INT-PATENT-CLASS-C08G-16/00 ..... N91-31307*
INT-PATENT-CLASS-C08G-73/10 ..... N91-31307*
INT-PATENT-CLASS-C22C-102 ..... N91-31270
INT-PATENT-CLASS-C22C-903 ..... N91-31270
INT-PATENT-CLASS-C22C-1900 ..... N91-31271
INT-PATENT-CLASS-C22C-1905 ..... N91-31268
INT-PATENT-CLASS-C22F-110 ..... N91-31268

INT-PATENT-CLASS-F02G-140 ..... N91-31174
INT-PATENT-CLASS-F02K-100 ..... N91-31176
INT-PATENT-CLASS-F02K-178 ..... N91-31175
INT-PATENT-CLASS-F02K-930 ..... N91-31207
INT-PATENT-CLASS-F02K-995 ..... N91-31207
INT-PATENT-CLASS-F16B-400 ..... N91-31127
INT-PATENT-CLASS-F16C-2902 ..... N91-31177
INT-PATENT-CLASS-F16L-5900 ..... N91-31206
INT-PATENT-CLASS-F42B-1512 ..... N91-31207
INT-PATENT-CLASS-F42B-15033 ..... N91-31182

INT-PATENT-CLASS-G01C-1916 ..... N91-31142
INT-PATENT-CLASS-G01F-1/00 ..... N91-31596*
INT-PATENT-CLASS-G01K-17/06 ..... N91-31608*
INT-PATENT-CLASS-G01K-17/16 ..... N91-31608*
INT-PATENT-CLASS-G01N-2318 ..... N91-31660
INT-PATENT-CLASS-G01R-2726 ..... N91-31598
INT-PATENT-CLASS-G01R-2726 ..... N91-31599
INT-PATENT-CLASS-G01S-104 ..... N91-31108
INT-PATENT-CLASS-G01S-302 ..... N91-31116
INT-PATENT-CLASS-G01S-502 ..... N91-31115
INT-PATENT-CLASS-G01S-7295 ..... N91-31512
INT-PATENT-CLASS-G02B-624 ..... N91-31946
INT-PATENT-CLASS-G03H-126 ..... N91-31600
INT-PATENT-CLASS-G05B-19/24 ..... N91-31885*
INT-PATENT-CLASS-G05B-19/42 ..... N91-31528*
INT-PATENT-CLASS-G05D-110 ..... N91-31182
INT-PATENT-CLASS-G06F-15/46 ..... N91-31885*
INT-PATENT-CLASS-G06F-15/50 ..... N91-31120*
INT-PATENT-CLASS-G06F-702 ..... N91-31511
INT-PATENT-CLASS-G06F-1562 ..... N91-31660
INT-PATENT-CLASS-G08B-108 ..... N91-31107
INT-PATENT-CLASS-G11C-29/00 ..... N91-31810*
INT-PATENT-CLASS-G015-352 ..... N91-31116

INT-PATENT-CLASS-H01L-21/306 ..... N91-31258*
INT-PATENT-CLASS-H01Q-136 ..... N91-31480
INT-PATENT-CLASS-H01Q-142 ..... N91-31481
INT-PATENT-CLASS-H01Q-904 ..... N91-31480
INT-PATENT-CLASS-H01Q-1310 ..... N91-31514
INT-PATENT-CLASS-H01Q-2106 ..... N91-31480
INT-PATENT-CLASS-H03H-970 ..... N91-31479
INT-PATENT-CLASS-H03H-1702 ..... N91-31513
INT-PATENT-CLASS-H03M-13/00 ..... N91-31810*
INT-PATENT-CLASS-H04J-102 ..... N91-31479
INT-PATENT-CLASS-H04K-3/00 ..... N91-31530*
INT-PATENT-CLASS-H04N-718 ..... N91-31693
INT-PATENT-CLASS-H05B-33/14 ..... N91-31950*

IS-M-670 ..... N91-31688 #

ISAL-90-0093 ..... N91-31284 #

ISBN-2-7170-0936-1 ..... N91-31098 #
ISBN-2-7170-0937-X ..... N91-31099 #
ISBN-2-7170-0938-8 ..... N91-31100 #
ISBN-2-7170-0939-6 ..... N91-31637 #
ISBN-2-7170-0940-X ..... N91-31101 #
ISBN-2-7170-0941-8 ..... N91-31102 #
ISBN-2-7170-0942-6 ..... N91-31103 #
ISBN-2-7170-0943-4 ..... N91-31587 #
ISBN-2-7170-0944-2 ..... N91-31187 #
ISBN-2-7170-0946-9 ..... N91-31104 #
ISBN-2-7170-0947-7 ..... N91-31105 #
ISBN-2-7170-0948-5 ..... N91-31588 #
ISBN-2-7170-0949-3 ..... N91-31188 #
ISBN-2-7170-0950-7 ..... N91-31589 #
ISBN-2-7170-0951-5 ..... N91-31590 #
ISBN-2-7170-0952-3 ..... N91-31847 #
ISBN-2-7170-0954-X ..... N91-31848 #
ISBN-2-7170-0955-8 ..... N91-31849 #
ISBN-2-7170-0956-6 ..... N91-31850 #
ISBN-2-7170-0957-4 ..... N91-31591 #
ISBN-2-7170-0958-2 ..... N91-31592 #
ISBN-2-7170-0959-0 ..... N91-31593 #
ISBN-2-7170-0960-4 ..... N91-31851 #
ISBN-2-7170-0962-0 ..... N91-31097 #
ISBN-2-7170-0963-9 ..... N91-31137 #
ISBN-90-6275-660-3 ..... N91-31118 #
ISBN-92-9092-104-08 ..... N91-31321 #

ISBN92-835-0618-9 ..... N91-31144 #

ISL-CO-224/878 ..... N91-31637 #

ISSN-0167-8590 ..... N91-32023 #
ISSN-0169-1615 ..... N91-31752
ISSN-0169-1708 ..... N91-31497
ISSN-0169-2690 ..... N91-31489 #
ISSN-0169-2690 ..... N91-31580 #
ISSN-0169-2690 ..... N91-31842 #
ISSN-0169-2690 ..... N91-31843 #
ISSN-0169-2690 ..... N91-31844 #
ISSN-0169-2690 ..... N91-31845 #
ISSN-0169-2690 ..... N91-31881 #
ISSN-0169-2690 ..... N91-31904 #
ISSN-0169-2690 ..... N91-31905 #
ISSN-0169-2690 ..... N91-31906 #
ISSN-0169-2690 ..... N91-31907 #
ISSN-0169-2690 ..... N91-31908 #
ISSN-0169-2690 ..... N91-31909 #
ISSN-0169-2690 ..... N91-31910 #
ISSN-0173-699X ..... N91-32002 #
ISSN-0178-0719 ..... N91-31957*
ISSN-0243-0177 ..... N91-31097 #
ISSN-0243-0177 ..... N91-31098 #
ISSN-0243-0177 ..... N91-31099 #
ISSN-0243-0177 ..... N91-31100 #
ISSN-0243-0177 ..... N91-31101 #
ISSN-0243-0177 ..... N91-31102 #
ISSN-0243-0177 ..... N91-31103 #
ISSN-0243-0177 ..... N91-31104 #
ISSN-0243-0177 ..... N91-31105 #
ISSN-0243-0177 ..... N91-31137 #
ISSN-0243-0177 ..... N91-31187 #
ISSN-0243-0177 ..... N91-31188 #
ISSN-0243-0177 ..... N91-31587 #
ISSN-0243-0177 ..... N91-31588 #
ISSN-0243-0177 ..... N91-31589 #
ISSN-0243-0177 ..... N91-31590 #
ISSN-0243-0177 ..... N91-31591 #
ISSN-0243-0177 ..... N91-31592 #
ISSN-0243-0177 ..... N91-31593 #
ISSN-0243-0177 ..... N91-31637 #
ISSN-0243-0177 ..... N91-31847 #
ISSN-0243-0177 ..... N91-31848 #
ISSN-0243-0177 ..... N91-31849 #
ISSN-0243-0177 ..... N91-31850 #
ISSN-0243-0177 ..... N91-31851 #
ISSN-0349-0467 ..... N91-31747 #
ISSN-0366-0885 ..... N91-31283 #
ISSN-0374-1257 ..... N91-31582 #
ISSN-0377-8312 ..... N91-31551 #
ISSN-0377-8312 ..... N91-31565 #
ISSN-0377-8312 ..... N91-31614 #
ISSN-0377-8312 ..... N91-31625 #
ISSN-0436-1199 ..... N91-31085 #
ISSN-0436-1199 ..... N91-31581 #
ISSN-0923-1714 ..... N91-31493 #
ISSN-0923-1714 ..... N91-31840 #
ISSN-0923-1714 ..... N91-31841 #
ISSN-0923-1714 ..... N91-31863 #
ISSN-0924-3275 ..... N91-31827 #
ISSN-0924-3275 ..... N91-31828 #
ISSN-0924-3275 ..... N91-31829 #
ISSN-0924-3275 ..... N91-31830 #
ISSN-0924-3275 ..... N91-31831 #
ISSN-0924-3275 ..... N91-31832 #
ISSN-0924-3275 ..... N91-31833 #
ISSN-0924-3275 ..... N91-31834 #

ISSN-0924-3275 ..... N91-31835 #
ISSN-0924-3275 ..... N91-31836 #
ISSN-0924-3275 ..... N91-31837 #
ISSN-0924-3275 ..... N91-31838 #
ISSN-0924-3275 ..... N91-31839 #
ISSN-0924-3275 ..... N91-31896 #
ISSN-0924-3275 ..... N91-31897 #
ISSN-0924-3275 ..... N91-31898 #
ISSN-0924-3275 ..... N91-31899 #
ISSN-0924-3275 ..... N91-31900 #
ISSN-0924-3275 ..... N91-31901 #
ISSN-0924-3275 ..... N91-31902 #
ISSN-0924-3275 ..... N91-31903 #
ISSN-0924-3275 ..... N91-31917 #
ISSN-0924-3275 ..... N91-31921 #
ISSN-0924-3275 ..... N91-31997 #
ISSN-0924-8374 ..... N91-31891 #
ISSN-0939-298X ..... N91-31185 #

ITLI-CT-91-04 ..... N91-31891 #

JUEL-2414 ..... N91-31283 #

K/QT-413 ..... N91-31300 #

KCP-613-4367 ..... N91-31257 #
KCP-613-4368 ..... N91-31653 #
KCP-613-4371 ..... N91-31251 #
KCP-613-4372 ..... N91-31819 #
KCP-613-4385 ..... N91-31652 #
KCP-613-4396 ..... N91-31657 #

KNMI-TR-129 ..... N91-31497

KNMI-WR-90-03 ..... N91-31752

L-16936 ..... N91-31143* #

LA-UR-91-941 ..... N91-31672 #
LA-UR-91-1652 ..... N91-31275 #
LA-UR-91-1722 ..... N91-31869 #
LA-UR-91-1723 ..... N91-31276 #
LA-UR-91-1777 ..... N91-31673 #
LA-UR-91-2081 ..... N91-31933 #
LA-UR-91-2119 ..... N91-31932 #
LA-UR-91-2120 ..... N91-31979 #
LA-UR-91-2129 ..... N91-31610 #
LA-UR-91-2144 ..... N91-31602 #
LA-UR-91-2170 ..... N91-31640 #
LA-UR-91-2248 ..... N91-31639 #
LA-UR-91-2259 ..... N91-31287 #
LA-UR-91-2295 ..... N91-31211 #
LA-UR-91-2314 ..... N91-31940 #
LA-UR-91-2317 ..... N91-31945 #
LA-UR-91-2342 ..... N91-31958 #
LA-UR-91-2346 ..... N91-31955 #
LA-UR-91-2377 ..... N91-31711 #
LA-UR-91-2386 ..... N91-31886 #
LA-UR-91-2389 ..... N91-31259 #
LA-UR-91-2390 ..... N91-31710 #
LA-UR-91-2440 ..... N91-31818 #
LA-UR-91-2541 ..... N91-31694 #

LA-12008-MS ..... N91-31929 #
LA-12102 ..... N91-31210 #
LA-12128-C ..... N91-31491 #
LA-12151-MS ..... N91-31477 #
LA-12152-MS ..... N91-31690 #

LAAS-89-395 ..... N91-31662 #
LAAS-91047 ..... N91-31524 #
LAAS-91135 ..... N91-31882 #

LBL-29415 ..... N91-32016 #
LBL-29967 ..... N91-31473 #
LBL-30520 ..... N91-31288 #
LBL-30563 ..... N91-31974 #
LBL-30677 ..... N91-31948 #
LBL-30878 ..... N91-32018 #
LBL-30899 ..... N91-31254 #
LBL-30917 ..... N91-31975 #
LBL-30942 ..... N91-31279 #
LBL-30946 ..... N91-32010 #
LBL-30950 ..... N91-31611 #

LR-649 ..... N91-31118 #

M-668 ..... N91-32006* #

MAD/PH-618 ..... N91-31930 #

MBB-FE22/S/PUB/0433/A ..... N91-31135 #
MBB-FE202/S/PUB/441 ..... N91-31088 #

MBB-UA-1189-90-PUB ..... N91-31871 #
MBB-UA-1190-90-PUB ..... N91-31186 #
MBB-UA-1191-90-PUB ..... N91-31304 #
MBB-UA-1192-90-PUB ..... N91-31317 #
MBB-UA-1193-90-PUB ..... N91-31086 #
MBB-UA-1201-90-PUB ..... N91-31183 #

MBB-UE-0015-90-PUB ..... N91-31705 #
MBB-UE-0018-90-PUB ..... N91-31706 #

MBB-UK-0131-90-PUB ..... N91-31087 #
MBB-UK-0132-91-PUB ..... N91-31198 #

MBB-Z-0336-90-PUB ..... N91-31635 #
MBB-Z-0337-90-PUB ..... N91-31134 #
MBB-Z-0339-90-PUB ..... N91-31949 #

MEMO-INF-90-39-REV ..... N91-31887 #
MEMO-INF-91-19 ..... N91-31493 #
MEMO-INF-91-22 ..... N91-31863 #
MEMO-INF-91-26 ..... N91-31840 #
MEMO-INF-91-31 ..... N91-31841 #

MEMO-909 ..... N91-31904 #
MEMO-910 ..... N91-31905 #
MEMO-911 ..... N91-31906 #
MEMO-912 ..... N91-31842 #
MEMO-913 ..... N91-31843 #
MEMO-914 ..... N91-31580 #
MEMO-915 ..... N91-31907 #
MEMO-916 ..... N91-31908 #
MEMO-917 ..... N91-31909 #
MEMO-918 ..... N91-31910 #
MEMO-919 ..... N91-31844 #
MEMO-920 ..... N91-31881 #
MEMO-921 ..... N91-31845 #
MEMO-938 ..... N91-31489 #

METRAVIB-RDS-1-007-67 ..... N91-31090 #

MIT/LCS/TM-455 ..... N91-31811 #

MMS-91/0003 ..... N91-31753 #

MPE-PREPRINT-196 ..... N91-31957*
MPE-PREPRINT-197 ..... N91-32009*
MPE-PREPRINT-198 ..... N91-32017

MPE-223 ..... N91-32002 #

MPIS-MITT-97 ..... N91-31582 #

MPIS-12/1990 ..... N91-31085 #
MPIS-12/1990 ..... N91-31581 #

MRL-TR-90-19 ..... N91-31109 #

MT-CWR-091-012 ..... N91-31280 #

MTL-TR-91-26 ..... N91-31311 #
MTL-TR-91-27 ..... N91-31245 #

NADC-91027-60 ..... N91-31141 #
NADC-91028-60 ..... N91-31808 #
NADC-91042-60 ..... N91-31768 #
NADC-91054-60-PT-1 ..... N91-31809 #

NAE-LTR-ST-1701 ..... N91-31125 #

NAS 1.15:4312 ..... N91-31751* #
NAS 1.15:4327 ..... N91-31874* #
NAS 1.15:102277 ..... N91-31775* #
NAS 1.15:102381 ..... N91-31208* #
NAS 1.15:102794 ..... N91-31078* #
NAS 1.15:103552 ..... N91-31606* #
NAS 1.15:104036 ..... N91-31138* #
NAS 1.15:104037 ..... N91-31139* #
NAS 1.15:104057 ..... N91-31201* #
NAS 1.15:104098 ..... N91-31531* #
NAS 1.15:104104 ..... N91-31687* #
NAS 1.15:104105 ..... N91-31677* #
NAS 1.15:104109 ..... N91-31082* #
NAS 1.15:104123 ..... N91-31595* #
NAS 1.15:104124 ..... N91-31879* #
NAS 1.15:104333 ..... N91-31178* #
NAS 1.15:104394 ..... N91-31648* #
NAS 1.15:104419 ..... N91-31876* #
NAS 1.15:104441 ..... N91-31181* #
NAS 1.15:104470 ..... N91-31235* #
NAS 1.15:104479 ..... N91-31654* #
NAS 1.15:104505 ..... N91-31218* #
NAS 1.15:104533 ..... N91-31216* #
NAS 1.15:105037 ..... N91-31194* #
NAS 1.15:105044 ..... N91-32003* #
NAS 1.15:105074 ..... N91-31813* #
NAS 1.15:105141 ..... N91-31220* #
NAS 1.15:105153 ..... N91-31212* #
NAS 1.15:105165 ..... N91-31605* #
NAS 1.15:105203 ..... N91-31911* #
NAS 1.15:105210 ..... N91-31106* #
NAS 1.15:105220 ..... N91-31977* #
NAS 1.15:105222 ..... N91-31217* #
NAS 1.15:105224 ..... N91-31196* #
NAS 1.15:105229 ..... N91-31708* #
NAS 1.15:105237 ..... N91-31597* #
NAS 1.15:105263 ..... N91-31318* #
NAS 1.21:7011(353) N91-31760*
NAS 1.26:4395 ..... N91-31470* #
NAS 1.26:4399 ..... N91-31609* #
NAS 1.26:4400 ..... N91-31684* #
NAS 1.26:4401 ..... N91-31685* #
NAS 1.26:4402 ..... N91-31686* #
NAS 1.26:182021 ..... N91-31692* #
NAS 1.26:183485 ..... N91-32007* #
NAS 1.26:183490 ..... N91-32020* #
NAS 1.26:183491 ..... N91-32021* #
NAS 1.26:183492 ..... N91-32022* #
NAS 1.26:183495 ..... N91-32012* #
NAS 1.26:184197 ..... N91-31607* #
NAS 1.26:184198 ..... N91-31204* #
NAS 1.26:184205 ..... N91-31215* #
NAS 1.26:184208 ..... N91-31853* #
NAS 1.26:184209 ..... N91-31214* #
NAS 1.26:185650 ..... N91-31890* #
NAS 1.26:186042 ..... N91-31492* #
NAS 1.26:186565 ..... N91-31488* #
NAS 1.26:187117 ..... N91-31213* #
NAS 1.26:187172 ..... N91-31499* #
NAS 1.26:187213 ..... N91-31219* #
NAS 1.26:187219 ..... N91-31209* #
NAS 1.26:187557 ..... N91-31926* #
NAS 1.26:187558 ..... N91-31927* #
NAS 1.26:187559 ..... N91-31923* #
NAS 1.26:187576 ..... N91-31679* #
NAS 1.26:187595 ..... N91-31888* #
NAS 1.26:187618 ..... N91-31889* #
NAS 1.26:187619 ..... N91-31576* #
NAS 1.26:187817 ..... N91-31947* #
NAS 1.26:188717 ..... N91-31961* #
NAS 1.26:188774 ..... N91-31723* #
NAS 1.26:188788 ..... N91-31083* #
NAS 1.26:188791 ..... N91-31678* #
NAS 1.26:188796 ..... N91-31820* #
NAS 1.26:188802 ..... N91-31200* #
NAS 1.26:188805 ..... N91-31750* #
NAS 1.26:188811 ..... N91-31928* #
NAS 1.26:188912 ..... N91-32009*
NAS 1.26:188913 ..... N91-31957*
NAS 1.60:3135 ..... N91-31143* #
NAS 1.61-1268 ..... N91-32006* #

NASA-CASE-ARC-11873-2 ..... N91-31258*
NASA-CASE-ARC-11909-1 ..... N91-31113*

NASA-CASE-GSC-12821-2 ..... N91-31530*
NASA-CASE-GSC-13239-1 ..... N91-31656*

NASA-CASE-LAR-13616-1 ..... N91-31950*
NASA-CASE-LAR-13854-1-CU N91-31120*
NASA-CASE-LAR-13910-2-CU N91-31307*
NASA-CASE-LAR-13952-2-SB N91-31596*
NASA-CASE-LAR-14096-1 ..... N91-31476*
NASA-CASE-LAR-14212-1-CU N91-31140*

NASA-CASE-LEW-14676-1 ..... N91-31529*
NASA-CASE-LEW-14967-1 ..... N91-31608*

NASA-CASE-MSC-21469-1 ..... N91-31655*
NASA-CASE-MSC-21585-1 ..... N91-31755*
NASA-CASE-MSC-21629-1 ..... N91-31803* #

NASA-CASE-NPO-11907-1-NP N91-31236*
NASA-CASE-NPO-17134-1-CU N91-31528*
NASA-CASE-NPO-17394-1-CU N91-31810*
NASA-CASE-NPO-17401-1-CU N91-31885*

NASA-CR-4395 ..... N91-31470* #
NASA-CR-4399 ..... N91-31609* #
NASA-CR-4400 ..... N91-31684* #
NASA-CR-4401 ..... N91-31685* #
NASA-CR-4402 ..... N91-31686* #
NASA-CR-182021 ..... N91-31692* #
NASA-CR-183485 ..... N91-32007* #
NASA-CR-183490 ..... N91-32020* #
NASA-CR-183491 ..... N91-32021* #
NASA-CR-183492 ..... N91-32022* #
NASA-CR-183495 ..... N91-32012* #
NASA-CR-184197 ..... N91-31607* #
NASA-CR-184198 ..... N91-31204* #
NASA-CR-184205 ..... N91-31215* #
NASA-CR-184208 ..... N91-31853* #
NASA-CR-184209 ..... N91-31214* #
NASA-CR-185650 ..... N91-31890* #
NASA-CR-186042 ..... N91-31492* #

NASA-CR-186565 N91-31488* #
NASA-CR-187117 N91-31213* #
NASA-CR-187172 N91-31499* #
NASA-CR-187213 N91-31219* #
NASA-CR-187219 N91-31209* #
NASA-CR-187557 N91-31926* #
NASA-CR-187558 N91-31927* #
NASA-CR-187559 N91-31923* #
NASA-CR-187576 N91-31679* #
NASA-CR-187595 N91-31888* #
NASA-CR-187618 N91-31889* #
NASA-CR-187619 N91-31576* #
NASA-CR-187817 N91-31947* #
NASA-CR-188717 N91-31961* #
NASA-CR-188774 N91-31723* #
NASA-CR-188788 N91-31083* #
NASA-CR-188791 N91-31678* #
NASA-CR-188796 N91-31820* #
NASA-CR-188802 N91-31200* #
NASA-CR-188805 N91-31750* #
NASA-CR-188811 N91-31928* #
NASA-CR-188912 N91-32009*
NASA-CR-188913 N91-31957*

NASA-RP-1268 N91-32006* #

NASA-SP-7011(353) N91-31760*

NASA-TM-4312 N91-31751* #
NASA-TM-4327 N91-31874* #
NASA-TM-102277 N91-31775* #
NASA-TM-102381 N91-31208* #
NASA-TM-102794 N91-31076* #
NASA-TM-103552 N91-31606* #
NASA-TM-104036 N91-31138* #
NASA-TM-104037 N91-31139* #
NASA-TM-104057 N91-31201* #
NASA-TM-104098 N91-31531* #
NASA-TM-104104 N91-31687* #
NASA-TM-104105 N91-31677* #
NASA-TM-104109 N91-31082* #
NASA-TM-104123 N91-31595* #
NASA-TM-104124 N91-31879* #
NASA-TM-104333 N91-31178* #
NASA-TM-104394 N91-31648* #
NASA-TM-104419 N91-31876* #
NASA-TM-104441 N91-31181* #
NASA-TM-104470 N91-31235* #
NASA-TM-104479 N91-31654* #
NASA-TM-104505 N91-31218* #
NASA-TM-104533 N91-31216* #
NASA-TM-105037 N91-31194* #
NASA-TM-105044 N91-32003* #
NASA-TM-105074 N91-31813* #
NASA-TM-105141 N91-31220* #
NASA-TM-105153 N91-31212* #
NASA-TM-105165 N91-31605* #
NASA-TM-105203 N91-31911* #
NASA-TM-105210 N91-31106* #
NASA-TM-105220 N91-31977* #
NASA-TM-105222 N91-31217* #
NASA-TM-105224 N91-31196* #
NASA-TM-105229 N91-31708* #
NASA-TM-105237 N91-31597* #
NASA-TM-105263 N91-31318* #

NASA-TP-3135 N91-31143* #

NCS-TIB-90-12 N91-31860 #

NHRC-90-29 N91-31770 #

NIKHEF-K/AMPS/91-04 N91-31943 #

NIST-855-05-91-34 N91-31242 #

NLR-MP-88050-U N91-31282 #
NLR-MP-88053-U N91-31133 #
NLR-MP-88054-U N91-31084 #
NLR-MP-88056-U N91-31119 #
NLR-MP-88059-U N91-31578 #

NLR-TP-89031-U N91-31878 #
NLR-TP-89146-U N91-31131 #
NLR-TP-89360-U N91-31081 #

NLR-TR-88001-U N91-31579 #

NMRDI-2-76-5622 N91-31114 #

NMRI-91-39 N91-31769 #

NOAA-TM-NWS-SR-134 N91-31744 #
NOAA-TM-NWS-SR-135 N91-31745 #

NOO-TN-01-91 N91-31754 #

NOSC/TD-2052 N91-31510 #

NPSCS-91-012 N91-32000 #

NRL-MR-6853 N91-31638 #
NRL-MR-6856 N91-31243 #
NRL-MR-6867 N91-31952 #
NRL-MR-6870 N91-31959 #

NRL-9311-PT-1 N91-31539 #
NRL-9316 N91-31501 #
NRL-9337 N91-31540 #
NRL-9343 N91-31502 #
NRL-9344 N91-31265 #
NRL-9345 N91-31508 #

NSMRL-1167 N91-31806 #

NSSDC-WDC-A-R/S-89-27 N91-31813* #
NSSDC-WDC-A-R/S-90-02 N91-32003* #

NTSB/ARC-91/01 N91-31110 #

ONERA-PV-1/8571-GY N91-31089 #

ONERA-RF-14/3641-PY N91-31925 #
ONERA-RF-25/7234-PY N91-31111 #
ONERA-RF-98/7154-PY N91-31112 #

ONERA-RS-14/3637-AY N91-31585 #

ONERA-RSF-85/1685-AY N91-31093 #
ONERA-RSF-88/1685-AY-158-A N91-31092 #

ONERA-RT-6/7256-RY-080-R N91-31234 #
ONERA-RT-10/3313-RY-090-R N91-31682 #
ONERA-RT-13/3641-PY N91-31924 #
ONERA-RT-35/5025-28 N91-31584 #
ONERA-RT-42/1621-RY-093-R N91-31586 #
ONERA-RT-50/3064-RY-093-R N91-31095 #
ONERA-RT-92/5094-PY N91-31136 #

ONERA-RTS-134/2149-AY-640-A N91-31094 #

ONERA/DERAT-37/5025-26 N91-31096 #

ONT-90-165 N91-31501 #

ORNL/M-1276 N91-31651 #

ORNL/SUB-85-27421/04 N91-31280 #

ORNL/TM-11746 N91-31190 #
ORNL/TM-11826 N91-31855 #

OTN-028386 N91-31706 #
OTN-028392 N91-31949 #
OTN-030547 N91-31198 #
OTN-030852 N91-31635 #
OTN-030861 N91-31705 #
OTN-030880 N91-31134 #
OTN-032761 N91-31871 #
OTN-032762 N91-31186 #
OTN-032763 N91-31304 #
OTN-032764 N91-31317 #
OTN-032766 N91-31086 #
OTN-032795 N91-31183 #
OTN-033083 N91-31087 #

PATENT-1-247-868 N91-31177
PATENT-1-249-609 N91-31294
PATENT-1-250-128 N91-31269
PATENT-1-250-926 N91-31107
PATENT-1-252-835 N91-31479
PATENT-1-253-363 N91-31268
PATENT-1-253-424 N91-31224
PATENT-1-253-724 N91-31600
PATENT-1-254-289 N91-31207
PATENT-1-254-292 N91-31116
PATENT-1-254-415 N91-31946
PATENT-1-254-637 N91-31115
PATENT-1-254-651 N91-31693
PATENT-1-255-929 N91-31271
PATENT-1-256-916 N91-31108
PATENT-1-257-987 N91-31270
PATENT-1-258-589 N91-31127
PATENT-1-258-924 N91-31660
PATENT-1-259-401 N91-31514
PATENT-1-262-571 N91-31481
PATENT-1-262-653 N91-31142
PATENT-1-263-181 N91-31480
PATENT-1-263-227 N91-31206
PATENT-1-263-443 N91-31599
PATENT-1-263-444 N91-31598
PATENT-1-264-072 N91-31513
PATENT-1-265-947 N91-31182

PATENT-1-271-231 N91-31511
PATENT-1-273-409 N91-31512
PATENT-1-274-075 N91-31126

PB91-164434 N91-31753 #
PB91-170282 N91-31114 #
PB91-176040 N91-31110 #
PB91-176685 N91-31744 #
PB91-176693 N91-31745 #
PB91-184960 N91-31645 #

PL-TR-91-2088 N91-31121 #

PMI-2335 N91-31189 #

PNL-7694 N91-31247 #
PNL-7715 N91-31716 #

R/D-6646-EE-02 N91-31960 #

RCC-376-91 N91-31740 #
RCC-378-91 N91-31739 #
RCC-379-91 N91-31742 #
RCC-380-91 N91-31741 #
RCC-701-90 N91-31507 #

RCC/FMG-702-91 N91-31503 #

RD/PA-14-227 N91-31184 #

RE-50-345/F N91-31231 #

REPT-90-6 N91-31774 #
REPT-90-071 N91-31846
REPT-90-072 N91-31884
REPT-90-074 N91-31995
REPT-90/05 N91-31475 #
REPT-91-021 N91-31994
REPT-431/91 N91-31285 #

RI/RD-87-164 N91-31213* #
RI/RD-91-157 N91-31214* #
RI/RD-91-158-PHASE-2 N91-31219* #

RL-TR-91-164 N91-31505 #

RSL-TR-8240-2 N91-31492* #
RSL-TR-8760-2 N91-31750* #

RTR-193-04 N91-31853* #

RUU-CS-90-24 N91-31827 #
RUU-CS-90-25 N91-31997 #
RUU-CS-90-28 N91-31896 #
RUU-CS-90-29 N91-31897 #
RUU-CS-90-30 N91-31828 #
RUU-CS-90-31 N91-31829 #
RUU-CS-90-32 N91-31898 #
RUU-CS-90-33 N91-31899 #
RUU-CS-90-34 N91-31830 #
RUU-CS-90-35 N91-31831 #
RUU-CS-90-36 N91-31832 #
RUU-CS-90-37 N91-31900 #
RUU-CS-90-38 N91-31833 #
RUU-CS-90-39 N91-31834 #
RUU-CS-90-40 N91-31835 #
RUU-CS-90-41 N91-31901 #
RUU-CS-90-42 N91-31917 #
RUU-CS-90-43 N91-31921 #
RUU-CS-91-01 N91-31836 #
RUU-CS-91-02 N91-31837 #
RUU-CS-91-03 N91-31838 #
RUU-CS-91-04 N91-31902 #
RUU-CS-91-05 N91-31903 #
RUU-CS-91-06 N91-31839 #

S/A-ANN-12-30-90 N91-31743 #

SAND-89-1724 N91-31702 #
SAND-90-0253 N91-31573 #
SAND-90-0844C N91-31248 #
SAND-90-0845C N91-31292 #
SAND-90-0846C N91-31293 #
SAND-90-2054C N91-31237 #
SAND-90-2281C N91-31689 #
SAND-90-3032C N91-31272 #
SAND-90-3106C N91-31978 #
SAND-90-7038 N91-31715 #
SAND-91-0061C N91-31309 #
SAND-91-0177C N91-31518 #
SAND-91-0210C N91-31868 #
SAND-91-0379C N91-31303 #
SAND-91-0589C N91-31971 #
SAND-91-0652C N91-31230 #
SAND-91-0872 N91-31802 #
SAND-91-0910C N91-31472 #

SAND-91-0938 ..... N91-31522 #
SAND-91-0946C ..... N91-31634 #
SAND-91-0955C ..... N91-31490 #
SAND-91-0956C ..... N91-31980 #
SAND-91-1157C ..... N91-31517 #
SAND-91-1220 ..... N91-31523 #
SAND-91-1296C ..... N91-31302 #
SAND-91-1467 ..... N91-31703 #
SAND-91-1578 ..... N91-31574 #
SAND-91-1659C ..... N91-31221 #
SAND-91-1731C ..... N91-31854 #
SAND-91-1737C ..... N91-31500 #
SAND-91-1784C ..... N91-31988 #
SAND-91-7003 ..... N91-31699 #
SAND-91-7004 ..... N91-31714 #
SAND-91-7009 ..... N91-31713 #
SAND-91-7066 ..... N91-31533 #

SAR-3 ..... N91-31723* #
SAR-4 ..... N91-31723* #
SAR-5 ..... N91-31723* #
SAR-6 ..... N91-31723* #

SK-1600-44-001-02-0 ..... N91-31483

SR-10 ..... N91-31121 #

SRI-ENV-91-292-6657-XXXIV ..... N91-31260 #

SRS/STD-TR89-90 ..... N91-31215* #

SSCL-MAN-0012 ..... N91-31817 #

SSD-TR-91-13 ..... N91-31612 #
SSD-TR-91-26 ..... N91-31805 #

ST-REPT-VOL-8-NO-2 ..... N91-32023 #

SU-SOL-91-9 ..... N91-31858 #

SU-TR-444 ..... N91-31920 #

TD-91-2007 ..... N91-31873
TD-91-2008 ..... N91-31872
TD-91-2021 ..... N91-31496

TIM-5834-2-1 ..... N91-31122 #
TIM-5834-2-2-VOL-2 ..... N91-31123 #
TIM-5834-4-1 ..... N91-31124 #

TIOS-91/003 ..... N91-31493 #
TIOS-91/006 ..... N91-31887 #

TNO-BOUW-BI-90-209 ..... N91-31577 #

TR-41 ..... N91-31266 #
TR-74 ..... N91-31264 #
TR-90-15 ..... N91-31880 #
TR-90-22 ..... N91-31824 #
TR-90-24 ..... N91-31825 #
TR-90-25 ..... N91-31895 #
TR-90-26 ..... N91-31996 #
TR-91-01 ..... N91-31826 #
TR-445 ..... N91-31919 #
TR-921 ..... N91-31644 #
TR-0090(5530-02)-1 ..... N91-31805 #
TR-0090(5935-03)-5 ..... N91-31612 #
TR-1991-18 ..... N91-31310 #

TR90-56 ..... N91-31914 #

TW-91-02 ..... N91-31918 #

UCRL-ID-103495-90 ..... N91-31658 #

UCRL-JC-104280 ..... N91-31316 #
UCRL-JC-105259 ..... N91-31717 #
UCRL-JC-106047 ..... N91-31298 #
UCRL-JC-106143 ..... N91-31315 #
UCRL-JC-106260 ..... N91-31748 #
UCRL-JC-106370 ..... N91-31642 #
UCRL-JC-106445 ..... N91-31718 #
UCRL-JC-106588 ..... N91-31698 #
UCRL-JC-106770 ..... N91-31274 #
UCRL-JC-107195 ..... N91-31572 #
UCRL-JC-107230 ..... N91-31815 #
UCRL-JC-107388 ..... N91-31314 #
UCRL-JC-107526 ..... N91-31749 #
UCRL-JC-107736 ..... N91-31252 #
UCRL-JC-107737 ..... N91-31719 #
UCRL-JC-107755 ..... N91-31763 #

UCRL-MA-107254 ..... N91-31675 #

UCRL-52000-91-2/3 ..... N91-32031 #

US-PATENT-APPL-SN-082766 ..... N91-31120*
US-PATENT-APPL-SN-140185 ..... N91-31950*
US-PATENT-APPL-SN-150169 ..... N91-31258*
US-PATENT-APPL-SN-172105 ..... N91-31528*
US-PATENT-APPL-SN-172105 ..... N91-31885*
US-PATENT-APPL-SN-192562 ..... N91-31120*
US-PATENT-APPL-SN-203178 ..... N91-31596*
US-PATENT-APPL-SN-218792 ..... N91-31307*
US-PATENT-APPL-SN-242254 ..... N91-31530*
US-PATENT-APPL-SN-264326 ..... N91-31885*
US-PATENT-APPL-SN-305675 ..... N91-31529*
US-PATENT-APPL-SN-311024 ..... N91-31810*
US-PATENT-APPL-SN-347558 ..... N91-31307*
US-PATENT-APPL-SN-347591 ..... N91-31258*
US-PATENT-APPL-SN-348223 ..... N91-31596*
US-PATENT-APPL-SN-378548 ..... N91-31803* #
US-PATENT-APPL-SN-410576 ..... N91-31236*
US-PATENT-APPL-SN-418320 ..... N91-31113*
US-PATENT-APPL-SN-486458 ..... N91-31655*
US-PATENT-APPL-SN-493529 ..... N91-31755*
US-PATENT-APPL-SN-531433 ..... N91-31608*
US-PATENT-APPL-SN-565090 ..... N91-31140*
US-PATENT-APPL-SN-591644 ..... N91-31476*
US-PATENT-APPL-SN-608657 ..... N91-31656*
US-PATENT-APPL-SN-921576 ..... N91-31530*

US-PATENT-CLASS-29-568 ..... N91-31656*
US-PATENT-CLASS-30-92 ..... N91-31655*
US-PATENT-CLASS-30-388 ..... N91-31655*
US-PATENT-CLASS-47-1.4 ..... N91-31803* #
US-PATENT-CLASS-47-62 ..... N91-31803* #
US-PATENT-CLASS-55-75 ..... N91-31803* #
US-PATENT-CLASS-73-178T N91-31120*
US-PATENT-CLASS-73-432.1 ..... N91-31596*
US-PATENT-CLASS-73-863.22 ..... N91-31755*
US-PATENT-CLASS-73-863.41 ..... N91-31755*
US-PATENT-CLASS-73-863.85 ..... N91-31755*
US-PATENT-CLASS-73-863.86 ..... N91-31755*
US-PATENT-CLASS-112-440 ..... N91-31236*
US-PATENT-CLASS-136-200 ..... N91-31608*
US-PATENT-CLASS-156-345 ..... N91-31258*
US-PATENT-CLASS-156-643 ..... N91-31258*
US-PATENT-CLASS-156-668 ..... N91-31258*
US-PATENT-CLASS-204-192.32 ..... N91-31258*
US-PATENT-CLASS-210-748 ..... N91-31803* #
US-PATENT-CLASS-228-2.5 ..... N91-31476*
US-PATENT-CLASS-228-107 ..... N91-31476*
US-PATENT-CLASS-244-75R N91-31140*
US-PATENT-CLASS-244-87 ..... N91-31140*
US-PATENT-CLASS-244-88 ..... N91-31140*
US-PATENT-CLASS-244-120 ..... N91-31140*
US-PATENT-CLASS-244-137.2 ..... N91-31113*
US-PATENT-CLASS-244-159 ..... N91-31803* #
US-PATENT-CLASS-244-163 ..... N91-31803* #
US-PATENT-CLASS-244-199 ..... N91-31140*
US-PATENT-CLASS-250-356.1 ..... N91-31608*
US-PATENT-CLASS-294-86.4 ..... N91-31656*
US-PATENT-CLASS-313-502 ..... N91-31950*
US-PATENT-CLASS-313-503 ..... N91-31950*
US-PATENT-CLASS-313-506 ..... N91-31950*
US-PATENT-CLASS-313-509 ..... N91-31950*
US-PATENT-CLASS-318-568.1 ..... N91-31528*
US-PATENT-CLASS-318-568.2 ..... N91-31528*
US-PATENT-CLASS-318-568.11 ..... N91-31885*
US-PATENT-CLASS-318-573 ..... N91-31528*
US-PATENT-CLASS-318-573 ..... N91-31885*
US-PATENT-CLASS-364-427 ..... N91-31120*
US-PATENT-CLASS-364-428 ..... N91-31120*
US-PATENT-CLASS-364-513 ..... N91-31528*
US-PATENT-CLASS-364-513 ..... N91-31885*
US-PATENT-CLASS-365-156 ..... N91-31810*
US-PATENT-CLASS-365-200 ..... N91-31810*
US-PATENT-CLASS-371-40.1 ..... N91-31810*
US-PATENT-CLASS-374-29 ..... N91-31608*
US-PATENT-CLASS-374-180 ..... N91-31608*
US-PATENT-CLASS-374-208 ..... N91-31608*
US-PATENT-CLASS-421-209 ..... N91-31529*
US-PATENT-CLASS-421-457 ..... N91-31529*
US-PATENT-CLASS-422-99 ..... N91-31755*
US-PATENT-CLASS-422-101 ..... N91-31755*
US-PATENT-CLASS-428-285 ..... N91-31236*
US-PATENT-CLASS-435-30 ..... N91-31755*
US-PATENT-CLASS-437-229 ..... N91-31258*
US-PATENT-CLASS-441-83 ..... N91-31113*
US-PATENT-CLASS-455-1 ..... N91-31530*
US-PATENT-CLASS-455-99 ..... N91-31530*
US-PATENT-CLASS-455-102 ..... N91-31530*
US-PATENT-CLASS-505-1 ..... N91-31529*
US-PATENT-CLASS-505-701 ..... N91-31529*
US-PATENT-CLASS-505-702 ..... N91-31529*
US-PATENT-CLASS-505-703 ..... N91-31529*
US-PATENT-CLASS-505-704 ..... N91-31529*
US-PATENT-CLASS-525-422 ..... N91-31307*
US-PATENT-CLASS-525-471 ..... N91-31307*
US-PATENT-CLASS-901-19 ..... N91-31528*
US-PATENT-CLASS-901-30 ..... N91-31656*

US-PATENT-4,936,146 ..... N91-31596*
US-PATENT-5,005,787 ..... N91-31803* #
US-PATENT-5,007,983 ..... N91-31258*
US-PATENT-5,014,340 ..... N91-31530*
US-PATENT-5,020,742 ..... N91-31113*
US-PATENT-5,021,518 ..... N91-31307*
US-PATENT-5,038,089 ..... N91-31885*
US-PATENT-5,038,473 ..... N91-31655*
US-PATENT-5,038,693 ..... N91-31236*
US-PATENT-5,044,063 ..... N91-31656*
US-PATENT-5,047,686 ..... N91-31950*
US-PATENT-5,047,700 ..... N91-31528*
US-PATENT-5,047,9421-CU N91-31120*
US-PATENT-5,048,023 ..... N91-31810*
US-PATENT-5,048,973 ..... N91-31608*
US-PATENT-5,049,492 ..... N91-31755*
US-PATENT-5,049,539 ..... N91-31529*
US-PATENT-5,050,789 ..... N91-31476*
US-PATENT-5,050,819 ..... N91-31140*

USAFA-TR-91-6 ..... N91-31861 #

USAFSAM-TR-90-25 ..... N91-31807 #

USARIEM-T11-91 ..... N91-31767 #

USCG/ONSCEN-4-91 ..... N91-31124 #
USCG/ONSCEN-01-91 ..... N91-31122 #
USCG/ONSCEN-02.2-91-VOL-2 ..... N91-31123 #

USGS-OFR-90-615 ..... N91-31998 #

VKI-LS-1991-02 ..... N91-31551 #
VKI-LS-1991-03 ..... N91-31565 #

VKI-1991-05-VOL-1 ..... N91-31614 #
VKI-1991-05-VOL-2 ..... N91-31625 #

W-9007 ..... N91-31892 #
W-9016 ..... N91-31577 #
W-9101 ..... N91-31916 #

WCAP-16 ..... N91-31746 #

WHH-114-0 ..... N91-31821 #

WL-TR-91-4012 ..... N91-31246 #

WMO/TD-409 ..... N91-31746 #

Appendix

NASA SCIENTIFIC AND TECHNICAL INFORMATION PROGRAM PRODUCTS AND SERVICES

The NASA Scientific and Technical Information (STI) Program provides for the collection and announcement of aerospace-related reports and literature obtained worldwide through agreements and exchanges. The result of the collection is the comprehensive NASA STI Database that covers aeronautics, space, and supporting disciplines.

The STI Database, documents generated or obtained by NASA, and products and services derived from or supporting the database are made available to the NASA research community and to the public. Descriptions and sources of these items are presented in the following pages.

Scientific and Technical Aerospace Reports (*STAR*) is an abstract journal, listing citations with abstracts for aerospace-related reports obtained from worldwide sources. *STAR* is issued on the 8th and 23rd of each month and announces current documents that have been entered into the NASA STI Database during the previous two weeks. The reports are of the following types:

- NASA, NASA contractor, and NASA grantee reports;
- Reports issued by other U.S. Government agencies, domestic and foreign institutions, universities, and private firms;
- Translations in report form;
- NASA-owned patents and patent applications;
- Other U.S. Government agency and foreign patents and patent applications;
- Domestic and foreign dissertations and theses.

Journal, book, and conference literature, journal translations, and certain foreign dissertations having the same subject scope as *STAR* are announced in a companion journal, *International Aerospace Abstracts* (*IAA*). *IAA* is issued on the 1st and 15th of each month and is available from the American Institute of Aeronautics and Astronautics, Technical Information Service, 555 West 57th Street, 12th Floor, New York, NY 10019.

ELIGIBILITY AND REGISTRATION FOR NASA STI PRODUCTS AND SERVICES

Organizations of the type listed below that have registered with NASA can receive products and services.

- NASA offices and installations, contractors, subcontractors, grantees, and consultants;
- Other U.S. Government agencies and their contractors;
- Libraries in the United States that have arrangements with NASA to maintain collections of NASA documents for public reference;
- Other organizations in the United States having a need for NASA documents in work related to aeronautics and space research;
- Organizations abroad that have established reciprocal documents exchange arrangements with NASA.

Only the central service points or central points of document acquisition and control within qualified organizations are eligible to register for NASA STI products and services. Domestic organizations that may be eligible to receive various classes of NASA publications and services should address their requests for registration or further information to:

NASA Center for AeroSpace Information
ATTN: Registration Services
P.O. Box 8757
Baltimore, MD 21240-0757
301-621-0153

Organizations abroad should direct requests to:

National Aeronautics and Space Administration
Director, Scientific and Technical Information Program
Code JTT
Washington, DC 20546
USA
703-271-5640

SUBJECT SCOPE

The subject scope of *STAR* and *IAA* includes all aspects of aeronautics and space research and development, supporting basic and applied research, and applications. Aerospace aspects of Earth resources, energy development, conservation, oceanography, environmental protection, urban transportation, and other topics of high national priority are also covered.

HOW TO USE *STAR* SUBJECT CATEGORIES

Abstracts in *STAR* are categorized by 10 major subject divisions that are divided further into 76 specific subject categories. The subject divisions and categories are listed in the Table of Contents together with a note for each that defines its scope and provides any cross-references. For example:

16 SPACE TRANSPORTATION
Includes passenger and cargo space transportation, e.g., shuttle operations; and space rescue techniques. For related information see also *03 Air Transportation and Safety* and *18 Spacecraft Design, Testing and Performance.* For space suits see *54 Man/System Technology and Life Support.*

CROSS-REFERENCES

Individual *STAR* abstracts are not ordinarily cross-referenced, except for certain conference reports or book translations that have had separate abstracts written for their component papers or chapters. Citations and abstracts of the components follow immediately after those of the parent document. When the subject content of a component differs sufficiently from the general content of the parent, a cross-reference citation also is printed at the end of the category to which it normally would have been assigned if it were independent.

DOCUMENTS ON MICROFICHE

Documents available on microfiche are designated by a pound sign (#) following the accession number.

LIMITED REPRODUCIBILITY

A note of limited reproducibility appears in the citation, if there are factors affecting the reproducibility of more than 20% of the document. These factors include faint or broken type, color photographs, black and white photographs, foldouts, dot matrix print, or some other factor that limits the reproducibility of the document. This notation also appears on the microfiche header with the specific factor checked off on a list visible in the second frame.

COLOR COPIES

An increasing number of NASA scientific and technical reports are being produced with color graphs, charts, illustrations, and photographs. An indication that a document has color pages follows the source and pricing (SAP) information in the *STAR* citation.

Registered users of the NASA Scientific and Technical Information Program will receive ordered documents with color at no additional cost, as long as stock copies of the document are available. Otherwise, an additional fee of $2.00 per color page will be charged. The NASA Center for AeroSpace Information staff will contact registered users to determine individual user's needs.

NASA PATENTS AND PATENT APPLICATIONS

Patents and patent applications owned by NASA are announced in *STAR* under appropriate subject categories and are referenced in the *STAR* indexes. In the Report/Accession Number Index, patents are indexed by the NASA Case Number, and the U.S. Patent Class. Patent applications are indexed by the NASA Case Number and the U.S. Patent Application Serial Number.

Printed copies of patents (which are not microfiched) are available for purchase from the U.S. Patent and Trademark Office.

NASA patent application specifications are sold in both paper copy and microfiche by the National Technical Information Service (NTIS). The US-Patent-Appl-SN-number should be used in ordering either paper copy or microfiche from NTIS.

When ordering patents, the U.S. Patent Number should be used, and payment must be remitted in advance, by money order or check payable to the Commissioner of Patents and Trademarks. Prepaid purchase coupons for ordering are also available from the U.S. Patent and Trademark Office.

The patents and patent applications announced in *STAR* are owned by NASA and are available for royalty-free licensing. Requests for licensing terms and further information should be addressed to:

National Aeronautics and Space Administration
Associate General Counsel for Intellectual Property
Code GP
Washington, DC 20546

SOURCES FOR DOCUMENTS

One or more sources from which a document announced in *STAR* is available to the public is given in each citation. The most commonly indicated sources and their acronyms or abbreviations are listed on page A-6. If the publication is available from a source other than those listed, the publisher and address will be displayed on the availability line or in combination with the corporate source line.

Avail: NTIS. Sold by the National Technical Information Service. Prices for hard copy (HC) and microfiche (MF) are indicated by a price code following the letters HC or MF in the *STAR* citation. Current values for the price codes are given in the tables on page A-7.

Initially distributed microfiche under the NTIS SRIM (Selected Research in Microfiche) is available at greatly reduced unit prices. For this service and for information concerning subscription to NASA printed reports, consult the NTIS Subscription Section, Springfield, VA 22161.

NOTE ON ORDERING DOCUMENTS: When ordering NASA publications (those followed by the * symbol), use the N accession number. NASA patent applications (only the specifications are offered) should be ordered by the US-Patent-Appl-SN number. Non-NASA publications (no asterisk) should be ordered by the AD, PB, or other *report number* shown on the last line of the citation, not by the N accession number. It is also advisable to cite the title and other bibliographic identification.

Avail: SOD (or GPO). Sold by the Superintendent of Documents, U.S. Government Printing Office, in hard copy. The current price and order number are given following the availability line. (NTIS will fill microfiche requests, as indicated above, for those documents identified by a # symbol.)

Avail: BLL (formerly NLL): British Library Lending Division, Boston Spa, Wetherby, Yorkshire, England. Photocopies available from this organization at the price shown. (If none is given, address inquiry to the BLL.)

Avail: DOE Depository Libraries. Organizations in U.S. cities and abroad that maintain collections of Department of Energy reports, usually in microfiche form, are listed in *Energy Research Abstracts.* Services available from the DOE and its depositories are described in a booklet, *DOE Technical Information Center - Its Functions and Services* (TID-4660), which may be obtained without charge from the DOE Technical Information Center.

Avail: ESDU. Pricing information on specific data, computer programs, and details on Engineering Sciences Data Unit (ESDU) topic categories can be obtained from ESDU International Ltd. Requesters in North America should use the Virginia address while all other requesters should use the London address, both of which are on page A-6.

Avail: Fachinformationszentrum, Karlsruhe. Sold by the Fachinformationszentrum Energie, Physik, Mathematik GMBH, Eggenstein Leopoldshafen, Federal Republic of Germany, at the price shown in deutschmarks (DM).

Avail: HMSO. Publications of Her Majesty's Stationery Office are sold in the U.S. by Pendragon House, Inc. (PHI), Redwood City, CA. The U.S. price (including a service and mailing charge) is given, or a conversion table may be obtained from PHI.

Avail: NASA Public Document Rooms. Documents so indicated may be examined at or purchased from the National Aeronautics and Space Administration, Public Documents Room (Room 126), 600 Independence Ave., S.W., Washington, DC 20546, or public document rooms located at NASA installations, and the NASA Pasadena Office at the Jet Propulsion Laboratory.

Avail: Univ. Microfilms. Documents so indicated are dissertations selected from *Dissertation Abstracts* and are sold by University Microfilms as xerographic copy (HC) and microfilm. All requests should cite the author and the Order Number as they appear in the citation.

Avail: US Patent and Trademark Office. Sold by Commissioner of Patents and Trademarks, U.S. Patent and Trademark Office, at the standard price of $1.50 each, postage free. (See discussion of NASA patents and patent applications below.)

Avail: (US Sales Only). These foreign documents are available to users within the United States from the National Technical Information Service (NTIS). They are available to users outside the United States through the International Nuclear Information Service (INIS) representative in their country, or by applying directly to the issuing organization.

Avail: USGS. Originals of many reports from the U.S. Geological Survey, which may contain color illustrations, or otherwise may not have the quality of illustrations preserved in the microfiche or facsimile reproduction, may be examined by the public at the libraries of the USGS field offices whose addresses are listed on page A-6. The libraries may be queried concerning the availability of specific documents and the possible utilization of local copying services, such as color reproduction.

Avail: Issuing Activity, or Corporate Author, or no indication of availability. Inquiries as to the availability of these documents should be addressed to the organization shown in the citation as the corporate author of the document.

FEDERAL DEPOSITORY LIBRARIES: To provide the general public with greater access to U.S. Government publications, Congress established the Federal Depository Library Program under the Government Printing Office (GPO), with 52 regional depositories responsible for permanent retention of material, inter-library loan, and reference services. (These libraries are not sales outlets.) At least one copy of nearly every NASA and NASA-sponsored publication, either in printed or microfiche format, is received and retained by the 52 regional depositories. A list of the regional GPO libraries, appears on page A-8. A local library can contact a regional depository library to help locate specific reports, or direct contact may be made by an individual.

PUBLIC COLLECTION OF NASA DOCUMENTS

An extensive collection of NASA and NASA-sponsored publications is maintianed by the British Library Lending Divison, Boston Spa, Wetherby, Yorkshire, England, for public access. The British Library Lending Division also has available many of the non-NASA publications cited in *STAR*.

European requesters may purchase facsimile copy or microfiche of NASA and NASA-sponsored documents, those identified by both the symbols # and * from ESA—Information Retrieval Service, European Space Agency, 8-10 rue Mario-Nikis, 75738 Paris CEDEX 15, France.

SUBMITTING DOCUMENTS

All users of this abstract service are urged to forward reports to be considered for announcement in *STAR*. This will aid NASA in its efforts to provide the fullest possible coverage of all scientific and technical publications that might support aeronautics and space research and development. If you have prepared relevant reports (other than those you will transmit to NASA, DOD, or DOE through the usual contract- or grant-reporting channels), please send them for consideration to the NASA Center for AeroSpace Information, P.O. Box 8757, Baltimore, MD 21240-0757.

Reprints of journal articles, book chapters, and conference papers are also welcome. These will be considered for announcement in *STAR*'s companion journal, *IAA*.

You may specify a particular source to be included in a report announcement if you wish; otherwise the report will be placed on a public sale at the National Technical Information Service. Copyrighted publications will be announced but not distributed or sold.

PURCHASE OF *STAR*

STAR is publicly available on annual subscription from the Superintendent of Documents, U.S. Government Printing Office, Washington, DC 20402.

STAR is available to registered users on annual subscription from the NASA Center for AeroSpace Information, ATTN: Registration Services, P.O. Box 8757, Baltimore, MD 21240-0757.

Microfiche of the abstract sections of *STAR* are available, on annual subscription only, from NTIS as PB91-911300, Attn: Subscriptions, 5285 Port Royal Road, Springfield, VA 22161. Annual subscription rates are $85.00 North America; $170.00 foreign. Abstract sections for previous years retroactive to 1964 are available at the current rates.

ADDRESSES OF ORGANIZATIONS

American Institute of Aeronautics and Astronautics
Technical Information Service
555 West 57th Street, 12th Floor
New York, New York 10019

British Library Lending Division,
Boston Spa, Wetherby, Yorkshire,
England

Commissioner of Patents and Trademarks
U.S. Patent and Trademark Office
Washington, DC 20231

Department of Energy
Technical Information Center
P.O. Box 62
Oak Ridge, Tennessee 37830

European Space Agency-Information Retrieval Service
ESRIN
Via Galileo Galilei
00044 Frascati (Rome) Italy

Engineering Sciences Data Unit International
P.O. Box 1633
Manassas, Virginia 22110

Engineering Sciences Data Unit International, Ltd.
251-259 Regent Street
London, W1R 7AD, England

Fachinformationszentrum Energie, Physik, Mathematik
GMBH
7514 Eggenstein Leopoldshafen
Federal Republic of Germany

Her Majesty's Stationery Office
P.O. Box 569, S.E. 1
London, England

NASA Center for AeroSpace Information
P.O. Box 8757
Baltimore, Maryland 21240-0757

National Aeronautics and Space Administration
Scientific and Technical Information Program (JTT)
Washington, DC 20546

National Technical Information Service
5285 Port Royal Road
Springfield, Virginia 22161

Pendragon House, Inc.
899 Broadway Avenue
Redwood City, California 94063

Superintendent of Documents
U.S. Government Printing Office
Washington, DC 20402

University Microfilms
A Xerox Company
300 North Zeeb Road
Ann Arbor, Michigan 48106

University Microfilms, Ltd.
Tylers Green
London, England

U.S. Geological Survey Library National Center
MS 950
12201 Sunrise Valley Drive
Reston, Virginia 22092

U.S. Geological Survey Library
2255 North Gemini Drive
Flagstaff, Arizona 86001

U.S. Geological Survey
345 Middlefield Road
Menlo Park, California 94025

U.S. Geological Survey Library
Box 25046
Denver Federal Center, MS914
Denver, Colorado 80225

NTIS PRICE SCHEDULES

(Effective October 1, 1991)

Schedule A
STANDARD PRICE DOCUMENTS AND MICROFICHE**

PRICE CODE	NORTH AMERICAN PRICE	FOREIGN PRICE
A01	$ 9.00	$ 18.00
A02	12.50	25.00
A03	17.00	34.00
A04-A05	19.00	38.00
A06-A09	26.00	52.00
A10-A13	35.00	70.00
A14-A17	43.00	86.00
A18-A21	50.00	100.00
A22-A25	59.00	118.00
A99	*	*
N01	60.00	120.00
N02	59.00	118.00
N03	20.00	40.00

Schedule E
EXCEPTION PRICE DOCUMENTS AND MICROFICHE**

PRICE CODE	NORTH AMERICAN PRICE	FOREIGN PRICE
E01	$11.00	$ 22.00
E02	14.00	28.00
E03	16.00	32.00
E04	19.00	38.00
E05	21.00	42.00
E06	24.00	48.00
E07	27.00	54.00
E08	30.00	60.00
E09	33.00	66.00
E10	36.00	72.00
E11	39.00	78.00
E12	43.00	86.00
E13	46.00	92.00
E14	50.00	100.00
E15	54.00	108.00
E16	59.00	118.00
E17	64.00	128.00
E18	69.00	138.00
E19	76.00	152.00
E20	88.00	176.00
E99	*	*

* Contact NTIS for price quote.

** Effective January 1, 1991, the microfiche copy of any new document entering the NTIS collection will be priced the same as the paper copy of the document.

IMPORTANT NOTICE

NTIS Shipping and Handling Charges

U.S., Canada, Mexico — ADD $3.00 per TOTAL ORDER

All Other Countries — ADD $4.00 per TOTAL ORDER

Exceptions — Does NOT apply to:

ORDERS REQUESTING NTIS RUSH HANDLING
ORDERS FOR SUBSCRIPTION OR STANDING ORDER PRODUCTS *ONLY*

NOTE: Each additional delivery address on an order requires a separate shipping and handling charge.

FEDERAL REGIONAL DEPOSITORY LIBRARIES

ALABAMA

AUBURN UNIV. AT MONTGOMERY LIBRARY
Documents Dept.
7300 University Drive
Montgomery, AL 36117-3596
(205) 244-3650 FAX: (205) 244-0678

UNIV. OF ALABAMA
Amelia Gayle Gorgas Library
Govt. Documents
Box 870266
Tuscaloosa, AL 35487-0266
(205) 348-6046 FAX: (205) 348-8833

ARIZONA

DEPT. OF LIBRARY, ARCHIVES, AND PUBLIC RECORDS
Federal Documents
Third Floor State Capitol
1700 West Washington
Phoenix, AZ 85007
(602) 542-4121 FAX: (602) 542-4400; 542-4500

ARKANSAS

ARKANSAS STATE LIBRARY
State Library Services
One Capitol Mall
Little Rock, AR 72201
(501) 682-2869

CALIFORNIA

CALIFORNIA STATE LIBRARY
Govt. Publications Section
914 Capitol Mall - P.O. Box 942837
Sacramento, CA 94237-0001
(916) 322-4572 FAX: (916) 324-8120

COLORADO

UNIV. OF COLORADO - BOULDER
Norlin Library
Govt. Publications
Campus Box 184
Boulder, CO 80309-0184
(303) 492-8834 FAX: (303) 492-2185

DENVER PUBLIC LIBRARY
Govt. Publications Dept. BS/GPD
1357 Broadway
Denver, CO 80203
(303) 571-2135

CONNECTICUT

CONNECTICUT STATE LIBRARY
231 Capitol Avenue
Hartford, CT 06106
(203) 566-4971 FAX: (203) 566-3322

FLORIDA

UNIV. OF FLORIDA LIBRARIES
Documents Dept.
Library West
Gainesville, FL 32611-2048
(904) 392-0366 FAX: (904) 392-7251

GEORGIA

UNIV. OF GEORGIA LIBRARIES
Govt. Documents Dept.
Jackson Street
Athens, GA 30602
(404) 542-8949 FAX: (404) 542-6522

HAWAII

UNIV. OF HAWAII
Hamilton Library
Govt. Documents Collection
2550 The Mall
Honolulu, HI 96822
(808) 948-8230 FAX: (808) 956-5968

IDAHO

UNIV. OF IDAHO LIBRARY
Documents Section
Moscow, ID 83843
(208) 885-6344 FAX: (208) 885-6817

ILLINOIS

ILLINOIS STATE LIBRARY
Reference Dept.
300 South Second
Springfield, IL 62701-1796
(217) 782-7596 FAX: (217) 524-0041

INDIANA

INDIANA STATE LIBRARY
Serials/Documents Section
140 North Senate Avenue
Indianapolis, IN 46204
(317) 232-3678 FAX: (317) 232-3728

IOWA

UNIV. OF IOWA LIBRARIES
Govt. Publications Dept.
Washington & Madison Streets
Iowa City, IA 52242
(319) 335-5926 FAX: (319) 335-5830

KANSAS

UNIV. OF KANSAS
Govt. Documents & Map Library
6001 Malatt Hall
Lawrence, KS 66045-2800
(913) 864-4660 FAX: (913) 864-5380

KENTUCKY

UNIV. OF KENTUCKY LIBRARIES
Govt. Publications/Maps Dept.
Lexington, KY 40506-0039
(606) 257-3139 FAX: (606) 257-1563; 257-8379

LOUISIANA

LOUISIANA STATE UNIV.
Middleton Library
Govt. Documents Dept.
Baton Rouge, LA 70803
(504) 388-2570 FAX: (504) 388-6992

LOUISIANA TECHNICAL UNIV.
Prescott Memorial Library
Govt. Documents Dept.
305 Wisteria Street
Ruston, LA 71270-9985
(318) 257-4962 FAX: (318) 257-2447

MAINE

TRI-STATE DOCUMENTS DEPOSITORY
Raymond H. Fogler Library
Govt. Documents & Microforms Dept.
Univ. of Maine
Orono, ME 04469
(207) 581-1680

MARYLAND

UNIV. OF MARYLAND
Hornbake Library
Govt. Documents/Maps Unit
College Park, MD 20742
(301) 454-3034 FAX: (301) 454-4985

MASSACHUSETTS

BOSTON PUBLIC LIBRARY
Govt. Documents Dept.
666 Boylston Street
Boston, MA 02117
(617) 536-5400 ext. 226
FAX: (617) 267-8273; 267-8248

MICHIGAN

DETROIT PUBLIC LIBRARY
5201 Woodward Avenue
Detroit, MI 48202-4093
(313) 833-1440; 833-1409
FAX: (313) 833-5039

LIBRARY OF MICHIGAN
Govt. Documents Unit
P.O. Box 30007
Lansing, MI 48909
(517) 373-0640 FAX: (517) 373-3381

MINNESOTA

UNIV. OF MINNESOTA
Wilson Library
Govt. Publications Library
309 19th Avenue South
Minneapolis, MN 55455
(612) 624-5073 FAX: (612) 626-9353

MISSISSIPPI

UNIV. OF MISSISSIPPI
J.D. Williams Library
Federal Documents Dept.
106 Old Gym Bldg.
University, MS 38677
(601) 232-5857 FAX: (601) 232-5453

MISSOURI

UNIV. OF MISSOURI - COLUMBIA
Ellis Library
Govt. Documents
Columbia, MO 65201
(314) 882-6733 FAX: (314) 882-8044

MONTANA

UNIV. OF MONTANA
Maureen & Mike Mansfield Library
Documents Div.
Missoula, MT 59812-1195
(406) 243-6700 FAX: (406) 243-2060

NEBRASKA

UNIV. OF NEBRASKA - LINCOLN
D.L. Love Memorial Library
Documents Dept.
Lincoln, NE 68588
(402) 472-2562

NEVADA

UNIV. OF NEVADA
Reno Library
Govt. Publications Dept.
Reno, NV 89557
(702) 784-6579 FAX: (702) 784-1751

NEW JERSEY

NEWARK PUBLIC LIBRARY
U.S. Documents Div.
5 Washington Street -
P.O. Box 630
Newark, NJ 07101-0630
(201) 733-7812 FAX: (201) 733-5648

NEW MEXICO

UNIV. OF NEW MEXICO
General Library
Govt. Publications Dept.
Albuquerque, NM 87131-1466
(505) 277-5441 FAX: (505) 277-6019

NEW MEXICO STATE LIBRARY
325 Don Gaspar Avenue
Santa Fe, NM 87503
(505) 827-3826 FAX: (505) 827-3820

NEW YORK

NEW YORK STATE LIBRARY
Documents/Gift & Exchange Section
Federal Depository Program
Cultural Education Center
Albany, NY 12230
(518) 474-5563 FAX: (518) 474-5786

NORTH CAROLINA

UNIV. OF NORTH CAROLINA - CHAPEL HILL
CB#3912, Davis Library
BA/SS Dept.—Documents
Chapel Hill, NC 27599
(919) 962-1151 FAX: (919) 962-0484

NORTH DAKOTA

NORTH DAKOTA STATE UNIV. LIBRARY
Documents Office
Fargo, ND 58105
(701) 237-8886 FAX: (701) 237-7138
In cooperation with Univ. of North Dakota, Chester Fritz Library
Grand Forks

OHIO

STATE LIBRARY OF OHIO
Documents Dept.
65 South Front Street
Columbus, OH 43266
(614) 644-7051 FAX: (614) 752-9178

OKLAHOMA

OKLAHOMA DEPT. OF LIBRARIES
U.S. Govt. Information Div.
200 NE 18th Street
Oklahoma City, OK 73105-3298
(405) 521-2502, ext. 252, 253
FAX: (405) 525-7804

OKLAHOMA STATE UNIV.
Edmon Low Library
Documents Dept.
Stillwater, OK 74078
(405) 744-6546 FAX: (405) 744-5183

OREGON

PORTLAND STATE UNIV.
Millar Library
934 SW Harrison - P.O. Box 1151
Portland, OR 97207
(503) 725-3673 FAX: (503) 725-4527

PENNSYLVANIA

STATE LIBRARY OF PENN.
Govt. Publications Section
Walnut St. & Commonwealth Ave. - P.O. Box 1601
Harrisburg, PA 17105
(717) 787-3752

SOUTH CAROLINA

CLEMSON UNIV.
Cooper Library
Public Documents Unit
Clemson, SC 29634-3001
(803) 656-5174 FAX: (803) 656-3025
In cooperation with Univ. of South Carolina, Thomas Cooper Library, Columbia

TENNESSEE

MEMPHIS STATE UNIV. LIBRARIES
Govt. Documents
Memphis, TN 38152
(901) 678-2586 FAX: (901) 678-2511

TEXAS

TEXAS STATE LIBRARY
United States Documents
P.O. Box 12927 - 1201 Brazos
Austin, TX 78711
(512) 463-5455 FAX: (512) 463-5436

TEXAS TECH. UNIV. LIBRARY
Documents Dept.
Lubbock, TX 79409
(806) 742-2268 FAX: (806) 742-1920

UTAH

UTAH STATE UNIV.
Merrill Library & Learning Resources Center, UMC-3000
Documents Dept.
Logan, UT 84322-3000
(801) 750-2684 FAX: (801) 750-2677

VIRGINIA

UNIV. OF VIRGINIA
Alderman Library
Govt. Documents
Charlottesville, VA 22903-2498
(804) 924-3133 FAX: (804) 924-4337

WASHINGTON

WASHINGTON STATE LIBRARY
Document Section
MS AJ-11
Olympia, WA 98504-0111
(206) 753-4027 FAX: (206) 753-3546

WEST VIRGINIA

WEST VIRGINIA UNIV. LIBRARY
Govt. Documents Section
P.O. Box 6069
Morgantown, WV 26506
(304) 293-3640

WISCONSIN

ST. HIST. SOC. OF WISCONSIN LIBRARY
Govt. Publications Section
816 State Street
Madison, WI 53706
(608) 262-2781 FAX: (608) 262-4711
In cooperation with Univ. of Wisconsin-Madison, Memorial Library

MILWAUKEE PUBLIC LIBRARY
Documents Div.
814 West Wisconsin Avenue
Milwaukee, WI 53233
(414) 278-2167 FAX: (414) 278-2137

WYOMING

WYOMING STATE LIBRARY
Supreme Court & Library Bldg.
Govt. Publications
Cheyenne, WY 82002
(307) 777-5920 FAX: (307) 777-6289

National Aeronautics and
Space Administration
Code JTT
Washington, D.C.
20546

Official Business

Penalty for Private Use, $300

SPECIAL FOURTH-CLASS RATE
POSTAGE & FEES PAID
NASA
PERMIT No. G27

NASA
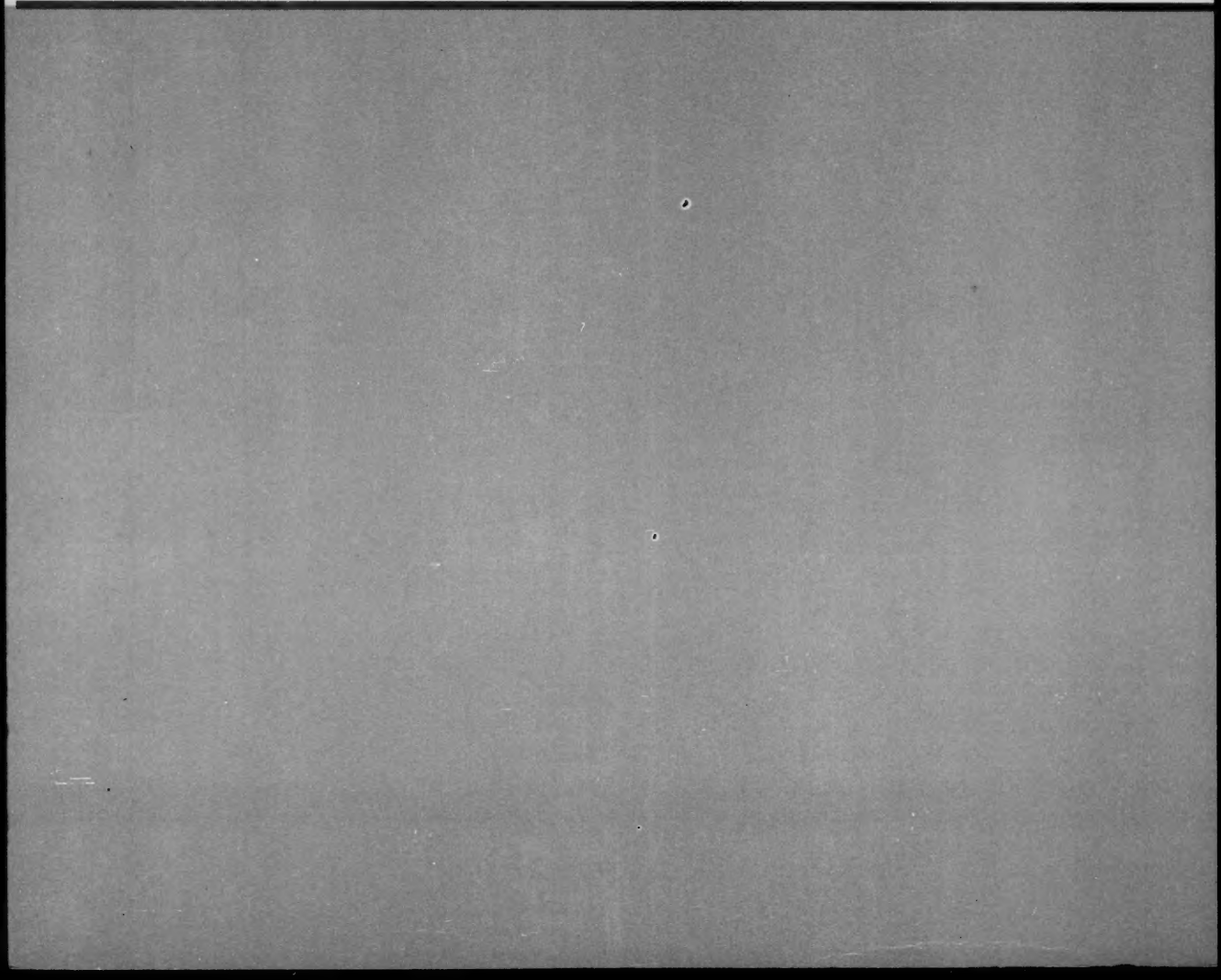
POSTMASTER: If Undeliverable (Section 158 Postal Manual) Do Not Return